BULLETIN OF THE
CHEMICAL SOCIETY OF JAPAN

Professor Masao KATAYAMA.

Professor Masao Katayama, the second son of Seigo Katayama, was born in Chayamachi near Okayama on September 11, 1877. In 1900 he finished the chemistry course in the Faculty of Science, Tokyo Imperial University, and continued to study as a post-graduate student.

In 1902 he was appointed to a professorship at the Higher Technical School of Tokyo and after three years he was sent to Europe as a Government Research Fellow. He studied there for three years, spending one half of the time in the Laboratory of Professor Lorenz in Zürich and the other half in the Laboratory of Professor Nernst in Berlin. In 1911 he was appointed Professor of Theoretical Chemistry of Tohoku Imperial University in Sendai. In 1919 he was called back to his *alma mater* to succeed Professor Joji Sakurai, now Privy Councillor and the President of the Imperial Academy, in the chair of Physical Chemistry in the Faculty of Science. This chair he has held continuously since then.

Outside the university he is also active as a member of the Imperial Academy and of the National Research Council; as the head of the Katayama Laboratory in the Institute of Physical and Chemical Research in Tokyo; on a committee of the Shanghai Science Institute; and as the Chairman of the Fifth Committee of the Japan Society for the Promotion of Scientific Research.

Professor Katayama's works on physical chemistry cover a notably wide scope, extending over the energetic and atomistic fields. Among them his studies on gas equilibrium and on surface tension are well known and cited in many chemical publications as important researches. The former was carried out with Professor Bodenstein for the dissociation of the vapour of sulphuric acid and nitrogen dioxide, and not only the result of the experiment but also the principle of the measurement was an important contribution to the study of gas equilibrium. The latter refers to the improvement of the Ramsay-Shields equation of surface tension which did not agree with the theory of corresponding states and failed to express the experimental result near the critical point. These two difficulties were overcome by the formula of Professor Katayama who took into consideration the effect of molecular attraction in the vapour phase. Under his direction many interesting researches have been carried out on electrochemistry, equation of state, chemical kinetics, atomic and mole-

cular structures, etc., but many of the results have been published under the names of his pupils. In addition to these brilliant works, Professor Katayama wrote a textbook of physical chemistry named "Kwagaku-Honron", in which the fundamental conceptions of physical chemistry are explained in an original manner and which is indisputably the best written in our language.

The papers published in the present number are dedicated to Professor Katayama by his pupils on the celebration of the sixtieth anniversary of his birthday. It is their heartfelt desire that Professor Katayama may long enjoy good health, and continue his activities on their behalf, as well as for the future development of physical chemistry in Japan.

December, 1937.

San-ichiro MIZUSHIMA.

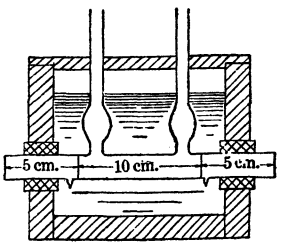
Rotatory Dispersion of Sugars in Liquid Ammonia and in Water.[1]

By Hikoichi SHIBA and Shintaro TANABE.

(Received January 11, 1938.)

We have attempted to study the nature of sugars in liquid ammonia. In the present paper are reported the results in the preliminary determination of their optical activities at the temperatures below the boiling point of the solvent. The optical rotations of sugars in this medium were measured by Sherry[2] at 20°C. for D-line. We were informed by the abstract that Shatenstein recently carried out polarimetric measurements with saponine at 20°C.

To observe the optical rotations at low temperatures, we constructed a polarimetric tube of fused quartz. It has, as shown in Fig. 1, two double windows of plane parallel plates. Both the chambers of the double windows were well evacuated, so that the disturbance by the frost or dew drops condensed on the window plates from the moisture in air was avoided and the field of view was kept clear even when it was cooled down to −70°C. The temperatures, at which we observed, were in the range from −35 to −70°C. and were kept constant within 1° without difficulty during a series of measurements by immersing the tube in a wooden tank of a sufficiently large capacity filled with alcohol and CO_2 snow and covering it externally with felt. We tried to make such a polarimetric tube of borosilicate glass but the glass plates of the windows had fatal strains for our purposes.



The polarimetric tube.

Fig. 1.

The polarimeter used was the three field type of Schmidt and Haensch with a monochromator as its accessory. For the light source the filament lamp 250 W for kinema projection was used through the monochromater which was calibrated with Hg-lines. Mercury, sodium, and cadmium vapour lamps were also used, being filtered with the monochromator. The sugars and the glucoside used were Kahlbaum's or Merck's products.

(1) This paper was read at the autumnal meeting of the Institute of Physical and Chemical Research (Nov. 21, 1935.)

(2) Sherry, *J. Phys. Chem.*, **11** (1907), 559.

For the comparison and the proof of purity of the materials, we determined accurately the rotatory dispersion in water, using the ordinary polarimetric tube 10 cm. long. The results of the measurements were briefly described in the following.

Aqueous Solutions. We determined the rotatory dispersions of *d*-glucose, *d*-fructose, *d*-galactose, α-methyl-*d*-glucoside, saccharose, lactose, and maltose in water with high accuracy. In these cases mercury lines ($\lambda = 0.612\,\mu$, 0.578, 0.546, 0.492, 0.436), cadmium lines ($\lambda = 0.644$, 0.509, 0.480), sodium line ($\lambda = 0.589$) were used except saccharose solutions which were observed with the filament lamp. The concentration of solutions is represented in molarities of anhydrous sugars and the specific rotation is evaluated for unit mass of them. Specific rotations obtained were graphed to test Drude's dispersion formula $[\alpha] = k_0/(\lambda^2 - \lambda_0^2)$ and to compare them with the data given by Grossmann and Bloch and by Wagner-Jauregg.[3] Good agreements were obtained as seen in Fig. 2–8. For saccharose such a comparison was omitted and for maltose the previous data of the dispersion to be utilized was not found.

In the cases where the multirotation was to occur, the measurements were carried out 3 or 4 days after preparing the solution. In the duration of preservation, care was taken not to be interfered by fermentation, avoiding the contact of the solutions with air.

Solutions in Liquid Ammonia. The optical rotations in liquid ammonia were measured with the filament lamp as the light source. The measurements were done in the day of preparation of the solution. The accuracy of the rotation measured in liquid ammonia is less than that in water because of using the special polarimetric tube, as mentioned above, at low temperatures. The fluctuation of the experimental values is within ±1% The sugars and glucoside in liquid ammonia were found to behave in the manner of simple rotatory dispersion, although some deviations are seen in the dispersion curve of lactose. The values of λ_0 and k_0 in Drude's formula were estimated from graphs and tabulated in Table 13. As is seen in Table 9, fructose in liquid ammonia showed small rotations with positive or negative sign. It may be roughly assumed that it has not optical activity under our conditions as well as in Sherry's observation at 20°C. Sherry reported that neither in methylamine nor in ethylamine fructose showed measurable optical activity. Such facts seem to suggest something of chemical change of ketose in these mediums.

(3) "International Critical Tables," Vol. II, 334.

The temperature coefficients of the specific rotation in liquid ammonia were determined for D-line with sodium vapour lamp, as shown in Table 14. We observed also sugars such as glucose, fructose, saccharose, and lactose dissolved in the mixture of water and ethyl alcohol in equal volumes at the room temperature and at low temperatures. The results are shown in Table 15.

Table 1. *d*-Glucose in water.

$^2/_3$ mol, 20-21°C., 3 days after dissolution, Hg-lamp.

λ (μ)	[α]
0.578	53.1
0.546	66.5
0.492	73.9
0.436	120.0

$\lambda_0 = 0.148$ $k_0 = 17.2$

Table 2. *d*-Fructose in water.

$^2/_3$ mol, 20-21°C., the day of dissolution, Hg-, Na-, Cd-lamps.

λ (μ)	[α]
0.644	—
0.612	−83.5
0.589	−93.0
0.578	−98.5
0.546	−110.0
0.509	−127.6
0.492	−128.7
0.480	−145.6
0.436	−181.0

$\lambda_0 = 0.152$ $k_0 = 29.8$

Table 3. *d*-Galactose in water.

$^1/_2$ mol, 21°C., 4 days after dissolution, Hg-, Na-, Cd-lamps.

λ (μ)	[α]
0.644	67.2
0.612	70.6
0.589	79.9
0.578	83.6
0 546	95.2
0.509	112.3
0.492	119.7
0.480	125.2
0.436	154.3

$\lambda_0 = 0.145$ $k_0 = 26.0$

Table 4. *α*-Methyl-*d*-glucoside in water.

$^2/_3$ mol, 20°C., 4 days after dissolution, Hg-, Na-, Cd-lamps.

λ (μ)	[α]
0.644	128.7
0.612	142.6
0.589	158.2
0.578	165.1
0.546	186.0
0.509	218.8
0.492	231.7
0.480	246.7
0.436	308.7

$\lambda_0 = 0.138$ $k_0 = 52.0$

Table 5. Saccharose in water.

0.292 mol, 28.3°C., filament lamp.

λ (μ)	[α]
0.623	57.3
0.589	64.7
0.578	66.4
0.546	76.1
0.517	86.7
0.492	96.4
0.458	105.5
0.436	115.9

1.168 mol, 28°C.

λ (μ)	[α]
0.623	57.8
0.610	60.4
0.600	62.5
0.589	64.8
0.578	67.7
0.565	71.0
0.546	76.6
0.530	81.8
0.510	89.2
0.492	95.7
0.470	105.2
0.450	116.4
0.436	125.0

$\lambda_0 = 0.141$ $k_0 = 21.2$

Table 6. Lactose in water.

1/3 mol, 19°C., 3 days after dissolution, Hg-, Na-, Cd-lamps.

λ (μ)	[α]
0.644	42.4
0.612	46.1
0.589	52.2
0.578	53.8
0.546	60.3
0.509	71.6
0.492	73.6
0.480	78.9
0.436	98 3

$\lambda_0 = 0.145$ $k_0 = 16.6$

Table 7. Maltose in water.

1/2 mol, 16°C., 4 days after dissolution, Hg-, Na-, Cd-lamps.

λ (μ)	[α]
0.644	113.9
0.612	124.6
0.589	138.7
0.578	144.7
0.546	164.4
0.509	191.8
0.492	205.0
0.480	216.5
0.436	271.0

$\lambda_0 = 0.173$ $k_0 = 43.6$

Table 8.
d-Glucose in liquid ammonia.

0.48 mol, −35°C., filament lamp.

λ (μ)	[α]
0.644	62.7
0.612	62.7
0.589	77.3
0.578	74.8
0.546	86.0
0.509	108.0
0.492	114.5
0.480	135.7
0.436	153.0

$\lambda_0 = 0.258$ $k_0 = 20.6$

Table 9.
d-Fructose in liquid ammonia.

0.46 mol, −36°C., filament lamp.

λ (μ)	[α]
0.612	+0.09
0.578	−4.18
0.546	−6.11
0.492	+5.47
0.436	−4.39

Table 10. *α*-Methyl-*d*-glucoside in liquid ammonia.

0.34 mol, −36°C., filament lamp.

λ (μ)	[α]
0.644	140.4
0.612	152.4
0.589	168.2
0.578	180.9
0.546	203.4
0.509	238.5
0.492	259.8
0.480	272.4
0.436	325.1

$\lambda_0 = 0.152$ $k_0 = 55.2$

Table 11.

Saccharose in liquid ammonia.

0.21 mol, −43°C., filament lamp.

λ (μ)	[α]
0.644	63.0
0.612	65.5
0.589	84.6
0.578	83.9
0.546	101.4
0.509	117.3
0.492	125.0
0.480	129.0
0.436	171.0

$\lambda_0 = 0.247$ $k_0 = 22.0$

Table 12.

Lactose in liquid ammonia.

0.19 mol, −51°C, filament lamp.

λ (μ)	[α]
0.644	40.4
0.612	59.0
0.589	62.1
0·578	71.0
0.546	83.4
0.509	96.3
0.492	104.5
0.480	107.0
0.436	122.7

$\lambda_0 = 0.214$ $k_0 = 19.6$

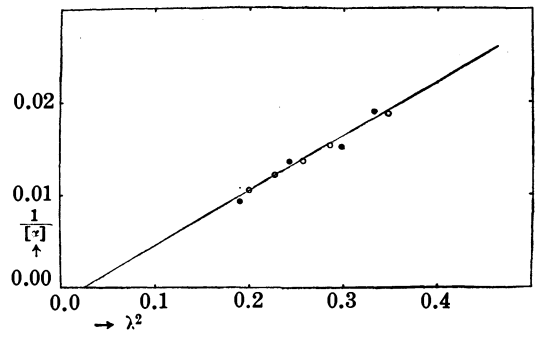


Fig. 2. *d*-Glucose in water. 20–21°C. ○ Grossmann and Bloch.

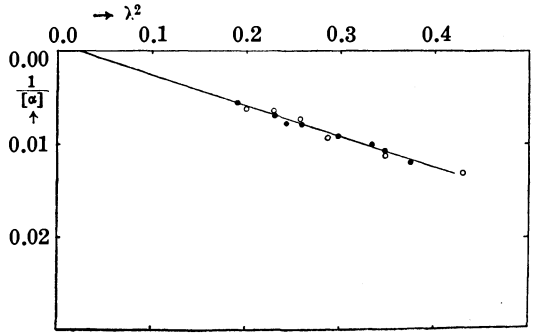


Fig. 3. *d*-Fructose in water. 20–21°C. ○ Grossmann and Bloch.

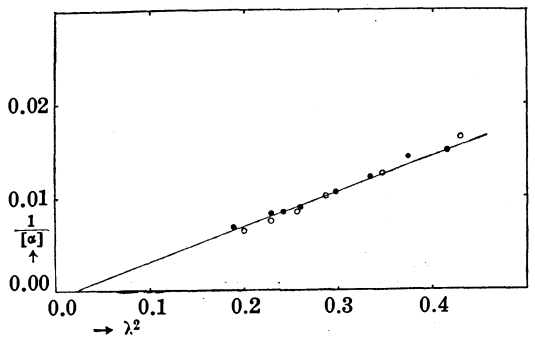


Fig. 4. *d*-Galactose in water. 21°C. ○ Grossmann and Bloch.

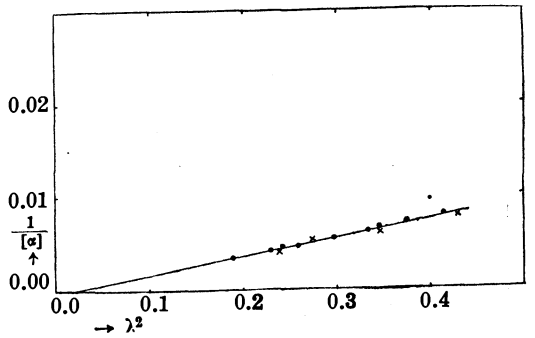


Fig. 5. *α*-Methyl-*d*-glucoside in water. 20°C. × Wagner-Jauregg.

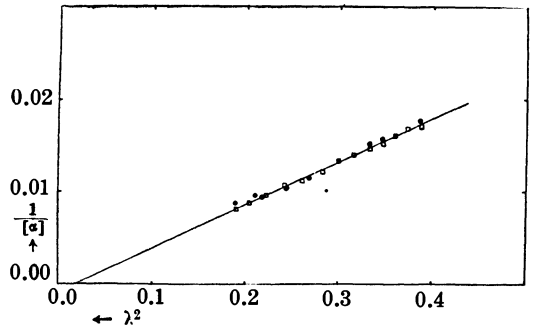


Fig. 6. Saccharose in water.
● 0.292 mol, 28.3°C. □ 1.168 mol, 28.0°C.

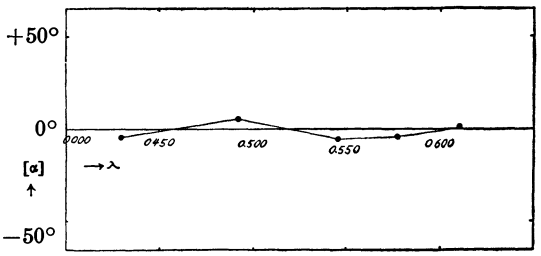


Fig. 10. *d*-Fructose in liquid NH_3, 0.46 mol, −36°C., filament lamp.

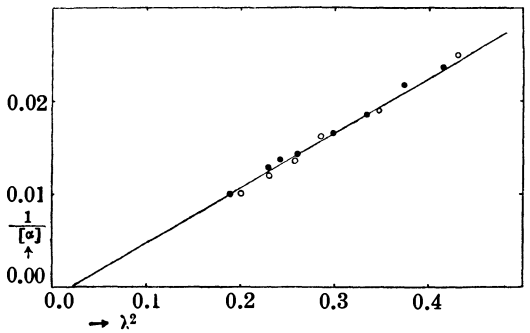


Fig. 7. Lactose in water. ○ Grossmann 19°C. and Bloch.

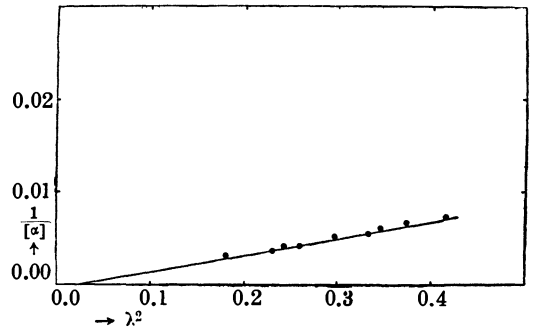


Fig. 11. α-Methyl-*d*-glucoside, in liquid NH_3, 0.34 mol, − 36°C., filament lamp.

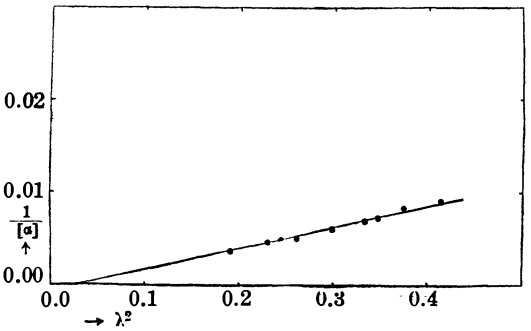


Fig. 8. Moltose in water. 16°C.

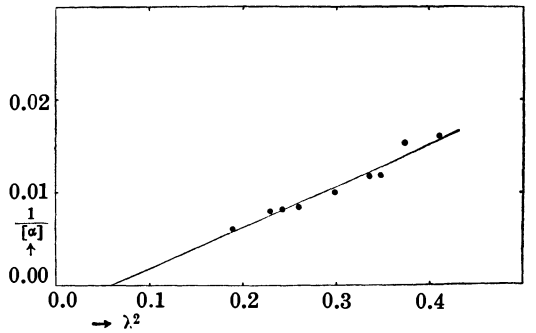


Fig. 12. Saccharose in liquid NH_3, 0.21 mol, −43°C., filament lamp.

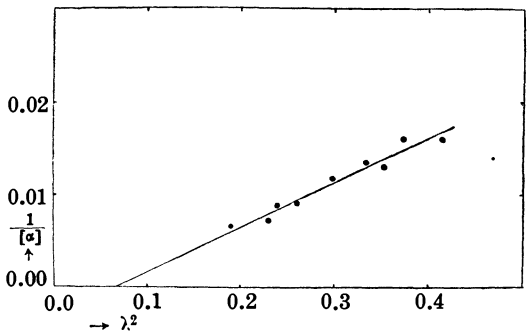


Fig. 9. *d*-Glucose in liquid NH_3, 0.48 mol, −35°C., filament lamp.

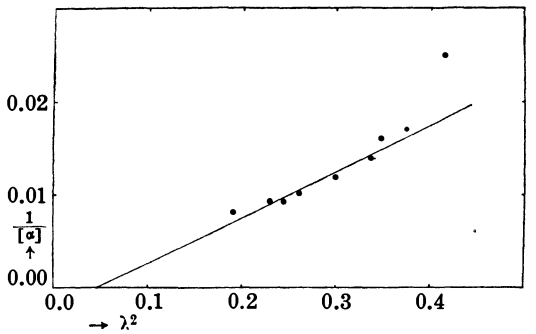


Fig. 13. Lactose in liquid NH_3, 0.19 mol, −51°C., filament lamp.

Table 13. Values of λ_0 and k_0 ($[\alpha] = k_0/(\lambda^2-\lambda_0^2)$).

	Aqueous solution			Solution in liquid NH_3		
	t °C.	λ_0 (μ)	k_0	t °C.	λ_0 (μ)	k_0
d-Glucose	21	0.148	17.2	−35	0.258	20.6
d-Fructose	20–21	0.152	29.8	−36	—	—
d-Galactose	21	0.145	26.0	—	—	—
α-Methyl-*d*-glucoside	20	0.138	52.0	−36	0.152	55.2
Saccharose	28	0.141	21.2	−43	0.247	22.0
Lactose	19	0.145	16.6	−51	0.214	19.6
Maltose	16	0.173	43.6	—	—	—

Table 14. Temperature coefficient of $[\alpha]_D$ in liquid ammonia.

	Concentration	t °C.	$[\alpha]_D$	$\frac{\Delta[\alpha]_D}{\Delta t}$	
d-Glucose	0.48 mol	−35	77.3	−0.26	
	0.48 mol	−62	84.2		
	3.5 g. in 100 c.c. solution	20	56.1		Sherry
	27.8 g. in 100 c.c. solution	20	55.3		Sherry
d-Fructose	0.46 mol	−36	[0]		
	—	20	0		Sherry
α-Methyl-*d*-glucoside	0.34 mol	−36	168.2	−0.31	
	0.34 mol	−54	173.6		
Saccharose	0.21 mol	−43	84.6	−0.20	
	0.21 mol	−63	88.6		
	8.2 g. in 100 c.c solution	20	76.0		Sherry
	48.8 g. in 100 c.c solution	20	73.6		Sherry
Lactose	0.19 mol	−42	60.5	−0.18	
	0.19 mol	−51	62.1		
	7.0 g. in 100 c.c. solution	20	33.2		Sherry
	27.8 g. in 100 c.c solution	20	32.5		Sherry

Table 15. Temperature coefficient of $[\alpha]_D$ in the mixture of water and ethyl alcohol (equal volumes).

	Concentration	t °C.	$[\alpha]_D$	$\frac{\Delta[\alpha]}{\Delta t}$
d-Glucose	0.5 g. in 100 c.c. solution	23 - 67	59.6 71.6	−0.13
d-Fructose	1 g. in 100 c.c. solution	23 −67.5	−64.8 −76.5	0.13
Saccharose	5 g. in 100 c.c. solution	20 −45	66.5 80.0	−0.20
Lactose	0.2 g. in 100 c.c. solution	23 −67.5	49.1 93.7	−0.53

Institute of Physical and Chemical Research, Tokyo.

X-Ray Spectroscopic Determination of Lanthanum, Neodymium and Gadolinium in the Presence of Other Rare Earth Elements.

By Kenjiro KIMURA.

(Received January 10, 1938.)

As is known, the separation of the rare earth elements from one another is, except cerium, so difficult and tedious that the usual chemical methods of analysis fail entirely when applied to the quantitative determination of each component in a rare earth mixture. Although some indirect methods proposed may be used for the analysis of a rare earth mixture of only a few components, most of them can not be applied to a complex mixture of the rare earths such as extracted from a natural mineral. The only reliable one that can be used even in such a case may be probably the X-ray spectroscopic method.[1]

(1) cf. A. Hadding, *Z. anorg. allgem. Chem.*, **122** (1922), 195; V.M. Goldschmidt and L. Thomassen, "Geochemische Verteilungsgesetze der Elemente," III, Kristiania (1924); P. Günther and G. Wilcke, *Z. physik. Chem.*, **119** (1926), 219; H. Schreiber, *Z. Physik*, **58** (1929), 619; P. Günther, A. Kotowski, and H. Lehl, *Z. anorg. allgem. Chem.*, **200** (1931), 287; I. Noddack, *Z. anorg. allgem. Chem.*, **225** (1935), 337; E. Minami, *Nachr. Ges. Wiss. Göttingen, Math.-physik. Klasse*, Fachgruppe IV, N.F. **1** (1935), 155.

The present author intends to estimate the amount of each of the rare earth elements in their mixture by comparing the intensity of their X-ray spectral lines with that of the reference elements. The method is in its principle quite similar to the one which was first proposed and investigated by G. von Hevesy, D. Coster, Y. Nishina and others[2] for the determination of hafnium content in zirconia-hafnia mixtures. The experimental results obtained with lanthanum, neodymium and gadolinium will be given in the present report.

The Determination of Lanthanum.[3]

For the determination of lanthanum in a mixture of the rare earths, the intensity of the $L\beta_2$ line of lanthanum is compared with that of the $L\beta_3$ line of cerium which is taken as the reference element. As the wavelength difference of the said two lines is only 8 X-Units, which corresponds to about 0.5 mm. on the photographic plate, the error of the estimation of the relative intensities due to the wrong exposure is practically eliminated.

Although cerium is an element that belongs to the rare earth group, it is comparatively easy to separate cerium alone from other rare earth elements by some chemical methods,[4] and there is no difficulty in ascertaining its amount present in a given sample, or in preparing a sample free from it. Since cerium can be completely precipitated from a solution with other rare earth elements in the form of hydroxide or oxalate, thorough mixing of the sample with the added reference substance can be easily attained without that tedious procedure of weighing and grinding which we have to follow when an element of quite different chemical properties is taken as the reference.

To a given sample of rare earth mixture is added a known quantity of cerium oxide, or lanthanum oxide if the cerium line of the original sample is stronger. The quantity added is to be varied until the two lines under consideration show an equal intensity on the photographic plate. If we know the concentration ratio CeO_2/La_2O_3 which makes the said two lines equally intense, we can easily calculate the amount of lanthana in the original sample from that of ceria present.

The actual procedure followed is given below.

(2) Hevesy and Coster, *Nature*, **111** (1923), 182; Coster, *Chem. News*, **127** (1923), 65; Coster and Nishina, *ibid.*, **130** (1925), 149; Kimura, *Z. physik. Chem.*, **128** (1927), 394.

(3) Read before the Chemical Society of Japan, April 3, 1930 and July 11, 1931, and published in Japanese in *J. Chem. Soc. Japan*, **54** (1933), 213.

(4) e.g. C. James and L. A. Pratt, *J. Am. Chem. Soc.*, **33** (1911), 1326; Paul H.M.-P. Brinton and C. James, *ibid.*, **41** (1919), 1080.

Materials and Experimental Procedure. The intensity of the lanthanum $L\beta_2$ line was compared with that of the cerium $L\beta_3$ line by using the oxide mixtures of lanthanum and cerium. The mixtures were prepared from cerium chloride and lanthanum chloride, which had been carefully purified, the former by the bromate method, the latter by the fractionation.

The high purity of the cerium salt used was shown by the X-ray spectroscopic analysis. It did not contain the detectable amount of any of other lanthanide elements.

It was also revealed by the X-ray method that the lanthanum salt prepared was free from neodymide elements. Although a few spectral lines of cerium and praseodymium were observed very faintly on the plate, the $L\beta_3$ line of cerium was not detected under the same experimental conditions that were followed in the case of the comparison of the relative intensities of the said two lines. Besides, the absorption bands due to some other rare earth elements were not observed with the concentrated solution of the lanthanum chloride used. Both the hydrogen peroxide test and the iodate test failed also to show the presence of cerium in it. Therefore, for the present purpose, the material may be assumed to be a pure lanthanum salt.

Solutions with appropriate known concentrations of lanthanum chloride and of cerium chloride were prepared. The proper volumes of each solution were pipetted and mixed thoroughly. By the addition of ammonium chloride and ammonia, the hydroxides of lanthanum and cerium were precipitated from the solution, filtered off, and ignited to oxides, which were used as a standard sample for the comparison of the relative intensities of the lanthanum $L\beta_2$ and the cerium $L\beta_3$ lines.

When a sample to be analysed was given, a mixture that could be used for the X-ray analysis was prepared from it by the following procedure. The original sample, if it consisted of rare earths only, was dissolved in dilute hydrochloric acid after fusion with sodium bisulphate if necessary, and a solution with the known concentration was prepared. But, if it contained some other elements which were precipitated with ammonia, the rare earths should be first extracted from it. By precipitation with oxalic acid, the rare earth elements and thorium could be separated from the other members of the analytical group of ammonia, such as iron, aluminium, zirconium, uranium, etc. Thorium in the oxalate precipitate was removed by applying the hydrogen peroxide method and thus a solution which contained the rare earth elements only was obtained. After the determination of the contents of cerium and total rare earth elements of the solution thus prepared, a definite volume of it was pipetted. To

it was added a known amount of the solution of cerium chloride, or that of lanthanum chloride according to the ratio CeO_2/La_2O_3 of the original sample. From this solution, the hydroxides of the rare earth elements were precipitated by the addition of ammonia, filtered off, and ignited to oxides.

With the oxide mixture thus prepared, the lanthanum $L\beta_2$ and the cerium $L\beta_3$ lines were photographed, using a metal X-ray tube and a vacuum spectrograph of Siegbahn's type. Calcite was used as the crystal. The width of the slit of the spectrograph was about 0.1 mm. The sample was put on the copper plate of the anticathode, which had been changed before each exposure. The X-ray lines were excited by cathode rays from the hot cathode of tungsten wire. The photograph was taken by 41 minutes' exposure at the applied tension of 15 kilo-volts (effective) and the current of about 2 milliamperes. During the exposure, the crystal was slowly rotated through an angle of 0.2 degree.

The spectral lines on the plates were examined under the magnifying glass. Instead of estimating the intensity ratio of the two lines under consideration, the quantity of the element added was varied until the said two lines became equally intense.

The photograph was taken repeatedly with the same sample, and the reproducibility of experiments was confirmed.

Experimental Results. (a) The relative intensities of the lanthanum $L\beta_2$ and the cerium $L\beta_3$ lines were compared by using $La_2O_3 - CeO_2$ mixtures as the samples. In Table 1 are given the results obtained, from which we know that the two lines under consideration show an equal intensity when the ratio CeO_2/La_2O_3 in weight is equal to 2.5(5).

(b) The presence of other rare earth elements might have some effects on the value of the balance ratio which was just determined to be 2.55 in the case of the mixture of lanthanum oxide and cerium oxide.

For the disturbing effects of a third element present in a sample, the following four cases were mentioned by G. von Hevesy[5]: (i) the case when a third element present has a stronger absorption effect on the line of longer wave-length; (ii) the case when a third element present has an absorption edge situated between the two lines to be compared; (iii) the case when a line of a third element present is situated between the absorption edges which correspond respectively to the two lines under comparison; (iv) the case when a line of a third element present lies near and on the short wave-length side of the absorption edges above mentioned.

(5) Hevesy, "Chemical Analysis by X-Rays and its Applications," 117, New York (1932).

In the present case there is no element of the rare earth group which has the absorption effects mentioned in (i) and (ii). As the wave-length difference of the absorption edges corresponding to the two lines to be compared is fairly large, some rare earth elements which have the excitation effects mentioned in (iii) and (iv) may come into consideration. But, as is seen in the following examples, these disturbing effects, if there be any, are generally very small and may be neglected in actual analyses.

Table 1.

CeO_2/La_2O_3 in weight	Intensity of La $L\beta_2$ compared with Ce $L\beta_3$
3.69	Weaker
3.06	Weaker
2.92	Weaker
2.81	Weaker
2.70	Weaker
2.65	Weaker
2.61	A little weaker
2.60	A little weaker
2.59	A little weaker
2.55	Nearly equal
2.54	Nearly equal
2.50	A little stronger
2.45	Stronger
2.39	Stronger
2.37	Stronger
2.20	Stronger
1.97	Stronger
1.80	Stronger
1.79	Stronger
0.87	Stronger

(c) As the examples, the amount of lanthanum oxide in several samples was determined. Sample No. 1 mainly consisted of the oxides of lanthanide elements of lower atomic numbers and was free from ceria. Sample No. 2 was a mixture of cerium earths, rich in neodymium and praseodymium. The amount of ceria in it was determined to be 29.35%. Sample No. 3 contained 49.6% of ceria, and less than 10% of yttrium earths; the remainder was cerium earths rich in neodymium. Sample No. 4 was a mixture of the rare earths; it contained 22.2% of ceria and about 10% of yttrium earths. It was rich in samaria.

Cerium oxide was added to Samples No. 1, No. 2, and No. 4, while lanthanum oxide was added to Sample No. 3 which was already rich in ceria. The relative intensities of the lanthanum $L\beta_2$ and the cerium $L\beta_3$ lines were compared with the results shown in Table 2.

Table 2.

(1) Sample No. 1.

$\frac{CeO_2 \text{ added}}{\text{Sample taken}}$ (%)	Intensity of La $L\beta_2$ compared with Ce $L\beta_3$
114	Stronger
120	Stronger
128	Nearly equal
137	Weaker
139	Weaker

(2) Sample No. 2.

$\frac{CeO_2 \text{ added}}{\text{Sample taken}}$ (%)	Intensity of La $L\beta_2$ compared with Ce $L\beta_3$
8.6	Weaker
7.7	Nearly equal
5.45	Nearly equal
3.9	Nearly equal
2.8	Stronger
2.5	Stronger
0.0	Stronger

(3) Sample No. 3.

$\frac{La_2O_3 \text{ added}}{\text{Sample taken}}$ (%)	Intensity of La $L\beta_2$ compared with Ce $L\beta_3$
44.3	Stronger
22.2	Stronger
17.7	Nearly equal (a little stronger)
15.5	Nearly equal
8.2	Weaker
4.4	Weaker
0.0	Weaker

(4) Sample No. 4.

$\frac{CeO_2 \text{ added}}{\text{Sample taken}}$ (%)	Intensity of La $L\beta_2$ compared with Ce $L\beta_3$
0.0	Stronger
2.29	Weaker
4.57	Weaker

If the balance ratio 2.55 which was determined with $La_2O_3-CeO_2$ mixtures also held true of these samples, the amount of the lanthanum oxide present in them might be easily calculated. Thus, the amount of the lanthanum oxide present in Sample No. 1 would be 128/2.55%, that in Sample No. 2, (5.45 + 29.35)/2.55%, that in Sample No. 3, (49.6/2.55 − 16)%, that in Sample No. 4, (22.2 + 2.29/2)/2.55%. But, if the presence of other rare earths had some disturbing effects, the value of the balance ratio which could be used for each sample respectively should be determined.

To know the effects of the other rare earth elements present and to determine the balance ratio for each sample, the following method which was similar to the one proposed by the present author[6] in the case of

(6) Kimura, *Z. physik. Chem.*, **128** (1927), 394.

the determination of hafnia in a mixture of the oxides of the elements precipitated by ammonia was tried.

Let x denote the percentage of lanthanum oxide to be determined, then

$$\frac{a}{x} = k \qquad (1),$$

where a is the amount of cerium oxide required to make the two lines under comparison equally intense, and k is the balance ratio CeO_2/La_2O_3 yet unknown.

To the sample is added first a known quantity of lanthanum oxide, and then cerium oxide is added until the lanthanum $L\beta_2$ and the cerium $L\beta_3$ lines again show an equal intensity. Let b denote the amount of lanthanum oxide added to the sample, and c, the amount of cerium oxide required to make the said two lines equally intense after the addition of b of lanthana. Then,

$$\frac{c}{x+b} = k \qquad (2).$$

From (1) and (2), we get

$$k = \frac{c-a}{b} \qquad (3).$$

If the value of k thus obtained were equal to or nearly equal to 2.55, i.e. the balance ratio determined with the oxide mixture of lanthanum and cerium, then the effects of the other rare earth elements in the sample should be negligible. If the value of k from (3) were different from 2.55, then we could use that value as the balance ratio special to the sample and thus the effects of the other rare earths could be eliminated automatically.

The value of k thus obtained for each sample is shown in Table 3.

Table 3.

Sample	a (%)	b (%)	c (%)	k found
No. 1	128	33.0	214	2.61
No. 2	34.8	9.9	59.7	2.52
No. 3*	49.6*	10.6*	76.2	2.51
No. 4	23.4	6.0	38.2	2.48

* Instead of x, $x+16$ was used.

As was seen from Table 3, the value of k thus found agreed with the balance ratio previously obtained for the mixtures of lanthanum oxide and cerium oxide within the error of experiments. Thus, the disturbing effects were almost negligible in these cases.

The amount of lanthanum oxide found by using the value of the balance ratio, k, obtained for each sample was given in Table 4 together with the amount determined by assuming it to be 2.55.

Table 4.

Sample	k	La_2O_3 (%)	La_2O_3 (%) $_{k=2.55}$
No. 1	2.61	49	50
No. 2	2.52	13.8	13.6
No. 3	2.51	3.8	3.5
No. 4	2.48	9.4	9.2

The Determination of Neodymium.[7]

For the determination of neodymium in a mixture of the rare earths, the intensity of the $L\alpha_1$ line of neodymium is compared with that of the $L\beta_1$ line of cerium, which is taken as the reference element. As the wavelength difference of the said two lines is only 14 X-Units, which corresponds to about 0.9 mm. on the photographic plate, the error of the estimation of the relative intensities due to the wrong exposure is practically eliminated.

Materials and Experimental Procedure. The relative intensities of the neodymium $L\alpha_1$ and the cerium $L\beta_1$ lines were compared by using the oxide mixtures of neodymium and cerium, which were prepared from their chlorides.

The solution of the cerium chloride which was prepared for the experiments with lanthanum was also used here. As for neodymium salt, two different samples were used, the one contained no lanthanide element except the negligible amount of lanthanum and cerium, the other, no lanthanide element except a trace of praseodymium. The amount of impurities was so small in both cases that they might be assumed for the present purpose to be pure neodymium salts.

(7) Read before the Chemical Society of Japan, June 14, 1930 and July 11, 1931, and published in Japanese in *J. Chem. Soc. Japan*, **54** (1933), 220.

As the procedure to prepare a sample to be put on the anticathode was quite similar to the one given already in the part of lanthanum of this report, its description will be omitted here. It must be mentioned only that the mixtures of the rare earths free from thoria and other oxides were used as the samples throughout this work.

The experimental conditions for the exposure were also the same as in the previous case, i.e. the photograph was taken by 41 minutes' exposure at the applied tension of 15 kilo-volts (effective) and the current of about 2 milliamperes.

Experimental Results. (a) With the oxide mixtures of neodymium and cerium, the relative intensities of the neodymium $L\alpha_1$ and the cerium $L\beta_1$ lines were compared. In Table 5 are shown the results obtained, from which we know that the two lines under consideration become equally intense when the ratio CeO_2/Nd_2O_3 in weight is equal to 0.71.[8]

Table 5.

CeO_2/Nd_2O_3 in weight	Intensity of Nd $L\alpha_1$ compared with Ce $L\beta_1$
1.98	Weaker
1.85	Weaker
1.76	Weaker
1.13	Weaker
0.99	Weaker
0.895	Weaker
0.804	Weaker
0.802	Weaker
0.710	Nearly equal
0.708	Nearly equal
0.702	Nearly equal
0.607	Stronger
0.503	Stronger
0.496	Stronger
0.401	Stronger

(b) It is somewhat peculiar that the balance ratio is less than unity. According to the experiments carried out by Y. Nishina and the

(8) The intensity ratio of the said two lines was also estimated by a microphotometer. In this case a little higher value 0.78 was obtained as the balance ratio CeO_2/Nd_2O_3.

present author, in which the intensity of the $L\beta_1$ line of a rare earth element of even atomic number was compared with that of the $L\alpha_1$ line of the element of atomic number higher by two by using the mixtures of the oxides of the two elements under consideration, the amount of the former element was generally greater than that of the latter when the said two lines showed an equal intensity. For examples, the balance ratio Gd_2O_3/Dy_2O_3 was equal to 2.1 for the gadolinium $L\beta_1$ and the dysprosium $L\alpha_1$ lines, the balance ratio Sm_2O_3/Gd_2O_3 was 2.5 for the samarium $L\beta_1$ and the gadolinium $L\alpha_1$ lines, and the balance ratio Nd_2O_3/Sm_2O_3 was 1.8 for the neodymium $L\beta_1$ and the samarium $L\alpha_1$ lines.

Only for the cerium $L\beta_1$ and the neodymium $L\alpha_1$ lines, as was shown by the experiments mentioned above, the balance ratio CeO_2/Nd_2O_3 was less than unity. The origin of this singular result might be traced back to the rapid disappearance of neodymium atoms from the surface layer of the anticathode spot compared with cerium atoms under the bombardment of the cathode rays. To ascertain this, the photographic plates different in time of exposure were compared. The plates taken with the samples remained on the anticathode after the bombardment of the cathode rays were also compared with the regular one. The tendency that the intensity ratio changed in favour of the cerium $L\beta_1$ line with the time of exposure was observed sometimes when the plates quite different in time of exposure were compared. But, the effect was not so clear as seen in the case of the comparison of the relative intensities of the barium $L\alpha_1$ and the titanium $K\alpha_1$ lines, investigated by M. Ishibashi.[9]

(c) The experiments were also carried out to know the effects of the presence of other rare earth elements. The absorption effects are expected by no element of the rare earth group. As for the excitation effects, only samarium and terbium may be mentioned. But as is seen in the following examples these effects are, if there be any, very small.

The following three samples were taken for the examples: Sample No. 5 mainly consisted of the oxides of lanthanide elements of lower atomic numbers and free from ceria; Samples No. 1 and No. 4 were the same as those which were used in the case of lanthanum.

Cerium oxide was added to Samples No. 1 and No. 5, while neodymium oxide was added to Sample No. 4 which was already rich in ceria.

The relative intensities of the neodymium $L\alpha_1$ and the cerium $L\beta_1$ lines were compared with the results shown in Table 6.

If the balance ratio 0.71 which was determined with $Nd_2O_3-CeO_2$ mixtures also held true of these samples, the amount of the neodymium

(9) Ishibashi, *Z. anorg. allgem. Chem.*, **202** (1931), 372.

Table 6.

(1) Sample No. 1.

$\frac{CeO_2 \text{ added}}{\text{Sample taken}}$ (%)	Intensity of Nd $L\alpha_1$ compared with Ce $L\beta_1$
34.19	Weaker
31.63	Weaker
30.74	Weaker
23.09	Weaker
20.70	Nearly equal (a little weaker)
18.89	Nearly equal (a little stronger)
11.40	Stronger

(2) Sample No. 5.

$\frac{CeO_2 \text{ added}}{\text{Sample taken}}$ (%)	Intensity of Nd $L\alpha_1$ compared with Ce $L\beta_1$
32.82	Weaker
26.47	Weaker
25.47	Weaker
22.70	Weaker
20.40	Weaker
18.21	Weaker
18.11	Weaker
16.40	Weaker
15.04	A little weaker
14.29	A little stronger
13.99	Stronger
13.74	Stronger
13.63	Stronger
11.82	Stronger
11.76	Stronger

(3) Sample No. 4.

$\frac{Nd_2O_3 \text{ added}}{\text{Sample taken}}$ (%)	Intensity of Nd $L\alpha_1$ compared with Ce $L\beta_1$
41.2	Stronger
25.5	A little stronger
23.1	A little weaker
20.6	Weaker
16.5	Weaker

oxide in them might be found by simple calculation. Thus, the neodymia content in Sample No. 1 would be $(20.70 + 18.89)/2 \times 0.71\%$, that in Sample No. 5, $(15.04 + 14.29)/2 \times 0.71\%$, and that in Sample No. 4, $\{22.2/0.71 - (25.5 + 23.1)/2\}\%$.

To see the effects of the presence of the other rare earths, the value of the balance ratio was determined for each sample by the method described in the case of lanthanum. The results obtained are shown in Table 7, where a denotes the amount of cerium oxide required to make the two lines under comparison equally intense, b, the amount of neo-

Table 7.

Sample	a(%)	b(%)	c(%)	k found
No. 1	19.8	64.13	66.28	0.73
No. 5	14.7	12.84	23.91	0.72
No. 5	14.7	25.67	32.86	0.71
No. 4*	22.2*	12.0*	30.2	0.67

* Instead of x, $x+24.3$ was used.

dymium oxide added to the sample and c, the amount of cerium oxide required to make the said two lines again equally intense after the addition of b of neodymia.

As was seen from Table 7, the value of k thus found agreed with the balance ratio obtained for the mixtures of neodymium and cerium oxides within the error of experiments.[10] Thus, the disturbing effects of the other rare earths were not observed in these cases. In Table 8, the amount of neodymium oxide found by applying to k the value obtained from the above experiments was compared with that calculated by assuming it to be 0.71.

Table 8.

Sample	k	Nd_2O_3(%)	$Nd_2O_3(\%)_{k=0.71}$
No. 1	0.73	27.	28.
No. 5	0.72	20.	21.
No. 5	0.71	21.	21.
No. 4	0.67	8.8	7.0

The Determination of Gadolinium.[11]

For the determination of gadolinium in a mixture of the rare earths, the intensity of the $L\alpha_1$ line of gadolinium is compared with that of the $L\beta_2$ line of neodymium, which is taken as the reference element. As the wave-length difference of the said two lines is only 10.5 X-Unites, which corresponds to about 0.7 mm. on the photographic plate, the error of the estimation of the relative intensities due to the wrong exposure is practically eliminated.

The neodymium content of a sample given should be previously estimated by the method described already in this report.

Materials and Experimental Procedure. The intensity ratio of the gadolinium $L\alpha_1$ and the neodymium $L\beta_2$ lines was determined with the mixtures of oxides of gadolinium and neodymium, which were prepared from their chlorides. Gadolinium chloride which did not show the presence of other lanthanide elements by the X-ray spectroscopic method was used for this work. The purity of neodymium chloride used was already given in the part of neodymium of the present report.

(10) The relatively low value of k found in the case of Sample No. 4 might be due to the excitation effect of samarium which was richly present in the sample, although it could not be yet confirmed.

(11) In collaboration with Mr. Yoshio Tsunoda. Read before the Chemical Society of Japan, July 14, 1934, and published in Japanese in *J. Chem. Soc. Japan*, **56** (1935), 81.

As the procedure of preparation of a sample to be put on the anti-cathode was quite similar to the one given already in the case of lanthanum, the description of it will be omitted here. It must be only mentioned that the mixtures of the rare earths free from thoria and other oxides were used throughout this work.

The apparatus used was the same as that described before. The photograph was taken by 41 minutes' exposure at the applied tension of 16 kilo-volts (effective) and the current of 2–5 milliamperes. The relative intensities of the lines were compared by a microphotometer with a photo-cell and a string-electrometer. The balance method used in the previous cases was also tried. Both results found agreed with each other.[12]

Experimental Results. (a) By using the mixtures of oxides of gadolinium and neodymium, the intensity of the gadolinium $L\alpha_1$ line was compared with that of the neodymium $L\beta_2$ line. The relative intensities of spectral lines were estimated by microphotometry.

The results obtained are shown in Table 9, where A_b denotes the deflection of the string of the electrometer expressed in divisions of the scale accessory to it at the background of the photographic plate, A_{Gd}, the deflection due to the gadolinium $L\alpha_1$ line, and A_{Nd}, that due to the neodymium $L\beta_2$ line. The density of the gadolinium $L\alpha_1$ line, denoted in Table 9 as D_{Gd}, can be expressed by $\log \frac{A_b}{A_{Gd}}$, while that of the neodymium $L\beta_2$ line, D_{Nd}, by $\log \frac{A_b}{A_{Nd}}$, and the intensity ratio of the said two lines, by D_{Nd}/D_{Gd} or $\log \frac{A_b}{A_{Nd}} : \log \frac{A_b}{A_{Gd}}$.

Table 9.

(1) Exposure at the current of 3 milliamperes.

Nd_2O_3/Gd_2O_3 in weight	A_b	A_{Nd}	A_{Gd}	D_{Nd}/D_{Gd}	D_{Nd}/D_{Gd} (Mean)
4.00	45.2	32.4	29.3	0.77	0.80
	45.2	32.2	30.0	0.83	
4.40	43.2	27.4	26.2	0.91	0.90
	42.7	28.0	26.4	0.88	
4.50	40.7	23.2	24.0	1.06	1.06
	40.7	23.4	24.2	1.06	

(12) In the case of neodymium given in this report and also in some other cases, a slight discrepancy was observed between the value obtained by microphotometry and that by the balance method. This was not the case with gadolinium.

Table 9.—(*Concluded*)

Nd_2O_3/Gd_2O_3 in weight	A_b	A_{Nd}	A_{Gd}	D_{Nd}/D_{Gd}	D_{Nd}/D_{Gd} (Mean)
5.00	41.7	14.4	16.2	1.13	1.13
	42.2	14.6	16.4	1.12	
6.00	36.7	27.2	29.0	1.27	1.27

(2) Exposure at the current of 5 milliamperes.

Nd_2O_3/Gd_2O_3 in weight	A_b	A_{Nd}	A_{Gd}	D_{Nd}/D_{Gd}	D_{Nd}/D_{Gd} (Mean)
4.40	39.8	20.3	19.3	0.93	0.92
	39.7	19.7	18.3	0.91	
4.50	41.3	27.0	29.3	1.24	1.20
	41.8	27.2	28.9	1.16	

(3) Exposure at the current of 2-3 milliamperes.

Nd_2O_3/Gd_2O_3 in weight	A_b	A_{Nd}	A_{Gd}	D_{Nd}/D_{Gd}	D_{Nd}/D_{Gd} (Mean)
4.40*	42.6	36.3	36.0	0.95	0.96
	42.3	35.3	35.1	0.97	
4.50**	42.3	32.3	32.8	1.06	1.07
	42.3	31.5	32.1	1.07	

* The photometer curve is shown in Fig. 1.

** The photometer curve is shown in Fig. 2.

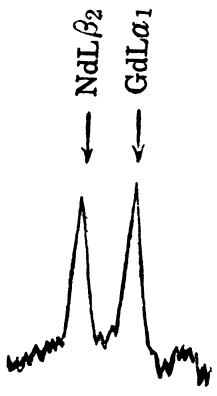


Fig. 1. $Nd_2O_3/Gd_2O_3 = 4.40$.

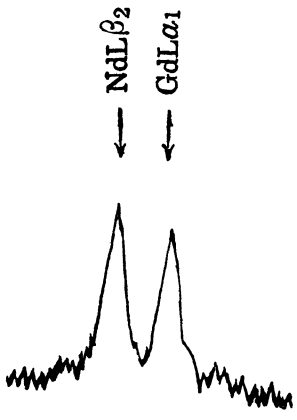


Fig. 2. $Nd_2O_3/Gd_2O_3 = 4.50$.

The balance ratio Nd_2O_3/Gd_2O_3, i.e. the ratio that makes D_{Nd}/D_{Gd} equal to 1.00, was found to be 4.46 from Table 9 (1), 4.43 from Table 9 (2), and 4.44 from Table 9 (3).

The photograph was also taken with the samples that remained on the anticathode after the bombardment of the cathode rays. The results are shown in Table 10. The balance ratio obtained was 4.47 and no sign of the change of the relative intensities was observed.

Table 10.

Nd_2O_3/Gd_2O_3 in weight	A_b	A_{Nd}	A_{Gd}	D_{Nd}/D_{Gd}	D_{Nd}/D_{Gd} (Mean)
4.40	39.9	23.3	21.4	0.86	0.87
	40.8	24.3	22.5	0.87	
4.50	39.8	24.7	25.3	1.05	1.05
	39.8	24.1	24.7	1.05	

From these experiments, the value 4.45 was taken as the balance ratio. A trial experiment with a sample which consisted of neodymium oxide and gadolinium oxide in the proportion of 4.45 to 1.00 showed, as was seen in Table 11, that the value was correct.

Table 11.

Nd_2O_3/Gd_2O_3 in weight	A_b	A_{Nd}	A_{Gd}	D_{Nd}/D_{Gd}	D_{Nd}/D_{Gd} (Mean)
4.45	39.0	26.3	26.6	1.03	1.01
	40.8	31.8	31.8	1.00	

(b) The experiments were also carried out to know the effects of other rare earth elements. The absorption effects are expected by no element of the rare earth group. As the wave-length difference of the absorption edges corresponding to the said two lines under comparison is fairly large, some rare earth elements may have the excitation effects.

The following three samples were used for the examples: Sample No. 6 consisted of the rare earths obtained from so-called gadolinium oxalate on sail which was not naturally pure and contained various rare earth elements; Sample No. 7 was a mixture of the rare earths rich in the elements of yttrium group; Sample No. 8 was the rare earths extracted from gadolinite found in Gihu Prefecture, Japan.

Various quantities of neodymium oxide were added to these samples respectively and the intensity ratio of the two lines under comparison was determined with the results shown in Table 12.

Table 12.

(1) Sample No. 6.

$\frac{Nd_2O_3 \text{ added}}{\text{Sample taken}}$ (%)	A_b	A_{Nd}	A_{Gd}	D_{Nd}/D_{Gd}	D_{Nd}/D_{Gd} (Mean)
0					0.59
11.4	43.5	34.0	36.0	1.30	1.28
	43.2	34.0	36.0	1.25	
9.8	39.8	33.3	33.3	1.00	1.00
	39.8	33.3	33.3	1.00	
8.6	40.5	35.0	34.2	0.86	0.88
	40.5	34.4	33.8	0.90	

(2) Sample No. 7.

$\frac{Nd_2O_3 \text{ added}}{\text{Sample taken}}$ (%)	A_b	A_{Nd}	A_{Gd}	D_{Nd}/D_{Gd}	D_{Nd}/D_{Gd} (Mean)
0					0.75
4.5	42.3	35.3	33.8	0.81	0.79
	41.8	35.1	33.3	0.77	
5.4	39.3	32.5	32.5	1.00	1.00
	38.8	31.3	31.3	1.00	
9.7	43.3	36.8	38.3	1.33	1.31
	43.3	37.5	38.7	1.28	

(3) Sample No. 8.

$\frac{Nd_2O_3 \text{ added}}{\text{Sample taken}}$ (%)	A_b	A_{Nd}	A_{Gd}	D_{Nd}/D_{Gd}	D_{Nd}/D_{Gd} (Mean)
0					0.54
12.2	42.3	34.1	37.3	1.71	1.66
	42.3	34.9	37.3	1.53	
9.2	41.2	33.0	34.4	1.23	1.29
	40.7	32.2	34.2	1.35	
7.4	42.8	38.0	38.1	1.02	1.01
	43.8	37.3	37.3	1.00	
6.1	37.3	27.3	25.8	0.85	0.82
	37.3	27.5	25.3	0.79	

From Table 12 (1), we knew that the addition of 9.4% of neodymium oxide to Sample No. 6 would make the said two lines equally intense. After the addition of this amount of neodymium oxide to the original sample, various quantities of neodymium oxide and gadolinium oxide were added in the proportion, $Nd_2O_3/Gd_2O_3 = 4.45$, and the relative intensities of the said two lines were compared. An example of the results obtained is shown in Table 13 (1).

Samples No. 7 and No. 8 were treated in a similar way. After the addition of 5.4% of neodymium oxide to Sample No. 7 or 7.4% of it to Sample No. 8, various quantities of neodymium oxide and gadolinium oxide were added in the proportion, $Nd_2O_3/Gd_2O_3 = 4.45$, respectively, and the relative intensities of the said two lines were compared. An example for each case is shown in Table 13 (2) and in Table 13 (3) respectively.

Table 13.

(1) Sample No. 6.

A_b	A_{Nd}	A_{Gd}	D_{Nd}/D_{Gd}	D_{Nd}/D_{Gd} (Mean)
37.8	27.3	27.7	1.05	1.01
37.8	26.9	26.7	0.98	

(2) Sample No. 7.

A_b	A_{Nd}	A_{Gd}	D_{Nd}/D_{Gd}	D_{Nd}/D_{Gd} (Mean)
30.3	25.7	25.9	1.03	1.01
30.3	24.5	24.5	1.00	

(3) Sample No. 8.

A_b	A_{Nd}	A_{Gd}	D_{Nd}/D_{Gd}	D_{Nd}/D_{Gd} (Mean)
40.3	24.6	26.0	1.13	1.13
40.3	24.6	26.0	1.13	

From the above experiments, we knew that the balance ratio 4.45 which was determined with the mixture of gadolinium and neodymium oxides also held true of Samples No. 6 and No. 7, and the effects of the other rare earth elements were not observed in these cases. A little low value 4.4 was obtained for Sample No. 8.[13] As the content of neodymium

(13) This might be due to the excitation effect of dysprosium richly present in the sample, although it could not yet be confirmed.

oxide in this sample was estimated to be 19.4% by the method described in the previous part of this report, the content of gadolinium oxide would be 6.1% if we took 4.4 for the balance ratio. It would be 6.0% if we assumed the balance ratio to be 4.45.

Table 14.

Allanite from Oyama.

MgO	1.29%
CaO	10.42
MnO	1.22
FeO	4.76
Fe_2O_3	9.70
Al_2O_3	16.03
La_2O_3	0.63
Ce_2O_3	5.96
Pr_2O_3	0.57
Nd_2O_3	3.80
Sm_2O_3	1.92
Gd_2O_3	1.02
Y_2O_3 etc.	4.19
ThO_2	2.11
SiO_2	34.65
H_2O	1.58
Total	99.85%

Applications.

These methods, combined with the other methods,[14] were applied in this laboratory to the analyses of chemical preparations as well as of minerals containing rare earth elements. As an example, the result of the analysis of allanite found in Oyama, Ehime Prefecture, Japan is given in Table 14.[15]

Summary.

(1) Lanthanum in a rare earth mixture can be determined by comparing the intensity of its $L\beta_2$ line with that of the cerium $L\beta_3$ line.

(2) Neodymium in a rare earth mixture can be determined by comparing the intensity of its $L\alpha_1$ line with that of the cerium $L\beta_1$ line.

(3) Gadolinium in a rare earth mixture can be determined by comparing the intensity of its $L\alpha_1$ line with that of the neodymium $L\beta_2$ line.

In conclusion, the author wishes to express his hearty thanks to Professor M. Katayama and to Professor Y. Shibata for their kind interests during the work. It is also the author's pleasant duty to acknowledge the valuable advice offered by Dr. Y. Nishina.

A part of the cost of this investigation was defrayed from the grant of the Nippon Gakujutsu Shinko-kwai (the Japan Society for the Promotion of Scientific Research) for which also the present author wishes to record his thanks.

Laboratory of Analytical Chemistry,
Chemical Institute, Faculty of Science,
Imperial University of Tokyo.

(14) For the determination of praseodymium, the intensity of the praseodymium $L\beta_2$ line was compared with that of the neodymium $L\beta_3$ line; vid. S. Shinoda, *J. Chem. Soc. Japan*, **56** (1935), 76. For the determination of samarium and also of neodymium, the intensity of the samarium $L\alpha_1$ line was compared with that of the neodymium $L\beta_1$ line by the wedge method proposed by S. Shinoda of this laboratory; vid. S. Shinoda, *J. Chem. Soc. Japan*, **56** (1935), 1483; *ibid.*, **58** (1937), 989.

(15) M. Ikawa, *J. Chem. Soc. Japan*, **58** (1937), 1261.

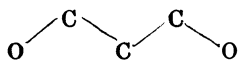
X-Ray Investigation of the Cubic Modification of Pentaerythritol, $C(CH_2OH)_4$.

By Isamu NITTA and Tokunosuké WATANABÉ.

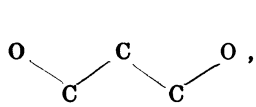
(Received December 28, 1937.)

It has been reported by L. Ebert,[1] that pentaerythritol, $C(CH_2OH)_4$, shows in the temperature range between 179.5 and 260.5°C., its melting point, another crystalline modification, which is optically isotropic, and that the heat of transition is estimated from the cooling curve to be several times as large as the heat of fusion. Now that the structure of the ordinary tetragonal modification has been determined independently by the present authors[2] and by Llewellyn, Cox, and Goodwin,[3] it will be of interest to make an X-ray investigation of the cubic modification to see if there exist some close relationships between the two structures.

The important features of the determined tetragonal structure may be summarized as follows: If the hydrogen atoms of the OH groups are not taken into consideration, the molecule $C(CH_2OH)_4$ in the crystal possesses approximately the symmetry of D_{2d}–$\bar{4}2m$, precisely S_4–$\bar{4}$, with one pair of primary alcohol radicals puckered upwards and the other downwards, namely,



and



all the bond angles of these atoms being approximately tetrahedral (Fig. 1). The molecules are arranged flat in a sheet parallel to the crystallographic c-plane, and the whole crystal is made up of such molecular layers. The linkage between neighbouring molecules in a layer is more or less firm by the interaction of the hydroxyl groups. The geometrical aspect of this linkage is such that four hydroxyl oxygen atoms, one out of each adjoining molecule, constitute a square, of which every side is presumably bridged over by a hydrogen atom (Fig. 2).

---

(1) L. Ebert, *Ber.*, **64** (1931), 114. See also K. Weissenberg, *Naturwissenschaften*, **15** (1927), 996; W. M. Cohn, *Z. Physik*, **50** (1928), 134.

(2) I. Nitta and T. Watanabé, *Nature*, **140** (1937), 365.

(3) F. J. Llewellyn, E. G. Cox, and T. H. Goodwin, *J. Chem. Soc.*, **1937**, 883.

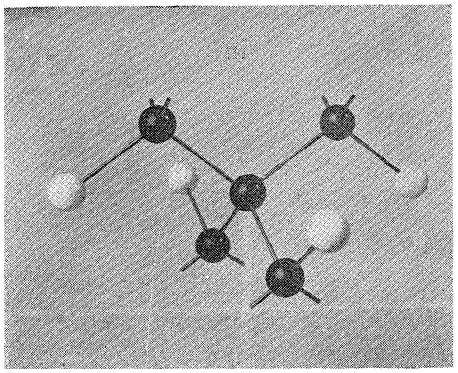


Fig. 1. Atomic configuration in tetragonal pentaerythritol, with C atoms shown as black and O atoms as white balls.

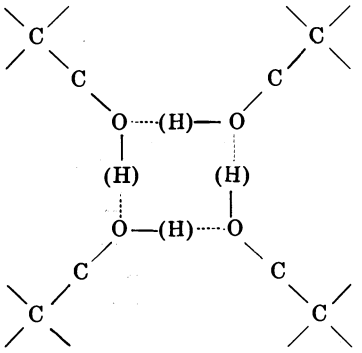


Fig. 2. Hydrogen bridges in tetragonal pentaerythritol.

In such closed hydrogen bridges, the "synchronized oscillations" may, according to Huggins,[4] cause an increased stability of the intermolecular linkage.

In the present experiment, material from Schering-Kahlbaum A. G. was fractionally crystallized from aqueous solution. The melting point of the sample was 257°C. Although the same sample was ascertained to melt, after sublimation, at a temperature higher than 260°C. as Ebert describes, such sublimate was not used.[5]

Since the old crystallographic choice of the principal axes of tetragonal pentaerythritol gives the value $c/a = 1.0236$ at a room temperature,[6] it was first examined by the Laue photographic method if the ratio c/a tends to unity as the temperature approaches to the transition point so that the transformation from tetragonal to cubic takes place rather continuously. Several Laue photographs were prepared at various temperatures up to 179.5°C. with the incident X-ray beam normal to the crystal slice cleaved along (001). The change of the ratio c/a was not found in the sense to decrease to unity. For example, the observed value was $c/a = 1.043$ at a temperature a little below the transition point. It was also found that the dissymmetrical intensity distribution of the Laue spots, (hkl) and (khl) in pairs, remains almost unaltered over the whole examined range of temperatures below 179.5°C. This implies that any torsional change of the atomic arrangement around a tetragonal axis does not sensibly occur. In other words, the molecular shape itself and the

(4) M. L. Huggins, *Nature*, **139** (1937), 550.

(5) For the ordinary and microscopic determination of the melting point our thanks are due to Mr. Z. Kochi at the Osaka Pharmaceutical College.

(6) P. Groth, "Chemische Krystallographie," Part III, 385.

relative orientation of the molecules in a (001) layer undergo practically no change up to the vicinity of the transition point. Thus it seems probable that the observed increase in the value of c/a is mainly due to the enlargement of the spacing $c/2$ between successive molecular layers. When the temperature of the crystal slice is raised above the transition point, the characteristic Laue pattern of the tetragonal modification is replaced by an assembly of a large number of smaller Laue spots distributed quite irregularly on the photograph, thus rendering our attempt unsuccessful to obtain Laue photographs of a single cubic crystal.

Debye-Scherrer photographs of the high temperature modification were made with the copper K radiation filtered through a nickel foil, the camera radius being 100 mm. and the angular range of the film ca. 70°. The temperature of the rotating sample was kept at 230°C. approximately. The films were protected by a paper screen in front of them from heat radiation of the electrical furnace, in which the sample was placed, and they were also water-cooled on the back side in order to prevent difficulties, such as their deformation and fogging, which will be caused by the elevation of the film temperature. It took about ten times as much time of exposure to obtain photographs with the appearance of the first seven lines as that necessary for good photographs of the tetragonal modification at ordinary temperatures. The obtained data are given in Table 1. It may be remarked here that Cohn[7] has already shown in his paper three powder photographs of pentaerythritol taken at 20, 140 and 230°C. respectively, of which he made no analysis of the obtained lines. Perhaps he regarded the third one of his photographs as solely due to the high temperature modification. However, it is now obvious from our present experiment that this is not a pure one but a mixed photograph due to both of the two modifications, indicating that his sample was not kept constantly at a temperature above the transition point.

As shown in Table 1, all the lines on the photographs are very well accounted for by a cubic face-centered lattice, the side of the unit cube being $a = 8.963$ A. at 230°C. Taking the number of molecules contained in the unit as four, the density of the crystal is computed to be $\rho = 1.255$ at 230°C., which is much lower than the value $\rho = 1.398$ at 25°C. for the tetragonal modification. As the volume increase of this tetragonal modification in the range from room temperatures to the transition point is estimated to be not much more than one per cent, the transformation should be accompanied by a considerable expansion of volume, and this is actually in accord with Ebert's and our observations. As for the re-

(7) W. M. Cohn, *Z. Physik*, **50** (1928), 134.

Table 1. Powder photographic data of cubic pentaerythritol.

l (mm.)	θ	$\sin\theta$	d (A.)	hkl	a (A.)
29.8	8°32′	0.1484	5.18_5	111	8.98_0
34.5	9°52′	0.1713	4.49_2	200	8.96_4
49.0	14° 4′	0.2431	3.16_5	220	8.95_1
60.4	17°18′	0.2974	2.58_7	222	8.96_1
70.1	20° 5′	0.3434	2.24_1	400	8.96_4
76.7	21°58′	0.3741	2.05_7	331	8.96_6
78.8	22°35′	0.3839	2.00_4	420	8.96_2
					mean 8.96_3

maining possible units for the crystal, it will be shown that either they contradict with the observed facts or they can be looked upon as improbable.

It is now required to arrange four molecules of $C(CH_2OH)_4$ in the face-centered cubic unit so as to furnish the crystal as a whole with the symmetry characteristic of the cubic system. However, such high symmetry cannot be afforded by the usual manner of arranging the four molecules of the symmetry S_4-$\bar{4}$, which is found in the case of tetragonal pentaerythritol. Thus it comes into question if the unit chosen above is wrong. In order, for the molecule of the symmetry S_4-$\bar{4}$, to yield a unit of cubic symmetry, their number in such unit must be some multiples of 3. After elimination on account of absurd values for the density of the crystal, there remains only one unit containing 12 molecules to be taken into consideration. In this case the side of such a unit becomes 12.67 A. and the underlying lattice simple or body-centered. However, the number of lines actually observed is too few to be accounted for in a natural way by such simple or body-centered lattice. Thus the unit of twelve molecules may also be eliminated. Returning to the original cubic face-centered unit containing four molecules, there arises a second question how it is possible to explain this peculiarity in the symmetry consideration. As in the cases of certain crystal structures,[8] a statistical explanation can be given to such phenomena; i.e. acquisition of higher molecular symmetry by some statistical means. In the present case of pentaerythritol, there will be three ways possible to realize such acquisi-

(8) See, for example, S. B. Hendricks and L. Pauling, *J. Am. Chem. Soc.*, **47** (1925), 2904; S. B. Hendricks, *Z. Krist.*, **74** (1930), 29; L. Pauling, *Phys. Rev.*, **36** (1930), 430; S. B. Hendricks, *Z. Krist.*, **84** (1932), 85; I. Nitta and T. Watanabé, *Sci. Papers Inst. Phys Chem. Research* (Tokyo), **26** (1935), 164.

tion. In the first one, the molecule is considered to keep the symmetry of S_4-$\bar{4}$; in the second, it is regarded to be non-rigid owing to the rotation about the single C–C bonds, of which the four directions from the central carbon atom are in angles of 109°28′; and in the third, both the molecular shape and the mutual orientation of the molecules are to be changed. All of these three possible ways will be taken into the following considerations to see which will give the best account for the observed intensities, the atomic separations in the molecule being assumed to be 1.54 A. for the C–C and 1.46 A. for the C–O bonds and the valency angles of the carbon atoms to be 109°28′.

On the assumption of the rigid molecule possessing the symmetry of S_4-$\bar{4}$, there are two extreme cases conceivable, in which the cubic symmetry of the statistical molecule is attained. The one case is that in which free spatial rotation of the molecule sets in so as to furnish it with the spherical symmetry (Case I). Then the corresponding space group is O_h^5-$Fm3m$ in the statistical sense. In the other case, which is rather statical, the whole crystal is constituted by a random distribution of three kinds of molecules, in equal concentration, the molecular $\bar{4}$-axis of each kind being parallel to each of the principal axes of the crystal (Case II). The space group is now statistically T_d^2-$F\bar{4}3m$. Intermediate of the above two, there is another important case, in which half of the molecules in Case II are rotated about the molecular axis through the angle of 90° (Case III). By the addition of these new orientations, the crystal acquires the cubic holohedral symmetry, the space group being again O_h^5-$Fm3m$. Among these three cases, it was found that Cases II and III account for the observed intensities fairly well, while Case I does not. The calculation of the intensities was made by assuming the molecular symmetry to be T_d-$43m$.

The second possibility of non-rigid molecule gives following important cases worth consideration, the four methylenic carbon atoms being assumed in all these cases as lying on the trigonal axes of the crystal. It is first conceivable that the hydroxyl groups rotate freely around the C–C bonds (Case IV, Fig. 3). Such arrangement corresponds to the space group T_d^2-$F\bar{4}3m$. However, this does not explain the observed intensity data. Next come two rather statical cases (Cases V and VI), in which each of the hydroxyl groups statistically take such three-fold positions, around the directions of the C–C bonds and at the same time in the planes defined by pairs of these C–C bonds, that the molecule may possess the symmetry of T_d-$\bar{4}3m$ (Fig. 4; black circles in Case V and open circles in Case VI). An atomic configuration of the molecule in Case V is closely related to Case II, followingly also to the original molecular shape, and

the calculated intensities are the same for both cases. The space groups in Cases V and VI are T_d^2-$F\bar{4}3m$. Though not satisfactorily, Case V explains the observed intensities much better than Case VI. Besides these,

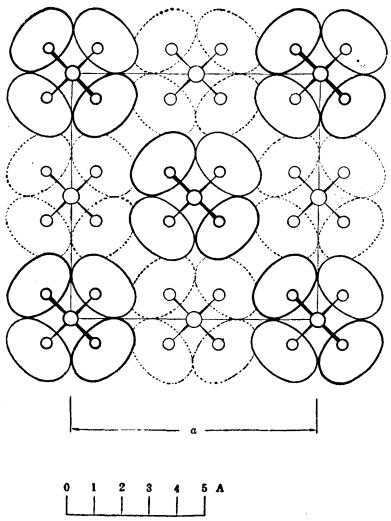


Fig. 3. Molecular arrangement of pentaerythritol in cubic form, corresponding to Case IV.

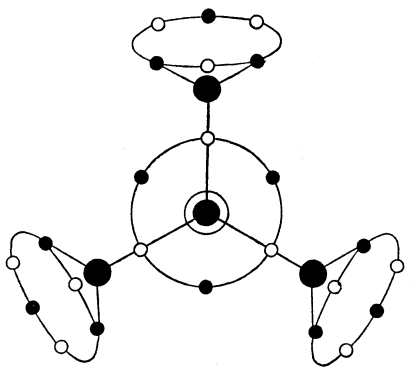


Fig. 4. Statistical atomic configurations of cubic pentaerythritol, $C(CH_2OH)_4$. The largest circle represents the central C, black circles the methylenic C atoms, and small circles the hydroxyl O atoms (black for Case V and white for Case VI).

there will be also another possible molecular symmetry of T-23. This seems, however, rather improbable in the present case of internal motions of non-rigid molecule.

The third possibility of non-fixed orientation of non-rigid molecules will now be discussed. In the first place, the spherical rotation of the molecule with freely rotating hydroxyl groups. This, however, does not seem to correspond to the observation. There comes next another case, in which half of the molecules of Case IV are rotated about the molecular axis through the angle of 90° as in Case III (Case VII). The mean molecular symmetry and the space group are O_h-$m3m$ and O_h^5-$Fm3m$ respectively. This case also does not explain the observed intensities. The same kind of change in the molecular orientations produces from Cases V and VI two new cases (Cases VIII and IX), to which the same molecular symmetry and the same space group as above can be given. The calculated intensities in Case VIII are the same as in Case III and explain the observed intensities fairly well, while Case IX fails. Perhaps it will be superfluous to note that the symmetry properties of Cases VII, VIII, and IX can be effected also by the rotations of molecular axes in azimuth.

After all these considerations, of which the resulting intensities are brought together in Table 2, following conclusions may be regarded as probable. Above the transition point, 179.5°C., pentaerythritol gives a cubic form, in which the central carbon atoms are arranged to build a cubic face-centered lattice, the distance between nearest molecular centers being calculated to be 6.338 A. from the side $a = 8.963$ A. of the unit. In this cubic modification, the layer structure of the tetragonal form is not retained any more, although fairly weakened hydrogen bonds seem to

Table 2. Calculated intensities for various possible cases.

hkl	I	II, V	III, VIII	IV	VI	VII	IX	X	$I_{obs.}$
111	206	327	306	262	280	260	220	287	v.v.s.
200	97.5	11.2	11.2	31	57.3	31	57.3	19.7	v.s.
220	62 3	1.8	1.8	1.8	1.2	1.8	1.2	1.8	—
311	49.5	3.1	2.2	5.0	11.0	0.7	1.2	1.3	v.v.w.
222	13.0	20.0	20.0	2.7	3.3	1.4	3.4	7.9	m.
400	4.0	0.0	0.0	0.3	2.2	0.3	2.2	0.0	v.v.w.
331	9.8	4.8	1.9	4.3	3.0	1.2	0.8	1.6	v.w.
420	8.2	2.2	2.2	0.0	1.5	0.0	1.5	0.7	v.w.
422	5.5	2.5	0.8	3.0	2.7	1.9	1.5	1.3	—
333 511	4.8	3.8 0.3	3.1 0.1	0.6 1.1	1.1 1.3	0.6 0.5	0.1 0.6	1.6 0.4	—

exist still. The molecule becomes non-rigid on account of rotation about the C–C bonds. This rotation, however, is not at all free, and the probability for the existence, accordingly the stability, of the atomic configuration, which corresponds to that observed in the molecule of the tetragonal modification, is outstandingly great among other possible configurations. By virtue of this rotation the orientation of the molecular $\bar{4}$-axis for such most stable atomic configuration can now and then be interchanged with each of the two directions, which are perpendicular to the original one. At the same time as the molecule becomes non-rigid, rotations of the molecule as a whole set in, but these are also not quite free. The most stable molecular orientations together with the most stable atomic configuration of the molecules are probably represented by what is described as Case VIII. Indeed, the actual motions in and of the molecules within the crystal will be very complicated and it will not be satisfactory to try to explain with any one of such models, rather statical in a certain sense, as above. Thus in order to make a better fit to the

observed intensities, it is necessary to take into account more cases in addition to Case VIII; for example, a weighted mean of Cases VIII and VII (Case X in Table 2). It will be added that, from the physical point of view, Case III does not probably represent the actual state of matter, though this can explain the intensities as well as Case VIII.

Perhaps it is interesting to notice that the molecular state in the cubic modification already approaches very much to that of the liquid state. This is fairly obvious from the very small heat of fusion.[1] The thermal vibrations of the molecular centers in the cubic crystal must be considerable chiefly because of the non-rigidity of the molecules. This is shown in the strong decrease of the intensity distribution with increasing angle on the powder photographs. In fact, a temperature factor $\exp(-B\sin^2\theta)$ with so large a constant B as 6.7 was used in the calculation of the intensities (Table 2).

It is well-known that the molecule of pentaerythritol was found in the molecular beam experiment of Estermann[9] to possess a dipole moment of approximately 2×10^{-18} E.S.U. Since a molecule of the symmetry of S_4-$\bar{4}$ cannot have a dipole moment, some intramolecular motions should be assumed in the molecule of pentaerythritol.[10] In this respect the non-rigidity of the molecule found in the present experiment may be looked upon as giving a concrete ground for this assumption, if in the molecular beam investigation above mentioned the temperature, not given in the paper of Estermann, is supposed to be enough high. On the other hand, no moment of pentaerythritol tetrabromide, of which the molecular structure in the gaseous state was determined by the electron diffraction study of de Laszlo[11] to be similar to that of the tetragonal pentaerythritol, will be interpreted by the non-rotation of the C–C bonds owing to the large volume and mass of the bromine atoms.

In conclusion, we wish to express our thanks to the Hattori Hôkôkwai for a grant.

Laboratory of Physical Chemistry, Faculty of Science,
Osaka Imperial University.

---

(9) J. Estermann, *Z. physik. Chem.*, B, **2**(1929), 287.
(10) Refer, for example, to L. Ebert, "Leipziger Vorträge," **1929**, p. 44.
(11) H. de Laszlo, *Compt. rend.*, **198** (1934), 2235.

On the Thermal Transition in Solid Deuterio-Ammonium Sulphate, $(ND_4)_2SO_4$.

By Isamu NITTA and Katsuji SUENAGA.

(Received December 28, 1937.)

In a previous paper[1] it has been reported that deuterio-ammonium chloride, ND_4Cl, shows like ordinary one the phenomenon of excessive specific heat with a discontinuity at about $-24°C.$, this being roughly by six degrees higher than the corresponding transition temperature of ordinary ammonium chloride. The work had been carried out in an attempt to get some closer informations concerning the nature of such peculiar kind of thermal transitions, which, according to the rather qualitative explanation of Pauling,[2] are due to the onset of rotations of the atomic groups in crystals. As a continuation of the investigation, thermal and dilatometrical measurements of the transition of deuterio-ammonium sulphate, $(ND_4)_2SO_4$, have now been made, of which an account will be given in the present paper.

The material used in the present experiment was prepared in the following way. The starting substances of the preparation were deuterium oxide from Norsk Hydro-Electrisk Kvaelstofaktieselskab, magnesium metal from Schering-Kahlbaum A. G., potassium nitrite, ammonium chloride and sulphur trioxide, the last three being pure chemicals of E. Merck. Using magnesium powder and chemical nitrogen from potassium nitrite and ammonium chloride, magnesium nitride, Mg_3N_2, was first produced. By the reaction of this nitride with deuterium oxide, heavy ammonia, ND_3, was then obtained and this was led into heavy sulphuric acid, D_2SO_4, from D_2O and SO_3, to produce the final material $(ND_4)_2SO_4$, the whole procedure being carried out in an evacuated system. The sample thus obtained was determined to contain 93.5 per cent of deuterium. A Debye-Scherrer photograph of this sample showed that the crystal structure is the same as that of ordinary ammonium sulphate, having the unit of practically the same dimensions.

By use of a micro-dilatometer of ordinary type, measurements were made with ordinary and heavy sulphates in a temperature range from

(1) I. Nitta and K. Suenaga, *Sci. Papers Inst. Phys. Chem. Research* (Tokyo), **32** (1937), 83. See also A. Smits and C. J. Muller, *Nature*, **139** (1937), 804.

(2) L. Pauling, *Phys. Rev.*, **36** (1930), 430.

−55 to −40°C. Carbon disulphide was chosen as the dilatometer liquid for the reason that the molecule of this compound contains no hydrogen atom. It is found from the measurements that both salts show quite similar volume-temperature curves and the transitions are accompanied by abrupt contraction of their volumes as the temperature is being raised, the relative change $\Delta V/V$ being approximately a half per cent for both salts. In the case of the ordinary salt the sudden change in volume occurs at −50.3°C. when the temperature is being lowered and −49.5°C. when raised. For the heavy salt the corresponding temperatures are −49.8 and −49.0°C. From these, the dilatometrical values of the transition temperatures are determined to be −49.9°C. for $(NH_4)_2SO_4$ and −49.4°C. for $(ND_4)_2SO_4$. Besides carbon disulphide, toluene was also used, in another dilatometer, to study the transition of ordinary ammonium sulphate with higher precision, and the result is given in Fig. 1. In spite of the early report that R. Ewald[3] failed to find out dilatometrically the transition of $(NH_4)_2SO_4$, it is certain from the present experiment that it really exists and can be observed by use of a dilatometer, if the temperature intervals are chosen small enough.

In order to confirm these obtained values for the transition points and, at the same time, to determine the heats of transition, cooling and heating curve measurements were also carried out with the aid of the same calorimeter as that used for the specific heat determination, which will be described below. The amount of sample taken was 8.35 g. in the case of the ordinary salt and 8.58 g. in the other. The heating curves were prepared with the energy supply of about 2 calories per minute. The obtained curves are shown in Fig. 2. Ordinary ammonium sulphate exhibits an arrest at −49.5°C. on heating and it shifts to −50.7°C. on cooling. The corresponding temperatures for the heavy ammonium sulphate are −48.9 and −50.2°C. Taking the mean of the both arrests on heating and cooling curves, the transition temperatures are given to be −50.1°C. for $(NH_4)_2SO_4$ and −49.6°C. for $(ND_4)_2SO_4$ in good agreement with the dilatometric values obtained above. From the data of the heating curves the heats of transition were determined for both ordinary and heavy salts. They are 210 at −49.5°C. for the former and 225 at −48.9°C. for the latter in calories per gram-ion of ammonium. These values are very remarkable in such a respect that Crenshaw and Ritter[4] gave from their specific heat measurement as the heat of transition of ordinary ammonium sulphate the value 485 cal./gram-ion, which is more

(3) R. Ewald, *Ann Physik*, **44** (1914), 1223.
(4) J. L. Crenshaw and I. Ritter, *Z. physik. Chem.*, B, **16** (1932), 143.

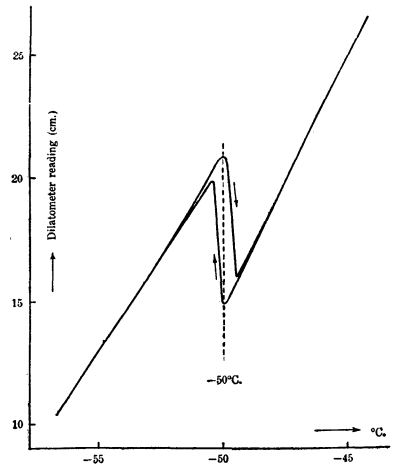


Fig. 1. Dilatometric curve of $(NH_4)_2SO_4$.
The liquid: toluene.
Sample taken: 8.02 g.

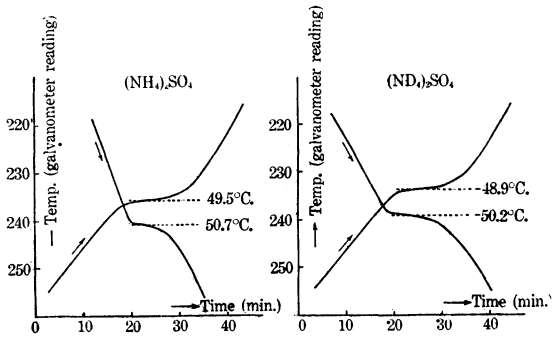


Fig. 2. Cooling and heating curves.

than double as large as the present value 210. This great disagreement seems to be due partly to the difficulty in computation of the heat of transition from the specific heat data and partly to their obtained data themselves, which are always somewhat too high as compared with the values of the present specific heat measurement (Table 1), and also judging from the molecular heat 44.80 cal. at 29°C. obtained by R. Ewald.[3]

The specific heats of ordinary and heavy ammonium sulphates were measured in the range from −180 to +25°C., using an improved vacuum calorimeter of the Nernst type. This calorimeter is made of copper and nickel-plated, its dimensions being 2 cm. in diameter and 4 cm. in height. There are six radial vanes, about 0.2 mm. thick, welded on the inside wall of this calorimeter in order to secure quick and effective conduction of heat into the crystalline sample. Being surrounded by a copper vessel, which is also nickel-plated and whose temperature can be controlled electrically, the calorimeter is put into an enclosed glass system to be evacuated. The samples taken were the same as those used for the cooling and heating curve measurements, viz. 8.35 g. of $(NH_4)_2SO_4$ and 8.58 g. of $(ND_4)_2SO_4$. In each measurement 5 to 20 calories of energy were supplied electrically to the calorimeter and the temperatures were measured by means of copper-constantan thermocouples. The obtained molecular heats C_p are shown in Tables 1 and 2. They are also plotted in form of the molecular heat-temperature curves in Fig. 3. The general

features of the curves are similar to those of ordinary and heavy ammonium chlorides. The discontinuous fall of specific heat begins at −50°C. in the case of ordinary ammonium sulphate and at −49.5°C. in the other. These temperatures of transition agree very well with those found on the volume-temperature and thermal analysis curves. As in

Table 1. Molecular heat of $(NH_4)_2SO_4$.

t°C.	Mol. heat	t°C.	Mol. heat	t°C.	Mol. heat
−180	19.5	−90	38.0	−47.5	42.3
−170	20.9	−80	43.0	−45	40.4
−160	22.6	−70	47.2	−40	40.9
−150	25.2	−60	55.2	−30	42.2
−140	26.8	−55	63.4	−20	43.3
−130	29.2	−52.5	70.7	−10	44.4
−120	31.4	−51.0	80.1	0	44.8
−110	33.6	−50.5	103.	+10	45.5
−100	36.4	−49	53.8	+20	46.0

Table 2. Molecular heat of $(ND_4)_2SO_4$.

t°C.	Mol. heat	t°C.	Mol. heat	t°C.	Mol. heat
−180	23.0	−90	47.2	−47.5	45.9
−170	25.2	−80	50.6	−45	44.8
−160	27.8	−70	54.2	−40	45.8
−150	30.2	−60	60.2	−30	45.9
−140	33.0	−55	67.8	−20	46.4
−130	34.2	−53	75.9	−10	47.2
−120	37.6	−51	92.3	0	48.3
−110	39.6	−50.5	107	+10	49.8
−100	43.2	−48.5	50.2	+20	50.6
				+25	51.5

the case of deuterio-ammonium chloride, the anomalous rise of the specific heat curve of the heavy sulphate begins at a relatively lower temperature as compared with that of the ordinary one. However, it is not certain whether this is characteristic of ND_4 ions, or due to the presence of lighter

components. Besides this peculiarity the curve for the heavy compound lies always higher than that for the ordinary one.

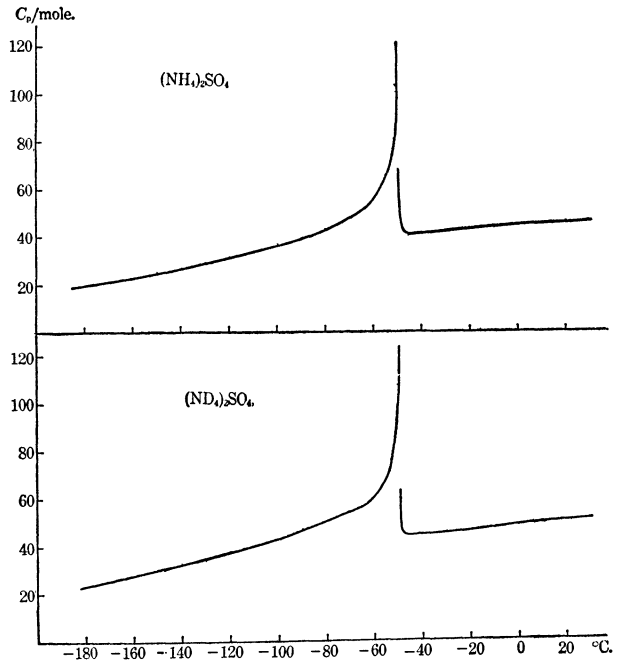


Fig. 3. Molecular heat-temperature curves.

For the reason of analogy, it would be natural from the observations on ordinary and heavy ammonium chlorides to expect that the transition point of heavy ammonium sulphate would be at least a few degrees higher than that of the ordinary sulphate. In the actual case, there was found a temperature shift of not more than a half degree. Perhaps this suggests that the phenomena of such transitions would not be so simple, if one tries to give a quantitative explanation of them. From the point of view of Pauling and Fowler,[5] it seems not impossible to imagine that, in the case of an oxy-acid, the interaction between deuterio-ammonium ion and the surrounding oxygen atoms would be weaker than that in the ordinary ammonium salt and that such effect would cancel out the opposing tendency of raising the transition temperature due to the doubling of the moment of inertia, brought about by the substitution of deuterium

(5) L. Pauling, *loc. cit.*; R. H. Fowler, *Proc. Roy. Soc.* (London), A, **149** (1935), 1; **A, 151** (1935), 1; see further his book, "Statistical Mechanics," 2nd Ed., 789 (1936).

in the rotating ammonium ion. Further discussion will be reserved until the investigation is extended to other deuterio-ammonium salts. Only it will be added that, though there are structurally two kinds of ammonium ions in the crystal lattice, the one is surrounded by nine and the other by ten oxygen atoms, there was found single transition point without any observable fine structure in the volume-temperature, thermal analysis, and molecular heat-temperature curves.

In conclusion, we wish to express our thanks to Mr. M. Koizumi for the determination of deuterium content and also to the Hattori Hôkôkwai for a grant.

Laboratory of Physical Chemistry, Faculty of Science,
Osaka Imperial University.

The Heat of Formation and the Specific Heat of Silicon Nitride.

By Shun-ichi SATOH.

(Received November 25, 1937.)

I. **Introduction.** The specific heat of silicon nitride has not yet been determined. Nor has the heat of formation of silicon nitride been measured directly in a calorimeter. The values so far reported in the literature are as follows: C. Matignon[1] obtained the value 159,300 cal. and W. B. Hincke and L. R. Brantley[2] reported the value 176,300 cal. at 1700°K. The object of the present paper is to determine the specific heat and from it the most probable value of the heat of formation of silicon nitride.

II. **Specimen.** (1) *Preparation of specimen.* For the preparation of silicon nitride, the following two methods were adopted: (a) In the first place, silicon amide was prepared by the action of ammonia on silicon tetrachloride:

$$SiCl_4 + 8\,NH_3 = Si(NH_2)_4 + 4\,NH_4Cl\ ,$$

(1) C. Matignon, *Bull. soc. chim.*, [4], **13** (1913), 791.
(2) W. B. Hincke and L. R. Brantley, *J. Am. Chem. Soc.*, **52** (1930), 48.

and then it was washed with liquid ammonia to remove ammonium chloride. Silicon amide thus purified was heated in nitrogen to 1200°C. and silicon nitride was obtained as follows[3]:

$$Si(NH_2)_4 \xrightarrow{0°C.} HNSi(NH_2)_2 \xrightarrow{100°C.} NSiNH_2 \xrightarrow{900°C.} HN(SiN)_2 \xrightarrow{1200°C.} Si_3N_4 .$$

Unfortunately, the product obtained in this way did not contain sufficient nitrogen.

(b) In the second place, purified nitrogen was passed over silicon (Kahlbaum) heated at 1300–1400°C. for ten hours (the method of L. Weiss and T. Engelhardt[4]). The silicon nitride thus obtained appeared greyish white and contained Si_2N_3, SiN, SiO_2, and some unchanged silicon. With the object of separating this unchanged silicon, SiN, and Si_2N_3, the nitrides were heated with 20% potassium hydroxide solution for seven hours. By this treatment, SiN was decomposed into silicon and nitrogen, and the silicon thus formed and the unchanged silicon are taken away as silicate. Next, the nitrides thus treated were put in a platinum dish containing 10 c.c. water mixed with 5 c.c. concentrated hydrofluoric acid and 5 c.c. concentrated nitric acid and left there for four days in order to take away Si_2N_3. The nitrides thus purified which contain Si_3N_4 and SiO_2 were washed with water and dried with alcohol and ether.

(2) *Analyses of specimen.* The nitrogen content of the above mentioned specimen was estimated by the method used by A. Dumas. The material to be analysed was intimately mixed with PbO and $PbCrO_4$ of equal quantity. The result thus obtained was 35.07% N. The silicon content was estimated by fusing the specimen with equal mixture of Na_2CO_3 and K_2CO_3. After dissolution in hydrochloric acid, the silica was filtered off and ignited. The result thus obtained was 58.44% Si. From the results shown above, the specimen may be considered to consist of 87.74% Si_3N_4 and 12.26% SiO_2.

III. **The Specific Heat of Silicon Nitride.** The mean specific heat of silicon nitride was measured by means of the ice calorimeter adopted by P. Oberhoffer[5]. The details of the measurement were already described in the measurement of the specific heat of aluminium nitride[6].

---

(3) F. Lengfeld, *Am. Chem. J.*, **21** (1899), 531; Em. Vigoroux and C. Hugot, *Compt. rend.*, **136** (1903), 1670; M. Blix and W. Wirbelauer, *Ber.*, **36** (1903), 4220; A. Stock and F. Zeidler, *Ber.*, **56** (1923), 986.

(4) L. Weiss and T. Engelhardt, *Z. anorg. allgem. Chem.*, **65** (1909), 38.

(5) P. Oberhoffer, "Dissertation Aachen," (1907).

(6) S. Satoh, *Sci. Papers Inst. Phys. Chem. Research* (Tokyo), **29** (1936), 19.

The measurement was carried out over the following three temperature intervals: 0–99.5, 0–316.4, and 0–585°C. The specimen was compressed and put into an aluminium cylinder of 8 mm. diameter and 2–3 mm. height. Over the above temperature intervals, the specific heat of pure aluminium was measured in order to see the correctness of the measurement.

(a) Measurement over the interval 0–99.5°C. Pure aluminium: 0.2193, 0.2171, 0.2175, mean: 0.2179. Specimen: 0.1761, 0.1766, 0.1753, mean: 0.1760.

The value of the mean specific heat of aluminium is in good agreement with that (0.2196) obtained by E. H. Griffiths and E. Griffiths[7]. The mean specific heat of the specimen is 0.1760 and this contains 87.74% Si_3N_4 and 12.26% SiO_2. When the correction was made on the assumption that the mean specific heat of SiO_2 in the specimen is 0.1862[8], the specific heat of pure Si_3N_4 became 0.1746.

(b) Measurement over the interval 0–316.4°C. Pure aluminium: 0.2308, 0.2321, mean: 0.2315. Specimen: 0.1972, 0.1956, mean: 0.1964.

The corresponding value of the mean specific heat of pure aluminium is not found in the literature but it is almost equal to that of the mean specific heat 0.2342 obtained by interpolating the values 0.2336 for 0–300°C. and 0.2374 for 0–400°C. which were determined by F. Wüst[9]. The mean specific heat of the specimen is 0.1964 and the author made the correction, assuming the mean specific heat of SiO_2 to be 0.2183[8], and obtained the mean specific heat of pure Si_3N_4: 0.1933.

(c) Measurement over the interval 0–585°C. Pure aluminium: 0.2440, 0.2434, 0.2448, mean: 0.2441. Specimen: 0.2188, 0.2190, 0.2195, mean: 0.2191.

The mean specific heat of pure aluminium is in accord with the value 0.2445 obtained by interpolating the values 0.2413 for 0–500°C. and 0.2452 for 0–600°C. which were shown by F. Wüst[9]. The mean value of the specimen is 0.2191, and making the correction on the supposition that the mean specific heat of SiO_2 is 0.2517[8], the mean specific heat of pure Si_3N_4 was found to be 0.2145.

The mean specific heat of pure silicon nitride (C_m) can be expressed by the following equation:

$$C_m = 0.1656 + 9.245 \times 10^{-5}t - 1.5 \times 10^{-8}t^2 .$$

(7) E. H. Griffiths and E. Griffiths, *Phil. Trans.*, A, **214** (1914), 319.

(8) "International Critical Tables," Vol. 5, 105.

(9) F. Wüst, A. Meuthen, and R. Durrer, *Forschungsarb. Gebiete Ingenieurw.*, **204** (1918), 42.

If C is the true specific heat and is expressed by the following equation:

$$C = C_0 + \alpha t + \beta t^2 ,$$

by integration, we have

$$\int_0^t C dt = \int_0^t [C_0 + \alpha t + \beta t^2] dt = C_0 t + \frac{1}{2}\alpha t^2 + \frac{1}{3}\beta t^3 = C_m t .$$

Hence $$C = \frac{d(C_m t)}{dt} .$$

Consequently, the true specific heat of pure silicon nitride can be expressed in the following equation:

$$C = 0.1656 + 1.847 \times 10^{-4} t - 4.5 \times 10^{-8} t^2 .$$

IV. **The Specific Heat of Silicon.** The specific heat of silicon was measured by A. Magnus[10]. By introducing $\beta\nu = 712$ into Debye's equation, C_v values can be obtained and C_p values computed from the equation

$$C_p - C_v = 1.42 \times 10^{-5} C_p^2 T$$

give a satisfactory result over a wide temperature range. But in order to simplify the calculation, the variation of the molecular heat of silicon with absolute temperature can be expressed in the following equation:

$$C_p = 3.724 + 4.816 \times 10^{-3} T - 2.186 \times 10^{-6} T^2 .$$

V. **The Heat of Formation of Silicon Nitride.** (1) *From the experimental formula.* From the equilibrium data of the reaction $Si_3N_4 = 3Si + 2N_2$ at high temperatures, the heat of formation of silicon nitride was calculated in the following way: The dissociation pressure of the above reaction at 1600°K. and 1800°K. was measured by W. B. Hincke and L. R. Brantley[2]:

$$\log P_{N_2} = -\frac{19250}{T} + 8.54 .$$

And the free energy equation is expressed as follows:

$$\Delta F^\circ = 176{,}300 - 78.35\, T.$$

Consequently, the heat of reaction at 1700°K. is 176,300 cal.

(10) A. Magnus, *Ann. Physik*, **70** (1923), 303.

As shown in Chapter III, the molecular heat of silicon nitride at 25°C. is 23.85 which can be obtained from the equation:

$$C_p = 0.1656 + 1.847 \times 10^{-4}t - 4.5 \times 10^{-7}t^2 .$$

As shown in Chapter IV, the atomic heat of silicon is expressed in the following equation:

$$C_p = 3.724 + 4.816 \times 10^{-3}T - 2.186 \times 10^{-6}T^2 .$$

According to G. N. Lewis and M. Randall[11], the molecular heat of nitrogen is:

$$C_p = 6.5 + 0.001\,T .$$

Thus in the reactant we have Si_3N_4: 23.85, and in the resultant, we have

$$3\,Si : 11.17 + 1.445 \times 10^{-2}T - 6.558 \times 10^{-6}T^2 ,$$

$$2\,N_2 : 13.00 + 2 \times 10^{-3}T ,$$

$$\therefore\ Si_3N_4 : 24.17 + 1.645 \times 10^{-2}T - 6.558 \times 10^{-6}T^2 .$$

Consequently in the whole system, the terms referring to the specific heats are

$$0.322 + 1.645 \times 10^{-2}T - 6.558 \times 10^{-6}T^2 .$$

Next, by combining the molecular heat terms with ΔH, the equation of the heat of reaction can be expressed as follows:

$$\Delta H = \Delta H_0 + 0.322\,T + 8.225 \times 10^{-3}T^2 - 2.186 \times 10^{-6}T^3 .$$

The free energy equation of the reaction is, therefore,

$$\Delta F^\circ = \Delta H_0 - 0.322T \ln T - 8.225 \times 10^{-3}T^2 + 1.093 \times 10^{-6}T^3 + IT .$$

From the equation $\Delta F^\circ = 176{,}300 - 78.35T$ obtained by W. B. Hincke and L. R. Brantley[2] we find that $\Delta F^\circ = 50{,}940$ at 1600°K. and $\Delta F^\circ = 35{,}270$ at 1800°K.

Introducing these values into the free energy equation, the values ΔH_0 and I can be obtained as shown below:

$$\Delta H_0 = 162{,}204 , \qquad I = -56.84 .$$

Hence, $\Delta H = 162{,}204 + 0.322\,T + 8.225 \times 10^{-3}T^2 - 2.186 \times 10^{-6}T^3 ,$

$$\Delta F^\circ = 162{,}204 - 0.322T \ln T - 8.225 \times 10^{-3}T^2 + 1.093 \times 10^{-6}T^3 - 56.84T .$$

(11) G. N. Lewis and M. Randall, "Thermodynamics," 80, (1923).

Consequently the heat of reaction at 25°C. is $\Delta H_{298} = 163{,}024$.
As shown in the above computation, the result obtained is as follows:

$$3Si + 2N_2 = Si_3N_4 + 163{,}024.$$

(2) *From the Nernst's heat theorem.* By the use of the Nernst's heat theorem, the author calculated the heat of formation of silicon nitride as follows: In the reaction $Si_3N_4 = 3Si + 2N_2$, the change of molecular number of the gaseous system is $\Sigma n = 2$.

If Q is the heat of reaction at any temperature and Q_0 is that at absolute zero, Q may be expressed in the following equation by the Nernst's heat theorem:

$$Q = Q_0 + \sum n \cdot 3.5T + aT^2 .$$

Differentiating with respect to T, we obtain

$$\frac{dQ}{dT} = \sum mC_p = 2 \times 3.5 + 2aT .$$

The molecular heat of each substance at 25°C. follows: Si_3N_4: $C_p = 23.85$; Si: $C_p = 4.965$; N_2: $C_p = 6.798$.
Accordingly,

$$a = \frac{3 \times 4.965 + 2 \times 6.798 - 23.85 - 7}{2 \times 298} = -0.003958 .$$

The chemical constant of N_2 is 2.6. So that $\Sigma nI = 2 \times 2.6 = 5.2$, and

$$\log K = -\frac{Q_0}{4.576T} + 3.5 \log T - \frac{0.003958}{4.576} T + 5.2 .$$

According to W. B. Hincke and L. R. Brantley[2]

$$\log P_{N_2} = -\frac{19250}{T} + 8.54 .$$

$$\log P_{N_2} = -3.49 \text{ at } 1600°K.$$

Hence, $\log K = \log P_{N_2}^2 = -\frac{Q_0}{4.576T} + 3.5 \log T - \frac{0.003958}{4.576} T + 5.2$,

$$-3.49 \times 2 = -\frac{Q_0}{4.576 \times 1600} + 3.5 \log 1600 - \frac{0.003958}{4.576} \times 1600 + 5.2 .$$

$$\therefore \quad Q_0 = 161{,}250 , \quad Q = Q_0 + 2 \times 3.5T + aT = 162{,}984 \text{ (at 25°C.)}.$$

This result is tantamount to that obtained by the experimental formula.

(3) C. Matignon[1] measured the equilibrium data of the reaction

$$3SiO_2 + 6C + 2N_2 = Si_3N_4 + 6CO$$

at 1700°K. and by the use of Nernst's approximate formula calculated the heat of formation of silicon nitride at room temperature to be 159,300 cal.

VI. **Discussion of the Result.** As shown above, the most probable value of the heat of formation of silicon nitride is

$$3Si + 2N_2 = Si_3N_4 + 163{,}000.$$

Comparison of the heat of formation of silicon nitride reported in the literature until now is as follows: 176,300 (W. B. Hincke[2]); 163,000 (S. Satoh); 159,300 (C. Matignon[1]).

The heats of formation of the nitrides of the elements: Na, Mg, Al, Si, P, S, and Cl which belong to the second series of the periodic table per one gram atom of nitrogen in the solid or liquid state are indicated in the following table in the order of their atomic numbers.

Atomic number	Nitrides	Heat of formation per one gram of nitrogen (kcal.)
11	(NaN_3)	− 1.7
12	Mg_3N_2	+57.6
13	AlN	+74.7
14	Si_3N_4	+40.7
15	P_3N_5	+16.3
16	SN	−31.9
17	NCl_3	−54.7

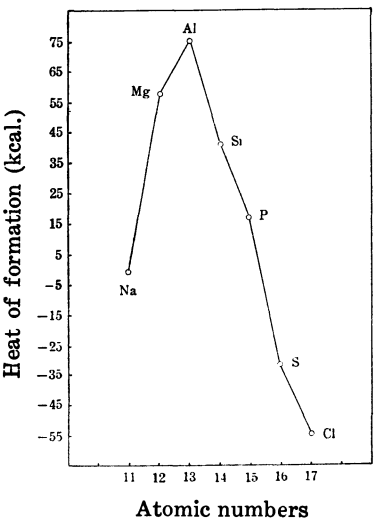


Fig. 1. Relationship between the heat of formation of nitrides of the elements belonging to the second series of the periodic table and their atomic numbers.

The heat of formation of sodium nitride is not yet known but the heat of formation of sodium azide is − 1.7 kcal. per one gram of nitrogen[12].

(12) E. Briner and P. Winkler, *J. chim. phys.*, **20** (1922), 203.

The heat of formation of magnesium nitride is 57.6 kcal.[13] and that of aluminium nitride is 74.7 kcal. as shown in the previous paper[6].

The heat of formation of silicon nitride is 40.7 kcal. as calculated above and that of phosphorus nitride is 16.3 kcal.[14]

The heat of formation of sulphur nitride is -31.9 kcal.[15] and that of nitrogen chloride is -54.7 kcal.[16]

In Fig. 1, the relation between the heats of formation of nitrides per one gram atom of nitrogen and their atomic numbers is shown graphically; the curve shows the maximum for aluminium. This bears a striking resemblance to the appearance of the maximum for beryllium in the curve showing the relationship between the heats of formation of nitrides of the elements belonging to the first series of the periodic table and their atomic numbers, which was reported in my last paper[17].

Summary.

As the specific heat of silicon nitride has not yet been determined, the mean specific heat of silicon nitride was measured by the ice calorimeter over three temperature intervals: 0–99.5, 0–316.4, and 0–585°C., and the equation of the true specific heat was obtained which holds good over the above temperature ranges:

$$C = 0.1656 + 1.847 \times 10^{-4}t - 4.5 \times 10^{-8}t^2 .$$

By using this value, the heat of formation of silicon nitride was computed from the dissociation pressure of silicon nitride at high temperatures. The result obtained is as follows:

$$3Si + 2N_2 = Si_3N_4 + 163{,}000.$$

The relationship between the heats of formation of nitrides of the elements belonging to the second series of the periodic table and their atomic numbers is discussed.

The Institute of Physical and Chemical Research, Tokyo.

---

(13) B. Neumann, C. Kröger, and H. Kunz, *Z. anorg. allgem. Chem.*, **207** (1932), 139.
(14) A. Stock and F. Wrede, *Ber.*, **40** (1907), 2923.
(15) M. Berthelot and Vieille, *Ann. chim. phys.*, [5], **27** (1882), 204.
(16) W. A. Noyes and W. F. Tuley, *J. Am. Chem. Soc.*, **47** (1925), 1336.
(17) S. Satoh, *Sci. Papers Inst. Phys. Chem. Research* (Tokyo), **29** (1936), 53.

The Theory on the Constitution of a Thermoreversible Gel.

By Fumio HIRATA.

(Received December 20, 1937.)

Introduction.

Concerning the constitution of thermoreversible gel, the present author has discussed elsewhere[1] the constitution and the sol-gel transformation of gelatine solution which gives a typical thermoreversible gel. It has been found that the theory of micellar constitution of gel is most adequate to explain the experimental results of the studies on the physicochemical properties of gel of gelatine and that the process of gelation may be explained on an assumption that the cause of gelation is in the fixation of the micelle particle in the system. By assuming that the micelle is of electric constitution and that the origin of rigidity of gel is in the mutually reacting electrostatical forces of these micelles, the experimental results of the measurement of rigidity have been examined, and an experimental equation has been found expressing the existence of a certain relation between the change of rigidity due to temperature and the change of dielectric constant of the intermicellar liquid of the gel due to the change of temperature. Taking into consideration the numerical values of modulus of rigidity and the concentration of the gel, and also the fact that the rigidity shows the maximum value at the isoelectric point of gelatine, it has been concluded that the mutually acting forces of the micelles may be considered to be of electric dipole nature.

In the present paper, the theoretical relation between the rigidity of gel and the dielectric constant of intermicellar liquid is investigated.

I. **Consideration on the Constitution of Thermoreversible Gel.** Among the theories on the constitution of gel, the theory that a gel is composed of micelles dispersed in a liquid, manifesting the elastic solid mass as a whole, seems to be most acceptable in the case of the gel of gelatine. The results of the studies made by the present author on the scattering of light by sol and gel of gelatine,[2] on the electrolytic conductivity of sol

(1) F. Hirata, *Rev. Phys. Chem.* (Japan), **11** (1937), 262; *Proc. Imp. Acad.* (Tokyo), **33** (1937), 266; *J. Chem. Soc. Japan*, **58** (1937), 1156 et seq.

(2) Duclaux and Hirata, *J. chim. phys.*, **30** (1933), 213.

and gel of gelatine,[3] on the ultrafiltration of sol of gelatine,[4] and on the refractive index of sol and gel of gelatine,[3] suggest that the process of gelation is nothing but the stoppage of the free translational and rotational motion, that is, of the Brownian motion of the micelles. It may be assumed that the direct forces of attraction and repulsion acting at a long distance are in action through the medium between the micelles in both sol and gel states. However, when the system is at high temperature, that is, in the sol state, the kinetic energy due to temperature of the micelles overcomes these forces in its action, and the micelles are free to move and consequently, the whole mass becomes a liquid. At lower temperature, that is, in the gel state, the intermicellar forces become superior in its action and these forces make the micelles take definite positions in the system. It may be said that the micelle is composed of an aggregate of particles of electric charges, and the rigidity of gel is the effect of the electrostatical forces of these micelles, which act through the intermicellar liquid. On the basis of the studies stated above, it may be assumed that the constitution of micelle is not affected by the change of temperature within the range of the present experiments. It follows, therefore, that the cause of the change of the rigidity of gel due to temperature exists not in the micelle itself but in the intermicellar liquid. Since the forces may be assumed to be of the electrostatical nature acting at a long distance through the intermicellar liquid, the change in the intermicellar forces may be ascribed to the change in the intermicellar liquid. If this assumption be correct, there must be a certain quantitative relation between the change of dielectric constant of the intermicellar liquid due to temperature and that of rigidity of the gel due to temperature.

II. **Method and Results of Measurement of Rigidity of Gel.** In order to investigate the constitution of thermoreversible gel, the study of the rigidity of gel, especially the study of the change of rigidity due to temperature must be one of the most important and the most direct process, for the difference between the gel and sol states in the case of thermoreversible gel seems to depend only on the difference of the mechanical rigidity of the colloidal system.

In the investigation of the constitution of gel from its rigidity, it is preferable to use a sample of as low concentration as possible for securing the simplicity of experimental conditions. In measuring the effect of temperature on the rigidity, it is necessary to use the method as ac-

(3) These experiments have been made in the author's laboratory. Cf. *J. Chem. Soc. Japan*, **58** (1937), 1156, et seq.

(4) Duclaux and Hirata, *J. chim. phys.*, **30** (1933), 229.

curate as possible, since the gel loses its rigidity as the temperature rises and turns into liquid in the end. Moreover, the method must be such as will allow the temperature of the sample remain constant and keep it free from desiccation. From these points of view, the method of Michaud[5] seems to be the most satisfactory one.

The method of measurement used by the present author is a modified form of the method of Michaud used in an experimental study on cellulosic solutions by Duclaux and the author.[6]

In this method of measurement[7] the sample is held in a glass capillary tube and the whole is kept in a water thermostat. If a pressure is applied to the sample at one end of the capillary tube, every point of the sample gel will be displaced parallel with the axis of the tube. Let l and R be the length and the radius of the capillary tube, respectively, X_0 be the displacement of the sample at a point on the axis of the capillary tube and μ be the modulus of rigidity of the gel, and the following relation will be obtained theoretically:[7]

$$\mu = PR^2 / 4lX_0 \qquad (1),$$

where P is the pressure applied.

The results of measurement of P and X_0 for the gel of gelatine at the isoelectric point $p\mathrm{H} = 4.7$ are given in Table 1 to 6. The concentration of this gel was 25.97 g./l. Taking P and X_0 as ordinate and abscissa, respectively, the relations are shown in Fig. 1. In this figure it is

Table 1. $t = 5.80 \pm 0.01$°C.

P (dyne/cm.^{2})	X_0 (cm.)	P/X_0
2.000×10^4	4.104×10^{-4}	4.873×10^7
2.961×10^4	6.156×10^{-4}	4.810×10^7
3.882×10^4	9.234×10^{-4}	4.204×10^7
5.373×10^4	12.31×10^{-4}	4.364×10^7
6.294×10^4	14.36×10^{-4}	4.382×10^7
7.255×10^4	15.39×10^{-4}	4.714×10^7

Table 2. $t = 11.69 \pm 0.01$°C.

P (dyne/cm.^{2})	X_0 (cm.)	P/X_0
1.999×10^4	5.130×10^{-4}	3.897×10^7
2.999×10^4	9.234×10^{-4}	3.248×10^7
3.950×10^4	10.26×10^{-4}	3.859×10^7
5.429×10^4	12.31×10^{-4}	4.410×10^7
6.272×10^4	14.36×10^{-4}	4.367×10^7
7.213×10^4	18.47×10^{-4}	3.906×10^7
8.173×10^4	20.52×10^{-4}	3.983×10^7

(5) Michaud, *Ann. phys.*, [9], **19** (1923), 63.
(6) Duclaux and Hirata, *J. chim. phys.*, **28** (1931), 538.
(7) Hirata, *Rev. Phys. Chem.* (Japan), **11** (1937), 262.

Table 3. $t = 15.00 \pm 0.01$°C.

P (dyne/cm.^{2})	X_0 (cm.)	P/X_0
1.940×10^4	5.130×10^{-4}	3.782×10^7
2.920×10^4	9.234×10^{-4}	3.162×10^7
3.900×10^4	9.234×10^{-4}	4.273×10^7
5.429×10^4	14.36×10^{-4}	3.779×10^7
6.330×10^4	16.42×10^{-4}	3.856×10^7
7.271×10^4	19.50×10^{-4}	3.730×10^7
8.192×10^4	20.52×10^{-4}	3.992×10^7

Table 4. $t = 18.00 \pm 0.01$°C.

P (dyne/cm.^{2})	X_0 (cm.)	P/X_0
2.017×10^4	8.208×10^{-4}	2.458×10^7
2.938×10^4	12.31×10^{-4}	2.386×10^7
3.918×10^4	19.49×10^{-4}	2.009×10^7
5.444×10^4	25.65×10^{-4}	2.123×10^7
6.404×10^4	25.65×10^{-4}	2.440×10^7
7.305×10^4	30.78×10^{-4}	2.373×10^7
8.245×10^4	33.86×10^{-4}	2.455×10^7

Table 5. $t = 20.50 \pm 0.01$°C.

P (dyne/cm.^{2})	X_0 (cm.)	P/X_0
4.895×10^3	5.130×10^{-4}	0.925×10^7
9.790×10^3	8.208×10^{-4}	1.193×10^7
1.469×10^4	14.36×10^{-4}	1.022×10^7
1.978×10^4	18.47×10^{-4}	1.068×10^7
2.428×10^4	20.52×10^{-4}	1.183×10^7
2.820×10^4	26.68×10^{-4}	1.057×10^7
3.290×10^4	31.81×10^{-4}	1.034×10^7
4.229×10^4	41.04×10^{-4}	1.030×10^7
5.189×10^4	48.22×10^{-4}	1.076×10^7
6.089×10^4	59.51×10^{-4}	1.021×10^7
6.931×10^4	68.74×10^{-4}	1.008×10^7
7.842×10^4	76.95×10^{-4}	1.019×10^7

Table 6. $t = 22.60 \pm 0.01$°C.

P (dyne/cm.^{2})	X_0 (cm.)	P/X_0
4.898×10^3	14.36×10^{-4}	3.411×10^6
9.992×10^3	30.76×10^{-4}	3.216×10^6
1.992×10^4	62.59×10^{-4}	3.176×10^6
2.978×10^4	92.34×10^{-4}	3.225×10^6
3.977×10^4	123.1×10^{-4}	3.232×10^6
5.937×10^4	179.6×10^{-4}	3.309×10^6
6.818×10^4	210.3×10^{-4}	3.247×10^6

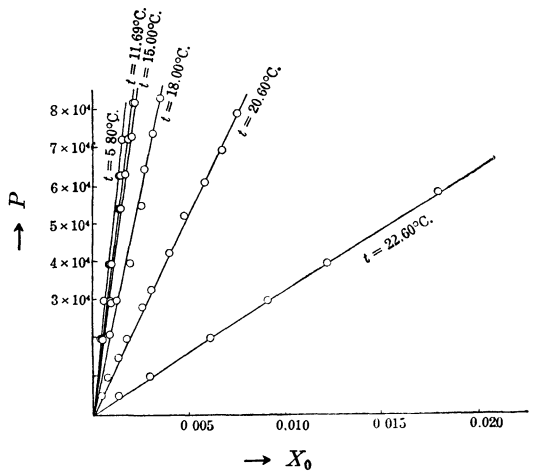


Fig. 1.

represented clearly that the relation between P and X_0 is perfectly linear, that is, the law of elasticity holds strictly within the range of the experimental temperatures and the pressures applied.

III. **Theoretical Relation between X_0 and ε.** As the magnitude of the modulus of rigidity has a direct connection with the displacement X_0, the change of rigidity due to temperature may be expressed in terms of the change of X_0 due to temperature. It is intended here to derive the theoretical relation which will hold between X_0

and ε, the dielectric constant of the intermicellar liquid of the gel for different temperatures.

In order to simplify the calculation, the micellar constitution of the gel of gelatine is assumed as shown in Fig. 2. Each micelle M which is supposed to be an electric dipole takes the position of each lattice point of a simple cubic lattice and the space between these micelles is supposed to be filled up by an intermicellar liquid.

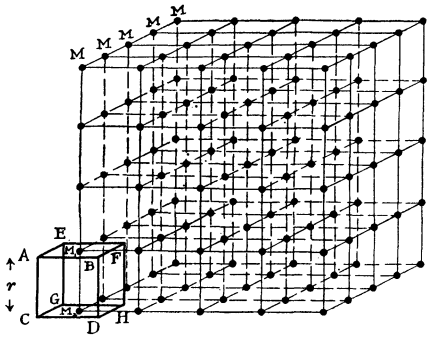


Fig. 2.

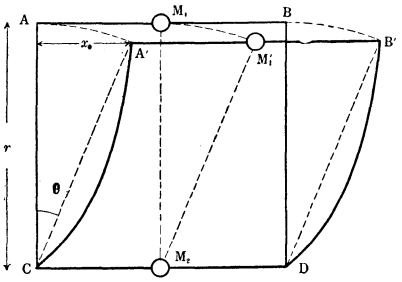


Fig. 3.

When such a gel is subjected to a holizontal shear, all the unit cube in the lattice will be deformed equally. Taking one of those unit cube, let us advance the consideration.

Let a unit cube be ABDC in Fig. 3, in which the cube is indicated by a cross section cut by a plane perpendicular to the side face ACGE of the cube ABCDEFGH in Fig. 2. M_1 and M_2 are the micelles which take the central position of each face shown as AB and CD in Fig. 3. If a pressure is applied at the side face AC, the base CD being fixed, the cube ABDC will be deformed and become the shape like A'B'DC. The micelle M_1 will be displaced to M_1' and the equilibrium of forces will be established. It is supposed that the mutual forces of M_1' and M_2 in the deformed state must produce the reactive elastic force. Let f_l be the direct active force between the micelles M_1' and M_2, and $f_l \sin\theta$ will be its horizontal component which appears in the horizontal direction. This component is nothing but the force which reacts as the rigidity of the cube. As already stated, the direct acting force is caused by the mutual action of the dipole micelles, the direct force between M_1' and M_2 is expressed in the following equation:

$$f_l = \frac{\gamma\sigma_0^2}{\varepsilon r^4} \qquad (2),$$

in which σ_0 represents the dipole moment of M_1' and M_2, γ the factor which is determined by the mutual orientation of the two dipole micelles in the deformed state, ε the dielectric constant of the medium which fills up the space between M_1' and M_2, and r the distance between the two micelles M_1' and M_2. The reactive horizontal force $-f_x$ will be given in the following form:

$$-f_x = -f_l \sin\theta$$

or

$$-f_x = -\frac{\gamma\sigma_0^2}{\varepsilon r^4}\sin\theta \qquad (3),$$

in which the negative sign of f_x indicates that the direction of the force is to the left.

When the temperature of gel changes, this horizontal force, $-f_x$ will be changed in its magnitude; for the rigidity of gel will change when the temperature of gel is changed. In equation (3), σ_0 and r may be assumed to be independent of temperature, but γ, ε and θ are supposed to change with temperature. In order to secure the simplicity of calculation, γ is assumed to be independent of the change of temperature.[8] Consequently, in this case only ε and θ are variable. If the measurement of rigidity, viz., the measurement of X_0 is executed for different temperatures but under a same constant pressure, the above force f_x may be taken as constant for the temperature of measurement. The following equation, therefore, is written for the reactive elastic force in the range of temperature of the measurements:

$$-f_x = k \qquad (4),$$

where k is a constant which is independent of temperature. From equations (4) and (3), we have

$$-\frac{\gamma\sigma_0^2}{\varepsilon r^4}\sin\theta = k \qquad (5).$$

If we summarize all of the constants in equation (5) which are independent of the change of temperature, by b, that is, $kr^4/\gamma\sigma_0^2 = b$, we get the following relation:

$$\sin\theta = -b\cdot\varepsilon \qquad (6).$$

Now we must find the relation between ε and $X_{0\cdot P}$. $X_{0\cdot P}$ means X_0 for a constant pressure P.

(8) As for the value of γ which gives the orientation polarization caused by the stress, it will be treated in a later report.

Next suppose, on the other hand, a cube of homogeneous gel of side length r. This cube is, in the microscopic point of view, is equivalent to the cube which is given in Fig. 1 as ABCDEFGH, but in the present case it is supposed to be an entirely homogeneous, isotropic, elastic mass. Only the dimension of the cubes is assumed to be equal in both cases. This cube is shown as ABDC in Fig. 4 which is shown as the cross section analogous to Fig. 3.

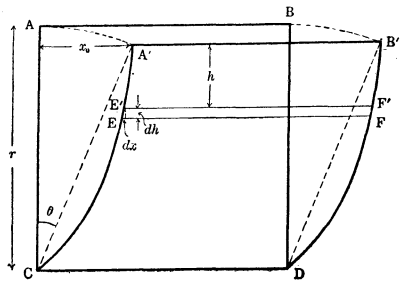


Fig. 4.

If pressure P is applied to the cube from the side face AC, the base CD being fixed, the cube ABDC will be deformed into A′B′DC when the equilibrium will be established. If we represent μ' as the modulus of rigidity of the gel under the deformed state, and consider the equilibrium condition of the acting and reacting forces which act horizontally to the plane E′F′, indicated in Fig. 3, of the infinitely thin gel block EFE′F′, we have the following equation:

$$Phr = -\mu' \frac{dx}{dh} r^2 \qquad (7).$$

The meaning of h, r, dh, dx in this equation is clearly shown in the figure. The left hand side of equation (7) represents the force that acts tangentially on the plane E′F′ in the right direction and the right hand side of the equation represents the reactive tangential force produced by the elastic property of the gel block EFF′E′. If we solve the equation (7), taking the limiting condition: $h = \sqrt{r^2 - x_0^2}$, when $x = 0$, we have

$$\frac{P}{2}(h^2 - r^2 + x_0^2) = -\mu' r x \qquad (8).$$

Putting $h = 0$ and $x = x_0$,

$$\frac{P}{2}(x_0^2 - r^2) = -\mu' r x_0 \qquad (9).$$

Rewriting, we have

$$\frac{P}{\mu'} = 2\frac{x_0}{r}\frac{r^2}{r^2 - x_0^2} \qquad (10).$$

We may write this equation in the following form, if we take the value of θ as the function of x_0, i.e., $\sin\theta = x_0/r$; $\cos\theta = \sqrt{r^2 - x_0^2}/r$,

$$\frac{P}{\mu'} = 2\sin\theta / \cos^2\theta \qquad (11).$$

If we express, on the other hand, the modulus of rigidity of the cube ABDC which is not deformed as μ, this modulus of rigidity μ must correspond to the value of μ measured directly by the method stated in paragraph II. In equation (1) of paragraph II, if we measure the value of X_0 under a constant pressure P, X_0 may be represented as $X_{0.P}$. Re-writing equation (1), we have

$$\frac{P}{\mu} = \frac{4lX_{0.P}}{R^2} \qquad (12).$$

To get the relation between μ and μ', it is necessary to determine the nature of the reactive elastic force. As already stated in the introduction of this paper, it may be concluded that the forces which cause the rigidity of gel is the electrostatic force between the dipole micelles of gelatine. Consequently, as the dipolar force are inversely proportional to the fourth power of the mutual distance of the micelles, the relation between μ and μ' may be represented in the following equation:

$$\frac{\mu'}{\mu} = \left(\frac{r}{r\cdot\cos\theta}\right)^4 = \frac{1}{\cos^4\theta} \qquad (13).$$

Combining equations (11) and (13), we have

$$\frac{P}{\mu} = 2\frac{\sin\theta}{\cos^2\theta}\frac{1}{\cos^4\theta} \qquad (14).$$

From equations (12) and (14), the following equation is given

$$\frac{4lX_{0.P}}{R^2} = 2\frac{\sin\theta}{\cos^6\theta} \qquad (15).$$

Changing the form, we get

$$\frac{4lX_{0.P}}{R^2} = 2\frac{\sin\theta}{(1-\sin^2\theta)^3} \qquad (16).$$

Neglecting the higher order of $\sin\theta$ in the denominator, we have

$$\frac{2lX_{0.P}}{R^2} = \frac{\sin\theta}{1-3\sin^2\theta} \qquad (17).$$

Now, putting the value of sin θ expressed in equation (6), equation (17) will be written as

$$\frac{2lX_{0\cdot P}}{R^2} = \frac{-b\cdot\varepsilon}{1-3b^2\varepsilon^2} \qquad (18).$$

This equation represents the relation between the values $X_{0\cdot P}$ and ε, and may be verified by using the results of the direct measurement of the modulus of rigidity.

If we change the form of equation (18), we have the following equation:

$$\frac{X_{0\cdot P}}{\varepsilon} = 3b^2X_{0\cdot P}\cdot\varepsilon - \frac{R^2}{2l}b \qquad (19).$$

If we put

$$3b^2 = \alpha$$

and

$$-b\frac{R^2}{2l} = \beta \qquad (20),$$

we have

$$\frac{X_{0\cdot P}}{\varepsilon} = \alpha\cdot X_{0\cdot P}\cdot\varepsilon + \beta \qquad (21),$$

where α and β are constant which are independent of temperature. This equation tells that, independent of temperature, the linear relation between $X_{0\cdot P}/\varepsilon$ and $X_{0\cdot P}\cdot\varepsilon$ exists for thermoreversible gels. In this form of relation, the result of calculation of the values of $X_{0\cdot P}$ and ε, and that of the observed values may conveniently be examined.

IV. **The Verification of the Relation Expressed by Equation (21).** The numerical data necessary to the verification of equation (21) are given in the following tables.

Table 7.

t	ε	$X_{0\cdot P}$	$X_{0\cdot P}/\varepsilon$	$X_{0\cdot P}\cdot\varepsilon$
5.80	85.73	$1.30_7\times10^{-3}$	$1.52_4\times10^{-5}$	0.112_1
11.69	83.51	$1.46_0\times10^{-3}$	$1.77_3\times10^{-5}$	0.123_6
15.00	82.19	$1.56_1\times10^{-3}$	$1.89_9\times10^{-5}$	0.128_5
18.00	81.07	$2.55_5\times10^{-3}$	$3.15_2\times10^{-5}$	0.206_7
20.50	80.15	$5.80_6\times10^{-3}$	$7.24_4\times10^{-5}$	0.465_3
22.60	79.38	$18.4_2\times10^{-3}$	$23.2_0\times10^{-5}$	1.46_2

Table 8.

t	$X_{0\cdot P}$ (calc.)	$X_{0\cdot P}$ (obs.)
5.80	$1.00_1\times10^{-3}$	$1.30_7\times10^{-3}$
11.69	$1.48_8\times10^{-3}$	$1.46_0\times10^{-3}$
15.00	$2.06_2\times10^{-3}$	$1.56_1\times15^{-3}$
18.00	$3.15_6\times10^{-3}$	$2.55_5\times10^{-3}$
20.50	$5.61_7\times10^{-3}$	$5.80_6\times10^{-3}$
22.60	$16.0_2\times10^{-3}$	$18.4_2\times10^{-3}$

All the values of $X_{0.P}$ in the table are the values determined under the pressure $P = 6 \times 10^4$ dyne/cm.^{2}. As for the values of ε, values of pure water have been adopted by reason that the gel is at its isoelectric point and that the measurement of electrolytic conductivity of the gel gives the values approximately equal to that of pure water. These values have been calculated by Drude's formula: $\varepsilon_t = 81.07[1 - 0.004583(t - 18) + 0.0000117(t - 18)^2]$. Taking the values of $X_{0.P}/\varepsilon$ and $X_{0.P}\cdot\varepsilon$ as the y-axis and the x-axis of co-ordinates respectively, their relation is shown in Fig. 5. It is clear from the figure that the relation represented by equa-

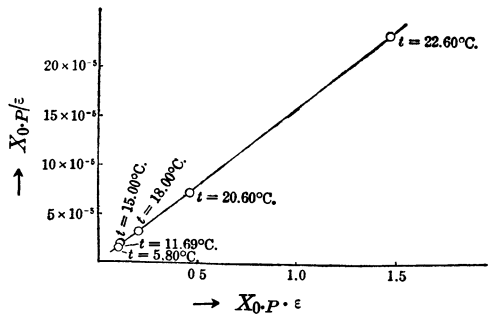
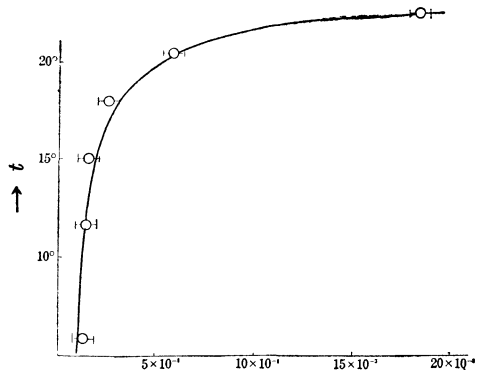


Fig. 5.



— ... calculated values.
○ ... observed value.
|—| ... range of the allowable experimental error of $X_{0.P}$.

Fig. 6.

tion (21) holds in the region of the experimental temperatures. If we calculate the constants α and β by the method of least square, using the numerical values given in Table 7, the following values are obtained:

$$\alpha = +1.602 \times 10^{-4},$$

$$\beta = -2.082 \times 10^{-6} \qquad (22).$$

Consequently, equation (21) may be written in the following form:

$$\frac{X_{0.P}}{\varepsilon} = 1.602 \times 10^{-4} X_{0.P} \cdot \varepsilon - 2.082 \times 10^{-6} \qquad (23).$$

By this equation and using the numerical values of ε, it is possible to calculate the values of $X_{0.P}$. The result of this calculation is given in Table 8, in which the calculated values are compared with the direct

observed values. In Fig. 6 the calculated values and the observed values of $X_{0.P}$ are plotted as a function of the experimental temperature, t, instead of ε. From the above tables and figures, the validity of equation (21) may be accepted. Next, if we combine equations (6) and (20), the constants α and β of equation (21) may be expressed in the following form:

$$\alpha = \frac{3\sin^2\theta}{\varepsilon^2},$$

$$\beta = \frac{R^2}{2l}\frac{\sin\theta}{\varepsilon} \qquad (24).$$

Consequently, if the values of $\sin\theta$ and ε corresponding to the experimental temperature are known, the constancy of α and β may be examined by the experimental data as follows. If we solve equation (17), the value of $\sin\theta$ will be given by the following equation:

$$\sin\theta = \frac{1}{6}\left(-\frac{R^2}{2lX_{0.P}} + \sqrt{\frac{R^4}{4l^2X_{0.P}^2}+12}\right) \qquad (25).$$

Taking values of R and l (in the present experiment, $R = 0.071$ cm. and $l = 10.01$ cm.)[9] and also that of $X_{0.P}$, the values of $\sin\theta$ for every experimental temperature will be obtained. These values are shown in

Table 9.

t	$\sin\theta$
5.80	0.5460
11.69	0.5497
15.00	0.5511
18.00	0.5612
20.50	0.5702
22.60	0.5750

Table 10.

t	α	β
5.80	$1.21_7\times10^{-4}$	$-1.60_3\times10^{-6}$
11.69	$1.30_2\times10^{-4}$	$-1.66_1\times10^{-6}$
15.00	$1.34_9\times10^{-4}$	$-1.58_3\times10^{-6}$
18.00	$1.43_8\times10^{-4}$	$-1.74_3\times10^{-6}$
20.50	$1.51_9\times10^{-4}$	$-1.79_5\times10^{-6}$
22.60	$1.57_5\times10^{-4}$	$-1.82_4\times10^{-6}$

Table 9. Adopting these values of $\sin\theta$, the numerical values of the constants α and β are computed and are shown in Table 10. If we take into consideration the magnitude of allowable experimental error of the measurement of $X_{0.P}$, it may be said that the calculated values of α and β show a good agreement with the values given in equation (20) and also

(9) F. Hirata, *Rev. Phys. Chem.* (Japan), **11** (1937), 262.

that these values are approximately independent of the change of temperature.

V. Conclusion. Although it is certain that there is a difference between the true configuration of micelles in the gel and the configuration assumed in the present theoretical calculation, the results of the verification described above will allow us to conclude that the assumptions adopted in the course of the theoretical treatment are acceptable, that is to say, the assumptions that the cause of the change of rigidity of gel due to temperature can be ascribed to the change of dielectric constant of intermicellar liquid due to temperature and that the nature of the intermicellar forces which cause the rigidity of gel must be an electric dipolar one.

Summary.

A relation has been derived theoretically between the dielectric constant of the intermicellar liquid and the rigidity of thermoreversible gel and the relation has been examined using the results of measurements of rigidity of the gel of gelatine.

Laboratory of Colloid Chemistry,
Kiriu Higher Technical School.

Constitution and Viscosity Association of High-molecular-weight Hydrocarbons.

By Bunnosuke YAMAGUCHI.

(Received December 4, 1937.)

In his previous paper[1] the author determined for a number of high-molecular-weight liquids a quantity which he called the viscosity association and found the existence of a linear relationship between their viscosity association and their temperature coefficients of viscosity. In the present paper the author attempts to establish by similar studies an empirical equation expressing such a relation, and to calculate by means of the equation the viscosity association of the high-molecular-weight hydrocarbons whose chemical structure and viscosity-temperature coefficients are known, with the object of studying their viscosity association in relation to their chemical structure.

The conception of the viscosity association and the method of its measurement were fully explained in the previous paper, but it will be helpful to give their outlines, as follows:

As indicated by the tangent drawn to the curve in Fig. 1 showing the change in viscosity with concentration of a solution of high-molecular-weight liquid in benzene, viscosity changes always approximately in linear proportion with concentration for dilute solutions not exceeding the concentration C. For higher concentrations the curve bends upward, showing that viscosity increases rapidly with concentration until it finally reaches η_a, which denotes the viscosity of pure solute A when the concentration becomes 100%. If we prolong the tangent qr until it intersects the ordinate at the extreme right, the point of intersection s indicates the viscosity η'_a which the solute would have, provided no special intermolecular forces have acted between the molecules of the solute, and consequently no particular association. Since the ratio η_a/η'_a denotes, as explained in the previous paper, a quantity proportional to that part which association takes in the viscosity of the solute, we express the quantity η_a/η'_a as A_v—viscosity association:

$$A_v = \frac{\eta_a}{\eta'_a} \qquad (1) .$$

(1) *Rept. Aeronaut. Research Inst., Tôkyô Imp. Univ.*, No. 102 (1934); *J. Chem. Soc. Japan*, **55** (1934), 353.

In determining the viscosity association, the value of η_a' may be calculated by applying Einstein's equation for the viscosity of a dilute suspensoid to solutions of such high-molecular-weight hydrocarbons as lubricating oils.

Einstein's equation of viscosity is

$$\eta = \eta_0\left(1+k\frac{v}{V}\right) \qquad (2),$$

where V is the total volume of solution, v the volume fraction of solute in the solution, and k a constant whose value, according to Einstein, is 2.5 independent of the size of the solute particles or molecules, provided they are spherical and of uniform size. It is however known from Eisenschitz's viscosity equation[2] and the studies of Kuhn[3] and Staudinger[4] that k depends on the molecular shape or structure of the solute.

If the solution contains g g. of solute and the density of the solute is d_a, equation (2) may be transformed into

$$\frac{\eta}{\eta_0}-1 = \eta_r-1 = k\frac{v}{V} = k\frac{g}{d_a V} = KC \qquad (3),$$

where $C = g\cdot 10^3/V$(g./l.), $K = k\cdot 10^{-3}/d_a$. Moreover, if the concentration is expressed in percentage C_p, the equation becomes

$$\frac{1}{d}\left(\frac{\eta}{\eta_0}-1\right) = K_p C_p \qquad (4),$$

where d denotes the density of solution and K_p a constant characteristic of the solute, whose value, however, must be independent of the concentration of the solution. Since K_p is proportional to k/d_a, $K_p d_a$ must depend on the structural character of the solute. If we determine the value of K_p for dilute solutions of a high-molecular-weight hydrocarbon to which equation (4) is applicable, the value of η_a' of the hydrocarbon is found by putting $C_p = 100$ in equation (4), seeing that the equation in this case becomes

$$\frac{1}{d_a}\left(\frac{\eta_a'}{\eta_0}-1\right) = K_p\cdot 100 \qquad (5),$$

---

(2) *Z. physik. Chem.*, A, **158** (1932), 78.

(3) *Z. physik. Chem.*, A, **161** (1932), 1.

(4) Staudinger, "Die Hochmolekularen Organischen Verbindungen," p. 56 and seq., Berlin.

rendering calculation of η'_a possible, so long as we know the density of the hydrocarbon d_a and the viscosity of the solvent η_0. For certain solutes, such as those having strong polarity and those of highly polymerized molecules, equation (4) is invalid, because it is found that for such compounds, K_p increases with increasing concentration, even though the solutions may be very dilute. As, however, it is possible, even in this case, to determine by the same equation the values of K_p for any solute at different concentrations, the value of K_∞ that K_p assumes at infinite dilution, in which the molecular association of the solute completely disappears, can be approximately determined by graphical extrapolation as described in the previous paper. We can therefore calculate the value of η'_a by inserting the value of K_∞ thus determined, instead of K_p, in equation (5), and accordingly determine the value of A_v.

The Experiment. (1) *Equation expressing the relation between the viscosity association and the viscosity-temperature coefficient of hydrocarbons.* In order to obtain an empirical equation representing the relation between their viscosity association and viscosity-temperature coefficients, careful measurements of viscosities at different temperatures as well as the determination of viscosity association were made of four samples of oils having different chemical compositions and viscosity characteristics. The method of experiment was similar to that used in the previous investigation. The determination of viscosity association was carried out at 25°C., with benzene as the solvent. Its viscosity and density at 25°C. were respectively 0.006043 poise and 0.8731. The results of the experiments are summarized in Table 1, in which the third column shows the relative viscosities of dilute solutions of oils at 25°C. and the fourth column the values of K_p calculated by equation (4). The values of η'_a and A_v, calculated by equations (5) and (1) for the oils, are also shown respectively in the fifth and sixth columns. The last column gives their mean temperature coefficients between 25 and 45°C. of both absolute and kinematic viscosities—$(\Delta\eta/\Delta t)_{25-45°C.}$ and $(\Delta\nu/\Delta t)_{25-45°C.}$. The values of their viscosities measured at various temperatures and their densities at 25°C. are given in Table 2. The result shows that the values of K_p for each oil, calculated for different concentrations of solution, are in every case almost identical, indicating that equation (4) holds good. The relation between the viscosity-temperature coefficient and the viscosity association of the oils is shown in Fig. 2 by circles. Since, in agreement with the results of the previous study, the viscosity-temperature coefficient increases in linear proportion with increase in the value of A_v, a linear relationship exists between them. In Fig. 2, dots, showing the

results for the oils used in the previous study (see Table 3), are found to fall almost on the same straight-line as do the small circles obtained in the present investigation. This straight-line may be expressed by

$$A_v = 4.5+1230\left(\frac{\Delta\eta}{\Delta t}\right)_{25\text{-}45^\circ\text{C.}} \qquad (6)\ .$$

The seventh column in Table 1 shows the ratio of viscosity association to density at 25°C. for each oil, and since

$$\frac{A_v}{d_a} = \frac{\eta_a}{d_a\eta'_a} = \frac{\nu_a}{\eta'_a} \qquad (1')\ ,$$

the value of the ratio can be obtained by the values of kinematic viscosity ν_a and η'_a at 25°C. As illustrated in Fig. 3, a linear relationship also exists between the ratio of A_v/d_a and the mean temperature coefficient of kinematic viscosity, the relation being expressed by

$$\frac{A_v}{d_a} = 4.5+1230\left(\frac{\Delta\nu}{\Delta t}\right)_{25\text{-}45^\circ\text{C.}} \qquad (7)\ ,$$

which is found to have the same numerical constants as equation (6).

Although in the foregoing cases, we have taken as the temperature coefficient of viscosity for oils its mean value between 25 and 45°C., it seems more reasonable to study their viscosity-temperature coefficients at 25°C. (if these are calculable) in relation to their viscosity association. As found by S. Erk and H. Eck,[5] the change in viscosity with temperature of mineral oils may be precisely expressed by Walther's equation[6]

$$(\nu+0.8)^{(T^m)} = k_1 \qquad (8)\ ,$$

where ν is the kinematic viscosity in centistokes and T the absolute temperature. As it has been confirmed that equation (8) holds fairly good for the oils used in the present investigation, the writer has used in calculating their viscosity-temperature coefficients at 25°C. the equation

$$\frac{d\nu}{dt} = -m(\log k_1)\frac{\nu+0.8}{T^{m+1}} \qquad (9)\ ,$$

which is derived by differentiating equation (8). In the calculation, the numerical values of the constants m and k_1 for each oil were obtained

(5) *Physik. Z.*, **37** (1936), 113.
(6) *Maschinenbau*, **10** (1931), 671; *Oel Kohle Erdoel Teer*, **12** (1936), 221.

by introducing into equation (8) its viscosities at 25 and 90°C. The results of calculation are given in Table 2. Fig. 4 gives the relation between the viscosity-temperature coefficients thus calculated and the viscosity association of the oils, showing that the relation is also a linear one. In this figure, dots show the results of similar calculations for two of the oils used in the previous study, namely, Aero Shell and Voltol.

(2) *Viscosity characteristics of viscous solutions of polystyrenes.* In order to ascertain on the one hand whether equation (7) holds similarly for viscous solutions of high-molecular-weight hydrocarbons as for liquid hydrocarbons or not, and on the other hand in order to observe the effect of molecular length of high-molecular-weight solutes upon both the viscosity association and the viscosity-temperature coefficient of the solutions, determination of the latter two quantities was carried out for viscous solutions of three polystyrenes that differ markedly in polymerization. In the experiments, the value of K_∞ of each polystyrene was determined by measuring the viscosities of its dilute solutions both in benzene and in ethyl acetate, the results being shown in Table 4, from which it will be seen that the value of K_∞ of each polystyrene differs according as whether benzene or ethyl acetate is used for the solvent in the determination, the value for benzene always greatly exceeding that for ethyl acetate. A similar fact was also found previously by Staudinger and Heuer[7] as well as by the present author,[8] the difference in K_∞ according to solvent being ascribed to difference in degree of solvation, with the conclusion that the molecules of polystyrene are practically not solvated in ethyl acetate, whereas they are greatly solvated in benzene. Therefore in calculating the η'_a of a polystyrene, instead of using its value of K_∞ determined in benzene, we should use that determined in ethyl acetate. As it is known that oils show no appreciable solvation either in benzene or in ethyl acetate, in the foregoing experiments, the values of K_p for oils determined in benzene were used in calculating η'_a, their values of K_p, as the example given in Table 5 shows, not virtually differing whether the solvent used is benzene or ethyl acetate.

In calculating η'_a for viscous polystyrene solutions in benzene, concerning which the relation between viscosity-temperature coefficient and viscosity association is to be studied, the following equation

$$\frac{1}{d_a}\left(\frac{\eta'_a}{\eta_0}-1\right)=K_\infty C_a \qquad (5')$$

(7) *Z. physik. Chem.*, A, **171** (1934), 129.
(8) *Kolloid-Z.*, **72** (1935), 51.

must be used instead of equation (5), where C_a and d_a respectively denote the concentration (%) and the density of the viscous solution whose η_a is to be obtained. Table 6 shows the values of η'_a and A_v/d_a thus calculated by equations (5′) and (1′) for six different solutions of polystyrenes in benzene, giving also their kinematic viscosities at 25 and 45°C. and their mean viscosity-temperature coefficients between 25 and 45°C. For these solutions, as will be seen from Fig. 5, a linear relationship exists between $(\Delta\nu/\Delta t)_{25-45°C.}$ and A_v/d_a, the straight-line being expressed by equation (7) as for oils. The degree of polymerization of the three polystyrenes used, which differs greatly, is believed to be nearly proportional to their values of K_∞. As will be seen from Table 6, solution No. 1 has a smaller value of A_v/d_a, and consequently a lower viscosity-temperature coefficient than solution No. 5, although the two have nearly the same viscosity at 25°C., the reason for which must be that the molecules of polystyrene I have a much longer structure than those of polystyrene III. Since the difference in viscosity-temperature coefficients between solutions 2 and 6, which have almost the same viscosity at 25°C., can also be explained similarly, it is concluded that for viscous solutions of high-molecular-weight hydrocarbons having the same viscosity at a certain temperature, the longer the molecule of solute, the lower is the temperature coefficient of viscosity. It is of interest, in this connection, to note that the solutions of polystyrene I have an extremely high viscosity index; for example, solution No. 3 shows a viscosity index of 180.

(3) *Constitution and viscosity association of high-molecular-weight hydrocarbons.* As already mentioned, the viscosity-temperature coefficient of a high-molecular-weight hydrocarbon or its solution is definitely related to its A_v value, and since the latter denotes the ratio η_a/η'_a, the former must be a function of η_a and η'_a. For this reason, in order to elucidate the relation between the chemical constitution and the viscosity-temperature coefficient of high-molecular-weight hydrocarbons, it behooves us to study the separate effects of chemical constitution on both η_a and η'_a. As to the effect of chemical structure on viscosity, i.e. η_a, various interesting conclusions have recently been obtained by Mikeska's elaborate investigation[9] on the viscosity characteristics of fifty-two synthetized hydrocarbons and also by Wiggins's study[10] on the constitution and viscosity characteristics of hydrocarbons. Since, as previously stated, $K_p d_a$ is dependent on molecular structure, it is evident from equation (5) that η'_a is likewise affected by chemical constitution. In order

(9) *Ind. Eng. Chem.*, **28** (1936), 970.
(10) *J. Inst. Petroleum Tech.*, **22** (1936), 305.

to study the effect of chemical constitution on $K_p d_a$ and η'_a, we selected twenty-three representative hydrocarbons out of the number which Mikeska synthetized in his investigation, and determined[11] their mean viscosity-temperature coefficients between 25 and 45°C. from his viscosity data, and calculated from the coefficients thus determined their values of $K_p d_a$ and η'_a with the aid of equations (7), (1'), and (5). A similar calculation was made also for 1,1-dicyclohexylhexadecane and 1-cyclohexyl-2-hexahydrobenzylheptadecane from the data of Landa and Čech.[12] The results are given in Table 7(a) and 7(b), from which the following interesting conclusions on the effect of chemical constitution on $K_p d_a$ and η'_a were drawn.

1. *Effect of length of side chain.* (a) A comparison of the results for compounds Nos. 26, 15, and 16 as well as of those for Nos. 1 and 2 leads to the conclusion that, for a given cyclic nucleus with a straight paraffinic side chain, the value of η'_a increases with length of side chain. (Compare also No. 11 with No. 13, No. 37 with No. 38, and No. 12 with No. 14.)

(b) The value of η'_a, as is evident from the results for compounds Nos. 15 and 28, is not appreciably affected by the number of side chains, provided the number of paraffinic carbon atoms attached to a given nucleus remains unchanged.

2. *Effect of straight chains as compared with branched chains.* A comparison of the results for compounds Nos. 2 and 3 as well as of those for Nos. 16 and 17 shows that, for a given number of carbon atoms, straight chains are more effective in increasing the value of η'_a than branched chains. (Compare also No. 12 with No. 13, and No. 38 with No. 39.)

3. *Effect of ring structure.* (a) A comparison of the results for compounds Nos. 1, 15, 40, and 48 indicates that, for a given paraffinic chain, the greater the complexity or the number of the cyclic rings attached to it—in other words, the more effective the cyclic groups in increasing the total length of the molecule, the higher is the value of η'_a. (Compare also No. 11 with No. 37, and No. 13 with No. 38.)

(b) Reduction of the aromatic to the corresponding hydro-aromatic rings slightly increases the value of η'_a. (Compare No. 15 with No. 37, No. 2 with No. 13, No. 3 with No. 12, No. 17 with No. 39, and No. 16 with No. 32 or No. 38.)

(11) For the determination, the extra- and inter-polation of their viscosities at 25 and 45°C. were made with the aid of the viscosity-temperature chart of Ubbelohde.

(12) *Collection Czechoslov. Chem. Commun.*, **6** (1934), 423.

4. *Effect of olefinic linkages in the side chain.* As will be seen from the results for compounds Nos. 3 and 5, and also from those for Nos. 17 and 18, an olefinic linkage in the side chain does not appreciably affect the value of η'_a.

5. *Effect of allocation of cyclic nucleus within the molecule.* According to a comparison made of the results for compounds Nos. 48 and 51, the effect of allocation of the cyclic nucleus within the molecule has no appreciable effect on the value of η'_a.

As already mentioned, the viscosity-temperature coefficient of a high-molecular-weight hydrocarbon depends not only on its η'_a, but also on its actual viscosity η_a. Although compounds Nos. 40 and 17 have almost the same value of η'_a, their temperature coefficients of viscosity differ considerably. This must be due to the difference in η_a which the effect of chemical structure brings about. The same may be said in the comparison of the viscosity-temperature coefficients of compounds Nos. 15, 28, and 51 having almost the same value of η'_a. Of these three compounds equally with eighteen paraffinic carbon atoms the one having normal chain has the lowest temperature coefficient of viscosity owing to its lowest viscosity. That compounds Nos. 32, 17, and 51, having nearly the same viscosity at 25°C., also differ much in the viscosity-temperature coefficient, is due to differences in the values of η'_a. As a rule, for such compounds of comparable viscosities, the greater η'_a, the lower the viscosity-temperature coefficient, whence it follows that the longer the molecule, the smaller the temperature coefficient of viscosity.

Since η'_a is related by equations (7) and (1′) to the temperature coefficient of viscosity in the form

$$\frac{1}{1.23\eta'_a} = \frac{1000}{\nu_a}\left[0.00366+\left(\frac{\Delta\nu}{\Delta t}\right)_{25-45°C.}\right] \qquad (7'),$$

an index that is expressed by $\frac{1000}{\nu_a}\left[0.00366+\left(\frac{\Delta\nu}{\Delta t}\right)_{25-45°C.}\right]$, if it be calculated for high-molecular-weight hydrocarbons, must be inversely proportional to their values of η'_a. Therefore, the relation of their chemical structure to their values of this index may at once be found, provided we have complete information on the effects of their chemical structure on their values of η'_a. Fig. 6 shows the variation in $(\Delta\nu/\Delta t)_{25-45°C.}$ and in the index for compounds Nos. 26, 15, and 16 with the number of carbon atoms in the side chain, indicating that the index decreases with length of side chain, whereas $(\Delta\nu/\Delta t)_{25-45°C.}$ increases.

The above mentioned conclusions are in some respects comparable with those made by Mikeska[9] on the relation between the chemical

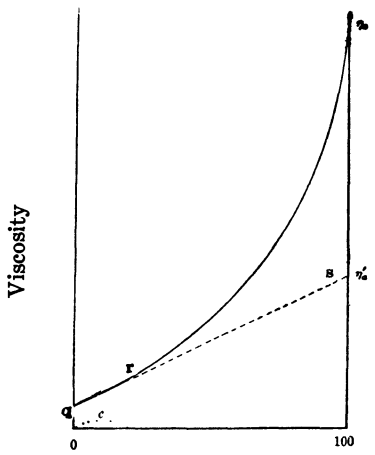


Fig. 1.

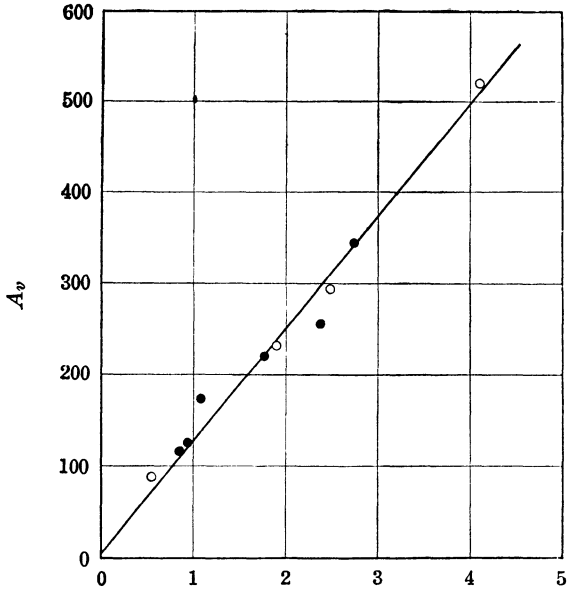


Fig. 2.

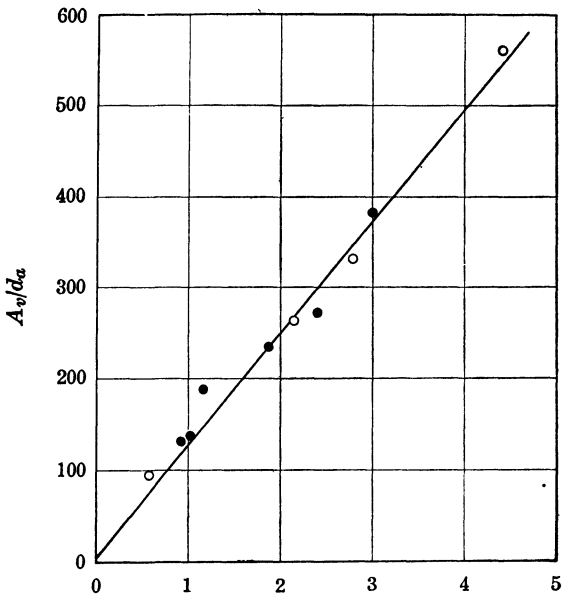


Fig. 3.

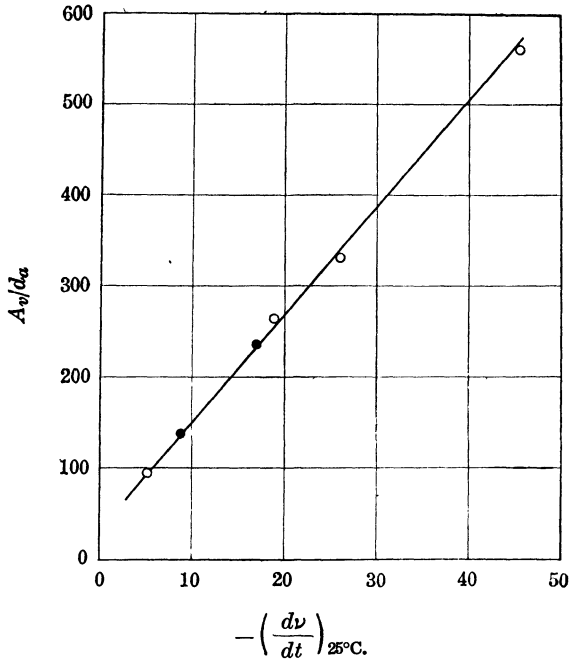


Fig. 4.

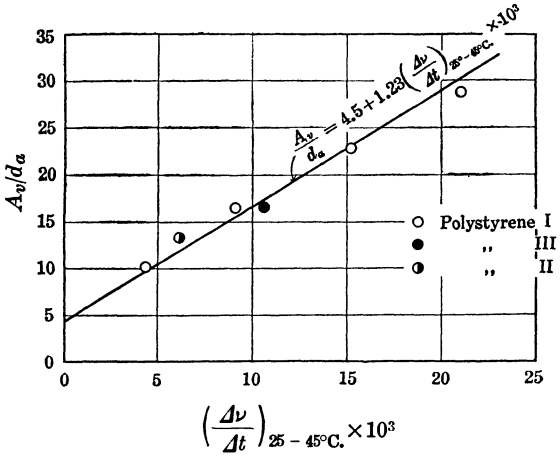


Fig. 5.

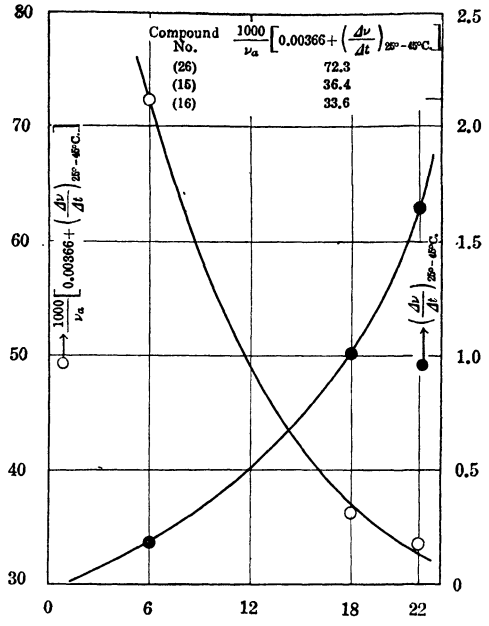


Fig. 6.

Table 1.

Oils	Conc. of benzene solution in % (C_p)	Density (d)	η_r	K_p		η'_a in poises	A_v	$\frac{A_v}{d_a}$	Mean viscosity-temperature coefficient between 25 and 45°C. $\frac{\Delta\eta}{\Delta t}$	Mean viscosity-temperature coefficient between 25 and 45°C. $\frac{\Delta\nu}{\Delta t}$
Mobile Oil S.R.N. (Mixed base)	2.525	0.8743	1.052	0.0238	0.0240	0.0195	520	561	0.410	0.441
	4.183	0.8751	1.087	0.0238						
	4.943	0.8755	1.105	0.0243						
Mobile Oil W. N. (Naphthenic)	2.706	0.8745	1.046	0.0195	0.0195	0.0169	87.9	94.9	0.0536	0.0577
	4.062	0.8752	1.070	0.0197						
Gargoyl Aero. H. (S. A. E. 60) (Paraffinic)	1.282	0 8733	1.035	0.0314	0.032	0.0232	294	331	0.248	0.279
	2.001	0.8734	1.056	0.0322						
	2.873	0.8735	1.083	0.0332						
	4.120	0.8737	1.121	(0.0336)						
Gargoyl Aero. W. (S. A. E. 50) (Paraffinic)	2.112	0.8731	1.054	0.0293	0.0311	0.0226	232	264	0.189	0.214
	3.015	0.8731	1.083	0.0315						
	3.949	0.8731	1.112	0.0325						

Table 2.

Oils	Density at 25°C. (d_a)	Viscosity			Mean viscosity-temperature coefficient between 25 and 45°C.		Constants in Walther's formula		$-\left(\frac{d\nu}{dt}\right)$ at 25°C. in centistokes	Viscosity index
		Temp. (°C.)	Kinematic visc. in stokes (ν)	Absolute visc. in poises (η)	$\frac{\Delta\nu}{\Delta t}$	$\frac{\Delta\eta}{\Delta t}$	m	log k_1		
Mobile Oil S. R. N.	0.9272	25	10.94	10.14	0.441	0.410	4.073	10.56	45.5	14
		45	2.133	1.952						
		90	0.2214	0.1966						
Mobile Oil W. N.	0.9253	25	1.609	1.489	0.0577	0.0536	4.266	10.90	5.13	58
		45	0.456	0.417						
		90	0.0815	0.0723						
Gargoyl Aero. H. (S. A. E. 60)	0.8871	25	7.680	6.813	0.279	0.248	3.427	8.948	26.0	109
		45	2.109	1.847						
		90	0.3043	0.2585						
Gargoyl Aero. W. (S. A. E. 50)	0.8790	25	5.953	5.233	0.214	0.189	3.403	8.864	19.0	97
		45	1.680	1.457						
		90	0.2538	0.2136						

Table 3.

Oils	Density at 25°C.	Kinematic viscosity		Absolute viscosity		$\left(\frac{\Delta\nu}{\Delta t}\right)_{25-45°C.}$	$\left(\frac{\Delta\eta}{\Delta t}\right)_{25-45°C.}$	$-\left(\frac{d\nu}{dt}\right)_{25°C.}$ in centistokes	A_v	$\frac{A_v}{d_a}$
		25°C.	45°C.	25°C.	45°C.					
Shell C. 2A.	0.8867	2.711	0.8663	2.404	0.7580	92.2×10^{-3}	82.3×10^{-3}	—	117	132
Aero Shell	0.9110	2.934	0.8990	2.673	0.8070	102×10^{-3}	93.3×10^{-3}	8.61	126	138
Mobile Oil A.	0.9215	3.212	0.8945	2.960	0.8140	116×10^{-3}	107×10^{-3}	—	174	189
Voltol	0.9359	5.013	1.263	4.692	1.172	187×10^{-3}	176×10^{-3}	16.9	220	235
Flugol	0.9405	6.594	1.800	6.202	1.491	240×10^{-3}	237×10^{-3}	—	256	272
Germ Oil	0.9039	7.755	1.747	7.010	1.560	300×10^{-3}	273×10^{-3}	—	345	382

Table 4.

Polystyrenes	Dilute solution in benzene					Dilute solution in ethyl acetate				
	Conc. in % (C_p)	Density (d)	η_r	K_∞		Conc. in % (C_p)	Density (d)	η_r	K_∞	
No. I	0.0945	0.8737	1.070	0.848	0.84	0.0992	0.8931	1.038	0.429	0.42
	0.1922	0.8738	1.143	0.852		0.2146	0.8934	1.083	0.433	
	0.2459	0.8739	1.178	0.828		0.4018	0.8938	1.157	0.437	
No. II	0.3075	0.8739	1.0961	0.358	0.36	0.2476	0.8935	1.046	0.208	0.20
	0.5056	0.8742	1.153	0.348		0.3981	0.8938	1.080	0.218	
	0.7069	0.8746	1.231	0.374						
No. III	0.4251	0.8746	1.0552	0.149	0.15	0.4943	0.8939	1.047	0.106	0.11
	0.6755	0.8746	1.0901	0.153		0.6630	0.8941	1.066	0.109	
	0.9242	0.8751	1.126	0.155						

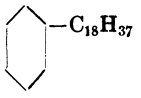
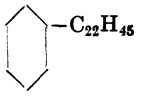
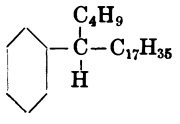
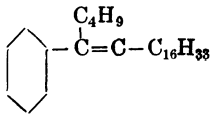
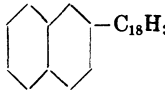
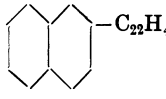
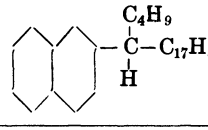
Table 5. Comparison of K_p of Mobile Oil S.R.N. in ethyl acetate and benzene.

Solvent	C_p (%)	Density (d)	η_r	K_p	
Ethyl acetate	2.902	0.8931	1.064	0.0247	0.0248
	4.898	0.8932	1.109	0.0249	
Benzene	2.525	0.8743	1.051	0.0238	0.0240
	4.183	0.8751	1.087	0.0238	
	4.943	0.8755	1.105	0.0243	

Table 6. Viscosity characteristics of viscous polystyrene solutions in benzene.

Solution No.	Polystyrenes	Conc. (%)	Density at 25°C. (d_a)	Kinematic viscosity in stokes		$\left(\frac{\Delta\nu}{\Delta t}\right)_{25-45°C.}$	K_∞ in ethyl acetate	η'_a	$\frac{A_v}{d_a}$
				25°C.	45°C.				
1	I	10.83	0.8915	0.3105	0.2244	0.00431	0.42	0.0306	10.2
2		13.82	0.8966	0.6168	0.4350	0.00909		0.0375	16.5
3		16.01	0.9007	0.9722	0.6690	0.0152		0.0426	22.8
4		17.62	0.9035	1.335	0.9147	0.0210		0.0464	28.8
5	III	36.82	0.9352	0.3130	0.1910	0.00610	0.11	0.0235	13.3
6	II	27.92	0.9193	0.6168	0.4043	0.0106	0.20	0.0371	16.6

Table 7 (a). Viscosity characteristics of aromatic hydrocarbons.

Compound No.	Structure	Empirical formula	Densiny at 25°C. (d_a)	Kinematic viscosity*		$\left(\frac{\Delta\nu}{\Delta t}\right)_{25-45°C.}$	$\frac{A_v}{d_a}$	η'_a	$K_p \cdot d_a$	Viscosity index
				25°C.	45°C.					
1		$C_{24}H_{42}$	0.8540*	0.133	0.0770	0.0028	7.94	0.0168	0.0178	196
2		$C_{28}H_{50}$	0.8513	0.197	0.115	0.0041	9.5	0.0207	0.0243	164
3		$C_{28}H_{50}$	0.8554	0.274	0.131	0.0073	13.5	0.0203	0.0236	138
5		$C_{28}H_{48}$	0.8675	0.228	0.117	0.0056	11.4	0.0200	0.0231	162
15		$C_{28}H_{44}$	0.906	0.378	0.177	0.0101	16.9	0.0224	0.0271	140
16		$C_{32}H_{52}$	0.8987	0.599	0.270	0.0165	24.8	0.0242	0.0300	144
17		$C_{32}H_{52}$	0.898*	0.630	0.265	0.0183	27.0	0.0233	0.0286	122

* Extrapolated values.

Table 7 (a).—(*Concluded*)

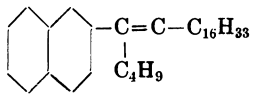
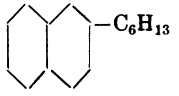
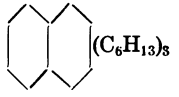
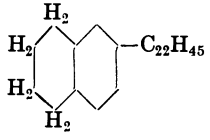
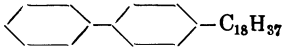
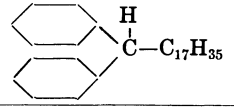
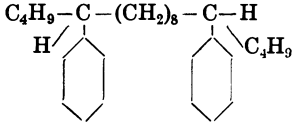
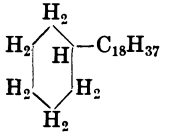
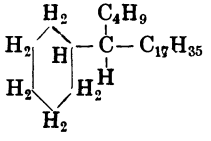
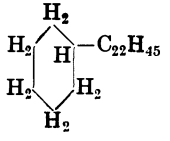
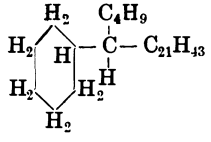
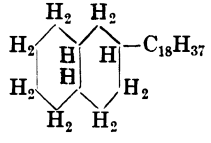
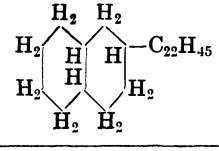
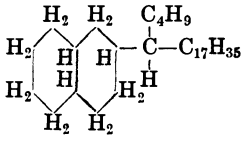
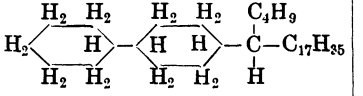
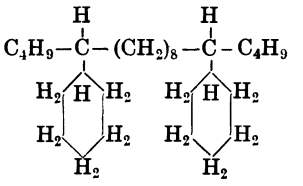
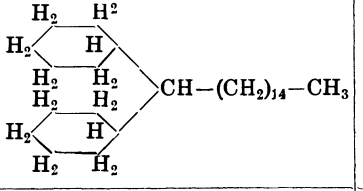
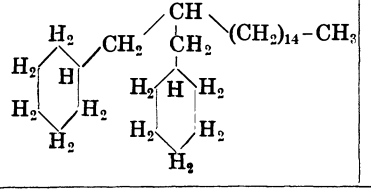
Compound No.	Structure	Empirical formula	Density at 25°C. (d_a)	Kinematic viscosity*		$\left(\frac{\Delta\nu}{\Delta t}\right)_{25-45°C.}$	$\frac{A_v}{d_a}$	η'_a	$K_p \cdot d_a$	Viscosity index
				25°C.	45°C.					
18		$C_{32}H_{50}$	0.9081	0.555	0.237	0.0159	24.1	0.0230	0.0281	116
26		$C_{16}H_{20}$	0.9575	0.0752	0.0396	0.00178	6.69	0.0112	0.0085	−66
28		$C_{28}H_{44}$	0.911	0.600	0.241	0.0180	26.6	0.0226	0.0274	98
32		$C_{32}H_{56}$	0.8786	0.629	0.286	0.0172	25.7	0.0245	0.0305	145
40		$C_{30}H_{46}$	0.9138*	0.452	0.213	0.0120	19.3	0.0234	0.0282	131
48		$C_{30}H_{46}$	0.9260*	0.467	0.199	0.0134	21.0	0.0222	0.0267	96
51		$C_{30}H_{46}$	0.9051	0.630	0.245	0.0193	28.2	0.0223	0.0269	92

Table 7 (b). Viscosity characteristics of naphthenic hydrocarbons.

Compound No.	Structure	Empirical formula	Density at 25°C. (d_a)	Kinematic viscosity*		$\left(\frac{\Delta v}{\Delta t}\right)_{25-45°C.}$	$\frac{A_v}{d_a}$	η'_a	$K_p \cdot d_a$	Viscosity index
				25°C.	45°C.					
11		$C_{24}H_{48}$	0.834*	0.204	0.106	0.0049	10.5	0.0194	0.0214	160
12		$C_{28}H_{56}$	0.8395	0.322	0.153	0.0085	15.0	0.0215	0.0255	140
13		$C_{28}H_{56}$	0.8327	0.313	0.156	0.0079	14.2	0.0220	0.0264	170
14		$C_{32}H_{64}$	0.8372	0.462	0.217	0.0123	19.6	0.0236	0.0290	149
37		$C_{28}H_{54}$	0.863	0.493	0.230	0.0132	20.7	0.0238	0.0294	144
38		$C_{32}H_{62}$	0.8673	0.772	0.339	0.0217	31.2	0.0247	0.0309	148

* Extrapolated values.

Table 7 (b).—(*Concluded*)

Compound No.	Structure	Empirical formula	Density at 25°C. (d_a)	Kinematic viscosity* 25°C.	Kinematic viscosity* 45°C.	$\left(\frac{\Delta v}{\Delta t}\right)_{25-45°C.}$	$\frac{A_v}{d_a}$	η'_a	$K_p \cdot d_a$	Viscosity index
39		$C_{32}H_{62}$	0.8615	1.00	0.390	0.0305	42.0	0.0238	0.0294	114
46		$C_{34}H_{66}$	0.867	1.52	0.541	0.0490	64.8	0.0235	0.0288	110
52		$C_{30}H_{58}$	—	1.033	0.363	0.0335	45.7	0.0226	0.0274	88
53**		$C_{28}H_{54}$	0.8791 at 20°C.	$\eta_{25°}$ =0.532	$\eta_{45°}$ =0.213	$\left(\frac{\Delta \eta}{\Delta t}\right)_{25-45°C.}$ =0.0160	A_v =24.2	0.0220	0.0264	98
54**		$C_{30}H_{58}$	0.8860 at 20°C.	$\eta_{25°}$ =0.481	$\eta_{45°}$ =0.197	$\left(\frac{\Delta \eta}{\Delta t}\right)_{25-45°C.}$ =0.0142	A_v =22.0	0.0219	0.0262	103

** For the calculation of $\left(\frac{\Delta \eta}{\Delta t}\right)_{25-45°C.}$, η'_a, and $K_p \cdot d_a$ of compounds Nos. 53 and 54, their values of absolute viscosity from Landa and Čech were used.

structure and the viscosity index of hydrocarbons, but none of his conclusions seem possible to explain the fact that compound No. 1, having a shorter side chain than compounds Nos. 2 and 13, is greater in viscosity index, as shown in the last column of Table 7, than the latter, whereas in the case of compounds Nos. 26, 15, 16, the shorter the side chain, the smaller is the viscosity index. No contradiction like this, however, is encountered in considering index $\frac{1000}{\nu_a}\left[0.00366+\left(\frac{\Delta\nu}{\Delta t}\right)_{25-45^\circ C.}\right]$ in relation to their chemical structure, for the reason that in the above two series of compounds η'_a invariably increases with length of side chain.

Aeronautical Research Institute,
Tokyo Imperial University.

On the Use of Interference Spectrographs for the Study of Fine Structures in Molecular Spectra.

By Sunao IMANISHI.

(Received December 13, 1937.)

Introduction. The high resolving powers conveniently obtainable, especially for the visible part of the spectrum, by the use of modern interference instruments may well be utilized for the study of a fine-structure in each rotational line of molecular band spectra, when the latter is suspected, by some reason or other, to be composed of several very closely situated components, or accompanied by satellites in close proximity to the main line. An individual band-line has usually a very small absolute intensity when compared with an atomic line; indeed, the total intensity associated with the emission of a single atomic line may be considered divided up into hundreds or more rotational lines of a whole band system belonging to a single molecular electronic transition. However, apart from the consequent increase in the time of exposure, which implies the necessity of taking much greater precautions against mechanical vibration and changes in the spectrograph due to temperature variation, the technique of photographing a fine-structure pattern of a band-line is the same in principle as with an atomic line.

As is well-known, a Michelson échelon grating or a Lummer-Gehrcke interference plate can magnify only a very small region of the spectrum without being overlapped by patterns of neighbouring "orders". Thus each such instrument has the so-called "range", characteristic of its construction and dependent on the wave-length. Two lines separated in wave-length farther than the range must therefore be resolved by means of an auxiliary or "coarse" dispersing system before or after sending the ray through the high-powered instrument to examine the individual structures. It is convenient, and only practicable for band study, to arrange matters so as to make the two dispersions at right angles to each other on the recording photographic plate, and we get a "crossed" spectrum, or a two-dimensional pattern of interference dots. In the case of a band spectrum each rotational line, at least at some distance from a head, must clearly be resolved from adjacent ones by the aid of this coarse dispersion.

When the region under examination is congested through overlapping of branches, or when treating a branch with very narrowly spaced rotational lines, the "coarse" dispersion may not be so coarse as one would be impressed by the word, since it is often necessary to use for this purpose a long focus plane grating or prism spectrograph, preferably of a small relative aperture to keep the patterns sharply defined; all these requirements pointing to still further prolongation of exposure time.

In the following are given brief descriptions of two studies in which such combined or "crossed" spectrographs were constructed and used.

Electronic Fine Structure in Helium Bands. The diatomic helium molecule, while formed with a very short life, has four electrons, two of which confine themselves in the molecular K-shell, not participating in the emission of visible light. With the remaining two valence electrons the system can have a set of singlet energy levels and a separate set of triplet levels, just like the He atom or the H_2 molecule with their two outer electrons. An inter-combination transition between a singlet and a triplet levels is extremely unlikely to occur in these light atomic or molecular systems, and any observed helium band should be classified either as a singlet-singlet transition with purely single rotational lines, or as a triplet-triplet transition with at least three very closely situated components corresponding to the theoretical spin fine-structures in the levels concerned, quite apart from any multiplication of branches caused by molecular rotation.

All these are very clear in theory and by analogy to other spectra, but, owing to the extreme smallness of spacings characteristic of the lightest atomic systems with their small nuclear charges, no direct experi-

mental evidence had existed as to the multiple nature of lines belonging to those bands classified as "triplets", until R. S. Mulliken and G. S. Monk published a paper[1] dealing with this problem, and found, for the first time, on photographs taken in high orders of a large concave grating spectrograph, a beginning resolution in lines of various bands having the $1s\sigma^2\ 2p\sigma\ 2p\pi\ ^3\Pi$ state either as the upper or the lower electronic level. They also found, in agreement with theoretical expectations, that no other level than the above $2p\pi\ ^3\Pi$ (notations for the inner three electrons will be omitted hereafter) had a fine-structure of measurable magnitude.

At the suggestion of G. H. Dieke, now of Johns Hopkins University, the writer had, independently of Mulliken and Monk, examined the expected fine-structures in the band λ 6400 Å, $3s\sigma\ ^3\Sigma \rightarrow 2p\pi\ ^3\Pi$, $0 \rightarrow 0$, with a 40 plate glass échelon. At λ 6400 Å the échelon had a range $\Delta\lambda_{max}$ of about 0.64 Å and a resolving power $\Delta\lambda/\lambda$ of about 3×10^5. The experimental arrangement for this work is roughly shown in Fig. 1.

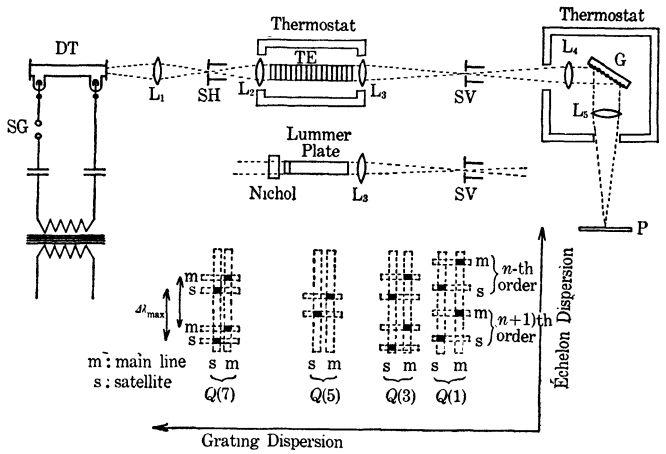


Fig. 1.

The source DT of helium bands is an end-on, sealed pyrex discharge tube of 1 m. length and 2 cm. internal bore, containing pure helium gas at about 4 cm. Hg pressure. A heavy condensed discharge is maintained through the discharge tube and a zinc or aluminium spark gap SG in series. The light from the source is condensed by a lens L_1 on the horizontal échelon slit SH, made parallel by a collimator lens L_2 and passes the échelon TE. The diffracted rays are projected by an achromatic lens L_2 of 1 m. focal length on to the second vertical slit SV of a coarse-analysing spectrograph L_4GL_5 and form here horizontal interference fringes.

(1) *Phys. Rev.*, **34** (1929), 1530.

The latter spectrograph contains a plane grating having 55,100 lines in its 9.3 × 7.6 cm.^{2} ruled area, and a camera lens of 3 m. focal length, giving a dispersion in the first order of about 3.2 Å per mm. on a photographic plate P. Thanks to the stigmatic nature of a plane grating spectrograph the directions of the two dispersions could be made perpendicular to each other as mentioned in the introduction, and the patterns produced on the plate are shown diagrammatically in the same figure, which may be compared with the final photograph obtained for the λ 6400 Å band reproduced in Fig. 3. The band happens to have a P-, a Q- and an R-branch and, fortunately, the λ 6402.246 Å line of neon, which was present in helium as an impurity, appears among the Q-lines nearly in a "double order" pattern, supplying a good standard for the determination of $\Delta\lambda_{\max}$.

The photograph shows a clear resolution of the one component of the triple structure in several rotational lines at the beginnings of the Q- and the P-branch as a weak satellite under each thick main line. R-lines are too weak at the beginning of the branch to give measurable patterns; each one of them, however, should have the same structure as the corresponding P-line labelled with the same rotational quantum number. The main lines themselves are still unresolved doublets, and on the original plate they do show obvious sign of resolution, as their dots are all rhomb-shaped, whereas if they were single the dots would be rectangular, defined by the parpendicular jaws of the two slits, just as the dots for the neon line are. But, as the source was not specially cooled with liquid air to suppress the Doppler effect, which may be quite appreciable with the light helium molecule, no quantitative measurement could be made of the separations in main lines. Result of measurements[2] for the resolved components is tabulated below in Table 1. According to H. A. Kramers the upper $3s\sigma\ ^3\Sigma$ state should also have a triple structure, but its spacings are far too smaller than those in the lower $2p\pi\ ^3\Pi$ state, as confirmed by Mulliken and Monk. Therefore the value given in the table under each line-notation can be taken as one of the two spacings in the respective rotational level in the lower $2p\pi\ ^3\Pi$ state. It decreases gradually as the rotational quantum number increases, exactly in accordance with theoretical calculations of the spin fine-structure for the rotating helium molecule. It may here be remarked that owing to special circumstances prevailing in the helium molecule, every other rotational level is lacking in each electronic state. Besides, lower levels for Q-lines and those for P- or R-lines are of different description or symmetry (c and d respectively). Hence, for this particular band, there is an odd sequence only of

(2) *Nature*, **125** (1930), 529; *Sci. Papers Inst. Phys. Chem. Research* (Tokyo), **14** (1930), 105.

the rotational quantum number for the Q-branch, and an even sequence only for the P- or the R-branch.

Table 1. Band λ 6400 Å

Line	$Q(1)$	$Q(3)$	$Q(5)$	$Q(7)$	$Q(9)$	$Q(11)$	$Q(13)$	$Q(15)$
$\Delta\nu_c$ (cm.$^{-1}$)	0.354	0.281	0.290	0.278	0.266	0.271	0.24	0.21
Line	$P(2)$							
$\Delta\nu_d$ (cm.$^{-1}$)	0.268							

Isotopic Constitution of Gold from Gold Hydride Bands. Early in 1935 gold remained one of a very few elements the isotopic constitution of which had not been determined quantitatively by the mass-spectrograph, owing to the difficulty of producing a suitable positive ion source. Its accepted chemical atomic weight is 197.21, and in analogy to the closely similar elements silver and copper, it seemed highly probable that it would be a mixture of practically only the two isotopes of odd mass-numbers 197 and 199, with an abundance ratio Au^{199}:Au^{197} of 1 to 8.3, or even 1 to 7.0, according as we take for the atomic mass unit (1/16)O or (1/16)O^{16} respectively.

On the other hand, Aston's famous "packing fraction" curve crosses the zero axis near at the mass number 197, and $+11 \times 10^{-4}$ seemed to be too large for the packing effect per proton for the gold atom,[3] a figure which we must assume if we consider this element to be constituted entirely of Au^{197}.

Now, in the domain of diatomic band spectra, we know of the gold hydride, AuH, spectrum, extensively investigated in emission as well as in absorption. It has a system extending from the near ultra-violet down into the visible region, with individual bands of the simplest structure having purely single and comparatively wide-spaced rotational lines. A preliminary calculation, based on the conventional and approximate theory of rotational and vibrational isotope shifts in diatomic bands, showed that if Au^{199} existed in the ratio of about 1 in 7 to Au^{197}, every rotational line near at λ 4000 Å should be accompanied by a satellite at a separation $\Delta\nu$ of about 0.14 cm.$^{-1}$, or $\Delta\lambda$ of about 0.024 Å, on its shorter wave-length side, standing in an intensity relation comparable with that of abundance.

(3) The packing fraction of gold is now obtained by Dempster (a short abstract of a report presented to the Chicago Meeting of the American Physical Society, November, 1937) as $+2.0\pm0.4$ ($\times10^{-4}$), by step-wise comparisons of gold with oxygen via copper[65]. From this the mass-spectrographic atomic weight of Au^{197} appears to be 197.039 ± 0.008.

This appeared a suitable problem for a reflecting échelon spectrograph the writer had for some time assembled out of parts, and an experiment was carried out in the following scheme (Fig. 2).

The light source S is a D.C. arc between gold poles burning in a hydrogen atmosphere of about 20 cm. Hg pressure, contained in a water-cooled metallic chamber. After passing a horizontal slit SH, and deflected by a small 45° prism RP, light enters a Littrow-mounted air-tight reflecting échelon chamber through a lens L_2 of 1.5 m. focus, projected back again by L_2, passes underneath RP, and fringes are formed on a vertical slit of a coarse-analysing prism spectrograph L_3PPL_4, which gives a linear dispersion of about 4 Å per mm. for λ 4000 Å. The reflecting échelon here used is made of 25 plane-parallel plates of fused silica, equal in thickness to about one-eighth of a wave-length, in optical contact, and platinized on its step surfaces. It has the range of about 0.1 Å and a theoretical resolving power of about 10^6 for the region aforementioned.

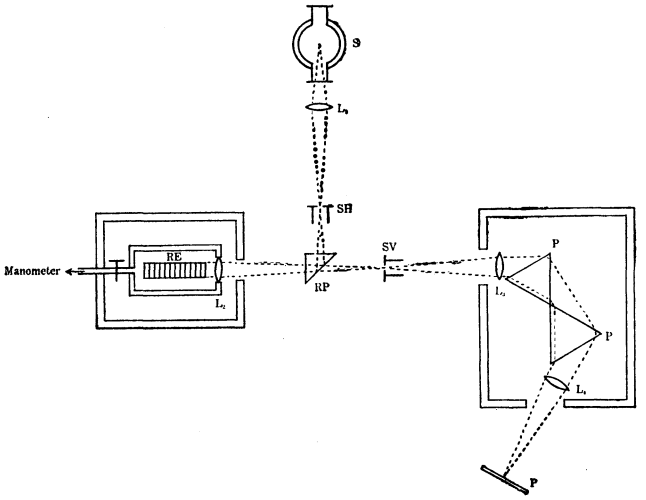


Fig. 2.

A reflecting échelon, first conceived also by Michelson, and constructed with a great precision of modern technique, is in principle no other than a kind of transmission échelon made of air, the steps of which are bounded by very rigid reflecting surfaces; and in passing twice through it, light suffers diffraction to give the enormous resolving power, which nearly matches that of a glass échelon of four times the plate number, with an added advantage of being perfectly free from weakening by absorption. Therefore it is essential to use it in a temperature-controlled air-tight box

to keep the refractive index of the surrounding air constant during an exposure. By a slight change of air pressure diffraction angles change, and we can have the same effect of changing over from the "single order"

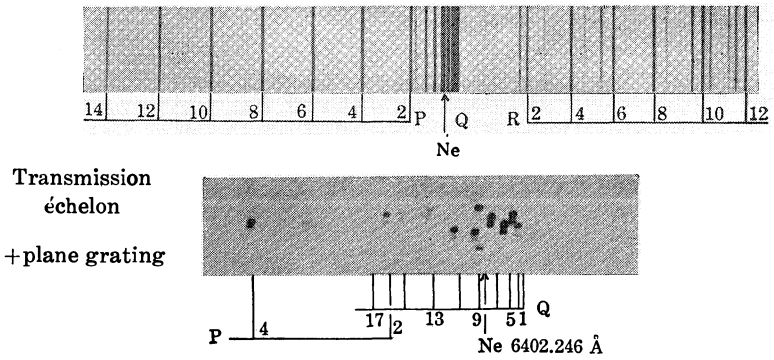


Fig. 3. He_2 band λ 6400 Å, $3s\sigma\,{}^3\Sigma \rightarrow 2p\pi\,{}^3\Pi$, $0 \rightarrow 0$. Plane grating.

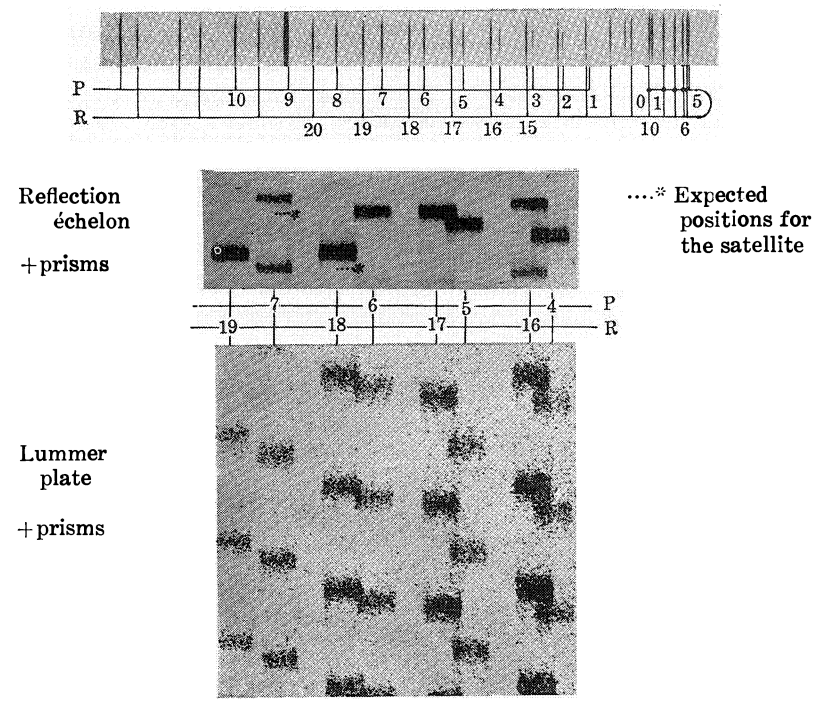


Fig. 4. AuH band λ 3973 Å, $^1\Sigma^* \rightarrow {}^1\Sigma$, $0 \rightarrow 1$. 15-Foot concave grating, 2nd order.

position into the "double order" one for a particular wave-length, just as by tilting an ordinary glass transmission échelon against the direction of incidence to alter path differences.

The final photograph obtained with this arrangement for the 0→1 vibrational band of the AuH $^1\sum^*\rightarrow{}^1\sum$ system at λ 3973 Å is shown in Fig. 4. Notwithstanding the circumstance that the source used was an ordinary arc only inefficiently cooled by running water, the main line in each pattern for every rotational member is sufficiently sharp to be regarded as purely single, and accompanied by no trace at all of a satellite, which should show up at a separation of about one-fifth of the range or the distance between the fringes of the main line in two consecutive orders, if it had an intensity about one-seventh of that of the latter.

This negative result[4] is quite against the expectation stated at the beginning of this section, but was confirmed by experiments using two alternative arrangements, in which the reflecting échelon was replaced by the 40-plate glass échelon described in the previous section, or a high-resolving quartz Lummer-Gehrcke plate; the patterns by the latter are shown also in the same reproduction (cf. Fig. 1 for the arrangement).

Meanwhile during this work, A. J. Dempster of Chicago University had elaborated a spark source of gold ions for his mass-spectrograph and communicated the same negative result to Nature,[5] stating in a more quantitative way that the ratio of Au^{199}:Au^{197} is much smaller than 1 in 500. Thus the complete agreement of the results obtained by the two quite independent methods, although the band-spectroscopic one is less direct than, and therefore of a supplementary nature to, the mass-spectrographic, confirmed the non-existence of a natural isotope of gold with mass number 199, and the hitherto accepted chemical atomic weight of this element seems, by the reason stated earlier, to need a revision.[3]

In conclusion, the writer wishes to express his most sincere thanks to Prof. M. Katayama of Faculty of Science, Tokyo Imperial University, for unchanging encouragements the writer received throughout his spectroscopic researches after graduation from the Department of Chemistry.

Institute of Physical and Chemical Research, Tokyo.

(4) *Nature*, **136** (1935), 476; *Sci. Papers Inst. Phys. Chem. Research* (Tokyo), **28** (1935), 129.

(5) *Nature*, **135** (1935), 993; also L. Sibaiya, working with hyper-fine structures of atomic gold lines using a Lummer-Gehrcke plate, arrived at the same conclusion, *Proc. Indian Acad. Sci.*, A, **2** (1935), 313.

Über den Austausch der Wasserstoffatome zwischen Pyrrol, Indol sowie ihren Methylderivaten und Wasser. I. Austausch der Wasserstoffatome zwischen Pyrrol und Wasser.[1]

Von Masao KOIZUMI* und Toshizo TITANI.

(Eingegangen am 20. Dezember 1937.)

Inhaltsübersicht. Die Austauschreaktion der H-Atome zwischen Pyrrol und Wasser wurde unter Verwendung des verdünnten schweren Wassers von verschiedenen Wasserstoffionenkonzentrationen untersucht. Die dabei gefundenen Tatsachen kann man kurz wie folgt zusammenfassen.

(1) Solange die H-Ionenkonzentration im verwendeten Wasser von $p\mathrm{H} = 14$ bis 2 bleibt, wird nur ein einziges und höchstwahrscheinlich an N gebundene H-Atom des Pyrrolmoleküls gegen die des Wassers sehr schnell ausgetauscht (die „erste" Austauschreaktion), aber selbst im Verlauf von zehn Stunden bei 30°C. treten keine weiteren H-Atome gegen die des Wassers auf, auch wenn 0.01 N saures schweres Wasser verwendet wird.

(2) Wenn dagegen die H-Ionenkonzentration in schwerem Wasser bis zu $p\mathrm{H} = 2$ bis 1 erhöht wird, setzt ziemlich plötzlich eine neue Art der Austauschreaktion (die „zweite" Austauschreaktion) ein, bei der mehr als ein H-Atom des Pyrrolmoleküls gegen die H-Atome des Wassers ausgetauscht werden. Diese neue „zweite" Austauschreaktion verläuft innerhalb der obenangegebenen pH-Grenzen mit gut messbarer Geschwindigkeit.

(3) Wenn wir aber die H-Ionenkonzentration in schwerem Wasser noch weiter erhöhen und dessen pH unterhalb 1 sinkt, wird die Austauschgeschwindigkeit so gross, dass sie sich fast unmessbar erweist.

(4) Bei Benutzung von fast reinem schwerem Wasser fanden wir, dass in dieser neuen „zweiten" Austauschreaktion die sämtlichen fünf H-Atome des Pyrrolmoleküls gegen die des Wassers austauschbar sind. Daraus folgt, dass der durchschnittliche Verteilungsquotient der D-Atome zwischen dem CH-Radikal des Pyrrolmoleküls und Wasser $k(\mathrm{CH}/\mathrm{H_2O}) = 0.70$ sein muss, wenn man den V.Q. zwischen dem NH-Radikal des Pyrrols und Wasser $k(\mathrm{NH}/\mathrm{H_2O}) = 0.88$ setzt.

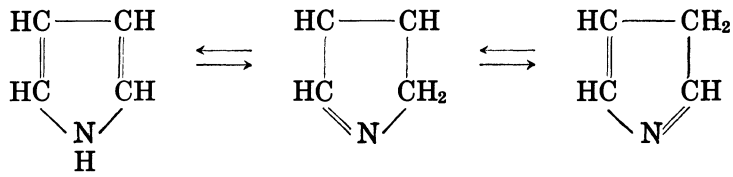
Das Auftreten der neuen „zweiten" Austauschreaktion kann man mit der Salzbildung des Pyrrolmoleküls und der daran folgenden tautomerischen Umwandlung desselben erklären.

---

* Früher Masao HARADA.

(1) Vorläufig mitgeteilt in diesem Bulletin, **12** (1937), 107.

Einleitung. Hauptsächlich auf Grund der chemischen Eigenschaften des Pyrrols nimmt man gewöhnlich von dieser Verbindung eine tautomerische Umwadlung an, wie das Schema (1) zeigt:[2]



(1)

Sollte eine solche Umwandlung wirklich stattfinden, dann liegt die Möglichkeit nahe, dass die sämtlichen H-Atome des Pyrrolmoleküls gegen die des Wassers ausgetauscht werden können, wenn man die beiden Substanzen zusammenschüttelt, obwohl die direkt an C gebundene H-Atome gewöhnlich nicht direkt austauschbar sind. Gegen diese Erwartung fanden wir aber in unserem früheren Versuch,[3] wo wir Pyrrol zusammen mit neutralem schwerem Wasser schüttelten, dass nur ein einziges und höchstwahrscheinlich an N gebundenes H-Atom des Pyrrolmoleküls gegen D-Atome des schweren Wassers ausgetauscht wurde, es aber selbst nach fünfzig Stunden bei 50°C. zu keinem Austausch weiterer H-Atome des Pyrrolmoleküls gegen die des Wassers kam. Im Anschluss an diesen Versuch führten wir nun einen ähnlichen Versuch nicht aber mit neutralem sondern alkalischem sowie saurem schwerem Wasser aus. Dabei fanden wir, dass die erwartete Austauschreaktion der sämtlichen H-Atome des Pyrrolmoleküls gegen die des Wassers oberhalb einer bestimmten H-Ionenkonzentration im verwendeten Wasser wirklich stattfand.

Austausch der H-Atome zwischen Pyrrol und Wasser bei verschiedenen H-Ionenkonzentrationen im letzteren. Eine genau bestimmte Menge (ca. 5 g.) von Pyrrol wurde zusammen mit einer bestimmten Menge (ca. 2 g.) von alkalischem bzw. saurem verdünntem schwerem Wasser in ein Glasrohr eingeschmolzen und bei bestimmter Temperatur (30°C.) aber verschiedener Länge geschüttelt. Das dazu benutzte alkalische bzw. saure schwere Wasser von bekanntem D-Gehalt sowie bestimmter H-Ionenkonzentration wurde dadurch bereitet, dass wir eine bestimmte Menge von ca. 3-prozentigem schwerem Wasser, dessen Gehalt an D genau bekannt war, mit einer bestimmten Menge von HCl- bzw. KOH-Lösung in gewöhnlichem Wasser versetzten. Nach gründlicher Zusammenschüttelung wurde das Wasser durch Abhebung vom Pyrrol abgetrennt und nach folgender Methode gereinigt. Bei der alkalischen Lösung wurde

(2) Vgl. H. Fisher und H. Orth, „Chemie des Pyrrols," Bd. I, Leipzig (1934).
(3) M. Harada und T. Titani, dies Bulletin, **11** (1936), 465.

das Wasser durch Destillation direkt vom zugesetzten Alkali befreit. Aber bei der sauren Lösung wurde sie zuerst unter Zusatz von kleinen Mengen von CaO neutralisiert und dann abfiltriert. Dabei fanden wir, als wir 1 N HCl-Lösung verwendeten, dass das Pyrrol während der Schüttelung gelb bis orange gefärbt wurde und bei der Neutralisation der damit geschüttelten wässrigen Lösung mit CaO eine weisse Trübung auftrat. Dieselbe Trübung trat auch in Erscheinung, aber in geringerem Masse, bei der Neutralisation von 0.1 N HCl-Lösung, nachdem es mit Pyrrol geschüttelt wurde. In den anderen Fällen blieb aber das Pyrrol während der Schüttelung vollkommen klar und farblos, und bei der Neutralisation der Lösung entstand keine Trübung. Das dadurch von Säure bzw. Alkali befreite Wasser wurde dann von dem darin ein wenig gelösten Pyrrol befreit, indem wir das Wasser zusammen mit gut getrocknetem Äther schüttelten. Der dabei wieder ins Wasser ein wenig gelöste Äther wurde durch die Behandlung des Wassers mittels Pumpenöls vollständig beseitigt.[3] Das so behandelte Wasser wurde dann auf übliche Weise gereinigt, indem wir es zunächst in Dampfform über Rotglut erhitztem CuO leiteten, dann unter Zusatz von Na_2O_2 und $KMnO_4$ in einem geschlossenen Rohr über Nacht erhitzten und zum Schluss im Vakuum zweimal destillierten. Die Dichte des so gereinigten Wassers bestimmten wir nach der Schwebemethode mittels eines kleinen Quarzschwimmers, um daraus die D-Konzentration in demselben kennen zu lernen. Die Reinheit des vom Wasser abgetrennten Pyrrols wurde in einem Fall, wo wir das Pyrrol mit 0.1 N HCl-Lösung schüttelten, durch die Bestimmung seines Siedepunktes geprüft. Dabei erwies er sich genau als derselbe (129–131°C.) wie vor dem Versuch.

Aus den wie oben ausgeführten Experimenten kann man die Zahl der austauschbaren H-Atome in einem Pyrrolmolekül durch Gl. (2) ausrechnen:

$$nk = 2\frac{M_w}{M_P}\frac{D_a - D_e}{D_e} \qquad (2),$$

wo n Zahl der austauschbaren H-Atome in einem Pyrrolmolekül, k Verteilungsquotient (V.Q.) der D-Atome zwischen Pyrrol und Wasser, M_w Molzahl des verwendeten schweren Wassers, M_P Molzahl des verwendeten Pyrrols, und D_a und D_e D-Konzentration im verwendeten schweren Wasser vor und nach dem Experiment ausdrücken. Aber weil die einzelnen H-Atome in einem Molekül streng genommen verschiedene Grösse von V.Q. k besitzen müssen, drückt das aus Gl. (2) ausgerechnete Produkt nk nichts anderes als die Summe derselben der einzelnen Arten von austauschbaren H-Atomen in einem gegebenen Molekül aus, wie Gl. (3) zeigt,

$$nk = \sum n_i k_i \,. \qquad (3).$$

Aus diesem Grund wollen wir das aus Gl. (2) errechnete Produkt nk weiter unten „Austauschäquivalent" eines gegebenen Moleküls nennen.

Das „Austauschäquivalent" nk des Pyrrolmoleküls, das wir unter Verwendung von verschieden alkalischem bzw. saurem schwerem Wasser gefunden haben, geben wir in Tabelle 1 wieder.

Tabelle 1.

Austauschäquivalent nk des Pyrrols bei verschiedenen Wasserstoffionenkonzentrationen.

Versuchsnr.	Normalität des benutzten Wassers	*p*H	Schüttelungsdauer in Stdn.	nk	Bemerkung
1	1 N KOH	14	1	0.92	
2	„ „	„	5	0.92	
3	neutral	7.00	5–50	0.88[3]	
4	0.01 N HCl	2.00	1	0.90	
5	„ „	„	5	0.88	
6	„ „	„	10	0.90	
7	0.024 N HCl	1.62	1	2.25	
8	„ „	„	3	3.53	
9	0.048 N HCl	1.32	1	3.29	
10	„ „	„	3	3.60	
11	0.1 N HCl	1.00	1	3.64	
12	„ „	„	5	3.74	Pyrrol blieb farblos, aber bei der Neutralisation der Lösung geringe Trübung ?
13	„ „	„	9	3.70	wie oben.
14	1 N HCl	0.00	2/3	3.81	Pyrrol wurde gelb gefärbt und bei der Neutralisation der Lösung trat weisse Trübung auf.
15	„ „	„	$2^1/_6$	3.76	wie oben.
16	„ „	„	5	3.64	Pyrrol wurde orange gefärbt, sonst wie oben.

Die Versuchsergebnisse in Tabelle 1 sind auch in der nebenstehenden Abbildung graphisch dargestellt, wo das gefundene nk gegen den *p*H des verwendeten schweren Wassers aufgetragen ist. Die Nummer bei jedem kleinen Kreis zeigt die Schüttelungsdauer in Stunden. Wie man aus dieser graphischen Darstellung sofort ersieht, hängt die Grösse des „Austauschäquivalents" nk des Pyrrolmoleküls stark von der H-Ionenkon-

zentration des damit geschüttelten Wassers ab. Bleibt nämlich die H-Ionenkonzentration im Wasser kleiner als 0.01 N (pH = 2), so bleibt auch der Wert von nk durchaus konstant und beträgt durchschnittlich 0.88.[4] Wenn dagegen die H-Ionenkonzentration im verwendeten Wasser 0.01 N (pH = 2) überschreitet, setzt plötzlich eine neue Art von Austauschreaktion ein und das Austauschäquivalent nk nimmt sprungweise bis auf 3.7 zu. Dieser letzte Wert bleibt aber wieder konstant bis zur höchsten H-Ionenkonzentration, die wir verwendeten.

Auf diese Weise können wir die Austauschreaktion der H-Atome zwischen Pyrrol und Wasser vorläufig in zwei Arten einteilen. Bei der gewöhnlichen „ersten" Art von Austauschreaktion, die bei kleinen H-Ionenkonzentrationen (pH $\geqq$ 2) im Wasser stattfindet, wird nur ein einziges und höchstwahrscheinlich an N gebundenes H-Atom gegen die des Wassers sehr schnell ausgetauscht. Wenn dagegen die H-Ionenkonzentration im Wasser bis pH $<$ 2 erhöht wird, setzt plötzlich eine neue „zweite" Art von Austauschreaktion ein, bei der mehr als ein H-Atom des Pyrrolmoleküls gegen die H-Atome des Wassers ausgetauscht werden. Diese „zweite" Austauschreaktion verläuft zwischen pH = 2 bis 1 mit gut messbarer Geschwindigkeit. Wenn aber der pH des Wassers unterhalb 1 sinkt, dann wird die Geschwindigkeit dieser „zweiten" Austauschreaktion fast unmessbar gross. Aber bei solchen enormen H-Ionenkonzentrationen im verwendeten Wasser fanden wir zugleich, wie schon oben in Tabelle 1 erwähnt, durch die Färbung des Pyrrols sowie die Trübung der damit geschüttelten Lösung bei der Neutralisation, ein deutliches Anzeichen für das Auftreten der Polymerisation des Pyrrolmoleküls.

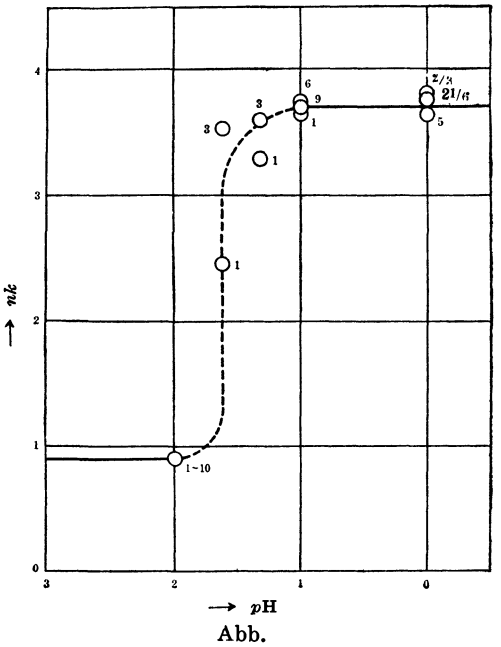


Abb.

Abhängigkeit des Austauschäquivalents nk des Pyrrols auf dem pH des damit geschüttelten Wassers und der Schüttelungsdauer.

(4) Rechnet man bloss aus den vorliegenden Versuchsergebnissen den Mittelwert von nk, dann ergibt er sich als 0.90 statt 0.88. Da aber dieser letztere Wert beim früheren Versuch (Fussnote (3)) nicht nur aus der Abnahme der D-Konzentration im schweren Wasser, sondern auch aus der Zunahme derselben im damit geschüttelten Pyrrol zugleich gerechnet wurde, muss er genauer als der erstere angesehen werden.

Bestimmung der Zahl der austauschbaren H-Atome bei der „zweiten" Austauschreaktion. Aus den oben angegebenen Versuchen fanden wir, dass das Austauschäquivalent des Pyrrolmoleküls bei der gewöhnlichen „ersten" Austauschreaktion $(nk)_1 = 0.88$, während es bei der neuen „zweiten" Austauschreaktion $(nk)_2 = 3.70$ beträgt. Aus diesem ersten Wert $(nk)_1$ darf man wohl schliessen, dass es sich bei der „ersten" Austauschreaktion um ein einziges und höchstwahrscheinlich an N gebundenes H-Atom handelt. Dagegen aus dem zweiten Wert $(nk)_2$ kann man nicht sofort über die Zahl der dabei austauschbaren H-Atome Schlüsse ziehen. Deshalb führten wir, um diese Zahl direkt zu bestimmen, einen besonderen Versuch aus. Bei diesem Versuch liessen wir nämlich eine kleine Menge von Pyrrol gegen eine überschüssige Menge des mit HCl angesauerten fast reinen schweren Wassers bis zum Austauschgleichgewicht reagieren.[5] Bezeichnet man dabei die Molzahl des Pyrrols mit M_P und die des schweren Wassers mit M_w, ferner den mittleren V.Q. der H-Atome zwischen diesen beiden Substanzen mit a, dann besteht zwischen den beiden H-Konzentrationen H_a und H_e im schweren Wasser vor und nach dem Versuch die Beziehung (4):

$$\frac{2M_wH_a+nM_P}{2M_w+nM_Pa} = H_e \qquad (4).$$

In dieser Beziehung (4) drückt n die Zahl der austauschbaren H-Atome in einem Pyrrolmolekül aus. Falls man aber, wie oben erwähnt, eine überschüssige Menge von fast reinem schwerem Wasser gegen eine kleine Menge von Pyrrol reagieren liess, dann sind die H-Konzentrationen H_a und H_e im ersteren beide sehr klein, und deshalb kann man die obige Gl. (4) wie folgt vereinfachen:

$$n = \frac{H_e-H_a}{(1-aH_e)} \cdot \frac{2M_w}{M_P} \fallingdotseq \left(H_e-H_a\right)\frac{2M_w}{M_P} \qquad (5).$$

Mittels dieser Gl. (5) konnten wir die Zahl n der austauschbaren H-Atome in einem Pyrrolmolekül bei der „zweiten" Austauschreaktion experimentell bestimmen. Dazu benutzten wir 99.4%iges schweres Wasser, das mit HCl auf ähnliche Weise wie schon oben erwähnt zu 0.1 bis 1 N angesauert war. Etwa 1 g. von diesem sauren schweren Wasser wurde zusammen mit ca. 0.03 bis 0.05 g. Pyrrol in einem Glasrohr unter Luft-

(5) Vgl. darüber G. Okamoto und S. Abe, *J. Chem. Soc. Japan*, **57** (1937), 1157 (japanisch); G. Okamoto, *J. Faculty Sci., Hokkaido Imp. Univ.*, Ser. III, **2** (1936), 81.

abschluss bei 30°C. etwa zwei Stunden lang geschüttelt, bis das Austauschgleichgewicht zustandekam. Dann wurde das schwere Wasser, auf ähnliche Weise wie schon oben erwähnt, vom Pyrrol geschieden, und die Dichte des so abgetrennten Wassers genau bestimmt, nachdem es neutralisiert und richtig gereinigt worden war. Die Bestimmung der Dichte des schweren Wassers führten wir ebenfalls nach der Schwebemethode mittels eines zu diesem Zweck besonders konstruierten Glasschwimmers aus. Da aber bei dem Blindversuch gefunden wurde, dass die Dichte des benutzten schweren Wassers während des Versuchs durch die Absorption der Feuchtigkeit aus atmosphärischer Luft durchschnittlich um 0.00033 ± 0.00001 vermindert wurde, und zwar diese Abnahme der Dichte des schweren Wassers der Zunahme des n-Wertes um etwa 0.5 entsprach, addierten wir der direkt gefundenen Dichte des schweren Wassers nach dem Versuch immer den oben angegebenen Wert und erst aus dieser korrigierten Dichte berechneten wir nach Gl. (5) die Zahl n der austauschbaren H-Atome. Die auf diese Weise erhaltenen Resultate geben wir in Tabelle 2 wieder, wo die Abnahme der Dichte des D_2O nach dem Experiment in der vierten Vertikalreihe schon auf die oben erwähnte Weise korrigiert ist.

Tabelle 2. Zahl n der austauschbaren H-Atome in einem Pyrrolmolekül bei der „zweiten" Austauschreaktion.

Versuchsnr.	Molzahl des Pyrrols M_P	Molzahl des D_2O M_w	Abnahme der Dichte des D_2O nach dem Exp.	n
1	0.000442	0.102	0.00135	4.9
2	0.000747	0.0712	0.00329	5.2
3	0.00118	0.0825	0.00454	4.8
4	0.000790	0.0682	0.00392	5.1

Aus diesem Versuch ersieht man sofort, dass bei der „zweiten" Austauschreaktion fünf, nämlich sämtliche, H-Atome des Pyrrolmoleküls gegen die des Wassers austauschbar sind.

Wir haben oben in Gl. (3) darauf hingewiesen, dass das Austauschäquivalent nk eines gegebenen Moleküls nichts anderes als die Summe aus den n_ik_i der einzelnen Arten der austauschbaren H-Atome in diesem Molekül ist. Demgemäss kann man das experimentell gefundene Austauschäquivalent nk des Pyrrolmoleküls wie folgt formulieren:

$$nk = n_N k_N + n_C k_C \qquad (6),$$

wo $n_N k_N$ das Austauschäquivalent des an N gebundene H-Atoms und $n_C k_C$ das der an C gebundenen H-Atome im Pyrrolmolekül ausdrückt. Da wir aber bei der „ersten" Austauschreaktion des Pyrrols $(nk)_1 = 0.88$, $n_N = 1$ und $n_C = 0$ gefunden haben, folgt aus Gl. (6) sofort, dass der V.Q. der D-Atome zwischen der NH-Gruppe des Pyrrols und Wasser $k_N = k(NH/H_2O) = 0.88$ liegt. Dagegen haben wir bei der „zweiten" Austauschreaktion $(nk)_2 = 3.7$ und $n_N + n_C = 5$ gefunden. Setzt man nun diese beiden Werte sowie die schon oben gefundene Werte von n_N $(= 1)$ und $k_N (= 0.88)$ in Gl. (6), dann ergibt sich, dass der mittlere V.Q. der D-Atome zwischen der CH-Gruppe im Pyrrol und Wasser

$$k_C = k(CH/H_2O) = \frac{3.70-0.88}{5-1} = 0.70$$

sein muss.

Wir möchten hier bemerken, dass der so gefundene V.Q. $k(CH/H_2O)$ des Pyrrolmoleküls erheblich kleiner als der des Benzolmoleküls ist, der von Koyano[6] bei 100°C. gleich 0.93 gefunden wurde. Daraus ersieht man, dass der V.Q. der D-Atome zwischen der CH-Gruppe, oder im allgemeinen einer bestimmten Atomgruppe, in einem gegebenen Molekül und Wasser ziemlich stark von der Molekülstruktur des ersteren beeinflusst wird.[7]

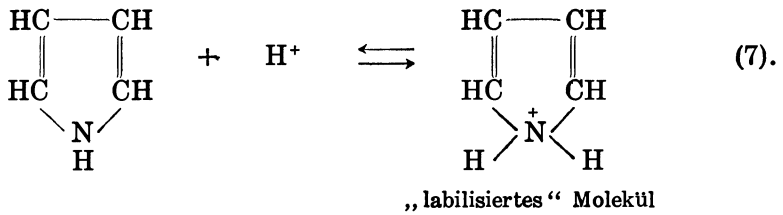
Diskussion. Eine der massgebenden Bedingungen für das Zustandekommen der „zweiten" Austauschreaktion, bei der alle H-Atome im Pyrrolmolekül gegen die des sauren Wassers ausgetauscht werden, ist ohne Zweifel die H-Ionenkonzentration im letzteren. Je grösser die H-Ionenkonzentration im verwendeten Wasser ist, desto leichter und schneller verläuft die „zweite" Austauschreaktion der H-Atome zwischen Pyrrol und Wasser, und bei genügend grossen H-Ionenkonzentrationen kann sie mit fast unmessbarer Geschwindigkeit verlaufen. Aber in diesem Gebiet der H-Ionenkonzentration tritt zugleich, wie schon oben erwähnt, ein deutliches Anzeichen für die Polymerisation des Pyrrolmoleküls auf. Es ist aber eine wohl bekannte Tatsache, dass das Pyrrol gegen Säuren sehr empfindlich ist. Behandelt man nämlich diese Substanz mit starken Säuren, so entsteht leicht Polymerisation und ergibt ein kompliziertes rot gefärbtes Polymerisationsprodukt (Pyrrolrot). In dem vorliegenden Versuch fanden wir auch, als wir das Pyrrol mit verhältnismässig stark saurer Lösung schüttelten, dass es gelb bis orange

(6) K. Koyano, *J. Chem. Soc. Japan*, **57** (1936), 933.

(7) Vgl. dazu K. Wirtz, *Z. physik. Chem.*, B, **34** (1936), 121; *Z. Elektrochem.*, **43** (1937), 662.

gefärbt und die damit geschüttelte wässrige Lösung bei der Neutralisation mit Kalk weiss getrübt wurde. Alle diese Tatsachen weisen ohne weiteres darauf hin, dass das Pyrrol in diesem Gebiet der H-Ionenkonzentrationen schon merklich polymerisationsfähig geworden war. Aber gerade bei dieser H-Ionenkonzentration trat die „zweite" Austauschreaktion am deutlichsten auf. Aus allen diesen Tatsachen spricht einwandfrei, dass es einen engen Zusammenhang zwischen der „zweiten" Austauschreaktion und Polymerisation des Pyrrolmoleküls geben und der massgebende Vorgang in den beiden Reaktionen die durch Säure bewirkte Lockerung der an C gebundenen H-Atome des Pyrrolmoleküls sein muss.

Aus diesem Grund sowie dem basischen bzw. schwach sauren Charakter der NH-Gruppe des Pyrrolmoleküls nehmen wir an, dass der erste Vorgang bei der „zweiten" Austauschreaktion sowie bei der Polymerisation des Pyrrolmoleküls unter dem Einfluss der Säuren, nichts anderes als die Salzbildung des Pyrrols bzw. die Anlagerung des Protons (bzw. Deuterons) an dem N-Atom desselben ist, wie das Reaktionsschema (7) zeigt:

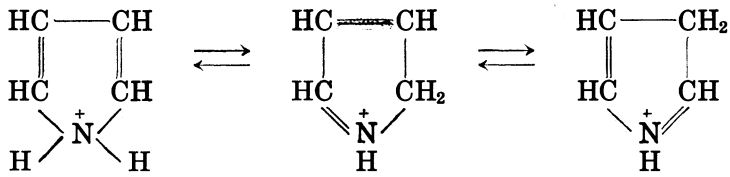


(7).

Durch diese Reaktion wird offenbar die Valenzzahl des N-Atoms von drei auf fünf vermehrt, und zugleich muss die Löslichkeit des Pyrrols im Wasser um einen gewissen Betrag vermehrt werden. Dabei muss man annehmen, dass das so gebildete positive Ion des Pyrrolmoleküls im Vergleich mit dem neutralen normalen Pyrrolmolekül viel reaktionsfähiger ist, oder mit anderen Worten die an C gebundenen H-Atome des Pyrrolmoleküls werden durch die Reaktion (7) mehr oder weniger gelockert. Infolgedessen kann das dadurch gebildete sogenannte „labilisierte" Pyrrolmolekül mittels seiner gelockerten H-Atome die Polymerisation oder die „zweite" Austauschreaktion der H-Atome leicht ausführen.

Was den eigentlichen Chemismus der „zweiten" Austauschreaktion des „labilisierten" Pyrrolmoleküls anbetrifft, so lassen sich noch keine sicheren Angaben machen. Aber allen Umständen nach, besonders infolge der leichten Beweglichkeit der H-Atome dieses Moleküls, liegt die Annahme nahe, dass es sich dabei um die tautomerische Umwandlung des Pyrrolmoleküls handelt. Obwohl die tautomerische Umwandlung des

normalen Pyrrolmoleküls nach dem Schema (1) aus dem vorliegenden Versuch sehr fraglich geworden ist, kann man solche für das bei der Reaktion (7) gebildete „labilisierte" Pyrrolmolekül nicht ganz ausschliessen. Vielmehr besteht die Annahme, dass die tautomerische Umwandlung bzw. Prototropie des „labilisierten" Pyrrolmoleküls nach dem Schema (8) viel leichter als beim normalen Molekül verlaufen kann.



(8)

Die Frage, ob diese Reaktion (8) oder im allgemeinen die „zweite" Austauschreaktion selbst durch die H-Ionen katalysiert wird, lässt sich nicht ohne weiteres beantworten. Aber aus dem Versuch mit Indol, dessen Ergebnisse später in diesem Bulletin veröffentlicht werden sollen, erwies es sich als höchstwahrscheinlich, dass dies wirklich der Fall ist. Doch davon soll später die Rede sein.

Zum Schluss möchten wir der Nippon Gakujutsu-Shinkohkai (der Gesellschaft zur Förderung der japanischen Wissenschaft) sowie der Hattori-Hohkohkai (der Hattori-Stiftung) für ihre finanzielle Unterstützung bei Ausführung der vorliegenden Arbeit unseren besten Dank aussprechen.

Schiomi-Institut für physikalische
und chemische Forschung
und
Physikalisch-chemisches Laboratorium
der Kaiserlichen Universität zu Osaka.

Über den Austausch der Wasserstoffatome zwischen Pyrrol, Indol sowie ihren Methylderivaten und Wasser.[1] II. Austausch der Wasserstoffatome zwischen Thiophen sowie Furan und Wasser.

Von Masao KOIZUMI und Toshizo TITANI.

(Eingegangen am 20. Dezember 1937.)

Inhaltsübersicht. Thiophen und Furan tauschen nicht ihre H-Atome unter denselben Versuchsbedingungen wie beim Pyrrol, d.h. bei Zimmertemperatur und unter Verwendung sauren Wassers, gegen die des Wassers aus. Die H-Atome dieser beiden Verbindungen können erst dann, wenn man diese Substanzen zusammen mit saurem Wasser unter Zusatz von Platinschwarz als Katalysator bei erhöhter Temperatur schüttelt, langsam gegen die des Wassers ausgetauscht werden. Dabei scheinen alle H-Atome der Verbindungen gegen die des Wassers ausgetauscht werden zu können. Aus diesen Versuchsergebnissen schliessen wir, dass bei der „zweiten" Austauschreaktion des Pyrrols, wo alle H-Atome desselben schnell gegen die des sauren Wassers ausgetauscht werden, nicht nur die Elektronenkonfiguration des Pyrrolmoleküls, sondern auch die chemischen Eigenschaften der NH-Gruppe bzw. des N-Atoms in demselben eine massgebende Rolle spielen.

Einleitung. Es wurde in unserem letzten Versuche,[1] als wir das Pyrrol zusammen mit saurem schwerem Wasser bei Zimmertemperatur schüttelten, gefunden, dass die an C gebundenen H-Atome des Pyrrolmoleküls bei einer bestimmten H-Ionenkonzentration im schweren Wasser ziemlich plötzlich austauschbar und schnell gegen D-Atome des letzteren ausgetauscht werden. Diese „zweite" Austauschreaktion des Pyrrols führten wir auf den chemischen Charakter der NH-Gruppe bzw. des N-Atoms des Pyrrolmoleküls sowie der dadurch bedingten tautomerischen Umwandlung desselben zurück. Aus diesem Grunde untersuchten wir nun die Austauschbarkeit der H-Atome von Thiophen und Furan gegen die des sauren Wassers, weil diese beiden Verbindungen wie bekanntlich mit Pyrrol isoelektronisch sind und ähnliche Elektronenkonfiguration wie dies besitzen.

Versuche mit Thiophen. Das Thiophen wurde chemisch rein von Kahlbaum bezogen und nach einmaliger Destillation direkt zum Versuch

(1) I. Mitteilung, dies Bulletin, **13** (1938), 85.

verwendet. Die sonstige Arbeitsmethode war im grossen und ganzen dieselbe wie im letzten Versuch mit Pyrrol.[1] Aber weil die H-Atome des Thiophens im Vergleich mit denen des Pyrrols sich schwerer austauschbar erwiesen, benutzten wir eine viel stärkere saure Lösung als beim Pyrrol. Jedoch konnten wir unter diesen milden Versuchsbedingungen überhaupt keine Austauschreaktion der H-Atome des Thiophens gegen die des Wassers erzielen, wie aus den Versuchen 1 und 2 in Tabelle 1 ersichtlich ist. Das dabei gefundene negative Austauschäquivalent *nk* ist selbstverständlich auf den Versuchsfehler zurückzuführen.

Tabelle 1. Versuche mit Thiophen.

Versuchsnr.	Benutzte Lösung	Temp. (°C.)	Schüttelungsdauer in Stdn.	Austauschäquivalent *nk*
1	1 N HCl	30	5	−0.08
2	3 N HCl	40	5	−0.04
3	1 N HCl + Platinschwarz	100	5	0.33
4	„ + „	150	5	2.11
5	„ + „	150	14	2.22
6	„ + „	150	30	2.80

Da auf diese Weise die unter den ähnlichen Verhältnissen wie beim Pyrrol ausgeführten Versuche 1 und 2 sich ganz negativ erwiesen, führten wir die übrigen Versuche 3 bis 6 unter verhältnismässig stärkeren Graden aus. Bei diesen Experimenten fügten wir nämlich der Lösung eine Menge von Platinschwarz als Katalysator hinzu und erhöhten die Temperatur bis auf 150°C. Die Schüttelung des Thiophens mit dieser Lösung dauerte in einem Fall sogar 30 Stdn. (Versuch 6). Bei dieser verhältnismässig heftigen Behandlung fanden wir erst die H-Atome des Thiophens langsam gegen D-Atome des schweren Wassers sich austauschen, wie aus der Schüttelungsdauer und dem dabei gefundenen Austauschäquivalent des Thiophens in Tabelle 1 ersichtlich ist. Dabei schienen alle H-Atome des Thiophens, nach der Grösse des gefundenen Austauschäquivalents *nk* zu urteilen, schliesslich ganz gegen D-Atome des schweren Wassers ausgetauscht werden zu können. Aber in diesen Fällen fanden wir schon immer den Beginn einer ziemlich merklichen Zersetzung des Thiophens, wie wir dies aus der Entwicklung des Schwefelwasserstoffs wahrnahmen.

Versuche mit Furan. Das Furan wurde durch die Zersetzung der Brenzschleimsäure unter Erhitzung dieser Verbindung auf 250 bis 270°C. im geschlossenen Rohr hergestellt. Die sonstige Verfahrungsart war

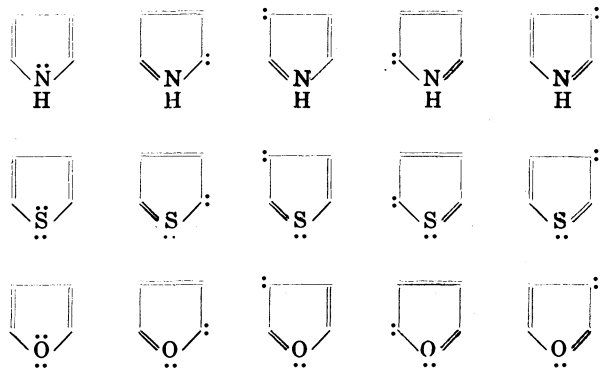
genau dieselbe wie beim Thiophen. Die Versuchsergebnisse geben wir in Tabelle 2 wieder.

Tabelle 2. Versuche mit Furan.

Versuchsnr.	Benutzte Lösung	Temp. (°C.)	Schüttelungs-dauer in Stdn.	Austausch-äquivalent *nk*
1	1 N HCl	40	5	−0.03
2	3 N HCl	40	5	0.07
3	1 N HCl + Platinschwarz	40	8	−0.02
4	„ + „	100	7	1.29
5	„ + „	100	34	2.72
6	neutrales schweres Wasser	100	20	0.07

Wie man aus Tabelle 2 ersieht, führt das Furan ebenso schwer wie Thiophen die Austauschreaktion der H-Atome aus und erst unter der katalytischen Mitwirkung des Platinschwarzes können die H-Atome des Furans gegen die des Wassers langsam ausgetauscht werden.

Diskussion. Pyrrol, Thiophen und Furan sind untereinander isoelektronisch und nach Pauling[2] können sie im Normalzustand fünf Arten von Elektronenkonfiguration besitzen, wie das folgende Schema zeigt:

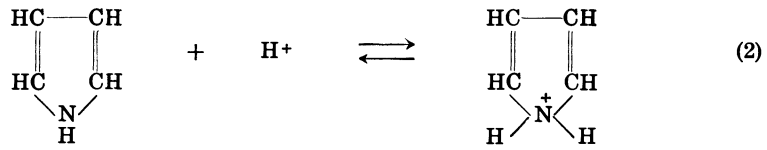


(1)

Schon allein aus diesem Vergleich der Elektronenkonfiguration in drei Arten der Moleküle liegt die Vermutung nahe, dass die H-Atome des Thiophens bzw. Furans ebenso leicht wie die des Pyrrols gegen die des Wassers austauschbar sein müssen. Aber in Wirklichkeit, wie in den

(2) L. Pauling, *J. Chem. Phys.*, **1** (1933), 607.

vorliegenden sowie in den letzten Versuchen gefunden wurde, gibt es einen enorm grossen Unterschied zwischen der Austauschbarkeit der an C gebundenen H-Atome des Pyrrols einerseits und der des Thiophens bzw. Furans anderseits. Dieser Befund weist ohne weiteres darauf hin, dass die Leichtaustauschbarkeit der an C gebundenen H-Atome des Pyrrolmoleküls nicht bloss mit der Elektronenkonfiguration in demselben im Normalzustand erklärt werden kann. Dafür muss man vielmehr den eigentlichen Charakter der NH-Gruppe bzw. des N-Atoms im Pyrrolmolekül in Betracht ziehen, wie wir schon in unserer letzten Mitteilung[1] darauf hingewiesen haben. Dort nahmen wir an, dass der erste massgebende Vorgang bei der „zweiten" Austauschreaktion des Pyrrols gegen saures Wasser die Anlagerung des Protons (bzw. Deuterons) an dem N-Atom des Pyrrolmoleküls und die dadurch bedingte Fünfwertigkeit des N-Atoms ist, wie das Schema (2) zeigt:



(2)

„labilisiertes" Molekül

Das durch die Reaktion (2) gebildete „labilisierte" Pyrrolmolekül kann nun ihren an C gebundenen H-Atome gegen die des Wassers leicht austauschen. Dabei ist die Annahme nicht von der Hand zu weisen, dass das „labilisierte" Pyrrolmolekül gemäss der Elektronenkonfigurationsänderung (1) eine tautomerische Umwandlung ausführt und dadurch die sämtlichen H-Atome in demselben eins nach dem anderen gegen die des Wassers ausgetauscht werden.

Zum Schluss sprechen wir der Nippon Gakujutsu-Shinkohkai (Der Gesellschaft zur Förderung der japanischen Wissenschaft) sowie der Hattori-Hohkohkai (der Hattori-Stiftung) für ihre finanzielle Unterstützung unseren wärmsten Dank aus.

Schiomi-Institut für physikalische und chemische Forschung
und
Physikalisch-chemisches Laboratorium der Kaiserlichen Universität zu Osaka.

Über den Gehalt der Kohlenhydrate an schwerem Sauerstoff.[1]

Von Noriyoshi MORITA, Kokiti GOTO und Toshizo TITANI.

(Eingegangen am 20. Dezember 1937.)

Inhaltsübersicht. Eine isotopische analytische Methode, nach der der Gehalt des gegebenen Wassers an schwerem Wasserstoff bzw. schwerem Sauerstoff im Vergleich mit gewöhnlichem Wasser ermittelt werden kann, wird angegeben. Nach dieser Methode wurde das Wasser, das bei der Verbrennung von Zucker, Baumwolle und Zedernholz in Luft, sowie von Zucker in elektrolytischem Sauerstoff gebildet worden war, isotopisch analysiert. Daraus fanden wir, dass die grössere Dichtigkeit des Wassers, das bei der Verbrennung dieser Substanzen in Luft gebildet wird, gewöhnlichem Wasser gegenüber fast ausschliesslich von der Anreicherung der schweren Isotope von Sauerstoff im ersteren herrührte. Zugleich wurde gefunden, dass der Wasserstoff im bei der Verbrennung gebildeten Wasser, infolgedessen im Zucker selbst, in der Form von Wasser gemessen, um etwa 1 γ schwerer als gewöhnlicher Wasserstoff ist. Zum Schluss ergab sich aus der isotopischen Analyse des Wassers, das durch die Reduktion des Sauerstoffs im Zucker mittels Wasserstoffs gewonnen wurde, dass der Sauerstoff im Zucker in der Form von Wasser gemessen um 5 ± 1 γ schwerer als gewöhnlicher Wassersauerstoff ist. Um die so aufgefundene Anreicherung der schweren Isotope von Wasserstoff und Sauerstoff im Kohlenhydrat zu deuten, werden einige Möglichkeiten angegeben.

Einleitung. Einige Autoren fanden bei ihren Versuchen, dass das Wasser, das bei der Verbrennung verschiedener Arten von wasserstoffhaltigen Substanzen, wie z.B. Kohlenwasserstoffe[2] und Kohlenhydrate[3] in Luft gebildet wurde, um 5 bis 8 γ dichter als gewöhnliches Wasser war,

(1) Vorläufig mitgeteilt in diesem Bulletin, **11** (1936), 695.

(2) R. D. Snow und H. L. Johnston, *Science*, **80** (1934), 210; C. H. Greene und R. J. Voskuyl, *J. Am. Chem. Soc.*, **56** (1934), 1649; M. Dole, *J. Am. Chem. Soc.*, **56** (1934), 999; *J. Chem. Phys.*, **2** (1934), 337, 548; N. S. Filippova, *J. Chem. Phys.*, **3** (1935), 316; *Compt. rend. acad. sci. U.R.S.S.*, **3** (1935), 29; S. H. Bertram und H. Mendel, *Chem. Weekblad*, **33** (1936), 687; A. Maillard, *Compt. rend.*, **203** (1936), 804.

(3) H. J. Emeléus, F. W. James, A. King, T. G. Pearson, R. H. Purcell und H. V. A. Briscoe, *J. Chem. Soc.*, **1934**, 1207, 1948; T. Titani und M. Harada, dies Bulletin, **10** (1935), 205, 261; K. Okabe und T. Titani, dies Bulletin, **10** (1935), 465.

und führten dies auf die Anreicherung des schweren Wasserstoffs bzw. Sauerstoffs in den untersuchten Verbindungen zurück. Aber diese Schlüsse sind durch den Befund[4] zum mindesten sehr fraglich geworden, dass der Luftsauerstoff um $7 \pm 1\,\gamma$ schwerer als der Wassersauerstoff, d.h. der im Wasser chemisch verbunden vorhandene Sauerstoff, ist. Nach diesem Befund kann das Wasser, das bei der Verbrennung der Substanz, die keinen Sauerstoff in sich enthält, wie z.B. Kohlenwasserstoff, in Luft gebildet wird, immer um einige γ schwerer als gewöhnliches Wasser sein, auch wenn der Wasserstoff in der Substanz gewöhnliche isotopische Zusammensetzung besitzt. Auf diese Möglichkeit haben wir schon in unserer früheren Abhandlung[5] hingewiesen. Aber die Sache liegt etwas anders bei der Verbindung, die Sauerstoff als einen Bestandteil in sich selbst enthält, weil sich in diesem Fall auch dieser Sauerstoff bei der Verbrennung der betreffenden Substanz an der Wasserbildung beteiligen kann. Dies ist z.B. der Fall bei verschiedenen Arten von Kohlenhydraten und kohlenhydrathaltigen Substanzen. Von diesen Substanzen fanden wir bei unseren früheren Versuchen,[6] dass das bei deren Verbrennung in Luft gebildete Wasser immer um 5 bis $8\,\gamma$ schwerer als gewöhnliches Wasser war. Aber bloss aus diesem Befund können wir aus dem eben erwähnten Grund nicht ohne weiteres schliessen, dass es sich dabei in diesen Substanzen um die wirkliche Anreicherung der schweren Isotope des Wasserstoffs bzw. Sauerstoffs handelte. Ebensowenig kann man den Schluss ziehen, dass die grössere Dichtigkeit des zur Verbrennung benutzten Luftsauerstoffs dem Wassersauerstoff gegenüber dabei eine Rolle spielte. Um auf diese Fragen einen sicheren Anhaltspunkt zu gewinnen, haben wir in der vorliegenden Arbeit drei Reihen von Versuchen durchgeführt. Im ersten Versuch wurde das Wasser, das bei der Verbrennung einiger Arten von Kohlenhydrat bzw. kohlenhydrathaltigen Substanzen in Luft gebildet wurde, nach dessen Gehalt an schweren Isotopen des Wasserstoffs und Sauerstoffs isotopisch analysiert. Dann im zweiten Versuch wurde das Wasser, das bei der Verbrennung von Rohrzucker in elektrolytischem Sauerstoff gebildet wurde, ebenfalls isotopisch analysiert. Und zum Schluss im dritten Versuch wurde der Gehalt des Zuckers an schwerem Sauerstoff im Vergleich mit gewöhnlichem Wasser bestimmt,

---

(4) N. Morita und T. Titani, dies Bulletin, **11** (1936), 36, 414; M. Dole, *J. Am. Chem. Soc.*, **57** (1935), 2731; *J. Chem. Phys.*, **4** (1936), 268; E. R. Smith und H. Matheson, *J. Research Natl. Bur. Standards*, **17** (1936), 625; T. O. Jones und N. F. Hall, *J. Am. Chem. Soc.*, **59** (1937), 259.

(5) N. Morita und T. Titani, dies Bulletin, **11** (1936), 419.

(6) T. Titani und M. Harada, dies Bulletin, **10** (1935), 205, 261; K. Okabe und T. Titani, dies Bulletin, **10** (1935), 465.

indem wir den Sauerstoff im ersteren zunächst durch Reduktion mit Wasserstoff möglichst vollständig in Wasser verwandelten und dessen Gehalt an schwerem Sauerstoff durch die isotopische analytische Methode direkt mit dem des gewöhnlichen Wassers verglichen.

Versuch I. Isotopische Analyse des bei der Verbrennung von Rohrzucker, Baumwolle und Zedernholz in Luft gebildeten Wassers. Bei unseren früheren Versuchen[6] fanden wir, dass die drei Arten von Wasser, die bei der Verbrennung von Rohrzucker (7.4 γ), Baumwolle (5.7 γ) und Zedernholz (4.5 γ) alle in Luft gebildet wurden, um den in den Klammern angegebenen Betrag schwerer als gewöhnliches Wasser waren. Da aber eben diese drei Arten von Wasser seitdem separat in Glasröhren aufbewahrt worden waren, wurden sie je nach deren Gehalt an schwerem Sauerstoff und Wasserstoff im Vergleich mit gewöhnlichem Wasser analysiert. Die analytische Methode besteht darin, dass das Probewasser und das damit zu vergleichende gewöhnliche Wasser beide durch Elektrolyse fast vollständig in ihre Bestandteile gespalten und der dabei entwickelte Sauerstoff separat in überschüssigem Protiumgas, d.h. praktisch deuteriumfreiem Wasserstoff, über erhitztem Platindraht katalytisch bis zu Wasser verbrannt wird.[7] Auf diese Weise erhält man zwei Arten von Protowasser, das eine aus dem Probewasser und das andere aus gewöhnlichem Wasser. Da aber in diesem Protowasser der Sauerstoff des respektiven Wassers als Ganzes enthalten sein muss, lässt sich der geringste Unterschied in der Isotopenzusammensetzung zwischen beiden Arten von Sauerstoff des Probe- und gewöhnlichen Wassers durch den Vergleich der Dichte der so gewonnenen beiden Arten von Protowasser ohne weiteres herausfinden. Falls z.B. das Protowasser aus dem Probewasser um Δs_2 schwerer als das aus gewöhnlichem Wasser wäre, dann muss dieser Dichteüberschuss auf die Anreicherung des schweren Sauerstoffs im untersuchten Probewasser zurückgeführt werden. Wir haben nach dieser Methode die oben angegebenen drei Arten von Wasser nach dessen Gehalt an schwerem Sauerstoff im Vergleich mit gewöhnlichem Wasser untersucht. Die dabei erhaltenen Resultate geben wir in Tabelle 1 wieder.

In dieser Tabelle zeigt Δs_1 in der ersten Vertikalreihe die früher gefundene Dichtezunahme des originalen Probewassers, das direkt bei der Verbrennung der betreffenden Substanz in Luft gebildet wurde, gewöhnlichem Wasser gegenüber. Deshalb muss Δs_1 offenbar von der Anreicherung der beiden schweren Isotope des Sauerstoffs und Wasserstoffs im untersuchten Wasser herrühren. Dagegen zeigt Δs_2 in der zweiten

(7) N. Morita und T. Titani, dies Bulletin, **11** (1936), 403.

Tabelle 1. Die isotopische Analyse des bei der Verbrennung von einigen Kohlenhydraten in Luft gebildeten Wassers.

Substanz	Δs_1 in γ	Δs_2 in γ	$\Delta s_1 - \Delta s_2$ in γ
Rohrzucker	+ 7.4	+ 6.2	+ 1.2
„	+ 7.4	+ 5.8	+ 1.6
Baumwolle	+ 5.7	+ 5.0	+ 0.7
Zedernholz	+ 4.5	+ 3.4	+ 1.1

Vertikalreihe die in dem vorliegenden Versuch gefundene Dichtezunahme des Protowassers, das aus dem betreffenden Probewasser hergestellt wurde, dem gewöhnlichen Protowasser gegenüber, das aus gewöhnlichen Wasser bereitet wurde. Notwendigerweise ist Δs_2 aus dem oben erwähnten Grund ausschliesslich auf die Anreicherung des schweren Sauerstoffs im untersuchten Wasser zurückzuführen. Infolgedessen kann man die Differenz $\Delta s_1 - \Delta s_2$ in der letzten Vertikalreihe der Tabelle als die Dichtezunahme des Probewassers gegen gewöhnliches Wasser wegen der Anreicherung des schweren Wasserstoffs im ersteren, folglich in der verbrannten Substanz selbst, ansehen. Auf diese Weise fanden wir, dass die grössere Dichtigkeit des Wassers, das bei der Verbrennung von Kohlenhydraten bzw. kohlenhydrathaltigen Substanzen in Luft gebildet wird, gewöhnlichem Wasser gegenüber grösstenteils von der Anreicherung des schweren Sauerstoffs im gebildeten Wasser herrührt. Dagegen kann der Wasserstoff in demselben Wasser, also im verbrannten Kohlenhydrat selbst, in der Form von Wasser gemessen nur um etwa 1 γ schwerer als der Wasserstoff in gewöhnlichem Wasser sein.

Versuch II. Isotopische Analyse des bei der Verbrennung von Rohrzucker in elektrolytischem Sauerstoff gebildeten Wassers. In diesem Versuche II haben wir denselben Rohrzucker, den wir im vorhergehenden Versuch I untersuchten, statt in Luft im elektrolytischen Sauerstoff verbrannt und das dabei gebildete Wasser auf dieselbe Weise wie oben isotopisch analysiert. Dazu wird 30 g. Zucker auf einem eisernen Schiffchen in ein Ende des Pyrexglasrohres hineingeschoben. Im anderen Ende des Rohres befindet sich eine Menge von Kupferoxyd, das aus reinem Kupfer und demselben elektrolytischen Sauerstoff, wie zur Verbrennung benutzt wird, hergestellt worden ist. Durch dieses Rohr wird der Sauerstoff, durch die Elektrolyse mit gewöhnlichem Wasser entwickelt, in der Richtung von Zucker nach Kupferoxyd mit einer Geschwindigkeit von ca. 300 c.c.

pro Minute geleitet, und zugleich wird das Rohr von aussen langsam erhitzt. Dadurch entsteht eine allmähliche Verbrennung des Zuckers und das dabei gebildete und abdestillierte Wasser wird in der mit Kohlensäureschneegemisch abgekühlten Flasche kondensiert abgefangen.

Auf diese Weise erhielten wir in zwei Experimenten, die wir beide mit 30 g. Zucker durchführten, jedesmal 15 g. Wasser. Dies entspricht 87% des theoretischen Wertes. Nachdem wir diese beiden Arten von Wasser separat gereinigt hatten, fanden wir das eine um 0.2 γ und das andere 1.0 γ schwerer als gewöhnliches Wasser. Da aber die Menge der beiden Wasser sich als zu wenig erwies, um weitere genauere Messungen auszuführen, wurden sie vereinigt und das so gewonnene Wasser nach dessen Gehalt an schwerem Sauerstoff und Wasserstoff auf dieselbe Weise wie beim Versuch I mit gewöhnlichem Wasser verglichen. Das Resultat ergab, dass das Protowasser aus diesem vereinigten Wasser um 0.2 γ leichter als gewöhnliches Protowasser war, wie in Tabelle 2 angegeben.

Tabelle 2. Die isotopische Analyse des bei der Verbrennung von Rohrzucker im elektrolytischen Sauerstoff gebildeten Wassers.

Substanz	Δs_1 in γ	Δs_2 in γ	$\Delta s_1 - \Delta s_2$ in γ
Rohrzucker	+ 0.2	− 0.2	+ 0.8
„	+ 1.0		

Da aber das untersuchte Wasser als Ganzes um 0.6 γ (= (0.2 + 1.0) /2) schwerer als gewöhnliches Wasser angesehen werden darf, folgt sofort, dass solch ein Anteil des Dichteüberschusses, der auf die Anreicherung des schweren Wasserstoffs im untersuchten Wasser, folglich im verbrannten Zucker selbst, zurückzuführen ist, gleich 0.8 γ (= 0.6 + 0.2) sein muss. Dieser Wert stimmt mit dem im Versuch I gefundenen innerhalb des Messfehlersbereichs sehr gut überein (vgl. Tabelle 1).

Der in diesem Versuch zur Verbrennung des Zuckers benutzte Sauerstoff wurde, wie oben erwähnt, durch die Elektrolyse mit gewöhnlichem Wasser hergestellt. Infolgedessen muss er in der Form von Wasser gemessen um etwa 1.6 γ leichter als gewöhnlicher Wassersauerstoff sein, wenn man den Trennfaktor der Sauerstoffisotope $k = 1.01$[8] setzt. Unter Benutzung dieses spezifisch leichten Sauerstoffs zur Verbrennung des Zuckers fanden wir aber den Sauerstoff im dabei gebildeten Wasser,

(8) N. Morita und T. Titani, dies Bulletin, **11** (1936), 414, 419.

wie oben erwähnt, nur um 0.2 γ leichter oder fast gleich schwer wie gewöhnlicher Wassersauerstoff. Dies weist ohne weiteres darauf hin, dass der Sauerstoff im verbrannten Zucker selbst auch um einige γ schwerer als gewöhnlicher Wassersauerstoff sein konnte. Diese Erwartung wurde tatsächlich im nächsten Versuch III einwandfrei bewiesen.

Versuch III. Isotopische Analyse des bei der Reduktion des Zuckers mittels Wasserstoffs gebildeten Wassers. Eine grosse Menge von Rohrzucker, den wir im Wasserstoffstrom erhitzten, wurde so vollständig zersetzt. Darauf wurde der im Zersetzungsprodukt gebildete Sauerstoff möglichst vollkommen in Wasser verwandelt und dessen Gehalt an schwerem Sauerstoff im Vergleich mit gewöhnlichem Wasser bestimmt. Die zur Zersetzung des Zuckers im Wasserstoffstrom benutzte Apparatur ist in der nebenstehenden Abb. schematisch angegeben. Der Destillierkolben Z, der aus langhalsigen Pyrexglaskolben besteht und den Inhalt von ca. 100 c.c. besitzt, enthält eine kleine Menge (ca. 25 g.) von Zucker, der von aussen langsam erhitzt wird, indem man den Wasserstoff durch das

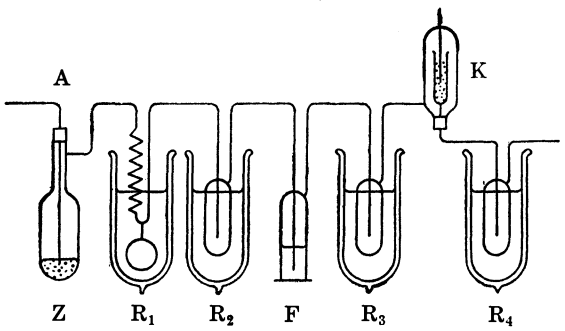


Abb. Zersetzungsapparatur des Zuckers.

Rohr A in den Kolben hineinleitet. Durch diese Prozedur wird der Zucker allmählich zersetzt und die dadurch gebildeten flüchtigen Substanzen, die hauptsächlich aus Wasser, Teer und einigen gasförmigen Verbindungen bestehen, werden zusammen mit dem Wasserstoffgas durch die Kühlflaschen R_1 bis R_4 nacheinander geleitet. Da die erste Flasche R_1 mit Eis und die zweite R_2 mit Kohlensäureschneegemisch je von aussen gut abgekühlt ist, wird dort Wasser und Teer aus dem Zersetzungsprodukt vollständig kondensiert angefangen, und zwar grösstenteils in der ersteren Flasche R_1. Der hier nicht kondensierte gasförmige Anteil des Zersetzungsprodukts, der hauptsächlich aus Kohlendioxyd und -monoxyd zusammen mit dem zugesetzten Wasserstoffgas besteht, wird dann, nachdem das Gasgemisch in der Flasche F mit Benzol gewaschen und von

dessen Dampf in der nächsten mit Kohlensäureschneegemisch abgekühlten Flasche R_3 befreit wird, durch das erhitzte Katalysatorrohr K und die Kühlflasche R_4 nacheinander geleitet. In diesem Katalysatorrohr, das mit Ni-ThO_2-Katalysator gefüllt ist, wird das Kohlendioxyd und -monoxyd mit dem zugleich befindlichen Wasserstoffgas bis zu Wasser reduziert und das so gebildete Wasser wird in der letzten mit Kohlensäureschneegemisch abgekühlten Flasche R_4 ausgefroren.

Am Ende jeder solchen Destillation, die wir immer mit einer Menge von 25 g. Zucker durchführten, fanden wir im Destillierkolben Z 7 bis 8 g. Zuckerkohle, in der Flasche R_1 10 bis 11 g. von gelb gefärbter stinkender Flüssigkeit, in der nächsten Flasche R_2 ebenfalls einige Tropfen von derselben Flüssigkeit, und in der letzten Flasche R_4 ca. 3 g. von fast reinem Wasser. In der Tat wiederholten wir dieselben Destillationen sechs bis elf mal nacheinander und sammelten die aus jeder Destillation erhaltene Flüssigkeit und Wasser zusammen. Die auf diese Weise aus den beiden Flaschen R_1 und R_2 gewonnene Flüssigkeit nennen wir zusammengefasst das Kondensat K_{12} und das Wasser aus der Flasche R_4 das Wasser W_4. Wir erhielten z.B. in einer Reihe von Versuchen, wo wir die Destillationen sechsmal wiederholten und deshalb insgesamt 150 g. Zucker zersetzt wurden, 45 g. Zuckerkohle, 65 g. von K_{12} und 18 g. von W_4.

Da das Wasser W_4 fast reines Wasser war, wurde es unmittelbar zur isotopischen Analyse verwendet. Dagegen, weil das Kondensat K_{12} neben Wasser noch eine beträchtliche Menge von organischen Verbindungen enthielt, wurde es einem weiteren Reinigungsprozess unterworfen. Zu diesem Zweck wird das Kondensat K_{12} unter dem Zusatz von einigen Tropfen von Schwefelsäure angesauert und zwischen Platinelektroden elektrolytisch gespalten. Das dabei entwickelte Knallgas enthält eine beträchtliche Menge von Kohlensäure, die durch die anodische Oxydation der im Kondensat befindlichen organischen Substanzen entsteht. Deshalb wird das Knallgas zuerst durch die Abkühlung mit flüssiger Luft von dieser beigemengten Kohlensäure befreit und dann unter dem Zusatz von einem kleinen Überschuss von Wasserstoff über erhitzter Kupferfolie bis zu Wasser rekombiniert. Das dadurch aus dem Kondensat K_{12} gebildete Wasser nennen wir Wasser W°_{12}. Die bei dieser Elektrolyse aus dem Elektrolyseurgas abgeschiedene Kohlensäure wird für sich auf dem Ni-ThO_2-Katalysator mittels Wasserstoffs bis zu Wasser reduziert. Das so gewonnene Wasser nennen wir Wasser W_{12}. Auf diese Weise erhielten wir, alles zusammen genommen, drei Arten von Wasser aus dem Zucker, nämlich W°_{12}, W_{12} je aus dem Kondensat K_{12} und das in der Flasche R_4 angefangene W_4. Das Mengenverhältnis dieser drei Arten von Wasser bei drei Reihen von Versuchen, die wir je mit 150 g., 280 g. und 250 g.

Zucker durchführten, geben wir in den dritten Vertikalreihen der Tabellen 3 wieder. Wie man daraus ersieht, konnten wir nach der oben angegebenen Methode 69 bis 73% des gesamten Sauerstoffs des Zuckers zu Wasser verwandeln.

Tabelle 3. Die isotopische Analyse des bei der Reduktion des Zuckers mittels Wasserstoffs gebildeten Wassers.

Versuch 1.

1. Menge des Zuckers in g.	2. Menge des Kondensats in g.	3. Menge der Arten von Wasser in g.	4. Δs in γ	5. Mittlerer Δs in γ
150	$K_{12} = 65$	$W^{*}_{12} = 33$ $W_{12} = 12$ $W_4 = 18$	2.6 4.2 5.9	3.9

Summe = 63 (73% des theoretischen Wertes)

Versuch 2.

1. Menge des Zuckers in g.	2. Menge des Kondensats in g.	3. Menge der Arten von Wasser in g.	4. Δs in γ	5. Mittlerer Δs in γ
280	$K_{12} = 107$	$W^{*}_{12} = 80$ $W_{12} = 19$ $W_4 = 15$	4.6 8.2 7.6	5.6

Summe = 114 (69% des theoretischen Wertes)

Versuch 3.

1. Menge des Zuckers in g.	2. Menge des Kondensats in g.	3. Menge der Arten von Wasser in g.	4. Δs in γ	5. Mittlerer Δs in γ
250	$K_{12} = -$	$W^{*}_{12} = 71$ $W_{12} = 21$ $W_4 = 13$	4.1 4.7 5.2	4.4

Summe = 105 (72% des theoretischen Wertes)

Die so gewonnenen drei Arten von Wasser wurden dann separat nach dessen Gehalt an schwerem Sauerstoff isotopisch analysiert. Die analytische Methode war genau dieselbe wie die im vorhergehenden Versuche I und II verwendete. Nämlich das Wasser wird zuerst elektrolytisch fast

vollständig in dessen Bestandteile gespalten und der dabei entwickelte Sauerstoff im überschüssigen Protiumgas bis zu Wasser verbrannt. Das so gewonnene Wasser wird hierauf sorgfältig gereinigt und dessen Dichte mit dem gewöhnlichen Protowasser, das aus gewöhnlichem Wasser auf ähnliche Weise wie oben hergestellt wird, mittels eines Quarzschwimmers verglichen. Auf diese Weise kann man die Dichtezunahme Δs des gegebenen Wassers wegen der Anreicherung des schweren Sauerstoffs in demselben im Vergleich mit gewöhnlichem Wasser finden. Die nach dieser Methode gefundene Dichtezunahme Δs der drei Arten von Wasser W_{12}°, W_{12} und W_4 ist in den vierten Vertikalreihen der Tabellen 3 wiedergegeben. Die dabei leicht ersichtliche grössere Dichtigkeit von W_{12} und W_4, die beide bei der Reduktion der Kohlensäure mittels Wasserstoffs gebildet wurden, im Vergleich mit W_{12}°, das bei der Rekombination des Knallgases erzeugt wurde, kann man dadurch erklären, dass die schweren Isotope des Sauerstoffs beim Austauschgleichgewicht zwischen Wasser und Kohlensäure stets in der letzteren angereichert werden. Aus diesem Grund errechneten wir den Mittelwert von Δs der drei Arten von Wasser W_{12}°, W_{12} und W_4 unter Berücksichtigung ihres Mengenverhältnisses und erhielten dadurch die Werte, die in den letzten fünften Vertikalreihen der Tabellen 3 wiedergegeben sind.

Aus den Ergebnissen der Tabellen 3 ersehen wir, dass der Sauerstoff in den untersuchten Arten von Wasser durchschnittlich um $5 \pm 1\,\gamma$ schwerer als gewöhnlicher Wassersauerstoff ist, falls man beide in der Form von Wasser vergleicht. Aber weil wir in diesen Versuchen, wie unter jeder Tabelle angegeben ist, mehr als zwei Drittel des gesamten Sauerstoffs im Zucker in Wasser verwandeln konnten, darf man wohl schliessen, dass der Sauerstoff im Zucker selbst auch den Dichteüberschuss von mindestens derselben Grössenordnung wie dem oben gefundenen gewöhnlichem Wassersauerstoff gegenüber besitzen muss.

Diskussion. *Wir haben aus den Versuchen I und II den Wasserstoff im Zucker um etwa 1 γ, dagegen aus dem Versuch III den Sauerstoff in demselben um etwa 5 γ, beide in der Form von Wasser gemessen, schwerer als der Wasserstoff bzw. Sauerstoff in gewöhnlichem Wasser gefunden.* Um diese Anreicherung der schweren Isotope des Wasserstoffs und Sauerstoffs im Zucker zu deuten, gibt es offenbar viele Erklärungsmöglichkeiten. Eine der wahrscheinlichsten Ursachen für die Anreicherung des schweren Wasserstoffs im Zucker ist, dass schwerer Wasserstoff durch den Isotopenaustausch zwischen Zucker und Wasser im ersteren akkumuliert wird. Harada[9] fand nämlich, dass beim Austauschgleichgewicht

(9) M. Harada, *J. Chem. Soc. Japan*, **57** (1936), 391.

des schweren Wasserstoffs zwischen Zucker und Wasser dieser um einen kleinen Betrag im Zucker angereichert wird, und der Verteilungsquotient der D-Atome zwischen den Hydroxylgruppen des Zuckers und Wasser $k = 1.10 \pm 0.1$ ist. Nach diesem Befund muss der gesamte Wasserstoff im Zucker in der Form von Wasser gemessen durchschnittlich um $0.7\,\gamma$ schwerer als der Wasserstoff in gewöhnlichem Wasser sein, wenn die beiden Substanzen sich im Isotopenaustauschgleichgewicht befinden. Dieser Wert ($0.7\,\gamma$) stimmt mit dem in den Versuchen I und II gefundenen Dichteüberschuss des Wasserstoffs im Zucker dem gewöhnlichen Wasserstoff gegenüber ($1\,\gamma$) hinreichend gut überein. Auf die Frage, ob man die grössere Dichtigkeit des Sauerstoffs im Zucker im Vergleich mit dem gewöhnlichen Wassersauerstoff auf ähnliche Weise wie oben mit der Austauschreaktion von O-Atome zwischen Zucker und Wasser deuten kann, können wir nicht sofort unumwunden antworten. In diesem Fall liegt auch die Möglichkeit vor, dass schwerer Sauerstoff bei der Assimilation der Kohlensäure von Pflanzen im gebildeten Kohlenhydrat angereichert wird.

Diese letzte Möglichkeit wurde auch schon von Greene und Voskuyl[10] angenommen, um die grössere Dichtigkeit des Luftsauerstoffs dem Wassersauerstoff gegenüber zu deuten. Die beiden Autoren nahmen an, dass atmosphärische Kohlensäure sich mit Wasser im Austauschgleichgewicht befindet, so dass der Sauerstoff in der ersteren um $10 \pm 1\,\gamma$ schwerer als gewöhnlicher Wassersauerstoff ist. Weiter nahmen sie an, dass die Pflanzen bei der Assimilation zwei O-Atome von CO_2 und ein O-Atome von H_2O aufnehmen und daraus ein Molekül von Sauerstoff an die Atmosphäre zurückgeben, so dass das übriggebliebene eine Sauerstoffatom in der Pflanzensubstanz Verwertung findet. Die Assimilationsreaktion verläuft demnach gemäss dem Schema (1).

$$\overset{*}{C}O_2 + H_2O = CH_2(2/3\ \overset{*}{O} + 1/3\ O) + (2/3\ \overset{*}{O} + 1/3\ O)_2 \qquad (1)$$

Unter dieser Annahme ergibt sich sofort, dass sowohl der Sauerstoff im gebildeten Kohlenhydrat (CH_2O) als auch im abgegebenen Sauerstoffmolekül (O_2) schwerer als gewöhnlicher Wassersauerstoff sein muss und zwar beide um $7 \pm 1\,\gamma (= 10 \times 2/3 + 0 \times 1/3)$. Diesen letzten Wert benutzten die beiden Autoren dazu, um den Dichteunterschied zwischen Luft- und Wassersauerstoff ($7\,\gamma$) zu deuten.

Nach dem oben angegebenen Chemismus der Assimilation muss der Sauerstoff im Kohlenhydrat, falls dieser weiter nicht ausgetauscht wird,

(10) C. H. Greene und R. J. Voskuyl, *J. Am. Chem. Soc.*, **58** (1936), 693.

ebenfalls um $7\,\gamma$ schwerer als gewöhnlicher Wassersauerstoff sein. Dagegen fanden wir in der vorliegenden Arbeit den Dichteüberschuss des Sauerstoffs im Zucker gewöhnlichem Wassersauerstoff gegenüber nur $5 \pm 1\,\gamma$. Die Diskrepanz zwischen diesen beiden Werten kann man eventuell durch den weiteren Austausch der O-Atome im Zucker gegen etwa die des Wassers erklären. Schliesst man aber diese Möglichkeit aus, so lässt sich der Unterschied auch wie folgt erklären: Man könnte z.B. annehmen, dass bei der Assimilation nicht die sämtlichen O-Atome von Kohlensäure und Wasser, sondern nur die Hälfte der O-Atome aus Kohlensäure, dagegen alle O-Atome aus Wasser von den Pflanzen aufgenommen werden, wie das Schema (2) zeigt.[11]

$$\begin{aligned} \overset{*}{C}O_2 + H_2O &= \quad \overset{*}{O} \quad + \quad C\overset{*}{O}\cdot H_2O \\ CO\cdot H_2\overset{*}{O} &= CH_2(1/2\ \overset{*}{O} + 1/2\ O) + (1/2\ \overset{*}{O} + 1/2\ O) \\ \hline \overset{*}{C}O_2 + H_2O &= CH_2(1/2\ \overset{*}{O} + 1/2\ O) + (3/4\ \overset{*}{O} + 1/4\ O)_2 \end{aligned} \qquad (2)$$

Aus diesem Reaktionsschema findet man ohne weiteres, dass der Sauerstoff im gebildeten Kohlenhydrat um $5 \pm 1\,\gamma\,(= 10 \times 1/2 + 0 \times 1/2)$, dagegen der im abgegebenen Sauerstoffmolekül um $8 \pm 1\,\gamma\,(= 10 \times 3/4 + 0 \times 1/4)$ schwerer als gewöhnlicher Wassersauerstoff sein muss. Der erste Wert stimmt offenbar mit dem im Versuch III von uns für Zucker experimentell gefundenen $(5 \pm 1\,\gamma)$ und der letztere mit dem bekannten Dichteunterschied $(7 \pm 1\,\gamma)$ zwischen Luft- und Wassersauerstoff hinreichend gut überein.

Bei der Verbrennung des Kohlenhydrates, der Gegenreaktion der Assimilation, treten dagegen die sämtlichen O-Atome in demselben gleich in der Reaktion ein, wie das Schema (3) zeigt.

$$CH_2\overset{*}{O} + O_2 = C(1/3\ \overset{*}{O} + 2/3\ O)_2 + H_2(1/3\ \overset{*}{O} + 2/3\ O) \qquad (3)$$

Nach diesem Reaktionsschema (3) muss das Wasser, das bei der Verbrennung des Zuckers in Luft gebildet wird, um $7 \pm 1\,\gamma\,(= 5 \times 1/3 + 7 \times 2/3 + 1)$ schwerer als gewöhnliches Wasser sein, weil der Sauerstoff im Zucker um $5\,\gamma$, der in Luft um $7\,\gamma$ und der Wasserstoff in Zucker um $1\,\gamma$, alles in der Form von Wasser gemessen, schwerer als der Sauerstoff bzw. Wasserstoff in gewöhnlichem Wasser ist. Der so be-

(11) Prinzipiell diesähnlicher Chemismus der Assimilation wurde schon so früh wie 1870 von A. v. Baeyer (*Ber.*, **3** (1870), 63) angegeben. Nach ihm verläuft die Reaktion nach dem folgenden Schema:

$$CO_2 = CO + O,$$
$$CO + H_2O + O = O_2 + H\cdot COH.$$

rechnete Wert ($7 \pm 1\,\gamma$) stimmt mit dem im Versuch I experimentell gefundenen gut überein. Falls man dagegen zur Verbrennung des Zuckers, wie im Versuch II, den elektrolytischen Sauerstoff benutzt, dessen Dichte um $1.6\,\gamma$ kleiner als gewöhnlicher Wassersauerstoff ist, dann kann das dabei gebildete Wasser nur um etwa $1 \pm 1\,\gamma (= 5 \times 1/3 + (-1.6) \times 2/3 + 1)$ dichter als gewöhnliches Wasser sein. Dieses Resultat stimmt wieder mit dem im Versuch II experimentell gefundenen gut überein.

Zum Schluss sprechen wir der Nippon Gakujutsu-Shinkohkai (der Gesellschaft zur Förderung der japanischen Wissenschaft) sowie der Hattori-Hohkohkai (der Hattori-Stiftung) für ihre finanzielle Unterstützung bei Ausführung dieser Versuche unseren wärmsten Dank aus.

Physikalisch-chemisches Laboratorium
der Kaiserlichen Universität zu Osaka
und
Schiomi-Institut für physikalische
und chemische Forschung.

Experimental Studies on the Electrochemical Polarisation Produced in the Cylindrical Mass of Litharge. I.

By Takewo TIKU.

(Received January 4, 1938.)

Introduction. It is well known that the oxides of lead in pasted state applied to the metal grid of lead or lead-antimony alloy are electrolytically transformed into the positive or negative active materials of the lead storage cell in dilute sulphuric acid solution. The above procedure is called the formation of pasted plates. As the negatives are grayish and the positives dark-brown or black, while litharge is yellow, the paste at the initial or final stage of the formation can be easily distinguished. In the intermediate stage of the formation of plates, it is observed that the paste in grids consists of two parts of different colours, displayed by litharge and by the positive or the negative material. The boundary between the two parts is to be regarded as the front of the formation. In the case of the negatives the front progresses from near the surface

of the paste, but in the case of the positives it starts from comparatively deep portion of the paste and reaches the surface at the end. From these features of the progress of the formation, the existence of some definite distribution of the electrochemical condition should be expected in the mass of litharge in the electrode plate.

The author intended to study the electrochemical polarisation in the mass of pasted litharge applying the direct electric potential through it, without using any metal electrodes attached to it.

Method of Producing Polarisation in the Mass of Litharge. In order to produce the positive and negative polarisations of the same kind as in the lead storage cell, the pasted mass of litharge must be placed in dilute sulphuric acid solution between two electrodes leading direct electric current. But, if the two electrodes are bridged with the electrolyte in any way, the portion of electric current passing through the mass of litharge shall be very small and the polarisation can hardly occur in it. In order to avoid this difficulty, a glass tube of moderate length was stuffed in its middle position with the pasted mass of litharge and the cavities at both sides of the mass were filled with dilute sulphuric acid solution, as is shown in Fig. 1. The pasted mass of litharge in the glass

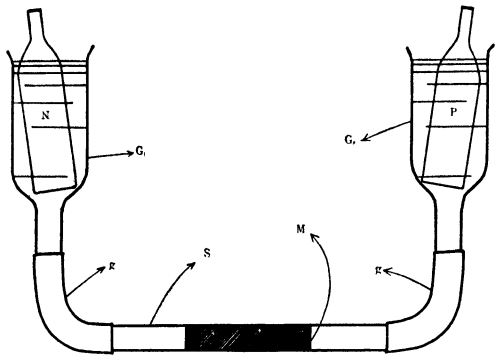


Fig. 1.

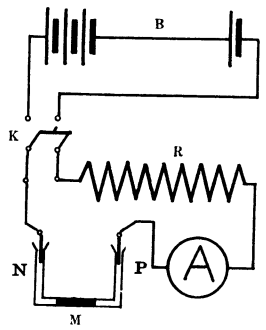


Fig. 2.

tube has a cylindrical form, its two bases being perpendicular to its axis. The length of the cylindrical mass was varied in the range of several centimeters.

In Fig. 1, S is the glass tube mentioned above, which was horizontally supported. M is the pasted mass of litharge. G_1 and G_2 are also glass tubes, supported nearly vertically, and connected to the both ends of S with rubber tubing g. Dilute sulphuric acid was poured into G_1 and G_2 and the small battery plates P and N were introduced as electrodes. The

mass M is thus sandwiched by the electrolyte. Direct electric potential was applied between P and N in the manner as shown in Fig. 2. B is a high tension battery, the voltage (v) of which is applied through the ohmic resistance R(8400 ohms) and the ammeter A when the key K is closed.

The pasted mass was made by mixing litharge powder and distilled water, the water being dropped on the powder till the paste attained the desired degree of stickiness. The consumption of the water was about 10% of the litharge in weight in every case. The litharge was put into the glass tube (the inner diameter about 0.7 cm.) as soon as possible and then the potential was applied. Density of the electrolyte used was about 1.20 at ordinary temperature. The value of v was about 66 volts.

After several hours application of v, chemical changes were observed to develop as follows. Around the positive end of the cylindrical mass several spots of grayish colour appeared in the field of buff colour and then the spots grew to be connected into each other. About this time dark brown and rather diffuse spots appeared at the negative side certain distance apart from the above. Then dendroidal figures began to grow from the former toward the latter and the latter proceeded to spread toward the more negative side. A typical appearance of patterns thus obtained are as drawn in Fig. 3. In Fig. 3, B is the former figure and

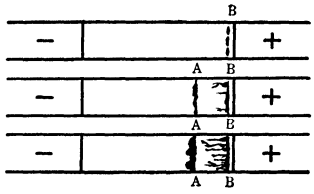


Fig. 3.

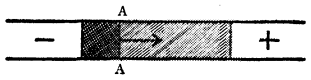


Fig. 4.

A the latter. Materials formed at A and B are ascertained to be lead-peroxide and lead respectively. These changes from litharge are of the same nature as in the formation of positive and negative electrodes of the lead storage cell, the electrolysis taking place in the mass itself.

Phenomena Observed before the Polarisation Patterns are Formed. In a few minutes after the application of the potential v, it was found that the colour of the negative end region of the mass turns slightly reddish, and this region spreads toward the positive side (Fig. 4). It was easily observed from the displacement of the boundary $\overline{AA}$ between two regions

of different colours toward the positive side. The average direction of the boundary $\overline{AA}$ appeared almost perpendicularly to the axis of the cylinder.

The velocity of $\overline{AA}$ diminished with time, and the displacement of $\overline{AA}$ became scarcely observable at the position certain distance apart from the positive end of the cylinder. Soon after, the polarisation patterns began to appear and the positive figure of the patterns appeared at the position of $\overline{AA}$, i.e., A in Fig. 3 is the place where $\overline{AA}$ ceased to move.

The current passing through the mass varied with time though the applied voltage v had nearly a constant value. This is shown in Fig. 5, the ordinate being the current, and the abscissa being the time after the application of v. The current gradually decreased with time at the beginning and reached minimum value within 10–90 minutes. At the next increasing stage, the fluctuation of current was so frequent that secure readings can hardly be obtained. It was during this period when

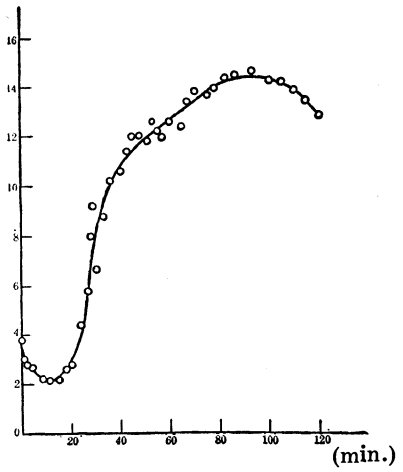


Fig. 5.

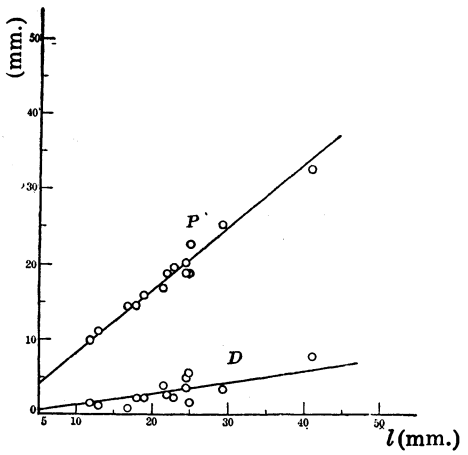


Fig. 6.

the polarisation patterns began to appear. After almost all the patterns shown in Fig. 3 were formed, the current did not change so much and maitained certain values for a while. The order of the currents was about several milliamperes.

On the Polarisation Patterns. It was experimented with several samples of different lengths. Apparent density of the mass in the glass tube before the application of the voltage was about 6.0 in every case. It was found that the position A where the positive figures are formed, was more distant from the positive end of the mass when the length l was larger. While the negative figures were formed at practically same posi-

tion near the positive end, within the range of a millimeter. The relative position of A with respect to l, can be known from Fig. 6. Here, P is the distance of A from the negative end of the mass, and D is the distance between A and B in Fig. 3. From the figure, it may be recognized that points showing P and D respectively distribute on a straight line. The inclinations of the lines for P and D are 0.83 and 0.14 respectively. These are the average values of P/l and D/l which are independent of the length. The above fact shows that the relative position where the positive figure of the polarisation pattern is formed is definite amount apart from the both ends of the cylindrical mass.

The type of the development of positive and negative patterns of the polarisation already described was observed to be similar to that of the Lichtenberg figure. But the dendroidal development of the positive Lichtenberg figure was observed in the negative patterns in our case and the positive patterns were alike the negative Lichtenberg figure. The dendroidal development of the negative patterns corresponds to the phenomenon observed in the negative deposition of metals in electrolysis.

The electrochemical patterns already described are not a superficial phenomenon occurring at the boundary between the mass and the glass tube. The cylindrical sample was cut perpendicularly to the axis and the sectional surface was examined. The results are as follows. (1) In the parts of $\overline{AA}$ and $\overline{BB}$ in Fig. 3, the positive or negative formation was completed over the whole sectional surface. (2) In the part between $\overline{AA}$ and the positive end, the polarity of the formation was positive or negative, and the pattern of either dull-grayish or dark-brown colour was found as spots in the sectional surface. In many cases, the positive was only of single big spot, while the negative was of several small ones. (3) In the part between $\overline{AA}$ and the negative end, no polarisation was found.

Observations with Different Kinds of Litharge and under Varied Conditions. Further experiments on the effects of the modification of litharge, the diameter of the mass, and the terminal voltage V upon the value of P/l were undertaken. The same experimental arrangement as before was used, and in addition to this a voltmeter (resistance 10000 ohms) was shunted between the electrodes to know the value of V. Estimation of P was made as follows in this case. After the polarisation patterns appeared, thin cerophane paper was fastened just around the glass tube and perspective figures of the patterns were drawn on the paper. Then the paper was taken off, spread in a plane and the average value of P was determined by rounding off the irregularities around the mass.

It was noticed that the value of P/l was not always 0.83, but it

varied in wide range under the same experimental conditions, according to the sample used. Litharge is found at ordinary temperature in red, yellow and buff modifications,[1] intermediate ones being often met with in commercial samples. Five different samples were examined in the experiment and the results obtained with them are as shown in Table 1.

Table 1.

Symbols for the different kinds of litharge	Colour of the powder	P/l	Remarks
(D), (C)	light greenish yellow	0.9	
(E)	yellowish red	0.2	
(A)	yellowish brown	0.6	for the battery use
(K)	yellow	0.8	"Bleioxyd—Kahlbaum zur Analyse"

The length and sectional diameter of the pasted cylindrical mass were about 23 mm. and 7 mm. respectively, the applied potential v was 110 – 120 volts. In pasting, 10 g. of the samples were taken and the necessary quantities Q of mixing water dropped into were as follows; 0.7 – 0.8 c.c. for (D) and (C), 1.15 c.c. for (E), 0.85 c.c. for (A), and 1.10 c.c. for (K). The room temperature was about 17 – 20°C. and the relative humidity about 70%. At the above compositions[2] the pastes attained the same degree of stickiness.

The apparent densities of them in the glass tube before the formation were about, 6.5 – 7.0 for (D) and (C), 6.5 for (E), 6.8 – 7.3 for (A), and 6.2 for (K) respectively.

From Table 1 it is known that the value of P/l is comparatively large with rather yellowish litharge, and small with reddish one. And this means that the boundary $\overline{AA}$ does not reach so near the positive end of the mass in the case of the reddish litharge, as for yellowish one. The samples (D) and (C) could not be distinguished by their appearance. The values of P/l for them were roughly 0.9 as shown in the Table 1. Precisely, the value for (C) was about 0.89, for (D) about 0.93, and the polarisation patterns in (C) appeared more elegantly than in (D). The sketches of the figures are shown in the next page.

(1) J.A. Smythe, "Lead," 234, (1923).

(2) In the previous work Q was 10% of the litharge, and the sample was rather reddish or brown.

The differences in the values of P/l for different samples will be considered to be the combined effect of the size of the particle, crystal form, purity and so on.

With the sample (C) described in Table 1, the polarisation phenomena were examined at different lengths and diameters of the mass and at varying series resistances. The composition of the paste was 10 g. of litharge and 0.7–0.85 c.c. of water. Applied voltage v was 110–120 volts.

(1) *Length.* Nineteen specimens of different lengths, 7.5–5.10 mm., were submitted to formation. Glass tubes for them were so chosen as the inner diameters were about 7.0 mm. The apparent densities were about 7.0.

The polarisation figures drawn on cerophane papers are shown in Fig. 7. Numerals in the nineteen figures are the lengths for themselves. The upside of each figure is the positive side. So the upper patterns are of negative and the lower zigzag patterns are of positive in each figure,

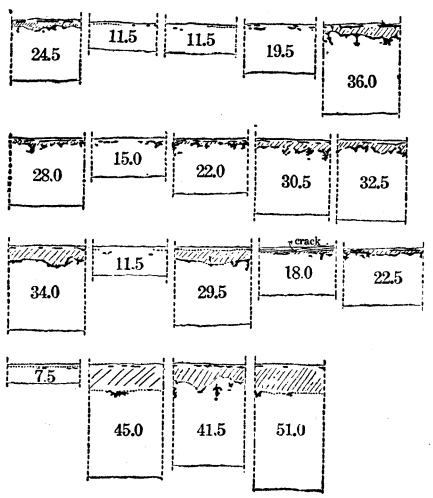


Fig. 7.

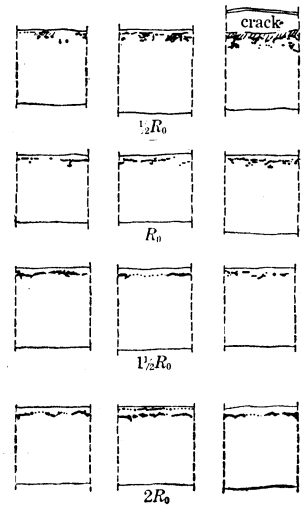


Fig. 8.

and dotted lines are the boundary $\overline{AA}$ where the patterns did not yet appear. The average values of P in these figures are plotted against the length l in Fig. 9. There exists a linear relationship for most points between P and l, which is represented by the straight line (1) in the figure. Several points, however, may be connected with the other straight line (2) also shown in the figure. The above straight lines pass through the origin. P/l estimated from (1) is 0.87, and from (2) is 0.78.

(2) *Thickness.* Thirteen kinds of the glass tube, the inner diameters of which were varied in 2–10 mm., were used to examine the effect of the thickness of the sample. The preparation of the specimens was the same as above. The length was about 25 mm. The value of P/l was about 0.9 or less in the average, and it showed a slight tendency to decrease with diminishing diameter. It would be the effect due to the fact that the apparent densities of the mass were found to diminish with increasing diameter. P/l may be affected by the hardness of the mass.

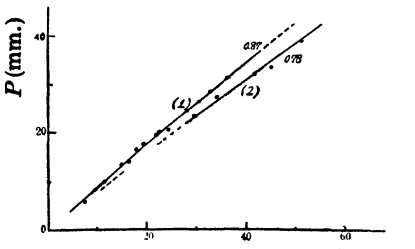


Fig. 9.

Table 2.

Value of series resistance	Time at maximum V (min.)	Maximum value of V (volts)
$1/2\ R_0$	5–10	80
R_0	15–25	62
$1\,1/2\ R_0$	20–30	50
$2R_0$	30–50	40-45

(3) *Series resistance.* Terminal voltage V and the current through the mass are changed by the value of the external series resistance R. R was 8400 ohms in the above experiments. The four cases when R was $\frac{1}{2}R_0$, R_0, $1\frac{1}{2}R_0$, and $2R_0$ (R_0=8400 ohms) were tested. The lengths and the diameters of the samples were 26–32 mm. and 6.5–6.7 mm. respectively. P/l took nearly the same value, about 0.9, in four cases. The polarisation patterns, however, grew rather finely as seen in Fig. 8 which was drawn in the same manner as Fig. 7 and their progress became slower at higher resistances. It would be due to the lowering of the field in the mass. The characteristic between V and the time changed with the series resistance as shown in Table 2.

Summary.

Litharge powder was mixed with distilled water and turned to pasted form. This was stuffed in glass tubes of moderate length at their middle portions, and direct electric current was passed through the mass. Positive and negative patterns due to electrolytic polarisation was produced in the mass facing each other at definite positions in the axial direction of the cylindrical mass, the position of the negative being near the positive end of the mass. The ratios of the distance P of the positive position from the negative end to the length l of the mass were found to be independent of the length in the average.

The value of P/l is affected by the modification of litharge, but not by the diameter, the length of the mass and the terminal voltage.

In conclusion, the author wishes to express his hearty thanks to Prof. M. Katayama of the Tokyo Imperial University for the interest in this work and the encouragement through the course of the experiment, and to Asst. Prof. D. Nukiyama of the University for his kind advices on this investigation.

Toyoda Research Laboratory, Imperial Invention Society,
Shimomeguro, Tokyo.

On the Catalytic Decomposition of Hydrogen Peroxide by Colloidal Platinum-carbonyl.

By Isamu SANO.

(Received November 25, 1937).

There have already been published a number of reports[1] on the catalytic decomposition of hydrogen peroxide by colloidal platinum. In the previous paper,[2] the author described the formation and behaviour of the platinum-carbonyl sol of red colour obtainable from the aqueous solution of chloroplatinic acid by the action of carbon monoxide. The present paper deals with the experiments on the catalytic decomposition of hydrogen peroxide by the colloidal platinum-carbonyl mentioned above and the colloidal platinum obtainable from it.

On passing carbon monoxide through the aqueous solution of chloroplatinic acid at ordinary temperature for some time, the colour of the solution changes from yellow to red, the platinum carbonyl sol being thus obtained. By dialyzing or standing in the air the red sol, it turns black to produce a platinum sol as prepared by Bredig's method.

---

(1) G. Bredig and M. v. Berneck, *Z. physik. Chem.*, **31** (1899), 258; G. Bredig and K. Ikeda, *Z. physik. Chem.*, **37** (1901), 1; T. S. Price and A. D. Denning, *Z. physik. Chem.*, **46** (1903), 89; D. A. MacInnes, *J. Am. Chem. Soc.*, **36** (1914), 878; M. A. Heath and J. H. Walton, *J. Phys. Chem.*, **37** (1933), 977, etc.

(2) I. Sano, this Bulletin, **9** (1934), 320.

Experimental. The hydrogen peroxide solution was obtained from "Oxyfull" by distillation under reduced pressure (50–60 mm. Hg, 85°C.) in a thoroughly steamed hard glass system, diluted with water to 20 times of volume and kept in a Pyrex flask. The reaction was carried out at 30.0°C. in a Erlenmeyer flask which was cleaned and steamed before use. Ninty-five c.c. of the hydrogen peroxide solution was placed in the flask, a definite volume of the red or black sol was added to it, and the solution thoroughly mixed by shaking. At the desired intervals of time, 5 c.c. was taken out from it, added to a mixture of 50 c.c. of water and 10 c.c. of dilute sulphuric acid (1:3), and titrated with a 0.10 N potassium permanganate solution. The sol added as catalyst, red or black, was inferred from calculation to contain 0.075 grams of platinum in one liter.

The results obtained are given in Tables 1, 2, 3, 4 and 5, where t denotes the time elapsed from the beginning in minutes, c the volume of the potassium permanganate solution equivalent to 5 c.c. of the reacting solution at time t in c.c. and k the velocity constant in the formula for unimolecular reaction, $k=(1/t)\log(c_0/c)$, c_0 being the initial concentration. k_p and k_T will be explained later.

Table 1. Five c.c. of red sol was added to 95 c.c. of hydrogen peroxide solution.

t	c	k
0	4.28 (c_0)	—
2	4.39	—
6	4.36	—
10	4.28	—
16.25	4.29	—
23.25	4.28	—
30	4.31	—
45	4.20	—
55	4.15	(0.000236)
60	4.08	(0.000350)
75	3.94	(0.000480)
90	3.82	0.000544
120	3.72	0.000508
150	3.55	0.000540
180	3.38	0.000569
240	3.16	0.000550
270	3.02	0.000559
450	2.39	0.000562

Table 2. Five c.c. of red sol was added to 95 c.c. of hydrogen peroxide solution.

t	c	k
0	4.31 (c_0)	—
2	4.27	—
6	3.37	(0.0178)
10	2.43	0.0249
18	1.53	0.0249
30	0.79	0.0246
45	0 36	0.0240
60	0.15	0.0243

Table 3a. Five c.c. of red sol was added to 95 c.c. of hydrogen peroxide solution.

t	c	k
0	4.25 (c_0)	—
2	4.24	—
5	4.09	(0.00340)
10	3.74	0.00560
15	3.53	0.00540
20	3.28	0.00565
30	2.90	0.00553
45	2.45	0.00531
75	1.71	0.00527

Table 3b. Two c.c. of red sol was added to 95 c.c. of hydrogen peroxide solution.

t	c	k
0	4.39 (c_0)	—
2	4.49	—
5.5	4.37	—
10	4.32	—
20	4.08	(0.00160)
30	3.93	0.00150
51	3.79	0.00124
60	3.70	0.00123
75	3.55	0.00123
90	3.43	0.00118
120	3.15	0.00120

Table 4a. Five c.c. of red sol was added to 95 c.c. of hydrogen peroxide solution.

t	c	k
0	4.27 (c_0)	—
2.17	4.35	—
5	4.25	—
10	4.30	—
15	4.18	—
20	4.08	—
25	3.91	(0.00152)
30	3.69	(0.00210)
35	3.38	(0.00300)
45	3.09	0.00311
60	2.72	0.00327
75	2.38	0.00339
90	2.06	0.00352
120	1.61	0.00353
150	1.32	0.00340
180	1.05	0.00338
210	0.83	0.00338
240	0.67	0.00335

Table 4b. Five c.c. of black sol (not dialyzed) was added to 95 c.c. of hydrogen peroxide solution.

t	c	k	k_p (p: −0.2)	k_T (γ: 0.0706)
0	4.28 (c_0)	—	—	—
2.2	2.91	0.0762	0.136	0.0322
5.3	1.99	0.0627	0.117	0.0322
12	1.00	0.0526	0.105	0.0333
20	0.54	0.0450	0.096	0.0318
30	0.24	0.0417	0.097	0.0322
45	0.08	0.0384	0.101	0.0318

Table 4c. Two c.c. of black sol (not dialyzed) was added to 95 c.c. of hydrogen peroxide solution.

t	c	k	k_p (p: −0.3)	k_T (γ: 0.0730)
0	4.44 (c_0)	—	—	—
2	3.61	0.0450	0.0683	0.0146
5.25	3.14	0.0287	0.0446	0.0106
10	2.58	0.0236	0.0377	0.0100
20	1.74	0.0203	0.0346	0.0105
30	1.24	0.0185	0.0331	0.0107
60	0.50	0.0158	0.0329	0.0110
123	0.11	0 0131	0.0352	0.0105

Table 5a. Five c.c. of red sol was added to 95 c.c. of hydrogen peroxide solution.

t	c	k
0	4.27 (c_0)	—
2	4.40	—
5	4.31	—
10	4.27	—
15	4.10	—
20	3.76	(0.00275)
30	3.02	(0.00500)
45	2.25	0.00618
60	1.74	0.00658
75	1.41	0.00641
90	1.14	0.00637
120	0.70	0.00654
150	0.46	0.00645

Table 5b. Five c.c. of black sol (dialyzed) was added to 95 c.c. of hydrogen peroxide solution.

t	c	k	k_p (p: −0.3)	k_γ (γ: 0.0523)
0	4.28 (c_0)	—	—	—
2.5	2.90	0.0676	0.107	0.0387
5	2.05	0.0639	0.107	0.0406
10.2	1.11	0.0553	0.106	0.0412
20	0.40	0.0515	0.112	0.0413
30	0.21	0.0436	0.106	0.0364

Table 5c. Two c.c. of black sol (dialyzed) was added to 95 c.c. of hydrogen peroxide solution.

t	c	k	k_p (p: −0.4)	k_γ (γ: 0.0719)
0	4.44 (c_0)	—	—	—
2	3.82	0.0327	0.0426	0.0104
5.1	3.22	0.0274	0.0370	0.0102
10	2.60	0.0232	0.0329	0.0100
20	1.80	0.0196	0.0300	0.0101
30	1.29	0.0179	0.0294	0.0103
45	0.80	0.0165	0.0301	0.0107
60	0.59	0.0146	0.0285	0.0100
90	0.29	0.0132	0.0303	0.0099

The red or black sols added as catalysts in the above experiments are summarized in Table 6.

Table 6. Carbon monoxide was passed through a 0.02% aqueous solution of chloroplatinic acid ($H_2PtCl_6 \cdot 6H_2O$) with nearly a constant velocity throughout the experiment. The red sol thus obtained contains 0.075 grams of platinum in one liter as described before.

Number of table	Time duration during which the gas was continually passed through the chloroplatinic acid solution in hours before the colour change	after the colour change	Time duration during which the red sol was left in the air in hours	Volume of sol added in c.c. red	black
1	0.5	0	2	5	—
2	1	0.5	2.5	5	—
3a	0.5	0.5	3.5	5	—
3b	0.5	0.5	2	2	—
4a	0.5	2.5	0	5	—
4b	0.5	2.5	one night	—	5 (not dialyzed)
4c	0.5	2.5	one night	—	2 (not dialyzed)
5a	0.5	4	0	5	—
5b	0.5	4	one night	—	5 (dialyzed)
5c	0.5	4	one night	—	2 (dialyzed)

Discussion. The above results are graphically represented in terms of the relationship between $\log(c_0/c)$ and t in Fig. 1, 2, 3, 4 and 5. If the catalytic decomposition of hydrogen peroxide by colloidal platinum proceeds in accordance with the formula for unimolecular reaction $-dc/dt = kt$ as exemplified by Bredig and his co-workers, it might be expected, particularly in Fig. 4 and 5, that there should exist a linear relation between $\log(c_0/c)$ and t.

In the case where the red sol is added as catalyst, the apparent concentration of hydrogen peroxide solution remains nearly constant—and sometimes even increases slightly—over a short time of the earlier stage and the reacting solution is of red tint throughout the period, suggesting the sol to exist unchanged. In time, the solution, however, will lose the red colour to become slightly tinged with black, and then, the decomposition reaction begins abruptly and proceeds rapidly. The induction period mentioned above is distinctly shown by the former parts of the curves 1, 2, 3a, 3b, 4a and 5a in Fig. 1, 2, 3, 4 and 5; while the latter

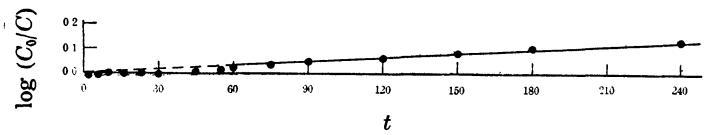


Fig. 1.

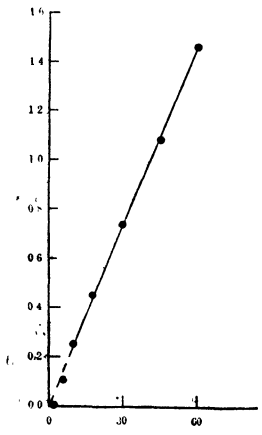


Fig. 2.

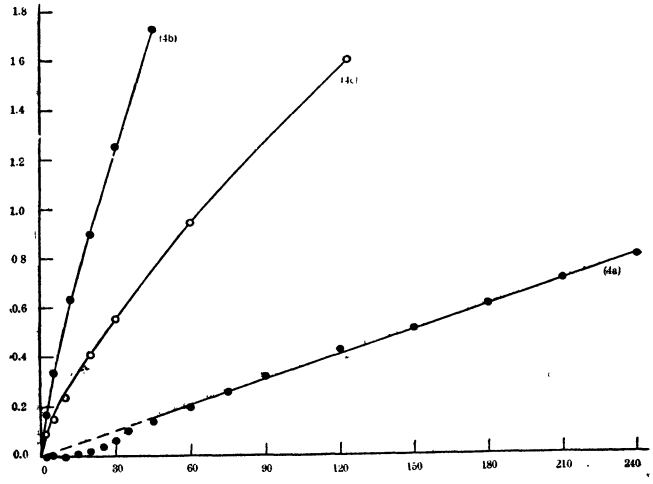


Fig. 4.

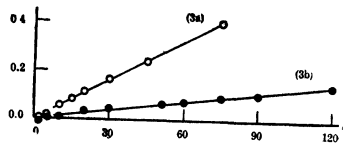


Fig. 3.

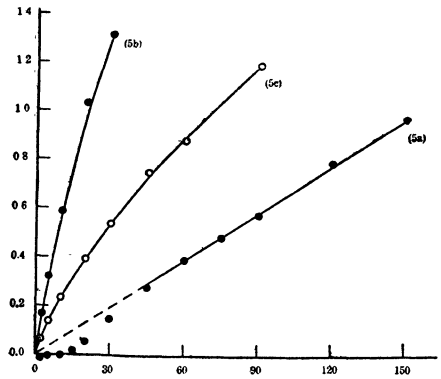


Fig. 5.

parts of these curves are linear and their extension lines passes through the origin, this indicating the reaction to proceed as unimolecular.

On adding the red sol to hydrogen peroxide solution, carbon monoxide considered to be retained in the colloidal particle as its essential constituent may be gradually set free, since the sol is diluted with hydrogen peroxide solution, and on subsequent titration, oxidized with potassium permanganate.[3] The apparent increase in the concentration of hydrogen peroxide solution during the induction period might probably be ac-

(3) J. W. Mellor, "A Comprehensive Treatise on Inorganic and Theoretical Chemistry," Vol. 5, 943.

counted for from such a point of view. Sooner or later, a certain limiting amount of carbon monoxide constituting the particle will be reached, when the particle may be more reasonably regarded as colloidal platinum rather than as colloidal platinum-carbonyl; that is to say, a sol of black colour as prepared by Bredig's method will be formed and hereupon, the induction period will be over.

Carbon monoxide remaining in the particle will, thenceforward, play the part of maintaining the catalytic activity of the colloid unaltered, as it may be considered for the gas either to volatilize from, or to act on oxygen[4] adsorbed by, the surface of the colloidal particle (The influence of oxygen adsorbed by the particle on the catalysis will be discussed below.), and thus render the portion of available surface covered with these free. The fact that, on adding the red sol to hydrogen peroxide solution as catalyst, the decomposition reaction proceeds as unimolecular after it passed through the induction period, may be explained by such a supposition.

In the case where the black sol obtained from the red one is added as catalyst, the decomposition reaction takes place immediately and proceeds rapidly, a curved line, instead of straight, being obtained between $\log(c_0/c)$ and t as shown in Fig. 4 and 5.

The velocity constants for unimolecular reaction k are given in the above tables. The constants, k_p and k_γ, are defined by the formulæ obtained by Freundlich[5] (1) and by the present author (2):

$$-\frac{dc}{dt} = k_p \cdot c^{1-p} \quad \text{or} \quad k_p = \frac{1}{p \cdot t}(c_0^p - c^p) \qquad (p \text{ a constant}) \quad (1),$$

and

$$-\frac{dc}{dt} = k_\gamma \frac{c}{1-\gamma c} \quad \text{or} \quad k_\gamma = \frac{1}{t}\left\{\log\frac{c_0}{c} - \gamma(c_0 - c)\right\} \qquad (\gamma \text{ a constant}) \quad (2).$$

The above-mentioned fact that the reaction deviates from unimolecular may probably be attributed to the retarding influence of oxygen evolved from hydrogen peroxide and subsequently adsorbed by colloidal platinum on the catalysis, subdivided platinum having a definite tendency to absorb oxygen.[6] From this point of view, the above formula (2) has been derived in the following manner: If θ represents the fraction of the available surface covered with molecules of oxygen, it follows,

(4) C. Paal, *Ber.*, **49** (1916), 548.

(5) H. Freundlich, "Kapillarchemie," Vol. 2, (1932).

(6) L. Woehler, *Ber.*, **36** (1903), 3492; C. Paal and C. Amberger, *Ber.*, **40** (1907), 2202; D. O. Shiels, *J. Phys. Chem.*, **33** (1929), 1181, etc.

according to Langmuir,[7] that for equilibrium between the adsorbed layer of molecules of oxygen and those in the surrounding medium, under the assumption that one molecule of oxygen occupies one elementary space of the surface,

$$a\mu(1-\theta) = \nu\theta ,$$

a being the fraction of the number of molecules of oxygen μ striking the surface in unit time which condense and $\nu\theta$ the number of molecules of oxygen which evaporate from the surface in unit time. On the other hand, the rate of decomposition of hydrogen peroxide $-dc/dt$ should be proportional to the number of molecules of hydrogen peroxide μ' striking the surface in unit time; hence

$$-\frac{dc}{dt} = k\mu'(1-\theta) ,$$

k being the velocity constant. Eliminating θ from these, it follows that

$$-\frac{dc}{dt} = \frac{k\mu'\nu}{\nu+a\mu} .$$

Although it might be assumed for μ to be proportional to c_0-c provided the oxygen evolved from hydrogen peroxide was wholly kept in the solution and adsorbed only to a small extent by the particles, the reaction was carried out in an open vessel as described above, and accordingly, it may be assumed for the present under the introduction of a constant β that μ should be proportional to $\beta(c_0-c)$, β being the average fraction of the amount of oxygen evolved which remains in the solution. Considering μ' to be proportional to the concentration of hydrogen peroxide solution c, the velocity of its decomposition should then be given by

$$-\frac{dc}{dt} = k_1\frac{c}{1-\gamma c}$$

which is the formula previously shown. k_1 and γ are the constants containing α, β, ν and k.

As seen in Fig. 4 and 5, the catalytic decomposition of hydrogen peroxide proceeds more rapidly with the black sol than with the red one. This fact may be rendered clear by the following consideration: As already described, the red sol turns black on account of the volatilization

(7) I. Langmuir, *J. Am. Chem. Soc.*, **38** (1916), 2286; **40** (1918), 1361.

of carbon monoxide retained in the particles of the sol and becomes catalytically active during the course of an induction period. The colloidal particles of platinum in the black sol thus formed might be considered to be contaminated with carbon monoxide more profoundly than those in the black sol obtainable by standing in the air over-night or dialyzing the red sol; hence, there should be a difference between the areas of active surface available for catalysis, from which may probably result the diversity in the rate of decomposition.

Summary.

(1) The catalytic decomposition of hydrogen peroxide by colloidal platinum-carbonyl as well as colloidal platinum obtainabe from it was examined.

(2) In the former case, the reaction proceeds as unimolecular after it passed through an induction period, while in the latter case, it deviates appreciaIy from unimolecular throughout the course of the reaction concerned.

(3) Some considerations were made on these facts.

The author wishes to express his cordial thanks to Professor J. Sameshima, under whose kind guidance this work has been carried out. The expense of the present experiments has been defrayed from the Committee on Catalysis in the Japan Society for the Promotion of Scientific Research.

Chemical Institute, Faculty of Science,
Imperial University of Tokyo.

Studies on the Oiliness of Liquids. V. Lubricants Consisting of Two or Three Chemical Compounds.

By Hideo AKAMATU.

(Received November 25, 1937.)

In the preceding papers,[1a][1b] the measurements of the coefficients of static friction of glass surfaces were described when some pure chemical compounds were used as lubricants. The present paper records the results when the lubricants consist of mixtures of chemical compounds.

In conclusion, we observed the good much evidence that a selective adsorption takes place on the friction surfaces. The idea of adsorption has already been applied to the boundary lubrication by some investigators, especially W. B. Hardy[2] to whom we owe the fundamental conception that a semi-polar molecule attaches to the friction surface anchoring itself by means of polar group and presenting to the liquid interface non-polar chain, forming a monomolecular orientated layer.

In the practical engineering, a well known patent "germ process" by Wells and Southcombe,[3] depends on the fact that the addition to mineral oil of small percentage of such compounds as fatty acids that lower the interfacial tension between water and oil gives exceptionally good lubricating values.

Wilson and Barnard,[4] W. G. Wilharm,[5] P. Woog,[6] and W. Bachmann[7] have observed the same results and agreed that there takes place adsorption of lubricant on the surfaces.

Most of these works, however, for the practical purposes, were dealing with the oil, the composition of which are very complex, so that it is difficult to postulate any mechanism. The present work deals with some binary or ternary solutions of pure chemical compounds, and the results

---

(1a) J. Sameshima, M. Kidokoro, and H. Akamatu, this Bulletin, **11** (1936), 659.

(1b) J. Sameshima and Y. Tsubuku, *ibid.*, **12** (1937), 127.

(2) W. B. Hardy and I. Doubleday, *Proc. Roy. Soc.* (London), A, **104** (1923), 25; W. B. Hardy, *Phil. Trans.*, A, **230** (1931), 1; W. B. Hardy and M. Nottage, *Proc. Roy. Soc.* (London), A, **138** (1932), 259.

(3) Wells and Southcombe, *J. Soc. Chem. Ind.*, **39** (1920), 51.

(4) Wilson and Barnard, *Ind. Eng. Chem.*, **14** (1922), 683.

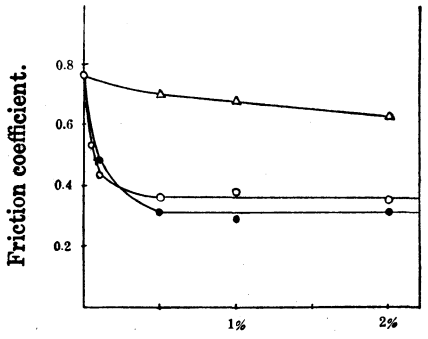
(5) W. G. Wilharm, *ibid.*, **18** (1926), 463.

(6) P. Woog, "Contribution a l'étude du graissage", Paris (1926).

(7) W. Bachmann and Brieger, *Kolloid-Z.*, **36** (1925), 142; **39** (1926), 334.

support the theories described above, suggesting a new point of view on the mechanism.

The method of measuring the static friction and the conditions were the same as described in the preceding paper.[1a] The friction surfaces consisted of a flat glass and a glass with a spherical surface.



△: *n*-Tetradecyl alcohol/Toluene.
○: Oleic acid/Toluene.
●: Palmitic acid/*m*-Xylene.

Fig. 1.

In carrying out the experiments with several binary solutions, it came to light that there was much evidence for tendency of selective character. This selectivity depends chiefly upon the polarity of the substance, and this appears most clearly when the mixture consists of polar and non-polar compounds. For example, when the lubricant is made by dissolving oleic acid ($\mu = 0.29$) in toluence ($\mu = 0.76$), the friction coefficient is nearly identical with that of pure oleic acid, being independent upon the concentration of oleic acid. Table 1 and Fig. 1 show how small amounts of a polar substance in a non-polar solvent is effective for the reduction of the friction of the solvent.

In the preceding paper,[1a] we have reported that the friction coefficient of hexane and nonane are 0.68 and 0.64 respectively. These data have been revised, since the samples formerly used may contain some unsaturated hydrocarbons as impurities. This time, hexane and nonane were shaken with fuming sulphuric acid for several days, dried over sodium metal and then distilled. With such samples, the friction coefficients are somewhat greater, that is 0.85 for hexane and 0.76 for nonane. It is supposed that heptane and octane have also values of this order. So it seems that the small amount of unsaturated hydrocarbons are still much effective. It is true also that the measurement of friction of a hydrocarbon is rather difficult, for it is readily contaminated while the measurements and the friction steps down gradually. Such a difficulty is little for polar compounds.

It is well known that, the molecules have to take orientation in such a manner as to prevent the abruptness of potential difference between the two neighbouring phases. In other words, the interfacial energy between polar compound and underlying solid surface, such as glass or metal, is smaller than that between a non-polar compound and solid sur-

Table 1. Polar solute and non-polar solvent.

Solute	Solvent	Conc. of solute (wt. %)	Friction coefficient
—	Toluene	—	0.76
—	*m*-Xylene	—	0.76
—	liq. Paraffin	—	0.55
—	*n*-Nonane	—	0.76
Oleic acid	Toluene	2	0.35
,,	,,	1	0.38
,,	,,	0.5	0.36
,,	,,	0.1	0.43
,,	,,	0.05	0.53
Palmitic acid	*m*-Xylene	4	0.32
,,	,,	2	0.31
,,	,,	1	0.29
,,	,,	0.5	0.31
,,	,,	0.1	0.48
Palmitic acid	*n*-Nonane	2	0.31
n-Tetradecyl alcohol	Toluene	2	0.63
,,	,,	1	0.68
,,	,,	0.5	0.70
,,	*n*-Nonane	2	0.54
Tripalmitin	*m*-Xylene	2	0.35
,,	,,	1	0.33
Stearic acid	liq. Paraffin	1 *	0.28
,,	,,	0.2 *	0.25
,,	,,	0.05	0.45
Benzoic acid	*m*-Xylene	2	0.59
Benzophenone	,,	3	0.77

(* This is not a true solution, but a mixture.)

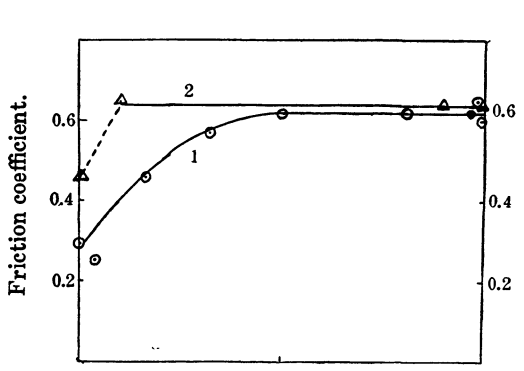
face, so that if such a solution, polar solute and non-polar solvent, be placed on the glass surface (polar) the polar molecules will attach to the surface preferentially with their polar groups facing to the surface, the phenomena will be like that on the water surface. Many investigations[8]

(8) H. N. Holmes and J. B. Thor, "Colloid Symposium Monograph VII," (1930), 213; W. Harkins and Gans, *J. Phys. Chem.*, **36** (1932), 86; J. J. Trillat and R. Vaille, *Compt. rend.*, **202** (1936), 2134.

have been carried out on polar and non-polar adsorption. On the other hand, the experiment on the spreading of liquid on solid surfaces,[9] or the electron diffraction analysis[10] supports this view directly.

It may be said that, in boundary lubrication, the oiliness depends only upon the adsorbed layer and the other part of solution does not impart the friction or oiliness, the non-polar solvent merely furnishing a medium. It seems that oiliness is merely depends on the friction between the surface with such adsorbed layers. Such a adsorption will be a dynamical equilibrium between the solid surface and the liquid in mass, so the orientation of the molecules will not be so complete as that deposited by Blodgett's[11] methods. It is natural, therefore, that the friction of the former is much greater than the latter.[12]

The same idea may be extended to the case when the solvent is also polar, but the phenomena become more complicate. The addition of a small quantity of a fatty substance is not effective generally. The results are shown in Table 2 and Fig. 2.

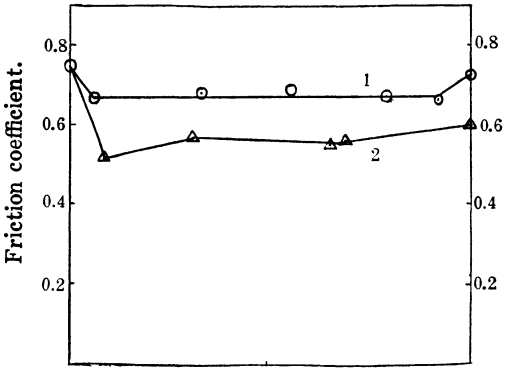


1. Oleic acid.
2. Glycol.

50%
Concentration.

1. Acetic acid.
2. *n*-Propyl alcohol.

Fig. 2 (a).



Water.

50%
Concentration.

1. Ethyl alcohol.
2. Acetic acid.

Fig. 2 (b).

There are some differences in the adsorbabilities or adhesion forces of molecules with active groups. If the adsorbabilities of the molecules composing the lubricant are alike each other, they will be adsorbed similarly and the value of the friction coefficient will be averaged. If, however, there is any disparity, one of them will be adsorbed preferentially

(9) R. Bulkley and Snyder, *J. Am. Chem. Soc.*, **55** (1933), 194.
(10) L. T. Andrew, *Trans. Faraday Soc.*, **32** (1936), 607.
(11) C. Blodgett, *J. Am. Chem. Soc.*, **57** (1935), 1007.
(12) H. Akamatu and J. Sameshima, this Bulletin, **11** (1936), 791.

Table 2.

Component 1	(wt. %)	Component 2	(wt. %)	Friction coefficient
—	—	Acetic acid	100	0.60
Oleic acid	1	,,	99	0.65
,,	2	,,	98	0.63
,,	3	,,	97	0.62
,,	19	,,	81	0.62
,,	50	,,	50	0.62
,,	68	,,	32	0.57
,,	84	,,	16	0.46
,,	96	,,	4	0.25
,,	100	—	—	0.29
Palmitic acid	4	Acetic acid	96	0.6—0.7
,,	2	,,	98	,,
Glycol	10	*n*-Propyl alcohol	90	0.64
,,	90	,,	10	0.65
—	—	*n*-Propyl alcohol	100	0.64
n-Tetradecyl alcohol	1	*n*-Propyl alcohol	99	0.64
,,	2	,,	98	0.66
Benzophenone	1	Glycol	99	.50
Hydroquinone	2	,,	98	0.46
—	—	Glycol	100	0.46
—	—	Dioxane	100	0.61
Palmitic acid	2	,,	98	0.5—0.6
Sebacic acid	2	,,	98	0.62
Ethyl alcohol	100	—	—	0.72
,,	91.6	Water	8.4	0.66
,,	78.8	,,	21.2	0.67
,,	54.7	,,	45.3	0.69
,,	32.4	,,	67.6	0.68
,,	6	,,	94	0.67
Acetic acid	68.4	Water	31.6	0.56
,,	64.6	,,	35.4	0.55
,,	30	,,	70	0.57
,,	8	,,	92	0.52
—	—	Water	100	0.75

and the friction depends on it only. Such a conception may be too simple, since there are many unknown factors affecting the friction. Hardy found, for example, that the temperature coefficient of a mixed lubricant is very complicated, although a single chemical substance has no temperature coefficient of friction. The present experiments were carried out at room temperature, 18–23°C., so the results may be considered as that of the constant temperature.

It has been observed, by some investigators, that the friction would be reduced with the interfacial energy between the lubricant and the friction surfaces, since the film would be stable. Of course, it seems the first essential condition to cover the active surface of the solid by adsorbed molecules. There is found no parallelism, however, between the interfacial energy and the oiliness. Molecules, which have the lower interfacial energy for the friction surface, are adsorbed preferentially by the surface. The friction, therefore, is determined by those surfaces with adsorbed layers, but the order of reducing the friction depends upon the properties of the individual molecules, molecular structure or other unknown properties. If the reducing power of friction is parallel with the stability of the film, the molecules which are adsorbed preferentially, must also be the better lubricant. But the fact is not so. With such a lubricant, as palmitic acid and acetic acid dissolved in *m*-xylene, the friction coefficient is nearly identical with that of acetic acid itself. It seems that acetic acid is adsorbed preferentially, but the molecular structure of acetic acid is not favourable to reduce the friction, in other words, in such a

Table 3. (Solvent: *m*-Xylene)

Solute	(%)	Friction coefficient	Solute	(%)	Friction coefficient
Acetic acid	4	0.49	Benzophenone	2	0.33
Palmitic acid	4		Palmitic acid	2	
Acetic acid	8	0.57	Benzoic acid	2	0.42
Palmitic acid	8		Palmitic acid	2	
Acetic acid	6	0.64	Oleic acid	2	0.64
Palmitic acid	2		Acetic acid	2	
n-Butyric acid	2	0.35	Tripalmitin	4	0.56
Palmitic acid	2		Acetic acid	4	
n-Butyric acid	5	0.31	Tripalmitin	1	0.58
Palmitic acid	5		*n*-Butyric acid	1	

case acetic acid behaves as an inhibitor. When the lubricant is a solution of palmitic acid and butyric acid in *m*-xylene, the friction coefficient is that of palmitic acid itself. When the lubricant consists of tripalmitin and butyric acid dissolved in *m*-xylene, the friction is identical with butyric acid. In those examples, the order of the adsorbability seems as follows; acetic acid, palmitic acid, butyric acid, tripalmitin. Several examples are shown in Table 3.

In conclusion the author wishes to express his gratitude for the kind advices of Prof. J. Sameshima, and for the grant defrayed by Japan Society for the Promotion of Scientific Research.

Summary.

The static boundary frictions were measured when some binary or ternary mixtures were placed on the glass surfaces. The results suggest that: (i) the friction is governed by the surfaces with adsorbed layer of lubricant, and (ii) the reducing power of friction depends upon the individual molecular constitution of the molecules which are adsorbed preferentially by the friction surface, rather than the stability of the film.

Selective adsorption by the glass surface has been investigated, and some examples has been reported.

Chemical Institute, Faculty of Science,
Imperial University of Tokyo.

Studes on the Oiliness of Liquids. VI[1]. Measurements of the Kinetic Friction Coefficients by the Method of Sliding Velocity.

By Tunetaka SASAKI.

(Received December 20th, 1937.)

The present paper describes the measurements of the kinetic friction coefficients by the sliding velocities of a slider on an inclined surface. It is generally accepted, as Amontons's rule, that the frictional force is independent of the contact area of two solids, and is simply proportional to the total pressure or load acting normally to the sliding surfaces. This rule is considered to be applicable to both kinetic and static friction so far as the condition of either dry friction or boundary lubrication is satisfied. In the case of static friction, the conditions of the measurement are relatively simple, while in the case of kinetic friction, it is rather complicated, because the friction is influenced, for instance, by the velocity of a body in motion and temperature rise caused by the friction, etc.

The published results on the influence of velocity on dry friction are rather conflicting. Coulomb pointed out that the velocity has almost no influence upon the dry friction between metals. On the other hand, Galton and Westinghouse,[2] and Smith[3] indicated that the friction decreases profoundly as the velocity increases. Jacob[4] determined the coefficients of kinetic and static frictions from the measurements of the critical angle of the frictional surface and concluded that on the contaminated surfaces the kinetic friction coefficient μ_k differs from the static friction coefficient μ_s considerably and the sliding motion is accelerated, while in the case of clean surfaces, μ_k is equal or nearly equal to μ_s and the motion is uniform.

The reports on the boundary lubrication are also complicated. Deeley,[5] working on boundary lubrication, found that μ_s was independent

(1) The first to fifth reports are published in the following: Sameshima, Kidokoro, and Akamatu, this Bulletin, **11** (1936), 659; Akamatu and Sameshima, *ibid.*, **11** (1936), 791; Sameshima and Miyake, *ibid.*, **12** (1937), 96; Sameshima and Tsubuku, *ibid.*, **12** (1937), 127; Akamatu, *ibid.*, **13** (1938), 127.

(2) Galton and Westinghouse, *Engineering*, **26** (1878), 153.

(3) Smith, Archibutt, and Deeley, "Lubrication and Lubricants," 843, (1927).

(4) Jacob, *Ann. Physik*, **38** (1912), 126.

(5) Deeley, *Proc. Phys. Soc.* (London), **32** (1920), 1s.

of the load and that at slow speeds, μ_k was practically equal to μ_s. On the other hand, Wilson and Barnard,[6] using Deeley's apparatus, observed that μ_k decreased with increasing speed, while Kimball,[7] Jenklin and Ewing[8] showed that at slow speeds μ_k exceeded μ_s and it increased with increasing speeds. Further, Jacob[4] indicated that when the frictional surfaces are separated by oily films, friction obeys the Coulomb's rule, the motion of a body is accelerated on the surface of the inclination exceeding a certain critical angle, and the value of μ_k is independent of the velocity. Recently, Beare and Bowden,[9] using the Deeley machine for measuring μ_k, further studied the problem of friction precisely and determined the constancy of μ_k over the wide range of velocity at various conditions of boundary lubrication.

Apparatus and Measurement. The apparatus employed in the present experiment has been constructed as shown in Fig. 1. In this figure, AB is a glass tube of 3 cm. in diameter and 60 cm. in length. A slider, shown in Fig. 2, has been made of a glass tube of 2 cm. in diameter,

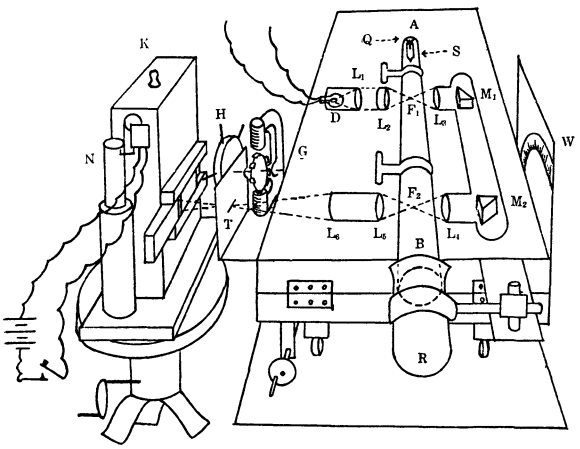


Fig. 1.

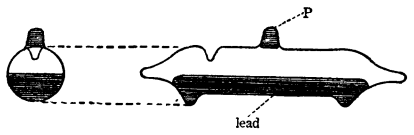


Fig. 2.

which is loaded with lead and carries a small projection P which serves to interrupts the optical paths in the tube AB. Again in Fig. 1, L_1, L_2, L_3, L_4, L_5, L_6, M_1, and M_2 are lenses and total reflexion prisms respectively. By this arrangement, the light from the source D is focussed

(6) Wilson and Barnard, *J. Ind. Eng. Chem.*, **14** (1922), 682.
(7) Kimball, *Am. J. Sci.*, [3], **13** (1877), 353.
(8) Jenklin and Ewing, *Phil. Trans.*, **167** (1877), 509.
(9) Beare and Bowden, *Phil. Trans.*, **234** (1935), 329.

at two points F_1 and F_2 in the tube AB and then, passing through the slit T, interrupted at constant time intervals by the projection H of a cynchronous motor G, it finally enters the time recorder box K, in which a photographic plate is made to slide down vertically, facing the light, with constant speed. The start of the plate is managed by the electromagnet N and a lever. The slider is held by the metal projection Q before its start and it rests, after each run, in the glass tube R containing cotton. The tube is made incline at a desired angle which is subsequently read by the protractor W.

The measurement is carried out as follows. At first the liquid under investigation is poured in the inclined tube, and the lever of the electromagnet N is pressed down to start the photographic plate. Then the slider is set in motion by releasing it from the support Q. Thus, the projection of the slider interrupts, as it runs down, at two points F_1 and F_2 of the optical path from the light source D to the photographic plate. On developing the plate, it gives the image of the line produced by D, having two dark spots caused by the interruption of the slider. At the same time, the cynchronous motor also marks a time scale on the line. Thus the time required for the passage between two points F_1 and F_2 can be measured to the accuracy of 1/50 second and therefore the mean velocity of the slider is calculated. The observations are undertaken at various inclinations of the tube.

In the measurement of the friction, the cleanliness of the sliding surfaces is important and it is necessary to remove the thin films of greasy matter on it. For this account, Hardy[10] paid special precautions for cleaning the surface. In the present experiment the following process has been adopted.[9] The tube is dipped in chromic acid mixture, washed carefully with soap solution, steaming with water vapour for 20 or 30 minutes, further with alcohol vapour for 20 or 30 minutes, and then finally dried by passing dried air through it. The slider is also cleaned by the same process prior to each experiment.

Calculation of the Kinetic Friction. In the present discussion it is assumed that the coefficient of the kinetic friction μ_k is constant and is independent of the sliding velocity, which has been verified in the present investigation. In Fig. 3 and in the following equations S_1 is distance between the starting point Q of the slider and F_1, S_2 distance between Q and F_2, T_1 time required to slide the distance S_1, T_2 time required to slide the distance S_2, m mass of the slider, θ angle of inclina-

(10) S. K. Hardy and W. B. Hardy, *Phil. Mag.*, [6], **38** (1919), 32.

tion of the tube, F driving force acting upon the slider along the tube, $v = 1/(T_2 - T_1)$ the quantity proportional to the mean velocity of the silder, G acceleration of the slider, and g gravity constant.

Then we obtain the following relations:

$$F = mg\sin\theta - \mu_k mg\cos\theta ,$$

$$G = \frac{F}{m} = g\sin\theta - \mu_k g\cos\theta \quad (1),$$

$$S_1 = \frac{1}{2} G T_1^2 \quad (2),$$

$$S_2 = \frac{1}{2} G T_2^2 \quad (3),$$

$$v = \frac{1}{T_2 - T_1} \quad (4).$$

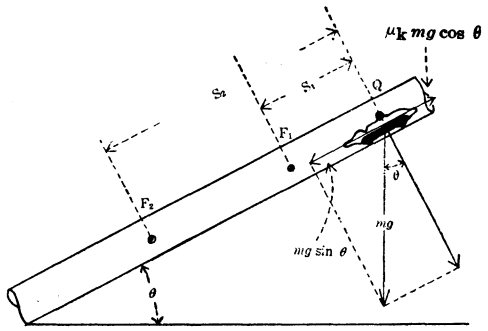


Fig. 3.

Eliminating T_1, T_2, and G from these four equations and expressing μ_k in terms of v and θ, we have the following equation:

$$\tan\theta - \frac{(\sqrt{2S_2} - \sqrt{2S_1})^2}{g} v^2 \sec\theta = \mu_k \quad (5).$$

In this equation the value $(\sqrt{2S_2} - \sqrt{2S_1})^2/g$ is constant and so $\tan\theta$ is linear to $v^2 \sec\theta$. In the figure drawn by plotting $\tan\theta$ against $v^2 \sec\theta$, the point of intersection of the straight line with the axis of $\tan\theta$ gives the value of μ_k.

In order to test the above conclusion several liquids were used to construct the diagram of $\tan\theta$ and $v^2 \sec\theta$. Some typical examples are shown in the following tables and figures. Table 1 and Fig. 4 show the

Table 1. Glycerin.

θ	$\tan\theta$	$T_2 - T_1$ (second)	$v^2 \sec\theta$	θ	$\tan\theta$	$T_2 - T_1$ (second)	$v^2 \sec\theta$
40°	0.838	0.114	100.5	18°	0.324	0.184	31.0
38	0.780	0.112	101.0	16	0.286	0.210	23.5
36	0.726	0.118	88.9	15	0.268	0.216	22.2
34	0.675	0.120	84.8	14	0.249	0.232	20.0
32	0.625	0.124	76.5	13	0.231	0.246	17.0
30	0.575	0.130	68.5	12	0.212	0.278	13.2
28	0.531	0.140	57.9	11	0.194	0.298	11.5
26	0.487	0.140	56 9	10	0.176	0.380	7.0
24	0.445	0.144	52.8	9	0.158	0.420	5.7
22	0.403	0.150	47.9	8	0.140	0.470	4.6
20	0.364	0.166	38.5				

existence of the linear relation between $\tan\theta$ and $v^2 \sec\theta$ as given by equation (5). Most of the other liquids under examination showed the similar results. The angle of inclination of the straight line calculated from equation (5) gives 46°10′ on the scale of diagram employed in Fig. 4. The angles for many liquids range between 40° and 50°. Some liquids deviate from the linear relation, an example of which is shown in Fig. 5.

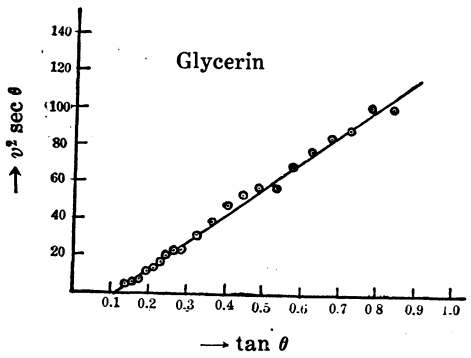


Fig. 4.

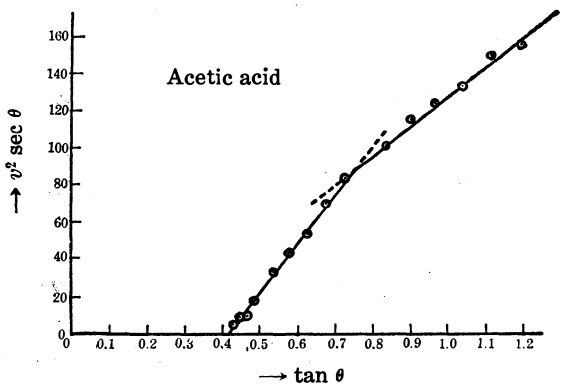


Fig. 5.

Examination of the Experimental Conditions. In order to test the reproducibility and to find the suitable experimental conditions, the following measurements were carried out on glycerin. The results are tabulated in Table 2, which gives the following conclusion. The reproducible value

Table 2.

Experimental conditions	μ_k (Glycerin)
(1) Using new tube of about 1 meter in length and new slider of 76.8 g. in weight.	0.10 0.10 0.09
(2) Using the above tube and slider after both of them have suffered abrasion by repeated experiments.	0.20 — —
(3) Using renewed tube of the same length as in (1) and renewed slider of 60.3 g. in weight.	0.10 — —

Table 2.—(*Concluded*)

Experimental conditions	μ_k (Glycerin)
(4) Using the same renewed tube as in (3) and abrased slider as in (2).	0.10 — —
(5) Using another new tube of 60 cm. in length and the abrased slider.	0.09 0.10 0.11

of μ_k can always be obtained with new tube and new slider, and it is independent of the length of the tube and the weight of the slider ((1), (3), and (5) in Table 2.), as is expected from equation (5). The value of μ_k remains unaltered so far as the glass tube is not abrased. The abrasion of both glass tube and slider increases the value of μ_k. In the present experiment the glass tube was always renewed when the reproducibility of μ_k with standard glycerin failed to exist.

Further it is necessary to start the slider with the force just to overcome the static friction. The excessive force imparts initial velocity to the slider which results the apparent decrease in the value of μ_k as shown in Table 3. In the experiments, pushing forces were controlled by the elastic strength of suitable spring arrangement. Too much force gives even a negative value of μ_k.

Table 3.

Force to overcome the static friction	Apparent μ_k of glycerin
Strongest	—0.03
Strong	0.05
Weak	0.10

Measurement of μ_k. The observed values of μ_k for water, alcohols, hydrocarbons, and fatty acid are tabulated in Table 4.

In the above observations, glycerin sometimes showed convex curves towards $\tan\theta$ axis owing perhaps to its high viscosity. When we plot the values of μ_k for alcohols against the numbers of carbon atoms in their molecules, the gradual decrease of μ_k with increasing numbers of carbon atoms is observed as in Fig. 6. These results may be compared with those of Beare and Bowden[9] or Sameshima and Miyake[1]. The μ_k value of water is large as is expected from the μ_s value of water.[1] The μ_k values

Table 4.

Lubricant	μ_k	Lubricant	μ_k
Glycerin	0.10	Hexane	0.34
Methyl alcohol	0.41	Heptane	0.16
Ethyl alcohol	0.34 (0.39)	Octane	0.24
Propyl alcohol	0.26	Nonane	0.31 (0.27)
Butyl alcohol	0.26 (0.23)	Acetic acid	0.42
Hexyl alcohol	0.15	Water	0.66 (0.69)

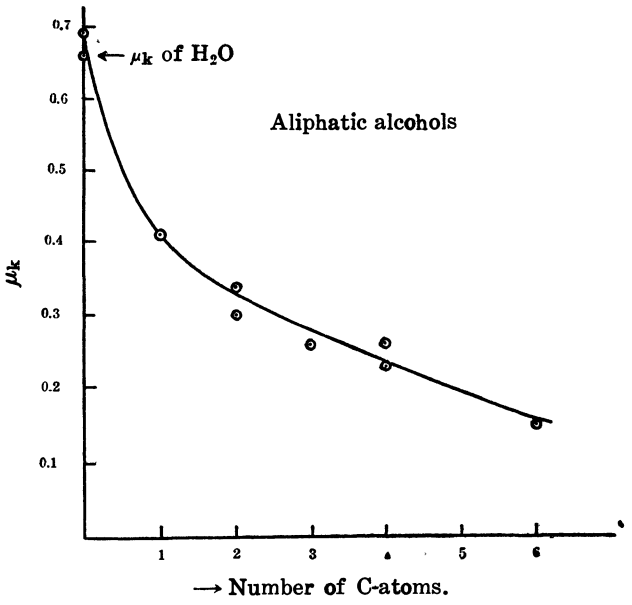


Fig. 6.

of hydrocarbons are irregular with respect to the numbers of carbon atoms in their molecules. Of the μ_k values of fatty acids series, only that of acetic acid was measured.

The author wishes to express his sincere gratitude to Professor J. Sameshima for his kind guidance. The expense for the experiments has been defrayed by a grant given to Professor Sameshima from Nippon Gakujutsu Shinkokwai (Japan Society for the Promotion of Scientific Research), to which the author's thanks are due.

Summary.

(1) Measurements of the kinetic friction coefficient have been made to study the oiliness of liquids. The method consists of the observation of the sliding velocity of a slider on an inclined surface lubricated with the liquid to be tested. Special apparatus has been constructed to measure the sliding velocity.

(2) It is confirmed that the kinetic friction coefficient is generally independent of the velocity over the range of the experiment (up to about 100 cm./sec.), and the following equation holds.

$$\tan\theta - \frac{(\sqrt{2S_2} - \sqrt{2S_1})^2}{g} v^2 \sec\theta = \mu_k$$

where v is the mean velocity of the slider on the surface of the inclination θ. The above equation lacks the viscosity term, so the conditons of the boundary lubrication are considered to be satisfied.

(3) The kinetic friction coefficients of glycerin, aliphatic hydrocarbons, aliphatic alcohols, acetic acid, and water have been measured.

Chemical Institute, Faculty of Science,
Imperial University of Tokyo.

Polymerisation of Tung Oil. I.

By Monzi TATIMORI.

(Received December 4, 1937.)

I. **Introduction.** It is well known that drying oils such as linseed, perilla, and tung oil are used for coating materials after special treatment generally called cooking.

Tung oil[1] is one of the most unsaturated oils and is important in paint and varnish industry. Its iodine value is about 260 as measured by hydrogenation method[2] and its polymerisation velocity is far greater than that of linseed oil. Therefore it has the disadvantage of gelation[3] and there are several devices and patents[4] to avoid it.

Most fatty oils are composed of glycerides of fatty acids such as stearic, oleic, linolic, and linolenic acid and obey the rule of proportionality between iodine value and density.[5] Tung oil, however, is an exception,[6] and it is supposed that the tung oil acids have distinctly different constitutions from that of linseed oil acids. There are many theories[7] on the constitutional formula of α-eleostearic acid, the main constituent of the tung oil acids. At present it is generally accepted that its most probable constitutional formula is

$$CH_3-(CH_2)_3-CH=CH-CH=CH-CH=CH-(CH_2)_7-COOH.$$[8]

The cooking of a drying oil at high temperatures in the absence of oxygen is accompanied by an increase in the viscosity, density, and apparent molecular weight of the oil and by a decrease in iodine value

(1) This oil is obtained from the seed of *Aleurites Fordii*, and is called Chinese wood oil.

(2) L. A. Jordan, *J. Soc. Chem. Ind.*, **53** (1934), 1.

(3) Gelation is the phenomenon that an oil solidifies suddenly and becomes an insoluble and unfusible mass.

(4) H. Brendel, *Farbe u. Lack*, **1932**, 145; H. Hardert, *ibid.*, **1928**, 558.

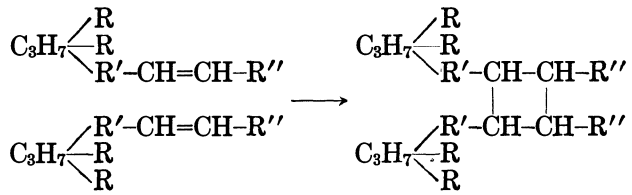
(5) K. Yokota and M. Tatimori, not yet published.

(6) The iodine value of tung oil is ca. 165 by Wijs method and is smaller than that of linseed oil.

(7) M. S. Cloez, *Compt. rend.*, **81** (1875), 469; **82** (1876), 501; **83** (1876), 943; M. L. Maquenne, *ibid.*, **135** (1902), 696; T. Kametaka, *J. Chem. Soc.*, **83** (1903), 1042; Fokin, *J. Russ. Phys.-Chem. Soc.*, **38** (1906), 419; R. Majima, *Ber.*, **42** (1909), 674.

(8) The formula was proposed by Boeseken and Ravensway, *Rec. trav. chim.*, **46** (1927), 619.

and saponification value, unless heat treatment is effected at unusually high temperature. Most authorities agree that these changes are due to the polymerisation of fatty acid radicals, although some investigators propose different hypothesis as to the exact mechanism.[9] According to Rhodes and Welz[10] the polymerisation of tung oil proceeds in the following schema, forming a tetramethylene linkage by the union of a pair of ethenoid groups,



(1).

While Fonrobert[11] supposed that tung oil polymerises after monomolecular reaction as can be concluded from the fact that the decrease in the evolution of heat is too small for bimolecular reaction, when tung oil is diluted by the addition of linseed oil.

It is desirable to study the polymerisation phenomena from the standpoint of chemical kinetics, as few papers have been published along this line. R. H. Kienle[12] studied the kinetics of the baking of tung oil film and found that it proceeds as a first order reaction. While Fuller[13] pointed out that the reaction constant calculated as the first order reaction is not constant, but has a maximum. J. Rinse[14] studied the polymerisation by measuring the refractive index. To compare polymerisation velocity for different temperatures he drew curves of refractive index and temperature, measuring time from the moment when the temperature reached 220°C. neglecting the polymerisation below 220°C. He did not treat the results kinetically. The present author studied the polymerisation of tung oil quantitatively and found that it is a second order reaction.

II. **Experimental Procedure.** An oil bath provided with an electric heater, a stirrer, and a mercury temperature regulator, was filled with

(9) By polymerisation of oil, we mean the result of changes by heating. There may be chances for reactions such as intramolecular and extramolecular polymerisation of glycerides, isomerisations of fatty acid radicals, and cracking and condensation of glycerine radicals.

(10) Rhodes and Welz, *Ind. Eng. Chem.*, **19** (1927), 68.

(11) Fonrobert, *Farben-Ztg.*, **40** (1935), 477, 505, 533, 560, 586.

(12) R. H. Kienle, *Ind. Eng. Chem.*, **22** (1930), 1370.

(13) Fuller, *ibid.*, **23** (1931), 1458.

(14) J. Rinse, *Rec. trav. chim.*, **51** (1932), 529.

soya bean oil and heated. The temperature was kept constant and a three necked 300 c.c. flask, which contained 250 g. of tung oil, was dipped in it and a gentle stream of carbon dioxide was passed over the surface of the oil. When the required temperature was reached the first 10 c.c. of the oil was taken as a sample in a test tube and chilled quickly by inserting it in cold water. The time was measured from that moment. Samples were withdrawn at suitable intervals and the run was continued until finally the oil gelatinised.

The material used had the following constants: density = 0.9418, refractive index $(n_D^{20}) = 1.5191$, iodine value (Wijs method) = 166.8, acid value = 1.8.

III. **Experimental Results.** For each sample density, iodine value, relative viscosity, and refractive index were measured.

Increase in density. The density was measured at 15°C. The results are shown in Fig. 1.

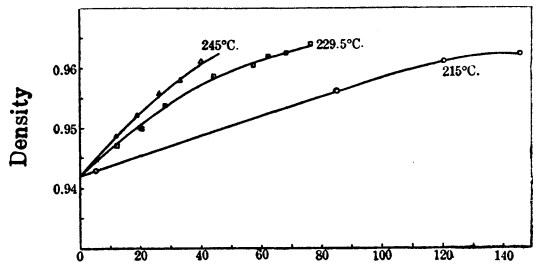


Fig. 1.

Decrease in iodine value. The iodine value is affected by the ratio of halogen solution to oil, by the duration of contact, and by the reaction temperature.

The Wijs reagent used was 0.1 N solution of iodine monochloride, with 2% excess of iodine to chlorine and the temperature was kept exactly at 20°C. during two hours.

If we denote by f the factor of thiosulphate solution for the titration of Wijs solution, by A the number of titration of blank Wijs solution, by B that of actual measurement, and by m the weight of oil, the iodine value is calculated as $(A - B)f/m$ and the ratio Z of halogen solution to oil as Bf/m.

Determinations for each sample were made for two or three values of Z, and the iodine value corrected for $Z = 239.9$ was obtained from the graph of log $[(A - B)f/m]$ versus log Z. The results are shown in Tables 1–3.

Increase in relative viscosity. Samples were dissolved in benzene to 2 and 3% and the viscosity was measured at 30°C. by an Ostwald viscometer described in the previous report.[15] The viscosity constant K_0 was

(15) M. Tatimori, *J. Soc. Chem. Ind., Japan*, **39** (1936), Suppl. binding, 473B.

Table 1. (206°C.)

Time of heating (min.)	Iodine value
0	—
30	163.7
60	158.1
90	154.3
120	150.4
150	147.9
180	144.9
210	141.1

Table 2. (230°C.)

Time of heating (min.)	Iodine value
0	160.6
8	157.8
16	154.4
24	151.7
32	148.7
40	146.8
48	144.6
56	142.3
64	140.1
72	139.2

Table 3. (245°C.)

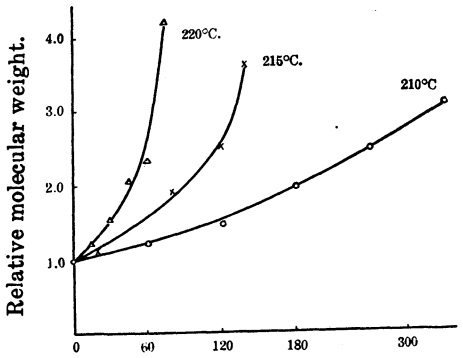
Time of heating (min.)	Iodine value
0	164.1
7	160.2
14	154.0
21	150.6
28	146.8
35	143.0
42	140.6

calculated by

$$\eta_{sp} = \frac{\eta_s - \eta_0}{\eta_0} = K_0C + K_1C^2 \qquad (2),$$

where η_{sp} denotes the specific viscosity, η_0 the viscosity of the solvent, η_s that of the solution, C the concentration, and K_0 and K_1 are constants. The author has already[16] discussed the meaning of K_0. For bodied linseed oil K_0 is approximately proportional to molecular weight.

Assuming K_0 to be a constant relating to the molecular weight of the solute, the relative molecular weight, i.e. the ratio of K_0 of bodied oil to that of raw oil, was calculated from the viscosity data and are shown in Fig. 2.



Time of heating in minutes.
Fig. 2.

Decrease in refractive index. Refractive index was measured by an Abbe refractometer at 20°C. The results are shown in Tables 5–10. The total amount of decrease in refractive index up to gelation is ca. 0.0081 in agreement with the J. Rinse's result.

IV. **Kinetics of Polymerisation.** *Theoretical consideration.* The molecule of tung oil is composed of three fatty acids, each of which having one active center of polymerisation. Therefore two types of polymerisation are possible, intramolecular polymerisation and extramolecular poly-

(16) M. Tatimori, *J. Soc. Chem. Ind., Japan*, **40** (1937), Suppl. binding, 19B.

merisation, and it is known[17] that both occur. In this case polymerisation velocity is given by the superposition of the first order and the second order reaction.

From the study of quantities such as iodine value and refractive index, we obtain the concentration of active radicals instead of that of molecules. In this case the concentration of active radicals should be taken into consideration, so that the polymerisation velocity can be expressed by a second order reaction formula,

$$\frac{dx}{dt} = K_2(a-x)^2 \qquad (3),$$

where x denotes the concentration of polymerised active radicals at time t, a the initial concentration of unpolymerised radicals, and K_2 is a reaction constant.

Then we have

$$K_2t = \frac{x}{a(a-x)} \qquad (4).$$

If we denote by n the refractive index at time t, by n_0 that for $t = 0$, and by n_∞ that for $t = \infty$, then $x = K'(n_0 - n)$ and $a = K'(n_0 - n_\infty)$. By inserting these to equation (4), and putting $K = K_2K'$, we have

$$Kt = \frac{n_0-n}{(n_0-n_\infty)(n-n_\infty)} \qquad (5).$$

Generally the reaction constant can be calculated from equation (5). In reactions such as saponification of esters, n_∞ or the quantity corresponding to it can be obtained by raising the temperature or by prolonging the time of reaction. In this case, the gelation occurs before the polymerisation proceeds to the end, so that the measurement of n_∞ is impossible. This is the difficulty in the kinetical treatment of the reaction. Therefore n_∞ must be calculated. A glance at equation (5) shows that, unknown n_∞ being contained in a quadratic form, it is difficult to calculate the most probable value of n_∞ from the experimental data.

By taking reciprocals of both sides, equation (4) can be transformed as follows,

---

(17) As for intramolecular polymerisation see E. Fonrobert and F. Pallauf, *Chem. Umschau Fette, Öle, Wachse Harze*, **33** (1926), 41; E. Rossmann, *Fette u. Seifen*, **44** (1937), 187. For extramolecular polymerisation see Rhodes and Welz, *Ind. Eng. Chem.*, **19** (1927), 68; Nagel and Grüss, *Wiss. Veröffentl. Siemens-Konzern*, **4** (1925), 284.

$$\frac{1}{aK_2t} = \frac{b}{t} = \frac{a}{x} - 1 \qquad (6),$$

in which a and b are constants.

The relation between $1/t$ and $1/x$ is linear, so that in a graph a straight line should be obtained. This is a conventional method to determine whether a reaction proceeds in the schema (1) or not. a and b can be obtained from the relation of $1/t$ versus $1/x$, and K_2 can be calculated by equation (6).

As an illustration of bimolecular reaction, the decrease of iodine value (at 215°C.) and that of refractive index (at 206°C.) are given in Tables 4–5 and Figures 3–4.

Table 4.

Time of heating (min.)	Iodine value	$\frac{1}{t} \times 10^2$	$\frac{1}{x} \times 10^2$
0	162.6	—	—
20	157.4	5.000	19.23
40	153.0	2.500	10.42
60	149.2	1.666	7.462
80	146.7	1.250	6.289
100	144.9	1.000	5.650
120	142.6	0.833	5.000
140	141.3	0.714	4.695

Table 5. (206°C.)

t	n_D^{20}	$\frac{1}{x} \times 10^{-2}$	$\frac{1}{t} \times 10^3$	K
0	1.5183	—	—	—
30	1.5169	7.14	33.33	0.203
60	1.51575	3.92	16.67	0.201
90	1.51465	2.74	11.11	0.209
120	1.5138	2.22	8.33	0.208
150	1.5130	1.89	6.67	0.210
180	1.5123	1.67	5.56	0.212
210	1.51175	1.53	4.76	0.211
240	1.51115	1.40	4.17	0.215
270	1.5110	1.37	3.70	0.198
				Mean 0.2074

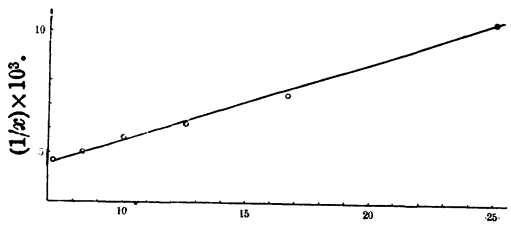


Fig. 3. Relation between reciprocals of iodine value and polymerisation time.

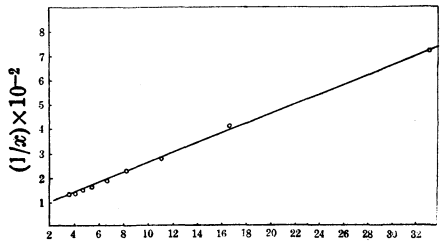


Fig. 4. Relation between reciprocals of refractive index and polymerisation time.

As the accurate measurements of iodine value of polymerised oil are difficult, refractive index is better for the study of the kinetics.

Reaction constants. The changes in refractive index of oils with time at various temperatures can exactly be expressed by equation (6).

Reaction constants were calculated from the refractive index and are given in Tables 5–10.

Table 6. (215°C.)

t	n_D^{20}	$\frac{1}{x} \times 10^{-2}$	$\frac{1}{t} \times 10^{3}$	K
0	1.5159	—	—	—
20	1.5149	10.00	50.00	0.297
40	1.51395	5.13	25.00	0.314
60	1.5131	3.57	16.67	0.324
80	1.5125	2.94	12.50	0.313
100	1.5118	2.44	10.00	0.324
120	1.51125	2.15	8.33	0.326
140	1.5111	2.08	7.14	0.293
				Mean 0.3130

Table 7. (224°C.)

t	n_D^{20}	$\frac{1}{x} \times 10^{-2}$	$\frac{1}{t} \times 10^{3}$	K
0	1.51695	—	—	—
15	1.5157	8.00	66.67	0.432
30	1.5146	4.26	33.33	0.453
46	1.5136	2.99	21.47	0.448
60	1.51275	2.38	16.67	0.466
75	1.5119	1.98	13.33	0.489
91	1.5113	1.77	10.99	0.481
				Mean 0.4614

Table 8. (229.5°C.)

t	n_D^{20}	$\frac{1}{x} \times 10^{-2}$	$\frac{1}{t} \times 10^{3}$	K
0	1.51595	—	—	—
8	1.51505	11.11	125.00	0.658
16	1.51425	5.88	62.50	0.664
24	1.5136	4.26	41.67	0.647
32	1.5130	3.39	31.25	0.644
41	1.5124	2.82	24.39	0.641
45	1.5121	2.60	22.22	0.653
50	1.5119	2.47	20.00	0.632
56	1.5116	2.30	17.86	0.625
64	1.5113	2.15	15.63	(0.605)
				Mean 0.6455

Table 9. (240°C.)

t	n_D^{20}	$\frac{1}{x} \times 10^{-2}$	$\frac{1}{t} \times 10^{3}$	K
0	1.5151	—	—	—
7.5	1.5140	9.09	133.3	0.999
15.0	1.5129	4.55	66.67	1.10
22.5	1.5121	3.33	44.45	1.09
30.25	1.51155	2.78	30.06	1.03
37.5	1.51045	2.41	26.67	1.02
45.0	1.51035	2.11	2.22	1.05
				Mean 1.049

Table 10. (245°C.)

t	n_D^{20}	$\frac{1}{x} \times 10^{-2}$	$\frac{1}{t} \times 10^{3}$	K
0	1.51555	—	—	—
7	1.5142	7.41	142.8	1.26
14	1.51295	3.85	71.43	1.44
21	1.5119	2.74	47.62	1.47
23	1.51115	2.27	35.71	1.41
35	1.5104	1.94	28.57	1.44
4	1.5100	1.80	23.81	1.34
				Mean 1.444

n_∞, n_G, and K are summarised in Table 11, where n_G is the refractive index just before the gelation.

Table 11.

Polymerisation temperature (°C.)	n_∞	n_G	K
245.0	1.5034	1.5100	1.444
240.0	1.5024	1.5104	1.049
229.5	1.5041	1.5113	0.6455
224.0	1.5034	1.5109	0.4505
215.5	1.5026	1.5111	0.3130
210.0	1.5026	1.5111	0.2447
206.0	1.5011	1.5110	0.2074
	Mean 1.5024		

Effect of temperature. The rate of polymerisation was determined at temperatures between 206 and 245°C.

In all cases the whole elapses can be expressed by a bimolecular reaction formula. The relation between reaction constant and temperature is shown in Fig. 5.

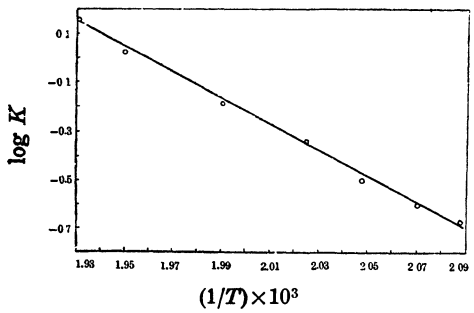


Fig. 5.

Table 12.

t°C.	K	K_1/K_2
240	1.065	1.67
230	0.635	1.62
220	0.392	1.55
210	0.250	

From Fig. 5 it will be seen that a linear relation exists between the logarithm of velocity coefficient and the reciprocal of polymerisation temperature, as can be expressed by the Arrehnius formula,

$$\ln K = C - \frac{Q}{RT} \qquad (7).$$

The values of C and Q were determined as: $C = 5.335$, $Q = 24{,}300$ cal. Temperature coefficient per ten degrees, which has a practical signifi-

cance, was calculated in the temperature range from 240 to 210°C. and is shown in Table 12.

Summary.

(1) Tung oil was polymerised up to gelation at various temperatures from 206 to 245°C. In the course of cooking, density, iodine value, relative viscosity, and refractive index were measured.

(2) Density, iodine value, and refractive index change rather quickly at the beginning but slowly towards the end of polymerisation. The viscosity changes, however, in opposite sense.

(3) The constants of raw oil and of polymerised oil just before the gelation are as follows.

	Raw oil	Polymerised oil
Density	0.9418	0.9631
Iodine value	166.8	140.5
K_0	3.36	13.4
Refractive index	1.5191	1.5109

(4) A new method to obtain the reaction constant is proposed for reactions of the type $A + A \rightarrow A_2$.

(5) This method was applied to the polymerisation of tung oil and the following conclusions were obtained.

(6) The polymerisation is a second order reaction as determined by both refractive index and iodine value.

(7) The polymerisation velocity was calculated between 206 and 245°C.

(8) The heat of activation was found to be ca. 24,000 cal.

(9) The temperature coefficients of the reaction per ten degrees is 1.55–1.67, in the temperature range from 210 to 240°C.

In conclusion, the author wishes to express his sincere thanks to Dr. K. Baba, Mr. T. Yoshioka, and Mr. K. Yokota for their kind guidance.

Laboratory of Hitachi Works, Hitachi Ltd.,
Sukegawa, Ibaraki Prefecture.

A Study of Passivity of Iron Using Electron Diffraction.

By Takeo IIMORI.

(Received December 22, 1937.)

Introduction. Since the discovery of passivity of iron in the eighteenth century, various explanations have been suggested. Lately, through careful experiments and studies, such as the electrolytic isolation of a transparent film by U. R. Evans[1] or the optical observations of L. Tronstad,[2] it has been shown that the phenomenon is definitely associated with a thin protective film on the surface of iron. However, the electron diffration method has not yet given a sufficiently satisfactory result in this study. G. P. Thomson's[3] examination of passive iron in nitric acid does not enable us to determine the composition of the film and the work of E. Rupp[4] merely suggests that the film might be α-Fe_2O_3.

The present author examined iron rendered passive in nitric acid or in a chromate solution by reflective diffraction of electrons from the surface film and also by transmissional diffraction, by first isolating the film. A part of this work has already been reported last year in a paper[5] from the Iitaka Laboratory and the present paper gives further details and also reports on the results of advanced experiments.

The Invisible Film. (a) *Isolation of an invisible film.* The isolation of an invisible film was carried out using the electrolytic method of U. R. Evans. A strip of electrolytic iron (0.15 mm. thick and 1 cm. wide) was cleaned by gentle polishing with emery papers of increasing fineness and then rendered passive by immersing it in a 0.1 N solution of potassium chromate. The passive strip was gently rinsed with water and the end, to be immersed into a 6% solution of sodium chloride contained in an electrolytic cell, was trimmed cross-wise after which it was immersed in the electrolytic bath to the depth of one centimeter. The cell was divided into an anodic and a cathodic section by means of a porous porcelain cylinder. With the passive strip as the anode electrolysis was immediately started, care being taken to maintain the current density constant at 6–7

(1) U. R. Evans, *J. Chem. Soc.*, **127** (1927), 1020.
(2) L. Tronstad, *Nature*, **127** (1931), 127.
(3) G. P. Thomson, *Proc. Roy. Soc.* (London), A, **128** (1930), 657.
(4) E. Rupp, *Kolloid-Z.*, **69** (1934), 375.
(5) I. Iitaka, S. Miyake, and T. Iimori, *Nature*, **139** (1937), 156.

milliamperes per square centimeter throughout the process. And also throughout the electrolysis, fresh sodium chloride solution was continually fed into the cell drop by drop while the excess was overflowed through a siphon. After continuing the electrolysis for some eighteen hours, two transparent, colorless but lustrous films were isolated, one from each side of the strip. The films were carefully scooped up with a piece of fine brass netting and transferred with the netting into water containing a small amount of alcohol and then thoroughly and carefully washed.

(b) *Transmissional electron diffraction by the film.* A piece of the film free from any stain whatsoever was selected, scooped up on a netting and then dipped first into a 50% solution of alcohol and next into a 95% alcohol. After the film was completely dried on a small piece of netting, it was placed with the net into an electron diffraction camera.

The electron beam used was accelerated with about 50 KV. potential (corresponding to about 0.05 Å in wavelength) ; the exact wavelength was determined from the diffraction pattern of zinc oxide used as a reference, the oxide being placed in the camera always ready for use immediately after each exposure.

In many cases, the films gave diffraction patterns composed up of only two or three vague rings attributable only to nearly amorphous substances; however, as shown in Table 1, in a few cases several rings were distinguished.

Table 1. Diffraction patterns of thin films.

Intensity	Spacing of rings (Å)				Indices of planes	Side of unit cube (Å)
	Exp. 1	Exp. 2	Exp. 3	Exp. 4		
m or *w*			4.5	4.6	(111)	8.0
w				2.96	(200)	8.37
s	2.5	2.53	2.54	2.53	(311)	8.43
s or *m*		2.07	2.09	2.08	(400)	8.32
w				1.63	(333), (511)	8.48
s	1.5	1.48	1.49	1.48	(440)	8.35
w				1.39?	(135)	8.45
					Mean	8.40 Å
			X-ray data[6]		8.380 Å for Fe_3O_4 8.322 Å for γ-Fe_2O_3	

(6) G. Hägg, *Z. physik. Chem.*, B, **29** (1935), 102.

The above table clearly indicates that the thin film is composed of either γ-Fe_2O_3 or Fe_3O_4 and not of α-Fe_2O_3. Many previous investigators, on the contrary, assumed the film to be α-Fe_2O_3. The magnetic property of the film, which is ferromagnetic, confirms without doubt the results as in above and proves that the film is either γ-Fe_2O_3 or Fe_3O_4 and also shows that the previous assumption is erroneous.

(c) *Invisible film on polished iron (not passive).* U. R. Evans[1] first ascertained through experiments that an invisible film similar to the one on passive iron also exists on iron polished in air but in this case. the cracks and pores present in the film in countless numbers make it vulnerable to reagents. A piece of non-passive electrolytic iron exposed for several hours to dry air after being polished, also yielded thin films by electrolysis; but in this case, unlike in the passive iron, the film always broke into fragments and were stained badly with rust. It was extremely difficult to select a sufficiently good film for a proper examination of its composition. Diffraction patterns obtained in a few cases were identical with that of Table 1, Exp. 2 or Exp. 1 and show that its composition is the same as that of passive iron.

Reflectional Election Diffraction with Passive Iron. (a) *Iron made passive in concentrated nitric acid.* Examination of iron made passive in concentrated nitric acid gave a result no more revealing than that obtained by G. P. Thomson[3] or E. Rupp.[4] The ring corresponding to 2.6 Å usually showed itself besides the iron pattern and merely indicates the existence of a thin oxide layer of a structure of the type similar to Fe_3O_4. Probably, the oxide layer cannot become any thicker in nitric acid so as to be detectable, because concentrated nitric acid has two properties, that of a strong oxidizer and that of a strong acid. It was observed, as a matter of fact, that iron made passive in a chromate solution after being highly polished, lost its luster and appeared as if etched when left in concentrated nitric acid overnight.

(b) *Iron made passive in potassium chromate solution.* In order to obtain a sufficiently thick protective film for study, potassium chromate solution was selected as the oxidizing reagent which also has the advantage of not dissolving the film. When a polished iron specimen was used, the diffraction pattern indicated no difference from that of non-passive iron; the pattern was identical with that of the invisible film, Table 1, Exps. 1 and 2. On the other hand, when iron etched with concentrated hydrochloric or nitric acid was used, at first a diffraction pattern similar to the one made passive in nitric acid was obtained; but a prolonged immersion in the chromate solution gradually made the iron pattern fainter, finally

turning it into the "Fe_3O_4 pattern". This change took place without any manifestation in the outward appearance of the specimen. (Fig. 2–5).

These results obtained by transmissional and reflectional diffraction of electrons by the protective film clearly indicate that the film on passive iron may be isolated without undergoing any change during the process and that its composition is either γ-Fe_2O_3 or Fe_3O_4.

Supplementary Experiments and Discussion. From examinations made thus far, it can be readily seen that the protective film on passive iron is composed of either γ-Fe_2O_3 or Fe_3O_4 and because the diffraction patterns are similar, it is impossible to make a distinction and consequently some other method must be resorted to in order to make the identification. Hence, the following experiments were carried out:

(a) *Passivity of Fe_3O_4.* When iron coated with Fe_3O_4 by heating in water vapor at 400°C. was immersed in a dilute nitric acid, the oxide coating rapidly dissolved away. On the other hand, when the iron coated with Fe_3O_4 was immersed in concentrated nitric acid, the oxide did not dissolve at all; subsequent immersion in a dilute nitric acid had no effect upon the oxide so treated. Further, treatment of the Fe_3O_4 coating with a chromate solution gave precisely the same result as above. It can therefore be seen that Fe_3O_4 can be rendered passive by treating it with an oxidizing agent. From the diffraction pattern and also from the outward appearance of the oxide film, it is seen that in the above treatment, passivity takes place without visible changes. It naturally follows that the passive state is produced by an oxide having the same diffraction as the superficial layer of Fe_3O_4 previously formed. With due regard of these phenomena, it is conceivable that the protective surface film of passive iron is probably also γ-Fe_2O_3.

(b) *The "unknown primary oxide".* A passive iron giving a good γ-Fe_2O_3 reflection pattern was heated in high vacuum at 600°C. in order to determine whether the oxide will actually transform into α-Fe_2O_3. Instead of this transformation, a very interesting phenomenon took place which is worthy of detailed description here. The heated specimen gave a pattern heretofore unknown among those given by various oxides of iron and in this paper the substance producing the pattern will be referred to as the "unknown primary oxide". This oxide was also obtained in the author's previous work[7] and it was found that its formation took place at a temperature between 200–300°C. or at 500°C. and at a very low pres-

(7) T. Iimori, *Nature*, **140** (1937), 218; *Sci. Papers Inst. Phys. Chem. Research* (Tokyo), **34** (1937), 60.

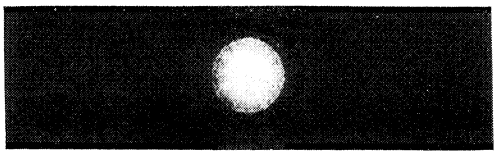


Fig. 1. The best photograph obtained from a protective film of passive iron.

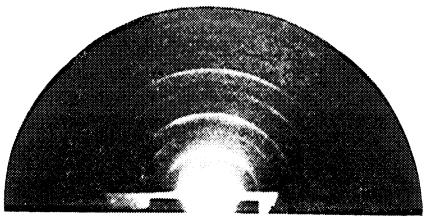


Fig. 2. Iron.

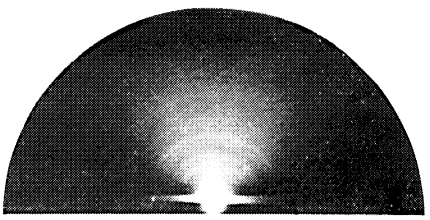


Fig. 5. Passive iron (immersed in a chromate solution 30 days).

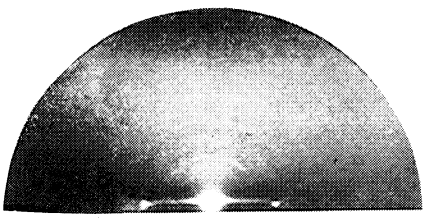


Fig. 3. Passive iron (immersed in a chromate solution 2 hours).

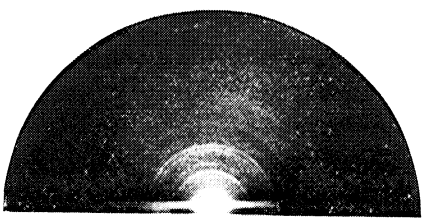


Fig. 6. γ-Fe_2O_3 (formed on etched iron in air at 300°C. and 10 mm.).

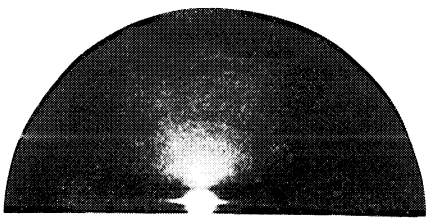


Fig. 4. Passive iron (immersed in a chromate solution 45 hours).

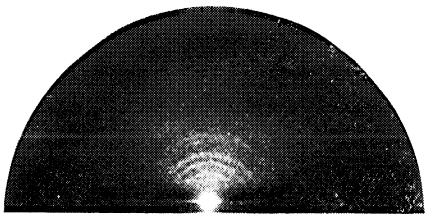


Fig. 7. The "unknown oxide" pattern formed by heating a passive iron at 600°C. in vacuum).

sure. Apparently, the formation of this unknown primary oxide takes place before that of either γ-Fe_2O_3 or Fe_3O_4. In the previous work, the rings obtained were quite vague but in the present case, the pattern was somewhat clearer and the rings identified are shown in Table 2.

Table 2. "Unknown primary oxide."

Spacing of rings (Å)	3.38	2.96	2.53	2.05	1.62	1.48	1.18
Intensity	*s*	*w*	*s*	*s*	*w*	*s*	*m*

Whether the oxide is simple or mixed is yet unknown, moreover, the exact condition favorable to its formation being still quite hazy further consideration cannot be made here. It is supposed, however, that the oxide is formed by the reduction of the protective film by migrating iron atoms.

(c) *Consideration with other experiments.* In the previous paper[7] by the present author, it was reported that the oxide formed on iron at lower temperatures is γ-Fe_2O_3 and the favorable pressure for the formation of Fe_3O_4 approaches that of vacuum as the temperature becomes low. Since the protective film on passive iron is the same as that formed on polished iron by mere exposure to dry air at room temperature, it is obvious that the surface film on passive iron is γ-Fe_2O_3 or, to say the least, some modification of ferric oxide.

Recently, on the basis of electrolytic experiments, U. R. Evans and H. A. Miley[8] are in the opinion that the oxide formed below 200°C. is γ-Fe_2O_3 because although being ferric it seems to be different from α-Fe_2O_3.

W. D. Bancroft and J. D. Porter[9] assumed the protective film on passive iron to be an adsorbed layer of FeO_3 and considered that the transformation from the unstable FeO_3 to the stable Fe_2O_3 occurs during the isolation of the film. But, in view of the fact that diffraction patterns obtained with the isolated film and with the unisolated one are identical, it might follow that the assumption of the existence of a protective film of FeO_3 is superfluous.

In conclusion, the experimental results described above and also their consideration infer that the protective film on passive iron is a layer of γ-Fe_2O_3 forming a perfectly compact covering.

(8) U. R. Evans and H. A. Miley, *J. Chem. Soc.*, **1937**, 1295.
(9) W. D. Bancroft and J. D. Porter, *J. Phys. Chem.*, **40** (1936), 37.

Summary.

The transmissional electron diffraction pattern of the isolated film from passive iron and the reflectional one obtained from iron rendered passive in a chromate solution are in both cases either γ-Fe_2O_3 or Fe_3O_4. Collaborating with the author's previous work and consideration of the passivity of Fe_3O_4, the protective oxide film is believed to be γ-Fe_2O_3.

The author wishes to express his sincere appreciation to Dr. I. Iitaka for his kind guidance and constant encouragement, and to Mr. S. Miyake for his valuable advices and assistance in electron diffraction technique. He also thanks to the Hattori Hôkô Kwai for the financial grant which was used for an improvement of our electron diffraction apparatus.

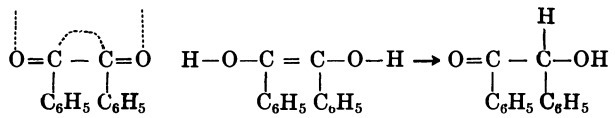
Iitaka Laboratory,
The Institute of Physical and Chemical Research, Tokyo.

Dipole Moments of Benzil and Stilbene Dichloride.

By Ken-iti HIGASI.

(Received December 20, 1937.)

In a famous paper[1] published in 1899, J. Thiele pointed out that benzil might be regarded as having conjugated double bonds. On reduction, its double bonds were supposed to move to the centre, giving an unsaturated glycol, and to prove this view, he succeeded in obtaining the *cis*- and *trans*-forms of the enolic diacetate.



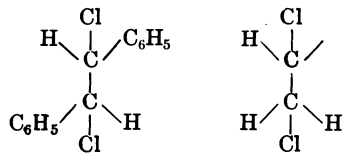
Benzil. Enolic isomer. Benzoin.

Translating this into modern words, the case for benzil may be said as intimately related to single bond-double bond resonance. If the C–C

(1) Thiele, *Ann.*, **306** (1899), 87, 142. See also Waters, "Physical Aspects of Organic Chemistry," 373, London (1935).

single bond aquires a considerable amount of double bond character due to this quantum mechanical resonance, intramolecular rotation should be greatly hindered, and its direct consequence would appear in the temperature independence of dipole moment.[2]

Having this view in mind, the dipole moment of benzil was measured in benzene and carbon tetrachloride at 25 and 50°C. The reason for choosing two different solvents is to check the specific action of solvents.



The dipole moment of α-stilbene dichloride in benzene and carbon tetrachloride was also studied. This substance resembles $CH_2Cl \cdot CH_2Cl$ in structural formula, the only difference being the existence of two C_6H_5 groups instead of two H atoms. From the comparison with the moment of $CH_2Cl \cdot CH_2Cl$ in the corresponding solvent, the effect of introducing big phenyl groups was sought.

Preparation of Materials. *Benzil.* Benzoin was first prepared from benzaldehyde and HCN and then was oxidised to benzil. Material thus obtained was recrystallised from alcohol and then from benzene. M.p. 95°C. Benzil was also synthesised from stilbene dichloride, and the dielectric study on it was made for comparison's sake.

α-Stilbene dichloride. This material was obtained by the addition of chlorine to stilbene (purest) of Fränkel and Landau. Recrystallised from alcohol and then from the mixture of benzene and hexane. M.p. 191°C. At first the material recrystallised from alcohol and dried was examined; and the slightly higher moment of 1.50 D was obtained; this seems to be due to the remaining alcohol.

Benzene, hexane, and carbon tetrachloride. Materials from the Schering-Kahlbaum A. G. and the Nippon Zyunyaku Co. were treated as in earlier work.[3]

Experimental Results. As the apparatus and the method of measurement of the dielectric constant were described in a previous paper,[3][4] only some improvements[5] which were made later will be reported here. In the oscillation circuit which contained the dielectric cell, a tetrode

(2) Kozima and Mizushima, *Sci. Papers Inst. Phys. Chem. Research* (Tokyo), **31** (1937), 296.
(3) Higasi, *ibid.*, **24** (1934), 57.
(4) Mizushima, Morino, and Higasi, *ibid.*, **25** (1934), 159.
(5) Cordial thanks are due to Mr. T. Sibata for his kindness in helping the writer in making these improvements.

bulb "Mazda" UY 236 with a screening grid and an indirectly heated cathode, were employed (Fig. 1.). For the switch which connects the dielectric cell to the oscillating circuit, a pen-form one (Fig. 2.) was used

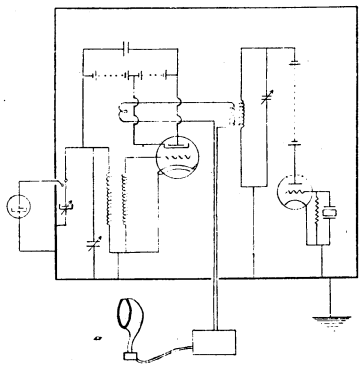


Fig. 1.

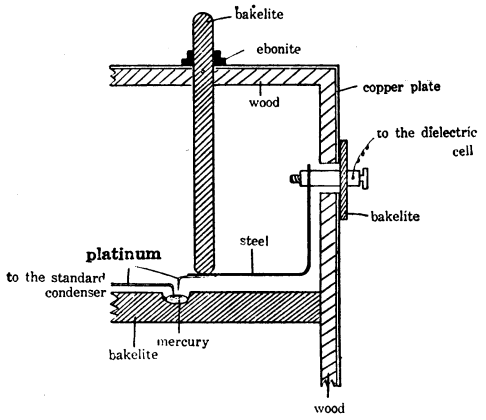


Fig. 2.

in the place of the former. A radio set of ordinary UY 24B, UY 47B, KX 12B type with a slight improvement was satisfactorily utilized for the purpose of amplifying the beat note.

Symbols and formulæ used in this article are as follows:

ω : the concentration of the solute in the gram percentage.

ε, ε_1 : the dielectric constant of the solution and the solvent respectively.

d, d_1 : the density of the solution and the solvent respectively.

p_{12}, p_1 : the specific polarization of the solution and the solvent,

$$p_{12}=\frac{\varepsilon-1}{\varepsilon+2}\cdot\frac{1}{d} \quad \text{and} \quad p_1=\frac{\varepsilon_1-1}{\varepsilon_1+2}\cdot\frac{1}{d_1}, \quad \text{respectively.}$$

P_2 : the molar polarization

$$P_2=M_2\left(p_1+\frac{p_{12}-p_1}{\omega}\right),$$

where M_2 denotes the molecular weight of the solute.

μ : the dipole moment, which is calculated in this article as follows,

$$\mu=0.01273\left[P_{2\infty}-(P_E+P_A)\right]^{\frac{1}{2}}T^{\frac{1}{2}}\fallingdotseq 0.01273(P_{2\infty}-(1+\delta)MR_D)^{\frac{1}{2}}T^{\frac{1}{2}}$$

$$\delta=0.05\sim0.15\ .$$

The estimation of the atomic polarisation in the determination of the dipole moment has been quite arbitrary and sometimes confusing. In the present case where the temperature dependence in moment is to be

examined, the total neglect of the atomic polarisation appears to be much more erratic. In this paper, the atomic polarisation was estimated as 5% of the molecular refraction, MR_D after Groves and Sugden[6] (denoted by μ) and also as 15% after Wolf's school[7] (denoted by μ'). As is clear by the results, the difference in the choice of the atomic polarization hardly affects the temperature dependence (See Table 2).

The results are shown in Table 1. The results on benzil from stilbene dichloride are also recorded in the same table. A glance at it will show that there is no difference in moment in benzene solution between this and the sample from benzaldehyde.

Discussion of Results. The dipole moment of benzil in benzene solution at 25°C. was found as 3.71 D by Hassel and Naeshagen[8] and 3.2 D by Sängewald and Weissberger.[9] The result of the present measurement, $\mu = 3.62$ D lies between them. The moment of α-stilbene dichloride

Table 1.

Benzil (prepared from benzoin).

In benzene at 25°C.

ω	ε	d	p_{12}	p_2	P_2
0.00	2 273	0.87336	0.34112	—	—
0.904	2.3379	0.87525	0.35238	1.587	333
1.610	2.3904	0.87684	0.36117	1.586	333
2.995	2.4951	0.87799	0.37883	1.599	336

$P_{2\infty} = 333$ c.c., $MR_D = 58.92$ c.c.,
$P_A = 5\% MR_D$, $P_E+P_A = 61.87$ c.c., $\mu = 3.62$D
$P_A = 15\% MR_D$, $P_E+P_A = 67.76$ c.c., $\mu' = 3.58$D

In benzene at 50°C.

0.00	2.225	0.84607	0.34269	—	—
0.904	2.2826	0.84824	0.35307	1.491	313
1.610	2.3281	0.84987	0.36106	1.484	312
2.995	2.4176	0.85342	0.37601	1.455	306

$P_{2\infty} = 313$ c.c., $P_E+P_A = 61.87$ c.c., $\mu = 3.62$D
$P_E+P_A = 67.76$ c.c., $\mu' = 3.58$D

(6) Groves and Sugden, *J. Chem. Soc.*, **1935**, 971.
(7) Wolf and Trieschmann, *Z. physik. Chem.*, B, **14** (1931), 346.
(8) Hassel and Naeshagen, *ibid.*, B, **6** (1929), 152.
(9) Sängewald and Weissberger, *Physik. Z.*, **30** (1929), 268.

In carbon tetrachloride at 25°C.

ω	ε	d	γ_{12}	p_2	P_2
0.00	2.232	1.58434	0.18374	—	—
0.6403	2.3094	1.58044	0.19225	1.512	318
0.910	2.3430	1.57888	0.19586	1.516	319
2.096	2.4912	1.57260	0.21114	1.491	314

$P_{2\infty} = 318$ c.c., $P_E + P_A = 61.87$ c.c., $\mu = 3.52$D
$P_E + P_A = 67.76$ c.c., $\mu' = 3.48$D

In carbon tetrachloride at 50°C.

0.00	2.183	1.53501	0.18424	—	—
0.6403	2.2497	1.53217	0.19193	1.385	291
0.910	2.2787	1.53097	0.19520	1.389	292
2.096	2.4104	1.52465	0.20974	1.400	294

$P_{2\infty} = 291$ c.c., $P_E + P_A = 61.87$ c.c., $\mu = 3.46$D
$P_E + P_A = 67.76$ c.c., $\mu' = 3.42$D

Benzil (prepared from stilbene dichloride)

In benzene at 25°C.

0.00	2.273	0.87353	0.34105	—	—
1.150	2.3569	0.87604	0.35551	1.599	336
1.491	2.3817	0.87708	0.35953	1.581	332

$P_{2\infty} = 334$ c.c., $P_E + P_A = 61.87$ c.c., $\mu = 3.63$D
$P_E + P_A = 67.76$ c.c., $\mu' = 3.59$D

In hexane at 25°C.

0.00	1.8871	0.66547	0.34293	—	—
0.524	1.9103	0.66729	0.34886	1.473	309
0.720	1.9182	0.66763	0.35100	1.463	307
1.442	1.9500	0.66966	0.35915	1.467	308

$P_{2\infty} = 308$ c.c., $P_E + P_A = 61.87$ c.c., $\mu = 3.45$D
$P_E + P_A = 67.76$ c.c., $\mu' = 3.41$D

α-Stilbene dichloride.

In benzene at 25°C.

ω	ε	d	p_{12}	p_2	p_2
0.00	2.273	0.87353	0.34105	—	—
0.767	2.2819	0.87548	0.34195	0.4584	115.1
1.254	2.2872	0.87658	0.34252	0.4583	115.1

$P_{2\infty} = 115.1$ c.c., $MR_D = 68.63$ c.c.
$P_A = 5\% MR_D = 3.4$ c.c., $P_E + P_A = 72.0$ c.c., $\mu = 1.45$D

In carbon tetrachloride at 25°C.

0.00	2.225	1.58411	0.18303	—	—
0.1925	2.2286	1.58340	0.18349	0.422	105.8
0.1928	2.2289	1.58339	0.18352	0.437	109.6

$P_{2\infty} = 108$ c.c., $P_E + P_A = 72.0$ c.c., $\mu = 1.32$D

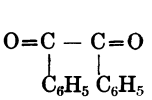
given by Weissberger and Sängewald[10] is recorded as 1.27 D in benzene at 25°C. in contrast to 1.45 D of the present author. The difference between them seems rather large, but on account of the small solubility of this substance in benzene, high accuracy cannot be claimed in an earlier work—in the present case, the accuracy being $\mu = 1.45 \pm 0.06$ D.

Table 2. Dipole moment of benzil.

Solvent / t°C.	C_6H_6		CCl_4	
	μ	μ'	μ	μ'
25	3.62	3.58	3.52	3.48
50	3.62	3.58	3.46	3.42

The result of the present work on benzil is summarised in Table 2. The values of benzene solution are quite independent of temperature, while those in carbon tetrachloride solution slightly decrease with rising temperature.

One must emphasize that this fact is incomprehensible by the ordinary chemical formula of benzil. If the carbon-carbon bond be purely single, from the analogy of $CH_2Cl{\cdot}CH_2Cl$,[4] it is clear that the stable internal position should correspond to the *trans*-position and measurable increase in moment with rising temperature should result. And if we can attribute the constancy in moment in the benzene solution to the abnormal action



(10) Weissberger and Sängewald, *Z. physik. Chem.*, B, **9** (1930), 133.

of the solvent, how can we explain the result obtained in carbon tetrachloride?

On the other hand, Hassel estimated the moment as 3.78 D, when free rotation occurs, and seemed to consider the agreement with the experimental value to be something more than mere coincidence. But free rotation, which is greatly hindered even in the case of $CH_2Cl{\cdot}CH_2Cl$ (with weaker mutual effect between the rotating groups), is very unlikely to occur.

From the result of Table 2, we may conclude as the following:

(1) The oscillatory rotation of the polar groups near the *trans*-position like that of $CH_2Cl{\cdot}CH_2Cl$ does not occur.

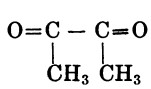
(2) The free rotation of the groups is improbable.

(3) Therefore, the carbon-carbon bond in benzil is different from the pure single bond.

As stated in the introduction, on account of the quantum mechanical resonance the carbon-carbon bond may acquire the double bond character. And the electronic structure of this bond has no longer the axial symmetry and tends to lock the groups either at the *cis*- or the *trans*-position. The dipole moment will be zero at the *trans*-position, while it will be very large at the *cis*-position.

The simplest explanation of the present experiment is to consider the existence of the *cis*-form only, (the *trans*-form having a much larger energy). From this assumption the constancy in the moment follows at once. Then we have to consider that the bond moments of this molecule become very different from the ordinary ones on account of the quantum mechanical resonance.

If, however, we consider the coexistence of the *trans*- and *cis*-configurations, the variation of the moment with temperature should result. And the observable value of the moment should be governed by the Maxwell-Boltzmann's law of distribution. The small decrease in the moment in CCl_4 solution might indicate this effect, but the temperature range of the present research is too small to draw a definite conclusion from it.



It is very interesting to note that diacetyl is reported to behave just like ethylene dichloride. According to Zahn,[11] its moment increases from 1.25 D at 66° to 1.48 D at 231°. Therefore in spite of its similar structure to benzil, its carbon-carbon bond does not show any marked deviation from the single bond. Although further studies are desirable

(11) Zahn, *Phys. Rev.*, ii, **40** (1932), 291.

to explain it, we should like to point out here that a similar behaviour in dipole moment was recently discovered by Mizushima and Kubo.[12]

Next, we will discuss the moment of α-stilbene dichloride.

Stilbene dichloride has two modifications (I and II of Fig. 3), and α-modification is supposed to be form I.

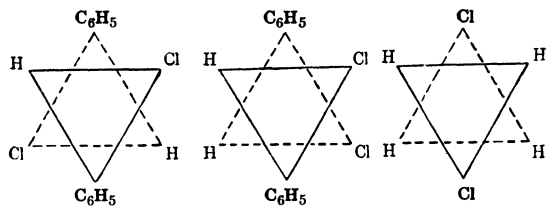


Fig. 3.

In Table 3 the comparison is made of the moments of this substance with those of ethylene dichloride in corresponding solvents.

As benzene is known to exert specific solvent action on ethylene dihalides, the results in carbon tetrachloride are first considered. It is remarkable that α-stilbene dichloride has almost the same moment as ethylene dichloride. As the moment of the rotating group $-CH(C_6H_5)Cl$ is supposed not to be much different from that of $-CH_2Cl$ (the moment of $C_6H_5CH_2Cl$ is 1.85 D in C_6H_6, while that of CH_3Cl is 1.86 D in vapour), this indicates that large phenyl groups do not exert a marked influence on the intramolecular rotation. This is easily understood by the consideration that in form I, the most stable position is the *trans*-position as regards to both phenyl groups and chlorine atoms, and the mutual effect of phenyl groups is not significant owing to large separation.

Table 3. Dipole moment at 25°C.

Solute \ Solvent	CCl_4	C_6H_6
$C_6H_5CHCl\cdot C_6H_5CHCl$	1.32	1.45
$CH_2Cl\cdot CH_2Cl$	1.36[4]	1.75[4]

The moment in benzene is larger than that in carbon tetrachloride. But this tendency is not so strong as it is observed in ethylene dichloride. As an explanation of anomalous behaviour of this substance in benzene, the formation of a loose-complex was proposed in which the mutual posi-

(12) Mizushima and Kubo, this Bulletin, **13** (1938), 174.

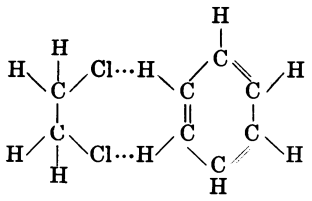


Fig. 4.

tion of two chlorine atoms tends to approach the *cis*-position[4] (Fig. 4.). According to this view, we might consider the case of *a*-stilbene dichloride as follows. This loose complex exists in the benzene solution of stilbene dichloride, too, giving a higher moment. But the two chlorine atoms cannot approach so near as in the case of ethylene dichloride because of the greater repulsion due to two phenyl groups.

Summary.

(1) The dipole moment of benzil was studied in three solvents and its temperature dependence was examined.

(2) The carbon-carbon bond of benzil is not a pure single bond and is probably a hybrid of single and double bonds. This is the result expected from Thiele's old idea of conjugated system and also from the quantum mechanical resonance.

(3) The dipole moment of *a*-stilbene dichloride was also studied in benzene and carbon tetrachloride solution. The result was compared with that of ethylene dichloride.

The research was conducted under the supervision of Professor M. Katayama and the author is specially indebted to Professor S. Mizushima for his guidance. Thanks are also due to Mr. T. Ando for discussions.

The Institute of Physical and Chemical Research,
Hongo, Tokyo.

Zur Theorie der Dielektrizitätskonstante des Gases unter hohem Druck.

Von Masaji KUBO.

(Eingegangen am 20. Dezember 1937.)

Nach der Debyeschen Dipoltheorie,[1] setzt sich die Molekularpolarisation polarer Verbindungen im Gas- oder Dampfzustand aus zwei Teilen, einem konstanten optischen Glied und einem von der Temperatur, aber nicht vom Druck abhängigen Dipolglied, zusammen, nämlich,

$$P = \frac{\varepsilon-1}{\varepsilon+2}V = a + \frac{b}{T} ;$$

wo P die Molekularpolarisation, ε die Dielektrizitätskonstante, V das Molekularvolumen und T die absolute Temperatur bedeutet. Die für das Material charakteristischen Konstanten a und b sind durch die Molekularkonstanten desselben bestimmt, und zwar

$$a = \frac{4\pi N\alpha}{3} , \qquad b = \frac{4\pi N\mu^2}{9k} ,$$

wo N die Avogadrosche Zahl, k die Boltzmannsche Konstante und α bzw. μ die Polarisierbarkeit bzw. das Dipolmoment bedeutet. Untersuchungen beim nicht zu hohen Druck haben bestätigt, dass die Debyesche Gleichung sich sehr gut bewährt hat und uns erlaubt, von der Temperaturabhängigkeit der Molekularpolarisation Rückschlüsse auf die Polarisierbarkeit und das Dipolmoment des freien Moleküls zu ziehen. Wir wollen nun über die Abweichung von dem Debyeschen Ausdruck beim hohen Druck diskutieren. Daran schon einige experimentelle Untersuchungen bis zu recht hohem Druck ausgeführt. Dafür ist die theoretische Forschung[2] von grosser Bedeutung, weil sie uns die Kenntnis über die Wechselwirkung der Moleküle untereinander liefert. Im folgenden wird eine Theorie entwickelt, die die Wechselwirkung der Dipole in Betracht zieht.

Wirken gar keine äusseren Kräfte, so ist die Verteilung im Raum der Dipole polarer Gasmoleküle statistisch ganz unregelmässig, d.i. keine

(1) Debye, „Polare Molekeln," (1929).

(2) Darunter ist die Arbeit von Keyes und Kirkwood (*Phys. Rev.*, **37** (1931), 202.) zu nennen. Sie berechneten statistisch den durchschnittlichen inneren Feld in einem Dielektrikum. Vergleiche ferner die Arbeit von Van Vleck (*J. Chem. Phys.*, **5** (1937), 556.).

Richtung in Bezug auf das raumfeste Koordinatensystem ist zur Orientierung des Dipols bevorzugt. Anders ist es beim molekülfesten Koordinatensystem. Wegen der gegenseitigen elektrostatischen Wechselwirkung, sind die Verteilung und die Orientierung der Moleküle nicht mehr unregelmässig, sondern von den Koordinaten abhängen. Es liegt also der Gedanke nahe, dass die von allen anderen Dipolen herrührende elektrische Feldstärke nicht mehr auf dem Anfangspunkt des Koordinatensystems verschwindet und eine kleine Beeinflussung ausübt.

Wir denken uns einen Raum, der polare Gasmoleküle mit dem Dipolmoment m enthält. Ferner wählen wir den Mittelpunkt eines beliebigen Moleküls als den Anfangspunkt der Polarkoordinaten (r, θ, φ), deren Pol oder z-Achse mit der Richtung des Dipols übereinstimmt. Wir bezeichnen mit f_z die z-Komponente der von einem Dipol auf dem Koordinatenanfangspunkt erregten elektrischen Feldstärke, der auf dem Punkt P (r, θ, φ) nach der Richtung (χ, ψ) orientiert ist, wobei χ den Winkel zwischen dem Radiusvektor r und der Richtung des Dipols auf dem Punkt P und ψ die Differenz der Azimute der beiden Dipole um ihre Verbindungslinie bedeutet. Ferner bezeichnen wir das elektrostatische Potential dieser zwei Dipole mit U. Da wir uns nur auf den nicht zu hohen Druck beschränken, ist die Wahrscheinlichkeit, dass mehr als zwei Moleküle gleichzeitig zusammenstossen, äusserst klein. Infolgedessen brauchen wir nur die Wechselwirkung zwischen zwei Dipolen behandeln. Nach dem Maxwell-Boltzmannschen Verteilungsgesetz, ist die Wahrscheinlichkeit, dass ein Molekül sich im Bereich $r \sim r + dr$, $\theta \sim \theta + d\theta$, $\varphi \sim \varphi + d\varphi$, $\chi \sim \chi + d\chi$ und $\psi \sim \psi + d\psi$ befindet, dem Ausdruck $\exp(-U/kT)$ proportional. Daher berechnet sich die von allen anderen Dipolen auf dem Koordinatenanfangspunkt erregte elektrische Feldstärke F_z nach der Formel

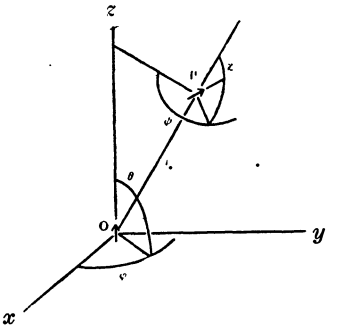


Abb. 1.

$$F = F_z = \int_{2\mathfrak{s}}^{\infty}\int_0^{\pi}\int_0^{2\pi}\int_0^{\pi}\int_0^{2\pi} f_z C \exp\frac{-U}{kT}\, r^2 \sin\theta \sin\chi\, dr\, d\theta\, d\varphi\, d\chi\, d\psi ,$$

wo C eine Konstante ist. Es ist ohne weiteres klar, dass F_x und F_y nach der Symmetrie verschwinden. Eine einfache Rechnung der Elektrostatik ergibt:

$$f_z = \frac{m}{r^3}(2\cos\theta\cos\chi - \sin\theta\sin\chi\cos\psi) ,$$

$$U = -mf_z = -\frac{m^2}{r^3}(2\cos\theta\cos\chi - \sin\theta\sin\chi\cos\psi) .$$

Wir wollen einfach annehmen, dass der Dipol auf dem Mittelpunkt des kugelförmigen Moleküls[3] liege und eine viel kleinere Ausdehnung als die Wirkungssphäre des Moleküls habe. Ferner nehmen wir an: Das Abstossungspotential, welches stark mit der abnehmenden Entfernung zwischen den zwei Molekülen zunimmt, werde unendlich gross für den Abstand, der kleiner als 2β ist (β = der Halbmesser der Wirkungssphäre des Moleküls), und das Dipolpotential spiele die Hauptrolle in der Wechselwirkung zwischen den beiden Molekülen. Dabei integrieren wir den Ausdruck über den ganzen Raum, ausschliesslich der Kugel, deren Mittelpunkt mit dem Koordinatenanfangspunkt zusammenfällt, und deren Halbmesser gleich 2β ist. Die obere Grenze der Integration nach r kann gleich unendlich gesetzt werden, weil die Ausdehnung des Raums viel grösser als β ist. Wenn man den Ausdruck $\exp(-U/kT)$ nach der Taylorschen Reihe entwickelt und integriert, so bekommt man:

$$F = \frac{4\pi^2 Cm^3}{9kT\beta^3}\left(1 + 1.250\times10^{-3}\frac{m^4}{k^2T^2\beta^6} + 1.156\times10^{-6}\frac{m^8}{k^4T^4\beta^{12}} + \cdots\right) .$$

In unserem Fall, wo wir uns nur mit den elektrischen Momenten von der gewöhnlichen Grössenordnung abgeben, werden unter den gewöhnlichen experimentellen Bedingungen das zweite und das dritte Glied usw. gegen das erste vernachlässigt. Um zu zeigen, dass die Näherung genügend genau ist, setzen wir z.B. für Ammoniak bei 150°C. die folgenden numerischen Werte ein, $m = 1.44\times10^{-18}$ e.s.E., $k = 1.37\times10^{-16}$ erg Grad^{-1}, $T = 423$°K. und $\beta = 1.82\times10^{-8}$ cm. Dann beträgt das zweite bzw. das dritte Glied nur zu 4.4×10^{-2} bzw. 1.4×10^{-3} mal das erste, und die obige Formel wird:

$$F = \frac{4\pi^2 Cm^3}{9kT\beta^3} .$$

Um die Konstante C zu bestimmen, berechnen wir die Anzahl der Moleküle, die sich in der Kugel (deren Mittelpunkt mit dem Koordinatenanfangspunkt zusammenfällt) vom Halbmesser l befinden wobei, l eine der Grössenordnung nach mit dem experimentellen Apparat vergleichbare Länge hat. Demnach

(3) Das kugelförmige Molekülmodell wird für Ammoniak gerechtfertigt, dessen drei Protonen sind in der Elektronenwolke des Stickstoffs eingehüllt.

$$1+\int_{2\beta}^{l}\int_0^{\pi}\int_0^{2\pi}\int_0^{\pi}\int_0^{2\pi} C\exp\frac{-U}{kT}\, r^2\sin\theta\sin\chi\, dr\, d\theta\, d\varphi\, d\chi\, d\psi = \frac{4\pi}{3}l^3 n\,,$$

wobei n die Anzahl der Moleküle pro Kubikzentimeter bedeutet. Erinnern wir uns, dass $l^3 n \gg 1$ und $l \gg \beta$, so erhalten wir

$$C = \frac{n}{4\pi}\,.$$

Deshalb

$$F = \frac{\pi m^3 n}{9kT\beta^3}\,.$$

Da das Molekül von diesem elektrischen Feld polarisiert wird, wird das elektrische Moment um den Betrag aF vergrössert:

$$m = \mu + aF = \mu\left(1+\frac{\pi a\mu^2 n}{9kT\beta^3}\right),$$

wobei wir m im Korrektionsglied mit μ ersetzen. Beim hohen Druck haben wir anstatt μ (das Dipolmoment des freien Moleküls) m (das wirkliche Dipolmoment unter hohem Druck) in den Debyeschen Ausdruck von P einzusetzen. Wir haben

$$P = \frac{4\pi N a}{3}+\frac{4\pi N m^2}{9kT} = \frac{4\pi N a}{3}+\frac{4\pi N\mu^2}{9kT}\left(1+\frac{\pi a\mu^2 n}{9kT\beta^3}\right)^2.$$

Da n gleich N/V ist,

$$P = \frac{4\pi N a}{3}+\frac{4\pi N\mu^2}{9kT}\left(1+\frac{2\pi N a\mu^2}{9kT\beta^3 V}\right).$$

oder

$$P = a+\frac{b}{T}+\frac{3ab^2}{8\pi N\beta^3 T^2 V}\,.$$

Das dritte Glied, das als Korrektionsglied zur Debyeschen Gleichung eingesetzt wird, hängt vom Druck ab. Wird P bei konstanter Temperatur als Funktion von $1/V$ aufgetragen, so erwarten wir nach der obigen Gleichung eine gerade Linie, die mit der Abszisse einen endlichen Winkel bildet. Daraus kann man β mittels der Gleichung

$$\beta = \sqrt[3]{\frac{3a(P_\infty - a)^2}{8\pi N\left(\frac{\partial P}{\partial(1/V)}\right)_T}}\,.$$

berechnen, wobei P_∞ die zum unendlichen Molekularvolumen extrapolierte Molekularpolarisation ($P_\infty = a + b/T$) bedeutet.

Zunächst wollen wir uns mit den nichtpolaren Gasen beschäftigen. Die Konstanz der Molekularpolarisation, d.h. die Gültigkeit des Clausius-Mosottischen Gesetzes, wurde nach vielen Messungen innerhalb der Messgenauigkeit bis zum sehr hohen Druck an Wasserstoff, an Stickstoff, an Methan und an Luft bestätigt.[4] Dies stimmt mit meiner Theorie gut überein, denn das dritte Glied, welches von dem Druck abhängt, für die nichtpolaren Verbindungen verschwindet.

Für die Molekularpolarisation des Kohlendioxyds fanden Keyes, Kirkwood und Uhlig[5] eine geringe Zunahme mit dem steigenden Druck, während Michels und Michels[6] eine geringe Tendenz zur Abnahme erhielten.[7]

Für Propan fanden Keyes und Oncley[8] eine fast lineare Zunahme der Clausius-Mosottischen Funktion mit der Dichte. Aber der Effekt ist nicht so ausgeprägt wie bei Kohlendioxyd.

Nun wenden wir uns den polaren Gasen zu. Leider ist Ammoniak das einzige, für welches Messungen über das grössere Druckintervall bis jetzt ausgeführt worden sind. Im Gegensatz zu nichtpolaren Gasen fanden Uhlig, Kirkwood und Keyes[5] eine deutliche Zunahme der Molekularpolarisation mit dem Druck. Wie aus der Abbildung 2 ersichtlich, zeigt die Molekularpolarisation bei konstanter Temperatur ein lineares Ansteigen mit $1/V$, was man von meiner Theorie erwartet.[9] Der daraus berechnete Molekularhalbmesser β ist in der Tabelle 1 wiedergegeben. Die dabei notwendige Konstante a wurde aus der zum unendlichen Molekularvolumen extrapolierte Molekularpolarisation P_∞ ermittelt und beträgt

(4) Tangl, *Ann. Physik*, **26** (1908), 59; Occhialini und Bodareu, *Ann. Physik*, **42** (1913), 67; Waibel, *Ann. Physik*, **72** (1923), 161; Broxon, *Phys. Rev.*, **37** (1931), 1338; **38** (1931), 2049; Jordan, Broxon und Walz, *Phys. Rev.*, **46** (1934), 66; Michels und Michels, *Phil. Mag.*, [7], **13** (1932), 1192; Michels, Jaspers und Sanders, *Physica*, **1** (1934), 627; Michels, Sanders und Schipper, *Physica*, **2** (1935), 753; Uhlig, Kirkwood und Keyes, *J. Chem. Phys.*, **1** (1933), 155; McNabney, Moulton und Beuschlein, *Phys. Rev.*, **47** (1935), 695.

(5) Keyes und Kirkwood, *Phys. Rev.*, **36** (1930), 754, 1570; Uhlig, Kirkwood und Keyes, *J. Chem. Phys.*, **1** (1933), 155.

(6) Michels und Michels, *Phil. Trans. Roy. Soc. London*, A, **231** (1933), 409.

(7) John (*Phil. Mag.*, [7], **22** (1936), 274.) versuchte die Dichteabhängigkeit der Clausius-Mosottischen Funktion von Kohlendioxyd durch die Raman-Krishnansche Theorie zu erklären.

(8) Keyes und Oncley, *Chem. Rev.*, **19** (1936), 195.

(9) Da Uhlig, Kirkwood und Keyes das Molekularvolumen von dem Druck nach der experimentell von Beattie und Lawrence (*J. Am. Chem. Soc.*, **52** (1930), 6.) gefundenen Beziehung zwischen Temperatur, Druck und Molekularvolumen berechneten, sind die Werte der Molekularpolarisation vom Fehler frei, der von der Abweichung des nach der Zustandsgleichung berechneten Molekularvolumens von dem wirklichen herrührt.

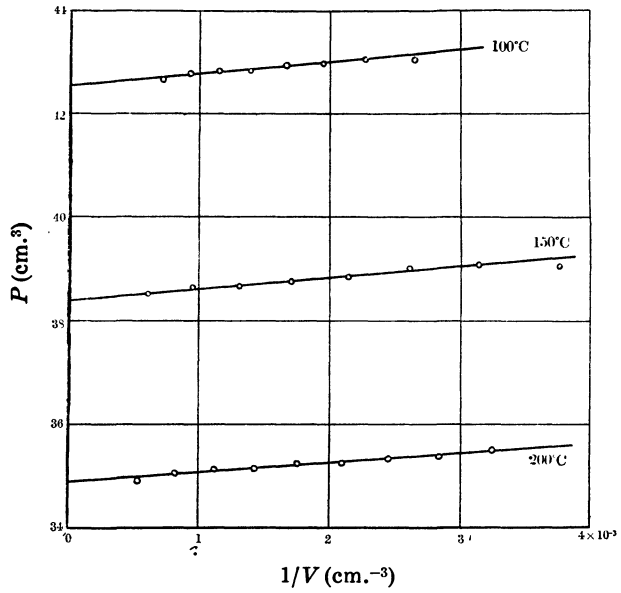


Abb. 2. Molekularpolarisation P von Ammoniak in Abhängigkeit von der Dichte $1/V$ für verschiedene Temperatur.

Tabelle 1.

t(°C.)	P_∞(cm.³)	$\frac{\partial P}{\partial(1/V)}$(cm.⁶)	$\beta \times 10^8$ (cm.)	Mittel	Messungen von
100	41.83	485	1.47	1.45	Keyes und Kirkwood
125	40.05	500	1.41		
150	37.72	410	1.44		
175	36.35	330	1.50		
100	42.55	235	1.90	1.82	Uhlig, Kirkwood und Keyes
150	38.40	225	1.78		
200	34.90	175	1.79		

6.2 cm.³. Zum Vergleich sind in Tabelle 2 die aus den anderen Methoden bestimmten Molekularhalbmesser zusammengestellt. Von den aus der inneren Reibung bestimmten Molekularhalbmessern, wurde der erste aus dem von Rankine und Smith[10] gemessenen gaskinetischen Stossquerschnitt (entnommen dem Tabellenwerk von Landolt-Börnstein), der zweite aus der Sutherlandschen Konstante und der Zähigkeit (Rankine und

(10) Rankine und Smith, *Phil. Mag.*, [6], **42** (1921), 601.

Tabelle 2.

Methode	$\beta \times 10^8$ (cm.)
Druckabhängigkeit der Molekularpolarisation	1.45 1.82
Innere Reibung	1.43 1.48 1.20
Van der Waalssche Zustandsgleichung	1.54

Smith[10] und Vogel,[11] entnommen dem Tabellenwerk von „International Critical Tables") berechnet und der dritte von Braune und Linke[12] gemessen. Auch die van der Waalssche Konstante wurde dem Tabellenwerk von Landolt-Börnstein entnommen. Die Übereinstimmung ist recht gut, wenn man in Betracht zieht, dass eine und dieselbe Messung der inneren Reibung des Gases für den Molekularhalbmesser sogar um 10 Prozent verschiedene Werte ergibt, je nachdem man dazu die Sutherlandsche oder die Reinganumsche Gleichung anwendet.[13]

Diese Theorie wird auch von ganz anderer Seite geprüft. Der elektrooptische Kerr-Effekt hängt eng mit den dielektrischen Eigenschaften zusammen, und zwar hat schon Oka[14] im Anschluss an meine Theorie eine Formel für die Druckabhängigkeit der Kerr-Konstante von Gasen abgeleitet. Auch hier ist das neu eingesetzte Korrektionsglied für nichtpolare Gase gleich Null, so dass bei diesen die bekannte Formel von Langevin und Born gelten muss, wie es auch Messungen an Kohlendioxyd, Methan, Athan und Äthylen bestätigen. Beobachtungen an polaren Gasen innerhalb grösserer Druckintervall sind leider bis heute noch nicht gemacht worden.

Herrn Professor Dr. M. Katayama und Herrn Professor Dr. S. Mizushima danke ich herzlich für ihre wertvollen Ratschläge und Unterstützungen.

Chemisches Institut, Wissenschaftliche Fakultät,
Kaiserliche Universität zu Tokyo.

(11) Vogel, *Ann. Physik*, **43** (1914), 1235.
(12) Braune und Linke, *Z. physik. Chem.*, A, **148** (1930), 195.
(13) Vergleiche dazu den Bericht von Titani (*Bull. Chem. Soc. Japan*, **8** (1933), 254.). Im allgemeinen gibt die Reinganumsche Gleichung einen höheren Wert für den Molekularhalbmesser als die Sutherlandsche Gleichung.
(14) Oka, *Proc. Phys.-Math. Soc. Japan*, [3], **19** (1937), 156.

Quantum Mechanical Resonance and Internal Rotation.

By San-ichiro MIZUSHIMA and Masaji KUBO.

(Received December 20, 1937.)

In a series of researches[1][2][3][4] on Raman spectra and electric dipole moments we have discussed the configuration of molecules having an internal degree of freedom. In some cases such as halogenated ethanes,[1] the intramolecular rotation around the C–C single bond is essentially governed by the exchange repulsion, dispersion attraction, and coulombic force between the atoms attached to the different movable groups of the molecule, the electronic structure of the rotation axis giving in itself no preference to any internal configuration. In other cases, however, where the axis acquires partially the character of a double bond due to the quantum mechanical resonance,[2][3][4] the electronic state of the bond has no more the axial symmetry and plays an important rôle in the hindrance of internal rotation,—a phenomenon which is inexplicable, even qualitatively, from the classical chemical theory. As the latter cases are of interest from the standpoint of stereochemistry we want to give further discussion on the resonance effect and especially on carboxylic resonance, supplementing some new experimental data of the dipole moments of the organic vapours.

The complete degeneracy between the two structures $R-C\begin{matrix}O^- \\ \diagdown \\ \diagup \\ O\end{matrix}$ and $R-C\begin{matrix}O \\ \diagup \\ \diagdown \\ O^-\end{matrix}$ in the case of carboxylic ion was treated in our previous communication[3] from the discussion of normal vibration of this ion and especially of the value of force constant for the C···O bond. If we attach a hydrogen atom to one of the two previously equivalent oxygen atoms of carboxylic ion to form acid molecule, the carboxylic resonance is inhibited to some extent and therefore a change in bond character takes place, as can at once be seen from the considerable change in the Raman

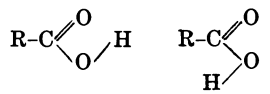
(1) Mizushima, Morino, and co-workers, *Physik. Z.*, **35** (1934), 905; **36** (1935), 600; **38** (1937), 459; *Sci. Papers Inst. Phys. Chem. Research* (Tokyo), **25** (1934), 159; **26** (1934), 1; **29** (1936), 63, 111, 188.

(2) Mizushima, Uehara, and Morino, this Bulletin, **12** (1937), 132.

(3) Morino and Mizushima, *Sci. Papers Inst. Phys. Chem. Research* (Tokyo), **32** (1937), 33.

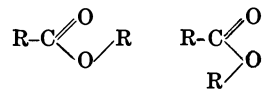
(4) Kubo, Morino, and Mizushima, *Sci. Papers Inst. Phys. Chem. Research* (Tokyo), **32** (1937), 129.

spectrum.[3] We have, however, good reason to believe that the resonance effect is here still large enough as to permit no internal oscillatory rotation of finite amplitude around the C–O axis. For this molecule we can consider the two configurations A and B in Fig. 1 which the resonance effect



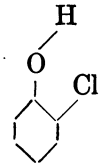
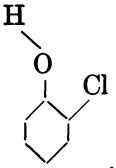
A B

Fig. 1. The two molecular configurations of carboxylic acid.



A B

Fig. 2. The two molecular configurations of carboxylic ester.

would allow, but according to the dipole measurement carried out by Zahn[5] almost all the molecules assume the A-form. This must be due to the coulombic attraction between the carbonyl and the hydroxyl bonds, which is superimposed upon the resonance effect, although this electrostatic effect alone is not sufficient to lock the molecule rigidly at the said position. In the case of *o*-chlorophenol the existence of the two molecular forms  and  predicted by the assumption of resonance[6] can be shown experimentally by the observation of the infrared absorption spectra, corresponding to the first,[7] second,[2] and third overtones[2] of the O–H vibration (each of them has two absorption maxima corresponding to these two molecular species). For the molecule of acetic acid vapour, however, we[8] have found only one absorption maximum for each of the second (9760 Å) and third overtones (7501 Å), which supplies with another experimental evidence as to the existence of the only one stable form of the carboxylic acid molecule (i.e. form A).

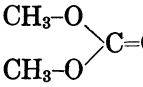
There will be some further inhibiting effect on the carboxylic resonance if we replace the hydrogen atom of the acid molecule by an alkyl radical to form ester molecule. The observed values of ester moments as well as their temperature independence show, however, that the resonance effect is still considerable and the molecules are locked at the position of A in Fig. 2 without performing oscillatory rotation about this

(5) Zahn, *Phys. Rev.*, **37** (1931), 1516; *Trans. Faraday Soc.*, **30** (1934), 804.
(6) Pauling, *J. Am. Chem. Soc.*, **58** (1936), 94.
(7) Wulf and Liddel, *J. Am. Chem. Soc.*, **57** (1935), 1464.
(8) Mizushima, Kubota, and Morino, to be published shortly.

stable position at all ordinary temperatures. So far as we know, such an observation has been carried out only by Zahn[9] and in view of the importance of this conclusion in stereochemistry, we have undertaken the reexamination of the dipole moment of methyl acetate in the vapour state. The result was that over a temperature range of 180° (from 34.5 to 209.2°C.) we could obtain a constant value 1.69_6 D of the ester moment in good agreement with that of Zahn's measurement.

The above conclusion as to the stable configuration of the ester molecule was obtained by comparing the observed value of moment with that calculated by vectorial addition for form A in Fig. 2. Although the quantum mechanical resonance makes the values of bond moments in the actual "mesomeric" molecule more or less different from those of the pure C=O, C−O, and O−R bonds respectively, there would scarcely be doubt that form A is the more stable. In any way the energy difference between the two molecular forms shown in Fig. 2 must be so large that we could almost speak of a normal and an excited state, otherwise we would find an observable temperature dependence of the ester moment according to the Maxwell-Boltzmann distribution. For the more exact treatment of the problem it is desirable to investigate the vibration spectra of esters, although the discussion of the normal vibration in this case must be much more difficult than that for carboxylic acid, whose O–H bond vibration can easily be separated from the other normal vibrations.

It is now very interesting to see to what extent such a resonance effect can hinder the intramolecular rotation, if we make a substitution in the ester molecule. When we replace the hydrogen atom of formic ester by a methyl group to form acetic ester, there is no change in the rigidity of the internal state which reveals itself in the observed value of dipole moment. If, however, we replace it by a methoxyl group to form methyl carbonate, the situation becomes quite different and as we reported in our previous communication,[4] the dipole moment of this vapour increases considerably as the temperature is raised (Compare Table 1),—i.e. while for carbonate ion there is complete degeneracy among the three structures


, 
, and 
, the electronic state of methyl carbonate can better be approximated by the classical formula  than in the case of carboxylic esters.

(9) Zahn, *Physik. Z.*, **33** (1932), 730.

Instead of methoxyl group we have next chosen chlorine as the substituent atom to study the effect of quantum mechanical resonance on the internal rotation of methyl and ethyl chloroformates. From the result of our dipole measurement in Table 1 it is easily shown that these molecules

Table 1. Dipole moments of several esters in the vapour state.

Dimethyl carbonate (P_E = 18.5 c.c.)		Methyl chloroformate (P_E = 16.7 c.c.)		Ethyl chloroformate (P_E = 21.2 c.c.)	
t(°C.)	m(D)	t(°C.)	m(D)	t(°C.)	m(D)
55.0	0.86	34.6	2.38	35.0	2.56
76.9	0.89	78.0	2.40	76.9	2.47
139.1	0.94	140.2	2.29	137.6	1.79
206.2	1.00_5	207.4	1.68	207.3	1.43

must exert internal oscillatory rotation, the amplitude of which is easily affected by the change of temperature. The C–O bond in the actual "mesomeric" molecule of these substances cannot, therefore, have such an amount of double bond character as in the case of simple carboxylic esters, for which practically the complete inhibition of internal rotation is realized at all ordinary temperatures by the said quantum mechanical force. To determine the stable configuration of these chloroformate molecules we have calculated the resultant moment as the function of the azimuthal angle φ, $\varphi = 0$ corresponding to the closest approach of the alkyl group to the chlorine atom (See Fig. 3). Assuming the values of the bond moments as m(C–Cl) = 1.86 D, m(C=O) = 2.75 D, and m(C–O) = 1.13 D, we obtain the maximum value of the resultant moment of 2.15 D for $\varphi = 0$, which decreases monotonously till it attains the minimum value of 1.58 D at $\varphi = \pi$. By comparing these calculated values with the observed (Table 1), we can easily understand that the stable internal position should correspond to that for $\varphi = 0$, although the quantitative comparison between them may be of small significance, because of the neglect of the mutual effect between bond moments as well as the resonance effect.

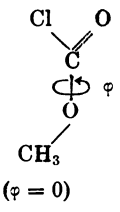


Fig. 3. Intramolecular rotation of methyl chloroformate.

Experimental.

Preparation of materials. Methyl acetate: Kahlbaum's sample "pure" was dehydrated over calcium chloride and subjected to fractional distillation; b.p. 57.2–57.7°C.

Methyl chloroformate: Kahlbaum's sample was purified by fractional distillation; b.p. 71.4–72.4°C.

Ethyl chloroformate: Takeda's sample was dehydrated over calcium chloride and fractionally distilled; b.p. 92.5–93.5°C.

The dielectric constant ε of the vapour was determined with the apparatus previously described[10] and the polarization P was calculated by means of the equation $P=[(\varepsilon-1)/(\varepsilon+2)]V$, in which V is the molar volume. The latter was calculated by using the van der Waals equation of state for methyl acetate. As the greatest deviation from the ideal gas law was less than 0.5% for this substance, we have used this law in evaluating the molar volume of the other two compounds, for which the van der Waals constants have not been reported.

The results of the measurements for methyl acetate are shown in Table 2. The polarization P was found to be a linear function of $1/T$, for which a least squares

Table 2. Dielectric constant ε and molecular polarization P of methyl acetate in the vapour state.

T(°K.)	p(mm.)	$(\varepsilon-1)\times10^6$	V(l.)	P(c.c.)	Mean
307.5	94.9	1126	202.0	75.92	
	131.7	1560	145.6	75.75	
	134.6	1611	142.4	76.55	
	147.8	1765	129.7	76.39	76.15
328.5	90.0	986	227.8	74.86	
	90.5	971	226.3	73.30	
	112.5	1198	182.1	72.78	
	162.6	1731	126.0	72.72	73.41
350.5	146.1	1412	146.8	69.20	
	190.8	1835	112.4	68.82	
	197.4	1898	108.7	68.80	
	208.8	2010	102.7	68.86	68.92
378.1	112.6	940	209.4	65.66	
	139.0	1150	169.7	65.06	
	145.6	1195	162.0	64.62	
	180.7	1489	130.6	64.85	65.05
410.5	171.6	1245	148.8	61.80	
	206.2	1478	123.7	61.00	
	209.9	1530	121.7	62.08	
	242.2	1785	105.3	62.71	61.90
482.2	221.4	1235	135.6	55.81	
	229.4	1229	130.9	53.60	
	234.6	1296	128.0	55.32	
	247.5	1358	121.3	54.93	54.91

(10) Kubo, *Sci. Papers Inst. Phys. Chem. Research* (Tokyo), **26** (1935), 242; **27** (1935), 65; **32** (1937), 26.

solution gives:

$$P = 18.1_5 + 1.785 \times 10^4/T.$$

From the second term of this equation we can calculate the value of dipole moment as 1.69_6 D and from the first that of atomic polarization as 0.6_5 c.c. by subtracting the molar refraction 17.5 c.c. extrapolated to infinite wave length. Thus in the accuracy attainable by the present experiment the dipole moment of this ester remains constant over the above temperature range.

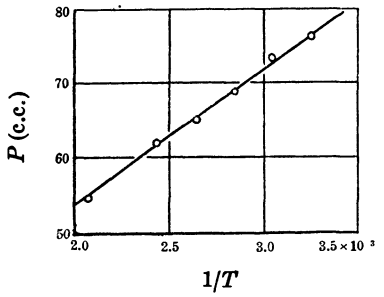


Fig. 4. The molecular polarization of methyl acetate.

The values of molecular polarization obtained by Zahn are in good agreement with those of the present measurement, but as he assumes the sum of electronic and atomic polarizations to be 19.4 c.c., his value of dipole moment decreases slightly with temperature from 1.69 D at 54.2°C. to 1.66 D at 243.3°C. and is equal to 1.67 D in the mean.

The experimental results for the two chloroformates are given in Table 3 and 4 and in Fig. 5. As can be expected for homologous series, the curves for the two

Table 3. Dielectric constant ε and molecular polarization P of methyl chloroformate in the vapour state.

T(°K.)	p(mm.)	$(\varepsilon-1)\times10^6$	V(l.)	P(c.c.)	Mean
307.7	112.9	2384	170.0	135.1	
	123.2	2565	155.7	133.1	
	136.2	2840	140.8	133.3	
	138.5	2813	138.5	130.0	132.9
351.1	125.1	2041	175.0	119.2	
	140.3	2329	156.1	121.1	
	141.0	2335	155.4	121.0	
	151.9	2492	144.3	119.9	120.3
413.3	137.0	1579	188.2	99.0	
	157.2	1769	164.0	96.7	
	157.6	1770	163.6	96.6	
	160.7	1780	160.5	95.2	96.9
480.5	204 5	1042	146.5	51.0	
	212.7	1152	141.0	54.2	
	215.4	1167	139.1	54.1	
	217.1	1201	138.0	55.2	54.6

Table 4. Dielectric constant ε and molecular polarization P of ethyl chloroformate in the vapour state.

T(°K.)	p(mm.)	$(\varepsilon-1)\times10^6$	V(l.)	P(c.c.)	Mean
308.1	56.3	1366	341.6	155.5	
	57.3	1405	335.6	157.2	
	64.5	1581	298.1	155.0	
	67.1	1600	286.6	152.8	155.1
350.0	56.8	1030	384.4	132.0	
	56.8	1016	384.4	130.1	
	58.6	1052	372.7	130.7	
	62.0	1127	352.2	132.4	131.3
410.7	78.7	645	325.6	70.0	
	79.1	672	324.0	72.6	
	79.7	664	321.5	71.2	
	87.5	746	293.0	72.8	71.7
480.4	70.7	354	424.0	50.0	
	73.5	375	407.9	51.0	
	74.2	359	404.0	48.3	
	75.6	377	396.2	49.8	49.8

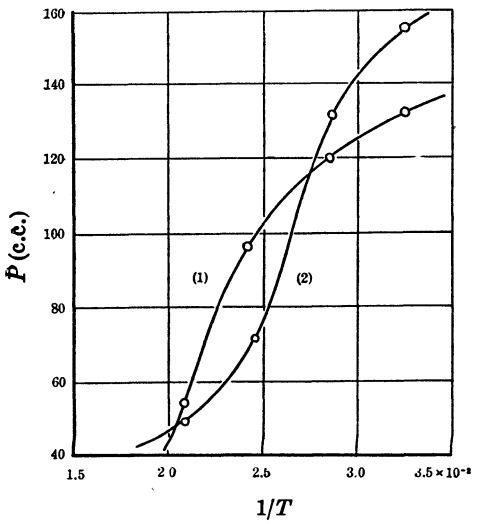


Fig. 5. The molecular polarizations of methyl chloroformate (1) and ethyl chloroformate (2).

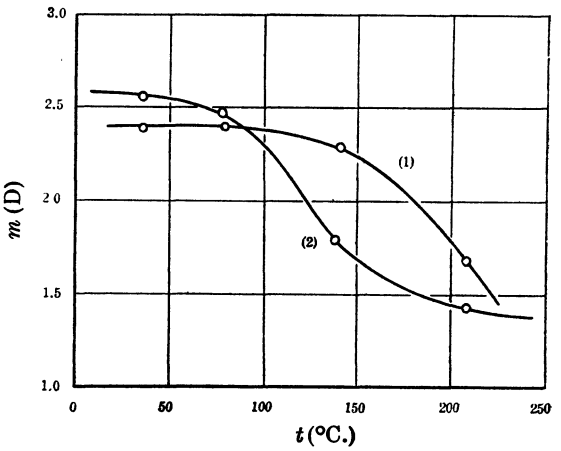


Fig. 6. The dipole moments of methyl chloroformate (1) and ethyl chloroformate (2).

compounds show an analogous behaviour. P is not here a linear function of $1/T$, indicating that the values of dipole moments change with temperature. To ascertain that no appreciable thermal decomposition took place in our measuring condenser we made the following observation in the case of ethyl chloroformate.[11] After the sample was evaporated to an appropriate pressure in the gas condenser previously evacuated, the cock was closed to separate the vapour chamber from the vessel containing the liquid sample, and the variation of pressure was carefully observed. After a few ten seconds the pressure attained a value, which remained constant. If decomposition had been occurring, there would have been the increase of pressure with time. The vapour was at last pumped out and was caught in a vessel cooled by the mixture of solid carbon dioxide and acetone. The colourless liquid, which condensed, showed the specific properties of the substance.

For these substances we have to calculate the dipole moments from the orientation polarization $P_O = P - P_A - P_E$ at each temperature. We assume, for each substance, that the atomic polarization amounts to 10% of the electronic polarization or the molar refraction extrapolated to infinite wave length. The values of dipole moments calculated by means of the usual relation $m = 0.0127\sqrt{P_O T}$ are shown in Table 1 and in Fig. 6. No data for the moment in the vapour state as well as in solution have been found in the literature to be compared with those of our observation on these two compounds.

We thank Prof. M. Katayama for his kind advices. Our thanks are also due to Nippon Gakujutsu-Shinkokai for a grant in aid of this research.

Summary.

The effect of single bond—double bond resonance upon the internal rotation was discussed for carboxylic acids and their derivatives. In acids and esters the strong carboxylic resonance imparts the double bond character to the C–O bond of the actual "mesomeric" molecule to such an extent that practically the complete inhibition of the internal motion is realized at all ordinary temperatures, while the replacement of hydrogen of H–COOR by chlorine or methoxyl group greatly reduces this double bond character, so that the internal oscillatory rotation of finite amplitude can take place about the C–O bond as axis.

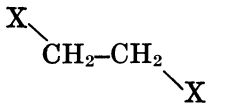
Chemical Institute, Faculty of Science,
Tokyo Imperial University.

(11) Ethyl chloroformate decomposes slowly from 250°C. as:
$ClCOOC_2H_5 \rightarrow C_2H_5Cl + CO_2$ (Beilstein).

The Motion of Ethylene Halide Molecules in Crystals as Revealed by the Raman Effect.

By San-ichiro MIZUSHIMA and Yonezo MORINO.

(Received December 20, 1937.)

The conspicuous difference in the Raman spectra of ethylene dihalides between the liquid and solid states reported in our previous paper was explained as due to the considerable change of the intramolecular state upon solidification.[1][2] Below the freezing point the molecules are almost all in the *trans* configuration  , while in the liquid state or in solutions there is a considerable deviation of the mean internal state from this stable position. (It was shown by our calculation[2] of normal vibrations that the Raman lines observed in the solid state all correspond to the symmetric vibrations to the centre of symmetry of the *trans* form.) The sharp drop of dielectric constant of ethylene chloride and bromide at the freezing point recently observed by White and Morgan is in conformity with our conclusion, which is discussed fully in their communication.[3]

In the vicinity of the unmodified line there seemed to exist other Raman lines which we could not resolve from the primary line in our former measurement. As it is doubtless important for the investigation of intermolecular state to confirm the existence of such low frequency lines, we have reexamined the Raman spectra of ethylene chloride and bromide with a spectrograph of our own construction having a larger dispersion and higher luminocity than the former one (dispersion 10 Å/mm. at 4000 Å). As was expected we could really observe fairly intense Raman lines in the said frequency region both as Stokes and anti-Stokes—for ethylene chloride at −40°C. a diffuse line was observed at 66 cm.$^{-1}$, and for ethylene bromide at 0°C. a line of the same nature at 49 cm.$^{-1}$, while for the latter substance at −40°C. two sharp and fairly intense lines appeared at 41 and 53 cm.$^{-1}$ respectively (see Figs. 1 and 2).

(1) Mizushima, Morino, and Noziri, *Nature*, **137** (1936), 945.

(2) Mizushima, Morino, and Noziri, *Sci. Papers Inst. Phys. Chem. Research* (Tokyo), **29** (1936), 63.

(3) White and Morgan, *J. Chem. Phys.*, **5** (1937), 655.

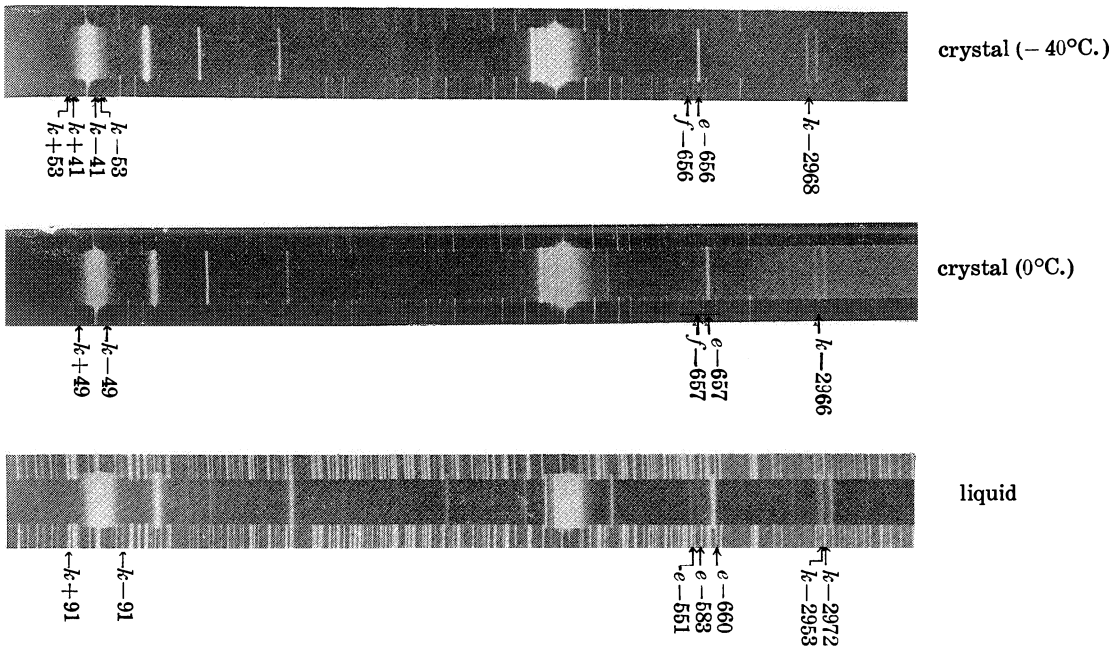


Fig. 1. Raman spectra of ethylene bromide.

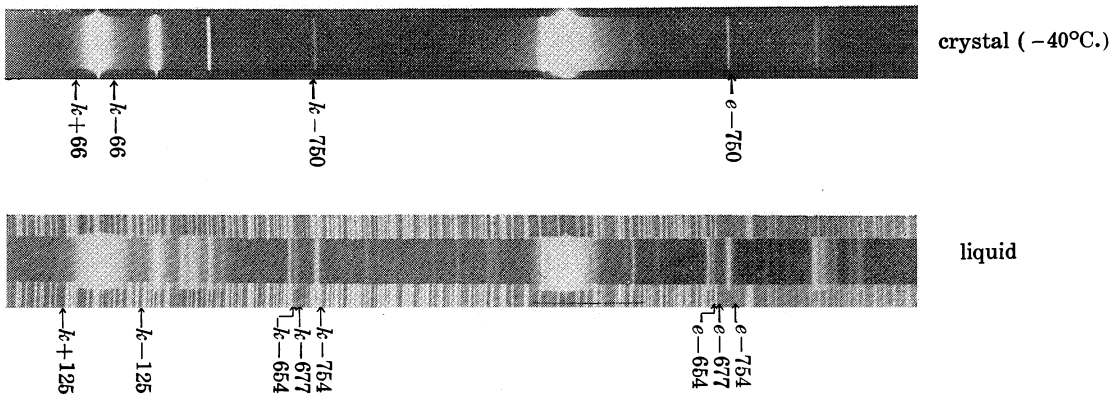


Fig. 2. Raman spectra of ethylene chloride.

It is very interesting to consider the observed change in Raman spectrum of the crystalline ethylene bromide in connection with the thermal transition observed at −24°C. by White and Morgan,[3] from which it may be concluded that these low frequency lines correspond to some motion of a molecule as a whole in the crystal lattice. There are two more reasons which would justify this conclusion: (1) we could observe no line (at least of the comparable intensity) in this frequency region of the liquid spectra, (2) the frequencies of these lines are too low to be identified with any of the internal normal vibrations,[4] as can be seen from our calculation for these molecules.[2]

Let us tentatively assume that these low frequency lines correspond to lattice frequencies and see how far we can treat our interesting experimental results with this assumption. In these crystals the van der Waals force between the halogen atoms would play the leading part in forming the molecular lattice, because of the greater polarizability of these atoms. This is also in conformity with the appearance of these lattice frequencies as the Raman effect, since there can also take place a considerable change in polarizability for the lattice vibration in such a crystal.

Before entering into the detailed discussion of this problem, we have to consider somewhat about the intramolecular state as revealed by the lines of higher frequencies. The values of Raman frequencies observed in the present experiment are no doubt of greater precision than those reported in our previous communication because of the larger dispersion of the spectrograph used. As far as, however, the conclusion given previously[2] is concerned, nothing need be changed. The disappearance of some of the liquid lines in the solid spectrum, which was the most important result of our previous experiment, has acquired further confirmation by the high luminocity of the present apparatus,—e.g. in the solid spectra we could observe distinctly the Raman lines excited by Hg-*f* and Hg-*g*, which correspond to the symmetric C–X vibrations (750 cm.$^{-1}$ for $C_2H_4Cl_2$ and 656 cm.$^{-1}$ for $C_2H_4Br_2$), but could find no trace of strong liquid lines to be found in their vicinity even by Hg-*e* excitation (654 cm.$^{-1}$ for $C_2H_4Cl_2$ and 551 cm.$^{-1}$ for $C_2H_4Br_2$). Thus it is quite sure that below the freezing point the molecule of ethylene halide is in a nearly pure *trans* state and the thermal transition observed for ethylene bromide at −24°C. has no effect on this intramolecular configuration.

(4) The intramolecular oscillatory rotation about the *trans* position (compare footnote (5)), which can have a frequency value of this order of magnitude, is not allowed in the Raman effect for the solid state, since this normal vibration is antisymmetric to the centre of symmetry of the *trans* configuration.

Returning to the problem of intermolecular motion, let us consider that the change in Raman spectrum of crystalline ethylene bromide is caused by the transition observed at −24°C. Then the said change of Raman lines must be due to the change in the molecular lattice. Now many thermal transitions are doubtless caused by the setting-in of molecular rotation in the crystal lattice, for which Pauling[5] first gave a theoretical treatment. The transition observed for ethylene bromide cannot, however, correspond to the onset of three dimensional molecular rotation in the crystal lattice, as can easily be seen from the following discussion. We have already stated that upon solidification the intramolecular rotation about the C–C axis is greatly restricted and the molecule assumes practically the pure *trans* form. This must be explained in terms of crystal forces. Such a specific effect of these forces in fixing the shape of the molecule would not be expected, if it were rotating about three axes. Taking into account our former result in Raman measurement,[1] White and Morgan explained the thermal transition of ethylene bromide observed by them as due to the onset of molecular rotation about only one axis, i.e. that of the zigzag Br–C–C–Br chain. Rotation about this axis does not contradict the existence of the said crystal forces which keep the molecules of the solid in a nearly pure *trans* state and it would not require a large amount of energy which is consistent with the small value of heat of transition estimated by White and Morgan.[3] The commencement of such a molecular rotation necessarily causes a change in the molecular field in the crystal lattice which affects the value of force constant and consequently the frequency of a normal vibration. The small frequency shifts observed for some of the lines of crystalline ethylene bromide (see Table 1) might be interpreted as due to such a change in the molecular field on passing through the transition point. That we have found no appreciable change in frequency on fusion (see Table 1), would then be of particular interest, when we consider that the molecules are rotating in the liquid state as well as in the solid state above the transition point. The experimental error in the reading of each line is different according to the character of the line and consequently

Table 1. Frequency changes in some of the high frequency lines of ethylene bromide.

Crystal		Liquid
−40°C.	0°C.	
2848	2857	2859
3020	3013	3013

(5) Pauling, *Phys. Rev.*, **36** (1930), 430; see also Smyth, *Chem. Rev.*, **19** (1936), 329.

we cannot treat these small frequency shifts for all lines with the same accuracy, although the complete treatment would be desirable from the view-point of the modern theory of the liquid state (quasi-crystalline structure). In this connection we want to mention the existence of a very diffuse line of the frequency of 91 cm.$^{-1}$ observed in the liquid spectrum. At the present stage we cannot conclude that this line corresponds to the line of 49 cm.$^{-1}$ observed for the solid at 0°C., indicating the quasi-crystalline structure of the liquid. It is also probable that this line corresponds e.g. to the intermolecular vibration of a conglomerate of molecules existing only in the liquid state. In any case this line has frequency too low to be indentified with any of the internal vibration of ethylene bromide molecule as can easily be seen from our previous calculation.[2]

The spectrum of crystalline ethylene chloride at −40°C. has only one Raman line in the region of the unmodified line and the nature of this line is similar to that of the corresponding line of crystalline ethylene bromide at 0°C. Moreover, on fusion there have been observed no appreciable frequency shifts of the two hydrogen vibrations (2874 cm.$^{-1}$ of solid to 2874 cm.$^{-1}$ of liquid and 3005 cm.$^{-1}$ of solid to 3004 cm.$^{-1}$ of liquid) corresponding to the two bromide lines discussed above. These may suggest that the molecule of ethylene chloride exerts one dimensional rotation around the axis of the zigzag Cl–C–C–Cl chain at this temperature and also at considerably lower temperatures, since there was found no transition point in the thermal measurement by White and Morgan down to −95°C. We have then to consider that the potential hump restraining the said one dimensional rotation in the crystal is smaller for ethylene chloride than for ethylene bromide and the molecules of the former substance can exert rotation at lower temperatures than those of the latter.

One might doubt if the thermal energy at −95°C. can give rise molecular rotation for ethylene chloride, while it cannot cause rotation for ethylene bromide below −24°C. The alternative possibility is that the molecules of ethylene chloride are fixed in the lattice or performing only the oscillatory rotation around the equilibrium orientations (this should not be confused with the intramolecular oscillatory rotation with which we have been dealing[6]). It is conceivable that because of the difference in size between chlorine and bromine atoms the potential hump acting against the one dimensional rotation becomes so large in the crystal of ethylene chloride as to permit no rotation below the freezing point. It is obviously too early at the present stage to give decision between these

(6) Mizushima, Morino, and co-workers, *Physik. Z.*, **35** (1934), 905; **36** (1935), 600; **38** (1937), 459; *Sci. Papers Inst. Phys. Chem. Research* (Tokyo), **25** (1934), 159; **26** (1934), 1; **29** (1936), 63, 111, 188; **31** (1937), 296; **32** (1937), 33, 129, 220.

two alternative possibilities. The investigation of the Raman spectrum of ethylene iodide, which we have already begun, might throw light on this problem.

We have no intention of giving here a conclusive explanation for our experimental result. The object of the present paper is to report these very interesting observations and to suggest a probable explanation for them.

Experimental.

In the present investigation we used a spectrograph of higher luminocity and a mercury lamp of stronger radiation than in our previous measurement. This together with the use of Agfa Isopan ISS film considerably reduced the time of exposure. For the crystals the longest exposure in the present experiment amounted to 15 hours, which would correspond to an exposure of more than two hundred hours with our previous apparatus. In order to investigate the region of the unmodified line, it is important to avoid as much as possible all parasitic light and stray reflections from the face of the crystals. This condition was secured by using carefully distilled liquids, which was allowed to solidify to a uniform mass. As the filters we have used, according to the suggestion of Ananthakrishnan,[7] dilute as well as con-

Table 2. The Raman spectra of $C_2H_4Cl_2$.

Solid state (−40°C.)			Liquid state					
			Present authors			Ananthakrishnan		
66	(4b)	$k\pm$						
	v							
	v		125	(5b)	$e\pm, k\pm$	123	(4b)	D
302	(5)	e, k	265	(5)	$e\pm, k, i$	263	(2)	P
	v		300	(8)	$e\pm, k, i$	302	(8)	P
	v		411	(5)	$e\pm, k, i$	411	(3)	D
	v		654	(8)	$e\pm, k, i, f$	654	(10)	PP
			677	(6b)	$e\pm, k, i$	675	(3)	D
750	(10)	e, k, i, f	754	(10b)	$e\pm, k, i$	754	(15b)	P
	v		881	(4)	e, k	880	(1)	D
	v		943	(5)	$e, [k]$	940	(2)	P
992	(3)	e, k	989	(2)	e, k			
			1031	(2)	e, k			
1059	(3)	e, k	1052	(4)	e, k	1052	(1)	P
			1145	(3)	e, k	1144	(1/2)	D
	v		1207	(5)	e, k	1206	(2)	D
1265	(2b)	k	1264	(3)	e, k	1262	(1)	D
1301	(5b)	k	1304	(6)	e, k	1302	(3)	P
			1393	(1)	e, k			
	v		1429	(6)	e, k	1429	(3)	D
1448	(2b)	e, k	1445	(4b)	e, k	1440	(1/2)	D
			2844	(3)	e, k	2844	(1)	?
2874	(3)	e, k, i	2874	(4)	e, k	2872	(1)	P
2964	(10)	e, k, i	2957	(10)	e, k, i	2956	(12b)	PP
3005	(6)	e, k, i	3004	(8b)	e, k, i	3002	(4b)	D

(7) Ananthakrishnan, *Proc. Indian Acad. Sci.*, A, **5** (1937), 76.

centrated solutions of iodine in carbon tetrachloride, which proved to be quite useful for our present purpose.

The results of our Raman measurement are shown in Tables 2 and 3, in which there is listed for each observed line: first, its frequency in cm.$^{-1}$; second, in parenthesis, its intensity as obtained by visual estimation; third, the mercury lines exciting it. The letter b following the number indicating the intensity, signifies a broad line and v in the columns of the solid spectra means the disappearance of the corresponding liquid line undoubtedly established in the accuracy of the present measurement. For the sake of comparison the experimental values of Ananthakrishnan[8] obtained for liquid ethylene chloride and bromide are inserted in the following tables.

Table 3. The Raman spectra of $C_2H_4Br_2$.

Solid state (−40°C.)	Solid state (0°C.)	Liquid state	
		Present authors	Ananthakrishnan
41 (4) $k\pm$	49 (3b) $k\pm$		
53 (3) $k\pm$			
v	v	91 (2b) $e\pm, k\pm$	92 (2b)
		132 (2) e	
187 (7) $e\pm, k+$	190 (7) $e, k+$	190 (10) $e\pm, k\pm$	189 (10) P
v	v	231 (3) e	228 (1b) P
		325 (1) e	320 (0) ?
v	v	355 (5) e, k	358 (2) D
		469 (1) e, k	470 (0) ?
v	v	551 (9) $e\pm, k, i, f$	551 (8) PP
v	v	583 (6b) $e\pm, k, i$	580 (2b) D
656 (10) e, k, i, f, g	657 (10) e, k, i, f	660 (10b) $e\pm, k, i$	659 (15b) P
			790 (0) ?
		836 (2) e	834 (1/2) D
		899 (3) e, k	895 (1) P
933 (0) k	934 (1) k	933 (2) e, k	930 (1b) P
		997 (0) e	
		1019 (1) e, k	
1057 (5) e, k, i	1056 (5) e, k	1053 (9) e, k, i	1051 (6) D
			1086 (??)
1157 (1) e		1169 (3) e, k	1169 (1/2) D
			1187 (0) D
1254 (8) e, k, i	1250 (8b) e, k	1255 (10b) e, k	1256 (10b) P
v	v	1276 (3) e, k	1295 (1s) P
v	v	1419 (3) e, k	1419 (1) D
1436 (3) [e], k	1438 (3) [e], k	1440 (5) e, k	1436 (2) D
2848 (2) e, k	2857 (3) e, k	2859 (4) e, k	2852 (1) PP
v	v	2953 (8) e, k, i	2950 (6) PP
2968 (8) e, k, i	2966 (10) e, k, i	2972 (10) e, k, i	2970 (8) PP
3020 (2) e, [k]	3013 (5) e, k, i	3013 (4b) e, [k]	3012 (2b) D

We thank Prof. M. Katayama and Prof. I. Nitta for their valuable advices. We are indebted to Hattori-Hôkôkai for a grant in aid of this research.

(8) Ananthakrishnan, *Proc. Indian Acad. Sci.*, A, **5** (1937), 285.

Summary.

In the region of the unmodified line there have been observed for crystalline ethylene halides some Raman lines which correspond to motions of a molecule as a whole, but not to internal normal vibrations. For ethylene bromide a considerable change in these low frequency lines was observed between the spectrum at −40°C. and that at 0°C. and it is highly probable that this change is caused at the transition temperature (−24°C.) observed in the thermal measurement. An explanation for these experimental results was suggested to identify these lines with lattice frequencies and to regard the transition point as the temperature at which the one dimensional molecular rotation sets in.

Chemical Institute, Faculty of Science,
Tokyo Imperial University.

The Normal Vibrations of Ethylene Halides.

By Yonezo MORINO.

(Received December 27, 1937.)

In the preceding article[1] it was established that the Raman lines observed in the solid state correspond to the symmetric vibrations of the *trans*-form of $C_2H_4X_2$, while those disappearing upon solidification to the antisymmetric vibrations, etc. This fact is very useful for the assignment of the fundamental frequencies of ethylene halides.

In our previous paper[2] we calculated the normal frequencies of $C_2H_4X_2$ considering CH_2-group as one particle, because it was chiefly in the lower frequency region that we were interested. To treat mathematically C-H vibrations as well as their effects on chain frequencies, we must consider the molecule as a system of eight particles having eighteen

(1) S. Mizushima and Y. Morino, this Bulletin, **13** (1938), 182. See also S. Mizushima, Y. Morino, and S. Noziri, *Nature*, **137** (1936), 945; *Sci. Papers Inst. Phys. Chem. Research* (Tokyo), **29** (1936), 63.

(2) S. Mizushima and Y. Morino, *Sci. Papers Inst. Chem. Phys. Research* (Tokyo), **26** (1934), 1.

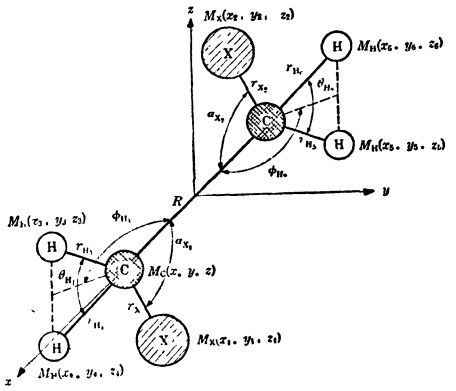


Fig. 1.

normal modes of vibrations. The equilibrium position of this system is the *trans*-form as shown in Fig. 1. It has the symmetry of C_{2h}, viz. one plane of symmetry and one centre of symmetry. The system makes a small vibration about this configuration. Let M_C, M_X, and M_H be the masses of carbon, halogen, and hydrogen atoms respectively, and x_i, y_i, z_i be their coordinates. The kinetic energy of this system T is easily separated as follows:

$$T = T_1 + T_2 + T_3 + T_4$$

where

$$T_1 = \frac{1}{4}M_C\left[(\dot{x}-\dot{x}')^2+(\dot{y}-\dot{y}')^2\right]+\frac{1}{4}M_X\left[(\dot{x}_1-\dot{x}_2)^2+(\dot{y}_1-\dot{y}_2)^2\right]$$
$$+\frac{1}{8}M_H\left[(\dot{x}_3+\dot{x}_4-\dot{x}_5-\dot{x}_6)^2+(\dot{y}_3+\dot{y}_4-\dot{y}_5-\dot{y}_6)^2+(\dot{z}_3-\dot{z}_4-\dot{z}_5+\dot{z}_6)^2\right],$$

$$T_2 = \frac{1}{4}M_C\left[(\dot{x}+\dot{x}')^2+(\dot{y}+\dot{y}')^2\right]+\frac{1}{4}M_X\left[(\dot{x}_1+\dot{x}_2)^2+(\dot{y}_1+\dot{y}_2)^2\right]$$
$$+\frac{1}{8}M_H\left[(\dot{x}_3+\dot{x}_4+\dot{x}_5+\dot{x}_6)^2+(\dot{y}_3+\dot{y}_4+\dot{y}_5+\dot{y}_6)^2+(\dot{z}_3-\dot{z}_4+\dot{z}_5-\dot{z}_6)^2\right],$$

$$T_3 = \frac{1}{4}M_C(\dot{z}-\dot{z}')^2+\frac{1}{4}M_X(\dot{z}_1-\dot{z}_2)^2$$
$$+\frac{1}{8}M_H\left[(\dot{x}_3-\dot{x}_4-\dot{x}_5+\dot{x}_6)^2+(\dot{y}_3-\dot{y}_4-\dot{y}_5+\dot{y}_6)^2+(\dot{z}_3+\dot{z}_4-\dot{z}_5-\dot{z}_6)^2\right],$$

and

$$T_4 = \frac{1}{4}M_C(\dot{z}+\dot{z}')^2+\frac{1}{4}M_X(\dot{z}_1+\dot{z}_2)^2$$
$$+\frac{1}{8}M_H\left[(\dot{x}_3-\dot{x}_4+\dot{x}_5-\dot{x}_6)^2+(\dot{y}_3-\dot{y}_4+\dot{y}_5-\dot{y}_6)^2+(\dot{z}_3+\dot{z}_4+\dot{z}_5+\dot{z}_6)^2\right].$$

The coordinates $x-x'$, $y-y'$, etc. belonging to the first part T_1 are totally symmetric, i.e. symmetric to the centre of symmetry as well as to the plane of symmetry. The coordinates $x+x'$, $y+y'$, etc. belonging to the second part T_2 are antisymmetric to the centre and symmetric

to the plane. The coordinates of the third part T_3 are symmetric to the centre and antisymmetric to the plane. The coordinates of the last part T_4 are antisymmetric both to the centre and to the plane. (See Table 1). It can be shown that the expression of the potential energy is also splitted into these four groups, although we assume the general quadratic form for it. The fundamental frequencies are thus separated into the four classes.

Table 1.

	Class I	Class II	Class III	Class IV
Centre of symmetry	sym.	antisym.	sym.	antisym.
Plane of symmetry	sym.	sym.	antisym.	antisym.
Coordinates of carbon atoms	$x-x'$ $y-y'$	$x+x'$ $y+y'$	$z-z'$	$z+z'$
Coordinates of halogen atoms	x_1-x_2 y_1-y_2	x_1+x_2 y_1+y_2	z_1-z_2	z_1+z_2
Coordinates of hydrogen atoms	$x_3+x_4-x_5-x_6$ $y_3+y_4-y_5-y_6$ $z_3-z_4-z_5+z_6$	$x_3+x_4+x_5+x_6$ $y_3+y_4+y_5+y_6$ $z_3-z_4+z_5-z_6$	$x_3-x_4-x_5+x_6$ $y_3-y_4-y_5+y_6$ $z_3+z_4-z_5-z_6$	$x_3-x_4+x_5-x_6$ $y_3-y_4+y_5-y_6$ $z_3+z_4+z_5+z_6$
Total number of coordinates	7	7	5	5
Conditions for translational motions		2		1
Conditions for rotational motions	1		2	
Number of normal coordinates	6	5	3	4
Selection rules for Raman-spectra	active	inactive	active	inactive
Selection rules for Infrared	inactive	active	inactive	active

The condition that the x-coordinate of the centre of gravity of the whole system is fixed, can be expressed by means of the coordinates belonging to Class II only:

$$M_C(\dot{x}+\dot{x}')+M_X(\dot{x}_1+\dot{x}_2)+M_H(\dot{x}_3+\dot{x}_5+\dot{x}_4+\dot{x}_6)=0\,.$$

The same holds for the y- and z-coordinates, thus we have

$$M_C(\dot{y}+\dot{y}')+M_X(\dot{y}_1+\dot{y}_2)+M_H(\dot{y}_3+\dot{y}_4+\dot{y}_5+\dot{y}_6)=0,$$

$$M_C(\dot{z}+\dot{z}')+M_X(\dot{z}_1+\dot{z}_2)+M_H(\dot{z}_3+\dot{z}_4+\dot{z}_5+\dot{z}_6)=0.$$

The conditions that the system is devoid of rotation are also given in a similar way. The number of the normal modes of vibrations belonging to each class is given by the difference between the number of the coordinates mentioned above and that of the conditions of this class. The vibrations of Classes I and III are active in the Raman effect, but inactive in the infrared. The vibrations of Classes II and IV are inactive in the Raman effect, but active in the infrared. These relations are summarized in Table 1.

It is very difficult to solve the secular equation for all the 18 frequencies. For the vibrations of Classes I and II, however, the solution can be obtained in the following way: For the potential energy of these classes we assume the following expression corresponding to a valence force system:

$$V=\frac{1}{2}k\overline{\Delta R}^2+\frac{1}{2}k_X(\overline{\Delta r}_{X_1}^2+\overline{\Delta r}_{X_2}^2)+\frac{1}{2}\delta_X r_X^2(\overline{\Delta\alpha}_{X_1}^2+\overline{\Delta\alpha}_{X_2}^2)$$
$$+\frac{1}{2}k_H(\overline{\Delta r}_{H_3}^2+\overline{\Delta r}_{H_4}^2+\overline{\Delta r}_{H_5}^2+\overline{\Delta r}_{H_6}^2)+\delta_H r_H^2(\overline{\Delta\phi}_{H_1}^2+\overline{\Delta\phi}_{H_2}^2)+\frac{1}{2}\beta_H r_H^2(\overline{\Delta\theta}_{H_1}^2+\Delta\theta_{H_2}^2),$$

where the notations are shown in Fig. 1.

In Class I, we have $\dot{x}=-\dot{x}'$, $\dot{y}=-\dot{y}'$, $\dot{x}_1=-\dot{x}_2$, $\dot{y}_1=-\dot{y}_2$, $\dot{x}_3=\dot{x}_4=-\dot{x}_5=-\dot{x}_6$, $\dot{y}_3=\dot{y}_4=-\dot{y}_5=-\dot{y}_6$, $\dot{z}_3=-\dot{z}_4=-\dot{z}_5=\dot{z}_6$, and $\Delta r_{X_1}=\Delta r_{X_2}$, $\Delta\alpha_{X_1}=\Delta\alpha_{X_2}$, $\Delta r_{H_3}=\Delta r_{H_4}=\Delta r_{H_5}=\Delta r_{H_6}$, $\Delta\phi_{H_1}=\Delta\phi_{H_2}$, $\Delta\theta_{H_1}=\Delta\theta_{H_2}$. Through complicated calculations similar to those given in our previous paper,[2] the secular equation which designates the six totally symmetric vibrations is found to be

$$\begin{vmatrix}
A_{11}\lambda^2-k, & A_{12}\lambda^2, & A_{13}\lambda^2, & A_{14}\lambda^2, & A_{15}\lambda^2, & A_{16}\lambda^2, \\
2A_{12}\lambda^2, & A_{22}\lambda^2-k_X, & A_{23}\lambda^2, & A_{24}\lambda^2, & A_{25}\lambda^2, & A_{26}\lambda^2, \\
2A_{13}\lambda^2, & A_{23}\lambda^2, & A_{33}\lambda^2-\delta_X r_X^2, & A_{34}\lambda^2, & A_{35}\lambda^2, & A_{36}\lambda^2, \\
2A_{14}\lambda^2, & A_{24}\lambda^2, & A_{34}\lambda^2, & A_{44}\lambda^2-2k_H, & A_{45}\lambda^4, & A_{46}\lambda^2, \\
2A_{15}\lambda^2, & A_{25}\lambda^2, & A_{35}\lambda^2, & A_{45}\lambda^2, & A_{55}\lambda^2-4\beta_H r_H^2, & A_{56}\lambda^2, \\
2A_{16}\lambda^2, & A_{26}\lambda^2, & A_{36}\lambda_2, & A_{46}\lambda^2, & A_{56}\lambda^2, & A_{66}\lambda^2-2\delta_H r_H^2,
\end{vmatrix}=0,$$

where A_{ij} are the coefficients defined by the masses of the atoms and the geometrical form of the molecule by means of the following relations:

$$\begin{cases} A_{11} = \frac{1}{2}M + 2a^2\rho , \\ A_{22} = M_X + b_1^2\rho , \\ A_{33} = M_X r_X^2 + c_1^2\rho , \\ A_{44} = 2M_H + b_2^2\rho , \\ A_{55} = 2M_H r_H^2 + d^2\rho , \\ A_{66} = 2M_H r_H^2 \cos^2\frac{\theta_H}{2} + c_2^2\rho , \end{cases}$$

$$\begin{cases} A_{12} = -\frac{1}{2}M_X \cos\alpha_X + ab_1\rho , \\ A_{13} = \frac{1}{2}M_X r_X \sin\alpha_X + ac_1\rho , \\ A_{14} = -M_H \cos\frac{\theta_H}{2}\cos\phi_H + ab_2\rho , \\ A_{15} = M_H r_H \sin\frac{\theta_H}{2}\cos\phi_H + ad\rho , \\ A_{16} = M_H r_H \cos\frac{\theta_H}{2}\sin\phi_H + ac_2\rho , \end{cases}$$

$$\begin{cases} A_{23} = b_1c_1\rho , \\ A_{24} = b_1b_2\rho , \\ A_{25} = b_1d\rho , \\ A_{26} = b_1c_2\rho , \\ A_{34} = c_1b_2\rho , \\ A_{35} = c_1d\rho , \\ A_{36} = c_1c_2\rho , \\ A_{45} = b_2d\rho , \\ A_{46} = b_2c_2\rho , \\ A_{56} = c_2d\rho , \end{cases}$$

and

$$\begin{cases} M = M_C + M_X + 2M_H , \\ -1/\rho = MR^2 + 4\left(M_X r_X^2 + 2M_H r_H^2 \cos^2\frac{\theta_H}{2}\right) \\ \qquad -4R\left(M_X r_X \cos\alpha_X + 2M_H r_H \cos\frac{\theta_H}{2}\cos\phi_H\right) , \\ a = -M_X r_X \sin\alpha_X + 2M_H r_H \cos\frac{\theta_H}{2}\sin\phi_H , \\ b_1 = M_X R \sin\alpha_X , \\ b_2 = -2M_H R \cos\frac{\theta_H}{2}\sin\phi_H , \\ d = 2M_H r_H R \sin\frac{\theta_H}{2}\sin\phi_H , \\ c_1 = -M_X r_X (2r_X - R\cos\alpha_X) , \\ c_2 = 2M_H r_H \cos\frac{\theta_H}{2}\left(2r_H \cos\frac{\theta_H}{2} - R\cos\phi_H\right) . \end{cases}$$

Putting $M_C = 12$, $M_H = 1.008$, $M_X = 79.92$, $r_H = 1.08$ Å, $r_X = 2.05$ Å, $R = 1.54$ Å and $\alpha = 109°28'$ for ethylene bromide, it is found that the cross terms A_{14}, $A_{15} \cdots A_{35}$, A_{36} are smaller than A_{11}, $A_{12} \cdots$, owing to the fact that the mass of hydrogen is small compared with that of bromine atom. If we neglect these cross terms, we have

$$\begin{vmatrix} A_{11}\lambda^2 - k, & A_{12}\lambda^2, & A_{13}\lambda^2, \\ 2A_{12}\lambda^2, & A_{22}\lambda^2 - k_X, & A_{23}\lambda^2, \\ 2A_{13}\lambda^2, & A_{23}\lambda^2, & A_{33}\lambda^2 - \delta_X r_X^2, \end{vmatrix} = 0 \qquad (1),$$

$$A_{44}\lambda^2 - 2k_H = 0 \qquad (2),$$

$$A_{55}\lambda^2 - 4\beta_H r_H^2 = 0 \qquad (3),$$

$$A_{66}\lambda^2 - 2\delta_H r_H^2 = 0 \qquad (4).$$

Equation (1) gives the chain frequencies of X-(CH_2)-(CH_2)-X. It can be reduced to the solution of the four body problem,[2] if $M_C + 2M_H$ is put equal to M and the distance r_H to zero. This shows that our former treatment for the chain frequencies is sufficiently correct in this approximation, even if we take the vibrations of hydrogen atoms into consideration. The latter three equations give the frequencies of CH_2-group, viz. equation (2) gives the C-H valency frequency, equation (3) that of the deformation of H-C-H angle, and equation (4) that of the deformation of CH_2-group relative to C-C axis.

These three hydrogen frequencies as well as the three chain frequencies should be active in the Raman effect in solid ethylene bromide. The higher frequencies of ethylene bromide in the solid state 2968 cm.$^{-1}$, 1436 cm.$^{-1}$, and 1254 cm.$^{-1}$ are assigned to the C-H frequencies, while the lower frequencies 187 cm.$^{-1}$, 656 cm.$^{-1}$, and 1057 cm.$^{-1}$ to the chain frequencies. The line 2968 cm.$^{-1}$ is identified with the C-H valency vibration; the line 1436 cm.$^{-1}$ with the deformation of H-C-H angle, and the line 1254 cm.$^{-1}$ with the deformation of CH_2-group relative to C-C axis. This assignment is in conformity with the results of Ta-You Wu[3] for C_2H_4 and of Trumpy[4] for *trans*-$C_2H_2Cl_2$. Ta-You Wu assigned the line 1440 cm.$^{-1}$ of C_2H_4 to the deformation frequency of CH_2-group. Trumpy observed that the frequency 1260 cm.$^{-1}$ of *trans*-$C_2H_2Cl_2$ decreased to 992 cm.$^{-1}$ on the insertion of D in place of H, showing that this frequency

(3) Ta-You Wu, *J. Chem. Phys.*, **5** (1937), 392.
(4) B. Trumpy, *Nature*, **135** (1935), 764.

is the deformation frequency of C-H to C-C axis. For ethylene chloride the corresponding three lines 2964 cm.$^{-1}$, 1448 cm.$^{-1}$, and 1301 cm.$^{-1}$, are identified with the totally symmetric vibrations of CH_2-groups. The force constants are thus obtained to be

$$\begin{cases} k_H = 5.19 \times 10^5 & \text{dyne/cm.} \\ \beta_H = 0.607 \times 10^5 & ,, \quad \text{for ethylene bromide,} \\ \delta_H = 0.308 \times 10^5 & ,, \end{cases}$$

and

$$\begin{cases} k_H = 5.18 \times 10^5 & \text{dyne/cm.} \\ \beta_H = 0.618 \times 10^5 & ,, \quad \text{for ethylene chloride.} \\ \delta_H = 0.330 \times 10^5 & ,, \end{cases}$$

For the vibrations of Class II, we obtain the following secular equation:

$$\begin{vmatrix} B_{11}\lambda^2-k_X, & 0, & B_{13}\lambda^2, & B_{14}\lambda^2, & B_{15}\lambda^2, \\ 0, & B_{22}\lambda^2-\delta_X r_X^2, & B_{23}\lambda^2, & B_{24}\lambda^2, & B_{25}\lambda^2, \\ B_{13}\lambda^2, & B_{23}\lambda^2, & B_{33}\lambda^2-2k_H, & B_{34}\lambda^2, & 0, \\ B_{14}\lambda^2, & B_{24}\lambda^2, & B_{34}\lambda^2, & B_{44}\lambda^2-4\beta_H r_H^2, & 0, \\ B_{15}\lambda^2, & B_{25}\lambda^2, & 0, & 0, & B_{55}\lambda^2-2\delta_H r_H^2, \end{vmatrix} = 0,$$

where

$$\begin{cases} B_{11} = M_X(M_C+2M_H)/M, \\ B_{22} = r_X^2 M_X(M_C+2M_H)/M, \\ B_{33} = 2M_H - 4\cos^2\frac{\theta_H}{2} M_H^2/M, \\ B_{44} = 2r_H^2 M_H - 4r_H^2 \sin^2\frac{\theta_H}{2} M_H^2/M, \\ B_{55} = 2r_H^2 \cos^2\frac{\theta_H}{2} M_H(M_C+M_X)/M, \end{cases}$$

and

$$\begin{cases} B_{13} = -2\cos\frac{\theta_H}{2}(\cos\alpha_X\cos\phi_H - \sin\alpha_X\sin\phi_H) M_H M_X/M, \\ B_{14} = 2r_H\sin\frac{\theta_H}{2}(\cos\alpha_X\cos\phi_H - \sin\alpha_X\sin\phi_H) M_H M_X/M, \end{cases}$$

$$\left\{\begin{aligned}
B_{15} &= 2r_H \cos\frac{\theta_H}{2}(\cos\alpha_X \sin\phi_H + \sin\alpha_X \cos\phi_H)M_H M_X/M\,,\\
B_{23} &= 2r_X \cos\frac{\theta_H}{2}(\cos\alpha_X \sin\phi_H + \sin\alpha_X \cos\phi_H)M_H M_X/M\,,\\
B_{24} &= -2r_X r_H \sin\frac{\theta_H}{2}(\cos\alpha_X \sin\phi_H + \sin\alpha_X \cos\phi_H)M_H M_X/M\,,\\
B_{25} &= 2r_X r_H \cos\frac{\theta_H}{2}(\cos\alpha_X \cos\phi_H - \sin\alpha_X \sin\phi_H)M_H M_X/M\,,\\
B_{34} &= 4r_H \cos\frac{\theta_H}{2}\sin\frac{\theta_H}{2}M_H^2/M\,.
\end{aligned}\right.$$

Neglecting the cross terms, we have

$$B_{11}\lambda^2 - k_X = 0 \qquad (5),$$

$$B_{22}\lambda^2 - \delta_X r_X^2 = 0 \qquad (6),$$

$$B_{33}\lambda^2 - 2k_H = 0 \qquad (7),$$

$$B_{44}\lambda^2 - 4\beta_4 r_H^2 = 0 \qquad (8),$$

$$B_{55}\lambda^2 - 2\delta_H r_H^2 = 0 \qquad (9).$$

Equations (5) and (6) express the antisymmetric valency and deformation frequencies of C-Cl bond and are the same as those derived in the previous paper.[2] Equations (7), (8), and (9) are those of the CH_2-groups. These vibrations are forbidden in the Raman effect for the *trans*-form of the molecule, and can be assigned to the lines disappearing in the solid spectra, for in the solid state the molecules of ethylene halides are in the *trans*-configuration, while in the liquid state it considerably deviates from this stable configuration. From the force constants obtained for the vibrations of Class I, we get the values 2978 cm.$^{-1}$, 1445 cm.$^{-1}$, and 1260 cm.$^{-1}$ for these lines. Actually ethylene bromide has the lines 2953 cm.$^{-1}$, 1419 cm.$^{-1}$, and 1276 cm.$^{-1}$, which disappear in the solid state and are to be assigned to the frequencies calculated. For ethylene chloride the observed lines 1429 cm.$^{-1}$ and 1393 cm.$^{-1}$ must be assigned to the calculated frequencies 1465 cm.$^{-1}$ and 1417 cm.$^{-1}$ respectively. Though in the C-H valency frequency region we have no line which vanishes and is to be assigned to the calculated frequency 2984 cm.$^{-1}$, comparison of its spectra with those of bromide suggests that the line corresponding to this frequency might overlap that of a symmetric vibration. (See Table 2.)

Table 2. Antisymmetric C–H vibrations.

	$C_2H_4Cl_2$		$C_2H_4Br_2$	
	$\nu_{calc.}$ (cm.$^{-1}$)	$\nu_{obs.}$ (cm.$^{-1}$)	$\nu_{calc.}$ (cm.$^{-1}$)	$\nu_{obs.}$ (cm.$^{-1}$)
ν(C—H)	2984	(2957) ?	2978	2953
δ(H-C-H)	1465	1429	1445	1419
δ(CH_2-C)	1417	1393	1260	1276

We have discussed eleven frequencies so far. It is easily seen from Table 1 that the remaining seven frequencies must be C-H vibrations except a vibration corresponding to the internal rotation. Thus we get as much lower frequencies as those of the four body problem X-(CH_2)-(CH_2)-X, even though we take the motion of hydrogen atoms into consideration. The conclusion of the previous paper with regard to these chain frequencies of ethylene halides is, therefore, not essentially modified by the consideration of the motion of hydrogen atoms.

In conclusion, the author wishes to express his cordial thanks to Prof. M. Katayama and Prof. S. Mizushima for their kind guidance and encouragement throughout the course of this study.

Chemical Institute, Faculty of Science,
Imperial University of Tokyo.

Über die Intensitätsverteilung der Faserdiagramme.

Von Yukichi GO, Saburo NAGATA und Jiro KAKINOKI.

(Eingegangen am 15. Januar 1938.)

I. **Einleitung.** Für die Entstehung der Faserstrukturen sind allgemein zwei Gründe massgebend, nämlich das natürliche Wachstum und die mechanische Deformation.

Als Wachstumsfaserstrukturen kann man nennen die von allen organischen Pflanzenfasern, ferner von tierischen Haaren und Wolle und vielleicht noch die von mineralischen Fasern.

Demgegenüber ist die Faserstruktur bei der Naturseide, Seidenstramin, Kunstseide, Zellwolle und den dünnen Metallfasern auf Einflüsse der mechanischen Deformation zurückzuführen.

Aber auch die oben angegebenen Fasern haben nicht immer die einfache Faserstruktur, sondern es können auch Spiralfaserstruktur,[1] Ringfaserstruktur und ganz allgemein noch abweichende Strukturen verschiedenen Grades vorliegen.

Im Folgenden wird nun die Intensitätsverteilung bei Röntgenaufnahmen dieser verschiedenen Faserstrukturen besprochen.

Über die Beziehung zwischen der Orientierung der Kristallite und der Intensitätsverteilung von Röntgenfaserdiagrammen existiert bisher nicht viele Literatur. Nach der allgemeinen qualitativen Systematisierung von K. Weissenberg,[1][2][3] hat O. Kratky[4] zum ersten Mal einen quantitativen Ausdruck für die Äquator-Reflexe der Spiralfaserstruktur abgeleitet, als er den Deformationsmechanismus der Faserstoffe untersuchte. I. Sakurada und K. Hutino haben für den Fall der Ringfaserstruktur die Intensitätsverteilung nicht nur für die Äquator-Reflexe, sondern auch für die allgemeinen Reflexe quantitativ diskutiert. Der noch allgemeinere Fall, nämlich der allgemeinen Reflexe der verschiedenen Faserstrukturen, wurde im hiesigen Laboratorium untersucht.[6] Beinahe zur gleichen Zeit hat C. Matano nach eigener Rechnungsweise ebenfalls den allgemeinen Fall behandelt.[7]

---

(1) K. Weissenberg, *Z. Physik*, **8** (1921), 20.
(2) K. Weissenberg, *Ann. Physik*, **69** (1922), 421.
(3) K. Weissenberg, *Z. Krist.*, **61** (1925), 58.
(4) O. Kratky, *Kolloid-Z.*, **64** (1933), 213.
(5) I. Sakurada und K. Hutino, *Sci. Papers Inst. Phys. Chem. Research* (Tokyo), **24** (1934), 193.
(6) Y. Go, J. Kakinoki und S. Nagata, *Rept. Japan. Assoc. Adv. Sci.*, **12** (1937), 128.
(7) C. Matano, *J. Soc. Chem. Ind. Japan*, **39** (1936), 478.

II. **Anwendung der Polanyi'schen Lagenkugel.** Für die Diskussion des Faserdiagrammes ist bekanntlich die Anwendung der Polanyi'schen Lagenkugel[8] am bequemsten. Jeder Kristallit des Aggregates wird durch Parallelverschiebung in den Mittelpunkt einer Einheitskugel gebracht und die Durchstosspunkte seiner Achsen an der Kugeloberfläche werden aufgesucht. Die „Dichte" oder „Belegungsdichte", welche diese „Repräsentationspunkte" an einer bestimmten Stelle haben, ist ein Mass für die Häufigkeit der entsprechenden Achsenrichtung. Die Dichteverteilung dieser „Repräsentationspunkte" auf der Lagenkugel zeigt den Ordnungszustand der Kristallite im Aggregat.

Für die Ermittlung der Intensitätsverteilung längs des Debye-Scherrer-Kreises jedoch muss in erster Linie die Dichteverteilung der Netzebenenrepräsentationspunkte auf der Lagenkugel entlang dem Reflexionskreise untersucht werden.

III. **Verhältnisse auf der Lagenkugel.** Die Lagenkugel für die Diskussion der Intensitätsverteilung ist in Abb. 1 abgebildet. Die Röntgenstrahlen gehen durch S_0 nach O. Eine zu untersuchende ideale Spiralfaser befindet sich im Punkte O und ihre Faserachse OF steht senkrecht zur Richtung S_0O. Da die Kristallitachse OC der Faser, welche mit der Symmetrieachse OF einen Winkel φ bildet, um diese gleichmässig verteilt ist, bildet der geometrische Ort von C einen Kreis, welcher OF als seine Achse besitzt.

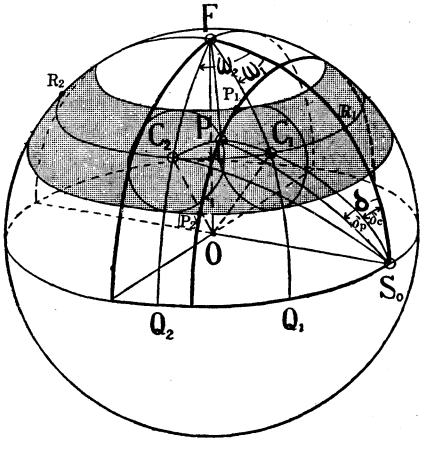


Abb. 1.

Die Normale von der Netzebene, welche bestimmten Netzebenenabstand „d" besitzt verteilt sich um OC herum gleichmässig mit dem bestimmten Winkel ρ. Der geometrische Ort der Repräsentationspunkte dieser Normalen bilden einen sogenannten „Netzebenenkreis" um die Achse OC.

Während die Kristallitachse OC um die Faserachse OF herum verteilt ist und ihre Repräsentationspunkte C folglich einen Kreis bilden, bestreicht der Netzebenenkreis eine Zone (auf der Abbildung schraffiert) auf der Lagenkugel. Alle Repräsentationspunkte der in Frage kommenden Netzebenen fallen also in diese Zone hinein. Diese Zone kann man die „Netzebenenzone" nennen.

(8) M. Polanyi, *Z. Physik*, **7** (1921), 149.

Im allgemeinen wenn die den bestimmten Netzebenenabstand „d" besitzende Netzebene die Röntgenstrahlen reflektiert, muss ihre Normale nach einer bestimmten Richtung gerichtet sein, welche die Bragg'sche Beziehung $n\lambda = 2d\sin\theta$ erfüllt. Der geometrische Ort der Repräsentationspunkte einer solchen Normale bildet einen sogenannten „Reflexionskreis" auf der Lagenkugel um die Achse OS_0, welche von dem Punkt S_0 den Abstand $90°-\theta$ besitzt.

Der Schnittpunkt von Reflexionskreis und Netzebenenkreis bildet einen Interferenzpunkt auf dem Debye-Scherrer-Kreis. Der Punkt P in Abb. 1 ist ein dieser Reflexionsstelle entsprechender Punkt auf der Lagenkugel.

Der Richtungswinkel δ einer Reflexionsstelle längs des Debye-Scherrer-Kreises wird auf der photographischen Platte von der Projektionslinie der Achse OF aus gemessen, und zwar von dem Punkte S_0 aus gesehen nach links als positiv. Dann ist der Winkel zwischen den beiden Hauptkreisen FS_0 und PS_0 kein anderer als δ.

IV. **Diskussion der Intensitätsverteilung.** Einerseits denken wir uns die Intensität an der Reflexionsstelle proportional der Anzahl der Kristallitachsen, welche in dem kleinen Bereich $d\delta$ ihren Einfluss ausüben.

Die Lage der Repräsentationspunkte C der Kristallitachse OC, deren Netzebenenkreis den Reflexionskreis im Punkte P schneidet, wird durch den Winkel ω bestimmt. Dabei ist ω der Winkel zwischen den Hauptkreisen FS_0 und FC, gemessen von F aus gesehen nach rechts als positiv. Die Zahl der Kristallitachsen ist dann proportional $d\omega$ und die gesuchte Intensität muss dem Werte $\frac{d\omega}{d\delta}$ proportional sein.

Andererseits kann man die Wanderungsgeschwindigkeit des Punktes P—längs des Reflexionskreises zwischen P_1 und P_2—mit $v = \frac{d\delta}{dt}$ annehmen, während die Kristallitachse OC mit der konstanten Geschwindigkeit $\frac{d\omega}{dt}$ = Konst. um ihre Achse rotiert. Nach der Beziehung $\frac{d\delta}{d\omega} \cdot \frac{d\omega}{dt} = \frac{d\delta}{dt}$ ist daher $\frac{d\omega}{d\delta} = \frac{1}{v}$. Also ist die gesuchte Intensität proportional $\frac{1}{v}$. Je schneller also der Punkt P längs des Reflexionskreises wandert, desto kleiner wird die Intensität der entsprechenden Reflexionsstelle im Diagramm. Unsere Aufgabe besteht nunmehr darin, den Wert von $\frac{d\delta}{d\omega}$ oder v auszurechnen. Der Winkel δ wird in zwei geteilt; δ_c ist derjenige zwischen den beiden Hauptkreisen CS_0 und FS_0, und δ_p der zwischen PS_0 und CS_0. .

$$\delta = \delta_c \pm \delta_p \tag{1}$$

$$\therefore \quad \frac{d\delta}{d\omega} = \frac{d\delta_c}{d\omega} \pm \frac{d\delta_p}{d\omega}$$

Aus den drei sphärischen Dreiecken PCS_0, FCS_0 und CQS_0 (Q ist der Schnittpunkt eines zu OF senkrecht stehenden und durch den Punkt S_0 gehenden Hauptkreises SQ mit dem Hauptkreis FC) können die folgenden drei Gleichungen abgeleitet werden.

$$\cos\delta_p = (\cos\rho - \cos\beta\sin\theta)\big/\sin\beta\cos\theta \tag{2},$$

$$\cos d_c = \cos\varphi\big/\sin\beta \tag{3},$$

$$\cos\beta = \sin\varphi\cos\omega \tag{4},$$

wobei β der Winkel zwischen OC und OS_0 ist.

Aus diesen drei Grundbeziehungen folgt:

$$\frac{d\delta}{d\omega} = \frac{\sin\varphi}{(1-\sin^2\varphi\cos^2\omega)}\Big\{\cos\varphi\cos\omega \pm \mu\sin\omega\,(\sin\varphi\cos\omega\cos\rho - \sin\theta) \times (\cos^2\theta - \sin^2\varphi\cos^2\omega - \cos^2\rho + 2\cos\rho\sin\theta\sin\varphi\cos\omega)^{\frac{1}{2}}\Big\} \tag{5},$$

$\pm$ ist bestimmt nach (1): $\mu = +1$ wenn $\sin\delta_p \geqslant 0$ und $\mu = -1$ wenn $\sin\delta_p < 0$.

Da im allgemeinen jeder Interferenzpunkt P zu zwei Netzebenenkreisen (C_1 und C_2 in Abb. 1) gehören kann, so müssen beide bei der Rechnung berücksichtigt werden. Dementsprechend sind auch für ω zwei Werte ω_1 und ω_2 möglich und wird nach jedem einzelnen bestimmt, nämlich $v_1 = \frac{d\delta}{d\omega_1}$ und $v_2 = \frac{d\delta}{d\omega_2}$.

$$v_1 = \left(\frac{d\delta}{d\omega}\right)_{\omega=\omega_1} = \frac{A}{A^2-B_1^2}\left\{\cos\varphi\cdot B_1 + \kappa_1\frac{(\cos\rho B_1 - \sin\theta A)\sqrt{\sin^2\varphi\cdot A^2 - B_1^2}}{\sqrt{A^2\cos^2\theta - B_1^2 - A^2\cos^2\rho + 2\cos\rho\sin\theta\cdot A\cdot B_1}}\right\}$$

$$v_2 = \left(\frac{d\delta}{d\omega}\right)_{\omega=\omega_2} = (B_1 \text{ und } \kappa_1 \text{ sind durch } B_2 \text{ und } \kappa_2 \text{ zu ersetzen}).$$

Wobei
$$A = 1-\cos^2\delta\cos^2\theta$$
$$B_1 = \sin\theta\cos\rho - \cos\varphi\cos\delta\sin\theta\cos\theta + \cos\theta\sin\delta\sqrt{c}$$
$$B_2 = \sin\theta\cos\rho - \cos\varphi\cos\delta\sin\theta\cos\theta - \cos\theta\sin\delta\sqrt{c}$$
$$c = \sin^2\varphi - \cos^2\rho - \cos^2\theta\cos^2\delta + 2\cos p\cos\varphi\cos\theta\cos\delta$$
κ_1 und κ_2 sind $+1$ oder -1.

Die gesuchte Intensität ist nun:

$$I \propto \left|\frac{1}{v_1}\right| + \left|\frac{1}{v_2}\right| \qquad (7),$$

Einige spezielle Fälle.

(A) Äquator-Reflexe der Spiralfaserstruktur $\rho = 90°$.

$$v_1 = \frac{A}{A^2-B_1^2}\left\{\cos\varphi B_1 + \frac{\sin\theta A\sqrt{\sin^2\varphi A^2-B_1^2}}{\sqrt{A^2\cos^2\theta - B_1^2}}\right\}$$
$$v_2 = \frac{A}{A^2-B_2^2}\left\{\cos\varphi B_2 - \kappa_2\frac{\sin\theta A\sqrt{\sin^2\varphi A^2-B_2^2}}{\sqrt{A^2\cos^2\theta - B_2^2}}\right\} \qquad (8)$$

κ_1 ist hierbei immer -1 und nur κ_2 muss wie folgt bestimmt werden:

(1) wenn $\cos\delta < \tan\varphi\tan\theta$
wenn $\cos\delta \lesseqgtr \cos\varphi\sin\theta$, $\kappa_2 = \pm 1$
wenn $\cos\delta = \cos\varphi\sin\theta$, $v_2 = \infty$ unabhängig von κ_2

(2) wenn $\cos\delta = \tan\varphi\tan\theta$ . . . . . $v_2 = -\tan\varphi$,, ,, ,, .

(3) wenn $\cos\delta > \tan\varphi\tan\theta$ . . . . . $\kappa_2 = -1$

(B) (i) Ringfaserstruktur (allgemeine Reflexe) $\varphi = 90°$.

$$v_{1,2} = \frac{A(\cos\rho B_{1,2} - \sin\theta A)}{\sqrt{A^2-B_{1,2}^2}} \times \{A^2\cos^2\theta - B_{1,2}^2 - A^2\cos^2\rho + 2\cos\rho\sin\theta A B_{1,2}\}^{-\frac{1}{2}} \qquad (9)$$

(ii) Äquator-Reflexe der Ringfaserstruktur $\varphi = 90°$, $\rho = 90°$.

$$v_1 = v_2 = (1-\cos^2\delta\cos^2\theta)\Big/\cos\delta\sin\theta\cos\theta \qquad (10)$$

Die Gleichungen (9) und (10) stimmen mit denjenigen überein, welche von Sakurada und Hutino abgeleitet wurden.

V. **Systematisierung der verschiedenen Diagramm-Typen.** Da die Intensität I nicht imaginär sein kann, kann

$$C = \sin^2\varphi - \cos^2\rho - \cos^2\theta\cos^2\delta + 2\cos\rho\cos\varphi\cos\theta\cos\delta$$

keinen negativen Wert haben und damit folgt:

$$\frac{\cos(\varphi-\rho)}{\cos\theta} \geqslant \cos\delta \geqslant \frac{\cos(\varphi+\rho)}{\cos\theta} \qquad (11).$$

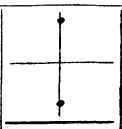
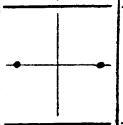
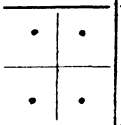
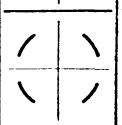
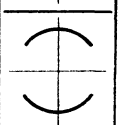
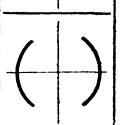
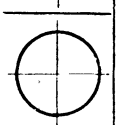
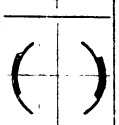
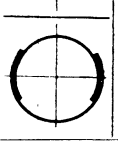
Unter Zugrundelegung dieser Bedingung kann man sämtliche möglichen Diagrammtypen systematisieren, wie es in der folgenden Tabelle 1 gezeigt wird.

Dabei scheiden von vornherein die zwei folgenden Fälle aus:

(1) Wenn $\theta > \rho+\omega$ ist, tritt kein Reflex auf.

(2) kann nicht 0 sein.

Tabelle 1.

1		$\begin{cases}\rho=0\\ \theta=\varphi\end{cases}$ $\begin{cases}\varphi=0\\ \theta=\rho\end{cases}$ $\begin{cases}\rho<\varphi\\ \rho<90^\circ-\varphi\\ \theta=\varphi+\rho\end{cases}$ $\begin{cases}\rho=\varphi\\ \rho<90^\circ-\varphi\\ \theta=2\varphi\end{cases}$ $\begin{cases}\rho>\varphi\\ \rho<90^\circ-\varphi\\ \theta=\rho+\varphi\end{cases}$
2		$\begin{cases}\rho=0\\ \varphi=90^\circ\end{cases}$ $\begin{cases}\rho=90^\circ\\ \varphi=0\end{cases}$
3		$\begin{cases}\rho=0\\ \varphi\neq 90^\circ\\ \theta<\varphi\end{cases}$ $\begin{cases}\varphi=0\\ \theta<\rho\neq 90^\circ\end{cases}$
4		$\begin{cases}\rho<\varphi\\ \rho<90^\circ-\varphi\\ \theta<\varphi-\rho\end{cases}$ $\begin{cases}\rho>\varphi\\ \rho<90^\circ-\varphi\\ \theta<\rho-\varphi\end{cases}$
5		$\begin{cases}\rho<\varphi\\ \rho<90^\circ-\varphi\\ \theta\geq\varphi-\rho\\ \theta<\varphi+\rho\end{cases}$ $\begin{cases}\rho=\varphi\\ \rho<90^\circ-\varphi\\ \theta<2\varphi\end{cases}$ $\begin{cases}\rho>\varphi\\ \rho<90^\circ-\varphi\\ \theta\geq\rho-\varphi\\ \theta<\rho+\varphi\end{cases}$
6		$\begin{cases}\rho<\varphi\\ \rho=90^\circ-\varphi\\ \theta<\varphi-\rho\end{cases}$ $\begin{cases}\rho<\varphi=90^\circ\\ \theta<90^\circ-\rho\end{cases}$ $\begin{cases}\rho>\varphi\\ \rho=90^\circ-\varphi\\ \theta<\rho-\varphi\end{cases}$ $\begin{cases}\rho=90^\circ>\varphi\\ \theta<90^\circ-\varphi\end{cases}$
7		$\begin{cases}\rho<\varphi=90^\circ\\ \theta=90^\circ-\rho\end{cases}$ $\begin{cases}\rho<\varphi\\ \rho=90^\circ-\varphi\\ \theta\geq\varphi-\rho\end{cases}$ $\begin{cases}\rho<\varphi\neq 90^\circ\\ \rho>90^\circ-\varphi\\ \theta\geq 180^\circ-(\varphi+\rho)\end{cases}$ $\begin{cases}\rho<\varphi=90^\circ\\ \theta>90^\circ-\rho\end{cases}$ $\rho=\varphi=45^\circ$ $\begin{cases}\rho=\varphi\neq 90^\circ\\ \rho>90^\circ-\varphi\\ \theta\geq 180^\circ-2\varphi\end{cases}$
8		$\begin{cases}\rho<\varphi\neq 90^\circ\\ \rho>90^\circ-\varphi\\ \theta<\varphi-\rho\end{cases}$ $\begin{cases}90^\circ\neq\rho>\varphi\\ \rho>90^\circ-\varphi\\ \theta<\rho-\varphi\end{cases}$ $\rho=\varphi=90^\circ$ $\begin{cases}\rho>\varphi\\ \rho=90^\circ-\varphi\\ \theta\geq\rho-\varphi\end{cases}$ $\begin{cases}90^\circ\geq\rho>\varphi\\ \rho>90^\circ-\varphi\\ \theta\geq 180^\circ-(\varphi+\rho)\end{cases}$
9		$\begin{cases}\rho<\varphi\neq 90^\circ\\ \rho>90^\circ-\varphi\\ \theta\geq\varphi-\rho\\ \theta<180^\circ-(\varphi+\rho)\end{cases}$ $\begin{cases}\rho=\varphi\neq 90^\circ\\ \rho>90^\circ-\varphi\\ \theta<180^\circ-2\varphi\end{cases}$ $\begin{cases}90^\circ\neq\rho>\varphi\\ \rho>90^\circ-\varphi\\ \theta\geq\rho-\varphi\\ \theta<180^\circ-(\varphi+\rho)\end{cases}$

Diese Tabelle zeigt natürlich nur die typischen Formen der Diagramme, gibt dagegen keine Auskunft über die Intensitätsverhältnisse.

Alle diese Reflexions- bzw. Diagramm-Typen können ebenfalls abgeleitet werden ohne die Beziehung (11) anzuwenden, und zwar mit Hilfe einer einfachen Betrachtung der Lagenkugel. Dieses hat bereits früher K. Weissenberg getan. Einer der von K. Weissenberg beschriebenen Fälle muss aber hier korrigiert werden. Für den Fall $\rho > \varphi$ wurde von ihm ein Diagrammtypus besprochen, der durch eine Intensitätsverdopplung in der vertikalen Mittellinie charakterisiert war. Aber wie man in der Tabelle 1 deutlich sieht, existiert diese Möglichkeit nicht.

Eine experimentelle Bestätigung hierfür konnte wie folgt durchgeführt werden. Ein Steinsalzkristall wurde um eine Achse herum gedreht, welche ihrerseits nochmals mit dem Neigungswinkel $\varphi = 51°10'$ (dem Spiralwinkel entsprechend) um eine zweite Achse rotierte. Bestrahlt man diesen rotierenden Kristall senkrecht zur zweiten Drehachse, dann erhält man ein der idealen Spiralfaserstruktur entsprechendes Diagramm. Trotzdem die Reflexionen der Ebenen (111), (200) und (220) die Bedingung $\rho > \varphi$ erfüllen, tritt dabei keine Intensitätsverdopplung in der vertikalen Mittellinie auf. Ein schematisches Bild und die Winkelverhältnisse werden in Abb. 2 und Tabelle 2 gezeigt.

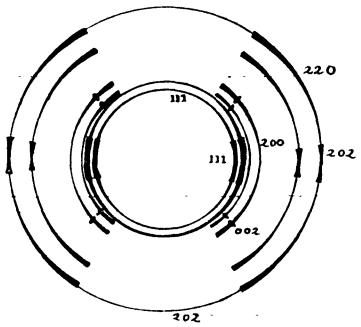


Abb. 2.

Tabelle 2.

φ=51° 10′ λ=Cu K_α K_β						
Index	λ	ρ	γ	δ_1	δ_2	Reflexe
111	α	54°41′	13°41′	0°	106°20′	
	β	54°41′	12°21′	0°	106°10′	
200	α	90°	15°51′	36°	144°	
	β	90°	14°18′	36°30′	143°30′	
002	α	0°	15°51′	49°20′	49°20′	
	β	0°	14°18′	49°40′	49°40′	
220	α	90°	22°42′	32°20′	147°40′	
	β	90°	20°42′	33°50′	146°10′	
202	α	45°	22°42′	0°	96°40′	
	β	45°	20°24′	0°	96°30′	

VI. **Vergleich der Intensitätsformeln von verschiedenen Autoren.** Jeder Autor hat nach eigenem Arbeitsprinzip die Verteilungsfunktionen ausgerechnet und ist zu verschiedenen Formeln gekommen, die aber beinahe gleiche Kurven zeigen. Diese Formeln müssen zunächst auf eine gleiche Bezeichnungsweise gebracht und dann zusammengestellt werden.

(1) *Spiralfaserstruktur.* (a) Allgemeine Reflexe.

(i) unsere Formel: $I \propto \left|\frac{1}{v_1}\right| + \left|\frac{1}{v_2}\right|$

$$v_{1,2} = \left(\frac{d\delta}{\delta\omega}\right)_{\omega_1,\omega_2} = \frac{A}{A^2-B_{1,2}^2}\left\{\cos\varphi\cdot B_{1,2} + \kappa_{1,2}\frac{(\cos\rho B_{1,2}-\sin\theta\cdot A)\sqrt{\sin\varphi\, A^2-B_{1,2}^2}}{\sqrt{A^2\cos^2\theta-B_{1,2}^2-A^2\cos^2\rho+2\cos\rho\sin\theta\cdot A\cdot B_{1,2}}}\right\}$$

$$A = 1-\cos^2\delta\cos^2\theta$$
$$B_1 = \sin\delta\cos\rho-\cos\varphi\cos\delta\sin\theta\cos\theta+\cos\theta\sin\delta\sqrt{c}$$
$$B_2 = \quad ,, \qquad ,, \qquad -\cos\theta\sin\delta\sqrt{c}$$
$$c = \sin^2\varphi-\cos^2\rho-\cos^2\theta\cos^2\delta+2\cos\rho\cos\varphi\cos\theta\cos\delta$$

(ii) Matano'sche Formel:

$$I \propto \frac{\sin\rho}{\sqrt{\sin^2\varphi-\cos^2\rho-\cos^2\theta\cos^2\delta+2\cos\theta\cos\rho\cos\varphi\cos\delta}}$$

$$\propto \frac{\sin\rho}{\sqrt{c}} \propto \frac{1}{\sqrt{c}} \quad (\sin\rho \text{ ist konstant bei einem bestimmten } \rho)$$

Die Matano'sche Formel ist viel einfacher als die von uns. Sie enthält nur den Ausdruck $\sqrt{c}$.

(b) Äquator-Reflexe. $\rho = 90°$.

(i) unsere Formel:

$$v_{1,2} = \frac{A}{A^2-B_{1,2}^2}\left\{\cos\varphi\cdot B_{1,2}-\kappa_{1,2}\cdot\frac{\sin\theta\cdot A\sqrt{\sin^2\varphi\, A^2-B_{1,2}^2}}{\sqrt{A^2\cos^2\theta-B_{1,2}^2}}\right\},$$

$$I \propto \left|\frac{1}{v_1}\right| + \left|\frac{1}{v_2}\right|.$$

(ii) Matano: $$I \propto \frac{1}{\sqrt{\sin^2\varphi-\cos^2\theta\cos^2\delta}}.$$

(iii) Kratky: $$I \propto \frac{\sin\varphi}{\sqrt{\sin^2\varphi-\cos^2\theta\cos^2\delta}} \propto \frac{1}{\sqrt{\sin^2\varphi-\cos^2\theta\cos^2\delta}}.$$

($\sin\varphi$ ist konstant bei einem bestimmten φ)

Hier stimmen die Formeln von Matano und Kratky überein.

(2) *Ringfaserstruktur.* (a) Allgemeine Reflexe.

(i) unsere Formel:

$$v_{1,2} = \frac{A(\cos\rho B_{1,2} - \sin\theta \cdot A)}{\sqrt{A^2 - B_{1,2}^2}} \times \left\{A^2\cos^2\theta - B_{1,2}^2 - A^2\cos^2\rho + 2\cos\rho\sin\theta A \cdot B_{1,2}\right\}^{-\frac{1}{2}},$$

$$I \propto \left|\frac{1}{v_1}\right| + \left|\frac{1}{v_2}\right|.$$

(ii) Matano: $$I \propto \frac{\sin\rho}{\sqrt{1-\cos^2\rho-\cos^2\theta\cos^2\delta}}.$$

(b) Äquator-Reflexe.

(i) unsere Formel: $$I \propto \frac{\cos\delta\sin\theta\cos\theta}{1-\cos^2\delta\cos^2\theta}.$$

(ii) Matano: $$I \propto \frac{1}{\sqrt{1-\cos^2\delta\cos^2\theta}}.$$

(iii) Kratky: $$I \propto \frac{1}{\sqrt{1-\cos^2\delta\cos^2\theta}}.$$

(iv) Sakurada u. Hutino: $$I \propto \frac{\cot\theta\cos\delta}{1+\cot^2\theta\sin^2\delta} = \frac{\cos\delta\sin\theta\cos\theta}{1-\cos^2\delta\cos^2\theta}.$$

Hier findet man zwei paarweise Übereinstimmungen, nämlich einerseits zwischen uns und Sakurada-Hutino, und andererseits zwischen Matano und Kratky.

Die zwei verschiedenen Funktionen sind in Abb. 3 graphisch dargestellt.

Die Kurven der Funktionen unterscheiden sich zu wenig von einander und auch die experimentelle Genauigkeit ist nicht gross genug, um die Richtigkeit der Funktionen einwandrei festzustellen.

Es ist also notwendig irgendeinen Fall herauszusuchen, bei dem die Funktionen schon qualitativ vershieden sind. Die Maximum- und Minimumpunkte der Funktionen wurden ausgerechnet und verglichen, aber leider findet man bei der Ringfaserstruktur in allen Fällen, und bei der Spiralfaserstruktur im Falle der Äquator-Reflexe keine Unterschiede. Nur bei den allgemeinen Reflexen der Spiralfaserstruktur ergibt sich die Möglichkeit einer Nachprüfung, da die Funktionen von uns und von Matano einen voneinander experimentell unterscheidbaren Minimumpunkt besitzen. Die Abb. 4 zeigt die Kurven für die Netzebene (021) der Cellulose; die ausgezogene Linie ist die nach unserer Funktion, die Gestrichelte Linie die nach Matano errechnete Kurve.

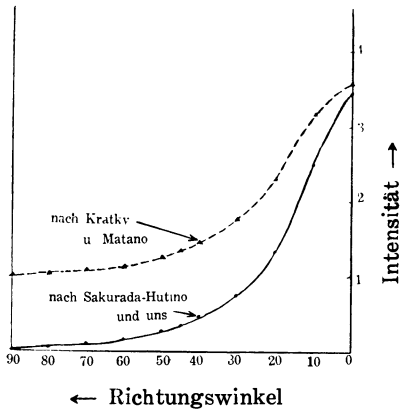


Abb. 3.

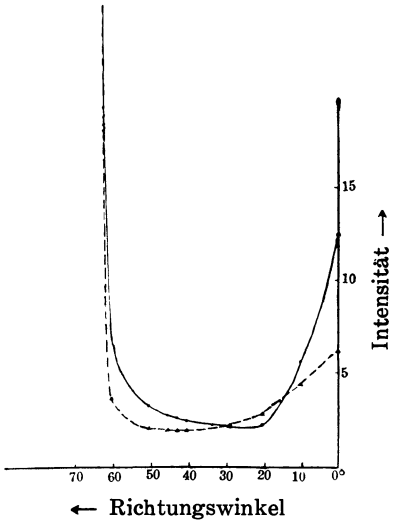


Abb. 4.

In unserer letzten Aufnahme konnten wir feststellen, dass die nach unserer Funktion errechnete Kurve mit dem experimentellen Ergebnis übereinstimmt.

VII. **Realisierung der verschiedenen Faserstrukturen durch Rotation des „Einkristalls"** Wie es schon im Paragraph V erklärt ist, kann man durch die doppelte Rotation des „Einkristalls" beliebige ideale Faserstrukturen realisieren. Hier zeigen wir das letzte Modell unserer Kamera und einige damit gemachte Aufnahmen.

Der Kristall K (Abb. 5) wird zunächst auf die Spitze einer Drehachse A gesetzt und mit einer konstanten Geschwindigkeit, welche durch einen kleinen synchronisierten Motor erzeugt wird, um eine bestimmte kristallographische Achse herum gedreht. Das ganze System lässt man dann nochmals um eine zweite Achse B (der Faserachse entsprechend) herum rotieren. Der Winkel φ zwischen den beiden Drehachsen A und B, welcher dem Spiralwinkel entspricht, ist beliebig regulierbar konstruiert. Durch die Blende S wird der Kristall senkrecht zur Achse B mit Röntgenstrahlen bestrahlt und das Diagramm wird auf einer flachen photographischen Platte oder einem zylindrisch gerollten Film F aufgenommen. Um längs des Debye-Scherrer-Kreises praktisch zu photometrieren, ist der zylindrisch gerollte Film geeignet, dessen Achse aber dabei mit dem Röntgenstrahlenbündel übereinkommen muss. Da das „Einkristall" der Cellulose selbst nicht hergestellt und daher auch nicht untersucht werden kann, so wird zur annäherungsweisen Realisierung beliebiger Faserstrukturen von

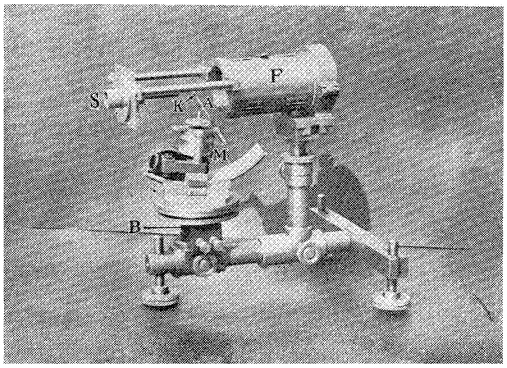


Abb. 5 Doppeldrehe-Kristall Kamera.

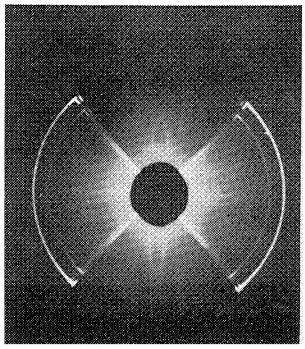


Abb. 6.

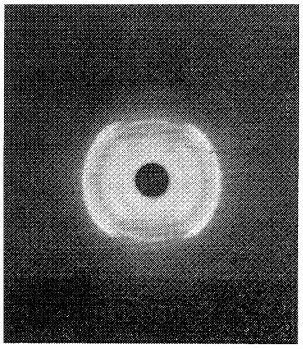


Abb. 7.

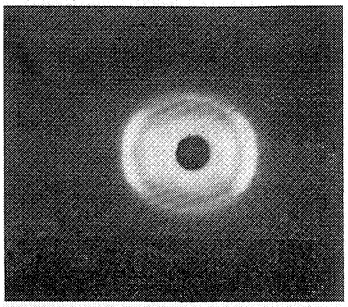


Abb. 8.

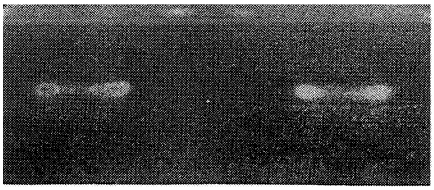


Abb 9.

Cellulose die Ramiefaser benutzt, da diese den besten Parallelitätsgrad der Kristallite aufweist.

Natürlich ist es nicht notwendig, bei der Ramiefaser die Achse A rotieren zu lassen, weil sie schon axiale Symmetrie besitzt; ferner ist es auch nicht möglich, damit die ideale Spiralfaserstruktur zu realisieren, sondern nur die reale.

Abb. 6 und 7 zeigen die Spiralfaserdiagramme von NaCl und Cellulose ($\varphi = 45°$), welche mit unserer Einrichtung aufgenommen sind. Die Intensitätsverteilungskurven dieser beiden Aufnahmen sind in Abb. 10 dargestellt.

Abb. 8 zeigt das Diagramm der natürlichen Spiralfaser der Agave.

Abb. 9 ist das auf dem zylindrisch gerollten Film aufgenommene Spiralfaserdiagramm der Cellulose mit dem Spiralwinkel 60°.

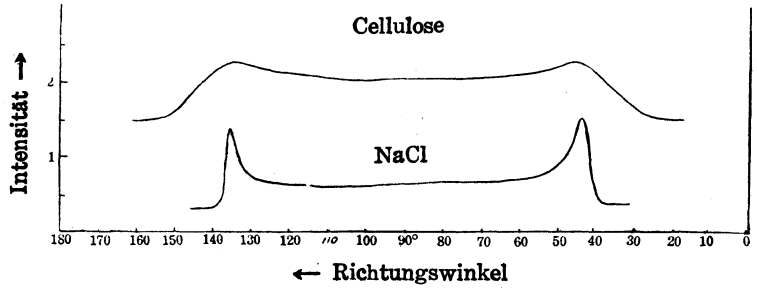


Abb. 10.

Schlussbetrachtung. Es wurde versucht, die Intensitätsverteilung des Faserdiagrammes quantitativ zu erfassen und eine allgemeine mathematische Funktion für die Intensitätsverteilung bei der idealen Spiralfaserstruktur zu finden. Eine solche Funktion schliesst die Intensitätsverteilung bei der Ringfaserstruktur und der einfachen Faserstruktur als Spezialfälle ein, und andererseits kann man sich das Diagramm der realen Faserstruktur aus einer Überlagerung vieler idealer Spiralfaserstrukturdiagramme zusammengesetzt denken.

Es wurde nun auf dem oben beschriebenen Wege eine Formel für die Intensitätsverteilung abgeleitet. Im Anschluss hieran konnte unter Zugrundelegung dieser Formel eine Systematisierung der verschiedenen möglichen Diagrammtypen vorgenommen werden.

Es wurde dann weiterhin ein genauer Vergleich unserer Formel mit den Formeln anderer Autoren vorgenommen. Hierbei zeigte es sich, dass die verschiedenen, auf verschiedenen Wegen erhaltenen Formeln von Kratky, Sakurada-Hutino, Matano und uns zwar sehr ähnlich sind, aber

doch kleine Abweichungen aufweisen. Für den praktischen Gebrauch—zum mindesten in den Fällen, wenn keine grösste Genauigkeit verlangt wird—ist die Benutzung der einfacheren und integriebaren Formel Matano's zu empfehlen.

Durch experimentelle Nachprüfung der nach Matano und uns errechneten Kurven in einem speziellen Fälle, in dem diese schon qualitativ verschieden sind, konnte gezeigt werden, dass die nach unserer Formel errechnete Kurve richtig ist.

Institut für Faserforschung,
Kaiserliche Universität zu Osaka.

On the Statistical Mechanical Treatment of the Absolute Rate of Chemical Reaction.

By Juro HORIUTI.

(Received December 20, 1937.)

By "chemical reaction" we understand simple rearrangements of chemical combinations among a group of atoms. It is the object of the present article to discuss in general the statistical method for treatment of the absolute reaction rate with a group of atoms having the following properties: (1) displacements of atoms take place adiabatically with regard to the electronic configuration; (2) classical mechanics holds for the motion of centres of gravity of atoms; (3) the group has more or less chance of interchanging energy with its surroundings at a definite temperature by interaction with radiation or with other material system; the interaction will be called "collision" in what follows; (4) the group can stably exist in the initial and the final state, which are distinctly different with each other in spacial relative configuration of atoms. Such a group of atoms will be called "chemical system" in what follows.

The rate constant of the reaction is now the probability with which the chemical system transits from the configuration of the initial state to that of final one per unit time. The transition and its probability will be treated with special reference to the configuration space, rather than

with reference to the phase space, since we are interested in the spacial rearrangements of atomic nuclei rather than in those of momenta. The representative point of our chemical system will thus move in the configuration space along a trajectory belonging to a definite energy state until interrupted by a collision and switched over to another trajectory. Time interval and the portion of trajectory marked off by two successive collisions will be called in what follows, "life time" and "free path" respectively. Further aspects of the motion of the representative point are those imposed by (4), i.e. the point may move about within either of two separate regions in the configuration space corresponding to the initial and the final state for a long time without traversing the critical regions intermediate between them. With this manner of representation the probability is now that with which a representative point escapes the initial region towards the final one. One may of course consider, if one prefers although it is not absolutely necessary, an assemblage of such points contained in the initial region, and use the terminology of the gas kinetic theory: the fraction of points out of the total contained in the initial region, which escape the latter per unit time, is the probability in question. It will be meant by the statistical equilibrium of the assemblage that the number of points contained in any assigned volume in the configuration space is proportional to the phase integral over the volume.

The probability will be dealt with for three different types of flow of points arising from different magnitudes of the free path. If the free path is small compared to the extension of the critical region and still less compared to that of the initial and the final regions, the representative point would, when situated at the critical regions, move back and forth and hesitate to reach either of regions. Even if it has once transited any fixed point on the critical region toward the final region, it would with almost equal probability, go back home as arrive at the destination and it is only with very small probability that one may expect it at the final region some time after the transition.

The assemblage of points, if it is at the distribution departing from that of statistical equilibrium, would thus flow with mass velocity less than that of thermal motion. Since momenta of points contained within any elementary volume, whose extention is larger than the free path, accord with Boltzmann's distribution because of sufficient collisions, the flow of points may be treated like diffusion if such volume is small enough.

According to (4) further, we have a steady flow in the neighbourhood of the critical region. In this case we may set up lines of flow and surfaces orthogonal to latters along which no resultant flow of points takes place. The main line of flow may duly be termed the "reaction co-

ordinate"[1][2] but the number of points which pass through the surface from the side of the initial region to that of the final region is by no means equal to that of the mass flow, the latter giving the reaction rate in this case.

This effect diminishes the reaction constant the more, the broader is the critical region measured along lines of flow and the more frequent are the collisions. So far as the latter frequency does not appreciably depend upon the temperature, the resulting depression is mainly imposed upon the temperature independent factor or the "collision factor" Z of the reaction constant $\mathfrak{k}$ as expressed by $\mathfrak{k} = Ze^{-\frac{U^*}{kT}}$ where U^* is the activation energy. The frequent occurrence of collisions in the present sense thus diminishes "collision factor".

This effect may account for the so-called slow reaction in the solution raised by Moelwyn-Hughes and Hinshelwood[3] where frequent collisions are expected.

In the other extreme case when the free path is large compared with the extension of both the initial and the final regions, the representative point, moving on a trajectory of a single energy state, is able to fly through both the regions over and over again without being hit by a collision. The reaction is completed by a timely collision when the representative point is just flying through the final region. This case was thoroughly discussed by Wigner from a different angle with special reference to the association reaction stabilised by three body collisions.[4]

The intermediate case is now that in which the free path is longer than the extension of the critical region but shorter than that of the initial and the final region. The representative point, when it has entered either of the regions, thus collides once at least and assumes an energy state in the region with a probability proportional to the Boltzmann factor but it traverses the critical region with one flight.

As to the manner of flow of points the following can be inferred. Suppose a surface S were stretched between the initial and the final region so that a point in the initial region has once at least to pass through it and that a large number of points exist in the initial region while none in the final region. The points which pass through the surface are those moving along trajectories which lead to the final region with a single pass through the surface or after once or many times passed in and out the

(1) Eyring, *J. Chem. Phys.*, **3** (1935), 107.
(2) Evans and Polanyi, *Trans. Faraday Soc.*, **31** (1935), 875.
(3) Moelwyn-Hughes and Hinshelwood, *J. Chem. Soc.*, **1932**, 230.
(4) Wigner, *J. Chem. Phys.*, **5** (1937), 720.

surface, and those moving on trajectories which pass the surface in and out without leading to the final region. The former group of points is assured of passage into the final region since none of them are struck out of their route in the critical region, the number of their passages per unit time being the point in question. If, on the other hand, the assemblage were at statistical equilibrium over the whole configuration space, the number of points in the initial region being the same as before, the total number of passages through the surface is increased by the number of in-and-out passages of trajectories which are traced by points coming from the final region: points from the final region which arrive at the initial region with a single pass through the surface contribute nothing to the total number since they do not encounter collisions within the critical region. The total number is thus the upper limit of that in question and the minimum value obtained by varying the surface is the best approximation. The minimum will give the exact number in question if it is the case that trajectories are not entangled within the critical region, which might be satisfied if the potential energy is not very complicated there. Such type of flow of points may be called "effusion". The reaction rate can be calculated as given below by counting the number of points falling on the surface S, and by minimizing the latter. The number is given by

$$-\frac{dN}{dt} = N\frac{\int^{S}\cdots\int c_1 e^{-\frac{\mu_1 c_1^2}{2kT}-\frac{E^*}{kT}} dq_2 dq_3 \cdots dq_n dp_1 dp_2 \cdots dp_n}{\int^{V}\cdots\int e^{-\frac{E}{kT}} dq_1 dq_2 \cdots dq_n dp_1 dp_2 \cdots dp_n} \qquad (1),$$

where $$E^* = E_K^* + U^*,$$

and $$E = \frac{1}{2}\mu_1 c_1^2 + E_K + U.$$

$q_1, q_2, \ldots, q_n$ are orthogonal curvilinear coordinates, q_1 being normal to the surface, n three times the number of nuclei of the chemical system, and p's conjugated momenta, while μ_1 and c_1 are respectively the reduced mass and the velocity associated with q_1. E is the total energy, E_K the kinetic energy in the degree of freedom 2, 3,..., n and U the potential energy where asterisks denote those quantities on surface S. Integration S is to be taken over whole S surface, over positive value of p_1 and over whole momentum space of remaining momenta and N the total number of representative points distributed over the region. Integration V is the phase integral of the initial region bounded by S. Integration over c_1 being carried through, the above equation becomes

$$-\frac{dN}{dt} = NkT\frac{\int^{S}\cdots\int e^{-\frac{E^*}{kT}}dq_2dq_3\cdots dq_n\,dp_2dp_3\cdots dp_n}{\int^{V}\cdots\int e^{-\frac{E}{kT}}dq_1dq_2\cdots dq_n\,dp_1dp_2\cdots dp_n} \qquad (2).$$

The integral in the numerator is nothing but the phase integral of the motion restricted on the surface S. A surface S_0 which minimizes the rate (2) will be called "critical surface". S_0 satisfies the condition:

$$\delta\int^{S}\cdots\int e^{-\frac{E^*}{kT}}dq_2dq_3\cdots dq_n\,dp_2dp_3\cdots dp_n = 0\ ,$$

since $N\Big/\int^{V}\cdots\int e^{-\frac{E}{kT}}dq_1dq_2\cdots dq_n\,dp_1dp_2\cdots dp_n$ remains unchanged by shifting surface S, because of the statistical equilibrium of points over the configuration space. Integrating over p, the variation equation becomes

$$\int^{S}\cdots\int^{i=2,3,\cdots,n}\Pi\sqrt{2\pi\mu_i kT}\,e^{-\frac{U^*}{kT}}\left(-\frac{1}{kT}\frac{\partial U^*}{\partial q_1}+\sum^{i=2,3,\cdots,n}\frac{1}{\rho_i}\right)(\delta q_1)^*dq_2dq_3\cdots dq_n=0,$$

or

$$\frac{1}{kT}\frac{\partial U^*}{\partial q_1} = \sum^{i=2,3,\cdots,n}\frac{1}{\rho_i} \qquad (3),$$

where μ_i's are reduced masses associated with i-th coordinates and ρ_i's principal radii of curvature.

The reaction rate can thus be calculated according to Eq.(2) by determining the critical surface by means of (3).

The present procedure will be discussed and exemplified in some special cases assuming the fulfilment of conditions for "effusion".

(i) Eq.(2) may be expressed in terms of partition functions by dividing both numerator and denominator throughout by h^n:

$$-\frac{dN}{dt} = N\frac{kT}{h}\frac{Q^*}{Q} \qquad (4),$$

where $$Q^* = \frac{1}{h^{n-1}}\int\cdots\int e^{-\frac{E^*}{kT}}dq_2dq_3\cdots dq_n\,dp_2dp_3\cdots dp_n\ ,$$

and $$Q = \frac{1}{h^n}\int\cdots\int e^{-\frac{E}{kT}}dq_1dq_2\cdots dq_n\,dp_1dp_2\cdots dp_n\ .$$

This is formally equivalent to the equations given by Eyring,[1] Wigner,[4] Evans and Polanyi[2] but different from those in the nature of the surface S for counting the passage of points; the method of the latter authors is equivalent to reckon the passage through a surface $\frac{\partial U}{\partial q_1} = 0$. In a special case when $\frac{\partial U}{\partial q_1} = 0$ happens to be a Cartesian plane Eq. (3) is satisfied and hence the difference in the two procedures vanishes.

In such a case Eq. (2) assumes the familiar form of the expression for effusion,

$$-\frac{dN}{dt} = N\sqrt{\frac{kT}{2\pi\mu_1}} \frac{\int^{S}\cdots\int e^{-\frac{U^*}{kT}} dq_2 dq_3 \cdots dq_n}{\int^{V}\cdots\int e^{-\frac{U}{kT}} dq_1 dq_2 \cdots dq_n} \qquad (5),$$

integrating over associated momenta, q_2, q_3, ..., q_n being now Cartesian coordinates. Integrals S and V give the area of the orifice and the volume of the containing vessel in the case of the effusion of real gas, where $U^* = U = \text{const.}$

(iia) The present procedure is applied to the association of two atoms, whose mutual potential energy $U(r)$ depending only on the distance r has no maximum. This is a case when the transition state method[1][2][4] can not be applied. Surface S is now $r_i > r > r_f$ in the six dimensional configuration space, where r_i and r_f are nuclear separations at the initial and at the final state respectively. Critical surface S_0 can be located by (3) that,

$$r = r_0,$$

where

$$\frac{1}{kT}\frac{\partial U^*}{\partial r_0} = \frac{2}{r_0} \qquad (6).$$

r_0 is such a distance that if two nuclei are destined to approach each other within r_0 they probably react, but not otherwise. This might be interpreted as the sum of collision radii of the two nuclei or when two atoms are identical as the collision diameter. It may be noted that r_0 depends on the temperature or on the mean relative velocity of the two nuclei. If, for instance, $U^*(r)$ is that of Coulomb attraction, the collision diameter is inversely proportional to the temperature.

(iib) If $U^*(r)$ has a maximum, the transition state method would reckon the passage of representative points through the surface $\frac{\partial U^*}{\partial r} = 0$, while the present one that through the surface $\frac{\partial U^*}{\partial r} = \frac{2kT}{r}$. Assuming

that $\frac{\partial U^*}{\partial r} = 0$ at $r = r_0' = 1\,\text{Å}$ and $-\frac{\partial^2 U^*}{\partial r^2} = 1 \sim 0.1\,\text{e.v./Å}^2$ in its neighbourhood, the ratio of the reaction rate v_T due to the transition state method to that due to the present procedure is calculated by Eq.(2) and Eq.(6)

$$\frac{v_T}{v} = \frac{r_0'^2}{r_0^2} e^{-\frac{U^*(r_0')-U^*(r_0)}{kT}} = 1.1 \sim 1.5 \quad \text{at} \quad 25°\text{C}.$$

The ratio is only trifling at room temperature but increases rapidly with increasing temperature.

Hokkaido Imperial University,
Sapporo.

The Mechanism of the Hydrogen Electrode Process. I. The Catalytic Mechanism.

By Juro HORIUTI and Go OKAMOTO.

(Received January 21, 1938.)

The elementary reaction underlying to the hydrogen electrode process such as the evolution of hydrogen at cathode or the consumption at anode may generally be formulated in the form,

$$2H^{+}B + 2\ominus \rightleftarrows H_2 + 2B ,$$

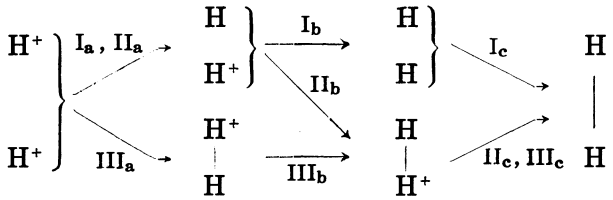
where B is the base of generalised sense due to Brönsted[1] and $\ominus$ the metal electron.

In the case when the two opposed processes are balanced we are dealing with the reversible hydrogen electrode. In the latter case hydrogen gas and the solution are catalytically interchanging their hydrogen atoms by way of the hydrogen electrode process. If further this is the only possibility of interchanging hydrogen atoms, the isotopic interchange reaction is simply a special case of the hydrogen electrode process, and we are enabled to observe the rate of electrode process in each direction at equilibrium by labelling it with a hydrogen isotope.

(1) Brönsted, *Rec. trav. chim.*, **42** (1923), 718.

The elementary process in question may take place through various possible intermediate states and any reaction step between successive intermediate states may possibly govern the rate, thus giving rise to various mechanisms.

Remembering that the elementary process of interest includes three acts i.e. neutralizations of two protons and the combination of them, all possible sequences of intermediate states can be schematically expressed as follows:



where parentheses show two protons (or a hydrogen atom and a proton) which are statistically independent of each other and dashes two such ones combined somehow with each other.

I shows the sequence of intermediate states—to be called "reaction path" hereafter—in which two protons are independently neutralised and subsequently combined with each other to form a hydrogen molecule, II that in which one of protons is neutralised, combined with the second one to form a hydrogen molecule ion, the latter being subsequently neutralised to form a hydrogen molecule and III that in which two protons are combined with each other and are neutralised one after another to form a hydrogen molecule.

Any transitions from an intermediate state to another can possibly be the rate determining step thus giving rise to different mechanisms. In usual attempts to find out the mechanism it was customary to restrict oneself to the reaction path I and to pick up the rate determining step from the two alternatives (I_a and I_b are identical) with a hope that a single mechanism thus found might rule over all hydrogen electrode processes.

Tafel[2] in old days considered that I_c was the rate determining step. This concept has found a considerable support in experiments of Bonhoeffer,[3] who has found that the series of catalytic activity of several metals for the recombination of active hydrogen ran parallel with that of cathodic overvoltage.

(2) Tafel, *Z. physik. Chem.*, **50** (1905), 641.
(3) Bonhoeffer, *Z. physik. Chem.*, **113** (1924), 199.

Le Blanc[4] maintained against the former that it was the neutralisation of proton which governed the rate. This was later supported by Volmer[5] and Frumkin,[6] who on the basis of this mechanism accounted for the well known Tafel's empirical relation between cathodic current i and overvoltage η,

$$\log i = -\frac{\alpha F\eta}{RT} + \text{constant, where } 0 < \alpha < 1 .$$

On the basis of the same mechanism but in language of wave mechanics Gurney[7] and Fowler[8] have also arrived at the explanation of the interesting empirical relation. In use of heavy hydrogen Horiuti and Polanyi[9] have later found that hydrogen gas and water were catalytically interchanging their hydrogen atoms in the presence of platinum black and that the interchange rates were appreciably affected by the hydrogen ion concentration and by addition of salts. The result of experiments seemed to direct to the fact that the rate determining reaction was associated with the change of electric charge of the elementary system since the change of concentrations of hydrogen ions and salts was known to affect the potential across the double layer at the interface where reactants were situated. This being however only compatible with I_a (or I_b) as the rate determining step, the claimed mechanism for the hydrogen electrode process seemed for some time convincing so far as one adheres to the customary manner of treating the mechanism.

Following consideration would, however, reveal that the usual concept does not suffice to understand general features of the hydrogen electrode process. Since the rate with which the elementary system passes through an intermediate state must be equal or greater than the total reaction rate, any assigned intermediate state imposes an upper limit upon the reaction rate. Topley and Eyring[10] have thus found that the energy of the state of neutral atoms on the reaction path I, if they were free ones wandering about in the solution as supposed by Fowler[8] and Gurney,[7] was too high for a reasonable magnitude of the reaction rate. It follows then that metals of large adsorption energy may give rise to the reaction path I by sheltering free atoms at the state of lower energy while such metals of very small adsorption energy as mercury practically blocks up

(4) Le Blanc, "Abhandlungen der deutschen Bunsen-Gesellschaften," No. 3, Halle (1910).
(5) Volmer, *Z. physik. Chem.*, *A*, **150** (1930), 209.
(6) Frumkin, *Z. physik. Chem.*, *A*, **164** (1933), 121.
(7) Gurney, *Proc. Roy. Soc.* (London), A, **134** (1931), 137; **136** (1932), 378.
(8) Fowler, *Trans. Faraday Soc.*, **28** (1932), 368.
(9) Horiuti and Polanyi, *Nature*, **132** (1933), 819, 931; **133** (1934), 142.
(10) Topley and Eyring, *J. Chem. Phys.*, **2** (1934), 222.

the reaction path I. The reaction in this case must have managed another path to pass through, if it has occurred at all.

On the basis of the more basic concept advanced above and of experiments with several different hydrogen electrode processes, the present authors have previously suggested that the step I_c governed the rate of hydrogen electrode process with electrodes of Ni, Cu, Fe, Ag, Au, and Pb (in alkaline solution) and II_c that of Hg, Sn, and Pb (in acidic solution).[11]

The former in which the recombination of two chemisorbed atoms was the rate determining step was called the catalytic mechanism and the latter in which the neutralization of hydrogen molecule ion governed the rate was called the electrochemical mechanism.[12]

These assignments of mechanisms have since been confirmed from various angles in this laboratory. Experimental confirmations were given to conclusions on the behavior of the hydrogen electrode process derived from respective mechanisms. Some quantitative conclusions have thus been derived on respective rates of the governing reactions by virtue of the statistical mechanical method, which could nicely account for behaviors of hydrogen electrode processes.[13][14] Tafel's empirical relation was thus quantitatively accounted for in both cases of mechanisms with special reference to the mutual interaction of hydrogen atoms and protons situated on the surface of the catalyst.

It is the object of the present paper to put forward some of our recent experimental evidences for the catalytic mechanism with special reference to nickel electrode. Experimental evidences for the electrochemical mechanism will be presented in a separate paper by Hirota in conjunction with one of the present authors.

Under the assumption that the adsorbed hydrogen atoms are practically non-polar and that the hydrogen electrode processes comprise the isotopic interchange reaction in the above sense, conclusions will be derived from the catalytic mechanism and confirmed by experiments in the following three cases.

(1) The rate determining step of the catalytic mechanism being the transition between neutral states i.e. chemisorbed hydrogen atoms

(11) Horiuti and Okamoto, *Sci. Papers Inst. Phys. Chem. Research* (Tokyo), **28** (1936), 231.

(12) According to the recent study of Ikusima in this laboratory it is very probable that the electrochemical mechanism is operative on the hydrogen electrode of platinum at least in the neighbourhood of the reversible equilibrium. The result will be published in a near future.

(13) G. Okamoto, J. Horiuti, and K. Hirota, *Sci. Papers Inst. Phys. Chem. Research* (Tokyo), **29** (1936), 223.

(14) Hirota and Horiuti, to be published in a near future.

and hydrogen molecule, the change of electrical potential at the interface cannot affect the reaction rate. It follows that the isotopic interchange rate between heavy hydrogen gas and aqueous solution will be insensitive to the change of hydrogen ion concentration or to the addition of salts contrary to the case of a platinum catalyst for which the rate with N/10 HCl solution was found 100 times as large as that with 1 N KOH + 1 N KCl solution according to a recent result of Ikusima.[15]

This conclusion was experimentally investigated by the following procedure. 4% shifted hydrogen gas of 104 mm. pressure was shaken with several different aqueous solution in a suitable vessel in the presence of annealed nickel wire of 0.1 mm. diameter and of 3300 m. length at 100°C.

The following table shows the results of experiments carried out with one and the same catalyst changing the solution from time to time, the interchange reaction rate being expressed by the first order rate, $k = \frac{1}{t} \log \frac{x_0}{x_t}$, where x_0 and x_t are atomic fractions of deuterium in hydrogen gas respectively before and after the reaction and t time of

Catalysed interchange reaction with different solutions at 100°C.

No. of exp.	Solution	Initial D-percent. $100\,x_0$	Final D-percent. $100\,x_t$	Time of shaking t (hr.)	Reaction rate $k\left(=\frac{1}{t}\log_{10}\frac{x_0}{x_t}\right)$
1	Neutral water	4.42	2.15	6.08	0.051
2	,,	,,	2.27	6.30	0.046
3	,,	,,	1.89	7.23	0.051
4	$\frac{N}{1000}$ KOH	,,	1.78	6.17	0.064
5	,,	,,	1.85	6.00	0.063
6	,,	,,	1.85	6.00	0.063
7	$\frac{N}{1000}$ KOH+$\frac{N}{10}$ KCl	,,	2.17	7.70	0.040
8	,,	,,	2.46	6.00	0.043
9	,,	,,	2.43	6.17	0.042
10	$\frac{N}{1000}$ KOH	,,	1.67	5.97	0.070
11	,,	,,	1.93	6.00	0.060
12	,,	,,	1.69	6.38	0.065
13	Neutral water	,,	2.29	6.00	0.048
14	,,	,,	2.01	8.00	0.043

(15) To be published in a near future.

shaking. One sees that experiments Nos. 1, 2, 3, 13, and 14 give good check with the activity of the catalyst. No appreciable variation of reaction rate being observed here contrary to the case of platinum, the conclusion from the mechanism was amply justified by experiments.

(2) From the catalytic mechanism it is expected that the electrode current behaves peculiarly when the electrode potential is suddenly raised or lowered. An experiment which confirmed the above expectation was described in our previous communication[11] and employed as one of the basis of concluding the catalytic mechanism. Here will be presented in a more improved form the experiment and the argument which connect the behavior of electrode current with the mechanism.

Let an anodically polarised hydrogen electrode be at a steady state or an anode at a constant polarization be steadily consuming hydrogen gas to form Brönsted's base[1] giving rise to a constant anodic current. Assuming the catalytic mechanism the state of affairs can be expressed by the following scheme:

$$\frac{1}{2}H_2 \underset{\overleftarrow{I}}{\overset{\vec{I}}{\rightleftarrows}} K-H \underset{\overleftarrow{\Im}}{\overset{\vec{\Im}}{\rightleftarrows}} H^+-B + \ominus \qquad (1),$$

where $^1/_2H_2$ denotes gaseous state, K − H chemisorbed state and $H^+ - B$ ionised state. Length of arrows schematically corresponds the relative frequencies of elementary reactions, latters being expressed in terms of electric currents by $\vec{I}$, $\overleftarrow{I}$, $\vec{\Im}$, and $\overleftarrow{\Im}$. Longer arrows above thus correspond to the positive resultant current i and shorter ones on the left to the governing step of the catalytic atomisation. The same thing, when expressed by above quantities, is

$$i = \vec{I}(\theta) - \overleftarrow{I}(\theta) = \vec{\Im}(\theta, \eta) - \overleftarrow{\Im}(\theta, \eta) \qquad (2a),$$

and

$$\vec{I} \ll \vec{\Im} \qquad (2b).$$

$\vec{I}$ and $\overleftarrow{I}$ are independent of the electrode potential because of neutral reactants and resultants but depend in general upon the degree of saturation θ of the catalyst's surface with chemisorbed atoms, while $\vec{\Im}$ and $\overleftarrow{\Im}$ depending in general on the both.

From the above equations we have

$$\frac{\overleftarrow{\Im}}{\vec{\Im}} = 1 - \frac{i}{\vec{\Im}}.$$

But since $i < \vec{I}$, according to (2b),

$$i \ll \vec{\mathfrak{I}} \,.$$

Hence we have

$$\vec{\mathfrak{I}}(\theta_1, \eta_1) \fallingdotseq \overleftarrow{\mathfrak{I}}(\theta_1, \eta_1) \,,$$

which expresses the partial equilibrium between adsorbed state and the ionised state.

If one changes η_1 suddenly to another value η_2 a new steady state is to be attained, being characterised by

$$\vec{\mathfrak{I}}(\theta_2, \eta_2) \fallingdotseq \overleftarrow{\mathfrak{I}}(\theta_2, \eta_2) \,.$$

θ_1 must now be readjusted to a new value θ_2 by removing or adding some hydrogen atoms to the chemisorbed state in order to attain the new steady state.

Since however,

$$\vec{I} > \overleftarrow{I} \,,$$

we have by Eq.(2b)

$$\overleftarrow{I} \ll \vec{\mathfrak{I}} \,,$$

and by Eq.(2a)

$$\vec{I} \ll \overleftarrow{\mathfrak{I}} \,,$$

which show that the excess or the defect of θ is readjusted almost exclusively through ionization or neutralization respectively. Since latter acts are associated with the transposition of electricity, the sudden change of the electrode current thus inserts and additional current to the steady value.

Fig. 1a shows the expected behavior of the anodic current when the electrode potential is suddenly raised. By a similar reasoning it is inferred for the case when the ionization governs the rate that the sudden change of the electrode potential will result merely in an abrupt change of steady current as shown in Fig. 1b without the initial peak as in the case of 1a.

For the experimental confirmation of the above conclusions a hydrogen electrode was constructed with a thin nickel wire A of 0.1 mm. diameter and of 67 m. length (200 cm.^{2} of apparent area) which was sealed in a glass vessel of 170 c.c. capacity as shown in Fig. 2 together with 110 c.c. of N/10 KOH solution and hydrogen gas of 580 mm. Hg pressure.

The vessel was shaken lengthwise to assure a dissolution equilibrium and the hydrogen electrode of nickel was polarised against a platinised

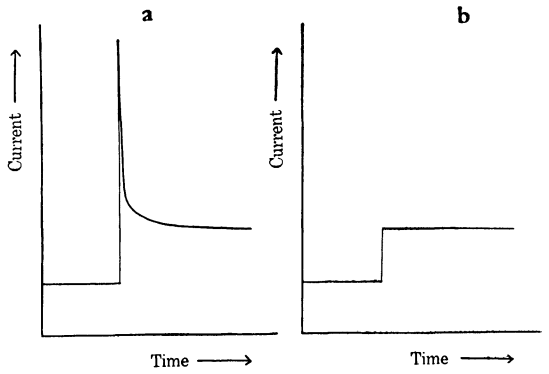


Fig. 1

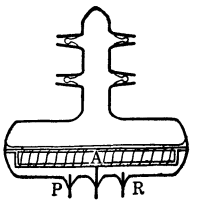


Fig. 2

platinum wire P sealed in the vessel. Anodic and cathodic polarization were determined against a reference electrode R.

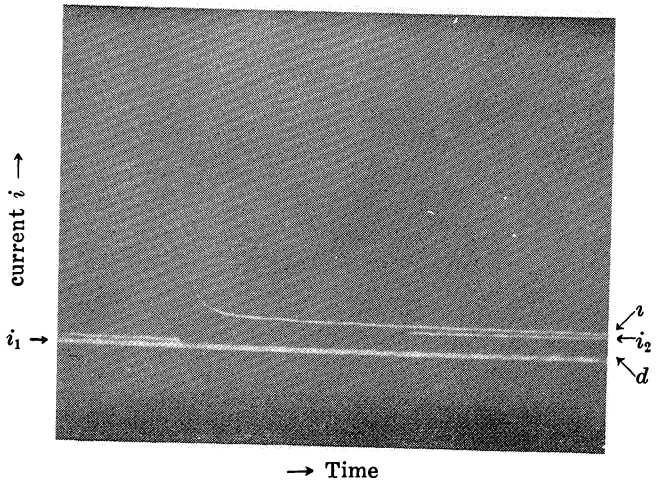
Over the whole range of electrode current (<0.2 microamp. cm.$^{-2}$) observed in the present experiment, the cathodic overvoltage was found to be negligible compared to the anodic one. This affords a sound basis to attribute observed aspects of current to the reaction at the anode. Moreover the diffusion of hydrogen gas toward the anode cannot be the governing process, for if it were the case, the thickness of the layer of solution adhered on the surface of the catalyst computed from the observed current, solubility of hydrogen gas and from the diffusion constant (10^{-5} cm.^{2}/sec.) amounts to the order of magnitude of 10 m., which is apparently impossible in our case. The genuine reaction rate at the anode in question could thus be observed by following the electrolytic current of the cell.

Actually the hydrogen electrode was kept at a fixed anodic polarization until a steady state was reached. The polarization was now suddenly raised by a small amount, the instantaneous current being followed by means of an oscillograph. Details of the experimental procedures and results are described in papers from this laboratory.[16]

The oscillograph record shows one of typical results of our observation. One sees that the theoretical conclusion is fully confirmed by the experiment.

(3) In the catalytic mechanism the rate of the electrode process at the steady state is governed by that of catalytic dissociation of hydrogen

(16) Okamoto, *J. Faculty Sci., Hokkaido Imp. Univ.*, Ser. III, Vol. II, No. 3 (1938), 116; Okamoto and Iijima, *Bull. Inst. Phys. Chem. Research* (Tokyo), **16** (1937), 1426 (printed in Japanese).



Temperature: 26°C.
Pressure: 580 mm. Hg.
η_1: 0.0114 volt.
η_2: 0.0226 volt.
i : instantaneous current.
i_1: initial steady current at η_1.
i_2: new steady current at η_2.
d: zero line.

Fig. 3. Oscillograph record.

molecules or of its reversed process. By formulating the latter at a given condition one could obtain an expression for the electrode current. Along this line Hirota in conjunction with present authors[13] arrived at the following expressions for the reaction rates in respective directions:

Catalytic atomization, $$\vec{v} = KGe^{-\frac{\varepsilon^*_{H_2}}{RT}}\frac{n}{Q_{H_2}} \qquad (3a),$$

Catalytic recombination, $$\overleftarrow{v} = KGe^{-\frac{\varepsilon^*_{H_2}}{RT}}\frac{1}{P^2} \qquad (3b),$$

where G is the number of adjacent pairs of metal atoms per unit area at which the catalytic atomization or the recombination takes place, $\varepsilon^*_{H_2}$ minimum potential energy of HH at the activated state, n the number of hydrogen molecules per unit volume and

$$Q_{H_2} = \frac{(2\pi mkT)^{\frac{3}{2}}2\pi^2 IkT}{h^5 \sinh\frac{h\nu_{H_2}}{2kT}} \cdot e^{-\frac{\varepsilon_{H_2}}{RT}} \quad \text{(State sum of a hydrogen molecule)},$$

$$K = \frac{kT}{h}(1-\theta)^2 e^{-\frac{u^*\theta}{RT}} \sum_{j}^{1\text{-}5} \frac{1}{2}\left(\sinh\frac{h\nu^*_{H_2,j}}{2kT}\right)^{-1}, \quad \frac{1-\theta}{\theta} = \frac{\sqrt{\frac{Q_{H_2}}{n}}}{q} \cdot e^{\frac{F(\eta_1-\eta_0)}{RT}},$$

$$q = e^{-\frac{\varepsilon_H + u\theta}{RT}} \sum_{j}^{1-3} \frac{1}{2}\left(\sinh \frac{h\nu_{H,j}}{2kT}\right)^{-1}, \quad \text{and} \quad P = \sqrt{\frac{Q_{H_2}}{n}} \cdot e^{\frac{F(\eta-\eta_0)}{RT}}.$$

Other notations have following meanings: θ: degree of saturation of chemisorbed atoms. $\varepsilon_{H_2} = -109.12$ kcal.[17]: potential energy of hydrogen molecule at the equilibrium position. $\varepsilon_H = -60$ kcal.[18]: heat of adsorption of a hydrogen atom. η: electrode potential. η_0: potential of reversible hydrogen electrode. $\nu^*_{H_2,j} = 936, 687, 1704, 368, 626$ (cm.$^{-1}$)[13]: normal vibrational frequencies of HH at the activated state. $\nu_{H,j} = 417, 479, 1900$ (cm.$^{-1}$)[13]: normal vibrational frequencies of H at the adsorbed state. $\nu_{H_2} = 4417.2$ (cm.$^{-1}$)[17]: harmonic frequency of a hydrogen molecule. $I = 4.65 \times 10^{-41}$ (g. cm.^{2})[17]: moment of inertia of hydrogen molecule. $u = 5.65$ kcal.[11]: repulsive potential of an adsorbed hydrogen atom due to surrounding ones at $\theta = 1$. $u^* = 6.70$ kcal.[13]: repulsive potential of HH at the activated state due to the surrounding chemisorbed atoms at $\theta = 1$.

Steady anodic current i is now expressed by

$$i = 2\epsilon KG e^{-\frac{\varepsilon^*_{H_2}}{RT}}\left(\frac{n}{Q_{H_2}} - \frac{1}{P^2}\right) \qquad (4),$$

where ϵ is the elementary charge, two charges being conveyed by one act at catalytic atomisation or recombination.

Eqs. (3a) and (3b) could be checked respectively by observations of individual rates of atomisation and the recombination labelled by deuterium while (4) by direct observations of anodic currents. But since estimations of $\varepsilon^*_{H_2}$ and G are associated with a considerable inaccuracy, the experimental confirmation was made other way round in the present work i.e. G was inversely calculated from experimental data of the anodic current as well as from those of the isotopic interchange reaction and two values thus obtained were compared with each other and with Z, the number of available metal atoms per unit area for the chemisorption of hydrogen atoms. G from two sources should coincide with each other and be of the same order of magnitude with Z whichever lattice plane of the electrode were active, so far as the catalytic mechanism were actually operative.

(17) Jeppesen, *Phys. Rev.*, **44** (1933), 195.
(18) Horiuti and Polanyi, *Acta Physicochim. U.R.S.S.*, **2** (1935), 505.

Evaluating K, n/Q_{H_2} and P by data given above G could be determined from observations of the absolute value and of its temperature coefficient of the anodic current or of the interchange reaction rate. Details of the experiments are given in a separate paper from this laboratory.[16]

The results were

$$G = 4 \times 10^{12} \quad \text{from the anodic current,}$$

$$G = 2 \times 10^{12} \quad \text{from the interchange reaction.}$$

Z was, on the other hand, obtained from the following quantitative analysis of the result of experiments (2).

The instantaneous current i or the excess of the rate of ionization of chemisorbed hydrogen atoms over that of neutralization will be assumed to vary linearly with θ,

or

$$i = \epsilon Zk\theta + \text{const.},$$

where ϵ is the elementary charge and k a proportionality constant. Denoting with i_2 and θ_2 corresponding quantities at the steady state reached some time after the raise of the anodic polarization, the above equation is

$$i - i_2 = \epsilon Zk(\theta - \theta_2) \qquad (5).$$

On the other hand the time rate, $-Z\frac{d\theta}{dt}$, of the decrease of chemisorbed atoms can similarly be expressed by

$$-Z\frac{d\theta}{dt} = Zk(\theta - \theta_2) - \{v(\theta) - v(\theta_2)\} \qquad (6),$$

where $v(\theta)$ is the supply of chemisorbed atoms due to the excess of the rate of the catalytic atomization of hydrogen molecules over that of recombination. Neglecting the second member on the right,[19] Eq.(6) is integrated in the form,

---

(19) $\varepsilon v(\theta_1)$ and $\varepsilon v(\theta_2)$ are steady currents respectively before and after the polarization was raised. According to Eq.(4) however the rate of the catalytic atomization varies monotonously from $v(\theta_1)$ to $v(\theta_2)$ along with the decrease of θ or $v(\theta_1) < v(\theta) < v(\theta_2)$. It follows then that $v(\theta_2) - v(\theta)$, which is smaller than $v(\theta_2) - v(\theta_1)$, can be neglected in comparison with $zk(\theta - \theta_2)$, since as seen from the oscillograph record, the total variation of the steady current $i_2 - i_1 = \varepsilon\{v(\theta_2) - v(\theta_1)\}$ is only a small fraction of $i - i_2$, or of $\varepsilon zk(\theta - \theta_2)$ by Eq.(5), at earlier stage immediately after the sudden raise of the anodic potential.

$$\log \frac{\theta - \theta_2}{\theta_1 - \theta_2} = -kt ,$$

time of switching being the origin of t.

By Eq. (5) we have

$$\log \frac{i - i_2}{i_0 - i_2} = -kt \qquad (7),$$

where

$$i_0 - i_2 = \epsilon Z k(\theta_1 - \theta_2) \qquad (8),$$

i_0 being the big initial current at $t = 0$.

Observed current was now analysed[20] according to Eq. (7) evaluating i_0 and k. From Eq. (8) we have immediately

$$Z = 2 \times 10^{12} ,$$

which is concordant with the forgoing two values of G affording another experimental support to the catalytic mechanism.

Hokkaido Imperial University,
Sapporo.

(20) According to a more detailed analysis, $i - i_2$ at the later stage is due to the outward diffusion of occluded hydrogen atoms in the metal. Cf. Reference (16).

The Mechanism of the Hydrogen Electrode Process. II. The Electrochemical Mechanism. The Existence of Hydrogen Molecule Ions on the Surface of the Electrode.

By Kozo HIROTA and Juro HORIUTI.

(Received January 21, 1938.)

Okamoto and one of the present authors[1] have previously suggested that it was the neutralization of hydrogen molecule ion adsorbed on the electrode-solution interface which governed the rate of the hydrogen electrode process on the mercury electrode. The proposed mechanism which was called the electrochemical mechanism has since been worked out and established by formulating the rate of the governing reaction by the statistical mechanical method, by deriving therefrom quantitative conclusions on the behavior of the hydrogen electrode process and by confirming latters by experimental data.[2] Especially Tafel's empirical relation[3] between electrolytic current i and the overvoltage η, i.e.

$$\log i = -0.5\frac{F\eta}{RT} + \text{const.},$$

and its range of validity was quantitatively derived from the theory.[2]

The present article deals with an experimental confirmation of one of direct conclusions from the theory i.e. the experimental verification of the existence of hydrogen molecule ion at the electrode-solution interface.

From the premise that the neutralization of hydrogen molecule ion is the slowest step it follows that hydrogen ions $(H^+)_{ads.}$ and hydrogen molecule ions $(HH^+)_{ads.}$ adsorbed on the interface must be at the partial equilibrium with each other and with ions H^+ in the bulk of the solution,

or $$(HH^+)_{ads.} \rightleftarrows (H^+)_{ads.} + H^+ + \ominus,$$

where $\ominus$ denotes metal electrons. Assuming the simple mass action law the electrical work required to transpose one mol of the reactant to the resultant is given by

(1) Horiuti and Okamoto, *Sci. Papers Inst. Phys. Chem. Research* (Tokyo), **28** (1936), 231.

(2) Hirota and Horiuti, to be published in a near future.

(3) Tafel, *Z. physik. Chem.*, **34** (1900), 200; **50** (1905), 649.

$$F\eta = -RT\ln\frac{n_{HH^+}}{n_{H^+}\cdot c_{H^+}} + \text{const.} \qquad (1),$$

from the condition that the total work should vanish at the equilibrium, where n_{HH^+} and n_{H^+} are respective numbers of the adsorbed elementary systems per unit area of the interface and c_{H^+} the concentration of H^+ in the bulk of the solution. It follows from Eq.(1)

$$\frac{n_{HH^+}}{n_{H^+}} \propto e^{-\frac{F\eta}{RT}} \qquad (2),$$

i.e. n_{HH^+} increases with negative polarization rapidly compared with n_{H^+}. By a more detailed statistical mechanical calculation taking the mutual interaction of $(HH^+)_{ads.}$ among themselves and with H^+ into account, $\frac{n_{HH^+}}{n_{H^+}}$ assumes the form,

$$\frac{n_{HH^+}}{n_{H^+}} = \kappa e^{-\frac{F\eta + u^{H^+}_{HH^+}\cdot\frac{n_{H^+}}{Z} - u^{HH^+}_{H^+}\cdot\frac{n_{HH^+}}{Z} + u^{HH^+}_{HH^+}\cdot\frac{n_{HH^+}}{Z}}{RT}} \qquad (3),$$

where κ is a constant independent of n_{HH^+}, n_{H^+} and of η.[4] Z is the

(4) In a separate work which will be published in a near future (Reference 2), the present authors have formulated and evaluated the constant κ with the result:

$$\kappa = Q_{HH^+}\Big/Q_{H^+}\cdot\sqrt{\frac{Q_{H_2}}{n}} = 1.0\times10^{-6}.$$

n is the number of hydrogen molecules per unit volume of the hydrogen gas of the hydrogen electrode to which the potential η is referred and Q_{H_2} the summation of states of a free hydrogen molecule expressed by

$$Q_{H_2} = \frac{(2\pi m_{H_2}kT)^{\frac{3}{2}}\,2\pi^2 I_{H_2}kT}{h^5\sinh\left(1-\frac{x}{2}\right)\cdot\frac{h\nu_0}{2kT}}\,e^{-\frac{\varepsilon^0_{H_2}}{kT}},$$

where m_{H_2} is the mass, I_{H_2} the moment of inertia, 6.21×10^{-21} g. cm.^{2}, ν_0 the harmonic frequency 4417.2 cm.$^{-1}$, x the anharmonicity constant 0.0297, and $\varepsilon^0_{H_2}$ the potential energy at the equilibrium position -109.12 kcal., numerical values being due to Jeppesen (*Phys. Rev.*, **44** (1933), 165).

Q_{H^+} and Q_{HH^+} are summation of states of respective elementary systems housed between a mercury atom and a water molecule at the interface being expressed by

$$Q_{H^+} = \int\frac{A^2}{h^2}\frac{1}{2}\left(\sinh\frac{h\nu_{H^+}}{2kT}\right)^{-1} e^{-\frac{\varepsilon_{H^+}}{kT}}\,d\sigma,$$

and

number of metal atoms per unit area of the metal surface and $u_{HH^+}^{H^+}$ is the potential exerted upon an adsorbed HH^+ by surrounding H^+ when $n_{H^+}=Z$. $u_{HH^+}^{HH^+}$ and $u_{H^+}^{HH^+}$ have similar meanings. $u_{HH^+}^{HH^+}$, for instance, was calculated by summing up quantum mechanical repulsive potentials[2] among HH^+ of interest and another HH^+ resting on one of surrounding metal atoms. Details of the calculation are left to the original paper.[2] Numerical values thus obtained are

$$u_{HH^+}^{HH^+} = 0.35 \text{ e.v.}, \quad u_{HH^+}^{H^+} = u_{H^+}^{HH^+} = 0.09 \text{ e.v.}$$

From the above result the followings can be deduced for the variation of population of HH^+ and H^+ with increasing cathodic potential.

At a sufficiently low cathodic potential charged particles at the interface consist almost exclusively of H^+. As the cathodic polarization is gradually increased, a point is reached when n_{HH^+} is no more negligible compared with n_{H^+}. From simplified Eq.(2) one sees that at room temperature a raise of cathodic polarization by 0.2 volts is sufficient to convert the ratio $\frac{n_{HH^+}}{n_{H^+}}$ from 10^{-2} to 10^{2}. Taking the mutual interaction of HH^+ and H^+ into account according to Eq.(3) another effect is expected at this turning point which can be subjected to an experimental verification.

Replacing the interface with the simplified model of Helmholtz's double layer and neglecting the concentration of negative ions on the cathode, the charge of the condenser $\epsilon(n_{H^+} + n_{HH^+})$ and its potential $\eta + \eta_0$ are related to each other by the formula,

$$-C(\eta+\eta_0) = \epsilon(n_{H^+}+n_{HH^+}) \qquad (4),$$

where η_0 is the absolute potential of the reference electrode, ϵ elementary charge and C the capacity of the double layer per unit area.

$$Q_{HH^+} = \int \frac{\sqrt{2\pi I_{HH^+} kT}}{h} \frac{1}{2^5} \prod_i^{1\cdots5} \left(\sinh \frac{h\nu_i}{2kT}\right)^{-1} e^{-\frac{\varepsilon_{HH^+}}{kT}} d\sigma ,$$

where $d\sigma$ is the elementary volume of the coordinate space of the water molecule's centre. Quantities in integrals, which are, in general, functions of σ, have the following meanings:

A : the phase integral of the motion of H^+ perpendicular to the axis through the centres of the mercury atom and the water molecule.

ν_{H^+} : the harmonic frequency of the vibration along the axis.

ν_i : the normal vibrational frequencies of the hydrogen molecule ion housed between the mercury atom and the water molecule.

I_{HH^+}: the moment of inertia of hydrogen molecule ion belonging to the single rotational degree of freedom around the $Hg-H_2O$ axis.

ε_{H^+} and ε_{HH^+}: the potential energies at equilibrium positions.

The total amount of charge required to create a unit area of new surface, E, is given by[5]

$$E = \epsilon (n_{H^+} + 2n_{HH^+}) \qquad (5).$$

When H^+ at the interface is replaced by HH^+ the charge required to create a unit area would increase by Eq.(5), the charge of the condenser being assumed to remain constant. But since an increase of HH^+ is associated with more or less decrease of H^+ due to repulsion, the increase in E due to neutralization to form H^+ might possibly be overcompensated by the decrease of the number of adsorbed H^+. Assuming C to be 19 microfarads according to Frumkin,[6] E could be expressed as the function of η by solving Eqs. (3), (4), and (5) simultaneously as shown by the dotted line in Fig. 1. The ordinate gives the number of elementary charge required to create a unit area and the absissa polarization referred to the decinormal calomel electrode. As was expected the curve shows a marked dip at the polarization where $(H^+)_{ads.}$ are replaced by $(HH^+)_{ads.}$.

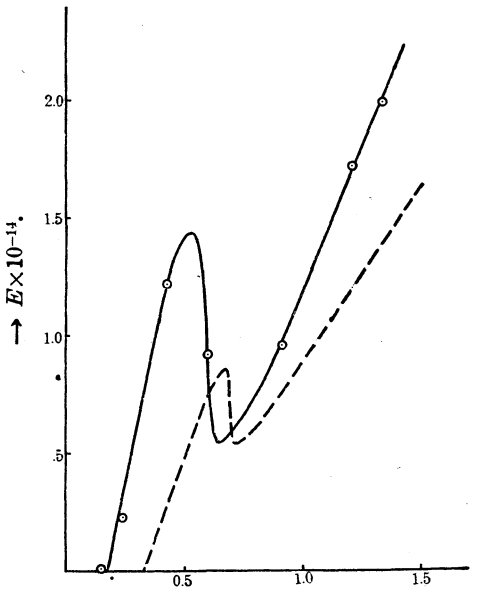
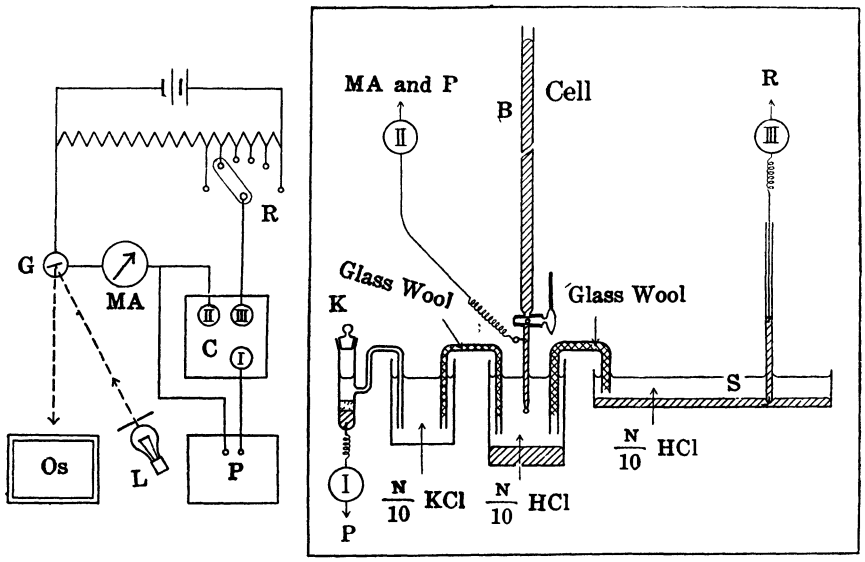


Fig. 1.

The above theoretical conclusion was subjected to an experimental investigation by the following procedure. Cathodically polarized mercury was slowly dropped into N/10 HCl solution, the current flowing was followed by an oscillograph and analysed to obtain the amount of charge E experimentally.

Fig. 2 shows the apparatus used. B is a burette of 60 cm. length and of 0.8 cm. diameter through its lower orifice of 0.3 mm. width mercury being dropped into the solution. S is a big mercury surface against which mercury drop is polarized at a constant potential. R is the switch which allows us to vary the potential stepwise. Solutions are combined with siphons packed with glass wool. The rate of dropping was varied from

(5) HH^+ requires another elementary charge for neutralization.
(6) Frumkin, *Z. physik. Chem.*, A, **164** (1933), 121.



MA: Microammeter. Os: Oscillograph. P: Potentiometer. G: Galvanometer.
C : Cell. K: Decinormal calomel electrode. L: Light source. R: Switch.

Fig. 2.

once per 2 sec. to once per 10 sec. Full size of a drop as determined by weighing was 0.0020 c.c. which was found independent of the rate of dropping but slightly of the polarization. Polarization was varied from -0.15 to -1.35 volts against decinormal calomel electrode at an interval of about 0.2 volts.

An oscillograph record was taken at a constant dropping rate but raising the polarization stepwise for every two or three drops. Here are shown two such ones taken both at 19°C. and respectively at the dropping rate once per 2.2 sec. and once per 7.1 sec. One sees that the current increases rapidly at first when a drop begins to grow but more and more slowly afterwards until the drop leaves the orifice when the current returns to the zero line to start a new course again.[7] Irregular discontinuities on the figure are due to switching from a polarization to another.

The record thus obtained being apparently contaminated with steady electrolytic currents the quantity of charge E in question was separated from the latter by the following analysis. The observed current at a given polarization and at a certain definite drop magnitude was plotted against the rate of increase of drop's area. The inclination of the straight line

(7) Instantaneous minus value of the current is due to the momentary diminution of the area after the mercury drop has been torn off at the orifice.

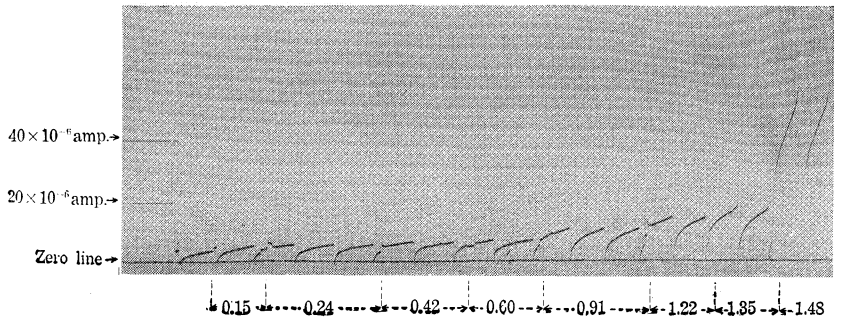


Fig. 3. Oscillograph record I. Dropping rate: Once per 7.1 sec.

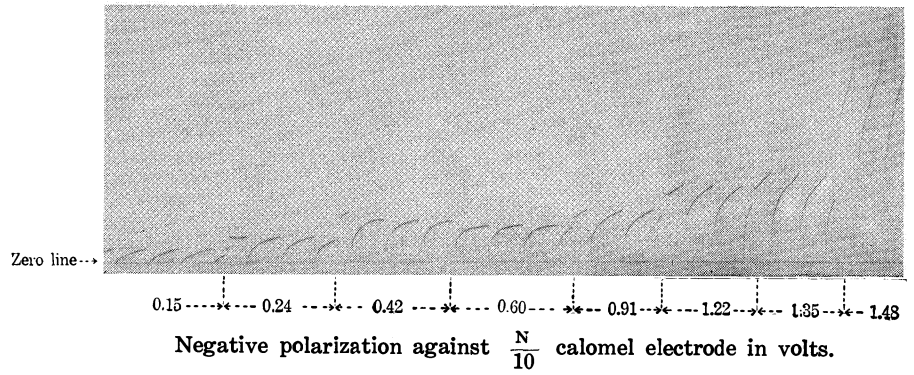


Fig. 4. Oscillograph record II. Dropping rate: Once per 2.2 sec.

gives the charge in question while its intercept at zero rate of increase of drop's area the electrolytic current which is a constant at a given polarization and at a definite surface area.

Experimental value of charge E expressed by the number of elementary charges per unit area was plotted against the polarization and shown by the full line in Fig. 1, the drop area being 0.159 cm.^{2} throughout.

One sees that the experiment satisfactorily confirms the strong dip on the theoretical curve derived from the claimed existence of hydrogen molecule ion at the interface. Quantitative disagreement would rather be shifted to the inaccuracy of *a priori* quantum mechanical calculation of interatomic potentials.

It is the pleasure of the present authors to express their sincere thanks to Professor M. Katayama for his valuable advices, his kind interests and encouragements throughout the forgoing three works.

Hokkaido Imperial University,
Sapporo.

Zur Kenntnis des Aufbaues thixotroper Systeme.

Von **Bunichi TAMAMUSHI.**

(Eingegangen am 22. Januar 1938.)

Freundlich[1] hat in seiner Monographie allgemeine Betrachtungen über die möglichen Ursachen der Thixotropie zusammengestellt. Bei der genannten Erscheinung handelt es sich sicherlich um die Wechselwirkung der abstossenden und anziehenden Kräfte zwischen den Teilchen der Sole oder Suspensionen, wenngleich die Meinungen über den feinen Mechanismus der Thixotropie auch noch divergieren. Bemerkenswert ist dabei der von Freundlich aufgestellte Zusammenhang zwischen Thixotropie und Koagulation, wonach die Thixotropie als Zwischenstufe von zwei extremen Zuständen, d.h. dem stabilen Solzustand einerseits und der vollkommenen Ausflockung anderseits, aufgefasst ist. Dieser bemerkenswerte Gedanke bedürfte jedoch noch weiterer experimenteller Unterstüztung.

Nun hat J. Russell,[2] der den Koagulationsprozess mit Suspensionen von einem englischen Ton (Oxford clay) untersucht hat, gefunden, dass sich die Koagulation mit sich vermehrender Elektrolytkonzentration in drei Typen A, B und C einteilen lässt, von denen A die partielle Koagulation mehr oder weniger lyophoben Charakters, B die thixotrope Gelatinierung und C die vollkommene Ausflockung lyophiler Natur darstellt. Eine ähnliche Erscheinung erkannte ich auch mit Suspensionen von einem Ton, der aus einem natürlichen japanischen Wasserstoffton durch Behandlung mit Natriumhydroxyd hergestellt wurde, indem man den Koagulationsprozess makroskopisch und ultramikroskopisch beobachtete. Diese Erfahrungen können im Grunde mit dem oben genannten Gedanken in Einklang gebracht werden.

Der untersuchte Natrium-Ton war thixotrop in seiner 10 prozentigen Suspension in destilliertem Wasser mit der Erstarrungszeit von etwa 6 Stunden. Durch Zusatz von 100–200 Millimol Natriumchlorid wird die Erstarrungszeit auf 15 Sekunden herabgesetzt, während die Suspensionen bei grösseren Elektrolytkonzentrationen unbeständig sedimentieren. Mit verdünnteren Suspensionen (0.4 und 2%) dieses Tons untersuchte man

(1) H. Freundlich, „Thixotropy" Actualités scientifiques et industrielles, No. 267, Paris (1935).

(2) J. L. Russell, *Proc. Roy. Soc.* (London), A, **154** (1936), 550.

die Koagulation unter Zusatz von NaCl, indem man das Sedimentvolumen nach einigen Tagen abliest und dann die Suspensionen durch ein neues Leitzsches Spaltultramikroskop beobachtet. Bei niedrigen Elektrolytkonzentrationen sedimentieren die Teilchen zum Teil, während die obere Flüssigkeit lange getrübt bleibt (partielle lyophobe Koagulation). Bei mittleren Elektrolytkonzentrationen (30–120 Millimol für 0.4 prozentige Suspension, und 15–60 Millimol für 2 prozentige Suspension), bilden die Teilchen mit den vielen Dispersionsmitteln eine uniforme, weiche, mehr oder weniger elastische Masse, wobei das Maximum des Sedimentvolumens aufgewiesen wird (thixotrope Gelatinierung). Bei höheren Elektrolytkonzentrationen flocken sich alle Teilchen in verhältnismässig kurzer Zeit vollkommen aus (lyophile Koagulation).

Noch einleuchtender war dieser Unterschied in den Typen der Koagulation im Feld des Ultramikroskops. Bei niederen Elektrolytkonzentrationen zeigen die Teilchen der Suspension lebhafte Brownsche Rotationsbewegung und teilweise noch Translationsbewegung. Mit steigender Elektrolytkonzentration werden diese Bewegungen allmählich schwächer, gleichzeitig sammeln sich die Teilchen zu Nebelflecken zusammen. In den optimalen Elektrolytkonzentrationen, wo das grösste Sedimentvolumen aufgewiesen ist, sieht man im Mikroskopfeld eine uniform ausgedehnte nebelartige Struktur, in der die Teilchen noch ganz schwache Brownsche Rotationsbewegung ausführen. Bei höheren Elektrolytkonzentrationen wird diese uniforme Struktur in mehrere irregular gebildete Flocken, die im Mikroskopfeld als dicke weisse Wolken glänzend erscheinen, umgewandelt, in denen die Teilchen bewegungslos dicht miteinander zusammenhalten. Im letzten Zustand sieht man jedoch noch einige Teilchen, die im Dispersionsmittel mehr oder weniger frei beweglich sind.

Ein analoges Verhalten findet man in denselben Ton-Suspensionen bei Zusatz von KCl, aber nicht bei Zusatz von $BaCl_2$ oder $AlCl_3$, in welchen letzteren Fällen die Koagulation in allen Elektrolytkonzentrationen fast gleichartig stattfindet, sodass sich kein merklicher Unterschied im Sedimentvolumen sowie im Flockungszustand erkennbar macht. Dies war auch der Fall, als man die Suspensionen von einem elektrodialysierten Wasserstoffton mit NaCl koagulieren liess. In allen diesen Fällen spielt sicherlich der Effekt der Entladung der Teilchen durch zugesetzte Ionen eine Hauptrolle, wobei die Teilchen überhaupt lyophob in dichte Packung eingepackt werden, welche gerade für das Entstehen der thixotropen Gelatinierung nachteilig ist. Die thixotrope Gelatinierung kommt also als eine Zwischenstufe des Koagulationsprozesses zustande, wobei die Teilchen zum Teil lyophob und zum Teil lyophil zu einer uniform gebildeten lockeren Struktur eingebaut sind.

Man könnte dann mit Freundlich[3] annehmen, dass die Thixotropie dadurch zutage tritt, dass die Teilchen in diesem Zustande in eine Gleichgewichtslage kommen, die einem schwachen Minimum der Potentialkurve der abstossenden und anziehenden Kräfte zwischen den Teilchen entspricht. Und zwar sind zwei Teilchen in dieser Gleichgewichtslage noch von einem mit ihrer Grösse vergleichbaren Abstande voneinander getrennt, welchen Abstand hindurch die anziehenden Kräfte wirken würden. Der durchschnittliche Abstand zwischen zwei Teilchen ist für den Fall der von Freundlich und Mitarbeitern[4] untersuchten 14 prozentigen Suspension von Bentonit, dessen Teilchengrösse im Mittel 0.1 μ ist, auf etwa 100 mμ geschätzt. Beinahe die gleichen Umstände gelten für die hier von mir untersuchten Ton-Suspensionen. Für den von mir früher untersuchten Fall der 33 prozentigen Kaolin-Suspensionen[5] bzw. Wasserstoffton-Suspensionen,[6] deren Teilchengrösse im Mittel 1 μ ist, ergibt sich der durchschnittliche Abstand gleich 1 μ, indem ein Teilchen etwa 10^{12} Wassermoleküle um sich trägt, unter Annahme, dass alle Teilchen für die Festigkeit des Systems verantwortlich sind. Die Anziehungskräfte, die in so grossem Abstande noch wirksam sind, kann man auf Grund der neuen quantenmechanischen Theorie der van der Waalsschen Kräfte begreifen.[7] Nach Kallmann und Willstätter,[8] welche versuchten die Londonsche Theorie auf kolloide Systeme zu übertragen, lassen sich die Kräfte zwischen zwei Teilchen folgendermassen ausdrücken: $U=\frac{16}{9}\pi^2 CN^2\left(\frac{r_0}{r}\right)^6$, worin r_0 den Teilchenradius und r den Abstand zwischen zwei Teilchen darstellt. Wie man sieht, ist dieser Ausdruck für einen bestimmten Wert von r_0/r unabhängig von der Teilchengrösse, und zwar für $r_0 \cong 2r$ wird diese Wechselenergie von der Grössenordnung einiger Zehntel Elektronvolt, die gerade gross genug, um das Zusammenhalten der Teilchen gegenüber der Temperaturbewegung aufrechtzuerhalten. Die grossen Teilchen können demnach bei relativ grossen Abständen noch mit Energie $>kT$ einander beeinflussen. Diese Schlussfolgerung macht eben die experimentellen Befunde, dass die Teilchen immer von Abständen, die ihrer Grösse vergleichbar sind, voneinander getrennt sind, verständlich. Dabei nimmt man allerdings an, dass der Typ der Koagulation mit der variierten Elektrolytkonzentration stetig von einem zum anderen übergeht, was an-

(3) H. Freundlich, „Thixotropy," S. 13, Paris (1935).
(4) H. Freundlich, O. Schmidt und G. Lindau, *Kolloid-Beihefte*, **36** (1932), 43.
(5) B. Tamamushi, *J. Chem. Soc. Japan*, **57** (1936), 132.
(6) B. Tamamushi, *Kolloid-Z.*, **79** (1937), 309.
(7) F. London, *Z. physik. Chem.*, B, **11** (1930), 222.
(8) H. Kallmann und M. Willstätter, *Naturwissenschaften*, **20** (1932), 952.

scheinend sowohl nach den Russellschen als auch nach meinen Erfahrungen berechtigt ist. Die Verwendung der neuerdings von Hamaker[9] formulierten Energiekurven soll demnach hier ausser Betracht gestellt werden.

Man beobachtete ferner eine hoch konzentrierte thixotrope Ton-Suspension (10%) unter Ultramikroskop und zwar im festen bzw. flüssigen Zustand. Im flüssigen Zustand, den man durch Hin- und Herbewegung der Gel in Quartzküvette mittels eines Handblasebalges erzielte, erkannte man deutlich Brownsche Rotationsbewegung der Teilchen, während sie nach dem Erstarren des Systems vollkommen bewegungslos wurden. Die Potentialenergie zwischen zwei ruhenden Teilchen übertrifft die kinetische Energie, aber sie muss jedoch genügend klein sein, damit die Struktur durch äusseren mechanischen Effekt leicht zerstört werden kann. Es handelt sich hier so zu sagen um ein stark gequelltes Gitter von sehr kleiner Gitterenergie.

Man stösst nun auf die Frage, ob die Teilchen im festen Zustand durch die Schicht des Dispersionsmittels einzeln voneinander getrennt sind, oder ob sie durch eine orientierte Anlagerung in einem dreidimensionalen Netzwerk, in welchem die Flüssigkeit durch die Netzarme in Kanälen oder in Tunneln gehalten wird, eingebaut sind. Auch wenn die Teilchen unter Ultramikroskop voneinander getrennt erscheinen, kann man nicht einfach daraufhin die erste Möglichkeit annehmen, da das Vorhandensein amikroskopischer Teilchen, die auch für die Thixotropie verantwortlich sind, nicht ausgeschlossen ist.

Rideal und Russell[10] schliessen sich lieber der zweiten Auffassung an, auf Grund der Tatsachen, (1) dass manchmal so verdünnte Sole, in denen man für die Dicke der angenommenen Lyosphere einen unbegreiflich grossen Wert gestatten muss, noch thixotrop sein können, und, (2) dass die thixotropen Sole im allgemeinen Teilchen enthalten, die anisometrisch sowie anisotrop sind.

Der erste Grund soll durch folgende Abschätzung anschaulich gemacht werden. Es sei hier angenommen, dass die Teilchen der Sole oder Suspensionen kugelförmig sind. Berechnet man die Zahl des Wassermoleküls, dessen Radius gleich 2.3×10^{-8} cm. gesetzt ist, die ein Teilchen durchschnittlich trägt, so ergibt sich Tabelle 1, worin einmal Lyosphere um die Teilchen und ein anderesmal dreidimensionales Netzwerk der Teilchen, in welchem die Flüssigkeit enthalten ist, angenommen ist.

---

(9) H. C. Hamaker, *Rec. trav. chim.*, **55** (1936), 1015; **56** (1937), 3, 727.

(10) E. K. Rideal und J. L. Russell, *Proc. Roy. Soc.* (London), A, **154** (1936), 540.

Tabelle 1.

Radius der Teilchen	Zahl des Wassermoleküle pro Teilchen					
	unter Annahme der Lyosphere		unter Annahme des dreidimensionalen Netzwerkes			
			Teilchen in einer Netzmasche			
	$r = r_0$	$r = \frac{1}{2} r_0$	4—5	10	40—50	100
1 mμ	6×10^2	2×10^2	2×10^2	10^3	2×10^4	10^5
10 mμ	6×10^5	2×10^5	2×10^5	10^6	2×10^7	10^8
100 mμ	6×10^8	2×10^8	2×10^8	10^9	2×10^{10}	10^{11}
1 μ	6×10^{11}	2×10^{11}	2×10^{11}	10^{12}	2×10^{13}	10^{14}
10 μ	6×10^{14}	2×10^{14}	2×10^{14}	10^{15}	2×10^{16}	10^{17}

Die Zahl der Wassermoleküle, die in der Netzwerkstruktur enthalten ist, ist also immer grösser als die in der Lyosphere, soweit eine Netzmasche mindestens aus 10 Teilchen besteht. Berechnet man ferner die Wassermoleküle pro Teilchen je nach der variierten Konzentration der Sole oder Suspensionen, indem man die Dichte des Teilchens gleich 2 setzt, so bekommt man die Ergebnisse der Tabelle 2, woraus man sieht, dass die grössere Zahl der Wassermoleküle bei geringeren Konzentrationen gerade nur durch die Netzwerkstruktur umfasst werden kann. Eine Lyosphere grösserer Dicke kann man allerdings nicht annehmen, soweit man für die Anziehungskräfte die Potentialenergie $>kT$ gestatten muss.

Tabelle 2.

Radius der Teilchen	Zahl der Wassermoleküle pro Teilchen je nach der Konzentration der Suspension			
	10%	1%	0.1%	0.01%
1 mμ	2.7×10^3	2.7×10^4	2.7×10^5	2.7×10^6
10 mμ	2.7×10^6	2.7×10^7	2.7×10^8	2.7×10^9
100 mμ	2.7×10^9	2.7×10^{10}	2.7×10^{11}	2.7×10^{12}
1 μ	2.7×10^{12}	2.7×10^{13}	2.7×10^{14}	2.7×10^{15}
10 μ	2.7×10^{15}	2.7×10^{16}	2.7×10^{17}	2.7×10^{18}

Es scheint demnach sehr berechtigt zu sein für thixotrope Systeme geringer Konzentrationen eine Struktur des dreidimensionalen Netzwerkes

anzunehmen, während eine Annahme der Lyosphere dabei unbefriedigend ist. Das sich die kugeligen Teilchen im Netzwerk linear einander anlagern werden, hat auch einen theoretischen Grund, welcher von Usher[11] angedeutet worden ist. Die neueren ultramikroskopischen Untersuchungen von Hauser und Reed[12] an Bentonit-Suspensionen sprechen auch für die Annahme der Strukturbildung des Netzwerkes.

Der zweite Grund, dass die Teilchen meistens anisometrisch und anisotrop sind, ist auch ohne Zweifel günstig für die Strukturbildung eines Netzwerkes oder einer Zone. Eine so orientierte Anlagerung der stark anisometrischen Teilchen könnte eventuell durch die regelmässige langsame Bewegung des Systems veranlasst werden, und dadurch wird das System schneller zur Erstarrung gebracht werden. Diese Erscheinung, die Rheopexy genannt ist, ist in der Tat zuerst von Freundlich und Juliusburger[13] z. B. bei thixotropen Gyps-Suspensionen und V_2O_5-Solen entdeckt worden. Immerhin müssen sich die Teilchen bei so orientierter Anlagerung in einem Gleichgewicht befinden, und sie müssen dabei locker, eventuell durch die Schicht des Dispersionsmittels getrennt, aneinander gebunden sein, sodass die Orientierung durch mechanischen Effekt leicht zerstört wird. Die Erstarrungszeit ist dann die Zeit, in der die einmal relaxierten Teilchen wieder zur Orientierung gebracht werden.

Wenn man nun die thixotrope Gelatinierung als Zwischenstufe der lyophoben und lyophilen Koagulation auffasst, so ergibt sich die Möglichkeit, dass das thixotrope System durch die Mischung von lyophoben und lyophilen Teilchen realisiert wird. Bary[14] deutete darauf hin, dass alle thixotropen Systeme eine Mischung von lyophoben und lyophilen Bestandteilen sind, wo die Gelatinierung durch die gegenseitige Orientierung dieser zwei Bestandteile zustande kommt.

Dass ein lyophobes, nicht thixotropes Material unter Zusatz eines lyophilen Materials thixotrop wird, ist in der Tat z. B. in der Rideal- und Russellschen Untersuchung[10] demonstriert worden, in welcher eine nicht thixotrope Quartz-Suspension bei Zusatz von einer sehr geringen Menge kolloidalen Aluminiumoxyds deutlich thixotrop gemacht werden konnte. Auch nicht thixotrope $BaSO_4$-Suspensionen werden durch Mischung mit Natrium-Ton thixotrop. Mit $BaSO_4$ allein, ist seine 30 prozentige Suspension weder thixotrop noch plastisch, während eine Mischung von 29.85 prozentigem $BaSO_4$ und 0.15 prozentigem Na-Ton in destilliertem Wasser

(11) Usher, *Proc. Roy. Soc.* (London), A, **125** (1929), 143.
(12) E. A. Hauser und C. E. Reed, *J. Phys. Chem.*, **41** (1937), 911.
(13) H. Freundlich und F. Juliusburger, *Trans. Faraday Soc.*, **31** (1935), 920.
(14) Bary, *Compt. rend.*, **196** (1933), 183.

bedeutende thixotrope und plastische Eigenschaften erwirbt.[15] Experimentiert man dabei mit gröberen Teilchen von $BaSO_4$ einerseits und mit feineren Teilchen anderseits, so tritt die Thixotropie bzw. Plastizität bei feineren Teilchen in stärkerem Masse auf. Hier erkennt man den Einfluss der Teilchengrösse auf die Thixotropie. Der Mechanismus, ob das lyophile Material durch nicht thixotrope lyophobe Teilchen adsorbiert wird, sodass sie genug Wasser um sich binden und demnach eine stark gelockerte Struktur bilden können, oder die beiden lyophilen und lyophoben Bestandteile durch eine orientierte Anlagerung zu einem Netzwerk eingebaut werden, kann doch von Fall zu Fall verschieden sein.

Um in den Mechanismus der Thixotropie weiter einzudringen, wäre es erwünscht Kenntnisse über die Mobilisierung bzw. Immobilisierung des Dispersionsmittels im flüssigen bzw. festen Zustande zu gewinnen, wozu wahrscheinlich die Messung des Dampfdrucks in den beiden Zuständen von Nutzen sein kann. Dieser von Herrn Professor Katayama freundlicherweise mündlich mitgeteilte Hinweis soll noch in Zukunft bearbeitet werden.

Zusammenfassung.

Auf Grund der Untersuchung des Koagulationsprozesses, die mit Suspensionen von einem Natrium-Ton durchgeführt wurde, ist festgestellt, dass die thixotrope Gelatinierung als Zwischenstufe von zwei extremen Zuständen, nämlich der partiellen lyophoben Koagulation einerseits und der vollkommenen lyophilen Ausflockung anderseits, auftritt.

Im Fall von konzentrierten thixotropen Suspensionen (grösser als etwa 10%), ist die Theorie der Lyosphere befriedigend, wobei man zwischen zwei Teilchen weitreichende van der Waalssche Kräfte annimmt. Dagegen bei thixotropen Systemen von geringeren Konzentrationen ist die Struktur eines dreidimensionalen Netzwerkes mit Recht annehmbar. Die Umstände, dass die Teilchen anisometrisch und anisotrop sind, begünstigen auch die Theorie der Strukturbildung eines orientierten Netzwerkes.

Dass ein thixotropes System durch Mischung von lyophilen und lyophoben Bestandteilen zu Tage tritt, wird demonstriert, indem man lyophoben nicht thixotropen $BaSO_4$-Suspensionen eine geringe Menge lyophilen Natrium-Ton zusetzt.

Nedzu Chemisches Laboratorium,
Musashi Hoch-Schule,
Itabashiku, Tokyo.

(15) Unveröffentliche Versuche von H. Sekiguchi.

The Adsorption of Helium on Charcoal below 78°K., and Production and Thermometry of Law Temperatures.

By Eizo KANDA.

(Received January 17, 1938.)

The production of lower temperatures by pumping off the adsorbed gas at a low temperature was first tried by Simon.[1] Recently Keyes and his coworkers[2] indicated, in the process of liquefying hydrogen, the practicability of refrigeration at temperatures near 40°K. by desorption of the hydrogen adsorbed at 63°K. The present author intended to obtain various low temperatures between the triple point of hydrogen (14.0°K.) and the boiling point of helium (4.2°K.) without using the helium liquefying apparatus. The desorption of helium is an excellent method for this purpose, but the adsorption of this gas on charcoal at such low temperatures has scarcely been studied.[3] The author determined the adsorption of helium below 78°K. The temperature below 14°K. was determined with the helium gas thermometer, and the resistance thermometers of constantan and of manganin were calibrated.

Adsorption of Helium. Helium gas used in the adsorption experiment was imported from America and its quality was 95%. The gas used for the gas thermometer was obtained through heating the monazite sand over 750°C., the crude gas was purified through the adsorption on charcoal cooled by liquid nitrogen and by liquid hydrogen respectively. Charcoal at 21°K. adsorbs even the traces of admixed gases together with a small part of helium. The apparatus was very analogous to that of Fig. 1 used in the adsorption experiment.

Experiment on Adsorption. The apparatus is shown in Fig. 1. The activated charcoal is in C. The volume of the gas adsorbed was measured with the burette B. The low temperature was obtained by means of liquid hydrogen or solid hydrogen. The amount of the adsorbent was almost 5 g.

The volume of the helium adsorbed per gram of charcoal at various temperatures and pressures is shown in Table 1. The adsorption isotherms are shown in Fig. 2.

(1) Simon, *Physik. Z.*, **27** (1926), 790.
(2) Keyes, Gerry, and Hicks, *J. Am. Chem. Soc.*, **59** (1937), 1426.
(3) Dewar, *Ann. chim. phys.*, [8], **3** (1904), 5.

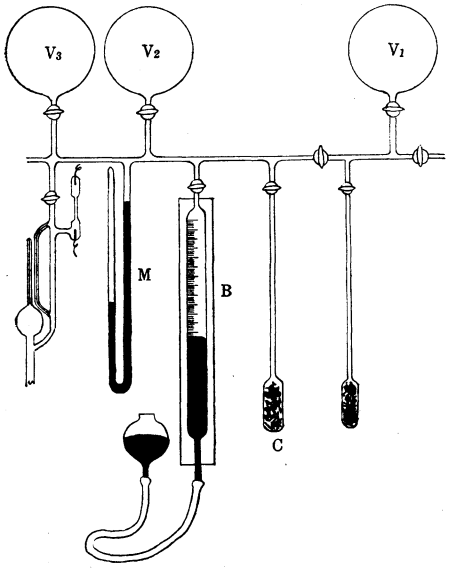


Fig. 1.

Table 1.

Temp. (°K.) \ Press. (cm.)	30	50	76
78.1	4	6	11
53.5	12	15	26
21.3	108	150	180
15.0	192	255	300
12.9	244	310	360

The heat of sorption was determined preliminarily with an evaporation method. It amounts to 1.2 kcal. per mol helium and is much smaller than Dewar's value.[3] The value calculated from the adsorption isotherms according to Clapeyron-Clausius equation deviates largely from the observed value.

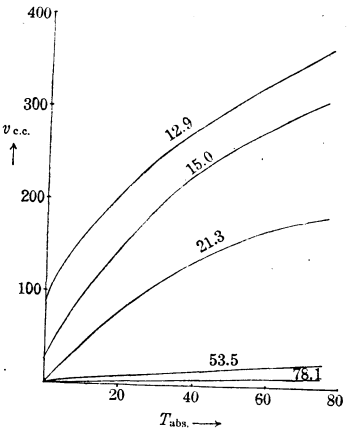


Fig. 2.

Production of Low Temperatures by Desorption. The apparatus was shown in Fig. 3.

Hydrogen or helium gas was introduced into C through V_2, and the charcoal in D was cooled by liquid hydrogen in the vessel B through the gaseous conduction. Helium gas was introduced into D through V_1 and was adsorbed on charcoal isothermally. After the saturation of adsorption was reached the gas for conduction in C was evacuated and the charcoal became adiabatic from the liquid hydrogen.

Adsorbed helium was pumped off as fast as possible. The temperature of the charcoal and the apparatus in D was lowered. In Fig. 3, G shows the bulb of the helium gas thermometer. The lowering of the

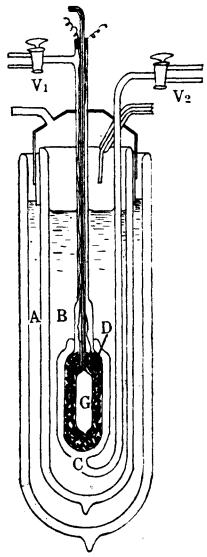


Fig. 3

temperature is dependent on (i) the dimension and adiabatic condition of the apparatus, (ii) the amount of charcoal, (iii) the amount of the adsorbed gas, (iv) the velocity of desorption, and (v) the initial temperature. In practice a large part of the heat of desorption was consumed against the thermal conduction from outward. The lowest temperature obtained in this trial was 5.8°K. To obtain any desired final temperature in certain apparatus containing the fixed amount of charcoal the author controlled the pressure of helium at which the adsorption took place. For example in an apparatus containing 17 g. of charcoal the various final temperatures reached are shown in Table 2. The initial temperature was 14.9°K.

The relation between the final temperature and the pressure at which the adsorption took place was shown in Fig. 4, where the amount of the charcoal was somewhat varied.

Table 2.

Pressure of helium (cm.)	Volume of adsorbed gas (l.)	Final temperature (°K.)
20	2.0	14.4
45	3.6	10.9
59	4.3	9.0
76	5.0	7.2
88	6.1	6.1

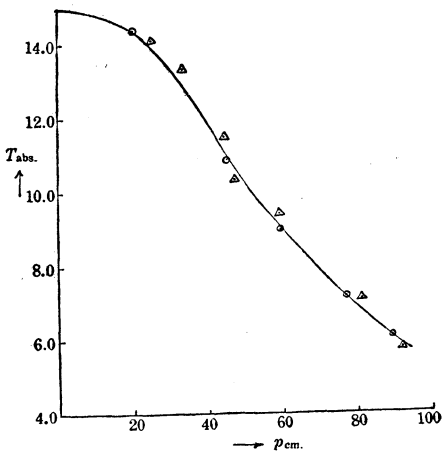


Fig. 4

Helium Gas Thermometer. The construction of the helium thermometer is very analogous to the hydrogen thermometer constructed by the present author,[4] but some modifications have been added. It is shown in Fig. 5. The thermometer bulb is of Pyrex glass and has a cylindrical cavity C in its centre for the resistance thermometer to be calibrated.

(4) Aoyama and Kanda, this Bulletin, **10** (1935), 472.

A is the adjustor of the mercury level having a thin iron plate and a screw.

The volume of the bulb V is 112.974 c.c. This volume, the capillary of the bulb, and the space of the mercury manometer have to be corrected for the thermal expansion. The linear expansion coefficient of the Pyrex glass is given in Table 3.

The temperature can be determined according to the equation:[4]

$$t = \frac{1}{\beta}\left[\frac{p_t V_0'}{p_0\left\{V_0 + \frac{V_s}{1+\beta t_s}\right\} - p_t \frac{V_s'}{1+\beta t_s}} - 1\right],$$

where V_s and t_s are the volume and the temperature of the dead space respectively, and p_0 is the pressure of the helium when the bulb is at 0°C. The pressure coefficient β of helium has a value $\beta = 0.00366072$.[5] To check the accuracy of the gas thermometer measurements the normal boiling point of hydrogen was determined. The vapour pressure tube of hydrogen was inserted into the cavity of the thermometer bulb and the whole was surrounded by liquid hydrogen. The equilibrium pressure in the vapour pressure tube and the temperature of the liquid hydrogen bath were measured (Table 4).

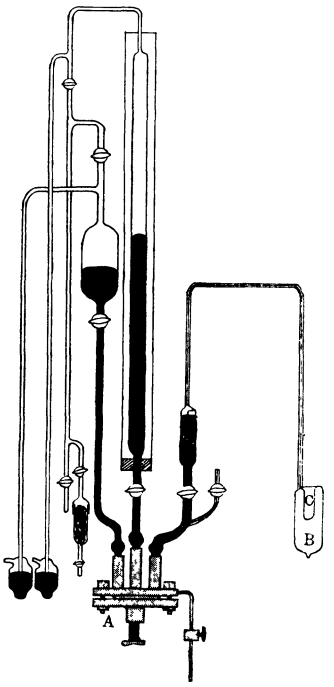


Fig. 5

Table 3.

T(°K.)	273	210	90	21
$\alpha \times 10^5$	0.35	0.30	0.10	0.05

Table 4.

p(mm.)	755.10	763.05	768.95	772.05
t(°C.)	−252.75	−252.72	−252.69	−252.68

(5) Keesom, Van der Horst, and Taconis, *Physica*, **1** (1933), 324.

The normal boiling point becomes −252.73°C. This is in good agreement with the values of other authors: Keesom, Bijl, and Van der Horst[6] −252.75°; Otto and Heuse[7] −252.78°; and Southard and Milner[8] −252.76°.

Calibration of Resistance Thermometer. The resistance thermometer is of a four lead type. The coil was set in the cylindrical cavity of the bulb of the gas thermometer and was buried by the charcoal. The results of calibration are shown in Table 5.

Table 5.

Constantan resistance thermometer. $R_0 = 49.150$

t(°C.)	R/R_0
−195.72	0.9945
−252.45	0.9728
−256.33	0.9687
−259.65	0.9637
−263.50	0.9544
−265.15	0.9487

Manganin resistance thermometer. $R_0 = 98.451$

t(°C.)	R/R_0
−194.98	0.9588
−252.66	0.9184
−254.95	0.9168
−257.32	0.9158
−259.81	0.9133
−262.40	0.9113
−264.51	0.9095
−266.59	0.9076
−267.33	0.9067

Both of constantan and manganin have very small temperature coefficients of electric resistance, but their resistances decrease monotonously down to the very low temperature near absolute zero. We can use them as thermometers for extreme low temperatures.

Summary.

The adsorption of helium on charcoal below to 78°K. was measured and the heat of sorption was determined. Systematical trials of the desorption method for the purpose of obtaining low temperatures without liquid helium were described. Resistance thermometers of manganin

(6) Keesom, Bijl, and Van der Horst, *Proc. Roy. Soc. Amsterdam*, **34** (1931), 78.
(7) Otto and Heuse, *Ann. Physik*, [5], **9** (1931), 486.
(8) Southard and Milner, *J. Am. Chem. Soc.*, **55** (1933), 4378.

and of constantan were calibrated with the helium gas thermometer down to 6°K.

The author wishes to express his sincere thanks to Prof. S. Aoyama who directed him throughout this work. He also wishes to express his heartful thanks to Prof. M. Katayama of Tokyo Imperial University who encouraged him incessantly. Thanks are also due to the Japan Society for the Promotion of Scientific Research for a grant.

Cryogenic Section, Research Institute
for Iron, Steel and Other Metals,
Tohoku Imperial University.

Hofmannscher Abbau von Domesticin-äthern.

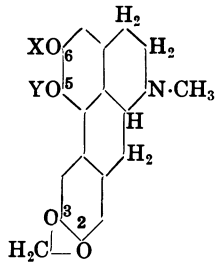
Von Hideo SHISHIDO.

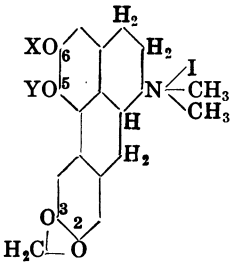
(Eingegangen am 17. Dezember 1937.)

In den früheren Mitteilungen wurden bisher die Synthesen von Domesticin-methyläther[1] (I, a), -äthyläther[2] (I, b) und einem Isomeren[3] (I, c) ausgeführt, wodurch die Konstitution weitgehend gestützt wurde. Es ist uns aber wünschenswert, den Hofmannschen Abbau dieser Domesticin-äther auszuführen, um die Konstitution des natürlichen Domesticins endgültig beweisen zu können.

Hierzu wurde zunächst der Domesticin-äther (I) in Jodmethylat (II) und dann durch Einwirkung von Alkali in Methinbase (III) umgewandelt. Diese letztere wurde in deren Jodmethylat (IV) und dann durch Behandlung mit Silberchlorid in Chlormethylat, und dieses durch Kochen mit Alkali in Vinyl-Verbindung (V) übergeführt. Weiter wurde die so erhaltene Vinyl-Verbindung durch Oxydation mittels Kaliumpermanganats in Phenanthren-carbonsäure (VI) und dann durch Decarboxylierung in ein Phenanthren (VII) umgewandelt.

Die oben angegebene Methinbase (III, a und b), Vinyl-Verbindung (V, a und b), Phenanthren-carbonsäure (VI, a und b) bzw. Phenanthren (VII, a und b) aus synthetischem Domesticin-methyläther bzw. -äthyläther ist identisch mit der aus natürlichen Substanzen. Aus diesem Resultat wurde es jetzt bekräftigt, dass die Konstitutionen des natürlichen Domesticins und seines Methyläthers, welche schon in den früheren Mitteilungen angegeben wurden,[4] ausser allem Zweifel feststehen.

I 

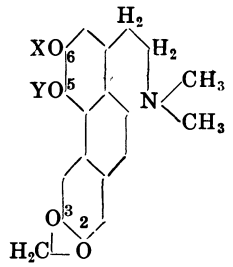
II 

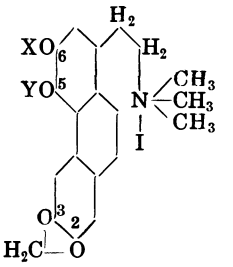
(1) Z. Kitasato und H. Shishido, *Ann.*, **527** (1937), 176.

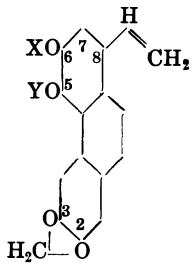
(2) Dieses Bulletin, **12** (1937), 150.

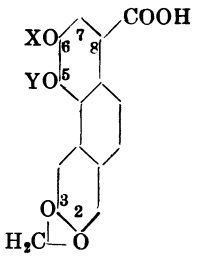
(3) *Ibid.*, **12** (1937), 419.

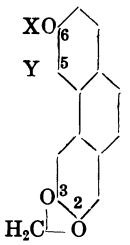
(4) Z. Kitasato und H. Shishido, *Ann.*, **527** (1937), 176; *Acta Phytochim.* (Japan), **9** (1937), 265.

III 

IV 

V 

VI 

VII 

I—VII, a: $X = CH_3$; $Y = CH_3$. (Domesticin-methyläther)
I—VII, b: $X = CH_3$; $Y = C_2H_5$. (Domesticin-äthyläther)
I—VII, c: $X = C_2H_5$; $Y = CH_3$. (*iso*-Domesticin-äthyläther)

Beschreibung der Versuche.

***d*-Domesticin-methyläther-jodmethylat** (II, a). 1 g. natürlicher Domesticin-methyläther wird in 15 c.c. Methanol gelöst und mit 3 c.c. Methyljodid 2–3 Stunden auf dem Wasserbad gekocht und dann das Lösungsmittel im Vakuum abgedampft. Der Abdampfungsrückstand wird aus Wasser umkrystallisiert und in Prismen erhalten, welche bei 105–107° schmelzen und zersetzen sich bei 117°. Diese Substanz ist in Methanol und Äthanol leicht und in Wasser schwerer löslich (Gef.: C, 52.16; H, 5.39. Ber. für $C_{21}H_{24}NO_4I$ (481): C, 52.39; H, 4.99%).

Methinbase von Domesticin-methyläther (III, a). 1 g. obiges Jodmethylat wird in 100 c.c. Wasser gelöst und mit 10 g. festem Kaliumhydroxyd anderthalb Stunden gelinde gekocht. Gebildete Krystalle werden mit Äther dreimal ausgezogen, die ätherische Lösung wird mit Wasser gewaschen und abgedampft. Der Abdampfungsrückstand wird aus Methanol umkrystallisiert und es werden Prismen vom Schmp. 133–134° erhalten (Gef.: C, 71.29; H, 6.91; N, 3.95. Ber. für $C_{21}H_{23}NO_4$ (353): C, 71.39; H, 6.52; N, 3.97%).

Des-*N*-methyl-domesticin-methyläther-jodmethylat (IV, a). 1 g. der Methinbase wird in 10 c.c. Methanol gelöst und dazu 3 c.c. Methyljodid hinzugefügt, so scheidet sich das Jodmethylat in schönen Krystallen ab. Das Jodmethylat wird aus 90%-igem Äthanol umkrystallisiert. Derbe Prismen vom Schmp. 292–294° unter Zers. (Gef.: C, 53.59; H, 5.32. Ber. für $C_{22}H_{26}NO_4I$ (495): C, 53.33; H, 5.25%).

2,3-Methylendioxy-5,6-dimethoxy-8-vinyl-phenanthren (V, a). 0.5 g. obiges Jodmethylat werden in 90%-igem Äthanol gelöst und mit einer genügenden Menge von frisch gefälltem Silberchlorid auf dem Wasserbad erwärmt. Dann wird das Reaktionsgemisch unter Zusatz von 150 c.c. Wasser bis zum vollständigen Verschwinden des Alkoholgeruchs erwärmt. Das Filtrat vom Silberjodid wird bis auf 100 c.c. eingeengt und mit 10 g. festem Kaliumhydroxyd eine Stunde gelinde gekocht, so scheidet sich die Vinyl-Verbindung in Krystallen ab. Man extrahiert sie mit Äther, wäscht die Ätherlösung mit verdünnter Salzsäure und dann mit Wasser, und dampft nach dem Trocknen mit Natriumsulfat den Äther ab. Der Abdampfungsrückstand wird nach Umkrystallisieren aus Äthanol[5] in langen Blättchen vom Schmp. 142–143° erhalten (Gef.: C, 74.14; H, 5.32. Ber. für $C_{19}H_{16}O_4$ (308): C, 74.03; H, 5.19%).

Das Trimethylamin, welches bei dieser Behandlung abgespalten wird, wird in 5%-iger Salzsäure aufgenommen und in das komplexe Chloraurat übergeführt. Blättchen vom Schmp. 246° (unter Zers.) (Gef.: Au, 49.45. Ber. für $(CH_3)_3N \cdot HCl \cdot AuCl_3$ (399.2): Au, 49.4%).

2,3-Methylendioxy-5,6-dimethoxy-phenanthren-8-carbonsäure (VI, a). 0.2 g. Vinyl-Verbindung werden in 30 c.c. Aceton gelöst und mit 0.6 g. Kaliumpermanganat, gelöst in einem Gemisch von je 10 c.c. Wasser und Aceton, bei 40–45° oxydiert. Nach übernächtigem Stehen wird Aceton abdestilliert und der Rückstand mit verdünnter Sodalösung gut ausgekocht und das Filtrat zweimal mit Äther ausgeschüttelt. Nun säuert man die Sodalösung mit Salzsäure an, extrahiert mit Äther und wäscht die ätherische Lösung dreimal mit Wasser. Der Abdampfungsrückstand des Äthers wird aus benzolhaltigem Äthanol umkrystallisiert, wobei sich gelbe Prismen vom Schmp. 252–253° bilden (Gef.: C, 66.13; H, 4.56. Ber. für $C_{18}H_{14}O_6$ (326): C, 66.26; H, 4.29%).

Methylester. 0.2 g. dieser Phenanthren-carbonsäure werden in üblicher Weise mit ätherischer Lösung von Diazomethan methyliert. Es krystallisiert aus Methanol in hellgelben Blättchen vom Schmp. 148–150° (Gef.: C, 67.36; H, 4.68; OCH_3, 27.18. Ber. für $C_{19}H_{16}O_6$ (340): C, 67.06; H, 4.71; OCH_3, 27.35%).

2,3-Methylendioxy-5,6-dimethoxy-phenanthren (VII, a). Zur Decarboxylierung[6] werden 0.2 g. obiger Phenanthren-carbonsäure mit 10 c.c. Chinolin und 0.52 g. Naturkupfer C (Schering-Kahlbaum) bis zur Beendigung der Kohlensäure-Entwicklung auf 190–200° 10 Minuten erhitzt und dann noch 20 Minuten gelinde gekocht. Das Reaktionsgemisch wird mit Äther verdünnt, vom Kupfer abfiltriert, etwa 10 Male mit 10%-iger Salzsäure, dann 3 Male mit 5%-iger Kalilauge ausgewaschen und die ätherische Lösung abgedampft. Das Phenanthren krystallisiert aus Methanol in langen Prismen vom Schmp. 127–128° aus (Gef.: C, 72.33; H, 5.14. Ber. für $C_{17}H_{14}O_4$ (282): C, 72.34; H, 4.96%).

***d,l*-Domesticin-methyläther-jodmethylat** (II, a). 1 g. synthetischer *d,l*-Domesticin-methyläther[7] wird mit Methyljodid in das Jodmethylat übergeführt wie bei dem oben angegebenen natürlichen Domesticin-methyläther. Das abgeschiedene Jodmethylat wird aus wasserhaltigem Methanol umgelöst und bildet dann dicke Prismen

(5) Die in Äthanol unlösliche Substanz schmilzt bei ca. 250–270° (unter Zers.) und scheint vielleicht ein polymerer Phenanthren-Körper sein.

(6) Vgl. E. Späth und K. Tharrer, *Ber.*, **66** (1933), 587.

(7) *Ann.*, **527** (1937), 176.

vom Schmp. 230–232° (Gef.: C, 52.33; H, 5.13. Ber. für $C_{21}H_{24}NO_4I$ (481): C, 52.39; H, 4.99%).

Überführung des *d,l*-Domesticin-methyläther-jodmethylats in Methinbase (III, a), **Des-*N*-methyl-jodmethylat** (IV, a), **Vinyl-phenanthren** (V, a), **Phenanthren-carbonsäure** (VI, a) **und 2,3-Methylendioxy-5,6-dimethoxy-phenanthren** (VII, a).

Die Überführung von diesen Substanzen in Methinbase wird genau wie bei natürlicher Substanz ausgeführt.

Die Methinbase krystallisiert aus Methanol in Prismen vom Schmp. 133–134° (Gef.: C, 71.37; H, 6.61; N, 3.96. Ber. für $C_{21}H_{23}NO_4$ (353): C, 71.39; H, 6.52; N, 3.97%). Die Mischprobe dieser Base mit derjenigen aus natürlicher Substanz zeigt keine Erniedrigung des Schmelzpunktes.

Das Des-*N*-methyl-domesticin-methyläther-jodmethylat wird aus 90%-igem Äthanol umkrystallisiert. Derben Prismen vom Schmp. 294–295° (unter Zers.) (Gef.: C, 53.40; H, 5.57. Ber. für $C_{22}H_{26}NO_4I$ (495): C, 53.33; H, 5.25%). Die Mischprobe mit demjenigen aus natürlicher Base gibt keine Erniedrigung des Schmelzpunktes.

Das 2,3-Methylendioxy-5,6-dimethoxy-8-vinyl-phenanthren krystallisiert aus Äthanol in langen Prismen vom Schmp. 141–142° (Gef.: C, 74.39; H, 5.30. Ber. für $C_{19}H_{16}O_4$ (308): C, 74.03; H, 5.19%). Es ist identisch mit demjenigen aus natürlicher Substanz (Mischprobe).

Die 2,3-Methylendioxy-5,6-dimethoxy-phenanthren-8-carbonsäure bildet aus benzolhaltigem Äthanol lange Prismen vom Schmp. 251–253° (Gef.: C, 66.49; H, 4.53. Ber. für $C_{18}H_{14}O_6$ (326): C, 66.26; H, 4.29%). Es ergibt keine Erniedrigung des Schmelzpunktes bei der Mischprobe mit demjenigen aus natürlicher Substanz.

Das 2,3-Methylendioxy-5,6-dimethoxy-phenanthren wird aus petrolätherhaltigem Methanol zu Prismen vom Schmp. 127–128.5° umkrystallisiert (Gef.: C, 72.51; H, 5.19. Ber. für $C_{17}H_{14}O_4$ (282): C, 72.34; H, 4.96%). Die Mischprobe mit demjenigen aus natürlicher Substanz ergibt keine Erniedrigung des Schmelzpunktes.

Darstellung von *d,l*-Domesticin-äthyläther-jodmethylat (II, b), **Methinbase** (III, b), **Des-*N*-methyl-jodmethylat** (IV, b), **Vinyl-phenanthren** (V, b), **Phenanthren-carbonsäure** (VI, b) **und 2,3-Methylendioxy-5-äthoxy-6-methoxy-phenanthren** (VII, b) **aus synthetischem *d,l*-Domesticin-äthyläther.**[8]

Diese Darstellung wird wie bei oben angegebenem Domesticin-methyläther ausgeführt.

Man stellt das *d,l*-Domesticin-äthyläther-jodmethylat mit Jodmethyl in Äthanol dar und krystallisiert aus Äthanol um. Es bildet Prismen vom Schmp. 225–227° (unter Zers.) (Gef.: C, 53.32; H, 5.46. Ber. für $C_{22}H_{26}NO_4I$ (495): C, 53.33; H, 5.25%).

Des-*N*-methyl-domesticin-äthyläther krystallisiert aus Äthanol in langen Prismen vom Schmp. 133–134.5° aus (Gef.: C, 71.62; H, 7.12; N, 3.97. Ber. für $C_{22}H_{25}NO_4$ (367): C, 71.93; H, 6.81; N, 3.81%). Mit demjenigen von natürlicher Herkunft gemischt (siehe unten), ergibt es keine Erniedrigung des Schmelzpunktes.

Des-*N*-methyl-domesticin-äthyläther-jodmethylat wird aus 90%-igem Äthanol umkrystallisiert. Derbe Prismen vom Schmp. 290–291° (unter Zers.) (Gef.: C, 54.18; H, 5.52. Ber. für $C_{23}H_{28}NO_4I$ (509): C, 54.22; H, 5.50%). Es ist identisch mit demjenigen aus natürlicher Substanz (siehe unten) (Mischprobe).

(8) Dieses Bulletin, **12** (1937), 153.

2,3-Methylendioxy-5-äthoxy-6-methoxy-8-vinyl-phenanthren krystallisiert aus Äthanol in langen Blättchen vom Schmp. 114–115.5° (Gef.: C, 74.73; H, 5.88. Ber. für $C_{20}H_{18}O_4$ (322): C, 74.53; H, 5.59%).[9]

2,3-Methylendioxy-5-äthoxy-6-methoxy-phenanthren-8-carbonsäure wird aus benzolhaltigem Äthanol umkrystallisiert. Prismen vom Schmp. 243–245° (Gef.: C, 67.10; H, 4.87. Ber. für $C_{19}H_{16}O_6$ (340): C, 67.06; H, 4.71%).

2,3-Methylendioxy-5-äthoxy-6-methoxy-phenanthren wird zweimal aus Methanol umkrystallisiert. Prismen vom Schmp. 134–135° (Gef.: C, 72.63; H, 5.62. Ber. für $C_{18}H_{16}O_4$ (296): C, 72.97; H, 5.41%).

Darstellung von Methinbase (III, b) *und Des-N-methyl-domesticin-äthyläther-jodmethylat* (IV, b) *aus natürlichem Domesticin-äthyläther.*

Diese Methinbase wird wie bei obigem Fall dargestellt und aus Äthanol umkrystallisiert. Sie bildet Prismen vom Schmp. 132–133° (Gef.: C, 71.60; H, 6.97; N, 4.14. Ber. für $C_{22}H_{25}NO_4$ (367): C, 71.93; H, 6.81; N, 3.81%).

Des-*N*-methyl-domesticin-äthyläther-jodmethylat krystallisiert aus 90%-igem Äthanol in derben Prismen vom Schmp. 290–291° (unter Zers.) (Gef.: C, 54.62; H, 5.89. Ber. für $C_{23}H_{28}NO_4I$ (509): C, 54.22; H, 5.50%). Das Jodmethylat bzw. die Methinbase aus natürlicher Substanz ist identisch mit demjenigen aus synthetischer Substanz.

Darstellung von *d,l-iso*-Domesticin-äthyläther-jodmethylat (II, c), Methinbase (III, c), Des-*N*-methyl-jodmethylat (IV, c), Vinyl-phenanthren (V, c), Phenanthren-carbonsäure (VI, c) und 2,3-Methylendioxy-5-methoxy-6-äthoxy-phenanthren (VII, c) aus synthetischem *iso*-Domesticin-äthyläther.[10]

Die Darstellung dieser Derivate wird wie bei obigen Fällen ausgeführt: *d,l-iso*-Domesticin-äthyläther-jodmethylat krystallisiert aus Äthanol in Prismen vom Schmp. 224–226° (unter Zers.) aus (Gef.: C, 53.17; H, 5.47. Ber. für $C_{22}H_{26}NO_4I$ (495): C, 53.33; H, 5.25%).

Da die Methinbase nicht leicht in krystallisierten Zustand zu bringen ist, wird sie auf folgende Weise gereinigt: 0.6 g. Jodmethylat werden in 60 c.c. Wasser gelöst und mit 6 g. Kaliumhydroxyd anderthalb Stunden gekocht. Das schwimmende Öl wird dreimal mit Äther ausgezogen und der Abdampfungsrückstand des Äthers wird in 10 c.c. Äthanol gelöst und mit einer Lösung von 0.175 g. Oxalsäure in 5 c.c. Äthanol hinzugefügt. Das so gebildete Oxalat krystallisiert aus 95%-igem Äthanol in Prismen vom Schmp. 195–197° (unter Zers.) aus (Gef.: C, 62.68; H, 6.33. Ber. für $C_{24}H_{27}NO_8$ (457): C, 63.02; H, 5.91%). Die Suspension dieses Oxalats in Natronlauge wird mit Äther ausgeschüttelt und der Abdampfungsrückstand des Äthers wird aus benzolhaltigem Petroläther zweimal umkrystallisiert. Die Methinbase bildet derbe Prismen vom Schmp. 117–118° (Gef.: C, 72.16; H, 7.07; N, 3.76. Ber. für $C_{22}H_{25}NO_4$ (367): C, 71.93; H, 6.81; N, 3.81%).

Des-*N*-methyl-*iso*-domesticin-äthyläther-jodmethylat krystallisiert aus 65%-igem Äthanol in derben Prismen vom Schmp. 289–290° (unter Zers.) aus (Gef.: C, 54.16; H, 5.58. Ber. für $C_{23}H_{28}NO_4I$ (509): C, 54.22; H, 5.50%).

---

(9) Als ein Nebenprodukt gewinnt man eine polymere Substanz vom Schmp. 250–260° (unter Zers.). Das abgespaltene Trimethylamin in dieser Behandlung wird auf übliche Weise in das komplexe Chloraurat übergeführt. Prismen vom Schmp. 252° (unter Zers.) (Gef.: Au, 49.33. Ber. für $(CH_3)_3N{\cdot}HCl{\cdot}AuCl_3$ (399.2): Au, 49.40%).

(10) Dieses Bulletin, **12** (1937), 419.

2,3-Methylendioxy-5-methoxy-6-äthoxy-8-vinyl-phenanthren wird aus Äthanol umkrystallisiert in langen Prismen vom Schmp. 119–120.5° (Gef.: C, 74.68; H, 5.82. Ber. für $C_{20}H_{18}O_4$ (322): C, 74.53; H, 5.59%).[11]

2,3-Methylendioxy-5-methoxy-6-äthoxy-phenanthren-8-carbonsäure krystallisiert aus Äthanol und dann aus benzolhaltigem Äthanol in Prismen vom Schmp. 235–236.5° aus (Gef.: C, 67.41; H, 5.00. Ber. für $C_{19}H_{16}O_6$ (340): C, 67.06; H, 4.71%).[12]

2,3-Methylendioxy-5-methoxy-6-äthoxy-phenanthren stallt nach dem Umlösen aus Methanol in derben Prismen vom Schmp. 126–128° (Gef.: C, 73.30; H, 5.63. Ber. für $C_{18}H_{16}O_4$ (296): C, 72.97; H, 5.41%).

Zum Schluss möchte ich Herrn Dr. Zenjiro Kitasato für seine freundliche Anregung und gütige Unterstützung meinen herzlichsten Dank aussprechen.

Chemisches Laboratorium des
Kitasato-Institutes, Tokyo.

---

(11) Das entwickelte Trimethylamin in dieser Reaktion wird als komplexe Chloraurat bestätigt. Ferner erhält man einen polymeren Körper vom Schmp. 240–250° (unter Zers.).

(12) Als ein Nebenprodukt werden neutrale gelbe Nadeln vom Schmp. 280–282° (unter Zers.) nach dem Umkrystallisieren aus Äthanol.

Nebenvalenzringverbindungen. IV. Über einige innerkomplexe Kobaltsalze der Oxyaldimine.*

Von Tokuichi TSUMAKI.

(Eingegangen am 17. Dezember 1937.)

Bei der Einwirkung von Kobaltacetat auf Salicylaldehyd und Äthylendiamin erhielten wir, wie schon mitgeteilt,[1] ein innerkomplexes Kobaltsalz, d.h. Salicylaldehyd-äthylendiimin-kobalt, welches aus heissem Benzol in schönen rotbraunen Nadeln krystallisiert.

Die rotbraunen Krystalle färben sich an der Luft, auch im Exsikkator, allmählich dunkelbraun und nehmen gleichzeitig an Gewicht zu, während sie im Vakuumexsikkator unverändert haltbar sind. Beim Stehenlassen der Krystalle findet also durch den Luftsauerstoff eine Oxy-

---

* Übersetzung einer Mitteilung, die in *J. Chem. Soc. Japan*, **58** (1937), 1288, auf Japanisch beschrieben.

(1) Pfeiffer, Breith, Lübbe und Tsumaki, *Ann.*, **503** (1933), 84.

dation statt. Erhitzt man die oxydierte Verbindung auf 100°, so verliert sie leicht wieder den Sauerstoff und nimmt an Gewicht bis zum ursprünglichen Werte ab, wobei die rotbraune Farbe zurückkehrt.

Nach meiner Ansicht, ist diese Oxydation eine Anlagerungsreaktion. Das Kobaltatom, welches die Stelle eines Zentralatoms des Komplexes einnimmt, bindet sich, wie weiter unten angegeben, locker an ein Sauerstoffmolekül, ganz in Analogie zur Bindungsweise des Oxyhämoglobins. Diese merkwürdige Anlagerung ist besonders auffallend bei dem pulverförmigen Kobaltsalze, welches aus der unten beschriebenen chloroformhaltigen Verbindung durch Abspaltung des Chloroforms erhalten wird. Die nähere Beschreibung folgt:

Löst man die aus Benzol umkrystallisierten rotbraunen Nadeln (Abb. 1) in Chloroform und lässt man die Lösung bei gewöhnlicher Temperatur unter vermindertem Druck verdunsten, so erhält man glänzende dunkelrote Prismen (Abb. 2). Die Verbindung enthält 1 Mol. Chloroform; diese gibt ihren Chloroformgehalt langsam an der Luft bei

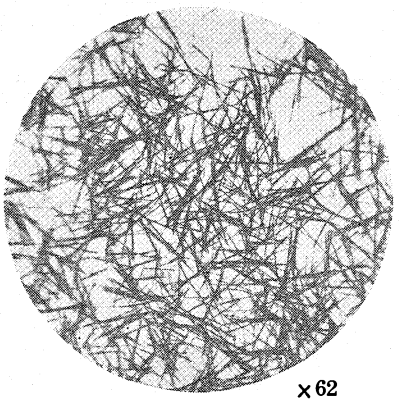


Abb. 1.

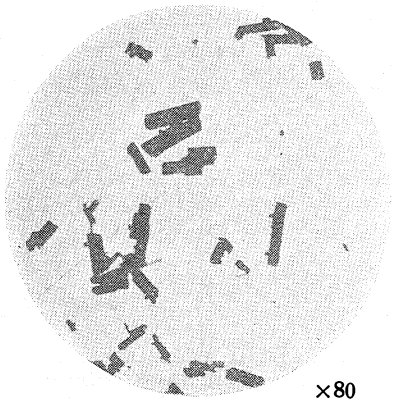
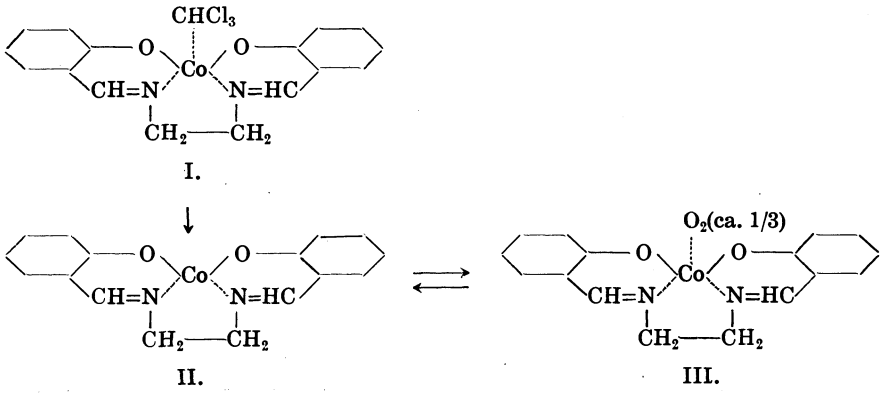


Abb. 2.

gewöhnlicher Temperatur ab und färbt sich dann allmählich dunkelbraun durch Oxydation. Im mit Chloroformdampf gesättigten Exsikkator ist sie unverändert haltbar. Beim Erhitzen der Verbindung auf 100° wird 1 Mol. Chloroform leicht abgegeben; der Erhitzungsrückstand ist ein rotbraunes Pulver. Das Pulver absorbiert schneller als die nadelförmigen Krystalle den Sauerstoff. Es färbt sich also nach einem Tage ganz schwarz und nimmt an Gewicht bis zum konstanten Werte zu. Erhitzt man das schwarze Pulver auf 100°, so verliert es auch leicht den Sauerstoff, wobei die rotbraune Farbe zurückkehrt. Die schwarze Substanz

verliert durch Erhitzen ungefähr 3.5-procentigen Sauerstoff; 1 Mol. Kobaltsalz enthält also ungefähr 1/3 Mol. Sauerstoff.



Die volumetrische Bestimmung des angelagerten Sauerstoffs wurde in einem Apparat (Abb. 3) durch Erhitzen der Substanz im Kohlensäurestrom auf 100° ausgeführt. Das abgespaltene Gas wurde über konzentrierter Kalilauge aufgefangen und gemessen. Das Gas erwies sich als Sauerstoff, weil es in alkalischer Pyrogallollösung völlig absorbiert wurde.

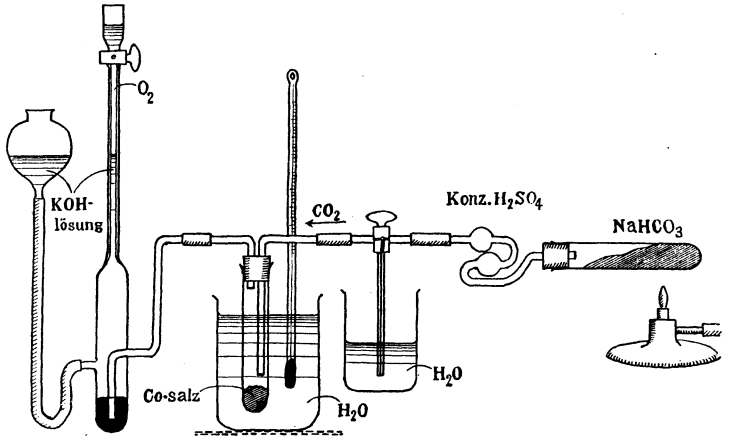
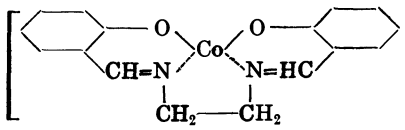


Abb. 3.

Lässt man nun die Chloroformlösung des Salicylaldehyd-äthylendiimin-kobaltes an der Luft stehen, so scheiden sich allmählich glänzende schwarzviolette Krystalle aus. Nach der Analyse und den Eigenschaften ist die Verbindung Salicylaldehyd-äthylendiimin-kobalti-hydroxyd (IV).



IV.

Die analogen innerkomplexen Verbindungen von Mangan und Eisen konnte ich, wie schon mitgeteilt,[2] durch analoge Methode darstellen. Aus Eisen-Verbindung konnte ich weiter das hämin-artige Chlorid, d.h. Salicylaldehyd-äthylendiimin-ferri-chlorid, darstellen.

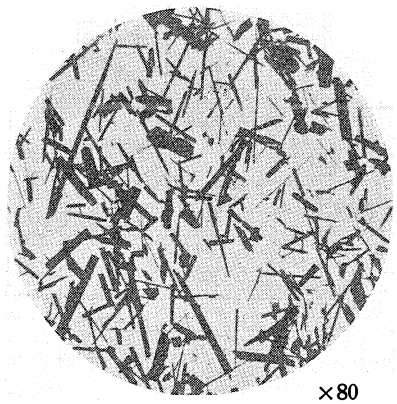
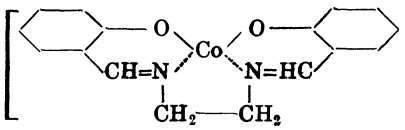


Abb. 4.

Lässt man nun die methylalkoholische Lösung von Salicylaldehyd-äthylendiimin-kobalti-hydroxyd nach Zusatz von wässriger Chlorammonium-Lösung stehen, so erhält man durch doppelten Umsatz Salicylaldehyd-äthylendiimin-kobalti-chlorid (V), ganz in Analogie mit der Entstehung von innerkomplexen Ferrichlorid. Das Kobalti-chlorid bildet schöne schwarzbraune Prismen (Abb. 4).



V.

Ein Versuch wurde gemacht um zu feststellen, ob das Salicylaldehyd-äthylendiimin-kobalt in verschiedenen Lösungsmitteln den Sauerstoff absorbieren könne, unter Bildung von Anlagerungsverbindung. Es gelang mir aber nicht, genaue Resultate zu erhalten, weil das Kobalto-salz in der Lösung, wie oben angegeben, bei Anwesenheit von wenig Wasser leicht in Kobalti-salz oxydiert wird. Um deutlich zu machen, dass die Erscheinung der obenerwähnten Absorption des Luftsauerstoffs durch das Kobaltsalz in festem Zustande nicht eine Adsorption des festen Körpers ist, sondern eine Anlagerung des Kobaltkomplexes, habe ich weiter eine spektrochemische Untersuchung über einige innerkomplexe Kobaltsalze ausgeführt.

(2) Pfeiffer, Breith, Lübbe und Tsumaki, *Ann.*, **503** (1933), 84; Tsumaki, *J. Chem. Soc. Japan*, **55** (1934), 1245; Tsumaki, dieses Bulletin, **10** (1935), 74; Tsumaki, *J. Chem. Soc. Japan*, **56** (1935), 1329.

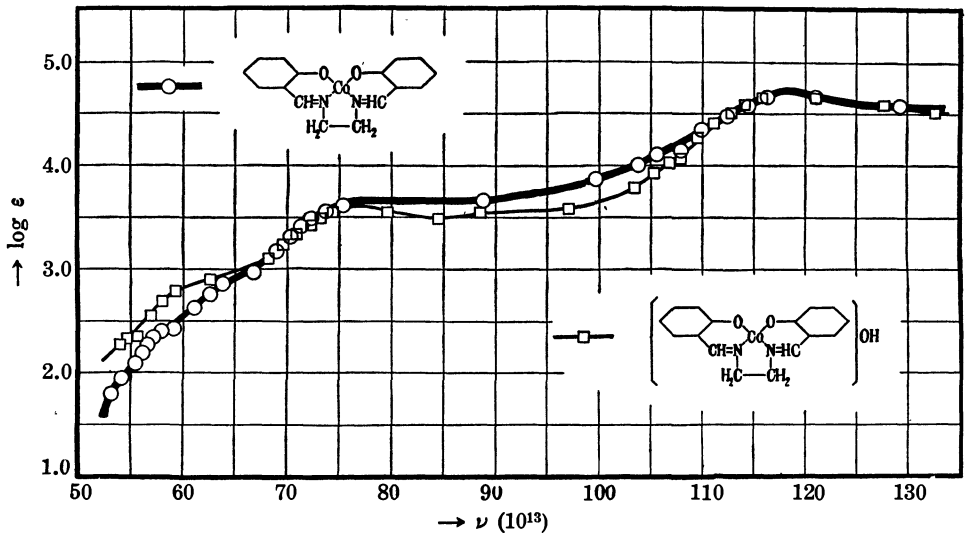


Abb. 5.

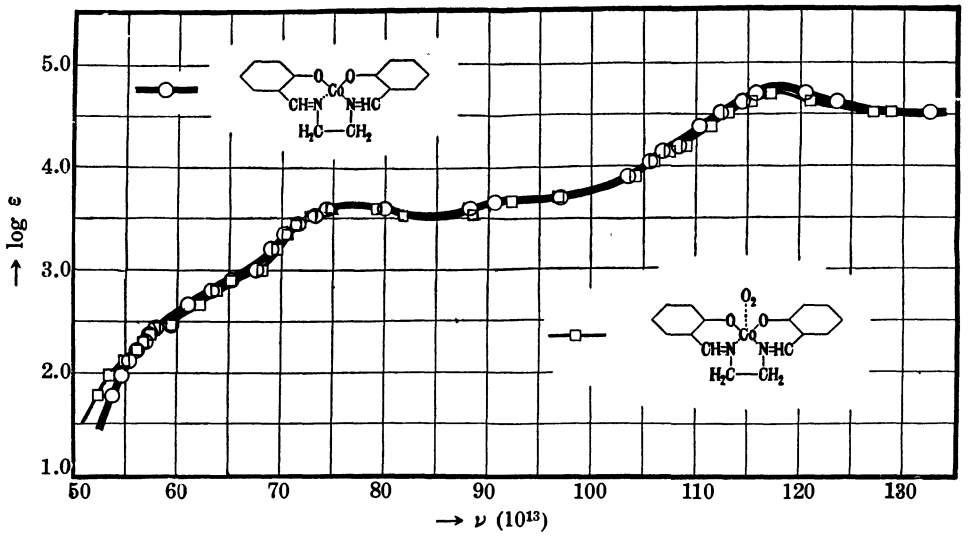


Abb. 6.

(1) Die Extinktionskoeffizienten der methylalkoholischen Lösung von Salicylaldehyd-äthylendiimin-kobalt wurden gemessen. Konzentration: 0.001 Mol/l. Schichtdicke: 5.0–0.02 cm. Die Absorptionskurve ist in Abb. 5 mit dicker Linie angegeben.

(2) Die Extinktionskoeffizienten der methylalkoholischen Lösung der Sauerstoff-Anlagerungsverbindung wurden gemessen. Konzentration:

0.0009 Mol/l. Schichtdicke: 5.0–0.02 cm. Das Resultat ist in Abb. 6 mit dünner Linie angegeben.

Die Differenz zwischen den beiden Kurven liegt darin, dass die Kurve der Anlagerungsverbindung bei $\nu = \text{ca. } 55 \times 10^{13}$ nach längeren Wellen verschoben ist.

(3) Erhitzt man die methylalkoholische Lösung der Anlagerungsverbindung auf dem Wasserbad, um den angelagerten Sauerstoff abzuspalten und misst man die Extinktionskoeffizienten, so erhält man die Absorptionskurve, wie in Abb. 6 mit dicker Linie gezeigt. Die Kurve stimmt recht gut, wie erwartet, mit der in Abb. 5 angegebenen Kurve des Kobalto-salzes überein. Durch Erhitzen gibt also die Anlagerungsverbindung in der Lösung leicht den Sauerstoff ab und geht wieder in das rotbraune Kobalto-salz über.

(4) Die Extinktionskoeffizienten von Salicylaldehyd-äthylendiimin-kobalti-hydroxyd wurden gemessen. Lösungsmittel: Methylalkohol. Konzentration: 0.001 Mol/l. Schichtdicke: 5.0–0.02 cm. Die Absorptionskurve ist in Abb. 5 mit dünner Linie angegeben.

Die Kurve ist etwas verschieden von den oben-erwähnten drei Kurven. Trotzdem finden wir in allen Fällen die Maximalabsorptionen der zweiten Absorptionsbanden bei $\nu = 77 \times 10^{13}$ und die der dritten Absorptionsbanden bei $\nu = 118 \times 10^{13}$.

Es ist sehr interessant, dass in allen Fällen die dritten Absorptionsbanden zur Erscheinung kamen, weil man dadurch die Konfiguration dieser Kobaltsalze bestimmen kann. Während die meisten Komplexsalze zwei Absorptionsbanden[3] im Sichtbaren und in der Nähe von Ultraviolett zeigen, haben einige Salze drei Absorptionsbanden. Zum Beispiel zeigte Y. Shibata[4] im Jahr 1915, dass Nitroamminkobalti-Verbindungen, wie $[Co(NH_3)_4(NO_2)_2{}^{(1)}_{(6)}]Cl$, $[Co(NH_3)_3(NO_2)_3]$ und $[Co(NH_3)_2(NO_2)_4]NH_4$, drei Absorptionsbanden haben. Nach seiner Ansicht, beruht die Erscheinung der dritten Bande auf ein Paar Nitro-Radikalen, die miteinander in Trans-Stellungen ihre Koordinationsstellen einnehmen.

Vor kurzem, fand R. Tsuchida mit seinen Mitarbeitern,[5] dass nicht nur Nitroamminkobalti-Verbindungen, sondern auch *trans*-Dichlortetramminkobaltichlorid $[Co(NH_3)_4Cl_2]Cl$ und einige andere Verbindungen die

(3) Shibata, *J. Chem. Soc. Japan*, **36** (1915), 118.

(4) Shibata, *J. Chem. Soc. Japan*, **36** (1915), 1246; Shibata und Maruki, *ibid.*, **37** (1916), 1142.

(5) Tsuchida, dieses Bulletin, **11** (1936), 721; Tsuchida und Kashimoto, *ibid.*, **11** (1936), 785; Tsuchida und Kobayashi, *ibid.*, **12** (1937), 83; Kobayashi, Hagitani und Mita, *J. Chem. Soc. Japan*, **58** (1937), 391; Kashimoto und Kobayashi, dieses Bulletin, **12** (1937), 350.

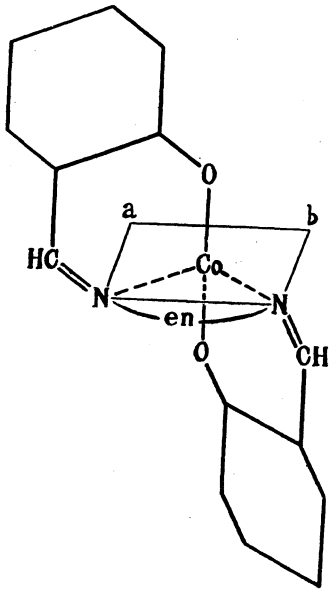


Abb. 7.

dritten Absorptionsbanden zeigen. Er zog daraus einen Schluss, dass die Theorie von Shibata erweitert werden könne, mit andern Worten, dass man die Theorie nicht nur auf Nitro-Radikale, sondern auch auf irgendwelche negative Reste, die miteinander in Trans-Stellungen die Koordinationsstellen einnehmen, anwenden könne.

Wendet man nun die Shibata-Tsuchidasche Theorie auf meine Kobalt-Komplexsalze an, so muss die Konfiguration der Salze so aufgestellt werden, dass zwei Sauerstoffatome im Salicylaldehydrest miteinander in Trans-Stellungen die Koordinationsstellen einnehmen. Zum Beispiel, soll das Salicylaldehyd-äthylendiimin-kobalt räumlich wie Abb. 7 formuliert werden, weil zwei Stickstoffatome im Äthylendiaminrest immer miteinander in Cis-Stellungen am Zentralmetallatom die Koordinationsstellen ausfüllen. Es besitzt also eine asymmetrische Konstitution.

Beschreibung der Versuche.

Salicylaldehyd-äthylendiimin-kobalt + $CHCl_3$. Man versetzt eine heisse Lösung von 4 g. Äthylendiamin-monohydrat in 180 c.c. Alkohol mit einer heissen Lösung von 16 g. Kobaltacetat in 80 c.c. Wasser, fügt in der Wärme 16 g. Salicylaldehyd hinzu und evakuiert sofort die Luft in dem Reaktionskolben. Es bildet sich rotbrauner Niederschlag, der schnell abgesaugt, mit Wasser gewaschen und auf Ton neben Chlorcalcium im Vakuumexsikkator getrocknet wird. Ausbeute 8 g. Beim Umkrystallisieren aus heissem Benzol erhält man schöne rotbraune Nadeln, die in Chloroform mit rotbrauner Farbe gut löslich sind. Verdunstet man die Chloroformlösung unter vermindertem Druck bei gewöhnlicher Temperatur, so erhält man glänzende dunkelrote Prismen, die schnell abfiltriert und im mit Chloroformdampf gesättigten Exsikkator neben Chlorcalcium getrocknet werden. Die Verbindung enthält 1 Mol. Chloroform; diese gibt ihren Chloroformgehalt langsam an der Luft bei gewöhnlicher Temperatur ab und färbt sich dann allmählich dunkelbraun durch Oxydation. Beim Erhitzen der Verbindung auf 100° wird 1 Mol. Chloroform abgegeben; der Erhitzungsrückstand ist ein rotbraunes Pulver. 0.0482 g. Substanz verloren bei 100° 0.0130 g. Chloroform. (Gefunden: $CHCl_3$, 26.97. Berechnet für $C_{16}H_{14}O_2N_2Co \cdot CHCl_3$: $CHCl_3$, 26.86%.)

Das abgegebene Chloroform wurde durch Isonitrilreaktion nachgewiesen. Die chloroformhaltige Verbindung ist leicht löslich in Äthylalkohol, Chloroform und Pyridin, wenig löslich in Benzol und Kohlenbisulfid und fast unlöslich in Tetrachlorkohlenstoff. In heissem Benzol ist sie leicht löslich.

Das chloroformfreie, rotbraune Pulver krystallisiert aus heissem Benzol in rotbraunen Nadeln, wie in Abb. 1 gezeigt. Die Verbindung erwies sich als Salicylaldehyd-äthylendiimin-kobalt. (Gefunden: Co, 18.47. Berechnet für $C_{16}H_{14}O_2N_2Co$: Co, 18.13%.)

Sauerstoff-Anlagerungsverbindung des Salicylaldehyd-äthylendiimin-kobaltes. Salicylaldehyd-äthylendiimin-kobalt in festem Zustande absorbiert an der Luft ungefähr 1/3 Mol. Sauerstoff und geht in die schwarze Sauerstoff-Anlagerungsverbindung über. Die Anlagerung findet besonders schnell mit dem pulverförmigen Kobaltsalze statt, welches aus der oben erwähnten, chloroformhaltigen Verbindung durch Erhitzen erhalten wurde.

Die volumetrische Bestimmung des angelagerten Sauerstoffes wurde in einem Apparate (Abb. 3) durch Erhitzen der Substanz im Kohlensäurestrom auf 100° ausgeführt. 0.0665 g. Anlagerungsverbindung: 1.64 c.c. O_2(19°, 759 mm.). 0.0308 g. Anlagerungsverbindung: 0.75 c.c. O_2(18°, 761 mm.). (Gefunden: 1/3 O_2, 3.29, 3.27. Berechnet für $C_{16}H_{14}O_2N_2Co \cdot 1/3O_2$: 1/3 O_2, 3.18%.)

Das aufgefangene Gas erwies sich als Sauerstoff, weil es in alkalischer Pyrogallollösung völlig absorbiert wurde.

Die Gewichtszunahme beim Stehenlassen des pulverförmigen Kobaltsalzes im Exsikkator und die Gewichtsabnahme beim Erhitzen der so erhaltenen schwarzen Anlagerungsverbindung sind gleichwertig. 0.0665, 0.0308, 0.2336 g. pulverförmige Substanz verloren bei 100° 0.0023, 0.0011, 0.0082 g. Sauerstoff. 0.0861 g. nadelförmige Substanz, welche zwei Monate lang im Exsikkator stehen gelassen wurden, verloren bei 100° 0.0033 g. Sauerstoff. (Gefunden: 1/3 O_2, 3.46, 3.57, 3.51, 3.83. Berechnet für $C_{16}H_{14}O_2N_2Co \cdot 1/3O_2$: 1/3 O_2, 3.18%.)

Die Anlagerungsverbindung ist leicht löslich in Chloroform, wenig löslich in Benzol und Äthylalkohol, fast unlöslich in Äther und unlöslich in Petroleumäther.

Salicylaldehyd-äthylendiimin-kobalti-hydroxyd. Löst man das Rohprodukt von Salicylaldehyd-äthylendiimin-kobalt in heissem Chloroform, filtriert man nach dem Erkalten den zurückbleibenden Niederschlag ab und lässt man das Filtrat an der Luft stehen, so scheiden sich nach einem Tage aus der dunkelbraunen Lösung glänzende schwarzviolette Krystalle aus, die abfiltriert, mit Chloroform gewaschen, auf Ton an der Luft getrocknet und dann bei 140° bis zur Gewichtskonstante erhitzt werden. (Gefunden: Co, 17.37; N, 8.47. Berechnet für $(C_{16}H_{14}O_2N_2Co)OH$: Co, 17.23; N, 8.19%.)

Die Krystalle sind leicht löslich in Eisessig, löslich in Methylalkohol und Pyridin, wenig löslich in Äthylalkohol, fast unlöslich in Chloroform und Kohlenbisufid und unlöslich in Benzol, Petroleumäther, Äther und Tetrachlorkohlenstoff. Erwärmt man die Verbindung mit verdünnter Schwefelsäure, so tritt Zersetzung unter Bildung von freiem Salicylaldehyd ein. Auch durch Kalilauge wird sie unter Bildung von Äthylendiamin zersetzt.

Salicylaldehyd-äthylendiimin-kobalti-chlorid. Man versetzt eine heisse Lösung von 1 g. Salicylaldehyd-äthylendiimin-kobalti-hydroxyd in 25 g. Methylalkohol mit 3 c.c. 1 N Essigsäurelösung, fügt 200 c.c. gesättigte wässrige Lösung von Ammoniumchlorid hinzu. Es entsteht eine tief-braune Lösung, aus der sich nach einem Tage schöne, schwarzbraune Prismen absetzen. Man filtriert sie ab, wäscht sie mit wässriger Lösung von Ammoniumchlorid, dann mit Wasser und schliesslich schnell mit verdünnter wässriger Methylalkohol. Ausbeute 0.7 g.

Die Substanz wurde vor der Analyse bei 160° bis zur Gewichtskonstante erhitzt. (Gefunden: Co, 16.29, 16.45; Cl, 9.63, 9.76; N, 7.76. Berechnet für $(C_{16}H_{14}O_2N_2Co)Cl$: Co, 16.35; Cl, 9.84; N, 7.77%.)

An dieser Stelle möchte ich Herrn Prof. Dr. R. Tsuchida und Herrn Dr. M. Kobayashi für ihre freundliche Unterstützung bei der Aufnahme der Absorptionsspektren meinen herzlichen Dank aussprechen.

Osaka-Hochschule, Osaka.

Quantitative Spectral Analysis. IX. Determination of Caesium by Emission-Spectra.

By Arata IWAMURA.

(Received January 7, 1938.)

I. **Introduction.** The chemical analysis of caesium contained in a sample solution, especially when caesium is contained in an insignificant amount, is exceedingly tedious in the process while less reliable in the outcome, principally owing to the difficulty of separating it from the other alkalies. The present writer has, nevertheless, tried to establish the definite method of quantitative analysis of caesium by means of emission-spectra.

II. **Sample Electrodes.** For the quantitative determination, the sample solution has been transformed into solid conductive electrodes in the following way: A sample solution of known or unknown caesium content and 20 c.c. of "sirupus simplex" of Jap. Ph. were mixed in a mortar. To this mixture 10 g. of carbon ("Nolit") were added and elaborately mixed and then heated in an air-oven for the express purpose of removing water contained in the mixture. When an appropriate consistency was thus obtained, it was moulded into tablets while hot, and they were further heated in an air-oven for further expelling any remaining volatile matter.

When the sample to be analysed was given in the form of solid substance, for example, such as ashes obtained from some plants or other, or some dry pulverized leaves, and stems of certain plants, or sometimes organic tissues of animals or insects, the sample was similarly rendered into the shape of tablets for sparking electrodes.

III. **The Apparatus Used and the Method of Experiment.** To excite sparks between a pair of electrodes, a transformer giving 10 kilovolts in the secondary circuit was used. Self-inductance of a magnitude of 5500 cm. was always inserted in the secondary circuit, but no capacity was inserted. The light emanating from an uncondensed spark between the electrodes was focussed by means of a lens on a slit of a constant deviation spectrograph. The dispersion of the spectrograph was 25 Å per mm. at $\lambda = 4560$ Å. The caesium lines at $\lambda = 4555.3$ and 4593.2 Å were detected, the former being more sensitive.

The method of analysis was consisted in drawing a density-concentration curve in connection with the line at 4555.3 Å so as to determine graphically the concentration of caesium chloride from the density of the caesium line in the spectrogram of an unknown sample. The so-called "method of comparison" was also tried, and both results were compared.

IV. **The Sensitivity of the Spectrographic Analysis.** The sensitivity of the spectrographic analysis of caesium chloride contained in the sample electrodes composed of carbon and "sirupus simplex" was determined in the same way as was already described.[1]

The relation between the percentage composition of caesium chloride in the electrodes and the intensity of the caesium line at $\lambda = 4555.3$ Å is shown in Table 1 and Fig. 1, where d representing the galvanometer deflection measuring the density of the line. The sensitivity was thus graphically found to be 2×10^{-4}% under the conditions of the experiment. (See Fig. 3, a and b.)

Table 1.

CsCl (%)	d (mm.) $\lambda = 4555.3$ Å
5×10^{-4}	3.2
15×10^{-4}	9.9
3.0×10^{-3}	17.6
5.0×10^{-3}	28.2

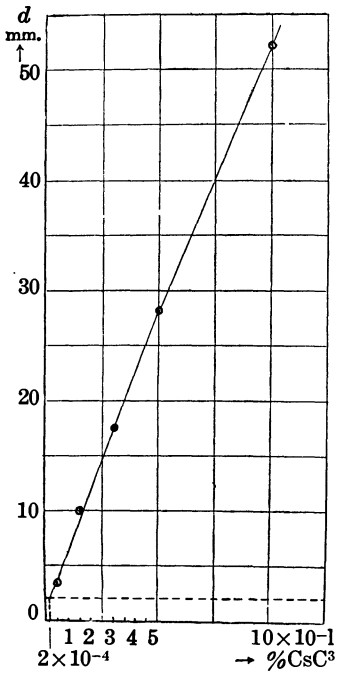


Fig. 1.

(1) *Mem. Coll. Sci., Kyoto Imp. Univ.*, A, **14** (1931), 51.

The sensitivity tried by means of employing the electrodes composed of zinc oxide and hydrochloric acid was found to be too low. The cause of this lower sensitivity shown in the electrodes cemented with zinc oxide can be understood when we compare the ionization potential of caesium with those of zinc, carbon, etc., as indicated in Table 2.

Table 2.

Elements	Cs	Zn	Mg	Ca	C	Na	Rb	K
1st ioniz. potential (volts)	8.88	9.35	7.61	6.09	11.24	5.12	4.16	4.32

V. **Examples of Analysis.** The results of analysing a sample by the graphical method of applying the density-percentage composition relation is shown in Table 3 and Fig. 2, the microphotometer records being given in Fig. 3, c and d.

Table 3.

CsCl (%)	d (mm.) $\lambda = 4555.3$ Å
x	3.3
3×10^{-3}	7.2
6×10^{-3}	11.5
1×10^{-2}	19.2
1.5×10^{-2}	19.0
2×10^{-2}	33.7

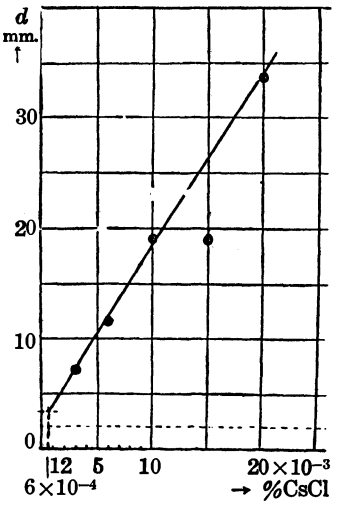


Fig. 2.

$x = 0.0006\%$ against the calculated value of 0.0005%.

The results of experiment showing how the method of comparison may be employed for the analysis of the same sample mentioned above, turned out to be as follows (see Fig. 4, a):

Let S denote the concentration of caesium chloride in the sample taken.

Ex. 1. $S = 0.0005\%$ CsCl.

CsCl (%)	d (mm.) $\lambda = 4555.3$ Å
0.0002	3.1
	4.9
S	8.0
	4.3
0.0008	12.3

By proportion we get,

$$6\times\frac{4.9}{9.2} = 3.2.$$

$$\therefore\ S = 0.0002+0.00032 = 0.00052.$$

$$\Delta = 100\times\frac{2}{50} = 4.0\%.$$

Ex. 2. $S = 0.0030\%$.

CsCl %)	d (mm.) $\lambda = 4555.3$ Å
0.0020	10.7
	7.3
S	18.0
	16.1
0.0050	34.1

By proportion we get,

$$30\times\frac{7.3}{23.4} = 9.$$

$$\therefore\ S = 0.0020+0.0009 = 0.0029.$$

$$\Delta = 100\times\frac{1}{30} = 3.3\%$$

Such a high order of accuracy can hardly be attained by any chemical method of analysis.

Another solid sample obtained from a plant was analysed by the density-percentage composition method and was found to contain 0.008% of caesium (or 0.011% as caesium chloride).

Another sample was similarly analysed and the content of CsCl was found to be 0.0143% as against the calculated value of 0.0150% (see Fig. 4, c and d), while by the graphical method from the density-percentage composition relation it was found to be 0.0155% as shown in Table 4.

Table 4.

No.	CsCl value	Method of comparison	%	Density-% relation	Δ (%)
1	0.0005	0.00052	4.0	0.0006	20.0
2	0.0030	0.0029	−3.3	—	—
3	0.0150	0.0143	−4.6	0.0155	4.1
4	—	—	—	0.011	—

Thus it is seen that both methods of analysis may be adopted for determining the amount of caesium chloride contained in solid electrodes with the results which agree with each other and also with the calculated value fairly well.

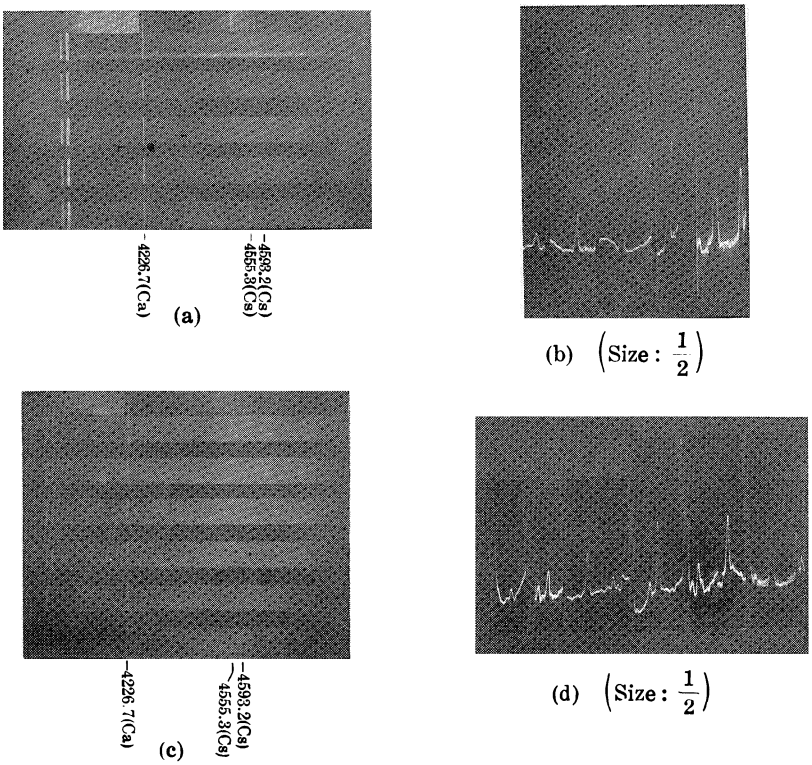

4226.7(Ca)
4593.2(Cs)
4555.3(Cs)
(a)
(b) (Size : 1/2)
4226.7(Ca)
4593.2(Cs)
4555.3(Cs)
(c)
(d) (Size : 1/2)

Fig. 3.

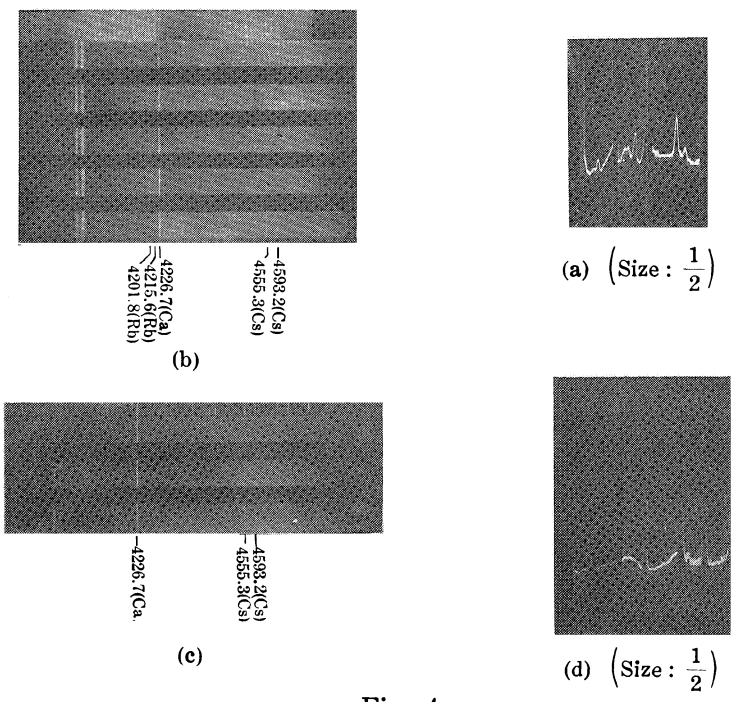

4226.7(Ca)
4215.6(Rb)
4201.8(Rb)
4593.2(Cs)
4555.3(Cs)
(b)
(a) (Size : 1/2)
4226.7(Ca.
4593.2(Cs)
4555.3(Cs)
(c)
(d) (Size : 1/2)

Fig. 4.

Summary.

(1) Solid sample electrodes were prepared from a caesium chloride solution, carbon and "sirupus simplex", and the amount of caesium chloride was spectrographically determined with a sensitivity of $2 \times 10^{-4}\%$.

(2) The analysis was conducted on sample electrodes containing 0.0005–0.015% of CsCl.

(3) Both the "method of comparison" and the graphical method were found to be applicable for the determination of caesium chloride with a fair degree of exactness, error being always caused within the permissible limit.

In conclusion, the present writer wishes to express his heartfelt and sincere thanks to Prof. M. Kimura, Phys. Inst., Imp. Univ. of Kyoto, for his supplying the writer with so many facilities during the years of experiment. Again, the writer wishes to express his high appreciation of the grant from the Imperial Academy towards this research.

Quantitative Spectral Analysis. X. Determination of Lithium by Emission-Spectra.

By Arata IWAMURA.

(Received January 7, 1938.)

I. **Introduction.** Although the process is very tedious, the ordinary chemical method employed for the estimation of lithium contained in a sample solid is less reliable in outcome, principally owing to the difficulty of separating it completely from other alkalies. The present writer tried to establish the direct method for the quantitative analysis of lithium by means of emission-spectra and then to apply the method to some sample clay, produced in the prefecture of Aichi, commonly employed as raw materials of the ceramic industry in our country.

II. **Sample Electrodes.** Sample solid electrodes containing varying amounts of lithium chloride were prepared from carbon, lithium chloride

and "sirupus simplex" by the method described in the preceding paper.[1] The lithium chloride taken for the experiment was obtained from Schering-Kahlbaum.

Sample electrodes containing clay were prepared by using the following mixture: 5 g. of clay (dried and powdered), 5 g. of carbon ("Nolit"), 10 c.c. of "sirupus simplex", and varying amounts of lithium chloride.

III. **Apparatus and Method of Experiment.** To excite arcs between a pair of electrodes, 220 volts alternating current was used. Self-inductance of a magnitude of 6000 cm. was inserted in the circuit. The light emanating from an arc between the sample electrodes was focussed on the slit of a glass-spectrograph of Nippon Kagakukikai Seisakusho make. The dispersion of the spectrograph was 96 Å per mm. at $\lambda = 6707.9$ Å.

The lithium lines at $\lambda = 6707.9$, 6103.6, 4971.9, and 4602.2 Å were detected, the first being the most sensitive.

The method of analysis was quite similar to that employed in the analysis of caesium reported in the preceding paper.[1]

IV. **The Sensitivity of the Sepectrographic Analysis.** The sensitivity of the spectrographic analysis of lithium chloride contained in a solid sample was thoroughly studied in the same way as was described in the previous paper.[2] The relation between the amount of lithium chloride contained in the solid sample and the intensity of the lithium line at $\lambda = 6707.9$ Å is shown in Table 1 and Fig. 1, d representing the galvanometer deflection measuring the intensity of the line.

Table 1.

LiCl (%) $\times 10^{-4}$	d (mm.)		Ratio (2)/(1)
	6707.9 Å (1)	6103.6 Å (2)	
0	1.5	1.8	1.2 (?)
1	4.3	1.8	0.42
2	5.7	2.0	0.35
3	10.0	2.6	0.26
4	11.9	4.0	0.34
8	19.0	6.5	0.34
			mean: 0.34

(1) This Bulletin, **13** (1938), 260.
(2) *Mem. Coll. Sci., Kyoto Imp. Univ.*, A, **14** (1931), 51.

The dotted-line in Fig. 1 denotes the density of the back ground of the plate and the broken line denotes the density of the lithium line emitted from the very minute trace of lithium contained in the electrode material originally.

The spectrogram shown in Fig. 2, a, and the corresponding microphotometer record Fig. 3, a–f, show that the sample contains very minute trace of lithium, i.e. $2 \times 10^{-5}\%$. (See also Fig. 1.)

The sensitivity was thus found graphically to be 0.00003% under the conditions of the experiment. The sensitivity with respect to the line at $\lambda = 6103.6$ Å was found analogously to be 0.0001%. See also the spectrogram and the corresponding microphotometer records shown in Fig. 2, a, and Fig. 3.

The ratio $d(2)/d(1)$ is calculated to be 0.34+ at a range of lithium chloride content varying from $1 \times 10^{-4}\%$ to $8 \times 10^{-4}\%$ as is shown in the 4th column of Table 1.

If the amount of lithium chloride to be determined is supposed to be exceedingly small, say $1 \times 10^{-4}\%$ to $3 \times 10^{-3}\%$, then the most sensitive line at $\lambda = 6707.9$ Å is to be selected. If lithium is contained in a larger amount the line at $\lambda = 6103.6$ Å should be selected. When the amount of lithium to be determined is much larger, say 0.005–0.05%, weaker excitation should be used, i.e. uncondensed high-tension spark or flame excitation. Fig. 2, b, is an example of uncondensed spark excitation adopted in the determination of lithium content as much as 0.05%. Spectrograms in Fig. 6 and Fig. 7 show how the line at $\lambda = 6707.9$ Å should not be used, because the intensity of the line does not vary as the percentage composition varies.

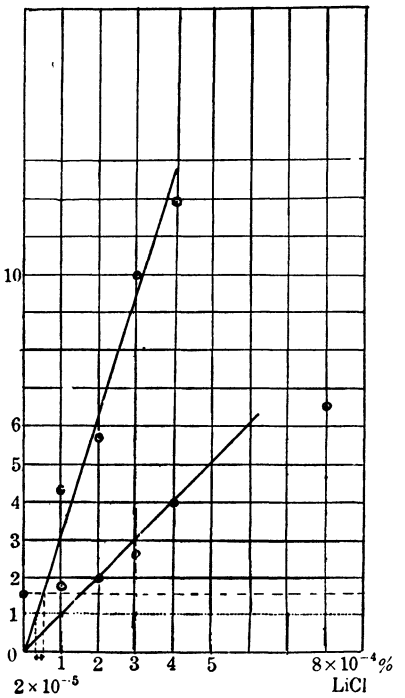


Fig. 1.

V. **Examples of Analysis.** The results of analysis showing how the method of comparison may be employed for the analysis, turned as follows:

Let S denote the percentage of LiCl in the sample taken, Δ the percentage deviation from the calculated value.

Ex. 1. $S = 0.0010\%$.

LiCl (%)	d (mm.) $\lambda = 6707.9$ Å
0.0005	17.4 — 2.6
S	20.0 — 5.1
0.0020	25.1

By proportion we get, $15 \times \frac{2.6}{7.7} = 5.1$.

$\therefore\ S = 0.0005 + 0.00051 = 0.00101$.

$$\Delta = 100 \times \frac{1}{100} = 1.0\%.$$

Ex. 2. $S = 0.0025\%$.

LiCl (%)	d (mm.) $\lambda = 6707.9$ Å
0.0010	20.2 — 10.1
S	30.3 — 5.2
0.0035	35.5

By proportion we get, $25 \times \frac{10.1}{15.3} = 16.5$.

$\therefore\ S = 0.0010 + 0.00165 = 0.00265$.

Another sample was analysed by exciting the sample electrodes with uncondensed sparks and the content of lithium chloride was found to be 0.0475% as against the calculated value of 0.0450%, the error being $100 \times \frac{25}{450} = 5.5\%$. (See Fig. 2, b.)

The results of analysis by the graphical method of applying the density-percentage composition relation is shown in Tables 2–4 and the spectrograms and their corresponding microphotometer records being given in Fig. 6 and Fig. 7.

The density-concentration method is favourably applicable in a range only, where the relation $d \infty c$ holds. With respect to the line at $\lambda =$ 6707.9 Å, these spectrograms are over-exposed or over-developed and they show that the densities do not vary proportionally as the content of lithium varies, while the line at $\lambda = 6103.6$ Å is normally exposed or normally developed. For this reason the line at $\lambda = 6103.6$ Å has been selected in the determination of lithium in the following cases. The reason why the ratio of (2)/(1) is not constant is also self-evident.

Table 2.

LiCl (%) $\times 10^{-2}$	d (mm.)		Ratio (2)/(1)
	6707.9 Å (1)	6103.6 A (2)	
x	20.9	1.7	0.08
1	23.6	3.3	0.14
2	24.6	5.9	0.24
3	34.0	12.0	0.35

$x = 0.001\%$ or $1 \times 10^{-3}\%$.

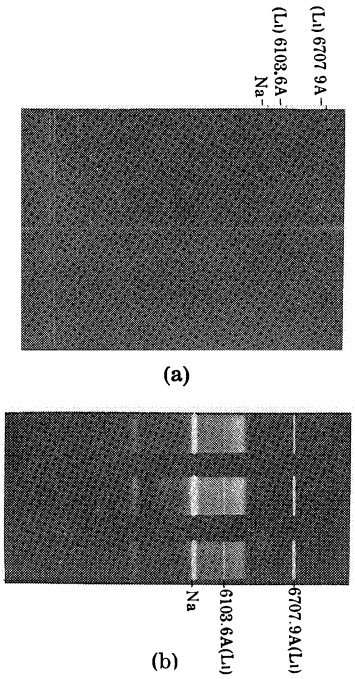
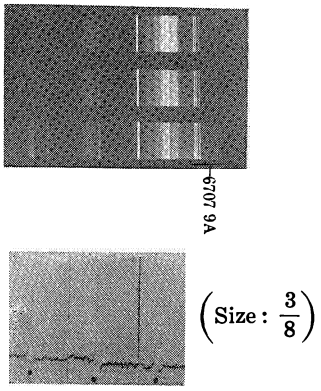
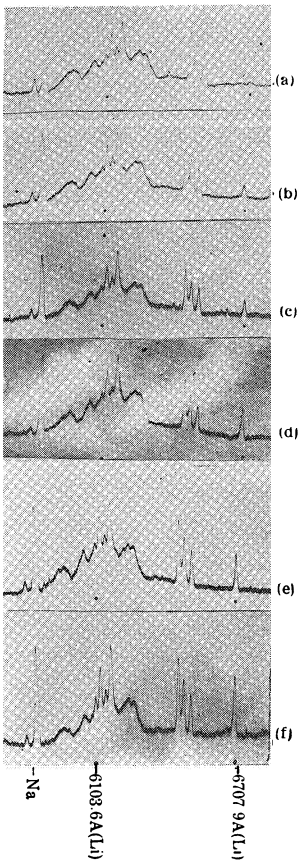


Fig. 2.



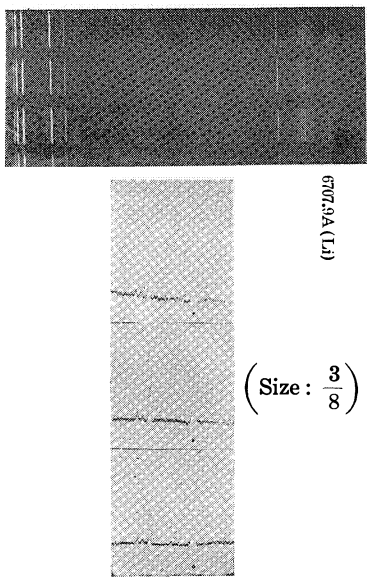
(Size : 3/8)

Fig. 4.



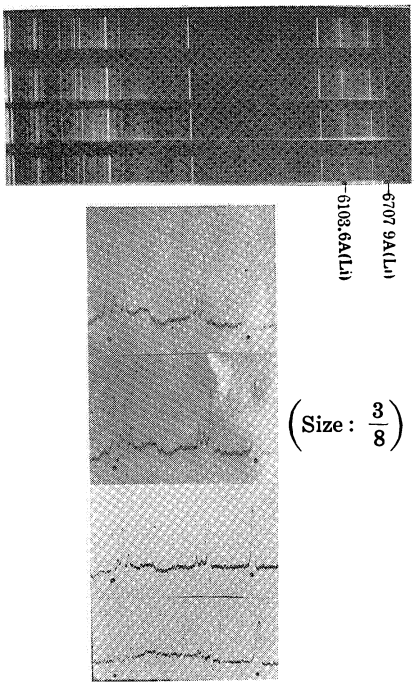
(Size : 3/8)

Fig. 3.



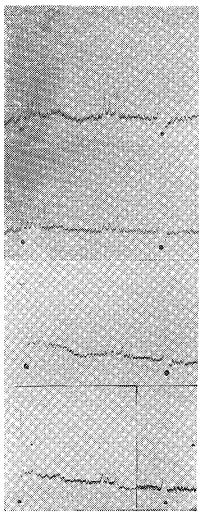
(Size : $\frac{3}{8}$)

Fig. 5.



(Size : $\frac{3}{8}$)

Fig. 6.



(Size : $\frac{3}{8}$)

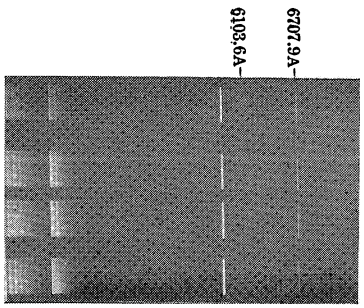


Fig. 7.

Table 3.

LiCl (%) $\times 10^{-4}$	d (mm.)		Ratio (2)/(1)
	6707.9 Å (1)	6103.6 Å (2)	
x	32.4	4.9	0.15
1	34.5	8.4	0.24
2	44.5	17.8	0.40
3	46.4	18.8	0.45

$x = 0.005\%$ or $5\times10^{-3}\%$.

Table. 4.

LiCl (%) $\times 10^{-3}$	d (mm.)		Ratio (2)/(1)
	6707.9 Å (1)	6103.6 Å (2)	
x	14.3	6.2	0.43
2	19.5	12.2	0.63
4	23.6	19.0	0.81
8	27.9	21.9	0.78

$x = 0.012\%$ or $12\times10^{-3}\%$.

The results of analysis is shown in Table 5.

Table 5.

No.	Comp. method found (%)	Calc. value (%)	Δ (%)	No.	Density-conc. relation $\times 10^{-3}$ (%)
1	0.00101	0.0010	1.0	5	1
2	0.00265	0.0025	6.0	6	5
3	0.0052	0.0050	4.0		
4	0.0475	0.0450	5.5	7	12

Such a high order of accuracy can hardly be attained by any chemical method of analysis.

In case, the lithium lines are observed in the spectrum of the carbon electrodes, the determination of lithium may be carried out by the method analogous to that previously described.[3]

(3) A. Iwamura, *Mem. Coll. Sci., Kyoto Imp. Univ.*, A, **14** (1931), 332.

Summary.

(1) Solid sample electrodes were prepared from carbon, "sirupus simplex" and varying amounts of lithium chloride, and the amount of lithium chloride was spectrographically determined with a sensitivity of $3 \times 10^{-5}\%$ with respect to the line at $\lambda = 6707.9$ Å, and with that of $1 \times 10^{-4}\%$ with respect to the line at $\lambda = 6103.6$ Å.

(2) The method of comparison was found to be applicable for the determination of lithium chloride throughout the range of 0.001–0.050%.

(3) Several samples containing lithium were analysed by the graphical method and were found to contain $1—12 \times 10^{-3}\%$ of lithium chloride.

(4) Several samples of clay produced in Seto and Inuyama were found to contain $3 \times 10^{-5}\%$ of lithium by the graphical method.

In conclusion, the writer wishes to express his high appreciation of the grant from the Imperial Academy towards this research.

Synthesis of *l*-Talose.[1]

By Shozo FUKUNAGA and Bennosuke KUBOTA.

(Received January 13, 1938.)

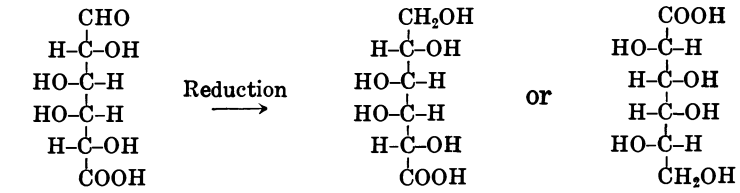
Among the sixteen theoretically possible aldohexoses, *l*-talose has been the last one yet unknown, nor have its derivatives been described except *l*-talomucic acid. Although its antipode *d*-talose has been already formed[2][3] from *d*-galactose derivatives easily obtainable from naturally occurring *d*-galactose, *l*-talose has not yet been synthesized, because no convenient natural source or no easy synthetical method has yet been found for preparing *l*-galactose or its derivatives in any large quantity.

The most convenient method of obtaining *l*-galactose derivatives seems to us to consist first in the reduction of *d*-galacturonic acid into *l*-galactonic acid as shown below:

(1) *l*-Talonic acid and some of its derivatives were already reported, *J. Chem. Soc. Japan*, **57** (1936), 551. See also this Bulletin, **12** (1937), 116.

(2) W. Bosshard, *Helv. Chim. Acta*, **18** (1935), 482.

(3) P. A. Levene and T. S. Tipson, *J. Biol. Chem.*, **93** (1931), 631; J. Komada, this Bulletin, **7** (1932), 211.



d-Galacturonic acid. *l*-Galactonic acid.

While it was obtained by W. N. Haworth, E. L. Hirst and their collaborators[4] from *d*-galactose by means of oxidation of its diacetone compound and subsequent reduction of *d*-galacturonic acid so formed, we have found in the course of our investigations in monoses[1] that it can be more easily prepared from barium salt of *d*-galacturonic acid directly obtained by hydrolysis of citrus pectic acid. We made attempt therefore to synthesize *l*-talose from *l*-galactonic acid prepared by this method.

Citrus pectic acid which is obtained from citrus pectin (orange pectin) by partial hydrolysis, is a polymeride of *d*-galacturonic acid described by K. P. Link and his collaborators.[5] Being hydrolized with dilute sulphuric acid, it gives *d*-galacturonic acid which is isolated in its barium salt according to Link's method. As it is rather unstable and very difficultly purified, the crude barium salt is submitted to reduction, directly after it has been converted into sodium salt, with 2.5 percent sodium amalgam. *l*-Galactonic acid so formed is purified through its cadmium salt, which, treated with hydrogen sulphide, gives *l*-galactonic lactone in crystalline form. It forms needles melting at 109.5–111°[6] with $[\alpha]_D^{18°} + 77°$ ($c = 1.76$ in water, after five minutes), and seems to be anhydrous form.

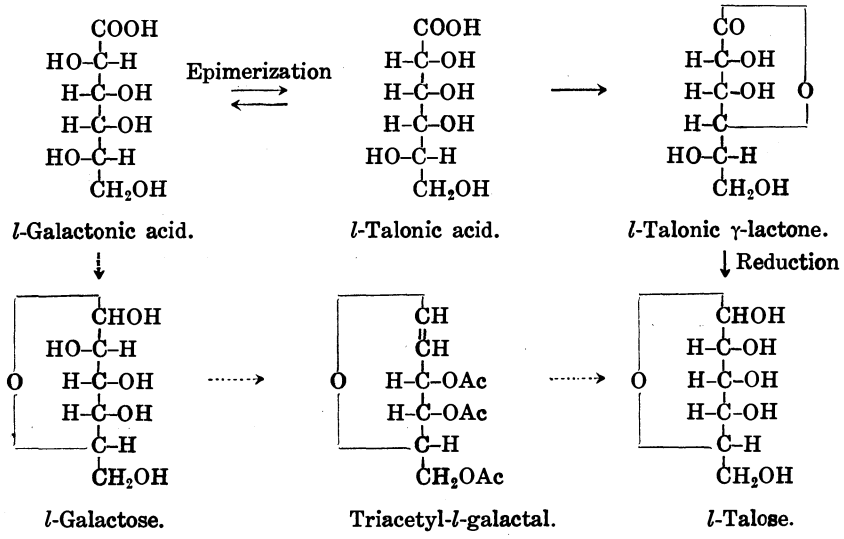
There are two methods of obtaining *l*-talose from *l*-galactonic acid. As it is more difficult and roundabout to synthesize *l*-talose through triacetyl-*l*-galactal according to Levene's method[3] in his synthesis of *d*-talose, *l*-galactonic acid is submitted to epimerization in order to turn it into *l*-talonic acid, the lactone of which is then reduced to *l*-talose in the same way as Bosshard did in his synthesis of *d*-talose,[2] as follows:

The epimerization is carried out by refluxing *l*-galactonic acid solution directly obtained from its cadmium salt for fifty hours with pyridine in the oil bath of 135° and *l*-talonic acid partially formed is conveniently separated in its potassium salt according to Bosshard, after the greater part of unchanged *l*-galactonic acid is removed in its cadmium salt.

(4) *J. Chem. Soc.*, **1933**, 1419, most recently by C. Glatthaar and T. Reichstein, *Helv. Chim. Acta*, **20** (1937), 1537.

(5) K. P. Link and P. Nedden, *J. Biol. Chem.*, **94** (1931), 307.

(6) All the melting points given in this paper are corrected.



l-Talonic acid crystallizes in needles with half a molecule of water like its antipode, melting at 124.5–125°, but when recrystallized from absolute ethyl alcohol, the anhydrous acid is obtained, white powder melting at 137–138° with $[\alpha]_D^{15°} - 18.2°$ ($c = 3.53$ in water, after five minutes). *l*-Talonic lactone can be crystallized in prisms melting at 133–134.5° with $[\alpha]_D^{17°} + 34.4°$ ($c = 1.17$ in water, after five minutes). Following some derivatives of *l*-talonic acid are obtained. Amide, white powder melting at 119–120.5° with $[\alpha]_D^{18°} + 13.3°$ ($c = 1.59$ in water). Phenylhydrazide, prisms melting at 161–162° with $[\alpha]_D^{18°} + 26.0°$ ($c = 2.21$ in water). According to O. F. Hedenburg and L. H. Cretscher,[7] the brucine salt of *d*-talonic acid is not a suitable derivative for the identification of the acid though many workers have written about it, because of its hygroscopic property and some uncertainty about its purity. On the contrary, the brucine salt of *l*-talonic acid is obtained in beautiful crystals from dilute ethyl alcohol which is by no means hygroscopic. It forms plates melting at 139–140° with $[\alpha]_D^{14°} - 23.7°$ ($c = 3.25$ in water), having the composition $C_6H_{12}O_7 \cdot C_{23}H_{26}O_4N_2 \cdot 2H_2O$.

The reduction of *l*-talonic lactone is carried out according to M. Steiger's advice described in preparation of *d*-ribose.[8] *l*-Talose is separated in its *o*-nitrophenylhydrazone. It forms orange leaflets melting at 148–149° with $[\alpha]_D^{14°} - 88°$ ($c = 0.171$ in methyl alcohol).

(7) *J. Am. Chem. Soc.*, **49** (1927), 478.
(8) *Helv. Chim. Acta*, **19** (1936), 193.

l-Talose is obtained in a colourless syrup with sweet taste from the *o*-nitrophenylhydrazone by decomposition with benzaldehyde. We have not yet succeeded in crystallizing it within a month notwithstanding our utmost efforts, while W. Bosshard described also that *d*-talose obtained by the similar method did not crystallize of itself without seeding.[9]

The equilibrium rotation of *l*-talose is calculated therefore from the reading of the *l*-talose solution directly obtained by the decomposition of known weight of its *o*-nitrophenylhydrazone, on the assumption that the conversion is quantitative. The results are $[\alpha]_D^{14^\circ} - 18.6^\circ$ ($c = 0.809$ in water, an hour after decomposition) and $[\alpha]_D^{14^\circ} - 19.8^\circ$ (after ten days), quite in agreement with the equilibrium rotation of Bosshard's *d*-talose, $[\alpha]_D^{20^\circ} + 20.6^\circ$ or Levene's, $[\alpha]_D^{27^\circ} + 19.7^\circ$.

It seems clear that *l*-talose, *l*-talonic acid, *l*-talonic lactone and their derivatives are now formed. The comparison of their properties with those of *d*-isomers are shown in Table 1 and 2.

Table 1. Talose and its *o*-nitrophenylhydrazone.

		Talose	*o*-Nitrophenylhydrazone
Authors' *l*-form	M.p.	—	148—149°
	$[\alpha]_D$	−19.8°(14°)	−88°(14°) (in methyl alcohol)
Bosshard's *d*-form[8]	M.p.	128—130°	148.5—149°
	$[\alpha]_D$	+ca. 30°→+20.6°(20°)	+88.3°(18°) (in methyl alcohol)

Table 2. Talonic acid and its derivatives.

		Acid anhydrous	Lactone	Phenyl-hydrazide	Amide	Brucine salt
Authors' *l*-form	M.p.	137—138°	133—134.5°	161—162°	119—120.5°	139 - 140°
	$[\alpha]_D$	−18.2°(15°)	+34.4°(17°)	+26.0°(13°)	+13.3°(18°)	−23.7°(14°)
d-Form[10]	M.p.	138°	132—134°	159°	121°	132° [11]
	$[\alpha]_D$	+19.0°(25°)	−34.7°(25°)	−25.4°(25°)	−13.1°(25°)	−26.15°(20°)

(9) The seeding crystal he used was obtained by the other method by Levene, see foot-note (2).

(10) From Tollens-Elsner, "Kurzes Handbuch der Kohlenhydrate," 4th Ed., 364, Leipzig (1935).

(11) The highest value recorded, but its purity was doubtful, P. A. Levene and G. M. Meyer, *J. Biol. Chem.*, **26** (1916), 362; **31** (1917), 624.

Experimental.

Preparation of Barium *d*-Galacturonate. Citrus pectic acid was hydrolized with dilute sulphuric acid according to K. P. Link and P. Nedden, but their method was a little modified. Citrus pectic acid (80 g.) was gradually added with stirring to boiling 2 5 percent sulphuric acid (4 litres) in a 5 litre flask equipped with a reflux condenser and a stirrer. The solution was refluxed in the oil bath of 110° for fifteen hours, being well stirred to prevent from charring and bumping. After the heating was finished, it was added with some kieselguhr, decanted and filtered from gelatinous residue. The filtration was very difficult, the solution was therefore filtered with a large filter paper over kieselguhr. The filtrate was then neutralized by heating to 70–80° with barium carbonate which was gradually added to the solution with stirring. Thus, we used barium carbonate in place of barium hydroxide solution for the neutralization of the solution, as this method had the advantages that neutralization of sulphuric acid and conversion of *d*-galacturonic acid formed into its barium salt were carried out at the same time and increase of volume of the solution was avoided. When the solution became not acid to congo red, it was decolourized with active carbon and filtered from barium sulphate after cooled. The filtrate and washings with hot water were united and concentrated in the bath below 50° in vacuum. During the concentration, brown gummy substance was precipitated which was filtered and the filtrate was decolourized twice with active carbon, further concentrated to about 100 c.c. in the bath below 45° in vacuum. After it was warmed with active carbon if necessary, the light brown solution was then poured into four volumes of 95 percent ethyl alcohol. Barium *d*-galacturonate was precipitated in almost white powder, which was filtered after standing overnight and dehydrated by washing successively with hot 95 percent and absolute ethyl alcohol. As the precipitate was very hygroscopic, the filtration and washing were carried out continuously lest it should be filtered off. But, when it was completely dehydrated, it became not so hygroscopic and was quickly dried by washing with dry ether. Faint yellow powder. Yield about 30 g. This was impure, but used directly for the reduction.

Reduction to *l*-Galactonic Acid and Separation in its Cadmium Salt. The crude barium *d*-galacturonate (25 g.) was dissolved in small volume of warm water, filtered from flocculent residue after it was warmed with active carbon for a while and excess of sodium sulphate was added to convert it into sodium salt. The filtrate and washings with hot water were united and the solution (about 500 c.c.) was reduced with 2.5 percent sodium amalgam at room temperature as follows: It was stirred vigorously in a thick-walled flask and 50 g. of the amalgam were added, while the solution was kept all the time to be slightly alkaline being not red to phenolphthalein by neutralizing with 20 percent sulphuric acid. The reduction was continued by adding 50 g. of fresh sodium amalgam each time after the amalgam was almost consumed, until the solution showed no reducing power against Fehling's solution. It took about forty hours and about 800 g. of the amalgam were consumed. The solution was then separated from mercury and filtered over active carbon. The filtrate was neutralized with dilute sulphuric acid to be acid to litmus but not acid to congo red and concentrated in vacuum until sodium sulphate separated out. After it was acidified with 20 percent sulphuric acid to become distinctly blue to congo red, it was poured into two litres of hot 95 percent ethyl alcohol. The alcoholic solution was filtered after standing overnight and the filtrate was concentrated in vacuum to expel alcohol after it was

diluted with water and finally concentrated to about 50 c.c. The excess of sulphuric acid was then removed quantitatively by warming the solution on the water bath with freshly precipitated wet barium carbonate. It was filtered over active carbon, the resulting *l*-galactonic acid solution was further concentrated in vacuum and heated on the boiling water bath for an hour with the excess of cadmium carbonate. After the evolution of carbon dioxide was ceased, some cadmium hydroxide was added to complete the neutralization. Carbon dioxide was then passed in the hot solution in order to remove the excess of cadmium hydroxide. The hot filtrate and washings with hot water separated cadmium *l*-galactonate in the cold, which was filtered after left for two days in cold place and washed with cold water. Some quantity of the salt was recovered from the mother liquor when concentrated and left for a long time. Recrystallized from large volume of boiling water. Yield about 9 g. White powder hardly soluble in cold water, having one molecule of water of crystallization. (Found: residue, 39.47. Calc. for $(C_6H_{11}O_7)_2Cd\cdot H_2O$: $CdSO_4$, 40.05 %.) When crystallized from dilute solution by gradual evaporation in the air at room temperature, needle crystals aggregating in cubes were obtained, which seemed to be tetrahydrate. (Found: residue, 35.66. Calc. for $(C_6H_{11}O_7)_2Cd\cdot 4H_2O$: $CdSO_4$, 36.27 %.)

l-Galactonic Acid and its Lactone. Cadmium *l*-galactonate was dissolved in about twenty times of boiling distilled water and quickly cooled. When it began to be turbid, it was decomposed with hydrogen sulphide, excess of which was avoided by testing with lead acetate in order to facilitate the filtration from cadmium sulphide. The filtrate was concentrated in vacuum and filtered over active carbon. Thus we obtained *l*-galactonic acid solution which separated needle crystals of the acid in the cold. It was used directly for the epimerization in the preparation of *l*-talonic acid.

The crystalline *l*-galactonic lactone was obtained as follows: The solution was concentrated in vacuum to a thick syrup and it was heated on the water bath for an hour in vacuum in order to complete the lactonization. The resulting lactone syrup was dissolved in absolute ethyl alcohol, filtered from flocculent precipitate and concentrated to a thick syrup, which began to crystallize in a few days in a vacuum desiccator over sulphuric acid. It was recrystallized twice from absolute alcohol, finally from dry ethyl acetate, and dried over P_2O_5 at 60° in vacuum. Small needles melting at 109.5–111°, with $[\alpha]_D^{18°} + 77°$ (35.3 mg. in 2 c.c. aqueous solution, $l = 2$ dm., $\alpha = +2.72°$).

Potassium l-Talonate, Epimerization of l-Galactonic Acid. The *l*-galactonic acid solution obtained from 30 g. of cadmium *l*-galactonate as described above, was concentrated to about 120 c.c., added with 9 c.c. pyridine and refluxed in the oil bath of 135° for fifty hours. The reflux condenser was then removed and the brown solution was heated for about twenty minutes with supply of water. When the greater part of pyridine was expelled, 10 g. of cadmium carbonate were gradually added to the solution and it was boiled gently with supply of water for half an hour more and some cadmium hydroxide freshly precipitated was added to neutralize the solution completely. The heating was then ceased and carbon dioxide was passed in the hot brown muddy solution to remove the excess of cadmium hydroxide. It was then left to stand two days in cold place and filtered from cadmium *l*-galactonate and carbonate. After the brown filtrate and washings with cold distilled water were decolourized with active carbon, the solution was concentrated to a thin syrup in vacuum. This syrup was left in ice-chest for two days and filtered from separated cadmium *l*-galactonate. Thus, the greater part of unchanged *l*-galactonic acid was removed, about 9 g.

of its cadmium salt being recovered. The filtrate and washings with small volume of cold distilled water were united and decomposed with hydrogen sulphide. The filtrate from cadmium sulphide was concentrated in vacuum, decolourized with active carbon and treated after W. Bosshard's method for separating talonic acid in its potassium salt as follows: The solution was divided in two portions, the nine tenths of its volume and the remainder. The former was exactly neutralized with carbonate-free potassium hydroxide solution and mixed with the latter. Thus, 90 percent of the acid was converted into its potassium salt. The solution was then concentrated in vacuum, decolourized and finally concentrated to a thin syrup. To this syrup methyl alcohol was added so far as constant turbidity did not occur and it was left in ice-chest. Potassium *l*-talonate crystallized out and was filtered after two days, washed with 70, 80 and 90 percent methyl alcohol respectively. It was dried in the air. Yield 4.7 g., some was recovered from the mother liquor when treated as above. Prisms melting at 166–168° with $[\alpha]_D^{15°}$ −2°, sufficiently pure for the next experiment.

l-Talonic Acid from its Potassium Salt. Potassium *l*-talonate was dissolved in distilled water and a volume of standard sulphuric acid solution slightly less than the calculated was added. The solution was concentrated in the bath below 50° in vacuum until sodium sulphate began to separate and precipitated by pouring into large volume of hot absolute ethyl alcohol. The warm solution was filtered from the precipitated salt, which was redissolved in small volume of warm water and precipitated again with absolute alcohol. The united warm alcoholic extracts separated needle crystals of *l*-talonic acid in the cold. When the filtrate was concentrated to a thin syrup at low temperature and added with several volumes of absolute alcohol, *l*-talonic acid crystallized out again. Recrystallized from dilute ethyl alcohol. Needles melting at 124.5–125°. But, when recrystallized from absolute ethyl alcohol, white powder melting at 137–138° with $[\alpha]_D^{15°}$ −18.2° (35.3 mg. in 1 c.c. aqueous solution, $l = 1$ dm., $\alpha = -0.64°$ after five minutes) was obtained. The former was hydrate and the latter anhydrous form. (Hydrate, found: C, 35.48; H, 6.63. Calc. for $C_6H_{12}O_7 \cdot \frac{1}{2}H_2O$: C, 35.28; H, 6.42%. Anhydrous acid, found: C, 36.87; H, 6.23. Calc. for $C_6H_{12}O_7$: C, 36.71; H, 6.17%.)

l-Talonic Lactone from l-Talonic Acid. The alcoholic solution of *l*-talonic acid obtained in the above experiment was directly used. It was concentrated to a thick syrup in vacuum, which was heated on the boiling water bath for an hour in vacuum to complete the lactonization. The syrup was then dissolved in absolute ethyl alcohol, filtered from flocculent precipitate and concentrated to a thin syrup in vacuum, which was easily crystallized by seeding or by concentrating in a vacuum desiccator. Recrystallized from absolute ethyl alcohol. Prisms melting at 133–134.5° with $[\alpha]_D^{17°}$ + 34.4° (23.4 mg. in 2 c.c. aqueous solution, $l = 2$ dm., $\alpha = +1.61°$, after five minutes) changing to + 29.3° after four days, showing that it was γ-lactone.

Derivatives of l-Talonic Acid. *Amide.* It was precipitated when dry ammonia was passed in the lactone solution in absolute alcohol. Recrystallized twice from absolute alcohol. White powder melting at 119–120.5° with $[\alpha]_D^{18°}$ + 13.3° (15.9 mg. in 1 c.c. aqueous solution, $l = 1$ dm., $\alpha = +0.21°$). (Found: N, 6.80. Calc. for $C_6H_{13}O_7N$: N, 6.63%.)

Phenylhydrazide. The equal weights of *l*-talonic acid and phenylhydrazine in a small volume of water were heated on the water bath for an hour with one drop of

dilute acetic acid. The phenylhydrazide separated when absolute alcohol was added to the solution. Recrystallized from absolute alcohol. Prisms melting at 161–162° with $[\alpha]_D^{13°} + 26.0°$ (44.2 mg. in 2 c.c. aqueous solution, $l = 2$ dm., $\alpha = +1.16°$). (Found: N, 9.35. Calc. for $C_{12}H_{18}O_7N_2$: N, 9.27%.)

Brucine salt. The equivalent weights of the lactone and brucine in small volume of water were heated for a while and several volumes of absolute alcohol were added to the solution. The brucine salt was crystallized out when it was left in cold place. Recrystallized by dissolving it in small volume of cold water and adding absolute alcohol. Plates melting at 139–140° with $[\alpha]_D^{14°} - 23.7°$ (65.0 mg. in 2 c.c. aqueous solution, $l = 2$ dm., $\alpha = -1.54°$). It was dihydrate, but not completely dehydrated by heating at 110° over P_2O_5 in vacuum (weight loss, 4.63%). When heated over its melting point in ordinary pressure, it solidified again after foaming, being completely dehydrated to the anhydrous form which melted towards 180° with decomposition. (Found: N, 4.61; H_2O, 5.79. Calc. for $C_6H_{12}O_7 \cdot C_{23}H_{26}O_4N_2 \cdot 2H_2O$: N, 4.47; H_2O, 5.75%.)

Reduction of *l*-Talonic Lactone into *l*-Talose. *l*-Talonic lactone (1.6 g.) was dissolved in distilled water (16 c.c.) and cooled to −2° in the freezing mixture. Sodium amalgam (38 g.) prepared from pure mercury in a porcelain mortar was added at a time with vigorous mechanical stirring, while the solution was kept constantly grey to congo red by neutralizing with 20 percent sulphuric acid drop by drop. In order to see the acidity all the time, we used fibres of congo red paper which were well washed and added in the flask at a white background at the beginning. The stirring was continued until the solution showed the reducing power corresponding to about 5 percent glucose solution against Fehling's solution, while the temperature was gradually raised to +6°. The reduction was then ceased, it took about 25 minutes and the amalgam was almost consumed. It was then separated from mercury, filtered over active carbon and neutralized with dilute sulphuric acid to become acid to litmus, but not acid to congo red. It was concentrated until sodium sulphate separated out, acidified with 20 percent sulphuric acid to become distinctly blue to congo red and gradually added with about eight volumes of absolute ethyl alcohol with stirring. It was filtered from sodium sulphate, which was digested with small volume of water on the water bath and precipitated again with absolute alcohol. The united alcoholic solution was concentrated over freshly precipitated barium carbonate in vacuum after diluted with water. It was then heated on the water bath for an hour with the excess of fresh barium carbonate. After the solution became neutral to litmus, it was filtered over active carbon and concentrated to a thin syrup, to which ten volumes of methyl alcohol were gradually added, digested in a mortar and filtered from precipitated barium *l*-talonate. The precipitate was dissolved in small volume of water and treated again as above with methyl alcohol. Thus, unchanged lactone was recovered as barium salt (about 0.35 g.). The united methyl alcoholic solution was concentrated to a thin syrup in vacuum. After it was precipitated again with methyl alcohol, the filtrate was concentrated to a syrup in vacuum. This syrup was then dissolved in absolute ethyl alcohol, filtered after standing for a while and concentrated again to a thick syrup. Thus, crude *l*-talose syrup (about 1.3 g.) was obtained.

***l*-Talose-*o*-nitrophenylhydrazone.** The *l*-talose syrup (1.3 g.) was converted into its *o*-nitrophenylhydrazone by heating it with *o*-nitrophenylhydrazine in methyl alcohol exactly after Bosshard's method for the *d*-isomer. Yield 1.4 g., corresponding to 46

percent of the theory when calculated from *l*-talonic lactone taken in the reduction. Recrystallized from absolute ethyl alcohol. Orange leaflets, melting at 148–149° with $[\alpha]_D^{14°} - 88°$ (17.1 mg. in 10 c.c. methyl alcohol solution, $l = 2$ dm., $\alpha = -0.30°$). (Found: N, 13.47. Calc. for $C_{12}H_{17}O_7N_3$: N, 13.33%.)

l-Talose from its o-Nitrophenylhydrazone. One gram of the *o*-nitrophenylhydrazone was heated on the water bath for an hour with 0.65 g. of benzaldehyde and 0.15 g. of benzoic acid in 40 c.c. of distilled water. It was then filtered from separated red voluminous precipitate of benzaldehyde-*o*-nitrophenylhydrazone and the filtrate was extracted several times with ether. When the aqueous solution was concentrated in vacuum, *l*-talose was obtained in a colourless syrup with sweet taste. Though we have left the syrup in a vacuum desiccator for a month and endeavoured to crystallize it, it has not yet been crystallized.

The Equilibrium Rotation of l-Talose. *l*-Talose-*o*-nitrophenylhydrazone (0.1532 g.) was decomposed with benzaldehyde in 6 c.c. of distilled water and treated as above. This *l*-talose solution was exactly diluted to 10 c.c. With this solution the rotation was directly measured and the specific rotation was calculated assuming that *l*-talose was formed quantitatively. The results were $[\alpha]_D^{14°} - 18.6°$ ($c = 0.809$ in water, $l = 1$ dm., $\alpha = -0.15°$, an hour after decomposition) and $[\alpha]_D^{14°} - 19.8°$ ($\alpha = -0.16°$, after ten days).

Summary.

(1) *l*-Talose is formed by the reduction of *l*-talonic lactone obtained from *l*-galactonic acid by means of epimerisation. It is a colourless syrup with sweet taste having a specific rotation of $-19.8°$ at 14°.

(2) *l*-Talonic acid (m.p. 137–138°, $[\alpha]_D^{15°} - 18.2°$) and *l*-talonic lactone (m.p. 133–134.5°, $[\alpha]_D^{17°} + 34.4°$) are obtained.

(3) Brucine salt of *l*-talonic acid (m.p. 139–140°, $[\alpha]_D^{14°} - 23.7°$) is suited for the identification of the acid. The amide (m.p. 119–120.5°, $[\alpha]_D^{18°} + 13.3°$) and the phenylhydrazide (m.p. 161–162°, $[\alpha]_D^{13°} + 26.0°$) are also obtained.

(4) *l*-Galactonic acid is conveniently prepared from citrus pectic acid.

In conclusion, the authors wish to express their hearty thanks to the Department of Education for a special grant for the research work.

Chemical Institute, Faculty of Science,
Imperial University of Tokyo.

The Oxidation of Methane.

By Haruki FUJIMOTO.

(Received January 20, 1938.)

The isolation of the oxygenated compound formed by the direct combination of methane with oxygen is very important not only from the viewpoint of the theory of hydrocarbon combustion but also for the utilization of natural gas.

H. L. Callendar[1] has conducted an experiment by passing hexane-air mixture through a heated tube, and identified a large number of products formed, such as aldehydes, acids, unsaturated hydrocarbons, tars and carbon in addition to CO_2 and H_2O, but no trace of hydroxy compound could be isolated. It woud, therefore, appear more likely that the combustion of the hydrocarbon in air begins with the formation of peroxides by the direct incorporation of the oxygen molecule in the hydrocarbon molecule.

Although according to the view of W. A. Bone, the hydroxylation theory is correct, all efforts to isolate the corresponding alcohol from the initial products of the slow interaction of paraffins with oxygen have been unsuccessful, apparently because under ordinary conditions the further oxidation of such an alcohol to the dihydroxy stage occurs too rapidly. And recently S. G. Hill and W. A. Bone[2] have reinvestigated the slow combustion of ethane showing that the initial product is not a peroxide but either alcohol or some less oxygenated body. Also D. M. Newitt and A. E. Haffner[3] have succeeded in obtaining substantial quantities of methyl alcohol by the direct interaction of oxygen and methane at a temperature of 340° and pressures of about 100 atmospheres. Thus, it was confirmed that slow oxidation of methane proceeds throughout in accordance with the hydroxylation theory.

Although there is considerable agreement that the main course of the oxidation of hydrocarbon proceeds in accordance with the hydroxylation theory, there has been some controversy as to whether the initial product is a hydroxylated molecule or peroxide. P. Mondain-Monval and B. Quanquin[4] have reported the very interesting fact that an air mixture

(1) *Engineering*, **123** (1927), 147, 182, 210.
(2) *Proc. Roy. Soc.* (London), A, **129** (1930), 434.
(3) *Ibid.*, A, **134** (1932), 591.
(4) *Compt. rend.*, **191** (1930), 299.

of hydrocarbon such as pentane or hexane, by passing through a tube heated to 300°C., was converted into aldehyde, CO_2 and an oily substance from which a peculiar substance was isolated which is very similar in chemical nature to peroxide CH_3OOH prepared by Rieche and Hitz by the interaction of H_2O_2 and dimethylsulphate in presence of potash.

In the investigations made heretofore, heat energy was applied for the activation of reacting substances, and in application of heat energy might give rise to some confusion in the theoretical consideration of hydrocarbon oxidation.

The present author, therefore, has studied the oxidation of methane by oxygen under influence of silent discharge, since the action of electric discharge can be controlled so as to obtain a definite initial compound in a pure state.

I. **Methane.** The sample used in this experiment is a natural gas from the Sinbara coal district, which shows after being mixed with oxygen the following compositions.

CH_4	H_2	C_nH_m	CO_2	CO	N_2	O_2
63.8	0.0	1.2	0.0	0.0	0.0	35.0

The gas was passed between two electrodes 4 mm. apart in two ozonizer discharges of 90 mm. diameter and 500 mm. long shown in Fig. 1.

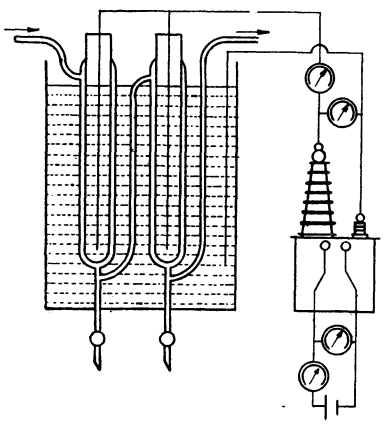


Fig. 1.

The rate of gas flow was about 30 litres per hour, and a current of 60 milliamperes at about 13000 volts was passed between the electrodes.

Methane and oxygen react violently with violent brushy sparks, and from 584 litres (N.T.P.) of the mixed gas there were formed 240 g. of liquid and 412 litres of gaseous substances. From the composition of the gases produced, as shown below, it was judged that the reaction took place in the tube.

CO_2	C_nH_m	O_2	H_2	CO	CH_4	N_2
3.4	0.8	2.06	3.9	7.4	61.5	2.5

120 l. (N.T.P.) CH_4 and 120 l. O_2 are transformed into 9.9 l. CO_2, 16.2 l. CO, 30.4 l. H_2 and 240 g. of a liquid; in other words, when methane was oxidised 21.7% of the product was carbon dioxide and carbon monoxide, and the remainder (78.3%) was a liquid. The liquid is colourless,

d = 1.1, n = 1.38, and was assumed to be a peroxide; it is unstable when heated, decomposes gradually on standing at ordinary temperature, has a remarkable oxidising effect on acidic potassium iodide solution and hydroquinone, and contains about 9% of active oxygen. When 240 g. of the liquid was heated on the water bath until no more gas evolved, 20 litres of a gas and 235 g. of liquid residue were formed. This gas consists of 96% H_2, 0.6% CO_2 and 1.0% CH_4. The residual liquid was fractionated and the density of each fraction was determined; the results are shown in Fig. 2. The fraction with b.p. 28–40°C. is supposed to be mainly methyl formate from its odour, boiling point and density, and its content was estimated to be 75% from methoxy value by Hewett's method and its ester value. The fraction with b.p. 60–70°C. is supposed to be methyl alcohol from its density. The fraction 98–107°C. is composed of 50% of formic acid, 7% of formaldehyde and the remainder is methyl alcohol and water. From the above results, the composition of the decomposition product is represented in mol percent as follows:

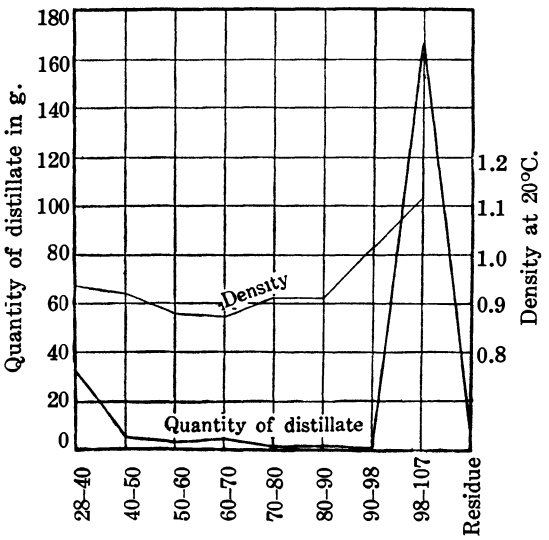


Fig. 2.

CO_2	CO	H_2	HCHO	HCOOH	$HCOOCH_3$	H_2O
8.4	13.5	41.3	7.3	33.6	14.2	74.0

In order to isolate this peroxide, the reaction product from methane and oxygen was neutralized with $MgCO_3$ under cooling with ice water and then extracted with ether. On evaporating the solvent under reduced pressure, there remained a viscous, oily residue; when cooled with ethyl alcohol brine solution to about −60°C., white crystals were deposited, filtered in a cold state and dried quickly by pressing with filter paper. The yield was 15% of the liquid product.

It melts at 62°C., and the results of elementary analysis and of molecular weight determination in benzene solution agree with those of dioxymethyl peroxide (Found: C, 25.47; H, 6.50; M.W., 108. Calc. for $C_2H_6O_4$: C, 25.53; H, 6.38%; M.W., 94; active oxygen, 17.0%). It decomposes ex-

plosively on heating, but can be kept without decomposition for a month at ordinary temperature, and shows not only oxidising action to potassium iodide solution and hydroquinone and titanium sulphate solution but reducing action to indigo solution. The active oxygen content was estimated to be 15.1%. The aqueous solution of the peroxide decomposes gradually on standing, and the reaction was accelerated by the presence of caustic alkali and also of metals such as Fe, Cu, Zn, Ni and Pt but not Al and Cr. The decomposition products are shown in Table 1.

Table 1. Decomposition products in weight percentage to the peroxide.

Decomposition products	By heating	By adding NaOH	By contact with Zn	By contact with Pt-black
HCOOH	80.5	95.0	26.6	30.2
HCHO	9.3	0.0	45.7	36.3
CH_3OH	0.9	0.9	6.8	1.0
$HCOOCH_3$	0.6	0.0	1.3	10.0

The chemical properties and physical character are very like those of dioxymethyl peroxide isolated by Wieland and Wingler[5] from the reaction of formaldehyde and hydrogen peroxide in an alkaline solution.

The chemical reaction of the compound will be explained easily by accepting the dioxy-methyl-peroxide formula for the peroxide but not methyl hydroperoxide CH_3OOH:

(1) The decomposition of the substance in aqueous solution described above is represented in the following scheme:

$$HOCH_2OOCH_2OH \rightarrow \begin{cases} HCOOH + H_2 \\ 2HCHO + H_2O_2 \\ HCOOCH_3 + H_2O_2 \end{cases}$$

(2) When the peroxide reacts with gaseous ammonia, a crystalline compound of explosive nature was formed, which agrees in analytical results and chemical character with hexamethylenetriperoxidediamine described by Baeyer and Villigar[6] (Found: C, 34.5; H, 6.0; active oxygen, 23.35. Calc. for $C_6H_{12}O_6N_2$: C, 34.6; H, 5.8; active oxygen, 23.06%).

$$3\,HOCH_2OOCH_2OH + 2NH_3 = \begin{matrix} CH_2OOCH_2 \\ N-CH_2OOCH_2-N \\ CH_2OOCH_2 \end{matrix} + 6H_2O$$

(5) *Ann.*, **431** (1923), 301.
(6) *Ber.*, **33** (1900), 2479.

II. **Ethane.** Ethane prepared from ethyl magnesium bromide and water, was mixed with oxygen in the following composition:

O_2	C_nH_m	C_2H_6	H_2
34.6	0.8	53.1	11.6

407 litres (N.T.P.) of the mixed gas were passed at a rate of 30 litres per hour into the reaction tube and produced 300 g. of the liquid product and 213 litres (N.T.P.) of gas which has the following composition:

CO_2	O_2	C_nH_m	CO	H_2	CH_4	C_2H_6	N_2
3.0	3.7	4.1	8.0	14.2	6.3	34.5	26.1

Hence, for the oxidation of ethane, conducted under conditions similar to those in the experiment with methane, it was estimated that 3 l. CO_2, 5 l. C_nH_m, 17 l. CO, 30 l. H_2, 14 l. CH_4 and 300 g. of the liquid product were yielded from 142 l. C_2H_6 and 133 l. O_2. The liquid product was supposed from its chemical behaviours to be composed of dioxyethyl peroxide $HO-\overset{CH_3}{\overset{|}{C}}H-O-O-\overset{CH_3}{\overset{|}{C}}H-OH$,[7] but it could not be isolated in a pure state owing to the difficulty of distillation at low pressure.

300 g. of the liquid reaction product was decomposed by heating on the water bath into 1.1 l. CO_2, 0.1 l. CO, 0.41 l. CH_4, 16.14 l. H_2 and 276 g. of liquid residue. The residue was fractionated by distillation into 10° fractions. Each fraction was examined for density and content of acid, aldehyde and ester; the results are shown in Fig. 3.

The first fraction (b.p. to 30°C.) contains ester and acetaldehyde, and the latter gives semicarbazone (m.p. 163°) and dimethon (m.p. 140°). The fraction 50–60°C. consists mainly of ester which is considered to be $HCOOC_2H_5$, yielding by hydrolysis 91 percent of the theoretical amount of formic acid and a trace of acetic acid. The fraction 70–80°C. contains ethyl alcohol as is evident from its density. The fraction 100–110°C. contains mostly water, and some quantity of formic acid and acetic acid in the proportion of about 7 : 2, and also formaldehyde (melting point of dimethon 188.5°C.). The last fraction is composed of ester.

It was concluded that dioxyethyl peroxide is transformed by thermal decomposition into the following substances:

(7) Rieche, "Alkylperoxyd und Ozonid," S. 53, (1931).

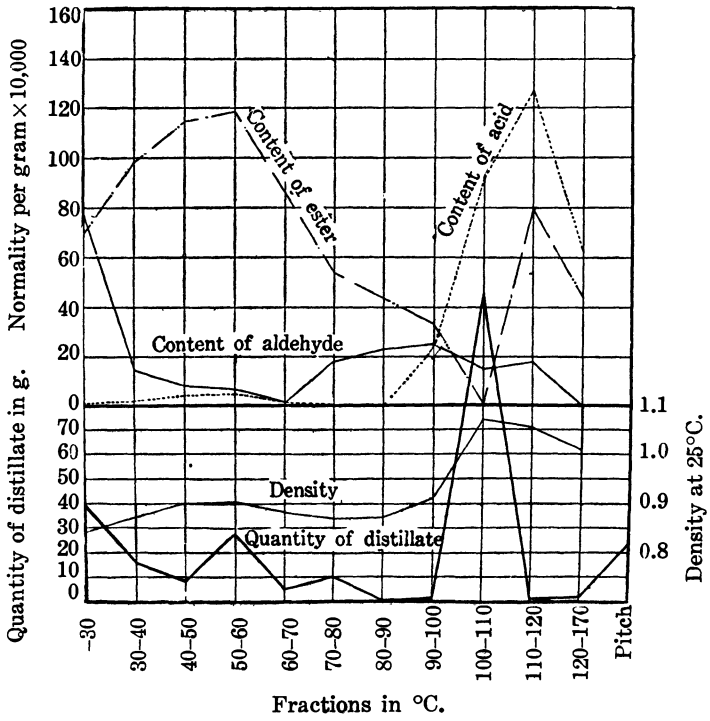


Fig. 3.

	(mol %)		(mol %)
CO_2	2.9	HCOOH	13.4
CO	12.0	CH_3COOH	4.3
H_2	32.5	Ester (mainly $HCOOC_2H_5$)	15.7
HCHO	3.1	H_2O	59.6
CH_3CHO	5.8		

These reaction products are very similar in proportion to those of oxidation of CH_3CHO by H_2O_2.[8]

Among these substances, formaldehyde and acetaldehyde were understood to be produced together with methylhydroperoxide by the disruption both of C–C and O–O linkings in the peroxide molecule:

$$HO-\underset{\displaystyle CH_3}{\underset{|}{CH}}-O-O-\underset{\displaystyle CH_3}{\underset{|}{CH}}-OH \rightarrow HCHO+CH_3CHO+CH_3OOH$$

The peroxide thus liberated, gives rise to HCOOH and HCHO as reported by Rieche and Hitz.[9] Formic acid ethyl ester is supposed to

(8) S. Bezzi, *Chem. Abstracts*, **27** (1933), 4773.
(9) *Ber.*, **62** (1929), 2458.

be formed by direct decomposition of the peroxide but not by Cannizzaro's reaction of the aldehydes:

$$\begin{matrix} HO-CH-O-O-CH-OH \\ \quad | \qquad\quad | \\ \quad CH_3 \qquad CH_3 \end{matrix} \rightarrow HCOOC_2H_5+CH_3OOH$$

III. **Butane.** By the interaction of butane and oxygen under the influence of silent discharge, dioxybutyl peroxide was formed and then, by distillation, isolated in a pure state. Its physical properties and analytical results are as follows: b.p. 55–60° (2 mm.); d_4^{25} 0.9373; n_D^{25} 1.4176; C, 53.84; H, 10.32; M.W., 138; active oxygen, 10.2 ($C_8H_{18}O_4$ requires C, 53.89; H, 10.18; M.W., 178; active oxygen, 9.0%).

IV. **Ethylene.** The experimental results shown in the oxidation of ethane, were explained by assuming that oxygen will attack the C–H bond of the molecule but not the C–C linking, and ethylene was then studied to investigate this assumption.

Ethylene gas was prepared by the dehydration of ethyl alcohol with sulphuric acid and mixed with oxygen in the following proportions:

CO_2	C_nH_m	O_2	CO	H_2	C_nH_{2n+2}	(*n*)	N_2
0.1	53.2	33.8	0.2	0.7	3.8	(2.7)	8.3

114 litres (N.T.P.) of the mixed gas were passed at the rate of 15 litres per hour into the reaction tube, and 59 g. of liquid reaction product and 66.7 litres of gas of the following composition resulted:

CO_2	C_nH_m	O_2	CO	H_2	C_nH_{2n+2}	(*n*)	N_2
4.4	43.1	12.2	12.2	7.8	4.8	(2.6)	15.5

From these data it appears that 31.8 l. (N.T.P.) ethylene by oxidation with 30.4 l. oxygen gave 2.8 l. CO_2, 7.9 l. CO, 4.4 l. H_2, and 59 g. of a peroxide. 246 g. of the impure peroxide (d_4^{25} 1.064, active oxygen 3.8%) yield by heating, 237 g. of liquid residue and gas of the composition 6.11 l. (N.T.P.) H_2, 0.2 l. CO_2, 0.04 l. CO, 0.25 l. C_nH_{2n+2}. The residue was fractionated and the distillates were examined for density and composition with the results shown in Fig. 4.

The fraction 40°C. consists of acetaldehyde (semicarbazone m.p. 163°C. and dimethon m.p. 140°C.) and ester. The fraction 50–60°C. consists mainly of $HCOOC_2H_5$, since by hydrolysis 94% formic acid was formed together with a trace of acetic acid. The fraction 100–110°C. is largely water with some formic acid and acetic acid in the proportion 7: 2.3, and formaldehyde (dimethon m.p. 189°C.).

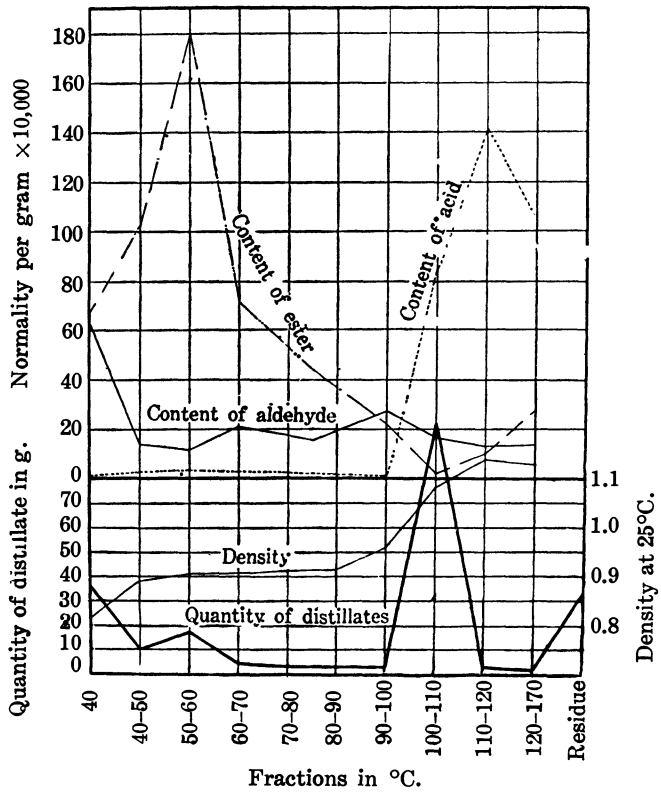


Fig. 4.

The peroxide obtained in an impure state from ethylene and oxygen will decompose by heating into the compounds which are shown below in comparison with those from ethane (Table 2). Since the results show slight difference in proportion of hydrogen and CO, it was concluded that the same dioxymethyl peroxide is formed both from ethane and ethylene: oxygen, as we expected, will combine with the C–H linking of the molecule.

$$2\,C_2H_4+2O_2 = HO-\underset{\displaystyle CH_3}{\underset{|}{CH}}-O-O-\underset{\displaystyle CH_3}{\underset{|}{CH}}-OH$$

$$2\,C_2H_6+2O_2 = HO-\underset{\displaystyle CH_3}{\underset{|}{CH}}-O-O-\underset{\displaystyle CH_3}{\underset{|}{CH}}-OH + H_2$$

The peroxide which was predicated by P. Mondain-Monval and B. Quanquin[4] as the first oxidation product from hydrocarbon by air, was actually isolated in some abundance by the author by the interaction of methane and oxygen under the influence of silent discharge, and the

Table 2.

Decomposition products	From ethylene	From ethane
CO_2	8.8%	2.9%
CO	24.8	12.0
H_2	17.0	32.5
HCHO	3.7	3.1
CH_3CHO	4.2	5.8
HCOOH	10.9	13.4
CH_3COOH	3.8	4.3
$HCOOC_2H_5$	14.7	15.7
H_2O	50.6	59.6

molecular structure was found to be $HOCH_2OOCH_2OH$ by a precise investigation of its physical and chemical properties.

Ethane, ethylene and butane gave the peroxide of chemical structure HOCH(R)–O–O–CHOH(R) by similar treatment in the electrical discharge of a mixture of hydrocarbon and oxygen, and the peroxides decomposed spontaneously into alcohol, aldehyde, acid and ester.

This fact emphasizes that the initial stage of the reaction is the excitation of the C–H bond of hydrocarbon but not of oxygen, since when an activated oxygen is present with an ethylenic compound, as in the case of ethylene and oxygen, a peroxide of another type should be formed, as postulated by S. Tanaka:[10]

$$CH_2{=}CH_2 + RCO_3H \rightarrow \underset{\underset{H}{|}}{H_2C}\!-\!\underset{\underset{O-O-COR}{|}}{CH_2} \rightarrow H_2C\!\!\begin{array}{c}\diagdown\\ \\ \diagup\end{array}\!\!CH_2 + RCO_2H \quad (O)$$

Theoretically, however, as to the mechanism of the formation of the peroxide from methane and oxygen, it may be considered that the initial step involves an excitation of either methane or oxygen molecules in the system.

According to the investigation by Sponer[11] methane exhibits absorption spectra of fundamental frequencies of 3022 cm.$^{-1}$ and 1304 cm.$^{-1}$ due to the oscillations of bonds shown in Fig. 5, and the electronic affinity of

(10) *J. Chem. Soc. Japan*, **53** (1932), 668.
(11) H. Sponer, "Molekülspektren," **I**, 82.

the oxygen molecule was assumed by Bradburg[12] and by Weiss[13] to be 1.6 volts and 2.7 volts respectively. When silent discharge operated on the mixture of methane and oxygen, the primary action might be dissociation of the electron pair forming the C–H bond of methane molecule, giving rise to partial ionisation. The activated molecule will then traverse the tube, picking up oxygen, forming a compound as a sort of dative peroxide of Milas[14]:

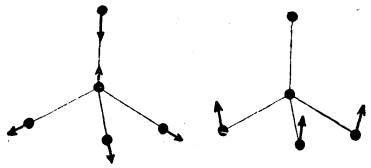
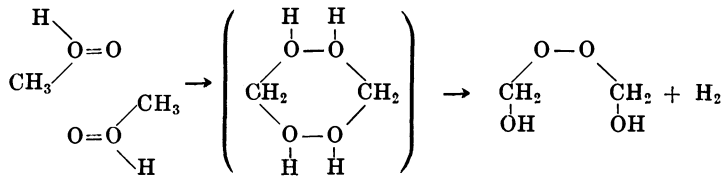
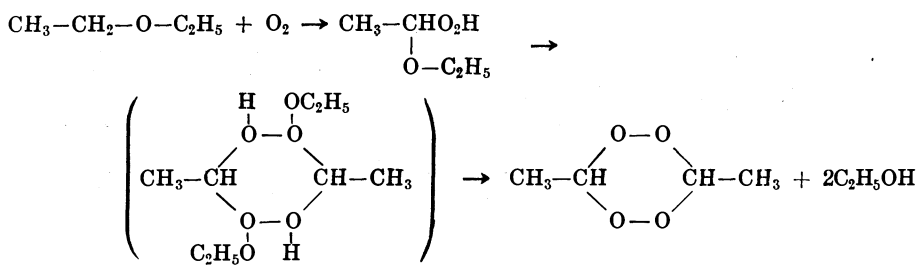


Fig. 5.

$$CH_3H' + O_2 = CH_3-\underset{\underset{O}{\|}}{OH}$$

The dative peroxide being of a polar nature will then transform by the halochromic action into the stabler peroxide form as explained in a manner similar to the autoxidation of diethyl-ether.[15]





Since Berthelot's classical work on the silent discharge in methane gas appeared, many investigators have used the silent discharge for transformation of the hydrocarbons into other substances, and also for the interaction of hydrocarbon and oxygen.

---

(12) *Phys. Rev.*, **44** (1933), 883.
(13) *Trans. Faraday Soc.*, **31** (1935), 966.
(14) *J. Phys. Chem.*, **38** (1934), 411.
(15) Rieche, "Alkylperoxyd und Ozonid," S. 74, (1931).

The most striking characteristic of the action of silent discharge on paraffin or on a mixture of paraffin and oxygen is the attack on the linkage of C–H of hydrocarbon molecule, and the result is similar in some respects to that which follows applying of heat energy.

In conclusion, the author wishes to express his sincere thanks to Rear Admiral Viscount M. Kawase, Rear Admiral R. Kinashi and Rear Admiral S. Nomura, the former and present Chiefs of the Scientific Research and Experimental Branch, for their kindness of enabling him to take part in this work, and also to Prof. S. Komatsu of Kyoto Imperial University whose advice and encouragement was valuable, and also to Mr. M. Mihara and Mr. T. Iwamoto, whose kind assistance enabled him to complete the experiment.

Über die chemische Natur der Taka-Amylase. II. Über das Molekulargewicht der Taka-Amylase.

Von Shiro AKABORI und Katuhiko KASIMOTO.

(Eingegangen am 31. Janur 1938.)

In der ersten Mitteilung[1] haben S. Akabori und K. Okahara in Bezug auf die chemische Natur der Taka-Amylase auf Grund der Tatsache, dass sie durch Proteinasen nicht spaltbar ist und durch Kollodiummembranen zu diffundieren vermag, den Schluss gezogen, dass sie weder ein Protein noch ein Polypeptid sein dürfte.

Für die weitere Entwicklung der Reinigungsmethode war es zunächst wünschenswert zu wissen, wie gross das Molekül der Taka-Amylase ist.

Für die Molekulargewichtsbestimmung kann man selbstverständlich bei den gewöhnlichen Enzympräparaten die kryoskopische Methode nicht anwenden.

Eine einfache, für nicht ganz reine Enzympräparate anwendbare Methode ist die Berechnung aus dem Diffusionskoeffizienten nach der Gleichung $D\sqrt{M} = \text{Konst.}$ Die Gültigkeit dieser Regel für mehrere organische Substanzen ist von v. Euler[2] und Oeholm[3] festgestellt

(1) Akabori und Okahara, dieses Bulletin, **12** (1937), 55.
(2) v. Euler, *Ann.*, **63** (1897), 273.
(3) Oeholm, *Z. physiol. Chem.*, **70** (1910), 378.

worden. Mit dieser Methode erhielten v. Euler und Kullberg[4] für Saccharase das Molekulargewicht 20,000.

Die Diffusionsgeschwindigkeit darf natürlich nicht im Zusammenhang mit der stofflichen Menge des Enzympräparats, sondern muss im Zusammenhang mit der Enzymwirkung verfolgt werden. Für diesen Zweck ist es unbedingt notwendig, die relative Enzymmenge, d.h. die Enzym-Einheiten möglichst genau zu bestimmen. Die Amylase-Einheiten werden gewöhnlich durch die Reaktionsgeschwindigkeitskonstanten bei bestimmten Verdauungsbedingungen gegeben, unter der Annahme, dass die Verdauung in monomolekularer Reaktion verläuft. Unseren Experimenten nach ist jedoch diese Annahme nur unter beschränkten Verdauungsbedingungen gültig. Wir haben deshalb zuerst versucht, die Bedingungen aufzufinden, bei denen die Maltosebildung in monomolekularer Reaktion verläuft und die Reaktionsgeschwindigkeitskonstante genau der Enzymmenge proportional ist. Für die Bestimmung der Enzym-Einheiten wandten wir die Methode von Willstätter und Schudel[5] unter den Verdauungsbedingungen von Willstätter, Waldschmidt-Leitz und Hesse[6] an. Der zeitliche Verlauf der Maltosebildung mit wechselnden Mengen Takadiastase ist aus Abb. 1 ersichtlich.

Zur Berechnung der Reaktionsgeschwindigkeitskonstante k dient die Gleichung

$$k = \frac{1}{t} \log \frac{a}{a-x}$$

worin t = die Versuchszeit in Minuten, a = die maximal entstehende Menge der Maltose und x = die zur Zeit t gebildete Maltosemenge.

Abb. 2 zeigt die Änderung von k in Abhängigkeit von Enzymmenge und Verdauungszeit.

Man ersieht aus Abb. 2, dass die Geschwindigkeitskonstante unter den Verdauungsbedingungen von Willstätter, Waldschmidt-Leitz und Hesse bei kleineren Mengen Enzym (weniger als A. E. = 0.016) und kürzeren Zeiten (5 bis 10 Minuten) der Enzymmenge proportional ist (Abb. 3).

Die Diffusionsgeschwindigkeit konnten wir in einfacher Weise mit Hilfe des Northrop- und Ansonschen Immersionsfilters[7] messen. Die Methode soll hier kurz erwähnt werden. Der angewandte Apparat wird in Abb. 4 wiedergegeben. L_1: konzentrierte Lösung. L_2: verdünnte

(4) v. Euler und Kullberg, *Z. physiol. Chem.*, **73** (1911), 335.
(5) Willstätter und Schudel, *Ber.*, **51** (1918), 780.
(6) Willstätter, Waldschmidt-Leitz und Hesse, *Z. physiol. Chem.*, **126** (1923), 143.
(7) Northrop und Anson, *J. Gen. Physiol.*, **12** (1926), 543.

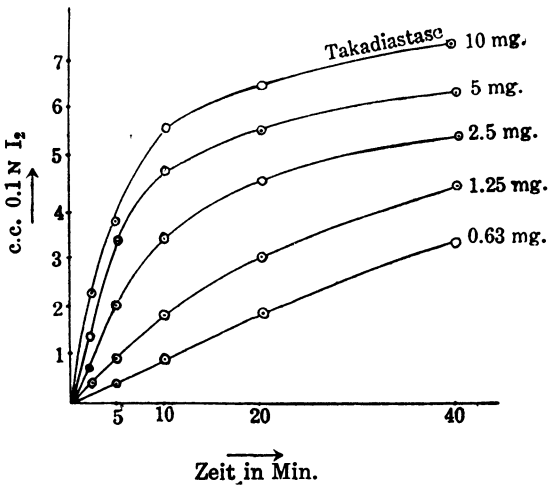


Abb. 1.

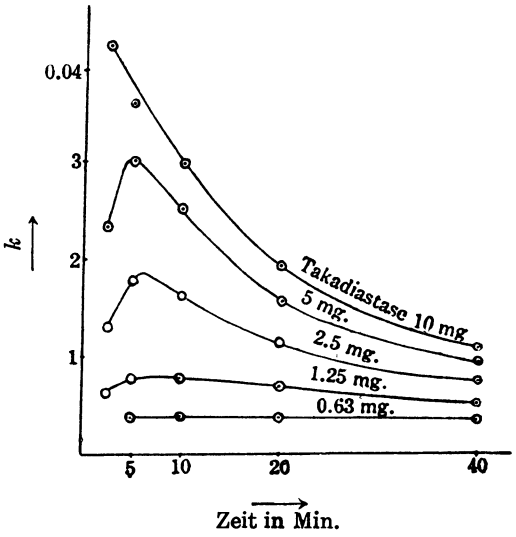


Abb. 2.

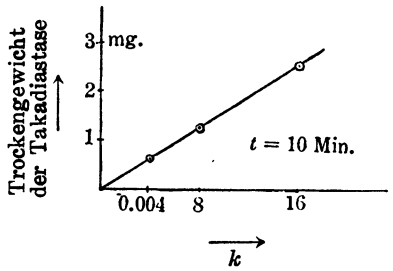


Abb. 3.

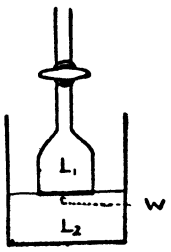


Abb. 4.

Lösung. W: Diffusionswand aus Glasfiltermasse. Wenn man einen ganz kleinen Bruchteil der gelösten Substanz durch die Diffusionswand diffundieren lässt, ist die Diffusionskoeffizient D durch folgende Formel gegeben:

$$D = \frac{hm}{Qt(C_1 - C_2)} \qquad (1),$$

wo m Menge der gelösten Substanz, die in der Zeit t von der Lösung L_1 in die Lösung L_2 diffundiert, h Dicke der Diffusionswand, Q Querschnitt der Diffusionswand, C_1 Konzentration der Lösung L_1, C_2 Konzentration der Lösung L_2, t Diffusionsdauer bedeutet.

Wenn man für L_2 reines Lösungsmittel anwendet, wird Gl. (1) wie folgt:

$$D = \frac{hm}{QtC_1} = K\frac{m}{tC_1} = KF \qquad (2),$$

wo

$$F = \frac{m}{tC_1} \qquad (3).$$

Wird F für eine bekannte und eine unbekannte Substanz gemessen, so kann das Molekulargewicht (M_x) der letzteren, auf dem Grund der Gleichung $D\sqrt{M} = \text{Konst.}$, nach folgender Gleichung (4) berechnet werden:

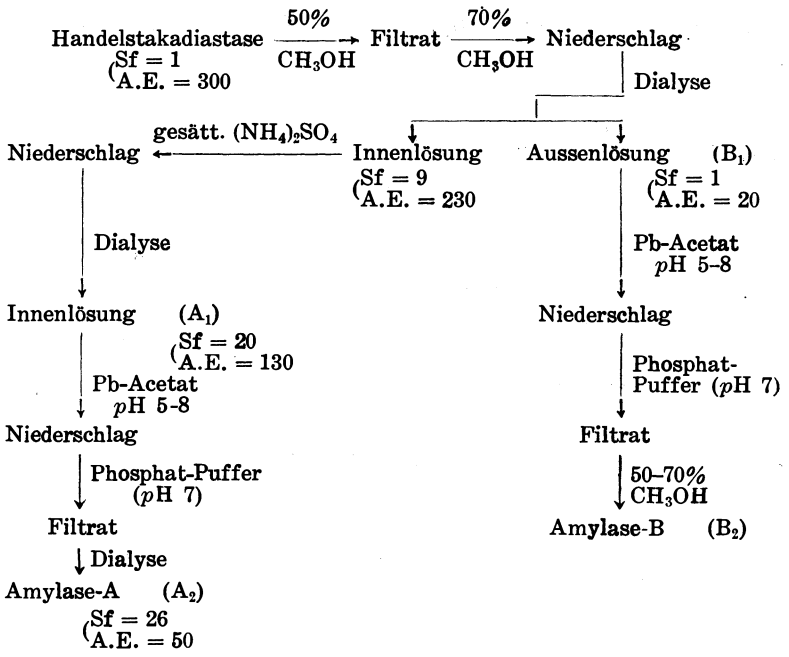
$$M_x = M\left(\frac{F}{F_x}\right)^2 \qquad (4).$$

Als Standardsubstanz nahmen wir *d*-Glukose, da deren Menge jodometrisch schnell bestimmt werden kann, und prüften die Genauigkeit der Methode bei Maltose und Methylstrychninbetain mit einem Immersionsfilter von 50 c.c. Inhalt bei 4°. (Herr Prof. M. Kotake hatte die grosse Freundlichkeit, uns Methylstrychninbetain zur Verfügung zu stellen, wofür wir zu besten Dank verpflichtet sind.)

Substanz	F	M(Ber.)	M(Gef.)
Glukose	0.0730	180	—
Maltose	0.0530	342	340
Methylstrychninbetain	0.0495	356	390

Man sieht also, dass die Diffusionsmethode mit befriedigender Genauigkeit anwendbar ist.

Reinigung der Taka-Amylase. Wie in der ersten Mitteilung beschrieben wurde, lässt sich der wirksame Bestandteil der Handelstakadiastase nicht durch 50%iges, sondern durch 70%iges Methanol ausfällen und geht bei der Dialyse mit einer Kollodiumhülse teilweise in die Aussenflüssigkeit. Das aus der Innenlösung gewonnene Amylasepräparat bezeichnen wir als Amylase-A und das aus der Aussenlösung gewonnene als Amylase-B. Das Reinigungsverfahren wird im folgenden Schema angegeben:



Die Molekulargewichtsbestimmung bei den Amylasepräparaten A_1, A_2, B_1 und B_2 gibt nach der Diffusionsmethode folgende Resultate:

Amylasepräparate	F	F_G	$(F_G/F)^2$	M
A_1	0.0196	0.0651	11.1	1990
A_2	0.0250	0.0732	8.6	1550
B_1	0.0426	0.0732	3.0	540
B_2	0.0445	0.0732	2.7	490

F_G bedeutet $\frac{m}{C_1 t}$ bei Glukose; s. Gl. (3).

Unseren Resultaten bei dieser Molekulargewichtsbestimmung kann natürlich noch kein grosses Gewicht beigelegt werden. Es ist aber wohl sicher, dass das Taka-Amylase-Molekül viel kleiner als ein gewöhnliches Eiweissmolekül ist. Merkwürdigerweise scheint der Träger der Taka-Amylase, im Gegensatz zum Falle des Flavinenzyms, keine grosse Rolle bei der Enzymwirkung zu spielen, denn bei dem Zusammenbringen der Aussen- und Innenflüssigkeit der Dialyse findet weder Aktivierung noch Hemmung statt.

Versuchsergebnisse. (a) *Diffusion der Glukose.* Anfangskonz. der Lösung 16.11%. $C_1 = 161.1$ mg./c.c.

Exp. Nr.	t	Diffundierte Glukose (mg.)
I	1	11.70
II	1	11.88
III	1	11.70
IV	1	11.97
		Mitt. 11.81

$F = 0.0732$

(b) *Diffusion der Maltose.* Anfangskonz. der Lösung 33.6%. $C_1 = 336$ mg./c.c.

Exp. Nr.	t	Diffundierte Maltose (mg.)
I	1	17.15
II	1	18.52
III	1	18.01
		Mitt. 17.89

$F = 0.0530$

$\left(\frac{F_G}{F}\right)^2 = 1.90$

Mol. Gew.

Gef.: 180 (Glukose) × 1.9 = 342

Ber. für $C_{12}H_{22}O_{11}$: 342

(c) *Diffusion des Methylstrychninbetains.* Die Bestimmung des Methylstrychninbetains wurde durch Messung der Intensität der mit konzentrierter Schwefelsäure und Kaliumbichromat erhaltenen Färbung mit Hilfe eines Kolorimeters ausgeführt.

Exp. Nr.	t	F
I	1	0.050
II	2	0.048
III	2	0.050
IV	1	0.051
V	3	0.048
VI	2	0.051
		Mitt. 0.0497

$\left(\frac{F_G}{F}\right)^2 = 2.2$

Mol. Gew.

Gef.: 390

Ber. für $C_{22}H_{26}N_2O_3$: 366

Ber. für $C_{22}H_{26}N_2O_3 \cdot 4H_2O$: 421

(d) *Amylasepräparat-B.* (i) B_1 im Schema. $C_1 = 0.2064$ A.E./c.c.

Exp. Nr.	t	Diffundierte A.E.
I	1	0.00913
II	1	0.00810
III	1	0.00913
		Mitt. 0.00879

$F = 0.0426$

$\left(\frac{F_G}{F}\right)^2 = 3.0$

Mol. Gew. = 540

(ii) B_2 im Schema. $C_1 = 0.343$ A.E./c.c.

Exp. Nr.	t	Diffundierte A.E.
I	1	0.0158
II	1	0.0131
III	1	0.0165
IV	1	0.0158
		Mitt. 0.0158

$F = 0.0445$

$\left(\frac{F_G}{F}\right)^2 = 2.7$

Mol. Gew. = 490

(e) *Amylasepräparat-A.* (i) A_2 im Schema. $C_1 = 1.558$ A.E./c.c.

Exp. Nr.	t	Diffundierte A.E.
I	1	0.0389
II	1	0.0381
III	1	0.0396
		Mitt. 0.0389

$F = 0.0250$

$\left(\frac{F_G}{F}\right)^2 = 8.6$

Mol. Gew. = 1550

(ii) A_1 im Schema. $C_1 = 0.930$ A.E./c.c.

Exp. Nr.	t	Diffundierte A.E.
I	2	0.0368
II	2	0.0371
III	2	0.0364
		Mitt. 0.0368

$F = 0.0196$

$\left(\frac{F_G}{F}\right)^2 = 11.1$

Mol. Gew. = 1990

Bei dieser Bestimmung haben wir ein anderes Immersionsfilter ($F_G = 0.0651$) benutzt als bei den übrigen Experimenten.

Zum Schluss möchten wir der Taniguchi Kogyo-Shoreikai (der Taniguchi-Gesellschaft zur Förderung der technischen Industrie) für die finanzielle Unterstützung, die diese Versuche ermöglicht hat, unseren herzlichen Dank aussprechen.

Chemisches Institut der Kaiserlichen Universität zu Osaka.

Über den Austausch der Wasserstoffatome zwischen Pyrrol, Indol sowie ihren Methylderivaten und Wasser. III. Austausch der Wasserstoffatome zwischen N-Methylpyrrol und Wasser.[1]

Von Masao KOIZUMI und Toshizo TITANI.

(Eingegangen am 31. Januar 1938.)

Inhaltsübersicht. Die Austauschreaktion der H-Atome zwischen *N*-Methylpyrrol $C_4H_4NCH_3$ und Wasser wurde unter Benutzung verdünnten schweren Wassers bei verschiedenen H-Ionenkonzentrationen untersucht. Dabei wurde gefunden, dass das *N*-Methylpyrrol, das keine ionisierbare (direkt austauschbare) H-Atome enthält, bei 30°C. und innerhalb zehn Stunden keine merkbare Austauschreaktion ausführt, solange die H-Ionenkonzentration im damit geschüttelten Wasser unterhalb 0.001 N (pH = 3) bleibt. Aber sobald die H-Ionenkonzentration im Wasser den letzteren Wert überschreitet, tritt ziemlich plötzlich eine neue Art der Austauschreaktion auf. Bei dieser neuen Reaktion werden alle vier H-Atome im Pyrrolkern des *N*-Methylpyrrols, ähnlich wie bei der „zweiten" Austauschreaktion des unsubstituierten Pyrrols, gegen die des Wasser ausgetauscht, und die Reaktionsgeschwindigkeit wächst stark mit der H-Ionenkonzentration im Wasser. Diese neue Art der Austauschreaktion des *N*-Methylpyrrols kann man unter derselben Annahme wie bei der „zweiten" Austauschreaktion des unsubstituierten Pyrrols, d.h. mit der Salzbildung des *N*-Methylpyrrols und der darauffolgenden tautomerischen Umwandlung des Pyrrolkerns, erklären.

Einleitung. Wir haben bei unserem früheren Versuche gefunden, dass das Pyrrol sein an N gebundenes H-Atom schnell gegen die des damit

(1) I. Mittl., dies Bulletin, **13** (1938), 85; II. Mittl., *ibid.*, **13** (1938), 95.

geschüttelten Wassers austauscht aber keine weiteren H-Atome, solange die H-Ionenkonzentration im letzteren unterhalb 0.01 N (pH = 2) bleibt („erste" Austauschreaktion). Dagegen wenn die H-Ionenkonzentration im Wasser diesen letzteren Wert überschreitet, tritt plötzlich eine neue Art von Austauschreaktion („zweite" Austauschreaktion) auf. Bei dieser neuen „zweiten" Austauschreaktion werden aber alle fünf H-Atome des Pyrrolmoleküls gegen die des Wassers austauschbar und die Reaktionsgeschwindigkeit wächst sehr stark mit der H-Ionenkonzentration im Wasser bis schliesslich die erstere sich fast unmessbar gross erweist. Diese neu gefundene „zweite" Austauschreaktion des Pyrrols haben wir unter der Annahme der Salzbildung des Pyrrols und der tautomerischen Umwandlung des dadurch gebildeten „labilisierten" Pyrrolmoleküls zu deuten versucht. Um nun diese Annahme weiter zu prüfen, haben wir in der vorliegenden Arbeit ähnliche Versuche mit *N*-Methylpyrrol ausgeführt. Diese Verbindung interessiert uns insofern als sie keine leicht ionisierbaren sogenannte „aktive" H-Atome in ihrem Molekül enthält.

Darstellung des Präparates. Das zu diesem Versuch benutzte *N*-Methylpyrrol wurde von Herrn Goto in unserem Laboratorium durch die Einwirkung von Methyljodid auf Pyrrolkalium in ätherischer Lösung dargestellt:

$$C_4H_4NK + CH_3I = C_4H_4NCH_3 + KI.$$

Das Rohprodukt, das zwischen 103 und 120°C. destillierte, wurde wiederholt fraktioniert destilliert und das Destillat, das zwischen 113 und 117°C. abdestillierte, wurde direkt zum Versuch verwendet. Das damit zu reagierende sauere schwere Wasser wurde auf dieselbe Weise wie bei den früheren Versuchen durch die Mischung des verdünnten schweren Wassers mit der HCl-Lösung in gewöhnlichem Wasser bereitet.

Experiment. Die Experimentalmethode war im grossen und ganzen dieselbe wie beim früheren Versuch mit Pyrrol.[1] Aber weil die Menge des zur Verfügung gestellten *N*-Methylpyrrols beschränkt war, arbeiteten wir immer mit einem Drittel des Materials weniger als bei den früheren Versuchen. Es wurden nämlich 1 bis 2 g. von *N*-Methylpyrrol zusammen mit ca. 0.4 g. von neutralem bzw. saurem verdünntem schwerem Wasser in einem zugeschmolzenen Glasrohr bei 30°C. verschiedener Zeitlänge geschüttelt. Dann wurde die Abnahme der Dichte des schweren Wassers schwebemetrisch bestimmt, nachdem es vom *N*-Methylpyrrol abgetrennt und richtig gereinigt worden war, und aus den so erhaltenen Experimentaldaten wurde schliesslich das Austauschäquivalent nk des *N*-Methylpyrrols auf die schon früher angegebene Weise berechnet. Die nachfolgende Tabelle gibt das so gefundene Austauschäquivalent des *N*-Methylpyrrols bei verschiedenen H-Ionenkonzentrationen im damit geschüttelten schweren Wasser wieder.

Tabelle. Austauschäquivalent des *N*-Methylpyrrols bei verschiedenen H-Ionenkonzentrationen.

Versuchs-nr.	Benutzte Lösung	*p*H	Schüttelungs-dauer in Stdn.	Austausch-äquivalent *nk*	Bemerkung
1	neutral	7.00	5	(0.35)	keine merkliche Änderung während des Versuchs.
2	0.00011 N HCl	3.96	5	0.12	
3	0.00105 N HCl	2.98	10	0.18	
4	0.002 N HCl	2.70	45±3	1.41	
5	0.01 N HCl	2.00	1.2	1.03	
6	0.01 N HCl	2.00	12.7	2.92	
7	0.03 N HCl	1.52	5	2.78	
8	0.8 N HCl	0.10	5	2.84	Die Lösung wurde gelb gefärbt.

Dieselben Ergebnisse sind auch zusammen mit denen des unsubstituierten Pyrrols, die wir beim früheren Versuch erhielten, in der nebenstehenden Abb. graphisch dargestellt, wo das gefundene Austauschäquivalent *nk* der beiden Substanzen gegen den *p*H des damit geschüttelten schweren Wassers aufgetragen ist. Die Nummer bei jedem kleinen Kreis zeigt die Schüttelungsdauer in Stdn. Aus dieser Abb. ersieht man ohne weiteres, dass das *N*-Methylpyrrol ebenso wie das unsubstituierte Pyrrol eine stufenweise Austauschreaktion ausführt, wenn die H-Ionenkonzentration im damit geschüttelten Wasser allmählich zunimmt. Solange die H-Ionenkonzentration im Wasser sehr klein und unterhalb 0.001 N (pH = 3.0) bleibt, bleibt auch das Austauschäquivalent *nk* des *N*-Methylpyrrols sehr klein und $nk = 0.12$ bis 0.18 (durchschnittlich 0.15). Daraus kann man wohl schliessen, dass das *N*-Methylpyrrol, das keine ionisierbare (direkt austauschbare) H-Atome in seinem Molekül enthält, unterhalb der eben genannten H-Ionenkonzentration überhaupt keine nennenswerte Austauschreaktion ausführt. Dagegen wenn die H-Ionenkonzentration im Wasser den oben genannten Wert 0.001 N (pH = 3.0) überschreitet, tritt ziemlich plötzlich, ähnlich wie bei der „zweiten" Austauschreaktion des unsubstituierten Pyrrols, eine neue Art von Austauschreaktion auf und das Austauschäquivalent des *N*-Methylpyrrols nimmt schliesslich bis auf 2.78 bis 2.92 (durchschnittlich 2.85) zu. Aber weil dieses Verhalten des *N*-Methylpyrrols sehr ähnlich wie das unsubstituierte Pyrrol bei seiner „zweiten" Austauschreaktion ist, liegt die Annahme sehr nahe, dass bei dieser neuen Austauschreaktion des *N*-Methylpyrrols alle vier H-Atome im Pyrrolkern aktive Rollen spielen, d.h. es sich hier um die „zweite"

Austauschreaktion des *N*-Methylpyrrols handelt, obwohl bei seiner „ersten" Austauschreaktion, wie oben gefunden, keine wirkliche Austauschreaktion stattfindet. Unter dieser Annahme können wir den mittleren Verteilungsquotient k der D-Atome zwischen der CH-Gruppe im

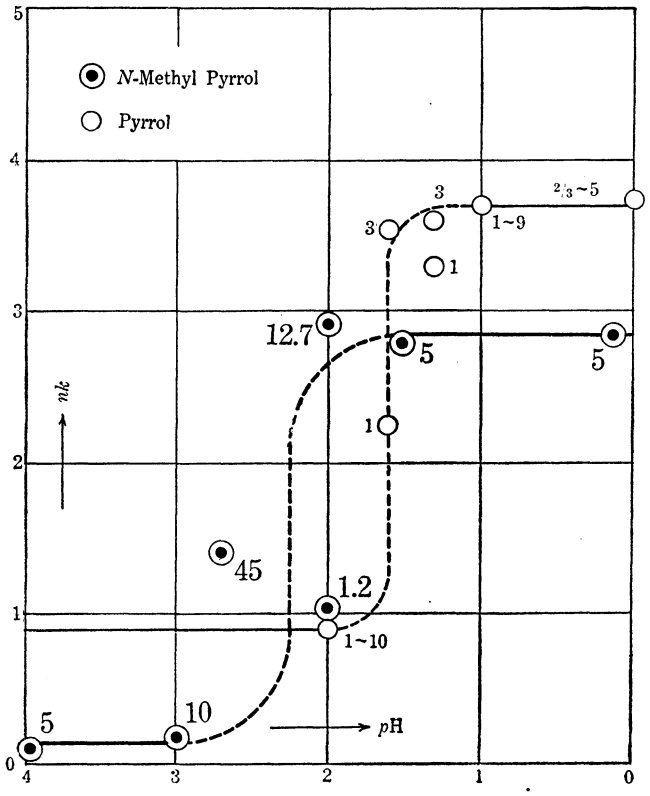


Abb. Abhängigkeit des Austauschäquivalents nk des *N*-Methylpyrrols und Pyrrols auf dem pH des damit geschüttelten Wassers und der Schüttelungsdauer.

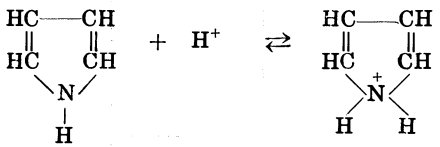
Pyrrolkern des *N*-Methylpyrrols und Wassers wie folgend ausrechnen. Dabei haben wir den kleinen Bruchteil ($nk = 0.15$) des Austauschäquivalents, der bei den kleinen H-Ionenkonzentrationen gefunden wurde, in Rechnung getragen.

$$k(\mathrm{CH/H_2O}) = \frac{\text{Austauschäquivalent}}{\text{Zahl der austauschbaren H-Atome}}$$

$$= \frac{2.85-0.15}{4} = 0.68.$$

Dieser Wert stimmt aber mit dem früher von Pyrrol bei seiner „zweiten" Austauschreaktion gefundenen Wert ($k = 0.70$) sehr gut überein. Dadurch erscheint die oben angegebene Annahme, dass bei der „zweiten" Austauschreaktion des *N*-Methylpyrrols ebenso wie beim unsubstituierten Pyrrol alle vier H-Atome im Pyrrolkern teilnehmen, weiter gesichert zu werden. Wir fanden ferner, wie aus der oben angegebenen Abb. ohne weiteres ersichtlich ist, dass die „zweite" Austauschreaktion des *N*-Methylpyrrols viel leichter d.h. bei kleinerer H-Ionenkonzentration als beim unsubstituierten Pyrrol aufzutreten vermag. Die „zweite" Austauschreaktion der letzteren Verbindung tritt nämlich erst bei 0.01 N (pH = 2.0), dagegen die der ersteren schon bei der zehnmal so kleineren Konzentration d.h. bei 0.001 N (pH = 3.0) deutlich auf. Von diesem Unterschied der Grenzwerte der H-Ionenkonzentration für die beiden Verbindungen wollen wir weiter unten sprechen.

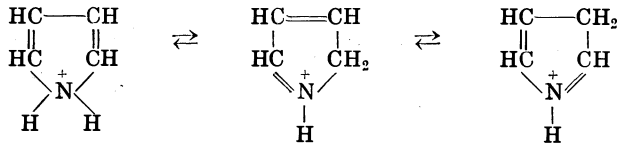
Diskussion. Die „zweite" Austauschreaktion des unsubstituierten Pyrrols wurde von uns dadurch gedeutet, dass zuerst ein Proton (bzw. Deuteron) am N-Atom des Pyrrolmoleküls angelagert und dadurch ein Pyrrolion bzw. ein „labilisiertes" Pyrrolmoleküls gebildet wird:



(1)

„labilisiertes" Molekül

Durch diese Salzbildung wird die Löslichkeit des Pyrrols in die Wasserphase, wo die Hauptreaktion verlaufen muss, um einen gewissen Betrag vergrössert. Aber zugleich werden die H-Atome im Pyrrolkern durch die Reaktion (1) mehr oder weniger gelockert und wegen dieser Leichtbeweglichkeit der H-Atome führt das so gebildete Pyrrolion bzw. „labilisiertes" Pyrrolmolekül eine tautomerische Umwandlung nach dem folgenden Schema aus:

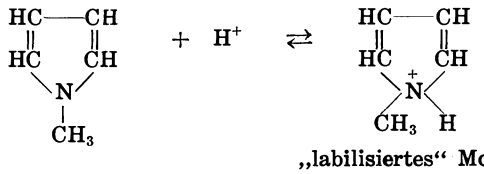


(2)

Durch diese Umwandlungsreaktion des Pyrrolkerns werden aber die H-Atome in demselben eins nach dem anderen gegen die des Wassers ausgetauscht, bis schliesslich alle H-Atome des ersteren durch die des letzteren ersetzt werden. Dabei ist auch denkbar, dass die Umwandlungsreaktion

(2) unter Mitwirkung der H-Ionen katalytisch durchgeführt wird. Auf diese Weise konnten wir das Auftreten der „zweiten" Austauschreaktion des unsubstituierten Pyrrols sowie ihre starke Abhängigkeit auf die H-Ionenkonzentration mindestens qualitativ erklären.

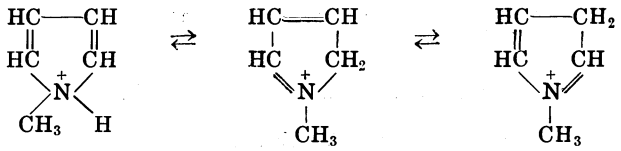
Genau denselben Chemismus können wir aber auch auf die in der vorliegenden Arbeit gefundene neue „zweite" Austauschreaktion des *N*-Methylpyrrols ohne weiteres anwenden. Der erste massgebende Vorgang ist demnach die Salzbildung des *N*-Methylpyrrols, wo die Wertigkeit seines N-Atoms von drei bis auf fünf vermehrt wird.



(3)

„labilisiertes" Molekül

Das so gebildete „labilisiertes" Molekül führt dann, höchstwahrscheinlich unter Mitwirkung der H-Ionen, eine tautomerische Umwandlung aus und dadurch werden die H-Atome im Pyrrolkern eins nach dem anderen gegen die des Wassers ausgetauscht.



(4)

Nach dem oben angegebenen Chemismus der „zweiten" Austauschreaktion ist der massgebende Vorgang die Salzbildungsreaktion ((1) bzw. (3)) des N-Atoms im Pyrrolkern. Aber auf Grund der wohl bekannten Tatsache, dass die Basizität der Aminogruppe durch die Ersetzung ihrer H-Atome mit Alkylradikale stark vergrössert wird, liegt die Annahme sehr nahe, dass die Basizität der Imidogruppe des Pyrrols durch die Ersetzung ihres H-Atoms mit einem Alkylradikal ebenfalls verstärkt wird. Wenn dies wirklich der Fall ist, dann muss das Gleichgewicht der Salzbildung (3) des *N*-Methylpyrrols bei einer bestimmten H-Ionenkonzentration mehr als bei (1) des unsubstituierten Pyrrols nach der rechten Seite hin verschoben sein. Folglich kann die „zweite" Austauschreaktion des *N*-Methylpyrrols leichter d.h. bei kleinerer H-Ionenkonzentration als die des unsubstituierten Pyrrols stattfinden. Diese theoretische Erwartung stimmt aber, wie schon oben gefunden, mit den Experimentalergebnissen sehr gut überein (vgl. Abb.), und dadurch erscheint der oben angegebene Chemismus der „zweiten" Austauschreaktion eine weitere Unterstützung

gefunden zu haben, obwohl dabei auch denkbar wäre, dass die Beweglichkeit der H-Atome im Pyrrolkern durch die Ersetzung des H-Atoms in der Imidogruppe mit dem Methylradikal um einen gewissen Betrag vergrössert werden kann.

Zum Schluss möchten wir der Nippon Gakujutsu-Shinkohkai (der Gesellschaft zur Förderung der japanischen Wissenschaft) sowie der Hattori-Hohkohkai (der Hattori-Stiftung) für ihre finanzielle Unterstützung bei der Ausführung der vorliegenden Arbeit unseren wärmsten Dank aussprechen.

Schiomi-Institut für physikalische
und chemische Forschung
und
Physikalisch-chemisches Laboratorium
der Kaiserlichen Universität zu Osaka.

Polymerisation von Styrol in schwerem Wasser und schwerem Alkohol. (Vorläufige Mitteilung.)

Von Masao KOIZUMI und Toshizo TITANI.

(Eingegangen am 4. Februar 1938.)

Heute wird allgemein angenommen,[1] dass die Polymerisation von Styrol oder gemeinhin gesagt die „Vinylpolymerisation" nach dem Schema der Kettenreaktion verläuft. Demnach besteht der ganze Prozess der Reaktion aus drei nacheinanderfolgenden Teilprozessen, nämlich (1) Keimbildungsprozess, (2) Wachstumsprozess und zuletzt (3) Abbruchsprozess. Obwohl jede Einzelheit dieser drei Teilprozesse noch nicht ganz einwandfrei auferklärt worden ist, liegt doch die Vermutung nahe, dass möglicherweise eine Lockerung der H-Atome in einem Molekül (beim Keimbildungsprozess) oder eine intra- bzw. intermolekulare Wanderung der H-Atome (bei den Wachstums- und Abbruchsprozesse) irgend eine aktive Rolle spielen kann. Falls dies wirklich der Fall wäre, dann liegt weiter die Möglichkeit vor, dass zusammen mit der Polymerisation die Austauschreaktion der H-Atome auftreten kann. Aus diesem Grund haben wir die Polymerisation von Styrol beim Vorhandensein von

(1) Vgl. z.B. H. Mark, *Naturwissenschaften*, **25** (1937), 753.

schwerem Wasser bzw. schwerem Alkohol ausführen lassen, um die eventuell mögliche Austauschreaktion herauszufinden. Beim Versuch mit schwerem Wasser wurde das Styrol zusammen mit verdünntem schwerem Wasser unter Luftabschluss in einem Glasrohr eingeschmolzen und bei 100°C. lange Zeit kräftig geschüttelt. Dagegen beim Versuch mit schwerem Alkohol wurde das Styrol in verdünntem schwerem Alkohol (C_2H_5OD) aufgelöst und die dadurch erhaltene Lösung wurde unter Luftabschluss in einem zugeschmolzenen Glasrohr bei 100°C. lange Zeit stehen gelassen. Durch diese beiden Versuche bemerkten wir aber keine nennenswerte Austauschreaktion zwischen Styrol und Wasser bzw. Alkohol, obwohl die Polymerisation von Styrol unter den oben genannten Versuchsbedingungen deutlich in Erscheinung trat. Man darf daher wohl schliessen, dass keine bis zu Austauschreaktion führende Lockerung bzw. Wanderung der H-Atome wenigstens beim Keimbildungs- und Wachstumsprozess stattfindet, wohl aber beim Abbruchsprozess. Bei diesem letzteren, wo die Stabilisierung des wachsenden Polymermoleküls eventuell durch die intra- bzw. intermolekulare Wanderung der H-Atome herbeigeführt wird, muss es aber mit den grössten Schwierigkeiten verbunden sein, diese gelockerten H-Atome durch Austauschreaktion direkt herauszufinden, da eben die Konzentration der gelockerten H-Atome bei diesem Prozess ausserordentlich klein angenommen werden muss.

Schiomi-Institut für physikalische
und chemische Forschung
und
Physikalisch-chemisches Laboratorium
der Kaiserlichen Universität zu Osaka.

Über den Austausch der Wasserstoffatome zwischen Pyrrol, Indol sowie ihren Methylderivaten und Wasser. IV. Austausch der Wasserstoffatome zwischen Indol und Wasser.[1]

Von Masao KOIZUMI und Toshizo TITANI.

(Eingegangen am 28. Februar 1938.)

Inhaltsübersicht. Die Austauschreaktion der H-Atome zwischen geschmolzenem Indol und Wasser wurde unter Benutzung von verdünntem schwerem Wasser untersucht. Dabei wurde gefunden, dass das Indol drei seiner H-Atome gegen die des Wassers und zwar in drei Stufen austauscht, wenn die H-Ionenkonzentration im letzteren allmählich zunimmt (vgl. Abb.).

Solange die H-Ionenkonzentration im Wasser zwischen pH = 7 (neutral) und etwa pH = 2.5 (0.003 N) bleibt, wird das eine an N gebundene H-Atom des Indolmoleküls schnell gegen die des Wasser ausgetauscht (die „erste" Austauschreaktion). Die daraufolgende „zweite" Stufe der Austauschreaktion tritt bei der H-Ionenkonzentration von etwa pH = 2.5 (0.003 N), d.h. am Ende der „ersten" Reaktion, ein und dauert bis auf etwa pH = 0.5 (0.3 N). Bei dieser „zweiten" Austauschreaktion wird zusammen mit dem an N gebundenen H-Atom noch ein an C verbundenes und zwar in der β-Stellung des Pyrrolkerns befindliches H-Atom austauschbar. Dagegen bei der letzten „dritten" Stufe der Austauschreaktion, die am Ende der „zweiten" Reaktion auftritt d.h. oberhalb der H-Ionenkonzentration von etwa pH = 0.5 (0.3 N) stattfindet, wird weiter ein an C und zwar in der α-Stellung des Pyrrolkerns verbundenes H-Atom gegen die des Wassers leicht austauschbar.

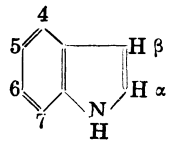
Neben dieser Austauschreaktion der H-Atome tritt aber zugleich, besonders bei den höheren H-Ionenkonzentrationen, die Polymerisation des Indolmoleküls deutlich auf, obwohl die letztere viel langsamer verlief als die erstere. Dabei wurde weiter gefunden, dass mindestens zwei Arten von Polymerisationsprodukten gebildet werden mussten.

Die hier gefundene eigenartige Austauschreaktion des Indols kann man ebenso wie beim Pyrrol mit der tautomerischen Umwandlung in engen Zusammenhang bringen. Dabei müssen die H-Ionen nicht nur auf die Bildung des reaktionsfähigen „labilisierten" Indolmoleküls sondern auch auf die weiteren Reaktionen des so gebildeten „labilisierten" Moleküls katalytisch wirken. Mit dieser Annahme können wir die hier gefundene stufenweise Austauschreaktion des Indols sowie das beim früheren Versuch gefundene ähnliche Verhalten des Pyrrols befriedigend erklären.

(1) I. Mitteil., dies Bulletin, **13** (1938), 85; II. Mitteil., *ibid.*, **13** (1938), 95.; III. Mitteil., *ibid.*, **13** (1938), 298.

Einleitung. Bei unserem früheren Versuch (I. Mittl.) wurde gefunden, dass das Pyrrol alle seine H-Atome zweistufig gegen die des Wassers austauscht, wenn die H-Ionenkonzentration im letzteren allmählich zunimmt. Bleibt nämlich die H-Ionenkonzentration im Wasser kleiner als 0.01 N (pH = 2.0), so tauscht das Pyrrol nur das eine an N gebundene H-Atom gegen die des Wassers aus (die „erste" Austauschreaktion). Wenn dagegen die H-Ionenkonzentration im Wasser diesen Wert überschreitet, tritt ziemlich plötzlich eine neue „zweite" Art von Austauschreaktion auf und dabei werden alle H-Atome im Pyrrolmolekül gegen die des Wassers leicht austauschbar. Neben dieser stufenweisen Austauschreaktion fanden wir zugleich ein deutliches Anzeichen für das Auftreten der Polymerisation des Pyrrolmoleküls. Anschliessend diesem Befund mit Pyrrol führten wir in der nächsten Arbeit (II. Mittl.) ähnliche Versuche mit Thiophen und Furan aus. Aber in diesem Fall konnten wir keine solche leichte Austauschbarkeit der an C gefundenen H-Atome herausfinden. Die H-Atome in diesen beiden Verbindungen liessen sich erst unter Mitwirkung des Platinkatalysators und nur bei erhöhten Temperaturen gegen die des sauren Wassers sehr langsam und kontinuierlich austauschen. Aus diesen Ergebnissen schlossen wir, dass die eingenartige Austauschreaktion des Pyrrols mit der tautomerischen Umwandlung seines Moleküls in engen Zusammenhang stehen und zwar die NH-Gruppe in demselben dabei eine massgebende Rolle spielen muss.

Aus diesem Grunde untersuchten wir nun die Austauschreaktion des Indols, weil diese Verbindung ihrer Molekülstruktur nach auch die Möglichkeit des ähnlichen Verhaltens wie beim Pyrrol besitzt.



Experiment der Austauschreaktion. Die Experimentalmethode war im grossen und ganzen dieselbe wie beim Pyrrol, ausgenommen die Arbeitstemperatur (vgl. I. Mittl.). Wir arbeiteten früher mit Pyrrol bei 30°C. Dagegen in der vorliegenden Arbeit wurde das Indol bei 60°C. mit verdünntem schwerem Wasser geschüttelt, um dadurch das Indol, dessen Schmelzpunkt bei 52°C. liegt, während des Versuchs vollkommen im flüssigen Zustand zu halten.

Etwa 3 g. Indol, das chemisch rein von Laire bezogen wurde, schüttelten wir in einem zugeschmolzenen Glasrohr unter Luftabschluss zusammen mit etwa 1 g. verdünntem schwerem Wasser von wechselnder

H-Ionenkonzentration verschieden lang bei 60°C. Darauf wurde das Wasser vom Indol durch die Destillation im Vakuum abgetrennt und die Dichte, folglich der Gehalt an D, des so abgeschiedenen Wassers, genau bestimmt, nachdem es auf ähnliche Weise wie beim Pyrrol richtig gereinigt worden war.

Aus den so erhaltenen Experimentaldaten berechneten wir, auf dieselbe Weise wie beim Pyrrol, das Austauschäquivalent nk des Indolmoleküls nach der folgenden Gl.(1) (vgl. Gl.(2) in der I. Mittl.):

$$nk = \frac{M_w}{M_j} \frac{D_a - D_e}{D_e} \qquad (1),$$

wo M_w die Molzahl des verwendeten schweren Wassers, M_j die des Indols, und D_a und D_e die D-Konzentration im verwendeten schweren Wasser vor und nach dem Experiment ausdrücken. Das Austauschäquivalent nk eines gegebenen Moleküls wird, wie früher erwähnt, durch die folgende Gl.(2) definiert (vgl. Gl.(3) in der I. Mittl.):

$$nk = \Sigma n_j k_j \qquad (2).$$

In dieser Gleichung zeigt n_j die Zahl der einer bestimmten Art austauschbarer H-Atome in einem gegebenen Molekül und k_j den Verteilungsquotient der D-Atome zwischen diesen Arten der H-Atome und denen des Wassers. Das so berechnete Austauschäquivalent nk des Indols bei verschiedener H-Ionenkonzentration im verwendeten Wasser ist in Tabelle 1 zusammengestellt, wo die Versuchsnr. in der ersten Vertikalreihe die zeitliche Reihenfolge der einzelnen Versuche zeigt.

Die Versuchsergebnisse sind auch in der nebenstehenden Abb. graphisch dargestellt, wo das gefundene Austauschäquivalent nk des Indols gegen den pH des damit geschüttelten schweren Wassers aufgezeichnet ist. Die Nummer bei jedem kleinen Kreis zeigt die Schüttelungsdauer in Stunden. Wie man aus dieser Darstellung ohne weiteres ersieht, führt das Indol mit allmählich zunehmender H-Ionenkonzentration die Austauschreaktion der H-Atome deutlich in drei Stufen aus.

Bei der „ersten" Stufe der Reaktion, die von neutral (pH = 7.0) bis auf etwa 0.003 N (pH = 2.5) dauert, wird nur ein und höchstwahrscheinlich an N gebundenes H-Atom des Indols gegen die des Wassers schnell ausgetauscht. Dagegen bei der „zweiten" Austauschreaktion, die am Ende der „ersten" Reaktion nämlich bei etwa 0.003 N (pH = 2.5) auftritt und bis auf etwa 0.3 N (pH = 0.5) dauert, wird dazu noch ein H-Atom, das an C gebunden ist, glatt gegen die des Wassers ausgetauscht. Bei diesem zweiten austauschbaren H-Atom handelt es sich, wie weiter unten noch

Tabelle 1. Austauschäquivalent *nk* des Indols bei verschiedenen H-Ionenkonzentrationen.

Versuchs-nr.	Normalität der benutzten Lösung	*p*H	Schüttelungs-dauer in Stdn.	*nk*	Bemerkung
1	neutral	7.00	5	1.05	
2	,,	,,	10	1.11	
7*	,,	,,	50	1.12	
10	0.001 N HCl	3.00	5	1.04	
11	,,	,,	50	1.05	Das Indol zeigt keine äusserliche Änderung während des Versuches.
13	0.005 N HCl	2.30	5	1.49	
15	,,	,,	50	1.70	
6*	0.01 N HCl	2.00	5	1.81	
5*	0.03 N HCl	1.52	5	1.72	
3*	0.3 N HCl	0.52	5	1.77	
14	0.8 N HCl	0.10	5	2.16	Nach der Schüttelung bleibt die Substanz auch bei der Zimmertemperatur ganz flüssig.
9	,,	,,	5	1.97	
12	,,	,,	20	2.17	
16*	,,	,,	50	2.20	Während der Schüttelung bei 60°C. wird die Substanz allmählich fest.
4*	3 N HCl	-0.48	5	2.28	
8	,,	,,	5	2.22	

(* vgl. Tabelle 2)

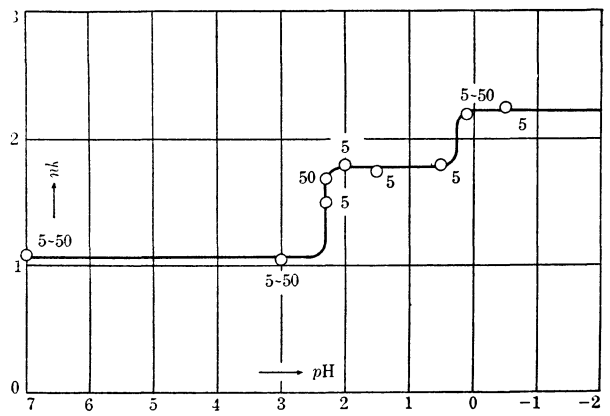


Abb. Abhängigkeit des Austauschäquivalents *nk* des Indols auf dem *p*H des damit geschüttelten Wassers und der Schüttelungsdauer.

zu erwähnen ist, höchstwahrscheinlich um das an C in der β-Stellung des Pyrrolkerns verbundene. Am Ende dieser „zweiten" Austauschreaktion

tritt aber weiter die „dritte" Stufe der Reaktion auf, und dadurch wird noch ein und zwar an C gebundenes H-Atom wieder leicht austauschbar. Diese letzte Stufe der Reaktion dauert, so weit wie wir untersuchten, mindestens bis auf etwa 3 N (pH = −0.5). Hinsichtlich der Lage und Art dieses zuletzt austauschbar werdenden H-Atoms liegt die Sache nicht so klar wie bei den anderen zwei, obwohl die α-Stellung im Pyrrolkern in der ersten Annährung die wahrscheinlichste ist. Auf diesen Punkt wollen wir weiter unten näher eingehen.

Bestimmung der Zahl der austauschbaren H-Atome bei der „dritten" Austauschreaktion. Über die Gesamtzahl n_{I} und n_{II} der austauschbaren H-Atome bei der „ersten" und „zweiten" Austauschreaktion gibt es wohl fast keinen Zweifel, dass $n_{\mathrm{I}} = 1$ und $n_{\mathrm{II}} = 2$ sind (vgl. weiter unten). Dagegen können wir in Bezug auf die Zahl n_{III} der bei der letzten „dritten" Stufe der Reaktion austauschbaren H-Atome nicht ohne weiteres sicher schliessen, dass $n_{\mathrm{III}} = 3$ ist, obwohl diese Zahl allen Umständen nach als sicher angenommen werden könnte. Aus diesem Grunde führten wir einen besonderen Versuch aus, um diese Zahl n_{III} direkt zu bestimmen. Das Verfahren war im grossen und ganzen dasselbe wie das frühere (vgl. I. Mittl.).

Es wurde nämlich eine kleine Menge von Indol genau abgewogen und dies zusammen mit einer überschüssigen Menge von ca. 1 N HCl-saurem fast reinem (92.5-prozentigem) schwerem Wasser bei 60°C. drei bis sechs Stunden lang unter Luftabschluss geschüttelt. Während dieses Verfahrens wandelte sich das Indol bald zu einer festen Masse um (Polymerisation! vgl. die Bemerkung in Tabelle 1). Dann wurde das Wasser vom Indol durch die Destillation im Vakuum abgetrennt und die Dichte des so abgeschiedenen Wassers, nachdem es zunächst unter Zusatz von gebranntem Kalk neutralisiert und dann sorgfältig gereinigt worden war, mittels eines zu diesem Zweck besonders konstruierten Glasschwimmers genau bestimmt. Die Zahl n_{III} der austauschbaren H-Atome in einem Indolmolekül bei der „dritten" Austauschreaktion wurde unter Benutzung der so gefundenen Abnahme der Dichte des schweren Wassers nach der folgenden Gl.(3) ausgerechnet (vgl. Gl.(5) in der I. Mittl.).

$$n_{\mathrm{III}} = \frac{2M_{\mathrm{w}}}{M_{\mathrm{j}}} \frac{(H_{\mathrm{e}} - H_{\mathrm{a}})}{(1 - \alpha H_{\mathrm{e}})} \qquad (3),$$

wo M_{w} und M_{j} je die Molzahl des zum Versuch verwendeten schweren Wassers und Indols, H_{a} und H_{e} den Gehalt an leichtem Wasserstoff des schweren Wassers vor und nach dem Experiment und α den mittleren Verteilungsquotient der H-Atome zwischen Indol und schwerem Wasser

darstellt. Bei der praktischen Ausführung der Berechnung setzten wir in der obigen Gl. (3) annährungsweise $a = 1$. Diese Vernachlässigung übte aber keinen merklichen Einfluss auf das Endresultat aus, weil wegen der überschüssigen Menge des schweren Wassers die H-Konzentration H_e in demselben nach dem Experiment immer sehr klein war (durchschnittlich $H_e = 10\%$). Die Versuchsresultate sind in der folgenden Tabelle 2 zusammengestellt.

Tabelle 2. Zahl n_{III} der austauschbaren H-Atome in einem Indolmolekül bei der „dritten" Austauschreaktion.

Versuchsnr.	Molzahl des D_2O M_w	Molzahl des Indols M_j	Abnahme der Dichte des D_2O nach dem Exp.	n_{III}
1	0.0546	0.000793	0.0018	2.7
2	0.0549	0.000803	0.00224	3.2
3	0.0622	0.000814	0.00164	2.7
4	0.0598	0.000881	0.00265	3.8
5	0.02345	0.000433	0.00275	3.2
6	0.1005	0.001034	0.00143	2.9

Aus den so gefundenen Werten von n_{III} in der letzten Vertikalreihe der Tabelle darf man wohl schliessen, dass bei der „dritten" Austauschreaktion drei H-Atome in einem Indolmolekül gleich austauschbar sind. Daneben bemerkt man aus diesem Versuchsergebnisse weiter, dass die Austauschreaktion der H-Atome im Vergleich mit der Polymerisation des Indols viel schneller verlaufen muss, weil abgesehen davon, dass das Indol durch die Polymerisation immer aus dem Reaktionssystem abgeschieden wurde, das Austauschgleichgewicht der H-Atome in jedem Fall richtig erreicht worden war.

Aus dem so gefundenen Wert von n_{III} $(= 3)$ sowie aus dem von vornherein sicheren Wert von n_I $(= 1)$ ergibt sich ohne weiteres, dass die Zahl der austauschbaren H-Atome bei der „zweiten" Austauschreaktion $n_{II} = 2$ sein muss. Auf diese Weise fanden wir nämlich, dass drei H-Atome des Indolmoleküls bei jeder Stufe der Reaktion eines nach dem anderen gegen die des Wassers ausgetauscht werden.

Experiment der Polymerisationsreaktion. Es fand sich, wie schon oben in Tabelle 1 bemerkt, ein deutliches Anzeichen für das Auftreten der Polymerisation des Indols besonders bei der grossen H-Ionenkonzentration. Als wir nämlich mit einer verdünnten unterhalb 0.03 N liegenden HCl-Lösung arbeiteten, blieb das geschmolzene Indol bei der

Arbeitstemperatur (60°C.) immer eine klare leicht bewegliche Flüssigkeit, und durch die Erkaltung zur Zimmertemperatur wurde es wieder ganz fest. Dagegen als wir das Experiment mit einer konzentrierten HCl-Lösung (0.8 N) durchführten, wurde das geschmolzene Indol während der Schüttelung allmählich zäh und selbst nach der Erkaltung erstarrte es nicht. Bei noch höherer H-Ionenkonzentration (3 N) wurde das geschmolzene während des Experiments ziemlich schnell schwer beweglich und zum Schluss ganz fest, abgesehen davon, dass die Arbeitstemperatur (60°C.) sicherlich oberhalb des Schmelzpunktes des reinen Indols (52°C.) lag. Alle diese Tatsachen weisen ohne weiteres darauf hin, dass neben der Austauschreaktion auch die Polymerisation des Indols bei der grossen H-Ionenkonzentration ziemlich deutlich vonstatten ging.

Obwohl die Polymerisation des Indols mit Hilfe von Säuren schon von vielen Autoren untersucht worden ist,[2] möchten wir hier einiges über unseren vorläufigen Versuch mitteilen, den wir im Anschluss an den Hauptversuch der Austauschreaktion durchführten. Das Experiment wurde folgendermassen ausgeführt. Das Indol, das beim Austauschversuch mit saurem schwerem Wasser geschüttelt und davon durch Destillation im Vakuum abgetrennt worden war, wurde dann mit einer bestimmten Menge von Benzol bei 29°C. so lange behandelt, bis keine Substanz mehr dadurch aufgelöst wurde. Bei diesem Versuch fanden wir, dass das Indol, das beim Austauschversuch mit verhältnismässig verdünnter HCl-Lösung geschüttelt worden war, durch die obige Behandlung restlos im Benzol aufgelöst und beim Verdampfen des Benzols wieder in festem Zustand abgeschieden wurde. Dagegen als wir beim Austauschversuch konzentriertere HCl-Lösung benutzten, blieb immer ein Teil des Indols unlöslich im Benzol und der darin lösliche Anteil beim Verdampfen des Benzols scheidete sich als eine gelbe schwer destillierbare Flüssigkeit ab. Die unterstehende Tabelle 3 gibt die Resultate einiger solcher analytischen Versuche, die wir mit dem zur Austauschreaktion benutzten Indol durchführten, wieder. Die Versuchsnr. in der ersten Vertikalreihe entspricht der des Hauptversuchs in Tabelle 1.

Aus diesem Resultat ersieht man sofort, dass gerade beim pH-Gebiet der „dritten" Austauschreaktion, d.h. unterhalb $p\mathrm{H} = 0.3$ (vgl. die Abb.), auch ziemlich starke Veränderung der Beschaffenheit (höchstwahrscheinlich Polymerisation) des Indols stattfindet. Eine diesähnliche Erscheinung liesse sich vielleicht auch beim pH-Gebiet der „zweiten" Austauschreaktion, d.h. zwischen $p\mathrm{H} = 2.3$ bis 0.3 auffinden, falls man dafür eine pas-

(2) Vgl. z.B. Oddo, *Gazz. chim. ital.*, **63** (1933), 898; O. Schmitz-Dumont und J. ter Horst, *Ber.*, **68** (1935), 240.

Tabelle 3. Analyse des beim Austauschversuch verwendeten Indols nach dessen Polymerisationsgrad.

Versuchs-nr.	Ergebnisse des Austauschversuchs				Ergebnisse der Analyse	
	Normalität der benutzten Lösung	*p*H	Schüttellungs-dauer in Stdn.	Austausch-äquivalent *nk*	Relative Menge des in Benzol unlöslichen Anteils	Beschaffenheit des in Benzol löslichen Anteils
7	neutral	7.0	50	1.12	0%	fest
6	0.01 N HCl	2.0	5	1.81	0	fest
5	0.03 N HCl	1.5	5	1.72	0	fest
3	0.3 N HCl	0.5	5	1.77	8	gelb flüssig
16	0.8 N HCl	0.1	50	2.20	50	gelb flüssig
4	3 N HCl	-0.5	5	2.28	64	gelb flüssig

sende analytische Methode ausfindig machen könnte. Aber in jedem Fall erscheint uns sehr interessant, dass ohne Rücksicht auf diese ziemlich starke Veränderung bzw. Polymerisation des Indolmoleküls die Austauschreaktion immer bis zum Gleichgewicht verlief. Man darf daher wohl schliessen, dass die Austauschreaktion im Vergleich mit der Polymerisation viel schneller vor sich ging, obwohl diese zwei Erscheinungen beide gleich durch die gelockerten bzw. beweglichen H-Atome hervorgerufen zu werden scheinen.

Diskussion. Wir fanden bei unserem früheren Versuch, wie schon oben in der Einleitung erwähnt, dass das Pyrrol bei allmählich zunehmender H-Ionenkonzentration seine H-Atome zweistufig gegen die des Wassers austauscht. Dagegen tauscht das Indol, wie sich aus der vorliegenden Arbeit ergab, drei seiner H-Atome mit zunehmender H-Ionenkonzentration dreistufig gegen die des Wassers aus. Über das „erste" austauschbare H-Atom des Indolmoleküls, das schon bei neutraler Lösung sehr schnell gegen das des Wassers ausgetauscht wird, besteht ebensowenig Zweifel wie über das „erste" austauschbare H-Atome des Pyrrols, dass es sich nämlich um das an N gebundene H-Atom handelt. Aber in Bezug auf die Art und Lage der anderen zwei H-Atome, die bei der „zweiten" und „dritten" Stufe der Reaktion beweglich werden, liegt die Sache nicht so einfach wie beim „ersten", und um darin Klarheit zu gewinnen, muss man noch andere Tatsachen insbesondere die chemischen Eigenschaften des Indols in Betracht ziehen. Bei den organisch-chemischen Arbeiten wird in der Regel angenommen, dass das in der β-Stellung des Indolmoleküls befindliche H-Atom viel reaktionsfähiger

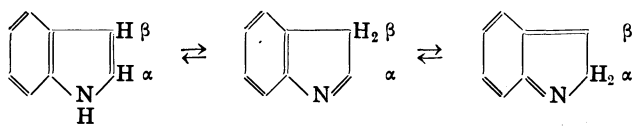
als das in der α-Stellung befindliche ist. Aus diesem Grunde sowie aus unseren eigenen Versuchen mit Methylindole, die später in diesem Bulletin veröffentlicht werden sollen, können wir mit ziemlich grosser Sicherheit schliessen, dass das „zweite" austauschbare H-Atom das an C in der β-Stellung des Indols verbundene H-Atom ist. Falls dies wirklich der Fall wäre, dann folgt die weitere natürliche Annahme, dass das „dritte" austauschbare H-Atom sich in der α-Stellung im Pyrrolkern befindet, obwohl es auch eine andere Möglichkeit gibt, dass dieses „dritte" H-Atom seinen Sitz nicht im Pyrrolkern sondern im Benzolkern des Indols finden kann. Aber gegen diese letzte Annahme sprechen u.a. die folgenden Tatsachen bzw. Überlegungen:

(1) Falls das „dritte" austauschbare H-Atom wirklich das im Benzolkern befindliche ist, dann müsste die „dritte" Austauschreaktion nicht so plötzlich wie beim wirklichen Fall sondern viel langsamer auftreten.

(2) Da die zwei H-Atome im Benzolkern, die sich in der 5- und 7-Stellung befinden, fast gleich leicht reaktionsfähig angenommen sind, müssten bei der „dritten" Austauschreaktion mindestens zwei H-Atome gleich austauschbar werden, wenn diese Stufe der Reaktion wirklich durch die im Benzolkern befindlichen H-Atome hervorgerufen werden würde.

(3) Der Verteilungsquotient der D-Atome bei der „dritten" Austauschreaktion wurde, wie weiter unten gezeigt wird, gleich 0.45 gefunden. Dieser Wert ist aber viel kleiner als der des Benzols (0.93),[3] dagegen nicht so klein im Vergleich mit dem des Pyrrols (0.70).

Wenn man auf diese Weise das „erste" austauschbare H-Atom das an N gebundene, das „zweite" das in der β-Stellung befindliche und das „dritte" das in der α-Stellung befindliche H-Atom annimmt, dann können wir die „zweite" und „dritte" Austauschreaktionen des Indols mit der tautomerischen Umwandlung seines Moleküls in Zusammenhang bringen, weil für diese Verbindung folgende drei Arten der Strukturformeln denkbar sind:

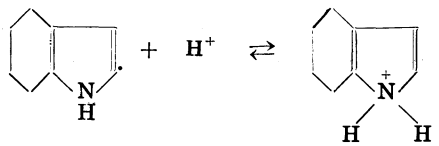


(i) (ii) (iii) (4).

(3) K. Koyano, *J. Chem. Soc. Japan*, **57** (1936), 933.

Wir können nämlich die „zweite" Austauschreaktion mit der tautomerischen Umwandlung zwischen den beiden Formen (i) und (ii), dagegen die „dritte" Stufe der Austauschreaktion mit der Umwandlung zwischen den Formen (i) und (iii) bzw. (ii) und (iii) wohl erklären. Dabei ist zu bemerken, dass die Formel (iii) die Strukturänderung im Benzolkern begleitet. Die verhältnismässig grosse Schwierigkeit, mit der die „dritte" Austauschreaktion stattfindet, kann daher mit der Schwierigkeit der Strukturänderung des Benzolkerns verbunden sein.

Als der erste massgebende Vorgang bei der Austauschreaktion des Indols kann man ebenso wie beim Pyrrol die Salzbildung, d.h. die Anlagerung des Protons (bzw. Deuterons) an dem N-Atom des Indolmoleküls annehmen:



(5).

„labilisiertes" Molekül

Das so gebildete „labilisierte" Molekül des Indols kann nun seine an C gebundenen H-Atome gegen die des Wassers leicht austauschen, indem es die tautomerische Umwandlung gemäss Gl. (4) ausführt. Mit dieser Annahme können wir das Auftreten der „zweiten" Austauschreaktion des Indols ebensogut wie die des Pyrrols erklären. Aber weil wir allein damit das weitere Auftreten der „dritten" Austauschreaktion des Indols schwer begreifen können, müssen wir, um dies befriedigend zu deuten, einen Schritt weiter tun und annehmen, dass die tautomerische Umwandlung des „labilisierten" Moleküls selbst auch durch die H-Ionen katalysiert wird. Die H-Ionen üben daher auf die Austauschreaktion sowie die Polymerisation des Indols bzw. Pyrrols dreierlei fördernde Einflüsse aus: (1) Die Vergrösserung der Löslichkeit des Indols bzw. Pyrrols im Wasser, worin der Meinung nach die Hauptreaktion verläuft, (2) die Bildung des reaktionsfähigen „labilisierten" Moleküls und (3) die katalytische Wirkung auf die tautomerische Umwandlung des so gebildeten „labilisierten" Moleküls. Unter dem Zusammenwirken aller dieser Einflüsse der H-Ionen kann die „zweite" bzw. „dritte" Austauschreaktion mit allmählich zunehmender H-Ionenkonzentration so plötzlich auftreten.

Wir geben in der folgenden Tabelle 4 den Mittelwert des Austauschäquivalents nk des Indols bei jeder Stufe der Austauschreaktion, der aus dem Resultat in Tabelle 1 errechnet wurde, wieder.

Die Werte k_N bzw. k_C in der letzten Vertikalreihe der Tabelle zeigen den mittleren Verteilungsquotienten der D-Atome zwischen dem NH- bzw.

Tabelle 4. Austauschäquivalent des Indols bei drei Arten der Austauschreaktionen.

Art der Austausch-reaktion	pH Grenze	Mittleres Austauschäquivalent nk	Anzahl der austauschbaren H-Atome n	k_N bzw. k_C
Erste	7—2.5	1.07 ± 0.04	1	1.07
Zweite	2.5—0.5	1.76 ± 0.04	2	0.69
Dritte	0.5	2.21 ± 0.04	3	0.45

CH-Radikal des Indols und Wasser, die wir aus den Werten von nk und n bei jeder Stufe der Reaktion nach der folgenden Methode errechnet haben. Gemäss der Definition des Austauschäquivalents (2) können wir

$$n_i k_i = 1.07,$$

$$n_i k_i + n_{ii} k_{ii} = 1.76,$$

$$\text{und} \quad n_i k_i + n_{ii} k_{ii} + n_{iii} k_{iii} = 2.21$$

setzen, wenn man mit n_i, n_{ii} und n_{iii} die Zahl der bei der „ersten", „zweiten" und „dritten" Austauschreaktion austauschbar werdenden H-Atome[4] und mit k_i, k_{ii} und k_{iii} deren Verteilungsquotienten ausdrückt. Da aber offenbar $n_i = n_{ii} = n_{iii} = 1$ ist, folgt ohne weiteres, dass

$$k_i = k(\mathrm{NH/H_2O}) = 1.07,^{[5]}$$

$$k_{ii} = k(\beta\text{-CH/H}_2\mathrm{O}) = 0.69,$$

$$\text{und} \quad k_{iii} = k(\alpha\text{-CH/H}_2\mathrm{O}) = 0.45$$

ist. Wir fanden bei unserem früheren Versuch (I. Mittl.), dass für Pyrrol $k(\mathrm{NH/H_2O}) = 0.88$ und $k(\mathrm{CH/H_2O}) = 0.70$ ist. Dieser letzte Wert stimmt mit dem $k(\beta\text{-CH/H}_2\mathrm{O})$ des Indols hinreichend gut überein, nicht aber mit dem $k(\alpha\text{-CH/H}_2\mathrm{O})$. Ebensowenig stimmt der Wert von $k(\mathrm{NH/H_2O})$ des

(4) Wir drücken mit n_I, n_{II} und n_{III} die Gesamtzahl der *austauschbaren* H-Atome bei jeder Stufe der Reaktion, dagegen mit n_i, n_{ii} und n_{iii} die Zahl der bei jeder Stufe der Reaktion gerade *austauschbar werdenden* H-Atome aus, so dass $n_I = 1$, $n_{II} = 2$ und $n_{III} = 3$, dagegen $n_i = n_{ii} = n_{iii} = 1$ ist.

(5) Wegen der isotopischen Fraktionierung des schweren Wassers bei dessen Abdestillation vom Indol kann dieser Wert $k(\mathrm{NH/H_2O})$ um einen kleinen Betrag zu gross sein. Dagegen ist der Wert $k(\alpha\text{-BH/H}_2\mathrm{O})$ möglicherweise wegen der starken Polymerisation des Indols ein wenig zu klein.

Indols mit dem des Pyrrols. Alle diese Tatsachen weisen ohne Zweifel darauf hin, dass der Verteilungsquotient ein und derselben Atomgruppe nicht nur von der Art des Moleküls, in welchem sie sich befindet, sondern auch von ihrer Lage in einem Molekül ziemlich stark beeinflusst wird (vgl. S. 92, I. Mittl.).

Zum Schluss möchten wir der Nippon Gakujutsu-Shinkohkai (der Gesellschaft zur Förderung der japanischen Wissenschaft) sowie der Hattori-Hohkohkai (der Hattori-Stiftung) für ihre finanzielle Unterstützung bei der Durchführung dieser Arbeit unseren besten Dank aussprechen.

Shiomi-Institut für physikalische
und chemische Forschung,
und
Physikalisch-chemisches Laboratorium
der Kaiserlichen Uuniversität zu Osaka.

Austauschreaktion der H-Atome zwischen Nitrophenole und Wasser. I. Austauschreaktion und Wasserstoffbindung.

Von Masao KOIZUMI und Toshizo TITANI.

(Eingegangen am 28. Februar 1938.)

Inhaltsübersicht. Die Austauschreaktion der H-Atome zwischen drei Arten der isomerischen Nitrophenole (*o*-, *m*- und *p*-Nitrophenole) und Wasser wurde in alkalischer Lösung bei 100°C. untersucht. Die dadurch gefundenen Tatsachen kann man kurz wie folgt zusammenfassen:

(1) Bei allen Arten der Nitrophenole wird das H-Atom der OH-Gruppe sehr schnell, fast momentan, gegen die des Wassers ausgetauscht.

(2) Daranschliessend tritt eine zweite Stufe der Reaktion auf, wo einige Zahlen der Kernwasserstoffatome langsam aber mit wohl messbarer Geschwindigkeit gegen die des Wassers ausgetauscht werden. Die Zahl der dieser Stufe der Reaktion beteiligenden Kernwasserstoffatome ist vermutlich zwei bei *o*-, drei bei *m*- und zwei bei *p*-Verbindung.

(3) Die Austauschreaktion der Kernwasserstoffatome hört mit dieser zweiten Stufe der Reaktion nicht ganz auf sondern dauert immer weiter, bis schliesslich alle Kernwasserstoffatome gegen die des Wassers ausgetauscht zu werden scheinen. Aber

diese letzte Stufe der Reaktion verläuft sehr langsam und sogar noch nach tausend Stunden wird kein Austauschgleichgewicht erreicht.

(4) Die Geschwindigkeit der zweiten Austauschreaktion ist bei der *m*- und *p*-Verbindung gegenseitig fast gleich gross, dagegen die der *o*-Verbindung erheblich klein im Vergleich mit der der anderen zwei Isomeren.

(5) Aus diesen Versuchsergebnissen kann man schliessen, dass die fördernde Wirkung der OH-Gruppe auf die Reaktionsfähigkeit der gegen diese Atomgruppe in *o*- und *p*-Stellung befindlichen Kernwasserstoffatome im Vergleich mit der störenden Wirkung der NO_2-Gruppe auf die gegen diese Atomgruppe in *o*- und *p*-Stellung befindlichen Kernwasserstoffatome unvergleichlich stark sein muss.

(6) Der grosse Unterschied der Reaktionsfähigkeit der Kernwasserstoffatome des *o*-Nitrophenols gegen die der anderen zwei Isomeren können wir mit der Annahme der intramolekularen Wasserstoffbindung zwischen den benachbarten OH- und NO_2-Gruppen der Verbindung erklären.

Einleitung. Die Austauschreaktion der H-Atome der verschiedenen Arten der aromatischen Verbindungen gegen die des Wassers ist der Gegenstand der Versuche vieler Autoren gewesen. Allen diesen bisherigen Versuchen nach erscheint die Austauschreaktion der Kernwasserstoffatome der allgemeinen Regel der Substitutionsreaktion zu folgen, die die gewöhnliche elektrophilische Substitutionsreaktion beherrscht.[1] Es wird z.B. gefunden,[2] dass die OH-Gruppe, die nach dieser Regel auf die eine Reihe der Substitutionsreaktion der gegen diese Atomgruppe in *o*- und *p*-Stellung befindlichen Kernwasserstoffatome fördernde Wirkung ausübt, auf die Austauschreaktion dieser derselben Kernwasserstoffatome ebenfalls günstig wirkt. Aber aus den organisch-chemischen Erfahrungen kennen wir ausser der OH-Gruppe noch viele andere Atomgruppen, die ebenso gut wie diese eine fördernde Wirkung besitzt, wie z.B. die NH_2-Gruppe. Dagegen gibt es auch andere Klassen der Atomgruppen, die gerade die entgegengesetzte Wirkung zeigen, wie z.B. die NO_2-Gruppe. Diese Atomgruppe übt auf die elektrophilische Substitutionsreaktion der gegen sie in *o*- und *p*-Stellung befindlichen Kernwasserstoffatome einen gewissen störenden Einfluss aus. Folglich erscheint uns sehr reizvoll eine Austauschreaktion der Kernwasserstoffatome mit solch einer aromatischen Verbindung auszuführen, die zwei Arten der Atomgruppen, von denen die eine fördernde die andere hingegen störende Wirkung besitzt, gleichzeitig in einem Molekül enthält. Aus diesem Grunde haben wir die Austauschreaktion der D-Atome der drei Arten der isomerischen Nitrophenole gegen verdünntes schweres Wasser ausgeführt. Solch eine Prüfung der Substitutionsregel an Hand der isotopischen Austauschreak-

(1) Vgl. z.B. C.K. Ingold, C.G. Raisin und C.L. Wilson, *J. Chem. Soc.*, **1936**, 1637.

(2) F.K. Münzberg, *Z. physik. Chem.*, B, **33** (1936), 23; K. H. Geib, *ibid.*, A, **180** (1937), 211.

tion hat aber einen anderen Vorteil gegenüber der üblichen Methode, die man bisher benutzte. Man untersucht nämlich bei den gewöhnlichen organisch-chemischen Arbeiten den Einfluss einer gegebenen Atomgruppe auf die Reaktionsfähigkeit der Kernwasserstoffatome dadurch, dass man die mit dieser angegebenen Atomgruppe substituierten Verbindung eine gewisse Substitutionsreaktion, wie z.B. Halogenierung bzw. Nitrierung, ausführen lässt und daraus über Ort und Lage der reaktionsfähigen Kernwasserstoffatome in diesem substituierten Molekül Schlüsse zieht. Aber diese Untersuchungsmethode kann nicht als ganz einwandfrei angesehen werden, weil, wie man aus der oben geschilderten Arbeitsweise ohne weiteres ersieht, die bei der tastenden Reaktion in den Benzolkern eingeführten Atome bzw. Atomgruppe ebenso gut wie die von vornherein darin befindliche Atomgruppe auf die frei bleibenden Kernwasserstoffatome irgendeine Wirkung ausüben kann. Infolgedessen kann man nach dieser Methode kaum zu einem ungestörten Bild der sukzessiven Substitutionsreaktion kommen. Gerade in diesem Punkt besitzt der Austauschversuch mit dem Wasserstoffisotop einen Vorteil, weil das schwere Isotop des Wasserstoffs mindestens in den „statischen" chemischen Eigenschaften praktisch identisch mit dem gewöhnlichen leichten Wasserstoffatom betrachtet werden kann.

Versuchsmethode. Eine genau abgewogene Menge von Nitrophenol wurde zusammen mit fast gleicher Menge des neutralen, sauren bzw. alkalischen verdünnten schweren (durchschnittlich 4-prozentigen) Wassers in einem Glasrohr in Vakuum eingeschmolzen und bei einer bestimmten Temperatur (100°C.) aber verschiedener Zeitlänge stehen gelassen. Dabei lösten sich *m*- und *p*-Nitrophenol restlos im Wasser auf. Hingegen wurde die *o*-Verbindung dadurch nicht ganz aufgelöst, und immer blieb eine kleine Menge derselben ungelöst auf dem Boden zurück. Aber dieser Unterschied konnte kaum einen Einfluss auf das Endresultat ausüben, weil, wie weiter unten gezeigt wird, die Austauschreaktion aller Arten der Verbindungen sehr langsam verlief. Nach einer bestimmten Zeit wurde das schwere Wasser durch die Destillation im Vakuum vom darin gelösten Nitrophenol abgetrennt und gereinigt. Die Reinigung des so abgeschiedenen schweren Wassers geschah je nach den Versuchsbedingungen der Hauptversuche auf verschiedene Weise. Als wir *m*- bzw. *p*-Nitrophenol mit neutraler bzw. alkalischer Lösung erwärmten und die Versuchsdauer nicht sehr lang währte, erwies sich das abgetrennte Wasser nach paarmaligen Destillationen im Vakuum genügend rein. Dagegen als wir *m*- bzw. *p*-Nitrophenol zusammen mit saurer Lösung erwärmten, neutralisierten wir die Lösung unter Zusatz von entwässertem K_2CO_3

und destillierten sie erst dann im Vakuum ab. Und beim Fall, wo die Erwärmung sehr lang dauerte, wurde das abgetrennte Wasser immer zuerst unter Zusatz von Na_2O_2 und $KMnO_4$ lange Zeit erwärmt und dann durch paarmalige Destillationen im Vakuum gereinigt. Beim Versuch mit *o*-Nitrophenol erwies es sich immer nötig, das abgetrennte Wasser zunächst in Dampfform über erhitztem CuO zu leiten und dann mit alkalischem $KMnO_4$ zu behandeln, um dies richtig zu reinigen. Dies rührte offenbar von der verhältnismässig leichten Zersetzbarkeit der *o*-Verbindung her. Die Dichte des so gereinigten Wassers wurde immer nach Schwebemethode mittels eines Quarzschwimmers genau bestimmt, um damit den Gehalt des Wassers an D zu erkennen.

Die Austauschbarkeit jeder Art von Nitrophenol drückten wir, wie bei dem anderen Versuche,[3] mit dem „Austauschäquivalent" des betreffenden Moleküls bei einem gegebenen Zeitpunkt aus. Das Austauschäquivalent nk eines gegebenen Moleküls wird im allgemeinen durch die folgende Gl.(1) definiert:

$$nk = \Sigma n_j k_j \qquad (1),$$

wo n_j und k_j die Zahl und den Verteilungsquotient einer bestimmten Art der austauschbaren H-Atome in einem Molekül ausdrückt, und die Summation für alle Arten der austauschbaren H-Atome in diesem Molekül ausgeführt werden muss. Das Austauschäquivalent nk des Nitrophenols kann man aus den oben erhaltenen Experimentalresultaten gemäss Gl.(2) leicht errechnen:

$$nk = \frac{2M_w}{M_o} \frac{C_a - C_e}{C_e} \qquad (2),$$

wo M_w die Molzahl des schweren Wassers, M_o die des Nitrophenols und C_a und C_e den D-Gehalt des schweren Wassers vor und nach dem Experiment ausdrückt.

Vorversuche. Um über die Austauschbarkeit der Kernwasserstoffatome der drei Arten der Nitrophenole die Vorkenntnis zu gewinnen, haben wir zunächst einige Versuche unter Benutzung der neutralen, sauren und alkalischen Lösung ausgeführt. Die dadurch erhaltenen Resultate sind in der folgenden Tabelle 1 zusammengestellt, wo C_a und C_e den Dichteüberschuss des verwendeten schweren Wassers vor und nach dem Experiment in γ-Einheiten ausdrücken (vgl. oben).

Durch diese Vorversuche fanden wir nämlich, dass nicht nur das Hydroxylwasserstoffatom sondern auch die Kernwasserstoffatome der

(3) Vgl. z.B. M. Koizumi und T. Titani, dies Bulletin, **13** (1938), 88.

Tabelle 1. Ergebnisse der Vorversuche.

a. Versuche mit neutraler Lösung (100°C.)

	Versuchs-dauer in Stdn.	M_w	M_o	$C_a - C_e$ in γ	C_e in γ	nk
o	2	0.0550	0.0215	660	2790	1.2
	50	0.0553	0.0217_5	667	2783	1.2
m	2	0.0551	0.0219	605	2845	1.07
	50	0.0550	0.0218	652	2798	1.17
p	2	0.110	0.0390	578	3039	1.07
	50	0.0562	0.0215	612	3005	1.07

b. Versuche mit 1 N HCl-Lösung (100°C.)

	Versuchs-dauer in Stdn.	M_w	M_o	$C_a - C_e$ in γ	C_e in γ	nk
o	—	—	—	—	—	—
m	50	0.0556	0.0216	611	2655	1.19
	260	0.0556	0.0216	673	2593	1.34
p	2	0.0568	0.0221	554	2712	1.05
	50	0.0592	0.0223	596	2670	1.18
	260	0.0563	0.0217	643	2623	1.27

c. Versuche mit 1 N KOH-Lösung (100°C.)

	Versuchs-dauer in Stdn.	M_w	M_o	$C_a - C_e$ in γ	C_e in γ	nk
o	50	0.0584	0.0212	636	2640	1.3
	150	0.0590	0.0217	654	3058	1.2
	260	0.0578	0.0216	674	2602	1.4
m	50	0.0647	0.0219	670	2606	1.52
	150	0.0576	0.0217	1172	2540	2.45
	260	0.0575	0.0208	1096	2180	2.78
p	2	0.119	0.0411	566	2710	1.21
	50	0.0581	0.0216	759	2983	1.37
	260	0.0890	0.0188	671	2605	2.64

Nitrophenole langsam aber deutlich gegen die des Wassers ausgetauscht werden, und zwar verläuft dieser Austausch der Kernwasserstoffatome in der alkalischen Lösung am schnellsten. Es wurde weiter gefunden, dass die Kernwasserstoffatome der *o*-Verbindung im Vergleich mit den anderen zwei Isomeren erheblich schwerer austauschbar sind, obgleich zwischen den letzteren zwei Isomeren keine deutlichen Unterschiede zu bemerken waren. Dieser Unterschied in der Reaktionsfähigkeit der *o*-Verbindung gegen die anderen zwei isomerischen Verbindungen tritt im weiter unten zu erwähnenden Hauptversuche noch deutlicher auf.

Hauptversuche mit alkalischer Lösung. Da aus dem vorhergehenden Vorversuche gefunden wurde, dass die Austauschreaktion der Kernwasserstoffatome der Nitrophenole am leichtesten in alkalischer Lösung verläuft, führten wir die Hauptversuche alle unter Benutzung der 3 N KOH-Lösung aus. Sonstige Arbeitsweise war genau dieselbe wie oben angegeben. Die Ergebnisse der Hauptversuche geben wir in den folgenden Tabelle 2 wieder.

Die Bedeutung der einzelnen Buchstaben in der ersten Horizontalreihe ist ohne weiteres klar (vgl. die Bemerkung bei der Gl.(2)), ausgenommen $(nk)_r$ in der letzten Vertikalreihe. Von dieser Quantität wollen wir weiter unten sprechen (vgl. S. 326). Die oben angegebenen Versuchsergebnisse stellen wir auch in der nebenstehenden Abb. 1 graphisch dar, wo das gefundene Austauschäquivalent *nk* der drei Arten der Nitrophenole gegen die Versuchsdauer aufgezeichnet ist. Wie man aus dieser graphischen Darstellung ersieht, kann man den ganzen Reaktionsverlauf jeder Verbindung etwa in drei Stufen einteilen, obwohl jede dieser Stufen nicht so scharf, besonders zwischen der zweiten und dritten Stufe der Reaktion, untereinander begrenzt ist, wie Münzberg[2] bei der Austauschreaktion der Polyphenole hinwies. Bei der ersten Stufe der Reaktion,

Tabelle 2. Ergebnisse der Hauptversuche.

a. Versuche mit *o*-Nitrophenol (100°C.)

Versuchsdauer in Stdn.	M_w	M_o	$C_a - C_e$ in γ	C_e in γ	*nk*	$(nk)_r$
2	0.0623	0.0216	821	3518	1.35	0.14
100	0.0636	0.0216	994	3345	1.75	0.34
260	0.0624	0.0216	1209	3130	2.23	0.58
812	0.0625	0.0218	1563	2776	3.23	1.08
1000	0.0630	0.0216	1609	2730	3.44	1.19

b. Versuche mit *m*-Nitrophenol (100°C.)

Versuchs-dauer in Stdn.	M_w	M_o	$C_a - C_e$ in γ	C_e in γ	nk	$(nk)_r$
2	0.0619	0.0216	857	3482	1.41	0.11
29	0.0628	0.0218	1278	3061	2.40	0.44
50	0.0638	0.0216	1361	2978	2.70	0.54
62	0.0633	0.0219	1453	2886	2.90	0.61
100	0.0629_5	0.0216	1579	2760	3.34	0.76
260	0.0629	0.0216	1645	2694	3.84	0.92
600	0.0626	0.0216	1834	2505	4.24	1.06
1000	0.0638	0.0216	1855	2484	4.41	1.11

c. Versuche mit *p*-Nitrophenol (100°C.)

Versuchs-dauer in Stdn.	M_w	M_o	$C_a - C_e$ in γ	C_e in γ	nk	$(nk)_r$
2	0.0612	0.0209	834	3505	1.38	0.16
50	0.0628	0.0216	1145	3194	2.09	0.51
100	0.0633	0.0216	1367	2972	2.70	0.82
260	0.0630	0.0216	1495	2844	3.11	1.02
600	0.0626	0.0216	1597	2742	3.38	1.16
1000	0.0635	0.0216	1667	2772	3.57	1.25

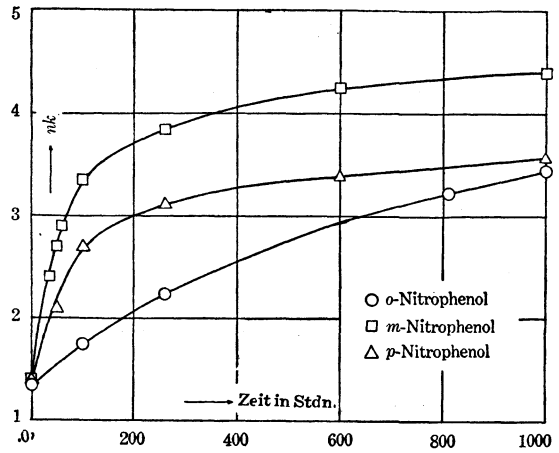
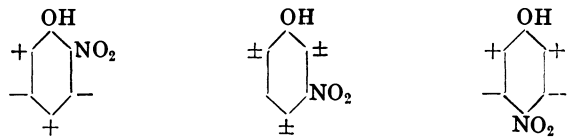


Abb. 1. Die Abhängigkeit des Totalaustauschäquivalents *nk* auf die Versuchsdauer.

die fast beim ersten Augenblick beendet wird, wird das Hydroxylwasserstoffatom sehr schnell durch das des Wassers ersetzt. Diese von vornherein schon zu erwartende Reaktion wird weiter dadurch bestätigt, dass der kleinste Wert des Austauschäquivalents ($nk = 1.05$ bis 1.07), der bei der neutralen Lösung gefunden wurde, sehr gut mit dem früher vom unsubstituierten Phenol gefundenen Verteilungsquotient der Phenolhydroxylgruppe ($k = 1.07$)[4] übereinstimmte. Dieser Wert wird aber beim vorliegenden Fall bald überschritten und das gefundene Austauschäquivalent nimmt mit der zunehmenden Versuchsdauer ziemlich schnell zu, und dadurch tritt die zweite Stufe der Reaktion auf, wo selbstverständlich einige Kernwasserstoffatome gegen die des Wassers ausgetauscht werden. Diese zweite Stufe der Reaktion beläuft sich aber nur bis auf etwa 100 bis 200 Stdn. und von da ab wird die Austauschgeschwindigkeit erheblich vermindert, obwohl diese sogar noch nach 1000 Stdn. nicht ganz bis auf Null herabgesetzt wird. Diese letzte nicht so scharf von der zweiten abgegrenzte Stufe der Reaktion wollen wir vorläufig die dritte Stufe nennen. Bei dieser dritten Stufe der Reaktion scheinen alle Kernwasserstoffatome der Nitrophenole schliesslich restlos gegen die des Wassers ausgetauscht zu werden.

Diskussion der Ergebnisse. Die organisch-chemische Erfahrung lehrt, dass die OH-Gruppe auf die elektrophilische Substitutionsreaktion der dieser gegenüber in der *o*- und *p*-Stellung befindlichen Kernwasserstoffatome fördernden Einfluss ausübt. Dagegen wirkt die NO_2-Gruppe auf dieselbe Reaktion vielmehr störend und zwar wird diese störende Wirkung am kleinsten auf das dieser Atomgruppe gegenüber in *m*-Stellung befindliche Kernwasserstoffatom angenommen. Nach dieser teils auch theoretisch aufgeklärten Substitutionsregel[5] können wir deshalb das folgende Schema für die Ersetzbar- bzw. Austauschbarkeit der Kernwasserstoffatome der drei isomerischen Arten der Nitrophenole aufstellen:



(3).

o-Nitrophenol *m*-Nitrophenol *p*-Nitrophenol

In diesem Substitutionsschema werden die Stellungen der Kernwasserstoffatome, deren Substitutionsreaktion durch die OH-Gruppe erleichtert

(4) M. Harada und T. Titani, dies Bulletin, **11** (1936), 465.
(5) Vgl. z.B. C.K. Ingold, *Chem Rev.*, **15** (1934), 225; G.W. Wheland und L. Pauling, *J. Am. Chem. Soc.*, **57** (1935), 2086; E. Hückel, *Z. physik. Chem.*, B, **35** (1937), 163.

wird, mit (+) Zeichen, dagegen die der Wasserstoffatome, deren Reaktion unter dem Einfluss der NO_2-Gruppe erschwert wird, mit (−) Zeichen gekennzeichnet. Infolgedessen ist aus diesem Schema bloss zu erwarten, dass zwei Kernwasserstoffatome der *o*-Verbindung ebenso leicht wie die der *p*-Verbindung austauschbar sind, dagegen die *m*-Verbindung keine leicht austauschbaren Kernwasserstoffatome in ihrem Molekül enthält, falls der störende Einfluss der NO_2-Gruppe ebenso stark wie die fördernde Wirkung der OH-Gruppe wäre. Diese rein theoretische Erwartung stimmt aber nicht immer mit den Versuchsergebnissen der vorliegenden Arbeit überein.

Erstens zeigte sich, dass die *o*-Verbindung, wie schon oben erwähnt, die Austauschreaktion der Kernwasserstoffatome viel schwerer als die anderen zwei isomerischen Verbindungen ausführt, und zweitens wurde gefunden, dass die drei Kernwasserstoffatome der *m*-Verbindung ebenso leicht wie zwei Wasserstoffatome der *p*-Verbindung gegen die des Wassers ausgetauscht werden. Diese beiden Tatsachen kann man deutlich aus der Abb. 2 ersehen. In dieser Abb. 2 wird statt des Totalaustauschäquivalents *nk* in Abb. 1 dessen „reduzierte" Wert $(nk)_r$ gegen die Versuchsdauer eingezeichnet. Diese Quantität $(nk)_r$, die schon in den letzten Vertikalreihen der Tabelle 2 angegeben werden, wurde dadurch berechnet, dass man vom Totalaustauschäquivalent *nk* das der OH-Gruppe $(nk)_{OH}$ abzieht und dann diese Differenz mit der Anzahl *n* der Kernwasserstoffatome, die bei der zweiten Stufe der Reaktion austauschbar angenommen werden (vgl. das Schema (3)), dividiert:

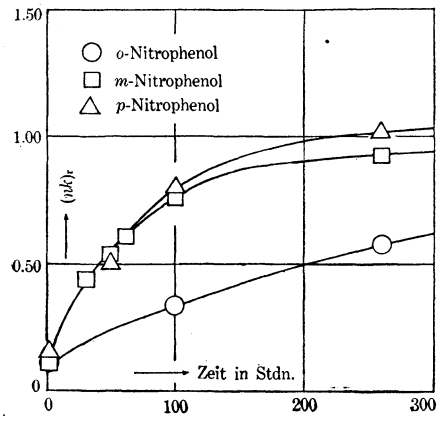


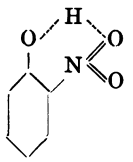
Abb. 2. Die Abhängigkeit des reduzierten Austauchäquivalents $(nk)_r$ auf die Versuchsdauer.

$$(nk)_r = \frac{nk-(nk)_{OH}}{n} \qquad (4).$$

Bei der praktischen Durchführung der Rechnung setzten wir $(nk)_{OH} = 1.07$ (Verteilungsquotient der OH-Gruppe) und für die *o*- und *p*-Verbindungen $n = 2$ dagegen für die *m*-Verbindung $n = 3$. Der so berechnete Wert von $(nk)_r$ kann deshalb als das mittlere Austauschäquivalent (bzw. Verteilungsquotient) eines der austauschbaren Kernwasserstoffatome in

einem Nitrophenolmolekül angesehen werden.[6] In Abb. 2 trugen wir das so berechnete $(nk)_r$ der drei Arten der Nitrophenole gegen die Versuchsdauer bis auf 300 Stdn.

Aus dieser Abb. 2 ersieht man sofort, dass die beiden Kurven der *m*- und *p*-Nitrophenole mindestens bis auf 100 Stdn. fast ganz übereinander liegen. Dies weist darauf hin, dass die drei Kernwasserstoffatome des *m*-Nitrophenols ebenso leicht wie die zwei H-Atome der *p*-Verbindung austauschbar sind, so dass die fördernde Wirkung der OH-Gruppe auf die Ersetzbarkeit der ihr gegenüber in *o*- und *p*-Stellung befindlichen Kernwasserstoffatome ungleich stärker als die störende Wirkung der NO_2-Gruppe auf die Reaktion der ihr gegenüber ebenfalls in *o*- und *p*-Stellung befindlichen Kernwasserstoffatome sein muss (vgl. Schema (3)). Die kleine Abweichung der beiden Kurven der *m*- und *p*-Verbindungen bei der längeren Versuchsdauer kann man auf das allmähliche Auftreten der dritten Stufe der Reaktion zurückführen, woran alle übrigen Kernwasserstoffatome der Austauschreaktion teilnehmen. Diese Schlüsse kann man weiteres dadurch bestätigen, dass der $(nk)_r$-Wert des *p*-Nitrophenols, das nur noch zwei Kernwasserstoffatome zur dritten Austauschreaktion übrig hat, bald deutlich grösser als der des *m*-Nitrophenols wird, das dazu nur ein H-Atom besitzt (vgl. Tabelle 2 und Schema (3)). Aus Abb. 2 ersieht man weiter, dass die Kurve des *o*-Nitrophenols immer erheblich tiefer als die anderen zwei Kurven liegt, d.h. die zwei austauschbar angenommenen Kernwasserstoffatome des *o*-Nitrophenols erheblich schwerer austauschbar im Vergleich mit den anderen zwei isomerischen Verbindungen sind (vgl. Schema (3)). Diese Eigentümlichkeit der *o*-Verbindung können wir aber mit der Annahme der intramolekularen Wasserstoffbindung zwischen den benachbarten OH- und NO_2-Gruppen dieser Verbindung wohl erklären. Es wird nämlich aus vielseitigen Versuchen heute im allgemeinen angenommen,[7] dass eine Art der Bindung mittels des Wasserstoffatoms zwischen den Sauerstoffatomen der OH- und NO_2-Gruppen gebildet ist, die sich gegenseitig in *o*-Stellung befinden, wie das folgende Schema zeigt:



(5).

(6) Es wird z.B. $(nk)_r = 0.93$, falls es sich um ein Kernwasserstoffatom eines reinen Benzolmoleküls handelt (vgl. K. Koyano, *J. Chem. Soc. Japan*, **57** (1936), 933).

(7) Vgl. z.B. E.N. Lassettre, *Chem. Rev.*, **20** (1937), 259.

Da aber die Ausbildung solch einer intramolekularen Wasserstoffbindung zwischen OH- und NO_2-Gruppe eine gewisse Menge der Valenzelektronen der Sauerstoffatome der beiden Atomgruppen in Anspruch nehmen muss, liegt die Annahme sehr nahe, dass die Wirkung dieser beiden Atomgruppen, besonders die fördernde Wirkung der OH-Gruppe, auf die Reaktionsfähigkeit der Kernwasserstoffatome dadurch stark geschwächt wird. Diese Annahme wird weiter dadurch gestützt, dass bei den *m*- und *p*-Verbindungen, in deren Moleküle wegen der grösseren Entfernung der OH- und NO_2-Gruppen keine Wasserstoffbindungen nachgewiesen werden, nicht nur der Reaktionsverlauf einander ähnlich ist sondern auch die Aktivierungsenergie der Austauschreaktion gegenseitig fast identisch ist, worauf in der nächsten Abhandlung hingewiesen werden soll.

Zum Schluss möchten wir der Nippon-Gakujutsu-Shinkohkai (der Gesellschaft zur Förderung der japanischen Wissenschaft) sowie der Hattori-Hohkohkai (der Hattori-Stiftung) für ihre finanzielle Unterstützung unseren wärmsten Dank aussprechen. Herrn T. Takagi, der bei der Ausführung der vorliegenden Arbeit uns sehr behilflich war, sind wir auch zu bestem Dank verpflichtet.

Shiomi-Institut für physikalische
und chemische Forschung,
und
Physikalisch-chemisches Laboratorium
der Kaiserlichen Universität zu Osaka.

Ein Versuch zur Austauschreaktion der Sauerstoffatome zwischen Carbonat-Ion und Wasser. (Vorläufige Mitteilung.)

Von Toshizo TITANI, Noriyoshi MORITA und Kokiti GOTO.

(Eingegangen am 28. Februar 1938.)

Die Untersuchung der Austauschreaktion der O-Atome zwischen verschiedenen Arten der Anionen und Wasser ist für uns insofern von Interesse als sie über die chemische Struktur des betreffenden Anions einiges Licht werfen kann. Aus diesem Grunde führten wir jetzt die Versuche mit einigen anorganischen Anionen aus. Obwohl diese unsere Versuche noch nicht ganz zum Abschluss gekommen sind, wollen wir dennoch eins der bisher gewonnenen Versuchsergebnisse vorläufig kurz mitteilen, weil über denselben Gegenstand schon einige Versuche von anderen Forschern vorliegen.(1) Das hier mitzuteilende Experiment haben wir mit Kaliumcarbonat durchgeführt. Dabei verfuhren wir folgendermassen. Etwa 10 g. von K_2CO_3 wurde zunächst im Vakuum bei ca. 250°C. fünf Stunden lang vollkommen getrocknet und dann in 20 c.c. schweres Wasser aufgelöst, dessen Gehalt an schwerem Sauerstoff durch fraktionierte Destillation um einen gewissen Betrag vergrössert worden war. Die so erhaltene Lösung wurde bei Zimmertemperatur über Nacht stehen gelassen, und dann das Wasser durch die Destillation im Vakuum vom Carbonat abgetrennt. Das so abgeschiedene Wasser versetzte man abermals mit 10 g. gut getrocknetem K_2CO_3 und behandelte es genau wie oben. Auf diese Weise wurde ein und dasselbe schwere Wasser (20 c.c.) dreimal mit 10 g. K_2CO_3, also insgesamt mit 30 g. K_2CO_3, behandelt. Nach dieser Behandlung wurde das Wasser richtig gereinigt und dessen Dichte mittels eines Quarzschwimmers genau bestimmt. Die Ergebnisse der zwei Reihen der Versuche geben wir in der folgenden Tabelle wieder.

Austauschreaktion der O-Atome zwischen K_2CO_3 und Wasser.

Δs_a in γ	$\Delta(s_a)_o$ in γ	Δs_e in γ	$\Delta s_a - \Delta s_e$ gef.	$\Delta s_a - \Delta s_e$ ber.
35.4	22.6	35.2	0.2	9.3
33.7	22.2	33.3	0.4	9.1

(1) E. Blumenthal und J.B.M. Herbert, *Trans. Faraday Soc.*, **33** (1937), 849; S.C. Datta, J.N.E. Day und C.K. Ingold, *J. Chem. Soc.*, **1937**, 1963.

In dieser Tabelle drücken Δs_a und Δs_e den gesamten Dichteüberschuss des benutzten schweren Wassers gewöhnlichem Wasser gegenüber vor und nach dem Experiment und $\Delta(s_a)_o$ solch einen Anteil des gesamten Dichteüberschusses Δs_a vor dem Experiment aus, der auf die Anreicherung der schweren Sauerstoffisotope zurückzuführen ist. Dieser letzte Wert $\Delta(s_a)_o$ wurde durch die isotopische Analyse des betreffenden Wassers[2] bestimmt. Aus dieser Tabelle ersieht man sofort, dass der anfängliche Dichteüberschuss des benutzten Wassers Δs_a durch die oben angegebene Behandlung mit K_2CO_3 nur um 0.2 bis 0.4 γ abnahm, wie aus der vierten Vertikalreihe der Tabelle offensichtlich ist. Hingegen müsste dann, falls es sich um den vollkommenen Austausch der O-Atome zwischen der gegebenen Menge des Carbonat-Ions und Wassers handelt, der Dichteüberschuss des benutzten Wassers durch diese Behandlung um 9.3 bis 9.1 γ abnehmen, wie in der letzten Vertikalreihe der Tabelle gezeigt ist. Diese theoretischen Werte berechneten wir aus dem Mengenverhältnis des Carbonat-Ions und Wassers unter der höchstwahrscheinlichen Annahme, dass der Verteilungsquotient der O-Atome zwischen diesen beiden Substanzen nahe gleich eins ist. Aus dem hier angegebenen Versuchsergebnis kann man daher sicher schliessen, dass es mindestens unter den hier benutzten Versuchsbedingungen zu keiner Austauschreaktion der O-Atome zwischen Carbonat-Ion und Wasser kam.

Physikalisch-chemisches Laboratorium
der Kaiserlichen Universität zu Osaka
und
Shiomi-Institut für physikalische
und chemische Forschung.

(2) Vgl. z.B. N. Morita, K. Goto und T. Titani, dies Bulletin, **13** (1938), 99.

The Addition of Hydrogen Bromide to Undecenoic Acid in Toluene Solution. I. The Effect of Reduced Nickel.

By Yoshiyuki URUSHIBARA and Matsuji TAKEBAYASHI.

(Received March 1, 1938.)

The effect of air on the addition of hydrogen bromide to undecenoic acid in toluene solution was first observed by one of the authors (Y. U.)[1] when he was at a synthetical experiment relating to carpaine with G. Barger and R. Robinson.[2] Later R. Ashton and J. C. Smith[3] investigated the problem in the light of the observations of M. S. Kharasch and co-workers,[4] who had found meanwhile the so-called peroxide effect in the addition of hydrogen bromide to unsaturated compounds. Smith and Kharasch with their co-workers have since published respectively several papers on the effect of peroxides and oxygen on the addition reactions of unsaturated compounds.

The present authors, studying the effects of various substances other than oxygen and peroxides on the addition of hydrogen bromide to allyl bromide, observed that reduced nickel and reduced iron influenced this reaction quite in the same way as oxygen.[5] Since, the effects of ferromagnetic metals as well as of oxygen and peroxides on the addition of hydrogen bromide or bromine to ethylenic compounds have been investigated in this laboratory.[6] Further, one of the authors[7] observed

(1) R. Robinson, *Chemistry & Industry*, **52** (1933), 219.
(2) *J. Chem. Soc.*, **1937**, 714.
(3) *J. Chem. Soc.*, **1934**, 435.
(4) *J. Am. Chem. Soc.*, **55** (1933), 2468, 2521, 2531; **56** (1934), 244.
(5) This Bulletin, **11** (1936), 692, 754; **12** (1937), 51.
(6) J. C. Smith gives an excellent summarizing article on "the 'Peroxide' or 'Oxygen' Effect," *Chemistry & Industry*, **56** (1937), 833. He quotes fully the present authors' works, and on page 836 of that article he writes, "They found a close parallel between the percentages of 1:3-dibromopropane from allyl bromide containing peroxide equivalent to x c.c. of oxygen and from pure allyl bromide to which x c.c. of oxygen had been added before sealing; the total yields of dibromo-compounds were also equal. ....." But, what the present authors intended to show by the results collected in Table 1 of the fifth paper on the addition of hydrogen bromide to allyl bromide, this Bulletin, **12** (1937), 140, is somewhat different from Smith's interpretation, and was really that "both the total yield of the product and the proportion of 1,3-dibromopropane in the product are greater in additions with peroxide-free allyl bromide in the presence of oxygen than in the additions with peroxide-containing allyl bromide in vacuum," and that "while the action of oxygen is very regular ..... the action of the peroxide is rather irregular ...." Discussions on these observations and conclusions drawn from them are given in the mentioned paper (p. 142).
(7) Y. Urushibara and O. Simamura, this Bulletin, **12** (1937), 507.

a close parallelism between the effects of oxygen and reduced nickel on the catalytic action of hydrogen bromide in the isomerization of iso-stilbene into stilbene. However, ferromagnetic metals have not yet been examined in other addition reactions except in an unsuccessful attempt with cinnamic acid and bromine.[8] Now the authors have returned to undecenoic acid, and the present paper records the results of experiments on the effect of reduced nickel on the addition of hydrogen bromide to undecenoic acid in toluene solution.

Undecenoic acid used was a commercial product (Kahlbaum, "extra pure") melting at 23.8° (corr.) and can be regarded fairly pure. It gave no colouration with ammonium thiocyanate and ferrous ammonium sulphate, being free from peroxide. Hydrogen bromide was prepared by the action of purified bromine on hot tetralin, washed by passing through cold tetralin and over moist red phosphorus, then dried with anhydrous calcium bromide and with phosphorus pentoxide. Toluene, free from thiophene, was redistilled over metallic sodium.

The apparatus is shown schematically in Fig. 1. The whole is made of Pyrex glass. A is a side tube of 22 mm. diameter and 120 c.c. capacity, B the reaction tube of 22 mm. diameter and 130 c.c. capacity, C the inlet tube of 7 mm. diameter for hydrogen bromide and hydrogen, and D the outlet for excessive hydrogen bromide and for evacuation. C was connected with the source of purified hydrogen bromide. Between them two three-way cocks were inserted, one way of the cock nearer to C being connected with the source of hydrogen through another three-way cock. These cocks were provided for manipulation of excluding air. During the passing of hydrogen bromide a calcium chloride tube was attached to D.

In experiments in presence of air undecenoic acid and toluene were directly mixed in B and hydrogen bromide was passed with cooling in ice water. In additions in vacuum (in absence of air) undecenoic acid was dissolved in a required amount of toluene in A, the volume of the solution was marked on A, and further 5–6 c.c. of the solvent was added. The excess of toluene was distilled off at room temperature by evacuation through D, while tube B was warmed in a hot water bath to avoid the condensation of toluene in it. In this way air was driven out. When the volume of the solution reached the mark, the stopcock of D was closed, B cooled in ice water, the contents of A decanted into B, and hydrogen bromide passed into the solution with caution. In experiments with reduced nickel, the catalyst was placed in B beforehand and heated in

(8) This Bulletin, **12** (1937), 506.

a hot water bath during the distillation of toluene as above. When the solution in A was reduced to the required volume, it was frozen by cooling in liquid air while the nickel in B was heated to 350–360°, evacuation being continued. The stopcock of D was closed, hydrogen introduced from C, and after a while the vessel evacuated again. This process was repeated three times, cooling of A and heating of B being continued. Then B was cooled to room temperature under evacuation. D was closed, A taken out of liquid air, and B immersed in ice water. The nickel was sometimes washed with hydrogen bromide gas. Then the solution in A was decanted on reduced nickel in B, and hydrogen bromide introduced.

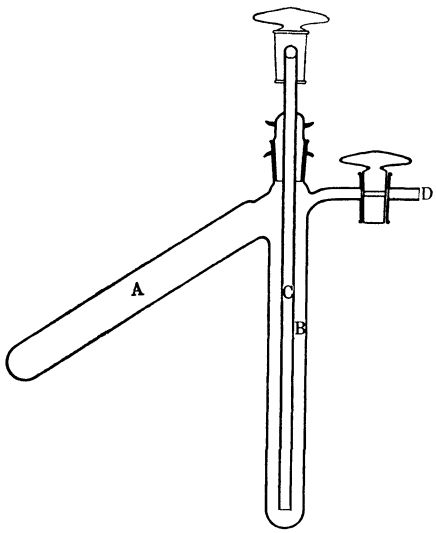


Fig. 1.

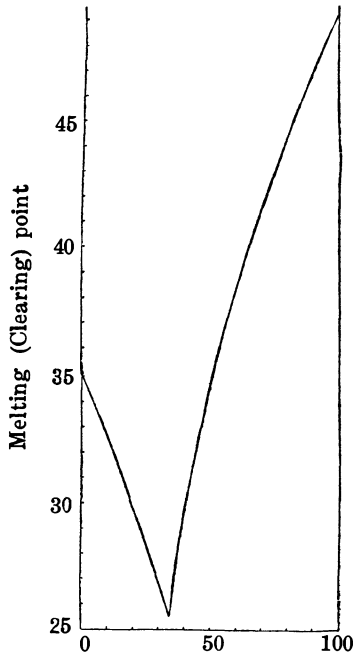


Fig. 2.

Hydrogen bromide was passed at 0°C. in the dark for one hour. The mixture was left to stand overnight at 0°C. in the dark. Toluene and the excess of hydrogen bromide were removed in vacuum at 50°, and the remaining substance was collected with toluene. When reduced nickel was used, the catalyst was filtered off and washed with toluene. The toluene solution was again evaporated in vacuum at 50°. The product was obtained always in quantitative yield, and did not decolourize bromine.

It was brought to crystallization by cooling to −5° if necessary, and pressed on cooled porous plates.

The proportion of 10- and 11-bromo-undecoic acids in the reaction product was determined by observing the melting (clearing) point. For this the data of Ashton and Smith[9] for the binary mixtures of the two bromo-acids were used. A melting points–composition curve (Fig. 2) was drawn and the compositions of the samples were obtained on the curve. To decide on which side of the eutectic point a sample fell, the melting points of mixtures with suitable amounts of 11-bromo-undecoic acid were observed.

No. of exp.	Undecenoic acid (g.)	Toluene (c.c.)	In presence of	Product	
				Melting point (°C.)	11-Bromo-acid (%)
1	5.0	5	None (vacuum)	34.5	2
2	3.68 (0.02 mol)	20	None (vacuum)	34.7	1
3	5.0	5	Hydrogen	34.7	1
4	5.0	5	Air	29.8	20
5	3.68	20	Air	48.7	97
6	5.0	5	Reduced nickel 3.0 g.	33.0	8
7	2.5	20	Reduced nickel 3.0 g.	25.5	34
8	2.5	20	Reduced nickel 3.0 g. HBr passed for 1.5 hrs.	31.1	42
9	3.68	20	Reduced nickel 1.2 g.	29.5	21
10	3.68	20	Reduced nickel 3.5 g. +Hydrogen	30.0	19
11	3.68	20	Reduced nickel 6.0 g.	25.6	34

The results of experiments are given in the accompanying table. As regards the effect of air the observations of Ashton and Smith were con-

(9) *J. Chem. Soc.*, 1934, 440.

firmed: In vacuum the product was nearly pure 10-bromo-undecoic acid no matter whether the solution was concentrated (Exp. 1) or dilute (Exp. 2). The effect of air, giving rise to the formation of 11-bromo-undecoic acid, was comparatively small in the concentrated solution (Exp. 4), while it was marked in the dilute solution (Exp. 5).

An effect similar to that of oxygen was observed with reduced nickel. Moreover, an analogous relation was found between the concentration of undecenoic acid and the effect of reduced nickel: the smaller the former the greater the latter (Exp. 6 and 7). Experiments on the relation between the amount of reduced nickel and the proportion of the 11-bromo-acid resulted as expected: as the former increased, so did the latter (Exp. 9 and 11). However, the effect of reduced nickel on the addition of hydrogen bromide to undecenoic acid in toluene solution has been found rather small compared with that of oxygen in view of the strong effect of the former in the case of allyl bromide. Hydrogen showed no significant effect (Exp. 3 and 10). The greater proportion of the 11-bromo-acid obtained on passing hydrogen bromide for a longer time (Exp. 8) was probably caused by correspondingly longer agitation of the reaction mixture.

While reduced nickel suffered no change during the reaction, reduced iron was attacked by hydrogen bromide or undecenoic acid in an addition in its presence.

Now experiments on the influence of antioxidants on the effect of oxygen and reduced nickel are under way, and the results will soon be ready for publishing.

The authors thank the Imperial Academy of Japan for a grant.

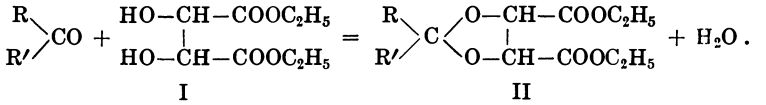
Chemical Institute, Faculty of Science,
Imperial University of Tokyo.

Distribution of Diethyl Tartrate between Ether and Aqueous Borate Solution and a Contribution to the Studies on the Equilibrium of the Boro-Diol Complex Formation.

By Yojiro TSUZUKI.

(Received March 10, 1938.)

Introduction. In the following condensation reaction, which takes place between a carbonyl compound and diethyl tartrate giving a bridged derivative of tartaric acid, the author[1] has been always successful in removing the unchanged ester (I) (which cannot otherwise be separated with ease) from the reaction product (II) by shaking the ethereal extract of the reaction mixture with saturated aqueous solution of borax.



I II

This success in the separation may probably be attributed to the circumstances that the unchanged ester (I), being a diol, forms some boro-diol complex with borate ion, while the reaction product (II), being insoluble in water, remains in the ethereal phase. It appears therefore that the tartaric ester can easily be transferred to the aqueous layer, although the ester by itself is freely soluble in ether as well as in water.

In the present work the author has made quantitative studies of this phenomenon, intending thus to demonstrate the efficiency of this process of separation.

The results of the measurements actually show that the distribution of diethyl tartrate between ether and water follows simply the distribution law, but in the system of ether and water containing borax the distribution coefficient C_2/C_1 is no more constant, and decreases with the increasing concentration of the ester. It can, however, be obviously shown that the use of borax solution in the extraction process is very advantageous, as was expected.

In order to give an interpretation of these phenomena, the author at first assumed the existence of the equilibrium of complex formation in the aqueous layer, which was later ascertained by the analysis of the experimental results. In consequence of this analytical studies the author

(1) Y. Tsuzuki, this Bulletin, **10** (1935), 255; **11** (1936), 362; **12** (1937), 487.

has succeeded in demonstrating clearly what is the favourable condition for extracting the ester from the ethereal solution.

Experimental Method. The distribution experiment was carried out in the usual way.[2] The determination of diethyl tartrate is made as follows: For the ethereal phase, ether is carefully evaporated up, and the residue is warmed with a known quantity of N/5 KOH and the excess of the alkali is titrated with N/10 HCl. For the aqueous borate phase, the solution is boiled with potassium hydroxide to saponify diethyl tartrate, and after the resulting alcohol is completely evaporated off, the residue is boiled with a known quantity of N $K_2Cr_2O_7$ to oxidize the liberated tartaric acid, and the excess of bichromate is determined by iodometry.[3]

Results of the Measurements. Distribution experiments were made in the systems of ether–water, ether–1/20 mol borax, and ether–N/4 KBO_2. The influence of temperature was also observed, except in the case of water–borax. The results are given in the accompanying tables and shown graphically in Fig. 1, where c_1 denotes the concentration (g. per 10 c.c. solution) of diethyl tartrate in the ethereal phase, and c_2 concentration (g. per 10 c.c. solution) of diethyl tartrate in the aqueous phase.

The distribution in the system of ether–water follows the Nernst distribution law, as shown in Table 1.

The results of the distribution measurement of diethyl tartrate between ether and aqueous borax solution (Table 2) shows that the ester is distributed in the latter phase much more than in pure water. By these quantitative experiments it can be understood that diethyl tartrate is effectively extracted out of the ethereal solution by shaking with borax solution. Thus it is shown that this extraction method is very useful in the purification process stated above.

It is also worthy of note that the ratio, c_2/c_1 diminishes with increasing concentration (c_1 or c_2).

The data of the distribution experiments between ether and 1/4 mol aqueous potassium borate (KBO_2) solution are given in Table 3, where it is seen that the distribution ratio, c_2/c_1 is yet in a marked degree greater than in the case of water–borax (Table 2), which is obviously shown graphically in Fig. 1.

(2) Ref. Eucken–Suhrmann, "Physikalisch-chemische Praktikumaufgaben," 158, Leipzig (1928).

(3) Determination of tartaric acid by bichromate method: Heidenhain, *Z. anal. Chem.*, **32** (1893), 357; K. Täufel and C. Wagner, *ibid.*, **67** (1925), 16; Wikul, *ibid.*, **68** (1926), 45.

Table 1. Distribution of diethyl tartrate between ether and water at 20°.

c_1	c_2	$k = c_2/c_1$
0.0172	0.0371	2.16
0.0271	0.0584	2.15
0.0446	0.101	2.26
0.0624	0.133	2.13
0.0910	0.211	2.31
0.114	0.257	2.26
0.228	0.519	2.28
		mean 2.22

Table 2. Distribution of diethyl tartrate between ether and 1/20 mol aqueous solution of borax at 20°.

c_1	c_2	c_2/c_1
0.0109	0.1271	11.7
0.0298	0.2355	7.88
0.0834	0.4159	4.98

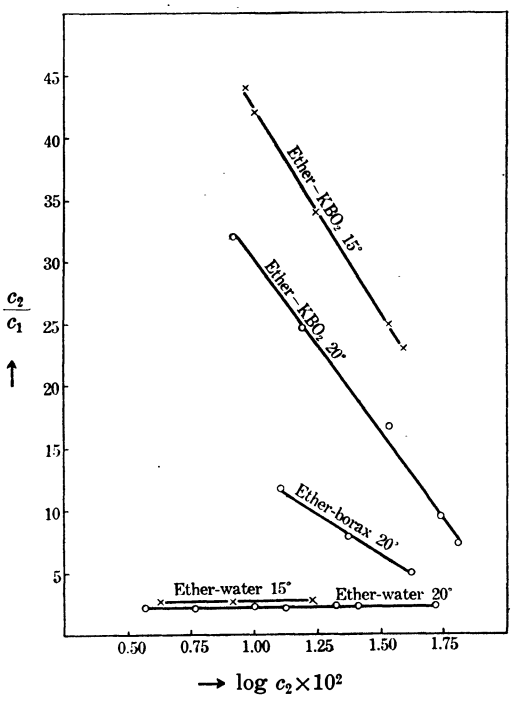


Fig. 1.

Table 3. Distribution of diethyl tartrate between ether and 1/4 mol aqueous potassium borate solution at 20°.

No. of experiment	c_1	c_2	c_2/c_1
I	0.0026	0.083	32.0
II	0.0063	0.155	24.7
III	0.0206	0.343	16.7
IV	0.0577	0.548	9.50
V	0.0876	0.640	7.31

As the ester is very soluble in the borate layer, the quantity of the ester distributed in the ethereal solution is greatly diminished, especially when the concentration of the ester is small. From this experiment we know that in the purification process the extraction of the ester by means of potassium borate is more effective than by the use of borax.

Influence of Temperature. In order to see the temperature influence on the distribution ratio, similar experiments were made at 15° for the systems of ether–water and of ether–1/4 mol aqueous potassium borate. The results are given in Tables 4 and 5.

Table 4. Distribution of diethyl tartrate between ether and water at 15°.

c_1	c_2	$k = c_2/c_1$
0.0164	0.0427	2.60
0.0316	0.0827	2.61
0.0613	0.1700	2.77

Table 5. Distribution of diethyl tartrate between ether and 1/4 mol aqueous KBO_2 solution at 15°.

No. of exp.	c_1	c_2	c_2/c_1
I	0.0021	0.093	44
II	0.0024	0.101	42
III	0.0051	0.177	34
IV	0.0136	0.343	25.1
V	0.0170	0.392	23.0

The distribution ratio $k = c_2/c_1$ in the system of ether–water (Table 4) becomes also nearly constant, but slightly greater than at 20°, while in the system of ether–1/4 mol KBO_2 (Table 5) the ratio c_2/c_1 is remarkably higher as compared with those at 20°. This relation will be clearly seen in Fig. 1.

Equilibrium between Diethyl Tartrate and Borate in the Aqueous Borate Layer.

The facts that the distribution coefficient in the system of ether–borate is inconstant as stated above, suggest that in the borate phase the ester exists not merely in free state, but rather combined with borate ion. The author now assumes that this "combined" ester is in equilibrium with the free ester, and the latter is, on the other hand, in constant ratio to the ester in the ethereal phase, in conformity with Nernst distribution law, as shown by the following scheme:

I. Ethereal layer: T Conc. of the ester $= c_1$

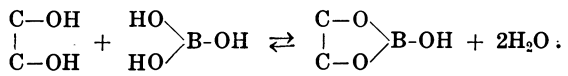
II. Aqueous layer: $BO_2' + T \rightleftarrows TB'$ Total conc. of the ester $= c_2$

$$\frac{[T]_{II}}{[T]_I} = k \quad \text{(Nernst distribution law),}$$

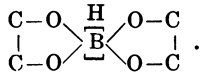
where T represents diethyl tartrate, TB′ complex ion of boro-tartrate, $[T]_I$ the concentration of diethyl tartrate in ethereal layer, $[T]_{II}$ the

concentration of "uncombined" diethyl tartrate in aqueous borate phase, and k the distribution coefficient in ether–water system.

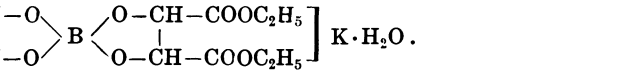
Reaction of Diethyl Tartrate with Borate Ion. Before entering the analysis of the equilibrium, we must investigate the type of the reaction. van't Hoff,[4] considering the facts that mannitol (with 6 hydroxyl groups) required 3 molecules of boric acid, and supposing that the high rotatory power of the complex, assumed the reaction of polyhydroxy-compounds with boric acid shown by the following scheme might be borne out by the cyclisation, since it was generally known that cyclisation in the molecule enhances the rotatory power of the compound.



On the other hand, Hermans[5] considered the complex was formed by the combination of two molecules of diol with one molecule of boric acid, the structure of which was of the cyclic nature containing pentavalent boron atom with the coordination number 4 in the centre of the complex molecule:



And later, in fact, Lowry[6] and Bancroft and Davis[7] isolated a complex compound of this structure, potassium boro-tartrate $KB(C_4H_4O_6)_2$, although it was a potassium salt of a different type of diol (hydroxy-carboxylic). B. Jones[8] described also the isolation of a complex of this sort, potassium ethyl boro-tartrate $C_{16}H_{24}O_{12}BK\cdot H_2O$, which was obtained by the action of boric acid and potassium carbonate on diethyl tartrate. The structure of this complex is considered as follows:



It was, however, demonstrated by H. T. Britton and P. Jackson[9] that in the complex of boro-tartaric acid the ratio, tartaric acid/boric acid is 1 or 2 according to the condition of the formation, by following the change in pH, conductivity, and optical rotation during the progressive

(4) "Die Lagerung der Atome in Raume," 3rd Ed., 90, Braunschweig (1908).
(5) *Proc. Acad. Sci. Amsterdam*, **26** (1925), 32.
(6) *J. Chem. Soc.*, **1929**, 2853.
(7) *J. Phys. Chem.*, **34** (1930), 2479.
(8) *J. Chem. Soc.*, **1933**, 951.
(9) *J. Chem. Soc.*, **1934**, 1002.

addition of sodium hydroxide to various tartaric-boric acid mixtures. And it was also shown by N. Vermaas[10] that between boric acid and diol (such as mannitol, sorbitol, fructose, etc.) two following equilibria exist:

$$\text{HB (boric acid)} + \text{D (diol)} \rightleftarrows \text{HBD} + 2H_2O\,,$$

$$\text{HBD} + \text{D} \rightleftarrows H^+ + BD_2^- + H_2O\,.$$

It may therefore be assumed that generally in the equilibrium between boric acid and diol both types of complex, i.e. mono-diol type and di-diol type exist, so that in the present case the equilibria between diethyl tartrate and potassium borate (KBO_2) may be considered as follows:

$$BO_2' + \text{T (diethyl tartrate)} \rightleftarrows TB'\begin{pmatrix}\text{complex ion of}\\ \text{mono-diol type}\end{pmatrix} + H_2O \qquad \text{(I)},$$

$$TB' + T \rightleftarrows T_2B'\begin{pmatrix}\text{complex ion of}\\ \text{di-diol type}\end{pmatrix} + H_2O \qquad \text{(II)}.$$

By applying the law of mass action to these equilibria, we have

$$K_1 = \frac{[TB']}{[BO_2'][T]} \qquad (1),$$

$$K_2 = \frac{[T_2B']}{[TB'][T]} \qquad (2),$$

$$K_1K_2 = K_3 = \frac{[T_2B']}{[BO_2'][T]^2} \qquad (3),$$

where the concentration of water is included in the equilibrium constant, as it may be regarded almost constant. The author will now inquire whether in the aqueous borate phase the above equilibria really exist or not. The relation of the concentrations of the substances in the equilibria are expressed as follows:

$$C_1 = \frac{[T]}{k}\,,$$

$$C_2 = 2[T_2B'] + [TB'] + [T] \qquad (4),$$

$$C_3 = [T_2B'] + [TB'] + [BO_2'] \qquad (5),$$

where k is distribution constant, C_1 concentration of diethyl tartrate in the ethereal phase, C_2 total concentration of diethyl tartrate in the aqueous borate phase, and C_3 total concentration of borate ion, all the concentrations being expressed in millimol per litre.

(10) *Rec. trav. chim.*, **51** (1932), 67, 955; J. Böeseken and N. Vermaas, *ibid.*, **54** (1935), 853.

Of these quantities, what can be analytically determined are C_1, C_2 and C_3. [T] can be estimated from the ratio k, in the case of ether–water system. Concentrations of other substances such as [T_2B'], [TB'] and [BO_2'] can not even indirectly be determined. But in a special case, when the sole product is of the mono-diol type (Reaction I), we are able to estimate [TB'] and [BO_2'] and thus calculate the equilibrium constant K_1. And in a similar way, if the sole product is of the di-diol type (Reaction II), we can estimate K_3.

Discussion of the Results. The experimental results already given in Table 3 are used for discussions on the equilibria considered above. The concentrations are now rewritten in millimol per litre and shown in Table 6, together with C_3 and [T].

Table 6.

No. of experiment	c_1	C_1	c_2	C_2	C_3	$[T]=C_1\times 2.22$
I	0.0026	1.3	0.0833	40.4	236	2.9
II	0.0063	3.1	0.155	75.4	234	6.9
III	0.0206	10.0	0.343	166.6	229	22.2
IV	0.0577	28.0	0.548	266	225	62.2
V	0.0876	42.5	0.640	310	223	94.4

Case 1. If K_3 is extremely small or $[T_2B']=0$,

then $$[TB'] = C_2 - [T],$$

and $$[BO_2'] = C_3 - [TB'].$$

K_1 can be calculated as shown in Table 7. K_1 is not constant and increases with the increasing concentration of diethyl tartrate.

Table 7.

No. of experiment	[T]	[TB']	[BO_2']	K_1
I	2.9	37.5	198	0.065
II	6.9	68.5	165	0.062
III	22.2	144	84.6	0.077
IV	62.2	204	21.2	0.155
V	94.4	216	7.0	0.327

Case 2. If K_1 is extremely small or $[TB'] = 0$,

then $[BO_2'] = (2C_3 + [T] - C_2)/2$,

and $[T_2B'] = C_2 + [BO_2'] - C_3 - [T]$.

K_3 can be calculated as shown in Table 8. K_3 is not also constant, and decreases with the increasing concentration of diethyl tartrate, which shows that reaction II is not dominant under this condition.

Table 8.

No. of experiment	[T]	$[BO_2']$	$[T_2B']$	K_3
I	2.9	217	18.4	0.0102
II	6.9	200	34.5	0.0036
III	22.2	157	72.2	0.00093
IV	62.2	123	102	0.000215
V	94.4	115	108	0.000105

We are, therefore, led to the conclusion that both equilibria equally exist in the solution. And if we give some appropriate value to K_3, then we may be able to make the value of K_1 nearly constant. For this purpose the following relations of the concentrations were derived from the formulæ (1), (3), (4) and (5):

$$[BO_2'] = \frac{C_3+[T]-C_2}{1-K_3[T]^2},$$

$$[TB'] = 2C_3+[T]-C_2-2[BO_2'].$$

Now if we put $K_3 = 8.5 \times 10^{-5}$ in the above formula, then K_1 becomes fairly constant, as shown in Table 9.

Table 9.

No. of experiment	[T]	$[BO_2']$	[TB']	K_1
I	2.9	199	37	0.065
II	6.9	166	67	0.059
III	22.2	88	137	0.070
IV	62.2	37	172	0.074
V	94.4	29	173	0.064
				mean 0.066

K_1 comes out nearly constant in a wide range of the concentration of the ester varying from 2.9 to 94.9, showing that the above considerations are reasonable.

Influence of Temperature on the Equilibrium. In exactly the same way as at 20°, calculations were made for the results of the distribution experiments at 15°. If we assume only one equilibrium, neither K_1 nor K_3 becomes constant also in this case, as shown in Tables 10–12.

Table 10.

No. of experiment	c_1	C_1	c_2	C_2	C_3	$[T] = C_1 \times 2.70$
I	0.0021	1.03	0.093	45	232	2.8
II	0.0024	1.2	0.101	49	234	3.1
III	0.0051	2.5	0.177	86	227	6.8
IV	0.0136	6.6	0.343	166	222	17.8
V	0.0170	8.3	0.392	190	225	22.4

Case 1. If K_3 is extremely small or $[T_2B'] = 0$,

then $[TB'] = C_2 - [T]$,

and $[BO_2'] = C_3 - [TB']$.

The values of K_1 are shown in Table 11.

Table 11.

No. of experiment	[T]	[TB']	$[BO_2']$	K_1
I	2.8	42	190	0.080
II	3.1	46	188	0.078
III	6.8	79	148	0.079
IV	17.8	149	73	0.114
V	22.4	168	57	0.134

Case 2. If K_1 is extremely small or $[TB'] = 0$,

then $[BO_2'] = (2C_3 + [T] - C_2)/2$,

and $[T_2B'] = C_2 + [BO_2'] - C_3 - [T]$.

The values of K_3 are given in Table 12.

However, if we assume the equilibria I and II coexist and put $K_3 = 4.5 \times 10^{-4}$, then we see also in this case that K_1 becomes nearly constant, as shown in Table 13.

Table 12.

No. of experiment	[T]	[BO_2']	[T_2B']	K_3
I	2.8	211	21.2	0.0131
II	3.1	211	22.9	0.0110
III	6 8	187	39.6	0.00463
IV	17.8	148	74.3	0.00158
V	22.4	141	83.8	0.00119

Table 13.

No. of experiment	[T]	[BO_2']	[TB']	K_1
I	2.8	191	40.6	0.077
II	3.1	189	44.2	0.075
III	6.8	151	72.6	0.071
IV	17.8	85.5	124	0.081
V	22.4	74.0	134	0.081
				mean 0.077

From the above considerations, the value of the equilibrium constant K_1 is estimated as follows: 0.077 at 15°C. and 0.066 at 20°C. By the aid of van't Hoff's reaction isochore

$$\frac{d \ln K}{dT} = \frac{Q}{RT^2},$$

the heat of reaction Q is evaluated as 5200 cals.

$$BO_2' + T \rightleftarrows TB' + Q.$$

This is a probable value to be expected of a reaction of this nature. Hermans[11] obtained as the heat of reaction values 3738—5450 cals. in the cases of analogous reactions of various cyclic diols with acetone.

Ratio of the Concentration of the Complex Ion of Mono-diol Type to that of Di-diol Type. This ratio can be expressed in the following terms from the relations (2) and (3):

$$\frac{[T_2B']}{[TB']} = K_2[T] = \frac{K_3}{K_1}[T].$$

(11) *Z. physik. Chem*, **113** (1924), 337.

The ratio must therefore increase with increasing [T], but may not amount to a high value, because the ratio K_3/K_1 is really found markedly small. Therefore, as an answer to an interesting question whether the main product of the reaction be TB′ or T_2B', the above considerations of these experimental results give a conclusion that under these conditions both reaction products exist, but the main product is that of the mono-diol type (TB′).

Distribution in the Ether—Boric Acid System. The author further measured the distribution of diethyl tartrate between ether and aqueous boric acid solution, the results of which are shown in Table 14.

Somewhat unexpectedly, the distribution ratio is found not only nearly constant, and independent of the concentration, but almost equal to that of ether–water system. We see that the presence of boric acid does not affect the distribution ratio, which shows clearly the inefficiency of the use of boric acid in the purification process already mentioned. This unexpected fact is, however, be explained by the following considerations:

Table 14. Distribution of diethyl tartrate between ether and 1/4 mol boric acid at 15°.

c_1	c_2	c_2/c_1
0.0305	0.0826	2.71
0.0618	0.1595	2.58
0.0921	0.2452	2.66
0.1212	0.3380	2.79

For the sake of generality, we assume at first that free boric acid can combine with the ester in both phases, the distribution coefficient of boric acid in ether–water system being known to be 1:44. Thus the equilibrium of distribution in the ether–boric acid system is represented by the following scheme:

$$\begin{array}{lc} \text{Ethereal phase:} & HBO_2+T \rightleftarrows TBH \\ & \downarrow\uparrow \quad \downarrow\uparrow \\ \text{Boric acid phase:} & HBO_2+T \rightleftarrows TBH \end{array}$$

By applying the law of mass action to these equilibria, we obtain:

$$K_e = \frac{[TBH]_e}{[HBO_2]_e[T]_e}; \qquad K_b = \frac{[THB]_b}{[HBO_2]_b[T]_b}.$$

If we take into account the following concentration relations:

$$C_1 = [T]_e + [TBH]_e; \qquad C_2 = [T]_b + [TBH]_b,$$

then the distribution ratio may be expressed as follows:

$$\frac{C_2}{C_1} = \frac{[T]_b(1+K_b[HBO_2]_b)}{[T]_e(1+K_e[HBO_2]_e)}$$

$$= k \times \frac{1+K_b[HBO_2]_b}{1+K_e[HBO_2]_e} .$$

The actual experimental results show that C_2/C_1 is nearly equal to k, so it must become

$$\frac{1+K_b[HBO_2]_b}{1+K_e[HBO_2]_e} = 1 .$$

To satisfy this relation the numerical values of the two terms, $K_b[HBO_2]_b$ and $K_e[HBO_2]_e$, must be either equal to each other or be by far smaller than 1. The latter case is considered to be natural. To explain this we take for simplicity only the mono-diol type of the reaction into consideration.

$$HBO_2 + T \rightleftarrows TBH \quad \text{(undissociated diethyl boro-tartrate)} \qquad (6)$$

$$TBH \rightleftarrows H^{\cdot} + TB' \qquad (7)$$

$$HBO_2 \rightleftarrows H^{\cdot} + BO_2' \qquad (8)$$

$$BO_2' + T \rightleftarrows TB' \qquad (9)$$

By applying the law of mass action to these equilibria, we have the following expressions:

$$K_1 = \frac{[TBH]}{[HBO_2][T]} ; \qquad k_1 = \frac{[H^{\cdot}][TB']}{[TBH]} ;$$

$$K_2 = \frac{[TB']}{[BO_2'][T]} ; \qquad k_2 = \frac{[H^{\cdot}][BO_2']}{[HBO_2]} .$$

It follows:

$$\frac{k_2}{k_1} = \frac{[BO_2'][TBH]}{[HBO_2][TB']} ; \qquad \frac{K_1}{K_2} = \frac{[BO_2'][TBH]}{[HBO_2][TB']} ; \qquad \frac{k_2}{k_1} = \frac{K_1}{K_2} .$$

As the boro-diol complex is generally a much stronger acid than boric acid, it follows:

$$k_1 \gg k_2 . \quad \therefore \quad K_2 \gg K_1 . \quad (K_2 = 0.077 \text{ at } 15^\circ) .$$

Now K_1 corresponds to K_b or K_e, so these numerical values must be very small. Consequently its product with the actual concentration of

boric acid, $K[HBO_2]$, may be regarded to be small as compared with 1. Thus the fact that the distribution ratio C_2/C_1 is nearly equal to k has been explained.

From the above experiments and the analysis of the results, we see that free boric acid comes into union with diethyl tartrate only in small proportions, and that the extraction of diethyl ester from the ethereal layer by means of boric acid is not favourable, owing to the fact that boric acid itself is soluble in ethereal phase. Thus it is shown both experimentally and theoretically that strongly dissociable borate KBO_2 favours the complex formation than borax, and consequently is suitable for the extraction of diol soluble in ether.

The author wishes to thank Professor M. Katayama for helpful discussions.

Summary

(1) The distribution of diethyl tartrate between ether and water containing boric acid, borax or potassium metaborate (KBO_2), has been measured.

(2) The results of the experiment on the system of ether–water have been found to follow simply the distribution law of Nernst.

(3) The distribution ratio in the system of ether–aqueous borate solution has been found to increase with the increasing electrolytic dissociation of borate, and this relation has been explained theoretically. The order of the magnitude of the distribution ratio to ether is water< borax<potassium metaborate.

(4) The equilibrium of boro-diol complex in the borate phase has been studied, and it has been shown that in the borate phase two complex compounds, i.e. those of mono-diol and di-diol types, must coexist, and the equilibrium constant (between ions) has been estimated.

(5) By the study of the temperature coefficient, the reaction of complex formation has been found to be exothermic and the heat of reaction has been estimated.

(6) The distribution of diethyl tartrate in the system of ether–water has been found indifferent to the addition of free boric acid, and this fact has been explained to be due to the insignificant dissociation of boric acid.

Musashi Higher School,
Itabashiku, Tokyo.

Electrolytic Reduction of N-Phenyl-succinimide.

By Buhei SAKURAI.

(Received March 14, 1938.)

The direct reduction of *N*-phenyl-succinimide to *N*-phenyl-pyrrolidine is so difficult that no chemical method has hitherto succeeded even in reducing one of the two carbonyls. By using a lead cathode Tafel[1] attained it electrolytically, but still his method was not fruitful to reduce both of the carbonyls.

Phenyl derivatives are generally seen to be less reducible than corresponding methyl or ethyl derivatives. So that, in electrolytic reduction of the former the more concentrated acid and the higher temperature are required.

As the present writer[2] had previously succeeded in completely reducing succinimide and its methyl and ethyl derivatives by using a zinc amalgam cathode, the trial was now undertaken to see whether the same method is successful to reduce *N*-phenyl-succinimide or not.

For the complete reduction of this substance far stronger reducing action seems necessary. But the use of the stronger sulphuric acid and the higher temperature are feared for destroying the reduction product, if any. Selection of the best conditions for the electrolytic reduction thus becomes very difficult. After many trials the present writer could obtain *N*-phenyl-pyrrolidine in a 30% yield by passing a current of high density, to a zinc amalgam cathode in a 50% sulphuric acid solution at a temperature of 25°.

N-phenyl-succinimide or succinanil used in the electrolysis was prepared after Menschtkin's method,[3] by fusing a mixture of succinic acid and aniline in a retort, and purified by recrystallizing the product from alcohol. It formed colourless needles melting at 156°.

In the reduction of this substance it must be noted that a 50% sulphuric acid solution which acts most effectively upon other substances of similar constitution is also fit for reducing phenyl-pyrrolidone into phenyl-pyrrolidine, but it is unfavourable for reducing phenyl-succinimide into phenyl-pyrrolidone, and for the latter purpose a 90% sulphuric acid

(1) Tafel, *Ber.*, **32** (1899), 74.
(2) B. Sakurai, this Bulletin, **10** (1935), 311; **11** (1936), 41.
(3) Menschtkin, *Ann.*, **162** (1873), 166.

is the most favourable. It is, therefore, not wise to employ a solution of 50% sulphuric acid from the start. It is advisable to divide the electrolysis into two stages: In the first stage the material is reduced to *N*-phenyl-pyrrolidone by passing a current of low density with a lead cathode, and in next stage the electrolysis is intensified for the completion of the reduction, using high current density, a zinc amalgam cathode and a dilute solution of 50% sulphuric acid.

The conditions of the electrolysis taken by the author are as shown in Table 1.

Table 1.

	First part of electrolysis	Second part of electrolysis
Cathode	Lead plate; 100 sq. cm. of area	Zinc amalgam; 15.8 sq. cm. of area
Catholyte	100 c.c. of 90% sulphuric acid to which 10 g. of *N*-phenyl-succinimide was added	Catholyte was diluted till H_2SO_4 becomes about 50%
Anode	Lead plate	Lead plate
Anolyte	50% sulphuric acid	50% sulphuric acid
Current density	5 amp. per 100 sq. cm.	95 amp. per 100 sq. cm.
Time of electrolysis	10 hours	24 hours
Current quantity	32.5 F. per mol	209 F. per mol
Temperature	55°	25°

In the electrolysis of the first stage, the vessel containing the catholyte was not cooled from outside. The temperature of the catholyte rose gradually up to 55° and the material wholly dissolved in the catholyte in the course of electrolysis. If all of the material is put in at a time, it makes the solution foamy owing to its small solubility. It is, therefore, convenient to add half of it at first, and waiting till all have been dissolved (some two hours are required), the other half is added to it. In 5 hours all were dissolved, but to complete the electrolysis the current was passed for another 5 hours.

Now lead cathode was replaced with zinc amalgam and the catholyte was diluted with 130 c.c. of water, and a spiral lead tube was inserted in it, through which water was passed. The vessel was kept in a tub in which cold water circulated, so as to cool the catholyte from inside and outside. The electrolyte was kept stirred vigorously, and electric current of 15 amp. was passed.

After the completion of the electrolysis a colourless liquid obtained was shaken with ether, and about 1.2 g. of needle crystals were obtained. After cooling with water, when the electrolytic solution was made alkaline with sodium hydroxide solution, dark-brown oily substance of peculiar smell appeared on the surface. By extracting it with ether 2.5 g. of oil were obtained. The first substance from the acid solution was proved to be *N*-phenyl-pyrrolidone, which, when crystallized from ether, melted at 68°.

The second substance obtained from the alkaline solution was brown nonvolatile oil having a peculiar smell, insoluble in water but easily soluble in alcohol or ether. The solution in ether showed a bright red colour. The oil is basic and gradually dissolves in a dilute acid solution. Its platinum double chloride forms yellow needles melting at 175° with decomposition. (Found: Pt, 27.8. Calculated for $(C_{10}H_{13}N)_2H_2PtCl_6$: Pt, 27.8%).

The above-mentioned properties thus far confirmed are identical with those of the *N*-phenyl-pyrrolidine[4] prepared in purely chemical manner.

The writer expresses his sincere thanks to Dr. Motooki Matsui, President of the Kyoto Imperial University, at whose suggestion this work was accomplished.

The Osaka Women's College,
Sumiyoshi, Osaka.

(4) Lyman C. Craig and R. M. Hixon, *J. Am. Chem. Soc.*, **52** (1930), 804.

On Experimental Conditions for the Half-shadow Polarimetry.*

By Ryutaro TSUCHIDA.

(Received March 23, 1938.)

Measurement of optical rotation of coloured substances is generally very difficult and consequently the accuracy of the measurement is considerably deteriorated especially in the spectral regions of their absorption bands. For the purpose of overcoming the difficulty, the author has carried out the following calculation, making use of a proposed definition of sensitivity of the measurement.

(1) The Position of the Analyser Corresponding to the Maximal Sensitivity. On traversing a layer of an optically active substance, a linearly polarised ray has only its plane of vibration changed in the spectral regions in which no absorption takes place. In the absorption bands, however, an elliptically polarised ray will result according to the circular dichroism of the substance. The incident plane polarised light whose amplitude is a_0 may be regarded as a resultant of two circularly polarised light of opposite sense and of equal amplitude $\frac{a_0}{2}$. After passing through d cm. of c mol/l. solution of an optically active substance, the two rays will have their amplitudes changed as follows,

$$\begin{cases} a_r = \frac{a_0}{2} e^{-\frac{1}{2}\varepsilon_r cd} \\ a_l = \frac{a_0}{2} e^{-\frac{1}{2}\varepsilon_l cd} \end{cases} \qquad (1)$$

where ε_l and ε_r denote the molar extinction coefficient of the substance for left and right circularly polarised light. Then a_L and a_K, the amplitudes corresponding to the major and the minor axis of the resultant elliptically polarised light may be expressed as

$$\begin{cases} a_L = \frac{a_0}{2}\left\{e^{-\frac{1}{2}\varepsilon_l cd} + e^{-\frac{1}{2}\varepsilon_r cd}\right\} \\ a_K = \frac{a_0}{2}\left\{e^{-\frac{1}{2}\varepsilon_l cd} - e^{-\frac{1}{2}\varepsilon_r cd}\right\} \end{cases} \qquad (2).$$

* Translation of an article published in Japanese. *J. Chem. Soc. Japan*, **56** (1935), 1312.

In half-shadow polarimetry two such elliptically polarised rays will be produced in front of the analyser and the angle between their major axes is equal to the aparture between the two vibration directions of the polariser i.e. 2θ.

Let the angle between the bisectrix and the vibration direction of the analyser be ω, then the intensities of the two rays after passing through the analyser are given by

$$\left.\begin{aligned} I_1 &= a_L^2\cos^2(\omega+\theta)+a_K^2\sin^2(\omega+\theta) \\ I_2 &= a_L^2\cos^2(\omega-\theta)+a_K^2\sin^2(\omega-\theta) \end{aligned}\right\}.$$

$$\therefore \quad I_1-I_2=(a_K^2-a_L^2)\sin 2\omega \sin 2\theta \tag{3}$$

$$I_1+I_2=2a_L^2(\cos^2\omega\cos^2\theta+\sin^2\omega\sin^2\theta) + 2a_K^2(\sin^2\omega\cos^2\theta+\cos^2\omega\sin^2\theta) \tag{4}.$$

When $I_1=I_2$, we obtain from (3)

$$\sin 2\omega = 0 \qquad \therefore \quad \omega = 0 \text{ or } \frac{\pi}{2}.$$

That is the two fields will be of equal brightness when ω takes the value 0 or 2π.

Next it must be decided which value of ω is more suitable for the measurement. As can be easily seen, the comparison of the brightness of the two fields will be easier when the difference between $\frac{\partial I_1}{\partial\omega}$ and $\frac{\partial I_2}{\partial\omega}$ is greater and the intensity is smaller. The following function S, therefore, will give the measure of sensitivity.

$$S=\left\{\frac{\partial(I_1-I_2)}{\partial\omega}\cdot\frac{1}{I_1+I_2}\right\}^2 \tag{5}.$$

From (3)

$$\frac{\partial(I_1-I_2)}{\partial\omega}=2\,a_K^2-a_L^2)\cos 2\omega\sin 2\theta \tag{6}.$$

Substituting (4), (6) and $\omega=0$ or $\omega=\frac{\pi}{2}$, we obtain from (5)

$$(S)_{\omega=0}=\left\{\frac{(a_K^2-a_L^2)\sin 2\theta}{a_L^2\cos^2\theta+a_K^2\sin^2\theta}\right\}^2$$

and

$$(S)_{\omega=\frac{\pi}{2}}=\left\{\frac{(a_L^2-a_K^2)\sin 2\theta}{a_L^2\sin^2\theta+a_K^2\cos^2\theta}\right\}^2 \tag{7}.$$

Since $\theta < \frac{\pi}{4}$ and consequently $\sin\theta < \cos\theta$,

$$(S)_{\omega=0} < (S)_{\omega=\frac{\pi}{2}} .$$

Thus the sensitivity should be greater, when the analyser is placed at right angles to the bisectrix of the acute angle between the major axes of the elliptically polarised rays. This conclusion coincides with our experience.

(2) **The Angle between the Two Vibration Directions of the Half-shadow Polariser.** Next let us determine the angle θ which gives the maximal value of S when the analyser is set so as to conform with the above conclusion.

From (7)

$$\left(\frac{\partial S}{\partial\theta}\right)_{\omega=\frac{\pi}{2}} = \frac{4(a_L^2-a_K^2)^2(a_K^2\cos^2\theta-a_L^2\sin^2\theta)\sin 2\theta}{(a_L^2\sin^2\theta+a_K^2\cos^2\theta)^3} .$$

Therefore $(S)_{\omega=\frac{\pi}{2}}$ will be maximal when

$$a_K^2\cos^2\theta-a_L^2\sin^2\theta = 0 \qquad \tan\theta = \pm\frac{a_K}{a_L} .$$

Substituting (2) in the relation, we obtain

$$\tan\theta = \frac{e^{-\frac{1}{2}\varepsilon_l cd}-e^{-\frac{1}{2}\varepsilon_r cd}}{e^{-\frac{1}{2}\varepsilon_l cd}+e^{-\frac{1}{2}\varepsilon_r cd}} = \frac{1-e^{\frac{1}{2}(\varepsilon_l-\varepsilon_r)cd}}{1+e^{\frac{1}{2}(\varepsilon_l-\varepsilon_r)cd}} .$$

When $(\varepsilon_l-\varepsilon_r)cd$ is small,

$$\theta \simeq \frac{1}{4}(\varepsilon_r-\varepsilon_l)cd \qquad (8).$$

Thus the angle between the two vibration directions of a half-shadow polariser which would give the maximal accuracy is theoretically $\frac{1}{2}(\varepsilon_r-\varepsilon_l)cd$, and depends on the concentration of the solution and the thickness of the layer as well as the circular dichroism of the substance. The circular dichroism, however, has been measured only for a limited number of optically active substances, and the above conclusion could not be applied to substances whose circular dichroism is unknown. Moreover, the intensity of available light-sources and the sensitivity of photographic plates are also limited and consequently the theoretical value of θ could not be attained in practical measurement.

For practical purpose the angle between the polarising prisms may be varied according to the following calculation. The light intensity after passing through the analyser is from (4) and (2)

$$I = \frac{I_1 + I_2}{2} = a_L^2 \sin^2\theta + a_K^2 \cos^2\theta$$

$$= \frac{a_0^2}{4}\left\{e^{-\varepsilon_l cd} + e^{-\varepsilon_r cd} - 2e^{-\frac{1}{2}(\varepsilon_l+\varepsilon_r)cd}\cos 2\theta\right\} .$$

Let the extinction coefficient of the racemic substance be ε, then

$$\varepsilon = \frac{\varepsilon_l + \varepsilon_r}{2} .$$

Assuming the initial intensity of the plane polarised light as $I_0 = a_0^2$,

$$I = \frac{I_0}{4} e^{-\varepsilon cd}\left\{e^{(\varepsilon-\varepsilon_l)cd} + e^{(\varepsilon-\varepsilon_r)cd} - 2\cos 2\theta\right\}$$

$$= \frac{I_0}{2} e^{-\varepsilon cd}(1-\cos 2\theta) = I_0 e^{-\varepsilon cd}\sin^2\theta .$$

$$\therefore \quad \sin^2\theta = \frac{I}{I_0} e^{\varepsilon cd} \qquad \theta \simeq \sqrt{\frac{I}{I_0}} e^{\frac{1}{2}\varepsilon cd} . \tag{9}$$

For the spectral regions in which no absorption bands exist, the ratio of I to I_0, which depends on the intensity of light source and the sensitivity of photographic plates used, is usually of the order of 10^{-2} to 10^{-3}.

Therefore $$\theta \simeq \sqrt{\frac{I}{I_0}} = 10^{-1} \sim 10^{-1.5} = 5.7^\circ \sim 1.8^\circ .$$

That is, the mean value of 2θ is 7.5°. In other words, for wave lengths for which no absorption takes place the angle of the vibration directions should be 7.5°. This conclusion is coincident with the fact that in ordinary fixed half-shadow polariser, the two parts of the split prism contain an angle of about 8°.

In the spectral regions of absorption bands, the angle 2θ should be adjusted so as to contain $7.5^\circ \times e^{\frac{1}{2}\varepsilon cd}$; or approximately $7.5^\circ \times (1 + \frac{1}{2}\varepsilon cd)$.

The author wishes to express sincere thanks to Prof. Y. Shibata for his kind interest in this work.

Chemical Laboratory,
Osaka Imperial University.

Der katalytische Isotopenaustausch des gasförmigen Sauerstoffs. I. Die Austauschreaktion der Sauerstoffatome zwischen Sauerstoff und Wasserdampf sowie Kohlendioxyd auf der Oberfläche des Platinschwamms und metallischen Platins.

Von Noriyoshi MORITA und Toshizo TITANI.

(Eingegangen am 29. März 1938.)

Inhaltsübersicht. Die Austauschreaktion der O-Atome zwischen gasförmigen Sauerstoff und Wasserdampf bzw. Kohlendioxyd auf der Oberfläche des Platinschwamms bzw. metallischen Platins wurde untersucht, indem wir das Gasgemisch aus den genannten Substanzen über die auf verschiedenen Temperaturen erhitzten Katalysatoren langsam leiteten. Beim Versuch mit Sauerstoff und Wasserdampf war der Gehalt des letzteren, hingegen beim Versuch mit Sauerstoff und Kohlendioxyd der des ersteren an schwerem Sauerstoff von vornherein angereichert worden, und aus dessen Abnahme nach dem Experiment wurde die Austauschreaktion untersucht. Durch diese Versuche wurde gefunden, dass die Austauschreaktion zwischen gasförmigem Sauerstoff und Wasserdampf auf Platinschwamm oberhalb etwa 550°C., dieselbe Reaktion auf metallischem Platin erst oberhalb 760°C., und die Reaktion zwischen gasförmigen Sauerstoff und Kohlendioxyd auf Platinschwamm oberhalb etwa 600°C. lebhaft stattfindet, bis das Austauschgleichgewicht schnell gebildet wird. Aber auch bei niedrigeren Temperaturen, d.h. bei etwa 300° bis 500°C. wird die Reaktion schon deutlich bemerkbar und zwar stimmt dieses Temperaturgebiet eben mit dem, wo die „zweite" aktivierte Adsorption des Sauerstoffs auf der Platinoberfläche einsetzt, nahezu überein. Daraus wurde geschlossen, dass bei der lebhaften Austauschreaktion des Sauerstoffgases auf der Platinoberfläche die aktivierte Adsorption des Sauerstoffs eine massgebende Rolle spielt. Es wurde weiter gefunden, dass die Austauschreaktion zwischen gasförmigen Sauerstoff und Wasserdampf um so vollständiger verläuft je langsamer das Reaktionsgemisch über dem Katalysator strömt, dagegen die Austauschgeschwindigkeit vom Mischungsverhältnis der beiden Substanzen in weiten Grenzen fast unabhängig ist.

Einleitung. Es gibt dafür kaum einen Zweifel, dass die Untersuchungen über den katalytischen Isotopenaustausch der O-Atome zwischen sauerstoffhaltigen Substanzen, insbesondere die zwischen gasförmigem Sauerstoff und anderen Sauerstoffverbindungen, über den Chemismus der Oxydationskatalyse einiges Licht werfen kann. Aus diesem Grunde haben wir die vorliegenden Versuche unternommen, und ein Teil der Versuchsergebnisse wurde bereits schon bekannt gegeben.(1) Aber weil durch die späteren Versuche die Experimentalresultate bei weitem vermehrt worden sind, wollen wir dies ausführlich, aber nach-

(1) N. Morita und T. Titani, dies Bulletin, **12** (1937), 104.

einander veröffentlichen, da die einmalige Veröffentlichung der ganzen bisher gewonnenen Versuchsergebnisse wegen des beschränkten Raumes nicht gestattet ist. Die von uns ausgeführten Versuche beschränkten sich hauptsächlich auf die Austauschreaktion der O-Atome zwischen gasförmigem Sauerstoff und Wasserdampf auf der Oberfläche verschiedener Arten der Metalle und Metalloxyde, obwohl von Zeit zu Zeit auch andere Arten der Austauschreaktion, wie z.B. die Reaktion zwischen Sauerstoff und Kohlendioxyd untersucht wurde. Das Hauptresultat, das bisher gewonnen wurde, ist, dass der vollständige Austausch der O-Atome fast immer stattfindet, wenn der betreffende Katalysator oberhalb einer bestimmten Temperatur erhitzt wird. Diese für einen gegebenen Katalysator charakteristische Grenztemperatur ist aber im allgemeinen nicht sehr hoch und liegt gewöhnlich zwischen 200° bis 800°C. Es liegt daher die Vermutung nahe, dass der schnelle und vollständige Austausch der O-Atome zwischen gasförmigem Sauerstoff und irgendeiner sauerstoffhaltigen Verbindung auf einem Oxydationskatalysator durch die aktivierte Adsorption des Sauerstoffs auf der betreffenden Katalysatoroberfläche herbeigeführt wird.

Die allgemeine Versuchsanordnung. Das Experiment wurde immer mit derselben Apparatur, die schematisch in Abb. 1 dargestellt ist, ausgeführt.

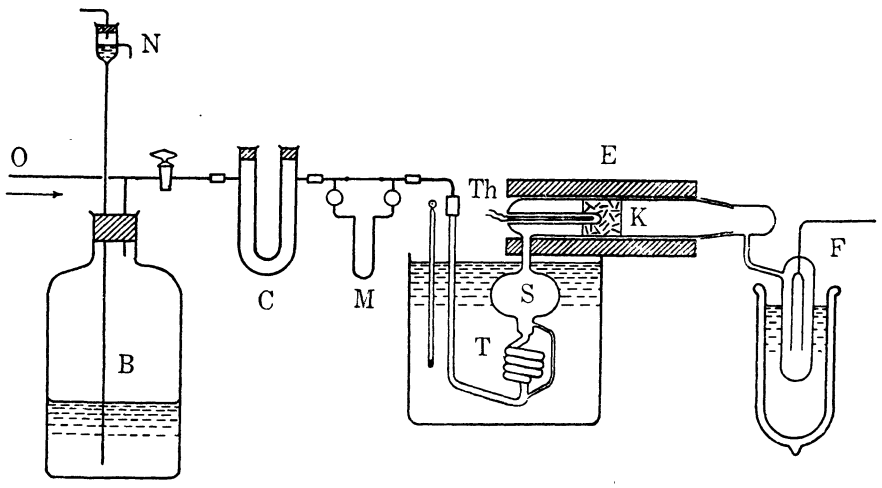


Abb. 1. [Die Versuchsanordnung.

Der gasförmige Sauerstoff wird durch die Elektrolyse der konzentrierten NaOH-Lösung in einem (nicht in der Abb. gezeigten) Elek-

trolyseur mit einer Nickelanode entwickelt. Dabei wird die Entwicklungsgeschwindigkeit des Sauerstoffs durch eine geeignete Wahl der Stromstärke durch den Elektrolyseur kontrolliert. In den meisten Fällen verwendeten wir dazu 12 Amp. elektrischen Strom, wodurch der Sauerstoff mit der Geschwindigkeit von 40 c.c. pro Minute (bei Zimmertemperatur und unter gewöhnlichem Druck gemessen) entwickelt wird. Der so entwickelte Sauerstoffstrom wird zunächst über das auf 400°C. erhitzte Kupferoxyd geleitet, um den Sauerstoff von darin zugemischtem Wasserstoff vollständig zu befreien. Dann wurde der Sauerstoff, nachdem er nacheinander mit Chromsäure-Schwefelsäure-Gemisch und NaOH-Lösung gewaschen worden ist, durch die Öffnung O in den Sauerstoffbehälter B hineingeleitet. Dieser letztere wird eingeschaltet, um den Druck infolgedessen die Strömungsgeschwindigkeit des Sauerstoffs mittels des Niveauapparats N konstant zu halten. Aus diesem Behälter B strömt der Sauerstoff durch das Chlorcalziumrohr C und den Strömungsmesser M in das Sättigungsgefäss S hinein. Dieses Gefäss S, das aus einer geräumigen Glaskugel und einer darunter zugeschmolzenen Glasschlange besteht, enthält in seinem Schlangenteil eine Menge schweres Wasser, dessen Gehalt an schwerem Sauerstoff durch die Destillation um einen gewissen Betrag vergrössert worden ist. Da dieses Gefäss S als Ganzes in einem Thermostat T eingetaucht ist, wird das Sauerstoffgas während seines Aufsteigens durch den Schlangenteil des Gefässes mit dem Dampf des schweren Wassers gesättigt, so dass durch die geeignete Wahl der Temperatur des Thermostats T ein Gasgemisch aus Sauerstoff und schwerem Wasserdampf von bestimmter Zusammensetzung gebildet werden kann. Hielt man z.B. die Temperatur des Thermostats T konstant auf 72°C., dann entstand im Sättigungsgefäss ein Gasgemisch von der Zusammensetzung $O_2:H_2O = 2:1$, da der Dampfdruck des gewöhnlichen Wassers bei dieser Temperatur gerade 1/3 Atm. beträgt und der des benutzten schweren Wassers infolge der geringen Anreicherung des schweren Sauerstoffs praktisch identisch mit der des gewöhnlichen Wassers betrachtet werden kann. Durch diese Zumischung des Wasserdampfs in den Sauerstoffstrom wird aber die Strömungsgeschwindigkeit des Gases mehr oder weniger vergrössert. Wenn z.B., wie oben erwähnt, der Partialdruck des Wasserdampfs im gebildeten Gasgemisch 1/3 Atm. beträgt, dann wird die Strömungsgeschwindigkeit um etwa 50% vermehrt, so dass, falls die Entwicklungsgeschwindigkeit des Sauerstoffs, wie in den meisten Fällen, gleich 40 c.c. pro Minute ist, dann die Strömungsgeschwindigkeit des gebildeten Gasgemisches (bei Zimmertemperatur und unter gewöhnlichem Druck gemessen) 60 c.c. pro Minute betragen muss. Das so gebildete Gasgemisch wird dann in das Kataly-

satorrohr K hineingeschickt. Dieses Rohr, das aus Quarzglas besteht und 2 cm. l. W. und 15 cm. Länge besitzt, enthält in seiner Mitte den zu untersuchenden Katalysator K und wird von aussen durch den elektrischen Ofen E auf einer konstanten Temperatur erhitzt. Die Temperatur des Katalysators wird mittels eins von aussen darin eingeschobenen Thermoelements Th gemessen. Das aus diesem Katalysatorrohr ausgeströmte Gasgemisch wird zum Schluss in die von aussen mit Kohlensäureschneegemisch abgekühlte Flasche F hineingeleitet und dort der Wasserdampf vollständig kondensiert aufgefangen.

Wenn auf diese Weise das im Sättigungsgefäss S befindliche schwere Wasser, dessen Volumen durchschnittlich 15 c.c. beträgt, durch das Katalysatorrohr K restlos abdestilliert und in der Flasche F vollständig kondensiert aufgefangen worden ist, wird es ausgegossen und dessen Dichte, nachdem es richtig gereinigt worden ist, mittels eines Quarzschwimmers im Vergleich mit der des gewöhnlichen Wassers genau gemessen. Das Messfehlerbereich liegt innerhalb $\pm 0.5\,\gamma$. Der so gefundene (endliche) Dichteüberschuss des schweren Wassers dem gewöhnlichen Wasser gegenüber wird dann mit dem anfänglichen Dichteüberschuss des benutzten schweren Wassers verglichen und aus deren Differenz wird der Schluss über die Austauschreaktion der O-Atome zwischen gasförmigem Sauerstoff und Wasserdampf auf der Oberfläche des betreffenden Katalysators gezogen.

Experiment 1. Austauschreaktion zwischen gasförmigem Sauerstoff und Wasserdampf auf Platinschwamm bei verschiedenen Temperaturen. Der Platinschwamm wurde dadurch hergestellt, dass wir käufliches „Platinchlorid" durch Erhitzung teilweise zersetzten und das dadurch erhaltene Rohprodukt im Katalysatorrohr mittels elektrolytischen Wasserstoffs bei ca. 200°C. vollständig reduzierten. Der so bereitete Platinschwamm besass das scheinbare Volumen von etwa 1.7 c.c. Das zu diesem Versuch benutzte an schwerem Sauerstoff angereicherte schwere Wasser wurde durch die fraktionierte Destillation des gewöhnlichen Wassers bereitet und besass den gesamten Dichteüberschuss von $22.2\,\gamma$, wovon $18.0\,\gamma$ von der Anreicherung des schweren Sauerstoffs herrührte, wie sich aus einer isotopischen Analyse ergab.[2] Etwa 15 c.c. dieses Wassers wurde ins Sättigunsgefäss (S in Abb. 1) hineingegossen, und durch dieses Wasser, das konstant auf 72°C. erwärmt war, leiteten wir den Sauerstoff, der durch die Elektrolyse des gewöhnlichen Wassers entwickelt wurde, mit der Geschwindigkeit von 40 c.c. pro Minute. Auf diese Weise erhielten wir die Strömung des Gasgemisches von der Zusammen-

(2) Vgl. z.B. N. Morita, K. Goto und T. Titani, dies Bulletin, **13** (1938), 99.

setzung $O_2:H_2O = 2:1$ mit der Geschwindigkeit von 60 c.c. pro Minute (vgl. oben). Das so gebildete Gasgemisch wurde dann über den Platinschwamm, der im Katalysatorrohr (K in Abb. 1) auf einer bestimmten Temperatur erhitzt war, so lange geleitet, bis das im Sättigungsgefäss befindliche 15 c.c. schwere Wasser durch das Katalysatorrohr in die Kühlflasche (F in Abb. 1) restlos abdestillierte. Dann wurde der endliche Dichteüberschuss Δs_e des abdestillierten Wassers, nachdem es richtig gereinigt worden war, mittels eines Quarzschwimmers genau gemessen und mit dem anfänglichen Dichteüberschuss Δs_a des betreffenden Wassers verglichen. Die so erhaltenen Versuchsergebnisse sind in Tabelle 1 zusammengestellt, wo die Versuchsnr. in der ersten Vertikalreihe die zeitliche Reihenfolge der einzelnen Versuche zeigt.

Tabelle 1. Austauschreaktion zwischen O_2 und H_2O auf Platinschwamm bei verschiedenen Temperaturen.

$O_2: H_2O = 2:1$, $\Delta s_a = 22.2\,\gamma$.

Versuchsnr.	Temperatur °C.	Δs_e in γ	$\Delta s_a - \Delta s_e$ in γ	Austauschmass $\%A$
3	300	21.5	0.7	4
4	400	19.3	2.9	17
7	430	14.2	8.0	47
8	470	9.1	13.1	78
1	500	12.1	10.1	60
9	540	6.5	15.7	93
10	580	5.9	16.3	96
5	600	5.9	16.3	96
2	730	5.0	17.2 } 16.9	102
6	800	5.7	16.5 }	98

Vom gesamten anfänglichen Dichteüberschuss $\Delta s_a (= 22.2\,\gamma)$ des verwendeten schweren Wassers rührten $18.0\,\gamma$, wie schon oben erwähnt, von der Anreicherung des schweren Sauerstoffs her. Dagegen war der damit zu reagierende elektrolytische Sauerstoff, in der Form von Wasser gemessen, um etwa $1\,\gamma$ leichter als gewöhnliches Wasser. Da aber diese beiden Substanzen im Verhältnis von $O_2:H_2O = 2:1$ vermischt und deren O-Atome miteinander ausgetauscht wurden, musste der anfängliche Dichteüberschuss Δs_a des schweren Wassers, wie eine einfache Rechnung ergibt, beim vollständigen Austausch um etwa $16 \pm 1\,\gamma$ abnehmen, d.h. $\Delta s_a - \Delta s_e = 16 \pm 1\,\gamma$ betragen, vorausgesetzt, dass schwerer Sauerstoff zwischen beiden Substanzen gleichmässig verteilt wird. Dieser Wert steht

aber sehr nahe dem Mittelwert (= 16.9 γ) der wirklich gefundenen Dichteabnahme ($\Delta s_a - \Delta s_e$) bei den letzten zwei Versuchen (Versuche 2 und 6). Wir nahmen deshalb an, dass bei diesen zwei Versuchen ein vollständiger Austausch wirklich erzielt wurde und unter dieser Annahme massen wir den Grad des Austausches durch den folgenden Quotient (1):

$$\%A = \frac{(\Delta s_a - \Delta s_e)}{16.9} \times 100 \qquad (1).$$

Das so berechnete sozusagen „prozentuale Austauschmass" $\%A$ geben wir in der letzten Vertikalreihe der Tabelle wieder.

Experiment 2. Austauschreaktion zwischen gasförmigem Sauerstoff und Kohlendioxyd auf Platinschwamm bei verschiedenen Temperaturen. Bei diesem Versuch wurde die Austauschreaktion der O-Atome zwischen gasförmigem Sauerstoff, dessen Gehalt an schwerem Sauerstoff vergrössert worden war, und gewöhnlichem Kohlendioxyd, das sich mit gewöhnlichem Wasser im isotopischen Austauschgleichgewicht befand, auf der Oberfläche des Platinschwamms unter Benutzung derselben Apparatur wie oben untersucht. Der dazu benutzte Platinschwamm war ebenfalls derselbe wie der beim letzten Versuche verwendete. Das schwere Sauerstoffgas wurde durch die Elektrolyse des Wassers, dessen Gehalt an schwerem Sauerstoff durch die fraktionierte Destillation vermehrt worden war, entwickelt. Das Wasser, das durch die Reduktion dieses Sauerstoffgases mittels Bombenwasserstoffs gebildet wurde, erwies sich um 17.5 γ schwerer als gewöhnliches Wasser. Dagegen war das Wasser, das durch die Reduktion des Sauerstoffs des zum Versuch benutzten Kohlendioxyds mittels Bombenwasserstoffs erhalten wurde, um 5.5 γ schwerer als gewöhnliches Wasser. Diese beide Substanzen wurden im Verhältnis von O_2:CO_2 = 1:1 vermischt und das so erhaltene Gasgemisch mit der Geschwindigkeit von 50 c.c. pro Minute (bei Zimmertemperatur und unter gewöhnlichem Druck gemessen!) über den auf verschiedenen Temperaturen erhitzten Platinschwamm geleitet. Das aus dem Katalysatorrohr ausgeströmte Gasgemisch wurde durch die Kühlflasche (F in Abb. 1), die mittels flüssiger Luft bis unter –150° bis –130°C. abgekühlt war, vom Kohlendioxyd befreit und das zurückgebliebene Sauerstoffgas mittels Bombenwasserstoffs bis zum Wasser reduziert. Das so gewonnene Wasser, das durchschnittlich etwa 10 c.c. betrug, wurde dann sorgfältig gereinigt und dessen Dichte mittels eines Quarzschwimmers genau bestimmt. Der endliche Dichteüberschuss Δs_e, der in der dritten Vertikalreihe der Tabelle 2 angegeben ist, ist nichts anderes als der des so gewonnenen Wassers aus dem reagierten Sauerstoff. Dagegen bedeutet der oberhalb

der Tabelle angegebene anfängliche Dichteüberschuss Δs_a den des Wassers, das durch die Reduktion des noch nicht reagierten Sauerstoffs mittels desselben Bombenwasserstoffs erhalten wurde.

Tabelle 2. Austauschreaktion zwischen O_2 und CO_2 auf Platinschwamm bei verschiedenen Temperaturen.

O_2: CO = 1 : 1, $\Delta s_a = 17.5\ \gamma$.

Versuchsnr.	Temperatur °C.	Δs_e in γ	$\Delta s_a - \Delta s_e$ in γ	Austauschmass $\%A$
1	390	15.9	1.6	27
4	460	15.5	2.0	33
2	520	14.5	3.0	50
5	600	12.3	5.2	87
3	690	11.0	6.5 } 6.0	108
6	820	12.0	5.5 }	92

Da das Sauerstoffatom des benutzten Sauerstoffgases, wie schon oben erwähnt, um 17.5 γ, dagegen das des Kohlendioxyd um 5.5 γ, beide in der Form von Wasser (dessen Wasserstoff der Bombenwasserstoff ist!) gemessen, schwerer als gewöhnliches Wasser waren und diese beiden Substanzen im Verhältnis von O_2:CO_2=1:1 vermischt wurden, musste das Wasser, das durch die Reduktion des vollständig ausgetauschten Sauerstoffs gebildet wurde, wie eine einfache Rechnung ergibt, um 11.5 γ schwerer als gewöhnliches Wasser sein, vorausgesetzt, dass schwerer Sauerstoff zwischen gasförmigem Sauerstoff und Kohlendioxyd gleichmässig verteilt wurde. Dieser Wert steht aber sehr nahe dem gefundenen Dichteüberschuss Δs_e des gebildeten Wassers bei den letzten zwei Versuchen (Versuche 3 und 6). Wir nahmen deshalb an, dass bei diesen zwei Versuchen das Austauschgleichgewicht erreicht wurde, und berechneten das prozentuale Austauschmass $\%A$ durch die folgende Gl. (2):

$$\%A = \frac{(\Delta s_a - \Delta s_e)}{6.0} \times 100 \qquad (2),$$

wo der Wert 6.0 den Mittelwert von $(\Delta s_a - \Delta s_e)$ bei den letzten zwei Versuchen ausdrückt. Wegen des verhältnismässig kleinen Dichteunterschiedes der Dichte des Sauerstoffs zwischen dem verwendeten Sauerstoffgas und Kohlendioxyd können wir keine grosse Genauigkeit für die hier gewonnenen Versuchsergebnisse beanspruchen. Doch zumindest dürfen wir annehmen, dass auch in diesem Fall oberhalb einer bestimmten Tem-

peratur (ca. 600°C.) ein vollständiger Austausch ziemlich schnell erzielt werden kann.

Experiment 3. Austauschreaktion zwischen gasförmigem Sauerstoff und Wasserdampf auf metallischem Platin bei verschiedenen Temperaturen. Der 0.07 bis 0.08 mm. dicke Platindraht, der insgesamt 3.3 g. wog, wurde in Spiralform zusammengerollt und, nachdem er durch heisse konzentrierte Kalilauge, Salzsäure und Salpetersäure nacheinander behandelt worden war, in das Katalysatorrohr (K in Abb. 1) hineingeschoben. Über diesen Platindraht, der auf verschiedene Temperaturen erhitzt war, wurde das Gasgemisch von der Zusammensetzung $O_2:H_2O = 2:1$ langsam geleitet. Die Strömungsgeschwindigkeit des Gasgemisches betrug, bei Zimmertemperatur und unter gewöhnlichem Druck gemessen, etwa 60 c.c. pro Minute. Die sonstige Arbeitsweise war im grossen und ganzen dieselbe wie beim Experiment mit Platinschwamm (Experiment 1). Die Versuchsergebnisse sind in Tabelle 3 zusammengestellt.

Tabelle 3. Austauschreaktion zwischen O_2 und H_2O auf metallischem Platin bei verschiedenen Temperaturen.

$O_2: H_2O = 2:1$, $\Delta s_a = 35.4\,\gamma$.

Versuchsnr.	Temperatur °C.	Δs_e in γ	$\Delta s_a - \Delta s_e$ in γ	Austauschmass $\%A$
4	400	35.3	0.1	0
2	450	35.4	0.0	0
5	540	33.6	1.8	9
1	610	29.5	5.9	30
3	760	18.3	17.1	88

Da vom gesamten anfänglichen Dichteüberschuss $\Delta s_a (= 35.4\,\gamma)$ des benutzten schweren Wassers $22.6\,\gamma$ auf die Anreicherung des schweren Sauerstoffs zurückzuführen war, dagegen der damit zu reagierende Sauerstoff, der durch die Elektrolyse des destillierten Wassers entwickelt wurde, in der Form von Wasser gemessen, um $1.6\,\gamma$ leichter als gewöhnliches Wasser war, so ergab eine einfache Rechnung, dass beim vollständigen Austausch die Dichteabnahme des schweren Wassers $(\Delta s_a - \Delta s_e) = 19.4\,\gamma$ sein musste. Dies wurde aber, wie aus Tabelle 3 offensichtlich ist, in diesem Fall auch bei der höchsten benutzten Temperatur noch nicht ganz erreicht. Wir berechneten deshalb das prozentuale Austauschmass $\%A$ unter Benutzung des oben angegebenen theoretischen Wertes der Dichteabnahme beim vollständigen Austausch durch die folgende Gl. (3):

$$\%A = \frac{(\Delta s_a - \Delta s_e)}{19.4} \times 100 \qquad (3).$$

Experiment 4. Die Austauschreaktion zwischen gasförmigem Sauerstoff und Wasserdampf auf metallischem Platin bei verschiedenen Strömungsgeschwindigkeiten. Obwohl von vornherein zu erwarten ist, dass sich das Austauschmass mit zunehmender Kontaktdauer des reagierenden Gasgemisches mit dem Katalysator vergrössert, erhielten wir dafür doch einen direkten Beweis durch das folgende Experiment. Das Gasgemisch von der Zusammensetzung $O_2:H_2O = 2:1$ wurde aus dem elektrolytischen Sauerstoff und schwerem Wasser hergestellt und dies über einen auf konstanter Temperatur (750°C.) erhitzten Platindrahtkatalysator mit verschieden grossen Geschwindigkeiten geleitet, indem wir die Stärke des elektrischen Stroms durch den sauerstoffentwickelnden Elektrolyseur verschieden gross wählten. Da aber die Temperatur des Sättigungsgefässes (S in Abb. 1) in jedem Fall konstant bei 72°C. gehalten war, wurde immer das Gasgemisch von derselben Zusammensetzung $O_2:H_2O = 2:1$ gebildet. Die durch diese Versuche gewonnenen Resultate geben wir in Tabelle 4 wieder, wo die Strömungsgeschwindigkeit des reagierenden Gasgemisches v in der zweiten Vertikalreihe bei Zimmertemperatur und unter gewöhnlichem Druck gemessen wurde.

Tabelle 4. Austauschreaktion zwischen O_2 und H_2O auf metallischem Platin bei verschiedenen Strömungsgeschwindigkeiten bei konstanter Temperatur (750°C.).

$O_2: H_2O = 2:1$, $\Delta s_a = 34.7\ \gamma$.

Versuchsnr.	v c.c./Min.	$(1/v)\times 10^3$	Δs_e in γ	$\Delta s_a - \Delta s_e$ in γ	$\%A$
3	100	10.0	31.9	2.8	15
2	60	16.7	29.1	5.6	31
6	55	18.2	28.4	6.3	35
4	45	22.2	28.8	5.9	33
5	35	28.6	27.1	7.6	42
1	25	40.0	19.6	15.1	83

Da das schwere Wasser den gesamten anfänglichen Dichteüberschuss $\Delta s_a = 34.7\ \gamma$ besass und wovon 21.0 γ von der Anreicherung des schweren Sauerstoffs herrührte, dagegen der damit zu reagierende elektrolytische Sauerstoff, in der Form von Wasser gemessen, um 1.6 γ leichter als gewöhnliches Wasser war, sollte die Dichteabnahme des schweren Wassers

($\Delta s_a - \Delta s_e$) beim vollständigen Austausch 18.1 γ betragen. Das prozentuale Austauschmass $\%A$ in der letzten Vertikalreihe der Tabelle wurde deshalb durch die folgende Gl. (4) berechnet:

$$\%A = \frac{(\Delta s_a - \Delta s_e)}{18.1} \times 100 \qquad (4).$$

Dieser Wert nimmt aber, wie aus der Tabelle klar hervorgeht, mit abnehmender Strömungsgeschwindigkeit des reagierenden Gasgemisches allmählich zu. In der nebenstehenden Abb. 2 zeichnen wir das gefundene prozentuale Austauschmass $\%A$ gegen den reziproken Wert der Strömungsgeschwindigkeit v des Gasgemisches auf. Aus dieser graphischen Darstellung ersieht man ohne weiteres, dass das prozentuale Austauschmass $\%A$ mit zunehmender Kontaktdauer des reagierenden Gasgemisches mit dem Katalysator proportional zunimmt.

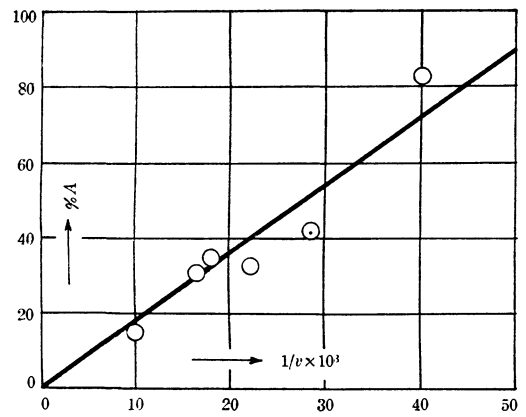


Abb. 2. Die Abhängigkeit des prozentualen Austauschmasses $\%A$ auf die Strömungsgeschwindigkeit v des reagierenden Gasgemisches.

Experiment 5. Austauschreaktion zwischen gasförmigem Sauerstoff und Wasserdampf auf Platinschwamm bei verschiedenen Mischungsverhältnissen der beiden Substanzen. Die Entwicklungsgeschwindigkeit des Sauerstoffs wurde immer konstant bei 40 c.c. pro Minute gehalten, indem wir durch den Elektrolyseur 12 Amp. elektrischen Strom schickten. Dagegen wurde die Temperatur des Sättigungsgefässes (S in Abb. 1) verschieden hoch gewählt, so dass das Gasgemisch aus Sauerstoff und Wasserdampf von wechselnden Zusammensetzungen entstand. Dies wurde dann über den Platinschwammkatalysator, der immer konstant auf 450°C. erhitzt war, langsam geleitet. Der dazu benutzte Platinschwamm war derselbe, der beim Experiment 1 verwendet wurde, und die sonstige Arbeitsweise war ebenfalls im grossen und ganzen dieselbe wie beim Experiment 1. Die Versuchsergebnisse sind in Tabelle 5 zusammengestellt, wo der Quotient in der zweiten Vertikalreihe das Mischungsverhältnis von gasförmigem Sauerstoff und Wasserdampf im reagierenden Gasgemisch darstellt.

Tabelle 5. Austauschreaktion zwischen O_2 und H_2O auf Platinschwamm bei verschiedenen Mischungsverhältnissen der beiden Substanzen.

Temperatur des Katalysators = 450°C., $\Delta s_a = 36.2\,\gamma$.

Versuchsnr.	Mischungsverhältnis $O_2 : H_2O$	v_r	Δs_e gef.	$\Delta s_a - \Delta s_e$ gef.	$\Delta s_a - \Delta s_e$ grenz.	$\%A$ gef.	$\%A$ red.
3	1 : 0.064	1.00	28.1	8.1	21.3	38	38
4	1 : 0.090	1.02	27.8	8.4	21.1	40	41
1	1 : 0.20	1.12	28.1	8.1	20.1	41	46
2	1 : 0.70	1.61	33.4	2.8	16.2	17	

Da aber die Entwicklungs- infolgedessen Strömungsgeschwindigkeit des Sauerstoffs immer konstant gehalten war, musste die Strömungsgeschwindigkeit des reagierenden Gasgemisches über den Katalysator je nach dessen Gehalt an Wasserdampf verschieden gross sein und zwar kann ihre relative Grösse aus der Zusammensetzung des Gasgemisches leicht errechnet werden. Die so berechnete relative Strömungsgeschwindigkeit v_r des Gasgemisches geben wir in der dritten Vertikalreihe der Tabelle wieder. Den Grenzwert der Dichteabnahme des schweren Wassers $(\Delta s_a - \Delta s_e)_{grenz}$ beim vollständigen Austausch, der in der sechsten Vertikalreihe der Tabelle angegeben ist, berechneten wir aus dem Dichteüberschuss ($= 20.4\,\gamma$) des schweren Wassers, der von der Anreicherung des schweren Sauerstoffs herrührte, sowie dem des Sauerstoffgases ($= -1.6\,\gamma$) in der üblichen Weise. Dann wurde aus diesem Grenzwert sowie der wirklich gefundenen Dichteabnahme $(\Delta s_a - \Delta s_e)_{gef.}$ in der fünften Vertikalreihe das Austauschmass $\%A_{gef.}$ in der zweiten letzten Vertikalreihe errechnet. Aber weil, wie im letzten Experiment 4 gefunden wurde, das Austauschmass $\%A$ mit der Strömungsgeschwindigkeit des Reaktionsgasgemisches umgekehrt proportional abnehmen muss, wurde das direkt gefundene Austauschmass $\%A_{gef.}$ unter Benutzung der in der dritten Vertikalreihe angegebenen relativen Geschwindigkeit v_r für den idealen Fall, wo die relative Geschwindigkeit $v_r = 1$ ist, umgerechnet. Den so reduzierten Wert des Austauschmasses $\%A_{red.}$ geben wir in der letzten Vertikalreihe der Tabelle wieder.

Aus diesem Experiment ersieht man, dass die Austauschgeschwindigkeit zwischen gasförmigem Sauerstoff und Wasserdampf durch das Mischungsverhältnis der beiden Gase nicht viel beeinflusst wird, obwohl bei sehr kleiner Konzentration des Sauerstoffs die Austauschgeschwindigkeit bis zu einem gewissen Grad abzunehmen scheint (Versuch 2).

Diskussion. Die Versuchsergebnisse, die in den Tabellen 1, 2 und 3 angegeben sind, stellen wir in der nebenstehenden Abb. 3 zusammenfassend graphisch dar, wo das prozentuale Austauschmass $\%A$, das in der letzten Vertikalreihe jeder Tabelle angegeben ist, gegen die Versuchstemperatur t aufgezeichnet ist. Aus dieser Abb. kann man die folgenden Schlüsse ziehen.

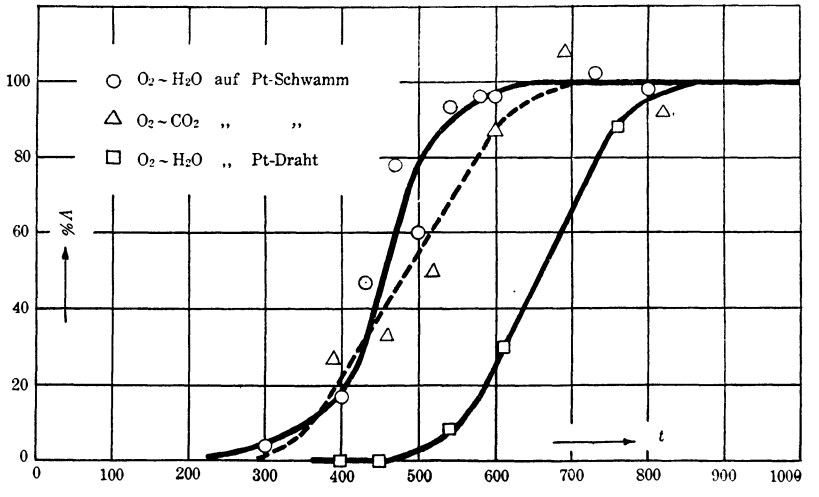


Abb. 3. Die Abhängigkeit des Austauchmasses $\%A$ von der Versuchstemperatur t.

(1) Die Austauschreaktion der O-Atome zwischen gasförmigem Sauerstoff und Wasserdampf auf der Oberfläche des Platinschwamms wird erst bei 300°C. bemerkbar und oberhalb 500°C. verläuft sie sehr schnell, bis der vollständige Austausch ziemlich leicht erreicht wird.

(2) Die Austauschreaktion zwischen gasförmigem Sauerstoff und Kohlendioxyd auf dem Platinschwamm wird ebenfalls zwischen 300° und 400°C. bemerkbar und oberhalb 600°C. wird ein vollständiger Austausch ebenso leicht wie beim (1) erreicht.

(3) Dagegen verläuft die Austauschreaktion zwischen gasförmigem Sauerstoff und Wasserdampf auf der Oberfläche des metallischen Platins viel langsamer als beim Platinschwamm und sogar bei 760°C. wird der vollständige Austausch unter den benutzten Versuchsbedingungen nicht ganz erreicht.

Diesen Unterschied der Austauschgeschwindigkeit auf Platinschwamm und metallischem Platin kann man aber auf die verschiedene Grösse der aktiven Oberfläche der beiden Katalysatoren zurückführen,

und in jedem Fall liegt die Annahme nahe, dass die aktivierte Adsorption des Sauerstoffs eine massgebende Rolle spielt. Diese Auffassung kann durch die folgenden Tatsachen bestätigt werden:

(1) Das Temperaturgebiet, wo die lebhafte Austauschreaktion stattfindet, liegt nicht sehr hoch, so dass die thermische Dissoziation der reagierenden Gase in homogener Gasphase keine massgebenden Einflüsse ausüben kann.

(2) Die Austauschgeschwindigkeit ist in weiten Grenzen vom Mischungsverhältnis der reagierenden Gase unabhängig und sie erscheint mit der abnehmenden Konzentration des Sauerstoffs endlich abzunehmen (Experiment 5).

(3) Die Austauschreaktion zwischen Sauerstoff und Kohlendioxyd auf Platinschwamm setzt fast bei derselben Temperatur wie die Reaktion zwischen Sauerstoff und Wasserdampf ein und verläuft ebenso leicht wie diese (Experiment 1 und 2, vgl. auch Abb. 3).

Die aktivierte Adsorption des Sauerstoffs auf der Oberfläche des metallischen Platins wurde von Reischauer[3] untersucht. Nach seinem Versuche gibt es zwei Arten der aktivierten Adsorption des Sauerstoffs auf der Platinoberfläche. Eine davon findet bei niedrigeren Temperaturen statt und bleibt fast ganz bis zum Schluss unterhalb etwa 250°C. Aber erhöht man die Temperatur weiter, so setzt eine neue „zweite" aktivierte Adsorption bei etwa 400°C. plötzlich ein und dauert bis zu noch höheren Temperaturen. Diesähnliche Eigentümlichkeit der Adsorption des Sauerstoffs auf der Platinoberfläche bei hohen Temperaturen wurde auch schon von Mond, Ramsay und Shields[4] bemerkt. Diese Autoren fanden nämlich, dass das Volumen des Sauerstoffgases, das bei verschiedenen Temperaturen durch eine bestimmte Menge des Platinschwarzes „okkuludiert" wird, zwischen 300° und 400°C. eventuell ein Maximum zeigt. Ob diese Erscheinung zu der oben erwähnten „zweiten" aktivierten Adsorption des Sauerstoffs in irgendeiner Beziehung steht, entzieht sich unsere Kenntnis. Ebensowenig ist der exakte Mechanismus der „zweiten" aktivierten Adsorption aufgeklärt worden. Aber die in der vorliegenden Arbeit gefundene Tatsache, dass die Austauschreaktion des Sauerstoffs eben bei 300° bis 400°C. deutlich bemerkbar wird, legt uns die Vermutung nahe, dass diese Reaktion mit der „zweiten" aktivierten Adsorption des Sauerstoffs in engem Zusammenhang stehen dürfte.

Die katalytische Austauschreaktion der O-Atome zwischen gasförmigem Sauerstoff und Wasserdampf wurde auch von Jones und Hall[5]

(3) H. Reischauer, *Z. physik. Chem.*, B, **26** (1934), 399.
(4) L. Mond, W. Ramsay und J. Shields, *Z. physik. Chem.*, **19** (1896), 25.
(5) T. O. Jones und N. F. Hall, *J. Am. Chem. Soc.*, **59** (1937), 259.

untersucht. Dabei verfuhren sie folgendermassen. Ein Platindraht wurde axial in ein Glasrohr gespannt und das zu reagierende Gasgemisch durch dieses Rohr langsam zirkuliert, während der Platindraht elektrisch auf verschiedene Temperaturen erhitzt wurde. Durch diese Versuchsanordnung fanden sie aber, dass die Austauschreaktion erst oberhalb 1800°K. deutlich stattfand, dagegen die Reaktion unterhalb 1500° bis 1600°K. kaum bemerkbar war. Aus diesem Befund schlossen die beiden Autoren, dass die hohe Temperatur eine der notwendigen Bedingungen für diese Austauschreaktion ist und deshalb nicht mit der aktivierten Adsorption, sondern mit der thermischen Dissoziation des Sauerstoffs in homogener Gasphase zu tun hat. Aber aus der oben skizzierten von diesen Autoren benutzten Versuchsanordnung zu urteilen, liegt die Vermutung nahe, dass wegen der kleinen Oberfläche des Katalysators im Vergleich mit der Gasphase die echte heterogene katalytische Reaktion kaum zu bemerken war, und es sich dabei hauptsächlich um die durch freie O-Atome veranlasste Austauschreaktion in homogener Gasphase handelte.

Zum Schluss möchten wir der Nippon Gakujutsu-Shinkohkai (der Japanischen Gesellschaft zur Förderung der wissenschaftlichen Forschungen) sowie der Hattori-Hohkohkai (der Hattori-Stiftung) für ihre finanzielle Unterstützung zur Ausführung dieser Arbeit unseren wärmsten Dank aussprechen.

Physikalisch-chemisches Laboratorium
der Kaiserlichen Universität zu Osaka
und
Siomi-Institut für physikalische
und chemische Forschung.

Iso-neoergosterol.

By Toshio ANDO.

(Received March 31, 1938.)

It was reported in the previous paper[1] that, along with neoergosterol, a new compound was isolated from the product of pyrolysis followed by the immediate distillation under high vacuum of ergopinacone, the dimolecular derivative prepared by the photochemical dehydrogenation of ergosterol. The new compound was considered to be an isomeride of neoergosterol $C_{27}H_{40}O$ and named iso-neoergosterol. It was then suspected that isoneoergosterol might be a stereoisomeride of neoergosterol, perhaps with regard to the carbon atom 3. However, further investigations have shown that iso-neoergosterol is not an isomeride of neoergosterol, but a molecular compound of the latter with a substance of formula $C_{28}H_{42}O$.[2] For convenience the name iso-neoergosterol is retained in this paper, although it is not appropriate to designate a substance not isomeric with neoergosterol.

Iso-neoergosterol is obtained from the more soluble part of the crude product in somewhat smaller quantity than neoergosterol and has a melting point 138–139° (corr.), $[\alpha]_D^{29°} = -59.1°$, and ultraviolet absorption maxima at 264 mμ (unsharp) and 277 mμ (sharp).[3] Its acetate melts at 108–109° (corr.), and has a specific rotation $[\alpha]_D^{23°} = -41.6°$.

Iso-neoergosterol yields easily a difficultly soluble digitonide with a decomposition point about 250°, while neoergosterol is not so easily precipitated by digitonin. Iso-neoergosterol gives distinctly the colour reactions of Liebermann-Burchard and of Rosenheim, while neoergosterol appears indifferent to these reactions. Thus it seems that iso-neoergosterol consists of a compound whose constitution is rather similar to that of ergosterol, the methyl group at the carbon atom 10 being yet reserved.

On acylation with 3,5-dinitrobenzoyl chloride and pyridin, iso-neoergosterol was separated into equal quantities of two different dinitrobenzoates:

---

(1) Y. Urushibara and T. Ando, this Bulletin, **11** (1936), 757.

(2) The epimeride of neoergosterol, epi-neoergosterol, was recently prepared by A. Windaus and M. Deppe, *Ber.*, **70** (1937), 76.

(3) Cordial thanks are due to Dr. K. Yamasaki for his kindness in taking absorption spectra.

3,5-dinitrobenzoate of neoergosterol, melting point 227–228° (corr.) with decomposition, $[\alpha]_D^{14°} = -6.7°$,[4] from the less soluble part, and a 3,5-dinitrobenzoate having presumably the composition $C_{35}H_{44}O_6N_2$, melting point 187.5–189.5° (corr.) with decomposition, $[\alpha]_D^{14°} = -72.9°$, from the more soluble part. The formula of the latter substance corresponds to the dinitrobenzoate of a compound $C_{28}H_{42}O$, and may be very probable in view of H. H. Inhoffen's hypothetical equation for the decomposition of ergopinacone:[5]

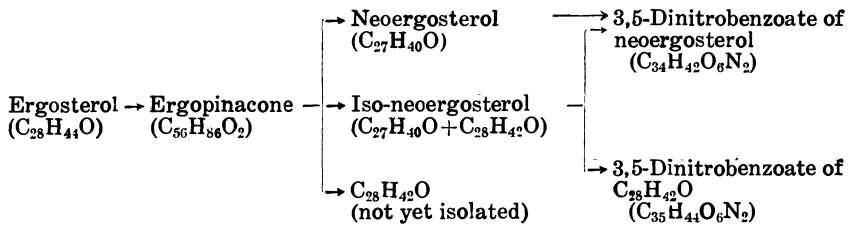
$$\underset{\text{Ergopinacone}}{C_{56}H_{86}O_2} \longrightarrow \underset{\text{Neoergosterol}}{C_{27}H_{40}O} + CH_4 + (C_{28}H_{42}O\,?)\,.$$

Dehydroergosterol $C_{28}H_{42}O$ gave a 3,5-dinitrobenzoate melting at 187.5–188.5° (corr.) with decomposition, namely at the same point as the dinitrobenzoate $C_{35}H_{44}O_6N_2$ from iso-neoergosterol, but a considerable depression of the melting point was observed with a mixture of the two substances.

Thus, iso-neoergosterol seems to be a molecular compound of neoergosterol and a compound $C_{28}H_{42}O$, an isomeride of dehydroergosterol. The isolation and investigation of the free compound $C_{28}H_{42}O$ are now in progress.

The easy precipitation of iso-neoergosterol by digitonin is undoubtedly due to the component $C_{28}H_{42}O$. However, the separation of iso-neoergosterol into its components by digitonin has not yet been successful, a substance with almost the same melting point as iso-neoergosterol being recovered.

From the quantitative point of view, at least one more compound of the same formula $C_{28}H_{42}O$, which does not combine with neoergosterol, may be expected and may be found in the more soluble part of the decomposition product of ergopinacone. Consequently, the changes involved may be expressed tentatively as follows:



(4) H. H. Inhoffen gives m. p. 218-220° (corr.), and $[\alpha]_D^{16°} = -13°$, *Ann.*, **497** (1932), 130.

(5) *Naturwissenschaften*, **25** (1937), 125.

Experimental.

Ergopinacone. Prepared from ergosterol (24 g.) according to the directions of H. H. Inhoffen.[4] Colourless silky needles (12.7 g.), m.p. 200–201° (corr.) with decomposition. In the Liebermann-Burchard test it gives red, violet, blue, green, and finally dark green colours; in the Rosenheim test, light pink, light violet, dark violet, then dark brownish violet colours.

Ergopinacone Diacetate. A solution of ergopinacone (300 mg.) in pyridin (55 c.c.) was mixed with acetic anhydride (4.5 g.). After a week the mixture was poured into water, the separating crystals were collected, washed with dilute acetic acid and with water, recrystallized twice from benzene-alcohol, and dried over phosphorus pentoxide in vacuum at 110°. Colourless fine needles (253 mg.) m.p. 205.5–206° (corr.) with decomposition (Found: C, 82.99; H, 10.13. Calculated for $C_{60}H_{90}O_4$:C, 82.31; H, 10.37%). $[\alpha]_D^{12°} = -209°$ (11.0 mg. in 1 c.c. chloroform solution, $l = 1$ dm., $\alpha_D^{12°} = -2.30°$), ultraviolet absorption maximum 267–268 mμ (unsharp) in 0.042% hexane solution. In the Liebermann-Burchard test the diacetate gives red, violet, blue, and then bluish green colours; in the Rosenheim test, pink, light violet, finally dark green colours. The diacetate is far more soluble and stable than the free pinacone.

Pyrolysis of Ergopinacone. Ergopinacone (11.3 g.) was subjected in portions of 1 g. to decomposition at 205–210° under the pressure of 0.2–0.3 mm. followed by the immediate distillation at 220–290° under 0.014–0.04 mm. Crystallization of the distillate (9.18 g., 81.3%) from ethanol by seeding yielded crude yellow crystals (5.15 g., 45.6% of ergopinacone, 56.2% of the distillate), m.p. 124–129° (corr.).

Neoergosterol. When the crude product (1.50 g.) was fractionally recrystallized from ethanol, pure neoergosterol (330 mg.) was first obtained from the less soluble part in colourless long needles, m.p. 153.5–154.5° (corr.). It gives neither Liebermann-Burchard nor Rosenheim reaction. The precipitation by digitonin occurs only slowly after several hours, and the precipitate melts and decomposes at about 210–260° to red brown liquid. The 3,5-dinitrobenzoate prepared from neoergosterol (80 mg.), recrystallized repeatedly from benzene-methanol, formed light yellow small plates (83 mg.), m.p. 222–223° (uncorr.) or 227–228° (corr.) with decomposition to yellow liquid (Found: C, 70.96; H, 7.39; N, 5.09. Calculated for $C_{34}H_{42}O_6N_2$: C, 71.06; H, 7.37; N, 4.88%). $[\alpha]_D^{12°} = -6.67°$ (15.0 mg. in 1 c.c. chloroform solution, $l = 1$ dm., $\alpha_D^{12°} = -0.10°$). The acetate of neoergosterol showed m.p. 123.5–124° (corr.), $[\alpha]_D^{28°} = +10.9°$ (13.8 mg. in 1 c.c. chloroform solution, $l = 1$ dm., $\alpha_D^{28°} = +0.15°$).

Iso-neoergosterol. The recrystallization of the more soluble part from methanol and then from acetone gave iso-neoergosterol (287 mg.) in colourless small fine needles, m.p. 138–139° (corr.), $[\alpha]_D^{29°} = -59.1°$ (12.7 mg. in 1 c.c. chloroform solution, $l = 1$ dm., $\alpha_D^{29°} = -0.75°$), ultraviolet absorption maxima in 0.043% hexane solution 264 mμ (unsharp) and 277 mμ (sharp).[6] In Liebermann-Burchard test it gives red, violet, deep blue, green, and finally dark green colours, while in Rosenheim test pink, light violet, dark bluish green, and finally dark brownish violet colours.

The acetate of iso-neoergosterol, m.p. 108–109° (corr.), $[\alpha]_D^{28°} = -41.6°$ (13.7 mg. in 1 c.c. chloroform solution, $l = 1$ dm., $\alpha_D^{28°} = -0.57°$), gives in Liebermann-Burchard

(6) Neoergosterol has an ultraviolet absorption maximum at about 268 mμ, H. H. Inhoffen, see note (4).

test violet, blue, dark green, and dark brownish violet colours, while in Rosenheim test, pink, light violet, greenish blue, dark green, and dark brownish violet colours.

Separation of Iso-neoergosterol into Components in the Forms of 3,5-Dinitrobenzoates. Iso-neoergosterol (250 mg.) was heated on a boiling water bath for 45 minutes with 3,5-dinitrobenzoyl chloride (390 mg.) and pyridin (3 c.c.) and the mixture was left to stand overnight. The crystals which separated out were collected, washed with cold methanol, with dilute acetic acid and with water, boiled with methanol, and then fractionally recrystallized from chloroform-methanol or benzene-methanol. Pure neoergosteryl 3,5-dinitrobenzoate was first obtained from the less soluble part in glittering light yellow small plates (150 mg.), melting at 227–228° (corr.) with decomposition to yellow liquid alone and in admixture with the specimen prepared from pure neoergosterol (Found: C, 71.01; H, 7.28; N, 5.03. Calculated for $C_{34}H_{42}O_6N_2$: C, 71.06; H, 7.37; N, 4.88%). $[\alpha]_D^{14°} = -6.74°$ (17.8 mg. in 1 c.c. chloroform solution, $l = 1$ dm., $\alpha_D^{14°} = -0.12°$).

From the more soluble part another 3,5-dinitrobenzoate was obtained in light yellow small plates (110 mg.), m.p. 184–186° (uncorr.) or 187.5–189.5° (corr.) with decomposition to wine-red liquid (Found: C, 71.57, 71.29; H, 7.60, 7.34; N, 4.80. Calculated for $C_{35}H_{44}O_6N_2$ or $C_6H_3(NO_2)_2COOC_{28}H_{41}$: C, 71.37; H, 7.54; N, 4.76%). $[\alpha]_D^{14°} = -72.9°$ (16.2 mg. in 1 c.c. chloroform solution, $l = 1$ dm., $\alpha_D^{14°} = -1.18°$). When mixed with the 3,5-dinitrobenzoate of dehydroergosterol, a depression of melting point was observed (mixed melting point 174.5–181.5°, corr.).

On adding water to the pyridin mother liquor of the crude 3,5-dinitrobenzoates and recrystallizing the precipitates repeatedly, a more quantity of 3,5-dinitrobenzoate identical with the above was obtained (37 mg.), m.p. 187.5–189.5° (corr.), $[\alpha]_D^{15°} = -72.1°$ (8.6 mg. in 1 c.c. chloroform solution, $l = 1$ dm., $\alpha_D^{15°} = -0.62°$).

The yield of neoergosteryl 3,5-dinitrobenzoate (150 mg.) was equal to that of the other 3,5-dinitrobenzoate $C_{35}H_{44}O_6N_2$ (147 mg. in total).

3,5-Dinitrobenzoate of Dehydroergosterol. Dehydroergosterol, m.p. 147–148° (corr.), prepared according to the directions of A. Windaus and O. Linsert,[7] was heated on a boiling water bath for 20 minutes with 3,5-dinitrobenzoyl chloride and pyridin. The crystals separating out on adding water to the reaction mixture were washed with dilute acetic acid and with water, boiled with methanol, and recrystalliized repeatedly from benzene-methanol. Yellow small needles, m.p. 184–185° (uncorr.) or 187.5–188.5° (corr.) with decomposition to deep red liquid (Found: N, 4.92. Calculated for $C_{35}H_{44}O_6N_2$: N, 4.76%).

Digitonin and Iso-neoergosterol. When digitonin (315 mg.) dissolved in 95% alcohol (35 g.) was added to a solution of iso-neoergosterol (92 mg.) in 95% alcohol (10 g.), there appeared instantly precipitates, the quantity of which increased rather rapidly. The digitonide was collected, washed with 95% alcohol and with ether, and then dried. Yield 272 mg. (68%). It sinters at about 196°, melts and decomposes gradually at about 203–254° (uncorr.). As K. Bonstedt[8] described that the digitonide of neoergosterol was easily decomposed to its components by extraction with benzene, the present author extracted the above digitonide first with benzene, dissolved the residue in pyridin and added ether. The precipitated digitonin was filtered off and

(7) *Ann*, **465** (1928), 148.
(8) *Z. physiol. Chem.*, **185** (1929), 165.

the filtrate was evaporated. The crystals which remained were repeatedly recrystallized from dilute acetone, colourless silky needles melting at 136–138.5° (corr.), and at 135–138.5° (corr.) in admixture with iso-neoergosterol. The yield was too poor to be investigated further.

In conclusion, the author wishes to express his hearty thanks to Prof. Y. Urushibara for his kind guidance and encouragement. The author's thanks are also due to Mr. Yasohachi Yamaguchi for his generous support of this work.

Chemical Institute, Faculty of Science,
Imperial University of Tokyo.

Recherches sur la concentration des ions d'hydrogène contenus dans les solutions aqueuses des ammines-cobaltiques complexes et sur leurs spectres d'absorption. IV. Solutions aqueuses des complexes renfermant la molécule d'éthylènediamine.[1]

Par **Taku UÉMURA** et **Naoichi HIRASAWA.**

(Reçu le 27 mars 1938.)

Ce mémoire est la suite du compte rendu sur la recherche en solution aqueuse des complexes du cobalt et du chrome, qui a été déjà publiée avec M. H. Suéda.[2] Le but de l'étude actuelle, déjà exposé dans les mémoires précédents, est une recherche pour connaître l'état des complexes en solution aqueuse en faisant varier la concentration des ions d'hydrogène (pH). Cette fois-ci, nous avons employé les complexes contenant des molécules d'éthylènediamine (NH_2–CH_2–CH_2–NH_2)[3] dans le noyau complexe où une molécule d'éthylènediamine joue le même rôle que deux molécules d'ammoniaque.

Corps étudiés et procédé expérimental. Dans les recherches actuelles, nous avons pris les onze composés suivants qui renferment la molécule NH_2–CH_2–CH_2–NH_2 dans leur radical complexe.

(1) $[Co\,en_3]Cl_3 \cdot 3H_2O$
(2) $[Co\,en_2Cl(H_2O)]Cl_2$ (deux espèces)
(3) $[Co\,en_2(H_2O)_2]Cl_3$ (cis et trans)
(4) $[Co\,en_2Cl_2]Cl$ (cis et trans)
(5) $[Co\,en_2OH(H_2O)]Cl_2 \cdot H_2O$ (cis)
(6) $[Co\,en_2OH(H_2O)]Br_2$ (trans)
(7) $[Co\,en_2NO_2(H_2O)](NO_3)_2$ (cis et trans)

Les conditions expérimentales que nous avons adoptées sont les suivantes, à savoir, solutions de 20 mm. ou 30 mm. d'épaisseur, 1/200 mol, 1/500 mol ou 1/5000 mol de concentration. La concentration des ions d'hydrogène a été déterminée en employant l'électrode d'antimoine et les coefficients d'extinction ont été mesurés au moyen du spectrographe en quartz français comme auparavant, avec une lampe à mercure en quartz comme source lumineuse. La plupart des photographies d'absorption ont été prises avec des plaques spéciales photographiques "Fuji" (marque japonaise).

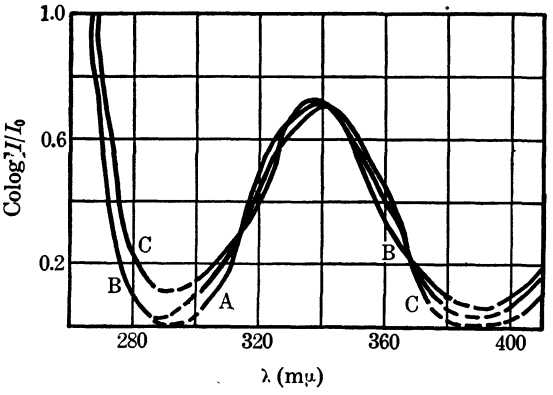
---

(1) Traduction du mémoire original japonais publié dans le Bulletin de la Faculté des Arts et Métiers de Tokyo (Tokyo Kogyô-Daigaku Gakuhô), **6** (1937), 217. Exposé lors de la Séance de la Société chimique du Japon, le 13 février 1937.

(2) T. Uémura et H. Suéda, ce bulletin, **10** (1935), 50, 85, 267; H. Suéda, *ibid.*, **12** (1937), 71.

(3) On la simplifie généralement moyennant la formule "*en*".

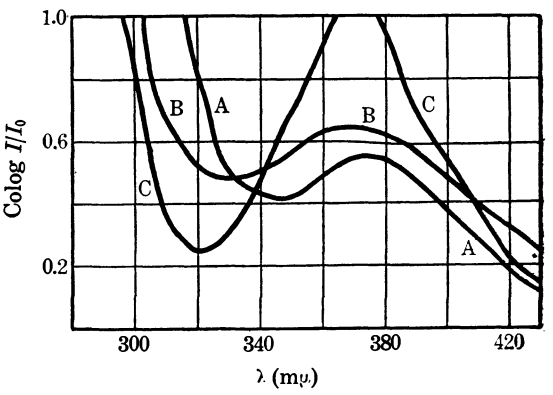
Relation entre la concentration des ions d'hydrogène (*p*H) et la courbe d'absorption des sels complexes. (1) $[Coen_3]Cl_3 \cdot 3H_2O$, *Chlorure de cobalti-triéthylènediamine.* Ce complexe a été préparé suivant les indications de Jörgensen.[4] Nous avons aussi consulté quelque comptes rendus spectrochimiques[5] sur le sel actuel. Une solution aqueuse de 1/200 mol du complexe a été préparée pour obtenir la figure 1 en employant 20 mm. d'épaisseur de solution. Quand on dissout ce composé dans l'eau, son *p*H est de 7.5 (courbe B – fig. 1) et ce *p*H change à 2.0 par l'addition de 1/200 titre HCl et à 10.6 par 1/200 liqueur titrée de NaOH (courbe A et C). Nous ne pouvons pas constater de grandes différences pour ces trois courbes A, B et C qui sont semblables au sel lutéo-cobaltique déjà étudié.[6] Le lutéo a eu son absorption maximum à 340 mμ de longueur d'onde et le présent corps a son absorption à peu près à la même position. Le pouvoir absorbant du corps actuel est cependant plus puissant que celui donné par le sel lutéo.



[Co en_3]Cl_3 (1/200 mol)

A: *p*H = 2.0 B: *p*H = 7.5 C: *p*H = 10.6

Fig. 1.



[Co $en_2Cl(H_2O)$]Cl_2 (cis) (1/500 mol)

A: *p*H = < 1; 5.9 B: *p*H = 7.1 C: *p*H = 8.8

Fig. 2.

(2) $[Coen_2Cl(H_2O)]Cl_2$ (*deux espèces*), *Chlorure de cobalti-chloro-diéthylènediamine-hydrine.* Deux isomères du composé sont déjà connus, et l'un, corps cis, peut être obtenu en appliquant la méthode de Werner[7]; quelques recherches spectrochimiques de ce complexe ont aussi

(4) S. M. Jörgensen, *J. prakt. Chem.*, [2], **39** (1889), 8.

(5) Y. Shibata et G. Urbain, *Compt. rend.*, **157** (1913), 593; Y. Shibata, *J. Coll. Sci., Imp. Univ. Tokyo*, **37** (1915), Art. 2, 6; C. Schleicher, Dissert. Zürich (1921), 23.

(6) Ce bulletin, **10** (1935), 52.

(7) A. Werner, *Ann.*, **386** (1912), 123; *Ber.*, **45** (1912), 3296.

été publiées par plusieurs auteurs.[8] Pour ce corps cis violet, nous avons pris des photographies pour observer son absorption avec la solution de 1/500 mol de concentration et de 50 mm. d'épaisseur.

La figure 2 nous montre une coïncidence de deux courbes: l'une est celle de solution neutre (pH = 5.9), l'autre celle de solution acide (obtenue par 1/200 titre HCl). La courbe A sur la figure 2 est superposée à ces deux courbes, et elle est aussi en même temps caractéristique de ce composé. La courbe B est formée par la solution du pH 7.1 en additionnant 1/500 liqueur titrée de NaOH. Elle est semblable à la courbe D de la figure 4 du composé $[Coen_2(H_2O)_2]Cl_3$(cis) (pH = 6.9). Ce résultat nous conduit à supposer que le noyau complexe $[Coen_2(H_2O)_2]^{+++}$ est d'abord formé en solution alcaline, et, de plus, une solution du pH plus fort (8.8) obtenu par l'addition de 1/200 liqueur titrée de NaOH intensifie considérablement son pouvoir absorbant. La production d'une absorption si forte nous permet de conclure à la formation du sel chloro-hydroxo ou aquo-hydroxo. Cependant, comme cette courbe C ressemble à celle du pH élevé du complexe $[Coen_2OH(H_2O)]Cl_2$(cis) (fig. 8), une relation $[Coen_2Cl(H_2O)]^{++}$ (cis) $\xrightarrow{\text{alcalin}}$ $[Coen_2OH(H_2O)]^{++}$ (cis) doit être reconnue. L'addition d'alcali à ce corps $[Coen_2Cl(H_2O)]Cl_2$ contribue probablement à le changer vers la fin en sel aquo-hydroxo en passant par celui diaquo.

L'autre isomère gris-vert, $[Coen_2Cl(H_2O]Cl_2 \cdot H_2O$, est synthétisé par la méthode indiquée par Meisenheimer et Kinderlen[9] qui ont assigné une forme trans à son sel préparé. Nous avons obtenu la figure 3 par ses photographies d'absorption en employant 50 mm. d'épaisseur de solution de 1/500 mol.

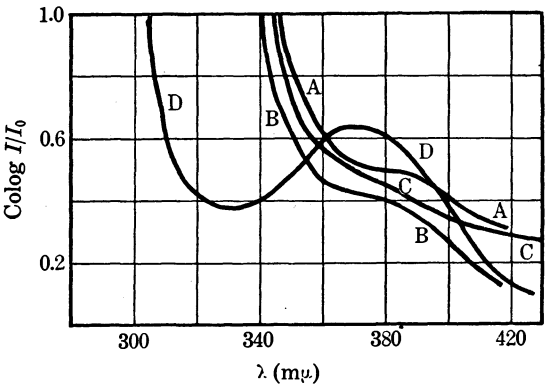
Le présent complexe est un solide gris-vert et donne une solution aqueuse verte qui vire rapidement au rouge-violet. Une solution acide peut cependant garder assez longtemps le vert, mais vire au rouge-violet par l'addition d'une base.

Comme nous pouvons l'observer sur la figure 3, la courbe C de la solution aqueuse (pH = 6.0) et les autres deux courbes A et B (pH faibles) n'ont pas d'absorption sélective, mais ne montrent qu'une translation de la fin d'absorption. La courbe D donnée par une solution de 1/200 liqueur titrée de NaOH (pH = 9.6) est bien différente de celles A, B et C qui n'indiquent pas clairement de leur modification en état neutre et acide. Cette courbe D est analogue à celle montrée par l'isomère cis (fig. 2), et, en même temps, elle n'est pas fort différente des courbes de

(8) K. Matsuno, *J. Coll. Sci., Imp. Univ. Tokyo*, **41** (1921), Art. 10, 18; C. Schleicher, *loc. cit.*; A. Uspensky et K. Tschibisoff, *Z. anorg. Chem.*, **164** (1927), 331.

(9) C. Meisenheimer et E. Kinderlen, *Ann.*, **438** (1924), 255.

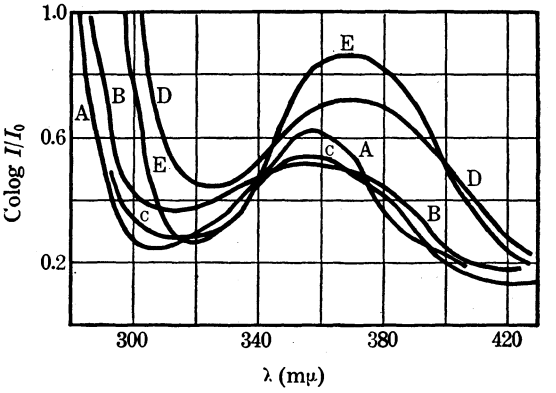
la figure 8 présentées par le noyau complexe [Coen_2OH(H_2O)](cis). C'est pourquoi, en renforçant le pH, c'est-à-dire en solution alcaline, le pouvoir absorbant croît et la forme cis s'y trouve en prenant probablement le type aquo-hydroxo.



[Co en_2Cl(H_2O)]Cl_2 (gris-vert) (1/500 mol)

A: pH < 1 B: pH = 5.3
C: pH = 6.0 D: pH = 9.6

Fig. 3.



[Co $en_2(H_2O)_2$]Cl_3 (cis) (1/500 mol)

A: pH = 1.4 B: pH = 5.8 C: pH = 5.9
D: pH = 6.9 E: pH = 10.1

Fig. 4.

(3) [Co$en_2(H_2O)_2$]Cl_3 (*cis et trans*), *Chlorure de cobalti-diéthylène-diamine-dihydrine.* Le composé cis de ces deux isomères est rouge-violet et s'obtient d'après la méthode de préparation indiquée par Werner.[10] Ces deux isomères, comme l'isomère cis du composé précédent, ont déjà été spectrochimiquement étudiés.[11] Le présent corps cis donne la figure 4 des courbes d'absorption avec ses solutions de 1/500 mol et de 50 mm. d'épaisseur.

En abandonnant ce complexe à lui-même, puisque sa couleur graduellement change, ses photographies d'absorption ont été aussitôt prises après la synthèse. Les trois courbes A, B et C, que sa solution aqueuse (pH = 5.8) et celles acides donnent, se ressemblent les unes aux autres tandis que la courbe D représentée par une solution alcaline (pH = 6.9 obtenu en additionnant 1/500 liqueur titrée de NaOH) est différente de celles des précédentes et son pouvoir absorbant augmente en montrant une influence bathochromique. Ce pouvoir absorbant devient encore plus fort en solution de pH plus élevé (10.1, par l'addition d'une solution de 1/200

(10) A. Werner, *Ber.*, **40** (1907), 265, 2121.

(11) K. Matsuno, *J. Coll. Sci., Imp. Univ. Tokyo*, **41** (1921), Art. 10, 18; A. Uspensky et K. Tschibisoff, *loc. cit.*

liqueur titrée de NaOH). Comme cette courbe E (fig. 4) est semblable à celle du pH fort donnée par $[Coen_2OH(H_2O)]Cl_2$(cis) (fig. 8), nous pouvons admettre la relation $[Coen_2(H_2O)_2]^{+++} \xrightarrow[\text{alcalin}]{} [Coen_2OH(H_2O)]^{++}$. Dans tous ces cas, le centre d'absorption des courbes du pH élevé se trouve au voisinage de 370 mμ.

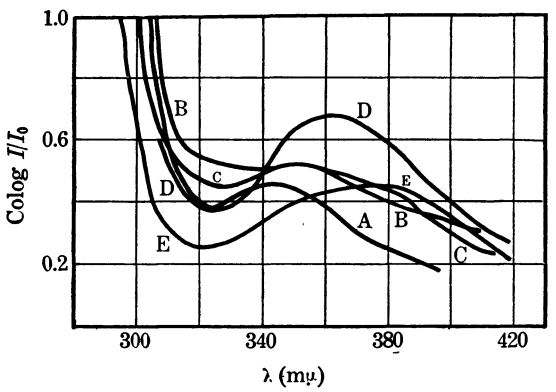
Le complexe trans, $[Coen_2(H_2O)_2]Cl_3 \cdot 2H_2O$, a été préparé suivant les indications données par Werner[12] et ses spectres d'absorption etudiés dans les mêmes conditions expérimentales que nous avons appliquées à l'isomère précédent, à savoir 1/500 mol de concentration et 50 mm. d'épaisseur de solution. Le complexe actuel est un solide rouge-brun qui donne une solution rouge-brun en le dissolvant dans l'eau. Cette couleur de solution aqueuse vire bientôt au rouge. La solution acide peut comparativement garder longtemps sa couleur originale, tandis que la solution basique vire rapidement au rouge. C'est pourquoi nous avons photographié aussitôt après la préparation du corps.

Ce complexe montre son pH à 5.8 en solution aqueuse (courbe C – fig. 5); les autres deux courbes A et B ont été respectivement obtenues par l'addition de 1/500 et de 1/200 titre HCl. Ces trois courbes ne montrent sensiblement pas leur absorption sélective, mais une autre solution alcaline du pH 6.8 préparée par l'addition de 1/500 liqueur titrée de NaOH donne une absorption sélective très nette (courbe D). La solution du pH plus fort (pH = 9.7) a été préparée en additionnant 1/200 liqueur titrée de NaOH et montre une diminution du pouvoir absorbant (courbe E).

La courbe A du présent corps (pH<1) est peut-être celle de l'absorption caractéristique du trans et les deux autres courbes B et C (pH = 5.5 à B et pH = 5.8 à C) suggèrent déjà quelques changements dans leur solution. Nous ne pouvons donc pas demander une précision absolue pour ces deux courbes B et C et nous avons aussi à admettre la stabilité faible du trans. L'absorption de solution aqueuse est ici plutôt semblable à celle donnée par les solutions alcalines. En observant les courbes de grands pH des solutions basiques, on peut admettre que $[Coen_2(H_2O)_2]^{+++}$ (trans) alcalinisé donne $[Coen_2OH(H_2O)]^{++}$ (trans). Cette relation est probablement acceptable en se référant aux courbes du corp $[Coen_2OH(H_2O)]Br_2$ (trans) (fig. 9) qui donnera un pouvoir absorbant plus faible que celui du type cis; d'où nous pouvons conclure que le présent isomère trans représente l'absorption du sel aquo-hydroxo du trans aux pH forts.

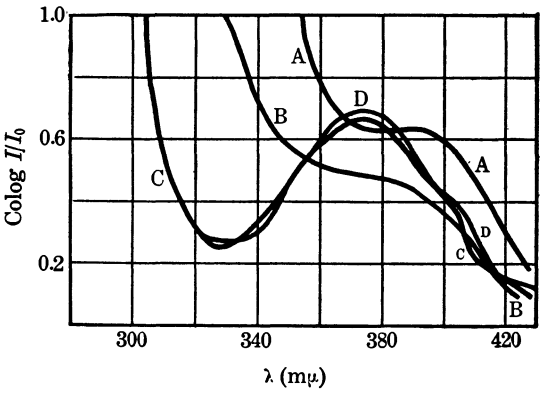
(4) $[Coen_2Cl_2]Cl$ (*cis et trans*), *Chlorure de cobalti-dichloro-diéthylènediamine.* L'isomère cis a été préparé d'après la méthode pro-

(12) A. Werner et C. Jantsch, *Ber.*, **40** (1907), 269; A. Werner, *Ann.*, **386** (1912), 97.



[Co $en_2(H_2O)_2]Cl_3$ (trans) (1/500 mol)
A: pH < 1 B: pH = 5.5 C: pH = 5.8
D: pH = 6.8 E: pH = 9.7

Fig. 5.



[Co $en_2Cl_2]Cl$ (cis) (1/500 mol)
A: pH = 5.9; 1.2 B: pH = 6.8
C: pH = 9.7 D: pH = 10.9

Fig. 6.

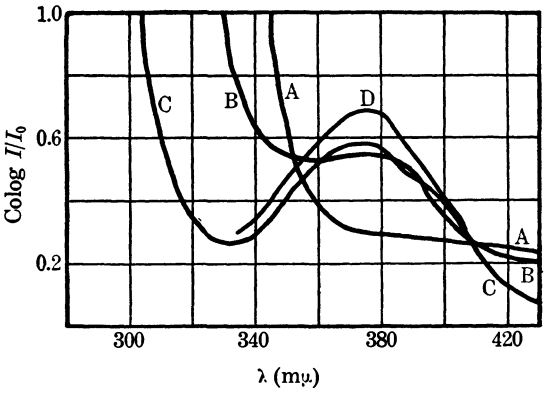
posée par Jörgensen.[13] C'est un complexe violet qui a été déjà étudié par plusieurs savants.[14] Nous l'avons photographié avec ses solutions de 1/500 mol de concentration et de 50 mm. d'épaisseur.

La solution aqueuse du composé montre son pH à 5.9 et sa courbe coïncide avec celle du pH 1.2 donnée par 1/500 titre HCl (courbe A – fig. 6). Cette courbe A est probablement caractéristique du présent complexe et bien que par l'addition de 1/500 liqueur titrée de NaOH (pH = 6.8) on obtienne la courbe B, l'absorption dans la région des longueurs d'onde plus courtes est moindre en courbe B qu'en courbe A. La courbe C du pH 9.7 (obtenu par l'addition de 1/200 liqueur titrée de NaOH) est bien différente des courbes A et B et montre son absorption maximum au voisinage de 370 mμ et minimum à 328 mμ. Cette courbe C est semblable à celles données par les deux sels $[Coen_2Cl(H_2O)]^{++}$ (fig. 2) et $[Coen_2(H_2O)_2]^{+++}$ (fig. 4), et on a déjà admis que ce complexe $[Coen_2Cl_2]^+$ (cis) change quantitativement au sel aquo-hydroxo. C'est pourquoi on peut facilement en déduire que cette courbe C donne l'absorption du sel aquo-hydroxo.

L'isomère trans obtenu par les indications de Werner[15] est un sel vert. Il a été déjà spectrochimiquement étudié[16] comme son isomère

(13) S. M. Jörgensen, *J. prakt. Chem.*, [2], **41** (1890), 448.
(14) G. Lifschitz et E. Rosenbohm, *Z. wiss. Phot.*, **19** (1920), 199; C. Schleicher, *loc. cit.*; A. Uspensky et K. Tschibisoff, *loc. cit.*
(15) A. Werner, *Ber.*, **34** (1901), 1733.
(16) A. Gordienko, Dissert. Zürich (1920), 90; Y. Shibata, *J. Coll. Sci., Imp. Univ. Tokyo*, **37** (1915), Art. 2, 24; G. Lifschitz et E. Rosebohm, *loc. cit.*; C. Schleicher, *loc. cit.*; A. Uspensky et K. Tschibisoff, *loc. cit.*

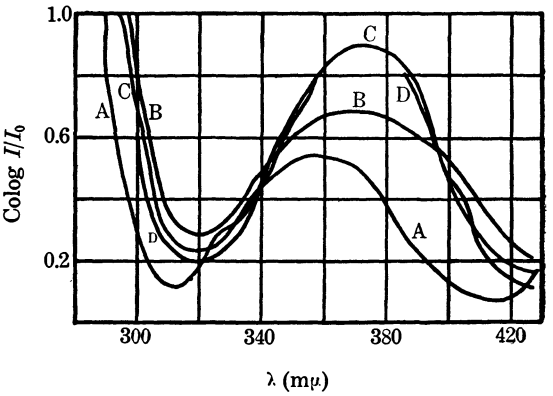
cis. Nous avons employé ses solutions de 1/500 mol de concentration et de 50 mm. d'épaisseur pour trouver l'absorption de ce composé. La solution aqueuse du sel actuel montre une valeur du pH à 5.3 et sa courbe d'absorption est parfaitement la même que celle représentée par une solution du pH<1 quand le sel se dissout dans HCl au titre 1/500 (courbe A – fig. 7.). Cette courbe A peut être considérée comme celle caracteristique du complexe en question. La courbe B, obtenue par une solution du pH 6.5 (par l'addition de 1/500 liqueur titrée de NaOH) est nettement différente de la courbe A, c'est-à-dire que dans ce cas, quelques modifications en solution ont déjà été produites. Les deux autres courbes C et D, obtenues respectivement de 1/200 (pH = 9.5) et de 1/150 liqueur titrée de NaOH (pH = 10.6), sont semblables à celle donnée par une solution du corps cis au pH fort (corbe C – fig. 6), d'où l'on peut conjecturer de la transformation du complexe trans en celui cis par l'addition de liqueur alcaline, ce qui a été déjà exposé dans certains mémoires. Les courbes C et D des grands pH sont analogues à celles données par le complexe aquo-hydroxo (cis) (fig. 8). On peut donc supposer la formation de celui-ci dans la solution du présent corps cis.



[Co en_2Cl_2]Cl (trans) (1/500 mol)

A: pH = <1; 5.3 B: pH = 6.5
C: pH = 9.5 D: pH = 10.6

Fig. 7.



[Co en_2OH(H_2O)]Cl_3 (cis) (1/500 mol)

A: pH = 1.7 B: pH = 6.4
C: pH = 8.6 D: pH = 10.4

Fig. 8.

(5) [Coen_2OH(H_2O)]$Cl_2 \cdot H_2O$ (*cis*), *Chlorure de cobalti-hydroxo-diéthylènediamine-hydrine.* Ce corps rouge a été synthétisé par la méthode proposée par Werner[17] et l'absorption mesurée avec ses solutions de 1/500 mol de concentration de 50 mm. d'épaisseur.

(17) A. Werner, *Ber.*, **40** (1907), 281.

La solution aqueuse du présent composé donne un *p*H 6.4, et 1.7 par 1/200 titre HCl, 8.6 par 1/500 liqueur titrée de NaOH et 10.4 par 1/200 liqueur titrée de NaOH. Nous avons montré ces résultats par les courbes A, B, C et D dans la figure 8. Nous y remarquons que l'augmentation des *p*H intensifie le pouvour absorbant des solutions, et l'absorption maximum se trouve aux environs des longueurs d'onde à 370 mμ à la valeur du *p*H fort.

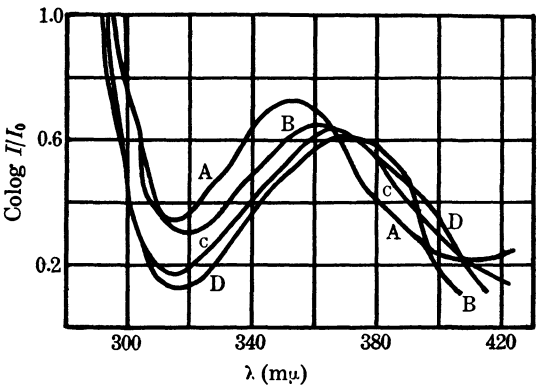
Les courbes d'absorption des grands *p*H données par $[Coen_2(H_2O)_2]Cl_3$ (cis) (fig. 4) et $[Coen_2Cl(H_2O)]Cl_2$ (cis) (fig. 2) sont analogues à celles montrées par des solutions alcalines du présent corps, d'où l'on peut facilement présumer que le présent complexe se forme dans les solutions alcalines des deux sels ci-dessus nommés. Une courbe de la solution acide (*p*H = 1.7) du présent corps (courbe A) est encore analogue à celle du *p*H faible de $[Coen_2(H_2O)_2]Cl_3$ (cis) (courbe A – fig. 4). Cela nous permet d'inférer l'existence de la relation suivante en solution: $[Coen_2(H_2O)_2]^{+++}$ (cis) $\underset{\text{acide}}{\overset{\text{alcalin}}{\rightleftarrows}}$ $[Coen_2OH(H_2O)]^{++}$ (cis).

(6) $[Coen_2OH(H_2O)]Br_2$ (*trans*), *Bromure de cobalti-hydroxo-diéthylènediamine-hydrine.* Nous avons préparé le présent complexe rose en appliquant la méthode publiée par Werner[18] et nous avons observé ses spectres d'absorption dans les mêmes conditions expérimentales que pour le corps précédent, à savoir 1/500 mol de concentration et 50 mm. d'épaisseur des solutions.

La solution aqueuse du présent complexe donne un *p*H 6.6 et ce *p*H est renforcé par l'addition d'alcali. Les solutions fortement alcalinisées présentent à peu près un même pouvoir absorbant et leur absorption maximum se trouve approximativement à la position analogue déjà montrée par son isomère cis. Cependant, ce corps trans manifeste un pouvoir absorbant bien plus faible que celui de cis. En comparant les deux figures 9 et 5, nous pouvons facilement saisir que le complexe $[Coen_2(H_2O)_2]Cl_3$(trans) change au complexe actuel par l'addition d'alcali. Mais, la solution acide du présent composé ne montre pas sa courbe d'absorption semblable à celle donnée par $[Coen_2(H_2O)_2]Cl_3$ (trans) en solution acide; ce qui différencie les sels trans et cis. C'est pourquoi nous ne pouvons qu'admettre une relation simple: $[Coen_2(H_2O)]^{+++}$ (trans) $\xrightarrow{\text{alcalin}}$ $[Coen_2OH(H_2O)]^{++}$ (trans).

(7) $[Coen_2NO_2(H_2O)](NO_3)_2$ (*cis et trans*), *Azotate de cobalti-nitro-diéthylènediamine-hydrine.* L'isomère cis a été difficile à préparer

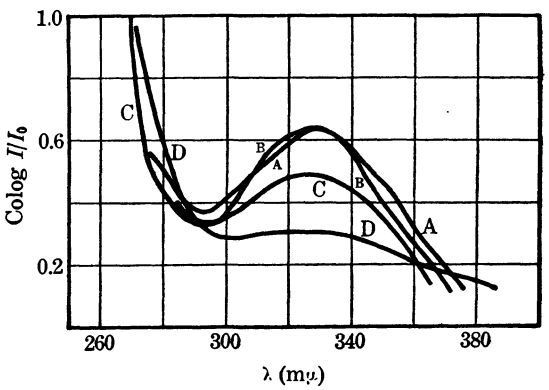
(18) A. Werner, *Ann.*, **386** (1912), 97.



[Co en_2OH(H_2O)]Br_2 (trans) (1/500 mol)

A: pH < 1 B: pH = 6.6
C: pH = 9.4 D: pH = 11.0

Fig. 9.



[Co en_2NO_2(H_2O)]$(NO_3)_3$ (cis) (1/5000 mol)

A: pH = 1.3 B: pH = 3.3
C: pH = 7.1 D: pH = 8.4

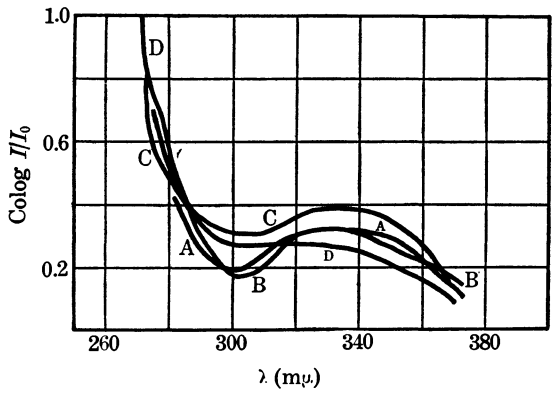
Fig. 10.

et nous l'avons obtenu par une méthode récemment publiée.[19] Comme son pouvoir absorbant est assez fort, pour observer ses spectres d'absorption nous avons préparé des solutions de 1/5000 mol de concentration et de 20 mm. d'épaisseur.

Le corps est un complexe rougeâtre et présente son pH à 7.1 quand il se dissout dans l'eau. Les courbes d'absorption (fig. 10) des pH faibles (pH = 1.3 ou 3.3) obtenues en additionnant de 1/2500 ou 1/5000 titre HCl ne sont pas différentes l'une à l'autre. Le pouvoir absorbant diminue en solution aqueuse (pH = 7.1 – courbe C) et l'absorption sélective disparaît en solution du pH plus fort (pH = 8.4 – courbe D), obtenue par l'addition de 1/2500 liqueur titrée de NaOH. Nous pouvons conclure de ces courbes d'absorption que ce composé ne montre pas de grands changements dans son radical complexe en solution acide, tandis qu'en solution basique on peut supposer la formation de l'azotate de cobalti-nitro-hydroxo-di-éthylènediamine ([Coen_2NO_2OH]NO_3) comme dans le cas du complexe cobalti-nitro-tétrammino-hydrine ([Co$(NH_3)_4(H_2O)NO_2](NO_3)_2$).[20] La solution purement aqueuse du corps actuel (courbe C) donc manifeste un état intermédiaire entre acide et basique, c'est-à-dire que nous pouvons admettre l'existence de l'équilibre [Co$en_2NO_2(H_2O)]^{++} \rightleftarrows$ [Coen_2NO_2·OH]$^+$. L'addition d'alcali, dans ce cas, permet d'inférer encore la formation de l'aquo-hydroxo au lieu de celle de nitro-hydroxo, mais cette supposition est peu plausible en comparant les deux figure 8 et 10.

(19) J. Meyer et O. Rampoldt, *Z. anorg. Chem.*, **214** (1933), 1.
(20) Ce bulletin, **12** (1937), 81.

L'isomère trans a été formé, comme le cas, suivant les indications de Meyer et Rampoldt.[19] C'est un complexe jaune et a été spectrochimiquement étudié, comme son isomère cis, avec des solutions de 1/5000 mol de concentration et de 20 mm. d'épaisseur. Nous pouvons facilement comprendre par la figure 11 que les courbes A et B des *p*H faibles données par ses solutions acides coïncident presque. Sa solution aqueuse montre un *p*H 7.2 en donnant une absorption maximum, mais son *p*H devient 7.7 quand ce complexe se dissout dans une solution de NaOH au titre 1/5000 et l'absorption sélective y disparaît (courbe D). Le corps actuel présente une absorption analogue à celle de son isomère précédent, à savoir sa solution acide donne l'absorption caractéristique du sel qui est un peu différente de son isomère (comparer figures 10 et 11). Le pouvoir absorbant est plus faible que celui du sel cis. Le changement d'absorption qui apparaît en solution neutre et alcaline est aussi semblable à son isomère cis, mais la distinction de ces deux isomères n'est pas très sensible. C'est pourquoi nous avons encore quelques doutes sur la formation du sel nitro-hydroxo(cis) en solution alcaline. Nous observons seulement que la solution alcaline du sel cis est rougeâtre tandis que celle de trans jaunâtre.



[Co $en_2NO_2(H_2O)](NO_3)_2$ (trans) (1/5000 mol)
A: *p*H = 2.9 B: *p*H = 3.8
C: *p*H = 7.2 D: *p*H = 7.7

Fig. 11.

Résumé.

(1) Les courbes d'absorption données par le complexe [Coen_3]Cl_3 sont peu influencées par la variation de la concentration des ions d'hydrogène.

(2) Les deux isomères cis et trans des trois complexes, [Coen_2 Cl(H_2O)]Cl_2, [Co$en_2(H_2O)_2$]Cl_3 et [Coen_2Cl_2]Cl manifestent des absorptions semblables qui donnent leur maximum aux environs des longueurs d'onde à 370 mμ, leur minimum à 320 mμ.

(3) D'après les études spectrochimiques, nous pouvons admettre les deux relations suivantes:

(a) $[Co\,en_2(H_2O)_2]^{+++}(cis) \underset{acide}{\overset{alcalin}{\rightleftarrows}} [Co\,en_2OH(H_2O)]^{++}(cis) \leftarrow [Co\,en_2Cl(H_2O)]^{++}(cis)$

(b) $[Co\,en_2(H_2O)_2]^{+++}(trans) \xrightarrow[alcalin]{} [Co\,en_2OH(H_2O)]^{++}(trans)$

(4) Les trois sels $[Co\,en_2(H_2O)_2]^{+++}$, $[Co\,en_2Cl(H_2O)]^{++}$ et $[Co\,en_2Cl_2]^{+}$ sont stables en solutions acides, assez instables en neutre et forment le sel $[Co\,en_2OH(H_2O)]^{++}$ en solutions alcalines.

(5) Les isomères cis et trans du sel $[Co en_2NO_2(H_2O)]$ perdent leur absorption sélective en solutions alcalines et le complexe cis peut probablement changer au $[Co en_2NO_2 \cdot OH]^{+}$ (cis) en se dissolvant dans l'alcali.

En terminant cette publication de nos études actuelles, nous tenons à exprimer nos sincères remerciements à l'autorité de la Faculté qui nous a bien encouragés pendant nos expériences et, en même temps, à la Société "Téjima Kogyô-Shikindan" qui a bien voulu nous aider à se charger d'une partie des dépenses de nos recherches.

Laboratoire de Chimie minérale, Faculté des Arts et Métiers de Tokyo (Tokyo Kogyô-Daigaku).

Absorption Spectra of Co-ordination Compounds. I.

By Ryutaro TSUCHIDA.

(Received May 7th, 1938.)

I. Introduction. It is already two decades since a number of facts were revealed of absorption spectra of metallic complexes by extensive studies of Y. Shibata[1] and his co-workers, pioneers in the field. Ever since, various hypotheses have been proposed as to the origins of absorption bands of these compounds, but none of those could satisfactorily explain, even qualitatively, the entire empirical facts already known.

According to Shibata,[1][2] the metallic complexes have generally two selective absorption bands, of which the first lies in the visible region and the second in the near ultra-violet.[3] Some complexes, however, give the third bands in the region of shorter wave-lengths. In more special cases, selective absorption bands due to ligands[4] themselves may superpose on those proper to the co-ordination combination.

The author has recently been studying the third bands of co-ordination compounds and has arrived at some conclusions on the origins of the first and the second band as well as the third. The present paper is an abbreviated summary of the results so far obtained.

II. The Third Band. The first systematic study on the third bands was carried out in 1915 by Y. Shibata,[5] who explained the third band of $[Co(NH_3)_4(NO_2)_2{}^{(1)}_{(6)}]X$ as due to the nitro-radicals co-ordinated in trans-position to each other, confirming his theory by several examples such as $[Co(NH_3)_3(NO_2)_3]$, $[Co(NH_3)_2(NO_2)_4]NH_4$, etc.,[6] and further determined the configuration of some compounds by ingenious application of

(1) Y. Shibata, *J. Coll. Sci., Imp. Univ. Tokyo*, 1915 to 1921; *J. Chem. Soc. Japan*, 1915 to 1922.

(2) Y. Shibata and G. Urbain, *Compt. rend.*, **157** (1913), 593; Y. Shibata, *J. Coll. Sci., Imp. Univ. Tokyo*, **37** (1915), Art. 2.

(3) In some cases, e.g., $[Ni(NH_3)_6]Cl_2$, $[Co(H_2O)_6]Cl_2$, etc., both the bands are shifted so immensely that the first and the second bands appear in the infra-red and the visible regions. T. Dreisch and W. Trommer, *Z. physik. Chem.*, B, **37** (1937), 37. On the contrary, in other cases, e.g., $[Ir\ en_3]X_3$, $[Rh\ en_3]X_3$, etc., the infra-red and the visible regions are transparent, all the bands being localized in the ultra-violet region. J. L. Lifschitz and E. Rosenbohm, *Z. physik. Chem.*, **97** (1921), 1; *Z. wiss. Phot.*, **19** (1920), 198.

(4) Throughout this article, the word ligand will be used in its original German sense, i.e., an ion or a molecule co-ordinated in a complex radical.

(5) Y. Shibata, *J. Chem. Soc. Japan*, **36** (1915), 1243.

(6) Y. Shibata, *J. Coll. Sci., Imp. Univ. Tokyo*, **37** (1916), Art. 8; Y. Shibata and K. Matsuno, *J. Chem. Soc. Japan*, **37** (1916), 160.

his theory on the third band as well as the experiment on the optical resolution of $[Co(NH_3)_2(NO_2)_2C_2O_4]M$.[7] During the investigation on the aquotization of $[Co(NH_3)_4Cl_2^{(1)}_{(6)}]Cl$, the present author[8] happened to find a third band for this complex, and extending Y. Shibata's theory, assumed that the third band is due to a pair or pairs of negative ligands co-ordinated in trans-positions.[9] A survey of the data available in the literature as well as our measurements of some complexes shows that the extended theory can be applied to all the third bands hitherto found with only one exception of $[Cr(NH_3)_5(NCS)](NCS)_2$.[10]

All the co-ordination compounds which have or seem to have at least a pair of negative ligands in trans-positions showed the third bands, but none of those deficient of the condition. The third bands confirmed or found in this laboratory are summarized in Table 1.

Table 1.

Complex compound	First band		Second band		Third band		$\nu_2-\nu_1$	$\nu_3-\nu_2$
	$\nu_1(10^{13})$	$\log\varepsilon$	$\nu_2(10^{13})$	$\log\varepsilon$	$\nu_3(10^{13})$	$\log\varepsilon$		
$[Co(NH_3)_4(NO_2)_2^{(1)}_{(6)}]Cl$[5][9]	67.9	2.32	87.0	3.54	119.6	4.08	19.1	32.6
$[Co(NH_3)_3(NO_2)_3]$[5][11]	68.8	2.21	86.9	3.45	120.4	3.81	18.2	33.5
$[Co(NH_3)_2(NO_2)_4]NH_4$[5][9]	69.0	2.56	85.9	3.67	119.0	3.85	16.9	33.1
$[Co(NH_3)_3(NO_2)_2Cl]$[11]	67.9	2.18	87.9	3.43	120.8	3.88	19.1	33.8
$[Co(NH_3)_3(NO_2)_2Br]$[11]	66.8	2.02	87.9	3.30	120.8	3.82	21.1	32.9
$[Co(NH_3)_2(NO_2)_2C_2O_4]NH_4$[12]	62.5	2.18	88.0	3.53	120.2	4.57	25.5	32.2
$[Co(NH_3)_4(NO_2)Cl_2^{(1)}_{(6)}]Cl$[9]	63.2	1.87	88.8	3.13	123.0	4.07	25.6	34.2
$[Co(ONO)_6]Na_3$[9]	62.0	2.34	82.4	3.75	114.0	3.95	20.4	31.6
$[Co(NH_3)_4Cl_2^{(1)}_{(6)}]Cl$[8]	<50	1.2	63	1.4	100	3.2	—	37
$[Co(C_2O_4)_3]K_3$[12]	49.6	2.09	71.8	2.19	123.0	4.42	22.2	51.2
$[Fe(CN)_6]K_3$[13]	71.8	3.03	99.4	3.20	114.0	3.05	27.6	13.6
$[PtCl_6]K_2$	67.0	1.58	84.0	2.58	115.6	4.11	17.0	31.6
$[Pt(NH_3)_2Cl_2^{(1)}_{(6)}]$	80.0	1.23	95.8	1.88	110.2	2.02	15.8	14.4
$[HgI_4]K_2$ (aq. soln. of KI)	—	—	93.6	4.40	112.8	4.66	—	19.2
KI_3[14] (mixed aq. soln. of KI and I_2)	—	—	84.4	4.09	104.4	4.21	—	20.0

(7) Y. Shibata and T. Maruki, *J. Coll. Sci., Imp. Univ. Tokyo*, **41** (1918), Art. 2; *J. Chem. Soc. Japan*, **37** (1916), 1142.
(8) R. Tsuchida, this Bulletin, **11** (1936), 721.
(9) R. Tsuchida and S. Kashimoto, this Bulletin, **11** (1936), 785.
(10) Y. Shibata, *J. Coll. Sci., Imp. Univ. Tokyo*, **41** (1918), Art. 6; Y. Shibata and K. Matsuno, *J. Chem. Soc. Japan*, **39** (1918), 661.
(11) M. Kobayashi, *J. Chem. Soc. Japan*, **58** (1937), 391.
(12) S. Kashimoto and M. Kobayashi, this Bulletin, **12** (1937), 350.
(13) S. Iimori, *J. Chem. Soc. Japan*, **36** (1915), 171.
(14) R. Tsuchida, this Bulletin, **10** (1935), 37.

From Table 1 it can be pointed out that the differences $\nu_3 - \nu_2$ for cobaltic complexes are about 33×10^{13}, while the differences $\nu_2 - \nu_1$ show values in a wide range from 17×10^{13} to 26×10^{13}.

The occurrence of the third band is independent of (1) the kind and valency of the central ion, (2) the sort of the ligand in question provided that it is of negative character, (3) the charge of the complex radical, and moreover, (4) the configuration, so long as the trans-pairing condition is fulfilled. It is a remarkable fact that not only the transition elements, but also others such as Hg^{++} and I^{+} can give rise to the third bands. It is also interesting that a chelate radical so complicated as dimethylglyoxime[15] shows a third band similar to those given by simple ions such as Cl^- and NO_2^-. Non-electrolytic complexes, e.g., $[Co(NH_3)_3(NO_2)_3]$, can have the third bands just as complex cations and anions. Complexes of planar structure, e.g., $[Pt(NH_3)_2Cl_2]$, and of linear type, e.g., I_3^-, give the third bands as well as those of octahedral configuration. In short, the third band is one of the general characteristics of absorption spectra of co-ordination compounds. According to the author's opinion, as will be discussed later, the third band is theoretically more important than the first which is the origin of the beautiful colour of the complex, and sometimes seems more useful in application even than the second which is the most important feature of the co-ordination compounds.

III. Theories on the Origins of the First and the Second Bands. The researches on the first and the second bands have been more active than those of the third, and consequently, as to the origins of these bands, there are various theories and hypotheses, which are briefly introduced here chronologically. Luther and Nikolopulos[16] assumed that the chemical linkage between the central metallic atom and the ligand gives rise to the first band. According to Shibata,[2][10][17] the first band is probably due to an electron of the central atom and the cause of the second band lies between the central metallic atom and the non-metallic atom of the ligand which combines directly with the former. By Lifschitz,[3] the first band is thought of as due to a group of electrons belonging to the central atom, and the second band is associated with the binding electrons of the co-ordinated group. According to Colmar and Schwartz[18] the first band is attributed partly to the central ion, because of an electronic

(15) C.f. Table 6.
(16) R. Luther and A. Nikolopulos, *Z. physik. Chem.*, **82** (1913), 361.
(17) Y. Shibata, "Spectrochemistry," Vol. I, Tokyo (1935).
(18) R. I. Colmar and F. W. Schwartz, *J. Am. Chem. Soc.*, **54** (1932), 3204.

transition, and partly to the internal vibrations of the atoms and ions making up the complex. Joos and Schnetzler[19] found that the absorption spectra of crystalline powder of chromic complexes at low temperatures, consist in several lines, and supported the theory of Deutschbein,[20] who explained the lines of Cr^{+++} as due to the electron transitions $3^4F - 3^2G$, the shift of lines being a kind of the Stark effect of the neighbouring atoms and molecules.

So far, there is no serious unreconcilable contradiction among these theories except that of Luther and Nikolopulos. Mead,[21] however, adopted Pauling's theory[22] and tried to explain both the first and the second band as equally due to energy differences between excited states of the co-ordination electrons. The opinion of Mathieu[23] on the first band is similar to that of Mead: viz., the first band is probably attributed to combination of the transitional energy of the co-ordination electrons and the vibrational energies of the central atom and the ligands. In brief, the matter stands thus. The opinions of various authors may find the point of agreement in attributing the second band to the co-ordination electrons. As to the first band, however, the theories may be divided into two groups: viz., Mead, Mathieu, Luther and Nikolopulos assumed the first band as due to co-ordination electrons, while most of the authors attributed the band to electrons belonging to the central metallic atom.

IV. The Origin of the First Band. Before dealing with the origin of the first band, it must be noticed here that the first and the second band could not be attributed to the same cause as was assumed by Mead.[21] Absorption spectra of cobaltic nitro-ammines and related compounds were taken and compared (Table 2).

As is seen from Table 2, the substitution of NO_2^- for NH_3 in nitro-ammine series has hypsochromic effect on the first band, while the same substitution has bathochromic effect on the second. If the first and the second band were to arise from causes of the same kind, one and the same substitution would have similar effects on both the bands.

On the other hand, the origin of the first band was attributed, as was stated in the preceding section (III), either to co-ordination electrons or to electrons in the central ion by various authors. It will, however, be highly improbable to attribute the first band to co-ordination electrons,

(19) G. Joos and K. Schnetzler, *Z. physik. Chem.*, B, **20** (1933), 1.
(20) O. Deutschbein, *Ann. Physik*, **14** (1932), 712.
(21) A. Mead, *Trans. Faraday Soc.*, **30** (1934), 1052.
(22) L. Pauling, *J. Am. Chem. Soc.*, **53** (1931), 1367.
(23) J. P. Mathieu, *Bull. soc. chim.*, [5], **3** (1936), 463.

Table 2.

Complex compound	First band		Second band		Third band		$\nu_2-\nu_1$	$\nu_3-\nu_2$
	$\nu_1(10^{13})$	$\log\varepsilon$	$\nu_2(10^{13})$	$\log\varepsilon$	$\nu_3(10^{13})$	$\log\varepsilon$		
Nitro-ammine complex								
$[Co(NH_3)_5NO_2]Cl_2$	65.8	1.95	92.6	3.12			26.8	
$[Co(NH_3)_4(NO_2)_2^{(1)}_{(2)}]Cl$	65.5	1.99	91.2	3.10			25.7	
$[Co(NH_3)_4(NO_2)_2^{(1)}_{(6)}]Cl$	67.9	2.32	87.0	3.54	119.6	4.08	19.1	32.6
$[Co(NH_3)_3(NO_2)_3]$	68.7	2.21	86.9	3.45	120.4	3.81	18.2	33.5
$[Co(NH_3)_2(NO_2)_4]NH_4$	69.0	2.56	85.9	3.67	119.0	3.85	16.9	33.1
Nitrito-complex								
$[Co(ONO)_6]Na_3$	62.0	2.34	82.4	3.75	114.0	3.95	20.4	31.6
$[Co(NH_3)_5ONO]Cl_2$	63.5	1.74	91.7	2.79			28.2	

so long as it has generally been accepted that the second band is due to those electrons.

With the aim of throwing light upon the subject, absorption spectra of $K_2[HgI_4]$ in KI solutions were measured, and two absorption maxima at 321 mμ ($\nu = 93.6 \times 10^{13}$) and 226 m$\mu$ ($\nu = 113 \times 10^{13}$) were observed.

Now a third band is expected for this compound, because of the negative ligands in trans-positions, and we know from experience that the third band of a co-ordination compound appears usually in the spectral region between 110×10^{13} and 120×10^{13}. Then the band at 113×10^{13} may possibly be regarded as the third band and the other at 93.6×10^{13}, consequently, the second. The co-ordination compound in question, therefore, lacks the first band, which would be impossible if the first band were due to the co-ordination electrons.

Comparing $K_2[Hg\,I_4]$ with other complexes which possess the first bands, we may notice at once the fundamental difference: viz., the central ions of the latter have unsaturated transition shells, while that of the former has not. Now we have come to the conclusion that the first band is attributed to electron transitions in the unsaturated transition shell of the central ion. Then the first band is one of the general characteristics of transition elements.

If we assume that the energy levels of the electron transitions are determined by the ligand co-ordinated in the direction of the transition, the effect of substitution of ligands on the first band will be qualitatively explained. It is now postulated that the electron transitions are depressed

by negative fields of the ligands and the stronger the field, the greater the depression.

For the purpose of unitary treatment of the different kinds of ligands, i.e., polar molecules, simple elementary ions, and radical ions, it will be convenient to introduce a quantity P, the work which would be done by the system if the ligand were to approach from infinity to the seat of co-ordination. Then a ligand which gives a larger energy of approach would have such negative field that will cause greater depression of the electron transition and consequently give rise to a first band of lower frequency. The greater the charge of the ligand and the larger the polarity and the polarizability as well, the greater will be the energy of approach P. Therefore, a simple elementary anion has generally stronger effect than a molecule. Of these anions, those which have larger polarizabilities must bring about larger depression than those which are less polarizable, and molecules which have larger dipole moments must have stronger effect than those of smaller moments. Thus the ligands, no matter whether they may be ions or molecules, could be arranged in the order of their effect on the energy levels. Arranging in the ascending order of P, we obtain a spectrochemical series for the first band: viz.,

$$NH_3,\ H_2O,\ F^-,\ Cl^-,\ Br^-,\ I^-.$$

The smaller the value P, the weaker the depression and the higher the frequency of the first band. The above series, therefore, shows the descending order of hypsochromic effect of the ligand on the first band. When a ligand is substituted for another which comes behind in the series, the first band is displaced towards the shorter wave-lengths, and, on the contrary, a substitution of a ligand for another ahead of it gives rise to a bathochromic effect. For example, H_2O is bathochromic than NH_3, but hypsochromic than Cl^-.

In order to verify the hypothesis, a number of complex compounds were prepared and their absorption spectra were taken. The results show that the above series coincides with that obtained from the measurements. For example, the first bands of $[Co(NH_3)_6]Cl_3$, $[Co(NH_3)_5H_2O]Cl_3$ and $[Co(NH_3)_5Cl]Cl_2$ are 63.6×10^{13}, 61.6×10^{13} and 58.7×10^{13} respectively (Table 3).

The effect of a radical ion on the first band is rather complicated, as it has its own poles which must be modified by neighbouring ions and molecules, and moreover, the effect may also vary according to the way in which it is co-ordinated. For example NO_2^- ion may be co-ordinated either with N or with O, as the case may be. In the former case it is

hypsochromic than NH_3 and in the latter, bathochromic.[24] The first bands of $[Co(NH_3)_5NO_2]Cl_2$, $[Co(NH_3)_5NH_3]Cl_3$ and $[Co(NH_3)_5ONO]Cl_2$ are 65.8×10^{13}, 63.6×10^{13} and 63.5×10^{13} respectively (Table 2).

Being thus unable to decide theoretically, positions of radical ions in the series of *P* have been found from experimental data as follows. In Tables 3, 4 and 5,[25] the complexes have been arranged in the order of frequencies of their first bands.

Table 3.

Ligand	Complex salt	First band		Second band	
		ν_1 (10^{13})	log ε	ν_2 (10^{13})	log ε
NO_2^-	$[Co(NH_3)_5NO_2]Cl_2$	65.8	1.95	92.6	3.12
NH_3	$[Cr(NH_3)_5NH_3]Cl_3$	65.0	1.48	86.0	1.44
	$[Co(NH_3)_5NH_3]Cl_3$	63.6	1.66	88.8	1.57
ONO^-	$[Co(NH_3)_5ONO]Cl_2$	63.5	1.74	91.7	2.79
H_2O	$[Co(NH_3)_5H_2O]Cl_3$	61.6	1.62	87.5	1.62
NCS^-	$[Cr(NH_3)_5NCS](NCS)_2$	61.6	1.82	(83)	1.67
	$[Co(NH_3)_5NCS]Cl_2$	60.2	2.14	(84)	2.60
NO_3^-	$[Co(NH_3)_5NO_3](NO_3)_2$	60.2	1.74	(83)	1.8
$SO_4^=$	$[Co(NH_3)_5SO_4]I$	60.0	1.70	85.5	2.76
OH^-	$[Co(NH_3)_5OH](NO_3)_2$	59.8	1.82	(82)	1.9
$C_2O_4^=$	$[Co(NH_3)_5C_2O_4]Br$	59.2	1.87	—	—
$CO_3^=$	$[Co(NH_3)_5CO_3]NO_3$	59.0	1.84	(82)	1.9
$S_2O_3^=$	$[Co(NH_3)_5S_2O_3]Cl$	58.2	1.76	(79)	2.15
Cl^-	$[Cr(NH_3)_5Cl]Cl_2$	58.7	1.53	80.0	1.54
	$[Co(NH_3)_5Cl]Cl_2$	57.5	1.64	82.8	1.66
$CrO_4^=$	$[Co(NH_3)_5CrO_4]NO_3$	55.6	2.14	78.4	3.54
Br^-	$[Co(NH_3)_5Br]Br_2$	55.4	1.68	(81)	2.8

(24) As will be seen in Table 2, successive substitution of NO_2 for NH_3 in the nitro-ammine series, causes gradual shift of the first band towards the shorter wave-lengths, but the first band of Fischer's salt, $K_3Co(NO_2)_6$, has by far the longest wave-length, betraying that it is hexanitritocobaltiate, $[Co(ONO)_6]K_3$, instead of hexanitrocobaltiate, $[Co(NO_2)_6]K_3$. R. Tsuchida, *J. Chem. Soc. Japan*, **59** (1938), 731.

(25) The absorption curves of the complexes in these tables as well as others will soon be published.

Table 4.

Ligand	Complex compound	First band		Second band	
		ν_1 (10^{13})	log ε	ν_2 (10^{13})	log ε
NO_2^-	$[Co(NH_3)_4(NO_2)_2^{(1)}_{(6)}]Cl$	67.9	2.32	87.0	3.54
	$[Co(NH_3)_4(NO_2)_2^{(1)}_{(2)}]Cl$	65.5	1.99	91.2	3.10
NH_3	$[Cr(NH_3)_4(NH_3)_2]Cl_3$	65.0	1.48	86.0	1.44
	$[Co(NH_3)_4(NH_3)_2]Cl_3$	63.6	1.66	88.8	1.57
H_2O	$[Co(NH_3)_4(H_2O)_2]Cl_3$	60.0	1.40	84.0	1.48
$C_2O_4^=$	$[Co(NH_3)_4C_2O_4]Br$	58.8	1.78	84.0	1.88
$CO_3^=$	$[Co(NH_3)_4CO_3]Br$	57.2	2.02	82.6	2.03
Cl^-	$[Co(NH_3)_4Cl_2^{(1)}_{(6)}]Cl$	<50	1.2	63	1.4

Table 5.

Ligand	Complex compound	First band		Second band	
		ν_1 (10^{13})	log ε	ν_2 (10^{13})	log ε
en	[Co *en*$_3$]Br_3	65.2	1.83	90.0	1.77
NH_3	$[Cr(NH_3)_6]Cl_3$	65.0	1.48	86.0	1.44
	$[Co(NH_3)_6]Cl_3$	63.6	1.66	88.8	1.57
ONO^-	$[Co(ONO)_6]Na_3$	62.0	2.34	82.4	3.75
NCS^-	$[Cr(NCS)_6]K_3$	53.1	2.08	70.8	2.00
H_2O	$[Cr(H_2O)_6]Cl_3$	52.5	1.02	73.6	1.20
$C_2O_4^=$	$[Co(C_2O_4)_3]K_3$	49.6	2.09	71.0	2.19

From Table 3, we obtain, experimentally, the spectrochemical series for the first band: viz.,

NO_2^-, NH_3, ONO^-, H_2O, NCS^-, NO_3^-, $SO_4^=$, OH^-, $C_2O_4^=$, $CO_3^=$, $S_2O_3^=$, Cl^-, $CrO_4^=$, Br^-.

Also from Table 4:

NO_2^-, NH_3, H_2O, $C_2O_4^=$, $CO_3^=$, Cl^-.

From Table 5:

en, NH_3, ONO^-, NCS^-, H_2O, $C_2O_4^=$.

All these series as well as the theoretical one above coincide with one another, and all the experimental rules by various authors[8][16][18][21][26]

(26) T. Uemura and H. Sueda, this Bulletin, **10** (1935), 267.

about the shifts of bands by substitutions of ligands may be included in the series.

The first band is expected to be more or less additive, as a complex may contain more than two kinds of ligands which have different *P*-values. The complexes which co-ordinate only one kind of ligand should naturally have narrower, symmetrical first bands than those which have ligands of different kinds, and among the latter, those which have ligands situated far apart in the spectrochemical series should have broader and less symmetrical first bands and sometimes these bands may be analysed into two or more components. For example $[Co(NH_3)_5Cl]Cl_2$ has broader and less symmetrical first band than $[Co(NH_3)_5NO_2]Cl_2$ or $[Co(NH_3)_5H_2O]Cl_3$ and may be analysed into the principal first band at about 57×10^{13} and an auxiliary first band at about 62×10^{13}. Mathieu,[23] Ernsberger and Brode[27] have tried to analyse the first bands into components.

V. Thermochemical Treatment of the Second Band. So long as the origin of the second band is concerned, opinions of various authors seem to find the point of agreement in attributing the second band to the co-ordination electrons. Whereas some of the co-ordination compounds lack the first bands and most of them the third, they never fail to give the second bands. This fact betrays the relation between the co-ordinate linkage and the second band. Another evidence is photochemical behaviour of co-ordination compounds. For example, $K_3[Co(C_2O_4)_3]$ is decomposed most readily by rays of the second band[28] and hydrolysis of $[Co(NH_3)_5C_2O_4]_2SO_4$ is accelerated most effectively by rays corresponding to its second band.[29] These and other photochemical changes show that the second band has direct relation to the formation and decomposition of the co-ordination compound: in other words, the co-ordination linkage is directly affected by the rays of the second band.

In order to explain these facts, it is now postulated that when a quantum of the second band is absorbed by a complex radical, one of the co-ordination links is split open and an excited ligand is produced in the original seat of co-ordination, e.g.,

$$[M\,A_6]^{n+} + h\nu_2 = [M\,A_5\{A\}]^{n+},$$

(27) M. L. Ernsberger and W. R. Brode, *J. Am. Chem. Soc.*, **56** (1934), 1842.

(28) I. Vranek, *Z. Elektrochem.*, **23** (1917), 336; F. M. Jaeger, *Rec. trav. chim.*, **38** (1919), 249.

(29) R. Schwarz and K. Tede, *Ber.*, **60** (1927), 65, 69; R. Schwarz and H. Weiss, *Ber.*, **58** (1925), 746.

$$[\mathrm{M\,X_6}]^{n-}+h\nu_2=[\mathrm{M^+\,X_5\{X^-\}}]^{n-},\ \text{etc.},$$

where {A} and {X} denote the excited molecule and ion respectively.

It is postulated here that the excited ligand thus produced by $h\nu_2$, recombine in most cases to form the original complex. It may sometimes be set free or sometimes be replaced by other ion or molecule, as the case may be, resulting in decomposition and substitution respectively. In case of recombination, the energy S is set free, which may be defined as co-ordination energy.

The relation of S to other energies may be shown by assuming the following cyclic process. (1) First the salt, say $\mathrm{MX_3}$, whose lattice energy is Φ_1, is separated into its constituent ions. (2) The ligands are brought to the positions of co-ordination. (3) And the next step is to excite the ligands till they are ready to enter into the co-ordination linkage with the central ion. (4) Then the combination takes place, setting the energy S free. (5) The last process is to form the complex crystal, whose lattice energy is Φ. The energy of approach in the process (2) is the same as P in the preceding section (IV), and that of excitation in the process (3) may be represented by R. Let Q be the heat of formation of the complex crystal from the component compounds of first order per one co-ordination, then

$$\mathrm{M\,X_3}+n\mathrm{A}=[\mathrm{M\,A}_n]\,\mathrm{X_3}+nQ,$$

and

$$Q=P-R+S+\frac{\Phi-\Phi_1}{n} \qquad (1a),$$

where n is the co-ordination number.

When the ligands are negative ions,

$$\mathrm{M\,X_3}+(n-3)\,\mathrm{K\,X}=[\mathrm{M\,X}_n]\,\mathrm{K}_{n-3},$$

and

$$Q=P-R+S+\frac{\Phi-\Sigma\Phi_1}{n} \qquad (1b),$$

where $\Sigma\Phi_1$ denotes the sum of the lattice energies of the compounds of first order.

Let Q' be the heat of formation of the complex radical from the central ion and the ligands, (1a) and (1b) will be equally reduced to

$$Q'=P-R+S \qquad (1').$$

It must be noticed here that the process (4) is the reverse reaction of the photochemical process by $h\nu_2$ mentioned above.

Hence

$$S = h\nu_2 \qquad (2).$$

Therefore, S may be found spectroscopically and Q and Φ's may also be determined experimentally. The value P could be calculated if the polarized state of the ligand in the position of co-ordination were exactly known. At present, however, we should be contented with approximate computation from its polarizability or dipole moment. And in special cases, R might be estimated. A few example of computing R are as follows.

(A) Mercuric chloride. This compound may be regarded as a co-ordination compound, as will be discussed in Part II[30] of this paper, and consequently the rules of absorption spectra so far obtained may be applied. As the molecule is of linear configuration,[31] a third band is expected (section II), nevertheless it will lack the first band (section IV). Therefore, the band of the longest wave-length, i.e., 205 mμ,[32] should be regarded as the second. The data necessary to calculate R are as follows. Latent heat of vaporization of mercury: $L = 13.8$ Cal. Ionization potentials: $V_{\mathrm{I}} = 10.38$ volts, $V_{\mathrm{II}} = 18.67$ volts. Heat of dissociation of chlorine: $D = 100$ Cal. Electron affinity of chlorine: $E = 88$ Cal. Polarizability of chlorine ion: $\alpha = 3.05 \times 10^{-24}$ e.s.u. Lattice energy of mercuric chloride: neglected. The second band: $\nu_2 = 146 \times 10^{13}\mathrm{sec}^{-1}$ ($\lambda_2 = 205$ mμ). Heat of formation of mercuric chloride: $2Q = 53.2$ Cal. Distance between Hg and Cl in the molecule: $d = 2.25$ Å.

$$\left.\begin{array}{l} (\mathrm{Hg}) \xrightarrow[-L=14]{\text{vaporization}} \mathrm{Hg} \xrightarrow[-J=e(V_{\mathrm{I}}+V_{\mathrm{II}})=667]{\text{ionization}} \mathrm{Hg}^{++} \\ \mathrm{Cl_2} \xrightarrow[-D=100]{\text{dissociation}} 2\,\mathrm{Cl} \xrightarrow[+2E=2\times 88]{\text{ionization}} 2\,\mathrm{Cl}^- \end{array}\right\} \xrightarrow[+2NP=2\times 313]{\text{approach}}$$

$$\xrightarrow[+2Q=53]{\text{combination}} [\mathrm{Cl\text{-}Hg\text{-}Cl}] \xleftarrow[+2NS=2Nh\nu_2=2\times 132]{\text{co-ordinate combination}} [\{\mathrm{Cl}^-\}\,\mathrm{Hg}\,\{\mathrm{Cl}^-\}] \xleftarrow[-2NR=x]{\text{excitation}}$$

From the cyclic process R may be found: viz., $NR = 116$ Cal.

(B) $[\mathrm{Ni(NH_3)_6}]\mathrm{Cl_2}$ and $[\mathrm{Ni(H_2O)_6}]\mathrm{Cl_2}$. The first bands of these compounds lie in the infra-red regions and the second bands are those whose maxima are at 568 mμ and 718 mμ respectively.

(30) It will be soon published.
(31) H. Braekken and W. Scholten, *Z. Krist.*, **89** (1934), 448.
(32) H. Fromherz and K. Lih, *Z. physik. Chem.*, A, **167** (1933), 103.

Complex salt	$6NQ$	λ_2	ν_2 (10^{13})	$Nh\nu_2$ ($= NS$)	NR
$[Ni(NH_3)_6]Cl_2$	86.4 Cal.	568 mμ	52.8	47.5 Cal.	$37.1+N\left(\frac{\Phi-\Phi_1}{6}+P\right)$ Cal.
$[Ni(H_2O)_6]Cl_2$	20.3 ,,	718 ,,	41.8	37.6 ,,	$34.2+\left(\frac{\Phi'-\Phi_1}{6}+P'\right)$,,

The lattice energy of $NiCl_2$, Φ_1 and the polarizability of H_2O being unknown, the values NR could not be calculated, but it may be assumed that $\Phi \simeq \Phi'$ and $P \simeq P'$. Hence the energies of excitation of NH_3 and H_2O in the ammine and the aquo-salt are nearly the same, in spite of the great difference between their heats of formation.

Summary.

(1) The origins of absorption bands of co-ordination compounds have been discussed.

(2) The first band is attributed to electron transitions in the unsaturated transition shell of the central ion. The band, therefore, appears only when the central ion is of a transition element.

(3) The shift of the first band by substitution of ligands may be explained by postulating that the electron transitions are more or less depressed by the negative field of the ligand, which may conveniently be represented by P, the energy of approach of the ligand, i.e., the work done by the ligand if it were to approach from infinity to the seat of co-ordination. The ascending order of P, i.e., the sequence of hypsochromic effect, is theoretically

$$NH_3,\ H_2O,\ F^-,\ Cl^-,\ Br^-,\ I^-.$$

The empirically obtained order of hypsochromic effect on the first band is

$$NO_2^-,\ NH_3,\ ONO^-,\ H_2O,\ NCS^-,\ NO_3^-,\ SO_4^=,$$
$$OH^-,\ C_2O_4^=,\ CO_3^=,\ S_2O_3^=,\ Cl^-, CrO_4^=,\ Br^-.$$

All the experimental rules so far obtained of the shifts of the first bands by substitutions of ligands may be explained by the hypothesis.

(4) The first band is more or less additive. The complexes which have ligands situated far apart in the spectrochemical series have broader and less symmetrical first bands than those which contain only one kind of ligands.

(5) The second band may be attributed to the co-ordination electrons, and is, therefore, the most general characteristic which a co-ordination compound should possess. Postulating that by absorption of a quantum $h\nu_2$ (ν_2 = frequency of the second band) the co-ordinate linkage is broken to produce an excited metastable ligand in the original seat of co-ordination, the following relations have been derived.:

$$Q = P - R + S + \frac{\Phi - \Sigma\Phi_1}{n},$$

and

$$S = h\nu_2,$$

where Q = heat of formation per co-ordination, R = activation energy, S = co-ordination energy, Φ = lattice energy of the co-ordination compound, Φ_1's = lattice energies of the component compounds of first order, and n = co-ordination number.

The author wishes to express sincere thanks to Professor Y. Shibata for his kind advice and encouragement. He is also indebted to Mr. M. Kobayashi and Mr. S. Kashimoto for their experimental assistance.

Chemical Department, Faculty of Science,
Imperial University of Osaka.

The Addition of Hydrogen Bromide to Allyl Bromide in the Presence of Various Substances. VII. The Effect of Nickel in the Form of Filings, and the Influence of Antioxidants on the Actions of Oxygen and Reduced Nickel.

By Yoshiyuki URUSHIBARA and Matsuji TAKEBAYASHI.

(Received March 31, 1938.)

In the presence of oxygen and peroxides hydrogen bromide adds slowly to allyl bromide and the product consists of nearly pure 1,2-dibromo-propane, while in the presence of oxygen or a peroxide the addition is rapid and 1,3-dibromo-propane is formed as the main product.[1] The addition of an antioxidant such as diphenylamine to the reaction mixture eliminates the effect of oxygen and peroxides.[1] Reduced nickel and reduced iron show an effect quite similar to that of oxygen so far as

(1) M. S. Kharasch and F. R. Mayo, *J. Am. Chem. Soc.*, **55** (1933), 2468.

the results of the reaction are concerned.[2] However, the action of these metals is not influenced by diphenylamine.[3] Further, it seems that no parallelism exists between the hydrogenating activity of reduced nickel and the effect on the addition: reduced nickel prepared at a temperature too high for a hydrogenating catalyst showed a very strong effect on the addition.[4] The present paper deals with an experiment on the effect of nickel filings and a comparative investigation of the influence of anti-oxidants on the actions of oxygen and reduced nickel. The results of experiments are summarized in the accompanying table.

Table.

Allyl bromide 24 g. (0.2 mol). Hydrogen bromide 20 g. (0.25 mol).
Addition in the dark at room temperature (12-15°). Reaction time 3 days.

Exp.	In presence of	Products		
		Total yield (%)	B. p. (°C./mm.)	1,3-Dibromo-propane (%)
1	None (vacuum)	25	28-32/10	4
2[5]	Oxygen 2.5 c.c.	53	42-51.5/9	96
3	Reduced nickel 3.5 g.	55	38-46.5/8	91
4	Nickel filings 7.0 g.	50	38-49.5/10	68
5	Diphenylamine 0.5 g. (1.5 mol %) Oxygen 2.0 c.c.	28	28-32/9	9
6	Diphenylamine 0.5 g. Reduced nickel 3.5 g.	55	43-55/12	81
7	Catechol 0.3 g. (1.5 mol %) Oxygen 2.0 c.c.	27	28-32/9	9
8	Catechol 0.3 g. Reduced nickel 3.5 g.	26	28-32/10	12
9	Hydroquinone 0.3 g. (1.5 mol %) Oxygen 2.0 c.c.	25	32-35/13	7
10	Hydroquinone 0.3 g. Reduced nickel 3.5 g.	29	35-40/14	20

Pure allyl bromide (24 g. or 0.2 mol) and hydrogen bromide (20 g. or 0.25 mol) were sealed in reaction tubes of Pyrex glass in addition of none (vacuum) (Exp. 1), oxygen (2.5 c.c.) (Exp. 2),[5] reduced nickel (3.5 g.) (Exp. 3), nickel filings (7.0 g.) (Exp. 4), oxygen (2.0 c.c.) and

(2) Y. Urushibara and M. Takebayashi, this Bulletin, **11** (1936), 692, 754; **12** (1937), 51.
(3) Y. Urushibara and M. Takebayashi, *ibid.*, **11** (1936), 754.
(4) Y. Urushibara and M. Takebayashi, *ibid.*, **12** (1937), 51.
(5) Exp. 12 of the fifth paper of this series, *ibid.*, **12** (1937), 140.

an antioxidant (1.5 mol%) (Exp. 5, 7, and 9), and reduced nickel (3.5 g.) and an antioxidant (1.5 mol%) (Exp. 6, 8, and 10). The substances used as antioxidants were diphenylamine (Exp. 5 and 6), catechol (Exp. 7 and 8), and hydroquinone (Exp. 9 and 10). The reaction tubes were shaken during daytime and left to stand still at night for three days in the dark at room temperature (12–15°C.). Then the yield and the composition of the products were determined.

Although it can be supposed that nickel filings might possess a comparatively small surface area in spite of the amount doubled and the nature of the surface might be quite different from that of the surface of reduced nickel, the filings exhibited an unexpectedly great effect (Exp. 4).

All the antioxidants so far used eliminated nearly completely the effect of oxygen (Exp. 5, 7, and 9), a confirmation of the results of Kharasch and Mayo,[1] while the effect of reduced nickel was diminished only slightly by diphenylamine (Exp. 6) in accord with previous observations[3] but rather heavily by catechol (Exp. 8) and by hydroquinone (Exp. 10). Parallel results have been obtained in the addition of hydrogen bromide to undecenoic acid as reported in the following paper.

An assurance that the effect of ferromagnetic metals is due to the action of the metals themselves and not of oxygen which might be present by chance was afforded by the fact that diphenylamine eliminates the effect of oxygen but not that of ferromagnetic metals.[3] This remains still true, but such an assurance could not have been obtained by the experiments with catechol and hydroquinone. However, that the ferromagnetic metals themselves are responsible for the effect observed in the addition in their presence was further established by the experiments with the metals which had never been in contact with oxygen (air) after repeated reduction in the reaction tube.[4]

Kharasch and co-workers[6] propose a hypothesis that bromine atoms are responsible for the effect of oxygen and peroxides in the addition of hydrogen bromide to unsaturated compounds. It is supposed that bromine atoms are produced by the action of oxygen or a peroxide on hydrogen bromide. However, it can not reasonably be assumed that reduced nickel would exhibit an oxidation-like effect on hydrogen bromide to produce bromine atoms, and, therefore, the influence of catechol and hydroquinone on the action of reduced nickel can hardly be attributed to the antioxidant effect of these substances. It is very probable that

(6) M. S. Kharasch, H. Engelmann, and F. R. Mayo, *J. Org. Chem.*, **2** (1937), 298.

the modes of influence of the antioxidants on the actions of nickel and oxygen are so much different as the modes of action of these catalysts on the addition. The authors will come back to this problem some other time.

Experimental.

Allyl bromide was purified by drying over calcium chloride and then redistilling in addition of hydroquinone. The absence of peroxides was ascertained by the test with ferrous ammonium sulphate and ammonium thiocyanate. Hydrogen bromide was prepared by the action of purified bromine on hot tetralin, washed by passing through cold tetralin and over moist red phosphorus, then dried with anhydrous calcium bromide and with phosphorus pentoxide. Diphenylamine and hydroquinone were purified by recrystallization from ligroin and from alcohol respectively, while commercial catechol (E. Merck) was used directly. Reduced nickel was prepared by reducing nickel oxide (Kahlbaum) with hydrogen at about 400°. Nickel filings were prepared from an ordinary thick nickel wire with a new file.

The experimental procedure was as follows. Exp. 5, 7 and 9: Allyl bromide (24 g. or 0.2 mol) and the antioxidant (1.5 mol per cent) were taken in the reaction tube, and cooled in a mixture of solid carbon dioxide and chloroform. Hydrogen bromide was passed into the tube until the required increase in the volume of the liquid (corresponding to 20 g. or 0.25 mol of hydrogen bromide) was reached (total volume 27 c.c.). Then the tube was cooled in liquid air, evacuated, and sealed off after admission of oxygen (2.0 c.c.). Exp. 1: Allyl bromide was taken in a mixing tube and hydrogen bromide condensed. Then the mixture was frozen in liquid air, the mixing tube was joined by fusion with the reaction tube, and the whole system was evacuated. The mixing tube was taken out of liquid air and the reaction tube was put into liquid air, whereby the mixture distilled into the reaction tube in vacuum. The tube was then sealed off without entrance of air. Exp. 3 and 4: Reduced nickel (3.5 g.) or nickel filings (7.0 g.) were taken in the reaction tube already joined with the mixing tube containing the frozen mixture of allyl bromide and hydrogen bromide, and, while the mixture was cooled in liquid air, the nickel was heated to 350–360° or above in the atmosphere of hydrogen, hydrogen being renewed three times by evacuation and introduction. Then the tubes were evacuated, the nickel cooled down, the mixing tube taken out of liquid air, and the reaction tube put into liquid air and sealed off in vacuum when the distillation of the mixture was over. Exp. 6, 8 and 10: The mixture of allyl bromide and the antioxidant was decanted in vacuum into the reaction tube cooled in solid carbon dioxide and chloroform after the reduced nickel was treated as mentioned above, and hydrogen bromide was passed into the reaction tube. The mixture was frozen in liquid air and sealed in vacuum.

The reaction tubes were slipped into iron pipes, and shaken during daytime at room temperature. After three days the reaction mixtures were treated according to the directions of Kharasch and Mayo,[1] and the compositions of the products were determined from the refractive indices, while the total yields from the weights.

Diphenylamine and hydroquinone gave yellow and brown colours respectively to the reaction mixtures in presence of oxygen, while catechol a reddish violet colour in presence of either reduced nickel or oxygen.

The authors thank the Imperial Academy of Japan for a grant.

Chemical Institute, Faculty of Science,
Imperial University of Tokyo.

The Addition of Hydrogen Bromide to Undecenoic Acid in Toluene Solution. II. The Influence of Antioxidants on the Actions of Oxygen and Reduced Nickel.

By Yoshiyuki URUSHIBARA and Matsuji TAKEBAYASHI.

(Received March 31, 1938.)

In the previous work of this series it was established that an effect similar to that of oxygen is exhibited by reduced nickel on the addition of hydrogen bromide to undecenoic acid in toluene solution.[1] Some of the results of the previous experiments are quoted in Table 1 for the sake of comparison. The present paper is concerned with a comparative investigation of the influence of antioxidants on the actions of oxygen (air) and reduced nickel. The results are given in Table 2.

Table 1.

Undecenoic acid (g.)	Toluene (c.c.)	In presence of	Product	
			Melting point (°C.)	11-Bromo-undecanoic acid (%)
3.68	20	None (vacuum)	34.7	1
3.68	20	Air	48.7	97
2.5	20	Reduced nickel 3.0 g.	25.5	34

(1) This Bulletin, **13** (1938), 331.

Table 2.

Undecenoic acid 2.5 g. Toluene 20 c.c. Hydrogen bromide passed for one hour at 0°C. in the dark.

Exp.	In presence of	Product	
		Melting Point (°C.)	11-Bromo-undecanoic acid (%)
1	Diphenylamine 0.5 g. (22 mol %) Air	40.0	65
2	Diphenylamine 0.5 g. Reduced nickel 3.0 g.	26.5	31
3	Catechol 0.3 g. (22 mol %) Air	33.5	6
4	Catechol 0.3 g. Reduced nickel 0.3 g.	33.0	8
5	Hydroquinone 0.3 g. (22 mol %) Air	34.2	3
6	Hydroquinone 0.3 g. Reduced nickel 3.0 g.	32.6	10

Hydrogen bromide was passed for one hour at 0°C. in the dark into the toluene solution of pure undecenoic acid (2.5 g.) in the presence of an antioxidant (22 mol% to the acid) and either air (Exp. 1, 3, and 5) or reduced nickel (3.0 g.) (Exp. 2, 4, and 6). Diphenylamine (Exp. 1 and 2), catechol (Exp. 3 and 4), and hydroquinone (Exp. 5 and 6) were used as antioxidants. The antioxidants were dissolved in toluene together with undecenoic acid. Hydroquinone was sparingly soluble in toluene and mostly remained undissolved. In other respects the reactions were run in the same way as described in the previous paper.[1]

The reaction mixtures were treated also in the same way as previously. Diphenylamine (hydrobromide) remaining in white solid in the toluene solution was filtered off at 0°C. after hydrogen bromide was removed in vacuum. Catechol gave a reddish violet colour to the reaction mixture in presence of either reduced nickel or air. Catechol and hydroquinone were washed out with water until the washings gave no colouration with ferric chloride. The reaction was always complete and the products did not decolourize bromine. The composition was determined from the melting point as previously.

The inhibiting influence of diphenylamine on the action of oxygen was found rather weak (Exp. 1). This may be attributed at least partly to the effect of the solvent and especially to the small solubility of diphenylamine hydrobromide in toluene, because R. Ashton and J. C. Smith[2]

(2) *J. Chem. Soc.*, **1934**, 435.

observed a marked influence of diphenylamine on the action of oxygen in the addition of hydrogen bromide to undecenoic acid in ligroin solution. Diphenylamine exhibited a negligibly small influence on the action of reduced nickel (Exp. 2). In view of the weak influence of diphenylamine on the action of reduced nickel in the addition of hydrogen bromide to allyl bromide,[3] it can be supposed that, even if the diphenylamine salt were more soluble in toluene, the inhibiting influence on the action of reduced nickel would not be much stronger. Catechol and hydroquinone exerted a strong inhibiting influence on the actions of both oxygen and reduced nickel (Exp. 3–6). There may be found a certain parallelism between the case of allyl bromide[3] and that of undecenoic acid. In both cases, in the amounts used, reduced nickel exhibited a greater effect on the addition than oxygen in the present of any of the antioxidants so far used, while the order of the extents of their effects was reversed in absence of the antioxidants. In this sense it may be said that the antioxidants exerted a greater inhibiting influence on the action of oxygen than on that of reduced nickel, even though their actions can not be correlated to each other, oxygen being a homogeneous, and reduced nickel a heterogeneous, catalyst, and the mechanisms of their actions being quite obscure. Further it may be pointed out that in both cases (allyl bromide and undecenoic acid) the action of oxygen was inhibited the most severely by hydroquinone while that of reduced nickel by catechol.

The authors thank the Imperial Academy of Japan for a grant.

Chemical Institute, Faculty of Science,
Imperial University of Tokyo.

(3) See the preceding paper, this Bulletin, **13** (1938), 400.

The Supposed Activation of Hydrogen Bromide by Oxygen. (Preliminary Note.)

By Yoshiyuki URUSHIBARA and Osamu SIMAMURA.

(Received May 5, 1938.)

In hopes of obtaining grounds for explaining the effects of oxygen and of ferromagnetic metals on the addition of hydrogen bromide to unsaturated organic compounds[1] and on the catalytic action of hydrogen bromide in the isomerization of isostilbene into stilbene,[2] the authors sealed reduced nickel freshly prepared and hydrogen bromide in a glass tube and the same in addition of oxygen in another, the amounts of all the substances being known, and examined the contents of the tubes after having placed them in the dark at room temperature for a fortnight. Unchanged hydrogen bromide was condensed by cooling in liquid air, and the pressure of the remaining gas mixtures was determined. Then the nickel was extracted with water and nickel and bromine in the resulting aqueous solutions were estimated. It was deduced that in absence of oxygen reduced nickel and hydrogen bromide underwent practically no change, while in presence of oxygen nearly all the hydrogen bromide introduced reacted with nickel to produce nickel bromide and hydrogen without giving rise to the formation of water. Thus oxygen was not brought to chemical reaction with any of reduced nickel, hydrogen bromide, hydrogen molecules, and hydrogen atoms, if any, and it is very probable that oxygen activated hydrogen bromide in the reaction with reduced nickel to produce nickel bromide and hydrogen. The experimental details and discussions will follow.

The authors thank the Japan Society for the Promotion of Scientific Research for a grant.

Chemical Institute, Faculty of Science,
Imperial University of Tokyo.

---

(1) This Bulletin, **11** (1936), 692, 754, 798; **12** (1937), 51, 138, 173; **13** (1938), 331, 400, 404.

(2) This Bulletin, **12** (1937), 507.

Die Vergleichung der Dichte des Leitungswassers von Osaka, Japan und von Cambridge, U.S.A.

Von Toshizo TITANI und Noriyoshi MORITA.

(Eingegangen am 28. April 1938.)

Inhaltsübersicht. Die Dichte des gereinigten Osaka- und Cambridge-Leitungswassers wurde untereinander verglichen. Daraus ergab sich, dass die beiden Wasser innerhalb $\pm 0.2\ \gamma$ dieselbe Dichte besitzen. Zu gleicher Zeit fanden wir, dass die zeitliche Schwankung der Dichte des Osaka-Leitungswassers innerhalb $\pm 0.1\ \gamma$ liegt. Die Änderung der Dichte des Wassers wegen der isotopischen Fraktionierung bei dessen Destillation und wegen der Veränderung des Sättigungsgrades der Luft in demselben wurde diskutiert und zugleich experimentell geprüft. Bei der genauen Vergleichung der Dichte des Wassers müssen die beiden zu vergleichenden Wasser unter möglichst gleichen Versuchsbedingungen gereinigt und behandelt werden.

Geschichtliche Einleitung. Eine der zuverlässigsten Methoden zur Bestimmung des Gehaltes des gewöhnlichen Wassers an schwerem Wasserstoff bzw. Deuterium liegt darin, dass man ein praktisch deuteriumfreies Wasser bzw. leichtes Wasser aus dem betreffenden Wasser bereitet und die Dichteabnahme des so gewonnenen leichten Wassers dem originalen Wasser gegenüber genau bestimmt.(1) Nach dieser Methode wurden schon ziemlich viele Arten von Wasser, meistens Leitungswasser, aus den verschiedensten Orten auf der Erde nach dessen Gehalt an Deuterium untersucht. Die Ergebnisse dieser vielen Versuche stimmen miteinander im allgemeinen gut überein, falls man dabei unter Umständen eine geeignete Korrektion in Rechnung bringt.(1) Aber trotzdem kann man noch bei genauerer Vergleichung einen kleinen Unterschied zwischen einzelnen Bestimmungen herausfinden. So wurde z.B. nach der oben erwähnten Methode von uns gefunden, dass das Vorkommenverhältnis von schwerem (D) und leichtem (H) Wasserstoff in Osaka-Leitungswasser $D:H = 1:5600$ ist.(1) Dagegen führten Greene und Voskuyl in Cambridge (U.S.A.) einen ähnlichen Versuch mit dem örtlichen Leitungswasser aus und erhielten einen Wert, der von unserem ein wenig verschieden war.(2) Da aber diese beiden Versuche nach ähnlicher Methode durchgeführt wurden, liegt nun die Vermutung nahe, dass es sich, wenn auch um einen kleinen, doch wirklichen Unterschied des Gehaltes an Deuterium bzw. der Dichte der beiden Arten von Leitungswasser handeln kann. Aus diesem

(1) N. Morita und T. Titani, dies Bulletin, **11** (1936), 403.
(2) Noch nicht veröffentlichte Arbeit.

Grund hat Herr Dr. Greene uns vorgeschlagen, die beiden örtlichen Leitungswasser gegenseitig auszutauschen und deren Dichte untereinander zu vergleichen. Diesem Vorschlage folgend schickten wir nach Cambridge eine Menge des Osaka-Leitungswassers und zugleich bekamen wir von Cambridge eine Menge des örtlichen Leitungswassers. Dabei versprachen wir zugleich, auf Ersuchen von Dr. Greene hin, die mit diesem Wasser erhaltenen Versuchsergebnisse am 14. Juni 1937 uns gegenseitig mitzuteilen. Die vorliegende Arbeit wurde von uns ausgeführt und zwar mit dem Resultat, dass das Versuchsergebnis, wie weiter unten noch zu erwähnen sein wird, mit dem von Dr. Greene und Dr. Voskuyl gut übereinstimmte.

Reinigung des Wassers. Das in diesem Versuch verwendete Cambridge-Leitungswasser wurde von Dr. Greene am 22. Dezember 1936 in Cambridge gesammelt und uns in einer reinen Blechbüchse in gutem Zustand übermittelt. Das damit zu vergleichende Osaka-Leitungswasser wurde von uns in hiesigem Laboratorium am 17. Dezember 1935 sowie am 25. Oktober 1937 gesammelt, und das erstere war bis zu diesem Versuch in einem zugeschmolzenen Glasrohr aufbewahrt. Alle diese Arten von Wasser wurden vor der Dichtebestimmung sorgfältig gereinigt. Da aber die Reinigung auf übliche Weise durch wiederholte Destillationen ausgeführt wurde, gaben wir dabei auf die Änderung der Dichte des Wassers wegen der isotopischen Fraktionierung bei der Destillation besonders acht. In der Praxis arbeiteten wir immer mit einer bekannten Menge von Wasser und bei dessen Destillation massen wir zugleich die Menge des Wassers, das am Anfang und Ende der Destillation weggeschüttet wurde. Der dabei benutzte Reinigungsprozess bestand aus nacheinander folgenden vier Stufen von Destillationen, nämlich (1), (2), (3) und (4).

(1) In der ersten Stufe der Destillation wurde ein verschiedenes Volumen von Wasser, das entweder 20 c.c., 25 c.c. oder 200 c.c. betrug, in einem Glaskolben mit einem Rückflusskühler unter Zusatz von einer kleinen Menge von KOH und $KMnO_4$ einige Stunden lang sieden gelassen und darauf abdestilliert. Dabei schütteten wir am Anfang der Destillation verschiedenes, aber wohl bekanntes Volumen des ersten Destillats weg und liessen zugleich am Ende der Destillation verschiedenes Volumen des Wassers im Destillierkolben zurück.

(2) Das Destillat aus der (1) Destillation wurde unter Zusatz einer kleinen Menge von P_2O_5 und $KMnO_4$ abermals abdestilliert. Dabei schütteten wir genau dasselbe Volumen des ersten Destillats wie bei der (1) Destillation weg und zugleich liessen wir am Ende der Destillation

ebenfalls genau dasselbe Volumen des Wassers wie bei der (1) Destillation im Destillierkolben zurück.

(3) Auf dieser Stufe der Destillation nahmen wir gegen (1) und (2) immer dieselbe Menge (ca. 15 c.c.) des Wassers aus dem Destillat (2) und destillierten dies unter Zusatz einer kleinen Menge von $Ba(OH)_2$ im CO_2-freiem Luftstrom ab.

(4) Diese letzte vierte Stufe der Destillation führten wir unter Verwendung der ganzen Menge des Destillats aus der (3) Destillation ebenfalls in CO_2-freiem Luftstrom aber ohne Zusatz und durch einen Pyrexkühler durch. Bei dieser (4) und der letzten (3) Destillation gossen wir am Anfang der Destillation immer dieselbe Menge des ersten Destillats weg und liessen zugleich am Ende der Destillation immer dieselbe Menge des Wassers im Destillierkolben zurück.

Auf diese Weise arbeiteten wir in den (1) und (2) Destillationen mit verschiedenen Volumen von Wasser; zugleich gossen wir am Anfang jeder Destillation verschiedene Menge des ersten Destillats weg und liessen am Ende der Destillation ebenfalls verschiedene Menge von Wasser im Destillierkolben zurück. Dagegen behandelten wir in den letzten beiden Destillationen (3) und (4) immer dieselbe Menge von Wasser unter genau denselben Versuchsbedingungen. Folglich, falls man irgendeine Änderung im Dichteunterschied zwischen zwei denselben Wasserarten infolge der ungleichen Reinigungsprozesse herausfinden kann, muss man die Ursache dafür ausschliesslich in den ungleichen Versuchsbedingungen bei den ersten zwei Destillationsprozessen (1) und (2) suchen.

Dichtevergleichung des Wassers. Die Dichte des wie oben gereinigten Wassers wurde in einigen Fällen ohne weiteres aber in den anderen Fällen nach dem Auspumpen der darin eingelösten Luft untereinander verglichen. Beim letzteren Fall wurde das gereinigte Wasser im Vakuum solange ausgepumpt bis keine Luftblasen mehr auftraten. Die Vergleichung der Dichte des Wassers führten wir nach der Schwebemethode mittels eines Quarzschwimmers bei 9.5°C. durch. Das Volumen des dazu benutzten Quarzschwimmers betrug ca. 1 c.c. und das des untersuchten Wassers ca. 12 c.c. Die dadurch erhaltenen Messergebnisse geben wir in Tabellen 1 und 2 wieder. Dabei führten wir die Dichtevergleichung nicht nur zwischen Osaka- und Cambridge-Leitungswasser (Tabelle 1), sondern auch zwischen zwei Wasserproben aus demselben Leitungswasser (Tabelle 2) durch, die aber bei den Reinigungsdestillationen (1) und (2) unter verschiedenen Bedingungen behandelt wurden. Die letzteren Versuche wurden zu dem Zweck durchgeführt, um daraus über den Einfluss der Destillation auf die Dichte des Wassers Kenntnis zu gewinnen.

Messergebnisse. Abkürzungen:

Osaka (35): das Osaka-Leitungswasser, das am 17. Dez. 1935 gesammelt wurde.

Osaka (37): das Osaka-Leitungswasser, das am 25. Okt. 1937 gesammelt wurde.

Cambridge (36): das Cambridge-Leitungswasser, das am 22. Dez. 1936 gesammelt wurde.

L: lufthaltig.

O: Luft ist möglichst vollständig ausgepumpt.

V: das Volumen des Wassers, das bei den Destillationen (1) und (2) (siehe oben) verwendet wurde.

V_a: das Volumen des ersten Destillats, das am Anfang der Destillationen (1) und (2) respektive weggegossen wurde.

V_e: das Volumen des Wassers, das am Ende der Destillationen (1) und (2) resp. im Destillierkolben zurückblieb und weggegossen wurde.

T: Ablesung des Beckmannthermometers, das bei der Dichtebestimmung nach Schwebemethode im Thermostat eingetaucht war.

ΔT: die Differenz zwischen T der beiden zu vergleichenden Wasserarten.

Δs: der Dichteunterschied zwischen zwei Wasserproben, der nach Gl. (1) aus ΔT berechnet wurde;

$$\Delta s = -79 \times \Delta T \qquad (1).$$

Δs (korr.): der korrigierte Dichteunterschied (siehe weiter unten).

Tabelle 1. Vergleichung der Dichte des Osaka- und Cambridge-Leitungswassers.

Versuchs-nr.	Wasserart	V c.c.	V_a c.c.	V_e c.c.	T	ΔT	Δs γ	Δs (korr.) γ
1	Osaka (35)L	20	1	1	4.381	−0.002	+0.2	+0.2
	Cambridge (36)L	20	1	1	4.383			
2	Osaka (37)O*	25	3	1	3.840	−0.002	+0.2	+0.2
	Cambridge (36)O**	25	3	1	3.842			
3	Osaka (35)L	200	2	2	3.826	−0.004	+0.3	+0.3
	Cambridge (36)L	200	2	2	3.830			
4	Osaka (37)O***	200	10	2	3.838	−0.004	+0.3	+0.3
	Cambridge (36)O****	200	10	2	3.842			

Tabelle 1.—(*Fortsetzung*)

Versuchs-nr.	Wasserart	V c.c.	V_a c.c.	V_e c.c.	T	ΔT	Δs γ	Δs (korr.) γ
5	Osaka (35)*L*	200	2	2	3.764	−0.006	+0.5	+0.1
	Cambridge (36)*L*	20	1	1	3.770			
6	Csaka (35)*L*	200	2	2	4.591	−0.009	+0.7	+0.3
	Cambridge (36)*L*	20	1	1	4.600			
7	Osaka (37)*O****	200	10	2	3.838	−0.004	+0.3	+0.3
	Cambridge (36)*O***	25	3	1	3.842			
8	Osaka (37)*O**	25	3	1	3.840	−0.002	+0.2	+0.2
	Cambridge (36)*O*****	200	10	2	3.842			

Tabelle 2. Änderung der Dichte desselben Leitungswassers wegen der verschiedenen Bedingungen bei den Destillationen.

Versuchs-nr.	Wasserart	V c.c.	V_a c.c.	V_e c.c.	T	ΔT	Δs γ
9	Osaka (35)*L*	200	2	2	3.829	−0.005	+0.4
	Osaka (35)*L*	20	1	1	3.834		
10	Osaka (37)*O*	200	10	2	3.838	−0.011	+0.9
	Csaka (37)*L*	200	10	2	3.849		
11	Osaka (37)*O****	200	10	2	3.838	−0.002	+0.2
	Osaka (37)*O**	25	3	1	3.840		
12	Cambridge (36)*O*****	200	10	2	3.842	±0.000	±0.0
	Cambridge (36)*O***	25	3	1	3.842		

*, **, ***, ****, resp. dasselbe Probewasser.

Diskussion der Ergebnisse. Wie man von vornherein erwarten kann und wirklich aus den oben angegebenen Tabellen ersieht, wird der direkt gefundene Dichteunterschied Δs zwischen zwei Wasserproben ziemlich stark von den Versuchsbedingungen bei deren Reinigungsprozess beeinflusst. Behandelt man nämlich bei den Reinigungsdestillationen (1) und (2) (vgl. oben) die gleiche Menge von Wasser unter möglichst gleichen Versuchsbedingungen, so erhält man innerhalb der Messfehlergrenze immer dieselben Ergebnisse, wie dies bei den Versuchen 1, 2, 3 und 4 in Tabelle 1 der Fall ist. Aus diesen Versuchen (1, 2, 3 und 4) folgt deshalb ohne weiteres, dass das Osaka-Leitungswasser durchschnittlich um $0.2 \pm 0.2\,\gamma$ schwerer als das Cambridge-Leitungswasser ist. Als wir

dagegen, wie bei den Versuchen 5 und 6 in Tabelle 1, das Volumen der beiden zu vergleichenden Wasser bei den Reinigungsprozessen (1) und (2) ungleich gross wählten, zeigte sich, dass der Dichteunterschied zwischen beiden Wasserarten deutlich zunahm. Durch diese ungleiche Behandlung konnten wir sogar zwischen denselben Wassersorten einen erheblichen Dichteunterschied herausfinden, wie dies beim Versuch 9 in Tabelle 2 der Fall ist. Alle diese Ergebnisse weisen ohne Zweifel darauf hin, dass das Wasser bei seiner Destillation eine ziemlich merkliche Änderung in seiner Isotopenzusammensetzung erleidet und dadurch seine Dichte verändern kann. Um diese teils schon wohl bekannte Tatsache zu vermeiden, verfährt man aber gewöhnlich so, dass man das Volumen des Wassers, das am Ende der Destillation im Destillierkolben zurückbleibt, möglichst gleich wie das des ersten Destillats wählt, das am Anfang der Destillation abdestilliert und weggeschüttet wird. Aber wie aus einer einfachen Rechnung sofort ersichtlich ist, kann man auf diese Weise die Änderung der Dichte des Wassers bei der Destillation nicht vollkommen vermeiden.

Bezeichnet man nämlich den isotopischen Trennfaktor der z.B. Wasserstoffisotope bei der Destillation des Wassers mit α, dann kann man die Konzentration des schweren Wasserstoffisotops D in dem ersten Destillat gleich $1/\alpha$ der im originalen Wasser setzen, wenn die D-Konzentration in demselben wie beim gewöhnlichen Wasser genügend klein ist. Dagegen muss die D-Konzentration im Wasser, das am Ende der Destillation im Destillierkolben zurückbleibt gleich $n^{\frac{\alpha-1}{\alpha}}$ der im originalen Wasser sein, falls das Volumen des ersteren $1/n$ des letzteren ist. Aus dieser Rechnung ersieht man deshalb, dass das Mittel- bzw. Hauptdestillat eine gewisse Änderung in seiner Isotopenzusammensetzung erleiden muss, wenn man das Volumen des ersten Destillats einfach gleich gross wie das des zurückbleibenden Wassers, d.h. $1/n$ des ganzen zu destillierenden Wassers wählt. Um diese Änderung der Dichte des Mitteldestillats zu vermeiden, muss man folglich das Volumen des wegzuschüttenden ersten Destillats um einige mal so gross wie das des zurückbleibenden Wassers wählen. Setzt man nun dafür den Faktor k, so kann er offenbar durch Gl. (2) errechnet werden, weil dabei die D-Konzentration c_m im Mitteldestillat gleich gross wie die c im originalen Wasser sein muss,

$$c_m = \frac{Vc - Vc\frac{k}{n}\frac{1}{\alpha} - Vc\frac{1}{n}n^{\frac{\alpha-1}{\alpha}}}{V - V\frac{k}{n} - V\frac{1}{n}} = c \qquad (2).$$

wo V das ganze Volumen des zu destillierenden Wassers ausdrückt. Aus dieser Gl. (2) folgt ohne weiteres, dass

$$k = \frac{n^{\frac{\alpha-1}{\alpha}} - 1}{1 - \frac{1}{\alpha}} \qquad (3)$$

ist. Das aber der Trennfaktor α der Wasserstoffisotope bei der Destillation des Wassers beinahe gleich 1 ist, so kann man diese Gl. (3) weiter wie folgt vereinfachen:

$$k = \frac{\alpha\left(1 + \left(\frac{\alpha-1}{\alpha}\right)\ln n - 1\right)}{\alpha - 1} = \ln n = 2.3 \log n \qquad (4).$$

Wenn man demnach das Volumen des ersten Destillats k/n mal, dagegen das des zurückbleibenden Wassers $1/n$-mal so gross wie das ganze Volumen des zu destillierenden Wassers wählt, dann kann das Wasser ohne Änderung der Dichte abdestilliert werden. Falls man dagegen, wie schon oben erwähnt, das Volumen des ersten Destillats und des zurückbleibenden Wassers einfacherweise beide gleich $1/n$-mal so gross wie das ganze Wasservolumen wählt, dann muss die Dichte des Mittel- bzw. Hauptdestillats des Wassers durch einmalige Destillation um einen gewissen Betrag Δs vermindert werden, und zwar wird dieser Betrag Δs offenbar durch Gl. (5) angegeben:

$$\Delta s = s\frac{(k-1)(1-1/\alpha)}{n-2} = s(\alpha-1)\frac{2.3 \log n - 1}{n} \qquad (5),$$

wo s die Dichteabnahme des deuteriumfreien Wassers dem gewöhnlichen Wasser gegenüber darstellt. Weil aber genau dieselbe Form von Gl. wie (5) auch für die Dichteänderung des Wassers wegen der Fraktionierung der Sauerstoffisotope gilt, kann man aus den beiden so gewonnenen Gln. die gesamte Dichteabnahme des Wassers bei einmaliger einfacher Destillation rechnerisch ermitteln. Die Tabelle 3 gibt die auf diese Weise berechnete Dichteabnahme des Wassers $\Delta s(\mathrm{H})$ und $\Delta s(\mathrm{O})$ wegen der Verarmung der schweren Isotope des Wasserstoffs und Sauerstoffs bei einmaliger Destillation mit verschiedenen Werten von n (siehe oben) wieder. Bei dieser Berechnung setzten wir in Gl. (5) $s(\mathrm{H}) = 17\,\gamma$, $\alpha(\mathrm{H}) = 1.05$ bzw. $s(\mathrm{O}) = 220\,\gamma$, $\alpha(\mathrm{O}) = 1.01$.

Tabelle 3. Dichteabnahme des Wassers bei einmaliger Destillation.

n	Δs (H)	Δs (O)	Δs (H)+Δs (O)
100	0.03	0.08	0.11
30	0.07	0.18	0.25
20	0.09	0.22	0.31
10	0.11	0.29	0.40

Gemäss dieser Berechnung muss die Dichte des Wassers um etwa 0.6 γ abnehmen, wenn man 20 c.c. Wasser zweimal destilliert und jedesmal 1 c.c. des ersten Destillats weggoss und zugleich dasselbe Volumen des Wassers am Ende der Destillation im Destillierkolben zurückliess. Dagegen beträgt die Abnahme der Dichte nur 0.2 γ, falls man statt 20 c.c. mit 200 c.c. arbeitet und immer 2 c.c. davon am Anfang und Ende der Destillation weggiesst. Folglich muss die Dichte des Hauptdestillats bei der ersteren Art der Destillation um etwa 0.4 γ weniger als die der letzteren sein, auch wenn wir dabei mit ein und derselben Wasserart arbeiteten. Dieser Wert stimmt aber mit dem Dichteunterschied, den wir beim Versuch 9 in Tabelle 2 mit Osaka-Leitungswasser experimentell fanden, sehr gut überein. Weil aber die Versuche 5 und 6 in Tabelle 1 mit Osaka- und Cambridge-Leitungswasser unter sonst genau denselben Versuchsbedingungen wie beim Versuch 9 ausgeführt wurden, können wir auch bei diesen beiden Versuchen 5 und 6 dieselbe Grösse des Dichteunterschieds wie beim Versuch 9, nämlich 0.4 γ, wegen der blossen isotopischen Fraktionierung erwarten. Zieht man aus diesem Grund aus dem direkt gefundenen Dichteunterschied $\Delta s = 0.5\ \gamma$ beim Versuch 5 und 0.7 γ beim Versuch 6 resp. den Betrag 0.4 γ ab, dann ergibt sich der so korrigierte Dichteunterschied Δs (korr.) = 0.1 γ beim ersteren und 0.3 γ beim letzteren Versuch. Diese beiden Werte stehen aber offenbar mit denen der anderen normal ausgeführten Versuche 1 bis 4 sehr gut im Einklang.

Bei den Versuchen 7 und 8 in Tabelle 1 sowie 11 und 12 in Tabelle 2 verwendeten wir ebenfalls wie bei den oben genannten Versuchen 5, 6 und 9 immer verschiedenes Volumen von zwei zu vergleichenden Wasser zu Reinigungsdestillationen. Aber weil wir bei diesen Versuchen, nämlich bei den Versuchen 7, 8, 11 und 12, das Volumen des Wassers, das am Ende der Destillation im Destillierkolben zurückblieb, nicht gleich sondern gemäss Gl. (4) $1/k$-mal so wenig wie das des ersten Destillats wählten, stimmte der direkt gefundene Dichteunterschied Δs ohne weiteres mit denen bei den anderen normal ausgeführten Versuchen sehr gut überein.

Wir konnten so den Einfluss der isotopischen Fraktionierung bei der Destillation des Wassers auf dessen Dichte richtig in Rechnung bringen. Der andere wichtige Moment für die Änderung der Dichte des Wassers liegt aber darin, dass die Menge bzw. der Sättigungsgrad der gelösten Luft im untersuchten Wasser unter Umständen variieren kann. Nach Marek[3] beträgt der Unterschied der Dichte des lufthaltigen und des luftfreien Wassers bei verschiedenen Temperaturen wie in Tabelle 4 angegeben ist.

Tabelle 4. Unterschied der Dichte s_L des lufthaltigen und s_O luftfreien Wassers (nach Marek):

Temp. °C.	0	5	8	9	10	15	20
$s_O - s_L$ in γ	2.5	3.3	3.4	3.3	3.2	2.2	0.4

Gemäss diesem Versuch verändert sich die Dichte des Wassers um etwa 0.1 γ, falls die Menge der darin gelösten Luft bei 10°C. um etwa 3% variiert. Dieser Einfluss muss aber bei der vorliegenden Arbeit insofern in Betracht gezogen werden, als wir die Destillate aus der letzten Reinigungsdestillation in einigen (in Tabellen mit *L* gekennzeichneten) Fällen ohne weiteres, dagegen in den anderen (in Tabellen mit *O* gekennzeichneten) erst nach dem möglichst vollständigen Auspumpen der gelösten Luft zur Dichtebestimmung verwendeten. Aber wie man aus den oben angegebenen Tabellen 1 und 2 ohne weiteres ersieht, war es unmöglich einen nennenswerten Unterschied zwischen den Ergebnissen dieser beiden Reihen von Versuchen herauszufinden, solange die zwei zu vergleichenden Wasserarten beide gleich lufthaltig oder ausgepumpt verglichen wurde. In dieser Hinsicht führten wir den Versuch 10 in Tabelle 2 weiter. Bei diesem Versuch verglichen wir die Dichte zwei derselben Osaka-Leitungswasser, von denen das eine lufthaltig, das andere dagegen möglichst vollständig ausgepumpt worden war. Dabei fanden wir, wie aus Tabelle 2 ersichtlich, dass das ausgepumpte Wasser um 0.9 γ dichter als das lufthaltige war. Obwohl wir damit keinen Dichteunterschied des luftfreien und lufthaltigen Wassers behaupten wollen, kann man daraus doch wohl schliessen, dass ein eventuell aufzutretender kleiner Unterschied in der Menge der gelösten Luft keinen merklichen Einfluss auf das Endresultat ausüben kann, solange die beiden zu vergleichenden

(3) Marek, *Ann. Physik*, [3], **44** (1891), 171; Landolt-Börnstein-Roth-Scheel, „Physikalisch-chemische Tabellen," 5. Aufl., Hw., I, 73.

Wasserarten unter möglichst gleichen Bedingungen behandelt und verglichen werden.

Aus diesem Grunde legten wir beim Vergleich der in der letzten Vertikalreihe der Tabelle 1 angegebenen korrigierten Werte Δs(korr.) des Dichteunterschiedes zwischen Osaka- und Cambridge-Leitungswasser gleiches Gewicht auf die Werte der beiden Reihen der Versuche, von denen eine mit lufthaltigem dagegen die andere mit ausgepumptem Wasser durchgeführt wurden. Bei diesem Vergleich ersieht man sofort, dass das Osaka-Leitungswasser durchschnittlich um $0.2 \pm 0.2\,\gamma$ dichter als das Cambridge-Leitungswasser ist. Aber weil dieser Betrag kaum ausserhalb des Messfehlerbereiches unserer Dichtebestimmung ($\pm 0.2\,\gamma$) liegt, so möchten wir lieber schliessen, dass die beiden Arten von Wasser innerhalb des Messfehlerbereiches dieselbe Dichte besitzen. Genau zu demselben Resultat kamen aber auch die Cambridge Forscher, Greene und Voskuyl. Die beiden Autoren teilten uns nämlich mit, dass bei ihrem Versuch das Osaka-Leitungswasser sich um $0.07\,\gamma$ dichter als das Cambridge-Leitungswasser erwies, aber dieser Betrag schon innerhalb ihres Messfehlerbereiches lag.

Aus diese Weise fanden wir, dass das untersuchte Osaka-Leitungswasser innerhalb $\pm 0.2\,\gamma$ dieselbe Dichte wie das Cambridger Wasser besitzt. Aber zugleich zeigte sich bei dem vorliegenden Versuch auch, dass das Osaka-Leitungswasser, das am 17. Dezember 1935 gesammelt wurde, innerhalb des Messfehlerbereichs ($\pm 0.1\,\gamma$) wieder genau dieselbe Dichte wie die des am 25. Oktober 1937 gesammelten Leitungswassers an demselben Ort besass. Damit versicherten wir uns der Tatsache, dass die Dichte des Osaka-Leitungswassers mindestens während dieser Jahresfrist sehr konstant geblieben ist.

Zum Schluss möchten wir nicht verfehlen, Herrn Dr. Greene in Cambridge, U.S.A., der zu dieser internationalen Arbeit Veranlassung gegeben hat, unsere Hochachtung und unseren Dank auszusprechen. Der Nippon Gakujutsu-Shinkohkai (der Japanischen Gesellschaft zur Förderung der wissenschaftlichen Forschungen) sowie der Hattori-Hohkohkai (der Hattori-Stiftung) sind wir auch für ihre finanzielle Unterstützung zu wärmsten Dank verpflichtet.

Physikalisch-chemisches Laboratorium
der Kaiserlichen Universität zu Osaka
und
Siomi-Institut für physikalische
und chemische Forschung.

Wiederbestimmung des Deuterium-Protium-Verhältnisses in gewöhnlichem Wasser.

Von Noriyoshi MORITA und Toshizo TITANI.

(Eingegangen am 28. April 1938.)

Inhaltsübersicht. Der Gehalt des Osaka- und Cambridge-Leitungswassers an Deuterium wurde durch die Erzeugung des deuteriumfreien (leichten) Wassers bestimmt. Dabei wurde bei beiden Arten der Wasser das gleiche gefunden, dass die Dichte des daraus erzeugten leichten Wassers bei 9.5 C.° um $16.9 \pm 0.5\,\gamma$ kleiner als die des respektiven originalen Wassers ist. Daraus folgte weiter, dass sich in den beiden Arten der Wasser D: H = 1: 6200 ± 200 verhält. Dieser Wert wurde mit den anderen veröffentlichten Daten verglichen und zugleich der Unterschied zwischen dem vorliegenden und dem von uns früher gefundenen Wert eingehend diskutiert.

Einleitung. Bei unserem früheren Versuch,[1] wo wir den Gehalt des Osaka-Leitungswassers an Deuterium durch die Erzeugung des leichten Wassers ermittelten, fanden wir, dass in diesem Wasser D: H = 1: 5600 ± 200 ist. Aber aus unserem letzten Versuch,[2] wo wir die Dichte des Osaka-Leitungswassers mit der des Cambridge-Leitungswassers verglichen, ergab sich, dass der oben angegebene Wert nicht als unwiderleglich angesehen werden kann. Folglich haben wir in der vorliegenden Arbeit die Bestimmung des D/H-Verhältnisses im Osaka-Leitungswasser von neuem wiederholt. Dabei wurde zugleich ein ähnlicher Versuch auch mit dem Cambridge-Leitungswasser durchgeführt, das von Dr. Greene in Cambridge, U.S.A. zur Dichtevergleichung beim letzten Versuch uns zur Verfügung gestellt worden war.

Die hier benutzte Methode beruht auf demselben Prinzip wie früher.[1] Man bereitet nämlich aus dem zu untersuchenden Wasser ein leichtes d.h. deuterium-freies Wasser durch die fraktionierte Elektrolyse und vergleicht die Dichte des so gewonnenen leichten Wassers mit der des originalen Wassers. Falls sich dabei die erstere bei 25°C. um Δs kleiner als die letztere erweist, kann das Atomverhältnis von D und H in gegebenem Wasser nach der folgenden Gl. (1) ohne weiteres berechnet werden:[3]

$$D/H = 9.419\Delta s - 1.01\,(\Delta s)^2 \qquad (1).$$

Bei dieser Ausrechnung von D/H aus Δs ist aber selbstverständlich

(1) N. Morita und T. Titani, dies Bulletin, **11** (1936), 403.
(2) T. Titani und N. Morita, dies Bulletin, **13** (1938), 409.
(3) Vgl. dies Bulletin, **11** (1936), 409.

Voraussetzung, dass das benutzte leichte Wasser vom Deuterium praktisch vollkommen frei ist, dagegen der Sauerstoff in demselben genau dieselbe Isotopenzusammensetzung wie der des originalen Wassers besitzt. Von diesen beiden wichtigen Voraussetzungen ist aber die letztere viel schwerer als die erstere zu erzielen, und gerade in diesem letzteren Punkt ergab sich, wie weiter unten noch zu erwähnen ist, dass unser früherer Versuch nicht ganz als einwandfrei angesehen werden kann. Aus diesem Grunde haben wir in der vorliegenden Arbeit auf die Gleichheit der Isotopenzusammensetzung des Sauerstoffs des leichten und des damit zu vergleichenden originalen Wassers unser besonderes Augenmerk gerichtet.

Experiment. Das Experiment wurde, wie schon oben erwähnt, zugleich mit dem Osaka- und Cambridge-Leitungswasser durchgeführt. Dabei verfuhren wir in der Praxis wie folgendermassen: Wir bereiteten zunächst ein deuteriumfreies Wasser allein aus dem Osaka-Leitungswasser durch fraktionierte Elektrolyse. Dann wurde das Protiumgas, das aus dem so gewonnenen deuteriumfreien Osaka-Wasser bei abermaliger Elektrolyse entwickelt wurde, mit dem Sauerstoff aus dem Osaka- bzw. Cambridge-Leitungswasser resp. zu Wasser rekombiniert. Die Entwicklung des Sauerstoffs aus dem Osaka- bzw. Cambridge-Wasser wurde ebenfalls durch Elektrolyse durchgeführt. Aber bei dieser Elektrolyse verwendeten wir nicht eine, wie bei dem früheren Versuch, sondern drei Arten von Elektrolyten, die alle aus dem originalen Osaka- bzw. Cambridge-Wasser bereitet wurden.

Der erste Elektrolyt wurde genau so wie beim früheren Versuch dadurch hergestellt, dass wir 15 c.c. des originalen Osaka- bzw. Cambridge-Leitungswassers mit 3 g. KOH versetzten. Der so bereitete Elektrolyt wurde in einem U-förmigen Glasrohr mit Platinanode langsam elektrolysiert. Dabei wurde dem Elektrolyt während der Elektrolyse von Zeit zu Zeit das originale Leitungswasser zugesetzt, um das Volumen des Elektrolyte annährend konstant zu halten. Und erst dann, als 15 c.c. Wasser ihm hinzugefügt worden waren, wurde er bis auf 3 c.c. herabelektrolysiert. Auf diese Weise wurden insgesamt 30 c.c. Wasser zur Elektrolyse verwendet und davon 27 c.c. vollkommen zersetzt. Den dadurch erzeugten Sauerstoff nennen wir weiter unten Sauerstoff I.

Nach der vollständigen Entwicklung des Sauerstoffs I blieben im Elektrolyseur nur noch 3 c.c. Elektrolyt. Dieser wurde dann unter Zusatz von originalem Leitungswasser wieder bis auf 15 c.c. aufgefüllt und der so bereitete Elektrolyt wurde weiter zur Entwicklung des Sauerstoffs, des Sauerstoffs II, benutzt. Dabei verfuhren wir auf genau dieselbe Weise wie bei der Erzeugung des Sauerstoffs I, d.h. das Volumen des

Elektrolyts wurde während der Elektrolyse unter Zusatz von originalem Leitungswasser stets konstant gehalten und erst dann, als 15 c.c. Wasser zugesetzt worden waren, wurde er bis auf 3 c.c. herabelektrolysiert. Die letzte Art von Sauerstoff, der Sauerstoff III, wurde unter Benutzung dieser 3 c.c. bei der Erzeugung des Sauerstoffs II im Elektrolysiergefäss zurückgebliebenen Elektrolyt, nachdem er unter Zusatz von originalem Leitungswasser wieder bis auf 15 c.c. aufgefüllt wurde, auf genau dieselbe Weise wie beim Sauerstoff I bzw. II entwickelt, d.h. unter stetiger Zufügung des originalen Wassers.

Die auf diese Weise aus Osaka- bzw. Cambridge-Leitungswasser erzeugten drei Arten von Sauerstoff wurden dann separat mit ein und demselben Protiumgas, das sich bei der Elektrolyse des oben aus Osaka-Leitungswasser bereiteten deuteriumfreien Wassers entwickelte, auf dem elektrisch bis auf Rotglut erhitzten Platinspiraldraht katalytisch zu Wasser rekombiniert. Dabei kontrollierten wir, wie beim früheren Versuch, die Strömungsgeschwindigkeit des Protiumgas ein wenig stärker als die doppelte des Sauerstoffs, um letzteren restlos reagieren zu lassen und dadurch die isotopische Fraktionierung des Sauerstoffs zu vermeiden. Die so erhaltenen drei Arten der leichten Wasser, die weiter unten resp. I. II. und III. leichtes Wasser genannt werden sollen, wurden dann separat sorgfältig gereinigt und deren Dichte mit der des betreffenden originalen Leitungswassers verglichen. Bei dieser Dichtevergleichung achteten wir besonders darauf, dass die beiden zu vergleichenden Wasserarten unter möglichst gleichen Bedingungen gereinigt und verglichen werden. In der Praxis wählten wir nämlich bei den Reinigungsdestillationen das Volumen der beiden zu vergleichenden Wasser möglichst gleich und verwendeten die Destillate aus der letzten Destillation direkt d.h. lufthaltig zur Dichtevergleichung.[2] Dies wurde aber bei 9.5°C. nach der Schwebemethode mittels Quarzschwimmers durchgeführt.

Ergebnisse. Die Ergebnisse der Experimente mit dem Osaka-Leitungswasser geben wir in Tabelle 1 und die mit dem Cambridge-Leitungswasser in Tabelle 2 wieder, wo ΔT die Differenz der Ablesung am Beckmannthermometer und Δs die daraus gemäss Gl. (2) errechnete Dichteabnahme des respektiven leichten Wassers dem originalen Wasser gegenüber ausdrücken:

$$\Delta s(\text{in } \gamma) = (79.7-6.9\Delta T)\Delta T^{(4)} \qquad (2).$$

(4) Diese Gleichung wurde aus der Änderung der Dichte des gewöhnlichen Wassers zwischen 9° und 10°C. nach der Methode der kleinsten Quadrate abgeleitet.

Tabelle 1. Dichteabnahme der aus Osaka-Leitungswasser bereiteten leichten Wasser dem originalen Wasser gegenüber.

Reihe der Versuche	Art des leichten Wassers	I	II	III
erste Reihe	ΔT	0.220°	0.214°	—
	Δs in γ	17.2	16.7	—
zweite Reihe	ΔT	0.225°	0.216°	0.215°
	Δs in γ	17.6	16.9	16.8

Tabelle 2. Dichteabnahme der aus Cambridge-Leitungswasser bereiteten leichten Wasser dem originalen Wasser gegenüber.

Reihe der Versuche	Art des leicht n Wassers	I	II	III
erste Reihe	ΔT	0.220°	—	—
	Δs in γ	17.2	—	—
zweite Reihe	ΔT	0.218°	0.210°	—
	Δs in γ	17.0	16.4	—

Wie aus diesen Tabellen ohne weiteres ersichtlich ist, erwies sich das I. leichte Wasser immer leichter als das II. und zwar durchschnittlich um 0.6 γ. Dagegen stimmten die Dichten des II. und III. leichten Wassers innerhalb des Messfehlerbereiches gut überein. Da aber der Wasserstoff in allen diesen Arten der leichten Wasser immer dasselbe Protium war, muss man den oben gefundenen Unterschied in der Dichte ausschliesslich auf die Verschiedenheit der Isotopenzusammensetzung des Sauerstoffs im respektiven leichten Wasser zurückführen. Dies weist aber weiter darauf hin, dass der Elektrolyt, aus dem der Sauerstoff I zur Bildung des I. leichten Wassers entwickelt wurde, betreffend der elektrolytischen Entwicklung des Sauerstoffs noch nicht im stationären Zustand befindlich

war und dieser erst bei der Entwicklung des Sauerstoffs II bzw. III erreicht wurde. Dieser Schluss fand weiter dadurch seine Bestätigung, dass der oben gefundene Dichteunterschied 0.6 zwischen dem I. und II. (bzw. III.) leichten Wasser mit dem theoretisch erwarteten Wert 0.4 γ hinreichend gut übereinstimmte, den wir bei unserem früheren Versuch zur Korrektion anwendeten.[5] So ist als sicher anzunehmen, dass der Sauerstoff im II. und III. leichten Wasser praktisch dieselbe Isotopenzusammensetzung wie das originale Leitungswasser besass.

Aber bezüglich des Wasserstoffs in diesen Arten der leichten Wasser muss man noch die folgende Tatsache in Betracht ziehen. Wir fügten nämlich dem deuteriumfreien Osaka-Leitungswasser immer eine kleine Menge KOH hinzu, um daraus das Protiumgas zur Bildung der genannten leichten Wasser elektrolytisch zu entwickeln. Dadurch kam aber eine minimale Menge Deuterium aus dem zugesetzten KOH in das deuteriumfreie Wasser und folglich in die damit hergestellten leichten Wasser hinein. Eine einfache Berechnung ergab, dass diese Zusetzung des Deuteriums die Dichte der dabei gebildeten leichten Wasser um 0.2 bis 0.3 γ vergrössern musste. Addiert man aus diesem Grunde zu der oben in den Tabellen angegebenen direkt gefundenen Dichteabnahme der II. und III. leichten Wasser noch diesen Betrag hinzu und nimmt weiter aus den so verbesserten Werten das Totalmittel, dann erhält man gemeinsam mit dem Osaka- und Cambridge-Wasser den Wert:

$$\Delta s = 16.9 \pm 0.5\,\gamma \qquad \text{bei } 9.5°\text{C.}$$

Dies stellt offenbar die Abnahme der Dichte des leichten Wasser, das praktisch von Deuterium frei ist, aber dessen Sauerstoff genau dieselbe Isotopenzusammensetzung wie das originale Wasser besitzt, dem Osaka- bzw. Cambridge-Leitungswasser gegenüber dar. Wenn man deshalb diesen Wert von Δs bei 9.5°C. auf 25°C. umrechnet[3] und weiter mit dem so umgerechneten Wert von Δs gemäss Gl. (1) das D/H-Verhältnis im Osaka- und Cambridge-Leitungswasser berechnet, dann ergibt sich gleich für die beiden, dass

$$\Delta s = 17.1 \pm 0.5\,\gamma \qquad \text{bei } 25°\text{C.}$$

und $$\text{D} : \text{H} = 1 : 6200 \pm 200$$

ist.

Diskussion. Wir fanden bei unserem letzten Versuch,[2] dass das Osaka-Leitungswasser innerhalb $\pm 0.2\,\gamma$ dieselbe Dichte wie das Cam-

(5) Vgl. dies Bulletin, **11** (1936), 408.

bridge-Leitungswasser besitzt. Bei der vorliegenden Arbeit fanden wir aber weiter, dass der Gehalt der beiden Arten von Wasser an Deuterium wieder ganz gleich ist. Die beiden Arten von Leitungswasser erwiesen sich somit nicht nur in ihrer Dichte, sondern auch in ihrer Isotopenzusammensetzung miteinander völlig ähnlich.

Die ausführliche Vergleichung der vorliegenden Werte von Δs und D/H mit den anderen veröffentlichten Daten, besonders mit solchen, die nach verschiedenen Methoden ermittelt wurden, wird auf die frühere Abhandlung[1] verwiesen und hier in Tabelle 3 möchten wir davon nur solche wiedergeben, die mit den vorliegenden im hinreichenden Einklang stehen.

Tabelle 3. D/H-Verhältnis in gewöhnlichem Wasser nach verschiedenen Autoren.

Beobachter	untersuchtes Wasser	angewandte Methode	D:H
Lewis und Macdonald[6]	Berkeley-Leitungswasser	Elektrolyse	1:6500
Edwards, Bell und Wolfenden[7]	Oxford-Leitungswasser	,,	1:6200
Johnston[8]	Columbus-Leitungswasser	leichtes Wasser	1:5900
Tronstad, Nordhagen und Brun[9]	Rjukan-Wasser	,,	1:6000
Hall und Jones[10]	Oberflächenwasser von Lake Mendota	,,	1:6400
Gabbard und Dole[11]	Wasser von Lake Michigan	,,	1:6900
vorliegende Arbeit	Osaka- und Cambridge-Leitungswasser	,,	1:6200

Die Methode, die von Lewis und Macdonald sowie von Edwards, Bell und Wolfenden benutzt wurde, beruht auf der Geschwindigkeit der Anreicherung des Deuteriums bei der Elektrolyse des gewöhnlichen

(6) G. N. Lewis und R. T. Macdonald, *J. Chem. Phys.*, **1** (1933), 341.
(7) A. J. Edwards, R. P. Bell und J. H. Wolfenden, *Nature*, **135** (1935), 793.
(8) H. L. Johnston, *J. Am. Chem. Soc.*, **57** (1935), 484, 2737.
(9) L. Tronstad, J. Nordhagen und J. Brun, *Nature*, **136** (1935), 515.
(10) N. F. Hall und T. O. Jones, *J. Am. Chem. Soc.*, **58** (1936), 1915.
(11) J. L. Gabbard und M. Dole, *J. Am. Chem. Soc.*, **59** (1937), 181.

Wasssers.[12] Dagegen ist das Prinzip, auf dem die Bestimmungsmethode der anderen Autoren beruht, im grossen und ganzen dasselbe wie die vorliegende Arbeit.

Bei unserem früheren Versuch[1] mit Osaka-Leitungswasser fand sich, dass die Dichteabnahme des daraus erzeugten leichten Wassers dem originalen Wasser gegenüber $\Delta s = 18.9 \pm 0.5\,\gamma$ bei 25°C. und folglich D : H = 1 : 5600 ± 200 ist. Vergleicht man diese Werte mit den vorliegenden ($\Delta s = 17.1 \pm 0.5\,\gamma$, und D : H = 1 : 6200 ± 200), dann ersieht man sofort, dass das damals erzeugte leichte Wasser um $1.8\,\gamma$ leichter als das vorliegende sein musste. Als Ursache für diese Diskrepanz können wir u. a. folgende drei Tatsachen in Betracht ziehen:

(1) Beim früheren Versuch berechneten wir die Dichteabnahme Δs des leichten Wassers aus der experimentell gefundenen Temperaturdifferenz ΔT am Beckmannthermometer nicht nach der oben angegebenen genaueren Form von Gl. (2), sondern nach der folgenden vereinfachten Gl. (3):[13]

$$\Delta s = 79 \times \Delta T \qquad (3).$$

Dadurch schätzten wir die Dichte des damals gebildeten Wassers um etwa $0.2\,\gamma$ zu leicht.

(2) Die Elektrolyte, die bei dem früheren Versuch zur Entwicklung des Protiumgas sowie des Sauerstoffs für die Herstellung des leichten Wassers benutzt wurden, sind die gleichen wie für das I. leichte Wasser bei der vorliegenden Arbeit. Deshalb musste das damals hergestellte leichte Wasser, genau so wie beim I. leichten Wasser, wegen der Zumischung des Deuteriums aus dem zugesetzten KOH um 0.2 bis $0.3\,\gamma$ zu schwer, dagegen der isotopischen Fraktionierung des Sauerstoffs wegen um etwa $0.6\,\gamma$ zu leicht und folglich beide zusammen um 0.4 bis $0.3\,\gamma$ zu leicht sein. Aber damals nahmen wir aus einer rechnerischen Ermittelung an, dass diese beiden Einflüsse innerhalb des Messfehlerbereiches sich untereinander auskompensierten.[5]

(3) Mit den oben geschilderten Tatsachen (1) und (2) können wir den gefundenen Unterschied $1.8\,\gamma$ bis auf etwas $1\,\gamma$ erklären. Der so übrig gebliebene Betrag $1\,\gamma$ ist aber mit der ungleich grossen isotopischen Fraktionierung des leichten und des damit zu vergleichenden originalen Leitungswassers bei deren Reinigungsdestillation zu erklären, weil wir

(12) Vgl. dies Bulletin, **11** (1936), 404.

(13) Diese Gleichung wurde damals nicht geschrieben.

damals das Volumen der beiden Arten der Wasser bei deren Reinigungsdestillation nicht gleich, sondern sehr verschieden gross wählten. Dass solch eine ungleiche Behandlung der beiden zu vergleichenden Wasser bei deren Reinigung eventuell einen merklichen Fehler hervorrufen kann, darauf wurde schon in unserer letzten Abhandlung[2] hingewiesen. Zieht man in der Tat das Mengenverhältnis der leichten und originalen Wasser, die bei der früheren Arbeit zu Reinigungsdestillationen verwendet wurden sowie die Zahl (vier Mal) der mit einer derselben Wasserart nacheinanderfolgend durchgeführten Destillationen in Rechnung, dann kann man wirklich den oben angegebenen Unterschied $1\,\gamma$ mit der isotopischen Fraktionierung befriedigend erklären.

Zum Schluss möchten wir Herrn Dr. Greene in Cambridge, U.S.A., der uns das bei der vorliegenden Arbeit untersuchte Cambridge-Leitungswasser zur Verfügung gestellt hat, unseren wärmsten Dank aussprechen. Der Nippon-Gakujutsu-Shinkohkai (der Japanischen Gesellschaft zur Förderung der wissenschaftlichen Forschungen) sowie der Hattori-Hohkohkai (der Hattori-Stiftung) sind wir auch für ihre finanzielle Unterstützung zu bestem Dank verpflichtet.

Physikalisch-chemisches Laboratorium
der Kaiserlischen Universität zu Osaka
und
Siomi-Institut für physikalische
und chemische Forschung.

Zur Kenntnis der Austauschgeschwindigkeit der Wasserstoffatome zwischen Zucker und Wasser.

Von Masao KOIZUMI* und Toshizo TITANI.

(Eingegangen am 27. Mai 1938.)

Inhaltsübersicht. Um über die Geschwindigkeit der Austauschreaktion der H-Atome zwischen der organischen Hydroxylgruppe und Wasser nähere Kenntnis zu gewinnen, führten wir mit Glucose, Fructose, Glycerin und Glykol Experimente aus, indem wir den D-Gehalt des Wassers, das aus der Lösung der betreffenden organischen Substanz in schwerem Wasser abdestilliert wurde, zu verschiedenen Zeiten nach der Herstellung der Lösung bestimmten. Durch diesen Versuch fanden wir, dass die Austauschreaktion im allgemeinen sehr schnell verläuft und das Austauschgleichgewicht spätestens in einer Minute (die kürzeste Zeit, die wir erzielen konnten) erreicht wird, gleichgültig ob wir dabei neutrale, saure bzw. alkalische Lösung benutzten. Weiter bestimmten wir den („scheinbaren") Verteilungsquotient α der D-Atome zwischen der Hydroxylgruppe einiger Hexosen und Wasser und fanden ihn als Mittelwert von $\alpha = 1.15$. Der „wahre" Verteilungsquotient dürfte um einige Prozent kleiner als dieser sein.

Einleitung. Wir teilten früher vorläufig mit,[1] dass die Austauschreaktion der H-Atome zwischen Glucose sowie Fructose und Wasser sehr schnell verläuft und es zum Austauschgleichgewicht, ohne Unterschied in neutraler, saurer bzw. alkalischer Lösung, spätestens innerhalb einer Minute komme. Zugleich fanden wir, obwohl nicht mitgeteilt wurde, dass der Verteilungsquotient der D-Atome zwischen Glucose bzw. Fructose und Wasser $\alpha = 1.1$ bis 1.2 ist. Bald darauf wurde aber ein ähnlicher Versuch von Orr[2] veröffentlicht, der zu einem dem unseren ganz entgegengesetzten Resultat führte. Er schloss nämlich aus seinem Versuch, dass das Austauschgleichgewicht zwischen Äthylalkohol und Wasser sich bei 25°C. erst nach 18 Stunden einstellt. Aus demselben Versuch fand er weiter, dass die Gleichgewichtskonstante der Reaktion:

$$C_2H_5OH + HDO \rightleftarrows C_2H_5CD + H_2O$$

$k = 1.11$ ist. Folglich muss der Verteilungsquotient der D-Atome zwischen Äthylalkohol und Wasser $\alpha = 2.22$ sein.[3] Dieser letztere Wert ist aber beträchtlich grösser als die von anderen Autoren für manche Arten der

* Früher Masao HARADA.

(1) M. Harada und T. Titani, dies Bulletin, **11** (1936), 55.

(2) W. J. C. Orr, *Trans. Faraday Soc.*, **32** (1936), 1033.

(3) Vgl. Gl. (4) in M. Harada und T. Titani, dies Bulletin, **11** (1936), 465.

organischen Hydroxylgruppe experimentell[4] bzw. rechnerisch[5] ermittelten, die im allgemeinen nicht viel von eins verschieden sind. Weiter ist der erste Schluss von Orr, dass die Austauschreaktion zwischen Alkohol und Wasser äusserst langsam verläuft, durch die späteren Versuche von Bonhoeffer und seinen Mitarbeitern[6] sehr fraglich geworden. Diese Autoren fanden nämlich, dass die Austauschreaktion zwischen Alkohol und Wasser ebenso leicht wie die zwischen leichtem (H_2O) und schwerem (D_2O) Wasser verläuft und das Austauschgleichgewicht fast unmessbar so schnell eingestellt wird.

In Anbetracht dieser Sachlage wird es nicht ganz zwecklos sein, die von uns früher durchgeführten und teils schon vorläufig mitgeteilten Versuche ausführlich zu beschreiben.

Versuche über die Austauschgeschwindigkeit. Wir führten diese Versuche mit Glucose, Fructose, Glycerin und Glykol aus. Beim Versuch mit Glucose verführen wir folgendermassen. Zuerst wird in einem mit geschliffener Mündung versehenen Glasrohr eine Lösung aus 2 bis 3 g. Glucose und 2 g. gewöhnlichem Wasser bzw. 1.5 N H_2SO_4 oder 0.5 N NaOH hergestellt. Die so hergestellte neutrale, saure oder alkalische Lösung von Glucose wird dann mit 1 c.c. von ca. 5 prozentigem schwerem Wasser versetzt und schnell damit gemischt. Nachdem unmittelbar darauf das Glasrohr mittels der geschliffenen Mündung mit einer Vakuumdestillationsanordnung verbunden worden, wird 50 bis 100 mg. Wasser aus der Lösung in das andere Glasröhrchen schnell abdestilliert, wozu durchschnittlich eine Minute erforderlich ist. Die so abdestillierte Wasserprobe wird zur Dichtebestimmung gesondert aufbewahrt. Dann werden aus derselben Lösung drei bis fünfmal zu verschiedenen Zeiten nach der Herstellung der Lösung kleine Wassermengen abdestilliert. Die letzte Probe wird frühestens nach zwanzig Stunden entnommen. Jede der so gesammelten Wasserproben wird durch zweimalige Destillation im Vakuum gereinigt und die Dichte des gereinigten Wassers mittels eines kleinen Glasschwimmers genau bestimmt. Die auf diese Weise mit Glucose durchgeführten Versuchsergebnisse sind in den folgenden Tabellen zusammengestellt. Die erste Horizontalreihe jeder Tabelle (t) gibt den mittleren Zeitpunkt jeder Abdestillation einer kleinen Menge des Wassers und die

(4) W. H. Hamill und W. Freudenberg, *J. Am. Chem. Soc.*, **57** (1935), 1427; A. I. Brodski, *J. Phys. Chem. (U.S.S.R.)*, **9** (1937), 755; vgl. auch M. Harada und T. Titani, dies Bulletin, **11** (1936), 465.

(5) K. Wirtz, *Z. physik. Chem.*, B, **34** (1936), 121.

(6) J. C. Jungers und K. F. Bonhoeffer, *Z. physik. Chem.*, A, **177** (1936), 430; K. Wirtz, *Z. Physik*, **101** (1937), 613; vgl. auch J. C. Jungers und K. Wirtz, *Bull. soc. chim. Belg.*, **45** (1936), 679.

zweite (Δs) den Dichteüberschuss des so abdestillierten Wassers gewöhnlichem Wasser gegenüber wieder. Dabei wurde der Dichteüberschuss des abdestillierten Wassers bei $t = 0$, d.h. vor dem Austausch, sowie der bei $t = \infty$, d.h. nach dem vollständigen Austausch, je rechnerisch ermittelt, indem wir den Verteilungsquotient der D-Atome zwischen der organischen Hydroxylgruppe und Wasser $\alpha = 1.1$ (vgl. weiter unten) und den zwischen flüssigem Wasser und Wasserdampf $\alpha = 1.04$[7] setzten.

Experiment 1. 2.3 g. Glucose wurden in 2.0 c.c. gewöhnlichen Wassers aufgelöst, und dieser Lösung wurde 1.0 c.c. von 4.7 prozentigem schwerem Wasser zugesetzt.

t in Min.	0	1	2½	1200	∞
$\Delta s \times 10^5$	(163)	123	130	122	(124)

Experiment 2. 2.8 g. Glucose wurden in 2.0 c.c. 1.5 N H_2SO_4 aufgelöst, und dieser Lösung wurde 1.0 c.c. von 4.7 prozentigem schwerem Wasser zugesetzt.

t in Min.	0	1⅙	12	70	1200	∞
$\Delta s \times 10^5$	(163)	123	122	123	122	(118)

Experiment 3. Genau wie Experiment 2, nur mit dem Unterschied, dass anstatt H_2SO_4 1.5N NaOH verwendet wurde.

t in Min.	0	1½	4½	40	3 Tage	4 Tage	∞
$\Delta s \times 10^5$	(163)	120	128?	120	123	121	(118)

Aus diesen Versuchen ersieht man ohne weiteres, dass das aus der Lösung bei verschiedenen Zeiten nach ihrer Herstellung, sogar möglichst unmittelbar nach der Vermischung des schweren Wassers, abdestillierte Wasser, innerhalb des Messfehlerbereichs immer denselben Dichteüberschuss besitzt und dieser direkt bestimmte Dichteüberschuss mit dem berechneten Wert beim vollständigen Austausch ($t = \infty$) hinreichend gut

(7) Vgl. J. Horiuti und G. Okamoto, dies Bulletin, **10** (1935), 503.

übereinstimmt, ohne Unterschied ob man dabei neutrale, saure bzw. alkalische Lösung benutzt. Wir können deshalb wohl schliessen, dass es zum Austauschgleichgewicht zwischen Glucose und Wasser spätestens in einer Minute (höchstwahrscheinlich noch viel schneller) kommt, gleichgültig ob man neutrale, saure oder alkalische Lösung verwendet.

Ähnliche Versuche führten wir auch mit Fructose aus. Aber in diesem Fall erwies sich der Dichteüberschuss des abdestillierten Wassers nicht so konstant wie bei der Glucose, wie aus den folgenden Tabellen ersichtlich ist.

Experiment 4. 2.8 g. Fructose lösten wir in 2.0 c.c. gewöhnlichen Wassers auf und setzten dieser Lösung 1.0 c.c. von 4.7 prozentigem schwerem Wasser zu.

t in Min.	0	4½	15	60	140	450	∞
$\Delta s \times 10^5$	(163)	106	106	115	117	118	(118)

Experiment 5. Genau wie Experiment 4, nur mit dem Unterschied, dass anstatt gewöhnlichen neutralen Wassers 1.5 N H_2SO_4 verwendet wurde.

t in Min.	0	1½	4½	11	45	160	310	∞
$\Delta s \times 10^5$	(163)	99		111	109	123	119	(118)

Experiment 6. Nachdem 2.8 g. Fructose in 2.0 c.c. 1.5 N NaOH aufgelöst worden, setzten wir dieser Lösung 1.0 c.c. 1.6 prozentigen schweren Wassers zu.

t in Min.	0	1½	4½	45	135	1620	3060	∞
$\Delta s \times 10^5$	(55)	15	22	30	37	42	42	(40)

Also fanden wir in diesen Versuchen mit Fructose am Anfang jedes Experiments immer einen abnorm kleinen Dichteüberschuss des abdestillierten Wassers, obwohl diese Abnormalität mit den weiteren einzelnen Destillationen nach und nach verschwand, bis schliesslich das abdestillierte Wasser den mit dem berechneten Wert gut übereinstimmenden

Dichteüberschuss zeigte. Um die Ursache hiervon festzustellen, führten wir einen Kontrollversuch unter Benutzung gewöhnlichen Wassers anstatt schweren Wassers aus.

Experiment 7. 2.8 g. Fructose wurden in 2.0 c.c. gewöhnlichen Wassers aufgelöst und dieser Lösung 1.0 c.c. gewöhnlichen Wassers zugesetzt.

t in Min.	0	1	4	15	90	1200	∞
$\Delta s \times 10^5$	(0)	−30	−11	−4	0	0	(0)

Bei diesem Kontrollversuch wurde gefunden, dass das am Anfang des Experiments abdestillierte Wasser deutlich eine kleinere Dichte als gewöhnliches Wasser besass, dass aber dieser Unterschied der Dichte des abdestillierten Wassers gewöhnlichem Wasser gegenüber mit den weiteren einzelnen Destillationen nach und nach verschwand. Dieses Resultat legt die Vermutung sehr nahe, dass die benutzte Fructose irgendeine flüchtige Verunreinigung bzw. Verunreinigungen enthielt und diese mit dem Wasser zusammen abdestillierte und so allmählich entfernt wurde, obwohl die Fructose genau wie die Glucose im voraus im Vakuum über Phosphorpentoxyd bei ca. 80°C. gut getrocknet worden war. Durch diese Annahme kann man den abnorm kleinen Dichteüberschuss des am Anfang der Experimente 4 bis 6 mit Fructose abdestillierten Wassers wohl erklären, weil wir dabei, genau so wie beim Kontrollversuch (Experiment 7), das aus der Lösung abdestillierte Wasser wegen seines kleinen Volumens nach zweimaliger Destillation im Vakuum ohne weitere besondere Reinigung direkt zur Dichtebestimmung benutzten. Zieht man diese Tatsache in Rechnung, so darf man auch von der Fructose schliessen, dass das Austauschgleichgewicht sich ebenso schnell wie bei der Glucose einstellt.

Wir führten die Versuche weiter mit Glycerin und Glykol aus. Die Versuchsanordnung war im grossen und ganzen dieselbe wie bei Glucose und Fructose, nur mit dem Unterschied, dass Glycerin bzw. Glykol ohne weiteres mit verdünntem schwerem Wasser vermischt und aus der so gebildeten Lösung eine kleine Menge von Wasser zu verschiedenen Zeiten nach der Vermischung im Vakuum abdestilliert wurde.

Experiment 8. Nachdem 6.065 g. Glycerin mit 2.0 c.c. von 3.3 prozentigem schwerem Wasser vermischt worden, destillierten wir aus der so hergestellten Lösung eine kleine Menge von Wasser zu verschiedenen Zeiten im Vakuum ab.

t in Min.	0	2	6	13	23	1350	∞
$\Delta s \times 10^5$	(347)	167	153	166	172	169	(175)

Experiment 9. Wir lösten 5.8 g. Glykol in 2.0 c.c. von ca. 4 prozentigem schwerem Wasser und destillierten aus dieser Lösung eine kleine Menge von Wasser zu verschiedenen Zeiten im Vakuum ab. Der Anfangs-D-Gehalt des benutzten Wassers wurde leider nicht genau bestimmt.

t in Min.	0	3	9	220	360	∞
$\Delta s \times 10^5$	(ca. 420)	215	211	206	222	(ca. 210)

Dass das Wasser beim Experiment 8 durch die Destillation im Vakuum hinreichend rein vom Glycerin abgetrennt werden konnte, wird aus dem folgenden Kontrollversuch ersichtlich.

Experiment 10. Ca. 6 g. Glycerin wurde in 2.0 c.c. gewöhnlichen Wassers aufgelöst und aus dieser Lösung eine kleine Menge von Wasser zu verschiedenen Zeiten im Vakuum abdestilliert. Die Dichte des so abdestillierten Wassers wurde, genau so wie bei den Hauptversuchen, erst dann bestimmt, nachdem es durch zweimalige Destillation im Vakuum gereinigt worden.

t in Min.	0	3	60	∞
$\Delta s \times 10^5$	(0)	−3	0	(0)

Aus diesen Experimenten 8 bis 10 darf man wohl schliessen, dass die Austauschreaktion zwischen Glycerin bzw. Glykol und Wasser ebenso leicht wie zwischen Glucose bzw. Fructose und Wasser verläuft und das Austauschgleichgewicht sehr schnell, höchstwahrscheinlich augenblicklich, eingestellt wird.

Bestimmung des Verteilungsquotienten der D-Atome zwischen Zucker und Wasser. Der Verteilungsquotient a der D-Atome zwischen Zucker und Wasser, der bekanntlich durch die folgende Gl. (1) definiert wird, wurde von Hamill und Freudenberg[4] unter Benutzung verhältnismässig konzentrierten schweren Wassers (10 bis 90%) für manche Arten von

Hexosen und ihren Derivaten bestimmt:

$$\alpha = \frac{\text{D/H in Zucker}}{\text{D/H in Wasser}} \qquad (1).$$

Dabei fanden die ebengenannten Autoren, dass ein einziger Verteilungsquotient nämlich $\alpha = 1.30$ mit genügender Genauigkeit auf alle von ihnen untersuchten Zuckerarten anwendbar war. Da aber konzentrierte schweres Wasser ausser Protiumdeuteriumoxyd (HDO) noch eine beträchtliche Menge von Deuteriumoxyd (D_2O) enthält, so liegt die Sache beim Austauschgleichgewicht in konzentriertem schwerem Wasser viel komplizierter als beim verdünnten schweren Wasser. Aus diesem Grunde benutzten wir in der vorliegenden Arbeit möglichst verdünntes schweres Wasser (ca. 1.5%) und bestimmten dadurch den Verteilungsquotienten der D-Atome zwischen Glucose, Fructose, Mannose sowie Rohrzucker und Wasser. Die sonstige Arbeitsweise war im grossen und ganzen dieselbe wie die von Hamill und Freudenberg. Eine abgewogene Menge von Zucker wird in eine ebenfalls abgewogene Menge des verdünnten schweren Wassers, vom wohl bekannten D-Gehalt, aufgelöst. Darauf wird das Wasser sofort, oder nachdem die Lösung verschiedene Zeit lang erwärmt worden, durch die Destillation im Vakuum möglichst vollständig vom Zucker abgetrennt. Das abgetrennte Wasser reinigten wir, indem wir es unter Zusatz von Kaliumpermanganat und Natriumperoxyd einige Stunden lang sieden liessen, es dann durch Destillation vom Zusatz befreiten und zum Schluss im Vakuum zweimal destillierten. Die Dichte, folglich der Gehalt an D, des so gereinigten Wassers wurde mittels eines Quarzschwimmers genau bestimmt. Der Verteilungsquotient α wurde dann durch die Gleichung:

$$\alpha = \frac{2M_w}{nM_z} \frac{D_a - D_e}{D_e} \qquad (2)$$

ohne weiteres berechnet. In dieser Gleichung bedeutet M_w: Molzahl des verwendeten schweren Wassers, M_z die des Zuckers, n: Anzahl der Hydroxylwasserstoffe in einem Zuckermolekül und D_a und D_e: D-Gehalt des Wassers vor und nach dem Versuch. Die so erhaltenen Versuchsergebnisse geben wir in Tabelle 1 wieder, wo D_a und D_e durch den Dichteüberschuss des betreffenden Wassers gewöhnlichem Wasser gegenüber ausgedrückt sind. Die beim Versuch verwendeten Zuckerarten wurden im voraus immer im Vakuum über Phosphorpentoxyd bei ca. 80°C. gut getrocknet.

Tabelle 1. Bestimmung des Verteilungsquotient einiger Zuckerarten

Zucker	Verwärmung der Lösung	$M_w \times 10^3$	$M_z \times 10^3$	D_a in γ	D_e in γ	Molzahl des abgetrennten Wassers $\times 10^3$	α
Glucose	80°C., 2 Stdn.	55 5	9.45	1475	999	48.5	1.12
,,	60°C., einige Zeit	148.7	16.5	1470	1129	139.	1.09
Fructose	ohne Erwärmung	55.5	4.55	1853	1493	50.7	1.18
,,	100°C., 20 Stdn. (unter vermindertem Druck)	55.5	22.2	1477	675	52.	1 18
Mannose	80°C., 2 Stdn.	54.5	12.7	1470	891	—	1.12
Rohrzucker	ohne Erwärmung	111.	10.3	1484	1025	107.	1.21

Wie aus der letzten Vertikalreihe der Tabelle 1 ohne weiteres ersichtlicht ist, unterscheiden sich die einzelnen Werte von α für die verschiedenen Zuckerarten nur wenig voneinander, so dass ein einziger Mittelwert von Verteilungsquotienten nämlich $\alpha = 1.15 \pm 0.05$ mit genügender Genauigkeit für alle oben angegebenen Zuckerarten gilt. Dieser Wert ist um ein wenig kleiner als der von Hamill und Freundenberg gefundene, nämlich $\alpha = 1.30$. Was diesen Unterschied anbetrifft, liegt aber die Vermutung nahe, dass der experimentell bestimmte Verteilungsquotient vom D-Gehalt des zum Versuch benutzten schweren Wassers abhängig ist, weil der D-Gehalt des von uns benutzten schweren Wassers nur ca. 2%, dagegen der des von Hamill und Freudenberg verwendeten Wassers viel grösser war und zwischen 10 bis 90% lag. Wir teilten deshalb die Versuchsergebnisse der eben genannten Autoren nach dem D-Gehalt des bei jedem Versuch benutzten schweren Wassers in zwei Gruppen und berechneten aus jeder Gruppe den resp. Verteilungsquotient. Das so erhaltene Resultat geben wir zusammen mit dem von uns in der vorliegenden Arbeit gefundenen Verteilungsquotient in Tabelle 2 wieder.

Tabelle 2. Abhängigkeit des experimentell bestimmten Verteilungsquotient vom D-Gehalt des benutzten Wassers.

D-Gehalt des benutzten Wassers	Verteilungsquotient	Beobachter
1.5%	1.15	Koizumi und Titani
10—20%	1.26	Hamill und Freudenberg
20—33%	1 40	,, ,,

Aus dieser Tabelle ersieht man ohne weiteres, dass der experimentell bestimmte Verteilungsquotient ziemlich deutlich vom D-Gehalt des benutzten Wassers abhängig ist und zwar mit zunehmendem D-Gehalt des Wassers allmählich zunimmt. Über die Ursache dieser Abhängigkeit des gefundenen Verteilungsquotient vom D-Gehalt des benutzten schweren Wassers können wir augenblicklich nichts Sicheres[8] sagen. Aber wenigstens aus den in Tabelle 2 angegebenen Experimentaltatsachen zu urteilen, möchten wir lieber den Verteilungsquotient, der unter Benutzung möglichst verdünnten schweren Wassers bestimmt wurde, nämlich $\alpha = 1.15$, als wahrscheinlicher annehmen.

Dieser kleinste Wert von Verteilungsquotient ($\alpha = 1.15$), der direkt experimentell bestimmt wurde, muss aber noch von „wahren" Verteilungsquotient so weit abweichen, als wir das schwere Wasser vom darin gelösten Zucker durch Destillation abtrennten und aus der Dichte des so abgeschiedenen Wassers den Verteilungsquotient berechneten. Bekanntlich erleidet das schwere Wasser durch die Destillation eine mehr oder weniger starke isotopische Fraktionierung und der zurückbleibende Anteil wird nach und nach mit den schweren Arten von Wasser angereichert. Deshalb muss der so bestimmte sozusagen „scheinbare" Verteilungsquotient offensichtlich um einen gewissen Grad grösser als der „wahre" Verteilungsquotient sein. Über die Absolutgrösse dieses Unterschiedes zwischen dem direkt bestimmten „scheinbaren "Verteilungsquotient und dem „wahren" Verteilungsquotient können wir im allgemeinen nichts Bestimmtes sagen, weil dieser Unterschied von vielen Faktoren, wie z.B. dem D-Gehalt des benutzten schweren Wassers, der Geschwindigkeit der Abdestillation des Wassers u.s.w. beeinflusst werden kann. Jedoch kann diese Abweichung des „scheinbaren" Verteilungsquotient vom „wahren" Verteilungsquotient nicht sehr gross sein, wenn man die Abdestillation des Wassers, wie in der vorliegenden Arbeit, ziemlich schnell ausführt, weil durch solch eine schnelle hochirreversible Destillation die isotopische Fraktionierung des Wassers in weitestem Masse begrenzt bzw. verhindert wird. Aus diesem Grunde dürfen wir wohl mit Recht annehmen, dass der „wahre" Verteilungsquotient zwischen Zucker und Wasser nicht viel von $\alpha = 1.1$ verschieden sein kann.

Okamoto[9] hat aus der von ihm direkt experimentierten Verteilung der D-Atome zwischen gasförmigem Wasserstoff und Wasser sowie Methylalkohol indirekt geschlossen, dass die D-Atome zwischen Wasser

(8) Vgl. M. Harada, *J. Chem. Soc. Japan*, **57** (1936), 391; A. I. Brodski, *J. Phys. Chem.* (*U.S.S.R.*), **9** (1937), 755.

(9) G. Okamoto, *Sci. Papers Inst. Phys. Chem. Research* (*Tokyo*), **31** (1937), 211; vgl. auch G. Okamoto und T. Kwan, *J. Chem. Soc. Japan*, **57** (1936), 1179.

und der Hydroxylgruppe des Methylalkohols, innerhalb des Messfehlerbereichs, gleichmässig verteilt werden müssen. Der Verteilungsquotient der D-Atome zwischen Methylalkohol und Wasser wurde auch von Wirtz[5] aus spektroskopischen Daten rechnerisch ermittelt. Dabei schätzte er, dass der Verteilungsquotient etwa $a = 1.1$ sein soll. Dieser Wert stimmt mit dem von uns in der vorliegenden Arbeit für Hexosen gefundenen bzw. geschätzten Wert sehr gut überein.

Zum Schluss möchten wir der Nippon Gakujutsu-Shinkohkai (der Japanischen Gesellschaft zur Förderung der wissenschaftlichen Forschungen) sowie der Hattori-Hohkohkai (der Hattori-Stiftung) für ihre finanzielle Unterstützung unseren besten Dank aussprechen.

Physikalisch-chemisches Laboratorium
der Kaiserlichen Universität zu Osaka
und
Siomi-Institut für physikalische
und chemische Forschung.

Absorption Spectra of Co-ordination Compounds. II.

By Ryutaro TSUCHIDA.

(Received May 16, 1938.)

A typical metallic complex has generally two absorption bands,[1] of which the first lies in the visible region and the second in the ultra-violet. In case the complex has negative ligands in trans-positions another band is expected, which is here called the third band.[2][3] Further, in special cases, selective absorption bands due to ligands themselves may be observed.

In Part I[4] of this series, the author discussed on the origins of the first and the second band, concluding that the former is attributed to

(1) Y. Shibata, *J. Coll. Sci., Imp. Univ. Tokyo*, **37** (1915), Art. 2; Y. Shibata and G. Urbain, *Compt. rend.*, **157** (1913), 593.

(2) Y. Shibata, *J. Chem. Soc. Japan*, **36** (1915), 1243.

(3) R. Tsuchida, this Bulletin, **11** (1936), 721; R. Tsuchida and S. Kashimoto, *ibid.*, **11** (1936), 785; R. Tsuchida and M. Kobayashi, *ibid.*, **12** (1937), 83.

(4) R. Tsuchida, *ibid.*, **13** (1938), 388.

electron transitions in an unsaturated transition shell of the central ion and the latter is due to a kind of reversible dissociation of ligands within the complex radical. The present paper deals with the origins of the third and the special bands as well as the relation between the absorption and the stability of the complex radical.

VI. Thermochemical Explanation of the Third Band. In order to explain the second band, it has been postulated in Part I[4] that, when a quantum of the second band is absorbed by a complex radical, one of the co-ordinate links is split open to produce in the original seat of co-ordination an excited ligand, which will recombine in most cases to regenerate the original complex: e.g.,

$$[\mathrm{M\ A_6}]^{n+} + h\nu_2 = [\mathrm{M\ A_5\{A\}}]^{n+},$$

$$[\mathrm{M\ X_6}]^{n-} + h\nu_2 = [\mathrm{M^+\ X_5\{X^-\}}]^{n-}, \quad \text{etc.},$$

where {A} and {X⁻} denote the excited molecule and ion respectively. Thus the frequency of the second band may be shown by the following relation.

$$S = h\nu_2 = -P + Q + R - \frac{\Phi - \Sigma\Phi_1}{n} \qquad (3),$$

where S = the co-ordination energy, P = the energy of approach, Q = the heat of formation of the complex from the component compounds of first order, R = the energy of activation of the ligand, Φ = the lattice energy of the complex, $\Sigma\Phi_1$ = sum of the lattice energies of the component compounds, and n = the co-ordination number.

For the third band, the author assumes a kind of neutralization between the central ion and one of the co-ordinating anion, in which an excited ionogen is produced in the position of co-ordination: e.g.,

$$[\mathrm{M\ X_6}]^{n-} + h\nu_3 = [\mathrm{M\ X_5\{X\}}]^{n-}, \quad \text{etc.},$$

where {X} denotes the excited ionogen. It is again assumed that the excited ionogen thus produced by $h\nu_3$ recombines, in most cases, to form the original complex and may be sometimes set free resulting in decomposition or substitution of ligands.

The photochemical neutralization may be treated thermochemically by assuming the following cyclic process. (1) First, the co-ordinate link is broken ($-S$). (2) The excited ion is converted into an ion in normal state ($+R$). (3) Then the ion is taken to infinity ($-P$). (4) The anion is deprived of the electron ($-E$). (5) The electron is given to the central

ion ($+J$). (6) The ionogen is again brought to the seat of co-ordination and then excited ($-R$).

Then

$$h\nu_3 = S+P+E+J \qquad (4),$$

where E = the electron affinity of the ligand, and J = the ionization energy of the central ion.

By means of the relation thus derived, several interesting facts may be explained.

(A) *Constancy of* $\nu_3 - \nu_2$. The differences, $\nu_3 - \nu_2$, are nearly equal for a series of similar compounds. The fact is especially remarkable in the nitro-ammine cobaltic series, in which $\nu_3 - \nu_2$ is nearly constant, while $\nu_2 - \nu_1$ varies in considerably wide range. (C.f. Section I.[4])

We obtain from the relations (2) and (4),

$$h\nu_3 - h\nu_2 = P+E-J .$$

Now for nitro-ammine cobaltic compounds, E and J are constant and P also may be regarded as constant, if we neglect the effect of neighbouring ligands. Therefore $\nu_3 - \nu_2$ is constant.

(B) *Estimation of the third ionization potential of cobalt.* Assuming the distance between the central ion and the negative charge of the nitro-radical of $[Co(NH_3)_2(NO_2)_4]Ag$[5] as 2.5 Å, we may roughly estimate the value P.

$$P = 27.4 \times 10^{12} \text{ ergs} = 17.5 \text{ e.v.}$$

$$h\nu_3 - h\nu_2 = 33h \times 10^{13} = 2.16 \times 10^{12} \text{ ergs} = 1.4 \text{ e.v.}$$

Hence $$J = P+E-(h\nu_3 - h\nu_2) = 20 \text{ e.v.}$$

This value of J seems too small for the third ionization of cobalt. The deviation might probably be attributed to the neglection of the polarization.

(C) *Third bands of non-metallic complexes.* Triiodide ion may be regarded as a non-metallic complex, of which the center and the ligands are all iodine ions, positive and negative. Then it should have a second band, while it should lack the first, the central ion being of an inert gas configuration. (Cf. Section IV.[4]) According to Mooney[6] the complex ion has a linear structure, and if we extend the hypothesis on the third band[4] to this non-metallic complex, here again a third band is expected.

(5) A. F. Wells, *Z. Krist.*, **95** (1936), 74.
(6) R. C. L. Mooney, *Z. Krist.*, **90** (1935), 143.

In fact, triiodide ion has two bands at 94×10^{13} and 113×10^{13}, which may possibly be regarded as the second and the third band respectively. (Cf. Section II.[4]) Allsopp[7] postulated that the twin bands have the origin in the simultaneous production during irradiation of iodine atoms in the normal and in the excited, metastable state. According to our hypothesis, however, the third band is due to a neutralization, in which iodine atoms in the normal and in the excited state are produced simultaneously just as was assumed by Allsopp. Absorption of the light energy corresponding to the second band produces an excited metastable ion.

(D) *The absorption bands of alkali halides.* Hilsch and Pohl[8] studied the absorption bands of crystals of alkali halides and explained the band of the longest wave-length as related to a neutralization of adjacent ions, e.g.,

$$Na^+ + Cl^- + h\nu = Na + Cl\ .$$

The energy was expressed by

$$h\nu = \Phi + E - J\ ,$$

where Φ = the lattice energy, J = the ionization energy of the alkali atom, and E = the electron affinity of the halogen atom. Born[9] modified the formula, by postulating "Lochenergie".

In order to extend the results of absorption spectra of co-ordination compounds, the author assumes further that the co-ordinate covalene may be considered as to consist of two parts, i.e., electro-valence and covalence, and these, in turn, may be explained as extreme cases of co-ordinate covalence: the electro-valence is an extreme case of co-ordinate covalence, in which the covalent linkage is so weak as may be neglected, and the covalence, the opposite extreme case, in which it lacks the electrostatic part. Then all the chemical linkages might be regarded as co-ordinate combination and consequently the results obtained for co-ordination compounds may be widely applied to various compounds.

Now sodium chloride, for example, should lack the first and the second band, because it has neither unsaturated transition shell nor co-ordinate bonds. In crystalline form, however, six chlorine ions are situated around a sodium ion, just as in a sexa-coördinated complex, every two of the former making a pair in trans-position to each other, and therefore a third band may be expected. Thus the band of the longest wave-length

(7) C. B. Allsopp, *Proc. Roy. Soc.* (London), A **158** (1937), 167.
(8) R. Hilsch and R. W. Pohl, *Z. Physik*, **59** (1928), 812.
(9) M. Born, *Z. Physik*, **79** (1932), 62.

in the ultra-violet region could be regarded as the third band and the relation (4) may be applied.

$$h\nu_3 = S+P+E-J\,.$$

Now P in this case is the work to bring Na^+ and Cl^- to infinity, i.e., the lattice energy Φ. And if we assume $S = 0$, the relation is reduced to

$$h\nu_3 = \Phi+E-J\,.$$

This is identical with the equation of Hilsch and Pohl, the latter being a special case of the relation (4).

(E) *Absorption spectra of various compounds of first order.* From the viewpoint suggested in (D), various binary compounds of the type M_mX_n, usually understood as compounds of first order, may be recognized as co-ordination compounds. A few examples are given here. Anhydrous chromic chloride may be regarded as a polynuclear complex compound. As is clear from its crystal structure,[10] every chromic ion is surrounded octahedrally by six chlorine ions and the entire crystal is of a layer lattice, each layer being built up of such octahedra having chlorine ions in common. Now, according to the author's opinion, the compound should have the first, the second and the third band.

It has already been stated that mercuric chloride could be regarded as a co-ordination compound, the second and the third band being expected. (Cf. Section V.[4]) As was discussed in (D), only the third band is expected for sodium chloride in crystalline state. Extending the idea on the opposite side, the author expects that stannic bromide, etc., should have the second and the third band.

In connection with this problem, the interesting research of the Joffés[11] must be referred to. They measured electrical conductivity of single crystals of cuprous oxide irradiating them with monochromatic lights. The spectrum of conductivity gives three maxima at 590 mμ, 420 mμ and 270 mμ, showing a curve quite similar to that of an absorption spectrum of a typical complex compound which has a third band. The crystal structure[12] shows that oxygen atoms are co-ordinated in trans-positions to each other referring to a copper atom, and this is the very structure for which a third band may be expected.

---

(10) N. Wooster, *Z. Krist.*, **74** (1930), 363.
(11) A. W. Joffé and A. T. Joffé, *Physik. Z. Sowjetunion*, **11** (1937), 241.
(12) P. Niggli, *Z. Krist.*, **57** (1922), 253.

VII. Extension of Trans-Pairing Hypotheses. It has long been known that the ligands co-ordinated in trans-position to each other are in special relation. The phenomenon of geometrical isomery is too well known. Drew, Cox and others[13] have shown that the four linkings to the ammonia molecules of tetrammine platinic salts are differentiated into two equivalent pairs which function independently, a closer relationship existing between the members of a pair than exists between either member of one pair and either member of the other. Cox and Preston[14] extended the theory. H. Sueda[15] assumed that the absorption spectra of complex compounds could be expressed as the sum of the characteristic absorption caused by the radicals situated at the trans-position, and analyzed second bands of various complex salts. Y. Shibata[2] explained the third bands of nitro-ammine cobaltic compounds by his trans-dinitro-theory. And the present author[3] extended Shibata's theory, explaining the third band as due to a pair or pairs of negative ligands in trans-positions.

As has been shown in the preceding section, it must be postulated in order to explain the third band that it has its origin in a kind of neutralization between the central cation and a ligand anion, but the postulate does not imply that the ligand must have another anion in its trans-position. The author should like to explain this point conventionally by the following hypothesis. In the process of the neutralization the electron must be transferred from the ligand to the central ion, during which the latter would undergo a great polarization, and this polarization in turn would cause in the ligand in trans-position further polarization of such a degree that anions only could correspond to it. In case there is a neutral ligand in the trans-position, it would resist the polarization and accordingly the neutralization would be prevenfed.

If we assume that the trans-pairing is due to polarization through the central ion as above, all the third bands could be explained. (Cf. Section II.[4]) Whereas in octahedral or square configuration the pair of ligands in trans-position only can have opposite co-ordination directions referred to the central ion, in tetrahedral configuration, however, any two ligands can have opposite components of co-ordination directions. Then another possibility of the third band must be admitted: viz., the third bands may be expected for tetrahedral molecules and ions such as SnI_4, CrO_4^-, etc., though they have no ligands in trans-positions. Thus

(13) H. D. K. Drew, F. W. Pinkard, W. Wardlaw, and E. G. Cox, *J. Chem. Soc.*, **1932**, 1004.

(14) E. G. Cox and G. H. Preston, *ibid.*, **1933**, 542.

(15) H. Sueda, *J. Chem. Soc. Japan*, **56** (1936), 406, 542.

the trans-diacido-hypothesis for octahedral and square configurations should be modified in its application to compounds of tetrahedral configuration.

VIII. Special Bands. We have seen that all the compounds which show the third bands have negative ligands co-ordinated in trans-positions and vice versa. The only exception in the literature is $[Cr(NH_3)_5(NCS)](NCS)_2$ which gives three bands in spite that it has only one negative ligand in co-ordination. Y. Shibata[16] proved that the special band is due to NCS radical itself when co-ordinated to any central metallic atom.

Then $[Co(NH_3)_5(NCS)]Cl_2$, $[Cr(NH_3)_2(NCS)_4]NH_4$ and $[Cr(NCS)_6]K_3$ should have the special bands. The author prepared these compounds as well as $[Cr(NH_3)_5(NCS)](NCS)_2$ and measured their absorption. The results are given in Table 6.

Table 6.

Complex compound	1st bd.		2nd bd.		Special bd.		3rd bd.		$\nu_s-\nu_2$	$\nu_3-\nu_2$
	$\nu_1(10^{13})$	log ε	$\nu_2(10^{13})$	log ε	$\nu_s(10^{13})$	log ε	$\nu_3(10^{13})$	log ε		
$[Co(NH_3)_5(NCS)]Cl_2$	60.2	2.14	(84)	2.60	98.0	3.20	—	—	14	
$[Cr(NH_3)_5(NCS)](NCS)_2$	61.5	1.82	(83)	1.67	100.4	3.56	—	—	17	
$[Cr(NH_3)_2(NCS)_4]NH_4$	57.5	1.95	(75)	1.75	99.6	4.17	(113)	3.9	25	38
$[Cr(NCS)_6]K_3$	53.1	2.08	70.8	2.00	98.6	4.40	(108)	4.3	28	37
[Co dg_2' Cl NH_3][17]	63.8	1.75	86.0	3.08	(101)	3.7	121.8	4.50	15	36
[Co dg_2' Cl *py*][18]	65.5	2.24	89.0	3.39	(102)	3.7	121.5	4.35	13	33

The special band of $[Cr(NH_3)_5NCS](NCS)_2$ is at $\nu = 100.4 \times 10^{13}$. $[Cr(NH_3)_2(NCS)_4]NH_4$ and $[Cr(NCS)_6]K_3$ give similar bands whose frequencies are 99.6×10^{13} and 98.6×10^{13} respectively. Whereas each of the first, the second and the third band of $[Cr(NCS)_6]K_3$ has a larger frequency than that of the corresponding band of $[Cr(NH_3)_2(NCS)_4]NH_4$, the position of the special band of the former is nearly the same as that of the latter. In these isorhodanato-complexes we may notice a peculiar group of atoms, M←N = C<, to which the special bands may be attributed. In [Co dg_2' Cl NH_3] and [Co dg_2' Cl *py*], the same group may

(16) Y. Shibata, *J. Chem. Soc. Japan*, **35** (1914), 807; *J. Coll. Sci., Imp. Univ. Tokyo*, **41** (1918), Art. 6.

(17) R. Tsuchida and M. Kobayashi, this Bulletin, **12** (1937), 83.

(18) S. Kashimoto and M. Kobayashi, *ibid.*, **12** (1937), 350.

again be found and accordingly similar special bands should be expected. In fact these dimethylglyoxime complexes show four bands each, of which those at about 100×10^{13} may be regarded as the special bands. Moreover, salicylaldehyde-ethylenediamine-cobalt which was recently reported by T. Tsumaki[19] has also a special band similar to those mentioned above and it may probably be due to the same origin.

We have seen that the spectra of a co-ordination compound consists of the first, the second, and the third band as well as special bands. The author, however, does not mean that a numbered band, say the third, is actually the third or there are at least three bands. For example, the third band of $[HgI_4]K_2$ is actually the second and that of rock salt, the first. Moreover, the third band of $[Co\,dg_2'\,Cl\,NH_3]$ is really the fourth, special band due to $M\leftarrow N=C<$ being the third numbered from the long-wave side.

Besides the absorption bands hitherto discussed, every co-ordination compound has the so-called end absorption, which is the superposition of special bands due to less effective ligands and their parts. By investigating shorter wave-lengths, we must naturally meet such bands. The special bands given in Table 6 are some of those which have comparatively longer wave-lengths.

As was discussed in Section I,[4] all the chemical combinations may be regarded as co-ordinate linkages or the extreme cases. The entire absorption spectrum of a compound may possibly be treated as a kind of superposition of co-ordination spectra of parts of the compound. For example, the spectrum of $[Co(NH_3)_5CrO_4]Cl$ may be analysed into spectra mainly of sexa-coördinate absorption unit, of which the center is Co and a quadri-coördinate unit whose center is Cr. These absorption units may be denoted as $[Co(NH_3)_5O-]$ and $[Cr\,O_3O-]$ for the sake of convenience. The former should have two bands, the first and the second, and the latter also two bands, the second and the third. Measurements show that the absorption bands due to $[Cr\,O_3O-]$ are slightly shifted towards the longer wave-lengths compared with those of $CrO_4^{=}$ alone: viz., the second band of the former is at 78×10^{13} and that of the latter, at 81×10^{13}. The first band of $[Co(NH_3)_5O-]$ is at 56×10^{13}, but the second is covered by the strongly absorbing second band of $[Cr\,O_3O-]$. The bands of $[Cr\,O_3O-]$ in this case may therefore, be called special bands of $[Co(NH_3)_5CrO_4]Cl$.

(19) T. Tsumaki, this Bulletin, **13** (1938), 252; *J. Chem. Soc. Japan*, **58** (1937), 1288.

IX. Stability of Co-ordination Compounds. There has been neither fixed definition nor generally accepted measure as to the stability of co-ordination compounds. The stability in solution must of course depend upon the nature of the solvent. The photochemical stability as was studied by Schwarz[20] could not be applied to compounds which do not undergo photochemical change.

Ephraim and his co-workers[21] have studied thermal decomposition of solid ammine complexes, but his definition of stability is applicable only to those complexes which are built up by Werner's auxiliary valences. In short, there is no definition of stability which would cover the entire field of co-ordination compounds. In order to establish such a definition, it is necessary to choose as the measure a property which is quite common to all co-ordination compounds. For this purpose spectroscopic data would give a fine measure. Luther and Nikolopulos[22] assumed that the first band is due to the linkage between the central atom and the ligand, and the strength of the linkage could be judged from the colour of the compound. In other words, they adopted the first band as the measure of stability. This hypothesis implies that the shorter the wave-length of the first band, the greater is the stability. According to this hypothesis, $[Co(NH_3)_5(NO_2)]Cl_2$, the most stable complex among the nitro-ammines, should have a first band of shorter wave-length than any other member of the series, but, as a matter of fact, the first band has lower frequency than those of less stable compounds such as $[Co(NH_3)_3(NO_2)_3]$ and $[Co(NH_3)_2(NO_2)_4]NH_4$. (Cf. Table 2.[4]) Moreover, the order of actual stability seems almost reverse to that of the frequency of the first band for the nitro-ammine cobaltic series. Thus the band could not be the true measure of stability, nevertheless it may be taken as a rough measure by the reason which will be shown later.

On the contrary, the frequency of the second band is precisely in the order of actual stability. In the nitro-ammine series, for example, $[Co(NH_3)_5(NO_2)]Cl_2$ has the highest frequency and $[Co(NH_3)_2(NO_2)_4]NH_4$ the lowest, the other members[23] being intermediate. Thus the second band may be adopted as the measure of stability, and consequently S may serve for the same purpose. From the

(20) R. Schwarz and K. Tede, *Ber.*, **60** (1927), 65, 69; R. Schwarz and H. Weiss, *ibid.*, **58** (1925), 746.

(21) F. Ephraim, *Ber.*, **45** (1912), 1322; **46** (1913), 3103, 3742; **47** (1914), 1828; **48** (1915), 41, 624, 629, 638, 1770, 2007; **49** (1916), 529; **50** (1917), 1069, 1088; **51** (1918), 130, 644, 706; **52** (1919), 236, 941; *Z. physik. Chem.*, **81** (1912), 513, 539; **83** (1913), 196.

(22) R. Luther and A. Nikolopulos, *Z. physik. Chem.*, **82** (1913), 361.

(23) It has already[4] been discussed that $[Co(ONO)_6]M_3$ does not belong to this series.

practical point of view alone, it is far advantageous to take the second band as the measure, because all the co-ordination compounds have the second bands whereas some of them lack the first as was shown in Part I.[4]

Substitution of NO_2^- for NH_3 in nitro-ammine complexes, gives rise to an instabilization of the complexes, or in other words, NH_3 is more hypsochromic than NO_2^-. The order of hypsochromic effect on the second band may be easily found for various ligands. In Tables 7 and 8, pentammine and tetrammine cobaltic complexes are arranged in the order of frequency of their second bands, i.e., the order of stability.

Table 7.

Ligand	Complex	ν_2 (10^{13})	log ε
NO_2^-	$[Co(NH_3)_5NO_2]Cl_2$	92.6	3.12
ONO^-	$[Co(NH_3)_5ONO]Cl_2$	91.7	2.79
H_2O	$[Co(NH_3)_5H_2O]Cl_3$	87.5	1.62
NCS^-	$[Co(NH_3)_5NCS]Cl_2$	(84)	2.60
OH^-	$[Co(NH_3)_5OH](NO_3)_2$	(84)	1.9
NO_3^-	$[Co(NH_3)_5NO_3](NO_3)_2$	(83)	1.8
Cl^-	$[Co(NH_3)_5Cl]Cl_2$	82.8	1.66
$CO_3^=$	$[Co(NH_3)_5CO_3]NO_3$	(82)	1.8
Br^-	$[Co(NH_3)_5Br]Br_2$	(81)	2.8

Table 8.

Ligand	Complex	ν_2 (10^{13})	log ε
NO_2^-	$[Co(NH_3)_4(NO_2)_2^{(1)}_{(2)}]Cl$	91.2	3.10
H_2O	$[Co(NH_3)_4(H_2O)_2^{(1)}_{(2)}]Cl_3$	84.0	1.48
$C_2O_4^=$	$[Co(NH_3)_4C_2O_4]Br$	84.0	1.88
$CO_3^=$	$[Co(NH_3)_4CO_3]Br$	82.6	2.03

From Table 7, we can find the hypsochromic order of ligands, i.e., the spectrochemical series for the second band:

NH_3, NO_2^-, ONO^-, H_2O, NCS^-, OH^-, NO_3^-, Cl^-, $CO_3^=$, Br^-.

It will be noticed that the series almost coincides with that of the first band. (Cf. Section IV.[4]) This fact may easily explained by the following consideration. We have seen in Section V,[4]

$$S = -P+Q'+R \qquad (1').$$

The smaller the value P, the greater will be the value S if Q' and R remain nearly equal. Thus the theoretical consideration for the first band given in Section IV[4] will also hold approximately for the second band. For example P for H_2O is smaller than that for Cl, but greater than that for NH_3. The ligand H_2O, therefore, forms more stable co-ordinate combination than Cl, but less stable linkage than NH_3.

From the same consideration it follows that the first and the second bands will be displaced side by side by a substitution, so long as Q' and R for the compounds remain nearly constant. In such cases we may be able to compare approximately the stability of these compounds by the position of the first bands, as has been proposed by Luther and Nikolopulos.[22] The first bands, however, fail sometimes to be the measure, as we have seen in the case of nitro-ammine cobaltic compounds. The first band is merely an approximate measure of stability after all.

In Table 9, symmetrical complex salts of iron, chromium and cobalt are shown all together in the order of the frequencies of the second bands. Here again it coincides with the order of actual stability, showing that the second band is the absolute measure of stability which covers the entire field of co-ordination compounds.

Table 9.

Linkage	Complex salt	ν_2 (10^{13})	log ε
Fe^{+++}—CN^-	$[Fe(CN)_6]K_3$	99.4	3.20
Co^{+++}—en	$[Co\ en_3]Br_3$	90.0	1.77
Co^{+++}—NH_3	$[Co(NH_3)_6]Cl_3$	88.8	1.57
Cr^{+++}—NH_3	$[Cr(NH_3)_6]Cl_3$	86.0	1.44
Co^{+++}—ONO^-	$[Co(ONO)_6]Na_3$	82.4	3.75
Cr^{+++}—H_2O	$[Cr(H_2O)_6]Cl_3$	73.6	1.20
Co^{+++}—$C_2O_4^=$	$[Co(C_2O_4)_3]K_3$	71.0	2.19
Cr^{+++}—NCS^-	$[Cr(NCS)_6]K_3$	70.8	2.00

The stability may sometimes be roughly compared without spectroscopic data. By dint of the relation (1′), we may be able to compare the stability of co-ordination compounds, of which Q's and R's are nearly equal. For example, the heats of formation[24] of $[Co(NH_3)_4Cl_2^{(1)}_{(6)}]Cl$ and $[Co(NH_3)_4Cl_2^{(1)}_{(2)}]Cl$ are 215 and 214 Cal. respectively, which may be regarded as equal, and R, i.e., the activation energy for Cl^- to combine with Co^{+++} may also be assumed as equal for this pair of isomers. Then we obtain from (1′) $S = -P +$ constant. If we neglect the polarization of Cl^-, the energy of approach, P, may be roughly calculated for the cis-form and the trans-isomer.

$$P_{trans} - P_{cis} = -\frac{e^2}{r}\left(\frac{1}{2} - \frac{1}{\sqrt{2}}\right) > 0 ,$$

where r denotes the distance between the central ion and the ligand.

Hence $P_{cis} < P_{trans}$.

Therefore $S_{cis} > S_{trans}$.

The cis-compound should, therefore, be more stable than its trans-isomer. Another example of geometrical isomery may be found in Table 2,[4] in which ν_2's of $[Co(NH_3)_4(NO_2)_2^{(1)}_{(2)}]Cl$ and $[Co(NH_3)_4(NO_2)_2^{(1)}_{(6)}]Cl$ are 91.2×10^{13} and 87.0×10^{13} respectively, the former thus being more stable.

In photochemical decomposition of $[Co(NH_3)_4(NO_2)_2]Cl$, however, the trans-form has been proved[20] to be more stable than the cis-isomer. This fact seems at first sight to contradict with the above conclusion, nevertheless this apparent discrepancy may be easily overcome by the following consideration.

When a complex radical absorbs $h\nu_2$, the co-ordinate link is split open and an excited ligand will be produced at the seat of co-ordination, as was shown in Section V.[4] Such excited state of a ligand may be reached otherwise, viz., by making the ligand approach to the central ion from infinity $(-P)$ and then giving it the energy of activation $(+R)$. The excited ligand which has the energy $(R - P)$, may either combine with the central ion to regenerate the original complex or leave the position of co-ordination resulting in decomposition or substitution. In other words, there may be assumed an intermediate metastable state prior to the formation or the destruction of the linkage.

(24) T. C. J. Ovenston and H. Terry, *J. Chem. Soc.*, **1936**, 1660.

$$[\mathrm{M\,A_5B}]+h\nu_2(=S) \rightleftarrows [\mathrm{M\,A_5\{B\}}] \rightleftarrows [\mathrm{M\,A_5}]+B+(R-P)\ ,$$

where {B} represents the excited ligand.

The greater the value S, the greater the stability of the complex in thermal reactions. During irradiation with $h\nu_2(=S)$, however, the energy of the intermediate excited state will sway the stability. The greater the energy $R-P$, the intermediate state will be the more readily decomposed. The stability in photochemical reaction, therefore, depends on the value $P-R$. We have seen above that

$$P_{\mathrm{cis}} < P_{\mathrm{trans}}\ .$$

Hence $$(P-R)_{\mathrm{trans}} > (P-R)_{\mathrm{cis}}\ .$$

Thus the trans-form is more stable in photochemical change than its cis-isomer.

X. Substitution of Ligands. Experience shows that the substitution of ligands which proceeds naturally occurs in the direction in which the value S increases, i.e., the second band is shifted towards the shorter wave-lengths.[25] In other words, the substitution reaction takes place so as to produce more stable substitution products. For example, $[\mathrm{Co(NH_3)_4Cl_2}]\mathrm{Cl}$ in aqueous solution changes step by step into $[\mathrm{Co(NH_3)_4(H_2O)_2}]\mathrm{Cl_3}$, the second band of the latter as well as those of the intermediate compounds showing the corresponding hypsochromic shifts from that of the initial compound.

This rule may be advantageously applied to judge the stability of complex compounds in solution. Whereas ligands which have larger S-values than H_2O, will form complexes stable in aqueous solution, complexes which contain ligands of smaller S-value than H_2O will be unstable in aqueous solution and aquotization will then take place. For example, the second bands of $[\mathrm{Co(NH_3)_6}]\mathrm{Cl_3}$, $[\mathrm{Co(NH_3)_5H_2O}]\mathrm{Cl_3}$ and $[\mathrm{Co(NH_3)_5Cl}]\mathrm{Cl_2}$ are respectively at 88.8×10^{13}, 87.5×10^{13} and 82.8×10^{13}. The luteo-salt is, therefore, very stable in aqueous solution, while the purpureo-salt changes gradually into the roseo-salt. The preparation of the purpureo-salt by adding hydrochloric acid to aqueous solution of the roseo-salt depends upon the fact that the former has much smaller solubility than the latter. It is the question of solubility and not of stability.

Extending the above consideration, we may now be able to discuss the possibility of methods of preparation of complex compounds. It is

(25) R. Tsuchida, this Bulletin, **11** (1936), 721.

possible to prepare by substitution reaction a complex compound whose S is larger than that of the material. The greater the difference in S, the easier the preparation. For example, the substitution of NH_3 for Cl^- should be much easier than that of NH_3 for H_2O.

Anhydrous chromic chloride $CrCl_3$ may be regarded as a polynuclear complex compound as was pointed out in Section VI. By simply keeping this salt in liquid ammonia, $[Cr(NH_3)_6]Cl_3$ is easily produced, but it is rather difficult to obtain the latter from $[Cr(H_2O)_6]Cl_3$ and liquid ammonia. These empirical rules and the hypothesis might be widely applied in explaining various chemical reactions as well as finding methods of preparation of co-ordination compounds. For this purpose the spectrochemical series for the second band given in Section IX may be of considerable service.

Summary.

(1) The absorption spectra of co-ordination compounds consist of the first, the second and the third bands as well as those due to ligands themselves. Some of the compounds may lack the first, the third, or both the bands, but none of them the second.

(2) Postulating that by absorption of a quantum $h\nu_3$ (ν_3 = the frequency of the third band) a kind of neutralization takes place between the central ion and one of the co-ordinated anion to produce an excited ionogen in the original seat of co-ordination, the following relation has been derived.

$$h\nu_3 = S+P+E-J,$$

where E = electron affinity of the anion, J = ionization energy of the central ion, S = co-ordination energy, and P = work of approach of the anion.

The ultra-violet absorption band of solid alkali halide has been explained as a special case of the third band.

(3) Besides the numbered bands, a co-ordination compound has generally some more bands due to ligands themselves. Examples of these special bands are given. The end absorption has also been explained.

(4) The co-ordination energy, $S(=h\nu_2)$, may be taken as the measure of stability of the co-ordination compound. The order of hypsochromic effect of ligands on the second band gives the order of strength of the co-ordinate linkages between the central ion and the ligands. The order of stability has been determined experimentally.

$$NH_3,\ NO_2^-,\ ONO^-,\ H_2O,\ NCS^-,\ OH^-,\ NO_3^-,\ Cl^-,\ CO_3^-,\ Br^-.$$

(5) Whereas the stability of co-ordination compounds may be defined by S as a rule, the photochemical stability, however, should be given by $P - R$, R being the activation energy. Both the stabilities were compared with illustrations.

(6) The substitution of ligands which proceeds naturally, takes place in the direction, in which the value S increases, or in other words, the second band is displaced towards the shorter wave-lengths. This rule and the spectrochemical series in (4) give the means of explaining as well as finding methods of preparation of various co-ordination compounds.

The author expresses sincere thanks to Professor Y. Shibata for his kind advice and encouragement. He is also indebted to Mr. S. Kashimoto and Mr. M. Kobayashi for their experimental assistance.

Chemical Department, Faculty of Science,
Imperial University of Osaka.

On the Relation between the Configuration of Metallic Complex Salts and their Absorption Spectra. II. *cis*-Trinitro-triammine-cobalt.[1]

By Hideo SUEDA.

(Received May 17, 1938.)

In a previous paper,[2] the assumption that the absorption band presented by complex salt solutions can be resolved into elements which are due to pairs of co-ordinated groups situated in trans-position and that these elements show an additive property in the same complex ion, was deduced from the comparison of absorption curves given by nitro-ammine cobaltic complex salts, and it was stated that it can be applied to $[Co(NH_3)_3(NO_2)_3]$ prepared by the ordinary method of S. M. Jörgensen.[3] That is, the author confirmed firmly the theory of Y. Shibata[4]

(1) Translated from the paper published in Japanese, *J. Chem. Soc. Japan*, **59** (1938), 47.

(2) This Bulletin, **12** (1937), 188.

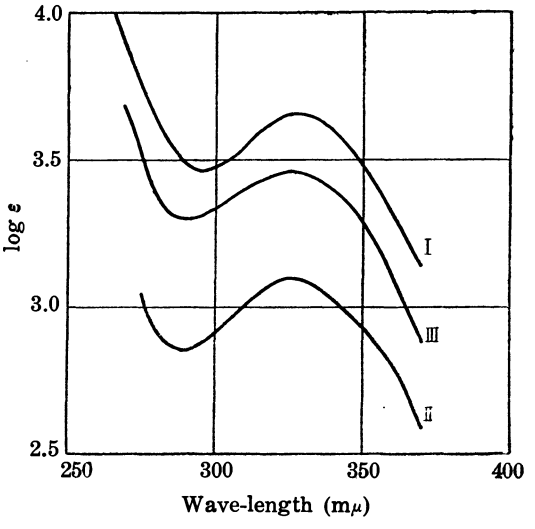
(3) H. Biltz and W. Biltz, "Übungsbeispiele aus der unorganischen Experimentalchemie," 3rd and 4th Ed. (1920).

(4) *J. Chem. Soc. Japan*, **30** (1915), 1243.

that the salt possesses trans-configuration. According to Werner's coordination theory, however, it is evident that cis-compound must also exist.

If *cis*-$[Co(NH_3)_3(NO_2)_3]$, of which nothing has ever been written, can be obtained, then such a salt must show, from the author's assumption, an absorption curve similar to that of $[Co(NH_3)_5(NO_2)]Cl_2$ and *cis*-$[Co(NH_3)_4(NO_2)_2]Cl$ and an absorption capacity three times that of the former and one and half times that of the latter. Since *cis*-$[Co(NH_3)_3(NO_2)_3]$ should show infallibly upon the author's assumption, it was prepared and tested.

$[Co(NH_3)_3(NO_3)_3]$ transforms into $[Co(NH_3)_3(H_2O)_3](NO_3)_3$ in water, and the latter has according to Y. Matsuno[5] a cis-configuration. Thus, if water molecules in $[Co(NH_3)_3(H_2O)_3](NO_3)_3$ can be replaced by nitro-radicals, then *cis*-$[Co(NH_3)_3(NO_2)_3]$ can be obtained. When the salt so prepared, it possessed a composition according to the above deduction and gave an absorption curve as indicated in Fig. 1, curve I. As the absorption curve differs from that of *trans*-$[Co(NH_3)_3(NO_2)_3]$, it can be considered as *cis*-$[Co(NH_3)_3(NO_2)_3]$. Curves II and III are absorption curves of $[Co(NH_3)_5(NO_2)]Cl_2$ and *cis*-$[Co(NH_3)_4(NO_2)_2]Cl$ respectively. As seen in Fig. 1, curves I, II and III are similar possessing maxima at wave-length 325 mμ. Extinction coefficient at the maximum of curve I is about 3.6 times that of curve II (the figure being slightly greater than expected) and about 1.6 times that of curve III.



I: *cis*-$[Co(NH_3)_3(NO_2)_3]$
II: $[Co(NH_3)_5(NO_2)]Cl_2$
III: *cis*-$[Co(NH_3)_4(NO_2)_2]Cl$

Fig. 1.

The results obtained above established the correctness of the prediction made from the author's assumption in his first paper. Moreover, according to Y. Shibata[4] and R. Tsuchida[6] *cis*-$[Co(NH_3)_3(NO_2)_3]$

(5) *J. Coll. Sci., Imp. Univ. Tokyo*, **41** (1921), Art 10, 14.
(6) This Bulletin, **11** (1936), 785.

should not possess the third absorption band, and, when measured down to nearly 250 mμ, no sign of such a band appeared.

Experimental.

To 5 g. of $[Co(NH_3)_3(NO_3)_3]$, prepared by the method of Jörgensen,[7] was added 50 c.c. water and on leaving the mixture to stand for 5 hours at about 10°C., a dark red solution was obtained. A small quantity remaining undissolved was removed by filtration, and to the filtrate was added 10 c.c. glacial acetic acid with cooling with ice. To the acidified solution 7 g. sodium nitrite was gradually added with constant stirring, the solution was left to stand for some time and filtered, and the filtrate left to stand for 24 hours in an ice box. Obtained crystals were washed thoroughly with cold water and recrystallized quickly from water, at a temperature not exceeding 50°C.

The recrystallized substance was analyzed for its hydrogen and nitrogen, the result being as follows. Found: H, 3.71; N, 32.7. Calculated for $[Co(NH_3)_3(NO_2)_3]$: H, 3.66; N, 33.9%.

Summary.

cis-$[Co(NH_3)_3(NO_2)_3]$ was prepared and its absorption band proved as being identical with that expected from author's assumption given in the first paper.

In conclusion, the author wishes to express his sincere thanks to Prof. Y. Shibata of the Imperial University of Tokyo, and to Assist. Prof. T. Uemura of the Tokyo University of Engineering for their kind encouragements.

Laboratory of Inorganic Chemistry,
Tokyo University of Engineering
(Tokyo Kôgyô-Daigaku).

(7) *Z. anorg. Chem.*, **5** (1894), 185.

Über den „Papain-Amylase-Symplex" (Über die chemische Natur der Taka-Amylase. III.)[1]

Von Shiro AKABORI und Katuhiko KASIMOTO.

(Eingegangen am 25. Mai 1938.)

Bei einem Versuch über die Wirkung von Papain auf Taka-Amylase haben wir zufällig beobachtet, dass sich beim Zusammenbringen der beiden Enzymlösungen ein Niederschlag bildet, der sowohl hohe Amylase wie Papain-Wirkung besitzt. Beim Verdünnen der Mutterlauge des obigen Niederschlags (N_1) mit destilliertem Wasser bildet sich wiederum ein neuer Niederschlag (N_2). N_2 hat stets höhere Aktivität als N_1. Dieselben Erscheinungen findet man sowohl bei der Aussen- wie Innenflüssigkeit der Dialyse von Taka-Amylase-Lösung mittels Kollodiumhülse. Man könnte wohl glauben, dass die Niederschlagsbildung darauf beruht, dass sich die beiden leicht in Wasser löslichen Stoffe, Taka-Amylase und Papain zu einem in Wasser schwer löslichen „Papain-Amylase-Symplex" verbinden. Der Symplex ist in destilliertem Wasser schwer, in Salzlösungen aber leicht löslich. Beim Verdünnen der Lösung mit Wasser wird der „Papain-Amylase-Symplex" wieder niedergeschlagen.

Behandelt man den in N-Acetatpuffer (pH = 5) gelösten „Papain-Amylase-Symplex" mit einem mit gleichem Puffer gewaschenen Aluminiumoxydpräparat (nach Brockmann), so wird die Amylase völlig absorbiert und das Papain bleibt in der Restlösung. Aus dieser Lösung, durch Aussalzen mit Ammoniumsulfat, Dialysieren mittels Kollodiumhülse und Fällen mit Aceton, gewinnt man auf zehn- bis zwanzigfach gereinigtes Papain als das Ausgangspapainpräparat. Aus dem Adsorbat lässt sich Amylase mit N/3 Phosphatpuffer (pH = 8) eluieren. Dieses Trennungsverfahren ist geeignet für die Reinigung von Papain, aber nicht für die Reinigung von Amylase, weil das so gewonnenes Amylasepräparat vom Phosphat schwer zu befreien ist.

Wir konnten nun Papain folgenderweise von Papain-Amylase befreien. Setzt man eine wässerige Lösung von hefe-nukleinsaurem Natrium zur Lösung der „Papain-Amylase" (N_2) in N-Acetatpuffer hinzu, so scheidet sich ein weisser Niederschlag aus, der aus nukleinsaurem Papain besteht. In der Mutterlösung bleibt die gesamte Amylase und überschüssige Nukleinsäure zurück. Diese lässt sich durch Zusatz einer wässerigen

(1) II. Mitteil. Ababori und Kasimoto, dies Bulletin, **13** (1938), 291.

Lösung von Benzidinchlorhydrat fällen. Aus der nach oben gewonnenen Amylase-Lösung erhält man durch Fällung mit Aceton ein hochaktives Amylasepräparat. Manchmal beobachtet man, dass die Amylasewirkung durch Benzidin stark gehemmt wird; z.B. verliert die Innenflüssigkeit der Dialyse und die daraus gewonnene „Papain-Amylase" (N_1) den grösseren Teil ihrer Wirkung durch Benzidin. Dagegen bleibt die Wirkung der Aussenflüssigkeit der Dialyse, der daraus gewonnenen „Papain-Amylase" (N_1 und N_2) und des N_2 aus der Innenflüssigkeit völlig unbeeinflusst vom Benzidin. Daraus darf man wohl den Schluss ziehen, dass im Taka-Amylase-Präparat eine Substanz vorkommt, welche unter Mitwirkung von Benzidin die Amylasewirkung hemmt, nicht durch Kollodiummembran diffundiert und leichter durch Papain als durch Amylase fällbar ist. Daher muss man zum Zweck der Reinigung der Amylase „Papain-Amylase" aus der Aussenflüssigkeit der Dialyse, oder „Papain-Amylase" N_2 aus der Innenflüssigkeit der Dialyse benutzen.

Die experimentellen Wege zur Reinigung der Taka-Amylase werden in der folgenden Tabelle schematisch angegeben.

Bei den nach oben über den „Papain-Amylase-Symplex" gereinigten Amylasen haben wir die Diffusionsgeschwindigkeiten nach der Northrop-Ansonschen Methode[2] gemessen und folgende Resultate gewonnen.

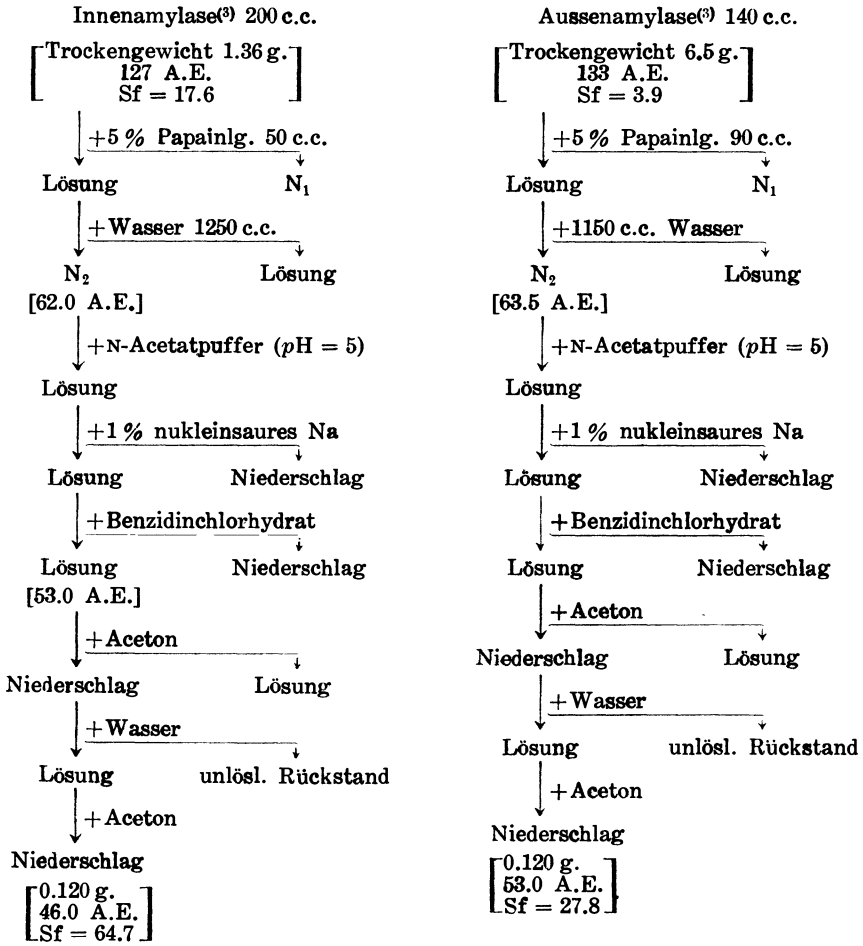
Gereinigte Amylase aus	D_G/D
1. Aussenamylase	2.76
2. Innenamylase	2.62

D_G bzw. D bedeuten die Diffusionskoeffizienten der Glucose bzw. des Enzyms.

Wenn man aus den obigen Resultaten das scheinbare Molekulargewicht des Enzyms berechnet unter der Annahme, dass der Diffusionskoeffizient der Quadratwurzel des Molekulargewichts umgekehrt proportional sei, so gewinnt man für die Aussenamylase das Mol. Gew. = 1370 und für die Innenamylase das Mol. Gew. = 1240.

In unserer früheren Publikation[1] über die chemische Natur der Taka-Amylase haben wir Ergebnisse bei der Molekulargewichtsbestimmung nach der Diffusionsmethode mitgeteilt. Seinerzeit hatten wir für das Molekulargewicht der Aussenamylase ca. 500 und für Innenamylase 1500–2000 gewonnen. Die über den „Papain-Amylase-Symplex" gereinigte Amylase hat also ein grösseres Molekulargewicht als die ursprüngliche Aussenamylase und ein kleineres als die ursprüngliche Innenamylase, und zwar scheint es fast gleich, ob man von Innen- oder auch von Aussen-Amylase ausgegangen ist.

(2) Northrop und Anson, *J. Gen. Physiol.*, **12** (1926), 543.



Mit Rücksicht auf die obigen experimentellen Resultate kann man wohl glauben, dass das eigentliche Taka-Amylase-Molekül verhältnismässig klein ist, sodass es durch Kollodiummembranen durchgehen kann, das Innenamylasepräparat jedoch irgendeine eiweissartige, hochmolekulare Substanz enthält, an die das Amylasemolekül locker gebunden ist, wodurch seine Diffusion verhindert worden ist. Die über den „Papain-Amylase-Symplex" gereinigte Amylase ist von ihrem natürlichen Begleiter befreit worden und zeigt daher dieselbe Diffusionsgeschwindigkeit. Was die Frage anbelangt, warum die gereinigte Amylase langsamer diffundiert

(3) Innen- bzw. Aussen-Amylase bedeutet die bei der Dialyse von Taka-Amylase-Lösung mittels Kollodiumhülse in der Innen- bzw. Aussenflüssigkeit befindliche Amylase.

als die nicht gereinigte Aussenamylase, so kann man noch nichts mit Sicherheit sagen, dürfte aber wohl folgendes vermuten: die Amylase-Moleküle werden sich wohl bei Nichtanwesenheit von Salzen zu grösseren Teilchen assozieren, bei Anwesenheit von Salzen dagegen einzeln peptisiert vorliegen.

Zum Schluss möchten wir der Taniguchi Kogyo-Shoreikai (der Taniguchi-Gesellschaft zur Förderung der technischen Industrie) für ihre finanzielle Unterstützung bei der Durchführung dieser Arbeit unseren besten Dank aussprechen.

Chemisches Institut der Kaiserlichen Universität zu Osaka.

Sedimentation Volume and Thixotropy.

By Hideo AKAMATU.

(Received June 2, 1938.)

The present paper describes on the apparent volume of the powder precipitated in the liquid medium, i.e. sedimentation volume.

In the case of a colloidal solution, the sedimentation volume of the particles depends upon the concentration of the electrolyte which is used to coagulate the sol. The sedimentation volume of the organosol varies by the dispersion medium, which has been studied by Wo. Ostwald,[1] A. v. Buzágh,[2] and W. D. Harkins.[3]

The present author has carried out some experiments on the sedimentation volume of powders in organic liquids, and found the parallelism between the sedimentation volume and the thixotropic nature of the system, some new examples of thixotropic systems being found.

Measurement of Sedimentation Volume. The powders which had been washed with water, and then with alcohol vapour and benzene vapour

(1) Wo. Ostwald and W. Haller, *Kolloidchem. Beihefte*, **29** (1929), 354.

(2) A. v. Buzágh, *Kolloidchem. Beihefte*, **32** (1931), 114.

(3) W. D. Harkins and D. M. Gans, *J. Phys. Chem.*, **36** (1932), 86; L. W. Ryan, W. D. Harkins, and D. M. Gans, *Ind. Eng. Chem.*, **24** (1932), 1288.

respectively, were dried in a high vacuum at 200–300°C., for four to five hours. The organic liquids were purified by the ordinary methods, the care being taken for drying.

In a graduated glass-stoppered test tube of 30 c.c. capacity, 15 c.c. of the liquid was taken, and the powder, after dried, was poured quickly into the test tube. The weight of the powder was known by the difference in weights of the test tube before and after the introduction of the powder. The tightly stoppered test tube was then shaken and allowed to stand in a large desiccator. The powders fell down to the bottom of the test tube in a few hours, however, it took usually about two or three weeks to attain the definite sedimentation volume. The reading of the sedimentation volume was taken when such an equilibrium had been attained.

Some examples are shown in Table 1 to illustrate the reproducibility of the experimental results. Table 2 shows the values obtained for various powders and liquids.

Table 1.

System	Sedimentation volume in c.c. per 1 g. of powder
Glass powder in Toluene	0.84 0.81 0.84 0.80
Zinc oxide in Ethyl alcohol	1.48 1.29
Graphite in Ethyl alcohol	1.70 1.78

Table 2. The sedimentation volume of powders settled in pure liquids.

Liquid \ Powder	Glass	ZnO	Talcum	$CaCO_3$	Graphite	Charcoal	Carbon black
Water	0.71		1.3	0.9	1.6	4.4	3.9
Ethylene glycol		1.3			1.9		3.8
Methyl alcohol		1.3			1.7		
Ethyl alcohol	0.69	1.4	1.4	0.8	1.7		
Acetone				1.1			
Toluene	0.82	2.5	1.9		1.8	4.1	3.8
Benzene				1.7			
Dioxane		1.9	1.7		1.7		3.6
Carbon tetrachloride	0.90	2.1		1.9			
Hexane				2.0			

The results show that if the powder is a polar substance, such as glass, zinc oxide, talcum and calcium carbonate, the sedimentation volume in nonpolar liquid is always larger than that in polar liquid, however, in the case of the nonpolar powder such as graphite, charcoal and carbon black, there are no disparity in the sedimentation volume according to the nature of the liquid.

W. D. Harkins and his coworkers[3] describes the fact that the monomolecular film of the fatty substance adsorbed on the pigment has a marked influence on the sedimentation volume of the pigment.

Experiments were, then, carried out for the solution instead of the pure liquid. The sedimentation volume of the glass powder in toluene containing a small quantity of oleic acid is much smaller than that in pure toluene. For example, the sedimentation volume of glass powder in toluene containing 1% oleic acid was 0.65 c.c. per 1 g. of powder. This volume corresponds to 79 percent of the volume settled in pure toluene. So small as 0.1% of oleic acid is sufficient to decrease in remarkable degree of the sedimentation volume of glass powder in toluene. The results are shown in Fig. 1 and Table 3.

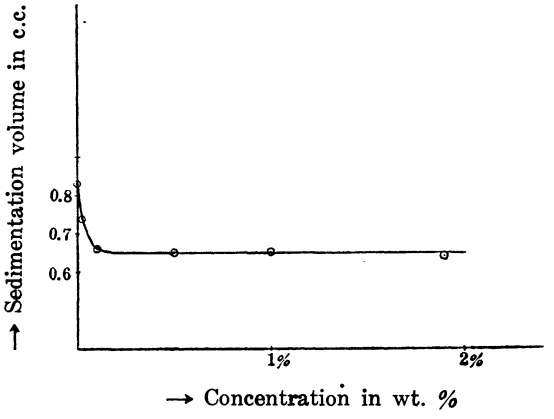


Fig. 1. Sedimentation volume of glass powder settled in Oleic acid/Toluene Solution.

Table 3.

Powder	Solvent	Solute	Sedimentation volume in c.c. per 1 g. of powder	Ratio
Glass	Toluene	—	0.82	1.00
,,	,,	Oleic acid 1%	0.65	0.79
,,	,,	Palmitic acid 2%	0.67	0.82
,,	,,	Tripalmitin 1%	0.68	0.82
,,	,,	Benzoic acid 1%	0.72	0.88
,,	,,	Acetic acid 5%	0.77	0.94
,,	Carbon tetrachloride	—	0.90	1.00
,,	,,	Palmitic acid 0.5%	0.64	0.71

Table 3.—(*Concluded*)

Powder	Solvent	Solute	Sedimentation volume in c.c. per 1 g. of powder	Ratio
Zinc oxide	Toluene	—	2.5	1.00
,,	,,	Hexyl alcohol 1%	1.5	0.60
,,	,,	Lecithin 1%	0.90	0.36
Talcum	Toluene	—	1.9	1.00
,,	,,	Palmitic acid 1%	1.6	0.84
Glass	Ethyl alcohol	—	0.69	
,,	,,	Palmitic acid 2%	0.68	
Zinc oxide	Ethyl alcohol	—	1.5	
,,	,,	Lecithin 1%	1.5	
Charcoal	Toluene	—	4.1	
,,	,,	Palmitic acid 1%	4.1	
,,	,,	,, 4%	4.2	
Graphite	Water	—	1.6	
,,	,,	Hexyl alcohol 0.3%	1.6	
,,	,,	Benzoic acid 0.2%	1.7	
,,	Ethyl alcohol	—	1.7	
,,	,,	Palmitic acid 2%	1.7	

In the fifth column of Table 3, the ratio of the sedimentation volume of a powder settled in the solution to that in the pure liquid is shown.

These results are classified in two groups, the one is the case in which the small quantity of the polar substance has marked influence to decrease the sedimentation volume, and the other is the case in which the addition of the polar substance shows no effect on the sedimentation volume. The first case has been observed when the system are made from the powder of polar substance and the solvent of nonpolar one. In those examples, it must be noticed, that the fatty substance, so-called, are especially effective to decrease the sedimentation volume, for example, oleic acid, palmitic acid or lecithin is more effective than acetic acid, benzoic acid or hexyl alcohol. The second case has been observed when the system consists of both the powder and the solvent of polar substances, or the powder of nonpolar one.

All of these results suggest that the selective adsorption and the molecular orientation take place on the surface of the powder. When

the powder is polar, the polar molecules of solute are strongly adsorbed from the nonpolar solvent taking good orientation. On the other hand, when the powder is nonpolar, the molecular orientation on the solid surface will not establish.

According to Ehrenberg's[4] theory, which seems most plausible to explain the large sedimentation volume, the particles must be loosely packed when they adhere each other by their contact point (the shape of the particles are not generally sphere), and they do not slip each other. On the other hand, if the adhesion force between the particles is weak, they will slip each other and finally they will take the close packing, so the sedimentation volume will become small.

When the suspension medium is water, the chief factor for weakening the adhesion force between the particles is the electrical charge presenting on the particles by adsorbing ions. So the sedimentation volume of aqueous suspension depends upon the concentration of the electrolyte in the solution. When the suspension medium is organic liquid, we

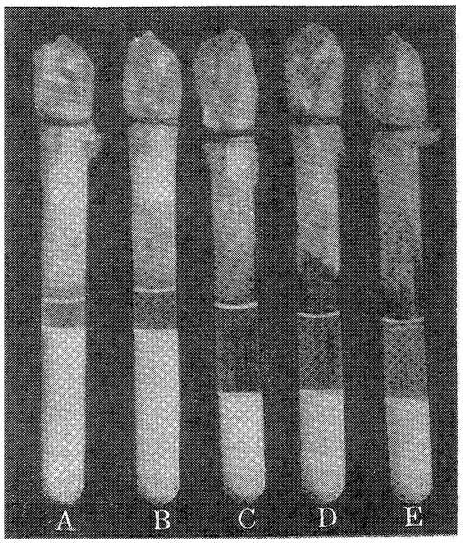


Fig. 2. Zinc oxide powder (about 7 g.) settled in

(A) Carbon tetrachloride
(B) Dioxane
(C) Ethylene glycol
(D) Ethyl alcohol
(E) *Methyl alcohol*

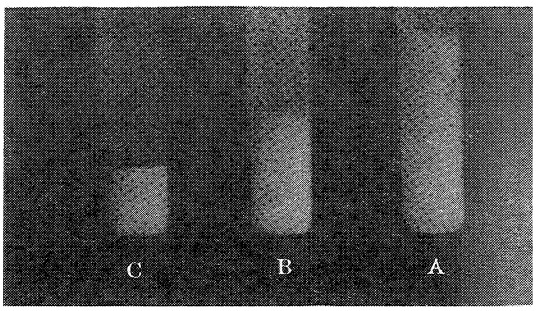


Fig. 3. Zinc oxide powder (about 4.5 g.) settled in

(A) Toluene
(B) Toluene containing 1% Hexyl alcohol
(C) Toluene containing 1% Lecithin

(4) A. v. Buzágh, "Kolloidik," 172, Dresden (1936).

may assume the dipole adsorption instead of the ion-adsorption. Present experimental results appear to suggest the close relationship to this assumption. We can not discuss, however, further since there are little data about the electro-kinetic potential of such a system consisting in solid-organic liquid interfaces.

Thixotropy. It can generally be said that there is the parallelism between the large sedimentation volume and thixotropic nature, for both of these phenomena occur by the loose packing of a system. The author has tested the thixotropic nature of the system consisting of powder and organic liquid, and found that a system which has large sedimentation volume shows always marked thixotropic nature.

For example, a thixotropic system was made by shaking in a test tube about 5 c.c. of toluene with 3.7 g. of calcium carbonate powder. This system is liquefied by shaking which is perceived by a fluid sound, while set to solid paste when shaking has stopped. However, syneresis occurred when this system left to itself for a few minutes, probably because of large particles.

Thixotropies have been tested on the combination of powders and liquids shown in Table 4.

Table 4.

Liquid \ Powder	Glass	ZnO	Talcum	$CaCO_3$	Al_2O_3	Graphite
Carbon tetrachloride	++	++	++	++	++	
Toluene	++	++	++	++	?	++
Benzene	++	+	++	·++	+	
Dioxane	++	+	+	+	—	
Hexane	+	+	+	++	?	+
Ethyl alcohol	—	?	—	—	—	—

++ distinctly thixotropic, + thixotropic, — no thixotropic

We come to conclusion from these results, that almost every kinds of powder can make a thixotropic system in the nonpolar liquid.

These are the macroscopic system, the particles being comparatively large, so it may not be called "the sol-gel transformation" in its proper meaning. It may be more natural to say that there occurs the phase inversion, viz., the powders are suspended in the liquid phase by shaking, while "the liquid sets in the powder" when stopped the shaking.

We saw, from the experiments described above, that the small quantity of the polar substance (surface active substance) decreases the

sedimentation volume in the nonpolar solvent. So the small quantity of the surface active substance destroy the thixotropic nature of the system. For example, a thixotropic system is obtainable from 5 c.c. of carbon tetrachloride and 6.4 g. of glass powder. If, however, the solution contained 1.6% palmitic acid beforehand, the system consisting in the same ratio as above is completely fluid on shaking and it does not set to solid paste when shaking has stopped. Furthermore, even after adding 14 g. of glass powder, the system shows no thixotropic nature. Some examples are shown in Table 5.

Table 5.

Powder	Liquid phase	Nature of the system
Glass 6.4 g.	CCl_4 5 c.c.	thixotropic
,,	CCl_4 solution 5 c.c. containing 1% Oleic acid	no thixotropic
,,	CCl_4 solution 5 c.c. containing 1.6% Palmitic acid	no thixotropic
Al_2O_3 9.5 g.	CCl_4 5 c.c.	thixotropic
,,	CCl_4 solution 5 c.c. containing 1% Oleic acid	no thixotropic
ZnO 1.6 g.	Toluene 5 c.c.	thixotropic
,,	Toluene solution 5 c.c. containing 1% Hexyl alcohol	thixotropic ?
,,	Toluene solution 5 c.c. containing 1% Lecithin	no thixotropic
$CaCO_3$ 3.7 g.	Toluene 5 c.c.	thixotropic
,,	Toluene solution 5 c.c. containing 1% Hexyl alcohol	no thixotropic

In conclusion, the author wishes to express his thanks to Professor J. Sameshima for his kind advices and encouragement.

Summary.

(1) Measurements were carried out on the sedimentation volume when a powder settled in an organic liquid or solution.

(2) A parallelism was found between the large sedimentation volume of the powder and thixotropic nature of the system.

Chemical Institute, Faculty of Science,
Imperial University of Tokyo.

Austauschreaktion der Sauerstoffatome zwischen Wasser und einigen organischen Verbindungen. (Vorläufige Mitteilung.)

Von Masao KOIZUMI und Toshizo TITANI.

(Eingegangen am 6. Juni 1938.)

Die Austauschreaktion der Sauerstoffatome zwischen Wasser und einigen organischen Verbindungen wurde unter Benutzung des an schweren Sauerstoffisotope angereicherten Wassers untersucht. Die dabei erhaltenen Hauptversuchsergebnisse sind in der folgenden Tabelle kurz zusammengefasst.

Substanz	Versuchs-temperatur °C.	Versuchsdauer in Stdn.	Anzahl der austausch-baren O-Atome in einem Molekül
Glucose	100°	0[1]–3	1
Benzaldehyd	110°	1–2	1
Benzoesäure	130°	1–5	1
Phenol	100°	24–48	<1
Bernsteinsäure	130°	1	2
,,	,,	2–5	4
Maleinsäure	100°	20–45	4
Fumarsäure	100°	3–45	2
Phthalsäure	100°	20	<1
Terephthalsäure	100°	20	<1

Das im Glucosemolekül leicht austauschbare eine O-Atom ist höchstwahrscheinlich das Carbonylsauerstoffatom. Dasselbe kann man auch von Benzoesäure und Fumarsäure sagen, wo nur die Hälfte ihrer O-Atome leicht austauschbar ist, besonders aus dem Grunde, da das Sauerstoffatom des Phenols sehr schwer austauschbar ist. Dieser Schluss erscheint weiter dadurch eine Stütze zu erfahren, dass Bernsteinsäure und Maleinsäure, deren letztere bekanntlich der Cisformstereoisomer der Fumarsäure ist, alle ihre O-Atome ziemlich leicht gegen die des Wassers austauschten. Dieses Resultat legte uns die Vermutung nahe, dass bei den zwei benachbarten Carbonylgruppen alle ihre O-Atome, vielleicht durch

(1) Glucose und Wasser wurden unmittelbar nach ihrer Vermischung abgetrennt.

die Zwischenbildung eines Anhydridmoleküls, durch die des Wassers ersetzt werden können. Dieser Vermutung zufolge untersuchten wir zunächst zwei ortisomerische aromatische Dicarbonsäuren, nämlich Phthal- und Terephthalsäure. Aber leider zeigten in diesem Fall die beiden Säuren, dass die Austauschreaktion äusserst schwer ausführbar ist. Die ausführliche Beschreibung der Arbeitsmethode der vorliegenden Arbeit soll später in diesem Bulletin folgen.

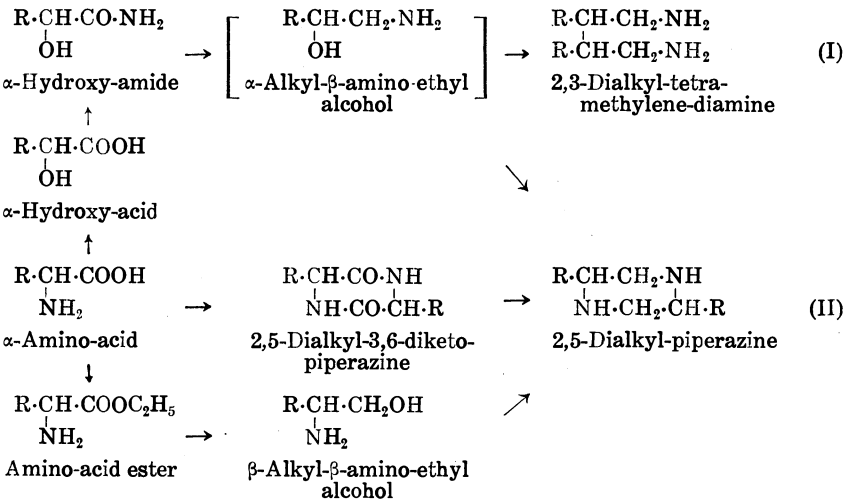
Siomi-Institut für
physikalische und chemische Forschung
und
Physikalisch-chemisches Laboratorium
der Kaiserlichen Universität zu Osaka.

On Some 2,5-Dialkyl-piperazines.[1]

By Haruomi ÔEDA.

(Received June 3, 1938.)

In the previous papers it was described that solid bases were obtained by catalytic hydrogenation of some α-hydroxy-amides and the author concluded that the bases correspond to 2,3-dialkyl-tetramethylene-diamines (I) which would result from further reduction of supposed primary products, α-alkyl-β-amino-ethyl alcohols.



Formula I was given from the facts that the observed molecular weights of the bases were double those of desoxy-amines and that such a condensation of two molecules of amino-alcohols with elimination of two hydroxyls by reduction might probably occur, when deduced in comparison with the work of Rupe and Ackermann.[2] Three kinds of "dialkyl-tetramethylene-diamine" (dimethyl, di-isobutyl and dibenzyl compounds) were mentioned in the previous papers.

After the publication of these papers, the author noticed another possible formula for these bases: i.e. piperazine formula (II). The pipera-

(1) Studies on Hydroxy-acids and Their Derivatives. VII. Correction to V and VI, this Bulletin, **12** (1937), 121, 377.

(2) *Helv. Chim. Acta*, **2** (1919), 221.

zines may be assumed to be formed from two molecules of β-amino-alcohols by dehydration. Similar reactions of alcohols with amines have been observed by many investigators, though a ring formation from β-amino-alcohol leading to piperazine nucleus could not be found as yet described.[3]

The compounds I and II can hardly be distinguished from each other by their analytical results[4] when the radical R is large or the base is analysed in the form of its derivatives. As already described in the previous paper, the author's base is found to behave as a secondary amine in sulphamide reaction. This fact favours formula II for these bases.

Among the three dialkyl-piperazines, the dimethyl and di-isobutyl compounds are known. Dimethyl-piperazine,[5] and its various derivatives are fully described in the literature, while the author's base is isolated in pure state only in the form of its benzoyl compound. Melting points of the benzoyl derivatives of the two bases coincide with each other showing 227–228°. On the other hand, no sufficient data for di-isobutyl-piperazine[6] are given in the literature to discuss its identity with the author's base.

For direct comparison of the two bases in question, the author tried to prepare di-isobutyl-piperazine by reducing the corresponding diketo-piperazine according to the description of Cohn.

Di-isobutyl-piperazine prepared from leucine anhydride was isolated as its hydrochloride (decomp. p. over 330°), though its yield was very poor. Free base (m.p. 80–83°), benzoyl compound (m.p. 222–223°) and benzene-sulphonyl compound (m.p. 211–213°) were prepared. The melting points given above coincide with those of the base and its derivatives isolated from leucic acid amide described in the previous paper. Mixed melting points also prove their identity.

---

(3) In some α-amino-aldehydes or α-amino-ketones, similar condensations which result in the formation of dihydro-pyrazine or pyrazine itself, in the presence of some oxidant, are described.

(4) In the previous papers, analytical results of the free bases, hydrochlorides, benzoyl derivatives, etc. are given. Difference of calculated values for the two formulæ in question becomes most notable in case of free bases. Calculated values for the two bases together with observed values are quoted from the previous paper as follows: Di-isobutyl base. Found: C, 72.24; H, 13.66; N, 14.22. Calculated for the piperazine, $C_{12}H_{26}N_2$: C, 72.73; H, 13.25; N, 14.15. Calculated for the tetramethylene-diamine, $C_{12}H_{28}N_2$: C, 71.94; H, 14.09; N, 14.00. Di-benzyl base. Found: C, 80.76; H, 8.54; N, 10.58. Calculated for the piperazine, $C_{18}H_{22}N_2$: C, 81.19; H, 8.35; N, 10.52. Calculated for the tetramethylene-diamine, $C_{18}H_{24}N_2$: C, 80.72; H, 9.02; N, 10.44.

(5) Hoyer, *Z. physiol. Chem.*, **34** (1901), 347.

(6) Cohn, *ibid.*, **29** (1900), 297. The base is isolated and analysed in the forms of its hydrochloride and platinum double chloride. No definite description is found of the free base and other derivatives.

Dibenzyl-piperazine is not found in the literature. Preparation of this base by reducing its diketo compound was unsuccessful, no trace of the piperazine being isolated when phenylalanine anhydride was reduced with sodium in ethyl or amyl alcoholic solution.

By reducing phenylalanine ester with sodium at 160°, Karrer[7] obtained β-benzyl-β-amino-ethyl alcohol, $C_6H_5 \cdot CH_2 \cdot CHNH_2 \cdot CH_2OH$. The preparation[8] was repeated by the present author and the expected amino-alcohol[9] was isolated in two different forms: the one melted at 71–73° and was optically inactive (its monobenzoyl compound, m.p. 148–149°), while the other melted at 92–94° and was optically active, $[\alpha]_D^{23} = -24.4°$ (its monobenzoyl compound, m.p. 169–171°). Besides the amino-alcohol, another solid base which was not described by Karrer, was isolated in a small quantity from the reaction mixture. It showed the same melting point (166–167°) as one of the solid bases[10] resulting from phenyl lactamide as described in the previous paper. Their identity was proved by the mixed melting point tests of the free bases as well as of their benzoyl compounds (m.p. 281–283°).

The amino-alcohol derived from phenylalanine is isomeric with the one which was assumed as an intermediate product in the previous paper, viz., α-benzyl-β-amino-ethyl alcohol, $C_6H_5 \cdot CH_2 \cdot CHOH \cdot CH_2NH_2$. If ring formation by dehydration occurs in these amino-alcohols, they give the same product, 2,5-dibenzyl-piperazine, and in fact, as shown above, the identical solid base was obtained by the reduction of either the hydroxy-amide or the amino-acid ester. This fact indicates that the compound is no doubt dibenzyl-piperazine.[11] The transformation of the amino-alcohols into the piperazine compound by dehydration might be favoured by the reaction temperature as high as 250° in the previous and 160° in the present experiments.

---

(7) *Helv. Chim. Acta*, **4** (1920), 97.

(8) Samples of natural leucine and phenylalanine which were the starting materials in the present preparations were the same as used in the preparation of amides of leucic acid and phenyl lactic acid in the previous work.

(9) Karrer isolated this amino-alcohol only in one form of its hydrochloride and no mention was given whether the starting material was active or racemic.

(10) In the previous paper another form of this base (m.p. 150–152°; its benzoyl compound, m.p. 198–200°) was isolated, but in the present experiment it could not be identified.

(11) If the bases resulting from the hydroxy-amide and the amino acid ester were products of further hydrogenation of the amino-alcohols (as considered in the previous paper), their formulæ would be $C_6H_5 \cdot CH_2 \cdot CH \cdot CH_2NH_2$ and $C_6H_5 \cdot CH_2 \cdot CH(NH_2) \cdot CH_2$
$C_6H_5 \cdot CH_2 \cdot CH \cdot CH_2NH_2$ $C_6H_5 \cdot CH_2 \cdot CH(NH_2) \cdot CH_2$.
They are isomeric with each other but never identical.

These considerations lead the author to conclude that 2,5-dialkyl-piperazine formulæ, instead of dialkyl-tetramethylene-diamine formulæ, are to be given to the solid bases described in the previous papers.

Experimental.

2,5-Di-isobutyl-3,6-diketo-piperazine (Leucine Anhydride.) Prepared from natural leucine by heating at 170° in the presence of glycerine.[12] M.p. 263° (uncorr.) or 270° (corr.) after recrystallisation from alcohol.

Reduction of Leucine Anhydride. The anhydride (10 g.) was added to absolute alcohol (dehydrated with metallic sodium, 500 c.c.). It dissolved completely when the mixture was kept boiling. Large excess of sodium (30 g.) was added to the boiling solution in small pieces through reflux condenser in the course of half an hour. After cooling, an equal volume of water was added and the alcohol was removed in vacuum. When the volume of the residue diminished to nearly half of the initial, the distillation was stopped. After removing precipitated unreacted anhydride, the filtrate was extracted with a large bulk of ether. After drying over caustic soda, ether was expelled from the extract and a little anhydride again crystallised out. Total yield of recovered anhydride corresponded to more than 10%, even when large excess of sodium was used. The residue (2.5 g.), after separation of the crystals, was distilled under reduced pressure through Widmer column and was separated into two fractions:

(I)	up to 100°	under 6 mm.	0.5 g.
(II)	over 100°	,,	1.2 g.

Fraction II tended to solidify in the receiver, while fraction I remained as viscous fluid. Both of the fractions were dissolved in ether separately and were extracted with dilute hydrochloric acid. From fraction I a hydrochloride very soluble in water was isolated, while from fraction II another hydrochloride insoluble in water was obtained together with the above soluble one.

Hydrochloride, Soluble in Water (a Base Left Undetermined). Crude sample from fraction I weighed 0.25 g. After decolouration with charcoal it crystallised from alcohol in colourless leaflets. The combined yield of pure sample from both fractions was 125 mg. M.p. 160–162° (uncorr.). No study on this hydrochloride was made.

Hydrochloride, Insoluble in Water (2,5-Di-isobutyl-piperazine). Crude sample weighed 0.2 g. After washing with alcohol it was dissolved in a large volume of hydrochloric acid and, after decolouration with charcoal, the solution was evaporated on the water bath. Colourless hydrochloride crystallised out while still hot before the solution completely dried up. It weighed 168 mg. Decomp. p. over 330°.

Free base. When the pure hydrochloride (50 mg.) was warmed with dilute caustic soda, free base separated out as an oil and turned to crystals on cooling. The separated base was dissolved in alcohol and filtered. After evaporation to a small

(12) Maillard, *Ann. chim.*, [9], **3** (1915), 83.

bulk, the free base was crystallised by adding water. M.p. 80–83°[13] after drying over caustic soda.

Benzoyl compound. The pure hydrochloride (33 mg.) was added to dilute caustic soda (2 c.c.) and benzoyl chloride was added drop by drop. Benzoyl compound was formed as sticky mass and turned to crystals on shaking. M.p. 217–218° (uncorr.) or 222–223° (corr.) after one recrystallisation from alcohol. No depression of melting point was observed when mixed with the sample described in the previous paper. (Benzoyl compound of the solid base from leucic acid amide melted at 223–224° (corr.) and its analytical result was given in the previous paper.)

Benzene-sulphamide. To a suspension of the free base in dilute caustic soda (50 mg. of the hydrochloride in 1 c.c.) benzene-sulphonyl chloride (2 drops, nearly equivalent) was added. Crude sulphamide (70 mg.) separated out as crystals. After recrystallisation from alcohol, it (39 mg.) melted at 206–208° (uncorr.) or 211–213° (corr.), alone or mixed with the sample described below. (Found: N, 5.69. Calculated for $C_{12}H_{24}N_2(C_6H_5SO_2)_2$: N, 5.85%.)

Benzene-sulphamide of "solid base from leucic acid amide". From the free base melting at 62–64° (50 mg.) and benzene-sulphonyl chloride (3 drops), crude sulphamide (78 mg.) was obtained just in the same way as above. When recrystallised from alcohol, the purified sample (19 mg.) melted at 205–207° (uncorr.) or 210–212° (corr.) and it was used in the above mixed melting point test.

Ethyl Ester of Phenylalanine. Prepared from natural phenylalanine and alcohol by dehydration with gaseous hydrochloric acid.[14] B.p. 135–136° under 8 mm.

Reduction of Phenylalanine Ester. Metallic sodium (45 g.) cut in small pieces was placed in a litre-flask which was immersed in an oil bath (160°). Mixture of the ethyl ester of phenylalanine (38 g.) and absolute alcohol (120 c.c.) was added drop by drop to the sodium through reflux condenser in the course of one hour. After interval of half an hour, a new bulk of alcohol (150 c.c.) was added and then the oil bath was detached. Alcohol was again poured until the metallic sodium completely disappeared. After cooling, water was added to dissolve separated alcoholate. The alcohol was removed in vacuum at 50–70° and the residue was concentrated also in vacuum until a light coloured oil separated in the flask.

The oil (not miscible with ether) and the water layer were separately extracted with a large bulk of ether. From the combined extract, after dehydration with sodium sulphate, ether was removed and the residue was concentrated to a small bulk on boiling water bath. Small amount of crystals gradually deposited on standing.

Dibenzyl-piperazine. The crystals were separated and washed with a little ether. After recrystallisation from alcohol, it melted at 163–164° (uncorr.) or 166–167° (corr.) and the sample amounted to 0.45 g. No depression of melting point was observed when the base was mixed with the base resulting from phenyl lactamide (m.p., the same; its analytical result was given in the previous paper).

---

(13) Solid base isolated from leucic acid amide, as already mentioned, shows different melting points 62-64° and over 80°). They are identical in analytical result and may be presumed to be mixtures of isomers. But their differentiation in the form of derivatives was unsuccessful.

(14) Fischer and Schöller, *Ann.*, **357** (1907), 1.

Benzoyl compound. Prepared from the above base (50 mg.) and benzoyl chloride (180 mg.) in alkaline medium (1.5 c.c. of 2N caustic soda). Crude benzoyl compound (79 mg.) separated, after washing with hot alcohol, was once recrystallised from glacial acetic acid. M.p. 274–276° (uncorr.) or 281–283° (corr.), alone or mixed with the benzoyl compound of the base resulting from phenyl lactamide (m.p., 280–282°; its analytical result was given in the previous paper).

β-Benzyl-β-amino-ethyl alcohol. After removal of dibenzyl-piperazine, the remaining syrup was subjected to vacuum distillation. The part distilling at 147–151° under 10 mm. was collected. It amounted to 4.4 g. and was colourless viscous fluid tending to crystallise after long standing. The crystals, after washing with a little benzene, on heating, softened at 65–70° and melted below 75°. By fractional recrystallisation from benzene it could be separated into two fractions. The part less soluble in benzene (1.27 g.) melted at 91–93° (uncorr.) or 92–94° (corr.) (Found: C, 71.63; H, 9.31;[15] N, 9.10%), $[\alpha]_D^{23} = -24.4°$ (28.25 mg. in 1.00 c.c. alcoholic solution; $l = 1$ dm.; $\alpha_D^{23} = -0.69°$). The part more soluble in benzene (0.94 g.) melted at 70–72° (uncorr.) or 71–73° (corr.) (Found: C, 71.78; H, 9.04; N, 9.29. Calculated for $C_9H_{13}ON$: C, 71.45; H, 8.67; N, 9.26%), $[\alpha]_D^{23}$ = almost null (−0.35°) (28.55 mg. in 1 c.c. alcoholic solution; $l = 1$ dm.; $\alpha_D^{23} = -0.01°$).

Benzoyl compound. The unfractionated mixture of the base (200 mg.) was dissolved in 2N caustic soda (6 c.c.) and benzoyl chloride (500 mg.) was added drop by drop with constant shaking. Crude benzoyl compound (250 mg.) separated could be differentiated into two fractions by fractional recrystallisation from benzene-alcohol (1:1). They were found, on analysis, to be mono-benzoyl derivatives. The part less soluble in the solvent (40 mg.) melted at 166–168° (uncorr.) or 169–171° (corr.) (Found: C, 75.34; H, 7.29; N, 5.45%). The more soluble part (51 mg.) melted at 146–147° (uncorr.) or 148–149° (corr.) (Found: C, 75.25; H, 7.14; N, 5.42. Calculated for $C_9H_{12}ON(C_6H_5CO)$: C, 75.25; H, 6.72; N, 5.49%).

The two forms of the benzoyl compound could be prepared from the fractionated free bases; the base with higher melting point giving the derivative with higher melting point and the lower one giving that with lower melting point.

In conclusion, the author expresses his sincere thanks to Mr. R. Suzuki, Director of the factory, for every facility given to the author and also to Dr. Y. Takayama for constant encouragements.

Chemical Laboratory, S. Suzuki (Ajinomoto) & Co., Ltd.
Kawasaki, near Tokyo.

---

(15) Determinations of carbon and hydrogen and measurements of optical rotation in this paper were done by Mr. Toshio Ando, to whom the author is very grateful.

Absorption Spectra of Co-ordination Compounds. III. Special Bands of Chromium Complexes.

By Ryutaro TSUCHIDA and Masahisa KOBAYASHI.

(Received June 16, 1938.)

It has been established by extensive studies of Y. Shibata[1] and his co-workers that the metallic complex has generally two absorption bands, of which the first appears usually in the visible region and the second in most cases in the ultra-violet. One of the present authors[2] has recently come to the conclusion that the first band is attributed to electron transitions in unsaturated transition shells of the central ions and the second band may be explained as due to a kind of incomplete dissociation of the complex radical brought about by irradiation, during which the co-ordinate bond is temporarily broken and the ligand is converted into an excited ion or molecule remaining in general in its seat of co-ordination. Moreover, some complexes may have the third bands[3] which are due to negative ligands co-ordinated in trans-positions to each other.[4] It has been postulated by the present author[5] that the third band is originated in a kind of neutralization between the central ion and one of the co-ordinated anions, during which the ligand is converted into an ionogen which recombines in most cases to regenerate the original complex.

According to the trans-anion hypothesis, $[Cr(NH_3)_5NCS](NCS)_2$ could not be expected to have a third band, nevertheless it shows three absorption bands in aqueous solutions[6] as well as in liquid ammonia.[7] Since rhodanate ion has no absorption band in the spectral regions in question when it is not co-ordinated, Y. Shibata[8] has explained the extra band of the rhodanato-complex as due to NCS-radical combined to the central metallic atom. Uzumasa, Okuno and Doi[9] have recently

(1) Y. Shibata, *J. Coll. Sci., Imp. Univ. Tokyo*, 1915 to 1921; *J. Chem. Soc. Japan*, 1915 to 1922.

(2) R. Tsuchida, this Bulletin, **13** (1938), 388.

(3) Y. Shibata, *J. Chem. Soc. Japan*, **36** (1915), 1243.

(4) R. Tsuchida, this Bulletin, **11** (1936), 721.

(5) R. Tsuchida, this Bulletin, **13** (1938), 436.

(6) Y. Shibata and K. Matsuno, *J. Chem. Soc. Japan*, **39** (1918), 661; Y. Shibata, *J. Coll. Sci., Imp. Univ. Tokyo*, **41** (1918), Art. 6.

(7) H. Shiba and T. Inoue, *J. Chem. Soc. Japan*, **56** (1935), 213.

(8) Y. Shibata, *J. Chem. Soc. Japan*, **35** (1914), 807.

(9) Y. Uzumasa, H. Okuno, and K. Doi, *J. Chem. Soc. Japan*, **59** (1938), 655.

illustrated the hypothesis by absorption bands of a number of rhodanates. Such bands are due to ligands themselves and, therefore, could be attributed neither to transition electrons of the central atom nor to co-ordination electrons of the co-ordination center in question. Being thus unable to be classified as any of the numbered bands, they are described here as special bands.

The present paper deals with some of such special bands taking chromium compounds as examples and also refers to the relation between absorption spectra and chemical properties.

Experimental.

The chromium complexes were prepared as described below and their absorption spectra in aqueous solutions were observed. The molar extinction coefficient ε is given by Beer-Lambert's law: $I = I_0 \times 10^{-\varepsilon cd}$, where c is the concentration in gram-ion per liter and d the thickness of the layer in cm. The absorption curves are given in Tables 1, 2 and 3.

$[Cr(H_2O)_6]Cl_3$ was prepared by the method of Bjerrum.[10] Spectrographic measurements: $c = 0.1$ mol/l. and $d = 15.0$ to 0.30 cm. The measurements were carried out at 20°C., as the complex undergoes tautomeric change at higher temperatures.

$[Cr(NH_3)_6]Cl_3$ was prepared by the method of Christensen[11] from anhydrous chromic chloride and liquid ammonia. Freshly prepared chromic chloride gives better yield of the luteo-salt. Spectrographic measurements: $c = 0.01$ mol/l. and $d = 5.00$ to 1.05 cm.

$[Cr(NH_3)_5Cl]Cl_2$ was partly prepared by the method of Christensen[11] and partly by our own. By introducing anhydrous chromic chloride in liquid ammonia the purpureo-salt and the luteo-complex are simultaneously produced, but of freshly prepared chromic chloride most portion is converted into the hexammine complex. The present authors heated hydrated chromic nitrate $Cr(NO_3)_3 \cdot 9H_2O$ with liquid ammonia at about 50°C. for a few hours in an autoclave. Excess of ammonia was evaporated and the residue was then treated with hydrochloric acid. Crude pentammine salt thus obtained was purified as usual. Spectrographic Measurements: $c = 0.005$ mol/l. and $d = 15.0$ to 1.05 cm.

$[Cr(NH_3)_5NCS](NCS)_2$. Werner and Halban[12] reported that they were unable to prepare the rhodanato-complex in crystalline form

(10) N. Bjerrum, *Z. physik. Chem.*, **59** (1907), 340.
(11) O. T. Christensen, *Z. anorg. Chem.*, **4** (1893), 229.
(12) A. Werner and J. v. Halban, *Ber.*, **39** (1906), 2669.

and it was still impure after second recrystallization. The colour according to the same authors is reddish brown to orange and their analysis gave 18.27% Cr for the theoretical value of 16.7% Cr.

The present authors prepared the salt by the same method and obtained it in two different crystalline forms after repeated recrystallization: yellowish pink crystalline powder and brownish red pyramidal crystals of about 1 mm. in length. The two forms are usually obtained as mixtures in various proportions according to conditions in recrystallization, and consequently the colour may be sometimes reddish brown and sometimes orange as has been described by Werner and Halban. Rapid precipitation from hot solutions gives yellowish pink form and slow crystallization from cold solutions the brownish red form. The chromium contents of the two forms were found to be 16.3% and 15.9% respectively, corresponding to theoretical values of 16.7% as $Cr(NCS)_3 \cdot 5NH_3$ and 15.8% as $Cr(NCS)_3 \cdot 5NH_3 \cdot H_2O$. The absorption of both the forms was measured. Spectrographic measurements: $c = 0.002$ mol/l. and $d = 15.0$ to 0.08 cm. The absorption curves thus obtained were identical, showing that the water molecule in the reddish brown form is merely the water of crystallization outside the complex radical.

$[Cr(NH_3)_2(NCS)_4]NH_4 \cdot H_2O$ was prepared by the method of Christensen.[13] Spectrographic measurements: $c = 0.001$ mol/l. and $d = 15.0$ to 0.04 cm.

$[Cr(NCS)_6]K_3 \cdot 4H_2O$ was prepared by the method of Roesler.[14] Spectrographic measurements: $c = 0.001$ mol/l. and $d = 15.0$ to 0.04 cm.

$[Co(NH_3)_5CrO_4]Cl$ was prepared by the method of Briggs.[15] Spectrographic measurements: $c = 0.001$ mol/l. and $d = 5.00$ to 0.02 cm.

K_2CrO_4. Spectrographic conditions: $c = 0.010$ and 0.002 mol/l. and $d = 1.05$ to 0.02 cm.

Discussion of the Results.

(1) Special Bands of Rhodanato-complexes. Whereas $[Cr(H_2O)_6]Cl_3$, $[Cr(NH_3)_6]Cl_3$ and $[Cr(NH_3)_5Cl]Cl_2$ have two bands each, the first and the second, $[Cr(NH_3)_5NCS](NCS)_2$ has three and $[Cr(NH_3)_2(NCS)_4]NH_4$ and $[Cr(NCS)_6]K_3$ have four bands each, just as could be expected from the author's hypotheses.[2][5]

As is clear from Fig. 1 and Table 1, substitution of NCS^- for NH_3 is bathochromic and at the same time hyperchromic for the first and the second band. Then the same substitution must be bathochromic also for

(13) O. T. Christensen, *J. prakt. Chem.*, **45** (1892), 216.
(14) J. Roesler, *Ann.*, **141** (1867), 185.
(15) S. H. C. Briggs, *J. Chem. Soc.*, **115** (1919), 70.

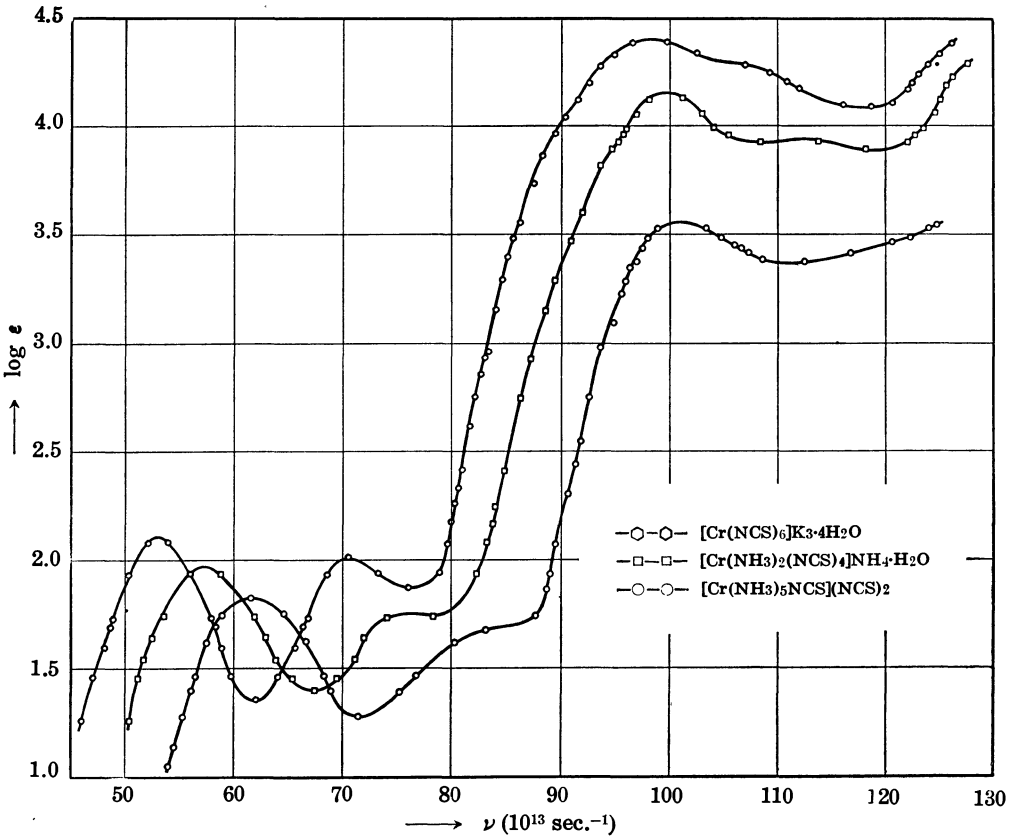


Fig. 1.

Table 1.

Complex compounds	1st bd.		2nd bd.		Special bd.		3rd bd.	
	$\nu_1(10^{13})$	log ε	$\nu_2(10^{13})$	log ε	$\nu_s(10^{13})$	log ε	$\nu_3(10^{13})$	log ε
$[Cr(NH_3)_5NCS](NCS)_2$	61.5	1.82	(83)	1.67	100.4	3.56		
$[Cr(NH_3)_2(NCS)_4]NH_4$	57.5	1.95	(75)	1.75	99.6	4.17	(113)	3.9
$[Cr(NCS)_6]K_3$	53.1	2.08	70.8	2.00	98.6	4.40	(108)	4.3
$[Co(NH_3)_5NCS]Cl_2$ [16]	60.2	2.14	(84)	2.60	98.0	3.20		
[Co dg'_2 NH_3Cl] [17]	63.8	1.75	86.0	3.08	(101)	3.7	121.8	4.50
[Co dg'_2 *py* Cl] [18]	65.5	2.24	89.0	3.39	(102)	3.7	121.5	4.35

(16) R. Tsuchida, *J. Chem. Soc. Japan*, **59** (1938), 592.
(17) R. Tsuchida and M. Kobayashi, this Bulletin, **12** (1937), 83. The symbol *dg'* denotes a dimethylglyoxime residue behaving as a monobasic acid.
(18) S. Kashimoto and M. Kobayashi, this Bulletin, **12** (1937), 350. The symbol *py* denotes a pyridine molecule.

the third band, so long as the following relation[5] should exist between the second and the third band.

$$h\nu_3 - h\nu_2 = P + E - J = \text{constant.}$$

For $[Cr(NH_3)_2(NCS)_4]NH_4$ and $[Cr(NCS)_6]K_3$, therefore, the third bands are those of the shortest wave-lengths. The band at about 100×10^{13} sec.$^{-1}$ which remains almost unaffected by the substitution is the special band due to Cr←N=C.

It is interesting to notice that the ε-value of the special band is approximately proportional to the number of NCS-radicals in the co-ordination. This fact shows that the special band is additive and the

Table 2.

Rhodanato-complexes	$\nu_s(10^{13}\text{sec.}^{-1})$	log ε	ε	Ratio
$[Cr(NH_3)_5NCS](NCS)_2$	100.4	3.56	36×10^2	1
$[Cr(NH_3)_2(NCS)_4]NH_4$	99.6	4.17	15×10^3	4
$[Cr(NCS)_6]K_3$	98.6	4.40	25×10^3	6.6

additivity in turn suggests that the absorption centers of the special band in a complex radical are fairly independent with one another, which could not be the case for the other numbered bands.

Whereas the second band of $[Cr(NCS)_6]K_3$ is isolated from the special band, those of $[Cr(NH_3)_2(NCS)_4]NH_4$ and $[Cr(NH_3)_5NCS](NCS)_2$, however, are partly superposed by their special bands. Further the second band of $[Co(NH_3)_5NCS]Cl_2$[16] is inexplicit, being almost entirely covered by its special band, which is due to the origin similar to that in the cases of rhodanato-chromic complexes. It has been shown by Shibata[19] that $[Co(NCS)_4]K_2$ has also a special band of similar origin. A peculiar group which may be represented by M←N=C is the common feature of all the above-mentioned complexes which have the special bands. Thus the special bands of $[Co\ dg_2'\ NH_3\ Cl]$[17] and $[Co\ dg_2'\ py\ Cl]$[18] might also be explained as due to the same group of M←N=C. In Table 1 are summarized the complexes which have the special bands due to M←N=C, where M is a metallic ion of any valency and of any kind, perhaps including hydrogen ion as in free thiocyanic acid.

(19) Y. Shibata, *J. Chem. Soc. Japan*, **35** (1915), 807; A. Hantzsch and Y. Shibata, *Z. anorg. Chem.*, **73** (1912), 309.

(2) Special Bands of Chromato-pentammine Cobaltic Salt. Being due to the unsaturated transition shell of the central ion, the first band[2] is expected for all the tervalent chromium complexes. For chromate ion, however, the first band could not be expected, as it has an electronic configuration similar to that of sulphate ion. The second and the third band are expected from the consideration given in the preceding paper[5] and are found at 81×10^{13} sec.$^{-1}$ and 110×10^{13} sec.$^{-1}$ respectively. The absorption curve is given in Fig. 2.

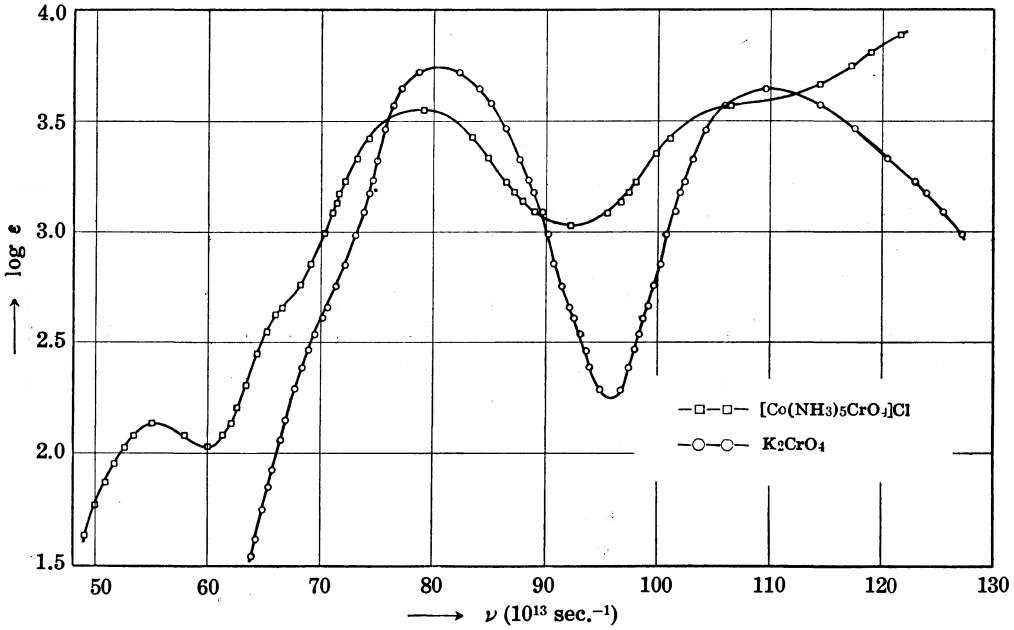


Fig. 2.

The absorption spectrum of $[Co(NH_3)_5CrO_4]Cl$ may be analysed into spectra mainly due to a sexa-coördinate absorption unit whose center is Co and a quadri-coördinate unit whose center is Cr. These absorption units may be denoted as $[(NH_3)_5Co–O–]$ and $[–O–CrO_3]$ for the sake of convenience. These two units are combined with each other having one oxygen atom in common. The former should have two bands, the first and the second, and the latter also two bands, the second and the third. As can be seen from Fig. 2, the absorption bands due to $[–O–CrO_3]$ are slightly shifted towards the longer wave-lengths compared with those of free CrO_4^- alone and the extinction coefficients at the absorption maxima of the former are considerably smaller than those of the latter: in other words, formation of co-ordinate linkage between Co^{+++} and CrO_4^- has a

bathochromic and a hypochromic effect upon the absorption bands of CrO_4^-. The first band of $[(NH_3)_5Co–O–]$ is at 55.6×10^{13} sec.$^{-1}$, but the second band is completely covered by the strongly absorbing second band of $[–O–CrO_3]$.

The bands of $[–O–CrO_3]$ in this case may be regarded as special bands of $[Co(NH_3)_5CrO_4]Cl$, if we take Co as the center of the entire complex. If we take Cr as the center, the bands of $[(NH_3)_5Co–O–]$ may be regarded as special bands as well. The special band, therefore, is relative to the absorption unit in question, and is essentially a numbered band of some other absorption unit.

We may notice that there are two kinds of special bands: viz., the bands which may be observed in the ligands themselves even when they are not combined in co-ordination and those which appear only when the ligands are co-ordinated. The special bands of the first kind may be represented by $[Co(NH_3)_5CrO_4]X$ and those of the second kind may be illustrated by $[Cr(NH_3)_5NCS]X_2$, etc.

(3) Stability and Absorption Spectra of Chromic Complexes. All the co-ordination compounds which contain tervalent chromium ions should

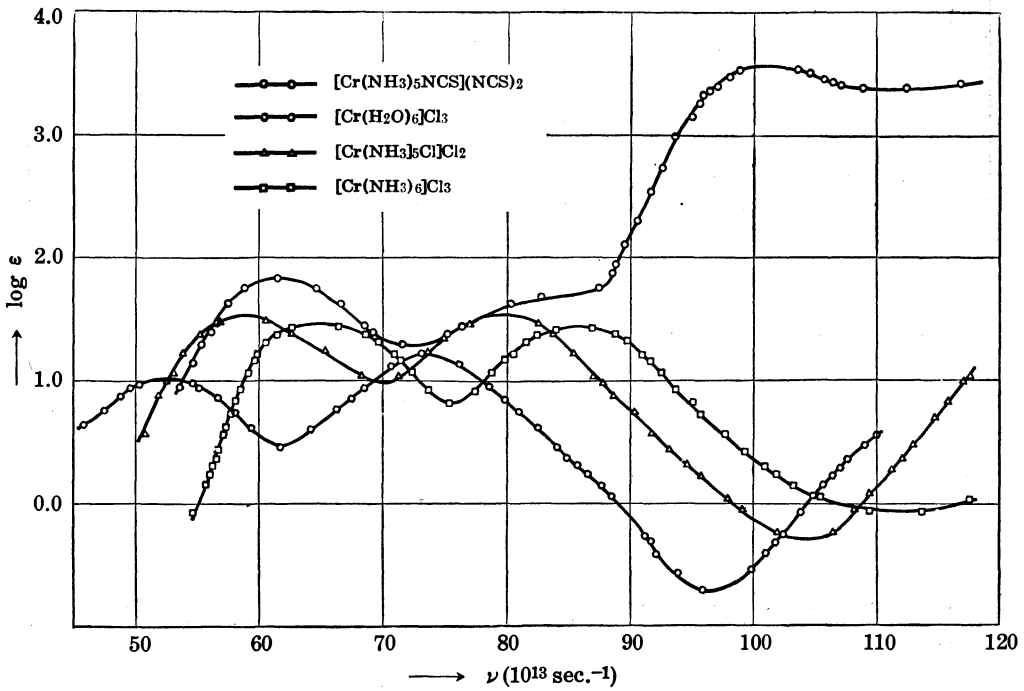


Fig. 3.

have the first and the second bands, the latter giving the measure of stability.[5] From the chromic complexes in Figs. 1 and 3, we may be able to find the spectrochemical series of ligands. Thus the hypsochromic order of ligands for the second bands of chromic complexes is NH_3, NCS^-, Cl^-. (Table 3). The hypsochromic order is from Table 4 NH_3, H_2O, NCS^-. Combining both series, we obtain NH_3, H_2O, NCS^-, Cl^-.

Table 3.

Chromic complexes	1st bd.		2nd bd.		Special bd.	
	$\nu_1(10^{13})$	log ε	$\nu_2(10^{13})$	log ε	$\nu_s(10^{13})$	log ε
$[Cr(NH_3)_5NH_3]Cl_3$	65.0	1.48	86.0	1.44		
$[Cr(NH_3)_5NCS](NCS)_2$	61.6	1.82	(83)	1.67	100.4	3.56
$[Cr(NH_3)_5Cl]Cl_2$	58.7	1.53	80.0	1.54		

Table 4.

Chromic complexes	1st bd.		2nd bd.		Special bd.		3rd bd.	
	$\nu_1(10^{13})$	log ε	$\nu_2(10^{13})$	log ε	$\nu_s(10^{13})$	log ε	$\nu_3(10^{13})$	log ε
$[Cr(NH_3)_6]Cl_3$	65.0	1.48	86.0	1.44				
$[Cr(H_2O)_6]Cl_3$	52.5	1.02	73.6	1.20				
$[Cr(NCS)_6]K_3$	53.1	2.08	70.8	2.00	98.6	4.40	(108)	4.3

As was discussed in the previous paper,[5] the spectrochemical series shows the order of the stability of the co-ordinate link between the central ion and the ligand. The above series indicates that chloro-pentammine and rhodanato-pentammine chromic salts are rather unstable in aqueous solutions. The absorption measurements of these complexes, therefore, were carried out with great precaution against the photo-chemical aquotization, using the solutions as fresh as possible by frequent preparations during the measurements.

It is interesting to notice that the above series for chromic complexes is coincident with the spectrochemical series for cobaltic complexes,[5] i.e., NH_3, NO_2^-, ONO^-, H_2O, NCS^-, OH^-, NO_3^-, Cl^-, $CO_3^=$, Br^-. We may, therefore, be able to discuss chemical properties of chromic complexes by dint of the spectrochemical series of cobaltic complexes, which have been far more thoroughly investigated than the former.

(4) **Applications of the Spectrochemical Series in Preparation.** Some of the chemical reactions used in preparing chromic complexes may be easily explained by the spectrochemical series. For example, Christensen's method[11] of preparing $[Cr(NH_3)_6]Cl_3$ and $[Cr(NH_3)_5Cl]Cl_2$ may be mentioned, in which anhydrous chromic chloride is simply kept in contact with liquid ammonia. Anhydrous chromic chloride may be regarded as a polynuclear complex compound, in which chromium atoms are surrounded by six chlorine atoms octahedrally just as in other chromic complexes. Then the rule[5] for substitutions in complex radicals may be applied to this compound: viz., the chlorine ions in complexes can be easily displaced by ammonia molecules, as Cl^- is far behind NH_3 in the spectrochemical series. The substitution takes place so readily that it proceeds rapidly even at the temperatures of liquid ammonia. Anhydrous chromic chloride when it is freshly prepared is almost entirely converted into the luteo-salt. The method of Christensen is, therefore. highly recommended for preparation of the luteo-salt, but it is rather inconvenient for preparing the purpureo-salt, especially when chromic chloride is too fresh. In short, the substitution of NH_3 for Cl^- in liquid ammonia is too rapid for preparing the purpureo-salt. Another method of preparing $[Cr(NH_3)_5Cl]Cl_2$ is based on the same principle. As NH_3 is ahead of H_2O in the series, $[Cr(H_2O)_6](NO_3)_3$ should be converted into $[Cr(NH_3)_6](NO_3)_3$ in liquid ammonia. It is evident from the positions of the ligands in the series that the substitution of NH_3 for H_2O is more difficult than for Cl^-: the latter is too rapid and the former is rather too slow for preparing $[Cr(NH_3)_5Cl]Cl_2$. The present authors, therefore, raised the temperature of liquid ammonia to about 50°C. in order to facilitate the dissociation of $Co-OH_2$ bonds.

Summary.

(1) Absorption spectra of several chromic complexes were measured and it was found that the spectrochemical series is coincident with that for cobaltic complexes.

(2) From the spectrochemical series was discussed the stability of the chromic complexes and some of the methods of preparation were explained.

(3) All the chromic complexes have the first and the second bands. $[Cr(NH_3)_5NCS](NCS)_2$ has another band in addition, which is due to the group $M\leftarrow N=C$ (M= a metal-ion of any kind and valency). $[Cr(NH_3)_2(NCS)_4]NH_4$ and $[Cr(NCS)_6]K_3$ have four bands each, the first, the second, the special and the third. The special bands are due to

the same origin as that of $[Cr(NH_3)_5NCS]X_2$ and the third bands are attributed to trans-pairing of the anions.

(4) Chromate ion, a quadri-coördinate complex, has not the first band, but the second and the third, as could be expected from the author's hypotheses.

(5) Absorption spectra of polynuclear compounds may be analysed into those of component complex radicals. For example $[Co(NH_3)_5CrO_4]Cl$ has three bands, of which one is the first band of the sexa-coördinate cobaltic complex and the other two are mainly the second and the third band of quadri-coördinate chromate radical. The second band of the former is almost entirely covered by the second band of the latter.

The authors wish to express sincere thanks to Prof. Y. Shibata for his kind encouragement. They are also indebted to Mr. M. Yanagi for his experimental assistance.

Chemical Department, Faculty of Science,
Imperial University of Osaka.

Synthesis of 3,4-Methylenedioxyphenyl-glyoxal.*

By Sin'iti KAWAI and Koichi ASHINO.

(Received June 23, 1938.)

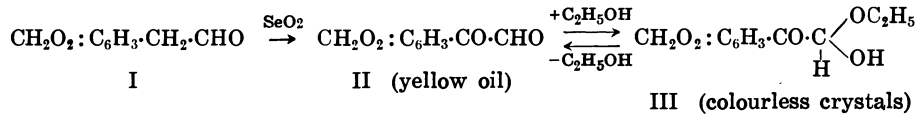
It is anticipated that the compound in the title will be obtained in yellow crystals or oil. Contrary to our expectation, when homopiperonal (I)[1] was oxidized with selenium dioxide in an alcoholic solution, colourless crystals with m.p. 107° were obtained. Further research upon the colourless compound revealed that it was nothing but the 3,4-methylenedioxyphenyl-glyoxal with one molecule of ethanol of crystallization (III). When the colourless compound was warmed with a boiling ethanol bath in Abderhalden's apparatus under reduced pressure (12 mm.) there remained a yellow oil (II).[2] This yellow oil regenerated the colourless crystals (III) when treated with ethanol.

---

* The same contents will soon be published in Japanese in *J. Chem. Soc. Japan*, **59** (1938), No. 8.

(1) Prepared by the ozonolysis of safrol. Compare S. Nagai, *J. Faculty Eng., Tokyo Imp. Univ.*, **13** (1923), 189.

(2) Since a part of the yellow oil (II) volatilizes with the ethanol of crystallization, the exact content of the latter can not be estimated with this apparatus.



I II (yellow oil) III (colourless crystals)

The disappearance of the yellow colour, the sign of α-diketones, in compound III can probably be attributed to the transformation of one of the carbonyl groups into the hemi-acetal form.

When compound III was treated with more than two molecules of phenylhydrazine, it gave the corresponding mono-phenylhydrazone. *o*-Phenylene-diamine, when mixed with compound III, produced the corresponding quinoxaline-derivative.

Experimental.

Molecular Compound between 3,4-Methylenedioxyphenyl-glyoxal and Ethanol (III). An alcoholic solution of homopiperonal (3.3 g.) and selenium dioxide (4 g.) was refluxed on a steam-bath for two hours. After cooling the selenium which precipitated in the meanwhile was filtered off and the filtrate was concentrated to a small bulk. The colourless crystals mingled with selenium which appeared in the meantime was collected and recrystallized from ether. Colourless long prisms, m.p. 107°. Yield 1 g. Found[3]: C, 58.30, 58.30; H, 5.62, 5.67. Calculated for $C_{11}H_{12}O_5$ (III): C, 58.48; H, 5.35%.) Fuchsine-sulphurous acid reaction was positive.

3,4-Methylenedioxyphenyl-glyoxal-mono-phenylhydrazone. Compound III (1 g.) and phenylhydrazine base (1.2 g.) were dissolved in glacial acetic acid which had been diluted with a little amount of water. Soon the mono-phenylhydrazone crystallized out, which was collected and recrystallized from ethyl alcohol, orange-yellow prisms, m.p. 140°. Yield 0.4 g. Found: N, 10.07. Calculated for $C_{15}H_{12}O_3$: N, 10.44%.

2-[3′, 4′-Methylenedioxyphenyl]-quinoxaline. Compound III (0.1 g.) and *o*-phenylene-diamine (0.6 g.) were dissolved in a small quantity of ethyl alcohol with gentle warming and then cooled. Soon the crystals of the quinoxaline derivative made their appearance, which were collected and recrystallized from ethyl alcohol, slightly yellow prisms, m.p. 167.5°. Yield 0.1 g. Found: C, 71.56; H, 4.07; N, 11.09. Calculated for $C_{15}H_{10}O_2N_2$: C, 71.99; H, 4.03; N, 11.20%.

Chemical Institute,
Tokyo-Bunrika University.

(3) The microanalyses of this compound according to Pregl's method, prosecuted by Kisaburo Yamagami, were successful only when they were carried out first in nitrogen stream and then in oxygen. The ordinary method gave a little too small values of carbon and hydrogen since the ethanol of crystallization burned suddenly at the commencement of the analyses.

Electrolytic Reduction of Glutarimide and Its Derivatives.

By Buhei SAKURAI.

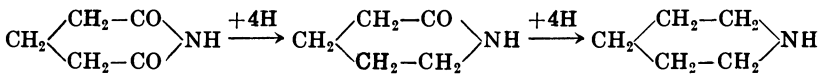
(Received June 25, 1938.)

As a rule reduction of acid imides is very difficult; complete reduction of even one of two carbonyl groups is often found unattainable by purely chemical means, that of both carbonyls being almost impossible. Electrolytically, however, reduction takes place with much ease, and by controlling the conditions of reduction properly it is not difficult to prepare the reduction product in some desired stage.

The results of electrolytic reduction of succinic acid imide,[1] undertaken by the author were previously communicated. The work was now extended to next higher dibasic acid imide, i.e. glutarimide, and the result so far obtained is here reported.

So far as the author could find in chemical literature, no one seems to have yet succeeded in getting piperidone or piperidine and their derivatives by direct reduction of glutarimide and its derivatives. Wallach[2] and L. Ruzicka[3] tried to reduce *N*-ethyl-piperidone with metallic sodium in alcoholic solution, and obtained a condensation product consisting of two molecules of piperidone but not *N*-ethyl-piperidine.

When electrolytically reduced, glutarimide and its derivatives change into piperidines passing through the stage of piperidones:



The first reduction takes place smoothly when lead is used as cathode in sulphuric acid solution. For the second reduction lead cathode prepared with a special care according to Lukes and Smetachova[4] should be used. The author found out that zinc amalgam is much more effective for the same purpose.

Of *N*-methyl-, *N*-ethyl-, and *N*-phenyl-glutarimides, the first two could be reduced easily and with comparatively little decomposition in an about 50% sulphuric acid solution, with lead cathode to *N*-methyl- and

(1) B. Sakurai, this Bulletin, **10** (1935), 311; **11** (1936), 41; **13** (1938), 350.
(2) Wallach, *Ann.*, **324** (1902), 285.
(3) L. Ruzicka, *Helv. Chim. Acta*, **4** (1921), 472.
(4) Lukes and Smetachova, *Collection Czechoslov. Chem. Commun.*, **5** (1933), 61.

N-ethyl-piperidones, respectively, and with zinc amalgam cathode to *N*-methyl- and *N*-ethyl-piperidines.

Glutarimide and *N*-phenyl-glutarimide are much more liable to decompose in the same sulphuric acid catholyte. So that, if careful attention be not paid to the concentration of sulphuric acid, fruitless results are obtained. It is to be noted that the concentrations of sulphuric acid which cause decomposition of glutarimide and *N*-phenyl-glutarimide differ widely from each other. In the case of glutarimide the most suitable concentration of sulphuric acid is 20–30%. If more concentrated, glutarimide begins to be decomposed to glutaric acid and ammonia and finally in the solution containing H_2SO_4 more than 70% complete decomposition takes place giving no reduction product. In the case of *N*-phenyl-glutarimide the solution containing 80–90% H_2SO_4 is found the most favourable for reduction. If H_2SO_4 becomes less concentrated than 60%, phenyl-glutarimide completely decomposes into glutaric acid and aniline, yielding no reduction product. Reduction from piperidone to piperidine does not differ in both cases, smooth reduction taking place in an about 50% acid solution. The degree of decomposition also differs according to the kind of cathode, and as zinc amalgam causes less decomposition than lead, it is preferable to use a 50% sulphuric acid solution from the beginning in the case of glutarimide, and to increase the concentration of sulphuric acid in electrolytic solution by adding concentrated sulphuric acid to it after the first reduction has been completed. As it is impossible to employ 50% acid and zinc amalgam cathode for *N*-phenyl-glutarimide, a 90% acid solution is to be used with lead cathode for the first reduction, and then the electrolytic solution is diluted to make H_2SO_4 50% and at the same time lead cathode is replaced with zinc amalgam before electrolysis is continued for the second reduction.

Experimental.

I. **Glutarimide,** $CH_2\langle{}^{CH_2-CO}_{CH_2-CO}\rangle NH$. Material was prepared after Bernheimer by fusing ammonium glutarate, and by recrystallizing the residue from alcohol. This forms colourless plates melting at 151°.

(1) *Reduction with lead cathode.* In order to obtain α-piperidone, electrolysis was undertaken under the following conditions. Cathode: lead, 100 sq. cm. Catholyte: 25% sulphuric acid with 3 g. of the imide dissolved in it. Current density: 5 amp. per 100 sq. cm. Current quantity: 7.2 F. per mol. Temperature: 20°.

The electrolytic bath was kept in a water tub full of cool water, and electrolyte was kept all the time stirred and cooled. After electrolysis colourless electrolyte was taken out, and treated with chloroform to extract unreduced material. Next

it was shaken with ether to extract glutaric acid produced through the decomposition of the material. After that the liquid was made alkaline with a saturated solution of sodium carbonate, when smell peculiar to α-piperidone came out. It was extracted with ether, and after expelling ether by evaporation about 3 c.c. of a liquid solution were obtained. It was put in a desiccator and then cooled in an ice-box, whereupon 0.4 g. (15%) of α-piperidone crystallized out. On recrystallizing it from ether colourless crystals melting at 38° were obtained. The platinum double chloride was obtained in yellow plates soluble in water or alcohol and melting at 176° with decomposition. Found: Pt, 32.05. Calculated for $\left[CH_2\begin{matrix}CH_2-CO\\CH_2-CH_2\end{matrix}NH\right]_2+H_2PtCl_6$: Pt, 32.07%.

From the above result, it is seen that, though the imide may be reduced to α piperidone, its greater part decomposes into glutaric acid and ammonia in the course of electrolysis.

To see how the decomposition of glutarimide is related to concentration of sulphuric acid a series of experiments were carried out varying concentration of sulphuric acid. The results were summarised in Table 1.

Table 1.

Conc. of sulphuric acid (%)	Unchanged material (%)	Glutaric acid (%)	α-Piperidone (%)
20	10	34	11
30	7.5	43	14
40	5.0	47	11
50	5.0	47	8.6
60	2.5	51	5.7
70	1.0	51	2.8
80	—	55	—
90	—	64	—

As is seen from the table, sulphuric acid of 20–30% seems to be most favourable for the production of α-piperidone.

(2) *Reduction with zinc amalgam cathode.* With the object of getting piperidine electrolysis was conducted using zinc amalgam as cathode under the following conditions. Cathode: zinc amalgam, 15.8 sq. cm. in area. Catholyte: 50% sulphuric acid 100 c.c. with 5 g. of imide dissolved in it. Anode: cylindrical plate of lead. Anolyte: 50% sulphuric acid. Current density: 88.6 amp. per 100 sq. cm. Current quantity: 70.8 F. per mol. Temperature: 25°.

Into the catholyte a spiral lead tube was inserted, through which cold water was passed, while the electrolytic bath itself was put in a water tub full of cool water to prevent the temperature from rising. The catholyte was kept stirred all the time. After electrolysis no glutarimide was detected in the catholyte, but about 0.5 g. (8.5%) of glutaric acid was isolated from it. When it was made alkaline by adding a saturated solution of sodium carbonate, there came out a strong smell re-

sembling that of ammonia. The alkaline solution was extracted with ether, and on the evaporation of ether about 3 c.c. of an aqueous liquid were obtained as the residue. This was made acidic by adding hydrochloric acid to it and evaporated to dryness on the water bath when 2.5 g. (47%) of piperidine hydrochloride was produced. Its platinum double chloride formed orange-red crystals easily soluble in water and alcohol, and melting at 198° with decomposition. Found: Pt, 33.60. Calculated for $\left[CH_2\begin{matrix}CH_2-CH_2\\CH_2-CH_2\end{matrix}NH\right]_2+H_2PtCl_6$: Pt, 33.62%.

The particularly noteworthy fact observed is that the decomposition of the material is less with zinc amalgam cathode than with lead cathode, in the solution containing sulphuric acid of the same concentration.

II. **α-Piperidone,** $CH_2\begin{matrix}CH_2-CO\\CH_2-CH_2\end{matrix}NH$. 1.5 g. of the piperidone obtained in the above experiment was subjected to 5 hours' electrolysis with zinc amalgam under the same conditions as above. As the result, 0.95 g. (52%) of piperidine hydrochloride was obtained, accompanied with a very little decomposition product. It is thus seen that piperidone is not so decomposable as glutarimide in sulphuric acid solution. The reason why the cathode of stronger reducing power, such as zinc amalgam, gives the better yield of reduction product is thus easily understood.

III. **N-Ethyl-glutarimide,** $CH_2\begin{matrix}CH_2-CO\\CH_2-CO\end{matrix}NC_2H_5$. *N*-Ethyl-glutarimide employed in the experiment was prepared by neutralizing glutaric acid with ethylamine and then subjecting the product to distillation at 250–260°. It is a colourless liquid.

(1) *Reduction with lead cathode.* To get *N*-ethyl-piperidone first, electrolysis, was undertaken under the following conditions. Cathode: lead plate 100 sq. cm. in area. Catholyte: 100 c.c. of 50% sulphuric acid in which 5 g. of imide was dissolved. Anode: cylindrical lead plate. Anolyte: 50% sulphuric acid. Current density: 5 amp. per 100 sq. cm. Current quantity: 26.3 F. per mol. Temperature: 28°.

The material dissolved readily in electrolytic solution. The electrolytic bath was kept cooled in a water tub in which cool water was caused to circulate. After the completion of the electrolysis the electrolytic solution was shaken with ether to extract glutaric acid. About 0.25 g. (5%) of it was obtained. Next, after greater part of acid was neutralized with sodium bicarbonate, the catholyte was made slightly alkaline with a saturated solution of sodium carbonate and then extracted with ether when 3.25 g. of a colourless liquid was isolated. It boils at 105–106°, and is easily soluble in water forming a weakly alkaline solution. Its platinum double chloride melts at 164° with decomposition. Found: Pt, 29.39. Calculated for $\left[CH_2\begin{matrix}CH_2-CO\\CH_2-CH_2\end{matrix}NC_2H_5\right]_2+H_2PtCl_6$: Pt, 29.40%. Yield of *N*-ethyl-piperidine in the above experiment is 72.1%.

In the reduction of *N*-ethyl-glutarimide, the concentration of sulphuric acid has close relation to the yield of reduction product; the greater the concentration, the smoother the reduction. If, however, the concentration becomes too great, it gives rise to the decomposition of the material, thereby lowering reduction rate.

Results of the electrolysis showing the relation between the concentration of sulphuric acid and yield of the piperidone are shown in Table 2.

Table 2.

Conc. of H_2SO_4 (%)	Glutaric acid (%)	*N*-Ethyl-piperidone (%)
20	5.4	5.5
30	6.5	44.0
40	7.6	55.0
50	10.8	71.5
60	11.9	77.0
70	16.2	60.5
80	43.2	27.5
90	59.4	5.5

From the table it is seen that if the concentration of sulphuric acid exceeds 70%, decomposition increases rapidly, causing the lowering of reduction rate, and 40–70% sulphuric acid gives the most favourable results.

(2) *Reduction with zinc amalgam cathode.* Next electrolysis for complete reduction was conducted under the following conditions. Cathode: zinc amalgam 15.8 sq. cm. Catholyte: 100 c.c. of 50% sulphuric acid in which 5 g. of imide was dissolved. Anode: cylindrical lead plate. Anolyte: 50% sulphuric acid. Current density: 98 amp. per 100 sq. cm. Current quantity: 126 F. per mol. Temperature: 15°.

The electrolysis was carried out by inserting a spiral lead tube into a cylindrical biscuit vessel containing catholyte. Cold water was caused to flow through the lead tube to cool it from inside, while the electrolytic bath itself was put in a water tub, in which cold water constantly circulates to cool the bath from outside. After completion of electrolysis neither the glutarimide nor glutaric acid was detected to exist in the bath. The electrolyte was now diluted with water of three times volume and after neutralizing the acid with sodium bicarbonate it was made slightly alkaline with a saturated solution of sodium carbonate. It was then subjected to steam distillation, when a substance smelling like ammonia came out. The distillate reacting alkaline to litmus paper was neutralized with hydrochloric acid and evaporated to dryness on the water bath. About 4.0 g. of a sticky substance was left as the residue. The platinum double chloride prepared from the residue crystallized in orange-red prisms from a mixture of absolute alcohol and a small quantity of petroleum ether. It melted at 202° with decomposition. Found: Pt, 30.74. Calculated for $\left[CH_2\begin{matrix}CH_2-CH_2\\ CH_2-CH_2\end{matrix}\!\!>\!NC_2H_5\right]_2+H_2PtCl_6$: Pt, 30.70%. The yield of *N*-ethyl-piperidine amounted to 75%.

IV. **N-Ethyl-piperidone,** $CH_2\begin{matrix}CH_2-CO\\ CH_2-CH_2\end{matrix}\!\!>\!NC_2H_5$. Instead of directly reducing *N*-ethyl-glutarimide, 2 g. of *N*-ethyl-piperidone was subjected to 5 hours' electrolysis under exactly the same conditions as the above experiment. As the result *N*-ethyl-piperidine was obtained with the yield of 52%.

V. **N-Phenyl-glutarimide,** $CH_2\langle^{CH_2-CO}_{CH_2-CO}\rangle NC_6H_5$. *N*-Phenyl-glutarimide was prepared from glutaric acid and aniline and purified by recrystallizing the product from absolute alcohol. It formed colourless needles insoluble in water but easily soluble in hot alcohol, and melted at 145°.

(1) *Reduction with lead cathode.* With a view to obtaining *N*-phenyl-piperidone, hitherto unknown, reduction was carried out under the following conditions. Cathode: lead plate 100 sq. cm. Catholyte: 100 c.c. of 90% sulphuric acid in which 5 g. of imide was dissolved. Anode: cylindrical lead. Anolyte: 50% sulphuric acid. Current density: 5 amp. per 100 sq. cm. Current quantity: 56.4 F. per mol. (8 hours). Temperature: 18°.

Electrolysis was carried out by cooling the electrolytic bath with circulating water and keeping catholyte constantly vigorously stirred. The imide partly remained undissolved at first, but gradually disappeared as electrolysis proceeded. After electrolysis the catholyte was diluted with three times as much water and filtered. The clear solution thus obtained was found to contain nothing to be extracted with ether. It was then made slightly alkaline with sodium bicarbonate and sodium carbonate, and from this alkaline solution about 3.5 g. (75%) of *N*-phenyl-piperidone was extracted in the form of brownish crystals. When it was recrystallized from alcohol it formed colourless needles melting at 98°. Found: C, 75.10; H, 7.47; N (determined as ammonia), 8.04%; mol. wt. (ebullioscopy in benzene), 170. Calc. for $C_{11}H_{13}ON$: C, 75.43; H, 7.43; N, 8.00%; mol. wt., 175. The platinum double chloride of this substance formed red-brown scaly crystals melting at 176° with decomposition. Found: Pt, 25.65. Calculated for $\left[CH_2\langle^{CH_2-CO}_{CH_2-CH_2}\rangle NC_6H_5\right]_2+H_2PtCl_6$: Pt, 25.69%.

As is obvious from the results of above experiment, the reduction of phenyl derivatives greatly differs from that of ethyl derivatives. For reduction of the former much more concentrated sulphuric acid solution is required. If more dilute sulphuric acid be used as in the reduction experiment for other imide derivatives, decomposition predominates over reduction, making reduction efficiency very bad. The relation existing between concentration of sulphuric acid and the yield of piperidone formed by reduction is shown in Table 3.

Table 3.

Conc. of sulphuric acid (%)	Unchanged material (%)	Glutaric acid (%)	*N*-Phenyl-piperidone (%)
90	—	—	76
80	10	—	54
70	—	48	36
60	20	58	—
50	25	64	—

Thus, high concentration of sulphuric acid favours the reduction. When concentration of sulphuric acid gets below 60% any reduction is effected no more. In

order to reduce *N*-phenyl-glutarimide without any loss in material it is necessary to maintain the concentration of sulphuric acid at a value not smaller than 80%.

(2) *Reduction with zinc amalgam cathode.* In the experiment conducted with the object of obtaining the final reduction product, *N*-phenyl-piperidine, it is inconvenient to work with zinc amalgam cathode in a concentrated sulphuric acid bath. Because not only it checks the passage of electricity, but also it causes decomposition of sulphuric acid. So that, it is advisable to divide the experiment into two stages. In the first stage electrolysis is carried out, as with lead cathode, in 90% sulphuric acid solution to reduce the imide to the piperidone stage and then the electrolytic solution is diluted to make concentration of H_2SO_4 as low as 50% and further electrolysis is carried out with zinc amalgam.

The first stage of reduction carried out with 5 g. of imide was followed by the second stage of reduction, for which the following conditions were employed. Catholyte: 100 c.c. of 90% sulphuric acid which was diluted with 130 c.c. of water. Cathode: zinc amalgam, 15.8 sq. cm. in area. Anolyte: 50% sulphuric acid. Anode: cylindrical lead plate. Current density: 79 amp. per 100 sq. cm. Current quantity: 101.5 F. per mol. (6 hours). · Temperature: 18°.

In the course of electrolysis, the electrolytic solution was cooled from both inside and outside. After electrolysis the catholyte contained some sulphur isolated by the decomposition of sulphuric acid. It was filtered and the filtrate was made alkaline with sodium bicarbonate and sodium carbonate solution, when oily *N*-phenyl-piperidine was isolated, which was extracted with ether. About 2.5 g. of the base (58% yield) was obtained. *N*-Phenyl-piperidine is a colourless oil, soluble in water, and easily produces a colourless soluble salt with hydrochloric acid. Its platinum double chloride is yellow crystals containing two molecules of water of crystallization, insoluble in water. It melts with decomposition. Found: Pt, 25.45. Calculated for $\left[CH_2\begin{<}CH_2-CH_2\\CH_2-CH_2\end{>}NC_6H_5\right]_2+H_2PtCl_6\cdot 2H_2O$: Pt, 25.42%.

In this connection the author expresses his heartfelt thanks to Dr. Motooki Matsui, Professor emeritus of the Kyoto Imperial University, for his cordial suggestions.

The Osaka Women's College,
Sumiyoshi, Osaka.

On the Silver Chromate Banding in Silicic Acid Gel.

By Toshizo ISEMURA.

(Received June 15, 1938.)

It was stated that silver chromate readily forms periodic banding in gelatine, but not in agar-agar or in silicic acid. But by suitably modifying the conditions, Bradford[1] could obtain the bands of silver chromate in agar-agar. On the other hand, Dhar and Chatteriji[2] concluded that the banding was formed by periodic coagulation of peptised sol. The silicic acid has not the peptising power on silver chromate, so that silver chromate does not form bands in silicic acid gel. This case is frequently pointed out as an example of the specific influence of the gel as a medium for the reaction. On the contrary to Dhar and Chatteriji's presentation, Hatschek[3] has succeeded in obtaining the bands of silver chromate in silicic acid gel. He had prepared the gel by an unusual method, based on the fact that the silicic acid is gelatinised on mixing a sodium silicate solution with a somewhat large quantity of potassium dichromate solution. After setting the gel he superposed a concentrated solution of silver nitrate on it. He could thus obtain the banding of silver chromate in silicic acid gel.

When we persuit the experiments of rhythmic precipitates in silicic acid gel, usually the gel is prepared as follows. One volume of sodium silicate solution is mixed with an equal volume of solution of some acid, pouring the water glass into the acid and mixing quickly and thoroughly, and then the inner electrolyte is added into it to adequate concentration. After setting the gel, diffusing electrolyte is superposed on it. The present author tried to make the silver chromate bands in the silicic acid gel which was made by this usual procedure. It was recognised with many experiments on the formation of rhythmic banding in silicic acid gel, that the concentration of the acid which is used to make a gel, that is to say, the hydrogen ion concentration of the gel, has a profound influence on whether the bands are formed or not. The fact that the formation of the rhythmic bands of silver chromate had been hitherto unobtainable seemed to be owing to the hydrogen ion concentration of the silicic acid

(1) Bradford, "Alexander's Colloid Chemistry, Theoretical and Applied," Vol. I, 790, New York (1926).

(2) Dhar and Chatteriji, *Kolloid-Z.*, **37** (1925), 89.

(3) Hatschek, *ibid.*, **38** (1926), 151.

gel. In the present study, the silicic acid gels were made by mixing equal volumes of sodium silicate solution (density 1.06) and nitric acid solutions having different concentration. The obtained results in these gels are summarised in the following table.

Table 1. $AgNO_3$ 5% ; 6.0 c.c. of Na_2SiO_3 (1.06) solution + 6.0 c.c. of HNO_3 + 0.4 c.c. of 5% $K_2Cr_2O_7$.

Concentration of HNO_3 N)	Nature of the rhythmic banding
0.67	Typical rhythmic precitates consisting of relatively coarse crystals of red black plates were obtained. The intervals between bands were large.
0.63	Typical rhythmic precipitates as shown in Fig. 1. (the left of the three) were obtained. Crystals were small needles.
0.58	At the top of the gel Liesegang bands accompanied by dendrites were recognised. In the middle, only dendrites were seen, and at the bottom again rhythmic bands appeared but they were those formed by diurnal cause.
0.55	The result was analogous to the case of 0.58 N. But the number of formed Liesegang bands was less.
0.50	No Liesegang band was formed. Dendrites and diurnal bands were seen.

With more concentrated nitric acid than 0.70 N, the silicic acid is not gelatinised. From the foregoing table we can recognise that in the gel of relatively high hydrogen ion concentration the silver chromate banding is formed. In the gel of low hydrogen ion concentration, the decomposition of sodium silicate is not complete, and the rest of sodium silicate reacts with silver nitrate, and so silver silicate is also formed. The silver chromate forms with this silver silicate either complicated bands accompanied by dendrites or only dendrites. The colour of the precipitates forming well-defined bands is red-black but the colour of dendritic bands or dendrites is reddish brown. As frequently stated in older literatures, the banding could not obtained in silicic acid gel, because of the comparatively narrow range of the acidity that is favourable to the band formation of silver chromate.

According to Hatschek's method, somewhat large quantity of potassium dichromate is needed, for it must gelatinise the silicic acid gel. As

the result of the existence of a large quantity of potassium dichromate, the obtained bands are close to each other and the empty spaces between the bands blurred and hardly discriminated. By the method which is now presented, we can regulate the concentration of potassium dichromate at will. The formed bands are more distinct being marked by gaps and empty spaces.

The influence of the kinds of acids which are used to make the gel, was also investigated. Of course, hydrochloric acid is inadequate for this purpose, because it unites with silver nitrate and precipitates an almost completely insoluble silver chloride. So, nitric, sulphuric and acetic acids were used.

Nitric acid is the most favourable, sulphuric acid comes next. Acetic acid forms silver acetate, that is somewhat difficultly soluble. And in the gel which is made by mixing sodium silicate solution and acetic acid, crystals of silver acetate grow in long needles. In the gel which is made from sodium silicate and sulphuric acid, silver sulphate crystals are also formed at the top of the gel, but this is not so remarkable as in the case of acetate. Fig. 1 shows the silver chromate banding in silicic acid gels. From left, the gels were made by mixing sodium silicate solution with nitric, sulphuric, and acetic acid respectively. Crystals formed in these gels are variously shaped. In many cases they are needles. At the bottom of a test-tube, the needle measures often more than 8 mm. long. But they are sometimes plates. These crystals were compared under a microscope, and observed that they consist of many small crystals. The needles were fern-like fronds under a microscope.

The plates are as shown in Fig. 2. The appearances of each crystals were rather different, but a single crystal separated from either a needle or a plate was the same. It crystallises in elongated hexagonal plates. Single crystals are taken in photograph and shown in Fig. 3.

As Hatschek[3] has already pointed out, Dhar and Chatteriji's coagulation theory[4] about the formation of rhythmic precipitates is not applicable. They support their theory with the non-formation of silver chromate bands in silicic acid.[2] But the last mentioned fact is clearly denied by the present experiments. Also the membrane theory is not correct, because the crystals in banding are separated from each other, no membrane formation being recognisable in the rhythmic precipitates, what may be observed in the photograph. The bands consist of well-

(4) Dahr and Chatteriji, *Kolloid-Z.*, **31** (1922), 15; **37** (1925), 2; **37** (1925), 89.

(5) Fischer and McLaughlin, *ibid.*, **30** (1922), 13; Traube and Takehara, *ibid.*, **35** (1924), 245.

developed crystals separated by relatively large spaces, allowing free passage to the diffusing electrolyte.

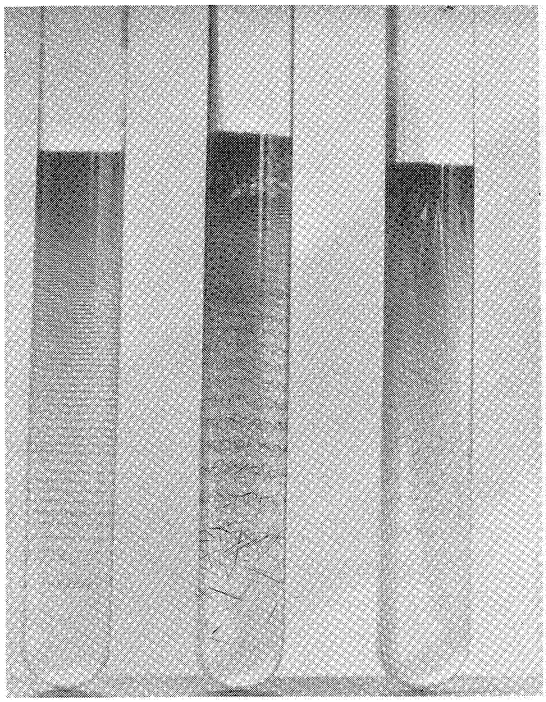
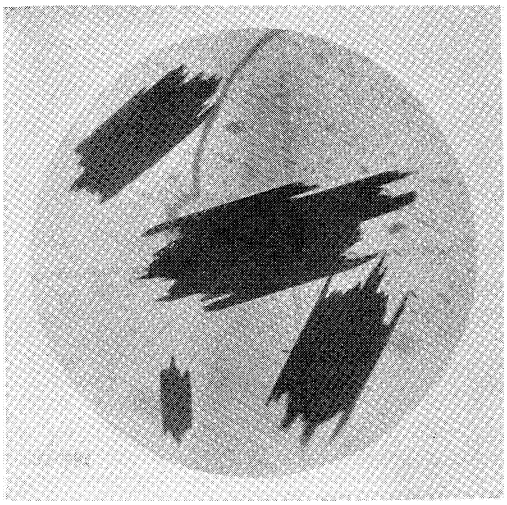
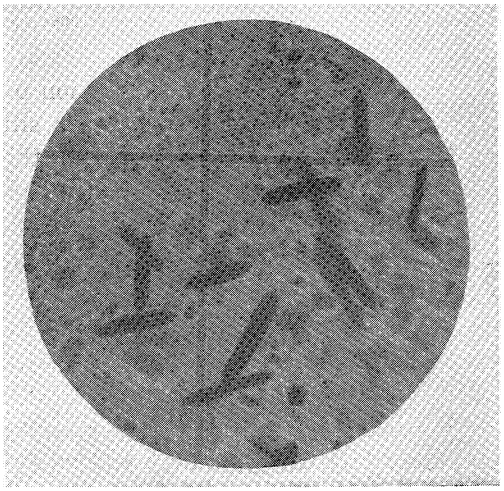


Fig. 1.



(×95)

Fig. 2.



(×310)

Fig. 3.

Summary.

(1) The formation of silver chromate bands in silicic acid gel which was made by a usual method, has been described.

(2) By this procedure, the concentration of chromate is regulated at will, and distinct banding is formed.

(3) The hydrogen ion concentration of the gel has a profound influence on the formation of rhythmic bands of silver chromate.

(4) Dhar and Chatteriji's theory and the membrane theory are not applicable.

In conclusion the author wishes to express his cordial thanks to Prof. J. Sameshima of the Tokyo Imperial University for his kind advices.

Kochi High School,
Kochi.

On the Calcium Phosphate Banding in Silicic Acid Gel.

By Toshizo ISEMURA.

(Received June 27, 1938.)

In regard to the formation of rhythmic precipitate of calcium phosphate in other medium than a silicic acid gel, several reports have been published. There have been the studies of Dogadkin,(1) Hatschek,(2) and Schemjakin(3) concerning the formation in a gelatine gel and those of Schemjakin on the phenomenon in an agar-agar gel. As to the rhythmic precipitation of this substance in a space between two pieces of glass and in capillary spaces without the aid of any gels, the studies of Doyle and Ryan(4) and Wo. Ostwald(5) can be mentioned. But the banding in a silicic acid gel have never been reported. Therefore, the present author has tried an experiment in order to know whether the Liesegang phenomenon of calcium phosphate could be caused or not in the silicic acid gel. And it was certified that calcium phosphate produced an extremely prominent rhythmic precipitate even in a silicic acid gel and that the banding

(1) *Kolloid-Z.*, **40** (1926), 33.
(2) *Kolloid-Z.*, **27** (1920), 225; *Biochem. J.*, **14** (1920), 418.
(3) *Kolloid-Z.*, **50** (1930), 58.
(4) *Brit Chem. Abstract*, A, **1929**, 1144; *Proc. Roy. Irish Acad.*, B, **38** (1929), 435.
(5) *Kolloid-Z.*, **40** (1926), 144.

was closely related to the hydrogen ion concentration of the medium or a silicic acid gel. The experimental result will be described in the following.

Although calcium salts were used as an inner electrolyte and sodium phosphate made diffuse into the gel in all the cases hitherto reported, whichever the inner electrolyte might be, calcium salts or sodium phosphate, as favourable a result was obtained in a silicic acid gel as in other gels. There was a marked difference between the silicic acid and other gels. Use of sodium phosphate as an inner electrolyte had rather a strong point that preparation of gel needed no special care. In use of calcium salts as an inner electrolyte, acetic acid, sodium silicate and calcium salt should be mixed in the order and the mixture stirred up rapidly. Unless these were mixed in this order or unless the mixture stirred up rapidly, white turbidities, which seemed to calcium silicate, were formed, partially coagulated, so that no transparent gel could be obtained. Use of sodium phosphate and the likes as an inner electrolyte, on the contrary, needed no special care. But in either case where a phosphate solution was added to diffuse into the gel containing a calcium salt or where a calcium salt solution was poured on the gel containing a phosphate, a rhythmic precipitate with very clear bands was obtained.

The following can be mentioned as one of the most favourable conditions. That is, for dissolving phosphate in a gel, mix 1 c.c. of a 8% solution of secondary sodium phosphate with 10 c.c. of a 0.75 N acetic acid and then add 10 c.c. of a 1.06 density solution of sodium silicate to it and allowed to stand to gelatinize. After the gel set firmly, a 2 mol solution of calcium nitrate was superimposed on it.

For dissolving calcium salt in a gel, after mixing the sodium silicate solution ($d = 1.06$) with 10 c.c. of 0.75 N acetic acid add 1.0 c.c. of a 10% calcium chloride solution to the mixture, while stirring up. After the gel set firmly, a 8% solution of secondary sodium phosphate was poured on it.

The right of Fig. 1 shows the bands formed by the former method and the left, those obtained by the latter method. Fig. 2 shows Liesegang rings of calcium phosphate formed on a glass plate by the former method.

The effect of the hydrogen ion concentration, inner electrolyte and its concentration, outer electrolyte and its concentration, concentration of gel, and, moreover, the effect of aging on the formation of this rhythmic precipitate have been examined, and the results are described in the following lines.

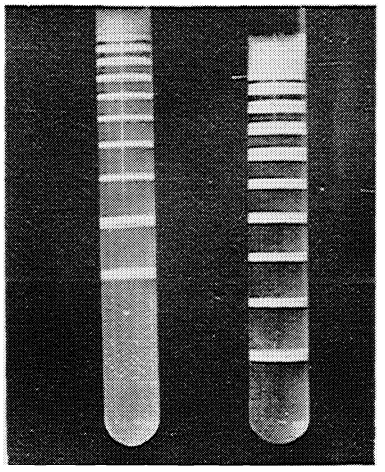


Fig. 1.

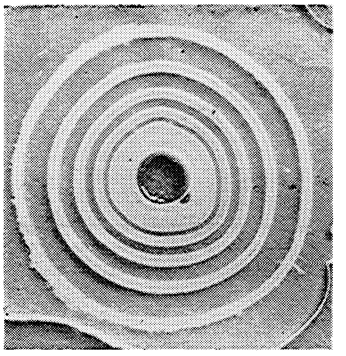


Fig. 2.

Effect of Hydrogen Ion Concentration. It has already been mentioned that the hydrogen ion concentration has a very marked effect on the formation of these bands. At first, the case where calcium chloride was used as the inner electrolyte will be described. If the hydrogen ion concentration was low in the addition of calcium chloride to a silicic acid sol, a partial coagulation occurred and produced a curdy precipitate; accordingly it was impossible to prepare a uniform gel. This is probably caused by the fact that the calcium salt was acted simultaneously by an amount of sodium silicate, which remained undecomposed, in the process of the formation of silicic acid by the action of acid, which was small in quantity.

In employment of a sol containing a little more concentrated acid, for instance, a sol which was prepared by mixing 0.66 N acetic acid and an equal volume of sodium silicate solution of 1.06 density, an uniform gel could be obtained. By diffusion of sodium phosphate into the gel, however, a long zone of white precipitate was formed, which was not rhythmic.

In a case where an acid was more concentrated, that is, in a case where a gel made from 0.75 N acetic acid and an equal volume of sodium silicate ($d = 1.06$) was used, the rhythmic precipitate could be formed. When the concentration was further more increased, the bands were hardly formed. In a gel composed of 1 N acetic acid and an equal volume of sodium silicate ($d = 1.06$), two or three incomplete bands were only formed on the contact surface of the diffusing solution and the gel.

In short, the formation of rhythmic bands was only possible in the gels which were made from 0.7–1 N acetic acid and an equal volume of a sodium silicate solution ($d = 1.06$). Especially 0.75–0.8 N acetic acid gave a favourable result. This can be seen in Table 1.

Table 1. Na_2SiO_3 ($d = 1.06$); $CaCl_2$ 0.08%; Na_2HPO_4 0.5 mol.

Conc. of acetic acid added (N)	Number of bands formed	Remarks
0.50		
0.66		A continuous zone of precipitate.
0.70	3	After a continuous precipitate as long as 4 cm., extremely thick bands were formed.
0.75	10	Typical rhythmic precipitate.
0.80	13	Typical rhythmic precipitate.
0.90	(15)	The bands were fragmental and incomplete but stood close.
1.00	(3)	Fragmental.

Equal volumes of Na_2SiO_3 and acetic acid were mixed. This result is in the case where the gel was filled to a height of 8 cm. of a test-tube of 1 cm. in internal diameter and 14 cm. in length.

The results were the same, where secondary sodium phosphate was used as the inner electrolyte. When a sodium silicate solution ($d = 1.06$) was mixed with an equal volume of 0.5, 0.6, and 0.7 N acetic acid respectively, the uniform gel could generally be obtained. When a calcium salt was allowed to diffuse into them, however, there formed only a zone of completely even white precipitate. When the acid or hydrogen ion is further more concentrated, the rhythmic precipitation may occur. As the concentration of acetic acid increased, the number of formed bands gradually decreased. No band was formed by the used of 2 N acetic acid. The results are given in Table 2.

Calcium phosphate was precipitated as the primary, secondary or tertiary calcium phosphate according to the value of pH of the gel in which the precipitation occurred. Therefore the primary salt can probably form no rhythmic bands on account of its solubility; while the secondary or tertiary salt can produce the rhythmic precipitate. When pH of the gel is high, the tertiary salt only formed, and it precipitates rather unrhythmical because a salt of too poor solubility, gives generally no rhythmic bands. Judging from these facts, the absence of rhythmic precipitate in this case is acknowledged.

Table 2. Na_2SiO_3 ($d = 1.06$); Na_2HPO_4 0.4%; $CaCl_2$ 30%.

Conc. of acetic acid (N)	*p*H	Number of bands formed	Remarks
0.60	8.98		Continuous precipitate formed.
0.70	7.72		,,
0.75	7.04	9	
0.80	6.01	7	
0.90	5.50	4	
1.00	5.30	3	
2.00	4.67	0	No precipitate formed.

The gel was made by mixing the equal volumes of sodium silicate and acetic acid. As much of the gel was taken as to fill to a height of 6 cm. of a test tube of 1.2 cm. in internal diameter and 11 cm. in length.

Inner Electrolyte and the Effect of Its Concentration. As already mentioned, calcium salts as well as sodium phosphate are usable as an inner electrolyte. At first the case of calcium chloride will be described. The experiment was conducted in a gel which was made from 0.75 N acetic acid and sodium silicate solution of 1.06 in density, containing calcium chloride in various composition from 0.004 to 5%.

The rhythmic precipitate was formed in any gels containing calcium chloride in higher concentrations than 0.017%. But when the amount of calcium chloride exceeds 5%, then a 0.5 mol solution of secondary sodium phosphate was hardly diffused into the gel and a stopper of precipitate was only formed on the surface contacting the gel. Yet generally, when calcium chloride was more concentrated, though all the other conditions were the same, the formed bands were large in number and stood close. If the concentration was beyond a certain limit, the bands increased their thickness, but the number of bands rather decreased. This was probably because by the osmotic pressure of the electrolytes in the gel. The diffusion became difficult into such a gel which contained so much inner electrolyte. The results are given in Table 3.

As much of a gel was taken as to fill to a height of 8 cm. of a test-tube of 1 cm. in internal diameter and 0.5 mol secondary sodium phosphate solution was allowed to diffuse in it. When calcium chloride was too much concentrated, the band of calcium phosphate which was formed on the contact surface of the gel and diffusing agent was broken by the osmotic pressure of calcium chloride solution. Then a new precipitate

Table 3. Outer electrolyte: Na_2HPO_4 0.5 mol.

Conc. of inner electrolyte $CaCl_2$ (%)	Number of bands formed	Remarks
5.00	0	Dendrites grew in the diffusing solution.
2.50	2	
1.50	8	The bands formed in the lower part of gel were fragmental.
0.50	9	
0.30	9	
0.15	11	
0.08	10	
0.03	6	
0.017	2	
0.010	0	
0.004	0	

The gel was made by mixing equal volumes of Na_2SiO_3 ($d = 1.06$) and acetic acid (0.75 N). The asterisk in the subsequent tables shows that such a gel was used.

was formed there and it grew in dendrites in the solution of secondary sodium phosphate as the diffusing solution. This seemed to be ascribed to the same cause as that the silicates of cobalt, nickel, and manganese, etc. grew in dendrites in a sodium silicate solution which is known as a "chemical garden" and that the copper ferrocyanide grew in a saccate form in a potassium ferrocyanide solution. An example is given in Fig. 3. It was a matter of course that this could be produced also when a sodium phosphate solution was added slowly to a concentrated solution of calcium chloride, or solid calcium salt.

When gels were prepared in the same conditions, except for employment of sodium phosphate as the inner electrolyte instead of calcium chloride, so far as the experiment is conducted in the range of 0.0125–1.25%, the gels containing the sodium phosphate in higher concentrations than 0.038%, always gave very clear rhythmic precipitates. If the inner electrolyte was small in concentration, the stopper of precipitate which was formed first of all, was large and the distances between the successive bands were large. Contrary to the case where calcium chloride was used as the inner electrolyte, if the inner elektrolyte was small in concentration, each band was rather thick. This was not because the precipitate was separated in abundance, but because the locality of the deposition was sharp in either side, having a certain

width. The relation between the concentration and the number of formed bands is given in Table 4, where each band was as thick as 5 mm. in the case of the least concentrated inner electrolyte.

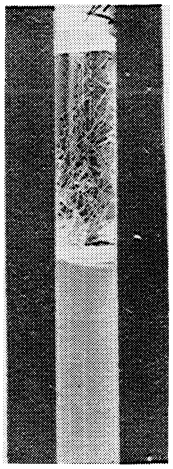


Fig. 3.

Table 4.* Outer electrolyte: $CaCl_2$ 30%.

Conc. of inner electrolyte Na_2HPO_4 (%)	Number of bands formed
1.25	13
1.08	12
0.87	10
0.54	8
0.13	5
0.07	3
0.038	2
0.0125	0

In experiment with the inner electrolyte of such other salts than secondary sodium phosphate, as primary potassium phosphate or tertiary sodium phosphate, 0.5 c.c. of each 0.5 mol primary or tertiary salt was added to each 10 c.c. of the sol composed of sodium silicate ($d = 1.06$) and an equal volume of 0.75 N acetic acid, in order to obtain a gel. In the gel containing the primary salt, the precipitate was formed rhythmically, while in the gel containing the tertiary salt, a continuous precipitate was obtained. But the rhythmic precipitation was recognised by adding half the quantity of the tertiary salt or by using 0.8 N acetic acid in preparation of the gel.

From the measurement of the pH in these cases, the rhythmic precipitation was possible in the gels of lower pH values than about 7.6. Therefore, it is not an important factor that which salt should be added, the primary, secondary, or tertiary one but the hydrogen ion concentration of the gel is an essential factor. The formation of the rhythmic precipitate was possible in the case where the pH was about 5.3–7.6; that is where the inner electrolyte was a mixture of the primary and secondary salts. Therefore it is supposed that the white bands formed are chiefly composed of the secondary calcium phosphate.

Outer Electrolyte and the Effect of Its Concentration. A sol was made by mixing 0.75 N acetic acid with an equal volume of sodium silicate solution ($d = 1.06$) and as much of calcium chloride was added to the sol as to become 0.1% in concentration. After the sol set to a gel, secondary sodium phosphate solutions of various concentration were poured on the gel. The experimental results are given in Table 5.

Table 5.* Inner electrolyte: $CaCl_2$ 0.1%.

Conc. of outer electrolyte Na_2HPO_4 (%)	Number of bands formed.
8.74	13
5.82	11
2.91	9
1.96	4
0.87	1

In this case, as much of the sol was taken as to fill to a height of 8 cm. of a test-tube of 1 cm. in inner diameter. The more concentrated sodium phosphate solution gives the more closeness of the bands and the more number of the bands.

Calcium chloride solutions of 5 to 30% were poured on the gel which was prepared in the same manner as the above and contains 0.5% of secondary sodium phosphate. In any case, the clear rhythmic precipitate was produced. The relation between the concentration and number of formed bands is given in Table 6.

Table 6.* Inner electrolyte: Na_2HPO_4 0.5%.

Conc. of outer electrolyte $CaCl_2$ (%)	Number of bands formed.	Remarks
30	8	These three agree completely and no difference is recognized among them.
25	8	
20	8	
15	8	The bands were close in proportion to the concentration of outer electrolyte.
10	8	
5	7	

In the case where the calcium chloride solutions of higher concentrations than 20% were used, no difference was recognized in the closeness and the total number of bands. This was a characteristic result. When the concentration was lower than 15%, the total number of formed bands was large in the case of the highly concentrated outer electrolyte, and

consequently the closeness of bands increased. This is a common rule in the formation of rhythmic precipitate.

Next, the effect of diffusion of different electrolytes into the fixed inner electrolyte was scrutinized. At first, primary potassium phosphate, secondary and tertiary sodium phosphate solutions of an equal concentration were respectively allowed to diffuse into silicic acid gels which were made from a sodium silicate solution ($d = 1.06$) and an equal volume of 0.75 N acetic acid, containing calcium chloride.

According to the experiment with gelatine gel, when the primary salt is allowed to diffuse in, no rhythmic precipitate is formed. In the silicic acid gel, there are the substances which act as a buffer solution on the hydrogen ion concentration. Therefore, it may form a rhythmic precipitate. When the primary salt was diffused, as a matter of course, the bands were formed at large intervals and the number of formed bands also was extremely small.

The diffusion of secondary sodium phosphate gave the most typical rhythmic precipitate, as already described. With tertiary sodium phosphate the rhythmic precipitate was formed, but the silicic acid gel was gradually peptized by the added solution of strong alkaline. On the other hand, the bands of calcium phosphate which had once been formed, received no effect by the alkalinity of the solution and remained unchanged, though they fell down slowly by their own weight to the level where there was still unpeptized gel. In the part where the peptization had not yet occurred, the rhythmic precipitate was successively formed, so that those bands piled up one after another.

Solutions of chloride, bromide, iodide and nitrate of calcium of the equal concentration made respectively diffuse into gels containing sodium phosphate as the inner electrolyte; the rhythmic precipitates were formed at the same distances and closeness, and scarcely any essential difference was found among them.

Effect of the Concentration of Gels. The acetic acid solution of an adequate concentration was added so as to be roughly $p\mathrm{H} = 6$ to the sodium silicate solutions of an equal volume, whose densities were respectively 1.06, 1.08 and 1.10. In any cases of the gels, the formation of the rhythmic precipitates could be observed. In the gel from the silicate solution of the density of 1.10, each stratum of precipitate somewhat blurred on either face and hardly grew into a clear band. Accordingly, the gels of as low concentrations as possible, are adequate for the present purpose of producing the rhythmic precipitate.

Effect of the Presence of a Third Substance. It was already known that the presence of a certain substance in the gel indifferent to the precipitation reaction, often had an effect on the formation and the properties of rhythmic bands. Hatschek, moreover, pointed out that in formation of the rhythmic precipitate of calcium phosphate in gelatine, some marked abnormalities were caused by the kinds of gelatine and impurities in it. The present author mixed the solutions of cane sugar, glucose, urea, potassium bromide and common salt, with the outer electrolyte in order to examine their effect as the third substance. As much of secondary sodium phosphate was added as to become 0.4% in concentration, to the sol which was made by mixing a sodium silicate solution ($d = 1.06$) and an equal volume of 0.75 N acetic acid. After the gel set firmly, the solution of outer electrolyte was put on it which had been prepared by mixing an equal volume of 2 mol calcium nitrate solution with cane sugar (1 and 2 mol solution), glucose (1 and 0.5 mol solution), urea (1 and 0.5 mol solution), sodium chloride (1 mol solution), and potassium bromide (1 mol solution), respectively. Pringsheim[6] states that when two salt solutions diffuse into a gel in opposite directions the reaction does not proceed beyond a thin film if the solutions are isotonic. A hypertonic solution continues to diffuse into a hypotonic and any precipitate formed is deposited in the latter. In accord with this idea, indifferent substances are often added to the solution on the top of the gel in order to ensure reaction below the gel surface. In the present case, however, when a third substance is added to the outer electrolyte, the increase in the diffusion velocity, which is determined by the osmotic pressure of the electrolyte will be very small, so that the effect on the formed rhythmic precipitate is negligible.

Next, the effect of a third substance added to the inner electrolyte was tested. The solution of a third substance was mixed with acetic acid solution to obtain a 0.8 N acetic acid solution and an equal volume of sodium silicate solution ($d = 1.06$) was poured into it. Then as much of secondary sodium phosphate was further added to the mixture as to be 0.4% in concentration. After gelatinized this sol to a firm gel, 2 mol solution of calcium nitrate was added to diffuse into it. When some organic compound (cane sugar, glucose and urea) was added as the third substance, at first, the bands were somewhat closer, but later rather thinner than those in the cases without the addition of the third substances.

(6) *Z. physik. Chem.*, **17** (1895), 473.

When, however, potassium iodide or bromide for instance, was added in the inner electrolyte (0.3 mol in the gel), some different results have been obtained. The first three or four bands could be produced although, whose particles were coarse, while those lower than the fourth or fifth bands composed of so coarse particles, that no distinct bands could be observed. The fact may be explained as follows. When an organic matter such as cane sugar, is added, the outer electrolyte is checked to diffuse into the gel by the osmotic pressure of the substance in the gel. Therefore, the concentration of the diffusing electrolyte inside the gel suffers a sharp gradient, so that the bands will deposit relatively close in the part contacting the diffusing solution, and afterward more thinly than the case where no third substance is added. The abnormalities caused by the presence of inorganic salts may be imputed to the fact that calcium phosphate has generally high solubility in the solutions of some other salts. An excess of the diffusing ion is readily brought forth in the vicinity of the part contacting the diffusing agent, so that the bands are formed. But tolerably deep inside of the gel, the minute change of solubility has a great effect on the velocity of separation of the precipitate. In the case of a high solubility, the separation of the precipitate is slow, and their particles are coarse; accordingly, the precipitate will deposit in abnormal bands.

Effect of Aging. Scott Blair, for the first time, reported that the rhythmic precipitate of silver chromate in a gelatine gel was greatly effected by the aging of the gel before superimposing the diffusing electrolyte.[7] The present author ascertained that this change of gel by the age was not really caused by the change of the structure of the gel.[8] Koenig,[9] on the other hand, advocated the effect of aging even in silicic acid gels, and reported that the abnormal bands were brought forth in an aged gel. But it was already mentioned that the normal rhythmic precipitate of copper chromate could be formed in a gel, which had elapsed a very long time.[8] It seemed, therefore, that the aging has no effect on bands in the case where there is no mutual action between the gel and inner electrolyte, especially in silicic acid gels. This view was confirmed by the rhythmic precipitates of calcium phosphate. The experiments have been conducted as follows. Five c.c. of a 0.5 mol sodium phosphate solution was added to 100 c.c. of a sol, which had been prepared by mixing sodium silicate solution ($d = 1.06$) and an equal volume of 0.75 N acetic

(7) *Phil. Mag.*, **49** (1925), 90.
(8) Isemura, this Bulletin, **8** (1933), 108.
(9) *J. Phys. Chem.*, **24** (1920), 466.

acid, and the mixture was separated into 12 test-tubes and let gelatinized. These test-tubes were kept in a thermostat at 25°C. and an equal volume of 0.5 mol calcium nitrate solution was poured on gels at 1, 3, 12 hours, 1, 2, 3, 4, 5, 9, 10, 12 and 15 days respectively after the setting of the gel. All these test-tubes made quite the same rhythmic precipitate, and cannot be noticed any difference among them. Thus the aging effect, generally, is not observed, provided the inner electrolyte does not react with the gel.

Summary.

(1) The formation of rhythmic precipitate of calcium phosphate in a silicic acid gel was described.

(2) The formation of this rhythmic precipitate was strongly affected by the hydrogen ion concentration of the gel.

(3) The effects of the concentrations of inner and outer electrolytes, and gel on this rhythmic precipitate, were studied.

(4) When the concentration of the inner electrolyte ($CaCl_2$), was sufficiently great, no diffusion of the outer electrolyte into the gel took place but reversely calcium salt diffuse into the outer electrolyte solution and dendrities were formed in the outer solution.

(5) The effect of the existence of a third substance in the gel and in the diffusing electrolyte, were also investigated. The existence of it in a diffusing electrolyte had almost no influence but the existence in a gel had some effects, especially in the case where bromide and iodide of potassium were used as the third substance.

In conclusion the author expresses his hearty thanks to Prof. J. Sameshima of the Tokyo Imperial University for his kind advices throughout the work.

Chemical Institute,
Faculty of Science,
Tokyo Imperial University,
Tokyo.

On the Composition of "Akebi" Seed Oil.

By Saburo KOMORI and Sei-ichi UENO.

(Received June 27, 1938.)

In Japan, "Akebi" seed oil is used for food locally in Iwate Prefecture, and the analytical constants of this oil have hitherto been reported by S. Uchida.[1] This oil has a peculiar characteristic, which is of extraordinarily high Reichert-Meissl value, but we have not any researches on the composition of it. The present authors have made a thorough examination on this oil, with the results that palmitic, stearic, oleic and linoleic acids were separated, and the presence of acetic acid was also confirmed.

I. The Seed Oil of "Mituba Akebi" (*Akebia lobata*, Decne.). The fruits of "Mituba Akebi", which ripen in October, are shown in Fig. 1. They contain numerous small black seeds as shown in Fig. 2, and 50 grains of the latter weigh 1.3 g. on the average.

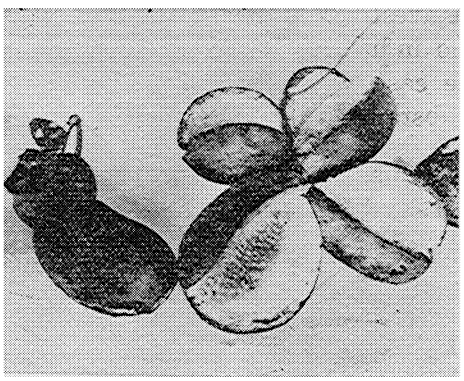


Fig. 1. Fruits of "Mituba Akebi."

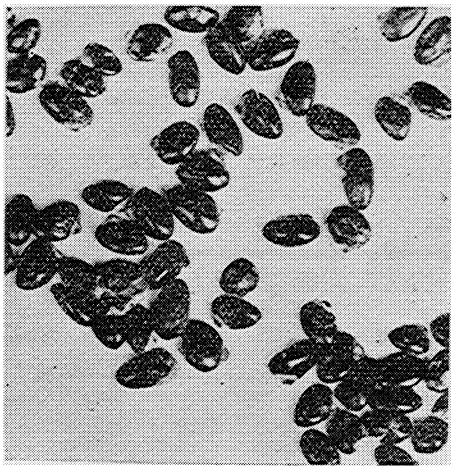


Fig. 2. Seeds of "Mituba Akebi" (life-size).

The seeds (350 g.) were ground, and by ether extraction, light yellow oil (97 g.) was obtained. The oil had the following characteristics: n_D^{20} 1.4652, d_4^{20} 0.9326, acid value 6.6, saponification value 254.9, iodine value

(1) *J. Soc. Chem. Ind.*, **35** (1916), 1091; *J. Soc. Chem. Ind., Japan*, **19** (1916), 33.

78.6, and Reichert-Meissl value 49.3. The sample oil (76 g.) was saponified and after the removal of unsaponifiable matter (0.7715 g.) by ether extraction, the soap solution was decomposed with dilute hydrochloric acid and mixed fatty acids (57 g.) were obtained.

(1) *Water soluble part.* The acidic solution, obtained by the decomposition of soap solution, was concentrated under reduced pressure after neutralisation. The concentrated solution was acidified, saturated with common salt, and extracted with large quantity of ether. The extracted substance had an irritative odour like acetic acid, and distilled at 108–114° under the ordinary pressure. The distilled substance was converted into *p*-bromophenacyl ester, two crystallisations from 75% ethyl alcohol gave an ester, m.p. 85.5–86°, which showed no depression of melting point when mixed with pure acetice acid *p*-bromophenacyl ester.

(2) *Water insoluble fatty acids.* The mixed fatty acids obtained as mentioned above formed a white semi-solid, which had n_D^{40} 1.4521, neutralisation value 203.3, iodine value 91.2. The mixed fatty acids (53 g.) were separated by the lead salt–alcohol method of Twitchell into solid and liquid portions as shown in Table 1.

Table 1.

	Yield	Neutralisation value	Iodine value
Solid acids	17.17 g. 32.4%	213.9	22.5
Liquid acids	67.6%	199.3	120.2

The solid fatty acids (15 g.) were fractionally redistilled as shown in Table 2.

Table 2.

Fraction	B.p./4 mm.	Yield (g.)	M.p.	Neutral. value	Iodine value
1	−175°	4.6	57.7−58.6°	217.4	7.6
2	175−180°	5.2	54.5−55.8°	215.2	19.4
3	180−184°	4.1	43.5−45.0°	209.0	41.3
Residue		0.8			

As the results of careful examinations of fractions 1 and 3, the authors isolated a large quantity of palmitic acid, and a small quantity of stearic acid.

The liquid acids obtained by the lead salt–alcohol method were converted into methyl esters and fractionally distilled as shown in Table 3.

Table 3.

Fraction	B.p./4 mm.	Yield (g.)	n_D^{20}	Saponif. value	Iodine value
1	176°	3.3	1.4541	190.2	112.2
2	176–177°	19.9	1.4545	189.1	116.7
3	177°	5.1	1.4550	189.4	117.5
Residue		1.1			

The saponification value of each fraction in Table 3 showed the non-existence of fatty acids having carbon numbers other than 18. In the fraction 2, oleic and linoleic acids were detected, as dihydroxystearic acid and tetrabromostearic acid respectively.

From the result of the above analysis, the mixed fatty acids of "Mituba Akebi" seed oil seemed to consist of the following composition: palmitic acid 23%, stearic acid 2%, oleic acid 53% and linoleic acid 22%.

II. The Seed Oil of "Itutuba Akebi" (*Akebia quinata*, Decne.). The seeds of "Itutuba Akebi" are comparatively larger than the seeds of "Mituba Akebi", and 50 grains of them weigh 4.03 g.

210 g. of the seeds were crashed, extracted with ether, and dark green oil (41 g.) was obtained. It had the following properties: n_D^{20} 1.4667, d_4^{20} 0.9354, acid value 2.0, saponification value 259.5, iodine value 77.3, Reichert-Meissl value 44.8, unsaponifiable matter 2.6%.

In the oil (28 g.) the existence of acetic acid was confirmed in the same way as the seed oil of "Mituba Akebi". The mixed fatty acids formed a dark green semi-solid, and their characteristics (n_D^{40} 1.4523, neutralisation value 205.1, iodine value 89.1), resembled very much those of the mixed fatty acids of "Mituba Akebi".

Department of Chemical Technology,
Faculty of Engineering,
Osaka Imperial University,
Japan.

Les spectres d'absorption des hydrocarbures azoïques et l'halochromie.

Par Taku UÉMURA et Yasuo INAMURA

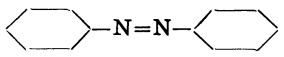
(Reçu le 9 juillet 1938.)

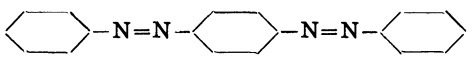
Nous avons déjà publié[1] sur les spectres d'absorption d'une vingtaine de composés azoïques mixtes et ceux de leurs isomères pour étudier spectrochimiquement de la production de tautomérie dans leurs solutions alcooliques. Les résultats obtenus des hydrocarbures azoïques sont montrés dans le présent mémoire qui est formé d'une partie des recherches des composés azoïques depuis longtemps étudiés dans notre laboratoire.

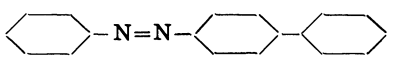
Corps étudiés et procédé expérimental. Les actuels hydrocarbures azoïques ont une forme générale Ar–N=N–Ar' où les radicaux, comme $-NH_2$, $-NO_2$, $-OH$ ou $-SO_3H$ ne sont pas substitués dans les noyaux aromatiques. On peut aussi nommer le hydrocarbure à ce qui contient d'alcoyle dans le radical aryle, mais puisque ces alcoyles dans les hydrocarbures n'influent pas sur l'absorption des rayons lumineux, nous avons exclu les pareils hydrocarbures et observé surtout les spectres d'absorption des composés monoazoïques.

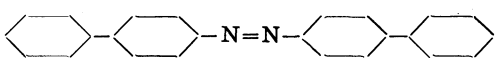
Le but de nos études actuelles est de trouver une courbe caractéristique de hydrocarbures azoïques et, en même temps, de savoir l'influence de la substitution du noyau aryle par un radical diphényl ou naphtalène. L'halochromie par l'acide sulfurique est aussi étudiée en comparant des courbes d'absorption de ces corps préparés.

Les composés que nous avons formés pour la présente recherche sont les suivants en notant leur couleur comme un solide:

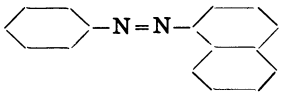
(1) Azobenzène  (orange)

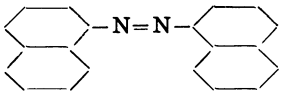
(2) Disazobenzène[2]  (brun)

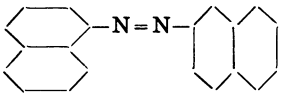
(3) Phénylazodiphényle[3]  (jaune)

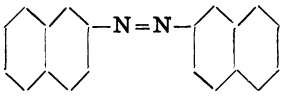
(4) Azodiphényle[4]  (jaunâtre)

(1) Ce bulletin **10** (1935), 169.
(2) C. Mills, *J. Chem. Soc.*, **67** (1895), 925.
(3) R. Pummerer et J. Binapfl, *Ber.*, **54** (1921), 2770, 2773, 2778, 2781.
(4) R. Pummerer et J. Binapfl, *ibid.*, **54** (1921), 2782.

(5) Benzène azo-α-naphtalène[5]  (rouge foncé)

(6) α,α′-Azonaphtalène[6]  (brun foncé)

(7) α,β′-Azonaphtalène[7]  (brun foncé)

(8) β,β′-Azonaphtalène[8]  (brun foncé)

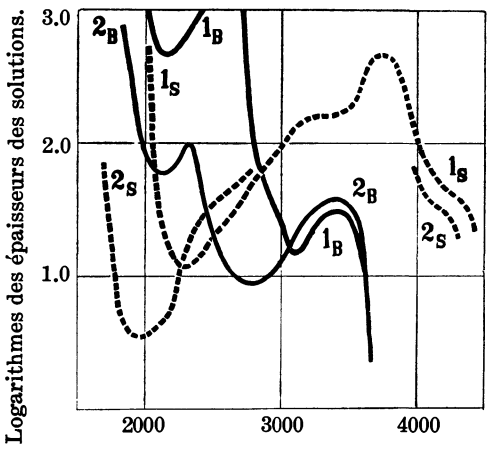
Le procédé d'expérience est presque le même que celui que nous avons déjà appliqué aux composés azoïques mixtes, à savoir en se servant du tube de Baly en quartz et du spectrographe en quartz (type E) de l'Anglais Adam Hilger, la source lumineuse par le courant continu (4 à 5 ampères à 100 volts) d'un arc métallique en fer. Les plaques panchromatiques "Fuji" (marque japonaise) ont été utilisées avec le révélateur du métol-hydroquinone en comptant 30 secondes comme temps de pose photographique pour obtenir des spectres d'absorption. Les solutions benzéniques pour photographier ont été préparées en dissolvant l'échantillon (2 à 15 mg.) dosé par un microbalance en fiole graduée (50 c.c.). Les concentrations de ces solutions sont variées de 1/1000 à 1/10000 mol pour les employer convenablement. L'observation de l'halochromie a été faite en adoptant l'acide sulfurique comme dissolvant. Nos courbes de Hartley-Baly obtenues par les photographies d'absorption sont calculées de l'épaisseur de solutions de 1/10000 mol de concentration et discutées du point spectrochimique.

Spectres d'absorption. *Composés azoïques d'une série benzénique. (Influences d'augmentation des radicaux azoïques).* La comparaison des courbes d'absorption de disazobenzène (courbe 2) et celle d'azobenzène (courbe 1), que nous avons pris comme une substance principale, est faite dans la figure 1. La première bande (longueur d'onde du centre: 466 mμ) ne change presque pas sa position centrale, mais on peut considérablement reconnaître un effet hyperchromique par l'augmentation

(5) R. Nietzki et R. Zehntner, *Ber.*, **26** (1893), 143.
(6) R. Nietzki et O. Goll, *ibid.*, **18** (1885), 3252.
(7) R. Nietzki et J. Göttig, *ibid.*, **20** (1887), 612.
(8) M. Lange, D.R.P., 78225; P. Friedlaender, "Fortschritte der Theerfarbenfabrikation," **4**, 1016.

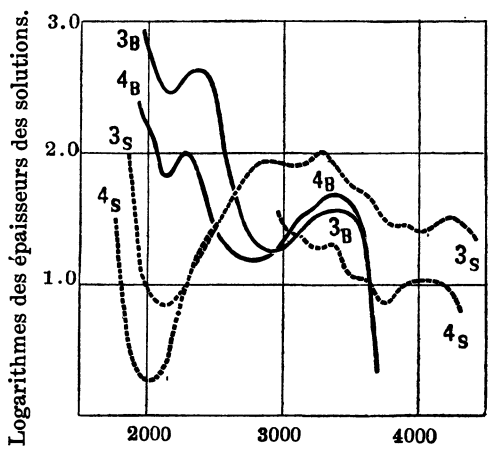
d'un radical azoïque. La deuxième bande (longueur d'onde du centre: 323 mμ en azobenzène) montre en disazobenzène à la longueur d'onde 376 mμ et exprime alors une influence bathochromique. Les variations de deux bandes d'absorption de ces composés peuvent être basées sur le nombre du radical azoïque. La bande halochromique en solution d'acide sulfurique change sa position de 429 mμ (azobenzène) à 513 mμ (disazobenzène) de longueur d'onde et cette transposition hyperchromique et bathochromique correspond à celle de première et deuxième bandes d'absorption produites par les solutions benzéniques. Seulement, la bande halochlomique donnée par l'azobenzène (courbe 1) montre une influence hypsochromique en la comparant avec la première bande de sa solution benzénique.

Composés azoïques d'une série diphényle. (*Influence du radical diphényle*). En substituant le noyau benzénique d'azobenzène par celui



1_B Azobenzène (Solution C_6H_6)
1_S ,, ,, (Solution H_2SO_4 conc.)
2_B Disazobenzène (Solution C_6H_6)
2_S ,, ,, (Solution H_2SO_4 conc.)

Fig. 1.



3_B Phénylazodiphényle (Solution C_6H_6)
3_S ,, ,, (Solution H_2SO_4 conc.)
4_B Azodiphényle (Solution C_6H_6)
4_S ,, ,, (Solution H_2SO_4 conc.)

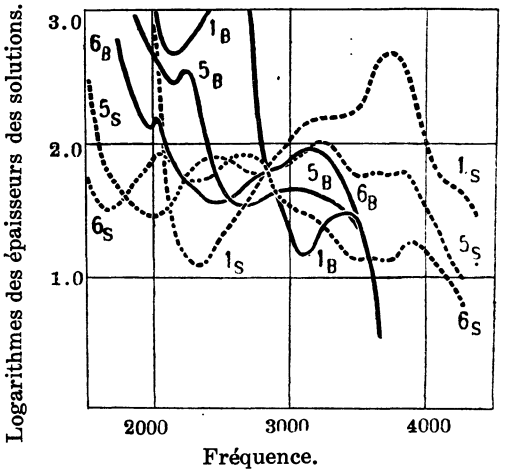
Fig. 2.

de diphényle, la couleur du cristal change au jaune ou au jaunâtre, tandis que celle d'azobenzène est orange, c'est-à-dire la couleur du cristal tourne de plus en plus pâle en remplaçant le radical benzénique par celui diphényle. L'absorption en solution benzénique manifeste cependant un effet hyperchromique et bathochromique (fig. 2). La première bande en solution benzénique d'azodiphényle (longueur d'onde du centre: 469 mμ) est plus

hyperchromique que celle de phénylazodiphényle (longueur d'onde du centre: 463 mμ), mais la deuxième bande de cette première substance montre encore une faible transposition bathochromique (de 342 mμ à 362 mμ de longueur d'onde centrale).

La bande halochromique est étroite et celle d'azodiphényle (courbe 4_s) est plus hyperchromique et plus bathochromique (de 470 mμ à 495 mμ) que celle de phénylazodiphényle (courbe 3_s) (fig. 2). Une sinuosité observée entre 3000 et 4000 de fréquence en bande halochromique est probablement une caractéristique du noyau diphényle.

Influence du noyau naphtalénique sur les spectres d'absorption. L'introduction du noyau naphtalénique dans les composés benzéniques grandit la largeur de la deuxième bande, et, en même temps, donne sensiblement un effet bathochromique (fig. 3). La longueur d'onde centrale de la deuxième bande d'azobenzène est 323 mμ; de benzène azo-α-naphtalène, 378 mμ et d'α,α'-azonaphtalène, 408 mμ. L'effet hyperchromique observé dans ces composés est moindre que celui des corps montrés dans les figures 1 et 2.



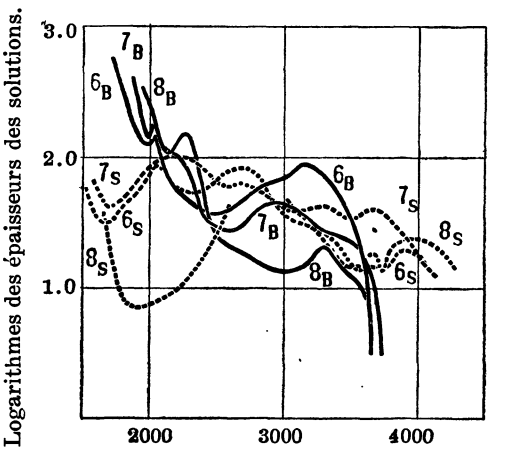
1_B Azobenzéne (Solution C_6H_6)
1_S ,, ,, (Solution H_2SO_4 conc.)
5_B Benzène azo-α-naphtalène (Solution C_6H_6)
5_S ,, ,, (Solution H_2SO_4 conc.)
6_B α,α'-Azonaphtalène (Solution C_6H_6)
6_S ,, ,, (Solution H_4SO_4 conc.)

Fig. 3.

La bande d'absorption par l'halochromie, comme on peut la trouver dans la figure 3, présente plutôt une influence hypochromique par l'augmentation du radical naphtalénique et, en comparant avec les autres hydrocarbures, les bandes halochromiques sont moins étroites en largeur.

Isomérie de position des hydrocarbures azonaphtaléniques et l'absorption des rayons lumineux. La figure 4 montre l'absorption des trois isomères de position des azonaphtalènes qui sont différents à la position connective entre deux radicaux naphtalénique et azoïque. Parmi les bandes d'absorption en solution benzénique, comme on voit à la figure 4, la première bande d'α,α'-azonaphtalène (courbe 6_B) est plus batho-

chromique que celle du β,β'-composé (courbe 8_B) (le centre des bandes se trouve à 520 mμ au corps α,α' et à 467 mμ au corps β,β') et on peut encore dire que le composé α,β' contient peut-être les bandes de ses isomères. Pour les deuxième bandes d'absorption, le corps α,α' se trouve au voisinage de celui α,β'; tandis que le composé β,β' a son centre dans la région de longueurs d'onde beaucoup plus basses (la position du centre est à 408 mμ pour α,α'; à 390 mμ pour α,β' et 333 mμ pour β,β'). Parmi ces trois isomères, le pouvoir absorbant du β,β' est le plus puissant, c'est-à-dire le plus hyperchromique.



6_B α,α'-Azonaphtalène (Solution C_6H_6)
6_S ,, ,, (Solution H_2SO_4 conc.)
7_B α,β'-Azonaphtalène (Solution C_6H_6)
7_S ,, ,, (Solution H_2SO_4 conc.)
8_B β,β'-Azonaphtalène (Solution C_6H_6)
S_S ,, ,, (Solution H_2SO_4 conc.)

Fig. 4.

La bande halochromique du composé α,α' est aussi semblable à celle du α,β' mais très différente de celle du β,β' (l'absorption par l'halochromie se trouve son centre à 599 mμ pour α,α'; à 588 mμ pour α,β' et à 527 mμ pour α,β'). Cette bande halochromique du β,β' est plus large et encore fort hyperchromique que celle des ses deux isomères. Les bandes produites par l'halochromie sont généralement divisées en de nombreuses petites bandes dans la région ultraviolette et c'est peut-être une caractéristique du noyau naphtalénique.

Halochromie des composés azoïques. M. P. Pfeiffer[9] a déjà exposé dans son ouvrage que les corps azoïques, comme des cétones ou des imines, forment des composés moléculaires avec des acides ou des sels métalliques et, dans ce cas, de nouveaux corps moléculaires formés montrent de couleurs plus profondes que les composés originaux, ce qui est une halochromie typique. Jusqu'à présent, la recherche sur l'halochromie a été principalement limitée aux cétones insaturées ou aux composés de série de triphénylméthane, et pour les corps azoïques, le sel hydrofluorique d'azobenzène ou ses autres sels comme perchlorate, hydrochlorique et

(9) P. Pfeiffer, "Organische Molekülverbindungen," 194, (1927).

azotate sont seulement connus. C'est pourquoi, le mémoire dans ce domaine est encore comparativement insuffisant.

On a déjà cependant publié, comme une conclusion spectrochimique, qu'une bande d'absorption étroite et nette est trouvée aux cétones. Nous avons aussi observé cette caractéristique en solutions d'acide sulfurique des hydrocarbures azoïques (figs. 1–4). Nous pouvons obtenir un cristal en appliquant le tetrachlorure d'étain en solution toluique de ces carbures azoïques et la couleur de ce cristal obtenu dans ce cas est même que celui déjà donné en solution d'acide sulfurique concentré. Tous ces résultats nous donnent une vérification expérimentale aux idées proposées par M. P. Pfeiffer, et nous pouvons donc assigner une formule développée $\left[\begin{matrix}Ar-N=N-Ar' \\ \quad H \quad\end{matrix}\right]^+X^-$ aux composés halochromiques, substances additives.

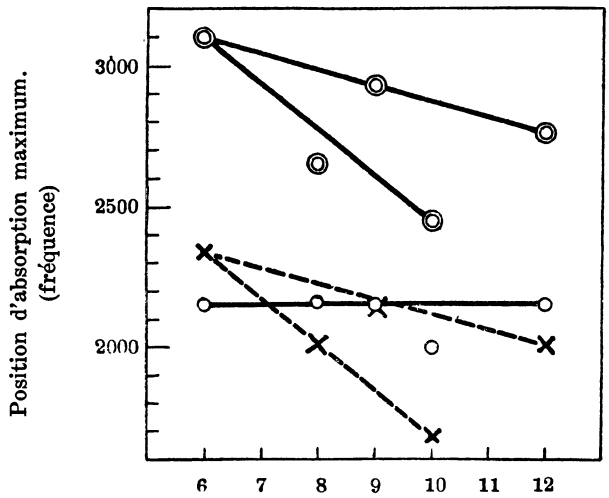
Si on fait recristalliser le précipité obtenu en versant la solution d'acide sulfurique concentré à la glace, le corps azoïque original est établi, ce qu'on nous conduit à penser que cette substance halochromique est celle d'addition. Mais quand on laisse cette solution d'acide sulfurique concentré à elle-même pendant de longues heures ou la chauffe, une sulfonation apparaît et quelquefois même une décomposition se produit.

La concentration d'acide sulfurique pour faire l'halochromie a une limite convenable, et quand nous diluons cette solution concentrée par l'addition de l'eau, l'hydrolyse se produit en se fanant subitement avec la précipitation. Si nous ajoutons alors l'acide sulfurique concentré pour renforcer sa concentration, la couleur se rétablit et la réaction est donc réversible. La limite de concentration d'acide sulfurique est 1.5 de densité pour l'azobenzène, et à peu près 1.6 pour les autres hydrocarbures azoïques.

Plus le poids moléculaire du composé devient grand, plus la concentration d'acide sulfurique doit être élevée pour faire colorer la solution. Quand nous déterminons un coefficient d'extinction d'une bande d'absorption halochromique donnée par des hydrocarbures azoïques, l'intensité des corps, comme une base, peut être connue. La variation de couleur des matières colorantes azoïques par un acide peut généralement être supposée de composé halochromique des hydrocarbures azoïques en tenant compte d'effet auxochromique des radicaux remplacés.

Régularité sur l'absorption des rayons lumineux par les hydrocarbures azoïques. L'absorption des rayons lumineux par des hydrocarbures azoïques est fondée sur le nombre d'une liaison double conjuguée dans le noyau aromatique (le noyau benzénique est supposé d'avoir trois liaisons doubles) et celui d'un radical azoïque, et la position du centre et l'intensité d'une bande en sont déterminées.

Les hydrocarbures azoïques montrent les deux bandes d'absorption (une large et une étroite) dans un dissolvant organique comme le benzène et ils donnent aussi la bande halochromique par l'acide sulfurique concentré qui a une forme caractéristique. La première bande d'absorption est peut-être due au radical azoïque, et sa position d'absorption maximum est cependant à peu près indépendante de l'augmentation du radical azoïque et du nombre des liaisons doubles conjuguées, puis son pouvoir absorbant est basé sur la nature du noyau introduit. Pour la deuxième bande au contraire, sa position, son intensité et sa forme sont considérablement influencées par des noyaux aromatiques insérés.



Nombre de liaison double dans les noyaux aromatiques.

6: Azobenzène
8: Benzène azo-α-naphtalène
9: Phénylazodiphényle
10: α,α′-Azonaphtalène
12: Azodiphényle

○ Première bande d'absorption (Solution C_6H_6)
◎ Deuxième bande d'absorption (,, ,,)
× Bande d'absorption halochromique (Solution H_2SO_4 conc.)

Fig. 5.

La variation du pouvoir absorbant d'une bande halochromique correspond à la première bande d'absorption en solution benzénique, tandis que la transposition d'une bande d'absorption à la deuxième bande.

La figure 5 nous exprime que l'invariabilité de la position centrale de la première bande d'absorption des hydrocarbures azoïques, l'azobenzène comme l'étalon, est montrée en solution benzénique. On peut encore observer en figure 5 que la deuxième bande d'absorption et la transposition de l'absorption maximum de la bande halochromique donnent une rela-

tion linéaire dans une homologue (série diphényle ou série naphtalénique) et en même temps parallèle.

Résumé.

Les résultats obtenus dans les recherches actuelles peuvent résumer comme suit:

(1) Les solutions benzéniques des hydrocarbures azoïques actuellement étudiés donnent une première absorption faible des rayons lumineux dans la région visible, et une deuxième dans la région ultraviolette.

(2) La position centrale de la première bande d'absorption n'exprime pas de grandes différences dans les hydrocarbures azoïques étudiés.

(3) Une transposition bathochromique de la deuxième bande d'absorption est sensiblement observée par l'augmentation du radical azoïque ou du nombre de liaison double, tandis que la première bande a une tendance à devenir moins nette.

(4) Pour la deuxième bande d'absorption, la série des composés naphtaléniques montre une largeur plus grande que celle benzénique et diphényle.

(5) Dans les présents hydrocarbures azoïques, la transposition d'absorption maximum de la deuxième bande en solution benzénique et celle par l'halochromie produite par l'acide sulfurique concentré exprime une relation linéaire et parallèle dans une homologue en augmentant le nombre de liaison double dans les noyaux aromatiques.

(6) La bande d'absorption halochromique donnée par une solution d'acide sulfurique concentré a une forme caractéristique, et les deux bandes d'absorption observées en solution benzénique n'y sont plus reconnues. La bande halochromique a généralement une forme étroite et elle est plus bathochromique que la deuxième bande en solution benzénique montrée par le même corps. Cependant son influence hyperchromique est quelquefois trouvée.

(7) La concentration d'acide sulfurique pour donner l'halochromie a une certaine limite. Quand on laisse une solution colorée à elle-même ou on la chauffe, elle se change chimiquement. La substance colorée obtenue par l'halochromie est peut-être une substance additive formée entre l'acide et le composé azoïque.

En terminant cet exposé, les auteurs sont très heureux d'exprimer leurs sincères remerciements envers la Société "Hattori-Hôkôkaï" qui a bien voulu se cherger d'une partie des dépenses de leurs recherches.

Laboratoire de Chimie minérale, Faculté des Arts et Métiers de Tokyo (Tokyo Kogyô-Daigaku).

On the Nature of Foam. I. Stability of the Foam Produced by the Aqueous Solutions of Alcohols and Acids.

By Tunetaka SASAKI.

(Received July 13, 1938.)

The phenomena of the foam formation have been studied for long time by numerous investigators referring, for example, to the brewing and soap industries, the process of flotation of minerals, priming of boiler water, and other practical cases, as well as on the theoretical standpoints. Attemps have been made to explain the mechanism of foaming.

The relation between the foaming and the surface tension which was considered to be the most important factor for the foam formation was studied by Ramsden,[1] Metcalf,[2] Freundlich,[3] Bartsch,[4] and others. They concluded that the foams are stabilised when there exist the difference in concentrations of the solute between the surface and the bulk of solution, the depression of the surface tension by adsorption, and the film formation. Ostwald and Steiner,[5] however, showed that there are stable foam systems of large surface tension, aqueous humic acid solution, for example, and that the lowering of the surface tension even breaks the foam. They pointed out that some other factors than the surface tension must be introduced to explain the mechanism of the foam formation. Further, the following factors are generally considered to affect the foam formation, and many reports have been published concerning them: orientation,[6] hydration,[6][7] adsorption,[8] rigidity[1][9][10] or structural viscosity,[5] electrical charge,[5][10] gelation,[1][4] and evaporation[6][11] of films or surface layers respectively. None of these factors in itself shows the simple relation to the foam formation. Accordingly,

(1) W. Ramsden, *Z. physik. Chem.*, **47** (1904), 336.
(2) M. V. Metcalf, *Z. physik. Chem.*, **52** (1905), 1.
(3) H. Freundlich, "Kapillarchemie," 1091, (1924).
(4) O. Bartsch, *Kolloid-Beihefte*, **20** (1925), 1; *Kolloid-Z.*, **38** (1926), 177.
(5) Wo. Ostwald and A. Steiner, *Kolloid-Z.*, **36** (1925), 342.
(6) D. Talmud and S. Suchowolskaja, *Z. physik. Chem.*, **154** (1931), 277.
(7) R. H. Bogue, *J. Am. Chem. Soc.*, **44** (1922), 1343.
(8) C. W. Foulk, *J. Ind. Eng. Chem.*, **21** (1929), 815; **23** (1931), 1283.
(9) O. Rohde, *Ann. Physik*, **19** (1906), 935.
(10) P. Rehbinder and E. Wenström, *Kolloid-Z.*, **53** (1930), 145.
(11) H. A. Neville and T. H. Hazlehurst, *J. Phys. Chem.*, **41** (1937), 545.

it is desirable, prior to the discussion of this problem, to analyse the phenomena of the foam formation precisely.

The most important property characterising the foam formation is the stability of foam. It can also be considered as the durability or the life time of foam. The other factor sometimes adopted but not so distinct is the foam producing power. This factor was vaguely considered by Bartsch[4] and lately explained by Foulk[8] to be the possibility of film formation when two surfaces in one liquid approaches each other, and was called "Balanced-layer theory". The following examples are given to explain the above consideration. When we shake the dilute aqueous solutions of saponin and acetic acid, following differences are observed. The foam of saponin solution is more stable but less foamy than that of acetic acid solution. Further, beer and champagne are both foamy but the foam of the former is more stable than that of the later. The foam formation, therefore, may be considered to consist of two factors,[12] namely the stability of foam and the foam producing power, but the latter factor is rather indistinct and quantitative measurements are only possible for the former, so it is desirable that we can explain the mechanism of the foam formation without considering the latter factor.

The measurement of the stability of foam is the important method for the study of the foam formation and is carried out by several means. For example, a vessel containing the solution under investigation is shaken and the volume or the height of foam produced and the duration of its existence are measured.[4] Sometimes the current of air or other gas of constant pressure and volume is passed through the solution instead of the shaking.[8][13] The former method is mainly applicable to the solution producing a stable foam such as the aqueous solution of saponin or soap. Other factors than the stability of foam may affect the results obtained by the former method. The latter method, however, gives quantities only proportional to the stability of foam, and is mainly applicable to the measurement of the unstable foam such as produced in the aqueous fatty acid or alcohol solution.

The present paper describes the measurements of the stabilities of foams of aqueous solutions of fatty acids and alcohols.

Apparatus and Measurement. The apparatus employed in the present experiment has been constructed as shown in Fig. 1. In this figure, A is a bottle containing glass wool and calcium oxide, B the foam produc-

(12) Practically bubble size must be considered still more.

(13) E. L. Lederer, *Z. angew. Chem.*, **47** (1934), 119.

ing tube, C paraffin-oil flow meter, D an empty bottle, E an air current controller consisting of a rubber tube and a screw cock, F an empty flask with a cock for the air leak. The foam producing tube B consists of a glass tube of 1.1 cm. in diameter carrying a porous plate at the bottom.

The measurement is carried out as follows: At first the inner tube of B is carefully cleaned by dipping in boiling water and steaming with water vapour, and dried by passing dry air through it. Then the constant volume (up to the height of 4.5 cm. from the bottom) of liquid for measurement is introduced in the tube by means of water jet pump connected at G, and the air current controller is properly adjusted, so as to obtain the condition in which the flow meter indicates a constant velocity of air current. Then, the air current, passing through the porous plate at the bottom of B, produces bubbles in the liquid, which go up and accumulate to make foam on the surface of the liquid. The height of the foam zone thus produced is measured by the scale attached to the tube. The air current of one atmospheric pressure is introduced into the tube at the velocity of 33.2 c.c./min. or 35 cm./min. in linear velocity, and 3 minutes are passed from the start to attain this velocity. Care is taken not to pass the air current too vigorously, otherwise the border between the bubble and foam zone becomes obscure.

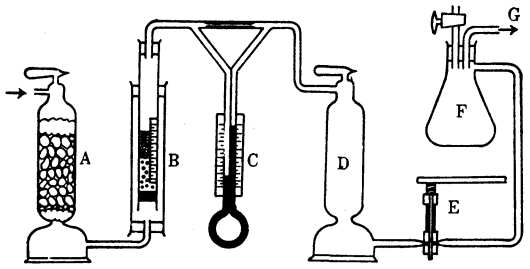


Fig. 1.

Now, we denote with H the height of foam at the stationary state, v the velocity of a bubble ascending the foam zone, and S the stability of the bubble in the foam zone. Then we obtain the following relation:

$$S \cdot v = H, \qquad \text{or} \qquad S = \frac{1}{v} \cdot H .$$

Therefore, if we assume v to be constant, the stability is proportional to the foam height, and we can determine the relative stability of foam if we measure the foam height at the constant velocity of the air current. The foam height has often been measured under the air current of constant static pressure,[8] but such a method, of course, cannot be used under the present experimental conditions. Thus, the diagrams are obtained by plotting the foam height against the time. The foam height at the time zero can be obtained by extrapolation which enables to cancel

the disturbances produced by the evaporation or other factors becoming distinctive in the course of time. Some of the examples of the results obtained by the above method for aqueous solution of *n*-butyl alcohol are shown in Table 1 and Fig. 2.

Table 1. *n*-Butyl alcohol. (0.5378 mol/liter).

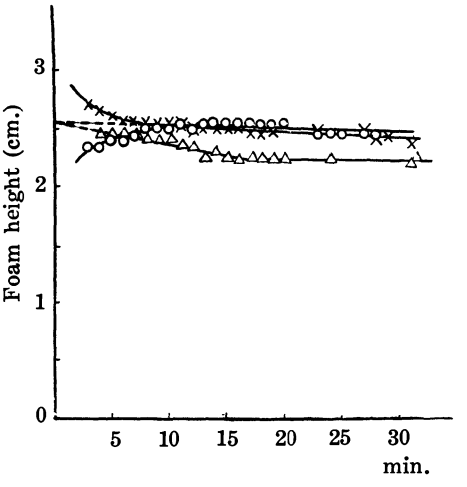
Time (minute)	Height of foam (cm.)			Time (minute)	Height of foam (cm.)		
	1	2	3		1	2	3
3	2.35	2.70	2.35	17	2.25	2.45	2.55
4	2.45	2.65	2.35	18	2.25	2.45	2.55
5	2.45	2.60	2.40	19	2.25	2.45	2.55
6	2.45	2.55	2.40	20	2.25	—	2.55
7	2.45	2.55	2.45	21	—	—	—
8	2.40	2.55	2.50	22	—	—	—
9	2.40	2.55	2.50	23	—	2.45	2.45
10	2.40	2.55	2.50	24	2.25	—	2.45
11	2.35	2.55	2.55	25	—	—	2.45
12	2.35	2.50	2.50	26	—	—	—
13	2.25	2.50	2.55	27	—	2.45	2.45
14	2.35	2.50	2.55	28	—	2.40	—
15	2.25	2.50	2.55	29	—	2.40	—
16	2.25	2.50	2.55	30	—	—	—
				31	2.20	2.35	—

In most cases, diagrams of straight lines are obtained differing in its direction even in the measurements under the same conditions, but the extrapolation of the lines to time zero generally gives the same value of H. There often occur the cases where the foam becomes very high at the beginning of the measurement, or it shows the irregular height with the time, but the stationary state is usually attained after such stages. In the worst case, about twenty minutes are necessary to attain the stationary state.

Prior to the principal experiments, the measurement of the foam height H is carried out at varying velocities of air current and at varying concentrations for the aqueous solution of *n*-hexyl alcohol in order to examine the relation $S \cdot v = H$. The results obtained are shown in Fig. 3.

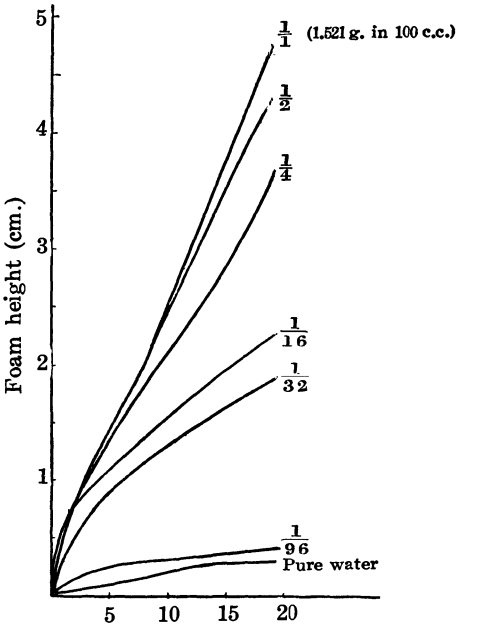
It is concluded from this experiment, that the following equation expresses more closely the relation between v and H.

$$S \cdot v = H - a \,.$$



n-Butyl alcohol.

Fig. 2.



Hexyl alcohol.

Fig. 3.

The correction term a varies with the concentration of the solution, and at slow velocity and optimum concentration, it takes a marked value, but at high speeds as are adopted in this experiment, the value is very small compared with H. So we shall consider the height H to be proportional to the stability S in the present experiment.

Experimental Results. The experimental results are shown in the diagrams (Fig. 4.–Fig. 11.). These diagrams are obtained by plotting the foam heights at the constant velocity of air current against the concentrations of the aqueous solutions of alcohols and fatty acids. At the same time, surface tensions are measured by Du Nöuy's apparatus and plotted against the concentrations. Table 2 shows the numerical data for the solution of *n*-butyl alcohol.

The following conclusions are obtained from the above experiments: (1) The stabilities of foams produced in the pure substances are zero or very small as can be seen from Figs. 4–11 or Table 3.

Measured heights of the foams never exceeded that of one bubble. This agrees with the known fact that the pure liquids do not foam on

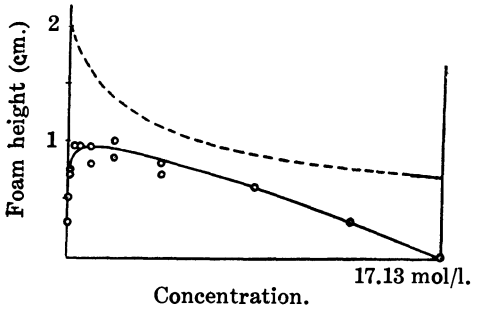


Fig. 4. Ethyl alcohol.

Fig. 4–Fig. 11.

1: Surface tension of the pure alcohol or acid.
2: Foam height of heterogeneous system.
3: Foam height of the pure alcohol or acid.

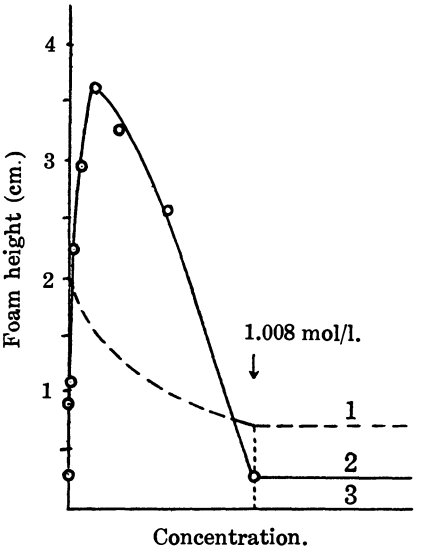


Fig. 5. *n*-Butyl alcohol.

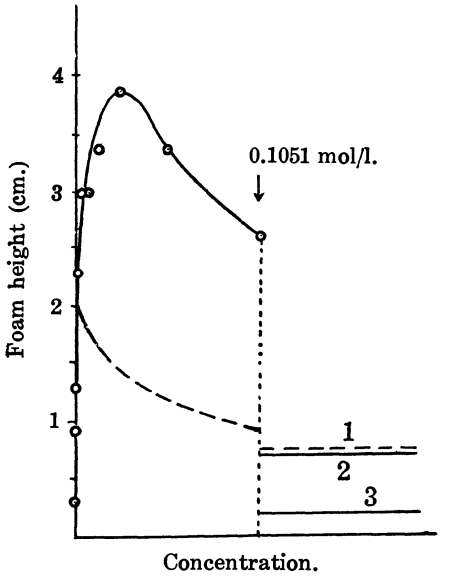


Fig. 6. *n*-Amyl alcohol.

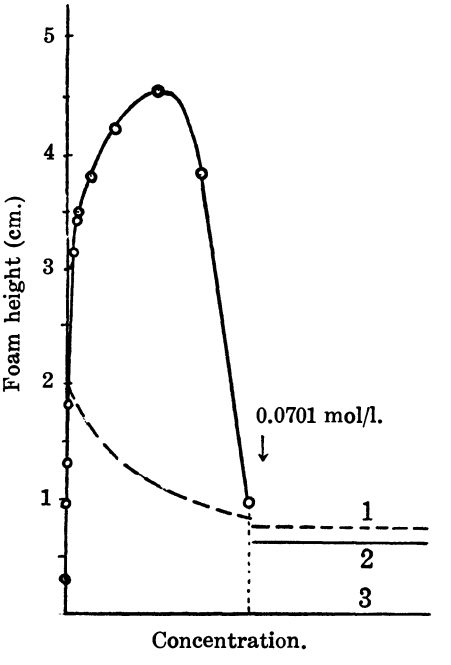


Fig. 7. *n*-Hexyl alcohol.

Table 2. *n*-Butyl alcohol.

Concentration (mol/liter)	Height of foam (cm.)	Surface tension (relative)
0	0.30	1.000
0.0021	0.90	0.998
0.0042	1.10	0.996
0.0084	—	0.981
0.0168	2.24	0.958
0.0336	—	0.908
0.0672	2.96	0.837
0.1345	3.60	0.743
0.2689	3.24	0.632
0.5378	2.54	0.504
1.0080*	0.25	0.372
Heterog. system	0.25	—
Pure butyl alcohol	0.00	0.371

* Saturated solution.

Table 3.

Substance	Height of foam (cm.)	Surface tension (relative)
Water	0.30	1.000
Ethyl alc.	0.00	0.342
n-Butyl alc.	0.00	0.371
n-Amyl alc.	0.20	0.376
n-Hexyl alc.	0.00	0.390
n-Octyl alc.	0.00	0.395
n-Decyl alc.	0.15	0.409
Formic acid	0.00	0.559
Acetic acid	0.00	0.393

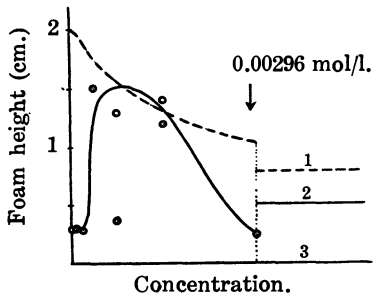


Fig. 8. *n*-Octyl alcohol.

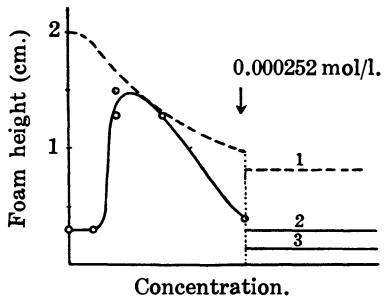


Fig. 9. *n*-Decyl alcohol.

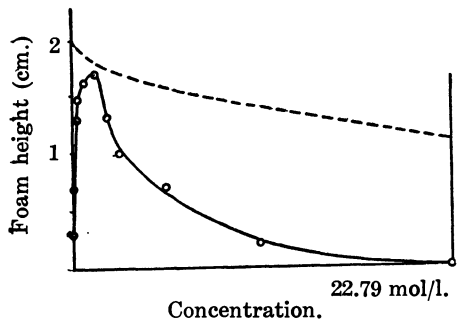


Fig. 10. Formic acid.

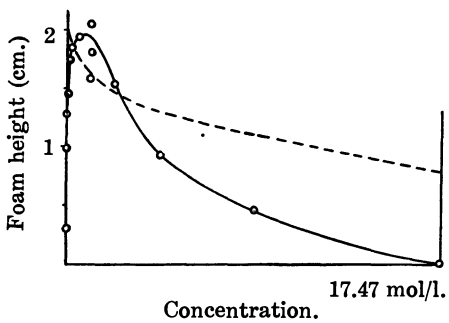


Fig. 11. Acetic acid.

agitation,[8] and is likely to indicate the existence of some relationship between the foam formation and the adsorption. It can also be seen from Table 3 that the absolute magnitude of the surface tension is not the determining factor for the foam formation.

(2) In the aqueous solutions of alcohols and fatty acids, the diagrams of stability and concentration show one marked maximum usually at the concentration where the surface tension falls rapidly with the dilution, namely in the region of the dilute solution. The measurement of stabilities for the solutions of *n*-octyl alcohol shows a remarkable irregularity.

Table 4.

Substance	Conc. of maximum stability		Foam height at maximum stability (cm.)	Surface tension	
	mol/liter	C/C_0*		relative	absolute (dyne/cm.)
Ethyl alc.	1.07	2/32	0.95	0.79	56.9
n-Butyl alc.	0.126	4/32	3.60	0.75	54.0
n-Amyl alc.	0.0131	8/32	3.85	0.81	58.3
n-Hexyl alc.	0.0350	16/32	4.56	0.68	48.6
n-Octyl alc.	0.00105	9/32	1.50	0.75	54.0
n-Decyl alc.	0.0000733	11/32	1.50	0.77	55.1
Formic acid	1.26	1.8/32	1.70	0.90	64.8
Acetic acid	0.819	1.5/32	1.95	0.85	61.2

* Concentration expressed by the fraction of saturated concentration.

In Table 4, the values of surface tension of alcohols in the solutions of maximum stability of foam range from 48 to 59 dynes/cm. They do not always agree with the results obtained by Bartsch[4] in which the maximum stabilities occurred in the solution of the surface tension near 61 dynes/cm. Although the surface tension shows no regularity, there can be seen a certain relationship between the concentration of maximum stability and the number of carbon atoms in the molecule of solute. Namely, the concentration of the maximum stability expressed by mols per liter decreases and that expressed by the fraction of the saturated concentration increases with increasing number of carbon atoms as are shown in Table 4 or in Fig. 12.[14]

(14) Logarithm of the solubility of fatty alcohol in water measured in this experiment is linear to the number of carbon atoms in its molecule.

(3) The foam height at maximum stability increases with increasing number of carbon atoms from ethyl to *n*-hexyl alcohol while decreases with further increase of carbon atom which is shown in Fig. 13. Thus, *n*-hexyl alcohol gives the maximum foam stability. The result may be compared with that obtained by Bartsch[4] who pointed out that iso-amyl alcohol has the maximum foam stability.

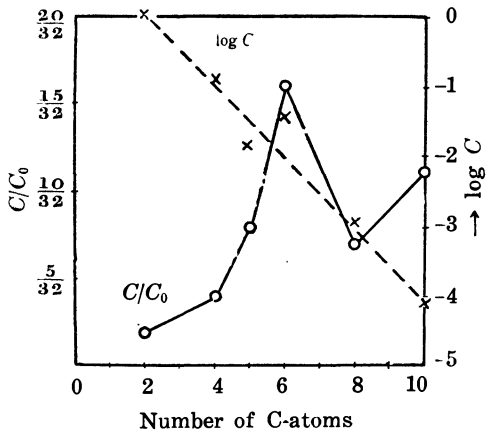
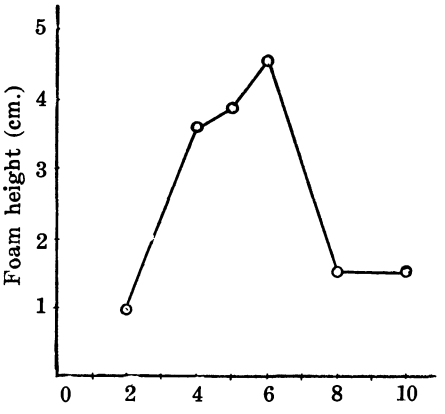


Fig. 12.



Aliphatic alcohols.

Fig. 13.

(4) In the heterogeneous systems of water and *n*-butyl alcohol or the higher homologue which has limited solubility in water, the stability of foam is very small, excepting the case of *n*-amyl alcohol as is shown in Table 5.

Table 5.

Substance	Foam height of heterogeneous system (cm.)
n-Butyl alcohol	0.25
n-Amyl alcohol	0.7
n-Hexyl alcohol	0.6
n-Octyl alcohol	0.5
n-Decyl alcohol	0.3

In the heterogeneous systems of water and surface active or polar substances such as fatty alcohols or acids, the stabilities of foams are usually zero or very small, the explanation of which being given in the preceding note.[15] Namely, the heterogeneous films containing drops of the excess component break the foam produced. In practice, hexyl alcohol or octyl alcohol which is

(15) Sasaki, this Bulletin, **11** (1936), 797.

used as the antifoam is the polar or surface active and hardly soluble substance and favours to produce such heterogeneous films.

On the other hand, there are many cases in which the foams are stabilized even in the heterogeneous systems. The examples are those which consist of an aqueous phase and various non-polar liquid phases of low surface tension, such as benzene or hexane. For instance, foams of the aqueous solution of acetic acid are killed by the addition of hexyl or octyl alcohol in excess, while stabilized by the addition of benzene or hexane in moderate excess.

The author wishes to express his sincere gratitude to Prof. J. Sameshima for his kind guidance. The expense for the experiments has been defrayed by a grant given to Prof. Sameshima from Nippon Gakujutsu Shinkokwai (Japan Society for the Promotion of Scientific Research), to which the author's thanks are due.

Summary.

(1) An apparatus for the measurement of the stability of foam has been described and the stability is measured by the height of the foam produced by the air current of a constant velocity.

(2) The relation between the velocity of the air current v and the height H of the foam produced was examined and the equation $S \cdot v = H - a$ has been obtained, in which S is the stability of foam and a a constant. The value a is negligible compared with H under the conditions of the present experiments.

(3) The measurements of the stabilities were carried out for the aqueous solutions of alcohols and fatty acids, from which several conclusions have been obtained.

Chemical Institute, Faculty of Science,
Imperial University of Tokyo.

Absorption Spectra of Salicylaldehyde-ethylenediimine and Related Compounds.

By Ryutaro TSUCHIDA and Tokuichi TSUMAKI.

(Received July 18, 1938.)

Introduction. One of the authors[1] (T.T.) has reported on a number of inner complexes of *o*-hydroxybenzaldehyde and *o*-hydroxybenzaldimine series. With the aim of throwing light upon the subject, the author[2] has measured the absorption spectra of salicylaldehyde-ethylenediimine-cobalt and determined its steric configuration by applying the trans-diacido-theory[3][4] of the third absorption bands of coordination compounds. On the other hand, the other of the authors[5][6] (R.T.) has been studying absorption spectra of coordination compounds and has come to a conclusion that every chemical linkage might be regarded as coordinate combination or its extreme case and, therefore, the results obtained for absorption spectra of coordination compounds may be widely applied to various inorganic compounds. This conclusion may be further extended even to organic compounds. In other words, entire absorption spectrum of a compound, inorganic or organic, may be regarded generally as a complicated superposition of spectra of a number of coordination groups, each atom in the compound being taken as a coordination center. And to all of these centers may be applied the theory of absorption spectra of coordination compounds.

For the purpose of acquiring further informations of the above-mentioned inner complex, the authors measured the absorption spectra of benzaldehyde-ethylenediimine (dibenzylidene-ethylenediamine), *o*-methoxybenzaldehyde-ethylenediimine, salicylaldehyde-ethylenediimine and *o*-hydroxyacetophenone-ethylenediimine and tried to explain, from the viewpoint of coordination chemistry, these absorption spectra and that of the inner complex as well.

---

(1) P. Pfeiffer, E. Breith, E. Lübbe, and T. Tsumaki, *Ann.*, **503** (1933), 84.
(2) T. Tsumaki, this Bulletin, **13** (1938), 252; *J. Chem. Soc. Japan*, **58** (1937), 1288.
(3) Y. Shibata, *J. Chem. Soc. Japan*, **36** (1915), 1243.
(4) R. Tsuchida, *J. Chem. Soc. Japan*, **59** (1938), 586.
(5) R. Tsuchida, this Bulletin, **13** (1938), 388.
(6) R. Tsuchida, this Bulletin, **13** (1938), 436.

Experimental. Benzaldehyde-ethylenediimine and *o*-methoxybenzaldehyde-ethylenediimine were prepared by the methods of Mason.[7] The molar extinction coefficients $\varepsilon (I = I_0 \times 10^{-\varepsilon cd})$ were measured. The solvent: ethyl alcohol. The concentration: 0.001 mol/l. The thickness of layer: 0.02–15.0 cm.

Salicylaldehyde-ethylenediimine and *o*-hydroxyacetophenone-ethylenediimine were prepared by the method of Mason[8] and that of one of the present authors[9] (T.T.) respectively. The absorption spectra were measured. The solvent: ethyl alcohol. The concentration: 0.0001 mol/l. The thickness of layer: 0.02–15.0 cm. The absorption curves are shown in Fig. 1.

Discussion of the Results. Prior to the discussion on the organic compounds in question, it will be more convenient to describe briefly the main features of the absorption spectra of coordination compounds. An absorption spectrum of a coordination compound generally consists of the first, the second and the third band, accompanied by a few special bands. The first band is due to electron transitions in the unsaturated transition shell of the central ion and is, therefore, one of the most remarkable characteristics of transition elements. The second band is the most general feature of coordination compounds and is due to a kind of incomplete dissociation of a ligand, i.e., a coordinated ion or molecule. It has been found[6] that the frequency of the second band gives the true measure of the strength of the coordinate link. The third band is attributed to a kind of neutralization between the central cation and a ligand anion and appears only when two or more anions are coordinated in trans-positions referring to the coordination center. Those bands which are not proper to the coordination center in question but are attributed to ligands themselves, are defined as special bands. A special band, however, is originally a certain numbered band referred to its own center. It is further known[10] that coordinate combination of a ligand has a bathochromic and hypochromic effect on the absorption bands proper to the ligand. In other words, a special band due to a ligand is less absorptive and has longer wave-length than the corresponding band of the ligand in free state.

Now benzaldehyde-ethylenediimine (I) shows one band at $\nu = 121 \times 10^{13}$ sec.$^{-1}$ *o*-Methoxybenzaldehyde-ethylenediimine (II) has two bands at

(7) A. T. Mason, *Ber.*, **20** (1887), 270, 272.
(8) A. T. Mason, *ibid.*, 271.
(9) P. Pfeiffer, E. Breith, E. Lübbe, and T. Tsumaki, *Ann.*, **503** (1933), 127.
(10) R. Tsuchida and M. Kobayashi, this Bulletin, **13** (1938), 471.

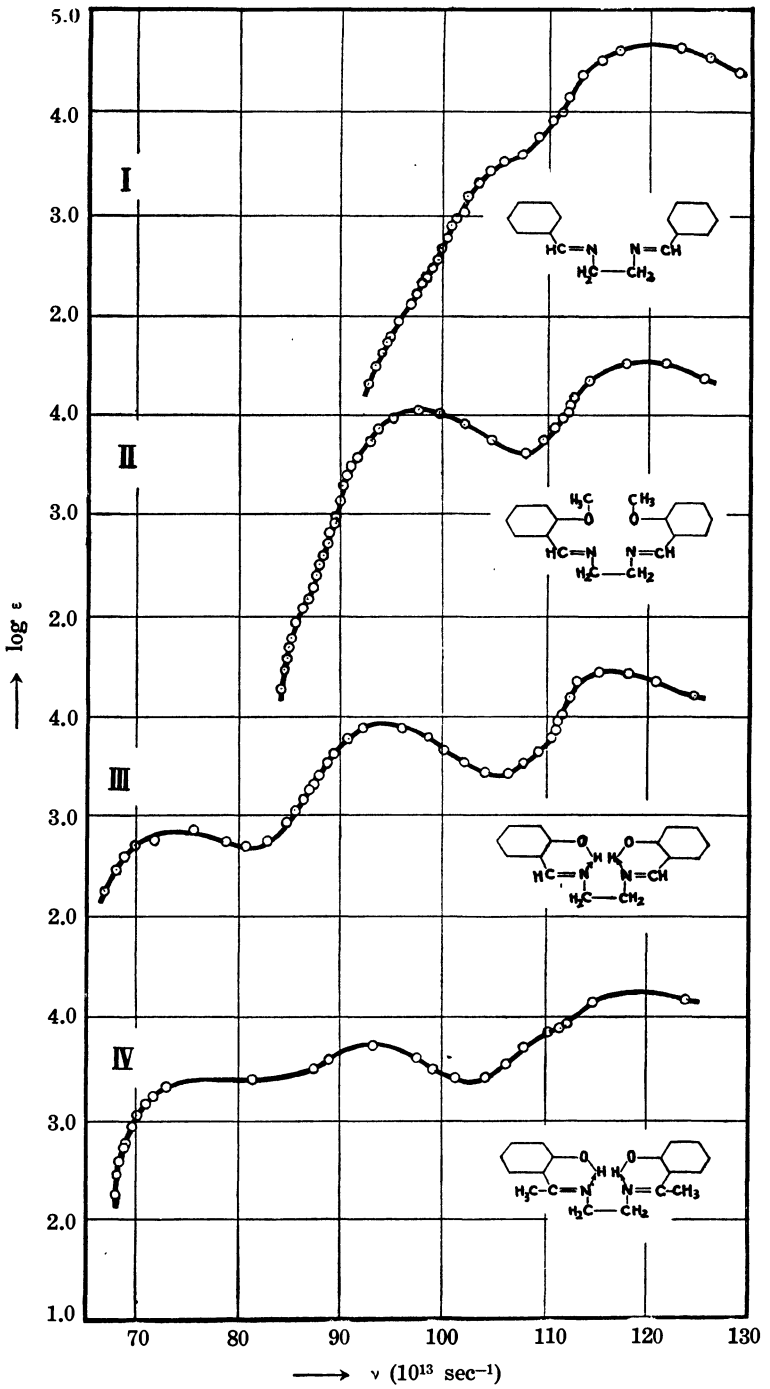

5.0
4.0
3.0
2.0
4.0
3.0
2.0
4.0
3.0
2.0
4.0
3.0
2.0
1.0
I
II
III
IV
log ε
70
80
90
100
110
120
130
ν (10¹³ sec⁻¹)

Fig. 1.

98×10^{13} sec.$^{-1}$ and 120×10^{13} sec.$^{-1}$, of which the latter is a special band proper to benzaldehyde-ethylenediimine(I), as can be seen from its frequency and extinction coefficients. The band at 98×10^{13} sec.$^{-1}$, accordingly, is attributed to CH_3O group. Salicylaldehyde-ethylenediimine (III) shows three bands at 75×10^{13} sec.$^{-1}$, 95×10^{13} sec.$^{-1}$ and 117×10^{13} sec.$^{-1}$ Both the absorption bands of the methoxy-derivative(II) are retained in this compound. The bathochromic and hypochromic effect on these special bands is remarkable: the frequencies of the special bands in salicylaldehyde-ethylenediimine(III) are 95×10^{13} sec.$^{-1}$ and 117×10^{13} sec.$^{-1}$ and the corresponding extinction coefficients are $\log^{-1} 3.9$ and $\log^{-1} 4.4$, whereas those of the absorption bands of methoxy-derivative(II) are 98×10^{13} sec.$^{-1}$, 120×10^{13} sec.$^{-1}$, $\log^{-1} 4.1$ and $\log^{-1} 4.5$ respectively. This fact as well as the band at 75×10^{13} sec.$^{-1}$ indicates that salicylaldehyde-ethylenediimine(III) has another absorption center which could not be found in its methoxy-derivative(II). The band at 75×10^{13} sec.$^{-1}$ is also found in the absorption spectrum of *o*-hydroxyacetophenone-ethylenediimine(IV), whose bands are at 75×10^{13} sec.$^{-1}$, 94×10^{13} sec.$^{-1}$ and 119×10^{13} sec.$^{-1}$, the corresponding extinction coefficients being $\log^{-1} 3.4$, $\log^{-1} 3.8$ and $\log^{-1} 4.3$. Of these the latter two are the special bands of the same origins as those of salicylaldehyde-ethylenediimine(III). The longest-waved band is seen only in the compounds (III and IV) containing OH group, but not in those (I and II) lacking the group. The band is, therefore, characteristic of the OH group, or rather of H in the group, as we have already distinguished the bands due to the absorbing center of O in the compounds (II, III and IV) which have either OH or OCH_3. In order to give rise to a band, the hydrogen atom should be a coordination center. Thus the band at 75×10^{13} sec.$^{-1}$ is attributed to the hydrogen bridge formed between the hydroxyl-group and the nitrogen atom. Then the band should be regarded as the second band of the absorbing center, O—H←N. Whereas Hilbert, Hendricks, Wulf, and Liddel[11] have supposed the existence of a hydrogen bond in a hydroxyl-compound, e.g., nitrophenol, by the absence of the hydroxyl-absorption band in the infrared region (6000 to 7500 cm.$^{-1}$), the present authors have now shown a hydrogen bond by the presence of a coordination band in the ultra-violet region.

The absorption bands of the compounds are summarized in Table 1 where the bands due to the same origin are shown in the same vertical column. Thus the bands under [a] are those which are common to all

(11) G. E. Hilbert, O. R. Wulf, S. B. Hendricks, and U. Liddel, *J. Am. Chem. Soc.*, **58** (1936), 548.

the compounds containing benzaldehyde-ethylenediimine, and those under [b] are attributed to the absorbing unit whose center is O. The bands under [c] are those due to the hydrogen bridge between the hydroxyl-group and the nitrogen atom.

Table 1.

	Compounds	[c]		[b]		[a]	
		$\nu(10^{13})$	log ε	$\nu(10^{13})$	log ε	$\nu(10^{13})$	o g
I	Benzaldehyde-ethylenediimine					121	4.7
II	*o*-Methoxybenzaldehyde-ethylenediimine			98	4.1	120	4.5
III	Salicylaldehyde-ethylenediimine	75	2.9	95	3.9	117	4.4
IV	*o*-Hydroxyacetophenone-ethylenediimine	75	3.4	94	3.8	119	4.3

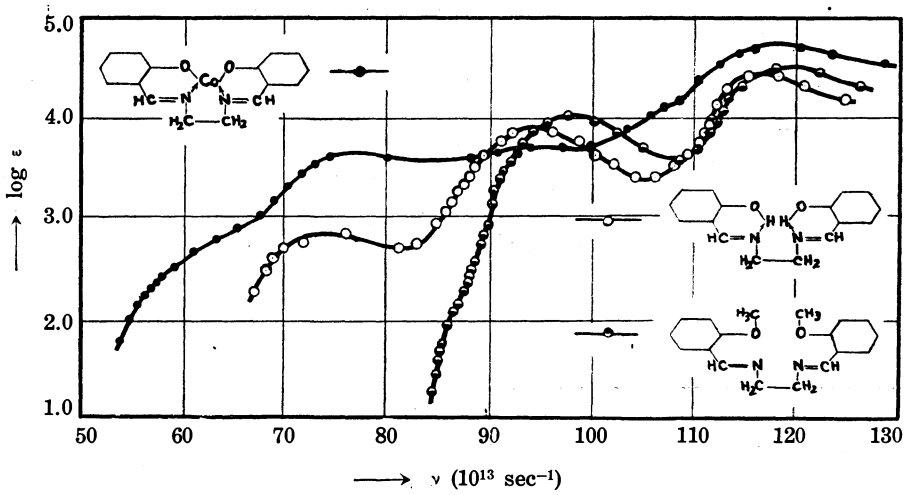


Fig. 2.

When salicylaldehyde-ethylenediimine (III) forms an inner complex with a metal ion, e.g., cobalt, the structure is quite similar to that of the original organic compound. The absorption spectrum of the inner complex[2] is shown in Fig. 2 together with those of salicylaldehyde-ethylenediimine (III) and *o*-methoxybenzaldehyde-ethylenediimine (II). The inner complex has five bands, viz., ca. 60×10^{13} sec.$^{-1}$, 77×10^{13} sec.$^{-1}$, 93×10^{13} sec.$^{-1}$, ca. 110×10^{13} sec.$^{-1}$ and 118×10^{13} sec.$^{-1}$ For this inner

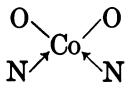
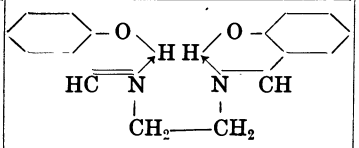
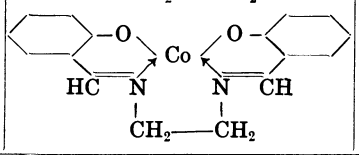
complex the second band of the absorbing center,  , is expected instead of the band due to hydrogen bridge, O—H←N. The band at 77×10^{13} sec.$^{-1}$ is the second band or the coordination band of the cobaltous ion as center, whereas the coordination band of the hydrogen bridge in salicylaldehyde-ethylenediimine is at 75×10^{13} sec.$^{-1}$ It is, therefore, evident that the coordinate link of cobalt with salicylaldehyde-ethylenediimine is more stable[6] than that of hydrogen in the organic compound, and the method of preparing the inner complex[1] may thereby be explained.[6] The longest-waved band at ca. 60×10^{13} sec.$^{-1}$ is the first band due to the incomplete transition shell of the cobaltous ion. The one at 93×10^{13} sec.$^{-1}$ is a special band due to the same origin as those in the column [b] in Table 1: viz., a band attributed to an absorbing unit, whose coordination center is oxygen. The band at about 110×10^{13} sec.$^{-1}$ is also a special band which belongs to the same class as those in the column [a] in the table, i.e., a special band common to all the benzaldehyde-ethylenediimine derivatives. Fig. 2 shows that the two bands of *o*-methoxybenzaldehyde-ethylenediimine(II) undergo the bathochromic and hypochromic effect in salicylaldehyde-ethylenediimine(III) and its inner cobaltous complex(V). The last band of the inner complex at 118×10^{13} sec.$^{-1}$ can not be a special band, as the maximal extinction coefficient is much greater than that of *o*-methoxybenzaldehyde-ethylenediimine(II). It is, therefore, the third band which is attributed to the neutralization between the central cobaltous ion and the phenolate residue. In Table 2 the

Table 2.

	Coordination compounds	1st band		2nd band		Special bands				3rd band	
						[b]		[a]			
		ν_1 (10^{13})	log ε	ν_2 (10^{13})	log ε	ν(10^{13})	log ε	ν(10^{13})	log ε	ν_3 (10^{13})	log ε
III				75	2.9	95	3.9	117	4.4		
V		ca. 60	2.5	77	3.7	93	3.5	ca. 110	4.2	118	4.8

absorption spectra of salicylaldehyde-ethylenediimine and its inner cobaltous complex are compared.

Thus the third band of the inner complex has been confirmed and the asymmetric configuration of the compound which had been reported in the previous paper[2] has thereby been corroborated.

Summary.

(1) Absorption spectra of benzaldehyde-ethylenediimine, *o*-methoxy-benzaldehyde-ethylenediimine, salicylaldehyde-ethylenediimine and *o*-hydroxyacetophenone-ethylenediimine have been measured, and the structures of the spectra have been qualitatively explained by the theories of absorption spectra of coordination compounds.

(2) The longest-waved band of salicylaldehyde-ethylenediimine as well as of *o*-hydroxyacetophenone-ethylenediimine has been explained as due to intramolecular formation of a hydrogen bridge between the hydroxyl group and the nitrogen atom. In other words an absorption band of a hydrogen bond has been found in the near ultra-violet region.

(3) The absorption spectrum of salicylaldehyde-ethylenediimine-cobalt has been explained and the steric configuration of the inner complex has thereby been corroborated.

The authors wish to express thanks to Mr. Z. Mita and Mr. M. Kobayashi for their assistance.

Chemical Department, Faculty of Science,
Imperial University of Osaka.

Über die chemische Natur des Papains. II.[1] Reinigung des Papains durch Taka-Amylase.

Von Shigeo OKUMURA.*

(Eingegangen am 18. Juli 1938.)

Die Münchner Schule hat die Reinigung des Papains mit Hilfe der Adsorption an Tonerde durchzuführen versucht, aber keine nennenswerten Erfolge[2] damit erzielt.

Vor kurzem haben Akabori und Kasimoto[3] die interessante Erscheinung beobachtet, dass das Papain durch Zugabe von Taka-amylaselösung fast völlig aus seiner konzentrierten Lösung gefällt wird. Der so gewonnenen Papain-Amylase-Niederschlag ist vermutlich ein Papain-Amylase-Symplex im Sinn R. Willstätters, da der Niederschlag die beiden enzymatischen Wirkungen von Papain und Amylase von hohem Reinheitsgrade besitzt. Während Papain, sowie Taka-amylase in Wasser leicht löslich ist, ist der „Symplex" im Wasser schwer, aber in Salzlösungen leicht löslich. Da Akabori und Kasimoto[3] die Bindung dieses Symplexes mittels Nukleinsäure auflösen konnten, ist von den genannten Autoren eine weitgehende Reinigung der Amylase erreicht worden. Der Verfasser hat sich bemüht, die Reinigung des Papains über den Papain-Amylase-Niederschlag durchzuführen, und gefunden, dass diese Arbeitsweise bessere Erfolge ergibt als die bisher angewandten üblichen Methoden.

„Papain-Amylase-Symplex" löst man in 2 N Essigsäure-Acetat-Puffer von pH = 5 und lässt die Lösung eine Säule von Aluminiumoxyd durchfliessen. Während Amylase dabei von dem Adsorbens festgehalten wird, geht Papain in die Restlösung über. Die Lösung enthält nun das Papain zu etwa 40% der angewandten Menge in sehr hohen Reinheitsgrade und die Aktivitätserhöhung steigt immer mehr und zwar bis zum Zwanzigfachen der Anfangsaktivität. Das so gereinigtes Papain ist aber infolge der Entfernung der Begleitstoffe sehr unbeständig und koaguliert bei der Dialyse der Lösung gegen Wasser zum grossen Teil. Wird die Adsorptionsrestlösung durch Zugabe von festem Ammoniumsulfat auf Sättigung gebracht, der dabei entstandene Niederschlag in wenig Wasser aufgelöst

---

* Früher Shigeo MAEDA.

(1) I. Mitteilung: dies Bulletin, **12** (1937), 319.

(2) *Z. physiol. Chem.*, **138** (1924), 184; **164** (1927), 10.

(3) *J. Chem. Soc. Japan*, **59** (1938), 563; dies Bulletin, **13** (1938), 453.

und gegen destilliertes Wasser bei 5° dialysiert, ist die Koagulierung des Enzyms bis zu einem gewissen Grade zu vermeiden. Aus der Innenlösung der Dialyse wird durch Fällung mit Aceton ein hochgereinigtes Papainpräparat gewonnen, das 48.46% C, 7.03% H und 13.7% N enthält. Der Tryptophangehalt beträgt 1.39%, also um die Hälfte weniger als der des Ausgangspräparats (3.43%). Während im gereinigten Präparat die SH-Reaktion mit Nitroprussidnatrium weder vor noch nach dem Behandeln mit Blausäure positiv verläuft, ist aber das Präparat, wie aus Tabelle 2 ersichtlich ist, durch Blausäure aktivierbar. Diese Aktivierung beobachtet man nur bei mehrstündiger Einwirkung des Enzyms auf Gelatine, nicht aber bei der Anfangsverdauung. Auf Grund der obigen Tatsachen glaubt der Verfasser Anhaltspunkte dafür gewonnen zu haben, dass die Blausäureaktivierung des Papains nicht auf der Aufspaltung der in dem Enzymkomplex enthaltenen –S–S– Gruppen in SH-Gruppen beruht,[4] wie bisher in zahlreichen Arbeiten ausschliesslich angenommen worden ist, sondern auf der Entfernung des Hemmungskörpers, der im Lauf der Verdauung entsteht oder im Papainpräparat vorkommt. Das Papain ist vielleicht ein spezielles Protein, das eine Aldehyd-Gruppe, aber keine –S–S– Gruppen oder SH-Gruppen trägt, wie der Verfasser schon in der I. Mitteilung erörtert hat.

Beschreibung der Versuche.

I. **Darstellung der Taka-amylaselösung.** 50 g. Taka-amylase wurden in 200 c.c. Wasser gelöst, mit 235 c.c. Methanol versetzt und der von dem abgeschiedenen Niederschlag abzentrifugierten Lösung wiederum 367 c.c. Methanol zugefügt. Der hierbei gewonnene zweite Niederschlag wurde abzentrifugiert, im wenig Wasser gelöst, mittels einer Kollodiumhülse gegen destilliertes Wasser dialysiert und die Innen- und Aussenlösung der Dialyse zur Reinigung von Papain angewandt.

II. **Papaineinheit und Papainwert.** Der Verfasser definiert diejenige Enzymmenge als Papain-Einheit [*P*-(*e*)], die unter den nachstehenden Verdauungsbedingungen einen COOH-Zuwachs entsprechend 1 c.c. einer 0.2 N KOH ergibt. Als Mass für den Reinheitsgrad wird der Papain-Wert [*P*-(*w*)] vorgeschlagen, welcher die Anzahl der Papain-Einheiten in 10 mg. Präparat angibt.

Ausführung der Bestimmung. Eine Mischung von 5 c.c. 5%iger Gelatinelösung, 5 c.c. N/5 Essigsäure-Acetat-Puffer (pH = 5) und (5 − x) c.c. destilliertem Wasser versetzt man mit x c.c. der zu bestimmenden unbekannten Menge von Papainlösung (Gesamtvolumen 15 c.c.). Nachdem die Mischung 10 Minuten bei 36° verblieben ist,

(4) W. Grassmann, *Z. angew. Chem.*, **44** (1931), 105; *Biochem. Z.*, **279** (1935), 131; Th. Bersin, *Ergeb. Enzymforsch.*, **4** (1935), 68; *Z. physiol. Chem.*, **220** (1933), 209; **222** (1934), 177; E. Maschmann, *ibid.*, **219** (1933), 99; **228** (1934), 141; *Biochem. Z.*, **277** (1935), 97.

wird sie unter Zusatz von Formol titriert. Bei der Bestimmung der Papain-Einheit darf der COOH-Zuwachs nicht über 0.2 Milliäquivalent (1.0 c.c. 0.2 N KOH) steigen; denn der COOH-Zuwachs ist bei den erwähnten Verdauungsbedingungen nur innerhalb der obigen Grenze der verwandten Enzymmenge proportional, wie in Abb. 1 graphisch dargestellt ist.

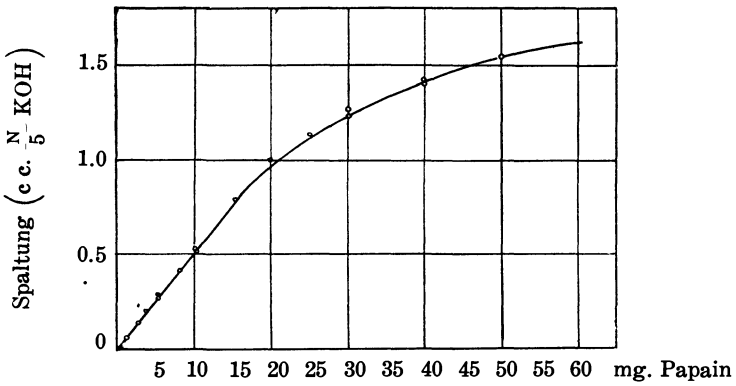


Abb. 1. Papainmenge und Grad der Hydrolyse.

III. **Vorreinigung des Papains.** 100 g. Handelspapain wurden mit 500 c.c. destilliertem Wasser durchgeschüttelt, 4–5 Stunden bei Zimmertemperatur stehen gelassen, abzentrifugiert und mittels einer Kollodiumhülse 17 Stunden lang bei 5° gegen Wasser dialysiert. Aus der Innenlösung (SH-Reaktion war sehr deutlich) wurde das Papain durch Zusatz von Aceton gefällt und über Schwefelsäure unter Vakuum getrocknet (SH-Reaktion war sehr schwach). 50 g. des getrockneten Papains ($[P\text{-}(e)]=390$, $[P\text{-}(w)]=0.06$) wurden in 250 c.c. N Essigsäure-Acetat-Puffer vom pH = 5 gelöst, zweimal mit je 30 g. Aluminiumoxyd behandelt, abzentrifugiert und in der Restlösung sowohl die Enzymmenge als auch der Reinheitsgrad bestimmt. Mittels dieser Behandlung kann man den Reinheitsgrad auf das Doppelte steigern ($[P\text{-}(e)]=330$, $[P\text{-}(w)]=0.14$).

IV. **Reinigung des Papains durch Amylase.** (1) *Versuche mit der Innenflüssigkeit der Dialyse von Taka-amylase.* Versetzt man 100 c.c. Papainlösung ($[P\text{-}(e)]=132$, $[P\text{-}(w)]=0.14$) mit einer überschüssigen Menge von 10%iger Taka-amylaselösung, so entsteht ein dunkelbrauner Papain-Amylase-Niederschlag N_1, welcher abzentrifugiert wird. Aus dem Filtrat lässt sich durch Zugabe der fünffachen Menge destillierten Wassers der zweite Niederschlag N_2 fällen. Der erste Niederschlag N_1 wird in 2N Essigsäure-Acetat-Puffer vom pH = 5 aufgelöst und nun durch eine mit Al_2O_3 gefüllte Röhre, welche vor der Adsorption mit der selben Pufferlösung gewaschen worden ist, sehr langsam hindurchgesaugt. Dabei wird die Amylase auf dem Adsorbens festgehalten, während das Papain in die Restlösung geht. Nach dreimaliger Adsorption wird das Papain durch Zugabe von festem Ammoniumsulfat ausgesalzen und die Suspension daraufhin mehrere Stunden in einem kalten Raum absitzen gelassen. Die klare obere Flüssigkeit wird mit einem Heber abgetrennt und die Suspension mittels einer Kollodiumhülse bei 5° dialysiert. Die Innenflüssigkeit filtriert man ab, fällt

mit dem sechsfachen Volumen an Aceton und trocknet im Vakuum über Schwefelsäure. Ein wie oben gereinigtes Papainpräparat zeigt einen Papain-Wert von 1.38.

Der zweite Niederschlag N_2 wird in gleicher Weise behandelt, wobei fast dasselbe Resultat ($[P\text{-}(w)] = 1.36$) gewonnen wird. Die Experimente wird in Tabelle 1 schematisch angegeben.

(2) *Versuche mit Aussenflüssigkeit der Dialyse von Taka-amylase.* Die Versuche mit der Aussenamylase (Amylase in der Aussenflüssigkeit der Dialyse) ergaben fast gleiche Resultate.

Tabelle 1.

Vorgereinigte Papainlösung 100 c.c.
$[P-(e)] = 132$; $[P-(w)] = 0.14$

Innenflüssigkeit der Amylase zugesetzt

Niederschlag N_1 $[P-(e)] = 74.90$; $[P-(w)] = 0.28$	Filtrat
	Zugabe von 5 Volumina Wasser
in 2 N CH_3COOH-CH_3COONa-Puffer (pH = 5) gelöst, adsorbiert an Al_2O_3	Niederschlag N_2 $[P-(e)] = 57.0$; $[P-(w)] = 0.27$
Restlösung	in 2 N CH_3COOH-CH_3COONa-Puffer (pH = 5) gelöst, adsorbiert an Al_2O_3
Ausgesalzen mit $(NH_4)_2SO_4$, dialysiert	Restlösung
Innenlösung	Ausgesalzen mit $(NH_4)_2SO_4$, dialysiert
Fällung mit 6 Volumina Aceton	Innenlösung
	Fällung mit 6 Volumina Aceton
Papain-Präparat $[P-(e)] = 30.0$; $[P-(w)] = 1.38$	Papain-Präparat $[P-(e)] = 24.0$; $[P-(w)] = 1.36$

V. **Aktivierung des gereinigten Papains.** Zu 10 c.c. der Adsorptionsrestlösung (Trockengewicht 2.6 mg. pro 1 c.c.) fügt man 10 c.c. einer 3%igen Blausäurelösung hinzu, lässt 2 Stunden lang in einem Thermostaten von 36° voraktivieren, versetzt dann 80 c.c. 5%ige Gelatin-lösung, pipettiert nach verschiedenen Zeiträumen je 10 c.c. ab und prüft die Aktivität mit Hilfe der Formoltitration. Die Versuchsresultate sind in Tabelle 2 zusammengestellt.

Tabelle 2.

COOH-Zuwachs (c.c. $^{N}/_{5}$ KOH)					
Stunde	$^{1}/_{6}$	1	3	5	24
ohne HCN	0.36	1.04	1.80	2.03	2.80
mit HCN	0.32	1.15	2.10	2.75	3.85

An dieser Stelle möchte ich Herrn Prof. S. Akabori und Herrn K. Kasimoto für ihre liebenswürdigen Ratschläge und freundliche Unterstützung meinen herzlichen Dank aussprechen.

Chemisches Institut der Kaiserlichen Universität zu Osaka.

Absorptionsspektren von Metallkomplexsalzen des 2,2′-Dipyridyls. II.

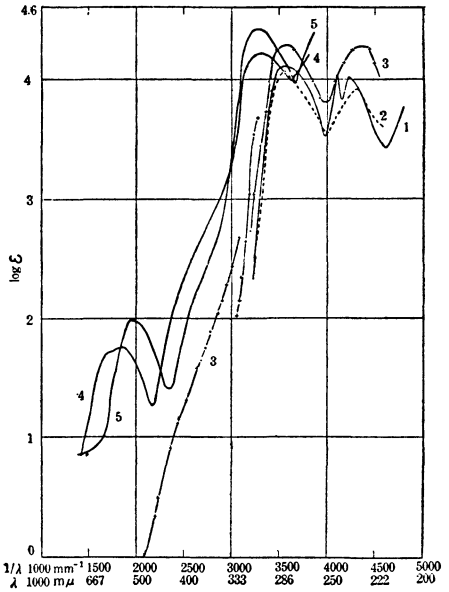
Von Kazuo YAMASAKI.

(Eingegangen am 23. Juli 1938.)

Die vorliegende Arbeit ist die Fortsetzung der vorangehenden Mitteilung[1] über die Absorptionsspektren der Dipyridyl-Metallkomplexe. Die hierein untersuchte Verbindungen sind 2,2′-Dipyridyl selbst, und $[Mn(Dip)_2]Cl_2$, $[Co(Dip)_2Cl_2]Cl{\cdot}2H_2O$ (Violeosalz) und $[Co(Dip)_2CO_3]Cl{\cdot}2H_2O$, hierbei *Dip* bedeutet Dipyridyl.

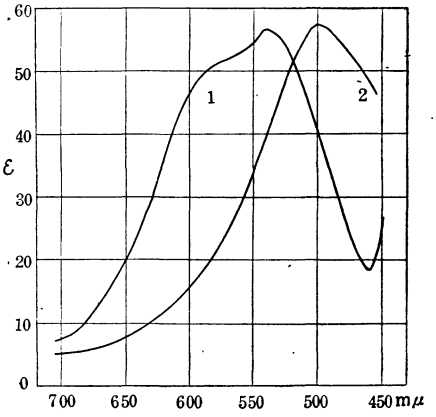
Die Absorptionsspektren wurden mit Hilfe von Quarzspektrographen (Hilger E2) nach der Henrischen Methode aufgenommen. In sichtbarem Gebiet wurde die Messung auch mit dem Nuttingschen Spektrophotometer durchgeführt. Als Lichtquelle dienten Eisen-Nickel Funken, Glühlampe und Wasserstofflampe je nach der Bedingungen. Die Absorptionskurven sind in den Abb. 1 und 2 gegeben, in welchen auf der Ordinate der molare Extinktionskoeffizient (ε) oder seine Logarithmen aufgetragen wurde.

(1) Dies Bulletin, **12** (1937), 390.



Kurve 1: 2,2′-Dipyridyl in Hexan.
„ 2: „ in Wasser.
„ 3: [Mn (*Dip*)$_2$] Cl$_2$.
„ 4: [Co (*Dip*)$_2$ Cl$_2$] Cl (Violeosalz).
„ 5: [Co (*Dip*)$_2$ CO$_3$] Cl.

Abb. 1.



Kurve 1: [Co (*Dip*)$_2$Cl$_2$] Cl (Violeosalz).
„ 2: Dasselbe nach Erhitzung.

Abb. 2.

2,2′-Dipyridyl: Die Absorptionsmessung dieser Substanz wurde nochmals von neuem durchgeführt, aber das Resultat zeigte keine Unterschiede zu der früheren Messung,[1] nämlich

In Hexan: $\lambda =$ 280 mμ, $\log \varepsilon = 4.12$;
„ 244 „ „ „ 4.03;
„ 235–236 „ „ „ 4.03.
In Wasser: $\lambda =$ 280 mμ, $\log \varepsilon = 4.1$;
„ 230–232 „ „ „ 3.93.

Wibaut und Spiers[2] haben das Absorptionsspektrum von dieselben Verbindung in Heptanlösung studiert. Nach ihren Angaben liegen die Banden an 2830 Å ($\log\varepsilon = 4.14$) und 2390 Å ($\log\varepsilon = 4.12$) und die Feinstruktur wurde ebenfalls nicht beobachtet.

(2) J. P. Wibaut und C. W. F. Spiers, *Rec. trav. chim.*, **56** (1937), 573.

$[Mn(Dip)_2]Cl_2$: 2 Mol $MnCl_2$ wurde in Wasser gelöst, mit 1 Mol Dipyridyl in Alkohol versetzt und die entstandene gelbe Lösung auf dem Wasserbad eingedampft. So erhaltene gelbe Krystalle sind ziemlich schwer löslich in kaltem Wasser. Die Analyse dieser neuen Verbindung ergab: Gefunden: Mn, 12.70; N, 13.95; Cl, 16.31. Berechnet für $Mn(Dip)_2Cl_2$: Mn, 12.55; N, 12.78; Cl, 16.20%. Es enthält kein Krystallwasser.

Die Absorption dieses Mn-Komplexes wurde in wässrigen Lösungen von Konzentration 1/200, 1/2000 und 1/10000 Mol untersucht.

$$\lambda = 280 \text{ m}\mu, \quad \log \varepsilon = 4.25^{(3)};$$
$$\text{,,} \quad 230\text{–}233 \text{ ,, ,} \quad \text{,,} \quad 4.25.$$

Wie ersichtlich aus der Absorptionskurve (Abb. 1) ist das Beersche Gesetz nicht gültig, und die Lagen der Absorptionsbanden im Ultraviolett stimmen gut mit den des freien Dipyridyls überein. Diese Tatsache zeigt, dass das Komplexsalz bei grosser Verdünnung die Zersetzung erleidet. Die analoge Erscheinung wurde auch bei $[Mn(Dip)_3]Cl_2$ beobachtet.[4]

$[Co(Dip)_2Cl_2]Cl \cdot 2H_2O$ (Violeosalz): Dieses Komplex wurde durch Oxydation des Gemisch von 2 Mol Dipyridyl und 1 Mol Kobaltchlorid hergestellt.[5] Die Aquotisierung dieses Salzes verursacht die allmähliche Veränderung der Lösungsfarbe. Die Absorptionsmessung der frischen Lösung ergibt:

$$\lambda = 540 \text{ m}\mu, \quad \log \varepsilon = 1.76 \ (\varepsilon = 57);$$
$$\text{,,} \quad 302 \text{ ,, ,} \quad \text{,,} \quad 4.20;$$

während, nach der Erhitzung von derselben Lösung etwa eine Stunde lang auf dem Wasserbad, die Bandenverschiebung nach Violett, zwar bis zu $\lambda = 500$ mμ, $\log\varepsilon = 1.76 \ (\varepsilon = 57.5)$ beobachtet wurde.

Vergleicht man die Lage der Banden in sichtbarem Teil mit den der anderen Violeosalze, so erkennt man, dass die Verwechselungen der Liganden in Komplexionen nur wenig auf die Bandenlage beeinflussen:

---

(3) Da das Salz sich in verdünnten Lösungen zersetzt, sind die ε-Werte dieser Banden nicht die wahre molare Extinktionskoeffizienten.

(4) G. T. Morgan und F. H. Burstall, *J. Indian Chem. Soc., Ray Commemoration Vol.* S. 15; "Inorganic Chemistry", S. 195 (1936).

(5) F. M. Jaeger und J. A. van Dijk, *Z. anorg. Chem.*, **227** (1937), 273. Wenn das Gemisch von $CoCl_2$ und Dipyridyl mit wenig HCl versetzt und im Exsikkator ohne Oxydation mit H_2O_2 eingedampft wird, entsteht eine grüne Salz aus der Masse. Über dieses Salz wird es später berichtet werden.

$[Co(NH_3)_4Cl_2]Cl$	: $\lambda = 540.\,m\mu$, $\varepsilon = 47$	Mathieu.[6]
$[Co(en)_2Cl_2]Cl$	: ,, 535 ,, , ,, 100	
,,	: ,, 530 ,, , ,, 95	Uspensky und Tschibisoff.[7]
Dasselbe nach der Erhitzung auf dem Wasserbad	: ,, 500 ,, , ,, 65	

$[Co(Dip)_2CO_3]Cl$[5]: Das Kohlenstoffdioxyd wurde in der mit Na_2CO_3 versetzten Lösung des Violeosalzes $[Co(Dip)_2Cl_2]Cl$ eingeleitet und die so entstandene rote Lösung eingedampft. Dunkelrote Krystalle. Die Absorptionsmessung dieser Lösung ergibt:

$\lambda = 510\ m\mu$, $\log \varepsilon = 1.98$;
,, 503 ,, , ,, 4.41.

Die Lagen der Banden der bisher untersuchten Carbonatosalze sind wie folgende:

$[Co(NH_3)_4CO_3]Br$: $\nu = 57.2 \times 10^{13}\ sec.^{-1}$ (525mμ), $\log \varepsilon = 2.02$ Tsuchida.[8]

$[Co(NH_3)_4CO_3]Cl$	: $\lambda = 526\ m\mu$	Shibata.[9]
$[Co(en)_2CO_3]Cl$	: ,, 526 ,,	

Die Bande des Dipyridylcarbonatosalzes wird demnach nach Violett um 15 mμ verschoben.

Der Vergleich der Wellenlängen der Banden von drei Dipyridylkomplexe: $[Co(Dip)_2Cl_2]Cl$, $[Co(Dip)_2CO_3]Cl$ und $[Co(Dip)_3]Cl_3$ ist hierunter angegeben:

$[Co(Dip)_3]Cl_3$: 450 mμ, 319, 307 mμ;
$[Co(Dip)_2Cl_2]Cl$: 540 ,, , 302 mμ;
$[Co(Dip)_2CO_3]$: 510 ,, , 303 ,, .

Also ersieht man, dass die erste Bande, durch die Substitution von einer Molekül des Dipyridyls durch 2 Cl^- oder CO_3^{--}, stark nach Rot verschoben wird.

---

(6) J. P. Mathieu, *Bull. soc. chim.*, [5], **3** (1936), 463.
(7) A. Uspensky und K. Tschibisoff, *Z. anorg. Chem.*, **164** (1927), 329.
(8) R. Tsuchida, dies Bulletin, **13** (1938), 395.
(9) Y. Shibata, *J. Coll. Sci., Imp. Univ. Tokyo*, **37**, Art. 2 (1915), 12.

Wie schon erwähnt in der ersten Mitteilung, sind die zwei Absorptionsbanden im Ultraviolett den allen Dipyridylkomplexsalzen ganz charakteristisch, indem die Bandenformen sich eine bedeutende Ähnlichkeit mit den des freien Dipyridyls zeigen und die eine von denen bei ca. 300 mμ und die andere bei 245 mμ liegen. Dagegen fehlt diese zweite Bande (245 mμ) den jetzt untersuchten drei Kobalti-Dipyridyl-Komplexsalzen, während die erste (ca. 300 mμ) ungefähr an der rechten Lage zum Vorschein kommt.

Diese im Ultraviolett befindlichen Banden stimmen jedoch nicht mit den des freien Dipyridyls (280 mμ und 230–232 mμ) in ihrer Wellenlängen überein; deswegen ist es sehr wahrscheinlich, dass sie den Dipyridylmoleküle die in koordinativer Bindung mit zentralem Metallatom stehen, zuzuschreiben. Nur sei es erwähnt, dass das $[Mn(Dip)_2]Cl_2$ in grosser Verdünnung, wegen der hydrolytischen Spaltung, die Banden der freien Dipyridyl-molekül zeigt.

Zusammenfassung.

Es wurden die Extinktionskurven von 2,2′-Dipyridyl im Hexan und Wasser, von $[Mn(Dip)_2]Cl_2$, $[Co(Dip)_2Cl_2]Cl$ (Violeosalz) und $[Co(Dip)_2CO_3]Cl$ im Wasser bei Zimmertemperatur zwischen 220 mμ und 700 mμ studiert. Die Zersetzung von $[Mn(Dip)_2]Cl_2$ in verdünnter Lösung wurde aus ihrem Kurvenverlauf deutlich wahrgenommen.

Es sei mir gestattet, Herrn Prof. Yuji Shibata für seine freundliche Anleitung und Ratschläge bei der Ausführung dieser Arbeit meinen herzlichen Dank auszusprechen.

Chemisches Institut, Naturwissenschaftliche Fakultät,
Kaiserliche Universität zu Tokyo.

Diffusion des an schwerem Wasserstoff sowie schwerem Sauerstoff angereicherten Wassers durch verdünntes Gelatingel.

Von Noriyoshi MORITA und Toshizo TITANI.

(Eingegangen am 30. Juli 1938.)

Inhaltsübersicht. Die Diffusion des Wassers, das an beiden Arten der schweren Isotope des Wasserstoffs und Sauerstoffs angereichert worden ist, durch verdünntes (etwa 5-prozentiges) Gelatingel wird nach zwei verschiedenen Methoden untersucht. Aus den ersten Reihen der Versuche (Versuch A) ergibt sich die Selbstdiffusionskonstante des Wassers durch verdünntes Gelatingel $D = 1.12$ cm.^{2}/Tag bei 6°C., dagegen aus den zweiten (Versuch B) $D = 1.83$ cm.^{2}/Tag bei derselben Temperatur. Die wahre Diffusionskonstante dürfte zwischen diesen beiden extremen Werten liegen. Aber in jedem Fall finden wir, dass das schwere Sauerstoffatom ebenso schnell wie das schwere Wasserstoffatom diffundiert. Daraus wird geschlossen, dass die eventuell vorhandene Extradiffusion der Wasserstoffatome durch dessen Austausch zwischen zwei benachbarten Wassermolekülen im Vergleich mit der gewöhnlichen Massendiffusion des Wassers vernachlässigt werden kann.

Einleitung. Nach dem Versuch von Wirtz[1] wurde gefunden, dass die Austauschreaktion der H- bzw. D-Atome zwischen leichtem und schwerem Wasser:

$$H_2O + D_2O \rightleftarrows 2HDO \qquad (1)$$

fast unmessbar so schnell stattfindet und das Austauschgleichgewicht wenigstens innerhalb 20 Sek., die kürzeste Zeit, die er erreichen konnte, schon vollständig hergestellt wird. Er schätzte weiter die obere Grenze der Reaktionszeit nach der Theorie von Hückel[2] sowie von Bernal und Fowler[3] für die anomale Beweglichkeit der H^+- und OH^--Ionen (Protonaustauschmechanismus!) und kam zu dem Ergebnis, dass diese etwa 1/100 Sek. oder kleiner als dies sein dürfte. Wenn der Austausch der H-Atome zwischen zwei benachbarten Wassermolekülen so schnell stattfindet, dann kann unter Umständen die Möglichkeit bestehen, dass Wasserstoffatome bei der Selbstdiffusion des Wassers schneller als Sauerstoffatome diffundieren. Diese Extradiffusion des Wasserstoffatom können wir durch die Untersuchung der Diffusion des schweren Wassers durch gewöhnliches Wasser (oder vice versa) ausfindig machen.

(1) K. Wirtz, *Z. Physik*, **104** (1937), 613.
(2) E. Hückel, *Z. Elektrochem.*, **34** (1928), 546.
(3) J. D. Bernal und R. H. Fowler, *J. Chem. Phys.*, **1** (1933), 515.

Aus dieser Erwartung bestimmten Orr und Butler[4] die Diffusionskonstante des schweren Wassers (HDO) durch gewöhnliches Wasser. Aber weil die von ihnen gefundene Diffusionskonstante D des schweren Wassers, die z.B. bei 0.1°C. $D = 1.26$ und bei 14.3°C. $D = 14.3$ cm.^{2}/Tag beträgt, in der Grössenordnung wohl im Rahmen der anderen normalen Substanzen, wie z.B. des Ammoniaks ($D = 1.00$ cm.^{2}/Tag bei 10°C.) liegt, kam man zum Schluss, dass die eventuell vorhandene Extradiffusion der Wasserstoffatome im Vergleich mit der gewöhnlichen Massendiffusion der Wassermoleküle vernachlässigt werden kann. Obwohl auf diese Weise auf die Nichtexistenz der Extradiffusion der Wasserstoffatome durch den Austauschmechanismus auf mittelbarem Wege hingewiesen wurde, untersuchten wir dies doch auf noch unmittelbarem Wege zu bestätigen. Wir liessen nämlich das an beiden Arten der schweren Isotope des Wasserstoffs und Sauerstoffs angereicherten Wasser durch gewöhnliches Wasser diffundieren und verglichen dadurch die Diffusionsgeschwindigkeit der Wasserstoff- und Sauerstoffatome.

Versuchsmethode. Da die Diffusion des schweren Wassers in einem vollkommen flüssigen Medium zu untersuchen nicht sehr leicht ausführbar war, benutzten wir in der vorliegenden Arbeit als Diffusionsmedium ein verdünntes Gelatingel anstatt reines Wassers. Wir bereiteten aus gewöhnlichem Wasser und Gelatin ein verdünntes Gelatingel und lassen das schwere Wasser dadurch diffundieren (oder vice versa). Dabei muss man natürlich davor sicher sein, dass die isotopische Zusammensetzung des benutzten schweren Wassers durch die eventuell aufzutretende Austauschreaktion der Wasserstoff- und Sauerstoffatome zwischen Wasser und Gelatin nicht beeinflusst wird. Dass aber dies wirklich nicht der Fall ist, bestätigten wir durch einen Kontrollversuch. Zu diesem Zweck bereiteten wir zunächst ein schweres Gelatingel, das etwa dieselbe chemische und isotopische Zusammensetzung wie die des beim Hauptversuch benutzten besass, indem wir 1.5 g. gewöhnliches luftgetrocknetes Gelatin in ca. 30 c.c. schweren Wassers auflösten. Das dazu benutzte schwere Wasser war an den beiden Arten der schweren Isotope angereichert worden und besass den gesamten Dichteüberschuss von 51.1 γ gewöhnlichem Wasser gegenüber, wovon etwa 57% (d.h. 29 γ) von der Anreicherung des schweren Sauerstoffs herrührte. Nachdem dieses schwere Gelatingel bei Zimmertemperatur einige Tage lang stehen gelassen worden, wurde das darin enthaltene Wasser durch die Destillation im Vakuum vollständig abdestilliert aufgefangen und dessen Dichte,

(4) W. J. C. Orr und J. A. V. Bulter, *J. Chem. Soc.*, **1935**, 1273.

nachdem es auf übliche Weise richtig gereinigt worden, genau bestimmt. Dies ergab aber in Übereinstimmung mit dem anfänglichen Dichteüberschuss des verwendeten Wassers, dass es um 51.4 γ schwerer als gewöhnliches Wasser ist und zwar davon 29.1 γ von der Anreicherung des schweren Sauerstoffs herrührt. Wir dürfen deshalb wohl schliessen, dass die isotopische Zusammensetzung des diffundierenden schweren Wassers durch die eventuell verlaufende Austauschreaktion zwischen Wasser und Gelatin, wenigstens unter den hier benutzten Versuchsbedingungen, praktisch nicht beeinflusst wird.

Bei der praktischen Durchführung der Diffusionsversuche unter Benutzung des Gelatingels können wir wenigstens drei Methoden in Betracht ziehen, wie schematisch in der nebenstehenden Abb. 1 gezeigt wird.

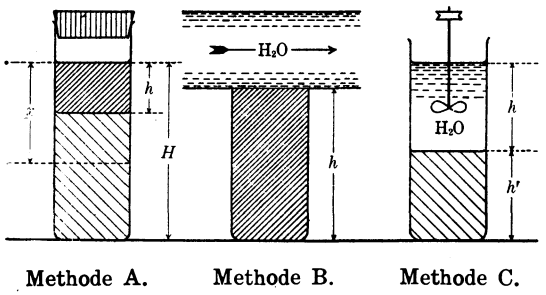


Abb. 1. Die schematische Darstellung der Messmethode der Diffusionskonstante des schweren Wassers durch Gelatingel.

Bei der Methode A füllen wir zunächst ein zylindrisches Gefäss vom Boden bis zur Höhe $(H-h)$ cm. mit dem aus gewöhnlichem Wasser bereiteten Gelatingel (der schräg aber grob gestrichene Teil in Abb. 1 A!) und darauf wird weiter ein Gelatingel aus schwerem Wasser (der schräg und dicht gestrichene Teil in Abb. 1 A!) um die Dicke h geschichtet, so dass die ganze Höhe der im Gefäss gebildeten Gelatinsäule H cm. beträgt. Unter dieser Vorrichtung diffundiert das schwere Wasser von der oberen schweren Gelatinschicht zur unteren leichten Gelatinschicht hinein, so dass die Dichte des Wassers, das in einem bestimmten Punkt in der unteren Schicht befindlich ist, mit der Zeit allmählich zunimmt. Wenn auf diese Weise die Dichte des um x cm. unter dem oberen Ende der Gelatinsäule befindlichen Wassers während der Zeit t um Δs über die des gewöhnlichen Wassers vermehrt worden ist, dann wird die Diffusions-

konstante D des schweren Wassers durch Gelatingel mittels Gl. (2) angegeben:[5]

$$\frac{\Delta s}{\Delta s_0} = \frac{h}{H} + \frac{2}{\pi} \sum_{n=1}^{\infty} \frac{1}{n} \sin \frac{n\pi h}{H} \cos \frac{n\pi x}{H} e^{-\left(\frac{n\pi}{H}\right)^2 Dt} \qquad (2),$$

wo Δs_0 den anfänglichen Dichteüberschuss des benutzten schweren Wassers gewöhnlichem Wasser gegenüber darstellt. Dabei benutzt man als Δs_0 und Δs entweder den gesamten d.h. zur Anreicherung der beiden Arten der schweren Isotope des Wasserstoffs und Sauerstoffs zurückzuführenden Dichteüberschuss oder den partiellen d.h. zur Anreicherung der nur einen Art der schweren Isotope des Wasserstoffs bzw. Sauerstoffs zurückzuführenden Dichteüberschuss, je nachdem ob es sich dabei um die Diffusion der beiden Arten oder nur der einen Art der H- bzw. O-Atome handelt.

Bei der Methode B füllen wir das gegebene zylindrische Gefäss ganz bis zur oberen Öffnung mit Gelatingel, das aus schwerem Wasser hergestellt worden (der schräg und dicht gestrichene Teil in Abb. 1 B!). Das so gefüllte Gefäss stellen wir nun in fliessendes, gewöhnliches Wasser, um das im Gelatingel befindliche schwere Wasser ins letztere diffundieren zu lassen. Wenn auf diese Weise der Dichteüberschuss des im Gelatin enthaltenen schweren Wassers während der Zeit t von Δs_0 bis unter Δs abgenommen hat, dann wird die Diffusionskonstante D des schweren Wassers durch das Gelatingel mittels Gl. (3) errechnet:[5]

$$D = -\frac{4h^2}{t\pi^2} \ln \left\{1 - \frac{\pi^2(\Delta s_0 - \Delta s)}{8\Delta s_0}\right\} \qquad (3).$$

Die Diffusionskonstante des Wassers durch Gelatingel können wir auch nach der Methode C in Abb. 1 bestimmen. In diesem Fall füllen wir das zylindrische Gefäss vom Boden bis zur Höhe h' mit dem Gelatingel, das aus gewöhnlichem Wasser hergestellt worden (der schräg aber grob gestrichene Teil in Abb. 1 C!) und darauf wird weiter eine Schicht schweren Wassers, das den anfänglichen Dichteüberschuss von Δs_0 besitzt, um die Dicke h gelegt. Diese letztere wird aber während des Versuchs tüchtig umgerührt, um deren Inneres durchaus homogen zu halten. Wenn auf diese Weise in einer bestimmten Zeitlänge t der Dichteüberschuss des oben geschichteten schweren Wassers vom anfänglichen Δs_0 bis unter zum endlichen Δs herabgesunken ist, dann können wir die

(5) Vgl. z.B. J. W. Mellor, „Higher Mathematics for Students of Chemistry and Physics", Longmans, Green & Co., London (1913).

Diffusionskonstante D des schweren Wassers durch das Gelatingel nach Gl. (4) ermitteln:[6]

$$\frac{\Delta s_0 - \Delta s}{\Delta s_0} = \frac{1}{2} - \sum_{n=1}^{\infty} \frac{8}{(2n+1)^2\pi^2} e^{-(2n+1)^2 \frac{\pi^2}{4} \frac{Dt}{h^2}} \qquad (4).$$

Bei dieser Gleichung setzten wir aber einfachheitshalber $h' = h$.

In der vorliegenden Arbeit bedienten wir uns unter den oben skizzierten drei Methoden der ersteren zwei, nämlich der Methode A und B. Die dadurch ausgeführten Versuche nennen wir weiter unten resp. Versuch A und B.

Versuch A. Wir benutzten als Messgefäss einen Glaszylinder von 5 cm. l.W. Diesen füllen wir zunächst von Boden bis zur Höhe $10 \times \frac{5}{6}$cm. $(= H-h)$ mit der Gelatinlösung, die aus gewöhnlichem Wasser und Gelatin bereitet worden und etwa 5 gewichtsprozentiges Gelatin enthält. Während der Erstarrung dieser Lösung bedecken wir diese mit gewöhnlichem Wasser, um dadurch ein Eintrocknen der Oberfläche des gebildeten Gelatingels zu verhüten. Dann wird das geschichtete Wasser abgegossen und unmittelbar darauf wird an dessen Stelle eine Schicht von schwerem Gelatingel sorgfältig hergestellt. Dabei geben wir besonders darauf acht, dass keine Luftblasen oder dergleichen bei der Grenzschicht der beiden Arten der Gelatingele eingeschaltet werden. Das zur Bereitung des schweren Gelatingels benutzte Wasser ist bei beiden Arten der schweren Isotope des Wassrstoffs und Sauerstoffs angereichert worden und besitzt den gesamten Dichteüberschuss von 40 bis 50 γ, wovon ca. 60% (d.h. 23 bis 30 γ) von der Anreicherung des schweren Sauerstoffs herrührt (vgl. weiter unten Tabellen 1). Da die Dicke der so hergestellten schweren Gelatinschicht $h = 10 \times \frac{1}{6}$ cm. beträgt, macht die Gesamthöhe der im Gefäss gebildeten Gelatinsäule $H = 10 \times \frac{5}{6} + 10 \times \frac{1}{6} = 10$ cm. aus. Dieses Gefäss wird, nachdem es mit einem Korkstöpsel (der senkrecht gestrichene Teil in Abb. 1 A) dicht geschlossen worden, in eine Kühlkammer geschoben und dort bei $6 \pm 1°$C. verschiedene Tagelängen stehen gelassen. Dies dauert beim ersten Versuch (A1) 11 Tage, beim zweiten (A2) 6 Tage und beim letzten (A3) 13 Tage. Hierauf wird das Gefäss aus der Kühlkammer herausgenommen und die darin befindliche Gelatinsäule sorgfältig herausgeschüttet. Dann werden aus

(6) H. W. March und W. Weaver, *Phys. Rev.*, **31** (1928), 1072; L. Friedman und E. O. Kraemer, *J. Am. Chem. Soc.*, **52** (1930), 1295.

dieser Gelatinsäule an einigen Stellen, die je um einen bestimmten Abstand (x cm.) von ihrem oberen Ende entfernt sind, senkrecht zu ihrer Achse, Scheiben von etwa 1 cm. Dicke abgeschnitten, und diese sofort im Vakuum der Destillation unterworfen, um das darin enthaltene Wasser vollständig abdestilliert aufzufangen. Die Dichte des so abgetrennten Wassers vergleichen wir, nachdem es auf die übliche Weise richtig gereinigt worden, mittels eines Schwimmers mit der des gewöhnlichen Wassers. Dabei bestimmen wir nicht nur den gesamten Dichteüberschuss des abgetrennten Wassers, sondern auch bei einigen ausgewählten Fällen solch einen Dichteüberschuss, der allein auf die Anreicherung des schweren Sauerstoffs zurückzuführen ist.[7] Diese beiden Arten von Dichteüberschuss unterscheiden wir in den unterstehenden Tabellen 1 resp. mit der Bezeichnung

Tabelle 1. Ergebnisse der Versuche A.

Versuch A1. $\Delta s_0(G) = 51.4 \pm 0.5\,\gamma$, $\Delta s_0(O) = 29.1 \pm 1\,\gamma$, $\Delta s_0(O)/\Delta s_0(G) = 57 \pm 2\%$, $t = 11$ Tage.

$9x/H$[8]	$\Delta s(G)$ in γ	$\Delta s(G)/\Delta s_0(G)$	$\Delta s(O)$ in γ	$\Delta s(O)/\Delta s(G)$ in %	Dt in cm.^{2}
0.7	13.1	0.255	—	—	12.6
6.9	4.8	0.093	2.3	48±21	12.2

Mittel $Dt = 12.4$ cm.^{2}

$\therefore\ D = 12.4/11 = 1.13$ cm.^{2}/Tag.

Versuch A2. $\Delta s_0(G) = 27.0 \pm 0.5\,\gamma$, $\Delta s_0(O) = 23.5 \pm 1\,\gamma$, $\Delta s_0(O)/\Delta s_0(G) = 64 \pm 3\%$, $t = 6$ Tage.

$9x/H$	$\Delta s(G)$ in γ	$\Delta s(G)/\Delta s_0(G)$	$\Delta s(O)$ in γ	$\Delta s(O)/\Delta s(G)$ in %	Dt in cm.^{2}
0.5	13.1	0.354	8.6	66±7	6.4
2.5	9.6	0.259	—	—	7.8
6.0	2.3	0.062	—	—	5.6
8.0	1.4	0.038	—	—	7.7

Mittel $Dt = 6.9$ cm.^{2}

$D = 6.9/6 = 1.12$ cm.^{2}/Tag.

(7) Die isotopische Analyse des Wassers führten wir nach der schon in der früheren Arbeit, wie z.B. N. Morita, K. Goto und T. Titani, dies Bulletin, **13** (1938), 99, beschriebenen Methode aus.

(8) Um die praktische Durchführung der Berechnung mittels Gl. (1) zu erleichtern, massen wir den Abstand x nicht in cm. sondern in der Einheit von $H/9$, wo H die Gesamtlänge der Gelatinsäule ausdrückt. Infolgedessen drückt der Wert $(9x/H)$ nichts anderes aus als die in dieser Einheit gemessene Länge des Abstands der untersuchten Gelatinschicht vom oberen Ende der Gelatinsäule.

Versuch A3. $\Delta s_0(G) = 37.0 \pm 0.5\,\gamma$, $\Delta s(O) = 23.5 \pm 1\,\gamma$,
$\Delta s_0(O)/\Delta s_0(G) = 64 \pm 3\%$, $t = 13$ Tage.

$9x/H$	$\Delta s(G)$ in γ	$\Delta s(G)/\Delta s_0(G)$	$\Delta s(O)$ in γ	$\Delta s(O)/\Delta s(G)$ in %	Dt in cm.^{2}
0.5	9.3	0.252	—	—	13.8
2.5	7.9	0.213	3.8	48 ± 13	14.0
6.0	5.1	0.138	3.1	61 ± 20	14.8
8.0	3.5	0.095	—	—	14.0

Mittel $D = 14.1_5$ cm.^{2}

$\therefore$ $D = 14.1_5/13 = 1.09$ cm.^{2}/Tag.

Totalmittel $D = 1.12$ cm.^{2}/Tag.

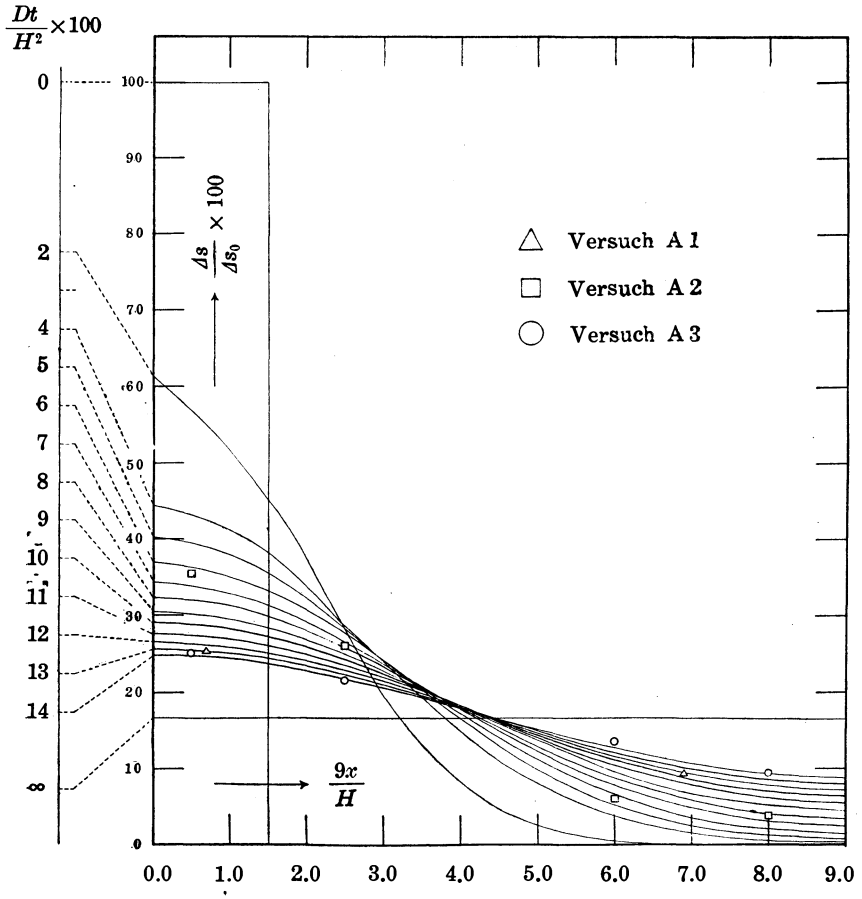


Abb. 2. Die Abhängigkeit von $(\Delta s/\Delta s_0)$ auf $(9x/H)$ bei verschiedenen ausgewählten Werten von (Dt).

(G) und (O). Der Dichteüberschuss $\Delta s_0(G)$ bzw. $\Delta s_0(O)$, der oberhalb jeder Tabelle angegeben ist, drückt den anfänglichen Dichteüberschuss des benutzten schweren Wassers aus.

Um aus den so direkt gefundenen Daten von $9x/H$ und $\Delta s(G)$ die Diffusionskonstante D des schweren Wassers, die unterhalb jeder Tabelle angegeben ist, zu bestimmen, benutzten wir eine graphische Methode. Weil in der vorliegenden Arbeit $H = 10$ cm. und $h/H = 1/6$ ist, wird Gl. (2) wie folgt vereinfacht:

$$\frac{\Delta s}{\Delta s_0} = \frac{1}{6} + \frac{2}{\pi} \sum_{n=1}^{\infty} \frac{1}{n} \sin \frac{n\pi}{6} \cos \frac{n\pi x}{10} e^{-\left(\frac{n\pi}{10}\right)^2 Dt} \qquad (5).$$

Die Kurven in Abb. 2. geben die mittels dieser Gl. (5) berechneten Werte von $(\Delta s/\Delta s_0)$ bei einigen ausgewählten Werten von $(Dt/H^2) \times 100$ $(= Dt,$ weil $H = 10$ ist) in Abhängigkeit von $(9x/H)$ wieder.[8] Zeichnet man deshalb die bei den Versuchen gefundenen Werte von $(\Delta s(G)/\Delta s_0(G))$ in dieser Abb. 2 ein, so liegen sie immer zwischen zwei Kurven, deren Dt-Wert untereinander um eins verschieden sind. Wir können daher den richtigen Wert von Dt für den angegebenen Wert von $(\Delta s(G)/\Delta s_0(G))$ durch die Interpolation bis auf ein Fünftel genau bestimmen. Die so bestimmten Werte von Dt geben wir in den letzten Vertikalreihen der Tabellen 1 wieder. Dann können wir die Diffusionskonstante D aus dem so ermittelten Wert von Dt ohne weiteres berechnen, weil die Versuchsdauer t schon wohl bekannt ist. Die auf diese Weise in drei untereinander unabhängig durchgeführten Versuchen gefundenen Werte von D stimmten aber, wie unter jeder Tabelle angegeben ist, untereinander hinreichend gut überein und der Totalmittelwert ergab $D = 1.12$ cm.^{2}/Tag.

Der auf diese Weise gefundene Wert von D stellt offenbar die Diffusionskonstante des schweren Wassermoleküls als Ganzes dar, weil wir als Δs_0 und Δs den gesamten Dichteüberschuss $\Delta s_0(G)$ und $\Delta s(G)$ benutzten. Wenn man dagegen statt $\Delta s_0(G)$ und $\Delta s(G)$ den Dichteüberschuss des Wassers, der allein auf die Anreicherung des schweren Sauerstoffs zurückzuführen ist, nämlich $\Delta s_0(O)$ und $\Delta s(O)$ verwendet, dann können wir die Diffusionskonstante der O-Atome ausfindig machen, und auf ähnliche Weise kann man auch die Diffusionskonstante der H-Atome berechnen. Aber weil erstens die direkt gemessenen Daten nicht ganz ausreichten, um solch eine Berechnung genau auszuführen und zweitens unser Zweck nicht in der Bestimmung der absoluten Grösse der Diffusionskonstante der H- und O-Atome sondern in der Vergleichung der Diffusionsgeschwindigkeit der beiden Arten der Atome liegt, verfuhren wir

folgendermassen. Wir berechneten nämlich aus dem gefundenen Wert von $\Delta s(O)$ und $\Delta s(G)$ das Verhältnis $\Delta s(O)/\Delta s(G)$ und dies verglichen wir mit dem anfänglichen $\Delta s_0(O)/\Delta s_0(G)$. Dabei ergab sich, wie aus den fünften Vertikalreihen der Tabellen ersichtlich ist, dass das Verhältnis $\Delta s(O)/\Delta s(G)$ sich in einer Reihe der Versuche hinreichend gut konstant verhielt, abgesehen davon in welcher Stelle der Gelatinsäule das Wasser geprüft wurde. Folglich darf man wohl schliessen, dass die schweren Sauerstoffatome ebensoschnell wie die schweren Wasserstoffatome diffundierten. Dasselbe Resultat gewannen wir auch im nächsten Versuch B, wo zur Bestimmung der Diffusionskonstante die Methode B in Abb. 1 benutzt wurde.

Versuch B. Ein Glaszylinder, dessen Höhe 10 cm. und dessen Inhalt ca. 30 c.c. beträgt, wird ganz bis zur oberen Öffnung mit dem aus schwerem Wasser bereiteten Gelatingel gefüllt und das ganze Gefäss in eine grosse Menge gewöhnlichen Wassers, das in einem Becherglas von ca. 3. *l.* Inhalt enthalten ist, eingetaucht. Dann wird das Becherglas in eine Kühlkammer getan und dort konstant bei $6 \pm 1°$C. gehalten. Dabei wird das Wasser, das im Becherglass ausserhalb des Gelatingefässes befindlich ist, während des Versuchs mittels eines elektrischen Rührwerkes sorgfältig umgerührt, um dessen Inneres stets homogen zu halten. Nach einer bestimmten Tagelänge, die von 6 bis 35 Tage dauert (vgl. Tabelle 2), wird das Gelatingefäss aus dem Becherglas herausgenommen und der Dichteüberschuss des im Gelatin enthaltenen Wassers auf dieselbe Weise wie beim Versuch A bestimmt. Die Diffusionskonstante D des schweren Wassers durch das Gelatingel wird dann mittels der schon oben angegebenen Gl. (3) ohne weiteres berechnet. Tabelle 2 gibt die so erhaltenen Versuchsergebnisse

Tabelle 2. Ergebnisse des Versuchs B.

t in Tage	$\Delta s(G)$ in γ	$\Delta s(O)$ in γ	$\Delta s(O)/\Delta s(G)$ in %	D in (cm.²/Tag.)
	$(\Delta s_0(G) =)$	$(\Delta s_0(O) =)$		
0	37.0±0.5	23.5± 1	64±3	—
6	29.9± ,,	—	—	1.82
14	23.3± ,,	13.7± ,,	59±4	1.77
21	18.8± ,,	—	—	1.81
35	12.8± ,,	7.0± ,,	55±8	1.90

Mittel $D = 1.83$ cm.²/Tag.

wieder, wo $\Delta s(G)$ und $\Delta s(O)$ ebenfalls wie in Tabellen 1 resp. den gesamten bzw. den zur Anreicherung des schweren Sauerstoffs allein zurückzuführenden Dichteüberschuss bedeutet.

Bei diesem Versuch B fanden wir nämlich die Diffusionskonstante D um ca. 0.7 grösser als beim Versuch A. Über die Ursache dieser Diskrepanz sind wir uns augenblicklich noch nicht ganz klar. Aber doch können wir wenigstens die folgenden Tatsachen in Betracht ziehen. Beim Versuch A, wo die zwei Arten der Gelatingele übereinander geschichtet wurden, gaben wir, wie schon oben erwähnt, besonders darauf acht, dass keine Zwischenschicht bei der Berührungsfläche der beiden Arten der Gelatingele gebildet wird. Aber aus der oben angegebenen Vergleichung der Versuchsergebnisse der beiden Reihen der Versuche A und B zu urteilen, erscheint doch beim Versuch A irgendeine Hemmung gegen die Diffusion des Wassers bei der Berührungsfläche der zwei Arten der Gelatingele vorhanden zu sein, obwohl wir über den exakten Charakter dieser Hemmung noch nichts Sicheres wissen. Dagegen beim Versuch B, wo wir das Gelatingel in gewöhnliches Wasser eintauchten, fanden wir immer, dass die Oberfläche des Gelatingel während des Versuches allmählich aufschwoll. Dies führt offenbar zur Vergrösserung der Diffusionsgeschwindigkeit des Wassers aus dem Gelatingel ins umgebende Wasser. Allen diesen Tatsachen nach möchten wir lieber schliessen, dass die wahre Diffusionskonstante D zwischen den hier angegebenen beiden extremen Werten liegen dürfte. Dieser Schluss findet weiter seine Bestätigung darin, dass der so geschätzte Mittelwert von D dem von Orr und Bulter[4] gefundenen nahe kommt.

Wir finden wiederum in diesem Versuch B, gut übereinstimmend mit Versuch A, und dies ist der Hauptzweck der vorliegenden Arbeit, dass es keine Unterschiede der Diffusionsgeschwindigkeit zwischen den H- und O-Atomen gibt, wie man dies aus dem konstant bleibenden Verhältnis des zur Anreicherung des schweren Sauerstoffs zurückzuführenden Dichteüberschusses $\Delta s(O)$ zum gesamten Dichteüberschuss $\Delta s(G)$ des Wassers im Gelatingel während des Diffusionsprozesses ohne weiteres ersehen kann (vgl. die vierte Vertikalreihe der Tabelle 2). Wir benutzten in der vorliegenden Arbeit als Diffusionsmedium nicht reines Wasser sondern ein wasserhaltiges Gelatingel. Aber weil der Gehalt des von uns benutzten Gelatingels an Gelatin sehr gering war (5 Gewichtsprozent!), darf man auch mit der Selbstdiffusion des Wassers durch reines Wassermedium denselben Schluss ziehen, nämlich, dass die eventuell vorhandene Extradiffusion der Wasseratome durch den Austauschmechanismus im Vergleich mit der gewöhnlichen Massendiffusion des Wassers vernachlässigt werden kann.

Diskussion. Um die anomal grosse Beweglichkeit der H^+- und OH^--Ionen zu deuten, nahmen Hückel[2] sowie Bernal und Fowler[3] an, dass das Proton bzw. Deuteron von einem Wassermolekül zum anderen springen kann, wie das folgende Schema zeigt:

$$(OH_3)^+ + OH_2 \rightleftarrows OH_2 + HOH_2^+ \qquad (6),$$

$$OH_2 + OH^- \rightleftarrows OH^- + HOH \qquad (7).$$

Dabei müssen die beiden benachbarten Wassermoleküle oder, im allgemein gesagt, Protonträger sich gegenseitig in einer geeigneten Lage befinden, um das Proton von einem zum anderen springen zu lassen. Solch eine geeignete Orientierung der zwei benachbarten Wassermoleküle findet aber nach Bernal und Fowler häufig genug statt, wo durch die Schema (6) und (7) die Extrabeweglichkeit der H^+- und OH^--Ionen befriedigend erklärt wird, vorausgesetzt, dass die Rotierbarkeit des Wassermoleküls bis zu einem gewissen Grad verhindert wird. Diese letztere Annahme steht aber mit der von ihnen angenommenen quasi-kristallinischen Struktur des flüssigen Wassers gut im Einklang.

Bei der Abwesenheit des äusseren Feldes muss der Protonsprung zwischen zwei benachbarten Wassermolekülen nach beiden Seiten mit gleicher Geschwindigkeit geschehen. Dies führt offenbar zur gleichmässigen Verteilung der Protonen und folglich des scheinbaren Systems OH_3^+ bzw. OH^- durch das gegebene Wasser. Dabei beträgt die Übergangsfrequenz der Protonen nach dem Schema (6) nach Hückel $\nu_{H^+} = 10^{10}$ bis 10^{11}/Sek. und nach Bernal und Fowler $\nu_{H^+} = 10^{12}$ bis 10^{13}/Sek. Da aber ein Liter Wasser 10^{-7} Mol OH_3^+ enthält und dies der atomaren Konzentration der H^+-Ionen von $10^{-7}/(2 \times 55.5) = 10^{-9}$ entspricht, wird die Frequenz ν_H, mit der die neutralen H-Atome durch den Protonsprung nach dem Schema (6) von einem Molekül zum anderen übergeführt werden:

$$\nu_H \leq 10^{13} \times 10^{-9} = 10^4/\text{Sek.} \qquad (8).$$

Die entsprechenden Werte der Übergangsfrequenz der Protonen nach dem Schema (7) bzw. der der Deuteronen nach dem Schema (6) und (7) müssen alle um einen gewissen Grad kleiner als der hier angegebene Wert (8) sein, wie man dies aus der geringeren Beweglichkeit der OH^--, OH_3^+ und OD^--Ionen schliessen kann.[9] Deshalb können wir den Wert (8) als

(9) Nach dem Experiment von W. N. Baker und V. La Mer, *J. Chem. Phys.*, **3** (1935), 406, unterscheiden sich die Übergangsfrequenzen der Protonen und Deuteronen um den Faktor $\sqrt{2}$ untereinander.

die obere Grenze der Übergangsfrequenz der H- bzw. D-Atome ansehen. Aber in jedem Fall darf man nicht übersehen, wie darauf schon von Bernal und Fowler hingewiesen wurde, dass es kein dasselbe H- bzw. D-Atom, sondern das Element H bzw. D ist, das mit der eben angegebenen Frequenz (8) durch das Wasser wandert. Falls dagegen ein und dasselbe H- bzw. D-Atom durch den Austauschmechanismus von einem Molekül zum anderen wandern muss, und zwar dies zur Extradiffusion der H- bzw. D-Atome führt, dann muss die Übergangsfrequenz offensichtlich viel geringer als der Wert (8) werden. Aber selbst wenn man diesen Wert (8) vorläufig als die alleroberste Grenze der Übergangsfrequenz des ein und desselben H- bzw. D-Atoms annimmt, wird doch die dadurch bedingte Extradiffusionsgeschwindigkeit der H- bzw. D-Atome im Vergleich mit der Geschwindigkeit der Massendiffusion des Wassers unvergleichbar so klein, wie man dies durch eine einfache Rechnung zeigen kann.

Wir können die Diffusionskonstante D einer Substanz A durch das Diffusionsmedium B nach dem Fickschen Gesetz wie folgt setzen:

$$D = -\frac{1}{q}\frac{\partial m}{\partial t}\Big/\frac{\partial c}{\partial x} \qquad (9)$$

wo $\partial m/\partial t$ die Menge der Substanz A ausdrückt, die in der Zeiteinheit durch den Querschnitt q nach der dies senkrechten Richtung x diffundiert, falls das Konzentrationsgefälle der Substanz A nach der Richtung x $-\partial c/\partial x$ beträgt. Bezeichnet man deshalb mit t die Zeit, die erforderlich ist, um das Molekül bzw. Atom A um die Strecke d nach der Richtung x zu transportieren, dann wird offenbar:

$$-\frac{\partial m}{\partial t} = \frac{qdc}{t} \quad \text{und} \quad \frac{\partial c}{\partial x} = \frac{c}{d} \qquad (10),$$

vorausgesetzt, dass das Konzentrationsgefälle um die Strecke d gleich c ist. Setzt man diese Beziehungen (10) in Gl. (9) ein, so erhält man die Gleichung:

$$D = d^2/t \qquad (11).$$

Setzt man deshalb bei der Extradiffusion der H-Atome den Abstand d in Gl. (11) gleich den Abstand zwischen den Schwerpunkten der zwei benachbarten Wassermoleküle, dann wird $1/t$ in dieser Gl. die Übergangsfrequenz ein und desselben H-Atoms zwischen zwei benachbarten Wassermolekülen. Den ersteren können wir offensichtlich:

$$d = (18.0/6.06 \times 10^{23})^{1/3} = 3 \times 10^{-8} \text{ cm}.$$

setzen. Betreffend der Grösse der letzteren, d.h. der Übergangsfrequenzen ein und desselben H-Atoms, wissen wir dagegen, wie schon oben erwähnt wurde, augenblicklich nichts Sicheres. Aber selbst wenn man diese, als die alleroberste Grenze, gleich dem oben angegebenen Wert (8) annimmt, wird doch die Extradiffusionskonstante D_{extra} der H-Atome, die unter Benutzung dieses Wertes nach Gl. (11) berechnet wird, so gering:

$$D_{\text{extra}} \leq (3 \times 10^{-8})^2 \times 10^4 \approx 10^{-11} \text{ cm.}^2/\text{Sek.}$$

$$\approx 10^{-6} \text{ cm.}^2/\text{Tag},$$

dass sie gegen die gesamte Diffusionskonstante $D (\approx 1 \text{ cm.}^2/\text{Tag})$ vollständig vernachlässigt werden kann.

Das hier angegebene Argument gilt selbstverständlich nur insofern, als sich kein äusseres Feld vorfindet. Wenn dagegen das letztere der Fall ist, dann treten ganz andere Verhältnisse ein und unter Umständen können die H-Atome schneller als die O-Atome übergeführt werden. Solch ein Versuch ist jetzt im Gang.

Zum Schluss möchten wir der Nippon Gakujutsu-Shinkohkai (der Japanischen Gesellschaft zur Förderung der wissenschaftlichen Forschungen) sowie der Hattori-Hohkohkai (der Hattori-Stiftung) für ihre finanzielle Unterstützung zur Ausführung dieser Arbeit unseren wärmsten Dank aussprechen.

Physikalisch-chemisches Laboratorium
der Kaiserlichen Universität zu Osaka
und
Siomi-Institut für physikalische
und chemische Forschung.

The Thixotropic and Plastic Behaviour of Suspensions of Barium Sulphate with Clay.

By Bunichi TAMAMUSHI and Yaichi SEKIGUCHI.

(Received July 30, 1938.)

I. There are such cases known, in which non-thixotropic and non-plastic systems become thixotropic and plastic on adding certain amounts of other materials. A non-thixotropic and non-plastic suspension of quartz powder in water becomes, for instance, plastic and thixotropic when a small amount of lecithin is added.(1) A small amount of clay (1–2%) contained in the Solnhofen-slate was found to be responsible for the extreme plasticity of the slate, whose chief constituent was calcium carbonate.(2) A non-thixotropic suspension of barium sulphate can be made thixotropic on adding a certain amount of bentonite.(3) The phenomenon, which appears thus to be a general one, is interesting not only from a theoretical point of view but also from a technical one. The baryte-suspension with bentonite used as a drilling fluid in boring for petroleum in the United States marks a rather curious example of the technical application of the phenomenon. The stability of dispersions of such drilling fluids were discussed by Ambrose and Loomis(3) as a function of *p*H of the dispersion medium. For controlling the properties of such artificial systems, basic studies from many sides would be desirable.

Now a sort of a natural hydrogen-clay found in Japan, possesses more or less plastic and thixotropic properties but in a less degree than bentonite(4) in the United States, owing to its lower degree of dissociation and consequently the smaller capacity of its particles for binding water molecules. The Japanese hydrogen clay(5) with exchangeable hydrogen ions, can however be turned into an alkali-clay by treating it with alkali-salts or alkali-hydroxides.(6) The alkali-clay thus obtained is highly thixo-

(1) H. Freundlich, *J. Soc. Chem. Ind.*, **53** (1934), 223.

(2) H. Freundlich and F. Juliusburger, *Trans. Faraday Soc.*, **30** (1934), 333.

(3) H. C. Lawton, H. A. Ambrose and A. G. Loomis, *Physics*, **2** (1932), 365; *ibid.*, **3** (1932), 185; H. A. Ambrose and A. G. Loomis, *ibid.*, **4** (1933), 265; *Ind. Eng. Chem.*, **25** (1933), 1019.

(4) H. Freundlich, O. Schmidt and G. Lindau, *Kolloid-Beihefte*, **36** (1932), 43.

(5) We would like to use this terminology instead of the widely used one: the Japanese acid clay.

(6) B. Tamamushi, *Kolloid-Z.*, **79** (1937), 309.

tropic and serves as a very effective adding material to make another non-thixotropic material such as barium sulphate or latex, thixotropic. The following experiments deal with the thixotropic and plastic properties of the suspensions of barium sulphate with various amounts of sodium-clay, where a certain correlation between thixotropy and related properties will be mentioned.

II. The natural hydrogen-clay taken at Itoigawa in Niigata prefecture, has a distinctly acidic reaction in its suspension in distilled water (*p*H of the ultrafiltrate of the suspension is equal to 5.8) and is slightly thixotropic in its concentrated suspensions (more than 35%) in water, whilst the sodium-clay formed by treating the former clay with dilute sodium hydroxide, is markedly thixotropic, its 10%-suspension in water solidifies on setting in about 60 minutes after strong shaking in a test tube of a diameter 14 mm. The sodium-clay greatly exceeds the hydrogen-clay in its swelling capacity in water according to the greater ability of the particles of the former clay in binding water molecules around them. The measurement of the swelling capacity was carried out by using the apparatus first designed by Freundlich, Schmidt and Lindau,[4] the result of which is shown in Table 1 and in Fig. 1.

Table 1.

Swelling capacity of hydrogen-clay (per 1 g.)		Swelling capacity of sodium-clay (per 0.1 g.)	
Time	Water taken in c.c.	Time	Water taken in c.c.
0''	0.000	0''	0.000
5	0.100	2' 59	0.100
13	0.200	6 35	0.200
21	0.300	10 18	0.300
27	0.400	21 20	0.400
35	0.500	38 25	0.500
44	0.600	54 10	0.550
52	0.700	1° 18 15	0.600
1' 02	0.800	2 2 5	0.650
1 14	0.900	3 2 0	0.693
1 46	1.000	3 17	0.700
2 42	1.050	4 4	0.725
4 51	1.100	4 30	0.735
6 32	1.125	5 0	0.745
34 30	1.165	5 40	0.760
1° 14	1.175	18 30	0.930
1 37	1.180	54	1.165
2 3	1.185		
3	1.185		

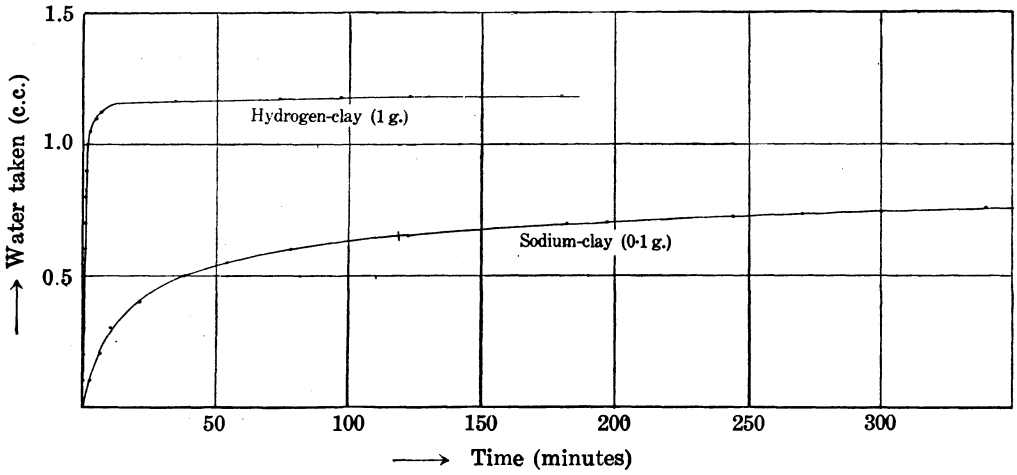


Fig. 1.

Moreover, the mass of the sodium-clay with a certain amount of water is strongly sticky and plastic, whereas the hydrogen-clay is rather brittle and non-plastic in the same conditions.

Now we prepared suspensions of barium sulphate according to the method of Weimarn[7] by the double decomposition of $Ba(CNS)_2$ and $MnSO_4 \cdot 7H_2O$, once with solutions of intermediate concentrations (N/5–N/10), and then with solutions of greater concentrations (about 5 N) of these salts. Consequently we obtained the suspensions of barium sulphate of smaller and larger particle size, radius of particles lying between about 2 μ and 10 μ, which was determined from the velocity of sedimentation by applying the Stokes formula.

The 25–30%-suspensions of barium sulphate without clay are certainly non-thixotropic, the suspensions of equal concentrations of solid matter with a small amount of the sodium-clay are however more or less thixotropic, as Table 2 shows.

It is to be remarked here that the suspensions with barium sulphate of larger particle size are thixotropic at the concentration of about 30%, while those with barium sulphate of smaller particle size are thixotropic at lower concentrations. The smaller size of particle is therefore advantageous to the thixotropy of the system.

It is further to be noticed that the suspensions with larger particles of barium sulphate seem to exhibit an optimum thixotropy at certain intermediate concentrations of the clay added, while those with smaller

(7) P. P von Weimarn, "Die Allgemeinheit des Kolloidzustandes," Dresden (1925).

Table 2.

With $BaSO_4$ of greater particle size.

Composition (%)		Remarks
$BaSO_4$	Clay	
29.85	0.15	thixotropic
29.41	0.59	optimumthixotropic
29.08	0.92	thixotropic
28.57	1.43	thixotropic

With $BaSO_4$ of smaller particle size.

Composition (%)		Remarks
$BaSO_4$	Clay	
24.88	0.12	unstable
24.51	0.49	thixotropic
24.23	0.77	thixotropic
23.81	1.19	rigid and thixotropic

particles of barium sulphate become more and more viscous on increasing the amount of the clay. This apparently strange behaviour of the system in thixotropy has however, as we shall see later on, a certain parallelism with the behaviour in other related properties.

III. Thixotropy is, as generally accepted, related to a loose packing of particles in suspension.[8] The volume of sedimentation, which is a good indicator for the degree of packing, was measured in the usual manner, 1 gram of the solid material being mixed with 10 c.c. of distilled water in a mess-cylinder, allowed to settle in an excess of liquid and the height of the powder settled down being determined after 24 hours. The results are shown in Table 3, in which the adopted values of the volume of sedimentation are the mean of several consecutive readings.

Table 3.

Composition of mixture (g.)		V. S. (c.c.)	Composition of mixture (g.)		V. S. (c.c.)
$BaSO_4$ (coarse)	Clay		$BaSO_4$ (fine)	Clay	
1.000	0.000	3.1	1.000	0.000	2.8
0.995	0.005	3.5	0.995	0.005	3.3
0.980	0.020	2.8	0.982	0.018	3.7
0.969	0.031	2.5	0.969	0.031	3.9
0.952	0.048	1.8	0.952	0.048	4.7
0.867	0.133	1.0	0.920	0.080	6.5
			0.831	0.169	9.1

As we see in the table, the volume of sedimentation is small in the suspensions of barium sulphate without clay and it increases steadily on

(8) H. Freundlich, "Thixotropy," 16, Paris (1935).

adding the clay, in the case of $BaSO_4$ of smaller particle size, whereas it attains maximum in the case of $BaSO_4$ of larger particle size. The maximum volume of sedimentation in the latter case corresponds to the optimum thixotropy found in the same case. The correlation between thixotropy and the volume of sedimentation is evident.

IV. Now, the paste of $BaSO_4$ with water is more or less plastic.[9] For practical purposes we may determine the so-called plasticity number,[10] which gives the difference between the amount of water required to make the material sticky and that to make it just wet enough to be rolled in small thin rods. This number of plasticity was found once for pure $BaSO_4$ to be equal to 8, the amount of water in parts necessary for 100 parts of solid matter being 20 for the lower limit and 28 for the upper one. The same number was then determined for the mixture of $BaSO_4$ (95 parts) and clay (5 parts) to be 20, as the amount of water in parts necessary for 100 parts of solid matter was found to be 35 for the lower limit and 55 for the upper one. It is therefore obvious that the plasticity of $BaSO_4$ increases remarkably on adding a certain amount of clay.

The plastic behaviour of colloidal systems may however be more definitely characterized by determining the so-called yield value of Bingham.[11] The determination of this value was executed in the following way, with suspensions of various compositions of $BaSO_4$ and clay once for $BaSO_4$ of smaller particle size and then for $BaSO_4$ of larger particle size.

The adopted method of measurement is the capillary tube method, the suspension being passed through a capillary tube under a certain pressure difference at the two ends of the tube, and the rate of flow being recorded. The radius of the capillary tube $R = 0.069$ cm., its length $l = 50.09$ cm., and the value of the pressure difference applied varied from 15 mm. to 200 mm. Hg. Under these experimental conditions, the rate of flow could be measured with 17%-suspensions of $BaSO_4$ of larger particle size, but with suspensions of $BaSO_4$ of smaller particle size the concentration must be lowered to about 12%, since the latter suspensions of higher concentrations were found to be too viscous.

The relation between the stress pressure P and the rate of flow V/t obtained are given graphically in Fig. 2–5.

(9) A. Atterberg, *Z. angew. Chem.*, **24** (1911), 928.
(10) R. Houwink, "Elasticity, Plasticity and Structure of Matter," 354, Cambridge (1937).
(11) E. C. Bingham, "Plasticity and Fluidity," New York (1922).

According to the theory of Bingham, the rate of the plastic flow in a capillary tube is expressed by the following equation:

$$\frac{V}{t} = \frac{\pi\mu R^4}{8l}\left(P - \frac{4}{3}p + \frac{p^4}{3P^3}\right),$$

where l is the length of the capillary tube, R its radius, P the pressure difference at the two ends of the tube, p a constant given by the relation:

$$p = \frac{2l}{R} f,$$

in which f is the friction or the yield value, and finally μ means a constant which is called the coefficient of mobility. The general feature of the curves in the above figures is justly represented by this equation.

For large values of the pressure applied, the last term of the equation becomes very small and the curve becomes nearly linear and coincides with its asymptote, namely:

$$\frac{V}{t} = \frac{\pi\mu R^4}{8l}\left(P - \frac{4}{3}p\right).$$

Putting herein $V/t = 0$, we obtain the intercept of the asymptote and from this we get the value of the true friction. From the inclination of the asymptote, we get further the value of $\frac{\pi\mu R^4}{8l}$ and consequently the value of the coefficient of mobility.

Applying the above relation to our experimental curves, we obtained the friction or the yield value f and the mobility coefficient μ in each case, the result being summarized in Table 4 and 5.

It is remarkable that in the case of $BaSO_4$ of larger particle size, the yield value attains its maximum at intermediate concentrations of the clay added, whereas it varies only in one direction with increasing amounts of clay in the case of $BaSO_4$ of smaller particle size. Such characteristic behaviour of the system in plastic flow may have a certain relation with what has been revealed in thixotropy and also in the packing of particles.

The existence of a definite yield value seems to be characteristic of all thixotropic systems. A system with a too low yield value might not be thixotropic. The mobility coefficient appears however to have no definite relationship with thixotropy, although a system with too low mobility would be unfavourable for the pronounced demonstration of the isothermal reversible sol-gel-transformation under the usual mechanical treatment.

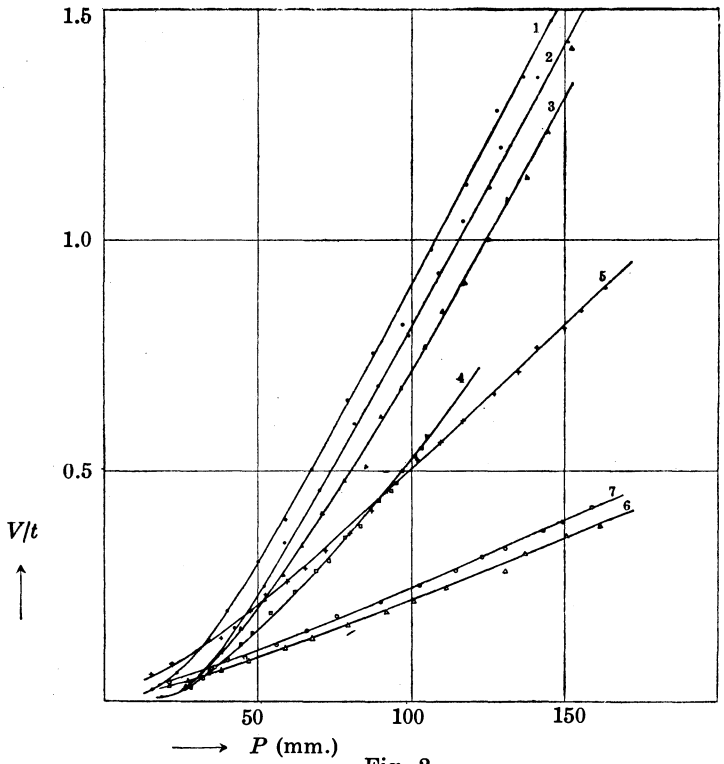

1.5
1.0
0.5
V/t
50
100
150
P (mm.)
1
2
3
4
5
6
7

Fig. 2.

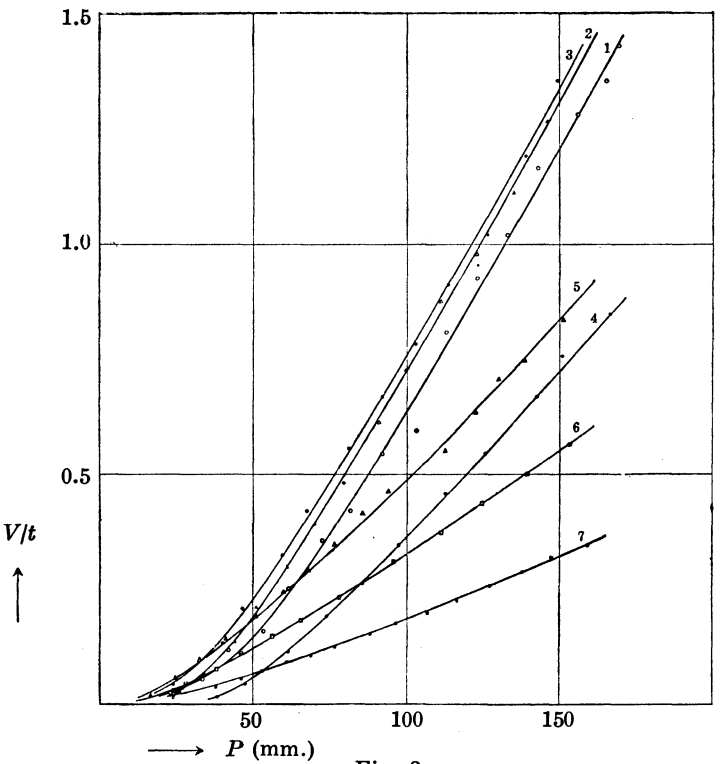

1.5
1.0
0.5
V/t
50
100
150
P (mm.)
1
2
3
4
5
6
7

Fig. 3.

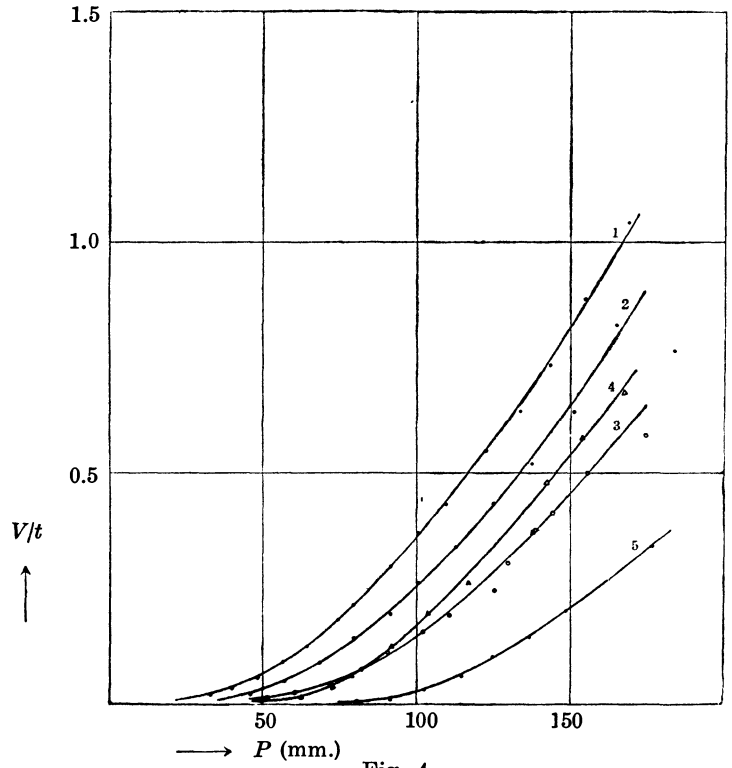


Fig. 4.

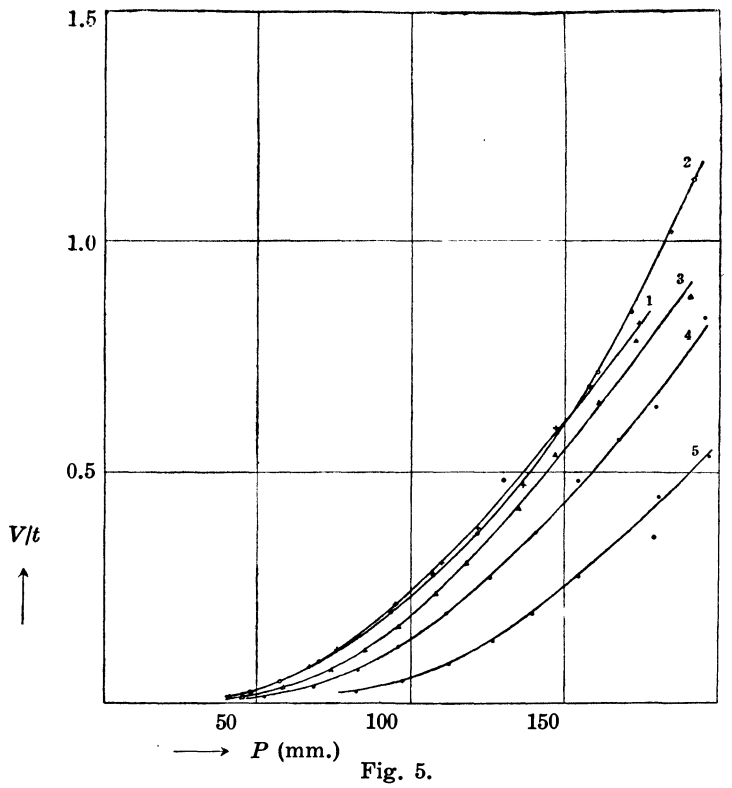


Fig. 5.

Table 4. With larger particles of $BaSO_4$.

Fig. No.	No. of curves in Fig.	Composition (%)		Yield value (dyne/cm^2.)	Mobility coef. (c. g. s.)
		$BaSO_4$	Clay		
2	1	17.0	0.00	1.72	10.58×10^7
	2	17.0	0.06	2.06	10.58
	3	16.9	0.61	2.54	10.36
	4	15.6	1.17	1.92	6.71
	5	15.4	2.22	1.17	5.25
	6	4.4	5.25	1.17	2.56
	7	0.0	5.48	1.10	2.74
3	1	17.00	0.00	2.81	9.00
	2	17.00	0.06	2.47	9.36
	3	17.00	0.19	2.40	9.75
	4	16.66	0.66	3.29	5.83
	5	16.45	1.22	1.65	5.43
	6	16.35	2.33	1.72	3.72
	7	15.95	3.37	2.06	2.39

Table 5. With smaller particles of $BaSO_4$.

Fig. No.	No. of curves in Fig.	Composition (%)		Yield value (dyne/cm^2.)	Mobility coef. (c. g. s.)
		$BaSO_4$	Clay		
4	1	17.00	0.00	4.94	8.66×10^7
	2	17.00	0.06	5.76	8.19
	3	17.00	1.13	6.17	6.03
	4	16.30	2.38	7.27	4.01
5	1	12.00	0.00	5.83	7.89
	2	12.00	0.03	6.31	8.83
	3	11.96	0.30	6.45	8.19
	4	11.92	0.60	6.65	6.95
	5	11.87	1.20	7.68	5.53

The values of the mobility coefficient obtained in the above are not quite certain owing to the narrow range of the pressure applied, nevertheless they show a general tendency to decrease with the increasing amount of the added clay.

V. Concerning the mechanism, how non-thixotropic $BaSO_4$-suspensions become thixotropic on adding the sodium-clay, it is not easy to give a conclusive explanation. The influence of electric charges of particles may be put aside, since both particles of $BaSO_4$ and of clay are equally negatively charged, which was demonstrated by the cataphoretic measurement under an ultramicroscope.

In non-thixotropic suspensions of $BaSO_4$, particles may be more or less independent of each other and they incline to settle in closer packing, whilst their independence will be lost when the clay is added, since the latter, adsorbed on the surface of $BaSO_4$-particles, will make the particles adhere to each other and thus facilitate the formation of a three dimensional net work in the whole system which favours thixotropy.[12]

Summary

(1) Non-thixotropic suspensions of $BaSO_4$ become thixotropic on adding certain amounts of a sodium-clay formed from a natural hydrogen-clay.

(2) The plasticity of the suspensions of $BaSO_4$ increases when the sodium-clay is added.

(3) The correlation among thixotropy, loose packing of particles (large volume of sedimentation), and isothermal plasticity, which is now generally accepted, is evident also in systems under investigation.

(4) A characteristic influence of the particle size of $BaSO_4$ on thixotropy and plasticity of the systems is mentioned.

Nedzu Chemical Laboratory,
Musashi Higher School,
Itabashiku, Tokyo.

(12) B. Tamamushi, this Bulletin, **13** (1938), 234.

The Isomerization of Isostilbene to Stilbene by Hydrogen Bromide in the Presence of Oxygen and of Ferromagnetic Metals.

By Yoshiyuki URUSHIBARA and Osamu SIMAMURA.

(Received May 5, 1938.)

In the previous paper[1] the authors reported that hydrogen bromide, in presence of oxygen, accelerated the isomerization of isostilbene to stilbene in the dark at room temperature in absence of solvents, while neither hydrogen bromide nor oxygen was active when present alone. However, M. S. Kharasch, J. V. Mansfield, and F. R. Mayo[2] observed that isostilbene in benzene solution was not isomerized to stilbene by hydrogen bromide even when the reactants were mixed in air (but the addition of a peroxide to the reaction mixture caused a rapid isomerization). With a view to obtaining an explanation of this apparent contradiction the present authors have studied the isomerization by hydrogen bromide in presence of oxygen in benzene solution.

Reduced nickel was found also to co-operate with hydrogen bromide to accelerate the isomerization of isostilbene to stilbene, although the effect of hydrogen bromide in presence of reduced nickel was much smaller than in presence of oxygen.[1] Another ferromagnetic metal, reduced iron, as well as other metals have now been examined in the isomerization by hydrogen bromide in absence of solvents, and reduced nickel in the isomerization in benzene solution. Further, the influences of antioxidants on the isomerization by hydrogen bromide in presence of oxygen or reduced nickel have been investigated.

Isostilbene was prepared, according to the directions of Schlenk and Bergmann,[3] by hydrogenating tolane in presence of palladium on barium sulphate, b.p. 110–110.5° under 1.2 mm., $n_D^{20°}$ 1.6130. Hydrogen bromide was prepared by the action of purified bromine on hot tetralin, washed by passing through cold tetralin and over moist red phophorus, then dried with anhydrous calcium bromide and with phosphorus pentoxide. Reduced nickel was prepared by reducing nickel oxide (Kahlbaum) with hydrogen, and reduced copper by grinding copper oxide in wire form (Merck) and reducing with hydrogen. Other materials were the purest commercial products, which were used directly or after purification.

(1) Y. Urushibara and O. Simamura, this Bulletin, **12** (1937), 507.
(2) *J. Am. Chem. Soc.*, **59** (1937), 1155.
(3) *Ann.*, **463** (1928), 115.

I. Isomerization in Presence of Oxygen in Benzene Solution. The experiments in benzene solution resulted similarly to those without the solvent: A benzene solution containing 5 per cent isostilbene was saturated with air and was made 0.01 N in hydrogen bromide by adding an appropriate amount of a concentrated benzene solution of hydrogen bromide in the dark at room temperature. After 20–30 minutes, the solution was washed with water, dried over anhydrous sodium sulphate, and evaporated. The residue, from which stilbene already began to crystallize out at the temperature of the boiling water bath (stilbene more than 50%), solidified to a crystalline mass on cooling. Thus it may be suspected that in the American investigators' experiments no sufficient oxygen was absorbed when the reactants were mixed in air or the result of the reaction was examined too soon.

When a much larger amount of hydrogen bromide was used (in presence of oxygen in benzene solution in the dark at room temperature), the first change was of course the isomerization of isostilbene to stilbene, but after 20 hours from beginning it was noticed that stilbene dibromide (m.p. 237°, identified with an authentic specimen) had been formed. This observation may favour the theory of bromine atoms by Kharasch and co-workers,[2] although they did not notice the effect of oxygen (air) on the isomerization of isostilbene to stilbene by hydrogen bromide in benzene solution.

II. Isomerizations in Presence of Reduced Iron and of Other Metals without Solvents, and in Presence of Reduced Nickel in Benzene Solution. In the same manner as in the previous experiments with reduced nickel,[4] the four metal catalysts, reduced iron, platinum black, palladium black, and reduced copper, were examined in their effects on the isomerization of isostilbene by hydrogen bromide. Reduced iron showed an effect comparable to that of reduced nickel, the crystals of stilbene beginning to appear in the course of ½–4 hours according to the amount of hydrogen bromide. The other metals gave also positive results, but it was more than 20 hours before crystals began to separate out. Although no exact comparison of the effects of these metals is possible, it may be mentioned that the ferromagnetic reduced nickel and reduced iron produce a stronger accelerating effect on the isomerization in co-operation with hydrogen bromide than the other metal catalysts so far used.

In the benzene solution (4 c.c.), containing 5–10 per cent isostilbene and 0.015–0.08 N hydrogen bromide, the formation of stilbene could not

(4) This Bulletin, **12** (1937), 508.

be demonstrated in presence of reduced nickel (0.1–0.5 g.) in the course of 1–4 days (in the dark at room temperature), a slightly viscous yellowish liquid being recovered. Such was also the case in absence of reduced nickel. However, in presence of reduced nickel and a large amount of hydrogen bromide a small quantity of stilbene was formed. Stilbene dibromide was not found in this case (examined on the fourth day). Thus it seems that the activity of reduced nickel is diminished to a great extent for the given concentrations of the reactants in benzene solution.

III. **Influences of Antioxidants.** When isostilbene, sealed with hydrogen bromide in a glass tube in absence of air, was exposed to sunlight, stilbene began to separate out in crystals in ½–1 minute and then the whole solidified instantly to a crystalline mass. The addition of catechol to isostilbene prevented the isomerization by hydrogen bromide in sunlight. Diphenylamine, which can eliminate more or less the effect of oxygen and peroxides in the addition of hydrogen bromide to unsaturated compounds, was found not to share with catechol the property of preventing the isomerization of isostilbene by hydrogen bromide in the light: When isostilbene containing diphenylamine was exposed to sunlight in presence of hydrogen bromide, stilbene separated out within a minute. It may be added here that in the dark isostilbene was not isomerized by diphenylamine either in presence or in absence of hydrogen bromide.(5)

Catechol prevented also the isomerization by hydrogen bromide in the heat: When isostilbene (0.2 c.c.) and hydrogen bromide (3 c.c.), sealed in a glass tube in absence of air, were heated in boiling water in the dark, the isomerization became noticeable in 30 minutes (stilbene crystallized out on cooling), while the addition of catechol (5 mg.) prevented this isomerization.

The influences of catechol and of diphenylamine on the isomerization of isostilbene by hydrogen bromide in presence of reduced nickel and of oxygen were also investigated.

Reduced nickel (20 mg.) was taken in a reaction tube, and isostilbene (0.2 c.c.) with catechol (5 mg.) in a side tube attached to the reaction tube. The nickel was heated at 330–350° in the atmosphere of hydrogen and then in vacuum, and cooled in vacuum. Hydrogen bromide (5 c.c.)

(5) According to G. R. Clemo and S. B. Graham, *J. Chem. Soc.*, **1930**, 213, dimethyl maleate is isomerized to dimethyl fumarate by primary and secondary amines. However, neither dimethyl maleate nor isostilbene was found to be transformed into the corresponding trans compound by diphenylamine.

was introduced, and the tube sealed off. The isostilbene containing catechol was decanted on the reduced nickel. After the mixture was left to stand in the dark at room temperature for a certain time, the tube was cut open in an aqueous solution of caustic soda, thus the access of air while hydrogen bromide was still present being avoided. In this experiment it was found that catechol prevented the isomerization of isostilbene by hydrogen bromide in presence of reduced nickel over 40 hours. On the other hand, diphenylamine could not prevent the isomerization under the same conditions as above. When isostilbene containing diphenylamine was first decanted on the reduced nickel and then hydrogen bromide was introduced, the result was the same (isomerization proceeded indifferently to diphenylamine).

Catechol prevented also the isomerization of isostilbene by hydrogen bromide in presence of oxygen, stilbene being not formed in the course of 20 hours. The inhibiting influence of diphenylamine on the isomerization by hydrogen bromide in presence of oxygen was also noticeable but weaker than that of catechol, about 20 per cent of isostilbene being transformed into stilbene in an hour.

Thus, the influences of the antioxidants on the isomerization of isostilbene by hydrogen bromide in presence of oxygen and of reduced nickel showed a certain parallelism to the influences of antioxidants on the effects of oxygen and of reduced nickel in the addition of hydrogen bromide to allyl bromide[6] and to undecenoic acid.[7] In every case, catechol eliminates to a great extent the effects of oxygen and of reduced nickel; on the other hand, diphenylamine, while it prevents more or less the action of oxygen, is incapable of influencing the effect of reduced nickel.

The authors express their hearty thanks to the Japan Society for the Promotion of Scientific Research (Nippon Gakujutsu Shinko-Kwai) for a grant.

Chemical Institute, Faculty of Science,
Imperial University of Tokyo.

(6) Y. Urushibara and M. Takebayashi, this Bulletin, **13** (1938), 400.
(7) Y. Urushibara and M. Takebayashi, *ibid.*, **13** (1938), 404.

On the Reaction of Gaseous Hydrogen Bromide with Reduced Nickel in the Presence of Oxygen.

By Yoshiyuki URUSHIBARA and Osamu SIMAMURA.

(Received July 14, 1938.)

In a preliminary note[1] the authors reported that in the dark at room temperature hydrogen bromide reacted with reduced nickel in presence of oxygen to give nickel bromide and hydrogen, while practically no reaction took place in absence of oxygen. The experimental details are given below:

In a glass tube with a capacity of 65 c.c. 0.5 g. of reduced nickel was taken; the air in the tube evacuated; hydrogen introduced; the nickel heated at 350–360° for ten minutes; the hydrogen evacuated thoroughly at the same temperature; and the tube with the nickel cooled down. With or without admission of 10 c.c. (4.3×10^{-4} mol) of oxygen, 45 c.c. (19.2×10^{-4} mol) of hydrogen bromide was introduced, and the tube was sealed off. The tube was left to stand in the dark or in diffuse light at room temperature for 14–15 days. A capillary seal attached to the tube was thrusted into an end of a piece of rubber tubing, the other end of which was connected with a trap and a manometer. The trap was evacuated and cooled in liquid air. The capillary seal inside the rubber tubing was broken from outside, and the pressure of the incondensable gases was read when the height of mercury in the manometer reached a stationary state. From the pressure and the approximate volume of the whole system the amount of the gases was calculated, the effect of cooling the trap on the pressure being taken into account. The reduced nickel, which showed no change in appearance in every case, was extracted with 25 c.c. of warm water. Aqueous caustic potash was added to the resulting solution; nickel hydroxide precipitated was collected and dissolved in hydrochloric acid; and nickel was estimated with dimethyl-glyoxime. Bromide ion in the filtrate from nickel hydroxide was determined by Volhard's method; and the amount of hydrogen bromide which reacted was calculated from the value of bromide ion. The results are given in Table 1.

In absence of oxygen, either in the dark (Exp. 1) or in diffuse light (Exp. 2), practically no reaction took place. Owing to the great percentage of error involved in the estimations of small amounts of the in-

(1) This Bulletin, **13** (1938), 407.

Table 1. Reduced nickel 0.5 g. Hydrogen bromide 45 c.c. (19.2×10^{-4} mol). At room temperature. Reaction time 14–15 days.

Exp. No.	Remarks	Incondensable gases (10^{-4} mol)	Found in the extract of reduced nickel			Hydrogen bromide which reacted (%)
			Ni (10^{-4} g. atom)	Br (10^{-4} g. atom)	Ni : Br	
1	No oxygen In the dark	0.4	0.9	2.0	1 : 2.2	10
2	No oxygen In diffuse light	0.5	0.8	2.3	1 : 2.9	12
3	Oxygen 10 c.c. (4.3×10^{-4} mol). In the dark	11	7.8	16.4	1 : 2.1	85

condensable gases and nickel bromide, the numerical values obtained in Exps. 1 and 2 are not exact.

In presence of oxygen as much as 85 per cent of hydrogen bromide introduced reacted (Exp. 3). If first reduced nickel were oxidized by oxygen and then hydrogen bromide reacted only with nickel oxide thus formed to give nickel bromide and water, nearly no incondensable gases would be left after 16.4×10^{-4} mol of hydrogen bromide reacted with nickel in presence of 4.3×10^{-4} mol of oxygen. On the other hand, if all hydrogen of the hydrogen bromide which reacted were converted into molecular hydrogen, the total amount of oxygen and hydrogen would be 12.5×10^{-4} mol. In fact, the amount of the incondensable gases was found to be 11×10^{-4} mol after reaction.

Thus, the authors drew the conclusion that in presence of oxygen hydrogen bromide reacted with reduced nickel to give nickel bromide and hydrogen without the formation of water, and then supposed the activation of hydrogen bromide by oxygen in this reaction. Such a hypothesis seemed not unreasonable in view of the following facts: Oxygen activates hydrogen bromide to isomerize isostilbene to stilbene[2] and affects the addition of hydrogen bromide to unsaturated organic compounds[3]; and, although reduced nickel shares such a property with oxygen,[2][4] it does not react with hydrogen bromide in absence of oxygen.

However, another possibility was that, if even a trace of water were produced by the oxidation of reduced nickel followed by the reaction of nickel oxide thus formed with hydrogen bromide, that trace of water might

(2) This Bulletin, **12** (1937), 507; **13** (1938), 566.
(3) *Ibid.*, **11** (1936, 692, 798; **12** (1937), 138, 173; **13** (1938), 331.
(4) *Ibid.*, **11** (1936), 692, 754; **12** (1937), 51; **13** (1938), 331, 400.

accelerate the reaction of hydrogen bromide with reduced nickel giving nickel bromide and hydrogen. Thus it seemed desirable to study the effect of water on the reaction of hydrogen bromide with reduced nickel and further to analyse the incondensable gases obtained in the reaction in presence of oxygen to know exactly the amount of hydrogen generated.

Table 2. Reduced nickel 0.5 g. Hydrogen bromide 45 c.c. (18.5×10^{-4} mol). At room temperature. In the dark. Reaction time 14–15 days.

Exp. No.	Added	Hydrogen produced (10^{-4} mol)	Found in the extract of reduced nickel			Hydrogen bromide which reacted (%)
			Ni (10^{-4} g. atom)	Br (10^{-4} g. atom)	Ni : Br	
4	Oxygen 10 c.c. (4.1×10^{-4} mol)	4.7	7.8	15.9	1 : 2.0	86
5	None, but reduced nickel exposed to air before use	4.3	6.4	12.2	1 : 1.9	66
6	Water 3 mg. (1.7×10^{-4} mol)	4.5	4.6	9.6	1 : 2.1	52
7	Water 3 mg. (1.7×10^{-4} mol)	5.4	5.5	11.5	1 : 2.1	62
8	None	0.6	0.9	2.2	1 : 2.4	12

In Table 2 another series of experiments carried out for this purpose are summarized. The procedure and the conditions of the experiments were the same as mentioned above unless otherwise stated below. To analyse the incondensable gases, oxygen was absorbed in alkaline pyrogallol and hydrogen was determined by the explosion method. The incondensable gases obtained in Exp. 4 was found to consist of 3.7×10^{-4} mol oxygen and 4.7×10^{-4} mol hydrogen. The percentage of hydrogen bromide which reacted was the same as in Exp. 3. The amount of hydrogen produced was found to be smaller than equivalent to that of nickel bromide formed.

In Exp. 5 reduced nickel was exposed to air before use, but treated in vacuum at room temperature before the introduction of hydrogen bromide; and the reaction took place without added oxygen. It was shown that the reaction of hydrogen bromide with reduced nickel was caused by combined or adsorbed oxygen on the reduced nickel. In the gas analysis no oxygen was detected and the amount of hydrogen was found smaller than equivalent to that of nickel bromide also in this case.

In Exps. 6 and 7, a trace of water (3 mg. or 1.7×10^{-4} mol) was added as follows: A tube containing 6 mg. of Glauber's salt was con-

nected with the reaction tube through a cock. The Glauber salt tube was cooled in liquid air, evacuated, filled with hydrogen, again evacuated, and the cock was closed. Reduced nickel in the reaction tube was treated as previously mentioned; the water of crystallization was vapourized into the reaction tube by opening the cock and heating the Glauber salt; the cock was closed again; and hydrogen bromide was introduced into the reaction tube. In this way, it was found that hydrogen bromide reacted with reduced nickel in presence of water but in absence of oxygen. Hydrogen was of course the only incondensable gas and its amount was equivalent to that of nickel bromide formed.

Thus, for the reaction of gaseous hydrogen bromide with reduced nickel in the presence of oxygen, although no evidence has been obtained to deny that oxygen may act also as a catalyst, it is the most probable that the reaction of hydrogen bromide with reduced nickel to give nickel bromide and hydrogen is accelerated by a trace of water supplied by the oxidation of reduced nickel followed by the action of hydrogen bromide on the oxide formed. The alternative, but less probable, mechanism of the formation of water may be the catalytic oxidation of hydrogen bromide by oxygen in presence of reduced nickel, freed bromine combining with reduced nickel.

To consider the matter more closely, adsorption should be taken into account. However, it is beyond the scope of the present study, which has been schemed with a view to obtaining grounds for explaining the effects of oxygen and of ferromagnetic metals on the addition of hydrogen bromide to unsaturated organic compounds[3][4] and on the isomerization of isostilbene to stilbene by hydrogen bromide,[2] and which has resulted in finding, perhaps, a combined case of the attack by a hydrogen halide on a metal preceded by the oxidation by oxygen and the activation of a hydrogen halide by a trace of water.

A reaction which seems to be of a similar type was reported by G. H. Bailey and G. J. Fowler,[5] who found that, when hydrogen bromide and oxygen were kept on mercury in the dark, hydrogen was produced together with water.

Further, the present authors observed reactions of different types with platinum black and with reduced copper: While platinum black and hydrogen bromide did not react in absence of oxygen, they gave in presence of oxygen a small amount (6 mg. from 0.2 g. platinum black, 45 c.c. hydrogen bromide and 10 c.c. oxygen in 17 days) of a substance which

(5) *J. Chem. Soc.*, **53** (1888), 755.

was not examined closely but was undoubtedly bromoplatinic acid, neither free bromine nor hydrogen being detected. Reduced copper and hydrogen bromide reacted nearly to the exhaustion of the latter either in presence or in absence of oxygen, cuprous bromide being formed in either case.

The authors thank the Japan Society for the Promotion of Scientific Research (Nippon Gakujutsu Shinko-Kwai) for a grant.

Chemical Institute, Faculty of Science,
Imperial University of Tokyo.

The Addition of Hydrogen Bromide to Undecenoic Acid in Toluene Solution. III. The Influence of the Impurities in Undecenoic Acid on the Effects of Oxygen and of Reduced Nickel.

By Yoshiyuki URUSHIBARA and Matsuji TAKEBAYASHI.

(Received July 23, 1938.)

The addition of hydrogen bromide to pure undecenoic acid in toluene solution in the absence of air (oxygen) yields nearly pure 10-bromo-undecanoic acid.[1][2] The presence of air (oxygen)[1] or reduced nickel[2] gives rise to the formation of more or less 11-bromo-undecanoic acid. The smaller the concentration of undecenoic acid in toluene solution, the greater the effect of either oxygen or reduced nickel.[2][3]

Antioxidants, such as diphenylamine, catechol and hydroquinone, eliminate to a greater or smaller extent the effects of oxygen and of reduced nickel on the addition of hydrogen bromide to undecenoic acid in toluene solution.[4] These substances are more effective in inhibiting the action of oxygen than of reduced nickel, and diphenylamine has practically no influence on reduced nickel.[4]

Ashton and Smith[1] observed, in the addition of hydrogen bromide to undecenoic acid in ligroin solution, that the impurities, originated from

(1) R. Ashton and J. C. Smith, *J. Chem. Soc.*, **1934**, 435.
(2) Y. Urushibara and M. Takebayashi, this Bulletin, **13** (1938), 331.
(3) Similar observations were made by Ashton and Smith in benzene solution in presence of air.
(4) Y. Urushibara and M. Takebayashi, this Bulletin, **13** (1938), 404.

the by-products in the preparation of undecenoic acid from ricinus oil, increased greatly the sensitiveness of undecenoic acid to oxygen, and as the impurities were removed, the undecenoic acid became less sensitive to oxygen.

In the present paper the authors deal with the influence of the impurities on the effects of oxygen and of reduced nickel in the addition of hydrogen bromide to undecenoic acid in toluene solution.

As the pure specimen of undecenoic acid a commercial product melting at 23.3–23.8° (corr.) (Kahlbaum, "extra pure") was used. The other specimen was prepared from ricinus oil and purified until it showed a melting point 20.5–21.7° (corr.). While the former was free from any traces of peroxides, the latter gave a very faint colouration with ammonium thiocyanate and ferrous ammonium sulphate. Even immediately after distilled in vacuum, the impure acid showed a slight peroxide reaction. Such a liability to form peroxides is a feature of impure undecenoic acid, and is caused probably by the presence of some aldehydes.[5] To protect the impure undecenoic acid, and even the pure if once its container was opened, from the formation of peroxides, they were kept in solid state in a refrigerator until use.

Hydrogen bromide was prepared by the action of bromine on hot tetralin and purified according to the directions of A. Klemenc.[6] Reduced nickel was prepared by reducing nickel oxide (Kahlbaum) with hydrogen.

The results of experiments are shown in Tables 1 and 2. Hydrogen bromide was passed into the solution of 1.3 g. undecenoic acid in 20 c.c. toluene (more dilute than in the previous experiments) at 0°C. in the dark for an hour. The fundamental procedure of the experiments was the same as described in the first paper.[2] Thus, the additions in vacuum and in the presence of air and of reduced nickel were carried out just in the same manner as done previously. The reactions with the admission of given amounts of oxygen were carried out in the same way as the reactions in vacuum, except that, just before the introduction of hydrogen bromide, the required volumes of oxygen were admitted and the reaction vessels were shaken for five minutes.

The reaction mixtures were treated in the same way as before, and the compositions of the products were determined by measuring the melting (clearing) points (compare Fig. 2 of the first paper). Although the reaction was always complete, the impurities in the starting material

(5) Compare Ashton and Smith, *J. Chem. Soc.*, **1934**, 436.

(6) A. Klemenc, "Die Behandlung und Reindarstellung von Gasen," 196, Leipzig (1938).

Table 1. Pure undecenoic acid, m.p. 23.3-23.8°.

Exp. No.	In presence of	Product	
		Melting point (°C.)	11-Bromo-undecanoic acid (%)
1	None (vacuum)	34.6	2
2	Oxygen 0.5 c.c.	30.2	19
3	,, ,,	30.6	17
4	,, 1 c.c.	30.0	19
5	,, ,,	29.8	20
6*	Air	48.7	97
7	Reduced nickel 3.0 g.	25.5	34

* Exp. 5 of the first paper (3.68 g. undecenoic acid in 20 c.c. toluene).

Table 2. Impure undecenoic acid, m.p. 20.5-21.7°.

Exp. No.	In presence of	Product	
		Melting point (°C.)	11-Bromo-undecanoic acid (%)
8	None (vacuum)	33.0	8−
9	Oxygen 0.5 c c.	43.4	76+
10	,, 1 c.c.	46.1	86+
11	Air	48.4	96+
12	Reduced nickel 3.0 g.	26.0	35−

might affect the melting points of the products. However, it can be considered that the impurities were removed when the crystallized products were pressed on porous plates. The numbers in the last column of Table 2 were obtained by assuming the products contained only the two bromo-undecanoic acids. The minus and plus signs indicate that the percentage of 11-bromo-undecanoic acid should be smaller and greater respectively if the impurities still contaminated the products and lowered their melting points.

In absence of air the pure undecenoic acid gave nearly pure 10-bromo-undecanoic acid (Exp. 1), while the impure starting acid a product containing perhaps a greater amount of 11-bromo-undecanoic acid (Exp. 8). No difference was found between the pure and the impure specimens in the reactions in air (Exps. 6 and 11), the amount of oxygen absorbed under the conditions of the experiments being sufficient for producing the maximum proportion of 11-bromo-undecanoic acid in either case. However, with the limited amounts of oxygen, a great difference

was observed between the pure and the impure specimens of undecenoic acid: With 0.5 or 1 c.c. oxygen, only about 20 per cent of the products from the pure undecenoic acid was 11-bromo-undecanoic acid (Exps. 2, 3, 4, and 5), while the proportion of 10- and 11-bromo-undecanoic acids was nearly reversed in the products from the impure starting acid (Exps. 9 and 10).

Thus, the impure undecenoic acid was found to be far more sensitive to oxygen than the pure acid in the addition of hydrogen bromide in toluene solution, although the greater sensitiveness of the impure acid remains to be explained chemically. A possible explanation may be that, as the impure acid is much more liable to form peroxides than the pure as mentioned above, the former might absorb oxygen (partly in the form of peroxides) more easily than the latter, and, therefore, more oxygen (a part regenerated from the peroxides by the action of hydrogen bromide) might be present in the impure acid than in the pure during the addition reaction. If so, the presence of more oxygen would be simply the cause of the apparent greater sensitiveness of the impure undecenoic acid to oxygen. Otherwise, the peroxides, if not decomposed by hydrogen bromide, might be more powerful than molecular oxygen in reversing the direction of addition of hydrogen bromide, although the molecular oxygen is more active than the peroxide from allyl bromide in the case of the addition of hydrogen bromide to allyl bromide.[7] Further, it may be also suspected that the impurities might act as oxygen carriers during the reaction. At any rate, nothing more concrete can be mentioned for the present.

On the other hand, the effect of reduced nickel seems not to be influenced by the impurities (Exps. 7 and 12). Even if the difference existing between Exps. 1 and 8 were taken into consideration or the impurities in the starting acid were assumed to affect the melting point of the product, it could be safely mentioned at least that the effect of reduced nickel was not increased by the impurities, contrary to the effect of oxygen. This may suggest the different mechanisms for the catalytic actions of oxygen and of reduced nickel, although their effects are very similar as seen from the results of the reactions which take place in their presence.

The authors express their hearty thanks to the Imperial Academy of Japan for a grant.

Chemical Institute, Faculty of Science,
Imperial University of Tokyo.

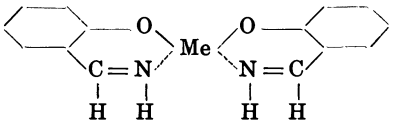
(7) This Bulletin, **12** (1937), 138.

Nebenvalenzringverbindungen. III. Über einige innerkomplexe Eisen- und Mangansalze der Oxyaldimine.*

Von Tokuichi TSUMAKI.

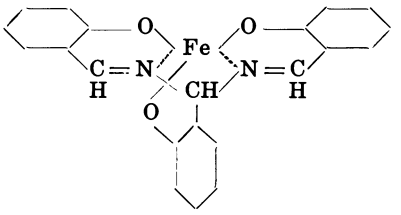
(Eingegangen am 25. August 1938.)

In der I. und II. Mitteilungen[1] ist beschrieben, dass aus den Oxyaldehyden und Oxyketonen mit Äthylendiamin und gewöhnlichen Metallsalzen eine Reihe von typischen Innerkomplexsalzen entsteht. Die Verbindungen dieser Art entstehen auch aus den Oxyaldehyden und Oxyketonen mit Ammoniak und verschiedenen Metallsalzen[2] (Formel I).



I.

Bei der Einwirkung von Ferrosulfat auf Salicylaldehyd und Ammoniak erhielt ich aber, wie in der zweiten Mitteilung erwähnt, ein innerkomplexes Ferrisalz von anderem Typus, d.h. Trisalicylaldehyd-diimineisen (Formel II).



II.

Bei der Reaktion findet also durch den Luftsauerstoff eine Oxydation des zweiwertigen Eisens zum dreiwertigen statt.

Lässt man nun auf eine Mischung von Salicylaldehyd und Ammoniak Ferrisalz (Eisenalaun) einwirken, so erhält man ein rotbraunes Pulver, aus dem ich durch Extrahieren mit Nitrobenzol fast schwarze Krystalle

---

* Übersetzung einer Mitteilung, die in *J. Chem. Soc. Japan*, **56** (1935), 1329, auf Japanisch beschrieben.

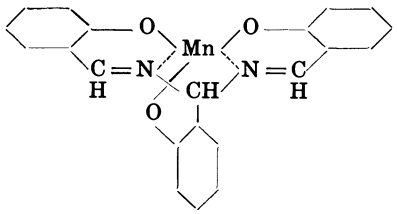
(1) I. Mitteilung: Pfeiffer, Breith, Lübbe und Tsumaki, *Ann.*, **503** (1933), 84; II. Mitteilung: Tsumaki, dies Bulletin, **10** (1935), 74.

(2) Pfeiffer, Buchholz und Bauer, *J. prakt. Chem.*, **129** (1931), 163; Pfeiffer, Breith, Lübbe und Tsumaki, *Ann.*, **503** (1933), 109.

des oben erwähnten Trisalicylaldehyd-diimin-eisens, welches 1 Mol. Nitrobenzol enthält, isolieren konnte.

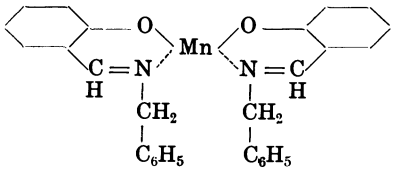
Eine Reaktion zwischen Hydrosalicylamid, Ammoniak und Ferrichlorid, dem vorher Ammoniak und Weinsäure zugesetzt sind, ist schon im Jahre 1840 von Ettling[3] untersucht worden. Er erhielt das Eisensalz des Salicylaldehydimids als ein gelbrotes Pulver und gab der Verbindung eine komplizierte Formel $C_{42}H_{36}O_3N_6+Fe_2O_3$; die später von Delépine[4] in $(C_7H_6ON)_3Fe$ vereinfacht und weiter von Pfeiffer[5] als Innerkomplexsalz $(C_7H_6ON>)_3Fe$ formuliert wurde. Die schwarzen Krystalle des Trisalicylaldehyd-diimin-eisens sind aber bei der Reaktion nicht isoliert worden.

Weiter habe ich Manganosalz auf Salicylaldehyd und Ammoniak wirken lassen. Da habe ich ein dunkelgelbes Pulver, welches wahrscheinlich ein Mangano-Komplexsalz ist, erhalten. Lässt man die Chloroformlösung der Verbindung über Nacht stehen, so wird das Manganosalz durch den Luftsauerstoff oxydiert und es scheidet sich allmählich aus der Lösung glänzende, fast schwarze Krystalle des Trisalicylaldehyd-diimin-mangans (Formel III) aus, in welchem das Manganatom dreiwertig ist.



III.

Bei der Reaktion zwischen Salicylaldehyd, Benzylamin und Manganacetat unter Luftabschluss erhält man rotgelbe Krystalle des Salicylaldehyd-benzylimin-mangans (Formel IV), die sich an der Luft durch Oxydation allmählich dunkelgelb färben.

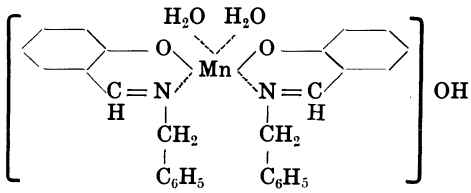


IV.

Lässt man Manganacetat auf Salicylaldehyd und Benzylamin in Alkohollösung an der Luft einwirken, filtriert die erhaltene schwarz-

(3) Ettling, *Ann.*, **35** (1840), 265.
(4) Delépine, *Bull. soc. chim.*, **21** (1899), 944.
(5) Pfeiffer, Buchholz und Bauer, *J. prakt. Chem.*, **129** (1931), 163.

braune Lösung ab und lässt das Filtrat an der Luft stehen, so scheiden sich glänzende, fast schwarze Krystalle aus. Beim Erwärmen der Krystalle mit verdünnter Schwefelsäure tritt Geruch nach Salicylaldehyd, beim Erwärmen mit Natronlauge Geruch nach Benzylamin auf. Beim schwachen Erhitzen mit Oxalsäure in Gegenwart von Schwefelsäure, erfolgt CO_2-Entwicklung. Das Manganatom in der Verbindung ist also dreiwertig. Nach der Analyse handelt es sich wahrscheinlich um die Verbindung: Salicylaldehyd-benzylimin-mangani-hydroxyd mit 2 Mol. Wasser (Formel V).



V.

Beschreibung der Versuche.

(1) **Trisalicylaldehyd-diimin-eisen.** Man erwärmt 4 g. Salicylaldehyd mit 10 g. 25-proz. Ammoniak und 150 c.c. Alkohol auf dem Wasserbad und fügt eine Lösung von 4.8 g. Eisenalaun in 80 c.c. Wasser hinzu. Es scheidet sich sofort ein rotbrauner Niederschlag aus, der nach dem Erwärmen auf dem Wasserbad abgesaugt und auf Ton an der Luft getrocknet wird. Man erwärmt den Niederschlag mit viel Alkohol und filtriert die dabei hinterbleibende Substanz ab, welche mit heissem Nitrobenzol umkrystallisiert wird. So erhält man fast schwarze Blättchen, die mit Alkohol gewaschen und im Vakuum über Chlorcalcium getrocknet werden. Ausbeute 1.5 g. Die Verbindung enthält 1 Mol. Nitrobenzol, das beim Erhitzen auf 150° abgegeben wird. Der Erhitzungsrückstand ist auch ein schwarzes Pulver. (Gefunden: Fe, 13.81; N, 6.98, 6.91. Berechnet für $C_{21}H_{15}O_3N_2Fe$: Fe, 14.00; N, 7.02%.)

(2) **Trisalicylaldehyd-diimin-mangan.** Man erwärmt 6 g. Salicylaldehyd mit 20 g. 25-proz. Ammoniak und 250 g. Alkohol und fügt eine Lösung von 4.8 g. Mangansulfat in 160 c.c. Wasser hinzu. Es scheidet sich sofort ein dunkelgelber Niederschlag aus, der schnell abgesaugt und auf Ton im Vakuumexsikkator über Natronkalk getrocknet wird. Man erwärmt das dunkelgelbe Pulver mit Chloroform, filtriert und lässt das erhaltene schwarzbraune Filtrat an der Luft stehen. So scheiden sich glänzende schwarzbraune Krystalle aus, die abfiltriert, mit Alkohol gewaschen und bei 110° getrocknet werden. Ausbeute 3.2 g. (Gefunden: Mn, 13.97; N, 6.90, 6.87. Berechnet für $C_{21}H_{15}O_3N_2Mn$: Mn, 13.80; N, 7.04%.)

Die Krystalle sind löslich in heissem Nitrobenzol und unlöslich in Alkohol und Chloroform.

(3) **Salicylaldehyd-benzylimin-mangan.** Man erhitzt ein Gemisch von 2.5 g. Salicylaldehyd, 5 g. Benzylamin und 100 g. Alkohol zum Sieden, fügt eine heisse Lösung

von 2 g. Manganacetat in 10 c.c. Wasser hinzu und evakuiert sofort die Luft in dem Reaktionskolben in einem Vakuumexsikkator. Aus der dunkelroten Lösung scheiden sich allmählich rotgelbe Prismen aus, die nach einem Tage abgesaugt, mit Alkohol gewaschen und im Vakuumexsikkator über Chlorcalcium getrocknet werden. Ausbeute 1.9 g.

Die Krystalle sind leicht löslich in Chloroform und Pyridin mit schwarzbrauner Farbe, wenig löslich in Alkohol und unlöslich in Äther, Petroleumäther und Wasser.

Die Krystalle färben sich an der Luft allmählich dunkelbraun durch Oxydation.

Die Verbindung ist ziemlich beständig gegen Alkali. Erwärmt man aber die Verbindung mit Kalilauge, so tritt Zersetzung unter Bildung von freiem Benzylamin ein. Durch verdünnte Schwefelsäure wird sie leicht unter Bildung von Salicylaldehyd zersetzt. (Gefunden: Mn, 11.37; N, 5.74. Berechnet für $C_{28}H_{24}O_2N_2Mn$: Mn, 11.56; N, 5.90%.)

(4) **Salicylaldehyd-benzylimin-mangani-hydroxyd+$2H_2O$.** Man erhitzt ein Gemisch von 2.5 g. Salicylaldehyd, 5 g. Benzylamin und 100 g. Alkohol, fügt allmählich eine Lösung von 2.5 g. Manganacetat in 12 c.c. Wasser hinzu und filtriert die erhaltene braune Lösung. Es scheiden sich aus dem Filtrat nach einigem Stehenlassen glänzende, fast schwarze Krystalle aus, die abfiltriert, mit Alkohol gewaschen und im Vakuumexsikkator über Chlorcalcium getrocknet werden. (Gefunden: Mn, 10.08, 10.10; N, 5.48. Berechnet für $C_{28}H_{25}O_3N_2Mn \cdot 2H_2O$: Mn, 10.40; N, 5.30%.)

Die Krystalle sind leicht löslich in Pyridin und Chloroform, löslich in Eisessig, wenig löslich in Äther und Alkohol und unlöslich in Wasser.

Erwärmt man die Verbindung mit Kalilauge, so tritt Zersetzung unter Bildung von freiem Benzylamin ein. Auch durch verdünnte Schwefelsäure wird sie unter Bildung von Salicylaldehyd zersetzt. Beim schwachen Erhitzen mit Oxalsäure in Gegenwart von verdünnter Schwefelsäure, erfolgt CO_2-Entwicklung.

Osaka-Hochschule, Osaka.

Nebenvalenzringverbindungen. V. Spektrochemische Untersuchungen über die innerkomplexen Metallsalze von Salicylaldehyd-äthylendiimin und seinen verwandten Verbindungen.

Von Tokuichi TSUMAKI.

(Eingegangen am 10. August 1938.)

In der IV. Mitteilung[1] habe ich die Absorptionskurve des innerkomplexen Kobaltsalzes von Salicylaldehyd-äthylendiimin angegeben und durch Anwendung der Shibata-Tsuchidasche Theorie,[2] dem Komplexsalze eine asymmetrische Konstitution zuerteilt, weil in der Kurve die dritte Absorptionsbande zur Erscheinung kam.

Später habe ich mit R. Tsuchida[3] die Absorptionsspektren des organischen Restes des obenerwähnten Komplexes gemessen und dadurch eine nähere Erklärung der Absorptionskurve des Komplexsalzes gegeben. Die sterische Konfiguration des Salzes ist dabei bestätigt worden.

Um tiefere Kenntnisse von den inneren Komplexsalzen der Salicylaldehyd-äthylendiimin-Reihe mit verschiedenen Metallen zu erhalten, habe ich nun die spektrochemischen Untersuchungen über diese Verbindungen ausgeführt.

(a) Salicylaldehyd-äthylendiimin-kupfer wurde nach Pfeiffer und Breith[4] dargestellt. Die Extinktionskoeffizienten wurden gemessen. Lösungsmittel: Methylalkohol. Konzentration: 0.0005 Mol/l. Schichtdicke: 0.02–5.0 cm. Die Absorptionskurve ist in Abb. 1 mit dicker Linie angegeben. Zur Vergleichung sind dabei die vor kurzem von mir[3] gemessenen Absorptionskurven des *o*-Methoxybenzaldehyd-äthylendiimins und Salicylaldehyd-äthylendiimins mit dünnen Linien gezeigt.

o-Methoxybenzaldehyd-äthylendiimin hat zwei Absorptionsbanden bei 98×10^{13} sek.$^{-1}$ und 120×10^{13} sek.$^{-1}$

Salicylaldehyd-äthylendiimin zeigt drei Banden bei 75×10^{13} sek.$^{-1}$, 95×10^{13} sek.$^{-1}$ und 117×10^{13} sek.$^{-1}$ Die Bande bei 75×10^{13} sek.$^{-1}$ ist, wie in der Mitteilung von Tsuchida und mir[3] erklärt, die zweite Bande, welche durch die Wasserstoff-Brücke zwischen Stickstoffatom und Hydro-

(1) Tsumaki, dies Bulletin, **13** (1938), 252.

(2) Shibata, *J. Chem. Soc. Japan*, **36** (1915), 1243; Tsuchida, *ibid.*, **59** (1938), 586; dies Bulletin, **13** (1938), 388; *ibid.*, **13** (1938), 436.

(3) Tsuchida und Tsumaki, dies Bulletin, **13** (1938), 527.

(4) Pfeiffer, Breith, Lübbe und Tsumaki, *Ann.*, **503** (1933), 84.

xylgruppe verursacht wird. Sie ist also die zweite Bande des absorbierenden Zentrums, O—H←N, in einer Nebenvalenzringverbindung. Die letzten zwei Banden des Salicylaldehyd-äthylendiimins sind die speciellen[3] Banden, welche den zwei Banden des *o*-Methoxybenzaldehyd-äthylendiimins entsprechen.

Nun dem Anschein nach hat das Kupfer-Komplexsalz des Salicylaldehyd-äthylendiimins, wie in Abb. 1 gezeigt, drei Absorptionsbanden bei 53×10^{13} sek.$^{-1}$, 84×10^{13} sek.$^{-1}$ und 111×10^{13} sek.$^{-1}$, während das Kobalt-Komplexsalz fünf Banden zeigt.[3] Die Kurve des Kupfer-Komplexes scheint aber bei näherer Betrachtung, wie weiter unten angegeben, auch fünf Banden zu enthalten.

Es ist bekannt,[5] dass die koordinative Bindung den Absorptionsbanden der Liganden einen bathochromisch-hypochromischen Einfluss gibt, mit anderen Worten, dass die speciellen Banden, die auf den Liganden beruhen, weniger absorbierend sind und längere Wellenlängen haben als die entsprechenden Banden der Liganden in freiem Zustande. Den Einfluss kann man auch bei der Vergleichung der Absorptionsbanden des Salicylaldehyd-äthylendiimins mit den des *o*-Methoxybenzaldehyd-äthylendiimins deutlich betrachten.

Wenn Salicylaldehyd-äthylendiimin ein inneres Komplexsalz des Kupfers bildet, müssen die speciellen Absorptionsbanden des Komplexes durch den bathochromisch-hypochromischen Einfluss im Gebiete der längeren Wellen als die Banden des *o*-Methoxybenzaldehyd-äthylendiimins erscheinen.

Die Absorption bei ca. 84×10^{13} sek.$^{-1}$ soll also eine specielle Bande und die zweite Bande des Komplexes enthalten.

Die Bande bei 53×10^{13} sek.$^{-1}$ ist die erste Absorptionsbande, die in der unvollständigen Übergangsschale des Kupri-ions begründet ist.[6]

Die Absorption bei ca. 111×10^{13} sek.$^{-1}$ kann nicht aus einer speciellen Bande bestehen, weil der maximale Extinktionskoeffizient grösser als der des *o*-Methoxybenzaldehyd-äthylendiimins ist.[7] Die Absorption enthält also ausser einer speciellen Bande noch die dritte[8] Absorptionsbande.

(b) *o*-Oxyacetophenon-äthylendiimin-kupfer wurde nach Pfeiffer und Tsumaki[4] dargestellt. Die Extinktionskoeffizienten wurden gemessen. Lösungsmittel: Methylalkohol. Konzentration: 0.0005 Mol/l.

(5) Tsuchida und Kobayashi, dies Bulletin, **13** (1938), 471.

(6) Tsuchida, *J. Chem. Soc. Japan*, **59** (1938), 731; dies Bulletin, **13** (1938), 388.

(7) Der maximale Extinktionskoeffizient der speziellen Bande muss durch den hypochromischen Einfluss viel kleineren Wert haben.

(8) Tsuchida, *J. Chem. Soc. Japan*, **59** (1938), 586; dies Bulletin, **13** (1938), 388; *ibid.*, **13** (1938), 436.

Schichtdicke: 0.02–5.0 cm. Die Absorptionskurve ist in Abb. 2 mit dicker Linie angegeben. Zur Vergleichung ist dabei die vor kurzem von mir[3] gemessene Absorptionskurve des *o*-Oxyacetophenon-äthylendiimins mit dünner Linie gezeigt. Die Absorptionskurve des Salzes wird mit analoger Weise mit der Erklärung der Kurve des Salicylaldehyd-äthylendiimin-kupfers analysiert.

Die Bande bei 56×10^{13} sek.$^{-1}$ ist die erste Absorptionsbande. Die Bande bei 85×10^{13} sek.$^{-1}$ ist die zweite Absorptionsbande. Die Bande bei 92×10^{13} sek.$^{-1}$ ist eine specielle Bande. Die Absorption bei 111×10^{13} sek.$^{-1}$ enthält eine specielle Bande und die dritte Bande.

(c) Salicylaldehydimin-kupfer wurde nach Ettling[9] dargestellt. Die Extinktionskoeffizienten wurden gemessen. Lösungsmittel: Methylalkohol. Konzentration: 0.0005 Mol/l. Schichtdicke: 0.02–15.0 cm. (Abb. 3).

Die Bande bei 52×10^{13} sek.$^{-1}$ ist die erste Bande. Die Absorption bei 84×10^{13} sek.$^{-1}$ enthält eine specielle Bande und die zweite Bande. Die Bande bei 105×10^{13} sek.$^{-1}$ ist eine specielle Bande. Die Bande bei 113×10^{13} sek^{-1} ist die dritte Bande.

(d) *o*-Oxyacetophenon-äthylendiimin-nickel wurde nach Pfeiffer und Lübbe[4] dargestellt. Die Extinktionskoeffizienten wurden gemessen. Lösungsmittel: Äthylalkohol. Konzentration: 0.0001 Mol/l. Schichtdicke: 0.08–15.0 cm. (Abb. 4).

Die Bande bei 75×10^{13} sek.$^{-1}$ ist die erste Absorptionsbande. Die Absorption bei 92×10^{13} sek.$^{-1}$ besteht aus einer speciellen Bande und der zweiten Bande. Die Absorption bei 120×10^{13} sek.$^{-1}$ enthält andere specielle Bande und die dritte Bande.

(e) Salicylaldehyd-äthylendiimin-magnesium wurde nach Pfeiffer und Tsumaki[4] dargestellt. Die Extinktionskoeffizienten wurden gemessen. Lösungsmittel: Methylalkohol. Konzentration: 0.0005 Mol/l. Schichtdicke: 0.02–15.0 cm. (Abb. 5).

Die Absorption bei ca. 90×10^{13} sek.$^{-1}$ scheint zwei Absorptionsbanden zu enthalten: eine specielle Bande bei ca. 91×10^{13} sek.$^{-1}$ und die zweite Bande bei ca. 82×10^{13} sek.$^{-1}$ Es fehlt der Kurve an der ersten Bande, weil Magnesium nicht das Übergangselement ist. Der maximale Extinktionskoeffizient der Absorptionsbande bei ca. 120×10^{13} sek.$^{-1}$ ist ungefähr gleich mit dem der entsprechenden Bande des *o*-Methoxybenzaldehyd-äthylendiimins. Trotzdem wird die Existenz der dritten Bande erlaubt, weil der Extinktionskoeffizient der speciellen Bande durch hypochromischen Einfluss einen kleineren Wert haben muss.

(9) Ettling, *Ann.*, **35** (1840), 265.

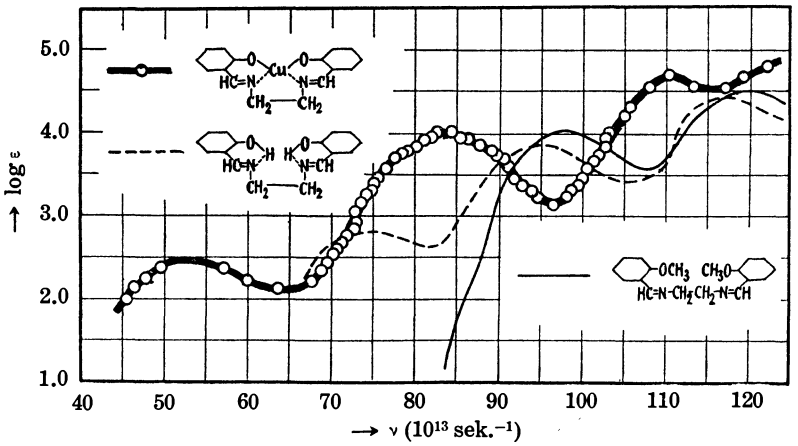


Abb. 1.

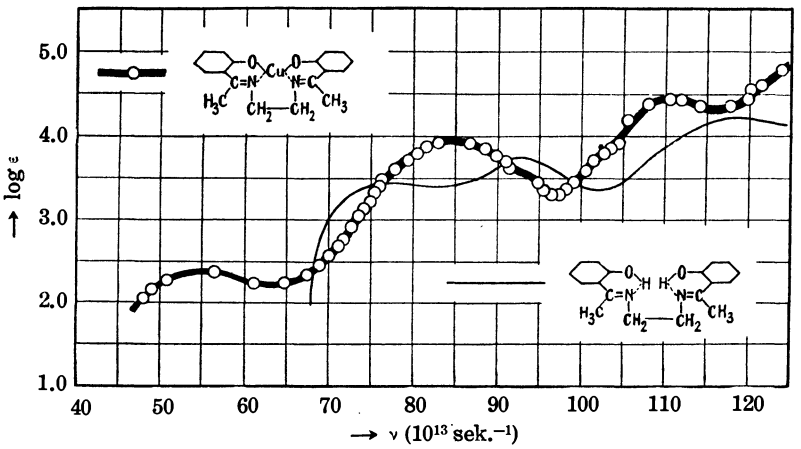


Abb. 2.

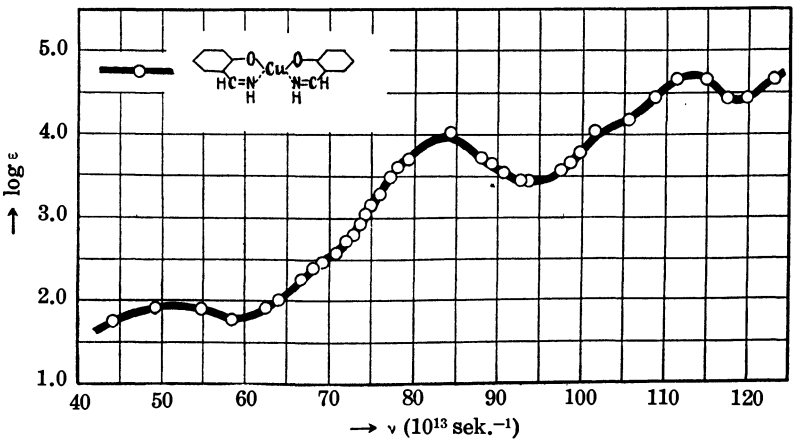


Abb. 3.

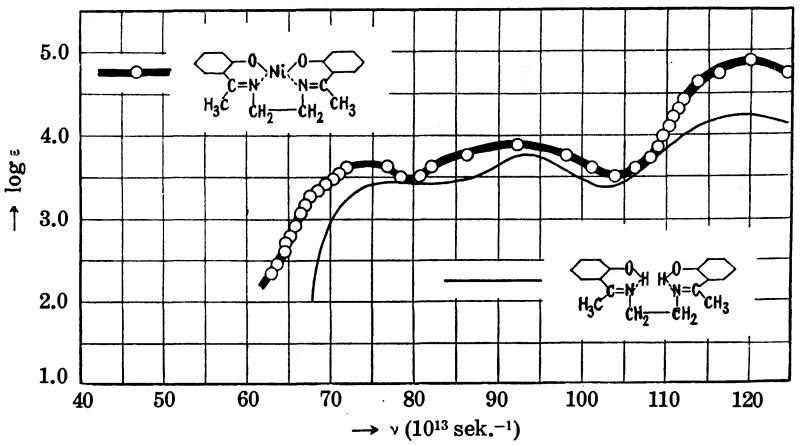


Abb. 4.

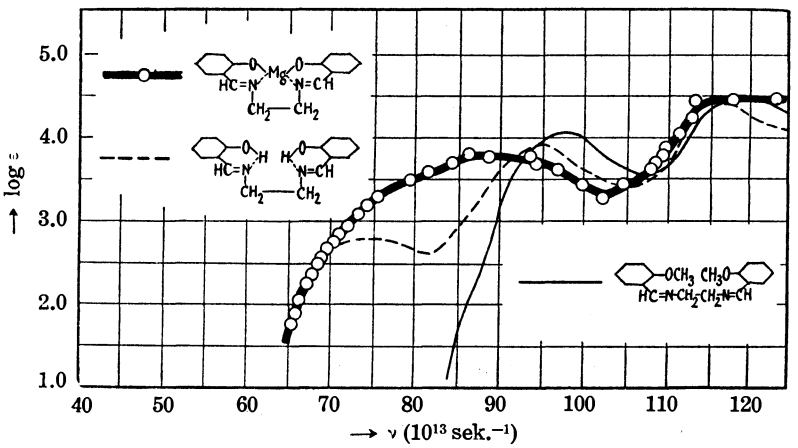


Abb. 5.

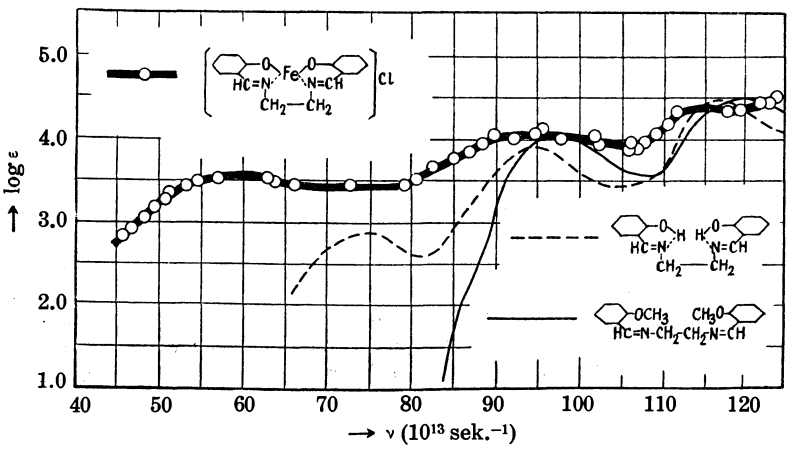


Abb. 6.

(f) Salicylaldehyd-äthylendiimin-ferri-chlorid wurde nach Pfeiffer und Tsumaki[4] dargestellt. Die Extinktionskoeffizienten wurden gemessen. Lösungsmittel: Äthylalkohol. Konzentration: 0.0001 Mol/l. Schichtdicke: 0.08–5.0 cm. (Abb. 6).

Die Bande bei 60×10^{13} sek.$^{-1}$ ist die erste Bande. Die Bande bei 93×10^{13} sek.$^{-1}$ besteht aus der zweiten Bande und einer speciellen Bande. Die Kurve hat noch eine Absorptionsbande bei 115×10^{13} sek.$^{-1}$ Der maximale Extinktionskoeffizient ist kleiner als der der entsprechenden Bande des *o*-Methoxybenzaldehyd-äthylendiimins und ungefähr gleich dem des Salicylaldehyd-äthylendiimins. Es ist schwer in diesem Falle zu versichern, ob der Extinktionskoeffizient der speciellen Bande des Komplexsalzes einen noch kleineren Wert zeigt, mit anderen Worten, ob die Existenz der dritten Bande erlaubt werden kann. In Erwägung der hypochromischen Neigung der speciellen Bande gibt es aber die Möglichkeit der Existenz der dritten Bande.

In allen Absorptionskurven der obenerwähnten Metall-Komplexsalze ausser dem Eisensalz kamen also mit Sicherheit die dritten Absorptionsbanden zur Erscheinung.

Wendet man nun die Shibata-Tsuchidasche Theorie über die dritten Bande auf diese Metall-Komplexsalze an, so muss die Konfiguration der Salze so aufgestellt werden, dass zwei Sauerstoffatome im organischen Rest miteinander in Trans-Stellungen die Koordinationsstellen einnehmen. Diese Metallsalze besitzen also wie das entsprechenden Kobaltsalz[1][3] eine asymmetrische Konstitution.

Zusammenfassung.

I. Mitteilung.[10] (1) Zahlreiche *o*-Oxyaldehyd- und *o*-Oxyketon-äthylendiimin-Komplexsalze, welche tricyclische orthokondensierte Nebenvalenzringe enthalten, wurden dargestellt. Als Metalle benutzte ich Nickel, Kobalt, Kupfer, Zink, Cadmium, Mangan, Eisen und Magnesium. Als die organischen Komponenten der Komplexe wurden Salicylaldehyd, Resobenzophenon und *o*-Oxyacetophenon gebraucht.

(2) Das häminartige Chlorid des Eisenkomplexes wurde dargestellt.

(3) Einige Komplexsalze von *o*-Oxyxanthon und *o*-Oxyanthrachinon wurden dargestellt.

---

(10) *Ann.*, **503** (1933), 84. In der Mitteilung habe ich mit P. Pfeiffer, E. Breith und E. Lübbe eine Untersuchung über tricyclische orthokondensierte Nebenvalenzringe mitgeteilt. Der Anteil der Mitarbeiter an der Darstellung der einzelnen Verbindungen ist durch die Anfangsbuchstaben ihrer Namen gekennzeichnet. Die vorliegende Zusammenfassung der I. Mitteilung enthält nur die Experimente, die ich selbst ausgeführt habe.

II. Mitteilung.[11] (1) Einige innerkomplexe Eisenverbindungen des Salicylaldehyd-äthylendiimins und Phenylnitrosohydroxylamins wurden dargestellt.

(2) Bei der Darstellung der Verbindungen habe ich in allen Fällen als Ausgangsmaterial Ferrosulfat gebraucht und das Eisen in den erhaltenen Substanzen ist immer dreiwertig.

(3) Bei diesen Reaktionen erhielt ich 2 Typen der komplexen Ferri-Verbindungen, d.h. $(>)_3Fe$ und $(>Fe<)_2O$. Die hämatinartige Hydroxyd-Form $(>Fe<)OH$ wurde auch erhalten, welche in alkalischer Lösung unbeständig ist und leicht in die Oxyd-Form $(>Fe<)_2O$ übergeht.

(4) Ein innerkomplexes Eisensalz von neuem Typus, d.h. Trisalicylaldehyd-diimin-eisen, wurde isoliert.

III. Mitteilung.[12] (1) Trisalicylaldehyd-diimin-Komplexsalze von Eisen und Mangan wurden untersucht.

(2) Die Mangan-Komplexverbindungen des Salicylaldehyd-benzylimins wurden dargestellt.

IV. Mitteilung.[1] (1) Salicylaldehyd-äthylendiimin-kobalt, welches aus Benzol in rotbraunen Nadeln krystallisiert, absorbiert in festem Zustande den Luftsauerstoff und geht in die schwarze Sauerstoff-Anlagerungsverbindung über. Erhitzt man die oxydierte Verbindung, so verliert sie leicht wieder den Sauerstoff und nimmt an Gewicht bis zum ursprünglichen Werte ab, wobei die rotbraune Farbe zurückkehrt. Das Kobaltatom bindet sich locker an ein Sauerstoffmolekül, ganz in Analogie zur Bindungsweise des Oxyhämoglobins.

(2) Diese merkwürdige Anlagerung ist besonders auffallend bei dem pulverförmigen Kobaltsalze, welches aus der chloroformhaltigen Verbindung durch Abspaltung des Chloroforms erhalten wird.

(3) Die qualitative und quantitative Bestimmung des angelagerten Sauerstoffs wurde ausgeführt.

(4) Um deutlich zu machen, dass die Erscheinung der Absorption des Luftsauerstoffs eine Anlagerung ist, habe ich eine spektrochemische Untersuchung ausgeführt.

(5) Durch Anwendung der Shibata-Tsuchidasche Theorie auf die Kobalt-Komplexsalze wurde die Konfiguration der Salze angegeben.

(6) Salicylaldehyd-äthylendiimin-kobalti-hydroxyd und Salicylaldehyd-äthylendiimin-kobalti-chlorid wurden dargestellt.

---

(11) Tsumaki, dies Bulletin, **10** (1935), 74.
(12) Tsumaki, dies Bulletin, **13** (1938), 579.

V. Mitteilung.[13] (1) Die Extinktionskoeffizienten von den innerkomplexen Kupfersalzen des Salicylaldehyd-äthylendiimins, *o*-Oxyacetophenon-äthylendiimins und Salicylaldimins, dem Nickelsalze des *o*-Oxyacetophenon-äthylendiimins, dem Magnesiumsalze des Salicylaldehyd-äthylendiimins und dem Salicylaldehyd-äthylendiimin-ferri-chlorid wurden gemessen.

(2) Die Absorptionskurven der Komplexsalze wurden erklärt durch Vergleichung mit den der organischen Liganden in freiem Zustande. In allen Kurven ausser dem Eisensalze kamen die dritten Absorptionsbanden zur Erscheinung. Beim Eisensalze gibt es die Möglichkeit der Existenz der dritten Bande.

(3) Durch Anwendung der Shibata-Tsuchidasche Theorie über die dritte Bande wurde die sterische Konfiguration der Salze festgestellt.

Bei diesen Untersuchungen wurden die unten beschriebenen 37 neuen Verbindungen dargestellt und charakterisiert:

1. Resobenzophenon-äthylendiimin-nickel.
2. *o*-Oxyxanthon-nickel.
3. *o*-Oxyxanthon-nickel + $2C_5H_5N$.
4. *o*-Oxyanthrachinon-nickel + $2C_5H_5N$.
5. *o*-Oxyanthrachinonimin-nickel.
6. *o*-Oxyanthrachinonimin-nickel + $2H_2O$.
7. Salicylaldehyd-äthylendiimin-ferrioxyd.
8. Salicylaldehyd-äthylendiimin-ferri-acetat.
9. Salicylaldehyd-äthylendiimin-ferri-benzoat.
10. Mandelsaures Salz des Salicylaldehyd-äthylendiimin-eisens.
11. Salicylaldehyd-äthylendiimin-ferri-*d*-campfer-β-sulfonat.
12. Salicylaldehyd-äthylendiimin-ferri-*d*-α-bromcampfer-α-sulfonat.
13. Salicylaldehyd-äthylendiimin-ferri-chlorid.
14. *o*-Oxyacetophenon-äthylendiimin-ferri-oxyd.
15. Salicylaldehyd-äthylendiimin-mangan + $C_2H_8N_2$.
16. Salicylaldehyd-äthylendiimin-mangani-hydroxyd.
17. Salicylaldehyd-äthylendiimin-magnesium.
18. Salicylaldehyd-äthylendiimin-zink + $\frac{1}{2}C_2H_8N_2$.
19. Salicylaldehyd-äthylendiimin-cadmium.
20. Salicylaldehyd-äthylendiimin-cadmium + C_5H_5N.
21. Salicylaldehyd-kobalt.
22. Salicylaldehyd-kobalt + $2H_2O$.
23. Salicylaldehyd-äthylendiimin-kobalt.
24. *o*-Oxyacetophenon-äthylendiimin-kupfer.
25. *o*-Oxyacetophenon-äthylendiimin.
26. Salicylaldehyd-äthylendiimin-ferri-hydroxyd + $2H_2O$.

(13) Tsumaki, dies Bulletin, **13** (1938), 583.

27. Trisalicylaldehyd-diimin-eisen.
28. Trisalicylaldehyd-diimin-eisen+$C_6H_5NO_2$.
29. Phenylnitrosohydroxylamin-ferrioxyd+$2C_2H_5OH$.
30. Phenylnitrosohydroxylamin-eisen.
31. Trisalicylaldehyd-diimin-mangan.
32. Salicylaldehyd-benzylimin-mangan.
33. Salicylaldehyd-benzylimin-mangani-hydroxyd+$2H_2O$.
34. Salicylaldehyd-äthylendiimin-kobalt+$CHCl_3$.
35. Sauerstoff-Anlagerungsverbindung des Salicylaldehyd-äthylendiimin-kobaltes.
36. Salicylaldehyd-äthylendiimin-kobalti-hydroxyd.
37. Salicylaldehyd-äthylendiimin-kobalti-chlorid.

An dieser Stelle möchte ich Herrn Prof. Dr. Paul Pfeiffer, Herrn Prof. Dr. Koichi Matsubara und Herrn Prof. Dr. Yuji Shibata für ihre freundlichen Ratschläge und Ermutigung meinen besten Dank aussprechen. Herrn Prof. Dr. Ryutaro Tsuchida danke ich auch herzlichst für seine freundliche Unterstützung bei der spektrochemischen Untersuchung.

Osaka-Hochschule, Osaka.

On Calcio-gadolinite, a New Variety of Gadolinite Found in Tadati Village, Nagano Prefecture.

By Toshio NAKAI.

(Received August 24, 1938.)

In May 1936, when the author with O. Nagashima was searching for minerals of the rare elements in Nagano Prefecture, a mineral which seemed to be gadolinite was found by us in the pegmatite region of Tukano, Tadati Village.(1) It occurs associated with several other rare minerals such as allanite, zircon, fergusonite, etc.

No good crystal for goniometric measurement has yet been found; however, by chemical and physical examinations mentioned below, the mineral was proved to be a variety of gadolinite containing a considerable

(1) This village is situated about 12 kilometers north-northeast of Naegi, one of the most famous places in Japan for its production of rare minerals.

quantity of calcium which seemed to replace a part of the rare earth elements. To this new variety of gadolinite, the author wishes to give the name "calcio-gadolinite."

The mineral occurs usually in a small massive state and rarely in imperfect prismatic crystals. Its colour is black and its streak greenish dark grey. It shows weak radioactivity. Its specific gravity determined by pycnometer method is 4.5 at 22°C.

The refractive indices of the mineral were determined by T. Sueno by means of the dispersion method using methylene iodide as dispersion medium and glass powder as standard. The result obtained is as follows:[2]

$$\alpha_D = 1.765\,; \quad \beta_D = 1.774\,; \quad \gamma_D = 1.787\,; \quad \beta_F - \beta_C = 0.018.$$

The pleochroism is very strong. Z(Dark brown) > Y(Light yellow) ≒ X(Light brown).

About 0.7 g. of the selected sample was taken for chemical analysis. The analysis was carried out by the method which was previously used by K. Kimura and M. Miyamoto[3] for the analysis of gadolinite from Yamaguti Village. The analytical result obtained is shown in Table 1.

Table 1. Analysis of calcio-gadolinite from Tadati.

CaO	11.91%	Ce_2O_3*	4.69%
MgO	0 14	$(La,Y)_2O_3$ etc.*	24.47
MnO	0.84	ThO_2	0.80
FeO	11.24	SiO_2	23.89
BeO	10.73	U_3O_8	0.10
Al_2O_3	1.68	H_2O (−)	0.14
Fe_2O_3	7.65	H_2O (+)	2.05
		Total	100.34%

* The mean atomic weight of the rare earth elements (including cerium) was found to be about 130 from the ratio, oxide/anhydrous sulphate.

With the sample of rare earths extracted from the mineral, L-series spectral lines of lanthanide elements were photographed using a vacuum spectrograph and a metal X-ray tube of Siegbahn's type. The relative intensities of the spectral lines are given briefly in Table 2.

From the result given in Table 2, this mineral is supposed to be rich in basic lanthanide elements such as lanthanum, cerium, praseodymium

(2) α, β, and γ were determined by S. Tsuboi's statistical method, *J. Geol. Soc. Tôkyô*, **25** (1918), 40.

(3) K. Kimura and M. Miyamoto, *J. Chem. Soc. Japan*, **57** (1936), 1200.

Table 2.

Elements	Relative intensities of lines
La, Ce, Pr, Nd	+ + +
Sm, Gd	+ +
Dy, Er	+
Eu, Tb, Ho, Tu, Yb, Lu	−

and neodymium and poor in terbide elements. It is very interesting to see that the type of the distribution of rare earth elements in this mineral is quite different from that in common gadolinite.[4]

By comparing the analytical result of this mineral with those of gadolinite, some resemblance between them may be recognised, especially in the amounts of beryllium oxide and silica, but the high content of calcium oxide and the low percentage of rare earths in the former mineral are remarkable enough to distinguish it from common gadolinite.

Now, the analytical result of the mineral of Tadati is expressed by the empirical formula,

$$Be_2(Fe^{II}, Fe^{III})\,(\Sigma Ce, Ca)_2\,Si_2(O,OH)_{10},$$

if the minor constituents are neglected. This formula may be derived from that of typical gadolinite, $Be_2Fe^{II}(\Sigma Y)_2Si_2O_{10}$, if we assume that about a half of the rare earth elements in the latter formula is replaced by calcium, a part of ferrous iron by ferric iron, and a part of oxygen by hydroxyl group. As mentioned already, the mineral of Tadati is unusually poor in lanthanide elements of higher atomic numbers, and it is quite possibly expected that calcium replaces chiefly the elements of yttrium group, ion radii of which bear closer resemblance to that of calcium.[5]

The powder diagram of the mineral was photographed by Debye-Scherrer's method using a metal X-ray tube of iron anticathode. The diagram obtained was proved to be almost identical with that of common gadolinite.

Thus, it can be evidently concluded that the mineral found in Tukano, Tadati Village, Nagano Prefecture, should be a variety of gadolinite which

(4) Cf. V. M. Goldschmidt and L. Thomassen, "Geochemische Verteilungsgesetze der Elemente," III, Kristiania (1924).

(5) Cf. V. M. Goldschmidt, "Geochemische Verteilungsgesetze der Elemente," VII, Oslo (1926).

contains a considerable quantity of calcium in the place of the rare earth elements. As far as the author knows, there is no variety of gadolinite on record which contains such a remarkable amount of calcium, and he believes he is justified in giving the name "calcio-gadolinite" to this mineral.

The radium content of the mineral was determined by the following method: A quantity of pulverized mineral was decomposed and brought into solution and the resulted solution was kept closed in a Curie bottle until the equilibrium was established between the radium contained and the radon generated from it. The generated radon was transferred into an ionization chamber and its radioactivity was measured by an electrometer which was previously calibrated with a standard solution of radium. The radium content of the mineral thus determined was $3.15 \times 10^{-8}\%$, i.e. 1 g. of the mineral contained 3.15×10^{-10} g. of radium.

As shown in Table 1, the mineral contains 0.10% of U_3O_8. Hence 1 g. of the mineral contains 0.00085 g. of uranium, and the ratio of radium to uranium in this mineral is

$$[\mathrm{Ra}] / [\mathrm{U}] = 3.71 \times 10^{-7}.$$

Therefore it can be presumed that in the mineral the equilibrium is established between radium and uranium.

In conclusion, the author wishes to express his hearty thanks to Professor K. Kimura for his kind advices and suggestions rendered during the course of this work. Thanks are also due to Professor T. Sueno of the Tokyo University of Engineering, who kindly measured the refractive indices of this mineral, and to Mr. O. Nagashima for his enthusiastic assistance in collecting the mineral used in this investigation. A part of the cost of this investigation was defrayed from the grant of the Nippon Gakujutsu Shinko-kwai (the Japan Society for the Promotion of Scientific Research) for which also the present author wishes to record his thanks.

Chemical Institute, Faculty of Science,
Imperial University of Tokyo.

Austauschreaktion der Wasserstoffatome zwischen Nitrophenol und Wasser. II. Chemismus der Reaktion.[1]

Von **Masao KOIZUMI** und **Toshizo TITANI.**

(Eingegangen am 30. August 1938.)

Inhaltsübersicht. Die Austauschreaktion der „zweiten" austauschbaren (vgl. I. Mitteil.) Kernwasserstoffatome des *m*- und *p*-Nitrophenols in alkalischer Lösung wird untersucht. Dabei wird zuerst eine Gleichung (Gl.(15)) abgeleitet, die uns mit Hilfe des direkt gefundenen Austauschäquivalents n_α der Verbindung bei verschiedenen Versuchsdauern die mittlere Geschwindigkeitskonstante $\bar{k}$ der Deuterierungsreaktion der Kernwasserstoffatome des Nitrophenols (graphisch) errechnen lässt. Unter Benutzung dieser Gl. wird die Geschwindigkeit der Austauschreaktion unter verschiedenen Versuchsbedingungen, d.h. mit verschiedener Konzentration des Alkalis, des Nitrophenols und des Wassers, untersucht. Aus allen diesen Versuchsergebnissen kommen wir zu dem Schluss, dass die Austauschreaktion der Kernwasserstoffatome des Nitrophenols in alkalischer Lösung hauptsächlich zwischen Phenolationen und neutralen Phenolmolekülen stattfindet, wie das folgende Schema zeigt:

$$NO_2{\cdot}C_6H_5{\cdot}O^- + NO_2{\cdot}C_6H_5{\cdot}OD \rightleftarrows NO_2{\cdot}C_6H_4D{\cdot}O^- + NO_2{\cdot}C_6H_5{\cdot}OH\,,$$

obwohl auch die Reaktion zwischen Phenolationen und neutralen Wassermolekülen, besonders bei geringerer Konzentration des Alkalis, nicht ganz ausgeschlossen werden kann.

Einleitung. Die im letzten Versuche[1] gefundenen Tatsachen kann man kurz wie folgt zusammenfassen:

(1) Drei isomerische Nitrophenole tauschen ihre Hydroxylwasserstoffatome sehr schnell, fast momentan, gegen die des Wassers aus (die „erste" Stufe der Reaktion).

(2) Daranschliessend tauschen sie aber einige ihrer Kernwasserstoffatome, besonders leicht in alkalischer Lösung und bei erhöhter Temperatur, gegen die des Wassers aus. Die Anzahl dieser „zweiten" austauschbaren Kernwasserstoffatome ist zwei bei *o*- und *p*-, dagegen drei bei *m*-Nitrophenol. Diese Anzahl der leicht austauschbaren Kernwasserstoffatome stimmt aber mit der, die nach der elektrophilen Substitutionsregel erwartet wird, gut überein, vorausgesetzt, dass die fördernde Wirkung der OH-Gruppe unvergleichbar stärker als die störende Wirkung der NO_2-Gruppe ist.

(3) Die Austauschreaktion der Kernwasserstoffatome kommt aber mit dieser „zweiten" Stufe der Reaktion nicht ganz bis zum Schluss,

(1) I. Mitteil.: dies Bulletin, **13** (1938), 318.

sondern verläuft weiter, bis schliesslich alle Kernwasserstoffatome der Nitrophenole durch die des Wasser ersetzt werden. Diese letzte „dritte" Stufe der Reaktion kann man aber durch ihre äusserst kleine Geschwindigkeit gegen die „zweite" Stufe ziemlich deutlich unterscheiden.

(4) Die Geschwindigkeit der „zweiten" Stufe der Reaktion ist beinahe gleich bei *m*- und *p*-Nitrophenol. Aber die Geschwindigkeit der *o*-Verbindung erheblich kleiner als die anderen zwei Isomeren. Dieser Unterschied der Reaktionsgeschwindigkeit des *o*-Nitrophenols gegen die anderen zwei Isomeren können wir vielleicht mit der Annahme erklären, dass beim *o*-Nitrophenol eine Wasserstoffbindung zwischen den benachbarten OH- und NO_2-Gruppen gebildet wird.

In der vorliegenden Arbeit behandelten wir dasselbe Problem in noch etwas quantitativerer Weise als bei der letzten, indem wir den Einfluss der Konzentrationsveränderung jedes Reaktionsteilnehmers auf die Geschwindigkeit der „zweiten" Stufe der Reaktion untersuchten, und zwar mit dem Zweck, um über den Chemismus der Reaktion einige Aufschlüsse zu gewinnen. Die Austauschreaktion des unsubstituierten Phenols in stark konzentrierter alkalischer Lösung wurde schon von Ingold und seinen Mitarbeitern[2] untersucht. Dabei kamen sie zu dem Schluss, dass die Reaktion hauptsächlich zwischen Phenolationen und neutralen Phenolmolekülen verläuft, indem die Hydroxylwasserstoffatome der letzteren gegen die Kernwasserstoffatome der ersteren ausgetauscht werden. Der von uns in der vorliegenden Arbeit mit Nitrophenol in verdünnter alkalischer Lösung gewonnene Schluss stimmt aber mit diesem gut überein.

Ausrechnung der Austauschgeschwindigkeitskonstante $\bar{k}$. Da die Austauschreaktion der D- bzw. H-Atome zwischen Nitrophenol und Wasser, wie bei den anderen ähnlichen Fällen, als eine reversible Reaktion verläuft, müssen wir die Geschwindigkeitskonstante $\bar{k}$ der Deuterierungsreaktion mit Hilfe der direkt gewonnenen Experimentaldaten mittelbar rechnerisch ermitteln. Dies führten wir in der Praxis folgendermassen aus.

Einfachheitshalber wollen wir zunächst die Abkürzungen, die weiter unten verwendet werden sollen, kurz zusammenstellen:

M_w: Gesamtmolzahl des zur Reaktion beteiligenden verdünnten schweren Wassers,

M_{ph}: Gesamtmolzahl des zum Versuch benutzten Nitrophenols,

V: Volumen der Lösung, die M_w Mol schweren Wassers und M_{ph} Mol Nitrophenols enthält,

(2) C. K. Ingold, C. G. Raisin und C. L. Wilson, *J. Chem. Soc.*, **1936**, 1637.

D_{w0}: D-Gehalt des schweren Wassers vor dem Versuch, d.h. am Anfang der „ersten" Stufe der Reaktion,

D_w: D-Gehalt des schweren Wassers nach dem Versuch, d.h. am bestimmten Zeitpunkt t während des Verlaufes der Reaktion,

D_{ph}: D-Gehalt des Kernwasserstoffs des Nitrophenols an demselben Zeitpunkt t wie oben bei D_w,

t: Versuchsdauer, d.h. die Zeitlänge t nach dem Anfang der Reaktion,

$\bar{k}$: mittlere Geschwindigkeitskonstante, mit der D-Atome bei der „zweiten" Stufe der Reaktion aus Wasser in eines der Kernwasserstoffatome des Nitrophenols eingeführt werden,

n_1: Anzahl der bei der „ersten" Stufe der Reaktion austauschbaren H-Atome. Da aber dies nichts anderes als das Hydroxylwasserstoffatom ist, so ist $n_1 = 1$,

n_2: Anzahl der bei der „zweiten" Stufe der Reaktion austauschbaren H-Atome, so dass $n_2 = 2$ für *o*- und *p*-Nitrophenol, aber $n_2 = 3$ für *m*-Nitrophenol ist (vgl. oben).

α_1: Verteilungsquotient der D-Atome zwischen OH-Gruppe des Nitrophenols und Wasser, so dass $\alpha_1 = 1.07$ bei 100°C. ist (vgl. I. Mitteil. S. 325),

α_2: Verteilungsquotient der D-Atome zwischen Kernwasserstoff des Nitrophenols und Wasser, so dass $\alpha_2 = 0.93$ bei 100°C. ist (vgl. I. Mitteil. S. 327).

Bei der praktischen Durchführung der Versuch bestimmten wir den D-Gehalt des Wassers D_w bei verschieden langer Versuchsdauer t. Oder mit anderen Worten ausgedrückt, massen wir die Abnahmegeschwindigkeit des D-Gehaltes des Wassers während des Verlaufes der Reaktion. Aber weil die „erste" Stufe der Reaktion sehr schnell verläuft und folglich sich immer im Austauschgleichgewicht befindet, dagegen die „dritte" Stufe der Reaktion im Vergleich mit der „zweiten" Stufe viel langsamer verläuft, darf man bei der Berechnung der Abnahmegeschwindigkeit des D-Gehaltes des Wassers nur die „zweite" Stufe der Reaktion in Rechnung ziehen. Wenn man deshalb annimmt, dass die Austauschreaktion als die Reaktion zweiter Ordnung zwischen Nitrophenol und Wasser verläuft, und die Reaktionsgeschwindigkeit jedes „zweiten" austauschbaren Kernwasserstoffatoms untereinander beinahe gleich ist,[3] so dass für jedes dieselbe mittlere Geschwindigkeitskonstante $\bar{k}$ anwendet werden kann,

(3) Diese Annahme darf wohl berechtigt sein, weil die „zweite" Stufe der Reaktion, wie in der letzten Mitteilung gezeigt wurde, ziemlich deutlich von der „dritten" begrenzt ist (vgl. Abb. 1 in I. Mitteil.).

dann können wir die Abnahmegeschwindigkeit der Konzentration des schweren Wassers [[HDO]] in der Lösung wie folgt setzen:

$$-\frac{d[[\mathrm{HDO}]]}{dt} = \bar{k} n_2 [[\mathrm{PhHOO}]] [[\mathrm{HDO}]] - \frac{\bar{k}}{\alpha_2} 2n_2 [[\mathrm{PhDOH}]] [[\mathrm{H_2O}]] \quad (1),$$

wo $[[\mathrm{H_2O}]]$, $[[\mathrm{HDO}]]$, $[[\mathrm{PhHOH}]]$ und $[[\mathrm{PhDOH}]]$ je die Gesamtkonzentration des leichten und schweren Wassers sowie die des leichten und schweren (kerndeuterierten) Nitrophenols in der Lösung ausdrückt. Bei dieser Gl.(1) nehmen wir weiter an, im Einklang mit dem wirklichen Fall, dass der D-Gehalt der Lösung genügend klein ist, so dass wir nur eine Art schweren Wassers sowie schweren Nitrophenols in Rechnung ziehen dürfen. Das erste Glied in der rechten Seite der Gl.(1) drückt die Geschwindigkeit der Deuterierungsreaktion der Kernwasserstoffatome des Nitrophenols und das zweite die der Gegenreaktion aus. Weil wir aber wegen der Kleinheit des D-Gehaltes der Lösung:

$$[[\mathrm{H_2O}]] = \frac{M_\mathrm{w}}{V}, \quad [[\mathrm{HDO}]] = \frac{2M_\mathrm{w}D_\mathrm{w}}{V}, \quad [[\mathrm{PhHOH}]] = \frac{M_\mathrm{ph}}{V} \quad \text{und}$$

$$[[\mathrm{PhDOH}]] = \frac{M_\mathrm{ph}D_\mathrm{ph}}{V}$$

setzen können, wird die obige Gl.(1) ohne weiteres wie folgt:

$$-\frac{dD_\mathrm{w}}{dt} = \frac{\bar{k}n_2 M_\mathrm{ph} D_\mathrm{w}}{V} - \frac{\bar{k}n_2 M_\mathrm{ph} D_\mathrm{ph}}{V\alpha_2} \quad (2).$$

Anderseits können wir:

$$2M_\mathrm{w}D_\mathrm{w0} = 2M_\mathrm{w}D_\mathrm{w} + \alpha_1 n_1 M_\mathrm{ph} D_\mathrm{w} + n_2 M_\mathrm{ph} D_\mathrm{ph} \quad (3)$$

setzen, weil die Gesamtmenge der D-Atome in der Lösung während des Verlaufes der Reaktion konstant bleiben muss. Aus dieser Gl.(3) folgt ohne weiteres, dass:

$$D_\mathrm{ph} = \frac{1}{n_2 M_\mathrm{ph}} \{2M_\mathrm{w}(D_\mathrm{w0} - D_\mathrm{w}) - \alpha_1 n_1 M_\mathrm{ph} D_\mathrm{w}\} \quad (4).$$

Setzt man deshalb diesen Wert von D_ph in Gl.(2) ein, so erhält man die Gl.:

$$-\frac{dD_\mathrm{w}}{dt} = \frac{\bar{k}}{V}\left\{D_\mathrm{w}\left(n_2 M_\mathrm{ph} + \frac{\alpha_1}{\alpha_2} n_1 M_\mathrm{ph} + \frac{2}{\alpha_2} M_\mathrm{w}\right) - \frac{2}{\alpha_2} M_\mathrm{w} D_\mathrm{w0}\right\} \quad (5).$$

Die Lösung dieser Gl. lautet aber:

$$\ln \frac{AD_{w1}-B}{AD_w-B} = \frac{\bar{k}At}{V} \tag{6},$$

wo

$$A = n_2M_{ph}+\frac{a_1}{a_2}n_1M_{ph}+\frac{2}{a_2}M_w \tag{7a},$$

$$B = \frac{2}{a_2}M_wD_{w0} \tag{7b},$$

und

$$D_{w1} = \frac{2D_{w0}M_w}{2M_w+a_1n_1M_{ph}} \tag{8}.$$

Dieser letztere Wert D_{w1} drückt offenbar den D-Gehalt des Wassers unmittelbar nach der Beendigung der „ersten" Stufe der Reaktion aus. Wir können deshalb aus Gl. (6) den D-Gehalt des Wasser D_w am willkürlichen Zeitpunkt t während des Verlaufes der „zweiten" Stufe der Reaktion errechnen und zwar lautet dieser:

$$D_w = \left\{(AD_{w1}-B)\, e^{-\frac{\bar{k}At}{V}}+B\right\}\Big/ A \tag{9}.$$

Bei der praktischen Ausführung der Versuche bestimmten wir das Austauschäquivalent na des Nitrophenols bei verschieden langer Versuchsdauer t. Diese erstere Quantität wird durch die Gl.:

$$na = \frac{2M_w}{M_{ph}}\frac{D_{w0}-D_w}{D_w} \tag{10}$$

definiert,[4] ganz gleichgültig, ob es sich dabei um die „erste" bzw. „zweite" Stufe der Reaktion handelt. Wir können deshalb das Austauschäquivalent n_1a_1 des Nitrophenols unmittelbar nach der Beendigung der „ersten" Stufe der Reaktion:

$$n_1a_1 = \frac{2M_w}{M_{ph}}\frac{D_{w0}-D_w}{D_{w1}} \tag{11}$$

setzen, und aus diesen beiden Gln. (10) und (11) folgt ohne weiteres, dass

$$na-n_1a_1 = \frac{2M_wD_{w0}}{M_{ph}}\left(\frac{1}{D_w}-\frac{1}{D_{w1}}\right) \tag{12}$$

(4) Vgl. Gl. (2) in I. Mitteil. Dabei ist zu beachten, dass $nk = n\alpha$, $M_o = M_{ph}$, $C_a = D_{w0}$ und $C_e = D_w$ ist.

ist. Setzt man nun in diese Gl. (12) den oben gewonnenen Wert von D_w (Gl. (9)) ein, so erhält man nach einer passenden Umformung die Gl.:

$$\ln \frac{n_1\alpha_1-(n\alpha-n_1\alpha_1)}{\left\{(n\alpha-n_1\alpha_1)+\frac{2M_w}{M_{ph}}+n_1\alpha_1\right\}\left(n_2\alpha_2+\frac{2M_w}{M_{ph}}+n_1\alpha_1\right)}$$

$$= \ln \frac{D_{w1}M_{ph}}{2D_{w0}M_w} + \ln \frac{AD_{w1}-B}{AD_{w1}} - \frac{\bar{k}At}{V} \qquad (13).$$

Diese Gl. (13) können wir aber unter Benutzung der Gln. (7b) und (8) weiter wie folgt vereinfachen:

$$V \ln \frac{\{n_2\alpha_2-(n\alpha-n_1\alpha_1)\}\left(\frac{2M_w}{M_{ph}}+n_1\alpha_1\right)}{\left\{(n\alpha-n_1\alpha_1)+\frac{2M_w}{M_{ph}}+n_1\alpha_1\right\}n_2\alpha_2} = -\bar{k}At \qquad (14).$$

Gemäss dieser Gl. (14) können wir nämlich die mittlere Geschwindigkeitskonstante $\bar{k}$ bei der „zweiten" Stufe der Reaktion aus dem direkt gefundenen Wert des Austauschäquivalentes $n\alpha$ bei einer bestimmten Versuchsdauer t berechnen. Für den praktischen Zweck der Berechnung von $\bar{k}$ wird diese Gl. (14) weiter wie folgt umgeformt (vgl. Gl. (7a)):

$$-X \log Y = \frac{\bar{k}}{2.303} t \qquad (15),$$

wo

$$X = \frac{V}{A} = \frac{V}{\left(n_2M_{ph}+\frac{\alpha_1}{\alpha_2}n_1M_{ph}+\frac{2}{\alpha_2}M_w\right)}$$

und

$$Y = \frac{1-\frac{n\alpha-n_1\alpha_1}{n_2\alpha_2}}{1+\frac{n\alpha-n_1\alpha_1}{\frac{2M_w}{M_{ph}}+n_1\alpha_1}} \qquad (16)$$

ist. Nach dieser Gl. (15) muss die Quantität $(-X\log Y)$ direkt proportional mit der zunehmenden Versuchsdauer t zunehmen und zwar drückt der Proportionalitätsfaktor nichts anderes als die Austauschgeschwindigkeitskonstante $\bar{k}/2.303$ aus. Wir können daher die Geschwindigkeitskonstante $\bar{k}$ graphisch ermitteln, indem wir die experimentell bestimmte Quantität $(-X\log Y)$ gegen die Versuchsdauer t einsetzen.

(Fortsetzung folgt.)

Der katalytische Isotopenaustausch des gasförmigen Sauerstoffs. II. Die Austauschreaktion der Sauerstoffatome zwischen Sauerstoff und Wasserdampf auf der Oberfläche amorphen Siliciumdioxyds, Quarzglases, Asbests sowie Bimssteins.[1]

Von Noriyoshi MORITA und Toshizo TITANI.

(Eingegangen am 30. August 1938.)

Inhaltsübersicht. Um über die Brauchbarkeit des Quarzglases, Asbests sowie Bimssteins als das Katalysatorrohr, Füllungsmittel sowie als den Katalysatorträger beim Versuch über die katalytische Austauschreaktion zwischen gasförmigem Sauerstoff und anderen gasförmigem sauerstoffhaltigen Verbindungen, wie z.B. Wasserdampf, Kenntnis zu gewinnen, wird der katalytische Austausch der O-Atome zwischen Sauerstoff und Wasserdampf auf der Oberfläche der genannten Substanzen sowie amorphen Siliciumdioxyds bei erhöhter Temperatur untersucht. Dabei wird gefunden, dass auf der Oberfläche amorphen Siliciumdioxyds unterhalb 650°C. fast keine Austauschreaktion stattfindet und sie erst oberhalb 700°C. bemerkbar wird. Wenn man das Reaktionsgemisch, das aus zwei Volumen Sauerstoffgases und einem Volumen Wasserdampfes besteht, durch das bis auf etwa 800°C. erhitzte Quarzrohr langsam leitet, kann man zu keiner nennenswerten Austauschreaktion kommen. Ebenso schwer findet die Reaktion auf der Oberfläche der Asbestfaser und des Bimssteins statt, wenn man das Gasgemisch bei ca. 800°C. über diese Substanzen leitet.

Einleitung. Beim Versuch über den katalytischen Austausch der O-Atome zwischen gasförmigem Sauerstoff und anderen gasförmigen sauerstoffhaltigen Verbindungen, dessen Ergebnisse teils schon mitgeteilt wurde[1] und teils später veröffentlicht werden soll, benutzten wir, wie schon in der letzten Abhandlung beschrieben, immer ein Quarzglasrohr als Katalysatorrohr. In der Mitte dieses Rohres füllen wir nämlich den betreffenden Katalysator und darüber wird das Reaktionsgasgemisch langsam durchgeleitet, während das ganze Rohr auf gewünschter Temperatur erhitzt wird. Dabei wird der Katalysator, der meistens grobkörnig ist, in seiner Lage im Mittelteil des Katalysatorrohres befestigt, indem wir die Katalysatormasse mit zwei Stöpseln aus Asbestfaser von beiden Seiten zusammenhalten. Weiter benutzten wir oft Bimsstein als den Träger des zu untersuchenden Katalysators. Deshalb erscheint es uns nötig im voraus zu bemerken, dass auf der Oberfläche dieser Substanzen bei der benutzten Temperatur, die meistens zwischen 200° und

(1) I. Mitteil.: dies Bulletin, **13** (1938), 357.

800°C. lag, keine nennenswerte Austauschreaktion zwischen gasförmigem Sauerstoff und Wasserdampf stattfindet. Aus diesem Grunde führten wir die vorliegende Arbeit durch. Die Versuchsmethode liegt darin, dass man das Reaktionsgasgemisch, das aus zwei Volumen elektrolytischen Sauerstoffs und einem Volumen schweren, an schwerem Sauerstoff angereicherten, Wasserdampfes besteht, resp. durch das mit amorphem Siliciumdioxyd, Asbestfaser und Bimsstein gefüllte Quarzrohr sowie durch das leere Quarzrohr bei einer bestimmten erhöhten Temperatur langsam leitet und dadurch die katalytische Aktivität dieser Substanzen für die Austauschreaktion der O-Atome zwischen Sauerstoff und Wasserdampf untersucht. Da die sonstige Arbeitsweise im grossen und ganzen dieselbe wie beim letzten Versuch[1] ist, so wird daraufhin verwiesen.

Experiment 1. Austauschreaktion zwischen gasförmigem Sauerstoff und Wasserdampf auf amorphem Siliciumdioxyd. Etwa 20 g. des käuflichen wasserfreien Natriumsilicats wurde in 300 c.c. Wasser aufgelöst und diese Lösung, die im voraus vom wenigen, unlöslich gebliebenen Rückstand abfiltriert worden war, wurde mit einer um ein wenig mehr als theoretisch berechneten Menge Salzsäure versetzt. Das dadurch gebildete Silicagel wurde dann von der Mutterlauge abfiltriert und bei 120°C. so lange (dies dauerte etwa 20 Stdn.) erwärmt, bis weisses Pulver entstand. Das so erhaltene Pulver des Silicagels wurde nochmals mit warmen Wasser wiederholt gewaschen, bis sich keine Cl-Ionen im abfiltrierten Wasser mehr nachweisen liessen. Dann wurde es wieder bei 100°C. gut getrocknet und zum Schluss im Porzellantiegel drei Stdn. lang rot geglüht.

Etwa 7 g. (scheinbares Volumen = ca. 12 c.c.) des so bereiteten amorphen Siliciumdioxyds füllte man in den Mittelteil des Katalysatorrohrs, das aus Quarzglas bestand, und darüber wurde das Reaktionsgasgemisch bei verschiedener Temperatur langsam geleitet. Das Reaktionsgasgemisch bestand aus 2 Volumen elektrolytischen Sauerstoffs und 1 Volumen an schwerem Sauerstoff angereicherten Wasserdampfes und die Strömungsgeschwindigkeit durch das Katalysatorrohr betrug, bei Zimmertemperatur und unter gewöhnlichem Druck gemessen, etwa 1 c.c. pro Sekunde. Der dabei benutzte elektrolytische Sauerstoff erwies sich, in der Form von Wasser gemessen, um 1.6 γ leichter, dagegen das schwere Wasser um 41.6 γ schwerer als gewöhnliches Wasser. Von diesem gesamten anfänglichen Dichteüberschuss Δs_a des schweren Wassers rührte aber, wie eine vollständige isotopische Analyse ergab, 26.1 γ von der Anreicherung des schweren Sauerstoffs her. Der auf diese Weise zusammen mit dem Sauerstoffgas aus dem Katalysatorrohr ausgeströmte Wasserdampf wurde dann durch Abkühlung mit Kohlensäureschneegemisch voll-

ständig ausgefroren und dessen Dichte, nach gründlicher Reinigung, schwebemetrisch genau bestimmt. Der Wert Δs_e in Tabelle 1 gibt den so ermittelten gesamten Dichteüberschuss des schweren Wassers nach dem Versuch, i.e. nach der Durchströmung wieder.

Tabelle 1. Austauschreaktion zwischen O_2 und H_2O auf amorphem SiO_2 bei verschiedenen Temperaturen.

$O_2 : H_2O = 2 : 1, \quad \Delta s_a = 41.6\gamma.$

Versuchsnr.	Temperatur °C.	Δs_e in γ	$\Delta s_a - \Delta s_e$ in γ	Austauschmass $\% A$
2(2)	500	41.5	0.1	0
1	600	40.8	0.8	4
4	650	41.6	0.0	0
3	680	38.5	3.1	14
5	800	34.7	6.9	31

Da aber vom gesamten anfänglichen Dichteüberschuss $\Delta s_a (=41.6\ \gamma)$ des zum Versuch benutzten schweren Wassers $26.1\ \gamma$, wie schon oben erwähnt wurde, auf die Anreicherung des schweren Sauerstoffs zurückzuführen war, so ergibt eine einfache Rechnung, dass beim vollständigen Austausch der schweren O-Atome zwischen dem verwendeten Volumen des Sauerstoffgases und Wasserdampfes der anfängliche Dichteüberschuss des letzteren um den Betrag von $22.2\ \gamma$ abnehmen müsste. Das prozentuale Austauschmass $\% A$ in der letzten Vertikalreihe der Tabelle 1 wurde deshalb nach der Gl. (1) berechnet:

$$\% A = \frac{\Delta s_a - \Delta s_e}{22.2} \times 100 \qquad (1).$$

Aus dem so gefundenen Werte von $\% A$ bei verschiedenen Temperaturen können wir wohl schliessen, dass auf der Oberfläche des amorphen Siliciumdioxyds unterhalb 650°C. keine nennenswerte Austauschreaktion zwischen Sauerstoffgas und Wasserdampf stattfindet und diese erst oberhalb 700°C. bemerkbar wird. Jedoch ist die katalytische Wirksamkeit des amorphen Siliciumdioxyds auch bei diesen erhöhten Temperaturen noch viel schwächer als die der anderen eigentlichen Austauschkatalysatoren, wie z.B. die des Platinschwammes, die in der I. Mittl. untersucht wurde.

(2) Zeitliche Reihenfolge.

Experiment 2. Austauschreaktion zwischen gasförmigem Sauerstoff und Wasserdampf auf der Wand des Quarzrohres. Wir benutzten zwei Arten des Quarzrohres zum Versuch. Das eine davon (Rohr A) war ein neu geblasenes und ganz durchsichtiges Quarzrohr, das etwa 40 cm. Länge und 22 mm. l.W. besass. Dagegen war das andere Rohr (Rohr B) das beim eigentlichen Austauschversuch schon mehrmals benutzte und folglich einigermassen undurchsichtig gewordene Quarzrohr. Dieses letztere Rohr, dessen Länge ebenfalls 40 cm. betrug, war aber um ein wenig schmaler als das erstere und besass 15 mm. l.W. Diese beiden Rohre wurden separat im elektrischen Ofen bis auf etwa 800°C. erhitzt und dadurch wurde das Reaktionsgasgemisch aus 2 Volumen Sauerstoffgases und 1 Volumen schweren Wasserdampfes mit der Strömungsgeschwindigkeit von 1 c.c. pro Sekunde (bei Zimmertemperatur und unter gewöhnlichem Druck gemessen!) langsam geleitet. Dass aber durch diese Behandlung keine nennenswerte Austauschreaktion wirklich zustande kam, können wir aus der unterstehenden Tabelle 2 ohne weiteres ersehen.

Tabelle 2. Austauschreaktion zwischen O_2 und H_2O auf der Wand des Quarzrohres.

$O_2 : H_2O = 2 : 1.$

Versuchsnr. (Art des Rohres)	Temperatur °C	Δs_a in γ	Δs_e in γ	$\Delta s_a - \Delta s_e$ in γ	$\%A$
A	830	38.8	38.5	0.3	2
B	760	31.7	30.8	0.9	5

Vom gesamten anfänglichen Dichteüberschuss Δs_a des benutzten schweren Wassers, der beim Versuch A und B, wie in der dritten Vertikalreihe der Tabelle gezeigt wird, resp. 38.8 γ und 31.7 γ betrug, rührte je 22.7 γ und 19.5 γ von der Anreicherung des schweren Sauerstoffs her. Deshalb müsste der gesamte Dichteüberschuss des schweren Wassers je um den Betrag von 19.4 γ und 16.9 γ abnehmen, falls die Austauschreaktion zwischen den angegebenen Volumen des Sauerstoffs und Wasserdampfes vollständig bis zum Ende stattfinden würde. Da aber die wirklich gefundene Dichteabnahme ($\Delta s_a - \Delta s_e$), die in der zweiten letzten Vertikalreihe der Tabelle wiedergegeben ist, bloss 2 bzw. 5% dieses theoretischen Wertes beträg ($\%A$ in der letzten Reihe!), so darf man beim eigentlichen Austauschversuch die katalytische Wirksamkeit der Wand des Katalysatorrohres im Vergleich mit der des darin befindlichen Katalysatoren ganz unbeachtet lassen.

Experiment 3. Austauscheraktion zwischen gasförmigem Sauerstoff und Wasserdampf auf Asbestfaser. Der Asbestfilter von Merck wurde mittels konz. Salzsäure mehrmals behandelt und zum Schluss mit destilliertem Wasser so lange gewaschen, bis keine Cl-Ionen mehr nachgewiesen wurden. Die so gereinigte Asbestfaser wurde dann im Trockenschrank gut getrocknet und etwa 9 g. davon füllte man in den Mittelteil des Katalysatorrohres. Das dazu benutzte Katalysatorrohr war das Quarzrohr A, das beim letzten Experiment 2 verwendet wurde. Die Zusammensetzung sowie die Strömungsgeschwindigkeit des Reaktionsgasgemisches war ebenfalls genau dieselbe wie beim letzten Experiment. Die so gewonnenen Versuchsergebnisse geben wir in Tabelle 3 wieder.

Tabelle 3. Austauschreaktion zwischen O_2 und H_2O auf Asbestfaser bei verschiedenen Temperaturen.

$O_2: H_2O = 2: 1, \quad \Delta s_a = 31.7\gamma.$

Versuchsnr.	Temperatur °C.	Δs_e in γ	$\Delta s_a - \Delta s_e$ in γ	Austauschmass $\% A$
3	600	31.5	0.2	1
4	800	30.5	1.2	7
1	800	28.2	3.5	21
2	870	28.1	3.6	21

Das Austauschmass $\% A$ in der letzten Vertikalreihe berechneten wir nach der Gl.:

$$\% A = \frac{\Delta s_a - \Delta s_e}{16.9} \times 100 \qquad (4),$$

weil vom gesamten anfänglichen Dichteüberschuss des benutzten schweren Wassers ($\Delta s_a = 31.7\ \gamma$), 19.5 γ auf die Anreicherung des schweren Sauerstoffs zurückzuführen war. Bei diesem Versuch fanden wir nämlich, dass bei erhöhten Temperaturen ein untrüglicher Austausch stattfand. Dass aber die Austauschreaktion auf dieser Höhe beim eigentlichen Austauschversuch als belanglos betrachtet werden darf, können wir aus der Tatsache verstehen, dass die Menge der beim eigentlichen Austauschversuch als das Füllungsmittel benutzten Asbestfaser weniger als ein Fünfzigstel der eben bei diesem Experiment 3 verwendeten war.

Experiment 4. Austauschreaktion zwischen gasförmigem Sauerstoff und Wasserdampf auf Bimsstein. Dieser Versuch ist in sofern nötig, als wir beim Austauschversuch Bimsstein oft als den Träger der anderen

Katalysatoren benutzten. Dass aber diese Substanz ebenso wenige katalytische Aktivität wie Asbest besitzt, können wir aus Tabelle 4 ohne weiteres ersehen. Der bei diesem Versuch benutzte Bimsstein war der „Bimsstein gekörnt" aus Kahlbaum. Dieser wurde aber vor dem Versuch weiter richtig gereinigt, indem wir ihn zunächst mit konz. Salzsäure dreimal behandelten und zum Schluss mit destilliertem Wasser so lange auswuschen, bis keine Cl-Ionen mehr nachgewiesen wurden. Etwa 35 g. davon wurde dann, nach vorausgehender gründlicher Trocknung, in dasselbe Quarzrohr, das beim letzten Experiment benutzt wurde, gefüllt und darüber wurde bei verschiedenen Temperaturen das Gasgemisch aus Sauerstoff und Wasserdampf langsam geleitet. Die Zusammensetzung und die Strömungsgeschwindigkeit des Gasgemisches war genau dieselbe wie beim letzten Experiment 3. Die Versuchsergebnisse sind in Tabelle 4 wiedergegeben.

Tabelle 4. Austauschreaktion zwischen O_2 und H_2O auf Bimsstein bei verschiedenen Temperaturen.

$O_2 : H_2O = 2 : 1, \quad \Delta s_a = 29.3\gamma$.

Versuchsnr.	Temperatur °C.	Δs_e in γ	$\Delta s_a - \Delta s_e$ in γ	Austauschmass % A
1	500	29.0	0.3	2
3	550	27.3	2.0	12
2	820	27.8	1.5	9

Das Austauschmass $\%A$, das in der letzten Vertikalreihe der Tabelle angegeben ist, errechneten wir mittels der Gl.:

$$\%A = \frac{\Delta s_a - \Delta s_e}{16.5} \times 100 \qquad (5),$$

da vom gesamten anfänglichen Dichteüberschuss des benutzten Wassers ($\Delta s_a = 29.3\ \gamma$), 19.0 γ von der Anreicherung des schweren Sauerstoffs herrührte. Das so berechnete prozentuale Austauschmass $\%A$ betrug aber sogar bei 820°C., der höchsten Temperatur, die wir benutzten, kaum 10%. Wir dürfen deshalb die katalytische Aktivität des Bimssteins gegen die der anderen eigentlichen Katalysatoren wohl unbeachtet lassen, wenn der erstere als der Träger der letzteren benutzt wird.

Zum Schluss möchten wir der Nippon Gakujutsu-Shinkohkai (der Japanischen Gesellschaft zur Förderung der wissenschaftlichen Forschungen) sowie der Hattori-Hohkohkai (der Hattori-Stiftung) für ihre finanzielle Unterstützung zur Ausführung dieser Arbeit unseren wärmsten Dank aussprechen.

Physikalisch-chemischcs Laboratorium der
Kaiserlichen Universität zu Osaka
und
Siomi-Institut für physikalische
und chemische Forschung.

Austauschreaktion der Sauerstoffatome zwischen Wasser und einigen organischen Verbindungen.

Von Masao KOIZUMI und Toshizo TITANI.

(Eingegangen am 30. August 1938.)

Inhaltsübersicht. Die Austauschreaktion der O-Atome zwischen Wasser und einigen organischen Verbindungen wurde unter Benutzung des an schwerem Sauerstoff angereicherten Wassers untersucht. Die dabei erhaltenen Versuchsergebnisse können wir kurz wie folgt zusammenfassen, wo n die Anzahl der austauschbaren O-Atome in einem organischen Molekül zeigt, wenn die betreffende Verbindung zusammen mit dem schweren Wasser bei der in den Klammern angegebenen Temperatur während der ebenfalls in den Klammern gezeigten Zeitlänge stehen gelassen bzw. geschüttelt wurde. Glucose $n \fallingdotseq 1$(100°C., 2–5 Stdn.), Benzaldehyd $n \fallingdotseq 1$(100°C., 1–2 Stdn.), Benzoesäure $n \fallingdotseq 1$(130°C., 2–5 Stdn.), Bernsteinsäure $n \fallingdotseq 4$(130°C., 2–5 Stdn.), Phenol $n \fallingdotseq 0$(100°C., 24–48 Stdn.), Malcinsäure $n \fallingdotseq 4$(100°C., 10–45 Stdn.), Fumarsäure $n \fallingdotseq 2$(100°C., 20 Stdn.), Phthalsäure $n \fallingdotseq 0$(100°C., 20 Stdn.), Terephthalsäure $n \fallingdotseq 0$(100°C., 20 Stdn.).

Einleitung. Die Austauschreaktion der H-Atome zwischen Wasser und verschiedenen organischen Verbindungen wurde, seitdem sie von Bonhoeffer und Brown[1] entdeckt worden war, von vielen Autoren eingehend untersucht und manche dieser Versuchsergebnisse haben uns einen wichtigen Anhaltspunkt für die Untersuchung der Molekülstruktur sowie der Reaktionsfähigkeit der verschiedenen organischen Verbindungen

(1) K.F. Bonhoeffer und G.W. Brown, *Z. physik. Chem.*, B, **23** (1933), 171.

gegeben. So liegt der Gedanke sehr nahe, dass ein ähnlicher Versuch über die Austauschreaktion der O-Atome der organischen Verbindungen auf diesem Gebiet der Isotopchemie einen weiteren Schritt leisten kann. Aus dieser Erwartung wurde der O-Atomenaustausch zwischen Wasser und organischen Verbindungen schon von einigen Autoren[2][3][4][5] unter Benutzung des an schweren Sauerstoff angereicherten schweren Wassers untersucht. Cohn und Urey[2] fanden z.B., dass die O-Atome der Hydroxyl- und Carboxylgruppe im allgemeinen gegen die des Wassers nicht leicht austauschbar sind, dagegen der Austausch zwischen Aceton bzw. Acetaldehyd und Wasser ziemlich leicht stattfindet. Dieses letztere Resultat wurde weiter durch den Versuch von Herbert und Lauder[3] bestätigt. Aber bei allen diesen Versuchen über den Austausch der O-Atome muss man darauf achten, dass sie von denen über den H-Atomenaustausch insofern verschieden ist, wie darauf schon von Cohn und Urey hingewiesen wurde, als die ersteren noch mehr qualitative Natur als die letzteren besitzen. Da bei der Austauschreaktion der H-Atome die Austauschbarkeit der betreffenden H-Atome meistens schon im voraus wohl bekannt bzw. zu erwarten ist, können wir den Versuch von vorn herein schon in mehr oder weniger quantitativer Weise beginnen. Dagegen haben wir beim O-Atomenaustausch über die Austauschbarkeit der betreffenden O-Atome in einem organischen Molekül im allgemeinen fast keine Vorkenntnis. Wir haben deshalb den Versuch über den O-Atomenaustausch zunächst von der qualitativen Seite anzupacken. Die vorliegende Arbeit wurde auch in dieser Linie ausgeführt. Deshalb sind die dabei erhaltenen Versuchsergebnisse noch von mehr oder weniger qualitativer Natur und weiter zeigen sie oft mit denen der schon veröffentlichten Arbeiten der anderen Autoren eine Duplizierung. Aber weil die von uns gefundenen Resultate nicht immer mit denen der anderen Autoren übereinstimmten, teilen wir auch solche doppelten Versuche ebenso eingehend wie die anderen zum erstenmal ausgeführten mit.

Allgemeine Bemerkung über den Versuch. Die in der vorliegenden Arbeit untersuchten Verbindungen sind: Glucose, Benzaldehyd, Benzoesäure, Bernsteinsäure, Phenol, Fumar- und Maleinsäure sowie Phthal- und Terephthalsäure. Ausserdem untersuchten wir auch Aceton. Aber

(2) M. Cohn und H. C. Urey, *J. Am. Chem. Soc.*, **60** (1938), 679; *J. Chem. Phys.*, **6** (1938), 175.

(3) J. B. M. Herbert und I. Lauder, *Trans. Faraday Soc.*, **34** (1938), 432.

(4) I. Roberts, *J. Chem. Phys.*, **6** (1938), 294.

(5) W. H. Mears, *J. Chem. Phys.*, **6** (1938), 295; I. Roberts und H. C. Urey, *J. Am. Chem. Soc.*, **60** (1938), 880.

leider konnten wir dabei zu keinen wiederholbaren Ergebnissen kommen. Das mit diesen Substanzen zu reagierende an schwerem Sauerstoff angereicherte schwere Wasser wurde durch die fraktionierte Destillation des gewöhnlichen Leitungswassers bereitet. Aber weil das so bereitete schwere Wasser nicht nur an schwerem Sauerstoff sondern auch an schwerem Wasserstoff angereichert war, wurde es im voraus betreffend seines Wasserstoffs normalisiert, d.h. der Gehalt dieses Wassers an schwerem Wasserstoff bis unter zu dem des gewöhnlichen Wassers herabgesetzt. Dies führten wir auf folgende Weise aus: Eine bestimmte Menge des zu normalisierenden Wassers wurde zunächst mit einer Menge Ammoniumchlorid zugesetzt. Die Menge des letzteren wählte man immer so, dass sie etwa ebensoviele H-Atome wie die im zu normalisierenden Wasser befindlichen enthielt. Die so bereitete Lösung, in welcher ein Teil des Ammoniumchlorids unlöslich auf dem Boden lag, wurde dann abwechselnd bis auf 100°C. erwärmt und wieder bis unter Zimmertemperatur abgekühlt, um dadurch den Austausch der H-Atome zwischen Wasser und Ammoniumchlorid zu vervollkommen. Dann wurde das Wasser, nachdem es durch die Destillation im Vakuum vom zuerst versetzten Ammoniumchlorid abgetrennt worden war, wieder mit frischem Salz zugesetzt und damit genau wie oben behandelt. Auf diese Weise wiederholten wir denselben Prozess mit ein und derselben Wasserprobe aber unter steter Erneuerung des zugesetzten Ammoniumchlorids fünf bis sechs Mal. Nach dieser Behandlung ergab die isotopische Analyse des resultierten Wassers, dass sein Dichteüberschuss von 25 bis 40 γ gewöhnlichem Wasser gegenüber ausschliesslich auf die Anreicherung des schweren Sauerstoffs zurückzuführen war. Deshalb konnten wir aus der Dichteabnahme des schweren Wassers nach dem Austauschversuch über die Anzahl der austauschbaren O-Atome im untersuchten organischen Molekül ohne weiteres zu einem Schluss kommen.

Um diese letztere Anzahl zu bestimmen, wurde eine bestimmte Menge des normalisierten schweren Wassers zusammen mit der ebenso gut abgewogenen Menge der organischen Verbindung in einem Glasrohr eingeschmolzen und bei einer bestimmten Temperatur, die meistens zwischen 100°C. und 130°C. lag, während einer bestimmten Zeitlänge stehen gelassen oder, falls die Substanz schwer löslich war, zusammengeschüttelt. Nach dieser Behandlung wurde das Wasser auf passendem Wege (Destillation im Vakuum bzw. Abheben!) von der organischen Verbindung abgetrennt und gereinigt. Zur Reinigung des durch organische Substanz verunreinigten Wassers benutzten wir beim Austauschversuch von H-Atomen als ein sehr wirksames Oxydationsmittel geglühtes Kupferoxyd, indem wir das Wasser in Dampfform über das bis auf Rotglut erhitzte

Kupferoxyd leiteten. Aber wir können diese Methode in der vorliegenden Arbeit über den O-Atomenaustausch nicht benutzen, weil das bis auf Rotglut erhitzte Kupferoxyd seine O-Atome ziemlich leicht gegen die des Wasserdampfes austauscht.[6] Deshalb führten wir die Reinigung des schweren Wassers in der vorliegenden Arbeit ausschliesslich unter Benutzung des Kaliumpermanganats durch. Das zu reinigende Wasser wurde nämlich unter Zusatz von Natriumperoxyd und Kaliumpermanganat lange Zeit sieden gelassen. Obwohl diese Reinigungsmethode nicht so wirksam wie die mit Kupferoxyd war, erwies sie sich doch hinreichend nützlich, wenn man die Kochdauer genügend lang ausdehnte und nötigenfalls denselben Prozess zweimal nacheinander wiederholte. Die Dichte des so gereinigten Wassers wurde, nachdem es wieder im Vakuum paarmal destilliert worden war, mittels eines Glasschwimmers genau bestimmt. Die Messgenauigkeit dürfte $\pm 1\,\gamma$ sein. Bezeichnet man den so ermittelten Dichteüberschuss des schweren Wassers vor und nach dem Experiment resp. mit Δs_a und Δs_e und Molzahl des zum Versuch verwendeten schweren Wassers und der organischen Verbindung je mit M_w und M_o, dann wird die Anzahl n der austauschbaren O-Atome in einem organischen Molekül mittels Gl.(1) ohne weiteres berechnet:

$$n = \frac{M_w}{M_o} \frac{\Delta s_a - \Delta s_e}{\Delta s_e} \qquad (1).$$

Bei dieser Gl. nehmen wir an, dass der Verteilungsquotient der schweren O-Atome zwischen Wasser und organischen Verbindungen beinahe gleich eins ist. Diese Annahme ist für den vorliegenden Zweck hinreichend, weil die Atomgewichte des leichten und schweren Sauerstoffs nur um einige Prozente von einander verschieden sind.

Versuch 1. Glucose. Die Lösung von Glucose in schwerem Wasser wurde in einem zugeschmolzenen Glasrohr bei 100°C. verschiedene Zeitlängen erwärmt. Dann wurde das Wasser durch die Destillation im Vakuum von Glucose abgeschieden. Die Reinigung des so abgeschiedenen Wassers führten wir durch einmalige Behandlung mit alkalischem Kaliumpermanganat und zweimalige Destillationen im Vakuum aus. Die dadurch erhaltenen Resultate geben wir in Tabelle 1 wieder. Aus diesem Resultat darf man wohl schliessen, dass Glucose bei 100°C. sogar nach 48-Stündiger Erwärmung nur eines seiner O-Atome gegen die des Wassers austauscht.

(6) Die noch nicht veröffentlichte Arbeit von N. Morita und T. Titani.

Tabelle 1. Glucose.

Nr.(7)	M_o	M_w	Δs_a in γ	Δs_e in γ	Temperatur °C.	Versuchsdauer in Stdn.	n
1	0.0171	0.0531	36	27	100°	$2^1/_3$	1.04
2	0.0161	0.0512	36	20	100°	20	2.5?
3	0.0158	0.0534	26	27	100°	$5^2/_3$	1.13
4	0.0189	0.0542	33	26	100°	48	0.77

Versuch 2. Benzaldehyd. Da das Benzaldehyd in Wasser schwer löslich ist, wurde das Aldehyd zusammen mit schwerem Wasser in einem zugeschmolzenen Glasrohr bei 110°C. verschiedene Zeitlängen kräftig geschüttelt. Danach wurde das Wasser durch Abhebung von Aldehyd abgetrennt und auf ähnliche Weise wie beim Versuch 1 gereinigt. Die Ergebnisse der Versuche sind in Tabelle 2 zusammengestellt, wo der mit K bezeichnete Versuch ein Kontrollversuch ist, der unter Verwendung des gewöhnlichen Wassers statt schweren Wassers durchgeführt wurde.

Tabelle 2. Benzaldehyd.

Nr.	M_o	M_w	Δs_a in γ	Δs_e in γ	Temperatur °C.	Versuchsdauer in Stdn.	n
1	0.0308	0.0531	33.5	21.2	110°	1	1.0
2	0.0347	0.0639	33.5	21.5	110°	2	1.0
K	0.0329	0.0473	0	-2	110°	1	—

Benzaldehyd tauscht nämlich bei 110°C. sein O-Atom ziemlich leicht gegen die des Wassers aus.

Versuch 2. Benzaldehyd. Da das Benzaldehyd in Wasser schwer löslich ist, wurde das Aldehyd zusammen mit schwerem Wasser in einem zugeschmolzenen Glasrohr bei 110°C. verschiedene Zeitlängen kräftig geschüttelt. Danach wurde das Wasser durch Abhebung von Aldehyd abgetrennt und auf ähnliche Weise wie beim Versuch 1 gereinigt. Die Ergebnisse der Versuche sind in Tabelle 2 zusammengestellt, wo der mit K bezeichnete Versuch ein Kontrollversuch ist, der unter Verwendung des gewöhnlichen Wassers statt schweren Wassers durchgeführt wurde.

(7) Zeitliche Reihenfolge.

Tabelle 3. Benzoesäure.

Nr.	M_o	M_w	Δs_a in γ	Δs_e in γ	Temperatur °C.	Versuchsdauer in Stdn.	n
1	0.0338	0.0391	26	17	130°	2	0.61
2	0.0333	0.0428	44	27	130°	2	0.81
3	0.0328	0.0458	32	13	130°	5	2.0?
4	0.0315	0.0536	32	22	130°	5	0.78
K1	0.0333	0.0457	0	-4	130°	2	—
K2	0.0299	0.0571	0	-5	130°	2	—
5	0.0331	0.0444	35	33	130°	1	0.08
6	0.0327	0.0467	35	23	130°	5	0.75
K3	0.0339	0.0483	0	0	130°	5	—

Versuch 4. Bernsteinsäure. Die Versuchsanordnung sowie Versuchsbedingungen waren im grossen und ganzen dieselben wie beim letzten Versuch 3 mit Benzoesäure. Aber unter diesen Versuchbedingungen tauschte Bernsteinsäure alle ihre vier O-Atome ziemlich leicht gegen die des Wassers aus, wie aus Tabelle 4 ersichtlich ist.

Tabelle 4. Bernsteinsäure.

Nr.	M_o	M_w	Δs_a in γ	Δs_e in γ	Temperatur °C.	Versuchsdauer in Stdn.	n
1	0.0411	0.0528	25	6	130°	2	4.0
2	0.0366	0.0431	25	4	130°	2	6.2
K	0.0410	0.0528	0	+1	150°	4	—
3	0.0361	0.0479	35	14	130°	1	1.9
4	0.0440	0.0462	35	8	130°	5	3.6

Versuch 5. Phenol. Die Abtrennung des schweren Wassers vom damit zusammengeschüttelten Phenol führten wir durch Abhebung aus. Aber weil das so abgeschiedene Wasser noch ziemlich beträchtlich von Phenol verunreinigt war, behandelten wir das Wasser mit alkalischem Permanganat zweimal nacheinander. Durch diese Behandlung wurde das Wasser praktisch vollkommen rein, wie der Kontrollversuch K in Tabelle 5 zeigt.

Das Hydroxylsauerstoffatom des Phenols ist diesem Versuch nach sehr schwer austauschbar und sogar nach 48-stündiger Erwärmung auf 100°C. liegt die gefundene Dichteabnahme des benutzten schweren Wassers kaum ausserhalb des Messfehlerbereiches.

Tabelle 5. Phenol.

Nr.	M_o	M_w	Δs_a in γ	Δs_e in γ	Temperature °C.	Versuchsdauer in Stdn.	n
1	0.0645	0.0540	40	39	100°	24	0.02
2	0.0704	0.0541	40	33	100°	48	0.16
3	0.0546	0.0478	40	35	100°	39	0.13
K	0.05	0.05	0	0	100°	24	—

Versuch 6. Maleinsäure und Fumarsäure. Da die Löslichkeit dieser beiden Säuren in Wasser auch bei 100°C. sehr gering war, benutzten wir bei der Ausführung des Austauschversuchs die in der nebenstehenden Abb. skizzierte Versuchsanordnung. Der dort gezeigte Apparat ist ganz aus Glas geblasen und das Reaktionsgemisch, das aus etwa 5 g. Säure und 1 c.c. schweren Wassers besteht, befindet sich am Boden des unteren geräumigen Teils A. Dieser Teil A wird zuerst von aussen durch das Kohlensäureschneegemisch gut abgekühlt, um dadurch das darin befindliche Reaktionsgemisch frieren zu lassen und der ganze Apparat durch die obere Mündung D gut evakuiert. Dann wird der Apparat an der Stelle D vom Vakuumapparat abgeschmolzen und das Kältebad um den unteren Teil A wird langsam durch das siedende Wasserbad gewechselt. Der durch diese Erwärmung von Reaktionsgemisch verdampfte schwere Wasserdampf geht durch den röhrenförmigen Teil B, der von aussen elektrisch erhitzt wird, zum Rückflusskühler C und das dort kondensierte Wasser kommt wieder bis zum unteren Teil A zurück. Auf diese Weise liess man eine bestimmte Menge schweren Wassers während der bestimmten Versuchsdauer über die im unteren Teil A befindliche und bis auf 100°C. erwärmte Säure zirkulieren. Die durch diese Versuchsanordnung gewonnenen Ergebnisse sind in Tabellen 6 und 7 zusammengestellt.

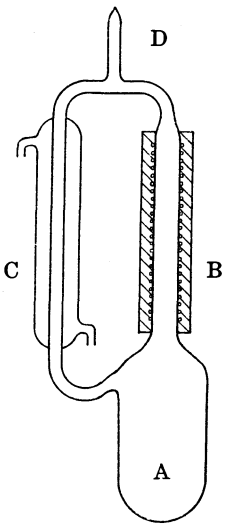


Abb. Austauschapparat für schwer lösliche Substanzen.

Tabelle 6. Maleinsäure.

Nr.	M_o	M_w	Δs_a in γ	Δs_e in γ	Temperatur °C.	Versuchsdauer in Stdn.	n
1	0.0438	0.0490	40	12	100°	20	2.6
2	0.0431	0.0486	40	6	100°	45	6.4
3	0.0397	0.0485	34	8.4	100°	10	3.7
K	0.044	0.055	0	0	100°		—

Tabelle 7. Fumarsäure.

Nr.	M_o	M_w	Δs_a in γ	Δs_e in γ	Temperatur °C.	Versuchsdauer in Stdn.	n
1	0.0471	0.0558	40	18	100°	3	1.4
2	0.0460	0.0473	40	16	100°	45	1.5
K	0.043	0.053	0	—1	100°	20	—

Diesem Versuch nach tauschte Maleinsäure alle ihre vier O-Atome ziemlich leicht gegen die des Wassers aus. Dagegen wurde bei Fumarsäure unter genau denselben Versuchsbedingungen nur etwa eine Hälfte der O-Atome in einem Molekül durch die des Wassers ersetzt.

Versuch 7. Phthalsäure und Terephthalsäure. Dieser Versuch wurde unter Verwendung derselben Versuchsanordnung und unter denselben Versuchbedinungen wie beim letzten Versuch 6 ausgeführt. Die dadurch gewonnenen Ergebnisse geben wir in Tabelle 8 wieder.

Tabelle 8. Phthalsäure und Terephthalsäure.

Substanz	M_o	M_w	Δs_a in γ	Δs_e in γ	Temperatur °C.	Versuchsdauer in Stdn.	n
Phthalsäure	0.0249	0.0501	40	37	100°	20	0.16
Terephthalsäure	0.0250	0.0521	40	35	100°	20	0.30

Zusammenfassung der Ergebnisse und Diskussion. Die in der vorliegenden Arbeit gewonnen Versuchsergebnisse sind in Tabelle 9 zusammengestellt.

Tabelle 9. Zusammenfassung der Ergebnisse.

Versuchsnr.	Substanz	Versuchsbedingungen	Anzahl der austauschbaren O-Atome in einem Molekül $!n$	Bemerkung
1	Glucose	100°C., 2 bis 48 Stdn.	1	teilweiser Austausch
2	Benzaldehyd	100°C., 1 bis 2 Stdn.	1	vollständiger Austausch
3	Benzoesäure	130°C., 2 bis 5 Stdn.	1	teilweiser Austausch
4	Bernsteinsäure	130°C., 2 bis 5 Stdn.	4	vollständiger Austausch
5	Phenol	100°C., 24 bis 48 Stdn.	0	fast kein Austausch
6	Maleinsäure	100°C., 10 bis 48 Stdn.	4	vollständiger Austausch
6	Fumarsäure	100°C., 3 bis 45 Stdn.	2	teilweiser Austausch
7	Phthalsäure	100°C., 20 Stdn.	0	fast kein Austausch
7	Terephthalsäure	100°C., 20 Stdn.	0	fast kein Austausch

Mit diesem verhältnismässig beschränktem Versuchsmaterial können wir natürlich nicht zu weitgehende Schlüsse ziehen. Aber wir wollen vorläufig die vorliegenden Versuchsergebnisse mit den veröffentlichten Daten von anderen Autoren vergleichen. Nach dem Versuch von Cohn und Urey,[2] von Herbert und Lauder[3] sowie von Roberts[4] wurde gefunden, dass die Carbonylsauerstoffatome der Aldehyde und Ketone verhältnismässig leicht, dagegen die Hydroxylsauerstoffatome der Alkohole äusserst schwer austauschbar sind. Diesem Befund nach erscheint das eine leicht austauschbare O-Atom im Glucosemolekül (vgl. Versuch 1) höchstwahrscheinlich das Carbonylsauerstoffatom zu sein. Das vorliegende Versuchsergebnis 2, dass Benzaldehyd sein O-Atom ziemlich leicht gegen die des Wassers austauscht, hat den oben zitierten Befund von Urey und anderen Autoren über die aliphatischen Aldehyde auch für die aromatischen erweitert. Dagegen stimmt das nächste Versuchsergebnis 3, dass Benzoesäure durch 2 bis 5-stündige Erwärmung auf 130°C. ihre O-Atome nur teilweise (etwa die Hälfte ihrer O-Atome) gegen die des Wassers austauscht, nicht ganz mit dem veröffentlichten Resultat von Roberts[4] überein. Dieser Forscher fand nämlich, dass die O-Atome der Benzoesäure schon durch 4-stündige Erwärmung bei 100°C. ohne jeden Zusatz restlos durch die des Wassers ersetzt werden.

Nach dem Versuch von Cohn und Urey sind die Carboxylsauerstoffatome mancher aliphatischen Carbonsäuren im allgemeinen nicht sehr leicht auszutauschen. Bernsteinsäure führte z.B., dem Versuch dieser

beiden Autoren nach, bei 25°C. sogar nach 44 Stunden keine Austauschreaktion aus. Der scheinbare Unterschied zwischen diesem Befund von Cohn und Urey und dem vorliegenden Versuchsergebnis 4, dass alle O-Atome der Bernsteinsäure durch 2 bis 5-stündige Erwärmung auf 130°C. verhältnismässig leicht ausgetauscht wurden, ist aber vom reaktionskinetischen Gesichtspunkt nicht unbegreiflich, weil die Versuchstemperaturen in beiden Reihen der Versuche ziemlich beträchlich untereinander verschieden sind. In der Tat erhielten wir auch bei unserem Versuch einen sicherlich kleineren Wert von n (etwa zwei), wenn die Versuchsdauer verhältnismässig kurz war (vgl. Versuch Nr. 3. in Tabelle 4). Cohn und Urey kamen weiter bei ihrem Versuch mit Phenol zu dem Ergebnis, dass diese Verbindung bei 25°C. sogar nach 44 Stdn. keine Austauschreaktion zeigt. Dieses Ergebnis wurde aber durch den vorliegenden Versuch 5 auch bei höherer Temperatur (100°C.) bestätigt. Das Phenolsauerstoffatom muss demnach als sehr schwer, vermutlich ebenso schwer wie das Alkoholsauerstoffatom, austauschbar betrachtet werden.

Das Ergebnis des Versuchs 6, dass die O-Atome der Maleinsäure viel leichter als die der Fumarsäure gegen die des Wassers ausgetauscht werden, ist insofern interessant, als diese beiden Säuren gegenseitig Stereoisomer sind, und zuerst ersuchten wir diesen Unterschied der Austauschbarkeit der O-Atome mit dem stereochemischen Strukturunterschied zu deuten. Wir können es uns z.B. so vorstellen, dass Maleinsäure (und Bernsteinsäure) ihre Carboxylsauerstoffatome unter Zwischenbildung der Anhydridmoleküle leichter als Fumarsäure gegen die des Wassers austauschen kann. Auf Grund dieser Vermutung untersuchten wir im nächsten Versuch 7 Phthalsäure und Terephthalsäure und zwar unter der Erwartung, dass die erstere die Austauschreaktion leichter als die letztere ausführen kann. Aber in Wirklichkeit fanden wir, wie aus Tabellen 7 und 8 ersichtlich, dass die Austauschreaktion für die beiden Säuren fast gleich so schwer ausführbar ist und in diesem Fall liegt die Annahme sehr nahe, dass diese schwere Austauschbarkeit grösstenteils auf die geringe Löslichkeit der beiden Säuren in Wasser zurückzuführen ist. Aus diesem Ergebnis kamen wir deshalb weiter zu dem Schluss, dass auch bei Malein- und Fumarsäure die Hauptursache für den Unterschied der Austauschgeschwindigkeit im Unterschiede der Löslichkeit zu suchen sein dürfte, obwohl auch die oben angegebene Möglichkeit der Zwischenbildung der Anhydridmoleküle nicht ganz ausgeschlossen werden kann. Dieser Schluss liegt, mindestens für den Fall mit Malein- und Fumarsäure, um so näher, als die Löslichkeit der Fumarsäure in Wasser nur etwa ein hunderstel der der Maleinsäure ist. Den Unterschied zwischen dem vorliegenden Versuchsergebnis mit Fumarsäure und dem von Cohn und

Urey,[2] die fanden, dass diese Säure überhaupt keine Austauschreaktion ausführte, können wir vielleicht auch aus demselben Grunde erklären, weil die von ihnen benutzte Temperatur (25°C.) viel niedriger als die vorliegende (100°C.) lag.

Zum Schluss möchten wir der Nippon-Gakujutsu-Shinkohkai (der Japanischen Gesellschaft zur Förderung der wissenschaftlichen Förschung) sowei der Hattori-Hohkohkai (der Hattori-Stiftung) für ihre finanzielle Unterstützung unseren wärmsten Dank aussprechen.

Siomi-Institut für physikalische
und chemische Forschung
und
Physikalisch-chemisches Laboratorium
der Kaiserlichen Universität zu Osaka.

Spectrochemical Study of Microscopic Crystals. I. Application of Microscopes in Spectrography.

By Ryutaro TSUCHIDA and Masahisa KOBAYASHI.

(Received September 9, 1938.)

For the purpose of studying absorption spectra of insoluble substances it is necessary to deal with them in solid state. As for soluble substances solid spectroscopy is also important from the viewpoint of avoiding solvent effects, specially for unstable compounds which would undergo change on dissolution. In most cases, however, fine transparent crystals which would yield sections large enough to be subjected to ordinary spectrophotometry are rarely obtained, and moreover, it is extremely difficult to prepare by polishing such crystals thin plane-parallel sections which have desired angular relations with crystal axes. Application of substances in powdery form which has been one of the most popular practices in solid spectroscopy is more favourable in procuring experimental materials, but it defies quantitative determination of absorption and even qualitative observation in the ultra-violet regions, because of the undesirable effect of light scattering. The authors could overcome these difficulties by simply making use of microscopes. In this new method microscopic crystals which are readily obtained in pure state may be directly used for spectrographic measurements. Extensive application of this method is expected in studying various pigments, lake colours and other insoluble substances as well as unstable compounds which would decompose on dissolution or in solutions. Pleochroism of microscopic crystals may also be measured by making use of a polarizing microscope. Especially pleochroism in the ultra-violet regions which can be investigated by means of a quartz optical system is expected to be of considerable importance in stereochemistry as well as in spectrochemistry. Further this method may find its application in micro-identification as has been proposed by I. Okada[1] whose chief purpose was to introduce into chemical researches petrographical methods of microscopic determination of refractive indices.

In the present paper is shown an example of this method. *cis*-Dichloro-tetrammine-cobaltic chloride readily undergoes aquotization in aqueous solution, as can be easily expected from the spectrochemical

(1) I. Okada, *J. Chem. Soc. Japan*, **47** (1926), 720.

series[2] in which the ligand Cl^- is far more bathochromic than H_2O. The absorption spectra of this unstable compound have been determined by means of a usual polarizing microscope.

Experimental. *cis*-Dichloro-tetrammine-cobaltic chloride was prepared by the method of R. Weinland.[3] Microscopic observation revealed that the salt thus obtained consists of rhombic prismatic crystals as shown in Fig. 1. The crystal shows straight extinction. Most crystals lie on their prismatic plane (110). Dichroism on the prismatic plane is violet and brownish red: when the crystal is oriented with its length parallel to the vibration direction of white rays it appears violet, whereas it is red when the vibrations are perpendicular to the c-axis. In other words one of the axial colours is violet and the resultant in the prismatic plane of the other two axial colours is brownish red.

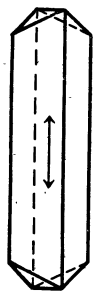
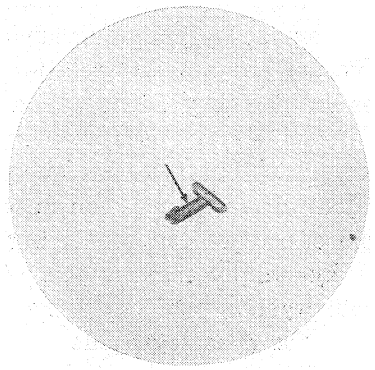


Fig. 1.



×165 $d = 0.0042$ cm.

Fig. 2.

The spectrographic experiments were carried out as follows. The most suitable crystal on a slide glass was chosen in the microscopic field. The crystal used for the measurements is shown by an arrow in the microphotograph in Fig. 2. The polarizing microscope was introduced between a light source of 200 watt incandescent lamp and a glass spectrograph. The position of the crystal was so adjusted that its image focused on the slit of the spectrograph is oriented with its c-axis parallel to the slit. The nicol was set also parallel to the c-axis. The spectrum was photographed, the time of exposure being t seconds. Next the crystal was

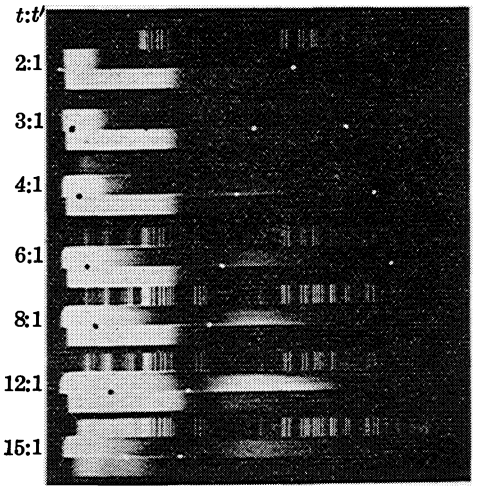
(2) R. Tsuchida, this Bulletin, **13** (1938), 445.

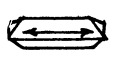
(3) Compare the manual by S. Shinoda and K. Harai on quantitative analysis and preparation of metallic complex salts, p. 151, Tokyo (1933).

slipped aside by a micrometer-screw on the microscope stage, so that the light traversed all the optical system except the crystal. The spectrum was taken, the exposure being t' seconds. The extinction coefficient ε in $I=I_0\times10^{-\varepsilon d}$ (d in cm.) for the wave-length at which the two spectra have equal opacity can be calculated by the following relation:

$$\varepsilon = \frac{0.9}{d} \log \frac{t}{t'} .$$

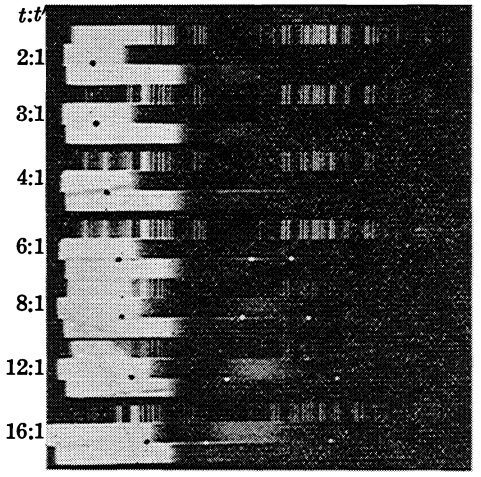
The thickness of the crystal was measured microscopically and for the purpose of finding wave-lengths, a spectrum of an iron arc was photographed side by side with the spectrum of the crystal. Extinction coefficients for various wave-lengths were measured by repeating the procedure for various combinations of t and t'. The absorption spectra thus obtained are shown in Fig. 3.





×165 d = 0.0042 cm.

Fig. 3.





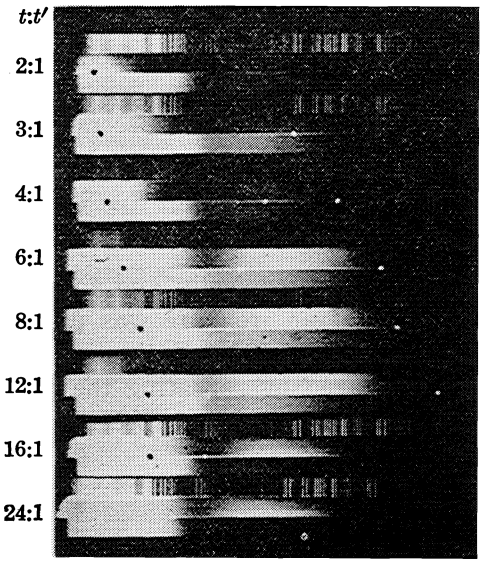
×165 d = 0.0042 cm.

Fig. 4.

Next the nicol was set perpendicular to the c-axis, while the crystal was kept in the same position parallel to the slit. The spectra was photographed just as in the former case. The set of the spectra are shown in Fig. 4.

Finally the nicol was removed and the procedure was repeated as in the former two cases. The spectra are shown in Fig. 5.

As is evident from the procedure, the size of the crystal sufficient for the measurements can be so small that its magnified image just covers the slit of the spectrograph.





×165 $d = 0.0042$ cm.

Fig. 5.

The absorption curves of the complex salt are given in Fig. 6, in which I shows the absorption giving rise to the facial colour on the prismatic plane (110) and II gives the absorption corresponding to the axial colour in the c-axis. The curve III is the resultant absorption in the plane containing the other two crystal axes. The facial extinction coefficients may be calculated as the mean values of those in the curves II and III. The maximal facial extinction coefficient thus calculated is $\log^{-1}$ 2.48 at 57.3×10^{13} sec.$^{-1}$ and coincides with the maximum of the curve I. The axial colours of the crystal axes, a and b, have not been determined. Nevertheless the additive nature[4] of the first bands of complex compounds has been confirmed.

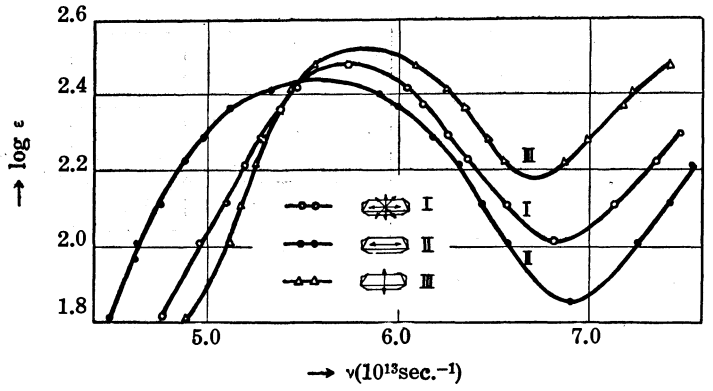


Fig. 6.

Summary.

A new method of measuring absorption spectra of microscopic crystals has been introduced. Application of a polarizing microscope

(4) R. Tsuchida, this Bulletin, **13** (1938), 396.

renders it possible to measure pleochroism of microcrystalline substances. An example is shown of *cis*-dichloro-tetrammine-cobaltic chloride.

The authors wish to express sincere thanks to Prof. Y. Shibata for his kind encouragement. They are also indebted to Mr. K. Umeda for his assistance.

Department of Chemistry, Faculty of Science,
Imperial University of Osaka.

Études spectrochimiques des matières colorantes complexes. I. Sur les complexes métalliques d'*o,o'*-dioxyazobenzène.

Par **Taku UÉMURA** et **Yasuo INAMURA.**

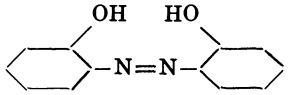
(Reçu le 12 septembre 1938.)

Introduction. En 1913 R. Bohn a trouvé un composé chromique de matière colorante azoïque qui est soluble dans l'eau. C'est l'origine des colorants complexes qui jouent aujourd'hui un rôle important à la teinture de laine. Pendant la grande guerre, les compagnies Ciba (suisse) et I.G. (allemand) ont réussi à fabriquer ces composés et une autre série des nouvelles matières colorantes, donnés par la marque "néolane" par la première et "palatinecht" par la seconde. Beaucoup de brevets sont déjà exposés depuis 1913, mais peu de recherches scientifiques ont été publiées sur ces corps complexes. Quant aux produits insolubles dans l'eau, c'est-à-dire les laques métalliques de ces colorants azoïques, on a plusieurs comptes rendus exposés. A. Werner[1] a déjà discuté sur la constitution chimique de ces composés. G. T. Morgan et J. D. M. Smith[2] ont constaté que les corps oxymonoazoïques devaient avoir un "chelate group" en traitant Eriochrome red B, Palatine chrome black 6B et Diamond black PV avec le sel cobaltique roséo. M. Elkins et L. Hunter[3] ont réussi à préparer quelques dérivés métalliques des corps *o*-oxyazoïques, et ils ont encore montré les constitutions de leurs substances obtenues. Les com-

(1) A. Werner, *Ber.*, **41** (1908), 1062.
(2) G. T. Morgan et J. D. M. Smith, *J. Chem. Soc.*, **125** (1924), 1731.
(3) M. Elkins et L. Hunter, *J. Chem. Soc.*, **1935**, 1598.

binaisons de cuivre ont été récemment formées par H. D. K. Drew et J. K. Landquist[4] qui ne donnent que des laques dans leur publication. F. A. Mason[5] a seul proposé une hypothèse sur la solubilité de "néolane", mais cela manque des preuves positives.

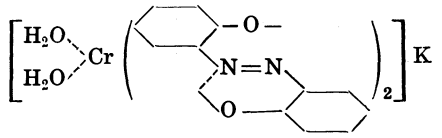
On sait que les matières colorantes de ce genre sont des dérivés d'*o,o'*dioxyazoïque ou ceux d'acide o-oxycarbonique et qu'on en conduit des combinaisons métalliques par les sels de chrome, cuivre, cobalt ou nickel. Nous avons tenté, dans le présent travail, de préciser les structures chimiques des produits métalliques d'*o,o'*-dioxyazobenzène



ou $C_{12}H_{10}O_2N_2$ (I), et de discuter sur la relation entre leur solubilité dans l'eau et leur constitution en profitant de leurs propriétés. Car, les sels métalliques actuellement étudiés seraient comparativement simples parmi les pareils colorants complexes.

Composés étudiés et leur constitution chimique. D'après la méthode indiquée qu'on trouve dans les brevets au début, nous avons traité l'*o,o'*-dioxyazobenzène avec l'hydroxyde de chrome en solution fortement alcaline. Dans ce cas, cependant, nous avons seulement reconnu le changement de couleur de cette substance organique, mais pas réussi à isoler un cristal pur. Nous avons donc employé le bichromate de potassium et l'acide lactique, et obtenu une poudre noire qui est certainement une vraie combinaison métallique. Enfin, puisque nous avons trouvé que le sesquichlorure de chrome est stable pour l'alcali en se décomposant très lentement, nous avons fait réagir ce sel chromique avec l'*o,o'*-dioxyazobenzène en solution d'hydroxyde de potassium et obtenu un cristal après la recristallisation par l'alcool. Ce produit préparé se dissout dans l'eau ou l'alcool, et en le faisant dissoudre dans la solution faiblement acide, on peut l'extraire de l'éther. Dans l'acide concentré, cela devient insoluble et se décompose en ses composants, mais il est très stable dans le milieu alcalin. On ne peut montrer une réaction du chrome qui doit être dans l'ion complexe. D'après notre analyse chimique, nous sommes capables d'assigner que le rapport de la matière colorante au chrome est 2:1. Si on peut admettre que l'*o,o'*-dioxyazobenzène a une structure plaine jointe par le "chelate ring", les six coordinations sont très probables pour appliquer au cas actuel, et ce ne serait pas téméraire de donner la formule suivante pour le cristal obtenu.

(4) H. D. K. Drew et J. K. Landquist, *J. Chem. Soc.*, **1938**, 292.
(5) F. A. Mason, *J. Soc. Dyers Colourists*, **48** (1932), 293.



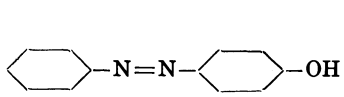
(II)

L'existence du chrome a été constatée par l'analyse qualitative et l'électrophorèse nous a montré le signe négatif de cet ion complexe. Si les deux molécules d'eau contenues dans le noyau complexe occupent deux positions en cis, on pourrait les dédoubler en deux isomères optiques que nous n'avons pu obtenir jusqu'au présent. C'est pourquoi nous pouvons supposer que notre nouveau composé renferme les deux molécules d'eau occupées en position en trans dans le radical complexe. Nous pouvons encore reconnaître les autres composés dont le rapport entre le colorant et le métal est 1:1 ou 1:3. Les complexes hydroxo ou polynuclaires sont aussi probablement existants, et nous avons l'intention de les étudier et de les exposer dans nos prochains mémoires.

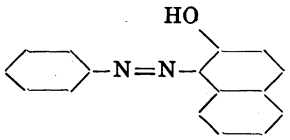
Outre le sel chromique que nous venons d'expliquer, nous avons aussi réussi à préparer deux autres complexes métalliques, celui de cobalt et de nickel. Pour synthétiser le sel cobaltiqué trivalent, le complexe purpuréo $[Co(NH_3)_5Cl]Cl_2$ a été utilisé envers le composé azoïque. Le composé cobaltique ainsi préparé est plus stable que celui de chrome contre l'acide, c'est-à-dire il ne se décompose pas dans la solution du *p*H bas si l'on ne l'échauffe. La couleur de sa solution est généralement rouge.

Notre sel de nickel a été formé en employant l'acétate de nickel. Ce nouveau corps se décompose dans la solution acide très peu et sa solution est rouge-orangeâtre. Comme le nickel est bivalent dans le noyau complexe où les nombres de coordination sont six, le sel formé se présente un ion complexe bivalent et deux atomes de potassium doivent être dans la molécule. L'analyse chimique et la mesure de la conductibilité électrique nous donnent les confirmations pour cette présomption.

Nous avons fait réagir les deux substances organiques suivantes sous la condition semblable,



(III)

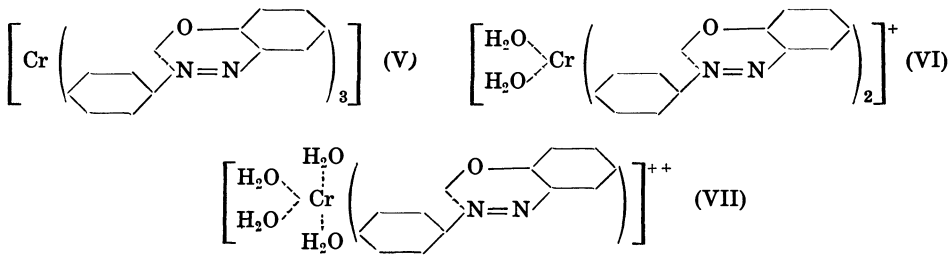


(IV)

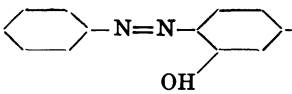
avec le chlorure de chrome, mais elles restaient invariables. On peut probablement dire que la "chelation" n'est pas formée avec le radical *p*-OH, car le résultat expérimental était négatif, c'est-à-dire le corps III n'a pas été métallisé. Quoiqu'il y ait un radical OH à la position ortho

comme le composé IV, il n'est pas suffisant d'obtenir un produit qui est soluble dans l'eau.

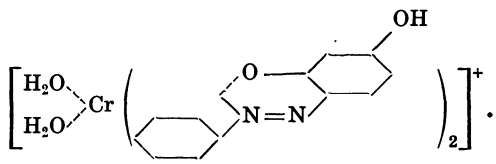
Les sels formés par la substance azoïque *o*-OH donneront les ions complexes suivants.



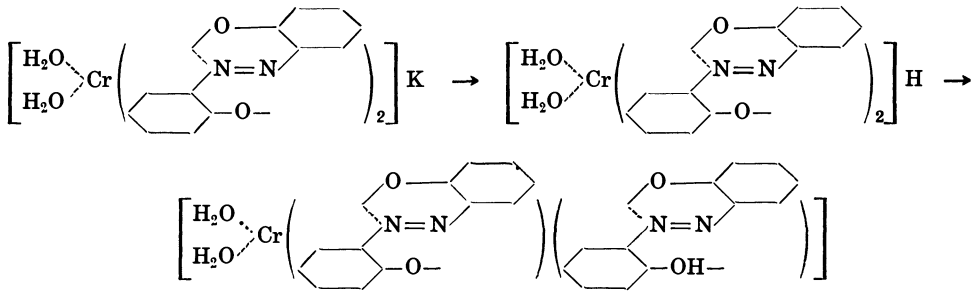
(V) (VI) (VII)

Le nouveau complexe chromique de potassium que nous avons réussi à préparer du colorant d'*o,o'*-dioxyazobenzène ne contient pas de groupement sulfonique, et il est cependant soluble dans l'eau, ce qui est une chose intéressante à étudier. Nous n'avons pas essayé de synthétiser des sels de sodium, mais nous croyons qu'il n'y aurait pas de grandes différences de ceux de potassium. On pourrait donc dire que le groupement sulfonique ne joue peut-être pas un grand rôle pour la solubilité dans l'eau des complexes azoïques. Pour former des complexes solubles, c'est important d'avoir deux radicaux OH. Il faut, cependant, encore procurer une raison qu'on a besoin de ces groupements OH qui occupent deux positions ortho et ortho' vis-à-vis de radical –N=N–. C'est ainsi que nous avons choisi le composé  (VIII) pour le faire métalliser.

Mais, ce corps VIII n'a pas donné l'action attendue avec des réactifs déjà employés. Toutes ces expériences nous conduisent à admettre que le groupement *p*-OH est beaucoup moins acide que celui d'*o*-OH, et que l'hydrogène de *p*-OH ne dissocie pas; en d'autres termes, ce *p*-OH est à peu près semblable à celui du corps monoazoïque déjà expliqué. Le corps VIII ne peut pas donner le sel de potassium mais donne un ion positif comme



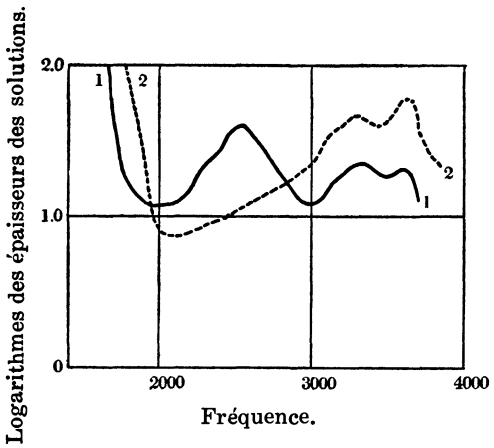
Le mécanisme de la teinture par des colorants comme "néolane" ou "palatinecht" sera expliqué comme suit:



Nous pouvons probablement supposer que la matière colorante complexe qui est soluble dans l'eau ainsi forme une laque insoluble en donnant un même effet lorsqu'on teint la laine avec le colorant acide et mordance avec le bichromate de potassium.

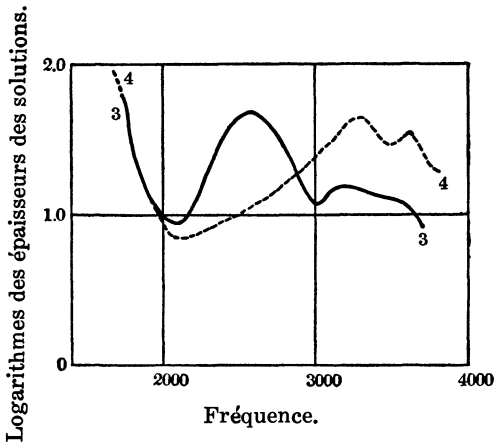
Partie expérimentale.

Spectres d'absorption. La figure 4 montre l'absorption d'*o,o'*-dioxyazobenzène en solution d'hydroxyde de potassium (ca. 1/10 N) et en celle d'acide sulfurique. Les figures 1 à 3 nous donnent les absorptions des sels de chromi-, cobalti- et nickélo-dioxyazobenzènedihydrine de potassium en solution aqueuse et en acide sulfurique. Les photographies d'absorption ont été prises en nous servant du spectrographe en quartz de l'Anglais Adam Hilger et les courbes ont été obtenues d'après le système proposé par Hartley et Baly. Tous ces trois sels complexes synthétisés en solution aqueuse ont montré des absorptions semblables en nous donnant une première absorption nette



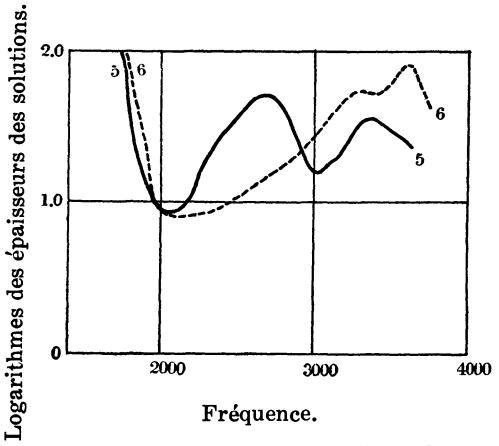
1. $[Cr(C_{12}H_8O_2N_2)_2(H_2O)_2]K\cdot 2H_2O$ (Solution H_2O)
2. $[Cr(C_{12}H_8O_2N_2)_2(H_2O)_2]K\cdot 2H_2O$ (Solution H_2SO_4 conc.)

Fig. 1.



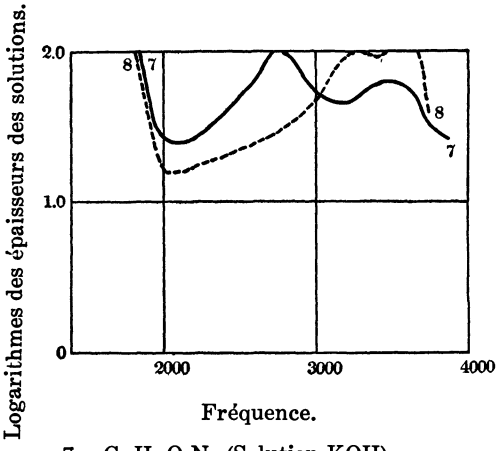
3. $[Co(C_{12}H_8O_2N_2)_2(H_2O)_2]K$ (Solution H_2O)
4. $[Co(C_{12}H_8O_2N_2)_2(H_2O)_2]K$ (Solution H_2SO_4 conc.)

Fig. 2.



5. $[Ni(C_{12}H_8O_2N_2)_2(H_2O)_2]K_2 \cdot 3H_2O$ (Solution H_2O)
6. $[Ni(C_{12}H_8O_2N_2)_2(H_2O)_2]K_2 \cdot 3H_2O$ (Solution H_2SO_4 conc.)

Fig. 3.



7. $C_{12}H_{10}O_2N_2$ (Solution KOH)
8. $C_{12}H_{10}O_2N_2$ (Solution H_2SO_4 conc.)

Fig. 4.

aux environs des longueurs d'onde à 500 mμ, malgré leur couleur différente des solutions. Nous en pourrons prouver que ces corps dissous aient chimiquement un type semblable en solution. Parmi ces trois complexes, le composé chromique est le plus bathochromique et celui de nickel le moins. En les comparant avec le colorant original (Fig. 4), un effet bathochromique et hyperchromique a été aisément trouvé. Cela nous revient à reconnaître qu'ils ont un même chromophore, c'est-à-dire un "chelate ring" joint le métal et le groupement azoïque qui se trouvent dans le radical complexe. Les trois courbes données par les combinaisons étudiées en solution d'acide sulfurique concentré coïncident grossièrement. Il est encore clair, d'après des courbes obtenues, que, en ajoutant l'acide sulfurique concentré, les complexes se décomposent en leurs composants, *o,o'*-dioxyazobenzène et sulfate métallique. Comme les absorptions données par les sulfates sont si faibles que leurs influences sur l'absorption ne sont pas sensiblement manifestées, et, dans ce cas, le spectre d'absorption ne montre que l'halochromie du colorant azoïque.

Lorsque les courbes des complexes sont élevées, dans les figures, à peu près 0.3 de logarithmes des épaisseurs des solutions à l'axe des ordonnées, elles se superposent sur celle donnée par le colorant original. C'est ainsi qu'on peut observer que une molécule du sel complexe renferme deux molécules du composé azoïque, car le logarithme de 2 vaut approximativement 0.3.

En utilisant l'acide sulfurique comme le solvant pour profiter l'halochromie des corps azoïques, on pourrait deviner quel colorant azoïque se trouve dans le noyau complexe des produits métalliques.

Mesure de la conductibilité électrique et de l'électrophorèse. Les expériences ont été faites pour déterminer la valence et la charge électrique des ions complexes.

Voici nos résultats expérimentaux de la mesure de la conductibilité électrique de nos trois corps.

Métal contenu	Ω (Résistance : ohm)	$\varkappa$ (Conductibilité spécifique)	c (Concentration : mol)	$\varkappa/c$ (Conductibilité moléculaire)
Chrome	4060	0.0000851	0.83×10^{-3}	1
Cobalt	2950	0.000117	1.17×10^{-3}	1
Nickel	1850	0.000187	0.97×10^{-3}	2

(température = 25°C.; constante de la batterie = 0.3456)

En supposant que le degré d'ionisation est semblable, ces mesures constatent que les ions complexes du chrome et du cobalt sont monovalents tandis que celui du nickel est bivalent comme nous les avions espérés.

En admettant que les solutions aqueuses de ces sels complexes ne soient pas colloïdales, nous étions capables d'observer l'électophorèse[6] que nous faisait comprendre que tous les ions complexes étudiés sont négatifs; car chaque ion coloré a passé vers l'anode.

Synthèse et analyse. (1) $[Cr(C_{12}H_8O_2N_2)_2(H_2O)_2]K\cdot2H_2O$. *Chromididioxyazobenzène-dihydrine de potassium.* Pour préparer ce sel complexe, on dissout 8.5 g. d'*o,o'*-dioxyazobenzène et 20 g. d'hydroxyde de potassium dans 100 g. d'eau. On y ajoute par de petites portions 3.2 g. de chlorure de chrome en poudre, et les chauffe au bain-marie en les agitant pendant deux heures. La solution rouge devient bordeaux et des cristaux métalliques s'y déposent. En les faisant recristalliser par l'eau, on obtient ainsi de jolis cristaux métalliques verts. Le sel préparé peut se dissoudre dans l'eau et dans l'alcool. Trouvé: Cr, 9.98; N, 9.71; H_2O, 6.22 (dans le radical complexe), 13.18 (somme totale). Calculé pour $[Cr(C_{12}H_8O_2N_2)_2(H_2O)_2]K\cdot2H_2O$: Cr, 10.02; N, 9.5; H_2O, 6.53 (dans le radical complexe), 12.27% (somme totale).

(2) $[Co(C_{12}H_8O_2N_2)_2(H_2O_2)]K$. *Cobalti-didioxyazobenzène-dihydrine de potassium.* On dissout 2 g. d'*o,o'*-dioxyazobenzène dans 50 c.c. de l'eau. On y ajoute 4 c.c. de la solution aqueuse d'hydroxyde de potassium (7.5 N), puis 2.5 g. du sel purpuréo cobaltique ($[Co(NH_3)_5Cl]Cl_2$). En les chauffant au bain-marie pendant dix heures, on y observe la formation des cristaux métalliques verts. On les fait recristalliser par l'alcool et puis par l'eau. Le complexe cobaltique obtenu se dissout dans l'eau ou dans l'alcool. Trouvé: Co, 10.76; N, 11.02; H_2O, 5.47. Calculé pour $[Co(C_{12}H_8O_2N_2)_2(H_2O)_2]K$: Co, 10.62; N, 10.04; H_2O, 6.45%.

(3) $[Ni(C_{12}H_8O_2N_2)_2(H_2O_2)]K_2\cdot3H_2O$. *Nickélo-didioxyazobenzène-dihydrine de potassium.* Ce corps complexe est synthétisé comme suit. En mélangeant 4 g. d'*o,o'*-dioxyazobenzène, 10 g. d'hydroxyde de potassium et 150 c.c. d'eau, on y ajoute 2.5 g. d'acétate de nickel dissous dans 10 c.c. d'eau, et les chauffe au bain-marie pendant cinq heures. Des cristaux métalliques s'y déposent et sont recristallisés dans l'eau. Trouvé: Ni, 10.76; N, 8.05; H_2O, 13.20. Calculé pour $[Ni(C_{12}H_8O_2N_2)_2(H_2O)_2]K_2\cdot3H_2O$: Ni, 10.46; N, 8.05; H_2O, 13.82%.

(6) C. Duval, *Compt. rend.*, **200** (1935), 2175.

Résumé.

(1) Nous avons réussi à préparer les trois complexes nouveaux de chrome, de cobalt et de nickel en utilisant l'*o,o'*-dioxyazobenzène et les sels métalliques.

(2) D'après les résultats des analyses chimiques, des conductibilités électriques et des électrophorèses, nous avons pu assigner leur constitution chimique.

(3) Leurs spectres d'absorption ont été observés dans l'eau et dans l'acide sulfurique.

(4) D'après leurs photographies d'absorption prises, nous pouvons constater que les nouveaux composés obtenu se décomposent au colorant original et au sulfate métallique par l'addition d'acide sulfurique concentré.

(5) Le rapport du métal au colorant dans le noyau complexe est supposé 1:2 pour nos nouveaux composés même d'après le calcul par des courbes d'absorption.

En terminant cette publication de nos présentes recherches, nous avons à exprimer nos sincères remerciements à la Société "Kéiméikaï" qui a bien voulu se charger d'une partie des frais de nos expériences, ainsi qu'à Monsieur M. Sékito de notre Faculté qui nous a permis de nous prêter son bienveillant concours dans nos mesures électrochimiques.

Laboratoire de Chimie minérale, Faculté des Arts et Métiers de Tokyo (Tokyo Kogyô-Daigaku).

Austauschreaktion der Wasserstoffatome zwischen Nitrophenol und Wasser. II. Chemismus der Reaktion.

(*Fortsetzung und Schluss.*)*

Von Masao KOIZUMI und Toshizo TITANI.

(Eingegangen am 30. August 1938.)

Einfluss der Alkalikonzentration auf die Austauschgeschwindigkeit der Kernwasserstoffatome des Nitrophenols. Unter Benutzung der im vorigen Abschnitt gewonnenen Gl.(15) untersuchten wir zunächst den Einfluss der Veränderung der Alkalikonzentration in Lösung auf die Austauschgeschwindigkeit des *m*- und *p*-Nitrophenols.(5) Dabei verfuhren wir folgendermassen: Wir bereiten aus verdünntem (etwa 4-prozentigem) schwerem Wasser und wasserfreiem Kaliumhydroxyd die Kalilauge von wohl bekannter Konzentration, die je 1, 2 und 3 N beträgt. Dann wird eine bestimmte Menge dieser Kalilauge zusammen mit der ebensogut abgewogenen Menge Nitrophenols in einem Glasrohr eingeschmolzen und verschiedene Zeitlängen auf 100°C. erwärmt. Nach der Beendigung der Erwärmung wird das schwere Wasser durch Destillation im Vakuum vom Nitrophenol und Alkali abgetrennt und dessen Dichte nach der Schwebemethode genau bestimmt, nachdem es im voraus auf die schon in I. Mitteil. beschriebene Weise gut gereinigt worden war. Wir berechnen jetzt aus dem so bestimmten D-Gehalt D_w des schweren Wassers nach dem Experiment und dem auf ähnliche Weise bestimmten anfänglichen D-Gehalt D_{w0} des Wassers, zusammen mit der Molzahl M_w des Wassers sowie der des Nitrophenols M_{ph} mittels Gl.(10) das Austauschäquivalent na bei der betreffenden Versuchsdauer t. Daraus wird weiter die Quantität $(-X \log Y)$ gemäss der Gl.(16) errechnet. Das dabei zur Berechnung von $(-X \log Y)$ erforderliche Volumen V der Lösung wird unter Benutzung der in Tabelle 1 angegebenen Daten über die Dichte der Lösung des Nitrophenols in Kalilauge, unter Umständen durch Extra- bzw. Interpolation, rechnerisch ermittelt. Diese Daten in Tabelle 1 erhielten wir,

---

* Fortsetzung aus S. 600 dieses Bandes.

(5) Die *o*-Verbindung wurde nicht untersucht, da sich nicht nur diese Verbindung in konzentrierter Alkalilösung ziemlich merklich zersetzbar erwies, sondern auch ihre Austauschgeschwindigket viel zu klein war, um die Geschwindigkeitskonstante genau zu ermitteln.

indem wir die Dichte der Lösung des Nitrophenols in gewöhnlicher (nicht schwerer) Kalilauge direkt pyknometrisch bestimmten.

Tabelle 1. Dichte der Lösung des Nitrophenols in Kalilauge verschiedener Konzentration bei verschiedenen Temperaturen.

Zusammensetzung der Lösung	Gewichtsverhältnis des Nitrophenols (G_{ph}) zu Kalilauge (G_w) G_{ph}/G_w	Temperatur (°C.)	Dichte der Lösung
m-Nitrophenol+1 N KOH	2.05	100	1.172
,, ,,	3.07	100	1.197
,, ,,	3.07	105	1.190
p-Nitrophenol+1 N KOH	2.26	100	1.178
,, ,,	3.07	100	1.202
,, ,,	3.07	104	1.198
p-Nitrophenol+3 N KOH	3.07	100	1.232

Die Zusammenstellung der so erhaltenen Versuchsergebnisse finden sich in Tabellen 2 und 3, wo die Zahlenwerte in jeder Vertikalreihe auf folgende Weise bestimmt bzw. berechnet sind:

1. Versuchsnummer.
2. Versuchsdauer t in Stdn.: vgl. oben.
3. Menge der Kalilauge G_w in g.: vgl. oben.
4. Konzentration der Kalilauge in N: vgl. oben.
5. Menge des Nitrophenols G_{ph} in g.: vgl. oben.
6. Volumen der Kalilauge bei 15°C. in Liter: aus 3. und der Dichte der betreffenden Kalilauge berechnet. Diese letztere beträgt bei 15°C. 1.05 für 1 N, 1.08 für 2 N und 1.13 für 3 N Kalilauge (vgl. 4.).
7. Volumen der Lösung bei 100°C. in Liter: vgl. oben.
8. (Analytische) Konzentration von KOH in Lösung [KOH]: aus 4., 6. und 7. berechnet. Aber weil die Menge des Nitrophenols in Lösung immer überwiegend grösser als die des Alkalis ist und deshalb das letztere (bis auf eine geringe hydrolytische Spaltung) fast ganz durch das erstere neutralisiert wird, haben wir in Wirklichkeit keine Hydroxylionen in der Lösung und wir können die hier angegebene analytische Konzentration des Alkalis [KOH] praktisch identisch mit der Konzentration der Phenolationen [PhO^-] ansehen.
9. Molzahl des (zum Austausch effektiven) Wassers M_w: Dies wird unter Berücksichtigung der austauschbaren H-Atome im zugesetzten Kaliumhydroxyd auf folgende Weise berechnet: Handelt es sich z.B. um 1 N KOH-Lösung (Dichte = 1.05 bei 15°C.), dann wiegt ein Liter

dieser Lösung bei 15°C. 1050 g. und diese Lösung enthält ein Mol d.h. 56 g. KOH und (1050−56) = 994 g. = 55.3 Mol H_2O. Da aber ein Mol KOH 0.5 Mol H_2O äquivalent ist, entspricht ein Liter von 1 N KOH-Lösung 55.3 + 0.5 = 55.8 Mol H_2O. Auf ähnliche Weise ersieht man ohne weiteres, dass ein Liter von 2 N und 3 N KOH-Lösung (Dichte = 1.08 und 1.13 bei 15°C.) resp. 53.7 + 1.0 = 54.7 Mol und 53.4 + 1.5 = 54.9 Mol H_2O entspricht. Unter Benutzung dieser Zahlenwerte sowie des Volumens der zum Versuch benutzen Kalilauge (vgl. 6.) können wir deshalb die Molzahl M_w des zum Austausch effektiven Wassers leicht berechnen.

10. Molzahl des Nitrophenols M_{ph}: aus 5. und dem Molekulargewicht des Nitrophenols (= 139.05) berechnet.
11. (Gesamt-)konzentration des (zum Austausch effektiven) Wassers [[H_2O]]: aus 7. und 9. berechnet.
12. Konzentration von (neutralen Wassermolekülen) H_2O in Lösung [H_2O]: Dies ist keine Konzentration des zum Austausch effektiven Wassers, sondern die der wirklich in Lösung befindlichen Wassermoleküle. Aber weil das Wasser nicht nur in der zur Lösung zugesetzten Kalilauge befindlich ist, sondern auch durch die Neutralisation von Kaliumhydroxyd durch Nitrophenol (und zwar ein Mol Wasser pro Mol Kaliumhydroxyd) erzeugt wird, so ist die gewünschte Konzentration der wirklich in Lösung befindlichen Wassermoleküle [H_2O], wie aus den in 9. erwähnten Tatsachen ohne weiteres ersichtlich ist, respt. um den Faktor (55.8 + 0.5)/55.8 = 1.009, (54.7 + 1.0)/54.7 = 1.018 und (54.9 + 1.5)/54.9 = 1.026 grösser als die in 11. angegebene Konzentration [[H_2O]], je nachdem ob es sich dabei um die 1 N, 2 N bzw. 3 N KOH handelt.
13. (Gesamt-)konzentration des Nitrophenols in Lösung [[PhOH]]: aus 7. und 10. berechnet.
14. Konzentration von (neutralen Nitrophenolmelkülen) PhOH in Lösung [PhOH]: Dies können wir aus 8. und 13. leicht berechnen, weil [PhOH] = [[PhOH]] − [PhO^-] ist.
15. Dichteüberschuss des (benutzten) schweren Wassers vor dem Experiment D_{w0} in γ: Dies wird, wie schon oben erwähnt wurde, nach Schwebemethode im Vergleich mit gewöhnlichem Wasser bestimmt, nachdem das zu untersuchende schwere Wasser durch die Destillation im Vakuum vom zugesetzten Kaliumhydroxyd befreit worden.
16. Dichteüberschuss des (benutzten) schweren Wassers nach dem Experiment D_w in γ: ähnlich wie bei 15. bestimmt.
17. Austauschäquivalent na (des Nitrophenols): mittels Gl.(10) unter Benutzung 9., 10., 15. und 16. berechnet (vgl. oben).

Tabelle 2. Versuch A. Kerndeuterierung des *m*-Nitrophenols bei verschiedener Alkalikonzentration (Temperatur = 100°C.).

1. Versuchs-nr.	2. Versuchs-dauer t in Stdn.	3. Menge der Kalilauge G_w in g.	4. Konzentration der Kalilauge in N	5. Menge des Nitrophenols G_{ph} in g.	6. Volumen der Kalilauge bei 15°C. $\times 10^3$ in Liter
1	50	1.163	1.00	3.043	1.107
2	150	1.038	,,	3.017	0.989
3	260	1.035	,,	2.891	0.986
4	48	1.017	2.00	3.030	0.942
5	95	1.008	,,	3.001	0.933
6	2	1.115	3.00	3.001	0.987
7	50	1.149	,,	3.001	1.016
8	62	1.140	,,	3.043	1.009
9	100	1.134	,,	3.001	1.003

7. Volumen der Lösung bei 100°C. $\times 10^3$ in Liter	8. Konzentration von KOH in Lösung = $[PhO^-]$	9. Molzahl des Wassers M_w	10. Molzahl des Nitrophenols M_{ph}	11. Konzentration des Wassers in Lösung $[[H_2O]]$	12. Konzentration von H_2O in Lösung $[H_2O]$
3.57	0.311 } Mittel	0.0617	0.0219	17.3 } Mittel	17.45 } Mittel
3.40	0.291 } 0.300	0.0550	0.0217	16.2 } 16.7	16.35 } 16.9
3.30	0.298 }	0.0549	0.0208	16.6 }	16.75 }
3.36	0.561 } 0.562	0.0515	0.0218	15.5 } 15.5	15.8 } 15.8
3.32	0.562 }	0.0511	0.0216	15.55 }	15.8 }
3.39	0.873 }	0.0541	0.0216	16.0 }	16.4 }
3.41	0.894 } 0.881	0.0558	0.0216	16.4 } 16.1	16.8 } 16.4
3.44	0.880 }	0.0554	0.0219	16.1 }	16.5 }
3.44	0.875 }	0.0551	0.0216	16.0 }	16.0 }

13. Konzentration des Nitrophenols in Lösung $[[PhOH]]$	14. Konzentration von PhOH in Lösung $[PhOH]$	15. Dichteüberschuss des schweren Wassers: vor dem Experiment D_{w0} in γ	16. Dichteüberschuss des schweren Wassers: nach dem Experiment D_w in γ	17. Austausch-äquivalent n_x	18. $(-X \log Y)$
6.14 } Mittel	5.83 } Mittel	3276	2606	1.45	0.00139
6.38 } 6.27	6.09 } 5.97	3712	2540	2.34	0.00562
6.30 }	6.00 }	3276	2180	2.66	0.00748
6.48 } 6.49	5.92 } 5.93	4133	2910	1.99	0.00397
6.50 }	5.94 }	4133	2753	2.38	0.00601
6.37 } 6.34	5.50 } 5.46	4339	3482	1.23	0.00059
6.34 }	5.45 }	4339	2978	2 36	0.00571
6.37 }	5.49 }	4339	2886	2.54	0.00686
6.28 }	5.40 }	4339	2760	2.92	0.00970

Tabelle 3. Versuch B. Kerndeuterierung des *p*-Nitrophenols bei verschiedener Alkalikonzentration (Temperatur = 100°C.).

1. Versuchs-nr.	2. Versuchs-dauer t in Stdn.	3. Menge der Kalilauge G_w in g.	4. Konzentration der Kalilauge in N	5. Menge des Nitrophenols G_{ph} in g.	6. Volumen der Kalilauge bei 15°C. $\times 10^3$ in Liter
10	2	2.142	1.00	5.714	2.04
11	50	1.046	,,	3.001	0.996
12	150	1.043	,,	3.071	0.994
13	260	1.601	,,	2.612	1.525
	(260)	—	—	—	—
14	48	1.161	2.00	3.044	1.075
15	95	1.084	,,	3.040	1.004
16	2	1.102	3.00	2.906	0.975
17	50	1.130	,,	3.001	1.000
18	95	1.119	,,	3.059	0.990
19	100	1.140	,,	3.001	1.009

7. Volumen der Lösung bei 100°C. $\times 10^3$ in Liter	8. Konzentration von KOH in Lösung = $[PhO^-]$	9. Molzahl des Wassers M_w	10. Molzahl des Nitrophenols M_{ph}	11. Konzentration des Wassers in Lösung $[[H_2O]]$	12. Konzentration von H_2O in Lösung $[H_2O]$
6.41	0.318 } Mittel	0.114	0.0411	17.8 } Mittel	18.0 } Mittel
3.36	0.297 } 0.303	0.0555	0.0216	16.5 } 16.9	16.65 } 17.0
3.40	0.292 }	0.0553	0.0221	16.3 }	16.25 }
3.62	0.422	0.0850	0.0188	23.5	23.5 }
—	(0.300)	—	—	—	—
3.46	0.622 } 0.606	0.0588	0.0219	17.2 } 16.8	17.5 } 17.1
3.41	0.590 }	0.0549	0.0219	16.3 }	16.6 }
3.41	0.858 }	0.0535	0.0209	15.7 }	16.1 }
3.38	0.888 } 0.875	0.0549	0.0216	16.2 } 16.0	16.6 } 16.2
3.44	0.864 }	0.0544	0.0220	15.8 }	15.8 }
3.38	0.896 }	0.0554	0.0216	16.4 }	16.4 }

13. Konzentration des Nitrophenols in Lösung $[[PhOH]]$	14. Konzentration von PhOH in Lösung $[PhOH]$	15. Dichteüberschuss des schweren Wassers: vor dem Experiment D_{w0} in γ	16. Dichteüberschuss des schweren Wassers: nach dem Experiment D_w in γ	17. Austausch-äquivalent n_α	18. $(-X \log Y)$
6.40 } Mittel	6.08 } Mittel	3276	2710	1.16	0.00046
6.43 } 6.44	6.13 } 6.14	3742	2983	1.31	0.00138
6.50 }	6.21 }	3712	2670	1.96	0.00617
5.19	4.77	3276	2605	2.52	0.01073
—	—	—	—	—	(0.00763)(6)
6.33 } 6.37	5.71 } 5.77	4133	3149	1.68	0.00312
6.42 }	5.83 }	3475	2471	2.05	0.00693
6.13 }	5.27 }	4339	3505	1.21	0.00081
6.39 }	5.50 }	4339	3194	1.83	0.00506
6.40 } 6.33	5.54 } 5.45	3243	2201	2.34	0.01094
6.39 }	5.49 }	4339	2972	2.36	0.01079

(6) Da die Alkalikonzentration beim Versuch 13 von den anderen drei Versuchen 10, 11 und 12 in derselben Versuchsreihe vielfach verschieden war, rechneten wir den bei diesem Versuch 13 direkt gefundenen Wert von $(-X \log Y)$, der 0.01073 beträgt,

18. (Die Quantität) $-X \log Y$: mittels Gl.(16) unter Benutzung 9., 10. und 17. berechnet (vgl. oben).

Zeichnet man die so gefundenen Werte von $(-X \log Y)$ (18. Reihen der Tabellen 2 und 3) gegen die Versuchsdauer t (2. Reihen der Tabellen), so erhält man für eine bestimmte Alkalikonzentration eine gute gerade Linie, wie aus den nebenstehenden Abbn. 1 und 2 offensichtlich ist und aus der Neigung dieser Linie gegen t-Achse kann die Geschwindigkeitskonstante $\bar{k}/2.303$ ohne weiteres gefunden werden (vgl. Gl.(15)). Die so gefundenen Werte von $\bar{k}/2.303$ geben wir in Tabelle 4 wieder.

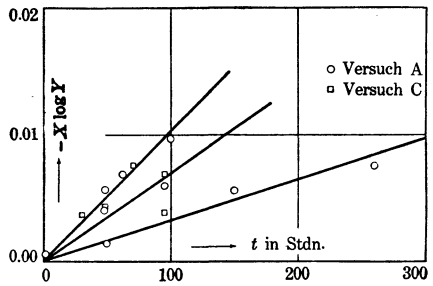


Abb. 1. *m*-Nitrophenol.

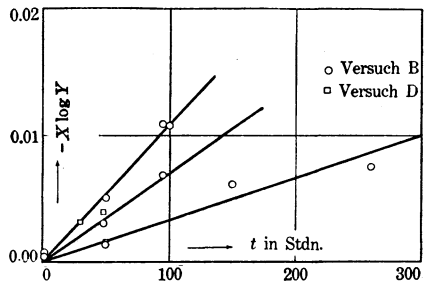


Abb. 2. *p*-Nitrophenol.

Tabelle 4. Austauschgeschwindigkeitskonstante $\bar{k}$ bei verschiedener Alkalikonzentration (Temperatur = 100°C.).

Nitrophenol	Alkalikonzentration [KOH]	Mittelwert [KOH]	Konzentration des Nitrophenols	$\bar{k}/2.303$	$\frac{\bar{k}/2.303}{[KOH]} \times 10^6$
meta	0.29–0.31	0.30	6.1–6.4	0.0000323	1.08
	0.56–0.56	0.56	6.5–6.5	0.0000696	1.24 } Mittel 1.16
	0.87–0.89	0.88	6.3–6.4	0.0001030	1.17
para	0.29–0.32	0.30	6.4–5.2	0.0000334	1.11
	0.59–0.62	0.60	6.3–6.3	0.0000706	1.18 } Mittel 1.18
	0.86–0.90	0.88	6.1–6.4	0.0001090	1.24

Wie aus der letzten Vertikalreihe dieser Tabelle 4 ersichtlich ist, ergibt sich aus diesem Versuch, dass die Geschwindigkeitskonstante $\bar{k}$

auf dieselbe Alkalikonzentration wie bei den anderen drei Versuchen, nämlich auf 0.300 N um, indem wir die weiter unten zu erwähnende Regel benutzten, dass die Quantität $(-X \log Y)$ bei einer bestimmten Versuchsdauer t mit zunehmender Alkalikonzentration direkt proportional zunimmt. Der so reduzierte Wert von $(-X \log Y)$ beim Versuch 13 beträgt 0.00763 und dieser Wert wurde bei der graphischen Ermittelung von $k/2.303$ (in Abb. 2) benutzt.

der „zweiten" Stufe der Reaktion mit zunehmender Alkalikonzentration [KOH] fast proportional zunimmt. Wir können deshalb wohl erwarten, dass bei dieser Stufe der Reaktion Phenolationen eine wichtige Rolle spielen müssen, weil ihre Konzentration $[PhO^-]$ in Lösung unter den hier benutzten Versuchsbedingungen proportional mit der des zugesetzten Alkalis [KOH] vermehrt wird (vgl. oben). Wir wollen deshalb weiter mehr oder weniger quantitativ diesen Schlüssen unser Augenmerk zuwenden.

Bezeichnet man mit

$[PhOH]$: die Konzentration der neutralen (undissozierten) Nitrophenolmoleküle,

$[PhOD]$: die der neutralen hydroxydeuterierten Nitrophenolmoleküle,

$[PhO^-]$: die der dissozierten Nitrophenolmoleküle, d.h. der Phenolationen,

$[OD^-]$: die der Deuteroxylionen

in Lösung, dann können wir die Abnahmegeschwindigkeit der Gesamtkonzentration des schweren Wassers $[[HDO]]$ in Lösung durch die Kernaustauschreaktion im allgemeinen wie folgt setzen:

$$-\frac{d[[HDO]]}{dt} = n_2\{k_1\overset{(i)}{[PhOH]}[HDO] + k_2\overset{(ii)}{[PhOH]}[OD^-] + k_3\overset{(iii)}{[PhOH]}[PhOD]$$
$$+ k_4\overset{(iv)}{[PhO^-]}[HDO] + k_5\overset{(v)}{[PHO^-]}[OD^-] + k_6\overset{(vi)}{[PhO^-]}[PhOD]\}$$
$$-(\text{Gegenreaktion}) \qquad (17),$$

wo die Konstante k_1, k_2 .... k_6 resp. die Austauschgeschwindigkeitskonstante zwischen je zwei Arten der Moleküle bzw. Ionen ausdrückt. Bei dieser Gl. (17) nehmen wir weiter an, dass der D-Gehalt der Lösung genügend klein ist, so dass immer nur monodeuterierte Moleküle bzw. Ionen in Rechnung gezogen werden dürfen. Wenn man nun das erste in { } geklammerte Glied in der rechten Seite der Gl. (17) mit dem ersten Glied der Gl. (1) vergleicht, so ersieht man ohne weiteres, dass zwischen der experimentell bestimmten mittleren Geschwindigkeitskonstante $\bar{k}$ und den einzelnen Geschwindigkeitskonstanten k_1, k_2 .... k_6 folgende Beziehung bestehen muss:

$$\bar{k} = k_1\frac{\overset{(i)}{[PhOH]}[HDO]}{[[PhOH]][[HDO]]} + k_2\frac{\overset{(ii)}{[PhOH]}[OD^-]}{[[PhOH]][[HDO]]} + k_3\frac{\overset{(iii)}{[PhOH]}[PhOD]}{[[PhOH]][[HDO]]}$$

$$\overset{\text{(iv)}}{+k_4\frac{[PhO^-][HDO]}{[[PhOH]][[HDO]]}}+\overset{\text{(v)}}{k_5\frac{[PhO^-][OD^-]}{[[PhOH]][[HDO]]}}+\overset{\text{(vi)}}{k_6\frac{[PhO^-][PhOD]}{[[PhOH]][[HDO]]}} \quad (18),$$

wo [[PhOH]] und [[HDO]] im Nenner jedes Gliedes je die Gesamtkonzentration des Nitrophenols und schweren Wassers in Lösung ausdrücken. Von diesen sechs Gliedern bzw. Teilreaktionen (i) bis (vi) können wir aber (i) und (iii) im Vergleich mit den anderen vier Gliedern vernachlässigen, weil, wie schon in I. Mitteil. gezeigt wurde, die Austauschreaktion in neutraler Lösung nur äusserst langsam verläuft. Ebenso wenig können die Teilreaktionen (ii) und (v) aus den folgenden Gründen aktive Rollen spielen. Erstens muss die Deuterierungskraft der OD^--Ionen, wie darauf schon von Ingold und seinen Mitarbeitern[2] hingewiesen wurde, viel schwächer als die der anderen Molekülarten in der Lösung wie z.B. Nitrophenolmoleküle und Wassermoleküle betrachtet werden. Zweitens dürfte die Konzentration der Deuteroxyl- bzw. Hydroxylionen, die unter den vorliegenden Versuchsbedingungen (die Menge des Nitrophenols ist überwiegend grösser als die des Alkalis!) allein durch die hydrolytische Spaltung der Phenolatmoleküle gebildet werden, zu klein sein, um die gefundene Reaktionsgeschwindigkeit damit zu deuten. Und drittens falls noch die Teilreaktion (v) die Hauptreaktion wäre, dann müsste die Reaktionsgeschwindigkeit mit zunehmender Alkalikonzentration nicht einfach proportional sondern viel schneller zunehmen. Auf diese Weise bleiben uns nur noch zwei Glieder bzw. Teilreaktionen (iv) und (vi) zu betrachten übrig. Die Geschwindigkeit dieser beiden Teilreaktionen muss, wie aus der Form der Gleichungen offensichtlich ist, mit zunehmender Alkalikonzentration annähernd proportional wachsen. Um zwischen diesen beiden Möglichkeiten zu unterscheiden, untersuchten wir nun den Einfluss der Veränderung der Konzentration der anderen zwei Reaktionsteilnehmer als Alkali, nämlich des Nitrophenols und des Wassers, auf die Reaktionsgeschwindigkeit.

Einfluss der Konzentration des Nitrophenols und des Wassers auf die Austauschgeschwindigkeit der Kernwasserstoffatome des Nitrophenols. Wenn man bei konstant bleibender Konzentration des Alkalis sowie des Nitrophenols die Konzentration des Wassers in Lösung vermindert, dann muss das vierte Glied (iv) in Gl.(18) fast unverändert bleibt, während das sechste (vi) sich vergrössert, weil bei konstant bleibender Alkalikonzentration auch die der Phenolationen $[PhO^-]$ konstant bleiben muss. Falls dagegen die Konzentration des Alkalis und des Wassers unverändert

bleibt, aber die des Nitrophenols vermindert wird, dann vergrössert sich das vierte Glied (iv), während das sechste (vi) fast unverändert bleibt. Wir können deshalb auf diese Weise zwischen diesen beiden Möglichkeiten (iv) und (vi) die Hauptreaktion unterscheiden. Aber weil es nicht möglich war allein die Konzentration des Wassers bzw. Nitrophenols zu verändern, verwendeten wir in den vorliegenden Versuchen C und D Wasser und Nitrophenol beide in bis zu einem gewissen Grad veränderten Mengen als in den letzten Versuchen A und B (vgl. Tabellen 2 und 3), und aus den so erhaltenen Versuchsergebnissen zogen wir den erwünschten Schluss auf mittelbarem Wege. Die Ergebnisse der so ausgeführten Versuche C und D sind in Tabellen 5 und 6 zusammengestellt, wo die Zahlenwerte in jeder Vertikalreihe auf dieselbe Weise wie bei den Versuchen A und B in Tabellen 2 und 3 bestimmt bzw. berechnet sind.

Um aus diesen Versuchsergebnissen über die Hauptreaktion den Schluss zu ziehen, verfuhren wir folgendermassen. Falls nämlich die Teilreaktion (iv) in Gl. (17) die Hauptreaktion wäre, dann müsste, wie aus der Form des entsprechenden Gliedes in Gl. (18) ohne weiteres ersichtlicht ist, die mittlere Geschwindigkeitskonstante $\bar{k}$, folglich die Quantität $(-X \log Y)$ bei einer bestimmten Versuchsdauer t, mit zunehmender Konzentration der Phenolationen $[PhO^-]$ direkt proportional zunehmen, aber zugleich müsste sie mit zunehmender Gesamtkonzentration des Nitrophenols [[PhOH]] in Lösung umgekehrt proportional abnehmen. Wenn dagegen die Teilreaktion (vi) in Gl. (17) die Hauptrolle spielt, dann muss die Quantität $(-X \log Y)$ bei einer bestimmten Versuchsdauer t mit zunehmender Konzentration der neutralen Phenolmoleküle [PhOH] bzw. [PhOD] sowie des Alkalis [KOH] und folglich der Phenolationen $[PhO^-]$ direkt proportional zunehmen, aber mit zunehmender Gesamtkonzentration des Nitrophenols [[PhOH]] sowie der des schweren Wassers [[HDO]] und folglich $[[H_2O]]$ umgekehrt proportional abnehmen. Wir können demnach unter Benutzung einer dieser Annahmen den Wert von $(-X \log Y)$, der bei einem Versuch in Tabellen 5 bzw. 6 (Versuch C und D) gefunden wurde, auf dieselbe Konzentration von $[PhO^-]$, [PhOH], [[PhOH]] und $[[H_2O]]$ wie beim entsprechenden Versuch in Tabellen 2 und 3 (Versuche A und B) umrechnen. Die so umgerechneten Werte von $(-X \log Y)$ geben wir in den 5. und 6. Vertikalreihen der Tabelle 7 wieder, wo $(-X \log Y)_{iv}$ in der 5. Vertikalreihe unter der ersteren Annahme, dass die Teilreaktion (iv) die Hauptreaktion ist, dagegen $(-X \log Y)_{vi}$ in der 6. Reihe unter der letzteren Annahme, dass die Teilreaktion (vi) die Hauptrolle spielt, je aus dem Werte von $(-X \log Y)$ in Tabellen 5 und 6 errechnet wurde.

Tabelle 5. Versuch C. Kerndeuterierung des *m*-Nitrophenols unter veränderten Versuchsbedingungen als beim Versuch A. (Temperatur = 100°C.).

1. Versuchs-nr.	2. Versuchs-dauer t in Stdn.	3. Menge der Kalilauge G_w in g.	4. Konzentration der Kalilauge in N	5. Menge des Nitrophenols G_{ph} in g.	6. Volumen der Kalilauge bei 15°C. $\times 10^3$ in Liter
20	95	1.040	1.00	2.030	0.990
21	48	1.017	2.00	2.042	0.942
22	95	1.081	,,	2.056	1.001
23	30	1.038	3.00	2.009	0·918
24	70	1.038	,,	2.001	0.918

7. Volumen der Lösung bei 100°C. $\times 10^3$ in Liter	8. Konzentration von KOH in Lösung = $[PhO^-]$	9. Molzahl des Wassers M_w	10. Molzahl des Nitrophenols M_{ph}	11. Konzentration des Wassers in Lösung $[H_2O]]$	12. Konzentration von H_2O in Lösung $[H_2O]$
2.62	0.378	0.0552	0.0146	21.1	21.3
2.57	0.733	0.0515	0.0147	20.1	20.5
2.58	0.775	0.0548	0.0148	21.4	21.8
2.67	1.03	0.0552	0.0145	20.7	21.2
2.66	1.04	0.0552	0.0144	20.8	21.3

13. Konzentration des Nitrophenols in Lösung [[PhOH]]	14. Konzentration von PhOH in Lösung [PhOH]	15. Dichteüberschuss des schweren Wassers: vor dem Experiment D_{w0} in γ	16. Dichteüberschuss des schweren Wassers: nach dem Experiment D_w in γ	17. Austausch-äquivalent $n\alpha$	18. $(-X \log Y)$
5.58	5.20	3742	2916	2.14	0.00380
5.72	4.99	4133	3143	2.21	0.00428
5.74	4.96	3475	2548	2.70	0.00658
5.43	4.40	3243	2575	1.98	0.00322
5.41	4.37	3243	2406	2.67	0.00662

Tabelle 6. Versuch D. Kerndeuterierung des *p*-Nitrophenols unter veränderten Versuchsbedingungen als beim Versuch B. (Temperatur = 100°C.).

1. Versuchs-nr.	2. Versuchs-dauer t in Stdn.	3. Menge der Kalilauge G_w in g.	4. Konzentration der Kalilauge in N	5. Menge des Nitrophenols G_{ph} in g.	6. Volumen der Kalilauge bei 15°C. $\times 10^3$ in Liter
25	50	1.047	1.00	2.050	0.998
26	48	1.016	2.00	2.009	0.941
27	30	1.154	3.00	2.005	1.021

7. Volumen der Lösung bei 100°C. $\times 10^3$ in Liter	8. Konzentration von KOH in Lösung $= [PhO^-]$	9. Molzahl des Wassers M_w	10. Molzahl des Nitrophenols M_{ph}	11. Konzentration des Wassers in Lösung $[[H_2O]]$	12. Konzentration von H_2O in Lösung $[H_2O]$
2.63	0.380	0.0556	0.0148	21.1	21.3
2.58	0.730	0.0514	0.0145	20.2	20.5
2.64	1.16	0.0560	0.0144	21.2	21.8

13. Konzentration des Nitrophenols in Lösung $[[PhOH]]$	14. Konzentration von PhOH in Lösung $[PhOH]$	15. Dichteüberschuss des schweren Wassers: vor dem Experiment D_{w0} in γ	16. Dichteüberschuss des schweren Wassers: nach dem Experiment D_w in γ	17. Austausch-äquivalent $n\alpha$	18. $(-X \log Y)$
5.63	5.25	3742	3162	1.39	0.00155
5.62	4.89	4133	3318	1.75	0.00384
5.46	4.30	3243	2681	1.63	0.00289

Der Wert $(-X \log Y)_{A,B}$ in der letzten 7. Vertikalreihe der Tabelle 7 stellt solch einen Wert von $(-X \log Y)$ dar, der in den Abbn. 1 und 2 für die angegebene Versuchsdauer t (4. Vertikalreihe der Tabelle 7) graphisch ermittelt wurde. Wenn man nun diesen Wert von $(-X \log Y)_{A,B}$ mit den resp. berechneten Wert von $(-X \log Y)_{iv}$ bzw.

Tabelle 7. Reduzierte Werte von $(-X \log Y)$ der Versuche C und D (Temperatur = 100°C.).

1. Nitrophenol	2. Versuchsnr.	3. Konzentration der benutzten Kalilauge	4. Versuchsdauer t in Stdn.	5. $(-X \log Y)_{iv} \times 10^5$	6. $(-X \log Y)_{vi} \times 10^5$	7. $(-X \log Y)_{A,B} \times 10^5$
meta	20	1 N	95	269	387	310
	21	2 N	48	289	444	340
	22	,,	95	423	695	660
	23	3 N	30	234	375	310
	24	,,	70	476	761	720
para	25	1 N	50	107	158	170
	26	2 N	48	278	400	340
	27	3 N	30	186	316	340

$(-X \log Y)_{vi}$ vergleicht, so ersieht man ohne weiteres, dass der letztere $(-X \log Y)_{vi}$ im allgemeinen besser als der erstere $(-X \log Y)_{iv}$ mit dem direkt gefundenen Wert $(-X \log Y)_{A,B}$ übereinstimmt, obwohl nur in einigen Fällen (wie z.B. Versuch 20 und 21) der Unterschied nicht ganz klar ist. Wenn man weiter die in Tabelle 7 angegebenen Werte von $(-X \log Y)_{vi}$ in Abbn. 1 und 2 einsetzt, so liegen die eingesetzten Punkte hinreichend gut auf den dort gezeichneten geraden Linien, wie aus den betreffenden Abbn. ersichtlich ist. Aus allen diesen Gründen möchten wir lieber schliessen, dass bei der Kerndeuterierungsreaktion des Nitrophenols die Teilreaktion (vi) in Gl. (17) eine Hauptrolle spielen muss, obwohl auch die Möglichkeit der Teilreaktion (iv), d.h. die Reaktion zwischen Phenolationen und Wasser, unter Umständen (bei geringerer Alkalikonzentration?), nicht ganz ausgeschlossen werden kann.

Wir fanden auf diese Weise, dass die Austauschreaktion der H-Atome zwischen Nitrophenol und Wasser in alkalischer Lösung hauptsächlich zwischen Phenolationen und neutralen Phenolmolekülen (bzw. neutralen Wassermolekülen) verläuft, indem die Kernwasserstoffatome der ersteren gegen die Hydroxylwasserstoffatome der letzteren ausgetauscht werden. Wir bestimmten weiter durch die Versuche über die Veränderung der Reaktionsgeschwindigkeit mit der Temperatur die Aktivierungsenergie dieser Reaktion. Über die Ergebnisse dieser Versuche wollen wir aber in der nächsten Abhandlung berichten.

Zum Schluss möchten wir der Nippon-Gakujutsu-Shinkohkai (der Japanischen Gesellschaft zur Förderung der wissenschaftlichen Forschun-

gen) sowie der Hattori-Hohkohkai (der Hattori-Stiftung) für ihre finanzielle Unterstützung unseren wärmsten Dank aussprechen. Herrn T. Takagi, der bei der Ausführung der vorliegenden Arbeit uns sehr behilflich war, sind wir auch zu bestem Dank verpflichtet.

Siomi-Institut für physikalische
und chemische Forschung
und
Physikalisch-chemisches Laboratorium
der Kaiserlichen Universität zu Osaka.

Über den Austausch der Wasserstoffatome zwischen Pyrrol, Indol, sowie ihren Methylderivaten und Wasser. V. Austausch der Wasserstoffatome zwischen N-Methylindol und Wasser.[1]

Von **Masao KOIZUMI, Yasukuni KOMAKI** und **Toshizo TITANI.**

(Eingegangen am 28. September 1938.)

Inhaltsübersicht. Die Austauschreaktion der H-Atome zwischen geschmolzenem *N*-Methylindol und Wasser wird bei 60°C. unter Benutzung verdünnten schweren Wassers untersucht. Das *N*-Methylindol, das keine ionisierbaren (direkt austauschbaren) H-Atome enthält, führt dementsprechend keine nennenswerte Austauschreaktion aus, solange die H-Ionenkonzentration im damit geschüttelten Wasser unterhalb etwa 0.03 N (pH$\geqq$ 2.5) bleibt („erste" Austauschreaktion). Dagegen wenn die H-Ionenkonzentration im Wasser diesen letzteren Wert überschreitet, tritt ziemlich plötzlich eine neue Art der Austauschreaktion auf und ein H-Atome in einem *N*-Methylindolmolekül wird leicht austauschbar („zweite" Austauschreaktion). Hauptsächlich aus dem Grunde, dass dieses letztere Verhalten des *N*-Methylindols sich dem des unsubstituierten Indols bei seiner „zweiten" Austauschreaktion ähnelt, schliessen wir, dass das H-Atom, das bei der „zweiten" Austauschreaktion des *N*-Methylindols austauschbar wird, das in β-Stellung an C-Atom gebundene H-Atom ist. Beim unsubstituierten Indol fanden wir, entsprechend der Austauschreaktion des in α-Stellung befindlichen H-Atoms, die „dritte" Austauschreaktion bei grösseren H-Ionenkonzentrationen. Aber im vorliegenden Fall mit *N*-Methylindol können wir, ausser der oben angegebenen „zweiten" Austauschreaktion, keine weitere stufenweise Austauschreaktion ausfindig machen, wenigstens solange die H-Ionenkonzentration unterhalb 3 N (pH$\geqq -0.5$) bleibt.

(1) I. Mitteil., dies Bulletin, **13** (1938), 85: II. Mitteil., *ibid.*, **13** (1938), 95; III. Mitteil., *ibid.*, **13** (1938), 298; IV. Mitteil., *ibid.*, **13** (1938), 307.

Einleitung. Im letzten Versuch (IV. Mitteil.) fanden wir, dass das Indol bei 60°C. drei seiner H-Atome in drei Stufen gegen die des damit geschüttelten Wassers austauscht, wenn man die H-Ionenkonzentration im letztern allmählich zunehmen lässt. Dieses eigenartige Verhalten des Indols lässt sich dadurch ermitteln, dass das Austauschäquivalent nk des Indols, das die Summe der Produkte aus der Anzahl n und dem Verteilungsquotient k der einzelnen austauschbaren Arten der H-Atome in einem organischen Molekül darstellt, mit zunehmender H-Ionenkonzentration nicht kontinuierlich sondern stufenweise zunimmt. Die nk-pH-Kurve des Indols zeigt zwei deutliche Sprünge bei zwei bestimmten pH-Werten (vgl. die unterstehende Abb.), nämlich bei $p\mathrm{H} = 2.5$ und $p\mathrm{H} = 0.5$. Zwischen jedem dieser Sprünge bleibt der nk-Wert unabhängig von pH in Lösung sowie von der Schüttelungsdauer konstant. Dadurch können wir die gesamte Austauschreaktion des Indols in drei Stufen bzw. Arten teilen; die „erste" Austauschreaktion findet zwischen $p\mathrm{H} = 7.0$ und 2.5 statt, die „zweite" zwischen $p\mathrm{H} = 2.5$ und 0.5 und die letzte „dritte" von $p\mathrm{H} = 0.5$ abwärts. Das so gefundene stufenweise Zuwachsen des Austauschäquivalents nk des Indols wird dadurch gedeutet, dass drei H-Atome des Indolmoleküls mit zunehmender H-Ionenkonzentration eines nach dem anderen stufenweise austauschbar wird: bei der „ersten" Austauschreaktion beteiligt sich das an N gebundene H-Atom, bei der „zweiten" das an C in β-Stellung gebundene H-Atom und bei der letzten „dritten" Stufe das an C in α-Stellung gebundene H-Atom an der Austauschreaktion.

Eine diesähnliche stufenweise Austauschreaktion führt auch Pyrrol und *N*-Methylpyrrol (bei 30°C.) aus, wie wir dies in der I. und II. Mitteil. berichtet haben. Aber in diesen Fällen findet die Austauschreaktion in zwei Stufen statt. Beim unsubstituierten Pyrrol findet die „erste" Austauschreaktion unterhalb der H-Ionenkonzentration von etwa 0.03 N ($p\mathrm{H} \geqq 1.5$) statt und dabei wird das eine an N gebundene H-Atom sehr schnell gegen die des Wassers ausgetauscht. Wenn die H-Ionenkonzentration in Lösung diesen letzten Wert überschreitet, tritt die „zweite" Austauschreaktion ziemlich plötzlich auf und dabei werden alle (vier) Kernwasserstoffatome des Pyrrols gleichzeitig austauschbar. Dagegen führt *N*-Methylpyrrol, das keine ionisierbaren H-Atome enthält, keine wirkliche Austauschreaktion beim pH-Gebiet aus, das ungefähr dem der „ersten" Austauschreaktion des unsubstituierten Pyrrols entspricht, wohl aber die „zweite" Austauschreaktion oberhalb der H-Ionenkonzentration von 0.001 N ($p\mathrm{H} \leqq 3$), wobei alle (vier) Kernwasserstoffatome gegen die des Wassers ausgetauscht werden. Aber, wie man ohne weiteres ersieht, liegt dieser Grenzwert der H-Ionenkonzentration für die „zweite" Aus-

tauschreaktion des *N*-Methylpyrrol deutlich niedriger als die des unsubstituierten Pyrrols.

Alle diese bisher gefundenen Tatsachen führten uns zum vorliegenden Versuch mit *N*-Methylindol. Diese Verbindung interessiert uns insofern, als ihre Beziehung in chemischer Struktur zum unsubstituierten Indol sich ähnlich wie die des *N*-Methylpyrrols zum unsubstituierten Pyrrol verhält.

Darstellung des Präparates. Das zum vorliegenden Versuch benutzte *N*-Methylindol wurde teils (Versuch 1 bis 8, vgl. die unterstehende Tabelle) von Y. K. und teils (Versuch 9 bis 21) von M. K. nach der Angabe von Herrn Prof. Akabori hergestellt:

Man lässt 7 g. Indol mit 5 g. Kalium in 250 g. gut getrocknetem Dioxan unter Luftabschluss reagieren, und das dadurch gewonnene Indolkalium in derselben Lösung weiter mit 25 g. Methyljodid umsetzen:

$$C_6H_4{\cdot}C_2H_2{\cdot}NK+CH_3I = C_6H_4{\cdot}C_2H_2{\cdot}NCH_3+KI\,.$$

Nach der Beendigung der Reaktion wird der grösste Teil des Dioxans durch Destillation unter gewöhnlichem Druck abdestilliert und der zurückgebliebene Anteil wird weiter der Dampfdestillation unterworfen. Das dadurch erhaltene an *N*-Methylindol angereicherte Destillat, das eine gelbe ölige Masse darstellt, wird dann mit Äther extrahiert und aus diesem Extrakt wird das *N*-Methylindol durch die fraktionierte Destillation unter vermindertem Druck abgeschieden. Dabei wurde der unter dem Druck von 20 mm. Hg zwischen 124.8° und 127.8°C. abdestillierte Anteil zum Versuch benutzt.

Austauschversuch. Die Experimentalmethode war im grossen und ganzen dieselbe wie beim letzten Versuch mit Indol, bis auf die Menge der bei einzelnen Versuche benutzten Proben, die im vorliegenden Fall wegen der beschränkten Menge der zur Verfügung gestellten Probe viel weniger war als beim letzten Versuch mit Indol. Ca. 0.8 g. (aber wohl abgewogene Menge) des *N*-Methylindols wird zusammen mit ebenfalls gut abgewogener Menge (etwa 0.15 c.c.) verdünnten schweren Wassers, das durch den Zusatz von verschiedenen Mengen von HCl angesauert ist, in einem zugeschmolzenen Glasrohr (unter Luftabschluss!) bei 60°C. verschiedene Zeitlängen geschüttelt. Bei dieser Temperatur bleibt das *N*-Methylindol während des Versuches vollkommen flüssig, und im Gegensatz zum letzten Versuch mit unsubstituiertem Indol können wir keine Anzeichen für die Polymerisation des *N*-Methylindolmoleküls bemerken. Um das schwere Wasser aus dem so behandelten Reaktionsgemisch abzutrennen, bedienten wir uns folgender zwei Methoden.

Methode a. Das schwere Wasser wird im Vakuum aus dem Reaktionsgemisch auf eine Menge gut entwässerten Calciumchlorids abdestilliert. Das auf diese Weise als das Kristallisationswasser des Calciumchlorids abgetrennte Wasser wird dann, nachdem das Hydrat im Vakuum einige Stunden lang gut abgesaugt worden ist, vom letzteren abdestilliert geschieden, indem wir das Hydrat im Vakuum stark erhitzen.

Methode b. In diesem Fall wird die Abtrennung des Wassers aus dem Reaktionsgemisch ebenfalls durch die Destillation im Vakuum durchgeführt. Aber weil das Wasser nicht wie bei der letzten Methode a auf Calciumchlorid sondern direkt ins leere Gefäss abdestilliert wird, enthielt das so gewonnene Destillat noch eine ziemlich beträchtliche Menge *N*-Methylindol. Das abdestillierte Wasser wird deshalb zunächst mit gut getrocknetem Äther kräftig geschüttelt und der dabei ins Wasser mehr oder weniger gelöste Äther durch die Behandlung mit Pumpenöl entfernt.[2]

Das schwere Wasser, das entweder nach der Methode a oder Methode b von *N*-Methylindol abgeschieden worden, wird immer auf übliche Weise unter Benutzung des alkalischen Kaliumpermanganats sorgfältig gereinigt und erst dann zur Dichtebestimmung verwendet. Die Dichtebestimmung des Wassers führten wir wie bisher mit Hilfe eines kleinen Glasschwimmers aus. Das Austauschäquivalent nk des *N*-Methylindols wird dann mittels Gl. (1) errechnet:

$$nk = \frac{M_w}{M_j} \frac{D_a - D_e}{D_e} \qquad (1).$$

In dieser Gl. bedeutet M_w und M_j je die Molzahl des zum Versuch verwendeten schweren Wassers und *N*-Methylindols und D_a und D_e resp. den Dichteüberschuss des benutzten schweren Wassers gewöhnlichem Wasser gegenüber vor und nach dem Experiment. Die so gewonnenen Versuchsergebnisse mit *N*-Methylindol geben wir in der folgenden Tabelle 1 wieder, wo die Versuchsnr. in der ersten Vertikalreihe die zeitliche Reihenfolge der einzelnen Versuche zeigt.

Zeichnet man das so gefundene Austauschäquivalent nk des *N*-Methylindols gegen den pH der damit geschüttelten Lösung, so erhält man die stufenförmige Kurve, die in der nebenstehenden Abb. gezeigt wird. Der Zahlenwert bei jedem kleinen Kreis in der Abb. gibt die Schüttelungsdauer in Stunden an. In derselben Abb. wird auch das Versuchsergebnis mit dem unsubstituierten Indol, das im letzten Versuch erhalten wurde, einge-

(2) Vgl. S. 468 der Arbeit: M. Harada und T. Titani, dies Bulletin, **11** (1936), 465.

Tabelle 1. Austauschäquivalent des *N*-Methylindols bei verschiedenen H-Ionenkonzentrationen.

Versuchs-nr.	Normalität der benutzten Lösung	*p*H	Schüttelungs-dauer in Stdn.	*nk*	Trennungs-methode
4	neutral	7.00	5	0.34	a
7	0.0001 N HCl	4.00	5	0.35	a
8	0.001 N HCl	3.00	5	0.31	b
10	„	„	5	0.23	b
13	„	„	12	0.41	b
16	0.01 N HCl	2.00	20	0.30	b
21	„	„	20	0.26	b
20	0.091 N HCl	1.04	21	1.02	b
9	0.1 N HCl	1.00	5	1.09	b
15	„	„	20	1.00	b
3	0.3 N HCl	0.523	5	0.96	a
5	0.8 N HCl	0.097	5	1.07	a
14	1 N HCl	0.00	5	1.02	b
11	„	„	20	1.26	b
17	„	„	20	1.06	b
2	3 N HCl	−0.523	5	1.26	a
18	„	„	20	1.16	b
19	„	„	21	1.10	b

tragen. Aus dieser Abb. ersieht man ohne weiteres, dass das *N*-Methylindol ebenso wie das unsubstituierte Indol eine stufenweise Austauschreaktion ausführt. Während nämlich die H-Ionenkonzentration in Lösung klein bleibt (kleiner als etwa 0.03 N, vgl. Abb.), ist das gefundene Austauschäquivalent des *N*-Methylindols auch sehr klein und beträgt durchschnittlich $nk \approx 0.30$. Aber wenn die H-Ionenkonzentration in Lösung wächst, so nimmt der Wert des Austauschäquivalents ziemlich plötzlich zu und innerhalb des *p*H-Gebietes 1.0 bis 0.0 beträgt es durchschnittlich $nk \approx 1.05$, obwohl bei noch grösserer H-Ionenkonzentration eine geringe vergrössernde Neigung des Austauschäquivalents bemerkbar ist. Weil dieses Verhalten des *N*-Methylindols sich der des im letzten Versuch unternommenen stufenweise Austauschreaktion des unsubstituierten Indols ähnelt, nennen wir das erste Gebiet der oben angegebenen Austauschreaktion des *N*-Methylindols, wo das Austauschäquivalent sehr klein bleibt, die „erste" Austauschreaktion, trotzdem es sich dabei höchstwahrscheinlich um keine wirkliche Austauschreaktion handelt. Dagegen soll das letzte Gebiet, wo das Austauschäquivalent grösser als eins beträgt

und deshalb die Austauschreaktion wirklich stattfinden muss, die „zweite" Austauschreaktion genannt werden. Der Grenzwert von pH zwischen diesen beiden Arten der Austauschreaktion liegt etwa bei $p\mathrm{H} = 1.5$ (0.03 N), wie man dies aus der Abb. ersieht.

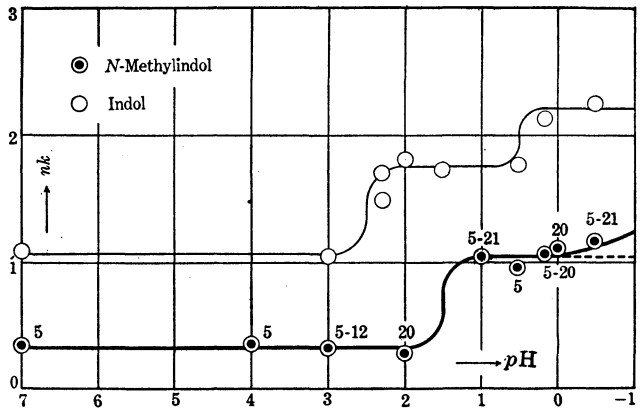


Abb. Abhängigkeit des Austauschäquivalents nk des N-Methylindols auf dem pH des damit geschüttelten Wassers und der Schüttelungsdauer.

Ein Spezialversuch. Bei allen in der obigen Tabelle 1 angegebenen Versuche wird das Austauschäquivalent nk aus dem Dichteüberschuss bzw. dem D-Gehalt des zusammen mit N-Methylindol geschüttelten schweren Wassers vor und nach dem Experiment unter Benutzung der Gl. (1) bestimmt. Aber bei einem anderen Versuch bestimmten wir dies aus dem anfänglichen Dichteüberschuss D_a des benutzten schweren Wassers sowie dem D-Gehalt des Wassers, das durch die Verbrennung des damit geschüttelten N-Methylindols gewonnen wurde. Wir schüttelten 0.0087 Mol (M_w) schweren Wassers, das durch den Zusatz von HCl bis auf 0.8 N angesauert war, zusammen mit 0.00585 Mol (M_j) N-Methylindol bei 60°C. etwa fünf Stunden lang. Das dazu benutzte schwere Wasser besass den anfänglichen Dichteüberschuss $D_a = 3312\,\gamma$. Dann wurde das schwere Wasser aus dem Reaktionsgemisch nach der Methode b abdestilliert weggenommen und das zurückgebliebene N-Methylindol in getrocknetem Luftstrom vollständig bis zum Wasser verbrannt. Nach der gründlichen Reinigung dieses Wassers, erwies es sich um $228\,\gamma$ ($= D_j$) schwerer als gewöhnliches Wasser. Das Austauschäquivalent nk des N-Methylindols wird somit mittels Gl. (2) errechnet:

$$nk = \frac{9D_j}{D_a - 9\frac{M_j}{2M_w}D_j} \qquad (2).$$

In dieser Gl. bedeutet die Anzahl 9 die der gesamten Wasserstoffatome in einem Molekül des *N*-Methylindols. Das aus diese Weise bestimmte Austauschäquivalent des *N*-Methylindols nk beträgt 0.78. Dieser Wert entspricht offensichtlich der „zweiten" Austauschreaktion, weil die H-Ionenkonzentration (0.8 N) des bei diesem Versuch benutzten schweren Wasser oberhalb des Grenzwertes (0.03 N) für die „zweite" Austauschreaktion liegt. Vergleicht man deshalb den oben angegebenen Wert (0.78) mit dem Mittelwert (1.05), der bei den Hauptversuchen in Tabelle 1 im Gebiet der „zweiten" Austauschreaktion gewonnen wurde, so ersieht man, dass der erstere um etwa $1.05 - 0.78 \approx 0.3$ kleiner als der letztere ist. Von diesem Unterschied soll später die Rede sein.

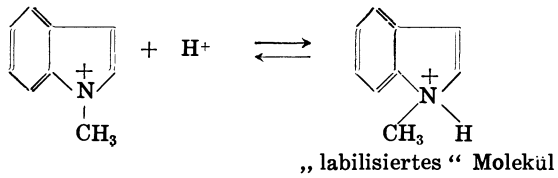
Diskussion. *N*-Methylindol enthält keine ionisierbaren d.h. direkt austauschbaren H-Atome in seinem Molekül. Wir dürfen deshalb den bei der „ersten" Austauschreaktion gefundenen kleinen Bruchteil des Austauschäquivalents, der durchschnittlich $nk \approx 0.30$ beträgt, wohl auf den konstanten Experimentalfehler zurückführen. Bei der „ersten" Austauschreaktion handelt es sich demnach um keine wirkliche Austauschreaktion. Bei der „zweiten" Austauschreaktion erhielten wir dagegen den endlichen Wert des Austauschäquivalents, und dieser beträgt, ausgenommen die um ein wenig gewachsenen Werte bei sehr grossen H-Ionenkonzentrationen, durchschnittlich $nk \approx 1.05$. Wenn wir deshalb den kleinen Bruchteil des Austauschäquivalents ($nk \approx 0.30$), der bei der „ersten" Austauschreaktion gefunden wurde, auf den konstanten Experimentalfehler zurückführen, so muss das wahre Austauschäquivalent bei der „zweiten" Austauschreaktion $nk \approx 1.05 - 0.30 \approx 0.75$ betragen. Dieser Wert stimmt aber mit dem Wert von $nk (= 0.78)$, das bei dem oben angegebenen Spezialversuch mit Hilfe des D-Gehaltes des durch die Verbrennung des mit schwerem Wasser behandelten *N*-Methylindols gewonnenen Wassers bestimmt wurde, hinreichend überein.

Der oben gefundene Wert des Austauschäquivalents des *N*-Methylindols bei der „zweiten" Austauschreaktion ($nk = 0.75$) liegt sehr nahe mit dem des unsubstituierten Indols bei seiner „zweiten" Austauschreaktion ($nk = 0.69$). Da aber die „zweite" Austauschreaktion des Indols, wie darauf schon im letzten Versuch hingewiesen wurde, höchstwahrscheinlich um die Austauschreaktion des einen in β-Stellung des Pyrrolkerns an C-Atom gebundenen H-Atoms handelt, so liegt die Annahme nahe, dass bei der „zweiten" Austauschreaktion des *N*-Methylindols ebenfalls das in β-Stellung an C-Atom gebundene H-Atome gegen die des Wassers ausgetauscht wird. Dieser Schluss wird weiter durch die in der nächsten

Abhandlung zu veröffentlichen Versuche mit α- und β-Methylindol bestätigt.

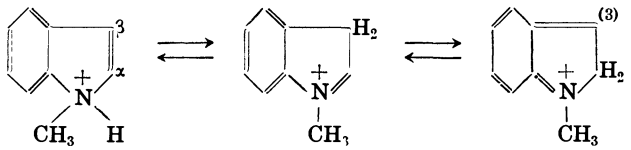
Beim unsubstituierten Indol fanden wir bei grösserer H-Ionenkonzentration (pH$\leqq$0.5) die „dritte" Austauschreaktion, bei der es sich höchstwahrscheinlich um die Austauschreaktion des in α-Stellung befindlichen H-Atoms handelt und das diesentsprechende Austauschäquivalent $nk = 0.45$ beträgt. Dagegen konnten wir beim vorliegenden Fall mit *N*-Methylindol keine solche „dritte" Austauschreaktion herausfinden, mindestens solange die H-Ionenkonzentration in Lösung unterhalb 3.0 N (pH$\geqq -1.5$) blieb, der höchsten Konzentration, die wir benutzten. Die bei sehr grossen H-Ionenkonzentrationen gefundene anwachsende Neigung des Austauschäquivalents des *N*-Methylindols dürfen wir lieber auf die von der Unstabilität dieser Verbindung in konzentrierter saurer Lösung herrührende minimale Zersetzung zurückführen. Vergleicht man weiter die nk-pH-Kurve des *N*-Methylindols mit der des unsubstituierten Indols (vgl. die Abb.), so ersieht man ohne weiteres, dass der Grenzwert der H-Ionenkonzentration für die „zweite" Austauschreaktion des *N*-Methylindols höher als der des unsubstituierten Indols liegt. Allen diesen Tatsachen nach erscheinen die Kernwasserstoffatome des Pyrrolrings des *N*-Methylindols viel schwieriger austauschbar bzw. reagierbar als die des unsubstituierten Indols zu sein. Derselben Ursache können wir vielleicht die in der vorliegenden Arbeit bemerkte Tatsache zuschreiben, dass das *N*-Methylindol im Gegensatz zum in der letzten Arbeit untersuchten unsubstituierten Indol auch bei ziemlich grossen H-Ionenkonzentrationen keine Anzeichen für Polymerisation aufweist.

Gemäss der Annahme, mit der wir die stufenweise Austauschreaktion von Pyrrol, *N*-Methylpyrrol sowie Indol zu erklären versuchten, können wir für die stufenweise Austauschreaktion des *N*-Methylindols folgende zwei Reaktionen in Betracht ziehen:



(3)

„ labilisiertes " Molekül



(4).

(3) Das chemische Verhalten des Indols zeigt, wie darauf schon in der letzten Mitteilung IV hingewiesen wurde, dass diese letzte Form der Umwandlung nur sehr schwer stattfinden kann.

Gemäss dieser Annahme können wir deshalb wohl erwarten erstens, dass das *N*-Methylindol ebenso wie beim unsubstituierten Indol ausserhalb der „zweiten" noch die „dritte" (um das α-H-Atom handelte) Austauschreaktion aufweisen wird, und zweitens, dass die „zweite" Austauschreaktion des *N*-Methylindols, wie das *N*-Methylpyrrol dem unsubstituierten Pyrrol sich gegenüber verhält, bei kleineren H-Ionenkonzentrationen als beim unsubstituierten Indol stattfinden wird. Aber in Wirklichkeit konnten wir gegen diese beiden Erwartungen keine „dritte" Austauschreaktion beobachten und weiter liegt der Grenzwert der H-Ionenkonzentration für die „zweite" Austauschreaktion des *N*-Methylindols deutlich höher als die für das unsubstituierte Indol. Daraus folgt ohne weiteres der Schluss, dass die Kernwasserstoffatome des Pyrrolrings im *N*-Methylindolmolekül viel schwieriger austauschbar sind als die des unsubstituierten Indols und für dieses dem Pyrrolderivat entgegengesetzte Verhalten des Indolderivats der angesetzte Benzolring im Indolmolekül eine massgebende Rolle spielen muss. Obwohl wir von diesem dirigierenden Effekt des Benzolrings auf die Austauschbarkeit der Pyrrolkernwasserstoffatome augenblicklich keine sichere Kenntnis haben,[4] liegt doch die Vermutung nahe, dass dieser Effekt mehr in der tautomeren Umwandlungsreaktion (4) als in der Salzbildungsreaktion (3) zu suchen sein dürfte.

Zum Schluss möchten wir der Nippon Gakujutsu-Shinkohkai (der Japanischen Gesellschaft zur Förderung der wissenschaftlichen Forschungen) sowie der Hattori-Hohkohkai (der Hattori-Stiftung) für ihre finanzielle Unterstützung bei der Durchführung dieser Arbeit unseren besten Dank aussprechen. Wir sind auch Herrn Prof. Akabori für seine freundlichen Ratschläge und Hilfe bei der Bereitung des in vorliegender Arbeit notwendigen Präparates zu herzlichem Dank verpflichtet.

Siomi-Institut für physikalische und chemische Forschung
und
Physikalisch-chemisches Laboratorium der Kaiserlichen Universität zu Osaka.

(4) Die Versuchsergebnisse des Pyrrols und des Indols bzw. des *N*-Methylpyrrols und des *N*-Methylindols können wir nicht ohne weiteres miteinander vergleichen, weil die Arbeitstemperatur beim Pyrrol und *N*-Methylpyrrol einerseits (30°C.) und die beim Indol und *N*-Methylindol anderseits (60°C.) miteinander nicht gleich ist.

On A New Sulphuric Acid Ester in the Mucus of *Charonia lampas*.

By **Tokuro SODA** and **Fujio EGAMI.**

(Received October 5, 1938.)

In the previous paper,[1] one (Soda) of us suggested the existence of a new sulphuric acid ester in the mucus of *Charonia lampas* and emphasized that the mucus is very rich in sulphur content but it contains nitrogen only in a small amount contrary to chondroitine sulphuric acid or similar compounds ever known.

As we have recently succeeded in isolating such a substance as suggested before, we will describe its properties. The mode of preparation is somewhat analogous to that of purification of heparin. Its sodium salt is precipitated by absolute alcohol in the state of colourless fiber just like cotton wool. In vacuum (80°) it loses about 10% of its weight. The results of analysis are as follows: N, 0.0–0.2%: Ehrlich's reaction for glucosamine is negative. Sulphate S, 15%; Lison's metachromatic reaction[2] for complex sulphuric acid esters is intensely positive. Uronic acid, 20%. Ash, 36% (Na_2SO_4).

By the action of sulfatase preparation obtained from the liver of *Charonia lampas*, it liberates sulphuric acid and gives reducing substances.

From the foregoing results, it may be regarded as a substance like mucoitine poly(probably tetra)-sulphuric acid, but without amino group. It has a far stronger inhibiting action upon blood coagulation than commercial heparin (Kahlbaum), and moreover it is proved that it can be used for tissue culture in place of heparin.

Chemical Institute, Faculty of Science,
Imperial University of Tokyo.

---

(1) *J. Chem. Soc. Japan*, **57** (1936), 981.
(2) *Bull. soc. chim. biol.*, **18** (1936), 225.

Eine Bemerkung über den Schmelzpunkt des Psoralens bzw. Ficusins.

Von Kunio OKAHARA.

(Eingegangen am 18. Oktober 1938.)

E. Späth und seine Mitarbeiter haben angegeben,[1] dass der Schmelzpunkt des synthetisierten Psoralens bei 171° liegt und so mit weit höher als der des natürlichen Produktes ist.

Das vom Verfasser aus den Blättern von *Ficus Carica* gewonnene Ficusin ist sicher von ein und derselben Struktur wie Psoralen, aber der Schmelzpunkt jenes Ficusins liegt bei 161–162°.[2] Auf seinen Wunsch hin hat der Verfasser Herrn Prof. E. Späth ein Ficusin-Präparat vom Schmelzpunkt 161–162° zugeschickt, welches in der Weise, wie nachher erwähnt wird, rein hergestellt wurde.

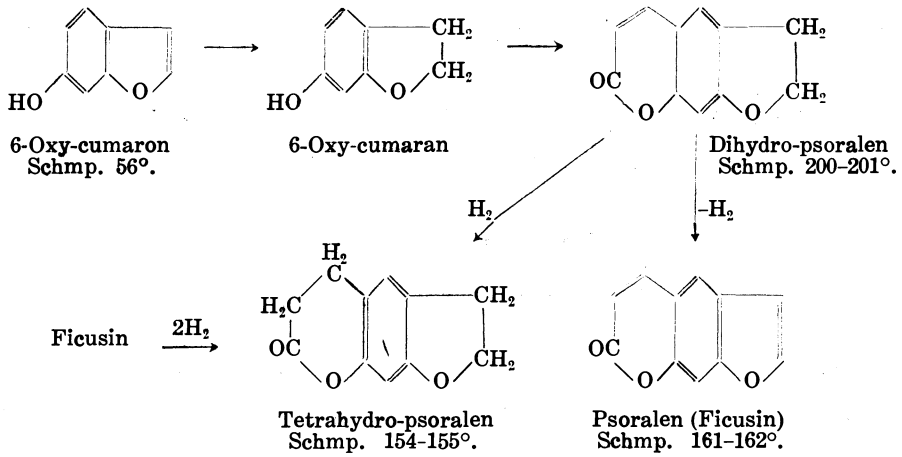
Nach E. Späth und seiner Mitarbeitern[3] zeigt aber das vom Verfasser zugeschickte Ficusin den Schmelzpunkt 165–166° (in Vakuumröhrchen 166–167°). Wenn man das Ficusin weiter reinigt, schmilzt es bei 168–169° und ergibt bei der Mischprobe mit dem synthetisierten Psoralen keine Schmelzpunktserniedrigung. Infolgedessen dürfte man von der Identität des Ficusins mit dem Psoralen sprechen.

In der Mitteilung über „die Identität von Ficusin mit Psoralen"[3] hat Prof. E. Späth meinen Namen in einer Form erwähnt, als ob ich auch sein Mitarbeiter wäre. Vor der Publikation habe ich jedoch keine darauf bezügliche Mitteilung von ihm erhalten. Ich habe ihm lediglich zum Zweck der Mischprobe mein Ficusin-Präparat zugeschickt.

Nun habe ich das frühere Ficusin-Präparat im Hochvakuum sublimiert, zweimal aus Toluol und dann weiter aus Methylalkohol umkrystallisiert. Der Schmelzpunkt blieb immer bei 161–162°. Infolgedessen habe ich die Experimente der Synthese des Psoralens von E. Späth und seinen Mitarbeitern[1] nachgeprüft. Die Versuche gingen folgenderweise.

---

(1) E. Späth, B. L. Manjunath, M. Pailer und H. S. Jois, *Ber.*, **69** (1936), 1087.
(2) K. Okahara, dies Bulletin, **11** (1936), 389.
(3) E. Späth, K. Okahara und F. Kuffer, *Ber.*, **70** (1937), 73.



Durch die obige Prüfung wurde es festgestellt, dass E. Späth wohl mit seiner Behauptung über die Identität von Ficusin mit Psoralen recht hat, dass aber seine Angaben über den Schmelzpunkt nicht richtig sein können. Der Schmelzpunkt des Psoralens (des Ficusins) liegt vielmehr bei 161–162°. Die von H. S. Jois und B. L. Manjunath angegebenen Schmelzpunkte von Psoralen[4] und seinen Derivaten[5] stimmen mit denjenigen des Verfassers überein.

Beschreibung der Versuche.

Versuch 1. 3.6 g. 6-Oxy-cumaron[6] (Schmp. 56°) werden in 40 c.c. Alkohol gelöst und unter Zusatz von 1 g. Platinoxyd in Wasserstoffatmosphäre reduziert. Dann wird mit Äther verdünnt, vom Katalysator abfiltriert und zur Trockne eingedunstet. Der Rückstand geht bei 105–110°/0.001–0.0005 mm. über und ergibt öliges, wohlriechendes Material in einer Menge von 3.1 g. Dieses Material lässt sich nicht krystallisieren, weshalb man es in der im folgenden beschriebenen Weise in das *p*-Nitrobenzoyl-Derivat überführt, das in schönen Krystallen erhalten wird.

Versuch 2. Werden 0.2 g. des obengenannten öligen Materials in 5 c.c. Pyridin gelöst und mit 0.3 g. *p*-Nitrobenzoylchlorid versetzt, so erhält man beim Erhitzen auf 80° eine gelbe Flüssigkeit. Wird die Reaktionsflüssigkeit bei Zimmertemperatur stehengelassen und dann mit Wasser versetzt, so scheiden sich gelbe Nadeln aus, welche abfiltriert und mit Wasser und Natriumcarbonat-Lösung gut ausgewaschen werden.

---

(4) H. S. Jois, B. L. Manjunath und S. Venkata Rao, *J. Indian Chem. Soc.*, **10** (1933), 41; *Chem. Zentr.*, **104** (1933), II, 77.

(5) H. S. Jois und B. L. Manjunath, *Ber.*, **70** (1937), 434.

(6) A. Sonn und E. Patschke, *Ber.*, **58** (1925), 96; P. Karrer, A. Glattfelder und F. Widmer, *Helv. Chim. Acta*, **3** (1920), 541.

Die aus Aceton umgelösten Krystalle schmelzen bei 161–162°. Ausbeute 0.56 g. (Gefunden: C, 60.88; H, 3.82; N, 4.92. Berechnet für $C_{15}H_{11}O_5N$: C, 61.02; H, 3.76; N, 4.71%).

Die durch Reduktion des 6-Oxy-cumarons gebildete Substanz ist 6-Oxy-cumaran, welches A. Sonn und seine Mitarbeiter[6] nicht zur Krystallisation bringen konnten, aber nach E. Späth[1] den Schmelzpunkt 61° hat.

Versuch 3. 0.6 g. 6-Oxy-cumaran werden mit 2.4 g. konz. Schwefelsäure und 0.6 g. Äpfelsäure im Ölbade auf 120° bis zum Aufhören des Schäumens erhitzt. Nach dem Erkalten wird die Reaktionsmasse mit wenig Wasser versetzt, mit Chloroform extrahiert und das Lösungsmittel bis zur Trockne abgedampft. Der Rückstand wird aus Methylalkohol umkrystallisiert. Das so erhaltene Dihydro-ficusin schmilzt bei 200–201°. Ausbeute 0.2 g. (Der Schmelzpunkt des Dihydro-psoralens von E. Späth beträgt 204°[1]).

Versuch 4. 30 mg. Dihydro-ficusin werden in 20 c.c. Alkohol gelöst und mit Wasserstoff und Platinoxydkatalysator bei Atmosphärendruck reduziert. Nach Beendigung des Reduktionsvorgangs wird die Lösung filtriert, das Produkt durch Eindampfen gewonnen und aus Alkohol umkrystallisiert. Schmp. 154–155°. Ausbeute 25 mg. Die Mischprobe dieser Krystalle mit Tetrahydro-ficusin[2] zeigt keine Schmelzpunktserniedrigung.

Versuch 5. Wird 0.1 g. Dihydro-ficusin mit 0.5 g. Palladiumschwarz gut vermengt und danach im Ölbade erhitzt, so tritt gegen 140° eine sehr lebhafte Reaktion ein. Man erhitzt das Reaktionsgemisch weiter bis auf 170°, zieht mit Aceton aus, dampft nach dem Filtrieren das Lösungsmittel ab, sublimiert im Hochvakuum, krystallisiert aus Toluol um und erhält so eine Substanz vom Schmelzpunkt 161–162° in einer Ausbeute von 50 mg. Bei der Mischprobe mit Ficusin bemerkt man keine Schmelzpunktserniedrigung.

Bei dieser Dehydrierung bleibt gelegentlich noch unverändertes Dihydro-ficusin zurück, indem die Reaktion ungenügend verläuft und dann das Produkt unscharf gegen 170° schmilzt. Auch kann der Fall einholen, dass das Dihydro-ficusin während der Reaktion sublimiert und an der oberen Wand des Gefässes krystallisiert. In diesem Fall geht auch die Dehydrierung unvollständig vor sich. Wenn E. Späth davon spricht, dass der Schmelzpunkt des von ihm synthetisierten Psoralens bei 171° ist, so mag es wohl mit Dihydro-psoralen verunreinigt gewesen sein.

Ich schliesse diese Bemerkung, indem ich Herrn Prof. Dr. S. Akabori für seine freundliche Unterstützung bei diesen Versuchen meinen besten Dank ausspreche.

Chemisches Institut der Kaiserlichen
Universität zu Osaka.

Der katalytische Isotopenaustausch des gasförmigen Sauerstoffs. III. Die Austauschreaktion der Sauerstoffatome zwischen Sauerstoff und Wasserdampf an der Oberfläche des Kupferoxyds.[1]

Von Noriyoshi MORITA und Toshizo TITANI.

(Eingegangen am 28. Oktober 1938.)

Inhaltsübersicht. Die Austauschreaktion der O-Atome zwischen gasförmigem Sauerstoff und Wasserdampf an der Oberfläche des Kupferoxyds wird bei verschiedenen Teperaturen untersucht. Die Reaktion wird erst bei etwa 650°C. bemerkbar und oberhalb 750°C. verläuft sie sehr lebhaft, bis ein vollständiger Austausch leicht erreicht wird. Bei diesem Versuch finden wir weiter, dass es einen kleinen Unterschied der katalytischen Aktivität zwischen den zwei Arten des benutzten Kupferoxyds gibt. Die eine Art des Kupferoxyds ist das direkt aus dem Handel bezogene. Dagegen wird die andere Art des Kupferoxyds durch die Reoxydation des einmal bis zum Kupfer reduzierten käuflichen Kupferoxyds eigens dazu hergestellt. Der Versuch zeigt, dass die letztere Art des Kupferoxyds bis zu einem gewissen Grad wirksamer als die erstere ist. Anschliessend an diesen Hauptversuch untersuchen wir die Austauschreaktion zwischen gasförmigem Sauerstoff und festem Kupferoxyd sowie die zwischen Wasserdampf und Kupferoxyd. Beim ersteren Fall können wir auch bei erhöhten Temperaturen (bis auf 900°C.) keine nennenswerte Austauschreaktion finden, wohl aber beim letzteren. In diesem Fall wird die Reaktion, ähnlich wie bei der oben erwähnten Reaktion zwischen Sauerstoffgas und Wasserdampf auf Kupferoxyd, bei etwa 650°C. bemerkbar und oberhalb 750°C. findet sie ziemlich lebhaft statt, bis schliesslich, unter den angegebenen Versuchsbedingungen, etwa ein Viertel bis ein Fünftel der O-Atome im Kupferoxyd gegen die des damit berührenden Wasserdampfes ausgetauscht werden. Es wird angenommen, dass bei der katalytischen Austauschreaktion zwischen gasförmigem Sauerstoff und Wasserdampf an der Oberfläche des Kupferoxyds eine intermediäre Verbindung zwischen dem Wasserdampf und Kupferoxyd gebildet und ihre Zersetzung in Wasserdampf, Sauerstoffgas und niedrigeres Oxyd des Kupfers eine massgebende Rolle spielt.

Einleitung. Wir haben früher (I. Mitteil.) die katalytische Austauschreaktion der O-Atome zwischen gasförmigem Sauerstoff und Wasserdampf an der Oberfläche des Platinschwamms untersucht. Dabei wurde gefunden, dass die Reaktion bei etwa 400°C. bemerkbar und dann mit steigender Temperatur immer lebhafter wird, bis schliesslich oberhalb 600°C. der vollständige Austausch leicht erreicht wird. Aber weil die Temperatur, wo sich diese Austauschreaktion bemerkbar macht, nahe der Temperatur liegt, wo die „zweite" aktivierte Adsorption des Sauer-

(1) I. Mitteil.: dies Bulletin, **13** (1938), 357; II. Mitteil.: dies Bulletin, **13** (1938), 601.

stoffgases an der Oberfläche des Platins eintritt, kommen wir zu dem Schluss, dass bei dieser Austauschreaktion die aktivierte Adsorption des Sauerstoffs am Platinschwamm ein massgebender Prozess sein wird. Im Anschluss an diesen Versuch untersuchten wir nun die katalytische Austauschreaktion zwischen gasförmigem Sauerstoff und Wasserdampf an der Oberfläche des Kupferoxyds. Diese letztere Substanz interessiert uns in so fern, als sie in sich selbst schon Sauerstoffatome enthält und deshalb der Mechanismus seiner katalytischen Wirkung auf den O-Atomenaustausch zwischen Sauerstoffgas und Wasserdampf etwas anders als beim Platinschwammkatalysator sein kann. Aus diesem Grunde untersuchten wir in der vorliegenden Arbeit nicht nur die Austauschreaktion zwischen Sauerstoffgas und Wasserdampf sondern auch die Reaktion zwischen Sauerstoffgas und festem Kupferoxyd sowie die zwischen Wasserdampf und Kupferoxyd. Mit Hilfe aller dieser Versuchsergebnisse versuchten wir über den Chemismus der katalytischen Austauschreaktion zwischen Sauerstoff und Wasserdampf an der Oberfläche des Kupferoxyds einen Schluss zu ziehen.

Experiment 1. Austauschreaktion zwischen gasförmigem Sauerstoff und Wasserdampf auf Kupferoxyd bei verschiedenen Temperaturen. Das vorliegende Experiment 1 sowie die weiter unten zu erwähnenden anderen zwei Versuche werden alle in derselben Apparatur durchgeführt, die beim früheren Versuch mit Platinschwamm benutzt wurde. Jede Einzelheit der Arbeitsweise wird deshalb auf die I. Mitteil. verwiesen. Etwa 15 c.c. an schwerem Sauerstoff angereichertes schweres Wasser wird ins Sättigungsgefäss eingelegt und konstant bei 72°C. gehalten. Durch dieses Wasser wird das Sauerstoffgas, das aus der Elektrolyse des gewöhnlichen destillierten Wassers entwickelt worden ist, langsam durchgeblasen. Das dadurch gebildete Gasgemisch von der Zusammensetzung $O_2 : H_2O = 2 : 1$ wird dann mit der Geschwindigkeit von 60 c.c. pro Minute (bei Zimmertemperatur und unter gewöhnlichem Druck gemessen!) durch das Katalysatorrohr geschickt. Dieses letztere, das aus Quarz besteht und 40 cm. Länge und 15 mm. l.W. besitzt, enthält in seiner Mitte den in Rede stehenden Kupferoxydkatalysator und wird von aussen auf gewünschte Temperatur erhitzt. Der aus dem Katalysatorrohr zusammen mit Sauerstoffgas ausgeströmte Wasserdampf wird vollständig kondensiert aufgefangen und dessen Dichte, nach sorgfältiger Reinigung, im Vergleich mit gewöhnlichem Wasser genau gemessen. Wenn wir deshalb den so gefundenen Dichteüberschuss des kondensierten Wassers mit der des originalen schweren Wassers vergleichen, können wir über die Austauschreaktion zwischen Sauerstoffgas und Wasserdampf einen Schluss ziehen.

Der in der vorliegenden Arbeit benutzte Kupferoxydkatalysator ist das „Kupferoxyd, drahtförmig" von Merck. Aber dies wird vor dem Gebrauch auf zwei verschiedene Arten behandelt. Bei einem Fall wird etwa 65 g. dieses Kupferoxyds in das Katalysatorrohr gefüllt und unter Durchleitung des Sauerstoffgases bis auf 700° bis 800°C. über Nacht erhitzt. Das so behandelte Kupferoxyd nennen wir weiter unten das Kupferoxyd I. Das andere, das Kupferoxyd II, wird dagegen aus demselben Kupferoxyd wie beim I dadurch bereitet, dass man dies, nachdem es zunächst mittels Wasserstoffgases bei ca. 550°C. vollständig bis zum Kupfer reduziert worden ist, durch Erhitzung (ca. 550°C.) im Sauerstoffstrom wieder bis zum Kupferoxyd oxydiert. Das dazu benutzte Sauerstoffgas wird aber durch die Elektrolyse des gewöhnlichen destillierten Wassers entwickelt. Deshalb muss der Sauerstoff im Kupferoxyd I um 7 γ schwerer, dagegen der im Kupferoxyd II um 1.6 γ leichter (beide in der Form von Wasser gemessen) als der gewöhnliche Wassersauerstoff sein, weil der erstere nichts anders als der Luftsauerstoff,[2] während der letztere der elektrolytische Sauerstoff aus gewöhnlichem destilliertem Wasser ist.[3] Die Ergebnisse der unter Benutzung dieser beiden Arten des Kupferoxyds durchgeführten Versuche geben wir in Tabellen 1 und 2 wieder. In diesen Tabellen stellt Δs_a und Δs_e resp. den Dichteüberschuss des benutzten schweren Wassers vor und nach dem Versuch dar, während $\Delta s_a(O)$ solch einen Anteil des gesamten anfänglichen Dichteüberschusses (Δs_a) des schweren Wassers zeigt, der auf die Anreicherung des schweren Sauerstoffs zurückzuführen ist.

Tabelle 1. Austauschreaktion zwischen O_2 und H_2O auf Kupferoxyd I bei verschiedenen Temperaturen.

$O_2 : H_2O = 2 : 1$, $\Delta s_a = 38.8\,\gamma$, $\Delta s_a(O) = 22.7\,\gamma$.

Versuchsnr.[4]	Temperatur °C.	Δs_e in γ	$\Delta s_a - \Delta s_e$ in γ	Austauschmass % A
3	620	37.2	1.6	8
5	680	36.3	2.5	13
1	730	29.9	8.9	46
4	800	17.6	21.2	109
2	850	15.5	23.3	120

(2) Vgl. z. B., N. Morita und T. Titani, dies Bulletin, **11** (1936), 414.
(3) Vgl. I. Mitteil.
(4) Zeitliche Reihenfolge.

Tabelle 2. Austauschreaktion zwischen O_2 und H_2O auf Kupferoxyd II bei verschiedenen Temperaturen.

$O_2 : H_2O = 2 : 1$, $\Delta s_a = 31.7\,\gamma$, $\Delta s_a(O) = 19.5\,\gamma$.

Versuchsnr.	Temperatur °C.	Δs_e in γ	$\Delta s_a - \Delta s_e$ in γ	Austauschmass $\% A$
4	490	30.0	1.7	10
2	500	30.0	1.7	10
3	680	22·4	9.3	55
1	760	12.4	19.3	114

Das prozentuale Austauschmass $\%A$ in der letzten Spalte der Tabellen 1 und 2 wird resp. nach der Gl. (1) bzw. (2) berechnet:

$$\%A = \frac{\Delta s_a - \Delta s_e}{19.4} \times 100 \qquad (1),$$

$$\%A = \frac{\Delta s_a - \Delta s_e}{16.9} \times 100 \qquad (2),$$

weil beim angegebenen Mischungsverhältnis des Sauerstoffgases und schweren Wasserdampfes der gesamte Dichteüberschuss des letzteren beim vollständigen Austausch seiner O-Atome gegen die des ersteren beim ersteren Versuch (Tabelle 1) um 19.4 γ und beim letzteren (Tabelle 2) um 16.9 γ abnehmen muss, wie es sich aus einer einfachen Rechnung ergibt. Dabei nehmen wir aber vorläufig an, dass die O-Atome im Kupferoxyd an dieser Austauschreaktion sich nicht beteiligen, obwohl diese Annahme, wie weiter unten gezeigt wird, nicht ganz der Wirklichkeit entspricht.

Zeichnet man das so berechnete Austauschmass $\%A$ bei verschiedenen Temperaturen gegen die letzteren auf, so erhält man, entsprechend Tabelle 1 und 2, Kurve I und II in der unten stehenden Abb. Beim Vergleich dieser zwei Kurven ersieht man ohne weiteres, dass das beim Versuch in Tabelle 2 benutzte Kupferoxyd II, das durch die Oxydation des einmal reduzierten käuflichen Kupferoxyds hergestellt worden ist, mehr oder weniger wirksamer als das direkt aus dem Handel bezogene Kupferoxyd I, das beim Versuch in Tabelle 1 benutzt wird. Aber in jedem Fall ist der Unterschied nicht sehr gross. Die Reaktion wird nämlich in beiden Fällen etwa bei 650°C. bemerkbar und dann wächst die Austauschgeschwindigkeit sehr stark mit der steigenden Temperatur an, bis schliesslich oberhalb etwa 750°C. ein vollständiger Austausch leicht hergestellt

wird. Bei diesen erhöhten Temperaturen erwies sich das gefundene prozentuale Austauschmass $\%A$ sogar grösser als 100%. Diese letztere Tatsache bzw. Diskrepanz weist aber ohne weiteres darauf hin, dass an der Austauschreaktion der O-Atome nicht nur Sauerstoffgas und Wasserdampf, wie oben angenommen, sondern auch das Kupferoxyd sich beteiligen muss. Aus diesem Grunde, sowie um über den Chemismus der vorliegenden katalytischen Reaktion zu einem greifbaren Ergebnis zu kommen, untersuchten wir demnächst die Austauschreaktion der O-Atome zwischen gasförmigem Sauerstoff und festem Kupferoxyd sowie die zwischen Wasserdampf und Kupferoxyd.

Experiment 2. Austauschreaktion zwischen gasförmigem Sauerstoff und festem Kupferoxyd. Etwa 750 g. Kupferoxyd wird im Exsikator aufbewahrt, nachdem es durch die etwa fünf stündige Erwärmung auf 120°C. im Trockenschrank möglichst vollständig getrocknet worden ist. Von diesem 750 g. Kupferoxyd wird aber bei jedem Austauschversuch je 150 g. zum Versuch gebraucht, indem wir dies im Mittelteil (etwa 25 cm. lang) des 40 cm. langen und 24 mm. weiten Quarzrohres füllen, so dass mit Hilfe der oben angegebenen Menge (750 g.) Kupferoxyd insgesamt fünf Austauschversuche durchgeführt werden können. Das im Quarzrohr gefüllte Kupferoxyd wird aber nicht ohne weiteres sondern nach der folgenden Vorbehandlung erst zum Versuch verwendet. Dies wird nämlich, genau so wie beim Kupferoxyd II in Experiment 1, zunächst durch die Erhitzung (550°C.) im Wasserstoffstrom ganz bis zum Kupfer reduziert und dann wieder mittels elektrolytischen Sauerstoffs aus gewöhnlichem destilliertem Wasser zum Kupferoxyd reoxydiert. Die Oxydierung wird dadurch ausgeführt, dass das reduzierte Kupferoxyd bis auf 550°C. erhitzt und darüber der elektrolytische Sauerstoff mit der Geschwindigkeit von 80 c.c. pro Minute über Nachtlang langsam geleitet wird. Das mit diesem Kupferoxyd zu reagierende Sauerstoffgas wird aus der Elektrolyse des an schwerem Sauerstoff angereicherten Wassers entwickelt. Der Dichteüberschuss, der lediglich auf die Anreicherung des schweren Sauerstoffs zurückgeführt werden kann, des dabei benutzten schweren Wassers beträgt 34.4 γ. Das so entwickelte an schwerem Sauerstoff angereicherte Sauerstoffgas wird dann mit reinem Stickstoffgas im Volumenverhältnis von $O_2 : N_2 = 2 : 1$ vermischt und durch das mit Kupferoxyd gefüllte Quarzrohr langsam geleitet. Die Durchströmungsgeschwindigkeit des Gasgemisches beträgt (bei Zimmertemperatur und unter gewöhnlichem Druck gemessen) 60 c.c. pro Minute. Das auf diese Weise aus dem Quarzrohr zusammen mit Stickstoffgas ausgeströmte Sauerstoffgas wird mit Bombenwasserstoff katalytisch bis zum Wasser

rekombiniert und die Dichte des so gewonnenen Wassers, dessen Menge durchschnittlich 10 c.c. beträgt, wird nach der sorgfältigen Reinigung genau bestimmt. Die dritte Spalte der Tabelle 3 gibt den Dichteüberschuss des bei jedem Versuch gewonnenen rekombinierten Wassers gewöhnlichem Wasser gegenüber wieder.

Tabelle 3. Austauschreaktion zwischen O_2 und festem CuO bei verschiedenen Temperaturen.

Versuchsnr.	Temperatur °C.	Dichteüberschuss des rekombinierten Wassers in γ	Dichteabnahme in γ	Austauschmass $\% A$
0*	610	36.3	0	—
1	500	35.3	1.0	4
2	600	33.5	2.8	10
3	700	32.9	3.4	12
4	800	33.2	3.1	11
5	900	33.0	3.3	12

*Kontrollversuch.

In dieser Tabelle 3 stellt der erste Versuch Nr. 0 den Kontroll- bzw. Vergleichsversuch dar, der unter sonst genau denselben Versuchsbedingungen wie bei den anderen Hauptversuchen nur mit dem leeren d.h. nicht mit Kupferoxyd gefüllten Quarzrohr durchgeführt wurde. Und die Dichteabnahme in der zweiten letzten Spalte der Tabelle 3 gibt den Unterschied des Dichteüberschusses des rekombinierten Wassers zwischen diesem Kontrollversuch Nr. 0 und den anderen Hauptversuchen wieder. Wir können deshalb mit Hilfe dieser gefundenen Dichteabnahme des rekombinierten Wassers das prozentuale Austauschmass $\% A$ bei jedem Versuch auf die übliche Weise berechnen, wenn die entsprechende Dichteabnahme beim vollständigen Austausch bekannt ist. Diese letztere beträgt aber, wie es sich aus einer einfachen Rechnung ergibt, $27.8\,\gamma$. Das prozentuale Austauschmass $\% A$ in der letzteren Spalte der Tabelle 3 wird somit mittels der Gl. (3) berechnet:

$$\% A = \frac{\text{(Gefundene Dichteabnahme)}}{27.8} \times 100 \qquad (3).$$

Das so berechnete Austauschmass $\% A$ erweist sich aber, wie auch aus der Kurve III in der unten stehenden Abb. ersichtlich ist, fast unabhängig von der Temperatur als sehr klein. Es beträgt sogar bei der höchsten

Temperatur (900°C.), die wir benutzten, kaum mehr als 10%. Wir möchten deshalb lieber annehmen, dass dieser kleine Bruchteil des Austauschmasses nicht viel mit der Austauschreaktion zwischen dem Sauerstoffgas und dem Kupferoxyd sondern vielmehr mit dem konstanten Experimentalfehler zu tun hat. Vielmehr liegt die Vermutung nahe, dass es sich dabei grösstenteils um die Austauschreaktion zwischen dem Sauerstoffgas und der von vornherein auf der Oberfläche des Kupferoxyds adsorbierten minimalen Menge des Wasserdampfes handelt (vgl. weiter unten bei der Diskussion).[5]

Experiment 3. Austauschreaktion zwischen Wasserdampf und festem Kupferoxyd bei verschiedenen Temperaturen. Wir führten zunächst drei Vorversuche aus, um über die Austauschbarkeit der O-Atome zwischen Wasserdampf und Kupferoxyd nähere Kenntnis zu gewinnen, und zwar die ersteren zwei durch das mit Kupferoxyd gefüllte und den letzteren durch das leere Quarzrohr. Bei jedem dieser ersteren zwei Versuche mit Kupferoxyd wird das Quarzrohr mit 118 g. Kupferoxyd I bzw. II gefüllt, das je auf die schon in Experiment 1 beschriebene Weise vorbehandelt worden ist, und darüber wird das Gasgemisch von der Zusammensetzung $N_2 : H_2O = 2 : 1$ aus Stickstoffgas und schwerem Wasserdampf mit der Geschwindigkeit von 60 c.c. pro Minute (bei Zimmertemperatur und unter gewöhnlichem Druck gemessen!) geleitet. Dagegen beim letzteren, einen Kontrollversuch wird dasselbe Gasgemisch durch dasselbe aber nicht mit Kupferoxyd gefüllte Quarzrohr mit derselben Geschwindigkeit wie bei den ersteren zwei Versuchen durchgeleitet. Das bei allen diesen Versuchen benutzte Gasgemisch aus Stickstoff und schwerem Wasserdampf wird dadurch bereitet, dass man das Stickstoffgas durch das bis auf 72°C. erwärmte schwere Wasser langsam durchbläst, d.h. auf dieselbe Weise wie bei der Bereitung des O_2–H_2O–Gemisches beim Experiment 1 nur unter Benutzung von Stickstoffgas anstatt Sauerstoffgases. Die sonstigen Versuchsbedingungen sind aus der Tabelle 4 ohne weiteres ersichtlich.

Die in der fünften Spalte der Tabelle 4 wiedergegebene Abnahme der Dichte des schweren Wassers nach dem Versuch Nr. 1 bzw. 2 zeigt, dass bei der benutzten Temperatur eine ziemlich lebhafte Austauschreaktion zwischen dem Wasserdampf und festem Kupferoxyd stattfindet. Wir

(5) Weil der Dissoziationsdruck des Kupferoxyds gemäss der Gl. $2CuO \rightleftarrows Cu_2O + \frac{1}{2}O_2$ bei 900°C. ca. 10 mm., bei 1000°C. ca. 100 mm. beträgt und bei 1050°C. Kupferoxyd unter dem atmosphärischen Druck direkt dissozieren kann, so ist es auch möglich, dass bei diesen erhöhten Temperaturen die Austauschreaktion der O-Atome zwischen gasförmigem Sauerstoff und festem Kupferoxyd direkt stattfindet.

Tabelle 4. Austauschreaktion zwischen H_2O und festem CuO bei erhöhten Temperaturen (Vorversuche).

$N_2 : H_2O = 2 : 1$, $\Delta s_a = 38.8\,\gamma$, $\Delta s_a(O) = 22.7\,\gamma$.

Versuchsnr.	das benutzte Kupferoxyd	Temperatur °C.	Δs_e in γ	$\Delta s_a - \Delta s_e$ in γ	% A	% CuO
1	CuO I	800	32.8	6.0	59	23
2	CuO II	810	29.1	9.7	63	25
3	ohne CuO	800	38.8	0.2	—	—

berechneten deshalb auf ähnliche Weise wie bei der Austauschreaktion zwischen Sauerstoffgas und Wasserdampf das prozentuale Austauschmass $\%A$ mit Hilfe der gefundenen Dichteabnahme des schweren Wassers ($\Delta s_a - \Delta s_e$) in der fünften Spalte der Tabelle 4 sowie des Grenzwertes der Dichteabnahme, die sich beim vollständigen Austausch ergeben würde. Da aber dieser letztere Grenzwert, wie eine einfache Rechnung zeigt, 10.1 γ beim Versuch 1 und 15.5 γ[6] beim Versuch 2 beträgt, so wird das Austauschmass $\%A = 59$ bis 63%.[7]

Bei dieser Berechnung von $\%A$ setzen wir aber stillschweigend voraus, dass die O-Atome des Kupferoxyds, ähnlich wie beim Wasserdampf, alle sich gleich leicht an der Austauschreaktion beteiligen können. Diese Voraussetzung entspricht aber insofern der Wirklichkeit nicht, als die O-Atome im Kupferoxyd wegen seiner Festigkeit nicht immer alle gleich leicht austauschbar sind. Wir müssen vielmehr annehmen, dass solche O-Atome des Kupferoxyds, die an bzw. in der Nähe der Oberfläche befindlich sind, viel leichter mit dem Wasserdampf in Berührung und folglich in Reaktion kommen können. Wir wollen deshalb vorläufig annehmen, dass nur ein Teil der in günstigster Lage befindlichen O-Atome des Kupferoxyds unter den angegebenen Versuchsbedingungen gegen die des Wasserdampfes vollständig ausgetauscht werden, während der übrige Anteil der O-Atome im Kupferoxyd ohne jede Veränderung bleibt. Mit

(6) Dieser Unterschied des Grenzwertes der Dichteabnahme zwischen Versuch 1 und 2 kommt vom Unterschied der Dichte des Sauerstoffs im benutzten Kupferoxyd, weil der des CuO I der Luftsauerstoff dagegen der des Cu II der elektrolytischer Sauerstoff ist (vgl. oben).

(7) Dieser Wert von % A kann höchstwahrscheinlich um einige Prozent zu gross sein, weil wir bei seiner Berechnung der eventuell vorhandenen Austauschreaktion des an der Oberfläche des benutzten Kupferoxyds von vornherein adsorbierten Wasserdamfes nicht Rechnung tragen. (vgl. oben beim Experiment 1).

Hilfe dieser Annahme können wir, auf die später in einer besonderen Abhandlung zu beschreibende Weise, das prozentuale Verhältnis *%CuO* der Sauerstoffatome im Kupferoxyd, die bei einem angegebenen Versuch als vollständig ausgetauscht angesehen werden, den gesamten Sauerstoffatomen im Kupferoxyd gegenüber leicht errechnen. Das so berechnete *%CuO* ergibt sich aber, wie die letzte Spalte der Tabelle 4 zeigt, 23 bis 25%.[8] Also fast ein Viertel der gesamten O-Atome im Kupferoxyd wird demnach unter den benutzten Versuchsbedingungen gegen die des Wasserdampfes vollständig ausgetauscht. Es liegt deshalb die Annahme nahe, dass die Austauschreaktion zwischen Wasserdampf und Kupferoxyd eigentlich sehr rasch stattfindet und ihr schneller Verlauf lediglich durch die Festigkeit des Kupferoxyds verhindert wird.

Da durch diese Vorversuche gefunden wurde, dass die O-Atome des festen Kupferoxyds gegen die des Wasserdampfes verhältnismässig leicht austauschbar sind, untersuchten wir nun dieselbe Reaktion bei verschiedenen Temperaturen. Das dazu benutzte Kupferoxyd wird auf genau dieselbe Weise wie beim vorhergehenden Experiment 2 bereitet und vorbehandelt.[9] Bei jedem Versuch wird etwa 150 g. dieses Kupferoxyds in demselben Quarzrohr wie beim Experiment 2 bis auf eine bestimmte Temperatur erhitzt und darüber wird das Gasgemisch aus Stickstoff und schwerem Wasserdampf, das ebenfalls wie beim vorhergehenden Vorversuch die Zusammensetzung von $N_2:H_2O = 2:1$ besitzt, mit der Geschwindigkeit von 60 c.c. pro Minute (bei Zimmertemperatur und unter gewöhnlichem Druck gemessen!) langsam geleitet. Die dadurch erhaltenen Versuchsergebnisse sind in Tabelle 5 zusammengestellt.

Das in der zweiten letzten Spalte der Tabelle 5 angegebene prozentuale Austauschmass *%A* wird nach der Gl.(4) berechnet:

$$\%A = \frac{\Delta s_a - \Delta s_e}{25.0} \times 100 \qquad (4).$$

Das so berechnete Austauschmass *%A* wächst, ähnlich wie beim katalytischen Austausch zwischen Sauerstoffgas und Wasserdampf an der Oberfläche des Kupferoxyds, mit zunehmender Temperatur ziemlich stark an (vgl. Kurve IV in der Abb.) und beträgt oberhalb 750°C. 40 bis

(8) Dieser Wert von *% CuO* kann aus demselben Grund, wie bei Fussnote (7) erwähnt wurde, um einige Prozent zu gross sein.

(9) In der Praxis verfuhren wir so, dass wir auf einmal 1500 g. Kupferoxyd auf die schon oben beim Experiment 2 erwähnte Weise getrocknet hatten, von denen wir die Hälfte (750 g.) zum Experiment 2 und die andere Hälfte zum vorliegenden Experiment benutzten.

Tabelle 5. Austauschreaktion zwischen H_2O und festem CuO bei verschiedenen Temperaturen.

$N_2 : H_2O = 2 : 1$, $\Delta s_a = 61.3\,\gamma$, $\Delta s_a(O) = 34.4\,\gamma$.

Versuchsnr.	Temperatur °C.	Δs_e in γ	$\Delta s_a - \Delta s_e$ in γ	% *A*	% *CuO*
1	400	58.4	2.9	12	—
2	500	56.9	4.4	18	—
3	660	56.1	5.2	21	7
4	800	49.5	11.8	47	15
5	900	47.4	13.9	56	19

60%. Das in der letzten Spalte der Tabelle 5 angegebene *%CuO*, das auf die schon oben erwähnte Weise berechnet wurde, zeigt, dass bei diesen erhöhten Temperaturen fast ein Fünftel der gesamten O-Atome im Kupferoxyd gegen die des Wasserdampfes vollständig ausgetauscht wird.

Diskussion. Die in der vorliegenden Arbeit gewonnenen Versuchsergebnisse sind in der nebenstehenden Abb. graphisch zusammengestellt. Daraus ersieht man, wie schon oben darauf hingewiesen wurde, dass die katalytische Austauschreaktion zwischen gasförmigem Sauerstoff und Wasserdampf an der Oberfläche des Kupferoxyds etwa bei 650°C. bemerkbar wird und oberhalb 750°C. sehr lebhaft stattfindet (Kurve I und II). Ähnlich verläuft die Reaktion zwischen Wasserdampf und Kupferoxyd (Kurve IV). Dagegen können wir zwischen gasförmigem Sauerstoff und Kupferoxyd, auch bei erhöhten Temperaturen, keine nennenswerte Austauschreaktion herausfinden (Kurve III). Es liegt deshalb die Annahme nahe, dass für den katalytischen Austausch zwischen Sauerstoffgas und Wasserdampf an der Oberfläche des Kupferoxyds nicht die aktivierte Adsorption des Sauerstoffs sondern die des Wasserdampfes an dem Kupferoxyd eine

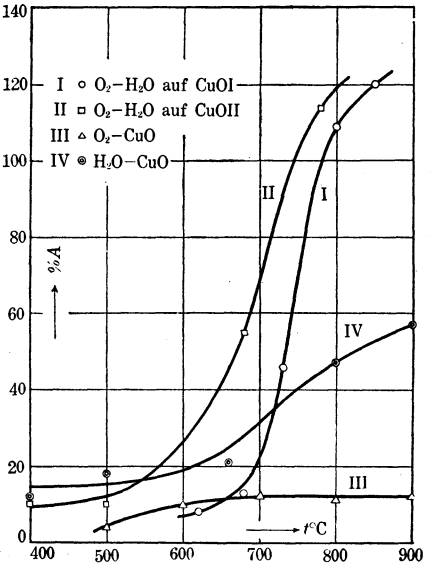


Abb. Die Abhängigkeit des Austauschmasses *%A* von der Versuchstemperatur *t*.

massgebende Rolle spielt. Diese Annahme liegt um so näher, da die Adsorption des Sauerstoffgases an der Oberfläche des Kupferoxyds sehr schwach,[10] dagegen die des Wasserdampfes an derselben Substanz verhältnismässig stark ist,[11] und unter Umständen das Anzeichen für die Chemisorption gefunden wird.[12] Guerout[13] fand z.B., dass bei Einwirkung des Wasserdampfes auf das Kupferoxyd das Kupferoxydul Cu_2O entsteht. Allen diesen Experimentaltatsachen nach können wir deshalb das Reaktionsschema des katalytischen Austausches der O-Atome zwischen gasförmigem Sauerstoff und Wasserdampf an der Oberfläche des Kupferoxyds etwa folgendermassen formulieren.

$$2CuO + H_2O = Cu_2O \cdot H_2O_2 \qquad (5),$$

$$Cu_2O \cdot H_2O_2 = Cu_2O + H_2O + \frac{1}{2}O_2 \qquad (6),$$

$$Cu_2O + \frac{1}{2}O_2 = 2CuO \qquad (7).$$

Durch Reaktion (5) wird ein Zwischenprodukt $Cu_2O \cdot H_2O_2$ zwischen dem Kupferoxyd und Wasserdampf gebildet. Dabei wird das erstere bis zum Kupferoxydul (im allgemeinen zum niedrigeren Oxyd) reduziert. Die so gebildete Zwischenverbindung wird aber nach dem Schema (6) zersetzt und dadurch wird Wasserdampf und gasförmiger Sauerstoff abgegeben. Die letzte Reaktion (7) zeigt die Wiederbildung des Kupferoxyds aus dem Kupferoxydul und gasförmigem Sauerstoff. Es ist ohne weiteres klar, dass durch die nacheinander folgende Zirkulation dieser drei Stufen der Reaktionen die O-Atome des Wasserdampfes und Sauerstoffgases unter Vermittelung der des Kupferoxyds gegeneinander allmählich ausgetauscht werden können.

Der dem oben angegebenen Reaktionsschema ähnliche Chemismus wurde schon von Neumann und seinen Mitarbeitern[14] angenommen, um die katalytische Oxydation der schwefligen Säure an der Oberfläche des Kupferoxyds zu erklären. Dabei nahmen sie an, dass die thermische Zersetzung des zuerst gebildeten Sulfats des niedrigeren Oxyds des Kupfers

(10) A. F. Benton, *J. Am. Chem. Soc.*, **45** (1923), 887.

(11) H. D. Draper, *J. Am. Chem. Soc.*, **50** (1928), 2637; H. Rose, *Pogg. Ann.*, **84** (1851), 480.

(12) Müller-Erzbach, *Wied. Ann.*, **25** (1885), 357.

(13) Guerout, *Compt. rend.*, **79** (1874), 221.

(14) B. Neumann, C. Kröger und R. Iwanowski, *Z. Elektrochem.*, **41** (1935), 821.

$Cu_2O \cdot SO_3$ in Kupferoxydul und Schwefeltrioxyd, d.h. die der oben angegebenen Teilreaktion (6) entsprechende Reaktion, ein massgebender Prozess ist. Bei der vorliegenden Austauschreaktion zwischen gasförmigem Sauerstoff und Wasserdampf kann auch diese zweite Stufe der Reaktion (6) der geschwindigkeitsbestimmende Prozess sein, obwohl wir dafür noch keine sichere experimentelle Stütze haben.

Wir haben oben beim Experiment 1 gefunden, dass das prozentuale Austauschmass $\%A$ zwischen Sauerstoffgas und Wasserdampf an der Oberfläche des Kupferoxyds bei höheren Temperaturen sogar über 100% steigt. Die Ursache für diese Diskrepanz ist aber jetzt klar. Dies kann nämlich teils auf die Austauschreaktion zwischen dem Wasserdampf und Kupferoxyd und teils auf die zwischen dem Sauerstoffgas und dem an der Oberfläche des Kupferoxyds von vornherein eventuell adsorbiert vorhandenen Wasserdampfe zurückgeführt werden.

Zum Schluss möchten wir der Nippon Gakujutsu-Shinkohkai (der Japanischen Gesellschaft zur Förderung der wissenschaftlichen Forschungen) sowie der Hattori-Hohkohkai (der Hattori-Stiftung) für ihre finanzielle Unterstützung zur Ausführung dieser Arbeit unseren wärmsten Dank aussprechen.

Physikalisch-chemisches Laboratorium
der Kaiserlichen Universität zu Osaka
und
Siomi-Institut für physikalische
und chemische Forschung.

Austauschreaktion der Sauerstoffatome zwischen einigen anorganischen Anionen und Wasser. (Vorläufige Mitteilung.)

Von **Toshizo TITANI** und **Kokiti GOTO.**

(Eingegangen am 1. November 1938.)

Es wurde von einigen Autoren gefunden,[1] dass die anorganischen Anionen, wie z.B. Phosphationen und Sulfationen, ihre O-Atome in alkalischer Lösung gegen die des Wassers austauschen. Die Reaktion

(1) E. Blumenthal und J. B. M. Herbert, *Trans. Faraday Soc.*, **33** (1937), 849; S. C. Datta, J. N. E. Day und C. K. Ingold, *J. Chem. Soc.*, **1937**, 1968.

wird nämlich durch die OH'-Ionen katalysiert. Nach unserem Versuch aber wird dieselbe Reaktion auch durch $H^{\cdot}$-Ionen katalysiert. Das Kaliumsulfat führt z.B. zu keiner nennenswerten Austauschreaktion in neutraler Lösung bei 180°C., sogar nicht nach 100 stündiger Erwärmung. Wenn man aber der Lösung von Kaliumsulfat eine Menge saures Kaliumsulfat $KHSO_4$ hinzufügt, so findet die Austauschreaktion der O-Atome statt, und durch 20 stündige Erwärmung bei 180°C. werden alle O-Atome von nicht nur HSO_4'-Ionen sondern auch von SO_4''-Ionen gegen die des Wassers ausgetauscht, wie man dies durch die Abnahme der Dichte des zur Herstellung der Lösung benutzten an schwerem Sauerstoff angereicherten schweren Wassers erkennt. Ebenso katalytisch wie $KHSO_4$ wirkt auch Salzsäure HCl. Erwärmt man z.B. die Lösung von Natriumchlorat $NaClO_3$ in schwerem Wasser ohne jeden Zusatz bis auf 100°C. 10 Stdn. lang, so findet keine nennenswerte Austauschreaktion statt. Wenn man dagegen derselben Lösung von $NaClO_3$ in schwerem Wasser eine Menge HCl zusetzt, so wird unter sonst denselben Versuchsbedingungen wie beim oben beschriebenen Kontrollversuch ohne jeden Zusatz fast die Hälfte der O-Atome von ClO_3'-Ionen gegen die des Wassers ausgetauscht. Die säure-katalysierte Austauschreaktion der O-Atome der Anionen kann vielleicht dadurch erklärt werden, dass aus den in Rede stehenden Anionen und zugesetzten $H^{\cdot}$-Ionen zuerst die freien Säuremoleküle gebildet werden und durch die reversible Spaltung dieser Säuremoleküle in Anhydridmoleküle und Wasser die O-Atome der Anionen durch die des Wassers eines nach dem anderen ersetzt werden. Die ausführliche Mitteilung der vorliegenden Arbeit soll später in diesem Bulletin veröffentlicht werden.

Physikalisch-chemisches Laboratorium
der Kaiserlichen Universität zu Osaka
und
Siomi-Institut für physikalische
und chemische Forschung.

On the Nature of Foam. II. The Foam Formation of Ternary System, Acetic Acid—Ethyl Ether—Water.

By Tunetaka SASAKI.

(Received November 21, 1938.)

It was reported in the preceding paper[1] that the maximum point of the foam stability of the binary mixtures such as water and alcohols or fatty acids occurs at the concentration where the gradient of surface tension is maximum. It was further confirmed that more stable foam can be obtained by the addition of a proper amount of ethyl ether to these solutions. The foaming properties of the ternary solutions is not yet studied quantitatively, though a few qualitative or semi-quantitative experiments have already been published by some authors.[2][3][4][5][6] The present paper describes the investigation on the foam formation of ternary liquid system, acetic acid—ethyl ether—water (AEW-system).

Experimental Procedure. In the ternary system of AEW, acetic acid is soluble both in ether and in water while ether is hardly soluble in water. Mutual solubility curve of this system is obtained by the measurement of the volume ratio in the liquid which shows the first indication of turbidity by the addition of the insoluble component to the homogeneous mixture of the other two. Fig. 1 is the diagram of AEW-system thus obtained, the data of which being shown in Table 1. Measurements were carried out at about 20°C.

The tie-line, i.e. the straight line connecting the two points on the mutual solubility curve which represents coexisting phases of a heterogeneous system can be obtained as follows: We take any one point in the heterogeneous region of the diagram, and draw a straight line so as its section made by the mutual solubility curve is divided at that point in two portions, the ratio of which is equal to that of the volumes of upper and lower coexisting phases. The tie-lines thus obtained are shown in Fig. 1.

---

(1) Sasaki, this Bulletin, **13**, (1938), 517.
(2) Wo. Ostwald and A. Steiner, *Kolloid-Z.*, **36** (1925), 342.
(3) C. W. Foulk, *J. Ind. Eng. Chem.*, **16** (1924), 1121; **21** (1929), 815.
(4) R. H. Bogue, *J. Am. Chem. Soc.*, **44** (1922), 1343.
(5) Wo. Ostwald and A. Quast, *Kolloid-Z.*, **48** (1929), 156.
(6) E. L. Lederer, *Z. angew. Chem.*, **47** (1934), 119.

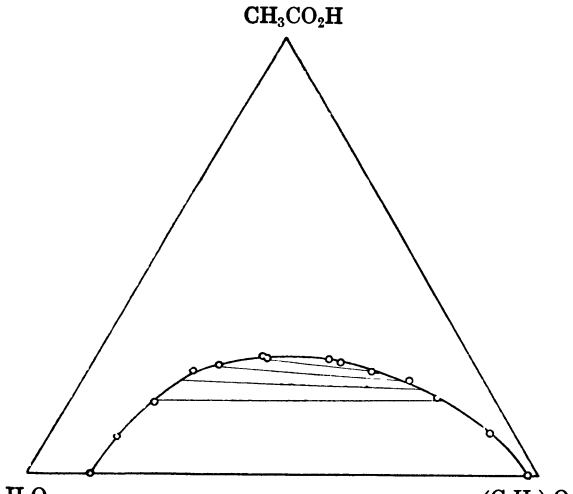


Fig. 1.

Table 1.

Volume ratio of limiting turbid mixture (about 20°C.).

Acetic acid	Ethyl ether	Water
0	12.3	87.7
0	98.0	2.0
8.7	13.5	77.8
9.5	85.7	4.8
16.7	16.7	66.6
17.8	71.5	10.7
21.6	64.0	14.4
23.8	20.6	55.6
23.8	55.6	20.6
25.0	25.0	50.0
25.8	48.4	25.8
26.4	46.0	27.6
26.5	33.8	39.7
27.0	32.5	40.5
60.0	40.0	∞
70.0	∞	30.0

Measurements of the foam formation were then undertaken for homogeneous and heterogeneous systems of AEW. The apparatus employed in the present experiment is different from that described in the preceding paper.[1] It has been constructed as shown in Fig. 2. In this figure, M is a synchronous motor, W a wheel carrying a crank, S a brake acting upon W, P a handle connected to the axis Q of the wheel W by a cord, R a spring pulling Q to S, and A a glass stoppered test tube with its support.

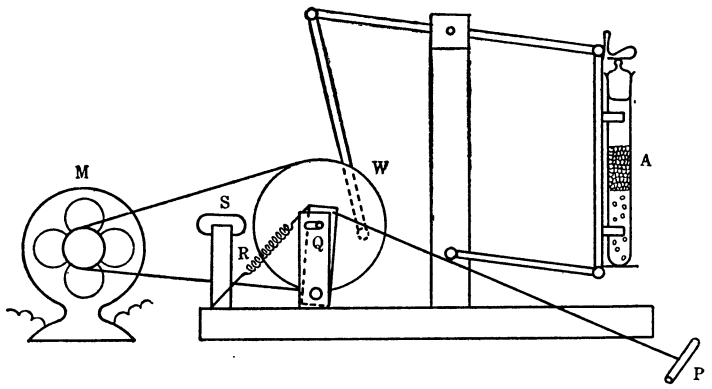


Fig. 2.

By pulling handle P, wheel W starts to rotate and test tube A vibrates up and down. If we release P, wheel W is pulled back by spring R, and

brake S acts to stop the wheel instantaneously. By this arrangement, the vibration can be made to start or stop sharply. Amplitude of the vibration is 12 cm. and the frequency is kept constant to 300 vibrations per minute throughout this experiment.

Measurement of the foam formation has been carried out as follows: First, a well stoppered test tube of 1.5 cm. in diameter and 15 cm. in length is washed carefully with soap solution and with chromic acid mixture successively, steamed with water vapour, and dried in an air bath. Then 10 c.c. of the liquid for measurement is introduced into the tube (up to the height of about 6 cm. from bottom) which is stoppered immediately and fixed on the shaking apparatus. Then the motor is set in motion and the test tube is brought into vibration by pulling the handle P. After continuing vibration for 10 seconds, it is stopped by releasing the handle and the two following quantities are measured: (1) Height of foam zone (H) which is measured immediately after the stop of vibration by reading the upper and lower meniscuses of foam zone by the scale attached to the test tube. (2) Time of duration of the foam zone (S) which is measured by recording the time required from the moment of stop of motion to the complete collapse of foam zone.

Table 2.

Composition in volume ratio			Height of foam, H(cm.)	Stability of foam, S(second)	Degree of foam formation, $S \cdot H$
Acetic acid	Ethyl ether	Water			
0	1.25	8.75	0	0	0
0	9.80	0.20	0	0	0
0.50	0	9.50	1.4	6.4	9.0
0.50	1.00	8.50	2.8	12.7	35.6
0.60	5.50	3.90	0	0	0
0.70	0	9.30	3.0	8.8	26.4
0.80	7.20	2.00	1.1	1.0	1.0
1.00	0.50	8.50	2.3	10.6	24.4
1.20	1.40	7.40	0	0	0
1.20	4.80	4.00	0	0	0
1.50	0	8.50	2.5	11.2	28.0
1.50	1.00	7.50	1.8	10.7	19.3
1.70	4.00	4.30	0	0	0
1.80	1.70	7.50	0	0	0
1.85	7.35	0.80	1.2	1.3	1.6
2.00	8.00	0	0	0	0
2.10	1.40	6.50	1.9	9.1	17.3
2.10	3.70	4.20	0	0	0
2.10	4.90	3.00	1.3	1.4	1.8
2.35	4.15	3.50	1.2	1.9	2.3
2.40	3.80	3.80	0	0	0
2.40	5.60	2.00	2.1	3.3	6.9
2.50	0	7.50	1.3	4.9	6.4
2.50	2.50	5.00	0	0	0

Table 2.—(*Concluded*)

Composition in volume ratio			Height of foam, *H*(cm.)	Stability of foam, *S*(second)	Degree of foam formation, *S*·*H*
Acetic acid	Ethyl ether	Water			
2.62	3.88	3.50	0	0	0
2.63	2.63	4.74	2.0	34.7	69.4
2.65	4.60	2.75	2.6	7.0	18.2
2.70	4.00	3.30	2.6	51.9	134.9
2.75	2.75	4.50	2.3	22.7	52.2
2.80	4.20	3.00	2.7	15.1	40.8
3.00	2.00	5.00	3.1	6.3	19.5
3.00	3.00	4.00	2.5	13.3	33.3
3.00	4.50	2 50	2.8	4.5	12.6
3.15	0.35	6.50	1.8	3.6	6.5
3.40	3.60	3.00	2.2	4.4	9.7
3.40	5.10	1.50	1.1	1.3	1.4
3.50	0	6.50	0.9	1.9	1.7
4.00	1.00	5.00	3.1	2.4	7.4
4.00	6.00	0	0	0	0
4.20	2.80	3.00	1.7	2.6	4.4
5.00	0	5.00	1.8	1.7	3.1
5.60	1.40	3.00	1.8	1.9	3.4
6.00	4.00	0	0	0	0
7.00	0	3.00	1.1	1.6	1.8
8.00	2.00	0	0	0	0

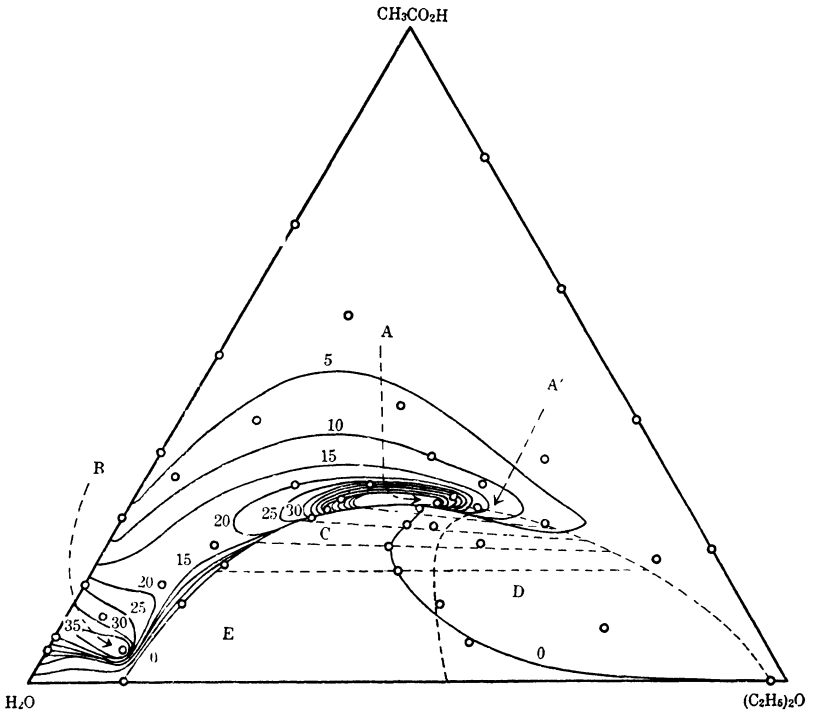


Fig. 3.

Experimental Results. The results of measurements are shown in Table 2.[7] In this table, S and H denote the time of duration and the height of foam zone respectively. As the measure of foam formation, S,[5][6][8] H,[2][4][9] or S/H[10] may be adopted. In this paper, however, both S and H were considered to be separate and independent factors characterizing the foam formation, and the product of them was employed as denoting the degree of foam formation. Fig. 3 is the diagram obtained from the above data and it represents the relation between composition and foam formation of AEW-system.

Discussion. The diagram of the foam formation, as a whole, is separated into two regions by the mutual solubility curve, namely homogeneous and heterogeneous regions.

(1) *Homogeneous region.* All systems of this region can froth, though widely differing in its degree, and the strong foam formations are observed in the vicinity of two points A and B in Fig. 3. Further, the surface of diagram has the steepest slope along the mutual solubility curve and along the straight line connecting the vertices of water and acetic acid, while it has gentle slope towards the straight line connecting water and ethyl ether.

The fact that the system near point B foams remarkably is explained from the results of the former experiments,[1] i.e. water—acetic acid system has the maximum foam stability at the region of such a dilute solution as its surface tension rapidly falls with dilution, and near this region point B exists. This can readily be seen in Fig. 3.

Foam formation also shows its maximum at point A and its degree far more exceeds that at B. The surface of diagram is remarkably projected near point A. For the explanation of the foam formation of systems near that point, it is necessary to study some other systems showing the same singularity upon the foam formation, or any other phenomena relating to it. As for an instance of the phenomenon exhibiting a similar singularity to foam formation, there is the critical opalescence of ternary systems consisting of benzene, ethyl alcohol and water or the analogous systems which were studied by Sata and his co-workers.[11] It is briefly explained as follows:

(7) Only a part of the data was shown for the economy of spaces.

(8) O. Bartsch, *Kolloid-Beihefte*, **20** (1925), 1.

(9) Wo. Ostwald and M. Meisser, *Kolloid-Beihefte*, **26** (1928), 1.

(10) P. A. Rehbinder and A. A. Trapeznikov, *Compt. rend. acad. sci. U. R. S. S.*, **18** (1938), 423.

(11) N. Sata and O. Kimura, this Bulletin, **10** (1935), 409; O. Kimura, *ibid.*, **11** (1936), 57; N. Sata and Y. Niwase, *ibid.*, **12** (1937), 86.

When we continue to add water to a homogeneous mixture of benzene and ethyl alcohol, the whole system gradually approaches to a region of heterogeneous system, becomes heterogeneous at last, and separates into two layers. Some systems show critical opalescence and anomalous increase in viscosity just before the separation into two layers, while others do not. There are optimum composition for initial benzene—ethyl alcohol mixture to show such critical opalescence on addition of water and the region of compositions of these opalescent systems is given by these authors as shown in Fig. 4. This is also a narrow region along a portion of the

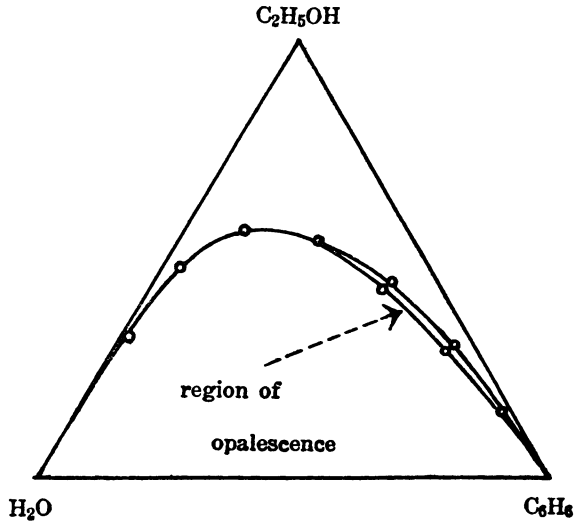


Fig. 4.

mutual solubility curve, and roughly corresponds to region A in Fig. 3. Taking into account of the above phenomena, a tentative explanation of the foam formation of systems near point A is made as follows:

When we trace the locus of middle points of tie-lines in the diagram of Fig. 3, we can find that region A is situated not far off the point of intersection of this locus and mutual solubility curve (A′ in the diagram). By the addition of small quantity of insoluble component (in this case water), any homogeneous system belonging to such a region can readily be converted into a heterogeneous one consisting of upper and lower layers of almost equal volumes, equal densities, and very small interfacial tension between them. Such conditions are generally considered to favour the formation of emulsion and consequently the foam is mechanically stabilized in such system like in most other colloidal solution.[2] Critical opalescence and anomalous viscosity which can only be seen in this region

also be explained as the typical phenomena of emulsion. Further, the aqueous solution of butyric acid was reported to show a similar critical foam formation.[2]

It has often been said that the foam of a solution vanishes at the moment when it touches ethyl ether or even the vapour of ethyl ether. This case, however, differs from the present condition, and belongs to the heterogeneous region or the formation of heterogeneous film by the condensation of ether vapour on the bubble wall, which is discussed in the later section. The mixture of the composition corresponding to region A in Fig. 3 has an outstanding power of foaming.

(2) *Heterogeneous region.* It can readily be seen from the diagram of Fig. 3, that the heterogeneous region is further divided into two parts, i.e. foamy and non-foamy regions.

(a) First, we will consider region C in Fig. 3 which is adjacent to region A. In a heterogeneous system belonging to this region, an upper layer consisting of water, acetic acid, and excessive ethyl ether is considerably smaller in volume compared with a lower layer consisting of acetic acid, ethyl ether, and excessive water, while the surface tension of the former is smaller than that of the latter, but not so markedly as in the system of region E. Table 3 shows these relations.

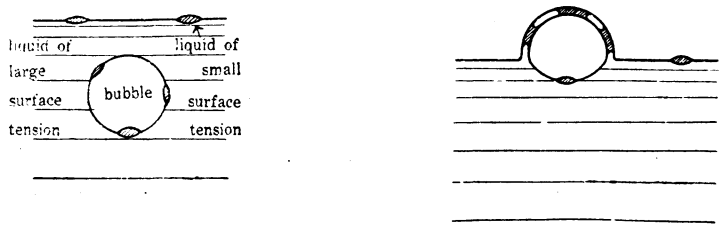
Table 3.

Composition in volume ratio			Surface tension (relative)		Foam formation	
Acetic acid	Ethyl ether	Water	Upper layer	Lower layer	$V_u < V_l$*	$V_u > V_l$
2.50	4.40	3.10	0 309	0.341	↑C region in Fig. 3, non-foamy.	D region in Fig. 3, slightly foamy.
2.20	4.30	3.50	0.301	0.368		
1.70	4.50	3.80	0.292	0.402	E region in Fig. 3, emulsion drop contains bubble.	
1.00	5.00	4.00	0.278	0.464		
0	5.50	4.50	0.261	0.632	↓	

* V_u and V_l denote volumes of upper and lower liquids respectively, coexisting in the corresponding heterogeneous system.

When we shake a system under such conditions, the upper layer of relatively small volume is dispersed in the lower one, and droplets of emulsion thus produced are then brought to the surface of bubbles formed at the same time by shaking, or they flock together in the free surface of dispersing medium. They finally spread upon the surface of the film enveloping the foam and flattly occupy a portion of it as is illustrated in

Fig. 5. Thus the patches of small surface tension make the film unstable and the bubbles will burst itself.[12] Heterogeneous systems consisting of fatty acids, alcohols, or any other water insoluble surface active substance and its aqueous solution as studied in the preceding experiments[1] also break the foam by the same reason.



Hatching indicates an upper layer of liquid of the heterogeneous system.

Fig. 5.



Fig. 6.

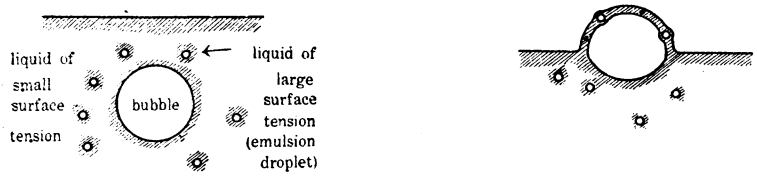


Fig. 7.

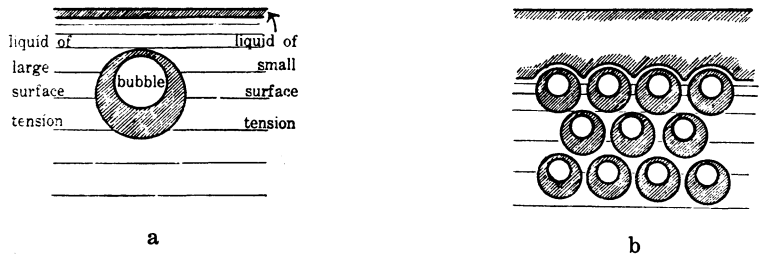


Fig. 8.

(12) Sasaki, this Bulletin, **11** (1936), 797.

(b) On the other hand, there can be a case where the foam is somewhat stabilized in a heterogeneous system in which a lower layer becomes to be dispersed in an upper one, or an upper layer of markedly lower surface tension is dispersed in a lower one on agitation. We may discuss the former case in this section.

Such a heterogeneous system usually consists of an upper layer of larger volume and a lower layer of smaller one as shown in the last column of Table 3, which corresponds to region D in Fig. 3. When we shake AEW-system belonging to this region, the lower layer of at least slightly larger surface tension is dispersed in the upper one which can readily be recognised from the appearance of breaking up of emulsion thus formed.[13] Droplets of such emulsion do not break films of foam produced in it simultaneously by agitation, for they either form droplets (and do not spread) on the surface of film in the case when they have slightly larger surface tension than dispersing medium, or they utterly escape from the surface of film when they have fairly larger surface tension than dispersing medium. These are schematically illustrated in Figs. 6 and 7 respectively. Accordingly, the system does not interfere with the foam produced in the dispersing medium, and so certain degree of foam formation can be expected in these cases.

(c) Next, the latter case of the section (b) will be discussed, that is the heterogeneous system composed of the droplets of markedly smaller surface tension in the medium of larger surface tension. In such a system, the volume of the upper layer (smaller surface tension) is usually smaller than that of lower one (larger surface tension) as shown in lower portion of the sixth column of Table 3, which corresponds to region E in Fig. 3.

When we shake AEW-system of this region, air bubbles produced at the same time in the dispersing medium readily and entirely go into the interior of emulsion droplets on account of large difference in surface tensions between both layers, so bubbles are covered with homogeneous films made of emulsion droplets which are again surrounded by the dispersing medium. These circumstances are readily understood from Fig. 8a. Thus, in the suitable system of this region, we can observe fairly stable emulsion drops containing air bubbles which gradually go up to, and accumulate at, the interface of ethyl ether—water as shown in Fig. 8b, though the foam formation cannot be observed.

In conclusion, the author wishes to express his hearty thanks to Prof. J. Sameshima for his kind guidance. The expense for the experi-

(13) It will be reported precisely upon this point in the latter paper.

ments has been defrayed from a grant given to Prof. Sameshima by Nippon Gakujutsu Shinkokwai (Japan Society for the Promotion of Scientific Research), to which the author's thanks are due.

Summary.

(1) The foam formation of the liquid ternary system of acetic acid—ethyl ether—water was measured by means of a shaking apparatus which was properly constructed for this purpose.

(2) The life time of foam produced and the height of foam zone have been measured.

(3) The diagrams were made between the degree of foam formation and the composition, and several conclusions were obtained on the foam formation of the mixture belonging to homogeneous and heterogeneous regions of the above ternary system.

Chemical Institute, Faculty of Science,
Imperial University of Tokyo.

On the Polymerization of Chloroprene as Revealed by the Raman Effect.

By Tutomu KUBOTA.

(Received November 26, 1938.)

Several authors[1][2][3] have applied the Raman spectra to the study of the polymerization mechanism, e.g., the polymerization of styrene[1][2] and methacrylic acid esters,[3] which is considered to proceed by the opening of the double bonds of monomers. The present paper deals with an analogous experimental research on the polymerization mechanism of chloroprene, one of dienes which have conjugate double linkages. Carothers and his co-workers[4] explained the polymerization mechanism of chloroprene as follows: the first step,

(1) Signer and Weiler, *Helv. Chim. Acta*, **15** (1932), 649.
(2) Mizushima, Morino, and Inoue, this Bulletin, **12** (1937), 136.
(3) Hibben, *J. Chem. Phys.*, **5** (1937), 706.
(4) Carothers, Williams, Collins, and Kirby, *J. Am. Chem. Soc.*, **53** (1931), 4203.

$$CH_2{:}C(Cl)\text{-}CH{:}CH_2 + CH_2{:}C(Cl)\text{-}CH{:}CH_2 + CH_2{:}C(Cl)\text{-}CH{:}CH_2 \quad (1)$$

$$\rightarrow \quad -CH_2\text{-}C(Cl){:}CH\text{-}CH_2\text{-}CH_2\text{-}C(Cl){:}CH\text{-}CH_2\text{-}CH_2\text{-}C(Cl){:}CH\text{-}CH_2\text{-} \quad (2)$$

and the second step,

$$\begin{matrix} -A-A-A-A-A-A-A-A-A- \\ -A-A-A-A-A-A-A-A-A- \\ -A-A-A-A-A-A-A-A-A- \end{matrix} \quad (2) \quad \rightarrow \quad \begin{matrix} -A-A-A-A-A-A-A-A-A- \\ -A-\underset{|}{A}-A-A-A-A-A-A-A- \\ -A-A-A-\underset{|}{A}-A-A-A-\underset{|}{A}-A- \end{matrix} \quad (3)$$

where A is a chloroprene unit. According to their theory, it is expected that the polymerized chloroprene will have a new C:C frequency which is nearly equal to that of 2-chlorobutene-(2), but is different from that of the monomer.

Raman spectra of monomeric chloroprene, polymerized chloroprene in the solid state, and 2-chlorobutene-(2) were photographed and the results are given in Table 1. When the liquid sample (monomer) solidifies,

Table 1.

Chloroprene (liquid)	Polychloroprene (solid)	2-Chlorobutene-(2)
158 (1b) e	158 (2b) e	—
249 (4b) e	248 (4b) e	230 (2b) e
—	—	339 (4) e,k
387 (3) e	387 (3) e	389 (0) e,k
—	—	433 (3) e,k
—	—	459 (3) e,k
518 (4) e	521 (4) e	523 (2) e,k
—	—	(544) (1) e
—	—	564 (0) e,k
629 (6) e	630 (6) e	606 (8) e,k
—	—	645 (0) e,k
—	—	670 (4) e,k
735 (0) e	735 (0) e	795 (0) e,k
882 (2b) e	882 (2b) e	—
923 (2b) e	921 (2b) e	—
1020 (2) e	1018 (2) e	1025 (0) e,k
—	—	(1115) (2) e
1214 (3) e	1216 (4) e	—
—	1260 (0) e	—

Table 1.—(*Concluded*)

Chloroprene (liquid)			Polychloroprene (solid)			2-Chlorobutene-(2)		
1287	(7)	e	1287	(7)	e	1287	(4)	e,k
1359	(0)	e	1359	(0)	e	—		
1381	(1)	e	1381	(1)	e	1380	(5)	e,k
1417	(6)	e	1419	(6)	e	1441	(8b)	e,k
1526	(1)	e	1526	(1)	e	—		
1581	(4)	e	1581	(4)	e	—		
1628	(15)	e,k	1628	(15)	e,k	(1633)	(4)	e,k
—			1658	(3)	e	1670	(7)	e,k
—			—			2857	(2b)	e,k
—			—			2918	(10)	e,i,k,q
—			—			2942	(2b)	e,k
—			—			2981	(5)	e,k,q
3015	(6)	e	3015	(6)	e	3025	(2b)	e,k
3113	(5b)	e	3109	(5b)	e	—		

the intensity of the C:C frequency of the monomer decreases slightly but there appears another frequency (1658 cm.$^{-1}$), which should be assigned also to the C:C frequency. The latter frequency is not much different from 1670 cm.$^{-1}$, the frequency due to the C:C bond of 2-chlorobutene-(2), the molecule of which has the methyl groups instead of the heavier groups of (2). From the intensities of the Raman lines it may be concluded that the polymerization proceeds linearly but not to a large extent. In the solid state, at least at the first stage, the larger part of chloroprene does not polymerize by the primary linkages but is held together by the van der Waals forces. Similar phenomena were also observed by Mizushima and his co-workers[2] about styrene and by Hibben[3] about methyl methacrylate.

The author thanks Prof. Mizushima for his kind advices and also expresses his thanks to Mr. K. Fuwa, Mr. A. Wada and Mr. R. Kitani for their kind encouragements.

Laboratory, Tokyo Electric Co.,
Kawasaki near Tokyo.

Austauschreaktion der Kernwasserstoffatome des Phenols. I. Austauschreaktion in alkalischer Lösung.

Von Masao KOIZUMI und Toshizo TITANI.

(Eingegangen am 29. November 1938.)

Inhaltsübersicht. Die Austauschreaktion des Phenols in der mit Alkali versetzten verdünnten schwerwässrigen Lösung kommt zur Untersuchung. Dabei wird der Versuch mit Hilfe der früher beim Versuch mit Nitrophenol entwickelten Methode nach der quantitativen Seite hin ausgeführt, indem die mittlere Geschwindigkeitskonstante $\bar{k}$ der Austauschreaktion der drei Kernwasserstoffatome des Phenolmoleküle bei verschiedenen Temperaturen zwischen 89° und 120°C. bestimmt wird. Die gefundenen Werte von $\bar{k}$ werden durch den Ausdruck wiedergegeben:

$$\log \bar{k} = (8.7 \pm 0.5) - \frac{24{,}800 \pm 800}{2.3\,RT} \quad \text{(Mol/Liter)}^{-1}\text{(Sek.)}^{-1}.$$

Diese Konstante $\bar{k}$ entspricht aber der stöchiometrischen Gl.:

$$C_6H_5OH + HDO = C_6H_4DOH + H_2O.$$

Dagegen findet die wirkliche Reaktion zwischen Phenolationen und neutralen Phenolmolekülen statt, wie etwa das folgende Schema zeigt:

$$C_6H_5O^- + C_6H_5OD = C_6H_4DO^- + C_6H_5OH.$$

Die Geschwindigkeitskonstante $\bar{k}_0$ für diese letzte Reaktion wird somit in der ersten Annährung durch den Ausdruck wiedergegeben:

$$\bar{k}_0 = 10^{10.8}\, e^{-\frac{24{,}800}{RT}} \quad \text{(Mol/Liter)}^{-1}\text{(Sek.)}^{-1}.$$

Die Reaktion dürfte deshalb als die normal verlaufende bimolekulare Reaktion aufgefasst werden können.

Einleitung. Die Austauschreaktion der Kernwasserstoffatome des Phenols in ziemlich konzentrierten alkalischen Lösungen wurde von Ingold und seinen Mitarbeitern[1] untersucht. Dabei kamen sie zu dem Schluss, obwohl ihre Versuchsmethode vielmehr qualitativer Natur war, dass die Reaktion zwischen Phenolationen und neutralen Phenolmolekülen verläuft. Denselben Schluss erhielten wir auch beim Austauschversuch mit drei isomerischen Arten der Nitrophenole in verdünnten alkalischen Lösungen.[2] Die dabei benutzte Versuchsmethode lässt uns aber den

(1) C. K. Ingold, C. G. Raisin und C. L. Wilson, *J. Chem. Soc.*, **1936**, 1637.
(2) M. Koizumi und T. Titani, dies Bulletin, **13** (1938), 318, 595, 631.

Reaktionsverlauf nicht nur von der qualitativen Seite sondern auch nach der quantitativen Seite hin verfolgen: sie lässt die Geschwindigkeitskonstante und folglich die Aktivierungsenergie der Reaktion ziemlich genau ermitteln. Wir haben deshalb unter Benutzung dieser Methode die Austauschreaktion des Phenols in saurer sowie in alkalischer Lösung untersucht. Der letztere Versuch, um welchen es sich in der vorliegenden I. Mitteilung handelt, interessiert uns in so fern, als wir dessen Ergebnisse, insbesonders die Aktivierungsenergie der Reaktion, mit der für die Nitrophenole[3] vergleichen können.

Versuche. Die Experimentalmethode ist im grossen und ganzen dieselbe wie die beim letzten Versuch mit Nitrophenole benutzte. Etwa 2 g. Phenol wird zusammen mit ca 1 g. KOH-alkalischen verdünnten schweren Wassers (beide Mengen sind genau gemessen!) in einem zugeschmolzenen und gut evakuierten Glasrohr bis auf eine bestimmte Temperatur während einer bestimmten Versuchsdauer erwärmt. Der D-Gehalt des dazu benutzten schweren Wassers ist ca 4% und die Alkalikonzentration beträgt immer ziemlich genau 1 N. Nach der Erwärmung wird das schwere Wasser durch die zweimal nacheinander folgend ausgeführte Destillation im Vakuum von Phenol abgetrennt. Da aber das so abgeschiedene Wasser noch eine ziemlich beträchtliche Menge von Phenol enthält, wird das Wasser zusammen mit einer Menge von gut getrocknetem Äther kräftig geschüttelt und der dabei im Wasser um ein wenig gelöste Äther durch die weitere Behandlung mit Pumpenöl beseitigt.[4] Das auf diese Weise vom Phenol vollständig befreite Wasser wird dann nach der üblichen Methode gründlich gereinigt und dessen D-Gehalt schwebemetrisch bestimmt. Bezeichnet man den so ermittelten D-Gehalt des schweren Wassers vor und nach dem Experiment resp. mit D_a und D_e, dann wird das Austauschäquivalent na des Phenols mittels der Gl.(1) ohne weiteres errechnet:

$$na = \frac{2(D_a - D_e)}{D_e} \frac{M_w}{M_{ph}} \qquad (1).$$

In dieser Gl.(1) bedeutet M_w und M_{ph} resp. die Molzahl des zum Versuch verwendeten schweren Wassers und des Phenols und das Austauschäquivalent na wird durch die Gl.(2) definiert:

$$na = \sum n_i a_i \qquad (2),$$

(3) Ein Teil der Arbeit, der sich hauptsächlich um die Aktivierungsenergie handelt, ist noch nicht veröffentlicht.

(4) Vgl. z.B. M. Harada und T. Titani, dies Bulletin, **11** (1936), 468.

Tabelle 1. Versuchsergebnisse.

Versuchs-nr.	Versuchs-dauer t in Stdn.	M_w	M_{ph}	$D_a - D_e$ in γ	D_e in γ	$n\alpha$
Versuchstemperatur = 88 5—89.0°C.						
24	8.5	0.0553	0.0218	1157	3112	1.89
25	12.5	0.0552	0.0216	1352	2917	2.38
26	18.0	0.0554	0.0218	1491	2778	2.74
Versuchstemperatur = 100.0°C.						
1	0.0	0.0553	0.0216	768	3249	1.21
8	0.0	0.0537	0.0216	871	3453	1.25
28	0.0	0.0549	0.0217	900	3421	1.26
29	0.0	0.0550	0.0212	858	3463	1.28
30	0.0	0.0553	0.0219	875	3446	1.28
17	4.5	0.0556	0.0217	1306	3025	2.21
16	6.0	0.0555	0.0216	1392	2939	2.43
2	6.0	0.0553	0.0216	1316	2701	2.49
7	8.0	0.0553	0.0216	1522	2802	2.78
6	15.0	0.0555	0.0219	1755	2569	3.46
5	25.5	0.0557	0.0218	1867	2457	3.89
3	45.0	0.0551	0.0219	1740	2277	3.85
4	48.0	0.0555	0.0217	1876	2448	3.92
Versuchstemperatur = 111.0~111 5°C.						
20	2.33	0.0552	0.0219	1420	2911	2.46
21	4.0	0.0555	0.0217	1637	2694	3.11
27	5.0	0.0551	0.0215	1698	2592	3.38
9	6.0	0.0557	0.0218	1720	2604	3.37
12	8.83	0.0555	0.0218	1890	2434	3.95
11	14.2	0.0555	0.0218	1873	2451	3.89
10	23.0	0.0554	0.0216	1870	2454	3.92
Versuchstemperatur = 122 0~122.5°C.						
19	1.2	0.0554	0.0218	1542	2789	2.81
18	1.7	0.0552	0.0218	1658	2673	3.14
14	3.0	0.0552	0.0219	1838	2486	3.73
15	6.0	0.0549	0.0217	1889	2442	3.91
13	9.0	0.0550	0.0218	1919	2405	4.03
22	10.0	0.0551	0.0220	1912	2419	3.96

wo n_i die Anzahl und a_i den Verteilungsquotienten der austauschbaren Arten der H-Atome bedeutet und die Summation für alle austauschbaren Arten der H-Atome in einem Molekül ausgeführt wird. Die auf diese Weise bei verschiedenen Versuchstemperaturen und Versuchsdauern gemessenen Werte vom Austauschäquivalent des Phenols sind in Tabelle 1 zusammengestellt, wo die Versuchsnr. in der ersten Spalte die zeitliche Reihenfolge der einzelnen Versuche zeigt und der D-Gehalt des schweren Wassers D_a und D_e durch den Dichteüberschuss gewöhnlichem Wasser gegenüber angegeben wird.

Dieselben Resultate geben wir auch in Abb. 1 graphisch wieder, wo das gefundene Austauschäquivalent na gegen die Versuchsdauer t eingezeichnet wird. Das Austauschäquivalent $(na)_0$ unmittelbar nach dem Beginn des Versuches, d.h. bei $t = 0$, besitzt, gemeinsam für alle vier Versuchstemperaturen, immer denselben Wert, nämlich 1.26. Dann

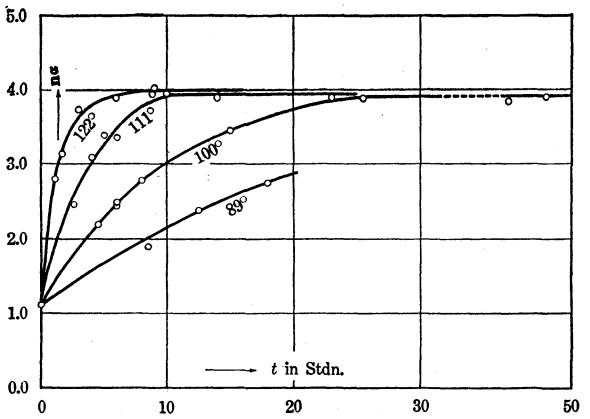


Abb. 1. Abhängigkeit des Austauschäquivalents $n\alpha$ von der Versuchsdauer t.

wächst na mit zunehmender Versuchsdauer allmählich an, bis schliesslich, nach genügend langer Zeit, ein Grenzwert $(na)_\infty$ erreicht wird. Dieser Verlauf der na-t-Kurve weist aber ohne weiteres darauf hin, dass das Hydroxylwasserstoffatom des Phenols sehr schnell, fast momentan, gegen die des Wassers ausgetauscht und dann einige Kernwasserstoffatome langsam, aber mit wohl bestimmbarer Geschwindigkeit, ausgetauscht werden. Was die sich an dieser Austauschreaktion beteiligenden Kernwasserstoffatome anbetrifft, so ist, aus dem anderen chemischen Verhalten des Phenols zu urteilen, ziemlich sicher, dass es sich um die in o-, o'- und p-Stellung befindlichen drei H-Atome handelt. Wir können deshalb mit Hilfe der gefundenen Werte von $(na)_0$ und $(na)_\infty$ den Ver-

teilungsquotienten (V.Q.) des Hydroxylwasserstoffs und Kernwasserstoffs des Phenols errechnen. Zunächst muss das anfängliche Austauschäquivalent $(na)_0$ den V.Q. des Hydroxylwasserstoffs ausdrücken, weil das Phenolmolekül nur ein solches Atom enthält. Aber der im vorliegenden Versuch gefundene Wert von $(na)_0$ (= 1.26) ist deutlich grösser als der früher von uns bestimmte V.Q. der Phenolhydroxylgruppe, nämlich 1.07.[5] Diesen Unterschied können wir auf die Verschiedenheit des Abtrennungsprozesses von Wasser aus der Lösung zurückführen. Beim früheren Versuch, dessen Hauptzweck die Bestimmung des Verteilungsquotienten war, trennten wir das Wasser vom Phenol dadurch ab, dass wir das letztere mittels Kohlenstofftetrachlorids aus der Lösung abzogen. Dagegen führten wir beim vorliegenden Versuch die Abtrennung durch die blosse Destillation im Vakuum aus. Deshalb liegt bei diesem letzteren Fall die Möglichkeit sehr nahe, dass die Verteilung der D-Atome wegen der Verschiebung des Austauschgleichgewichts während des Destillationsprozesses günstig für den Hydroxylwasserstoff des Phenols verschoben wird. Wir haben vielmehr mit dem hier gefundenen Wert von $(na)_0$ (= 1.26) dem „scheinbaren" Verteilungsquotienten des Hydroxylwasserstoffatoms zu tun. Aber in jedem Fall darf man, aus den folgenden Gründen, die Differenz $na-(na)_0$ als das wahre Austauschäquivalent des Kernwasserstoffs des Phenols ansehen. Denn erstens erhielten wir für $(na)_0$ immer einen wiederholbaren Wert (= 1.26), obwohl dies vom wahren V.Q. verschieden ist (vgl. Tabelle 1 bei 100.0°C.) und zweitens kann die Verschiebung des Austauschgleichgewichts des Kernwasserstoffs während des Destillationsprozesses bei der Abtrennung (die höchstens eine Stunde dauert) wegen der Kleinheit der Austauschgeschwindigkeit wohl ausser Acht gelassen werden. Nimmt man deshalb an, wie schon oben erwähnt, dass die sich an der Austauschreaktion beteiligenden Kernwasserstoffatome die in *o*-, *o'*- und *p*-Stellung befindlichen drei H-Atome sind, dann können wir den V.Q. dieser H-Atome mittels der Gl.(3) ohne weiteres errechnen:

$$\text{V.Q.} = \frac{(na)_\infty - 1.26}{3} \qquad (3).$$

Der so berechnete Wert von V.Q. stimmt, wie die letzte Spalte der Tabelle 2 zeigt, mit dem für unsubstituiertes Benzol gefundene V.Q., der nach Koyano[6] bei 100°C. 0.93 beträgt, hinreichend gut überein, obwohl wir zwischen beiden Werten einen untrügbaren Unterschied finden können. Dieselbe Neigung, dass der V.Q. von Phenole um ein wenig kleiner als

(5) M. Harada und T. Titani, dies Bulletin, **11** (1936), 465.
(6) T. Koyano, *J. Chem. Soc. Japan*, **57** (1936), 929.

der des unsubstituierten Benzols ist, wurde auch von Geib[7] und Münzberg[8] bei ihren Arbeiten mit Polyphenole gefunden. Wir ersehen weiter aus dieser Tabelle 2, dass der Wert von $(n\alpha)_\infty$ und folglich der V.Q. der Kernwasserstoffs bis zu einem gewissen Grad von der Temperatur abhängt.

Tabelle 2. Verteilungsquotient der Kernwasserstoffatome des Phenols.

Versuchs-Temperatur °C.	$(n\alpha)_\infty$	$(n\alpha)_\infty - 1.26$	V. Q. $= \frac{(n\alpha)_\infty - 1\,26}{3}$
89	3.90[9]	2.64	0.88
100	3.92	2.66	0.89
111	3.94	2.68	0.89
122	3.98	2.72	0.91

Geschwindigkeitskonstante und Aktivierungsenergie. Wenn wir die Austauschreaktion des Phenols in wässriger Lösung als die reversible bimolekulare Reaktion zwischen Phenol und Wasser auffassen, können wir die mittlere Geschwindigkeitskonstante $\bar{k}$ für die (stöchiometrische) Reaktion (4) graphisch ermitteln:

$$C_6H_5OH + HDO = C_6H_4DOH + H_2O \qquad (4).$$

Die Bestimmungsmethode beruht auf genau demselben Prinzip wie das beim früheren Versuch mit Nitrophenole benutzte. Wir bedienen uns nämlich der folgenden Beziehungen zwischen der Geschwindigkeitskonstante $\bar{k}$, dem Austauschäquivalent $n\alpha$ und der Versuchsdauer t:[10]

(7) K. H. Geib, *Z. physik. Chem*, A, **180** (1937), 211.

(8) F. K. Münzberg, *Z. physik. Chem.*, B, **33** (1936), 23, 39.

(9) Dieser Wert wurde, aus dem Bedürfnis der weiteren Berechnung, mit Hilfe der Daten bei den anderen Temperaturen extrapoliert ermittelt.

(10) Vgl. Gl. (15) und (16) in der zweiten Arbeit von Fussnote 2. Beim vorliegenden Fall wird in dieser letzteren Gl. (16) $n_2 + \frac{\alpha_1}{\alpha_2} n_1 = 4.2$, $\frac{2}{\alpha_2} = 2.2$, $n\alpha - n_1\alpha_1 = n\alpha - 1.26$, $n_2\alpha_2 = (n\alpha)_\infty - 1.26$ und $n_1\alpha_1 = 1.07$ gesetzt, weil die Austauschreaktion des Hydroxylwasserstoffatoms als die „erste" und die der Kernwasserstoffatome als die „zweite" Stufe der Reaktion aufgefasst werden kann. Der Grund dafür, dass für den Ausdruck $(n\alpha - n_1\alpha_1)$, $n_1\alpha_1 = 1.26$ dagegen für $(n_1\alpha_1)$ allein $n_1\alpha_1 = 1.07$ gesetzt wird, liegt darin, dass der Ausdruck $(n\alpha - n_1\alpha_1)$ bzw. $(n_1\alpha_1)$ resp. als Ganzes bzw. als sich selbst das „wahre" Austauschäquivalent des Kernwasserstoffs bzw. Hydroxylwasserstoffs ausdrücken muss (vgl. dazu die Diskussion bei Gl. (3)).

$$-X \log Y = \frac{\bar{k}}{2.303} t \qquad (5),$$

wo

$$X = \frac{V}{4.2M_{ph} + 2.2M_w} \quad \text{und} \quad Y = \frac{1 - \dfrac{n\alpha - 1.26}{(n\alpha)_\infty - 1.26}}{1 + \dfrac{n\alpha - 1.26}{\dfrac{2M_w}{M_{ph}} + 1.07}} \qquad (6).$$

Das (in Liter gemessene) Volumen der Lösung V, wird mit Hilfe des in Tabelle 3 angegebenen spezifischen Volumens der Lösung bei in Rede stehender Temperatur berechnet. Dieses letztere wurde aber direkt pyknometrisch bestimmt.

Tabelle 3. Spezifisches Volumen der Lösung.

Temperatur °C.	89	100	111	122
Spez. Volumen in c.c.	0.9879	0.9980	1.0077	1.0170

Tabelle 4. Geschwindigkeitskonstante bei verschiedenen Temperaturen.

Versuchs-temperatur °C.	Versuchs-dauer t in Stdn.	$-X \log Y$	$\bar{k}/2.303$	$\log(\bar{k}/2\,303)$	$1/T$
89	8.5 12.5 18.0	0.00103 0.00145 0.00209	0.000116 ~ 0.000118	−3.936 ~ −3.928	0.002762
100	4.5 6.0 8.0 15.0	0.00119 0.00154 0.00217	0.000264 ~ 0.000270	−3.578 ~ −3.569	0.002681
111	2.33 4.0 5.0 6.0	0.00159 0.00294 0.00385 0.00382	0.00070 ~ 0.00074	−3.155 ~ −3.131	0.002604
122	1.17 1.67 3.0	0.00222 0.00298 0.00561	0.00178 ~ 0.00183	−2.750 ~ −2.737	0.002532

Die unter Benutzung dieser Werte des spezifischen Volumens sowie der des bei verschiedenen Versuchsdauern gefundenen Austauschäquivalents na mittels Gl. (6) berechneten Werte von $(-X \log Y)$ geben wir in der dritten Spalte der Tabelle 4 wieder.[11]

Zeichnet man die berechneten Werte von $(-X \log Y)$ gegen die Versuchsdauer t, so erhält man für jede bestimmte Versuchstemperatur, wie Gl. (5) fordert, eine gute gerade Linie in Abb. 2 und aus der Neigung dieser Linie gegen die t-Achse wird die Geschwindigkeitskonstante $\bar{k}/2.303$ graphisch ermittelt. Die so gefundenen Werte von $\bar{k}/2.303$ geben wir in der vierten Spalte der Tabelle 4 wieder.

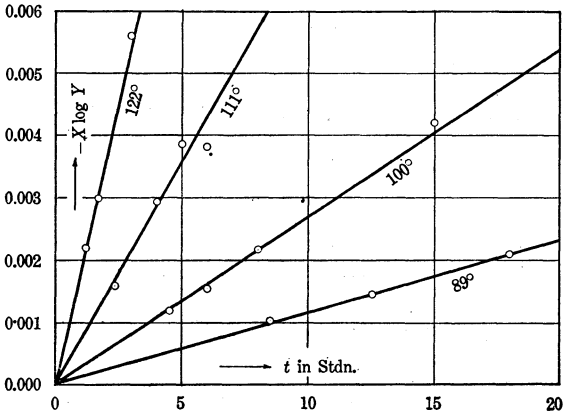


Abb. 2. Graphische Ermittelung der Geschwindigkeitskonstante $\bar{k}$.

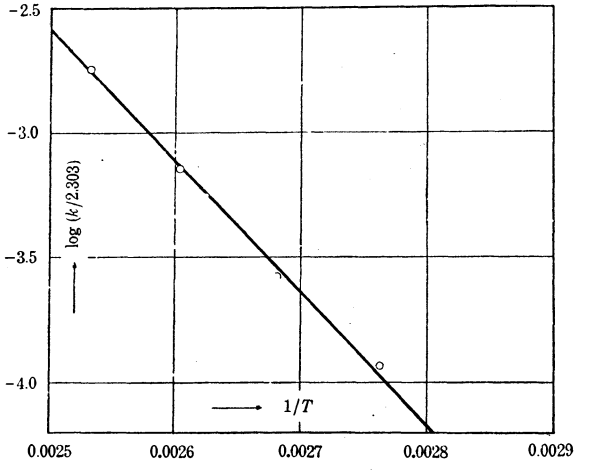


Abb. 3. Abhängigkeit der Geschwindigkeitskonstante $\bar{k}$ von der absoluten Temperatur T.

(11) Die Daten von sehr langer Versuchsdauer wurden nicht benutzt.

Da wir auf diese Weise die Geschwindigkeitskonstante $\bar{k}$ bei vier verschiedenen Temperaturen bestimmt haben, können wir die Aktivierungenergie der Reaktion nach der üblichen Methode ohne weiteres bestimmen. In der nebenstehenden Abb. 3 zeichnen wir die aus Tabelle 4 entnommenen Werte von $\log(\bar{k}/2.303)$ gegen die ebenfalls in Tabelle 4 angegebenen reziproken Werte der absoluten Temperatur $1/T$ ein. Die dadurch gewonnene gerade Linie können wir durch den Ausdruck:

$$\log(\bar{k}/2.303) = (11.0 \pm 0.5) - \frac{24{,}800 \pm 800}{4.574\,T} \text{ (Mol/Liter)}^{-1}\text{(Stunde)}^{-1} \quad (7),$$

bzw.: $$\bar{k} = 10^{8.7 \pm 0.5}\, e^{-\frac{24{,}800 \pm 800}{RT}} \text{ (Mol/Liter)}^{-1}\text{(Sekunde)}^{-1} \quad (8)$$

wiedergeben.

Die so ermittelte Konstante $\bar{k}$ ist aber, wie aus der Ableitung der Gl.(5) und (6) ohne weiteres ersichtlich ist,[12] für die schon oben angegebene stöchiometrische Reaktion (4) einzusetzen, so dass diese Konstante $\bar{k}$ durch Gl.(9) definiert wird:

$$-\frac{d[[\text{HDO}]]}{dt} = k\,[[C_6H_5OH]]\,[[\text{HDO}]] \quad (9),$$

wo $[[C_6H_5OH]]$ und $[[\text{HDO}]]$ resp. die gesamte (analytische) Konzentration des Phenols bzw. schweren Wassers bedeutet. Dagegen muss die wirkliche Reaktion, wie schon oben in der Einleitung erwähnt wurde, zwischen Phenolationen und neutralen Phenolmolekülen, etwa nach dem folgenden Schema, verlaufen:

$$C_6H_5O^- + C_6H_5OD = C_6H_4DO^- + C_6H_5OH \quad (10),$$

und somit wird die Geschwindigkeitskonstante $\bar{k}_0$ für diese grundlegende Reaktion(10) durch Gl.(11) bestimmt:

$$-\frac{d[C_6H_5OD]}{dt} = \bar{k}_0\,[C_6H_5O^-]\,[C_6H_5OD] \quad (11),$$

wo $[C_6H_5O^-]$ und $[C_6H_5OD]$ resp. die wirkliche Konzentration von Phenolationen und schweren Phenolmolekülen bedeutet. Da aber die Austauschreaktion der Hydroxylwasserstoffatome sehr schnell stattfindet und folglich die beiden schweren Molekülarten HDO und C_6H_5OD sich immer im Gleichgewicht befinden müssen, darf man die beiden Geschwindigkeiten (9) und (11) praktisch gleich setzen. So wird:

(12) Vgl. dazu die Arbeit: M. Koizumi und T. Titani, dies Bulletin, **13** (1938), 595.

$$\bar{k}_o = \bar{k}\frac{[[C_6H_5OH]]\,[[HDO]]}{[C_6H_5O^-]\,[C_6H_5OD]} = \bar{k}\frac{2[[C_6H_5OH]]\,[[H_2O]]}{[C_6H_5O^-]\,[C_6H_5OH]} \qquad (12).$$

Aber weil in der ersten Annäherung $[C_6H_5OH] = [[C_6H_5OH]] - [C_6H_5O^-]$ und $[C_6H_5O^-] = [[KOH]]$ gesetzt werden kann, folgt ohne weiteres, dass

$$\bar{k}_o = 10^{2.1}\,\bar{k} \qquad (13)$$

ist und mit Hilfe dieser Beziehung (13) und der schon oben angegebenen Gl.(8) erhält man für die Geschwindigkeitskonstante $\bar{k}_0$ der grundlegenden Reaktion (10) den Ausdruck:

$$\bar{k}_o = 10^{10.8}\, e^{-\frac{24,800}{RT}} \qquad (14).$$

Der Stossfaktor ($= 10^{10.8}$) für die vorliegende Reaktion (10) ist also von fast derselben Grössenordnung wie der für die von Geib[7] untersuchte Austauschreaktion von Resorcin in saurer Lösung. Deshalb liegt die Annahme nahe, dass die hier untersuchte Reaktion von Phenol in alkalischer Lösung ebenso wie die Reaktion von Resorcin in saurer Lösung, als die normal verlaufende bimolekulare Reaktion in Lösung aufgefasst werden darf. Dagegen ist die gefundene Aktivierungsenergie ($= 24,800$ cal.) der vorliegenden Reaktion (4) bzw. (10) um etwa 4.3 Kcal. grösser als die der Austauschreaktion von Resorcin in saurer Lösung. Aber weil nach Geib die Aktivierungsenergie derselben Reaktion in alkalischer sowie neutraler Lösung etwa ebenso hoch wie in saurer ist, liegt die Vermutung nahe, dass die Aktivierungsenergie der Austauschreaktion der Wasserstoffatome im Benzolkern sich mit der Zunahme der im Kern eingeführten Anzahl der Hydroxylgruppen allmählich vermindert. Über den Mechanismus der Reaktion soll später, erst nach der Beendigung der nächsten Versuche in saurer Lösung diskutiert werden.

Zum Schluss möchten wir der Nippon-Gakujutzu-Shinkohkai (der Japanischen Gesellschaft zur Förderung der wissenschaftlichen Forschungen) sowie der Hattori-Hohkohkai (der Hattori-Stiftung) für ihre finanzielle Unterstützung bei der Ausführung der vorliegenden Arbeit unseren wärmsten Dank aussprechen.

Siomi Institut für physikalische und chemische Forschung
und
Physikalisch-chemisches Laboratorium der Kaiserlichen Universität zu Osaka.